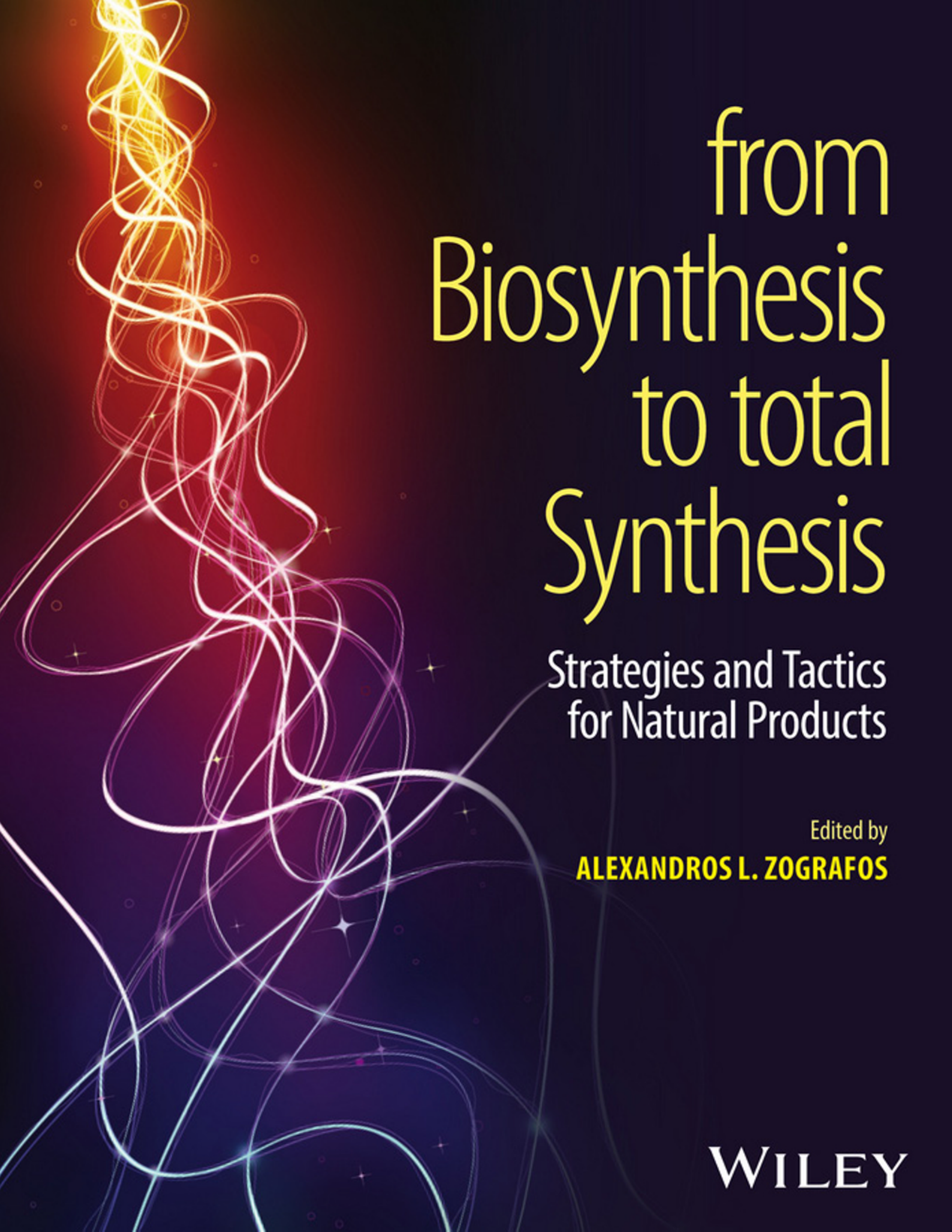


# from Biosynthesis to total Synthesis

## Strategies and Tactics for Natural Products

Edited by

**ALEXANDROS L. ZOGRAFOS**

WILEY

# FROM BIOSYNTHESIS TO TOTAL SYNTHESIS

# FROM BIOSYNTHESIS TO TOTAL SYNTHESIS

## Strategies and Tactics for Natural Products

Edited by

**ALEXANDROS L. ZOGRAFOS**
Aristotle University of Thessaloniki, Greece

WILEY

Copyright © 2016 by John Wiley & Sons, Inc. All rights reserved

Published by John Wiley & Sons, Inc., Hoboken, New Jersey
Published simultaneously in Canada

No part of this publication may be reproduced, stored in a retrieval system, or transmitted in any form or by any means, electronic, mechanical, photocopying, recording, scanning, or otherwise, except as permitted under Section 107 or 108 of the 1976 United States Copyright Act, without either the prior written permission of the Publisher, or authorization through payment of the appropriate per-copy fee to the Copyright Clearance Center, Inc., 222 Rosewood Drive, Danvers, MA 01923, (978) 750-8400, fax (978) 750-4470, or on the web at www.copyright.com. Requests to the Publisher for permission should be addressed to the Permissions Department, John Wiley & Sons, Inc., 111 River Street, Hoboken, NJ 07030, (201) 748-6011, fax (201) 748-6008, or online at http://www.wiley.com/go/permissions.

Limit of Liability/Disclaimer of Warranty: While the publisher and author have used their best efforts in preparing this book, they make no representations or warranties with respect to the accuracy or completeness of the contents of this book and specifically disclaim any implied warranties of merchantability or fitness for a particular purpose. No warranty may be created or extended by sales representatives or written sales materials. The advice and strategies contained herein may not be suitable for your situation. You should consult with a professional where appropriate. Neither the publisher nor author shall be liable for any loss of profit or any other commercial damages, including but not limited to special, incidental, consequential, or other damages.

For general information on our other products and services or for technical support, please contact our Customer Care Department within the United States at (800) 762-2974, outside the United States at (317) 572-3993 or fax (317) 572-4002.

Wiley also publishes its books in a variety of electronic formats. Some content that appears in print may not be available in electronic formats. For more information about Wiley products, visit our web site at www.wiley.com.

***Library of Congress Cataloging-in-Publication Data***

Names: Zografos, Alexandros L., editor.
Title: From biosynthesis to total synthesis : strategies and tactics for natural products / edited by Alexandros L. Zografos.
Description: Hoboken, New Jersey : John Wiley & Sons, Inc., [2016] | Includes bibliographical references and index.
Identifiers: LCCN 2015037375 (print) | LCCN 2015047240 (ebook) | ISBN 9781118751732 (cloth) | ISBN 9781118753569 (Adobe PDF) | ISBN 9781118753637 (ePub)
Subjects: LCSH: Organic compounds–Synthesis. | Biosynthesis.
Classification: LCC QD262 .F76 2016 (print) | LCC QD262 (ebook) | DDC 572/.45–dc23
LC record available at http://lccn.loc.gov/2015037375

Set in 10/12pt Times by SPi Global, Pondicherry, India

Printed in the United States of America

10 9 8 7 6 5 4 3 2 1

*Dedicated to my mother, father and wife*

# CONTENTS

**LIST OF CONTRIBUTORS** **xiii**

**PREFACE** **xv**

**1 From Biosyntheses to Total Syntheses: An Introduction** **1**
*Bastien Nay and Xu-Wen Li*

1.1 From Primary to Secondary Metabolism: The Key Building Blocks, 1
1.1.1 Definitions, 1
1.1.2 Energy Supply and Carbon Storing at the Early Stage of Metabolisms, 1
1.1.3 Glucose as a Starting Material Toward Key Building Blocks of the Secondary Metabolism, 1
1.1.4 Reactions Involved in the Construction of Secondary Metabolites, 3
1.1.5 Secondary Metabolisms, 4
1.2 From Biosynthesis to Total Synthesis: Strategies Toward the Natural Product Chemical Space, 10
1.2.1 The Chemical Space of Natural Products, 10
1.2.2 The Biosynthetic Pathways as an Inspiration for Synthetic Challenges, 11
1.2.3 The Science of Total Synthesis, 14
1.2.4 Conclusion: A Journey in the Future of Total Synthesis, 16
References, 16

**SECTION I ACETATE BIOSYNTHETIC PATHWAY** **19**

**2 Polyketides** **21**
*Françoise Schaefers, Tobias A. M. Gulder, Cyril Bressy, Michael Smietana, Erica Benedetti, Stellios Arseniyadis, Markus Kalesse, and Martin Cordes*

2.1 Polyketide Biosynthesis, 21
2.1.1 Introduction, 21
2.1.2 Assembly of Acetate/Malonate-Derived Metabolites, 23
2.1.3 Classification of Polyketide Biosynthetic Machineries, 23
2.1.4 Conclusion, 39
References, 40

2.2 Synthesis of Polyketides, 44
2.2.1 Asymmetric Alkylation Reactions, 44
2.2.2 Applications of Asymmetric Alkylation Reactions in Total Synthesis of Polyketides and Macrolides, 60
References, 83
2.3 Synthesis of Polyketides-Focus on Macrolides, 87
2.3.1 Introduction, 87
2.3.2 Stereoselective Synthesis of 1,3-Diols: Asymmetric Aldol Reactions, 88
2.3.3 Stereoselective Synthesis of 1,3-Diols: Asymmetric Reductions, 106
2.3.4 Application of Stereoselective Synthesis of 1,3-Diols in the Total Synthesis of Macrolides, 117
2.3.5 Conclusion, 126
References, 126

**3 Fatty Acids and Their Derivatives 130**
*Anders Vik and Trond Vidar Hansen*

3.1 Introduction, 130
3.2 Biosynthesis, 130
3.2.1 Fatty Acids and Lipids, 130
3.2.2 Polyunsaturated Fatty Acids, 134
3.2.3 Mediated Oxidations of ω-3 and ω-6 Polyunsaturated Fatty Acids, 135
3.3 Synthesis of ω-3 and ω-6 All-*Z* Polyunsaturated Fatty Acids, 140
3.3.1 Synthesis of Polyunsaturated Fatty Acids by the Wittig Reaction or by the Polyyne Semihydrogenation, 140
3.3.2 Synthesis of Polyunsaturated Fatty Acids via Cross Coupling Reactions, 143
3.4 Applications in Total Synthesis of Polyunsaturated Fatty Acids, 145
3.4.1 Palladium-Catalyzed Cross Coupling Reactions, 145
3.4.2 Biomimetic Transformations of Polyunsaturated Fatty Acids, 149
3.4.3 Landmark Total Syntheses, 153
3.4.4 Synthesis of Leukotriene $B_5$, 158
3.5 Conclusion, 160
Acknowledgments, 160
References, 160

**4 Polyethers 162**
*Youwei Xie and Paul E. Floreancig*

4.1 Introduction, 162
4.2 Biosynthesis, 162
4.2.1 Ionophore Antibiotics, 162
4.2.2 Marine Ladder Toxins, 165
4.2.3 Annonaceous Acetogenins and Terpene Polyethers, 165
4.3 Epoxide Reactivity and Stereoselective Synthesis, 166
4.3.1 Regiocontrol in Epoxide-Opening Reactions, 166
4.3.2 Stereoselective Epoxide Synthesis, 172
4.4 Applications to Total Synthesis, 176
4.4.1 Acid-Mediated Transformations, 176
4.4.2 Cascades via Epoxonium Ion Formation, 179
4.4.3 Cyclizations under Basic Conditions, 181
4.4.4 Cyclization in Water, 182
4.5 Conclusions, 183
References, 184

**SECTION II MEVALONATE BIOSYNTHETIC PATHWAY 187**

**5 From Acetate to Mevalonate and Deoxyxylulose Phosphate Biosynthetic Pathways: An Introduction to Terpenoids 189**
*Alexandros L. Zografos and Elissavet E. Anagnostaki*

5.1 Introduction, 189
5.2 Mevalonic Acid Pathway, 191
5.3 Mevalonate-Independent Pathway, 192
5.4 Conclusion, 194
References, 194

**6 Monoterpenes and Iridoids 196**
*Mario Waser and Uwe Rinner*

6.1 Introduction, 196
6.2 Biosynthesis, 196
6.2.1 Acyclic Monoterpenes, 197
6.2.2 Cyclic Monoterpenes, 197
6.2.3 Iridoids, 200
6.2.4 Irregular Monoterpenes, 202
6.3 Asymmetric Organocatalysis, 203
6.3.1 Introduction and Historical Background, 204
6.3.2 Enamine, Iminium, and Singly Occupied Molecular Orbital Activation, 207
6.3.3 Chiral (Brønsted) Acids and H-Bonding Donors, 213
6.3.4 Chiral Brønsted/Lewis Bases and Nucleophilic Catalysis, 218
6.3.5 Asymmetric Phase-Transfer Catalysis, 220
6.4 Organocatalysis in the Total Synthesis of Iridoids and Monoterpenoid Indole Alkaloids, 225
6.4.1 (+)-Geniposide and 7-Deoxyloganin, 226
6.4.2 (–)-Brasoside and (–)-Littoralisone, 227
6.4.3 (+)-Mitsugashiwalactone, 229
6.4.4 Alstoscholarine, 229
6.4.5 (+)-Aspidospermidine and (+)-Vincadifformine, 230
6.4.6 (+)-Yohimbine, 230
6.5 Conclusion, 231
References, 231

**7 Sesquiterpenes 236**
*Alexandros L. Zografos and Elissavet E. Anagnostaki*

7.1 Biosynthesis, 236
7.2 Cycloisomerization Reactions in Organic Synthesis, 244
7.2.1 Enyne Cycloisomerization, 245
7.2.2 Diene Cycloisomerization, 257
7.3 Application of Cycloisomerizations in the Total Synthesis of Sesquiterpenoids, 266
7.3.1 Picrotoxane Sesquiterpenes, 266
7.3.2 Aromadendrane Sesquiterpenes: Epiglobulol, 267
7.3.3 Cubebol–Cubebenes Sesquiterpenes, 267
7.3.4 Ventricos-7(13)-ene, 270
7.3.5 Englerins, 271
7.3.6 Echinopines, 271
7.3.7 Cyperolone, 273

7.3.8 Diverse Sesquiterpenoids, 276
7.4 Conclusion, 276
References, 276

**8 Diterpenes** **279**
*Louis Barriault*

8.1 Introduction, 279
8.2 Biosynthesis of Diterpenes Based on Cationic Cyclizations, 1,2-Shifts, and Transannular Processes, 279
8.3 Pericyclic Reactions and their Application in the Synthesis of Selected Diterpenoids, 284
8.3.1 Diels–Alder Reaction and Its Application in the Total Synthesis of Diterpenes, 284
8.3.2 Cascade Pericyclic Reactions and their Application in the Total Synthesis of Diterpenes, 291
8.4 Conclusion, 293
References, 294

**9 Higher Terpenes and Steroids** **296**
*Kazuaki Ishihara*

9.1 Introduction, 296
9.2 Biosynthesis, 296
9.3 Cascade Polyene Cyclizations, 303
9.3.1 Diastereoselective Polyene Cyclizations, 303
9.3.2 "Chiral proton ($H^+$)"-Induced Polyene Cyclizations, 304
9.3.3 "Chiral Metal Ion"-Induced Polyene Cyclizations, 308
9.3.4 "Chiral Halonium Ion ($X^+$)"-Induced Polyene Cyclizations, 313
9.3.5 "Chiral Carbocation"-Induced Polyene Cyclizations, 319
9.3.6 Stereoselective Cyclizations of Homo(polyprenyl)arene Analogs, 319
9.4 Biomimetic Total Synthesis of Terpenes and Steroids through Polyene Cyclization, 319
9.5 Conclusion, 328
References, 328

**SECTION III SHIKIMIC ACID BIOSYNTHETIC PATHWAY** **331**

**10 Lignans, Lignins, and Resveratrols** **333**
*Yu Peng*

10.1 Biosynthesis, 333
10.1.1 Primary Metabolism of Shikimic Acid and Aromatic Amino Acids, 333
10.1.2 Lignans and Lignin, 335
10.2 Auxiliary-Assisted $C(sp^3)$–H Arylation Reactions in Organic Synthesis, 336
10.3 Friedel–Crafts Reactions in Organic Synthesis, 344
10.4 Total Synthesis of Lignans by $C(sp^3)$─H Arylation Reactions, 353
10.5 Total Synthesis of Lignans and Polymeric Resveratrol by Friedel–Crafts Reactions, 357
10.6 Conclusion, 375
References, 375

**SECTION IV MIXED BIOSYNTHETIC PATHWAYS– THE STORY OF ALKALOIDS 381**

**11 Ornithine and Lysine Alkaloids 383**

*Sebastian Brauch, Wouter S. Veldmate, and Floris P. J. T. Rutjes*

11.1 Biosynthesis of L-Ornithine and L-Lysine Alkaloids, 383
11.1.1 Biosynthetic Formation of Alkaloids Derived from L-Ornithine, 383
11.1.2 Biosynthetic Formation of Alkaloids Derived from L-Lysine, 388
11.2 The Asymmetric Mannich Reaction in Organic Synthesis, 392
11.2.1 Chiral Amines as Catalysts in Asymmetric Mannich Reactions, 394
11.2.2 Chiral Brønsted Bases as Catalysts in Asymmetric Mannich Reactions, 398
11.2.3 Chiral Brønsted Acids as Catalysts in Asymmetric Mannich Reactions, 404
11.2.4 Organometallic Catalysts in Asymmetric Mannich Reactions, 408
11.2.5 Biocatalytic Asymmetric Mannich Reactions, 413
11.3 Mannich and Related Reactions in the Total Synthesis of L-Lysine- and L-Ornithine-Derived Alkaloids, 414
11.4 Conclusion, 426
References, 427

**12 Tyrosine Alkaloids 431**

*Uwe Rinner and Mario Waser*

12.1 Introduction, 431
12.2 Biosynthesis of Tyrosine-Derived Alkaloids, 431
12.2.1 Phenylethylamines, 431
12.2.2 Simple Tetrahydroisoquinoline Alkaloids, 433
12.2.3 Modified Benzyltetrahydroisoquinoline Alkaloids, 433
12.2.4 Phenethylisoquinoline Alkaloids, 436
12.2.5 Amaryllidaceae Alkaloids, 438
12.2.6 Biosynthetic Overview of Tyrosine-Derived Alkaloids, 442
12.3 Aryl–Aryl Coupling Reactions, 442
12.3.1 Copper-Mediated Aryl–Aryl Bond Forming Reactions, 443
12.3.2 Nickel-Mediated Aryl–Aryl Bond Forming Reactions, 446
12.3.3 Palladium-Mediated Aryl–Aryl Bond Forming Reactions, 447
12.3.4 Transition Metal-Catalyzed Couplings of Nonactivated Aryl Compounds, 450
12.4 Synthesis of Tyrosine-Derived Alkaloids, 456
12.4.1 Synthesis of Modified Benzyltetrahydroisoquinoline Alkaloids, 456
12.4.2 Synthesis of Phenethylisoquinoline Alkaloids, 460
12.4.3 Synthesis of Amaryllidaceae Alkaloids, 462
12.5 Conclusion, 468
References, 469

**13 Histidine and Histidine-Like Alkaloids 473**

*Ian S. Young*

13.1 Introduction, 473
13.2 Biosynthesis, 473
13.3 Atom Economy and Protecting-Group-Free Chemistry, 480

13.4 Challenging the Boundaries of Synthesis: PIAs, 488
13.5 Conclusion, 497
References, 499

**14 Anthranilic Acid–Tryptophan Alkaloids** **502**
*Zhen-Yu Tang*

14.1 Biosynthesis, 502
14.2 Divergent Synthesis–Collective Total Synthesis, 508
14.3 Collective Total Synthesis of Tryptophan-Derived Alkaloids, 510
14.3.1 Monoterpene Indole Alkaloids, 510
14.3.2 Bisindole Alkaloids, 512
References, 517

**15 Future Directions of Modern Organic Synthesis** **519**
*Jakob Pletz and Rolf Breinbauer*

15.1 Introduction, 519
15.2 Enzymes in Organic Synthesis: Merging Total Synthesis with Biosynthesis, 520
15.3 Engineered Biosynthesis, 526
15.4 Diversity-Oriented Synthesis, Biology-Oriented Synthesis, and Diverted Total Synthesis, 533
15.4.1 Diversity-oriented Synthesis, 535
15.4.2 Biology-oriented Synthesis, 536
15.4.3 Diverted Total Synthesis, 539
15.5 Conclusion, 541
References, 545

**INDEX** **548**

# LIST OF CONTRIBUTORS


**Elissavet E. Anagnostaki,** Department of Chemistry, Laboratory of Organic Chemistry, Aristotle University of Thessaloniki, Thessaloniki, Greece and Research and Development Department, Pharmathen S.A., Thessaloniki, Greece

**Stellios Arseniyadis,** School of Biological and Chemical Sciences, Queen Mary University of London, London, United Kingdom

**Louis Barriault,** Department of Chemistry, University of Ottawa, Ottawa, Ontario, Canada

**Erica Benedetti,** Laboratoire de Chimie et Biochimie et Pharmacologiques et Toxicologiques, CNRS-Université Paris Descartes Faculté des Sciences Fondamentales et Biomédicales, Paris, France

**Sebastian Brauch,** Institute for Molecules and Materials, Radboud University Nijmegen, Nijmegen, The Netherlands

**Rolf Breinbauer,** Institute of Organic Chemistry, Technische Universität Graz, Graz, Austria

**Cyril Bressy,** Aix Marseille Université, Centrale Marseille, CNRS, Marseille, France

**Martin Cordes,** Institute for Organic Chemistry and Center of Biomolecular Drug Research (BMWZ), Leibniz Universität Hannover, Hannover, Germany and Helmholtz Center for Infection Research (HZI), Hannover, Germany

**Paul E. Floreancig,** Department of Chemistry, Chevron Science Center, University of Pittsburgh, Pittsburgh, PA, USA

**Tobias A. M. Gulder,** Department of Chemistry and Center for Integrated Protein Science Munich (CIPSM), Biosystems Chemistry, Technische Universität München, Munich, Germany

**Trond Vidar Hansen,** School of Pharmacy, University of Oslo, Oslo, Norway

**Kazuaki Ishihara,** Department of Biotechnology, Graduate School of Engineering, Nagoya University, Nagoya, Japan

**Markus Kalesse,** Institute for Organic Chemistry and Center of Biomolecular Drug Research (BMWZ), Leibniz Universität Hannover, Hannover, Germany and Helmholtz Center for Infection Research (HZI), Hannover, Germany

**Xu-Wen Li,** Shanghai Institute of Material Medica, Chinese Academy of Science, Shanghai, China

**Bastien Nay,** Muséum National d'Histoire Naturelle and CNRS (UMR 7245), Unité Molécules de Communication et Adaptation des Microorganismes, Paris, France

**Yu Peng,** State Key Laboratory of Applied Organic Chemistry, Lanzhou University, Lanzhou, China

**Jakob Pletz,** Institute of Organic Chemistry, Technische Universität Graz, Graz, Austria

**Uwe Rinner,** Institute of Organic Chemistry, Johannes Kepler University Linz, Linz, Austria and Department of Chemistry, College of Science, Sultan Qaboos University, Muscat, Oman

**Floris P. J. T. Rutjes,** Institute for Molecules and Materials, Radboud University Nijmegen, Nijmegen, The Netherlands

**Françoise Schaefers,** Department of Chemistry and Center for Integrated Protein Science Munich (CIPSM), Biosystems Chemistry, Technische Universität München, Munich, Germany

**Michael Smietana,** Institut des Biomolécules Max Mousseron, CNRS, Université de Montpellier, ENSCM, France

**Zhen-Yu Tang,** Department of Pharmaceutical Engineering, College of Chemistry and Chemical Engineering, Central South University, Changsha, China

**Wouter S. Veldmate,** Institute for Molecules and Materials, Radboud University Nijmegen, Nijmegen, The Netherlands

**Anders Vik,** School of Pharmacy, University of Oslo, Oslo, Norway

**Mario Waser,** Institute of Organic Chemistry, Johannes Kepler University Linz, Linz, Austria

**Youwei Xie,** Max-Planck-Institut für Kohlenforschung, Mülheim, Germany

**Ian S. Young,** Bristol-Myers Squibb Company, Chemical Development, New Brunswick, NJ, USA

**Alexandros L. Zografos,** Department of Chemistry, Laboratory of Organic Chemistry, Aristotle University of Thessaloniki, Thessaloniki, Greece

# PREFACE

*There is pleasure in the pathless woods,*
*there is rapture in the lonely shore,*
*there is society where none intrudes,*
*by the deep sea, and music in its roar;*
*I love not Man the less, but Nature more.*
*Lord Byron*

The first time I came across with the idea of editing a book that merges selected chapters of *biosynthesis* and *total synthesis* was when I was teaching postgraduate courses of natural product synthesis at Aristotle University of Thessaloniki. This period, I realized that the best way to teach youngsters synthesis was to start from the very origin of inspiration, *nature* and its tools: *biosynthesis*.

Over the last decades, biosynthesis is filling our gaps of understanding the complex mechanisms of nature and provides useful sources of inspiration not only in the way natural products can be synthesized but also by directing synthetic chemists in developing atom-economical, efficient synthetic methods. Several are the examples that mimic biosynthetic guidelines, from modern iterative alkylations and aldol reactions to C─H oxidations that compile nowadays the modern toolbox of organic synthesis.

The handed book is constructed in the logic of presenting the parallel development of biosynthesis and organic methodology and how these can be applied in efficient syntheses of natural products. The book is divided into four sections each representing the four major biosynthetic pathways of natural products, namely, acetate, mevalonate, shikimate biosynthetic pathways, and the mixed biosynthetic pathways of alkaloids. These sections are divided into chapters that represent selected classes of natural products, for example, lipids, sesquiterpenoids, lignans, etc. Each of these chapters is further divided into three distinct subchapters: (a) biosynthesis, (b) methodological section, and (c) application of the described methodology in the total synthesis of the described family of natural products. By this way, the readers can be focused in the direct comparison between biosyntheses and the developed methodologies to construct the crucial for each class of natural product carbon bonds. Although the book, as it develops, is focused on presenting the power of biosynthesis and how this power can be applied in providing inspiration for the efficient synthesis of natural products, it was not the authors will to present only biomimetic total syntheses but rather to exploit the modern synthetic methodologies and recognize their disabilities for further improvement.

Of course this book will not have been realized without the excellent work of renowned scientists worldwide working either in the field of biosynthesis or total synthesis, who collected the existing knowledge on biosynthesis, analyzed the existing modern methodologies, and presented a bouquet of selected total syntheses. Throughout our

endeavor to complete this book, I learned many things from their expertise but I also realized that only with tight collaborations you can build long-lasting friendships. I would like to thank them all once again for their trust and effort to complete this book. We all hope that the current work will contribute to a better understanding of the current status of organic chemistry and to the discovery of novel *strategies and tactics* for the synthesis of natural products.

Alexandros L. Zografos
September 2015
Thessaloniki, Greece

# 1

# FROM BIOSYNTHESES TO TOTAL SYNTHESES: AN INTRODUCTION

Bastien Nay[1] and Xu-Wen Li[2]

[1] *Muséum National d'Histoire Naturelle and CNRS (UMR 7245), Unité Molécules de Communication et Adaptation des Microorganismes, Paris, France*

[2] *Shanghai Institute of Material Medica, Chinese Academy of Science, Shanghai, China*

## 1.1 FROM PRIMARY TO SECONDARY METABOLISM: THE KEY BUILDING BLOCKS

### 1.1.1 Definitions

The primary and secondary metabolisms are traditionally distinguished by their distribution and utility in the living organism network. *Primary metabolites* include carbohydrates, lipids, nucleic acids, and proteins (or their amino acid constituents) and are shared by all living organisms on Earth. They are transformed by common pathways, which are studied by biochemistry (Fig. 1.1). *Secondary metabolites* are structurally diverse compounds usually produced by a limited number of organisms, which synthesize them for a special purpose, like defense or signaling, through specific biosynthetic pathways. They are studied by natural product chemistry. This distinction is not always so obvious and some compounds can be studied in the context of both primary and secondary metabolisms. This is especially true nowadays with the use of genetic and biomolecular tools, which tend to make natural product sciences more and more integrative. However, an important point to remember is that the primary metabolism furnishes key building blocks to the secondary metabolism. It would be difficult to describe in detail the full biosynthetic pathways in this section. We tried to organize the discussion as a *vade mecum*, synthetically gathering information from extremely useful sources, which will be cited at the end of this chapter.

### 1.1.2 Energy Supply and Carbon Storing at the Early Stage of Metabolisms

The sunlight is essential to life except in some part of the deep oceans. It provides energy for plant photosynthesis that splits molecules of water into protons and electrons and releases $O_2$ (Scheme 1.1). A proton gradient inside the plant chloroplasts then drags a transmembrane ATP synthase complex that produces adenosine triphosphate (ATP) while electrons released from water are transferred to the coenzyme reducer nicotinamide adenine dinucleotide phosphate hydride (NADPH). A major function of chloroplasts is to fix $CO_2$ as a combination to ribulose-1,5-bisphosphate (RuBP) performed by RuBP carboxylase (rubisco), forming an instable "$C_6$" β-ketoacid. This is cleaved into two molecules of 3-phosphoglycerate (3-PGA), which is then reduced into 3-phosphoglyceraldehyde (3-PGAL, a "$C_3$" triose phosphate) during the Calvin cycle. This is one of the major metabolites in the biosynthesis of carbohydrates like glucose and a biochemical mean for storing and retaining carbon atoms in the living cells.

### 1.1.3 Glucose as a Starting Material Toward Key Building Blocks of the Secondary Metabolism

Glucose-6-phosphate arises from the phosphorylation of glucose. It is the starting material of glycolysis, an important process of the primary metabolism, which consists in eight enzymatic reactions leading to pyruvic acid (PA)

*From Biosynthesis to Total Synthesis: Strategies and Tactics for Natural Products*, First Edition. Edited by Alexandros L. Zografos.
© 2016 John Wiley & Sons, Inc. Published 2016 by John Wiley & Sons, Inc.

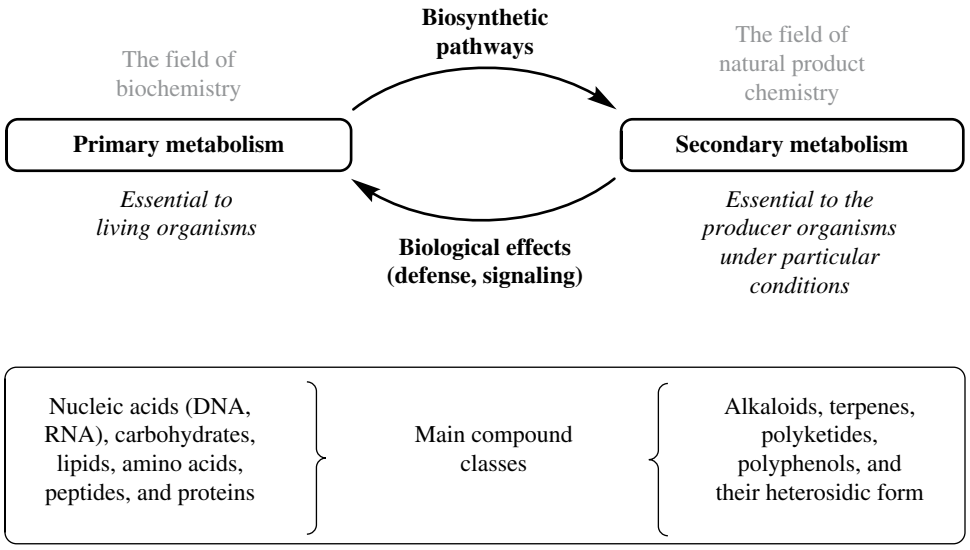
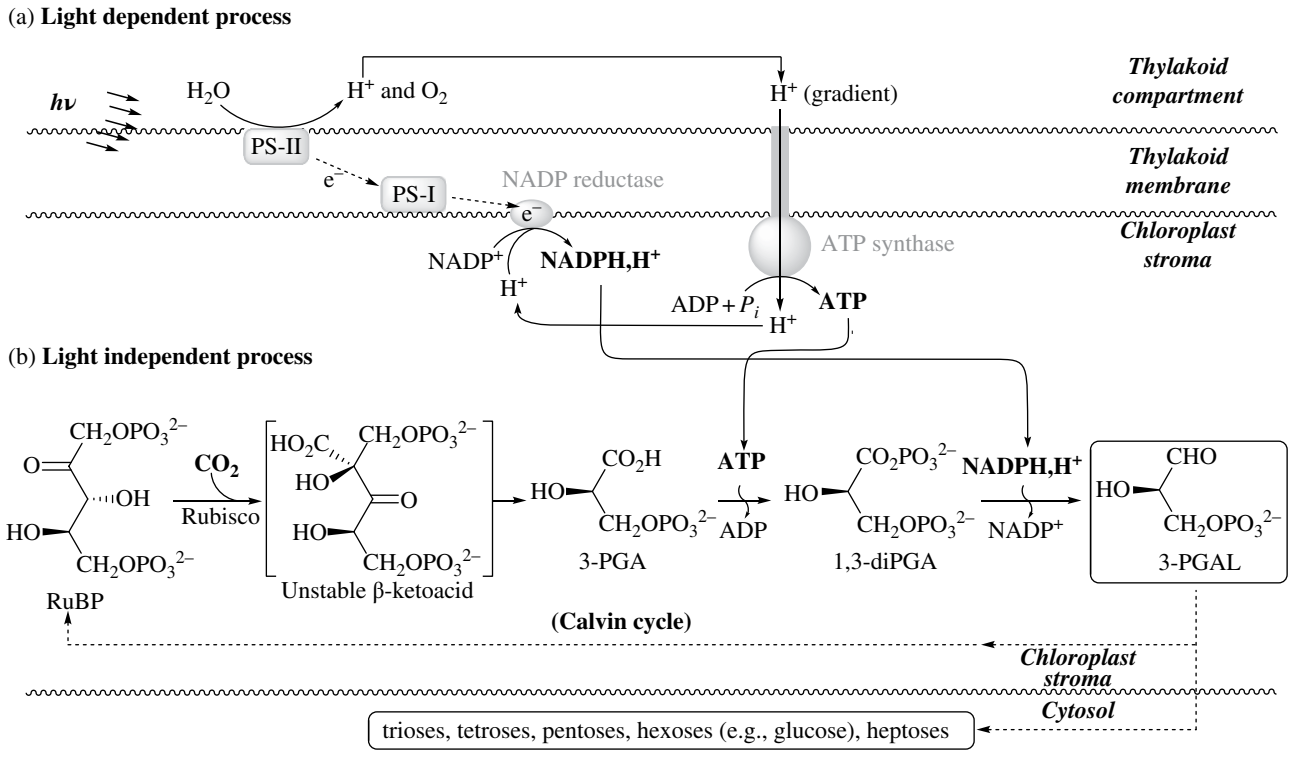
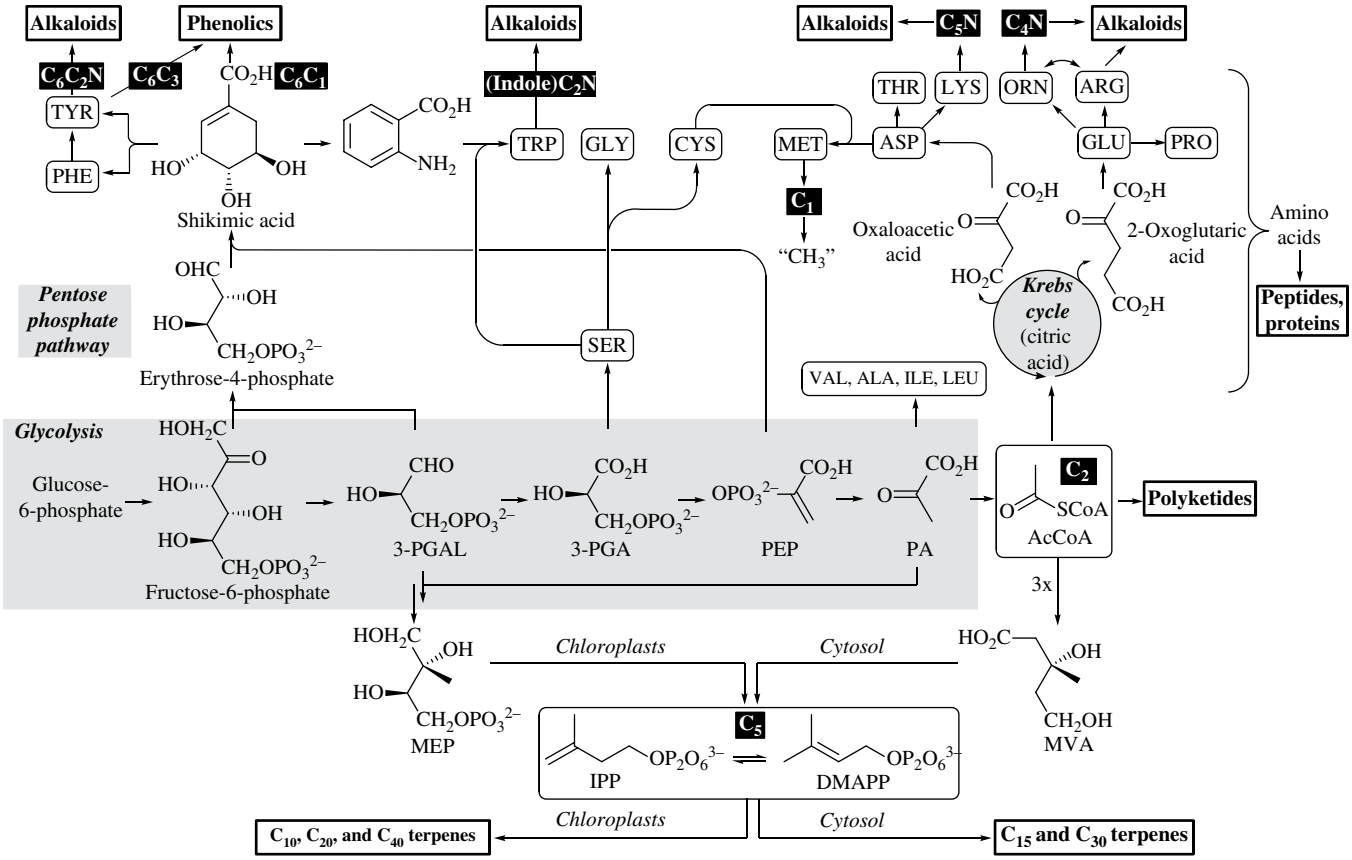



**FIGURE 1.1** Primary *versus* secondary metabolisms.




**SCHEME 1.1** The photosynthetic machinery (PS-I and PS-II, photosystems I and II).

(Scheme 1.2). Important intermediates for the secondary metabolism are produced during glycolysis. Glucose, glucose-6-phosphate, and fructose-6-phosphate can be converted to other hexoses and pentoses that can be oligomerized and enter in the composition of heterosides. Additionally, fructose-6-phosphate connects the pentose phosphate pathway, leading to erythrose-4-phosphate toward shikimic acid, which is a key metabolite in the biosynthesis of aromatic amino acids (phenylalanine, tyrosine, or $C_6C_3$ units) and $C_6C_1$ phenolic compounds. The next important intermediate in glycolysis is 3-PGAL, which can be redirected toward methylerythritol-4-phosphate (MEP) in the



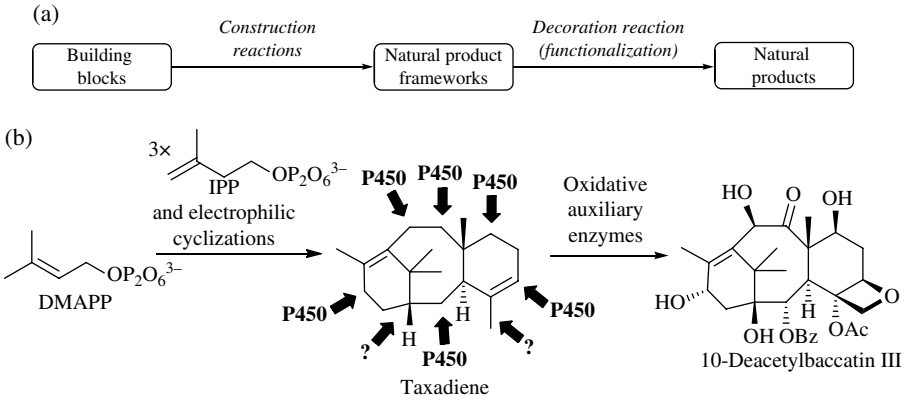

**SCHEME 1.2** The building block chart, involving glycolysis, and the Krebs cycle.

chloroplast. MEP is a starting block in the biosynthesis of terpenes through $C_5$ isoprene units (isopentenyl diphosphate (IPP) and dimethylallyl diphosphate (DMAPP)), especially those in $C_{10}$, $C_{20}$, and $C_{40}$ terpenes. 3-PGA is a precursor of serine and other amino acids, while phosphoenolpyruvate (PEP), the precursor of PA, is also an intermediate toward the previously mentioned shikimic acid. Lastly, PA is not only a precursor of the fundamental "$C_2$" acetyl coenzyme A (AcCoA) unit but also an intermediate toward aliphatic amino acids and MEP.

AcCoA is the building block of fatty acids, polyketides, and mevalonic acid (MVA), a cytosolic precursor of the $C_5$ isoprene units for the biosynthesis of terpenes in the $C_{15}$ and $C_{30}$ series (mind it is different from the MEP pathway, in product, and in cell location). Finally, AcCoA enters the citric acid or Krebs cycle, which leads to several precursors of amino acids. These are oxaloacetic acid, precursor of aspartic acid through transamination (thus toward lysine as a nitrogenated $C_5N$ linear unit and methionine as a methyl supplier), and 2-oxoglutaric acid, precursor of glutamic acid (and subsequent derivatives such as ornithine as a nitrogenated $C_4N$ linear unit). All these amino acids are key precursors in the biosynthesis of many alkaloids.

### 1.1.4 Reactions Involved in the Construction of Secondary Metabolites

Most reactions occurring in the living cells are performed by specialized enzymes, which have been classified in an international nomenclature defined by an enzyme commission (EC) number. There are six classes of enzymes depending on the biochemical reaction they catalyze: EC-1, oxidoreductases (catalyzing oxidoreduction reactions); EC-2, transferases (catalyzing the transfer of functional groups); EC-3, hydrolases (catalyzing hydrolysis); EC-4, lyases (breaking bonds through another process than hydrolysis or oxidation, leading to a new double bond or a new cycle); EC-5, isomerases (catalyzing the isomerization of a molecule); and EC-6, ligases (forming a covalent bond between two molecules). Many subclasses of these enzymes have been described, depending on the type of atoms and functional groups involved in the reaction and, if any, on the cofactor used in this reaction. For example, several cofactors can be used by dehydrogenases like NAD(P)/NAD(P)H, FAD/$FADH_2$, or FMN/$FMNH_2$. For a description of this classification, the reader can refer to specialized Internet websites like ExplorEnz [1]. What is important to realize is that most enzymes are substrate specific and have been selected during




**SCHEME 1.3** (a) From building blocks to natural products and (b) the example of 10-deacetylbaccatin III.

evolution to perform specific transformations, making natural products with often and yet unknown functions.

Secondary metabolites arise from specific biosynthetic pathways, which use the previously defined building blocks. The bunch of organic reactions involved in these biosyntheses allows the construction of natural product frameworks, which are finally diversified through "decoration" steps (Scheme 1.3). It is not the purpose of this introductive chapter to describe in detail all biosynthetic pathways and the reader can refer to excellent books and articles, which have been published elsewhere [2, 3].

The reactions involved in the construction of natural product skeletons will be described later for representative classes of compounds. The identification of the building block footprint in the natural product skeleton will be emphasized as much as possible, sometimes referring to biogenetic speculations [4]. After the framework construction, the decoration steps will involve as diverse reactions as aliphatic C─H oxidations (e.g., involving a cytochrome $P_{450}$ oxygenase) occasionally triggering a rearrangement, heteroatom alkylations (e.g., methylation by *S*-adenosylmethionine) or allylation (by DMAPP), esterifications, *heteroatom* or C-glycosylations (leading to heterosides), radical couplings (especially for phenols), alcohol oxidations or ketone reductions, amine/ketone transaminations, alkene dihydroxylations or epoxidations, oxidative halogenations, Baeyer–Villiger oxidations, and further oxygenation steps. At the end of the biosynthesis, such transformations may totally hide the primary building block origin of natural products.

### 1.1.5 Secondary Metabolisms

***1.1.5.1 Polyketides*** Polyketides (or polyacetates) are issued from the oligomerization of $C_2$ acetate units performed by polyketide synthases (PKS) and leading to $(C_2)_n$ linear intermediates [5, 6]. If the $(C_2)_n$ intermediates arise from successive Claisen reactions performed by ketosynthase domains (KS, in nonreducing PKS), a highly reactive poly-β-ketoacyl intermediate $H{-}(CH_2C{=}O)_n{-}OH$ is formed, leading to phenolic and aromatic products through further intramolecular Claisen condensations. Furthermore, highly reducing PKSs are made of specialized enzymatic subunits working in line or iteratively to functionalize each $C_2$ linker bond as $CH(OH)CH_2$ (by ketoreductases (KR)), then as $HC{=}CH$ (by dehydratases (DH)), and as $CH_2CH_2$ (by enoyl reductases (ER)), leading to a high degree of functionalization of the final product (Fig. 1.2). By these iterative sequences, highly reduced polyketides, which can be either linear, macrocyclized, or polycyclized depending on the reactivity of the biosynthetic intermediates, can be formed [7]. With the same logic, fatty acids are also biosynthesized by fatty acid synthases.

Moreover, the PKS enzyme can be hybridized with nonribosomal peptide synthetase (NRPS) domains (see also "NRPS metabolites and peptides" in the "Alkaloids" section), leading to the acylation of an amino acid by the $(C_2)_n$ acyl intermediate. As previously, the functionalization of the acyl chain depends on the PKS enzyme, and the PKS/NRPS products are also extremely diversified (e.g., hirsutellone B; Fig. 1.2) [8].

***1.1.5.2 Terpenes*** Terpenes are derived from the oligomerization of the $C_5$ isoprene units DMAPP and IPP. Both precursors are prompt to generate either an allylic cation (the diphosphate is a good leaving group) or a tertiary carbocation, respectively, which makes the IPP easy to react with DMAPP (Scheme 1.4). This reaction happens in the active site of a terpene synthase, which activates the departure of the diphosphate group from DMAPP, thanks to Lewis acid activation (a metal like $Mg^{2+}$, $Mn^{2+}$, or $Co^{2+}$ is present in the enzyme active site [9]). This leads to geranyl ($C_{10}$, monoterpene precursor) or farnesyl ($C_{15}$, sesquiterpene precursor) diphosphate, depending on the location of the enzyme (chloroplast for the MEP pathway or cytosol for the MVA pathway). Geranylgeranyl ($C_{20}$, diterpene) and

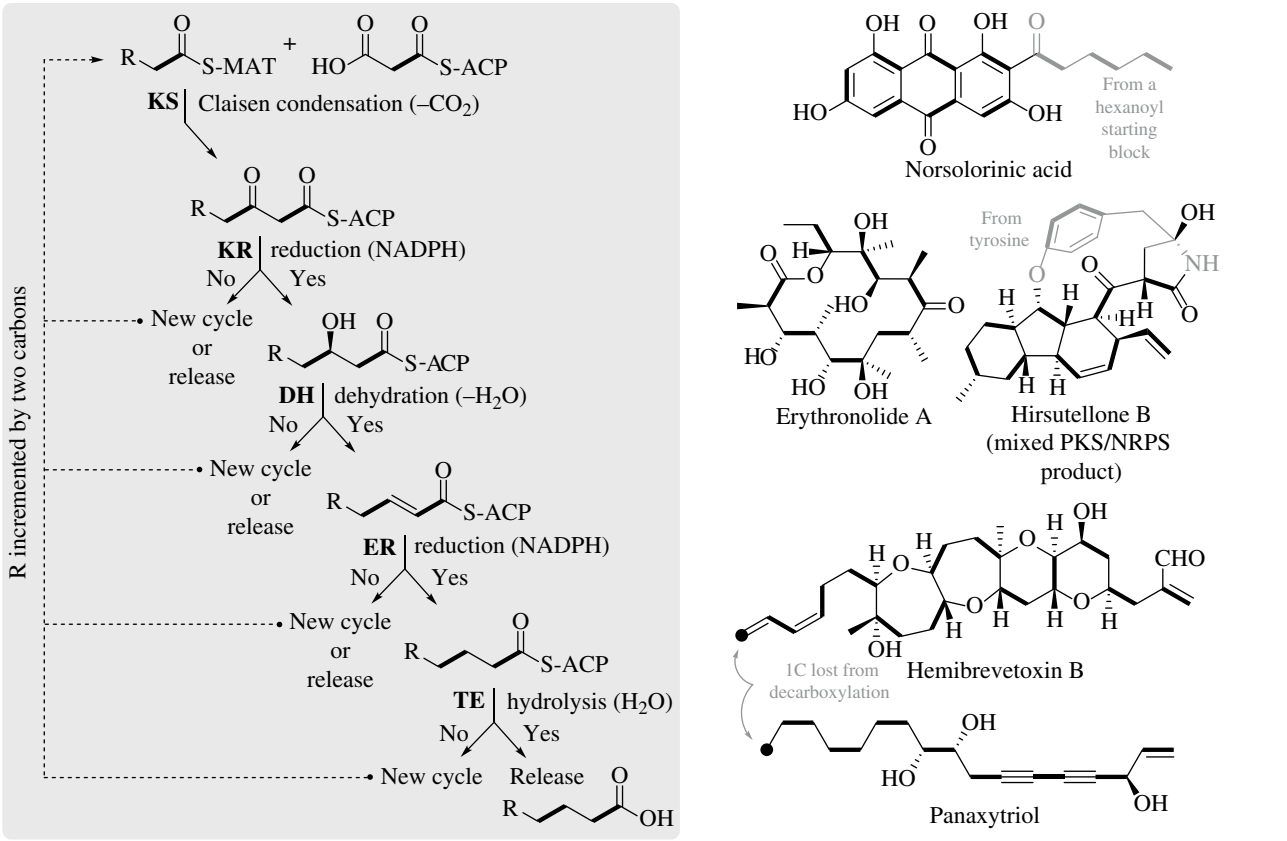
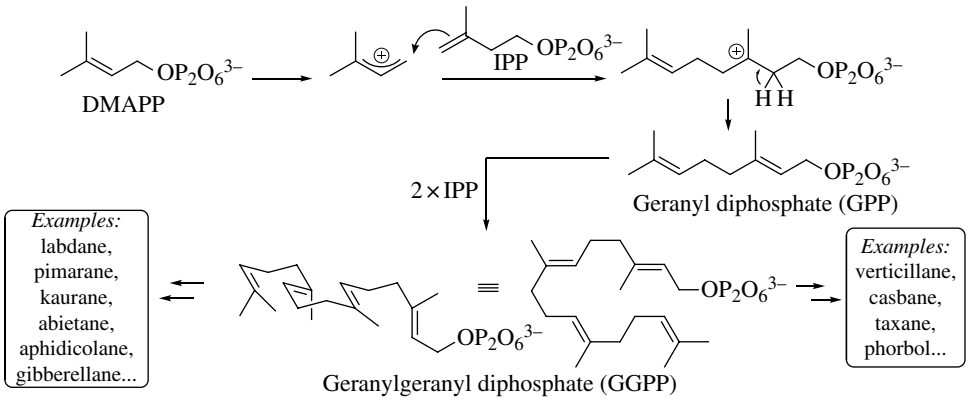



**FIGURE 1.2** Chemical logic of polyketide construction leading to variable functionalization of the elongated acyl chain and examples of resulting chemical diversity. ACP, acyl carrier protein; DH, dehydratase; ER, enoyl reductase; KR, ketoreductase; KS, ketosynthase; MAT, malonyl acyl transferase; TE, thioesterase.




**SCHEME 1.4** Early assembly of $C_5$ units in terpene biosynthesis, leading to diterpenes ($C_{20}$).

farnesylfarnesyl ($C_{30}$, triterpene precursor) diphosphates can also be obtained by further additions of IPP, leading to longer linear intermediates.

The cyclization of linear precursors is achieved by specialized cyclases, which generate a poorly functionalized natural product framework [10, 11]. Auxiliary enzymes such as oxygenases then increase the complexity and the diversity of compounds by further functionalization (Scheme 1.3b) [12]. A high degree of oxidation can be observed in compounds like thapsigargin, paclitaxel, or bilobalide (Fig. 1.3). The biosynthesis of this last compound, for example, involves a high oxygenation pattern, two Wagner–Meerwein rearrangements, and several oxidative cleavages leading to the loss of five carbons. The resulting natural products can

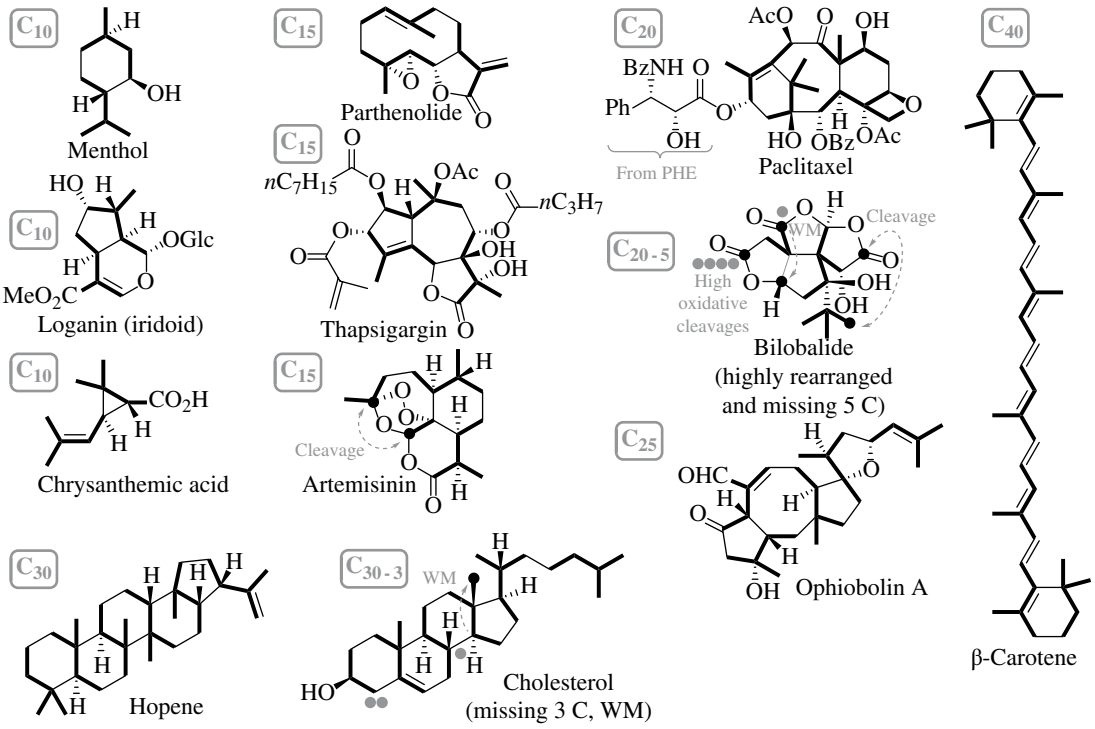



**FIGURE 1.3** Chemical diversity in the terpene series (WM, Wagner–Meerwein shifts; ●, lost carbons; bold bonds are remnant of primary building blocks).

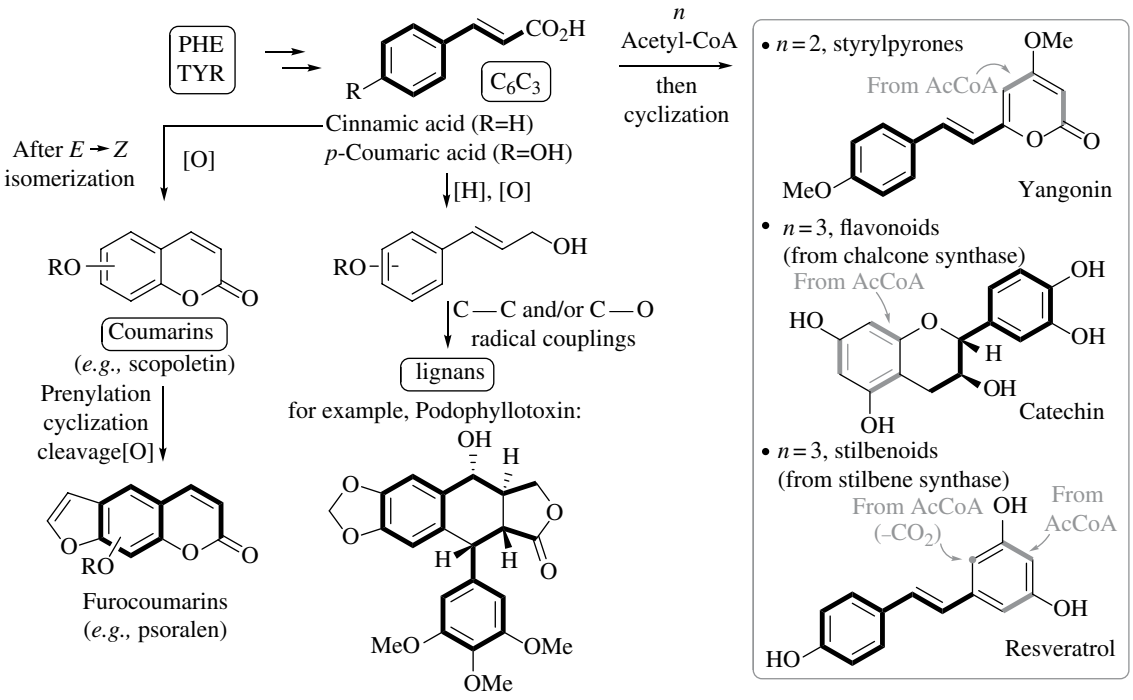
thus be extremely modified, with structures whose biogenetic origin is far from being obvious at first sight and cannot be determined without further experiments such as isotopic labeling.

***1.1.5.3 Flavonoids, Resveratrols, Gallic Acids, and Further Polyphenolics*** We have previously discussed the polyketide origin of some phenolic compounds based on the $(C_2)_n$ motif. Other polyphenols like gallic acids are directly derived by the aromatization of shikimic acid ($C_6C_1$ building block; Scheme 1.2) [13]. The $C_6C_3$ building blocks are available from the conversion of phenylalanine and tyrosine into cinnamic and *p*-coumaric acids, respectively, and then by further hydroxylation steps (Scheme 1.5). These can dimerize into lignans (e.g., podophyllotoxin) [14, 15] through radical processes or converted to low molecular weight compounds like eugenol, coumarins, or vanillin [16]. The coenzyme A thioesters of these $C_6C_3$ acids can be used as initiator units by specialized ketosynthases for an elongation by two acetyl units, leading to aromatic polyketides like styrylpyrones or diarylheptanoids (e.g., curcumin) [17]. Important compounds from this metabolism are flavonoids ($C_6C_3C_6$) [18] and stilbenoids ($C_6C_2C_6$) (a decarboxylation occurs during the aryl cyclization) [19], which are synthesized by chalcone synthase and stilbene synthase, respectively. Flavonoids (e.g., catechin) and stilbenes (e.g., resveratrol) are present in large amounts in fruits and vegetables and may exert their radical scavenging properties *in vivo*.

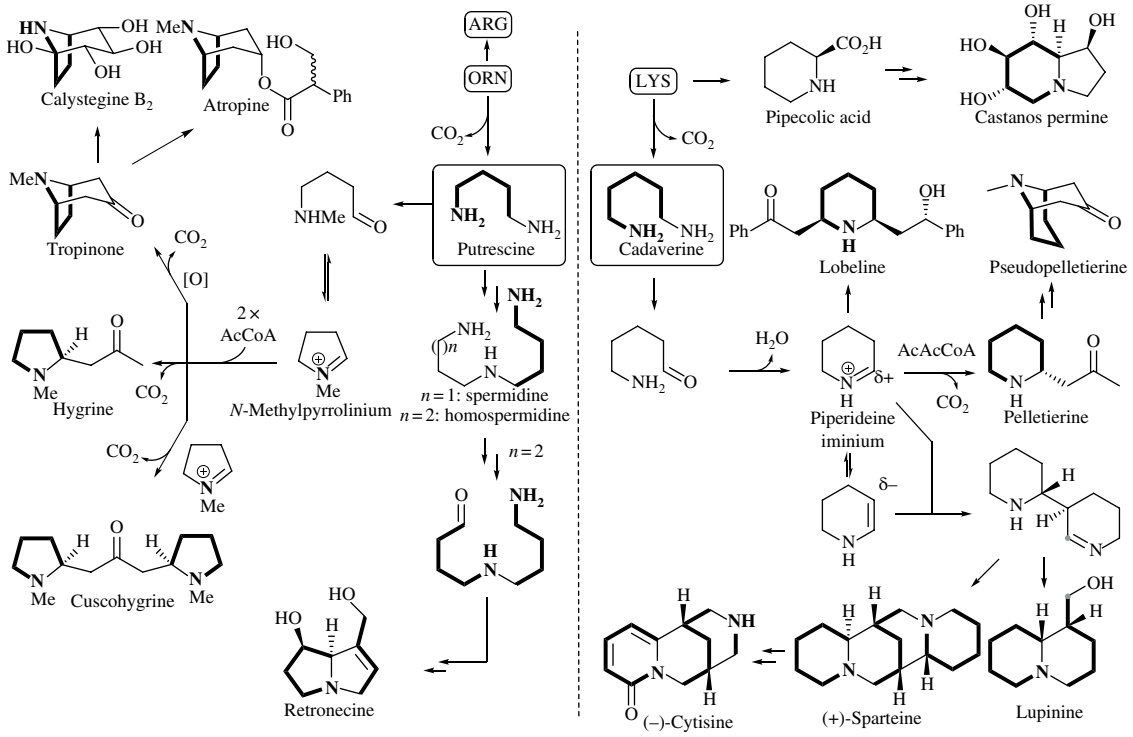
***1.1.5.4 Alkaloids*** Alkaloids are nitrogen-containing compounds. The nitrogen(s) can be involved in an amine function, conferring basicity to the natural product (like "alkali"), or in less or nonbasic functions such as an amide, a nitrile, an isonitrile, or an ammonium salt (quaternary amines). For amines, protonation often occurs at physiological pH and may condition their biological activity. In many cases, the nitrogen is biogenetically derived from an amino acid. We will thus discuss alkaloids according to their amino acid origin.

*Alkaloids Derived from the Krebs Cycle (Lysine and Ornithine Derived)* As shown previously (Scheme 1.2), the Krebs cycle is a crucial metabolic process, which leads to α-ketoacids (oxaloacetic and 2-oxoglutaric acids). Their enzymatic transamination affords the two amino acids—aspartic acid and glutamic acid—which are the direct biosynthetic precursors of amino acids lysine and ornithine, respectively. These in turn produce cadaverine, a "$C_5N$" unit, and putrescine, a "$C_4N$" unit, which are major components for the biosynthesis of important alkaloids, as will be discussed later (Scheme 1.6). Additionally, ornithine is a precursor of arginine, another important amino acid.

ORNITHINE-DERIVED ALKALOIDS (INCORPORATING THE $C_4N$ UNIT) Putrescine is derived from the decarboxylation of ornithine and is a precursor of linear polyamines like spermine. After enzymatic methylation of one amine of putrescine

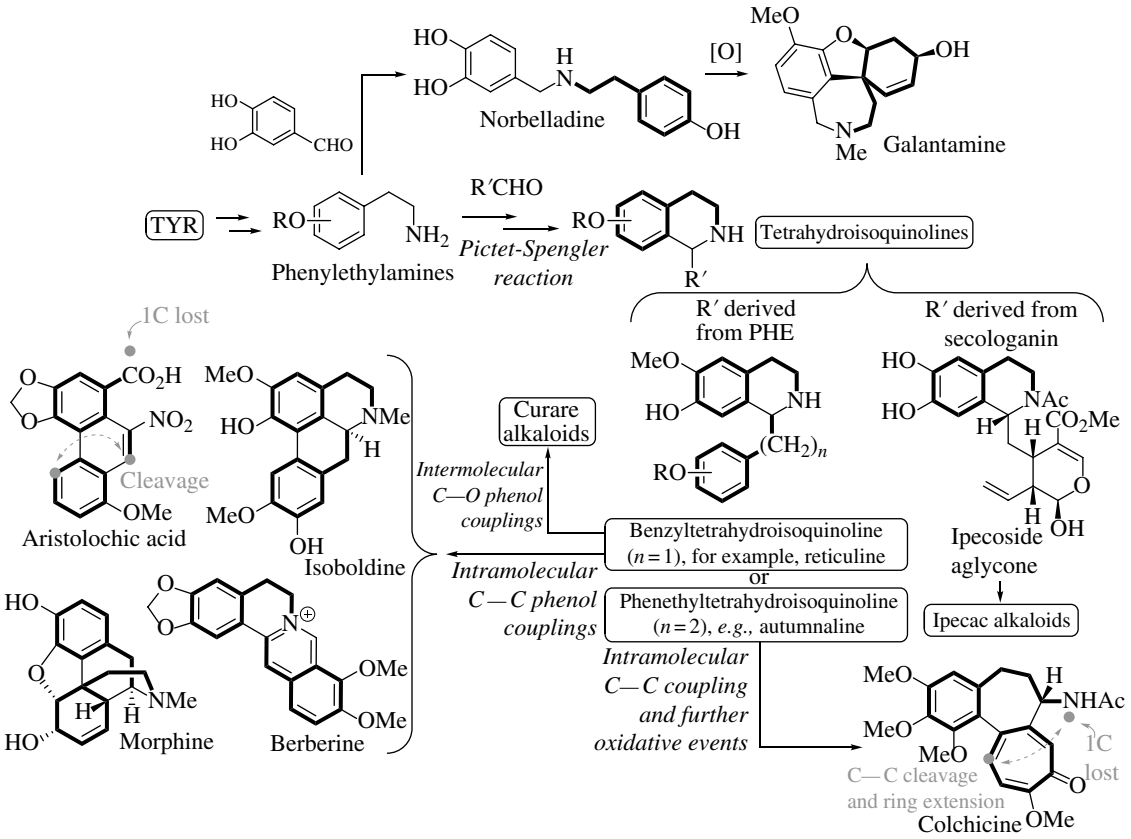



**SCHEME 1.5** The phenylpropanoid biosynthetic pathways.




**SCHEME 1.6** Lysine- and ornithine-derived alkaloid biosynthetic pathways (mind the structural similarities).

in the presence of *S*-adenosylmethionine, transamination of the other affords γ-(*N*-methylamino)aldehyde [20]. The resulting cyclic iminium is a key intermediate in the formation of many medicinally important alkaloids such as the plant-derived compounds cocaine, atropine, or the calystegines [21, 22]. Indeed, this iminium is a Mannich acceptor, which can react with various nucleophiles, the first of those being the carbanion of acetyl-CoA. Thus, after a stepwise




**SCHEME 1.7** Tyrosine-derived alkaloid biosynthetic pathways (double head arrows figure bond cleavages during biosynthetic processes).

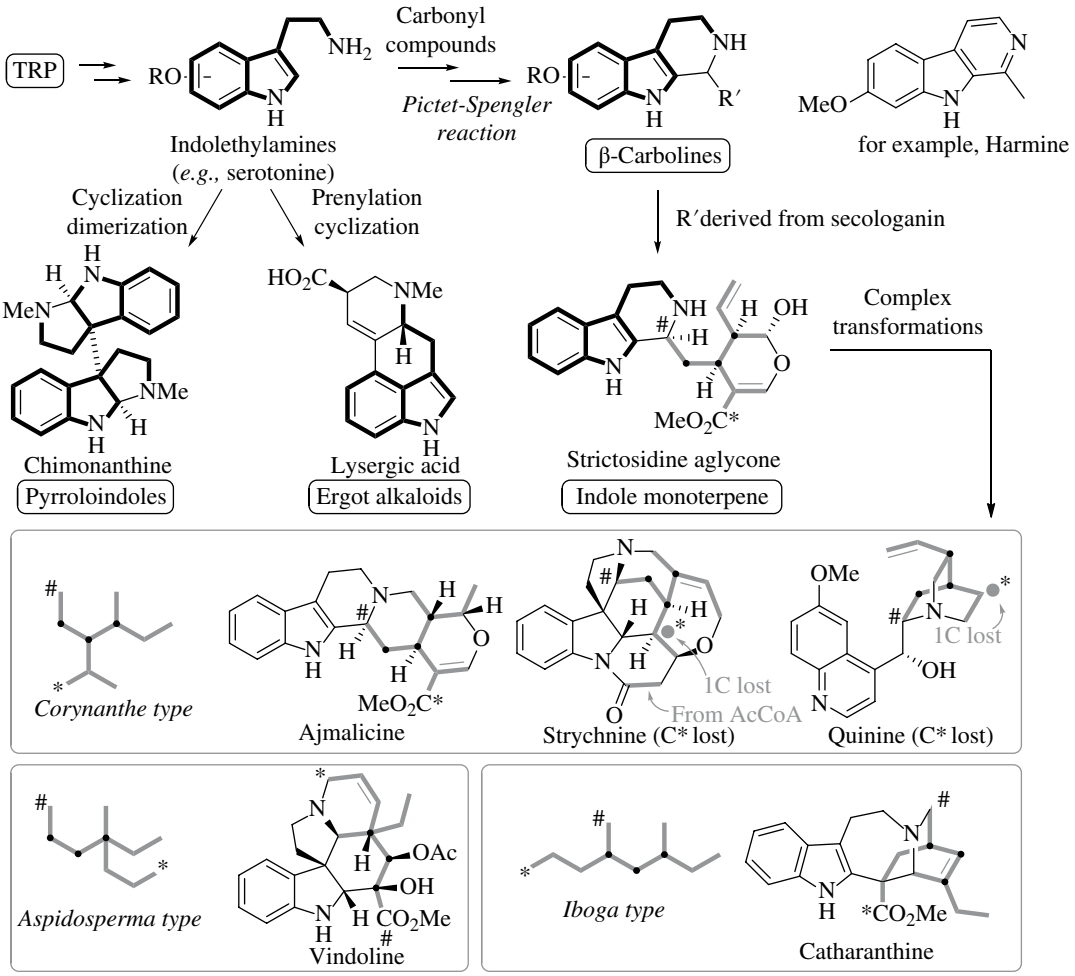
elongation by two AcCoA units, either decarboxylation can occur, leading to the acetonylpyrrolidine hygrine, or a second Mannich reaction by the intramolecular attack of the acetoacetate anion onto an oxidation-derived pyrrolinium, leading to the tropane skeleton (tropinone). The acetoacetyl-CoA intermediate can also react intermolecularly with another pyrrolinium cation, leading to cuscohygrine after decarboxylation. Finally, the pyrrolizidine alkaloids [23] are derived from homospermidine, which, when submitted to terminal oxidative deamination, leads to the bicyclic skeleton of retronecine and further *Senecio* alkaloids. We can mention herein that ornithine is a biosynthetic precursor of arginine, bearing a guanidine function, which is an intermediate toward the toxic compounds tetrodotoxin and saxitoxin (not shown).

LYSINE-DERIVED ALKALOIDS (INCORPORATING THE $C_5N$ UNIT) From lysine to piperidine alkaloids, the biosynthetic steps parallel the one previously described from ornithine. Indeed, the oxidative deamination of cadaverine affords a δ-amino aldehyde, which cyclizes through imine formation into piperideine. Protonation results in a Mannich acceptor, which is able to react with various nucleophiles such as β-ketothioester anions. The first product of these reactions is pelletierine, which can further react through an intramolecular Mannich reaction leading to pseudopelletierine. Quinolizidines [24] can also be formed, first from the Mannich reaction of the piperideine acceptor with the corresponding enamine nucleophile and then after additional transformation steps, leading, for example, to lupinine, sparteine, or cytisine.

Indolizidine alkaloids [15] such as castanospermine and swainsonine are formed from pipecolic acid, an amino acid derived from lysine, which can be elongated by malonyl-CoA followed by ring closure. When protonated, these alkaloids are oxonium mimics strongly inhibiting glycosidases.

*Tyrosine- and Phenylalanine-Derived Alkaloids* Tyrosine and phenylalanine amino acids are bearing the phenylethylamine moiety of many medicinally relevant alkaloids. Further hydroxylations on the aromatic carbocycle or on the aliphatic part can be observed. Methylations can occur on phenolic oxygens and on the amine, leading to catecholamines (adrenaline, noradrenaline, dopamine). Arylethylamines are also usual to react with endogenous aldehydes through Pictet–Spengler reactions [25], leading to important biosynthetic intermediates (Scheme 1.7) like:

- Reticuline from the reaction with 4-hydroxyphenylacetaldehyde toward benzyltetrahydroisoquinoline alkaloids:




**SCHEME 1.8** Tryptophan-derived alkaloid biosynthetic pathways (gray parts: monoterpenic units).

morphine, berberine, tubocurarine, isoboldine, or the highly modified aristolochic acid [26, 27]

- Automnaline from the reaction with 3-(4-hydroxyphenyl) propanal toward phenylethyltetrahydroisoquinoline alkaloids: colchicine, cephalotaxine, or schelhammericine [28, 29]
- Ipecoside from the reaction of dopamine with secologanin toward terpene tetrahydroisoquinoline alkaloids: ipecoside or emetine

Lastly, norbelladine (top of Scheme 1.7) is issued from the reductive amination of 3,4-dihydroxybenzaldehyde (derived from phenylalanine) with tyramine (derived from tyrosine) and constitutes a biosynthetic node leading to Amaryllidaceae alkaloids such as galantamine, crinine, or lycorine depending on the topology of phenolic couplings. In all these biosynthetic routes, radical phenolic couplings are key reactions for C─C and C─O bond formations and rearrangements [30, 31].

*Tryptophan-Derived Indole and Indole Monoterpene Alkaloids* As for alkaloids derived from tyrosine and phenylalanine, those derived from tryptophan are formed after decarboxylation of the amino acid (into tryptamine) and possible hydroxylation of the aromatic carbocycle (e.g., serotonin) and N-methylation (e.g., psilocin). As previously, tryptamine can also react through Pictet–Spengler reactions to form tetrahydro-β-carbolines, which can be aromatized, for example, into harmine (Scheme 1.8) [16].

When the aldehyde partner of the Pictet–Spengler reaction with tryptamine is the terpene secologanin, strictosidine is formed as an entry toward the vast monoterpene indole alkaloids [32, 33]. Hydrolysis of the glucosidic part releases the strictosidine aglycone bearing an aldehyde, while iminium formation and further cyclization and reduction can lead to ajmalicine (from oxocyclization) or yohimbine (from carbocyclization). These alkaloids are referred to as from the *Corynanthe* type, with the monoterpene carbon skeleton unmodified. Although it misses one carbon and has a very

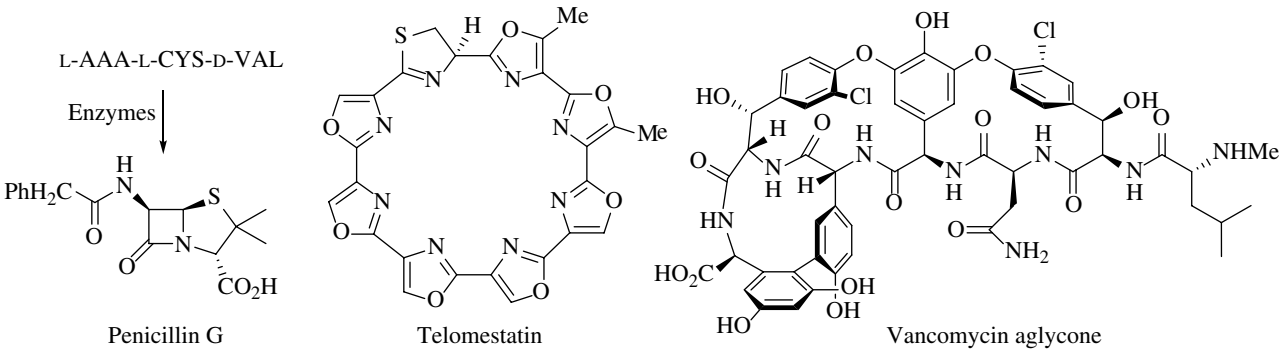



**FIGURE 1.4** Structural diversity of nonribosomal peptide compounds (AAA, α-aminoadipic acid).

different structure, strychnine is related to the *Corynanthe* alkaloids, incorporating two carbons from acetyl-CoA. Highly modified monoterpene skeletons are derived from the *Corynanthe* core through C─C bond breaking and reorganization, leading to *Iboga*-type (e.g., catharanthine) and *Aspidosperma*-type (e.g., vindoline) alkaloids. The anticancer drug vinblastine is a heterodimer resulting from the nucleophilic attack of vindoline on a Mannich acceptor resulting from catharanthine, found in Madagascar periwinkle (*Catharanthus roseus*). The heteroaromatic compounds ellipticine, camptothecin, and quinine are also derived from a *Corynanthe*-type precursor, although in this case the biosynthetic relationship may not be obvious due to deep modifications of the skeleton.

Finally, two important classes of compounds have to be mentioned since they have inspired many synthetic chemists. The pyrroloindole alkaloids result from the cyclization of tryptamine, as found in physostigmine (formed by a cationic mechanism after methylation in position 3 of the indole; not shown) or in chimonanthine (presumably formed by a radical coupling mechanism; Scheme 1.8). The ergot alkaloids are derived from the 3,3-dimethylallylation on position 4 of the indole in tryptophan whose further cyclization and oxidation processes afford the natural products (e.g., lysergic acid, Scheme 1.8, and ergotamine), which have had important medical applications [34].

*NRPS Metabolites and Peptides* NRPS enzymes assemble amino acids, including nonproteinogenic ones, into oligopeptides. The enzymes contain several modules, and especially an adenylation domain (A), which specifically selects and activates the amino acid to be transferred as a thioester on the nearby peptidyl carrier protein (PCP) [2]. A condensation module (C) then catalyzes the formation of the peptide bonds between the newly introduced amino acyl-PCP (bearing a free amine) and the elongated peptidyl-PCP thioester. At the end of the elongation, a cyclization can occur into cyclopeptides, but the peptide can also be transferred to auxiliary enzymes like methyltransferases, glycosyltransferases, or oxidases (vancomycins are typical products of such functionalizations) [35, 36]. The formation of heterocycles is also frequently encountered in this metabolism, as in penicillins that are derived from the tripeptide α-aminoadipoyl-cysteinyl-valine or telomestatin (Fig. 1.4) [2].

*Other Alkaloid Origins* There are many other nitrogen sources involved in alkaloid biosyntheses, for example, nicotinic acid (originated from aspartic acid and intermediate in nicotine and anabasine biosyntheses) and anthranilic acid (originated from tryptophan and intermediate toward acridines or aurachins). The amination reaction (e.g., through transamination of carbonyl compounds) is also a way to introduce nitrogens in natural products, for example, from fatty acids, steroids (toward *Solanum* alkaloids or cyclopamines), or other terpenoids (aconitine and atisine have diterpene skeletons, while *Daphniphyllum* alkaloids are triterpene derivatives). Finally, nucleic acids can also be precursors of alkaloids like the well-known caffeine.

## 1.2 FROM BIOSYNTHESIS TO TOTAL SYNTHESIS: STRATEGIES TOWARD THE NATURAL PRODUCT CHEMICAL SPACE

### 1.2.1 The Chemical Space of Natural Products

Natural products occupy an important place in human communities as demonstrated by their vast use from ancient times to nowadays, like dyes, fibers, oils, perfumes, agrochemicals, or drugs. Broadly, both primary and secondary metabolites could be classified as natural products, while the latter, as discussed previously, are usually regarded as the "natural products" owing to their complexity and diversity arising from a variety of biosynthetic pathways. The structural chemical diversity found among

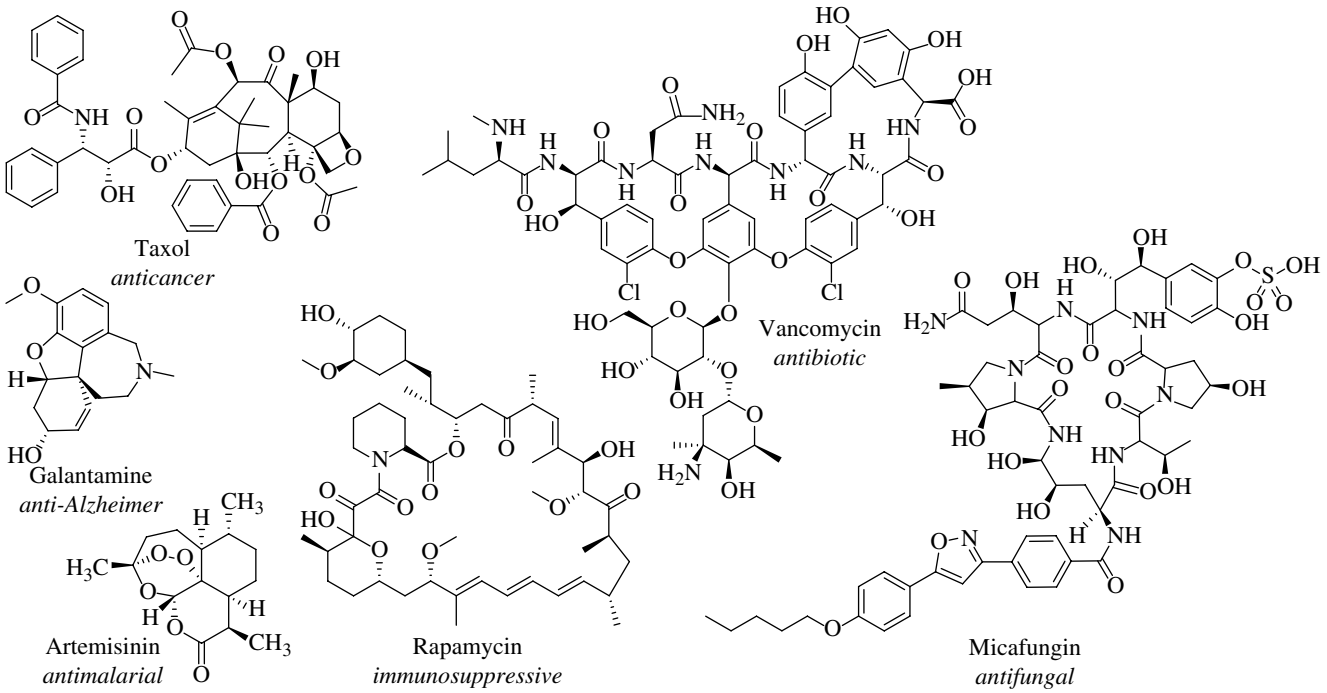
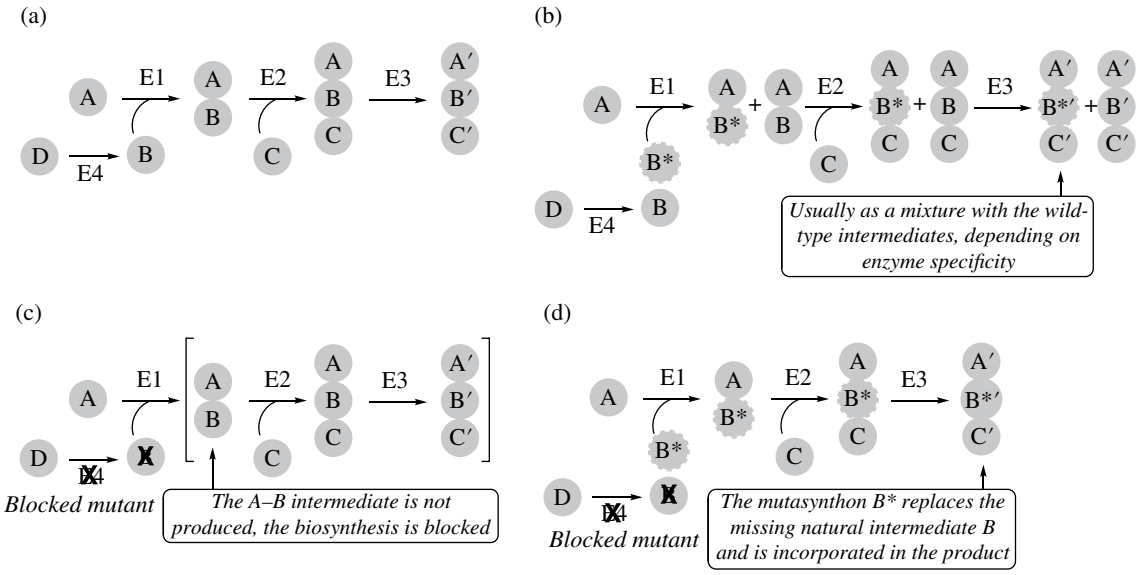



**FIGURE 1.5** Some famous natural products currently used as drugs.

all living organisms, defining the chemical space of natural products [37], is the consequence of their evolution, occurring as an adaptation of organisms to their environment. It is commonly believed that secondary metabolites are produced as messengers by living organisms or as weapons against enemies, and thus they should have certain biological activities in a medicinal point of view [38]. Indeed, natural products are regarded as one of the main sources of medicines (Fig. 1.5). From the traditional medicinal extracts to every single bioactive molecule, the methods of extraction, purification, identification, and biological investigation of natural products have been well established. Their complex structures and interesting properties have attracted synthetic chemists to accomplish their total syntheses and that of medicinally relevant analogs, sometimes in the industrial context [39]. Thus, targeting the chemical space of natural products has never been more relevant than today. Although the discovery of natural products demands time and labor-consuming manipulations, it is worth to notice that the knowledge on this chemical space is still continually growing while biological advances allow for discovering and understanding potential targets. However, increasing the chemical space of human-made compounds based on natural products should benefit from transdisciplinary collaborations such as the use of coupled biosynthetic and chemical synthetic methods to design original "unnatural natural products" [40].

### 1.2.2 The Biosynthetic Pathways as an Inspiration for Synthetic Challenges

***1.2.2.1 Precursor-Directed Biosyntheses and Mutasynthetic Strategies to Increase the Chemical Space of Natural Products*** As the genetics and biochemistry of natural product biosynthesis are better understood, novel biosynthetic techniques have been developed to study and generate new diversity in natural product analogs (Scheme 1.9). Precursor-directed biosynthesis (PDB) is considered as the earliest example of combining chemical and biological methods for the generation of complex natural product analogs [41, 42]. This approach, compared with the biosynthetic pathway of wild-type metabolites (Scheme 1.9a), involves the feeding of analogs of the natural biosynthetic building blocks to the living organisms (Scheme 1.9b), usually bacteria or fungi, which incorporate the modified precursors into the biosynthesized compound. Mutasynthesis, also termed as mutational biosynthesis (MBS), involves the inactivation of a key step of the biosynthesis in a mutant microorganism (Scheme 1.9c), which can then be fed by various modified or advanced building blocks (mutasynthons; Scheme 1.9d) [43]. These mutasynthons could not be incorporated by the wild type due to specificities of the enzymatic machinery. Build up on PDB, MBS eliminates the natural biosynthetic intermediate, thus generating a less complex mixture of metabolites and making the purification or yield of target products better.



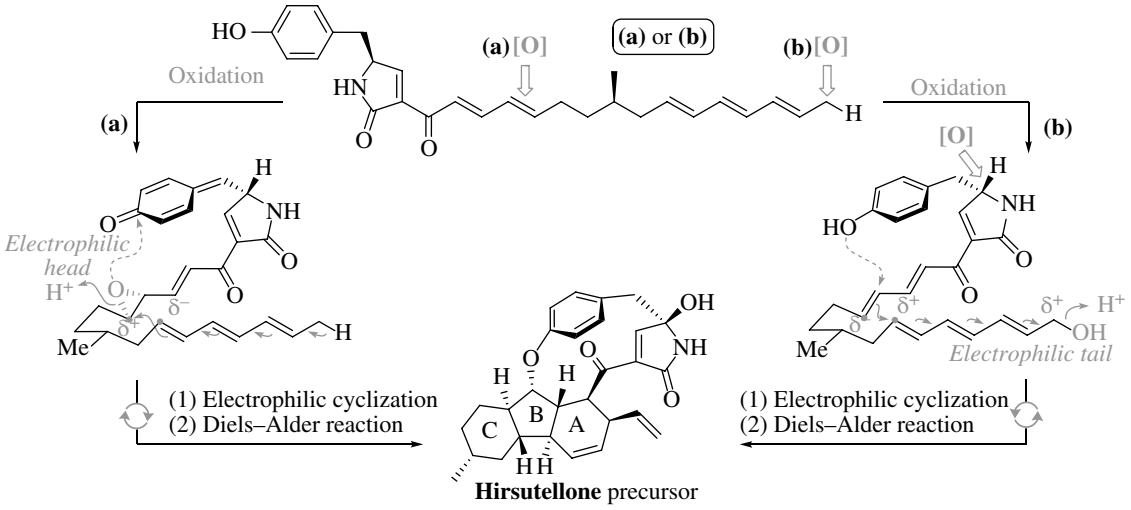

**SCHEME 1.9** (a) Biosynthetic pathway of wild-type metabolites; (b) precursor-directed biosynthesis: the modified synthon B* replaces the natural synthon B; (c) biosynthetic pathway blocked by a mutation (the enzyme E4 is not functional); (d) mutasynthesis: a mutasynthon B* is introduced to replace B and is incorporated in the biosynthesis, leading to a "mutated" natural product.

Both approaches can potentially greatly increase the diversity of natural compounds.

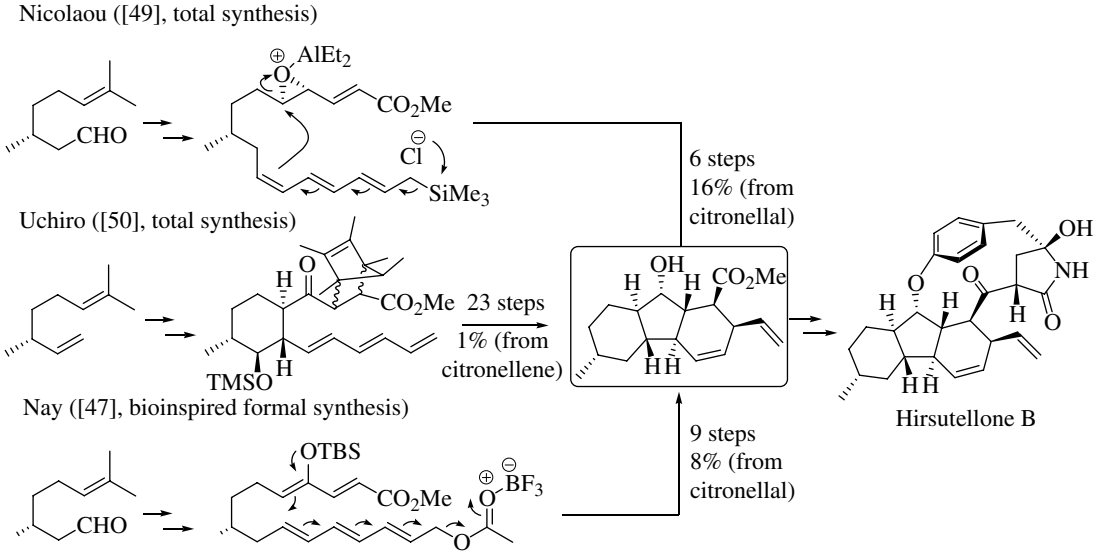
***1.2.2.2 The Biomimetic Strategy: A Bridge between Biosynthesis and Total Synthesis*** During the past century, synthetic chemists were endeavoring to discover more efficient strategies to access complex natural products. The chemical synthesis of tropinone by Robinson in 1917 [44], one of the first biomimetic ones, is a fantastic example of an early efficient synthesis, which consisted in a multicomponent process between succinaldehyde, methylamine, and calcium acetonedicarboxylate [45]. Since then, the construction of natural products by chemical methods inspired by nature's biosynthetic pathways has attracted many synthetic chemists and participated in the progress of organic chemistry. As discussed in the book *Biomimetic Organic Synthesis* coedited by one of us (B.N.), an increasing number of total syntheses have been termed "biomimetic" or "bioinspired" during the last 20 years, meaning the use of a synthetic tactic that follows or mimics a hypothetical or proven biosynthetic pathway. Concomitantly, the biosynthesis of natural products has been more and more understood, thanks to genetic and enzymatic studies. Therefore, as a bridge between biosynthesis and total synthesis, biomimetic synthesis is able to overcome some drawbacks of conventional strategies, as it often relies on the self-assembling properties of a key reactive intermediate [46].

Tremendous works dealing with bioinspired total syntheses of secondary metabolites have thus been achieved, providing new insights in the reactivity of biomimetic precursors and occasionally leading to controversy or unresolved questions [47]. An interesting example goes to hirsutellones, a family of fungal PKS/NRPS compounds (also regarded as alkaloids due to their nitrogen) with intriguing structures and a significant antitubercular activity [7]. Their biosynthesis has been hypothesized by Oikawa who proposed a key linear precursor of the related compounds GKK1032A$_2$, made from one tyrosine, nine AcCoA, and several methylations by *S*-adenosylmethionine [48]. We applied this hypothesis to the less methylated hirsutellones (Scheme 1.10). Two different biosynthetic pathways can be proposed for the polycyclization. Pathway (a) involves the selective oxidation of one of the dienoyl double bonds ($C_\gamma$=$C_\delta$) to generate an epoxide and of the phenol. This "electrophilic head" would then be attacked in a conjugated ene reaction involving the triene and initiating the cyclization. Formation of the bent paracyclophane would then be followed by a stereoselective intramolecular Diels–Alder (IMDA) reaction leading to the complete tricyclic core of the natural product. Pathway (b) involves the allylic oxidation at the terminal methyl group of the triene to release an allylic alcohol or cation as an "electrophilic tail." The polycyclization would then be initiated through reverse electronic activation compared to pathway (a), forming the first cyclohexane ring before the IMDA reaction occurs.

Nicolaou et al. [49] and Uchiro et al. [50] achieved the total syntheses of hirsutellone B in 2009 and 2011, respectively. We recently described a formal total synthesis by forming the key decahydrofluorene (tricyclic) core of hirsutellone in a biomimetic strategy following pathway (b) [47]. As for the synthesis of this important synthetic




**SCHEME 1.10** Biosynthetic hypotheses for the biosynthesis of hirsutellones. Pathway (a) would involve the transient loss of aromaticity of the phenol and then rearomatization with bending of the paracyclophane, while pathway (b) would involve the direct attack of the phenol with concomitant formation of the bent macrocycle. The IMDA reaction would proceed lately.



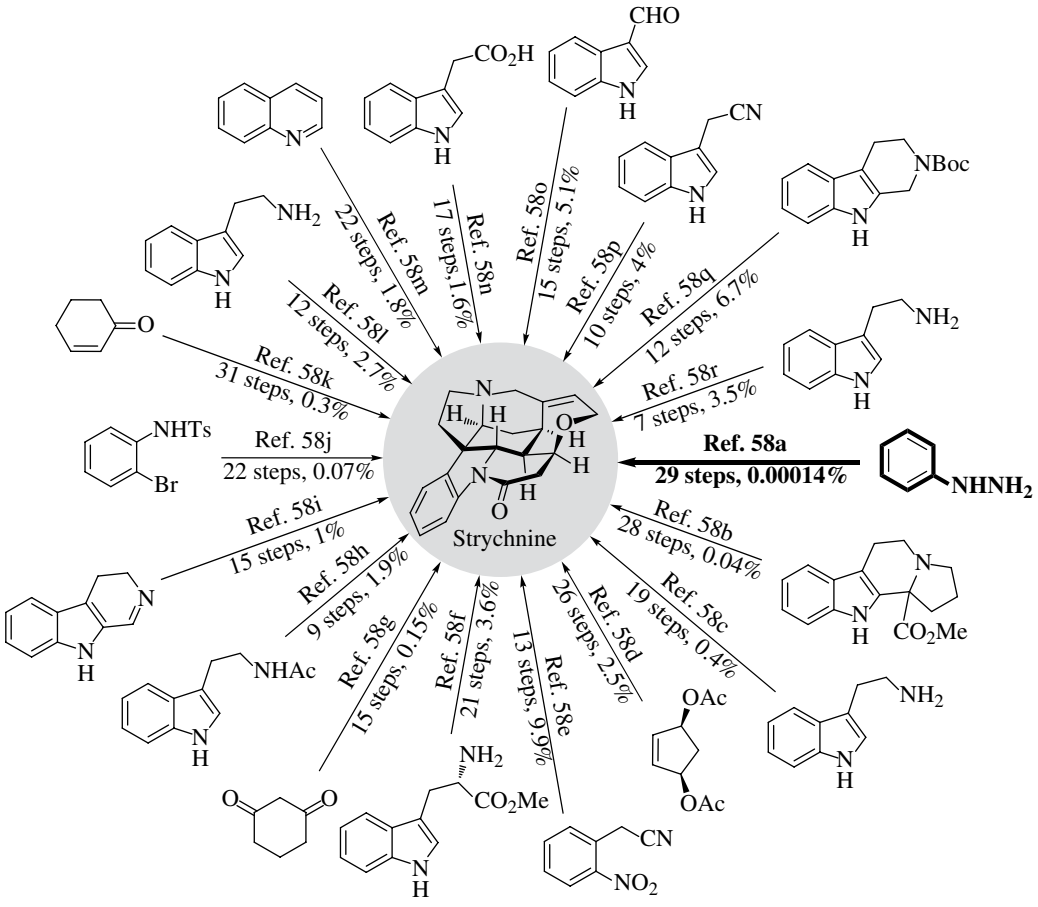

**SCHEME 1.11** Biomimetic and conventional strategies toward hirsutellones: Nicolaou's total synthesis was not originally reported as biomimetic but supports the proposed tail-to-head biosynthetic pathway; Uchiro reported a conventional total synthesis; we reported a biomimetic formal synthesis leading to Nicolaou's intermediate, supporting the head-to-tail biosynthetic pathway.

intermediate with eight stereocenters, Uchiro's nonbiomimetic strategy took 23 steps from *R*-(–)-citronellene with 1% global yield (Scheme 1.11). In comparison, Nicolaou's synthetic strategy, involving an $Et_2AlCl$-triggered cascade cyclization, decreased the number of reaction steps to six steps starting from *R*-(+)-citronellal and with 16% overall yield. Although this was not claimed as biomimetic by the authors, this work supports the "tail-to-head" biosynthetic pathway (a) (Scheme 1.10) and nicely reveals the efficiency of biosynthetically related cascade reactions. We reported an alternative biomimetic synthesis of the tricyclic core of hirsutellones by a reverse "head-to-tail" cyclization strategy using nine steps and with 8% brsm global yield (Scheme 1.11) [47]. Interestingly, our strategy supports the biosynthetic pathway (b), thus confirming that both biosynthetic routes are possible. However, thanks to recent biosynthetic experiments using the isotopically labeled precursor ($^{18}$O-*phenol*)-L-tyrosine, we demonstrated that the phenolic oxygen is incorporated in analogous natural products, pyrrocidines, thus giving clues to biosynthetic pathway (b) [51].

### 1.2.3 The Science of Total Synthesis

***1.2.3.1 The Evolution of Total Synthesis and Its Significance Today*** The vast utility of total synthesis and its connections with other research fields can be illustrated by a selection of key words, some of them deeply resonating with current major societal challenges: medicinal chemistry and new drugs, pharmacology, agrochemicals, biosynthetic studies, synthetic methodologies, structure determination, physical organic chemistry, catalysis, green resources, or bioinspiration. Back to the nineteenth century, the first organic synthesis of urea from ammonium cyanate, an inorganic substance, was accomplished by Wöhler in 1828 and raised the curtain of total synthesis. Total synthesis had then, for a time, played an essential role on elucidating the structure of natural products, and it is still the case nowadays when the determination of relative and absolute configurations cannot be achieved by analytic methods. With the improvement of analytical chemistry, and as chemistry and biology are better understood, the role of total synthesis slowly changed. A variety of new reactions, catalysts, and technologies have been developed for total synthesis. Most importantly, total synthesis is playing a key role for new drug discovery, chemical biology, or even material science. As introduced in the former part, a lot of natural products and derivatives were developed to provide new drugs against human diseases (Fig. 1.5), of which total synthesis enabled a larger amount of products available for further studies [52] and challenged optimized strategies for their industrial production [35]. As striking examples, we can cite Paterson's synthesis of discodermolide at the 60 g scale for anticancer clinical studies by Novartis [53], or the recent industrial production of the antimalarial drug artemisinin by Sanofi, using a semisynthetic strategy starting from a biotechnologically available advanced intermediate [54, 55].

***1.2.3.2 Strychnine as a Case Study: A Classic among the Classics*** Herein, we would like to illustrate the evolution of total synthesis by one of the most famous natural products, strychnine (Scheme 1.12). For decades, strychnine was regarded as one of the most challenging natural products to be synthesized [56]. The correct structure of strychnine was determined by Woodward and Brehm in 1948, one century after its discovery [57]. Since then, this remarkable natural product witnessed the evolution of total synthesis.




**SCHEME 1.12** The 18 total syntheses of strychnine (1954–2011) [58a–r].

The landmark synthesis of strychnine was reported by Woodward and coworkers in 1954, 6 years after its structure determination [58].

Since then, many synthetic chemists have been confronted with strychnine, which is a classic among the classics of total synthesis. Overall, 18 total syntheses of strychnine have been reported so far [58a–r], the shortest one in only 7 linear steps from tryptamine by Vanderwal [58r], to be compared with the earliest total synthesis of Woodward in 29 linear steps from phenylhydrazine [53a]. The efficiency of these works can be evaluated by looking at the overall yields, from 0.00014% [58a] to nearly 10% yield [58e]. For sure, these improvements not only took benefits from Corey's retrosynthetic "Logic of Chemical Synthesis" but also from those famous chemists's creativity and from new achievements in synthetic and catalytic methodologies. Indeed, new methodological concepts have arisen by the last 20 years, such as those of ideal synthesis [59], atom economy, step economy, redox economy, and sustainable approaches [60].

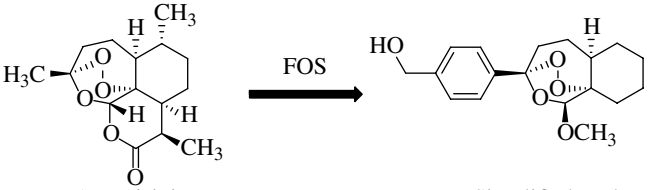
The efficiency of total synthesis should then benefit to the growing research efforts in chemical biology and drug discovery in the future, in connection with recently designed strategies like diversity-oriented synthesis (DOS) and function-oriented synthesis (FOS).

***1.2.3.3 DOS and FOS: Two Strategies to Optimize Biological Hits and Synthetic Efficacy*** Classical combinatorial chemistry has allowed for the synthesis of vast amounts of products, yet poorly overlapping the chemical space of natural products, essentially due to their limited structural diversity and drug-likeness. Chemists are thus searching for ever more efficient ways to generate rapidly more complex and diverse functional compounds. As discussed before, precursor-directed biosynthesis and mutasynthesis have been developed by biochemists and exemplify a biological mean to diversify structures in a natural product series. In addition, organic chemists have designed new strategies for this purpose, such as DOS and FOS.

*DOS and Divergent Total Synthesis* DOS, often compared with the classical target-oriented synthesis (TOS), is using forward synthetic analysis with the aim of transforming various building blocks, through planned reactions, to efficiently generate complex and diverse compounds matching with a large portion of the chemical space. To some extent, this is the opposite way as the well-established retrosynthetic analysis of TOS. The strategy of DOS mainly relies on the variation of three parameters [61]: (1) the building blocks, to introduce a vast number of functional groups in the skeleton; (2) the stereochemistry, which can be introduced by various stereoselective reagents; and (3) the molecular skeleton, which could achieve the highest level of structural complexity and diversity by using different synthetic methods, such as multicomponent reactions, combinational synthesis, folding pathway, and branched pathway [62]. In any case, DOS greatly increases the chemical space to enable more biological and pharmaceutical investigation.

Using an analogous strategy, diverse natural products were synthesized through collective natural product synthesis or divergent total synthesis. This powerful concept was applied by MacMillan and coworkers to the asymmetric synthesis of six monoterpene indole alkaloids using organocascade catalysis (strychnine, aspidospermidine, vincadifformine, akuammicine, kopsanone, and kopsinine) [63]. Dai and coworkers exploited the combination of a biosynthetically inspired strategy with such a divergent approach for the synthesis of seven monoterpene indole alkaloids (mersicarpine, leuconodines B and D, leuconoxine, melodinine E, leuconolam, and rhazinilam) [64]. In the taiwaniaquinoid series, four natural products were synthesized by Li and coworkers after two to three steps from a common intermediate prepared on the gram scale [65]. Such collective strategies are more and more encountered in the literature, taking advantage of a common synthetic route leading to key intermediates to access entire families of compounds rather than a sole natural product target.

*FOS* The common problem encountered with total synthesis is the high complexity of natural products, which often takes many steps to be achieved and lowers overall yields. One way to solve this problem is, as discussed before, to think and design efficient synthetic strategies, for example, using redox or step economy, to shorter the route. Another approach is to design less complex synthetic targets by maintaining or improving selected functions involved in the biological activity, which is the so-called FOS. FOS is based on the study of complex targeted molecules with the aim of shortening the synthetic work to develop diverse simplified but still functional targets, keeping key structural features to effect biological functions [66]. FOS is thus deeply related to drug discovery. Many simplified small compounds can indeed be proposed from structure–activity relationship studies. For example, the famous antimalarial artemisinin gave simplified but functional analogs with potent *in vitro* antimalarial activities in the same range of $IC_{50}$ as that of the natural product (Scheme 1.13) [67]. Other than DOS, which focuses on structure complexity and diversity, FOS concentrates more




Artemisinin
$IC_{50}$ = 9.2 nM

Simplified analog
$IC_{50}$ = 15 nM

**SCHEME 1.13** The FOS strategy toward a simplified but still potent analog of the antimalarial artemisinin.

on the functional groups involved in the biological functions, while both of them are somehow inspired by total synthesis.

### 1.2.4 Conclusion: A Journey in the Future of Total Synthesis

The future of total synthesis is written in our laboratory notebooks. It will not only be conditioned by new synthetic achievements and new methodologies and technologies improving the efficacy of experiments but also by their applications to answer questions from new horizons. All of us will agree, as it was said by others, that total synthesis is marked by beauty and it has sometimes been compared with art. Not so many fields can respond to such criteria, and it is due to the free creativity we are able to exert. In theory, total synthesis could provide any compound, from the simplest to the most complex ones. But can we provide enough material for deepened studies in other research fields [52]? Indeed, our products, once achieved, are not to be stored indefinitely in tiny flasks. They should lead to new projects, new questions, and new answers.

Thus, how studying in depth the biological, the chemical, and the physical properties of a natural product when its natural source is rare, low producing, and sometimes no more available? This question is in the hand of two scientific communities: the biotechnological and the synthetic chemist ones. Let's bet that we will still answer many of such questions by continuing to improve qualitatively and quantitatively our productivity by making our syntheses simpler and faster (and thus, as we may say, more "elegant") and by being the driving forces in building strong interdisciplinary bridges.

*Further Reading on Total Synthesis and Biosynthesis*

- J.-N. Bruneton, *Pharmacognosie, phytochimie, plantes medicinales*, Tec & Doc Lavoisier: Paris (2009)
- E. J. Corey and X.-M. Cheng, *The Logic of Chemical Synthesis*, Wiley: New York (1989)
- J. Cossy and S. Arseniyadis, *Modern tools for the synthesis of complex bioactive molecules*, Wiley: Hoboken (2012)
- P. M. Dewick, *Medicinal natural products, a biosynthetic approach*, Wiley: Chichester (2009)
- T. Hudlicky and J. W. Reed, *The way of synthesis*, Wiley-VCH: Weinheim (2007)
- K. C. Nicolaou and E. J. Sorensen, *Classics in total synthesis*, Wiley-VCH: Weinheim (1996)
- K. C. Nicolaou and S. A. Snyder, *Classics in total synthesis II*, Wiley-VCH: Weinheim (2003)
- K. C. Nicolaou and J. S. Chen, *Classics in total synthesis III*, Wiley-VCH: Weinheim (2011)
- E. Poupon and B. Nay (Eds), *Biomimetic Organic Synthesis*, Wiley-VCH: Weinheim (2011)

The reader interested in biosynthetic pathways can also refer to the interactive KEGG atlas (biosynthetic pathways) available on Internet: http://www.kegg.jp/kegg/atlas/.

## REFERENCES


1. http://www.enzyme-database.org/class.php (accessed September 28, 2015).
2. T. D. H. Bugg, *Nat. Prod. Rep.* 2001, **18**, 465–493.
3. P. M. Dewick, *Medicinal natural products, a biosynthetic approach*, Wiley: Chichester (2009): refer to Chapter 2 for a description of the construction mechanisms.
4. R. Thomas, *Nat. Prod. Rep.* 2004, **21**, 224–248.
5. C. Hertweck, *Angew. Chem. Int. Ed.* 2009, **48**, 4688–4716.
6. M. A. Fischbach, C. T. Walsh, *Chem. Rev.* 2006, **106**, 3468–3496.
7. X.-W. Li, A. Ear, B. Nay, *Nat. Prod. Rep.* 2013, **30**, 765–782.
8. D. Boettger, C. Hertweck, *ChemBioChem* 2013, **14**, 28–42.
9. S. Frick, R. Nagel, A. Schmidt, R. Bodemann, P. Rahfeld, G. Pauls, W. Brandt, J. Gershenzon, W. Boland, A. Burse, *Proc. Natl. Acad. Sci. U.S.A* 2013, **110**, 4194–4199.
10. Example of the trichodiene synthase: M. J. Rynkiewicz, D. E. Cane, D. W. Christianson, *Proc. Natl. Acad. Sci. U.S.A* 2001, **98**, 13543–13548.
11. Example of taxadiene synthase: R. Croteau, R. E. B. Ketchum, R. M. Long, R. Kaspera, M. R. Wildung, *Phytochem. Rev.* 2006, **5**, 75–97.
12. L. M. Podust, D. H. Sherman, *Nat. Prod. Rep.* 2012, **29**, 1251–1266.
13. L. Pouységu, D. Deffieux, G. Malik, A. Natangelo, S. Quideau, *Nat. Prod. Rep.* 2011, **28**, 853–874.
14. T. Umezawa, *Phytochem. Rev.* 2003, **2**, 371–390.
15. L. B. Davin, N. G. Lewis, *Phytochem. Rev.* 2003, **2**, 257–288.
16. F. Bourgaud, A. Hehn, R. Larbat, S. Doerper, E. Gontier, S. Kellner, U. Matern, *Phytochem. Rev.* 2006, **5**, 293–308.
17. D. Yu, F. Xu, J. Zeng, J. Zhan, *IUBMB Life* 2012, **64**, 285–295.
18. K. Saito, K. Yonekura-Sakakibara, R. Nakabayashi, Y. Higashi, M. Yamazaki, T. Tohge, A. R. Fernie, *Plant Physiol. Biochem.* 2013, **72**, 21–34.
19. J. Chong, A. Poutaraud, P. Hugueney, *Plant Sci.* 2009, **177**, 143–155.
20. S. Biastoff, W. Brandt, B. Dräger, *Phytochemistry* 2009, **70**, 1708–1718.
21. A. J. Humphrey, D. O'Hagan, *Nat. Prod. Rep.* 2001, **18**, 494–502.
22. B. Dräger, *Nat. Prod. Rep.* 2004, **21**, 211–223.
23. D. Ober, E. Kaltenegger, *Phytochemistry* 2009, **70**, 1687–1695.
24. D. S. Seigler, *in Plant secondary metabolism*, Springer US, Boston (1999), pp. 546–567.
25. J. Stöckigt, A. P. Antonchick, F. Wu, H. Waldmann, *Angew. Chem. Int. Ed.* 2011, **50**, 8538–8564.

26. J. Ziegler, P. J. Facchini, R. Geißler, J. Schmidt, C. Ammera, R Kramell, S. Voigtländer, A. Gesell, S. Pienkny, W. Brandt, *Phytochemistry* 2009, **70**, 1696–1707.
27. V. Sharma, S. Jain, D. S. Bhakuni, R. S. Kapil, *J. Chem. Soc. Perkin* 1982, **1**, 1153–1155.
28. A. R. Battersby, R. B. Herbert, E. McDonald, R. Ramage, J. H. Clements, *J. Chem. Soc. Perkin* 1972, **1**, 1741–1746.
29. H. Abdelkafi, B. Nay, *Nat. Prod. Rep.* 2012, **29**, 845–869.
30. J. Eichhorn, T. Takada, Y. Kita, M. H. Zenk, *Phytochemistry* 1998, **49**, 1037–1047.
31. A. M. Takos, F. Rook, *Int. J. Mol. Sci.* 2013, **14**, 11713–11741.
32. S. E. O'Connor, J. J. Maresh, *Nat. Prod. Rep.* 2006, **23**, 532–547.
33. J. Stöckigt, S. Panjikar, *Nat. Prod. Rep.* 2007, **24**, 1382–1400.
34. C. L. Schardl, D. G. Panaccione, P. Tudzynski, *in The Alkaloids: Chemistry and Biology*, Vol. **63**, G. A. Cordell (Ed.), Elsevier: Amsterdam (2006), 45–86.
35. G. Yim, M. N. Thaker, K. Koteva, G. Wright, *J. Antibiot.* 2014, **67**, 31–41.
36. B. K. Hubbard, C. T. Walsh, *Angew. Chem. Int. Ed.* 2003, **42**, 730–765.
37. C. M. Dobson, *Nature* 2004, **432**, 824–828.
38. L. H. Caporale, *Proc. Natl. Acad. Sci. U.S.A* 1995, **92**, 75–82.
39. A. Bauer, M. Brönstrup, *Nat. Prod. Rep.* 2013, **31**, 35–60.
40. T. Liu, Y.-M. Chiang, A. D. Somoza, B. R. Oakley, C. C. C. Wang, *J. Am. Chem. Soc.* 2011, **133**, 13314–13316.
41. D. E. Cane, F. Kudo, K. Kinoshita, C. Khosla, *Chem. Biol.* 2002, **9**, 131–142.
42. C. J. B. Harvey, J. D. Puglisi, V. S. Pande, D. E. Cane, C. Khosla, *J. Am. Chem. Soc.* 2012, **134**, 12259–12265.
43. (a) A. Kirschning, F. Hahn, *Angew. Chem. Int. Ed.* 2012, **51**, 4012–4022; (b) S. Weist, R. D. Süssmuth, *Appl. Microbiol. Biotechnol.* 2005, **68**, 141–150; (c) K. Weissman, *Trends Biotechnol.* 2007, **25**, 139–142.
44. R. Robinson, *J. Chem. Soc. Trans.*, 1917, **111**, 762–768.
45. J. W. Medley, M. Movassaghi, *Chem. Commun.* 2013, **49**, 10775–10777.
46. E. Gravel, E. Poupon, *Eur. J. Org. Chem.* 2008, 27–42.
47. X.-W. Li, A. Ear, L. Roger, N. Riache, A. Deville, B. Nay, *Chem. Eur. J.* 2013, 16389–16393.
48. H. Oikawa, *J. Org. Chem.* 2003, **68**, 3552–3557.
49. K. C. Nicolaou, D. Sarlah, T. R. Wu, W. Zhan, *Angew. Chem. Int. Ed.* 2009, **48**, 6870–6874.
50. H. Uchiro, R. Kato, Y. Arai, M. Hasegawa, Y. Kobayakawa, *Org. Lett.* 2011, **13**, 6268–6271.
51. A. Ear, S. Amand, F. Blanchard, A. Blond, L. Dubost, D. Buisson, B. Nay, *Org. Biomol. Chem.* 2015, **13**, 3662–3666.
52. C. A. Kuttruff, M. D. Eastgate, P. S. Baran, *Nat. Prod. Rep.* 2014, **31**, 419–432.
53. (a) S. J. Mickel, G. H. Sedelmeier, D. Niederer et al., *Org. Proc. Res. Dev.* 2004, **8**, 92–100 (Part 1); (b) S. J. Mickel, G. H. Sedelmeier, D. Niederer et al., *Org. Proc. Res. Dev.* 2004, **8**, 101–106 (Part 2); (c) S. J. Mickel, G. H. Sedelmeier, D. Niederer et al., *Org. Proc. Res. Dev.* 2004, **8**, 107–112 (Part 3); (d) S. J. Mickel, G. H. Sedelmeier, D. Niederer et al., *Org. Proc. Res. Dev.* 2004, **8**, 113–121 (Part 4); (e) S. J. Mickel, D. Niederer, R. Daeffler et al., *Org. Proc. Res. Dev.* 2004, **8**, 122–130 (Part 5).
54. C. J. Paddon, P. J. Westfall, D. J. Pitera et al., *Nature* 2013, **496**, 528–532.
55. (a) J. Dhainaut, A. Dlubala, R. Guevel, A. Medard, G. Oddon, N. Raymond, J. Turconi (Sanofi –Aventis, Fr.) WO 2011/026865 (2011); (b) V. Kraft, G. Kretzschmar, K. Rossen (Sanofi –Aventis, Fr.) WO 2011/030223 (2011).
56. J. S. Cannon, L. E. Overman, *Angew. Chem. Int. Ed.* 2012, **51**, 4288–4311.
57. R. B. Woodward, W. J. Brehm, *J. Am. Chem. Soc.* 1948, **70**, 2107–2115.
58. (a) R. B. Woodward, M. P. Cava, W. D. Ollis, A. Hunger, K. Schenker, *J. Am. Chem. Soc.* 1954, **76**, 4749–4761; (b) P. Magnus, M. Giles, R. Bonnert, C. S. Kim, L. McQuire, A. Merritt, N. Vicker, *J. Am. Chem. Soc.* 1992, **114**, 4403–4405; (c) M. E. Kuehne, F. Xu, *J. Org. Chem.* 1993, **58**, 7490–7497; (d) S. D. Knight, L. E. Overman, G. Pairaudeau, *J. Am. Chem. Soc.* 1993, **115**, 9293–9294; (e) V. H. Rawal, S. Iwasa, *J. Org. Chem.* 1994, **59**, 2685–2686; (f) M. E. Kuehne, F. Xu, *J. Org. Chem.* 1998, **63**, 9427–9433; (g) D. Solé, J. Bonjoch, S. García-Rubio, E. Peidró, J. Bosch, *Angew. Chem. Int. Ed.* 1999, **38**, 395–397; (h) M. J. Eichberg, R. L. Dorta, K. Lamottke, K. P. C. Vollhardt, *Org. Lett.* 2000, **2**, 2479–2481; (i) M. Ito, C. W. Clark, M. Mortimore, J. B. Goh, S. F. Martin, *J. Am. Chem. Soc.* 2001, **123**, 8003–8010; (j) M. Nakanishi, M. Mori, *Angew. Chem. Int. Ed.* 2002, **41**, 1934–1936; (k) T. Ohshima, Y. Xu, R. Takita, S. Shimizu, D. Zhong, M. Shibasaki, *J. Am. Chem. Soc.* 2002, **124**, 14546–14547; (l) G. J. Bodwell, J. Li, *Angew. Chem. Int. Ed.* 2002, **41**, 3261–3262; (m) Y. Kaburagi, H. Tokuyama, T. Fukuyama, *J. Am. Chem. Soc.* 2004, **126**, 10246–10247; (n) H. Zhang, J. Boonsombat, A. Padwa, *Org. Lett.* 2007, **9** 279–282; (o) G. Sirasani, T. Paul, W. Dougherty Jr., S. Kassel, R. B. Andrade, *J. Org. Chem.* 2010, **75**, 3529–3532; (p) C. Beemelmanns, H.-U. Reissig, *Angew. Chem. Int. Ed.* 2010, **49**, 8021–8025; (q) S. B. Jones, B. Simmons, A. Mastracchio, D. W. C. MacMillan, *Nature* 2011, **475**, 183–188; (r) D. B. C. Martin, C. D. Vanderwal, *Chem. Sci.* 2011, **2**, 649–651.
59. (a) P. A. Wender, *Nat. Prod. Rep.* 2014, **31**, 433–440; (b) T. Gaich, P. S. Baran, *J. Org. Chem.* 2010, **75**, 4657–4673.
60. T. Newhouse, P. S. Baran, R. W. Hoffmann, *Chem. Soc. Rev.* 2009, **38**, 3010–3021.
61. (a) M. D. Burke, G. Lalic, *Chem. Biol.* 2002, **9**, 535–541; (b) D. R. Spring, *Org. Biomol. Chem.* 2003, **1**, 3867–3870.
62. C. Cordier, D. Morton, S. Murrison, A. Nelson, C. O'Leary-Steele, *Nat. Prod. Rep.* 2008, **25**, 719–737.
63. S. B. Jones, B. Simmons, A. Mastracchio, D. W. C. MacMillan, *Nature* 2011, **475**, 183–188.
64. Y. Yang, Y. Bai, S. Sun, M. Dai, *Org. Lett.* 2014, **16**, 6216–6219.
65. J. Deng, R. Li, Y. Luo, J. Li, S. Zhou, Y. Li, J. Hu, A. Li, *Org. Lett.* 2013, **15**, 2022–2025.
66. P. A. Wender, V. A. Verma, T. J. Paxton, T. H. Pillow, *Acc. Chem. Res.* 2008, **41**, 40–49.
67. G. H. Posner, P. M. O'Neill, *Acc. Chem. Res.* 2004, **37**, 397–404.

# SECTION I

# ACETATE BIOSYNTHETIC PATHWAY

# 2

# POLYKETIDES

FRANÇOISE SCHAEFERS AND TOBIAS A. M. GULDER

*Department of Chemistry and Center for Integrated Protein Science Munich (CIPSM), Biosystems Chemistry, Technische Universität München, Munich, Germany*

## 2.1 POLYKETIDE BIOSYNTHESIS

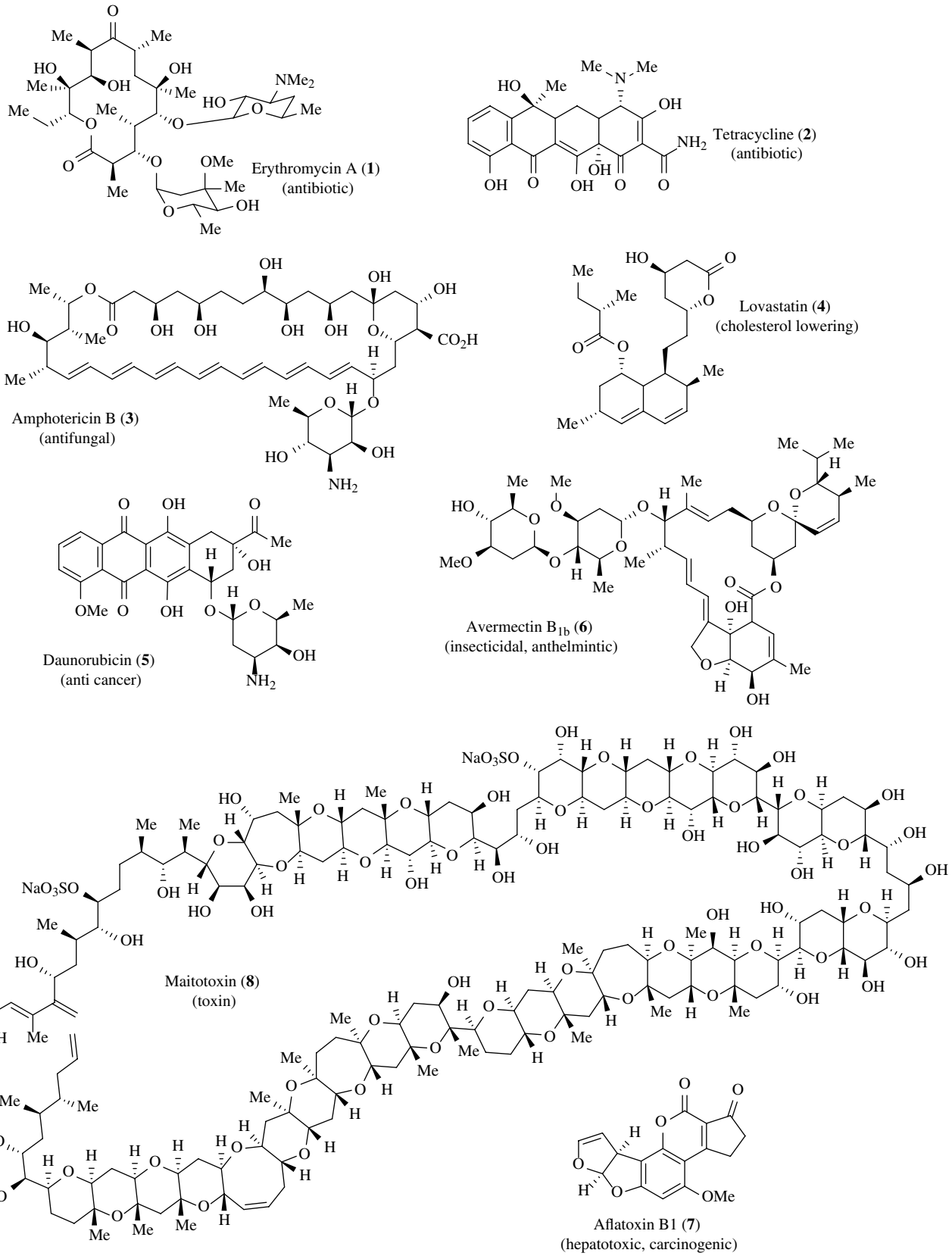
### 2.1.1 Introduction

Polyketides are a fascinating class of natural products with highly diverse, often complex structures combined with a likewise impressive breath of strong and selective biological activities. Because of these extraordinary properties, polyketides continue to fascinate and inspire medicinal, synthetic, and natural product chemists and biochemists alike. This appeal of polyketides can easily be illustrated by some representative examples shown in Scheme 2.1. From a structural point of view, this limited selection already comprises a tremendous diversity, from small aromatic and aliphatic polycyclic compounds, to densely functionalized and stereochemically challenging macrolides, up to strikingly large and complex polyethers. In addition, these compounds exhibit a multitude of different biological properties with many important clinical applications: erythromycin A (**1**) [1] and tetracyclines [2], for example **2**, are widely applied antibiotics. The polyene amphotericin B (**3**) is an effective agent against various systemic fungal infections and shows antiprotozoal activity [3]. Lovastatin (**4**) is an effective cholesterol-lowering agent and has served as a blueprint for the development of a large set of synthetic statins [4]. The DNA intercalating agent daunorubicin (**5**) is a potent anticancer chemotherapeutic [5]. The avermectin family of antiparasitics, exemplified by **6**, have been instrumental for the treatment of severe maladies caused by parasitic worms, in particular onchocerciasis (river blindness) [6]. The biomedical significance of this small selection of polyketides is underlined by the fact that they—and/or synthetic derivatives inspired by them—can all be found on the World Health Organization's List of Essential Medicines [7].

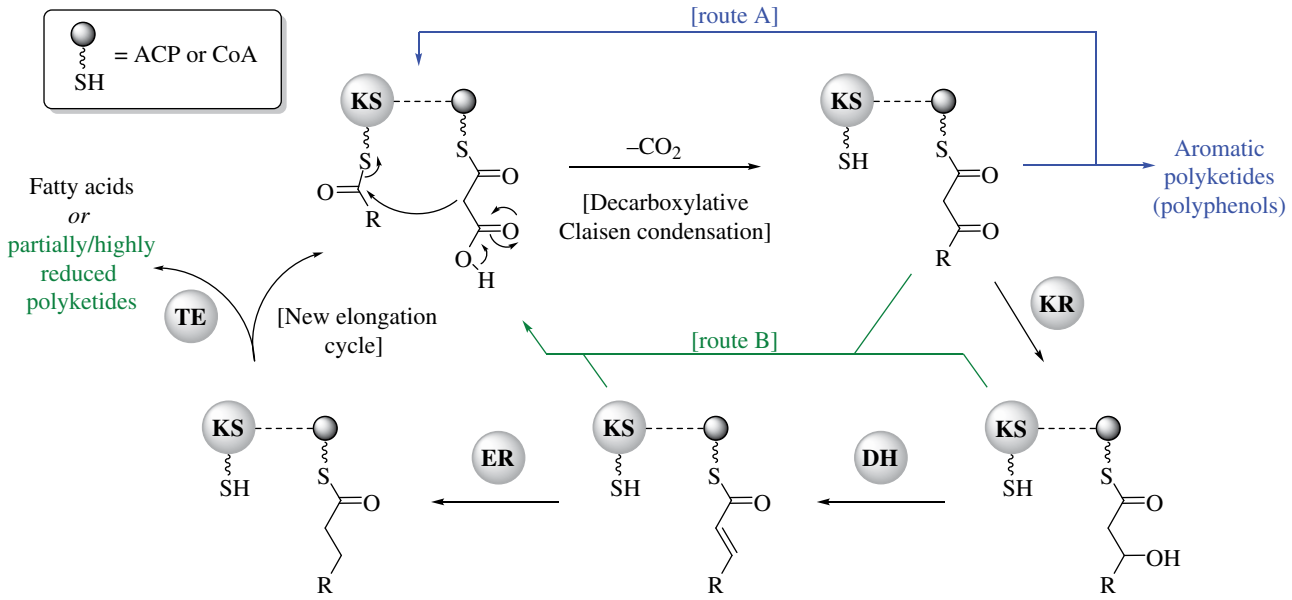
Besides these desirable biomedical properties, the impact of the biological activity of polyketides on mankind also extends to detrimental effects. Prominent examples are the aflatoxins, such as B1 (**7**), produced by *Aspergillus* sp. [8]. This group of compounds exhibits acute hepatotoxic effects and strongly increases the risk of developing liver cancer upon chronic exposure [9]. The compounds can primarily be detected on dried goods, such as corn, nuts, fruits, and spices, but also find their way into fresh produce, such as meat or milk. Aflatoxin levels in food are thus tightly regulated (with typical tolerance levels in between 0 and 30 μg/kg). Another impressive example is maitotoxin (**8**), the largest nonpolymeric, nonpeptidic organic molecule isolated from nature until today [10]. This giant polyether is produced by dinoflagellates (e.g., *Gambierdiscus toxicus*) and moves up the food chain to ultimately enrich in fish, for example, in *Ctenochaetus striatus* (called maito in Tahiti) from which **8** was initially discovered. Ingestion of such contaminated food leads to the severe illness ciguatera. This effect is caused by the tremendous toxicity of **8** ($LD_{50}$ of 50 ng/kg in mice).

Equally impressive as the polyketide structural and functional diversity are the enzymatic machineries that evolved to produce these fascinating secondary metabolites,

*From Biosynthesis to Total Synthesis: Strategies and Tactics for Natural Products*, First Edition. Edited by Alexandros L. Zografos.
© 2016 John Wiley & Sons, Inc. Published 2016 by John Wiley & Sons, Inc.




**SCHEME 2.1** Selection of structurally and functionally diverse polyketide natural products **1–8**.




**SCHEME 2.2** Biosynthetic routes to fatty acids and polyketides.

almost exclusively employing simple acetate and malonate building blocks for core structure assembly. Within this chapter, we discuss the logic of biosynthetic polyketide assembly. This diverse topic has been comprehensively reviewed in excellent general articles in recent years [11–15]. We herein focus on the introduction of the basic mechanisms and concepts of polyketide core structure assembly using a number of well-studied representative examples, thus allowing to compare the biosynthetic versus chemical synthetic strategies (see following chapters) to assemble such beautiful small molecules.

### 2.1.2 Assembly of Acetate/Malonate-Derived Metabolites

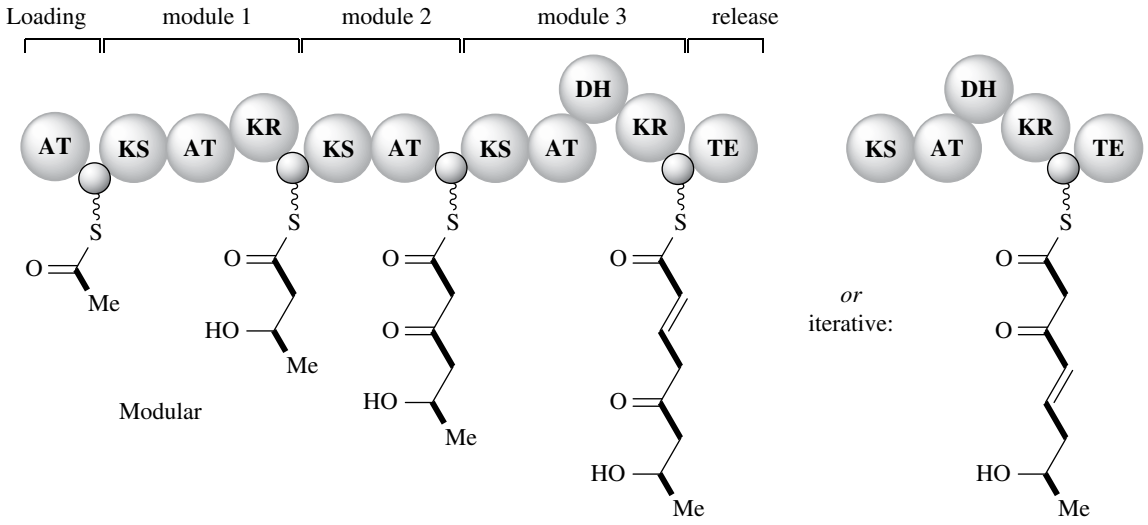
The basic principle of polyketide assembly is highly related to that of fatty acid biosynthesis [14, 16]. In both biosynthetic systems, an acyl-primed ketosynthase (KS) catalyzes chain extension by decarboxylative Claisen condensation with malonate activated by its attachment to coenzyme A or an acyl carrier protein (ACP) via a thioester bond (Scheme 2.2). In fatty acid synthases (FASs), the resulting ketone is reduced to the corresponding alcohol by a ketoreductase (KR), dehydrated by action of a dehydratase (DH) to give the alkene with subsequent double-bond reduction by an enoyl reductase (ER) yielding the saturated system (cf. Section 3.2). The latter can then be transferred onto the KS domain and enter the next cycle of chain extension and complete reduction. This homologation process facilitates the assembly of long-chain saturated fatty acids, for example, palmitic acid, after seven cycles, which will ultimately be released from the catalytic system by saponification of the linkage to the thiol activating group, for example, catalyzed by a thioesterase (TE) domain [16].

Remarkably, polyketide synthases (PKSs) utilize the identical, small set of biosynthetic reactions to generate the tremendous structural diversity observed in the polyketide natural product family. The diversification of core structures accessible by PKSs when compared to FASs is achieved by flexible application of the reductive transformations processing the ß-keto groups resulting from chain extension. The class of aromatic polyphenols thereby can be accessed by omitting reductions (Scheme 2.2, route A). Alternatively, the oxidation state at the ß-carbon can individually be controlled after each elongation step to keep ketones, alcohols, or double bonds in the respective positions (Scheme 2.2, route B), leading to highly or partially reduced PKS products. Together with an increased flexibility concerning the acyl and malonyl building blocks combined with further post-PKS modifications—such as hydroxylation, halogenation, or glycosylation tailoring reactions—this strategy gives rise to a virtually inexhaustible diversity of possible product structures.

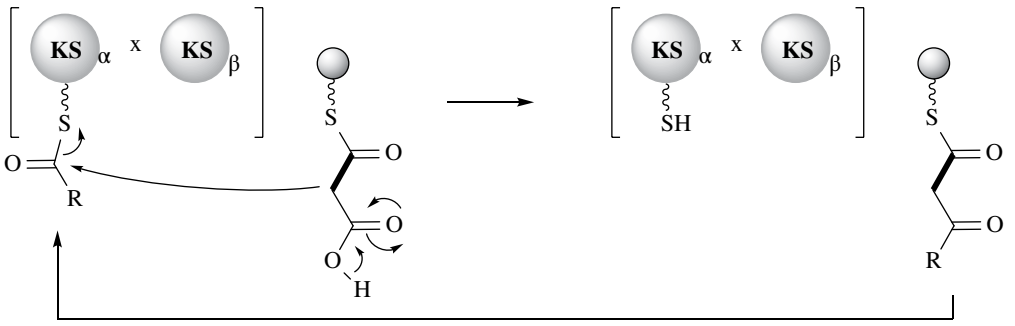
### 2.1.3 Classification of Polyketide Biosynthetic Machineries

Depending on the overall structural organization of the individual catalytic units, their exact function, and precursor requirements, PKSs can roughly be classified into three substantially different types (Scheme 2.3) [11–13]. In analogy to the FAS classification, type I PKSs are multifunctional megaenzymes bearing all catalytic units on a large polypeptide [14, 17–22]. Type II PKSs are dissociable complexes

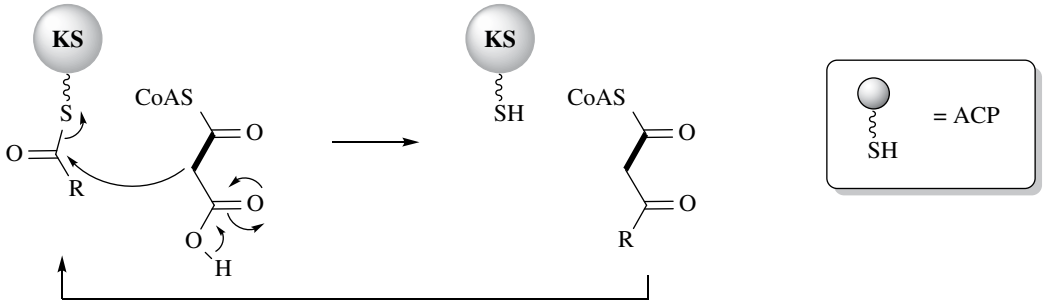
(a)




(b)




(c)




**SCHEME 2.3** Classification of PKSs. (a) Type I PKS. (b) Type II PKS. (c) Type III PKS.

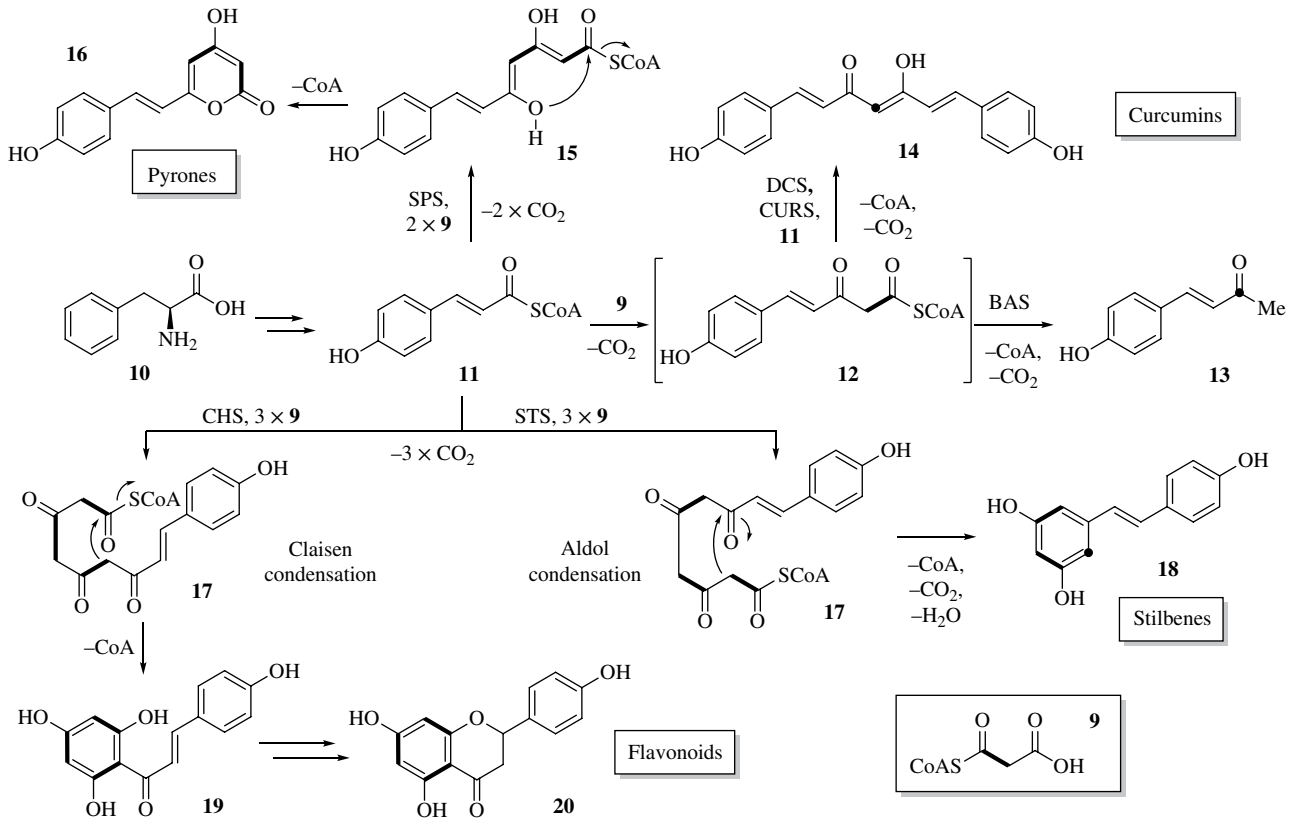
of individual proteins with single functions [23–26]. Both these systems rely on thiotemplate mechanisms in which the substrates and growing polyketide intermediates are covalently attached to the biosynthetic proteins via thioester bonds. The additional type III PKSs, by contrast, only require a single KS active site and utilize free, that is, coenzyme A-bound rather than ACP-bound building blocks for polyketide assembly [27–31].

The three types of PKSs are not equally distributed across the kingdoms of life and, owing to their structural and functional differences, generate distinct types of products [13]. The type III (mainly found in plants, some in bacteria and fungi) and type II (only bacteria) PKSs produce aromatic natural products by iterative use of their respective catalytic units with no to little reductive alterations. Fungal iterative type I PKSs are capable of crafting both aromatic and structurally diverse reduced polyketides. These PKSs are often further classified as nonreducing (NR), partially reducing (PR), or highly reducing (HR), depending on the degree of reductive processing during chain assembly [20]. Despite the iterative use of the overall PKS system, each individual catalytic domain can optionally be employed in each elongation cycle, thus facilitating biosynthesis of highly complex products. Bacterial iterative type I PKSs have long thought to be rare, but a number of interesting examples encoding structurally challenging molecules, such as enediynes [32, 33] or polycyclic tetramate macrolactams [34, 35], have been identified in recent years. Finally, modular type I PKSs that have so far only been found in bacteria and few protists exclusively generate reduced, often highly elaborate natural products [17]. In these systems, each PKS module contains all catalytic domains responsible for the incorporation and the desired reductive processing of a single $C_2$-building block. This so-called colinearity principle facilitates a direct translation of PKS module organization into expected product structure and *vice versa* [17], a convenient correlation not currently possible for any of the other types of PKSs. In recent years, however, a new subtype of modular type I PKSs emerged. The most prominent difference to previous textbook PKSs is the lack of individual AT domains in each module but instead the presence of a single AT domain outside the modular PKS structure that is acting on all ACPs in *trans* [36]. Many of these *trans*-AT PKSs feature module skipping or repeated utilization of certain modules as well as domain architectures deviating from the predictable, long-known *cis*-AT PKS standards. While this complicates product prediction significantly, recent detailed insights into precursor selection mechanisms are beginning to demystify *trans*-AT PKSs.

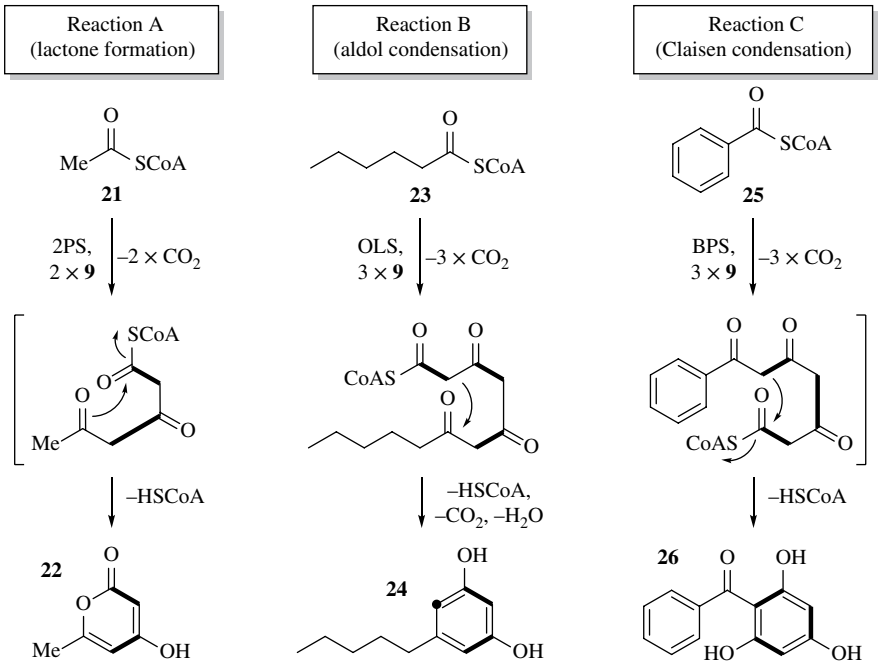
Although the organization of PKSs into types I to III will continue to be challenged by newly discovered systems that do not match the scheme [37, 38], it is extremely useful to explain fundamental differences in polyketide biosynthetic diversity. We will thus adhere to this classification and will begin to introduce the seemingly simplest type III PKS systems.

***2.1.3.1 Type III PKSs in Plants, Bacteria, and Fungi*** Type III PKSs are proteins of about 40–45 kDa size forming homodimers that bear two catalytically active sites, each facilitating product formation by decarboxylative condensation of malonyl-CoA (**9**) with a starter unit (cf. Scheme 2.3c) [27–31]. The broad product spectrum of such systems is a result of their high flexibility concerning the number of elongation steps, the final chain termination/cyclization chemistry, and starter unit selection. Among the best-studied type III PKSs are those involved in the biosynthesis of phenylpropanoids in plants. Starting from L-phenylalanine (**10**), deamination by phenylalanine ammonia lyase (PAL), *p*-hydroxylation by cinnamic acid 4-hydroxylase (C4H), and activation of the carbonyl by 4-coumaroyl:CoA ligase (4CL) by thioester formation with coenzyme A yield the central precursor *p*-coumaroyl-CoA (**11**) [39]. Alternatively, **11** is accessible by direct deamination of L-tyrosine with tyrosine ammonia lyase (TAL) in some microorganisms and grasses [40–42]. Compound **11** now serves as the starter unit for many plant-derived type III PKSs (Scheme 2.4). Decarboxylative elongation with one unit of **9** catalyzed by benzalacetone synthase (BAS) to **12** with concomitant hydrolysis and decarboxylation yields *p*-hydroxybenzalacetone (**13**) [43]. Similar elongation of **11** with **9** catalyzed by diketide-CoA synthase (DCS) in the presence of curcumin synthase (CURS) results in the formation of the curcuminoid carbon skeleton, for example, of bisdemethoxycurcumin (**14**) [44, 45]. Notably, curcumins are also directly accessible from cinnamoyl-CoA precursors by action of a single enzyme, curcuminoid synthase (CUS) [46]. Elongation of **11** by two units of **9** catalyzed by styrolpyrone synthase (2PS) gives **15**, which is directly cyclized by intramolecular lactonization to give pyrone **16** [47]. Such pyrone formation is also catalyzed by 4-coumaroyltriacetic acid synthase (CTAS) [48]. The latter, however, uses three units of **9** for chain extension, thus resulting in the longer-chain *p*-coumaroyl triacetic acid lactone. Both chalcone synthase (CHS) and stilbene synthase (STS) likewise use three units of **9** to give intermediate **17** [49]. In STS, this is further processed by Aldol condensation to give stilbenes, such as resveratrol (**18**) [50]. Alternatively, CHS catalyzes Claisen condensation producing chalcone **19**, the precursor of flavonoids, such as naringenin (**20**) [51].

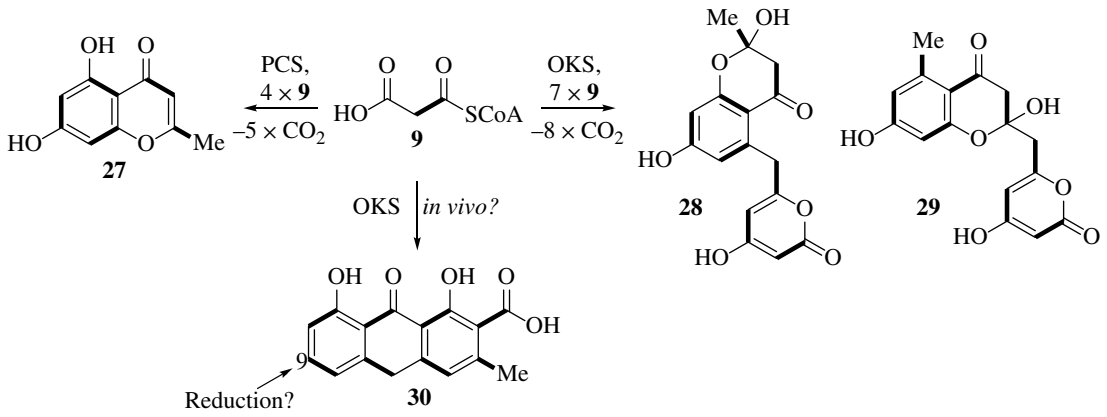
Although Scheme 2.4 presents only a small selection of currently characterized plant type III PKSs, it contains all important basic reactions of this class of enzymes. Besides sole elongation chemistry, here leading to **13** or **14**, cyclization reactions allow further diversification by either (A) lactonizations to give pyrones, (B) aldol condensations to resorcinols or resorcylic acids, or (C) Claisen condensations yielding phloroglucinols (Scheme 2.5). Using




**SCHEME 2.4** Type III PKS involved in phenylpropanoid biosynthesis in plants.




**SCHEME 2.5** Selected examples of plant type III PKSs utilizing diverse starter units.



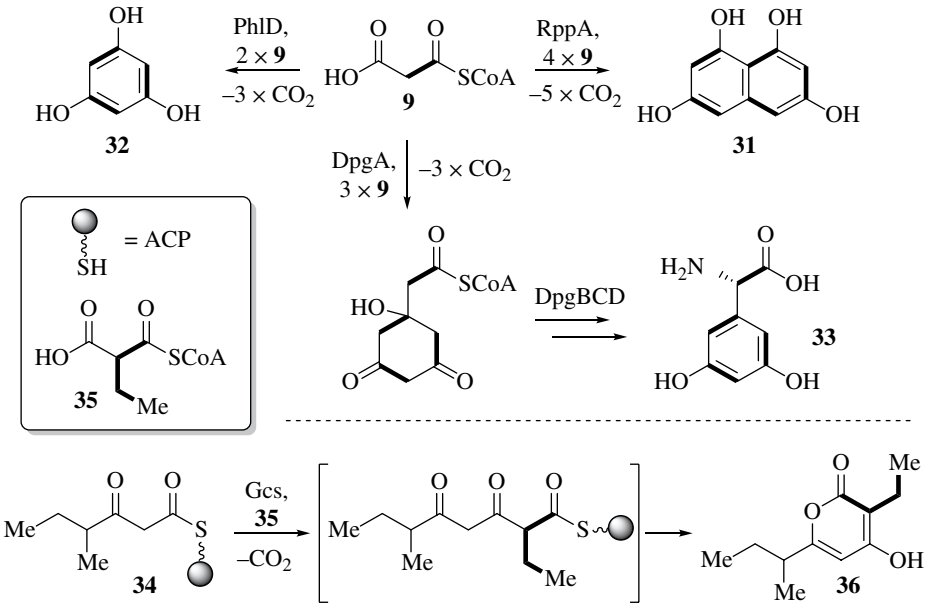

**SCHEME 2.6** Recent examples of plant type III PKSs producing long-chain products.

this set of reactions A–C, variations in starter units facilitate access to further chemical diversity. For example, extension of acetyl-CoA (**21**) with two units of **9** catalyzed by 2-pyrone synthase (2PS) gives pyrone **22** [47]. Threefold extension of hexanoyl-CoA (**23**) with **9** catalyzed by olivetol synthase (OLS) produces olivetol (**24**) [52], a central building block in cannabinoid biosynthesis. Benzophenone synthase (BPS) extends benzoyl-CoA (**25**) by three $C_2$ units leading to benzophenone **26** [53].

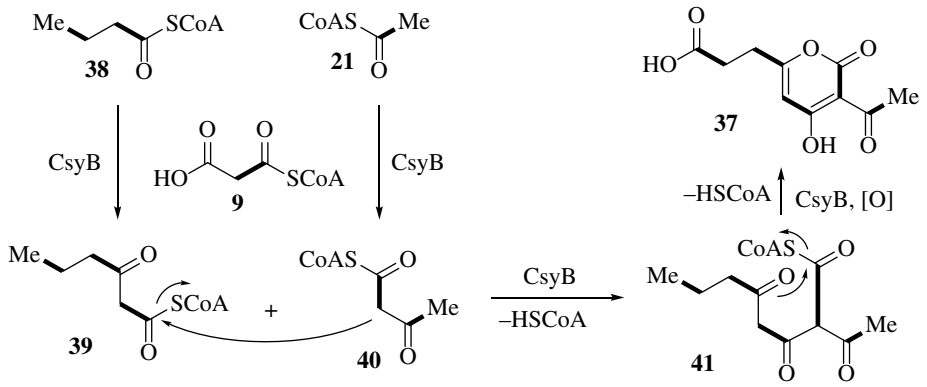
As suggested by the aforementioned examples, most type III PKSs in plants catalyze two or three chain-extension cycles. However, currently characterized systems range from one to eight elongation reactions. Two interesting enzymes for long-chain assembly were discovered in *Aloe* sp., pentaketide chromone synthase (PCS) [54], and oktaketide synthase (OKS) [55]. *In vitro*, PCS was shown to utilize five units of **9** to form chromones **27** (Scheme 2.6). By homologation of eight units of **9**, OKS unexpectedly yielded SEK4 (**28**) and SEK4b (**29**), two compounds previously known as shunt products from bacterial type II PKSs [56]. While chromones, comparable to **27**, could indeed also be PKS products *in vivo*, for example, leading to aloesin-type secondary metabolites known from *Aloe* sp., OKS is thought to require an enzymatic partner *in vivo* [30]. A KR might be involved in the reduction of the carbonyl function at C-9 of a theoretical, linear octaketide precursor, which subsequently would allow to funnel OKS biosynthesis toward chrysophanol-related natural products, such as **30**. Similar KR activity-mediated product control can be found in many bacterial type II PKS systems (cf. Section 2.1.3.2).

Type III PKSs have long been thought to exclusively occur in plants. This changed with the discovery of the 1,3,6,8-tetrahydroxynaphthalene (**31**, THN) synthase RppA from *Streptomyces griseus* in 1999 [57, 58], which meanwhile was identified in a number of other actino- and proteobacteria [59–62]. RppA catalyzes the formation of **31** by decarboxylative fusion of five malonyl-CoAs (**9**) and cyclization of the resulting linear precursor (Scheme 2.7). Since the discovery of RppA, type III PKS biochemistry in bacteria has been extended by a number of other enzymes. This included phloroglucinol (**32**) synthase PhlD from *Pseudomonas fluorescens* [63] and DpgA from *Amycolatopsis orientalis* [64], which, together with DpgBCD, assembles 3,5-dihydroxyphenylglycine (**33**), an important amino acid building block in glycopeptide antibiotics [65]. Further examples include type III PKSs involved in bacterial alkylresorcinol/-quinone (e.g., ArsB, SrsA, FtpA) [66–68], and -pyrone (e.g., ArsC, BpsA, PKS18) [69–71] biosynthesis. Some of these enzymes exhibit properties unknown for plant-derived congeners: for example, ArsB and ArsC derive their long-chain alkyl starter units from the type I FAS ArsA by direct interaction with the respective ACP [66], and SrsA and FtpA do not only accept **9** but also methylmalonyl-CoA as extender unit [67, 68]. These unusual features are combined in the type III PKS Gcs from *Streptomyces coelicolor* that not only preferentially accepts an ACP-bound, branched starter unit **34** [72] but is also capable of extending it with ethylmalonyl-CoA (**35**) to ultimately yield germicidin C (**36**) [73].

Only in very recent years, the first type III PKSs from fungi have been identified and functionally studied. CsyA from *Aspergillus oryzae* [74] and 2′-oxoalkylresorcylic acid synthase (ORAS) from *Neurospora crassa* [75, 76] were shown to produce tri- and tetraketide pyrones from long-chain fatty acid acyl-CoAs using malonyl-CoA (**9**) extender units. ORAS furthermore is capable of assembling resorcylic acids and resorcinols from linear tetra- and pentaketide precursors. AnPKS from *Aspergillus niger* likewise crafts tri- and tetraketide pyrones from fatty acid acyl-CoAs, but additionally is capable of accepting benzoyl-CoA starter units [77]. CsyB from *A. oryzae* exhibits a very uncommon reactivity (Scheme 2.8). It is the key enzyme in the biosynthesis of csypyrone B1 (**37**) [78]. CsyB-mediated formation of **37** is achieved by unprecedented fusion of two ß-ketoacyl-CoA units **39** and **40** derived from decarboxylative extension of a butyryl-CoA (**38**) and acetyl-CoA (**21**), respectively




**SCHEME 2.7** Selected examples of type III PKS systems in bacteria.



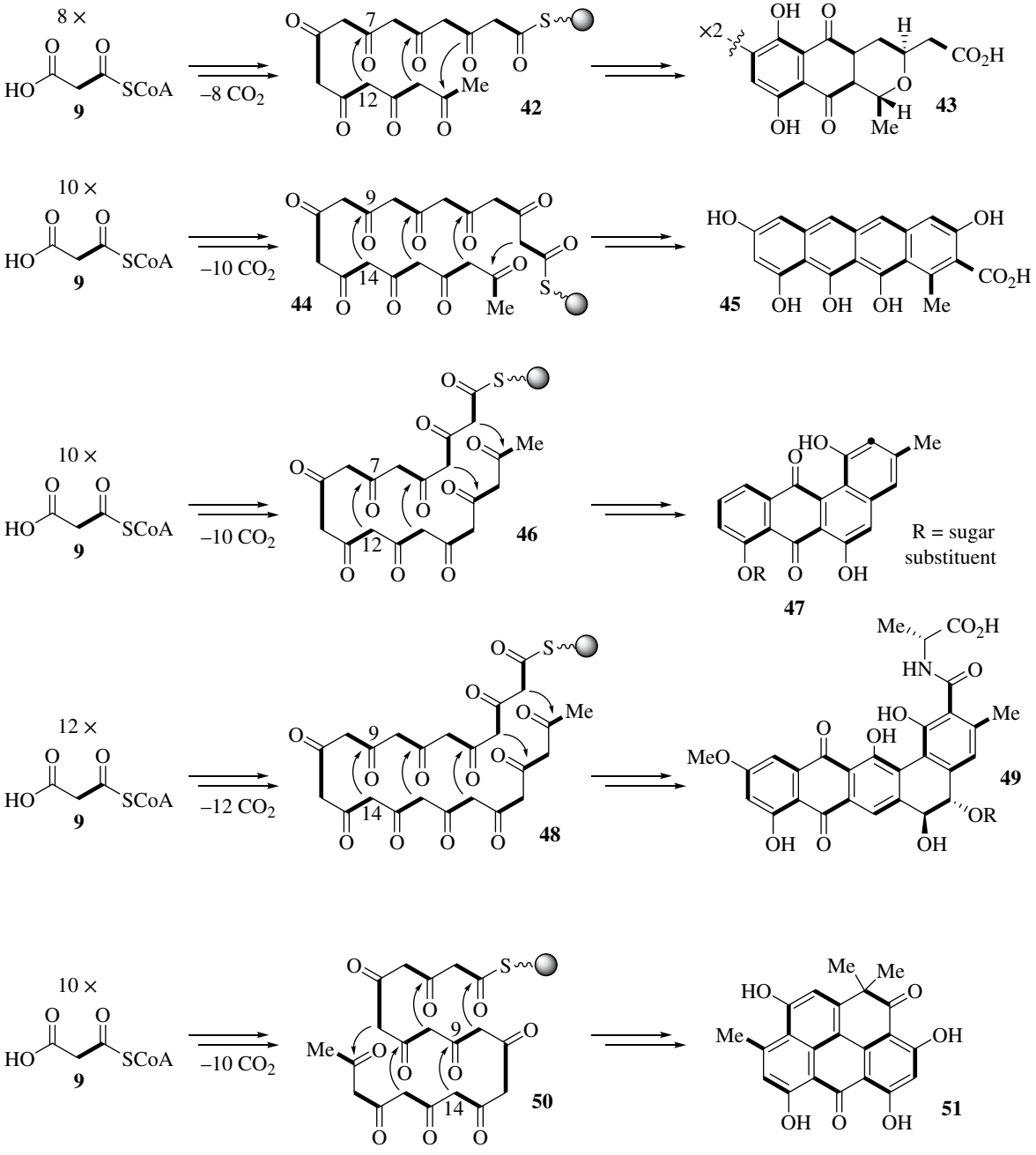

**SCHEME 2.8** Csypyrone B1 (**37**) biosynthesis catalyzed by CsyB, a fungal type III PKSs.

[79, 80]. Subsequent cyclization of intermediate **41** and oxidation delivers **37** (Scheme 2.8).

As these few examples of novel bacterial and fungal systems clearly indicate, many seemingly firm rules in type III PKS biosynthesis will continue to be challenged with an increasing number of such PKSs from diverse organisms being identified and functionally studied.

***2.1.3.2 Type II PKS Systems in Bacteria*** Many biomedically important aromatic natural products are derived from bacterial type II PKSs [23]. Within these biosynthetic machineries, individual enzymes form a functional complex, the so-called minimal PKS. This is composed of a KSα/KSβ heterodimer and a dissociated ACP that serves as product tether (cf. Scheme 2.3b). ACP loading with building blocks is catalyzed by a malonyl-CoA:ACP transacylase (MAT), an activity that can be provided by FabD from fatty acid biosynthesis [81], or might alternatively also be achieved by self-acylation [82, 83]. While KSα catalyzes iterative, decarboxylative chain extension of a starter unit exclusively utilizing malonyl-CoA (**9**), KSβ lacks the necessary active site cysteine residue to perform this function. Thus, it is not directly involved in chain elongation chemistry, but rather in chain initiation [84] and in control of the length of the final polyketide intermediate (hence its additional name CLF = chain length factor) [85–87].

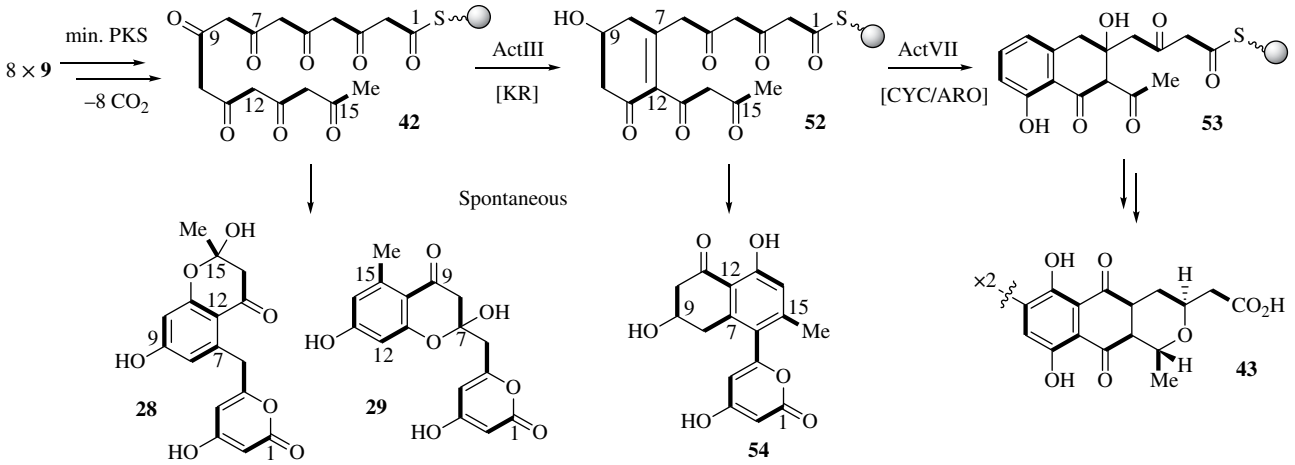
In most bacterial type II PKS products, the polyketide precursor is composed of eight (octaketides, e.g., precursor **42**, toward benzoisochromanes such as actinorhodin (**43**) [88]), ten (decaketides, e.g., precursors **44** and **46** toward tetracenomycins **45** [89] and angucyclines such as landomycin (**47**) [90]), or twelve (dodecaketides, e.g., precursor **48** leading to pentangular polyphenols such as pradimicin (**49**) [91]) $C_2$-building blocks (Scheme 2.9), with the largest




**SCHEME 2.9** Typical type II PKS intermediates (R group indicates further glycosylation).

known example to date being the pentadecaketide fredericamycin [92]. The linear polyketide precursor molecules seem to generally be preorganized in a U-shaped manner [13]. Cyclization by aldol condensation thus leads to linear or angular polycyclic products with no more than two sides of any ring being annealed to another ring system. An interesting exception to this general rule is resistomycin (**51**), which results from cyclization of an S-shaped decaketide precursor **50** [93]. The predominant lack of reductive processing of the intermediate polyketide chain results in the characteristic alternating 1,3-oxygenation pattern in type II PKS products, which in some cases is obscured to some extent by post-PKS oxygenation.

As indicated in Scheme 2.9, the cyclization of the first aromatic ring predominantly occurs between C-12 and C-7 or C-14 and C-9. Furthermore, in each type II PKS pathway, all subsequent cyclization reactions of the highly reactive polyketide intermediate need tight control. Besides significant contributions of the minimal PKS in precursor protection and potentially also in control of the first ring cyclization,

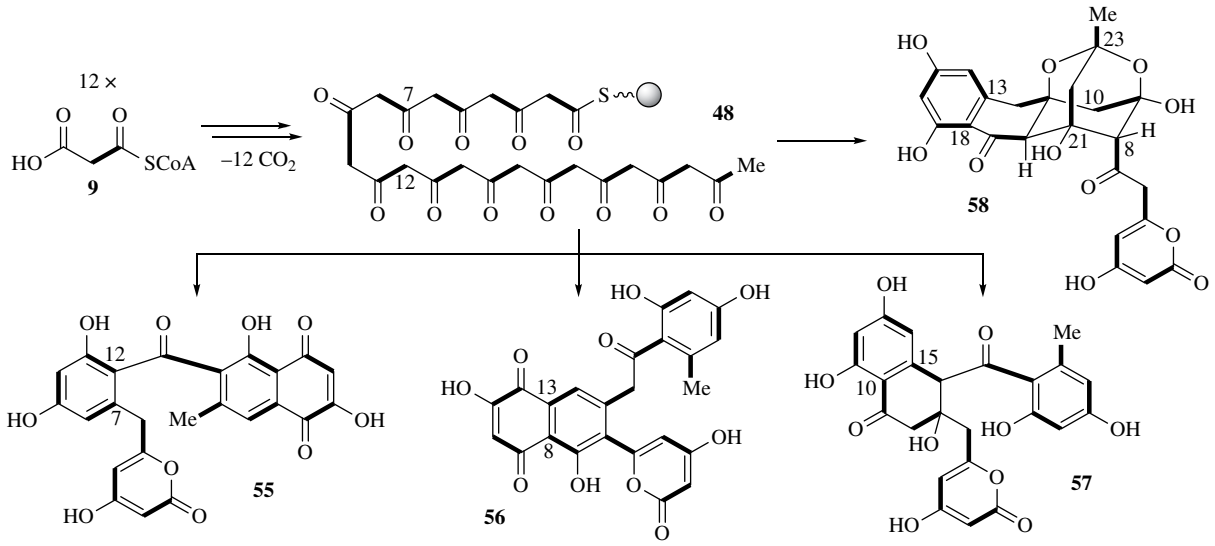



**SCHEME 2.10** Control of the regiochemistry in ring formation in the biosynthesis of actinorhodin (**43**).

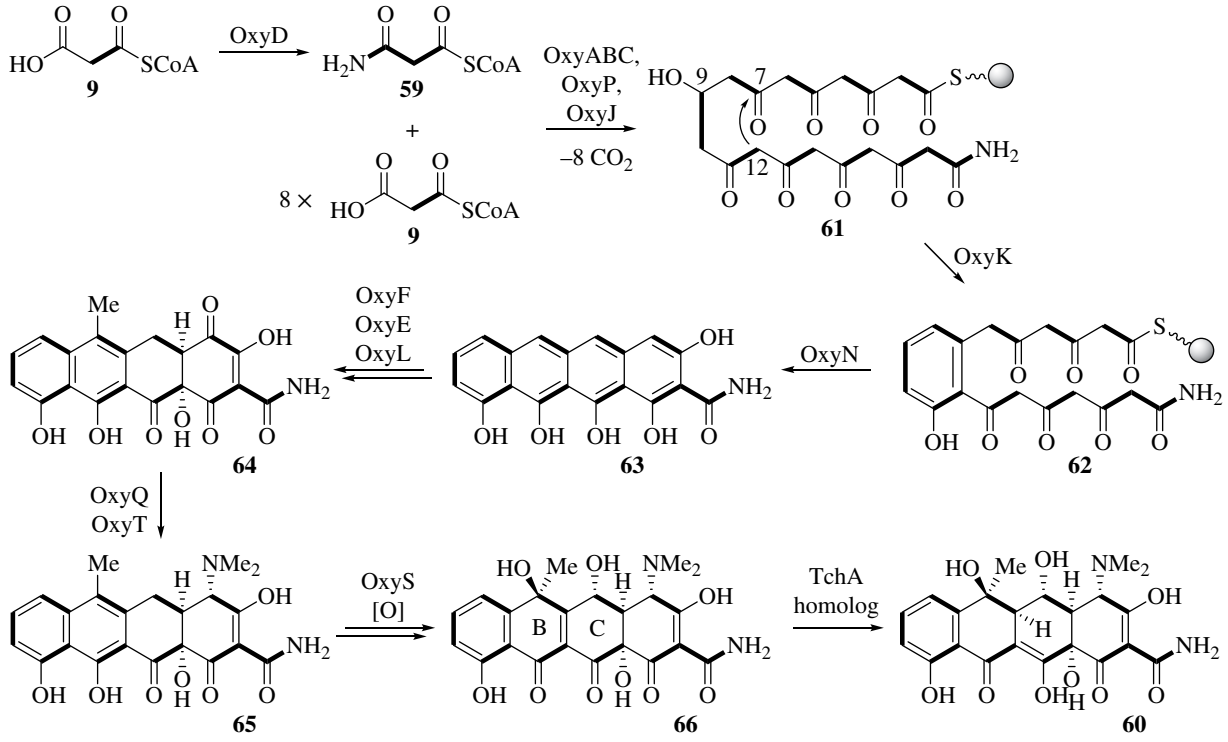
correct folding and thus cyclization of the polyketide are further orchestrated by cyclases (CYC), aromatases (ARO), and a primary KR, the latter almost exclusively reducing precursor chains at C-9. The impact of these important chaperone-like accessory biocatalysts was comprehensively summarized in an excellent recent article by Tang et al. [94]. We thus herein focus on two instructive examples, starting with the exceptionally well-studied biosynthesis of actinorhodin (**43**) [24]. If control over first ring cyclization regioselectivity toward **43** is assumed for the *act* minimal PKS alone, exclusive formation of C-12 to C-7 cyclized PKS products would have to be expected (Scheme 2.9). However, investigations into the product spectrum of the minimal PKS revealed the formation of SEK4 (**28**), with the expected C-12 to C-7 cyclization, together with SEK 4b (**29**) with a C-10 to C-15 connectivity [56] (Scheme 2.10). This clearly rules out an exclusive control of first ring cyclization by the minimal PKS and rather points toward a mere temporal protection of the growing polyketo chain against undesired cyclization within the KS complex. If the KR ActIII is employed in addition, selective reduction at C-9 leads to an exclusive C-12 to C-7 cyclization as shown in intermediate **52**, ultimately leading to mutactin (**54**) [95] (Scheme 2.10). The interplay of the minimal PKS with the KR and the altered structure and conformation of the C-9-reduced substrate thus apparently facilitate strict control over first ring cyclization outcome. The second ring is selectively formed by action of the CYC/ARO Act VII to give **53**, which is ultimately converted into actinorhodin (**43**) by action of the remaining pathway-specific enzymes [24].

The lack of cyclization control by minimal PKSs alone was also impressively demonstrated by expression of the type II PKS *whiE* from *Streptomyces coelicolor* [96]. This led to the formation of more than 30 structurally highly diverse polyketides, with first ring cyclization ranging from C-12 to C-7 as in TW93e (**55**), C-8 to C-13 as in TW93f (**56**), C-10 to C-15 as in TW93g (**57**), and C-13 to C-18 leading to the unprecedented 2,4-dioxaadamantane structure TW93h (**58**) (Scheme 2.11).

In addition to shaping diverse structures by flexible control of cyclization regiochemistry with the aforementioned enzymes, type II PKSs are also capable of incorporating diverse starter units, for example, short-chain fatty acids or benzoate, by interaction with ACPs from type III PKS systems loaded with the respective molecule (which in turn can be derived from FAS or type I PKSs) or by dedicated transferases [97]. An interesting example of an unusual starter unit is malonamate (**59**) found in the class of tetracycline natural products, such as oxytetracycline (**60**) [98, 99]. The amide functionality in **59** is installed by action of the amidotransferase OxyD, either using malonyl-CoA (**9**) or ACP-bound malonate as the substrate [100] (Scheme 2.12). Enhanced priming of the minimal PKS OxyABC with **59** versus acetate is supported by the thiolase OxyP that shows preferential activity toward acetyl-ACP hydrolysis, thus policing starter unit selection [101]. Elongation of the starter unit with eight building blocks **9** and selective reduction at C-9 by KR OxyJ lead to theoretical intermediate **61**. Cyclization by the first ring CYC/ARO OxyK [102] results in **62**, which gets elaborated to the tetracyclic core structure pretetramid (**63**) by CYC OxyN [103]. Further post-PKS tailoring of the structure by C-methylation (OxyF) and oxygenation (OxyE and OxyL) yields 4-keto-anhydrotetracycline (**64**), which upon reductive amination (OxyQ) and di-*N*-methylation (OxyT) gives anhydrotetracycline (**65**) [104]. Oxygenation of the B-ring by OxyS (also named OtcC) and of the C-ring by an additional oxygenase delivers **66** [105]. In analogy to the chlortetracycline pathway, the last reduction step to **60** is likely catalyzed by a homolog of the reductase TchA [106]. This series of methylation, oxygenation, and reduction tailoring steps thus establishes the highly functionalized, bioactive oxytetracycline (**60**) structure [98, 99].



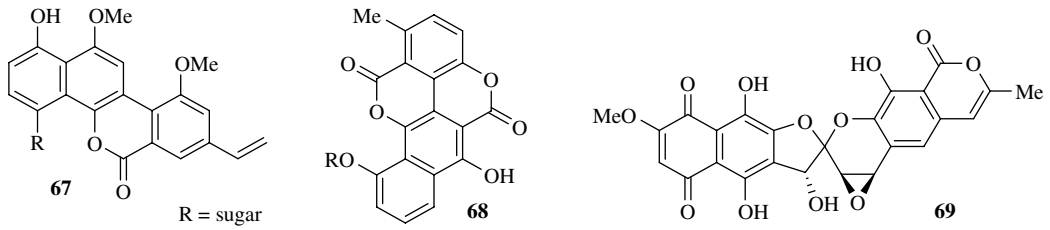
**SCHEME 2.11** Products of the minimal type II PKS *whiE* formed by spontaneous cyclization.



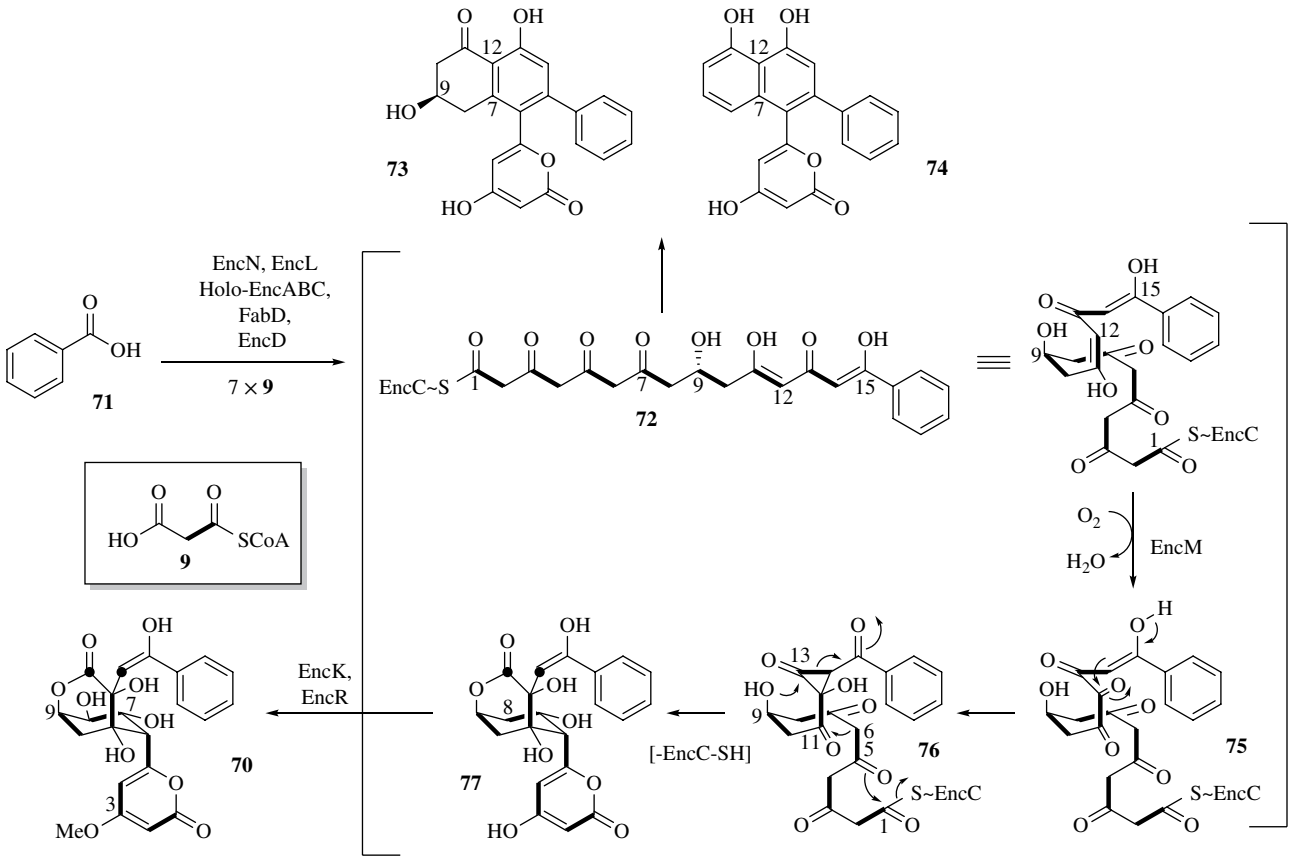
**SCHEME 2.12** Biosynthesis of oxytetracycline (**60**).

Besides rather conservative oxidative functionalization of type II PKS products by tailoring enzymes, PKS core structures are in some pathways heavily modified by extensive oxidative rearrangement reactions. Examples for such processes are found in the biosynthesis of the gilvocarcins, such as **67**, resulting from the rearrangement of an angucyclic precursor of type **47** [107] (cf. Scheme 2.9); of chartreusin (**68**), derived from linear tetracyclic systems comparable to **45** [108]; or of griseorhodin A (**69**) [109], derived from a hexacyclic angular aromatic precursor molecule (Scheme 2.13) [13, 23].

This small selection nicely illustrates the potential of oxidative post-PKS tailoring steps to restructure type II PKS architectures [13, 23]. Nonetheless, the resulting products remain to be aromatic polyketides. The single most impressive deviation from this typical type II PKS product

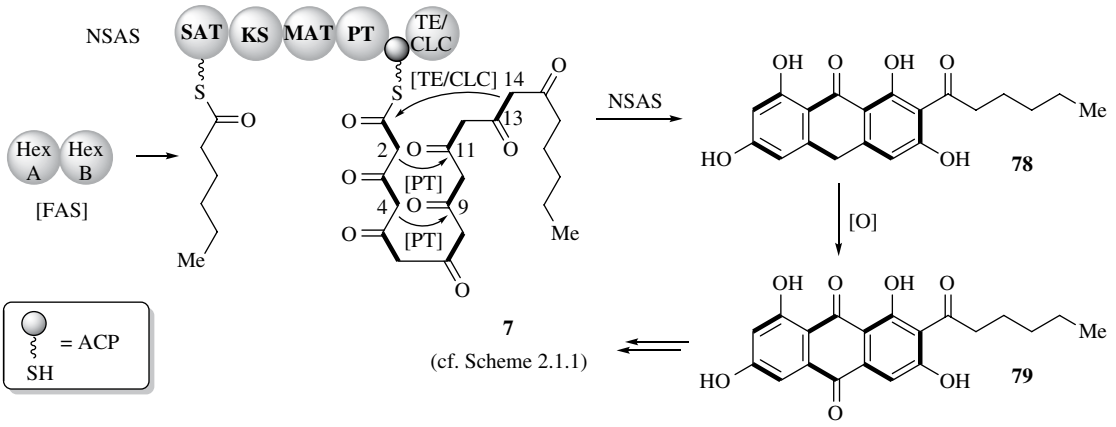



**SCHEME 2.13** Selection of unusual type II polyketides derived from oxidative core structure rearrangements.




**SCHEME 2.14** Biosynthesis of the highly unusual type II PKS product enterocin (**70**).

space is found in the biosynthesis of enterocin (**70**) in *Streptomyces maritimus* [110] (Scheme 2.14). In this case, the benzoate:ACP ligase EncN transfers a benzoate starter unit **71** to the ACP EncC of the enterocin minimal PKS EncABC [111]. Efficient loading of this precursor is controlled by the type II TE EncL that selectively cleaves misprimed starter units, for example, acetate, from EncC [112], similar to the function of OxyP in the biosynthesis of **60** earlier [101]. Subsequent attachment of elongating **9** onto EncC is catalyzed by a homolog of the MAT FabD [113]. Interestingly, this set of enzymes alone does not produce any isolable, benzoate-primed polyketides. With the additional KR EncD, however, selective C-9 reduction leads to theoretical intermediate **72**. This suggests that EncD serves an important catalytic role that helps to direct product assembly and that it likely reduces the nascent polyketide chain during elongation rather than after its complete assembly [114]. Without any further enzymes, **72** spontaneously cyclizes to wailupemycins, for example, by the common C-12 to C-7 cyclization pattern yielding wailupemycins F (**73**) and G (**74**) and thus leading to typical aromatic type II PKS products [113]. In the presence of the flavoprotein EncM, however, oxidation at C-12 to the corresponding ketone **75** precedes the formation of cyclopropanone **76**. Subsequent lactone formation between the alcohol function at C-9 with concomitant cleavage of the C–C bond between C-13 and C-14 and two further cyclization reactions (from the oxygen at C-5 to C-1 and from C-6 to C-11) furnishes intermediate




**SCHEME 2.15** Biosynthesis of norsolorinic acid (**79**) by a fungal type I iPKS.

**77** [115, 116]. The oxygenation reaction at C-12 by EncM, which induces this Favorskii-type rearrangement sequence, remarkably proceeds via a flavin-*N*-5-oxide [117]. The catalytic activity of this single enzyme thereby reroutes the cyclization outcome, leading to the highly unusual enterocin core structure **77**. The biosynthetic assembly of enterocin (**70**) is completed by action of the SAM-dependent methyltransferase (MT) EncK, which methylates the hydroxyl group at C-3, and the cytochrome P450 hydroxylase EncR that mediates C-8 hydroxylation [113].

As the biosynthesis of enterocin (**70**) impressively demonstrates, type II PKSs are not limited to the biosynthesis of polycyclic, aromatic structures. Undoubtedly, future research on this type of PKSs will continue to reveal unprecedented biosynthetic features.

***2.1.3.3 Type I PKS Systems in Fungi and Bacteria*** Type I PKSs are multidomain monomodular (iterative type I PKS, iPKS) or multimodular (modular type I PKS) systems in which the catalytic domains are located and covalently linked within large multifunctional enzymes (cf. Scheme 2.3a) [13]. These proteins can thus reach enormous sizes and are therefore also often referred to as megasynthases. With only a few exceptions, fungi typically harbor monomodular type I iPKSs [21, 22]. Fungal PKSs are further classified according to the degree of reductive processing of the assembled polyketide chain as NR, PR, and HR [20]. Owing to the PKS domain organization in a single protein and the programmed, iterative use of these catalytic units, biochemical and mechanistic investigations of these systems have been extremely challenging. It is thus not surprising that the elucidation of many important fungal type I PKS functions was mostly achieved within the last two decades. In the following section, we will briefly introduce some of the key features of fungal type I PKSs, exemplarily using the norsolorinic acid (NR) and lovastatin (HR) synthases.

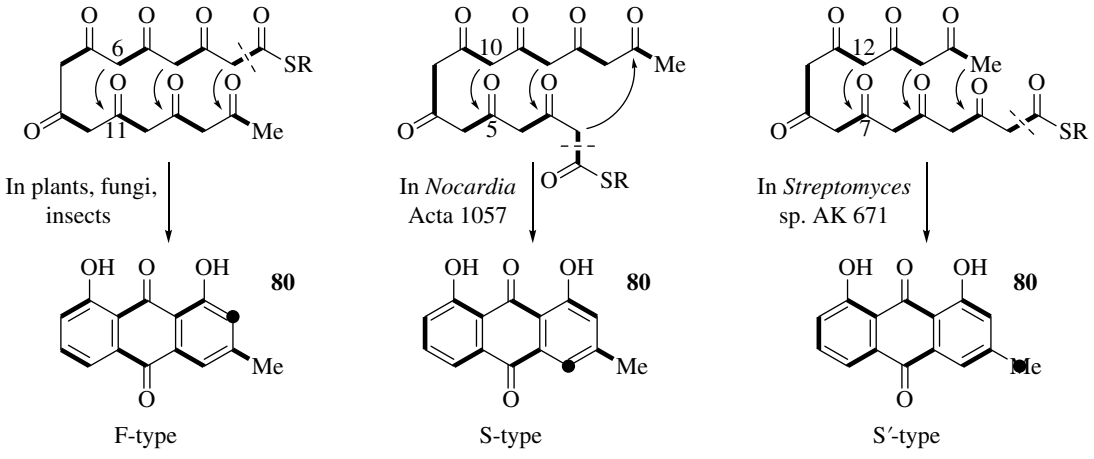
Fungal NR type I iPKSs produce aromatic compounds, structurally highly related to bacterial type II PKS structures [21]. One of the best-studied examples is norsolorinic acid synthase (NSAS) that encodes **79**, the first isolable precursor in sterigmatocystin and aflatoxin biosynthesis [118] (Scheme 2.15). Early isotope labeling and genetic experiments suggested the starter unit to be hexanoate [119, 120]. This building block is provided by HexAB, homologs of fungal α- and β-FAS subunits clustered with NSAS [121, 122]. The exact domain organization of NSAS was elucidated by bioinformatic analysis using the Udwary–Merski algorithm (UMA) [123]. This revealed the presence of six discrete domains, four of which were identified by their conserved sequences to be KS, MAT, ACP, and a terminal TE–Claisen cyclase (TE/CLC) domain. In addition, an amino-terminal domain was predicted, which was later identified to be responsible for hexanoate loading and thus named starter unit transacylase (SAT) [124]. Remarkably, SAT utilizes an active site cysteine residue for activating hexanoate as a thioester, in contrast to the common serine-mediated oxoester activation found in MAT domains. Finally, a product template (PT) domain was postulated, which was thought to be responsible for chain length control and stabilization of the growing polyketide chain [123]. In fact, PT sequences were shown to cluster according to the structures of their respective products [125]. The exact roles of these individual domains were recently firmly established in an impressive deconstruction approach [126]. After homologation of the hexanoate starter to the ACP-bound octaketide precursor, PT mediates regioselective Aldol condensation reactions between C-4/C-9 and C-2/C-11 [127]. As shown before for WA PKS [128], TE/CLC subsequently catalyzes a C-14 to C-1 Claisen reaction to form the third ring system while cleaving **78** from the synthase [129]. In the absence of TE/CLC, the control of the selectivity of this off-loading mechanism is lost. This leads to the formation of **78** along with the respective pyrone resulting from nucleophilic attack of the C-13 oxygen function onto the thioester bond (not shown). Compound **78** gets transformed into norsolorinic acid (**79**) by oxidation. By a complex

series of reactions, **79** is ultimately restructured to yield aflatoxins, such as **7** [8] (cf. Scheme 2.1).

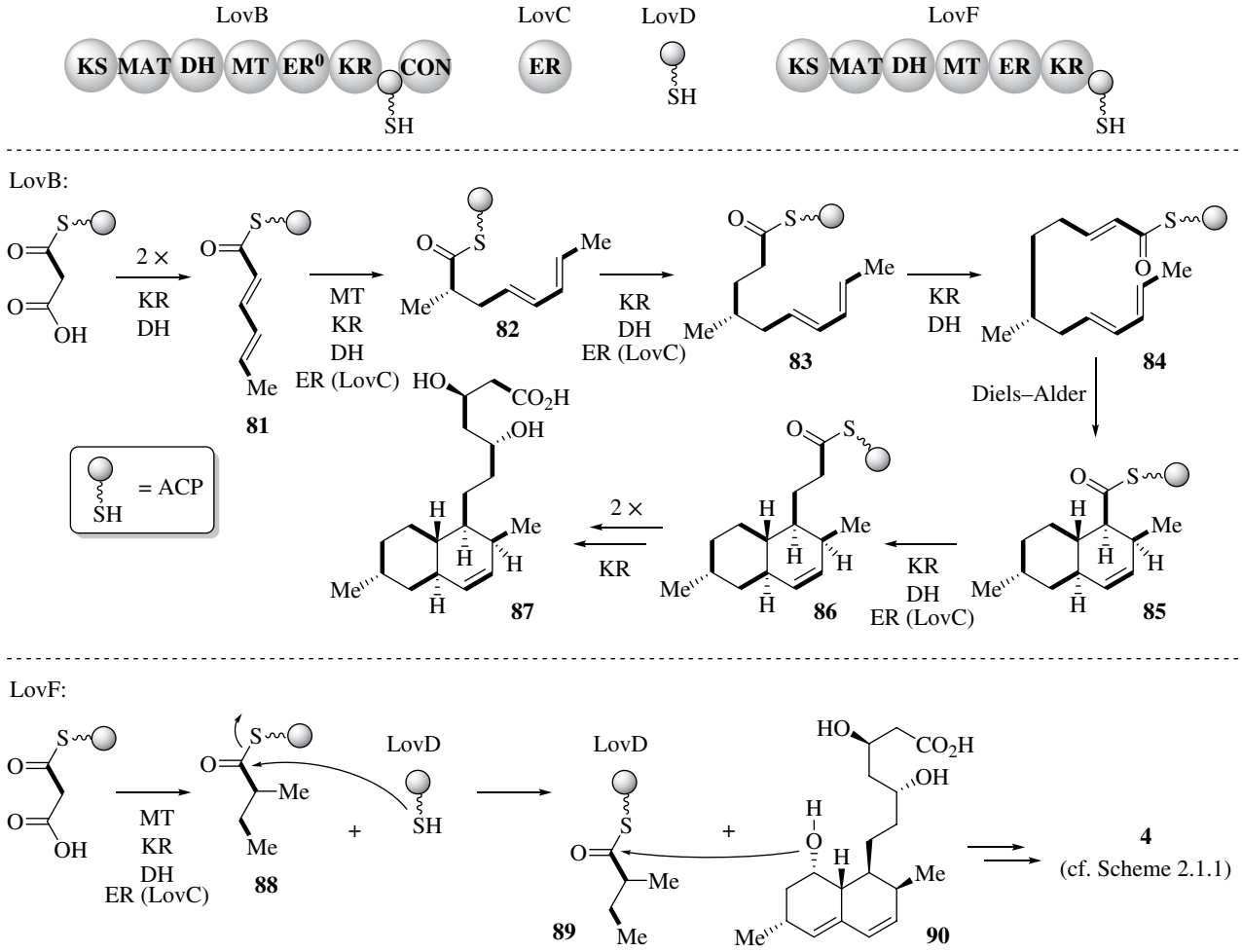
As exemplified by **79**, the products formed by fungal iPKSs strongly resemble bacterial type II PKS products. However, differences in folding of the linear polyketide backbone result in different cyclization regiochemistry. This almost exclusively leads to the incorporation of three intact $C_2$ units in the ring system first cyclized in bacteria, referred to as S-type folding (from ***S****treptomyces*), whereas only two $C_2$ units are found in the first ring in case of eukaryotes (F-type folding from **f**ungi) [130]. This phenomenon was illustrated by comparative isotope labeling studies elucidating the folding pattern of the ubiquitous octaketide chrysophanol (**80**) in higher plants, fungi, and insects when compared to that observed in the bacterial strains *Streptomyces* sp. AK 671 and *Nocardia* Acta 1057 [131] (Scheme 2.16). Indeed, in all eukaryotic producers of **80**, the expected F-type folding was observed [132]. *Nocardia* Acta 1057 and *Streptomyces* sp. AK 671 even provided two distinguishable S-type folding patterns, likely resulting from different first ring cyclization events, that is, C-10 to C-5 and C-12 to C-7, respectively [132, 133].

The natural products derived from fungal HR type I PKSs open an entirely different structural space. A prototypical example of such a system is the biosynthetic machinery encoding lovastatin (**4**). The HR PKS LovB (lovastatin nonaketide synthase (LNKS)) of this pathway contains functional KS, MAT, DH, KR, ACP, and C-MT domains in addition to a terminal CON domain resembling NRPS condensation domains and a nonfunctional ER ($ER^0$) [134, 135] (Scheme 2.17). Heterologous expression experiments in *Aspergillus nidulans* [136] and gene deletion and chemical complementation studies in *Aspergillus terreus* [137] revealed that the free-standing ER LovC is additionally required for the production of the first isolable intermediate of lovastatin biosynthesis, dihydromonacolin L (**87**). It is acting as *trans*-ER, a concept also found in other fungal HR type I PKSs [22]. The complex programming of the activity of the individual catalytic domains of LovB during each elongation reaction was beautifully illuminated by complete reconstitution of the LovB/C enzymatic machinery [138]: after priming, LovB catalyzes two rounds of chain extension with concomitant action of KR and DH to give enzyme-bound sorbic acid (**81**). Without NADPH in the enzymatic assays, reduction cannot take place and the non-reduced triketide precursor does not get further elaborated but rather gets cleaved off the PKS by nonenzymatic pyrone formation (not shown). Further extension and C-methylation at the newly introduced α-C-atom are followed by KR, DH, and ER (LovC) activity to give **82**. If the enzymatic system lacks SAM, therefore preventing C-methylation, also no ER activity is observed, neither at this nor at any later stage of polyketide assembly. This consequently leads to polyunsaturated pyrone or ketone shunt products (not shown) [135, 138]. The activity of the MT thus controls downstream ER processing and is therefore decisive for the selective formation of **87**. Further elongation with complete reduction to **83**, followed by extension and partial reduction to **84**, sets the stage for a Diels–Alder reaction to furnish decalin **85**. The Diels–Alder reaction is controlled by LovB [139], potentially involving the biochemically yet uncharacterized CON domain [22]. Further extension of **85** with full reduction gives **86**, which gets elaborated into **87** by two additional elongation steps with reductive processing by the KR only. This example clearly demonstrates the high degree of complexity in programming the activity of the individual catalytic domains of LovB during a particular elongation step and the utility of LovC acting as *trans*-ER. The recent crystal structure of LovC provides first explanations into the molecular interactions of LovB and LovC during polyketide assembly [140].

In addition to the decalin core structure **87**, lovastatin (**4**) bears a short, branched side chain. This building block is assembled by LovF, a second HR type I PKS [135]. The




**SCHEME 2.16** Different folding patterns in the biosynthesis of chrysophanol (**80**) in eukaryotes and prokaryotes.

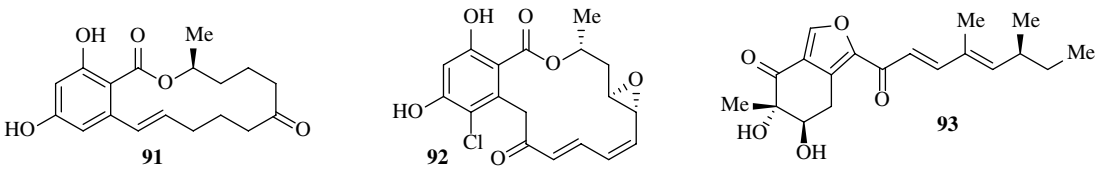



**SCHEME 2.17** HR fungal type I PKS machinery encoding lovastatin (**4**).

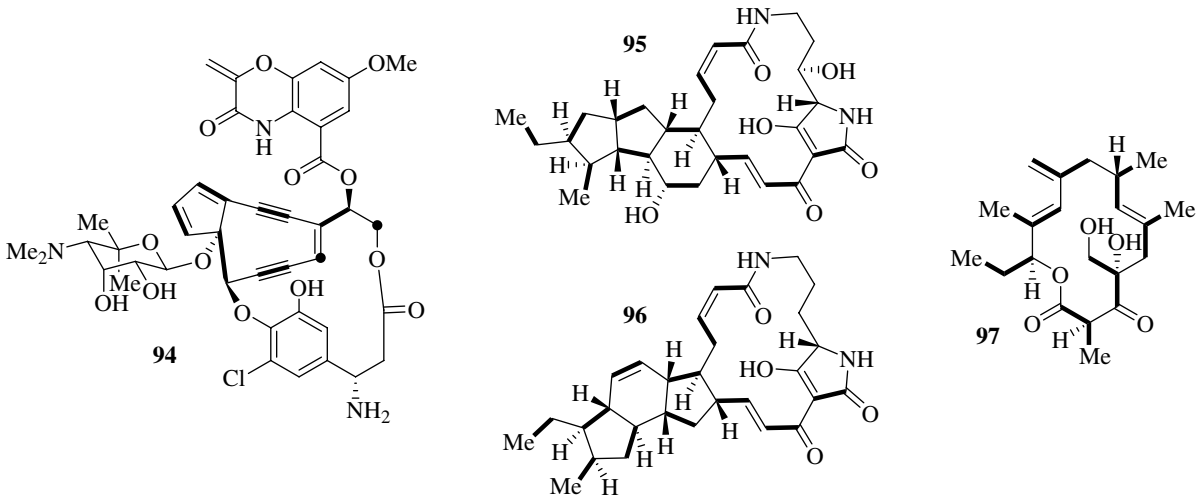
domain architecture of LovF is almost identical to that of LovB (Scheme 2.17). However, it is devoid of a terminal CON domain and contains an active ER. After priming, LovF catalyzes a single elongation cycle with all processing domains active, thus leading to the C-methylated intermediate **88**. The free-standing ACP LovD intercepts this precursor to give **89** [141]. Nucleophilic attack of the hydroxyl group located at the decalin core of **90**, which in turn is derived from **87** by oxidative tailoring to the thioester functionality in **89** followed by intramolecular lactone formation, concludes lovastatin (**4**) biosynthesis.

The interplay of two PKSs is a common theme in fungal polyketide biosynthesis [22]. This strategy allows to expand the structural space covered by such PKSs without further complicating the programmed teamwork of domains within a single iterative PKS. Lovastatin (**4**) biosynthesis thereby represents an example of convergent PKS interactions, where two independently acting PKSs assemble their products that finally get fused by action of an additional enzyme, in this case the ACP LovD. However, there are also many examples of sequential interplay of PKSs, where one synthase provides a precursor that gets further elaborated by a second PKS. In the biosynthesis of norsolinic acid (**79**; cf. Scheme 2.15), for example, the hexanoate starter unit is assembled by the FAS HexAB, transferred to NSAS, and further processed to ultimately yield **79** [122]. The transfer of the building block in such cases is thought to be catalyzed by direct interactions of the ACP of the first PKS with the SAT of the second [142]. Such dual PKS systems also facilitate the biosynthesis of molecules bearing structural features of both, NR and HR PKS products. Typical examples are the resorcylic acid lactones (RALs), such as zearalenone (**91**) [143, 144] or radicicol (**92**) [145] (Scheme 2.18). In some cases, the NR PKS-derived aromatic residue furthermore gets heavily modified by post-PKS processing, as, for example, in asperfuranone (**93**) biosynthesis [146].

Iterative type I PKSs were thought to almost exclusively occur in fungi or, in the rare bacterial cases, to provide rather simple building blocks, for example, for typical modular type I bacterial PKSs [13]. However, more and more evidence



**SCHEME 2.18** Fungal natural products originating from dual HR/NR type I PKS systems.

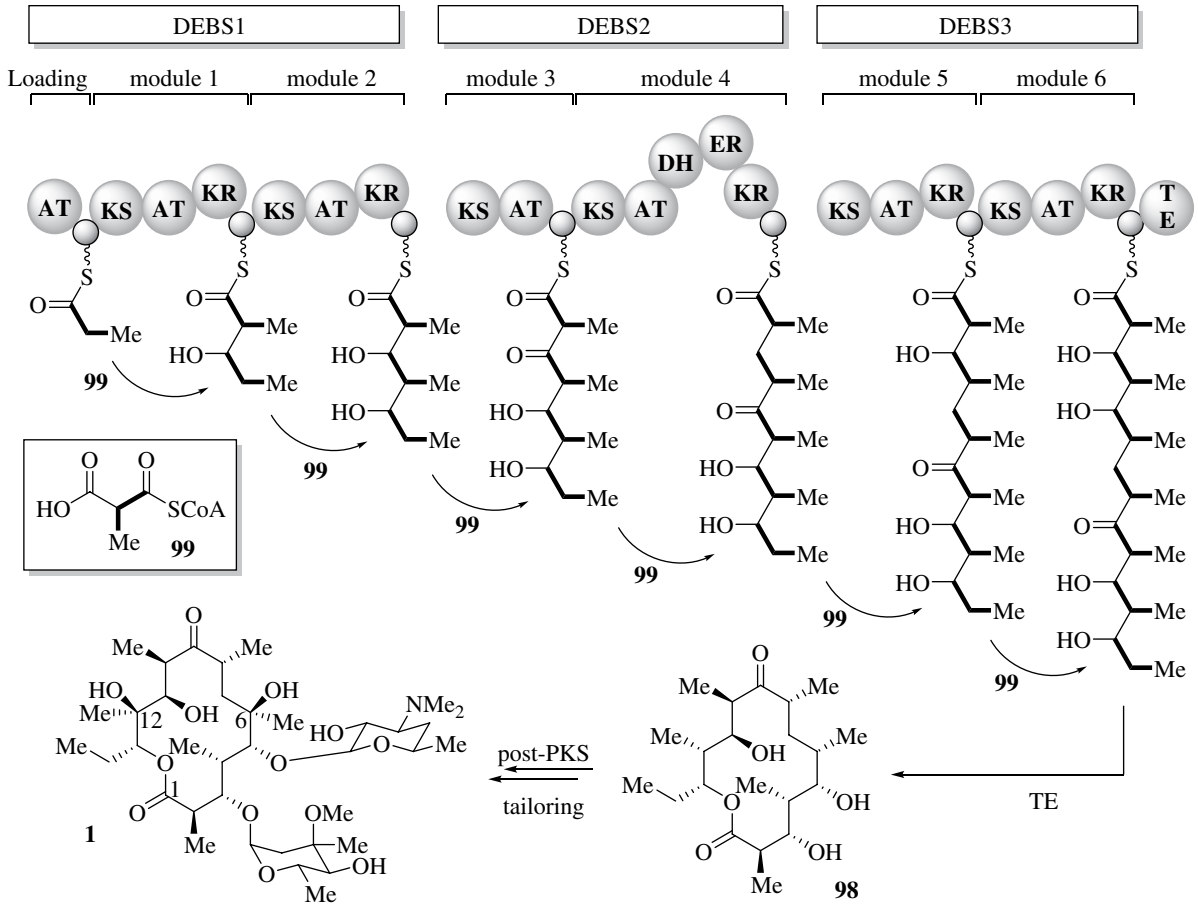


**SCHEME 2.19** Selection of natural products derived from uncommon bacterial type I iterative PKSs.

underlining the importance of iterative type I PKSs in bacterial secondary metabolism is uncovered. For example, the polyketide core structure of enediynes, such as C-1027 (**94**) (Scheme 2.19) [32] or calicheamicin (not shown) [33], is assembled by such synthases. In addition, a single iterative PKS module is also involved in the biosynthesis of polycyclic tetramate macrolactams, such as HSAF (**95**) [147] or ikarugamycin (**96**) [34, 35]. Very recently, even the complex programming of different oxygenation states in the iterative PKS machinery encoding the 14-membered galbonolide macrolides, for example, galbonolide B (**97**) in *Streptomyces* spp., has been discovered [148, 149]. These emerging examples clearly indicate that further unexpected pathways involving iterative type I PKSs await being discovered, not only in fungi but also in bacteria and likely in other organisms.

The vast majority of bacterial type I PKSs, however, is encoded on large, multimodular megaenzymes that closely resemble assembly line processes [17]. In these systems, each elongation step is catalyzed by an individual module that is also equipped with the catalytic domains necessary for the desired reductive processing of the β-carbonyl of the elongated intermediate to either the alcohol (KR), the alkyne (KR, DH), or the alkene (KR, DH, ER). The nascent polyketide precursor thereby moves across the PKS during assembly, ultimately reaching the terminal ACP domain. Typically, a TE domain catalyzes final cleavage of the PKS-bound intermediate by either hydrolysis or macrocyclization [150].

The prototypical example of such modular type I PKSs is DEBS that assembles 6-deoxyerythronolide B (**98**), the PKS precursor of erythromycin (**1**) [151–153]. The landmark discovery of this giant enzymatic machinery (total size of the PKS > 1 MDa), independently by Katz et al. [154] and Leadlay et al. [155], also largely contributed to a dramatic shift of biosynthetic research, from elaborate feeding experiments to modern biomolecular approaches. DEBS is composed of 28 domains distributed over 7 modules on three large PKS proteins DEBS 1–3 (Scheme 2.20). Each of the six elongation modules catalyzes the incorporation of propionate by decarboxylative Claisen-type condensation utilizing methylmalonate (**99**) as building block. Modules 1, 2, 5, and 6 all only contain KR, leading to secondary alcohols at the β-positions in the intermediates bound to the respective ACP domains. Module 3 is devoid of any reductive domain, thus retaining the β-carbonyl. The presence of KR, DH, and ER in module 4 leads to full reduction of the respective β-carbon of the intermediate attached to the ACP of this module. Upon full assembly of the polyketide chain, product release is achieved by TE-catalyzed macrolactone formation to yield **98**. The observed absolute configuration in **98** is installed by perfect stereocontrol during the KR-mediated reduction events [153]. Further post-PKS tailoring reactions, that is, stereoselective C-6 and C-12 hydroxylation and two glycosylations, conclude the biosynthesis of erythromycin (**1**) [151, 152].

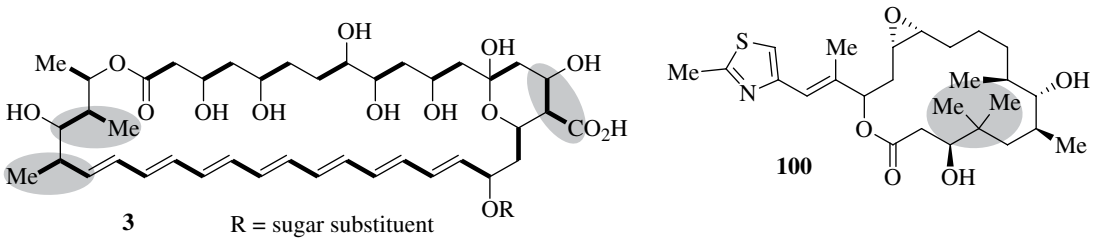



**SCHEME 2.20** DEBS, a prototypical example of a bacterial type I modular PKS.

While the modular structure of such type I PKSs causes high metabolic costs because of the resulting huge enzymatic machineries that need to be assembled, it also facilitates biosynthesis of highly complex natural product scaffolds. The structural space accessible by these PKSs is further enlarged by their ability to incorporate different α-substituted building blocks by employing the respective 2-substituted malonate precursors, thus leading to alkyl-branched products. This flexibility is a result of the individual AT domains in each module that can selectively activate different extender units. An example for the selective incorporation of methyl branches can be found in amphotericin biosynthesis, where 16 malonates and 3 methylmalonates (gray label) are incorporated into the final structure, for example, **3** [156] (Scheme 2.21). Furthermore, optional MT domains are capable of introducing methyl or even dimethyl branches, for example, in the biosynthesis of epothilones (**100**, gray label) [157].

The biosynthesis of many complex bacterial PKS products largely follows the aforementioned assembly line logic [17], although exceptions exist [158]. The observed collinearity makes these systems ideal targets for the controlled generation of novel "unnatural" natural products by modifications of the overall PKS modular architecture [159] or individual catalytic functions. In the case of DEBS, this has led to, that is, the generation of a large set of derivatives of **98** by altering functions of individual catalytic domains within the megasynthase [160]; the reconstitution of mono-, bi-, or trimodular PKS substructures [161–164]; and the remarkable complete reconstitution of the entire DEBS machinery with protein extracts [165] or even purified proteins [166]. Such experiments have strongly contributed to our current understanding of PKS assembly lines. In addition, extensive structural studies on these PKSs are beginning to provide deep mechanistic insights into their functions [153, 167–170], recently culminating in high-resolution structures of a complete pikromycin PKS module [171, 172].

The aforementioned textbook knowledge on type I bacterial PKSs is mainly based on investigations targeting systems from actinomycete bacteria. These organisms have long been studied because of their proven track record to biosynthesize numerous bioactive small molecules. In recent years, however, natural product researchers have started to interrogate unusual bacterial taxa, for example, bacteria from remote habitats, symbiotic bacteria, or pathogens.

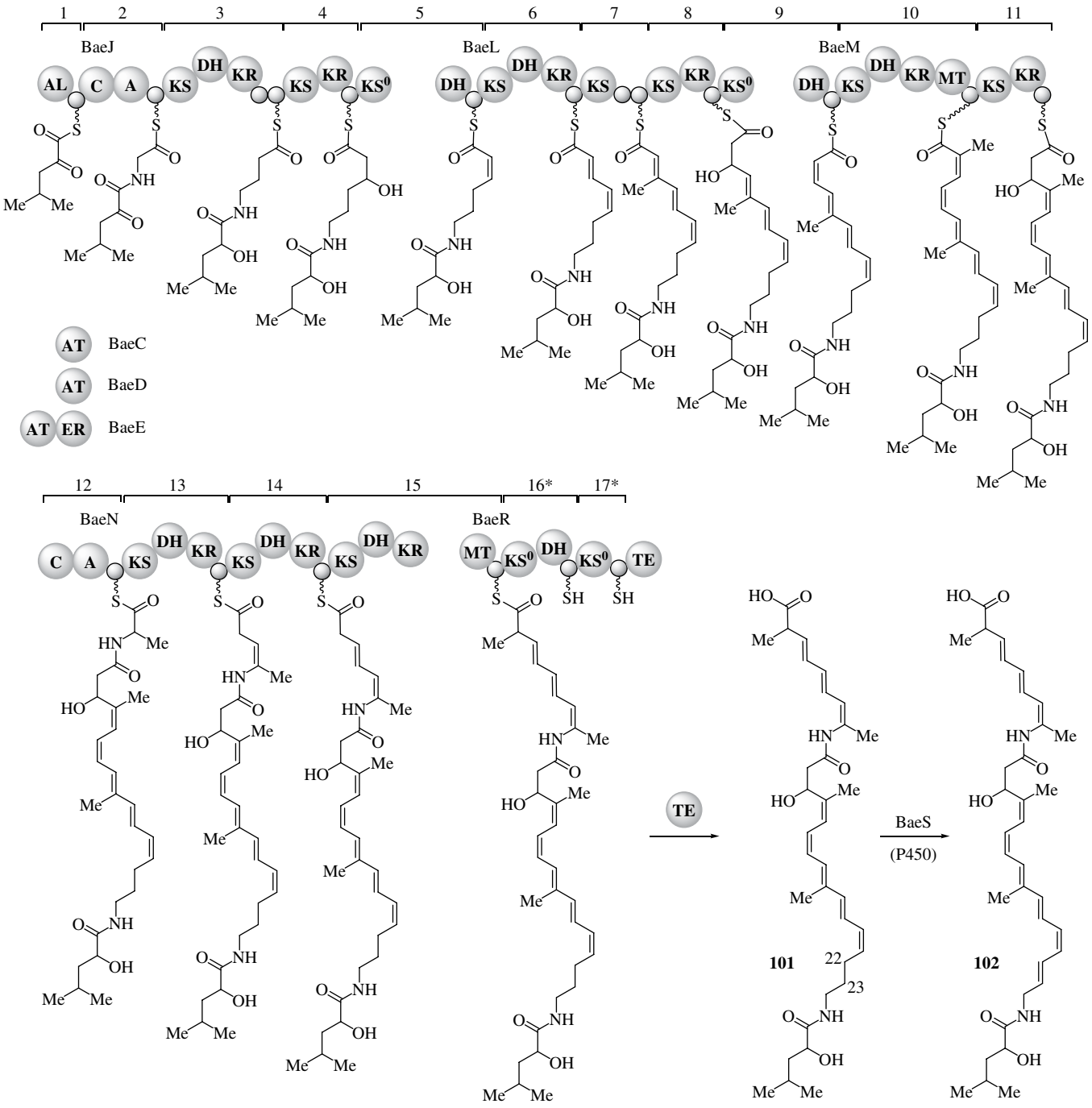



**SCHEME 2.21** Incorporation of alkyl branches into amphotericin B (**3**) and epothilone A (**100**).

This has led to the discovery of a new class of multimodular type I PKSs [173, 174]. In these PKSs, all individual modules lack the AT domains. The PKS building blocks are instead provided by a free-standing AT acting in *trans*. These systems were consequently named *trans*-AT PKSs (or "AT-less" PKSs), as opposed to the classical *cis*-AT PKSs described in the preceding text [36]. Interestingly, phylogenetic analyses of multimodular PKSs showed that *cis*- and *trans*-PKSs have evolved independently from FAS [175] following two different modes of evolution. While *cis*-PKSs predominantly evolve by duplication of individual modules with subsequent alterations in domain composition [176], *trans*-AT PKSs derive from multiple genetic parts by extensive horizontal gene transfer [177].

Importantly, *trans*-AT PKSs do not adhere to the collinearity principle of their *cis*-AT counterparts [36]. For example, individual modules might be used more than once or might be completely omitted. Furthermore, while *cis*-PKSs only comprise eight different module architectures, depending on the presence/absence of the optional domains (none, KR, KR/DH, KR/DH/ER, each with or without MT), more than 50 variations can be found in *trans*-AT PKSs. This diversity in module structures gives rise to a large number of catalytic features, including ß-branching cassettes, dehydrating bimodules leading to *cis*-configured double bonds, etc. [178]. A detailed discussion of all features of this remarkable class of PKSs would thus clearly exceed the scope of this article. We instead selected a single, representative example to briefly introduce some intriguing features of *trans*-AT PKS systems, the biosynthetic machinery encoding bacillaene (**102**). It was initially discovered as *pksX* in *Bacillus subtilis* 168 as the first *trans*-AT PKS to be identified [179, 180]. An almost identical cluster (*bae*, Scheme 2.22) was later found in *Bacillus amyloliquefaciens* and firmly linked to the production of **101** and **102** by gene deletion experiments [181]. Within *bae* (*pksX*), the *trans*-AT BaeC (PksC) loads all ACPs with malonyl-CoA [182]. The acyl-CoA ligase (AL) in module 1 attaches the α-ketoisocaproate starter unit to the first ACP [183]. This building block gets elongated by a nonribosomal peptide synthetase (NRPS) module (module 2) using glycine. Due to the modularity of both, bacterial PKS type I and NRPS biosynthetic enzymes, hybrid PKS/NRPS products encoded by a combination of PKS and NRPS modules are a common theme [17], in particular in *trans*-AT PKSs [36]. Two noncanonical reactions are catalyzed within module 3: the DH not only reduces the glycine-derived β-carbonyl after elongation, as expected, but remarkably also the remote ketone function of the starter unit [183]. In addition, full reduction to the alkane is observed, although no ER is located in module 3. This catalytic activity is instead provided in *trans* by BaeE [184]. The next step is likewise unusual. The dehydrating bimodule 4/5 catalyzes the formation of a *cis*-configured double bond [185]. The same catalytic activity is conferred by bimodule 8/9 further downstream. The next unusual modification is catalyzed by module 7, a so-called β-branching module, which introduces a methyl branch *via* a mechanism resembling exomethylene bond formation in mevalonate-dependent isoprenoid biosynthesis [182]. Another intriguing feature of this PKS is the introduction of an enamine structural portion in module 13 by double-bond generation in β,γ-position [186]. The last two modules, 16* and 17*, seem to be superfluous for the production of **101** and **102**. Remarkably, virtually all intermediates of the complex biosynthetic pathway have been structurally characterized. This was facilitated by the deletion of the terminal TE domain, which unexpectedly led to the hydrolytic cleavage of pathway intermediates from all modules [185]. These results were not only instrumental for understanding bacillaene biosynthesis in detail but also led to the discovery of a proofreading enzyme that cleaves stalled intermediates from *trans*-AT PKSs. This activity is provided by enzymes previously annotated as AT, in this case BaeD, that rather possesses TE-like activity [187]. After final cleavage of **101** off the synthase by the terminal TE, the biosynthesis of bacillaene (**102**) is concluded by oxidation at C-22/C-23 catalyzed by the cytochrome P450 BaeS [185].

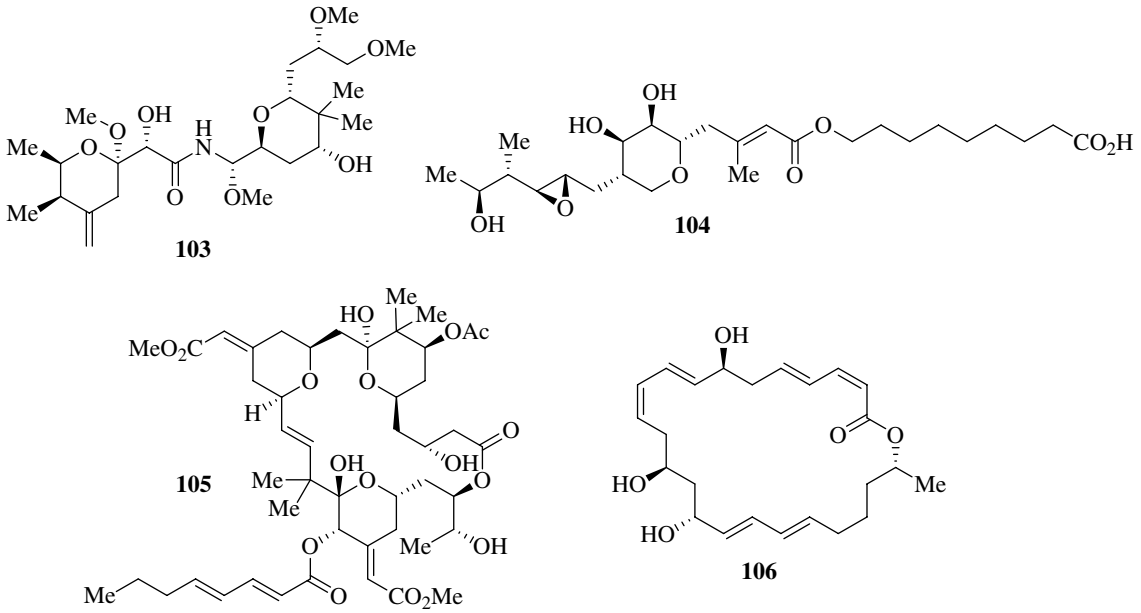
The aforementioned example nicely showcases the catalytic versatility of *trans*-At PKSs. It is thus not surprising that many structurally complex, biologically highly active secondary metabolites have meanwhile been attributed to *trans*-AT PKSs. Examples include pederin (**103**) [173], mupirocin (**104**) [188], bryostatins (**105**) [189, 190], and macrolactins (**106**) [181, 191] (Scheme 2.23).




**SCHEME 2.22** The bacterial type I modular *trans*-AT PKS encoding bacillaene (**101**).

### 2.1.4 Conclusion

Within this chapter, we strived to introduce the mechanistic principles of polyketide core structure assembly. Despite the structural diversity of polyketide natural products, there are only few different catalytic domains facilitating a small number of basic reactions—common to all types of PKSs—that are crucial for product biosynthesis. By smart recombination of these catalytic units, nature has succeeded in generating a combinatorial library of bioactive small molecules with a structural and biological diversity that is virtually inexhaustible. The structural and functional space covered by these molecules is further expanded by post-PKS functionalization reactions catalyzed by so-called tailoring enzymes. This includes reorganization of the entire PKS




**SCHEME 2.23** Representative examples of natural products derived from *trans*-AT PKSs: pederin (**103**), mupirocin (**104**), bryostatins (e.g., **105**), and macrolactins (e.g., **106**).

core (cf. Scheme 2.23) [13] but also subtle changes by group transfer reactions (e.g., glycosylation, alkylation) [192, 193] or oxidative transformations (e.g., hydroxylation, halogenation, phenol-oxidative cross coupling) [194–198]. The final steps in the biosynthesis of PKS-derived polyethers are in impressive example of oxidative tailoring discussed in Section 4.2. Investigations into the chemistry and biochemistry of these fascinating natural products will undoubtedly continue to reveal fascinating new chemical structures, biological activities, and biocatalytic potential for decades of natural product research.

## REFERENCES


1. S. Pal, *Tetrahedron* 2006, **62**, 3171–3200.
2. I. Chopra, M. Roberts, *Microbiol. Mol. Biol. Rev.* 2001, **65**, 232–260.
3. A. C. Mesa-Arango, L. Scorzoni, O. Zaragoza, *Front. Microbiol.* 2012, **3**, 1–10.
4. J. A. Tobert, *Nat. Rev. Drug Discov.* 2003, **2**, 517–526.
5. G. Aubel-Sadron, D. Londos-Gagliardi, *Biochimie* 1984, **66**, 333–352.
6. W. C. Campbell, *Curr. Pharm. Biotechnol.* 2012, **13**, 853–865.
7. For WHO Model List of Essential Medicines, see here: http://www.who.int/medicines/publications/essentialmedicines/en/ (accessed on October 22, 2015).
8. M. Abrar, F. M. Anjum, M. S. Butt, I. Pasha, M. A. Randhawa, F. Saeed, K. Waqas, *Crit. Rev. Food. Sci. Nutr.* 2013, **53**, 862–874.
9. T. W. Kensler, B. D. Roebuck, G. N. Wogans, J. D. Groopman, *Toxicol. Sci.* 2011, **120**, S28–S48.
10. M. Murata, T. Yasumoto, *Nat. Prod. Rep.* 2000, **17**, 293–314.
11. D. A. Hopwood, *Chem. Rev.* 1997, **97**, 2465–2498.
12. J. Staunton, K. J. Weissman, *Nat. Prod. Rep.* 2001, **18**, 380–416.
13. C. Hertweck, *Angew. Chem. Int. Ed. Engl.* 2009, **48**, 4688–4716.
14. S. Smith, S. C. Tsai, *Nat. Prod. Rep.* 2007, **24**, 1041–1072.
15. C. D. Reeves, *Crit. Rev. Biotechnol.* 2003, **23**, 95–147.
16. B. J. Rawlings, *Nat. Prod. Rep.* 1998, **15**, 275–308.
17. M. A. Fischbach, C. T. Walsh, *Chem. Rev.* 2006, **106**, 3468–3496.
18. B. J. Rawlings, *Nat. Prod. Rep.* 2001, **18**, 231–281.
19. B. J. Rawlings, *Nat. Prod. Rep.* 2001, **18**, 190–227.
20. R. J. Cox, *Org. Biomol. Chem.* 2007, **5**, 2010–2026.
21. R. J. Cox, T. J. Simpson, *Meth. Enzymol.* 2009, **459**, 49–78.
22. Y.-H. Chooi, Y. Tang, *J. Org. Chem.* 2012, **77**, 9933–9953.
23. C. Hertweck, A. Luzhetskyy, Y. Rebets, A. Bechthold, *Nat. Prod. Rep.* 2007, **24**, 162–190.
24. A. Das, C. Khosla, *Acc. Chem. Res.* 2009, **42**, 631–639.
25. B. J. Rawlings, *Nat. Prod. Rep.* 1999, **16**, 425–484.
26. B. Shen, *Top. Curr. Chem.* 2000, **209**, 1–51.
27. M. B. Austin, J. P. Noel, *Nat. Prod. Rep.* 2003, **20**, 79–110.
28. K. Watanabe, A. P. Praseuth, C. C. Wang, *Curr. Opin. Chem. Biol.* 2007, **11**, 279–286.
29. J.-L. Ferrer, M. B. Austin Jr. C. Stewart, J. P. Noel, *Plant Physiol. Biochem.* 2008, **46**, 356–370.
30. I. Abe, H. Morita, *Nat. Prod. Rep.* 2010, **27**, 809–838.
31. D. Yu, F. Xu, J. Zeng, J. Zhan, *IUBMB Life* 2012, **64**, 285–295.

32. W. Liu, S. D. Christenson, S. Standage, B. Shen, *Science* 2002, **297**, 1170–1173.
33. J. Ahlert, E. Shepard, N. Lomovskaya, E. Zazopoulos, A. Staffa, B. O. Bachmann, K. Huang, L. Fonstein, A. Czisny, R. E. Whitwam, C. M. Farnet, J. S. Thorson, *Science* 2002, **297**, 1173–1176.
34. J. Antosch, F. Schaefers, T. A. Gulder, *Angew. Chem. Int. Ed. Engl.* 2014, **53**, 3011–3014.
35. G. Zhang, W. Zhang, Q. Zhang, T. Shi, L. Ma, Y. Zhu, S. Li, H. Zhang, Y. L. Zhao, R. Shi, C. Zhang, *Angew. Chem. Int. Ed. Engl.* 2014, **53**, 4840–4844.
36. J. Piel, *Nat. Prod. Rep.* 2010, **27**, 996–1047.
37. R. Müller, *Chem. Biol.* 2004, **11**, 4–6.
38. B. Shen, *Curr. Opin. Chem. Biol.* 2003, **7**, 285–295.
39. M. Kaneko, E. I. Hwang, Y. Ohnishi, S. Horinouchi, *J. Ind. Microbiol. Biotechnol.* 2003, **30**, 456–461.
40. D. A. Scott, P. M. Hammond, G. M. Brearley, C. P. Price, *J. Chromatogr.* 1992, **573**, 309–312.
41. J. Rösler, F. Krekel, N. Amrhein, J. Schmid, *Plant. Physiol.* 1997, **113**, 175–179.
42. J. A. Kyndt, T. E. Meyer, M. A. Cusanovich, J. J. Van Beeumen, *FEBS Lett.* 2002, **512**, 240–244.
43. I. Abe, Y. Takahashi, H. Morita, H. Noguchi, *Eur. J. Biochem.* 2001, **268**, 3354–3359.
44. Y. Katsuyama, T. Kita, N. Funa, S. Horinouchi, *J. Biol. Chem.* 2009, **284**, 11160–11170.
45. Y. Katsuyama, T. Kita, S. Horinouchi, *FEBS Lett.* 2009, **583**, 2799–2803.
46. Y. Katsuyama, M. Matsuzawa, N. Funa, S. Horinouchi, *J. Biol. Chem.* 2007, **282**, 37702–37709.
47. S. Eckermann, G. Schröder, J. Schmidt, D. Strack, R. A. Edrada, Y. Helariutta, P. Elomaa, M. Kotilainen, I. Kilpeläinen, P. Proksch, T. H. Teeri, J. Schröder, *Nature* 1998, **396**, 387–390.
48. T. Akiyama, M. Shibuya, H. M. Liu, Y. Ebizuka, *Eur. J. Biochem.* 1999, **263**, 834–839.
49. J. Schröder, G. Schröder, *Z. Naturforsch. [C]* 1990, **45**, 1–8.
50. M. B. Austin, M. E. Bowman, J. L. Ferrer, J. Schroder, J. P. Noel, *Chem. Biol.* 2004, **11**, 1179–1194.
51. J. L. Ferrer, J. M. Jez, M. E. Bowman, R. A. Dixon, J. P. Noel, *Nat. Struct. Biol.* 1999, **6**, 775–784.
52. F. Taura, S. Tanaka, C. Taguchi, T. Fukamizu, H. Tanaka, Y. Shoyama, S. Morimoto, *FEBS Lett.* 2009, **583**, 2061–2066.
53. L. Beerhues, *FEBS Lett.* 1996, **383**, 264–266.
54. I. Abe, Y. Utsumi, S. Oguro, H. Morita, Y. Sano, H. Noguchi, *J. Am. Chem. Soc.* 2005, **127**, 1362–1363.
55. I. Abe, S. Oguro, Y. Utsumi, Y. Sano, H. Noguchi, *J. Am. Chem. Soc.* 2005, **127**, 12709–12716.
56. H. Fu, D. A. Hopwood, C. Khosla, *Chem. Biol.* 1994, **1**, 205–210.
57. N. Funa, Y. Ohnishi, I. Fujii, M. Shibuya, Y. Ebizuka, S. Horinouchi, *Nature* 1999, **400**, 897–899.
58. N. Funa, Y. Ohnishi, Y. Ebizuka, S. Horinouchi, *J. Biol. Chem.* 2002, **277**, 4628–4635.
59. J. Cortés, J. Velasco, G. Foster, A. P. Blackaby, B. A. Rudd, B. Wilkinson, *Mol. Microbiol.* 2002, **44**, 1213–1224.
60. S. Li, S. Grüschow, J. S. Dordick, D. H. Sherman, *J. Biol. Chem.* 2007, **282**, 12765–12772.
61. J. Zeng, R. Decker, J. Zhan, *Appl. Biochem. Biotechnol.* 2012, **166**, 1020–1033.
62. F. Gross, N. Luniak, O. Perlova, N. Gaitatzis, H. Jenke-Kodama, K. Gerth, D. Gottschalk, E. Dittmann, R. Müller, *Arch. Microbiol.* 2006, **185**, 28–38.
63. W. Zha, S. B. Rubin-Pitel, H. Zhao, *J. Biol. Chem.* 2006, **281**, 32036–32047.
64. C. C. Tseng, S. M. McLoughlin, N. L. Kelleher, C. T. Walsh, *Biochemistry* 2004, **43**, 970–980.
65. H. Chen, C. C. Tseng, B. K. Hubbard, C. T. Walsh, *Proc. Natl. Acad. Sci. U S A* 2001, **98**, 14901–14906.
66. A. Miyanaga, N. Funa, T. Awakawa, S. Horinouchi, *Proc. Natl. Acad. Sci. U S A* 2008, **105**, 871–876.
67. M. Funabashi, N. Funa, S. Horinouchi, *J. Biol. Chem.* 2008, **283**, 13983–13991.
68. T. Hayashi, Y. Kitamura, N. Funa, Y. Ohnishi, S. Horinouchi, *Chembiochem* 2011, **12**, 2166–2176.
69. N. Funa, H. Ozawa, A. Hirata, S. Horinouchi, *Proc. Natl. Acad. Sci. U S A* 2006, **103**, 6356–6361.
70. C. Nakano, H. Ozawa, G. Akanuma, N. Funa, S. Horinouchi, *J. Bacteriol.* 2009, **191**, 4916–4923.
71. P. Saxena, G. Yadav, D. Mohanty, R. S. Gokhale, *J. Biol. Chem.* 2003, **278**, 44780–44790.
72. J. A. Chemler, T. J. Buchholz, T. W. Geders, D. L. Akey, C. M. Rath, G. E. Chlipala, J. L. Smith, D. H. Sherman, *J. Am. Chem. Soc.* 2012, **134**, 7359–7366.
73. L. Song, F. Barona-Gomez, C. Corre, L. Xiang, D. W. Udwary, M. B. Austin, J. P. Noel, B. S. Moore, G. L. Challis, *J. Am. Chem. Soc.* 2006, **128**, 14754–14755.
74. D. Yu, J. Zeng, D. Chen, J. Zhan, *Enzyme Microb. Technol.* 2010, **46**, 575–580.
75. N. Funa, T. Awakawa, S. Horinouchi, *J. Biol. Chem.* 2007, **282**, 14476–14481.
76. S. B. Rubin-Pitel, H. Zhang, T. Vu, J. S. Brunzelle, H. Zhao, S. K. Nair, *Chem. Biol.* 2008, **15**, 1079–1090.
77. J. Li, Y. Luo, J. K. Lee, H. Zhao, *Bioorg. Med. Chem. Lett.* 2011, **21**, 6085–6089.
78. Y. Seshime, P. R. Juvvadi, K. Kitamoto, Y. Ebizuka, I. Fujii, *Bioorg. Med. Chem.* 2010, **18**, 4542–4546.
79. M. Hashimoto, T. Koen, H. Takahashi, C. Suda, K. Kitamoto, I. Fujii, *J. Biol. Chem.* 2014, **289**, 19976–19984.
80. T. Mori, D. Yang, T. Matsui, M. Hashimoto, H. Morita, I. Fujii, I. Abe, *J. Biol. Chem.* 2015, **290**, 5214–5225.
81. W. P. Revill, M. J. Bibb, D. A. Hopwood, *J. Bacteriol.* 1995, **177**, 3946–3952.
82. T. S. Hitchman, J. Crosby, K. J. Byrom, R. J. Cox, T. J. Simpson, *Chem. Biol.* 1998, **5**, 35–47.

83. A. L. Matharu, R. J. Cox, J. Crosby, K. J. Byrom, T. J. Simpson, *Chem. Biol.* 1998, **5**, 699–711.
84. C. Bisang, P. F. Long, J. Cortés, J. Westcott, J. Crosby, A. L. Matharu, R. J. Cox, T. J. Simpson, J. Staunton, P. F. Leadlay, *Nature* 1999, **401**, 502–505.
85. R. McDaniel, S. Ebert-Khosla, D. A. Hopwood, C. Khosla, *Science* 1993, **262**, 1546–1550.
86. R. McDaniel, S. Ebert-Khosla, D. A. Hopwood, C. Khosla, *J. Am. Chem. Soc.* 1993, **115**, 11671.
87. Y. Tang, S.-C. Tsai, C. Khosla, *J. Am. Chem. Soc.* 2003, **125**, 12708–12709.
88. P. L. Bartel, C. B. Zhu, J. S. Lampel, D. C. Dosch, N. C. Connors, W. R. Strohl, J. M. Beale Jr., H. G. Floss, *J. Bacteriol*. 1990, **172**, 4816–4826.
89. W. Bao, E. Wendt-Pienkowski, C. R. Hutchinson, *Biochemistry* 1998, **37**, 8132–8138.
90. M. K. Kharel, P. Pahari, M. D. Shepherd, N. Tibrewal, S. E. Nybo, K. A. Shaaban, J. Rohr, *Nat. Prod. Rep.* 2012, **29**, 264–325.
91. B. C. Kim, J. M. Lee, J. S. Ahn, B. S. Kim, *J. Microbiol. Biotechnol.* 2007, **17**, 830–839.
92. E. Wendt-Pienkowski, Y. Huang, J. Zhang, B. Li, H. Jiang, H. Kwon, C. R. Hutchinson, B. Shen, *J. Am. Chem. Soc.* 2005, **127**, 16442–16452.
93. K. Jakobi, C. Hertweck, *J. Am. Chem. Soc.* 2004, **126**, 2298–2299.
94. H. Zhou, Y. Li, Y. Tang, *Nat. Prod. Rep.* 2010, **27**, 839–868.
95. D. H. Sherman, M. J. Bibb, T. J. Simpson, D. Johnson, F. Malpartida, M. Fernandez-Moreno, E. Martinez, C. R. Hutchinson, D. A. Hopwood, *Tetrahedron* 1991, **47**, 6029–6043.
96. Y. Shen, P. Yoon, T. W. Yu, H. G. Floss, D. Hopwood, B. S. Moore, *Proc. Natl. Acad. Sci. U S A* 1999, **96**, 3622–3627.
97. B. S. Moore, C. Hertweck, *Nat. Prod. Rep.* 2002, **19**, 70–99.
98. L. B. Pickens, Y. Tang, *Metab. Eng.* 2009, **11**, 69–75.
99. L. B. Pickens, Y. Tang, *J. Biol. Chem.* 2010, **285**, 27509–27515.
100. W. Zhang, B. D. Ames, S. C. Tsai, Y. Tang, *Appl. Environ. Microbiol.* 2006, **72**, 2573–2580.
101. P. Wang, X. Gao, Y. H. Chooi, Z. Deng, Y. Tang, *Microbiology* 2011, **157**, 2401–2409.
102. H. Petkovic, A. Thamchaipenet, L. H. Zhou, D. Hranueli, P. Raspor, P. G. Waterman, I. S. Hunter, *J. Biol. Chem.* 1999, **274**, 32829–32834.
103. W. Zhang, K. Watanabe, C. C. Wang, Y. Tang, *J. Biol. Chem.* 2007, **282**, 25717–25725.
104. W. Zhang, K. Watanabe, X. Cai, M. E. Jung, Y. Tang, J. Zhan, *J. Am. Chem. Soc*. 2008, **130**, 6068–6069.
105. N. Peric-Concha, B. Borovicka, P. F. Long, D. Hranueli, P. G. Waterman, I. S. Hunter, *J. Biol. Chem.* 2005, **280**, 37455–37460.
106. T. Nakano, K. Miyake, H. Endo, T. Dairi, T. Mizukami, R. Katsumata, *Biosci. Biotechnol. Biochem.* 2004, **68**, 1345–1352.
107. M. K. Kharel, L. Zhu, T. Liu, J. Rohr, *J. Am. Chem. Soc.* 2007, **129**, 3780–3781.
108. Z. Xu, K. Jakobi, K. Welzel, C. Hertweck, *Chem. Biol.* 2005, **12**, 579–588.
109. Z. Yunt, K. Reinhardt, A. Li, M. Engeser, H. M. Dahse, M. Gütschow, T. Bruhn, G. Bringmann, J. Piel, *J. Am. Chem. Soc.* 2009, **131**, 2297–2305.
110. J. Piel, C. Hertweck, P. R. Shipley, D. M. Hunt, M. S. Newman, B. S. Moore, *Chem. Biol.* 2000, **7**, 943–955.
111. M. Izumikawa, Q. Cheng, B. S. Moore, *J. Am. Chem. Soc.* 2006, **128**, 1428–1429.
112. J. A. Kalaitzis, Q. Cheng, D. Meluzzi, L. Xiang, M. Izumikawa, P. C. Dorrestein, B. S. Moore, *Bioorg. Med. Chem.* 2011, **19**, 6633–6638.
113. Q. Cheng, L. Xiang, M. Izumikawa, D. Meluzzi, B. S. Moore, *Nat. Chem. Biol.* 2007, **3**, 557–558.
114. C. Hertweck, L. Xiang, J. A. Kalaitzis, Q. Cheng, M. Palzer, B. S. Moore, *Chem. Biol.* 2004, **11**, 461–468.
115. L. Xiang, J. A. Kalaitzis, G. Nilsen, L. Chen, B. S. Moore, *Org. Lett.* 2002, **4**, 957–960.
116. L. Xiang, J. A. Kalaitzis, B. S. Moore, *Proc. Natl. Acad. Sci. U S A* 2004, **101**, 15609–15614.
117. R. Teufel, A. Miyanaga, Q. Michaudel, F. Stull, G. Louie, J. P. Noel, P. S. Baran, B. Palfey, B. S. Moore, *Nature* 2013, **503**, 552–556.
118. M. P. Brown, C. S. Brown-Jenco, G. A. Payne, *Fungal Genet. Biol.* 1999, **26**, 81–98.
119. D. S. J. McKeown, C. McNicholas, T. J. Simpson, N. J. Willett, *J. Chem. Soc. Chem. Commun.* 1996, 301–302.
120. P. K. Chang, J. W. Cary, J. Yu, D. Bhatnagar, T. E. Cleveland, *Mol. Gen. Genet.* 1995, **248**, 270–277.
121. T. S. Hitchman, E. W. Schmidt, F. Trail, M. D. Rarick, J. E. Linz, C. A. Townsend, *Bioorg. Chem.* 2001, **29**, 293–307.
122. C. M. Watanabe, C. A. Townsend, *Chem. Biol.* 2002, **9**, 981–988.
123. D. W. Udwary, M. Merski, C. A. Townsend, *J. Mol. Biol.* 2002, **323**, 585–598.
124. J. M. Crawford, B. C. Dancy, E. A. Hill, D. W. Udwary, C. A. Townsend, *Proc. Natl. Acad. Sci. U S A* 2006, **103**, 16728–16733.
125. A. M. Bailey, R. J. Cox, K. Harley, C. M. Lazarus, T. J. Simpson, E. Skellam, *Chem. Commun.* 2007, 4053–4055.
126. J. M. Crawford, P. M. Thomas, J. R. Scheerer, A. L. Vagstad, N. L. Kelleher, C. A. Townsend, *Science* 2008, **320**, 243–246.
127. J. M. Crawford, T. P. Korman, J. W. Labonte, A. L. Vagstad, E. A. Hill, O. Kamari-Bidkorpeh, S. C. Tsai, C. A. Townsend, *Nature* 2009, **461**, 1139–1143.
128. I. Fujii, A. Watanabe, U. Sankawa, Y. Ebizuka, *Chem. Biol.* 2001, **8**, 189–197.
129. T. P. Korman, J. M. Crawford, J. W. Labonte, A. G. Newman, J. Wong, C. A. Townsend, S. C. Tsai, *Proc. Natl. Acad. Sci. U S A* 2010, **107**, 6246–6251.
130. R. Thomas, *Chembiochem* 2001, **2**, 612–627.

131. G. Bringmann, A. Irmer, D. Feineis, T. A. Gulder, H. P. Fiedler, *Phytochemistry* 2009, **70**, 1776–1786.
132. G. Bringmann, T. F. Noll, T. A. Gulder, M. Grüne, M. Dreyer, C. Wilde, F. Pankewitz, M. Hilker, G. D. Payne, A. L. Jones, M. Goodfellow, H. P. Fiedler, *Nat. Chem. Biol.* 2006, **2**, 429–433.
133. G. Bringmann, T. A. Gulder, A. Hamm, M. Goodfellow, H. P. Fiedler, *Chem. Commun.* 2009, 6810–6812.
134. L. Hendrickson, C. R. Davis, C. Roach, D. K. Nguyen, T. Aldrich, P. C. McAda, C. D. Reeves, *Chem. Biol.* 1999, **6**, 429–439.
135. J. Kennedy, K. Auclair, S. G. Kendrew, C. Park, J. C. Vederas, C. R. Hutchinson, *Science* 1999, **284**, 1368–1372.
136. J. L. Sorensen, J. C. Vederas, *Chem. Commun.* 2003, 1492–1493.
137. J. L. Sorensen, K. Auclair, J. Kennedy, C. R. Hutchinson, J. C. Vederas, *Org. Biomol. Chem.* 2003, **1**, 50–59.
138. S. M. Ma, J. W. Li, J. W. Choi, H. Zhou, K. K. Lee, V. A. Moorthie, X. Xie, J. T. Kealey, N. A. Da Silva, J. C. Vederas, Y. Tang, *Science* 2009, **326**, 589–592.
139. K. Auclair, A. Sutherland, J. Kennedy, D. J. Witter, J. P. Van den Heever, C. R. Hutchinson, J. C. Vederas, *J. Am. Chem. Soc.* 2000, **122**, 11519–11520.
140. B. D. Ames, C. Nguyen, J. Bruegger, P. Smith, W. Xu, S. Ma, E. Wong, S. Wong, X. Xie, J. W. Li, J. C. Vederas, Y. Tang, S. C. Tsai, *Proc. Natl. Acad. Sci. U S A* 2012, **109**, 11144–11149.
141. X. Xie, M. J. Meehan, W. Xu, P. C. Dorrestein, Y. Tang, *J. Am. Chem. Soc.* 2009, **131**, 8388–8389.
142. J. Foulke-Abel, C. A. Townsend, *Chembiochem* 2012, **13**, 1880–1884.
143. Y. T. Kim, Y. R. Lee, J. Jin, K. H. Han, H. Kim, J. C. Kim, T. Lee, S. H. Yun, Y. W. Lee, *Mol. Microbiol.* 2005, **58**, 1102–1113.
144. I. Gaffoor, F. Trail, *Appl. Environ. Microbiol.* 2006, **72**, 1793–1799.
145. H. Zhou, K. Qiao, Z. Gao, J. C. Vederas, Y. Tang, *J. Biol. Chem.* 2010, **285**, 41412–41421.
146. Y. M. Chiang, E. Szewczyk, A. D. Davidson, N. Keller, B. R. Oakley, C. C. Wang, *J. Am. Chem. Soc.* 2009, **131**, 2965–2970.
147. Y. Li, H. Chen, Y. Ding, Y. Xie, H. Wang, R. L. Cerny, Y. Shen, L. Du, *Angew. Chem. Int. Ed. Engl.* 2014, **53**, 7524–7530.
148. H. J. Kim, S. Karki, S. Y. Kwon, S. H. Park, B. H. Nahm, Y. K. Kim, H. J. Kwon, *J. Biol. Chem.* 2014, **289**, 34557–34568.
149. C. Liu, J. Zhu, Y. Li, J. Zhang, C. Lu, H. Wang, Y. Shen, *Chembiochem* 2015, **16**, 998–1007.
150. M. E. Horsman, T. P. Hari, C. N. Boddy, *Nat. Prod. Rep.* 2015, **32**, DOI: 10.1039/C1034NP00148F.
151. J. Staunton, B. Wilkinson, *Chem. Rev.* 1997, **97**, 2611–2629.
152. D. E. Cane, *J. Biol. Chem.* 2010, **285**, 27517–27523.
153. C. Khosla, D. Herschlag, D. E. Cane, C. T. Walsh, *Biochemistry* 2014, **53**, 2875–2883.
154. S. Donadio, M. J. Staver, J. B. McAlpine, S. J. Swanson, L. Katz, *Science* 1991, **252**, 675–679.
155. J. Cortes, S. F. Haydock, G. A. Roberts, D. J. Bevitt, P. F. Leadlay, *Nature* 1990, **348**, 176–178.
156. P. Caffrey, S. Lynch, E. Flood, S. Finnan, M. Oliynyk, *Chem. Biol.* 2001, **8**, 713–723.
157. I. Molnar, T. Schupp, M. Ono, R. Zirkle, M. Milnamow, B. Nowak-Thompson, N. Engel, C. Toupet, A. Stratmann, D. D. Cyr, J. Gorlach, J. M. Mayo, A. Hu, S. Goff, J. Schmid, J. M. Ligon, *Chem. Biol.* 2000, **7**, 97–109.
158. L. Katz, *Methods Enzymol.* 2009, **459**, 113–142.
159. H. G. Menzella, R. Reid, J. R. Carney, S. S. Chandran, S. J. Reisinger, K. G. Patel, D. A. Hopwood, D. V. Santi, *Nat. Biotechnol.* 2005, **23**, 1171–1176.
160. R. McDaniel, A. Thamchaipenet, C. Gustafsson, H. Fu, M. Betlach, G. Ashley, *Proc. Natl. Acad. Sci. U S A* 1999, **96**, 1846–1851.
161. R. Pieper, R. S. Gokhale, G. Luo, D. E. Cane, C. Khosla, *Biochemistry* 1997, **36**, 1846–1851.
162. R. S. Gokhale, S. Y. Tsuji, D. E. Cane, C. Khosla, *Science* 1999, **284**, 482–485.
163. S. Y. Tsuji, D. E. Cane, C. Khosla, *Biochemistry* 2001, **40**, 2326–2331.
164. G. A. Roberts, J. Staunton, P. F. Leadlay, *Eur. J. Biochem.* 1993, **214**, 305–311.
165. R. Pieper, G. Luo, D. E. Cane, C. Khosla, *Nature* 1995, **378**, 263–266.
166. B. Lowry, T. Robbins, C. H. Weng, R. V. O'Brien, D. E. Cane, C. Khosla, *J. Am. Chem. Soc.* 2013, **135**, 16809–16812.
167. C. Khosla, Y. Tang, A. Y. Chen, N. A. Schnarr, D. E. Cane, *Annu. Rev. Biochem.* 2007, **76**, 195–221.
168. A. L. Edwards, T. Matsui, T. M. Weiss, C. Khosla, *J. Mol. Biol.* 2014, **426**, 2229–2245.
169. A. Rittner, M. Grininger, *Chembiochem* 2014, **15**, 2489–2493.
170. K. J. Weissman, *Nat. Prod. Rep.* 2015, **32**, 436–453.
171. S. Dutta, J. R. Whicher, D. A. Hansen, W. A. Hale, J. A. Chemler, G. R. Congdon, A. R. Narayan, K. Hakansson, D. H. Sherman, J. L. Smith, G. Skiniotis, *Nature* 2014, **510**, 512–517.
172. J. R. Whicher, S. Dutta, D. A. Hansen, W. A. Hale, J. A. Chemler, A. M. Dosey, A. R. Narayan, K. Hakansson, D. H. Sherman, J. L. Smith, G. Skiniotis, *Nature* 2014, **510**, 560–564.
173. J. Piel, *Proc. Natl. Acad. Sci. U S A* 2002, **99**, 14002–14007.
174. Y. Q. Cheng, G. L. Tang, B. Shen, *Proc. Natl. Acad. Sci. U S A* 2003, **100**, 3149–3154.
175. J. Piel, D. Hui, N. Fusetani, S. Matsunaga, *Environ. Microbiol.* 2004, **6**, 921–927.
176. H. Jenke-Kodama, T. Börner, E. Dittmann, *PLoS Comput. Biol.* 2006, **2**, e132.
177. T. Nguyen, K. Ishida, H. Jenke-Kodama, E. Dittmann, C. Gurgui, T. Hochmuth, S. Taudien, M. Platzer, C. Hertweck, J. Piel, *Nat. Biotechnol.* 2008, **26**, 225–233.

178. T. A. Gulder, M. F. Freeman, J. Piel, *Top. Curr. Chem.* 2011, 1–55, Epub DOI: 10.1007/128_2010_113.

179. C. Scotti, M. Piatti, A. Cuzzoni, P. Perani, A. Tognoni, G. Grandi, A. Galizzi, A. M. Albertini, *Gene* 1993, **130**, 65–71.

180. A. M. Albertini, T. Caramori, F. Scoffone, C. Scotti, A. Galizzi, *Microbiology* 1995, **141**(Pt 2), 299–309.

181. X. H. Chen, J. Vater, J. Piel, P. Franke, R. Scholz, K. Schneider, A. Koumoutsi, G. Hitzeroth, N. Grammel, A. W. Strittmatter, G. Gottschalk, R. D. Süssmuth, R. Borriss, *J. Bacteriol.* 2006, **188**, 4024–4036.

182. C. T. Calderone, W. E. Kowtoniuk, N. L. Kelleher, C. T. Walsh, P. C. Dorrestein, *Proc. Natl. Acad. Sci. U S A* 2006, **103**, 8977–8982.

183. C. T. Calderone, S. B. Bumpus, N. L. Kelleher, C. T. Walsh, N. A. Magarvey, *Proc. Natl. Acad. Sci. U S A* 2008, **105**, 12809–12814.

184. S. B. Bumpus, N. A. Magarvey, N. L. Kelleher, C. T. Walsh, C. T. Calderone, *J. Am. Chem. Soc.* 2008, **130**, 11614–11616.

185. J. Moldenhauer, X. H. Chen, R. Borriss, J. Piel, *Angew. Chem. Int. Ed. Engl.* 2007, **46**, 8195–8197.

186. J. Moldenhauer, D. C. Götz, C. R. Albert, S. K. Bischof, K. Schneider, R. D. Süssmuth, M. Engeser, H. Gross, G. Bringmann, J. Piel, *Angew. Chem. Int. Ed. Engl.* 2010, **49**, 1465–1467.

187. K. Jensen, H. Niederkrüger, K. Zimmermann, A. L. Vagstad, J. Moldenhauer, N. Brendel, S. Frank, P. Pöplau, C. Kohlhaas, C. A. Townsend, M. Oldiges, C. Hertweck, J. Piel, *Chem. Biol.* 2012, **19**, 329–339.

188. A. K. El-Sayed, J. Hothersall, S. M. Cooper, E. Stephens, T. J. Simpson, C. M. Thomas, *Chem. Biol.* 2003, **10**, 419–430.

189. M. Hildebrand, L. E. Waggoner, H. Liu, S. Sudek, S. Allen, C. Anderson, D. H. Sherman, M. Haygood, *Chem. Biol.* 2004, **11**, 1543–1552.

190. S. Sudek, N. B. Lopanik, L. E. Waggoner, M. Hildebrand, C. Anderson, H. Liu, A. Patel, D. H. Sherman, M. G. Haygood, *J. Nat. Prod.* 2007, **70**, 67–74.

191. K. Schneider, X. H. Chen, J. Vater, P. Franke, G. Nicholson, R. Borriss, R. D. Sussmuth, *J. Nat. Prod.* 2007, **70**, 1417–1423.

192. S. Singh, G. N. Phillips Jr., J. S. Thorson, *Nat. Prod. Rep.* 2012, **29**, 1201–1237.

193. S. Martinez Cuesta, N. Furnham, S. A. Rahman, I. Sillitoe, J. M. Thornton, *Curr. Opin. Struct. Biol.* 2014, **26**, 121–130.

194. H. Aldemir, R. Richarz, T. A. Gulder, *Angew. Chem. Int. Ed. Engl.* 2014, **53**, 8286–8293.

195. C. T. Walsh, T. A. Wencewicz, *Nat. Prod. Rep.* 2013, **30**, 175–200.

196. L. C. Blasiak, C. L. Drennan, *Acc. Chem. Res.* 2009, **42**, 147–155.

197. P. K. Sydor, G. L. Challis, *Methods Enzymol.* 2012, **516**, 195–218.

198. L. M. Podust, D. H. Sherman, *Nat. Prod. Rep.* 2012, **29**, 1251–1266.

Cyril Bressy[1], Michael Smietana[2], Erica Benedetti[3], and Stellios Arseniyadis[4]

[1] *Aix Marseille Université, Centrale Marseille, CNRS, Marseille, France*
[2] *Institut des Biomolécules Max Mousseron, CNRS, Université de Montpellier, ENSCM, France*
[3] *Laboratoire de Chimie et Biochimie et Pharmacologiques et Toxicologiques, CNRS-Université Paris Descartes Faculté des Sciences Fondamentales et Biomédicales, Paris, France*
[4] *School of Biological and Chemical Sciences, Queen Mary University of London, London, United Kingdom*

## 2.2 SYNTHESIS OF POLYKETIDES

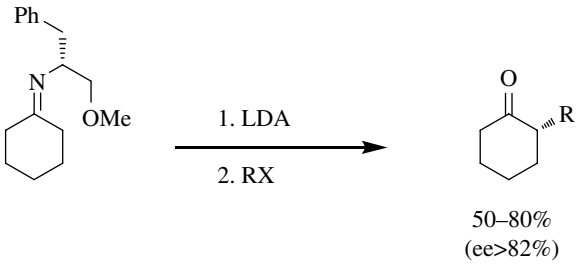
### 2.2.1 Asymmetric Alkylation Reactions

Nature has always been capable of performing specific synthetic transformation in a highly regio, chemo-, and stereoselective fashion using complex chiral machinery (please refer to Section 2.1). Thanks to a rich synthetic evolution over the past century, organic chemists have been able to rival nature by developing some particularly effective and selective synthetic tools and applying them to the synthesis of complex natural products; the asymmetric alkylation is definitely one of them.

#### *2.2.1.1 Enders Alkylation*

*Introduction* The regiocontrolled α-alkylation of aldehydes and ketones focused tremendous attention between the 1950s and the 1970s [1]. Fundamental solutions emerged with the development of nitrogenated equivalents of enolates as first described by Stork, who brought important contributions in this area by developing the enamine [2] and the metalloenamine [3] alkylations. As a matter of fact, these seminal works were essential in the development of stereoselective processes for the α-alkylation of carbonyl compounds. Meyers described the diastereoselective alkylation of chiral imines through the formation of an azaenolate intermediate [4] with moderate to good levels of selectivity using a chiral auxiliary based on a phenylalanine derivative (Scheme 2.24).

In 1976, Corey and Enders reported the use of an α-lithiated *N*,*N*-dimethylhydrazone as an efficient equivalent of an enolate, leading to the metallation on the less hindered position. In the same paper, they developed a mild oxidative protocol for the cleavage of the hydrazone using a methanolic/aqueous solution of sodium periodate. The same year,



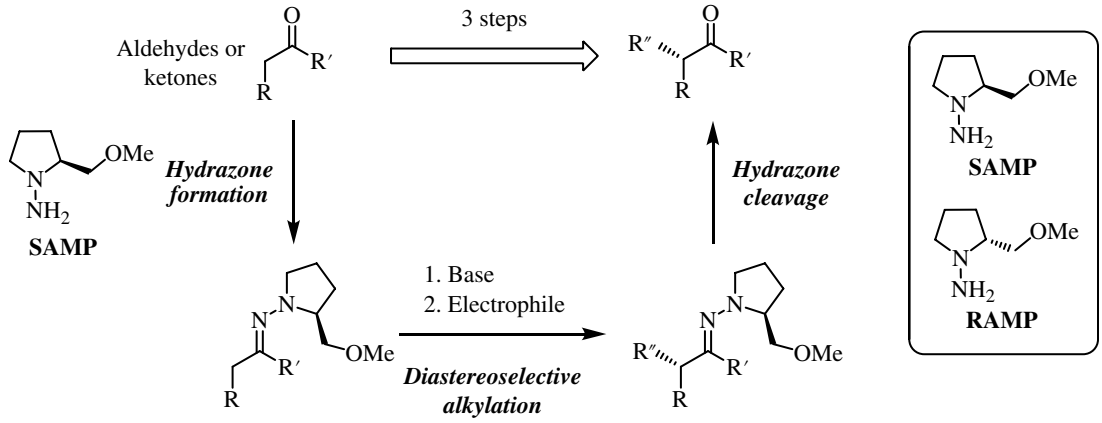

**SCHEME 2.24** Stereoselective Myers' alkylation.

Enders introduced a three-step protocol allowing to diastereoselectively alkylate ketones [5] (Scheme 2.25). This procedure was eventually extended to aldehydes [6]. Hence, the carbonyl compound is first converted to the corresponding chiral hydrazone using SAMP or RAMP hydrazine. The diastereoselective alkylation then takes place by forming the azaenolate intermediate in the presence of a strong base and treating it with an electrophile. The resulting alkylated product finally undergoes auxiliary cleavage to afford the desired compound [1, 7].

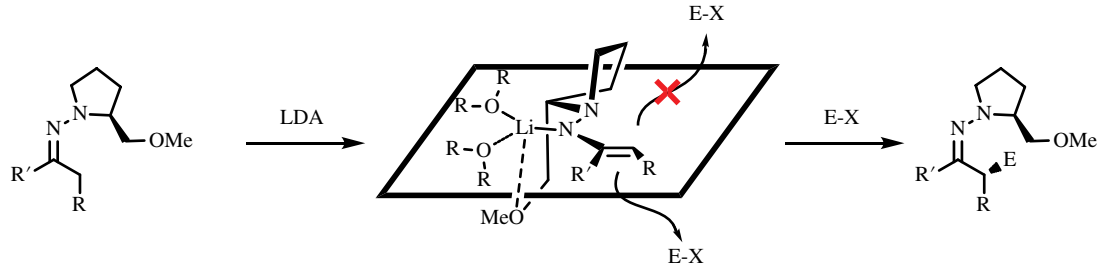
Based on experimental and theoretical data, a model was proposed to explain the observed diastereoselectivity. Hence, the azaenolate intermediate adopts an (*E*) geometry for the C═C bond and a (*Z*) geometry for the C—N bond, leading to a four-atom plane. The methoxymethyl group points out of the plan and chelates the lithium atom, which rigidifies the intermediate species. The pyrrolidine moiety brings more steric hindrance to the *si*-face of the azaenolate (the R is here considered as an alkyl group) and thus favors the approach of the electrophile with good to excellent facial discrimination (Scheme 2.26).

*Preparation of RAMP and SAMP Hydrazones* (*S*)-1-Amino-2-methoxymethylpyrrolidine **4** or SAMP is prepared from (*S*)-proline **1** in a four-step sequence involving an initial reduction to prolinol **2**, followed by the formation of the corresponding *N*-nitrosamine **3** using EtONO, which is eventually reduced to the hydrazine **4** (Scheme 2.27). The synthesis of its enantiomer, (*R*)-1-amino-2-methoxymethylpyrrolidine **7** or RAMP, requires six steps starting from glutamic acid **5**. The latter undergoes a dehydrative cyclization to pyroglutamic acid **6** followed by an esterification using diazomethane and a reduction with $LiAlH_4$ to afford the (*R*)-prolinol, which is then converted to the hydrazine using the exact same protocol as previously.

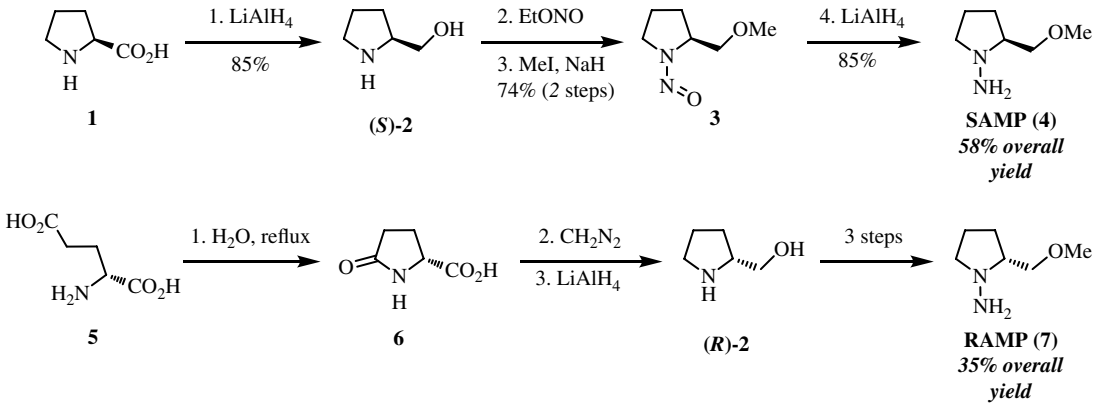
The preparation of the corresponding hydrazones from SAMP and RAMP differs depending on the carbonyl moiety (Scheme 2.28). Indeed with aldehydes, the synthesis requires solvent-free conditions at 0°C, while with ketones, the hydrazones are prepared under harsher conditions such as refluxing benzene with a catalytic amount of acid or in



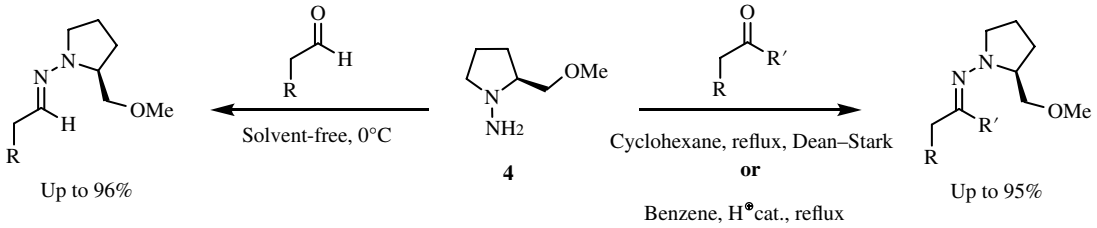

**SCHEME 2.25** Ender's protocol for the asymmetric [alkylation of aldehydes and ketones].



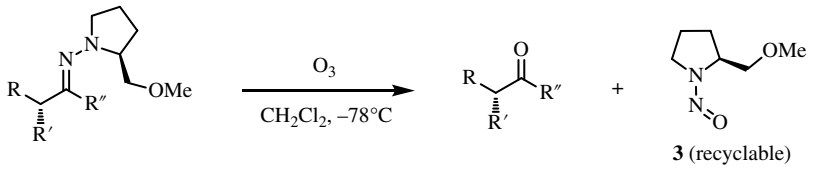

**SCHEME 2.26** Model for the diastereoselective alkylation of SAMP hydrazone.




**SCHEME 2.27** SAMP and RAMP synthesis.




**SCHEME 2.28** Condensation of SAMP with aldehydes and ketones to form hydrazones.




**SCHEME 2.29** Oxidative cleavage of SAMP hydrazones using ozone.

cyclohexane under water separation conditions (Dean–Stark apparatus).

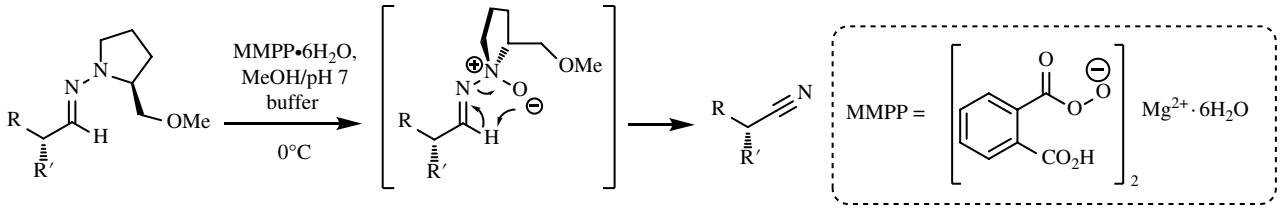
Interestingly, while the *E*/*Z* diastereomeric ratio of the resulting hydrazones usually varies, this does not impact the stereochemical outcome of the diastereoselective alkylation.

*Cleavage of the Hydrazones* The removal of the chiral auxiliary is a crucial step due to the possible racemization or epimerization of the resulting carbonyl compound. A number of methods are available in the literature with both advantages and drawbacks depending on the sensitivity of the substrates. In this paragraph, we will mainly focus on the protocols that are well established and that have actually been used in the context of natural product synthesis. Two main groups of chiral auxiliary cleavage conditions can be distinguished: the oxidative and the hydrolytic cleavages.

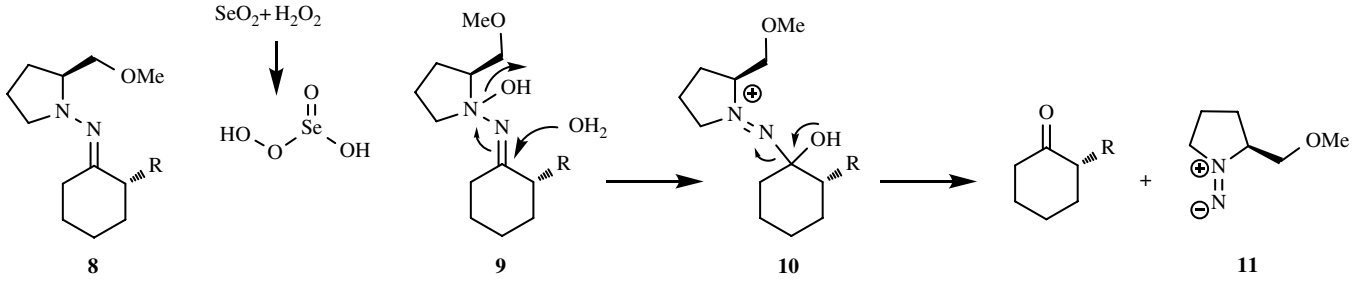
Among the oxidative cleavages, ozone is probably one of the most employed procedures. It is one of the two methods employed by Enders in his seminal paper published in 1976 [8]. This protocol allows to break the C=N double bond to afford the corresponding carbonyl compound along with *N*-nitrosamine **3**, a precursor of the SAMP hydrazine which can thus be recycled (Scheme 2.29).

The group of Enders found that magnesium monoperoxyphthalate hexahydrate (MMPP) could be used as a chemoselective oxidant capable of promoting the removal of the hydrazone without racemizing the product [9]. The mild conditions (MMPP·$6H_2O$, MeOH/pH 7 buffer, 0°C) were found to be applicable to substrates bearing an alkenyl moiety, affording the desired ketones in a limited amount of time (typically 5 min to 2 h). Interestingly, the same conditions applied to the hydrazones derived from aldehydes afford the corresponding nitrile [10]. The proposed mechanism involves the oxidation of the pyrrolidine nitrogen to form the hydrazone *N*-oxide, which undergoes a spontaneous aza-Cope elimination (Scheme 2.30).

In 2009, Smith had to come up with new conditions for the oxidative cleavage of Enders' auxiliary as all the known methods failed to provide the desired product without any




**SCHEME 2.30** Proposed mechanism for the conversion of SAMP hydrazones to nitriles.



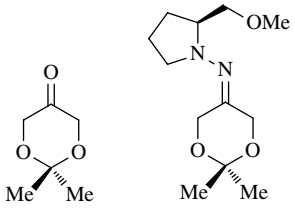

**SCHEME 2.31** Proposed mechanism for the oxidative cleavage of SAMP hydrazones under the Smith conditions.

epimerization [11]. In the context of the total synthesis of nodulisporic acid, his group found that $SeO_2$ and $H_2O_2$ in MeOH with a pH 7 phosphate buffer at room temperature were the best conditions to safely remove the chiral auxiliary. Mechanistically, $H_2O_2$ oxidizes $SeO_2$ into peroxyselenous acid, which promotes the oxidation of the pyrrolidine nitrogen (Scheme 2.31). The resulting intermediate is then hydrolyzed to form the desired ketone along with a diazene byproduct.

Concerning the hydrolytic cleavage conditions, one method was reported by Enders in his seminal study in 1976 [8]. The latter consists in the alkylation of the nitrogen with an excess of iodomethane to form the corresponding ammonium salt, which is hydrolyzed in a biphasic HCl 1 M/*n*-pentane system. In 1998, Enders described very mild conditions using a saturated aqueous solution of oxalic acid in ether, which allowed to hydrolyze the hydrazones without racemization [12]. This protocol has also the advantage of recycling the chiral SAMP hydrazine.

It is worth pointing out that a reductive treatment using $LiAlH_4$ followed by a hydrogenolysis with Raney nickel affords the corresponding amines [13], while the treatment of the hydrazones with propan-1,3-dithiol in the presence of $BF_3.Et_2O$ leads to the corresponding dithianes [14].

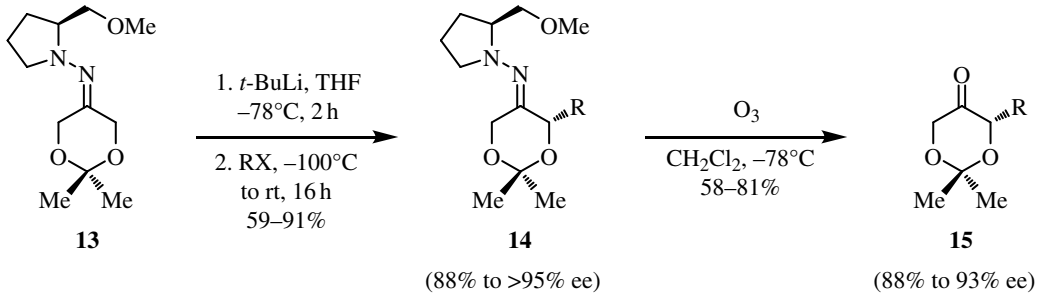
*Iterative Strategy for the Synthesis of Polyacetates* Enders identified 2,2-dimethyl-1,3-dioxan-5-one **12** [15] as a particularly interesting building block for the synthesis of polyacetates using the SAMP/RAMP hydrazone strategy [16]. Indeed, this building block can play the role of a synthetic equivalent of dihydroxyacetone phosphate (DHAP) involved in various biosynthetic processes. More specifically, this method appeared to be particularly useful for the preparation of *anti*-1,3-polyols [17].



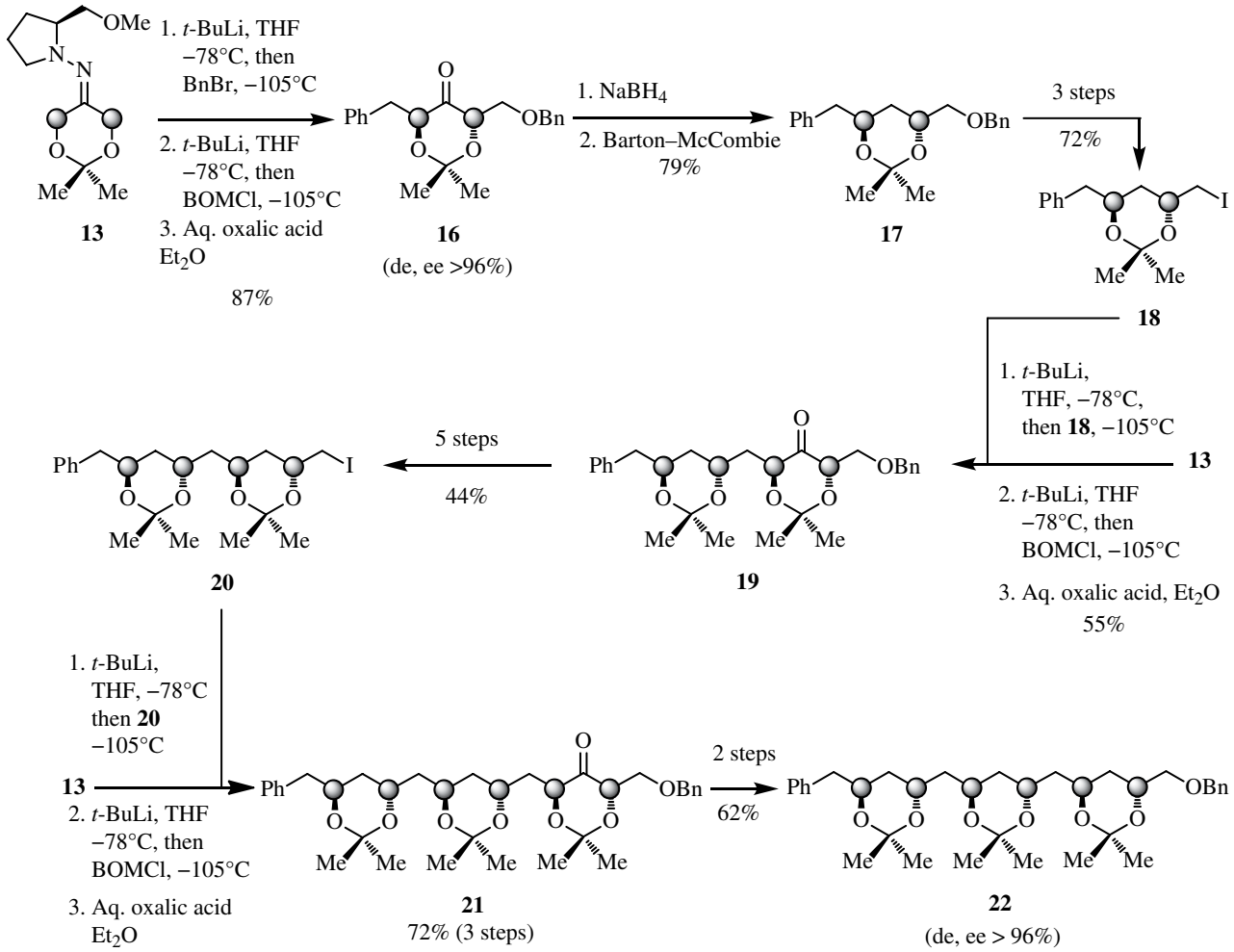
**12`** **13**

The deprotonation of chiral hydrazone **13** is obtained using *tert*-butyllithium as the base at −78°C in THF. The reaction mixture is then cooled to −100°C before the electrophile is added, and the reaction is allowed to warm to room temperature overnight. The corresponding alkylated product **14** is obtained in moderate to good yields with excellent diastereoselectivities ranging from 88% to >95%. Ozonolysis finally releases the ketone without any noticeable erosion of the enantioselectivity (Scheme 2.32).

In 1999, Enders used this method in an iterative fashion to synthesize *anti*-1,3-polyols (Scheme 2.33). The sequence required two diastereoselective alkylations at the α- and α′-positions of the hydrazone before cleavage of the chiral auxiliary using an aqueous solution of oxalic acid in ether. The reduction of the resulting ketone followed by a Barton–McCombie deoxygenation furnished the corresponding acetal **17**, which was converted to the iodide intermediate **18** upon three additional steps. The latter was then used as an

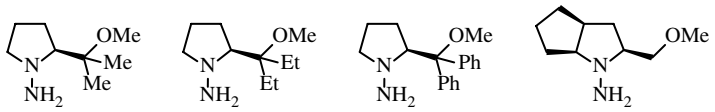



**SCHEME 2.32** Diastereoselective alkylation of 2,2-dimethyl-1,3-dioxan-5-one hydrazone.



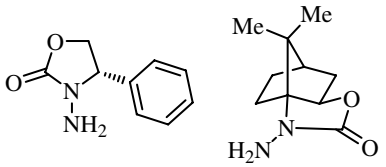

**SCHEME 2.33** Iterative diastereoselective alkylation.

electrophile in a subsequent alkylation reaction. Protection of the resulting primary alcohol as a BOM ether followed by cleavage of the chiral auxiliary eventually afforded compound **19** bearing a bis-2,2-dimethyl-1,3-dioxan unit. The five-step sequence to the corresponding iodide derivative was then repeated before a new double diastereoselective alkylation with hydrazone **13** was performed leading, after hydrolysis, to ketone **21**. A final deoxygenation afforded the title polyol unit with an excellent enantio- and diastereoselectivity. Hence, in order to obtain compound **22** bearing six stereogenic centers, 3 equivalents of SAMP hydrazone were necessary.




**SADP** **SAEP** **SAPP** **RAMBO**

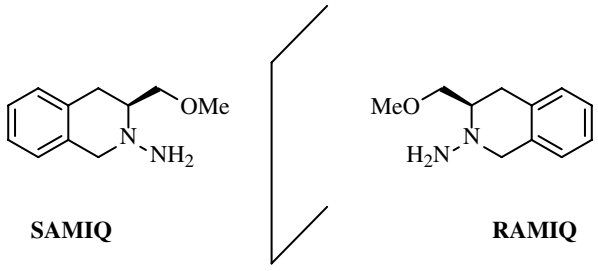
**SCHEME 2.34** Sterically demanding analogs to SAMP/RAMP hydrazines.




**SCHEME 2.35** Efficient *N*-amino cyclic carbamates for stereoselective alkylations.

*Enders-Type Alkylations with Related Reagents* Several related reagents were developed after the appearance of the SAMP and RAMP hydrazones. More sterically demanding hydrazines such as SADP, SAEP, SAPP [18], or SAMBO [19] were prepared and used in various diastereoselective transformations (Scheme 2.34).

In 2008, Lim and Coltart described the use of *N*-amino cyclic carbamates (ACC) (Scheme 2.35) as chiral auxiliaries [20]. These hydrazines have the advantage of easily forming hydrazones even with ketones; moreover their removal is usually rapid and nearly quantitative under mild conditions (few minutes with PTSA in acetone at rt). In addition, the C═O bond provides a useful anchoring point during the formation of the azaenolate and enhances the acidity of the hydrogen atoms at the α-position of the hydrazone. Hence, the deprotonation is fast and does not require low temperatures (−40°C versus −110°C to −78°C for SAMP and RAMP hydrazones) to afford good diastereoselectivities.




**SAMIQ** **RAMIQ**

Recently Pan and Liu unveiled two SAMP and RAMP hydrazine analogs, namely, (*S*)/(*R*)-2-amino-3-methoxymethyltetrahydro-quinoline, also called SAMIQ and RAMIQ hydrazines [21]. Interestingly, instead of building their chiral auxiliaries around the proline framework, the authors used (*S*)- and (*R*)-phenylalanine. The tetrahydroquinoline moiety was prepared *via* a Pictet–Spengler annulation with formaldehyde. These chiral auxiliaries were evaluated for their chiral induction in various Michael additions and were shown to induce excellent stereoselectivities ranging between 95.3 and >99.5% ee. Compared to the SAMP/RAMP hydrazones, these new hydrazones have the advantage of containing a chromophore and being often crystalline.

*Utilization of Enders' Alkylation with Other Electrophiles* Enders' hydrazones were also shown to react with other electrophiles than alkyl halides. Indeed, several carbon-centered electrophiles could be used such as aldehydes and ketones through aldolization reactions [22], various Michael acceptors [23], aziridines [24], but also some unconventional electrophiles such as THF in the presence of trialkylsilyl trifluoromethane sulfonate or cyclopropenes with the zinc azaenolate [25].

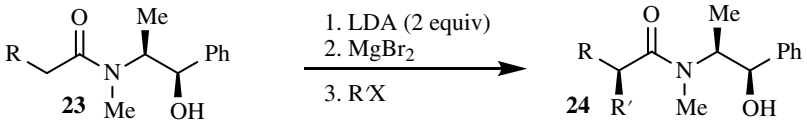
Several carbon–heteroatom bonds can also be formed by reaction with the deprotonated intermediate form. We can quote the formation of C–O bonds [26], C–S bonds [27], C–N bonds [28], C–Si bonds [29], and even C–P bonds [30].

*Conclusion* The SAMP/RAMP hydrazone methodology developed by Enders almost 40 years ago dominated the field of diastereoselective α-alkylation of aldehydes and ketones. Due to its generality and robustness, this method cannot be circumvented. The recent development made by Coltart in 2008 is the first remarkable improvement since the initial discovery.

### *2.2.1.2 Myers' Alkylation*

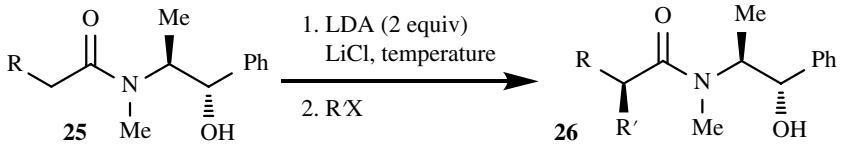
*Seminal Works by Larchevêque* In the late 1970s, the group of Larchevêque explored the alkylation of carboxamides using ephedrine **23** as chiral auxiliary [31, 32]. Both enantiomers of this alkaloid are commercially available and relatively cheap. Initial conditions involved the use of 2 equivalents of LDA in ether at room temperature to slowly metalate the carboxamides before the addition at 10°C of the iodoalkane in the presence of HMPT. These conditions afforded a moderate diastereoselectivity of the α-alkylation (dr = 76:24). Nevertheless the transmetalation by the addition of $MgBr_2$ after deprotonation with LDA (Table 2.1) improved significantly the diastereoselectivity (dr = 95:5). Additional examples with other electrophiles also gave results with interesting selectivities (100/0 > dr > 90:10). Unfortunately this group did not find satisfactory conditions to cleave the

**TABLE 2.1 Diastereoselective Alkylation of Ephedrine Carboxamides**




| Entry | R | R′X | Yield (%) | dr |
|---|---|---|---|---|
| 1 | Me | Etl | 75 | 90:10 |
| 2 | Me | $(Et)_2SO_4$ | 95 | 90:10 |
| 3 | Me | *n*-Bul | 95 | >95:5 |
| 4 | Et | *n*-Bul | 93 | 95:5 |
| 5 | Et | BnCl | 95 | 100:0 |

**TABLE 2.2 Diastereoselective Alkylation of Pseudoephedrine Carboxamides**

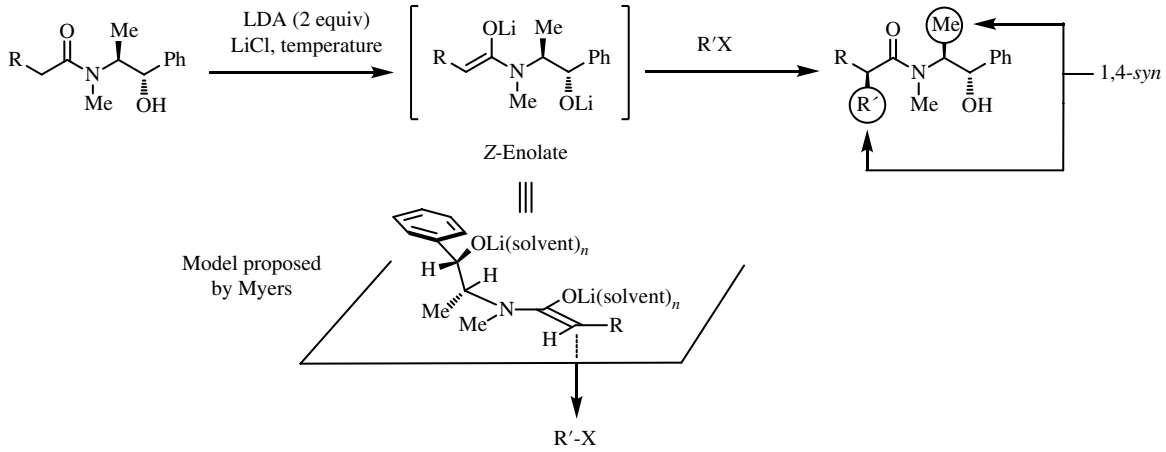



| Entry | R | R′X | Temperature (°C) | Time (h) | Yield (%) | Crude de (%) | Isolated de (%) |
|---|---|---|---|---|---|---|---|
| 1 | Me | BnBr | 0 | 0.2 | 90 | 94 | >99 |
| 2 | Me | *n*-Bul | 0 | 1.5 | 80 | 98 | >99 |
| 3 | Me | BOMBr | −78 | 1.5 | 80 | 98 | 98 |
| 4 | Bn | Mel | 0 | 1 | 99 | 94 | 94 |
| 5 | Bn | Mel | −78 | 8 | 95 | 97 | 97 |
| 6 | Bn | *n*-Bul | 0 | 1.5 | 90 | 98 | 98 |
| 7 | *n*-Bu | Mel | 0 | 1 | 94 | 94 | 94 |
| 8 | *n*-Bu | Mel | −78 | 6 | 89 | 96 | 96 |
| 9 | *n*-Bu | BnBr | 0 | 0.7 | 87 | 98 | >99 |
| 10 | Ph | Etl | 0 | 0.7 | 92 | 96 | >99 |

chiral auxiliary without altering the enantioselectivity of the final product, which hampered the use of the method in natural product synthesis.

*From Ephedrine to Pseudoephedrine Carboxamide* More than a decade after the seminal work of Larchevêque, Myers and coworkers described the alkylation of carboxamides derived from pseudoephedrine [33, 34]. Both enantiomers of pseudoephedrine are also readily available and quite inexpensive. The preparation of the carboxamides consists in the coupling between commercially available pseudoephedrine and an acyl chloride or an anhydride. The corresponding carboxamides are often crystalline and can be easily purified by recrystallization. Myers found slightly modified conditions in order to obtain high levels of diastereoselectivity in the alkylation process. The deprotonation occurs also with LDA but in the presence of 6 equivalents of anhydrous lithium chloride, which improve two crucial parameters: (i) the global kinetics of the reaction (typically 1.5 h) and (ii) the completion of the reaction. Without LiCl the pseudoephedrine propionamide alkylation with *n*-butyl iodide gives only 32% of the desired product at 0°C after 5 h, while the reaction with LiCl affords complete conversion after 1.5 h at the same temperature and 80% yield. The role of LiCl remains unclear but seems to modify the aggregation state. The alkylated products are isolated in excellent yields (80–95%) and high diastereoselectivities (90–98% de), which could be improved by recrystallization (96–99% de). The most commonly employed electrophiles include primary alkyl iodides and primary alkyl bromides, both of which can be used in the absence of toxic HMPT in comparison with Larchevêque's protocol. Secondary alkyl iodide can also be used; however, the reactions need to be performed at reflux and the yields are usually lower than the ones obtained when using primary alkyl halides [35] (Table 2.2).

The alkylation of the *Z*-enolate intermediate (Scheme 2.36) occurs on the same face as the methyl group (mnemonic). In a model, Myers proposed the alkyl halides approach by




**SCHEME 2.36** Model and mnemonic for Myers' alkylation.

the *si*-face of the enolate, which is stabilized by allylic strain and solvent interactions to the conformer shown in Scheme 2.36.

The reaction with β-branched primary alkyl iodides provides an iterative method to prepare deoxypropionates. The alkylations are then performed at room temperature and afford high yields (>90%) and excellent diastereoselectivities even when the pseudoephedrine carboxamide reacts with chiral β-branched primary alkyl iodides in a mismatched fashion (dr = 142:1 – 1:199) (Table 2.3).

*Cleavage of Pseudoephedrine Auxiliary* In contrast to the ephedrine auxiliary, which is difficult to cleave once the alkylation is performed, the pseudoephedrine moiety can be readily removed under various conditions with a limited impact on the ees [36].

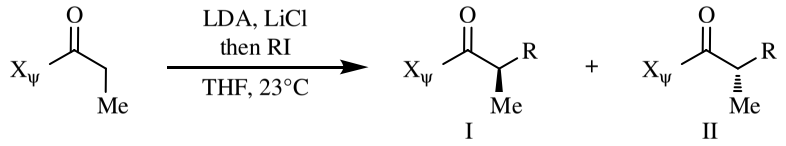
HYDROLYSIS INTO CARBOXYLIC ACIDS The pseudoephedrine-derived carboxamides were cleanly converted to the corresponding carboxylic acids with a minimum amount of epimerization using a 1:1 mixture of concentrated sulfuric acid and dioxane at reflux (Table 2.4, entry 1). Basic hydrolytic conditions could also be used to obtain the corresponding carboxylic acid using, for example, *tetra*-butylammonium hydroxide (5 equiv) in a 1:4 mixture of *tert*-butanol and water at reflux; however these conditions do induce a slight epimerization (Table 2.4, entry 2). Myers also tried to employ Lewis acids such as $FeCl_3$, which were found to reduce the epimerization process, but the reactions are usually more sluggish (at least 48 h) with in some cases incomplete conversions (Table 2.4, entry 3). Finally Myers developed an alternative one-pot three-step protocol (Table 2.4, entry 4) involving an N to O acyl transfer using methanesulfonic acid in refluxing THF (typically 1–3 h), the formation of an amine–borane complex by the addition of lithium borohydride (to avoid the acyl group from shifting back), and a final saponification using an aqueous sodium hydroxide solution.

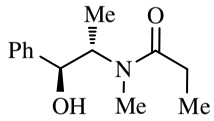
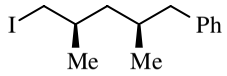
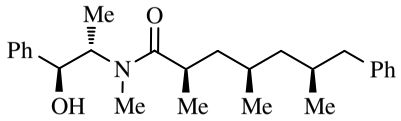
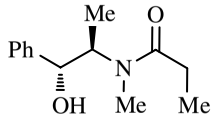
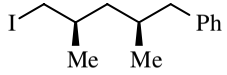
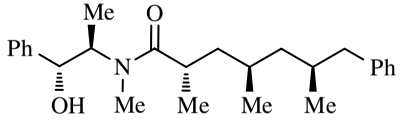
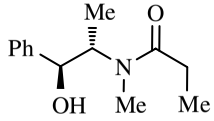
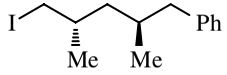
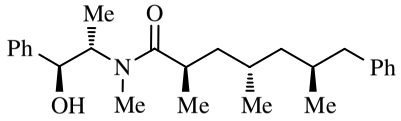
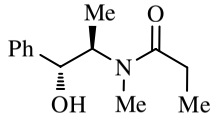
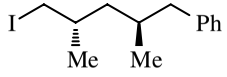
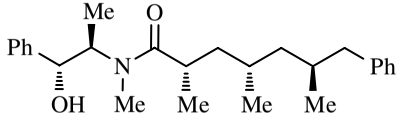
REDUCTION TO THE CORRESPONDING ALDEHYDE Lithium triethoxyaluminum hydride [$LiAlH(OEt)_3$] was found to readily convert pseudoephedrine carboxamides to the corresponding aldehyde with only limited erosion of the ees (Table 2.5). To do so, a solution of the pseudoephedrine carboxamide in THF is added at −78°C to a suspension of $LiAlH(OEt)_3$ (2.3 equiv) in hexanes. The reaction mixture is then warmed to 0°C before a dilute acidic aqueous solution (typically HCl 0.5 M) is added, resulting in the formation of the desired aldehyde along with the pseudoephedrine aminal **27**. To avoid the formation of the byproduct, the quenching can be performed using a 1 M aqueous solution of hydrochloric acid and 10 equivalents of trifluoroacetic acid.

REDUCTION TO THE CORRESPONDING ALCOHOL Various conditions were also developed to convert the pseudoephedrine carboxamides to the corresponding primary alcohol [50]. Indeed, after extensive studies, the group of Myers unveiled lithium pyrrolididotrihydroborate (LPT) and lithium amidotrihydroborate (LAB) as appropriate reagents for this transformation (Table 2.6). LPT, for instance, triggers the formation of the primary alcohol in high yields and barely any erosion of the chiral information even for some particularly sensitive substrates such as the one derived from α-phenylacetamide. Nonetheless, LAB appears to be a superior reducing agent than LPT as it allows to cleanly convert pseudoephedrine carboxamides to the corresponding alcohols at room temperature with no or very limited epimerization.

TRANSFORMATION INTO KETONES BY THE ADDITION OF ORGANOLITHIUM SPECIES It was shown that the addition of an excess of an organolithium species on a pseudoephedrine carboxamide affords the corresponding ketone. In practice, the reaction proceeds through the deprotonation of the free hydroxyl group followed by the addition of the

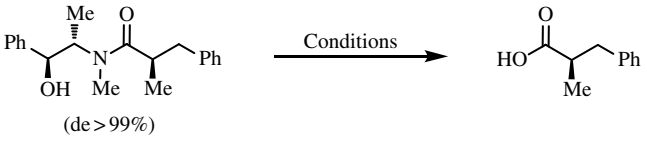
**TABLE 2.3 Myers' Alkylation with β-Branched Primary Alkyl Iodides**




| Entry | Carboxamide | Electrophile ($R^I$) | Product | Yield (%) | Ratio I:II |
|---|---|---|---|---|---|
| 1 |  |  |  | 93 | 142:1 |
| 2 |  |  |  | 96 | 1:70 |
| 3 |  |  |  | 93 | 66:1 |
| 4 |  |  |  | 94 | 1:199 |

organolithium species on the carbonyl center. The tetrahedral intermediate species is stable for a few minutes before the addition of diisopropylamine (1 equiv) scavenges the excess of organolithium reagent. The reaction mixture is eventually quenched with acetic acid in $Et_2O$ (10% v/v), and the resulting ketone is isolated in usually good to excellent yields (54–97% yield) and with limited stereochemical erosion (88–>95% ee) (Table 2.7).

**TABLE 2.4 Hydrolysis of Pseudoephedrine Carboxamides to Carboxylic Acids**

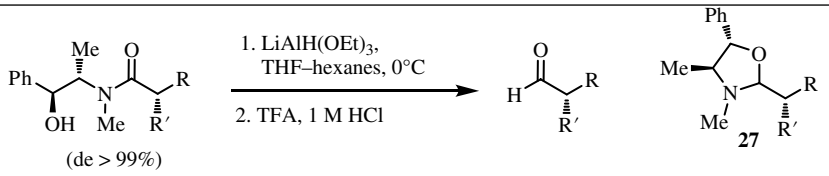



(de > 99%)

| Entry | Conditions | Yield (%) | ee (%) |
|---|---|---|---|
| 1 | $H_2SO_4$ : dioxane (1:1) reflux | 95 | 97 |
| 2 | *n*-$Bu_4NOH$ (5 equiv) *t*-BuOH : $H_2O$ (1:4), reflux | 93 | 94 |
| 3 | $FeCl_3$ (5 equiv) $H_2O$:dioxane (4:1), reflux | 94 | 98 |
| 4 | 1) MsOH (1.5 equiv), THF, reflux 2) $LiBH_4$ (1.5 equiv), 23 °C 3) NaOH (5 equiv), $H_2O$, 23 °C | 94 | 98 |

*Diastereoselectivity of Myers' Alkylations Monitored by NMR Analysis* Various methods allow to measure the diastereoselectivity of a given Myers' alkylation. Those methods include NMR analysis, which is often hampered by the presence of rotamers, and gas chromatography of the corresponding acetates or trimethylsilyl ethers. In 2007, Myers found a practical way of determining the diastereoselectivity by forming of a cyclic iminium salt (Scheme 2.37) [37]. Indeed after 2 min in the presence of triflic anhydride and pyridine in dichloromethane at 0°C, the pseudoephedrine carboxamide spontaneously undergoes cyclization to the corresponding cyclic iminium salt **28**. In the process, the stereogenic center bearing the *in situ* generated triflate deals with a highly stereospecific inversion of configuration. Most importantly, the $^1H$ NMR analysis of the cyclic iminium is generally much more convenient than the initial amide especially for diastereoselectivities that exceed 90%.

**TABLE 2.5 Reduction of Pseudoephedrine Carboxamides into Aldehydes**



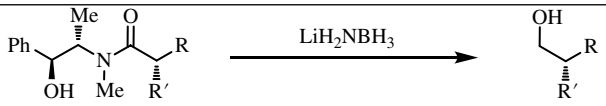

(de > 99%)

Selected examples:



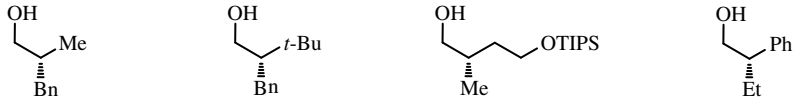

76%, 95% ee | 75%, 98% ee | 80%, 97% ee | 80%, 90% ee

**TABLE 2.6 Reduction of Pseudoephedrine Carboxamides into Primary Alcohols**



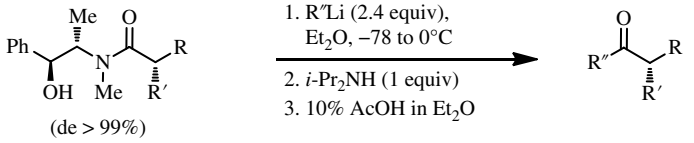

(de > 99%)

Selected examples:

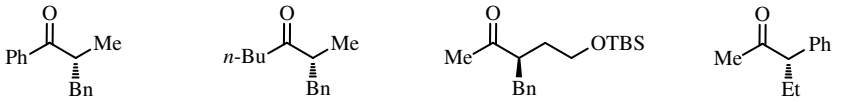



90%, >99% ee | 89%, >95% ee | 91%, >95% ee | 83%, 92% ee

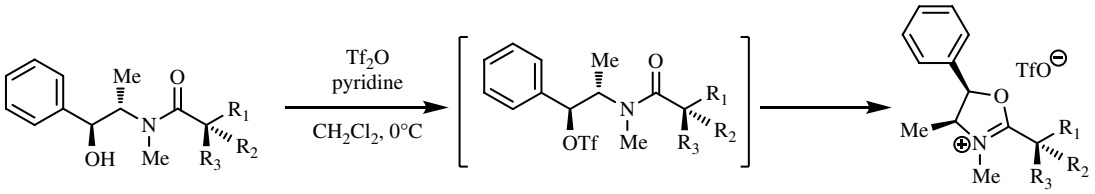
**TABLE 2.7 Conversion of Pseudoephedrine Carboxamides into Ketones**




Selected examples:

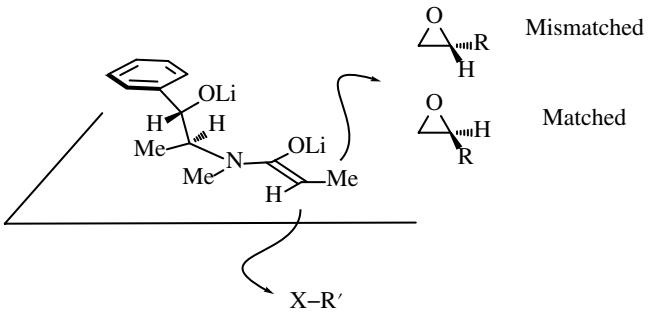


| 94%, >95% ee | 89%, >95% ee | 92%, >95% ee | 54%, 88% ee |
|---|---|---|---|




**28**

**SCHEME 2.37** Transformation of pseudoephedrine carboxamides into cyclic iminium salt.




**SCHEME 2.38** Model for the alkylation of pseudoephedrine amides with epoxides.

*Utilization of Myers' Alkylation with Other Electrophiles* Pseudoephedrine carboxamides were also used as pronucleophile with a wide variety of electrophiles. Rapidly after his seminal paper, Myers explored the possibility of using epoxides as electrophiles [38]. Surprisingly, the approach of the epoxide occurred from the opposite face of the enolate compared to alkyl halides (Scheme 2.38).

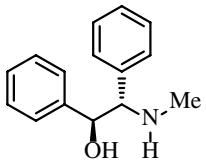
The group of Badia in Spain also explored the possibility of using other types of electrophiles [39]. Interestingly, the aldolization of zirconium enolates with various electrophiles afforded excellent *syn*-diastereoselectivities. Imines were also employed as electrophiles in Mannich reaction with lithium enolates [40] affording to *anti*-β-aminoesters in excellent level of selectivities.

In 2004, researchers from Merck laboratories explored Michael additions on pseudoephedrine carboxamide-derived enolates [41]. A singular salt effect was observed as the presence of LiCl in the reaction mixture led to the *syn*-adduct, while the absence of LiCl afforded the *anti*-adduct.

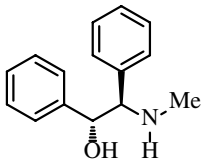
More recently Scheidt [42] tried to condense pseudoephedrine carboxamide enolates onto acylsilanes, but unfortunately no adduct was formed.

*Myers-Type Alkylations with Different Carboxamides* In 2012, Myers described the diastereoselective alkylation of (1*S*,2*S*)- and (1*R*,2*R*)-2-methylamino-1,2-diphenylethanol carboxamides **29** and **30** [43] (Scheme 2.39). This study unveiled several advantages of these chiral auxiliaries over the more traditional pseudoephedrine carboxamides:

- Pseudophenamines are not exposed to commercial restriction compared to pseudoephedrines that are regulated.
- Similar or better diastereoselectivities were observed when using pseudophenamine amides compared to pseudoephedrine amides.
- The pseudophenamine carboxamides present physical properties facilitating isolation (greater propensity to



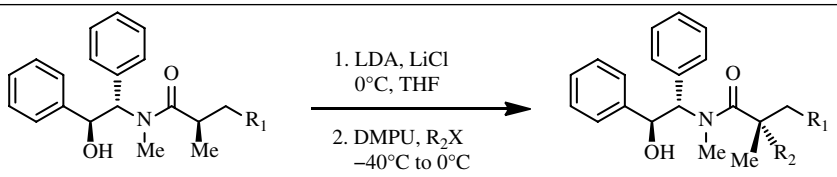

(−)-(1*S*,2*S*)-Pseudophenamine (**29**)



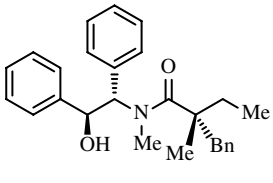

(+)-(1*R*,2*R*)-Pseudophenamine (**30**)

**SCHEME 2.39** Structures of (1*S*,2*S*)- and (1*R*,2*R*)-pseudophenamines.

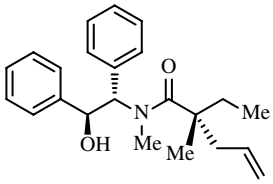
**TABLE 2.8 Stereocontrol of Quaternary Centers by Diastereoselective Alkylation of Pseudophenamine Amides**



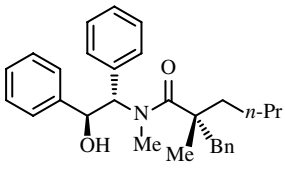

Selected examples:



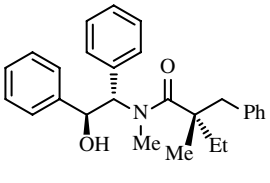

85%
dr > 19:1
(dr > 19:1)[a]




99%
dr > 19:1
(dr = 14:1)[a]




87%
dr > 19:1
(dr = 8.3:1)[a]




85%
dr = 9.9:1
(dr = 6.2:1)[a]

[a] dr obtained with the corresponding pseudoephedrine amides.

be in a crystalline form) and analysis (well-defined NMR signals) in comparison with the corresponding pseudoephedrine carboxamides.

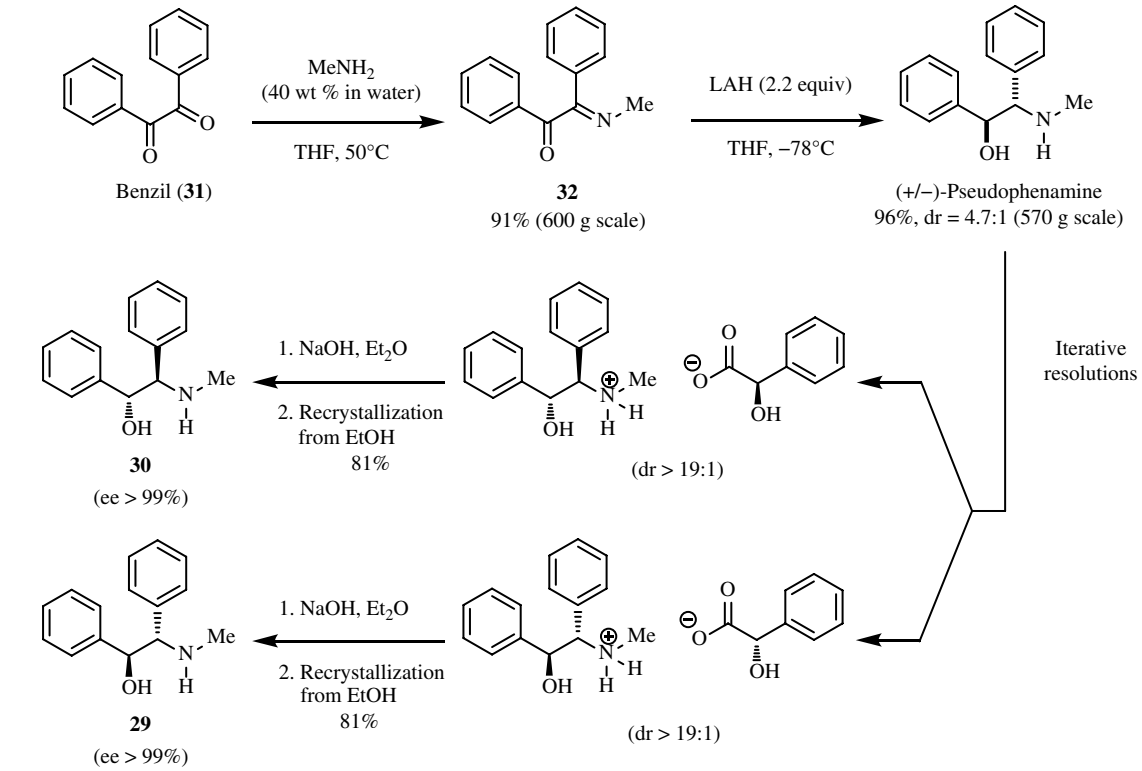
Interestingly the use of α,α-disubstituted pseudophenamine amides allowed significant improvements, especially when trying to generate quaternary stereogenic centers [44] (Table 2.8).

A short and scalable synthesis of (+)- and (−)-pseudophenamines was recently described by the same group. The synthetic sequence began with the formation of monoimine derived from benzyl (Scheme 2.40). The reduction of the corresponding iminoketone **32** with lithium aluminum hydride provided racemic pseudophenamine in a 4.7:1 diastereoisomeric ratio and 96% yield. Iterative resolutions with mandelic acid afforded both diastereoisomers with excellent optical purity (dr > 19:1) giving around 100 g of each enantiomer (starting from 570 g of a racemic mixture) in roughly 92% ee. A subsequent recrystallization from absolute ethanol provided more than 80 g of each enantiomer in optically pure form (ee > 99%).

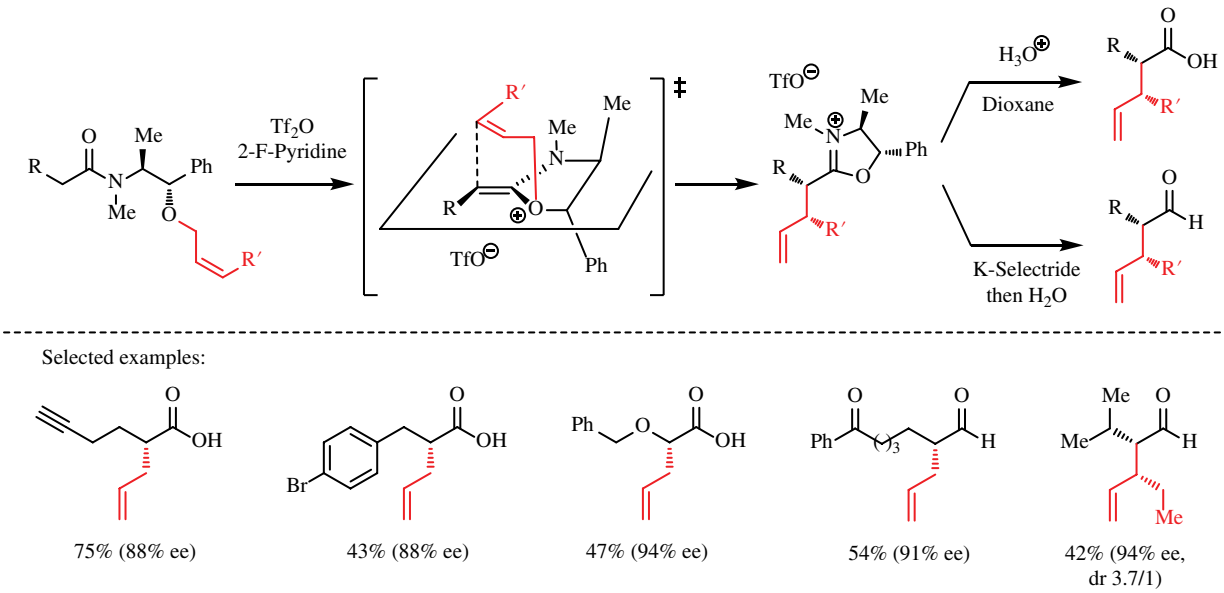
This new chiral auxiliary was recently used with success in aldolization processes affording *syn*-β-hydroxy-α-amino acids in a highly selective fashion [45].

The group of Maulide recently reported a singular method to alkylate pseudoephedrine-derived carboxamides [46]. Their strategy, also referred to as "traceless α-allylation," relies on the use of the O-allylated form of Myers' carboxamides. When submitted to electrophilic activation conditions in the presence of triflic anhydride and 2-fluoropyridine (Scheme 2.41), the carboxamides cyclize to the corresponding iminium before a Claisen rearrangement takes place, leading to the sigmatropic transfer of the allyl group. The resulting iminium bearing now a new stereogenic center at the α-position can be converted either to the corresponding carboxylic acid ($H_3O^+$ in dioxane) or aldehyde (K-selectride and then $H_2O$) depending on the reaction conditions. Due to the mild conditions, the reaction is tolerant toward a large variety of functional groups including nitriles, ketones, esters, alkenes, alkynes, ethers, and halides, and enantioselectivities are usually high ranging from 87% to 97% ee.

*Conclusion* The Myers' alkylation appears year after year to be a simple and robust method to create new carbon–carbon bonds in a highly diastereoselective fashion even with complex precursors. As such, this alkylation process is undoubtedly an unavoidable method in the modern toolbox of the synthetic organic chemist.



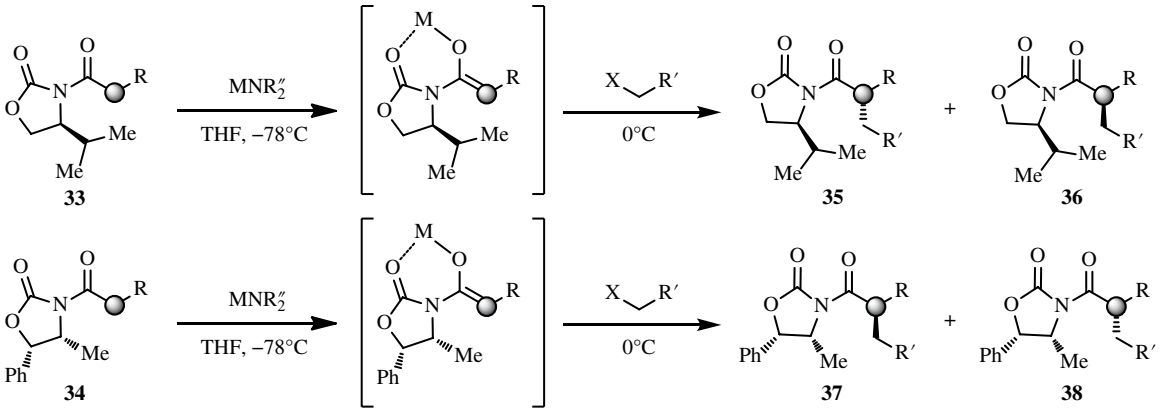

**SCHEME 2.40** Synthesis of (+)- and (−)-pseudophenamines by Myers.




**SCHEME 2.41** Traceless α-allylation.

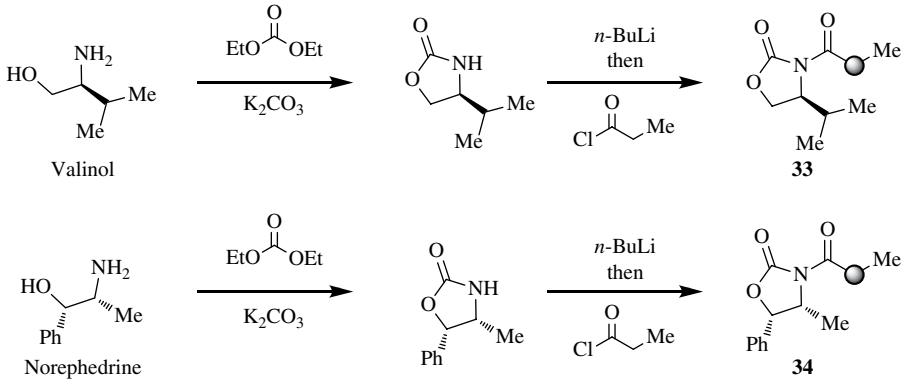
### *2.2.1.3 Evans' Alkylation*

*Seminal Work* In the early 1980s, Evans introduced the use of chiral oxazolidinones as auxiliaries in asymmetric synthesis [47]. These chiral auxiliaries found use in a variety of synthetic transformations, including the diastereoselective alkylation of enolates, usually generated using a hindered base such as LDA or NaHMDS in THF at −78°C [48]. Under these conditions, the *Z*-enolate is predominantly formed as the metal is chelated by the oxygen atom of the enolate and the carbonyl of the oxazolidinone, thus providing a face discrimination (Scheme 2.42). The alkylation occurs in typically 2–4 h at 0°C using 3 equivalents of the electrophile,




| Entry | Imide | Alkylating reagent | dr (crude) **35**:**36** or **37**:**38** | dr (purified) **35**:**36** or **37**:**38** | Yield (%) |
|---|---|---|---|---|---|
| 1 | **33** (R = Me) | $PhCH_2Br$ | 98:2 | >99:1 | 92 |
| 2 | **34** (R = Me) | $PhCH_2Br$ | >99:1 | >99:1 | 78 |
| 3 | **33** (R = Me) | $CH_2=CH\text{-}CH_2Br$ | 98:2 | >99:1 | 71 |
| 4 | **34** (R = Me) | $CH_2=CH\text{-}CH_2Br$ | 98:2 | >99:1 | 75 |
| 5 | **33** (R = Me) | EtI | 94:6 | >99:1 | 36 |
| 6 | **34** (R = Me) | EtI | 88:12 | >99:1 | 53 |
| 7 | **33** (R = Et) | MeI | 89:11 | 99:1 | 79 |
| 8 | **34** (R = Et) | MeI | 87:13 | >99:1 | 82 |

**SCHEME 2.42** Diastereoselective alkylation of enolate derived from acyloxazolidinones.



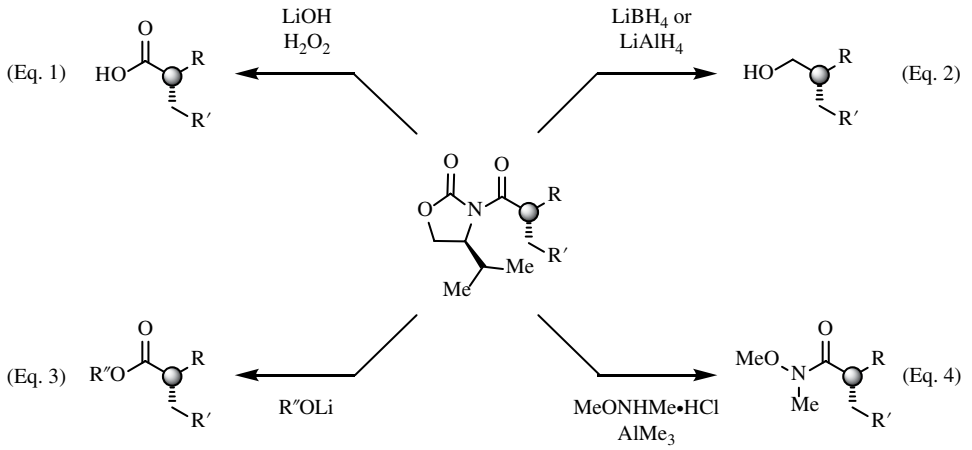

**SCHEME 2.43** Preparation of chiral Evans imides.

and the diastereoselectivity is usually excellent (dr > 99:1). As a general trend, activated alkylating agents such as iodomethane, benzylbromide, or allylbromide give excellent results both in terms of yields and selectivities. Interestingly, alkyl triflates can be used when less reactive electrophiles do not provide the desired alkylated product [49].

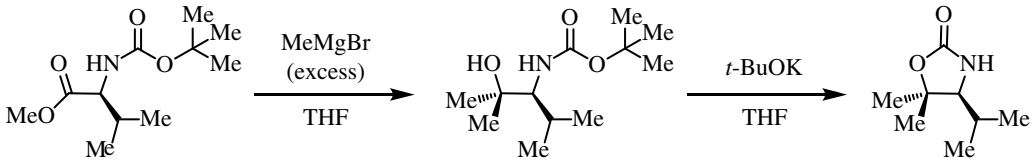
*Preparation of Acylated Oxazolidinones* The Evans diastereoselective alkylation precursors are generally prepared in two steps starting from the corresponding β-aminoalcohols, which are themselves prepared by reduction of the related optically active α-amino acids (typically valine, phenylalanine, and phenylglycine) or available from natural sources such as norephedrine (Scheme 2.43). The reaction between the aminoalcohol and phosgene provides the oxazolidinone; however, diethylcarbonate can also be a friendly alternative to phosgene or triphosgene [50]. The acylation of the oxazolidinones requires deprotonation with *n*-BuLi and then treatment with an acyl chloride to afford the desired acyloxazolidinones.

*Cleavage* Several protocols have been developed in order to remove the chiral auxiliary without eroding the chiral information obtained during the diastereoselective alkylation process (Scheme 2.44).

Hence, the hydrolysis of the imide can be performed using LiOH [51]; however, when the substrates are too hindered, the regioselectivity of the hydroxide addition can be altered leading to the ring opening of the oxazolidinone. To




**SCHEME 2.44** Posttransformations of alkylated chiral imides.

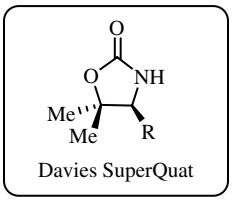



**39** **40** **41**
62% (2 steps)

**SCHEME 2.45** Preparation of *i*-Pr SuperQuat.

limit this undesired side reaction, $HOO^-$ can be used (Scheme 2.21, Eq. 1) [52]. The reduction of the imide can also be envisioned using $LiBH_4$ or $LiAlH_4$ (Scheme 2.21, Eq. 2) [53]. Interestingly, the imides can also undergo transesterification using lithium alcoholates (Scheme 2.21, Eq. 3) or transamidation using a mixture of $AlMe_3$ and MeONHMe. HCl (Scheme 2.21, Eq. 4) [54].

*Related Chiral Auxiliaries for Diastereoselective Alkylation*


Davies SuperQuat

In 1995, Davies and Sanganee introduced a new chiral auxiliary derived from Evans' oxazolidinones [55, 56]. The so-called SuperQuat incorporates a gem-dimethyl group at the 5 position of the oxazolidinone, which provides particular properties that are distinct from the traditional Evans auxiliaries. Their preparation follows a slightly different synthetic route [57] starting from the Boc-protected methylester of the corresponding amino acid (**39**). Hence, the addition of MeMgBr affords the tertiary alcohol **40**, which can then be converted to the corresponding oxazolidinone **41** using potassium *tert*-butoxide (Scheme 2.45).

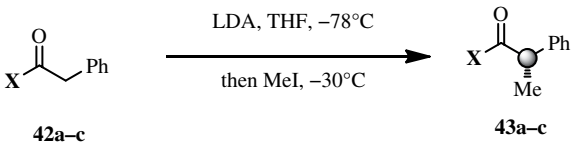
In many cases the diastereoselectivities obtained using Davies' SuperQuat are higher than the ones obtained using Evans' oxazolidinones (Scheme 2.46).

The explanation of this improved diastereoselectivity can be rationalized by a conformational effect induced by the added gem-dimethyl group [58]. Indeed the steric hindrance produced by the two methyl groups forces the isopropyl to rotate and offer a better shielding effect (Scheme 2.47). This explanation was confirmed by NOE experiments [59].

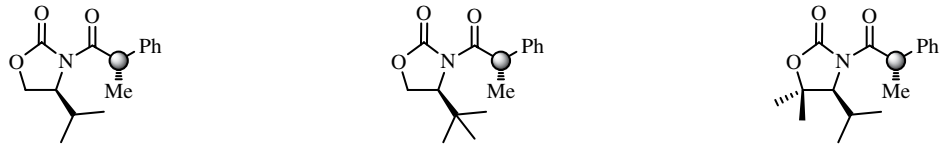
As previously mentioned the Evans oxazolidinones are sensitive to alcaline hydrolysis (e.g., with LiOH) as they can undergo ring opening to form the undesired "endocyclic products." Interestingly, Davies' SuperQuat prevents this side reaction to occur as the gem-dimethyl group provides shielding to the endocyclic C=O. This was confirmed by submitting both Evans- and Davies-derived pivaloyloxazolidinones to LiOH (Scheme 2.48). Indeed, with the Evans oxazolidinone, a mixture of endo- and exocyclic products was obtained, while only the exocyclic product was formed when using the SuperQuat.

In addition, in contrast to Evans' auxiliary, it is possible to effectively cleave Davies' auxiliary and isolate the corresponding aldehyde with no erosion of the selectivity using DIBAL at −78°C followed by a treatment with a saturated aqueous solution of $NH_4Cl$ (Scheme 2.49). Under these conditions, the chiral auxiliary can be recovered in over 90% yield and reused [60].

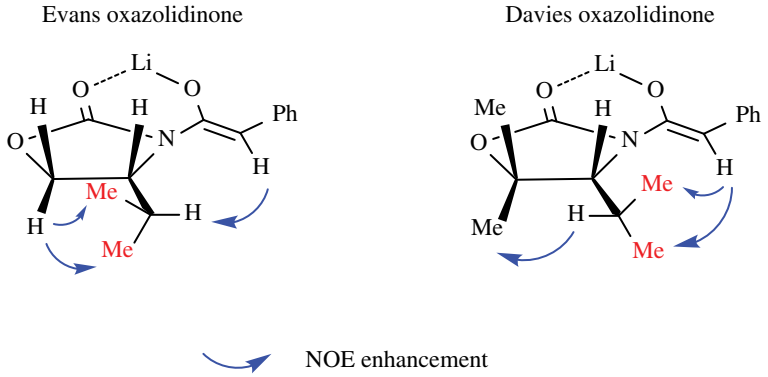
More recently, the group of Brigaut described the use of chiral 4-phenyl-2-trifluoromethyloxazolidine as an excellent chiral auxiliary in the diastereoselective alkylation of



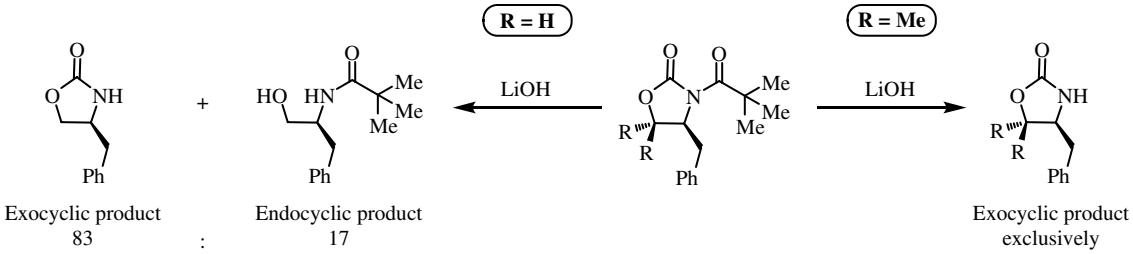

Selected examples:




**SCHEME 2.46** Comparison of selectivities induced by *i*-Pr, *t*-Leu oxazolidinones, and *i*-Pr SuperQuat auxiliaries during diastereoselective alkylation.




**SCHEME 2.47** Conformational impact of the gem-dimethyl group in SuperQuat enolate.

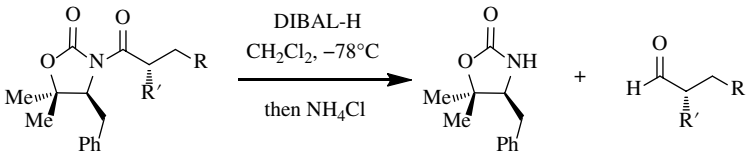



**SCHEME 2.48** Comparison between the Evans and the Davis oxazolidinones over hydrolysis by LiOH.

enolates (Scheme 2.50) [61]. This new chiral auxiliary affords high levels of diastereoselectivity on a large range of alkyl halides. DFT calculations suggest an interaction between the sodium atom and a fluorine atom of the $CF_3$ group, which rigidifies the enolate intermediate [62].

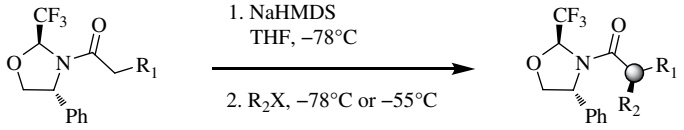
*Other Electrophiles* Other electrophiles can be used in order to obtain new C–C, C–O, C–N, and C–X bonds in a diastereoselective fashion (Scheme 2.51), the most common one being perhaps aldehydes, which can undergo diastereoselective aldolization with the concomitant control of two new stereogenic centers [63] (Scheme 2.51, Eq. 1). This transformation uses boron enolates to react with the aldehydes through a Zimmerman–Traxler transition state (please refer to Section 2.3 for a detailed description).

Some more or less conventional electrophiles can also be used to generate new C–C bonds in a diastereoselective fashion. These include orthoesters, which require the use of titanium enolates [64] (Scheme 2.51, Eq. 2), and acyl chlorides, which lead to the formation of β-ketoimides bearing a stereogenic center between the two C═O [65] (Scheme 2.51, Eq. 3) and Michael acceptors [66] (Scheme 2.51, Eq. 4).




| Entry | R | Imide R′ | dr | Aldehyde | |
|---|---|---|---|---|---|
| | | | | Yield (%) | ee (%) |
| 1 | Ph | Me | 92.5:7.5 | 87 | 87 |
| 2 | Ph | Allyl | 93:7 | 76 | 87 |
| 3 | Ph | Prenyl | 97:3 | 74 | 94 |
| 4 | *i*-Pr | Bn | 95.5:4.5 | 95 | 91 |
| 5 | Me | Bn | 97:3 | 95 | 94 |

**SCHEME 2.49** Reductive cleavage of Davis oxazolidinones.




Selected examples:



78% (de > 99%) | 74% (de > 99%) | 78% (de > 99%) | 71% (de > 99%)

**SCHEME 2.50** Diastereoselective alkylation of *N*-acyl oxazolidines by Brigaut.

Oxygenation can also be performed using the chiral enolates derived from Evans' imides and an oxaziridine [67] (Scheme 2.51, Eq. 5), while C–N bonds can be generated diastereoselectively using either di-*tert*-butyl azodicarboxylate [68] (Scheme 2.51, Eq. 6) or trisyl azide [69] (Scheme 2.51, Eq. 7). Finally, *N*-bromosuccinimide (NBS) was also shown to react with Evans' enolates to form C–Br bonds stereoselectively [70] (Scheme 2.51, Eq. 8).

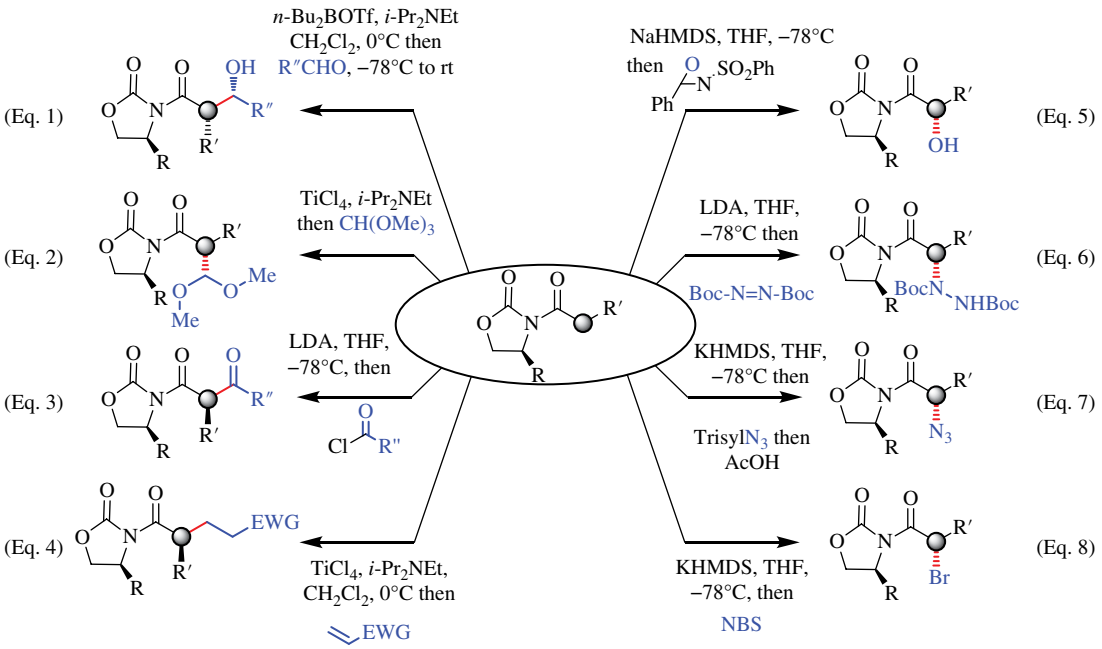
*Conclusion* After the chiral hydrazones developed by Enders, Evans introduced the chiral oxazolidinones, which appeared to be particularly useful not only for the diastereoselective alkylation of azaenolates but also on a wide range of asymmetric transformations, finding applications in the synthesis of some of the most architecturally appealing and complex natural products.

## 2.2.2 Applications of Asymmetric Alkylation Reactions in Total Synthesis of Polyketides and Macrolides

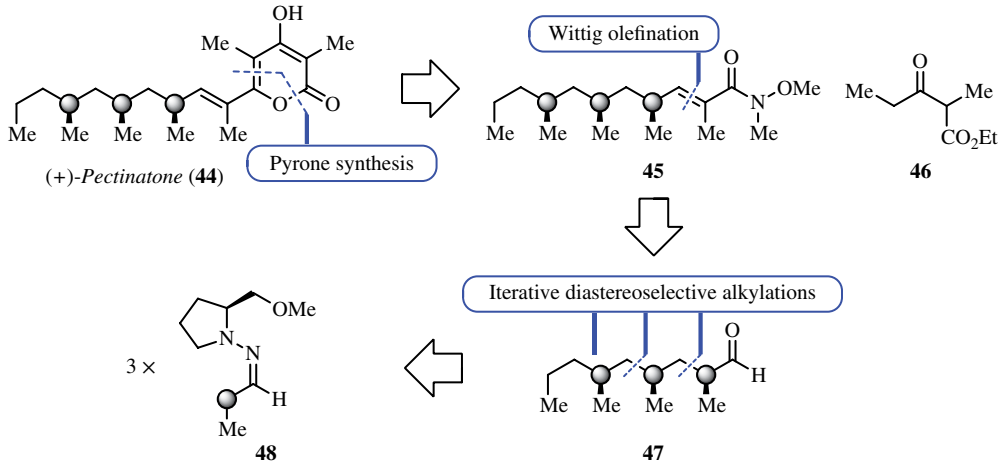
### *2.2.2.1 Applications of Enders' Alkylation Reaction*

*(+)-Pectinatone [71]* (+)-Pectinatone is a marine natural product isolated from *Siphonaria* sp. mollusks displaying antibacterial, antifungal, and cytotoxic activities [72]. This molecule presents a pyrone core with a deoxypolypropionate side chain. Birkbeck and Enders applied the iterative diastereoselective alkylations strategy using chiral SAMP hydrazone [71] (Scheme 2.52). Their retrosynthetic analysis involved a late-stage introduction of the pyrone heterocycle by the condensation of the Weinreb amide **45** and the β-ketoester **46**. Weinreb amide **45**, on the other hand, would be obtained through a Wittig olefination starting from aldehyde **47**, which in turn would be built using iterative alkylations of hydrazone **48**.

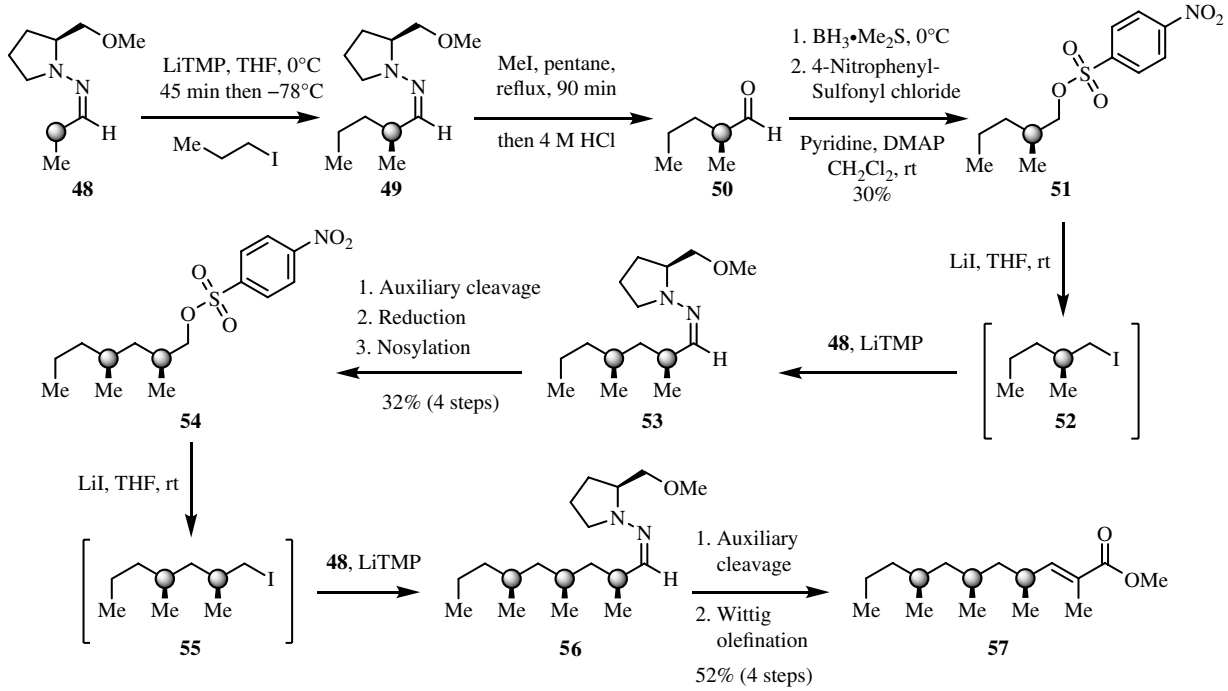
The synthesis of (+)-pectinatone began with the diastereoselective alkylation of hydrazone **48** using lithium tetramethylpiperidide (LiTMP) and iodopropane, which led to the formation of the corresponding alkylated product **49** with a high diastereoselectivity (de = 94%) (Scheme 2.53). The hydrazone was then cleaved using the salt method (MeI in refluxing pentane and then 4 M HCl), and the resulting aldehyde **50** was reduced with borane dimethyl sulfide complex and subsequently converted to the corresponding nosylate **51**. Substitution of the *para*-nitrobenzene sulfonate with lithium iodide eventually led to the volatile chiral iodide **52**, which was subsequently engaged in an alkylation



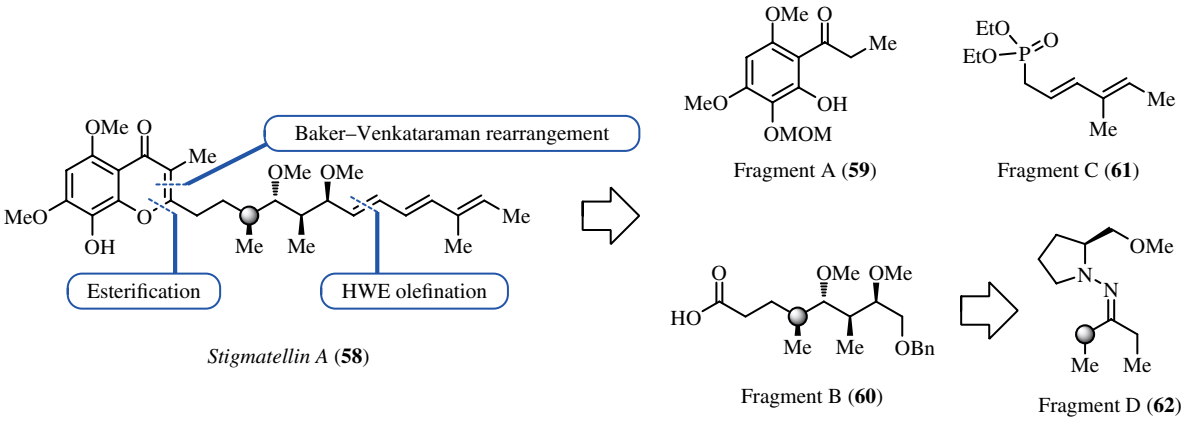

**SCHEME 2.51** Versatility of the Evans chiral oxazolidinones.




**SCHEME 2.52** Retrosynthetic analysis of (+)-pectinatone by Enders.

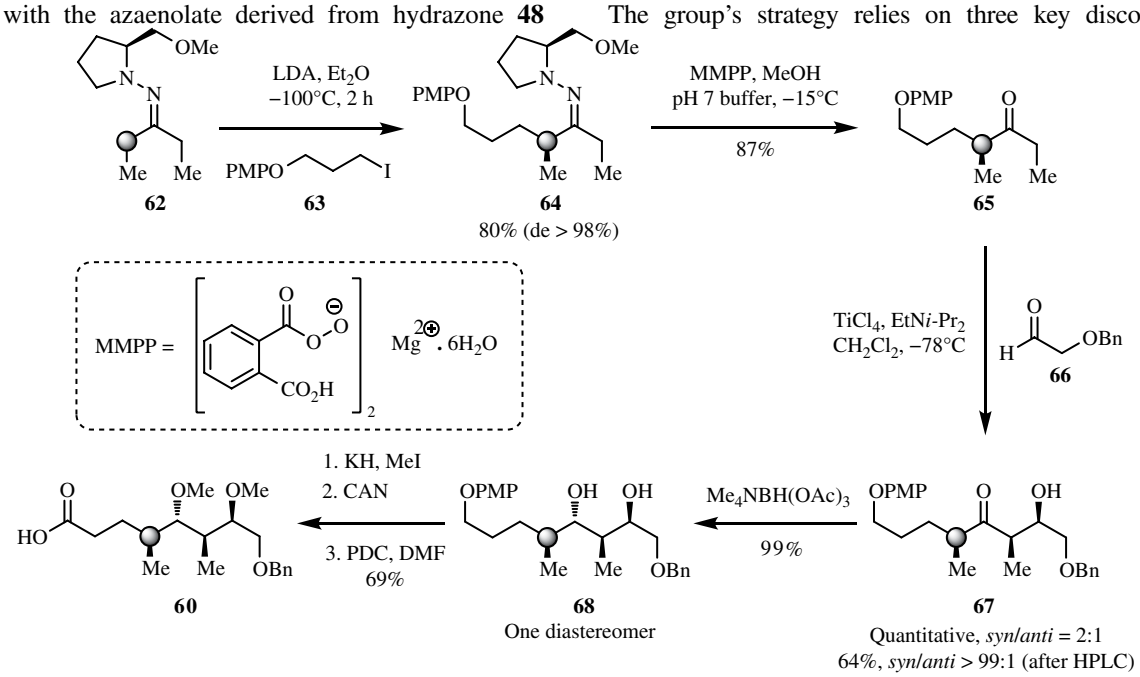



**SCHEME 2.53** Synthesis of intermediate **57** in the synthesis of (+)-pectinatone by Enders.




**SCHEME 2.54** Retrosynthetic analysis of stigmatellin A by Enders.

reaction with the azaenolate derived from hydrazone **48**. The group's strategy relies on three key disconnections:

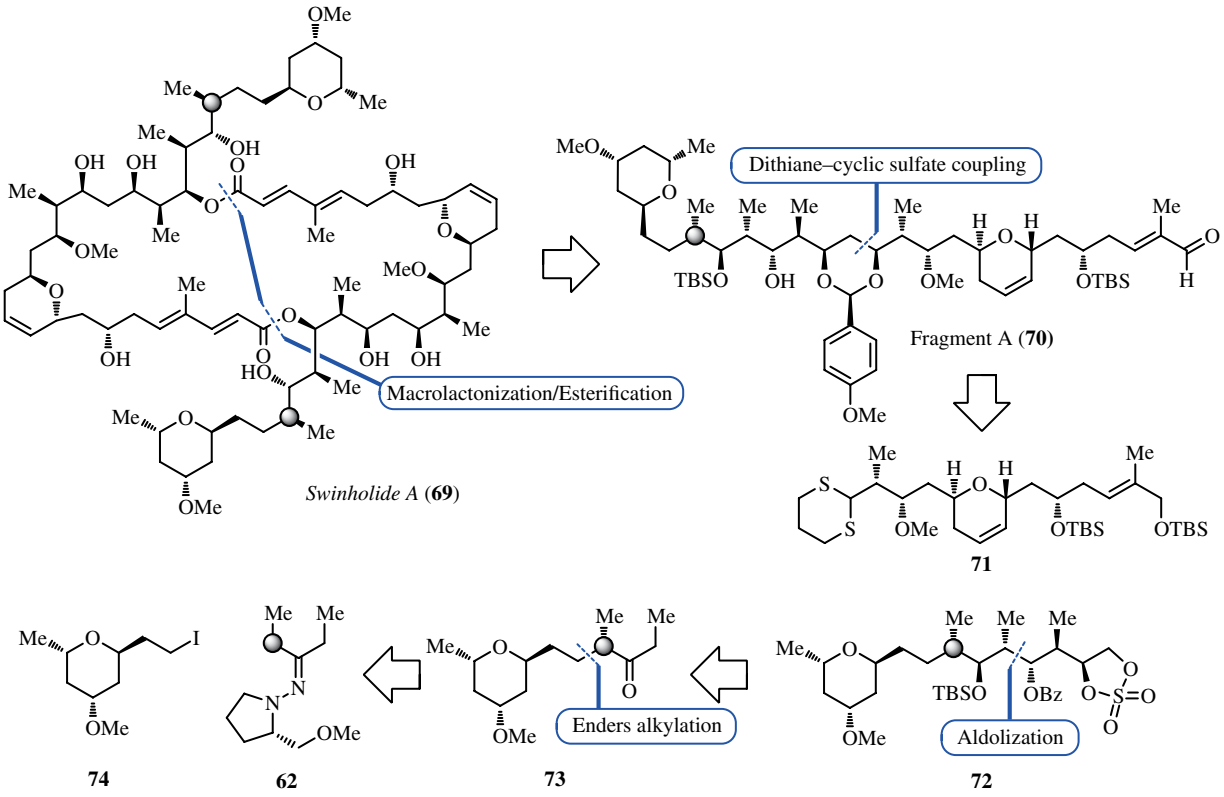



**SCHEME 2.55** Preparation of fragment **B** in the total synthesis of stigmatellin A.

affording **53** with a good diastereoselectivity (de = 86%). The auxiliary cleavage/reduction/nosylation sequence was then repeated to afford intermediate **54**, which was once again converted to an iodide intermediate and engaged in another diastereoselective alkylation reaction. Removal of the chiral auxiliary followed by a Wittig olefination eventually led to the desired ester **57**.

*Stigmatellin A [24]* In 2000, the Enders group achieved the first total synthesis of stigmatellin A (**58**) [73], a natural product isolated by Höfle et al. [74] from myxobacterium *Stigmatella aurantiaca*, which is a powerful inhibitor of electron transport in mitochondria and chloroplasts. an esterification between the functionalized phenol **59** and the central fragment **60**, a Baker–Venkataraman rearrangement at the origin of the chromone formation, and a Horner–Wadsworth–Emmons olefination involving phosphonate **61** to introduce the polyenic portion. The central fragment **60** bearing the *anti–anti–syn* stereotetrad was envisioned using a SAMP hyd8razone-mediated alkylation (Scheme 2.54).

The preparation of fragment B relied on a diastereoselective alkylation of the SAMP hydrazone D followed by a diastereoselective aldolization (Scheme 2.55). Hence, in the presence of LDA in $Et_2O$, the hydrazone was deprotonated and condensed with the alkyl iodide **63**. The alkylated product **64** was obtained in 80% yield and excellent

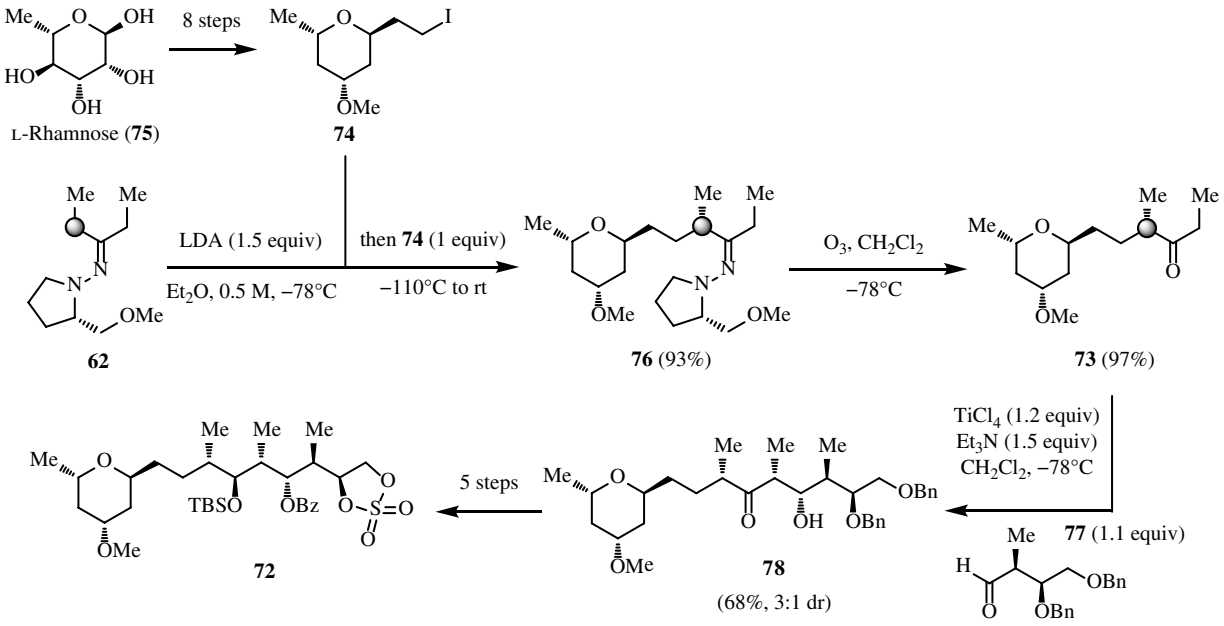



**SCHEME 2.56** Retrosynthetic analysis of swinholide A by Nicolaou.

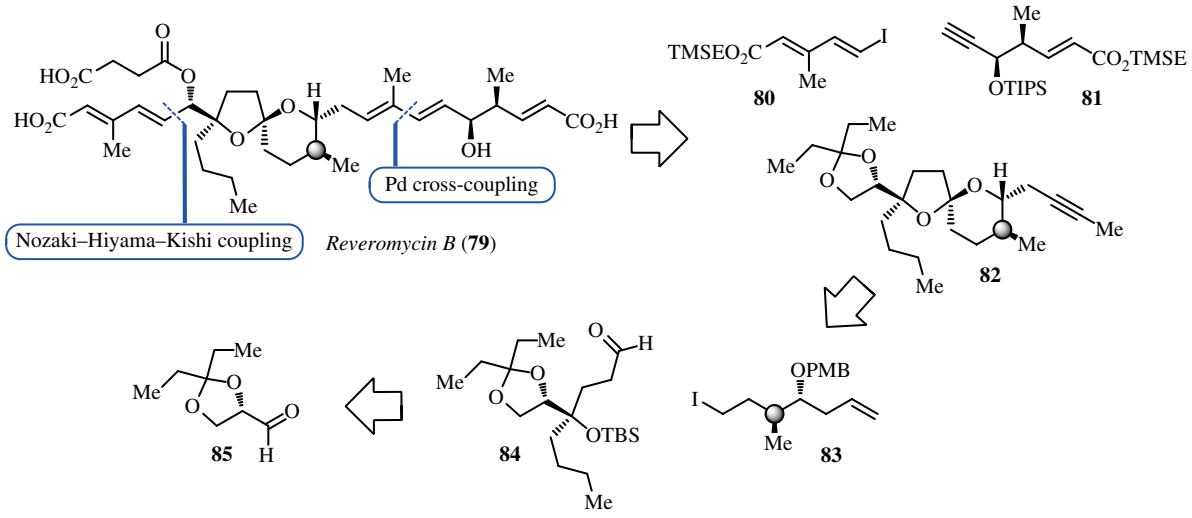
diastereoselectivity (de > 98%). The latter was then converted to the corresponding ketone with concomitant cleavage of the chiral auxiliary using MMPP. The aldolization between ketone **65** and 2-benzyloxyacetaldehyde **66** under Evans' conditions with $TiCl_4$ and Hünig's base led to the corresponding β-hydroxy ketone **67** in quantitative yield albeit with a poor diastereoselectivity (*syn*/*anti* = 2:1). Preparative chiral HPLC separation eventually afforded the aldol product as a single stereoisomer, which was engaged in an Evans–Chapman–Carreira reduction with tetramethylammonium triacetoxyborohydride [$Me_4NBH(OAc)_3$] to give the *anti*-diol **68** in quantitative yield as a single diastereomer. Finally, alkylation of the hydroxyl groups followed by the deprotection of the PMP ether and the oxidation of the corresponding alcohol afforded fragment B in 69% yield.

*Swinholide A [75]* In 1996, Nicolaou's group reported the total synthesis of swinholide A (**69**) [75] after several efforts [76]. This 44-membered macrolide, which was isolated from *Theonella swinhoei* by Carmely et al. [77], exhibits an impressive cytotoxic activity [78] by interacting with the actin cytoskeleton [79]. Due to its interesting C2 symmetry, Nicolaou and coworkers envisioned to build the macrolide core through the dimerization of a monomer after esterification and macrolactonization (Scheme 2.56). The retrosynthetic analysis led to fragment **A** at the origin of both sides, the latter being prepared through an anion coupling between dithiane **71** and the cyclic sulfate **72**. The latter would in turn be obtained by aldolization using ketone **73**, which would itself result from an Enders diastereoselective alkylation between hydrazone **62** and the iodotetrahydropyran **74**. Finally, this iodotetrahydropyran would be prepared starting from L-rhamnose (**75**).

The synthesis of **72** started with the transformation of L-rhamnose (**75**) into the 2,6-*trans*-iodopyran **74** in an eight-step sequence featuring a Lewis acid-mediated allylation using allyltrimethylsilane and a double Barton–McCombie deoxygenation (Scheme 2.57). This 2,6-*trans*-iodopyran was then engaged in an Enders alkylation with the azaenolate derived from hydrazone **62** to afford the corresponding alkylated product **76** in 93% yield. The chiral auxiliary was then removed by ozonolysis to afford ketone **73**, which was used in a titanium-mediated aldolization reaction ($TiCl_4$, $Et_3N$) with aldehyde **77** to obtain the corresponding β-hydroxyketone **78** in 68% yield and a 3:1 diastereoisomeric ratio. Additional Hoveyda–Evans *anti*-reduction, protecting group modifications and cyclic sulfate generation afforded the C18–C31 fragment **72**. With this synthesis, the authors proved that a complex electrophile could be employed; moreover this diastereoselective alkylation/aldolization




**SCHEME 2.57** Synthesis of the C18–C31 fragment of swinholide A by Nicolaou.

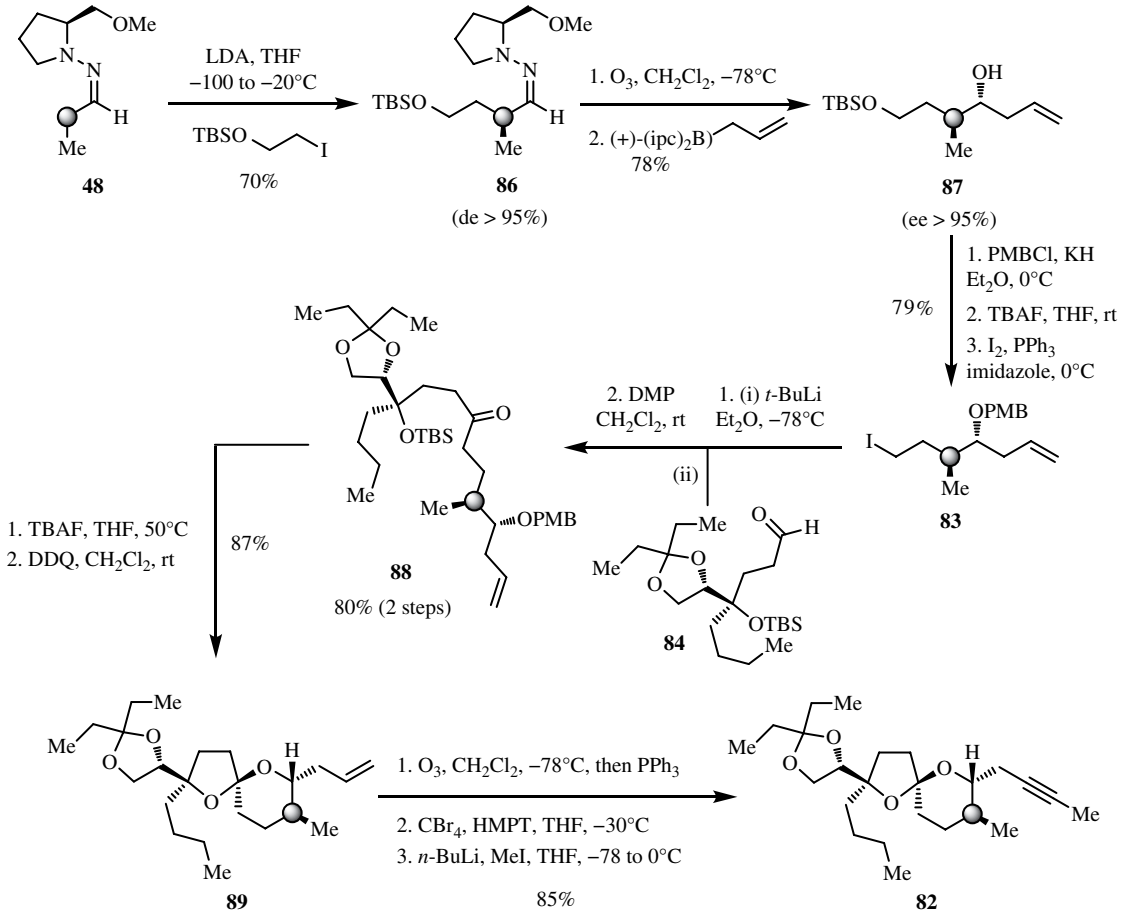



**SCHEME 2.58** Retrosynthetic analysis of reveromycin B by Theodorakis.

sequence furnished a convergent approach generating as much as six stereogenic centers in a limited amount of steps.

*Reveromycin B [81a]* Reveromycin B belongs to a group of four natural products isolated from soil actinomycete, which are characterized by a spiroketal core bearing two functionalized unsaturated side chains [80]. This natural product inhibits eukaryotic cell growth. In 1999, Drouet and Theodorakis described the first total synthesis of reveromycin B [81] in which the side chains were introduced at a late stage using transition metal-catalyzed cross couplings of vinyl iodide **80** with terminal alkyne **81** (Scheme 2.58). The spirocyclic core, on the other hand, was envisioned through a ketalization after assembly of the precursor by condensing iodide **83**, synthesized using a SAMP hydrazone diastereoselective alkylation, to aldehyde **84**.

The synthesis of the spiroketal core represented the major challenge of this work (Scheme 2.59). It started with an Enders diastereoselective alkylation using the SAMP hydrazone **48** to afford the alkylated product **86** in good yield and high diastereoselectivity. An oxidative cleavage under ozonolysis conditions of the hydrazone provided the corresponding aldehyde, which was subsequently engaged in a Brown



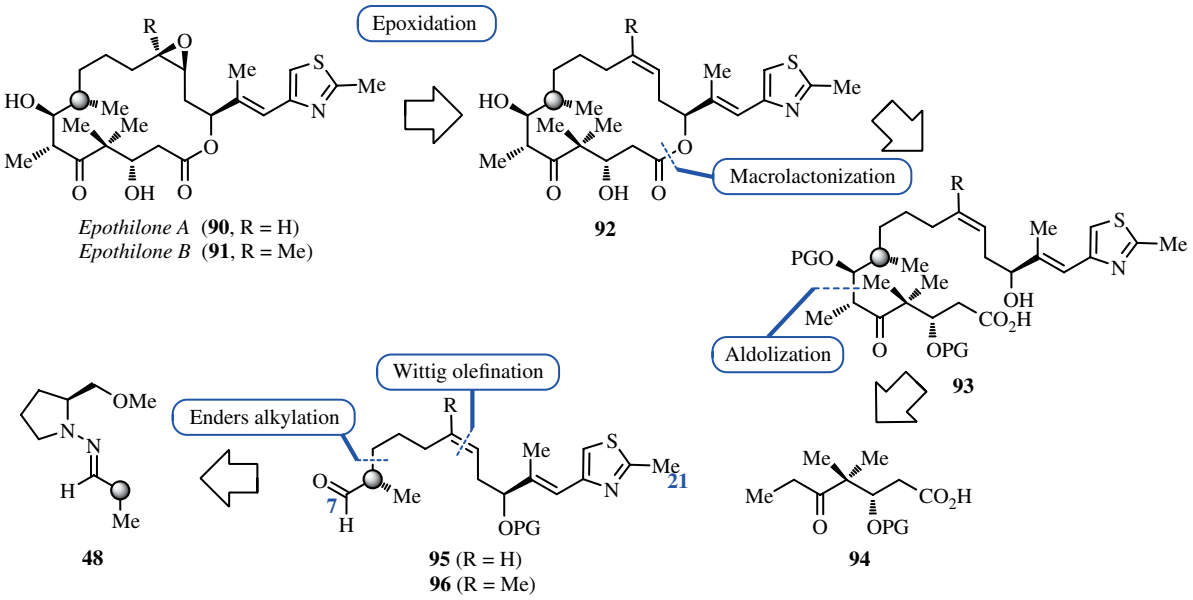

**SCHEME 2.59** Preparation of the spiroketal core of reveromycin B by Theodorakis.

allylation to form the homoallylic alcohol **87**. Protection of the secondary alcohol followed by deprotection of the silyl ether in the presence of TBAF and iodination of the resulting primary alcohol afforded iodide **83** in 62% overall yield. The latter was then converted to the corresponding organolithium species and reacted with aldehyde **84**. The resulting alcohol was eventually oxidized with Dess–Martin periodinane (DMP) giving the ketone **88** in 81% yield over two steps. The deprotection of the hydroxyl groups caused the spontaneous spiroketalization resulting in the formation of compound **89**, which was finally converted to the desired alkyne **82** through a three-step sequence involving the oxidative cleavage of the terminal alkene under ozonolysis conditions and a Corey–Fuchs alkynylation.

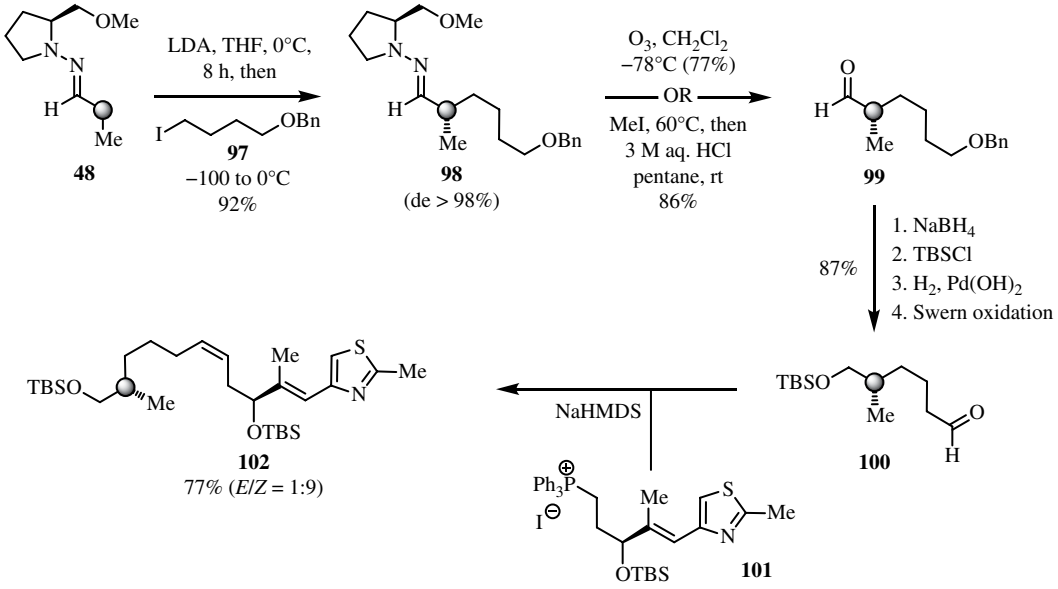
*Epothilones A and B [82]* In 1997, Nicolaou and coworkers reported the total synthesis of epothilones A (**90**) and B (**91**), two natural products isolated from myxobacteria *Sorangium cellulosum* [82]. These molecules exhibit impressive antitumor activities due to important microtubule binding affinities. Their retrosynthetic analysis relied on a late-stage epoxidation and a macrolactonization (Scheme 2.60). The synthesis of the two macrolactone precursors, on the other hand, was envisioned through an aldolization between ketoacid **94** and aldehydes **95** and **96**, the latter being elaborated using SAMP hydrazone diastereoselective alkylations.

The synthesis of the C7–C21 fragments of epothilones A (**95**, Scheme 2.61) and B (**96**, Scheme 2.62) slightly differed due to the nature of the R group. Hence, compound **95** was prepared through an Enders alkylation between hydrazone **48** and the iodo compound **97** affording the alkylated product **98** as a single diastereoisomer. Ozonolysis or alkylating hydrolysis conditions were then employed to remove the chiral auxiliary and afford the corresponding aldehyde **99**, while four additional steps were required to convert this last intermediate to aldehyde **100**. The latter finally underwent a Wittig olefination with **101** to afford the desired C7–C21 fragment **102** with a good diastereoselectivity (*Z*/*E* = 9:1).

To prepare the C7–C21 fragment of epothilone B, a different pathway was taken (Scheme 2.62). First a Wittig reaction was conducted between aldehyde **103** and the ylide **104** to afford triene **105** as a single diastereomer. Three steps were then necessary to convert the ester moiety into a methyl group (**106**) and three additional steps allowed to obtain iodide **107**. The latter was then engaged




**SCHEME 2.60** Retrosynthetic analysis of epothilones A and B by Nicolaou.

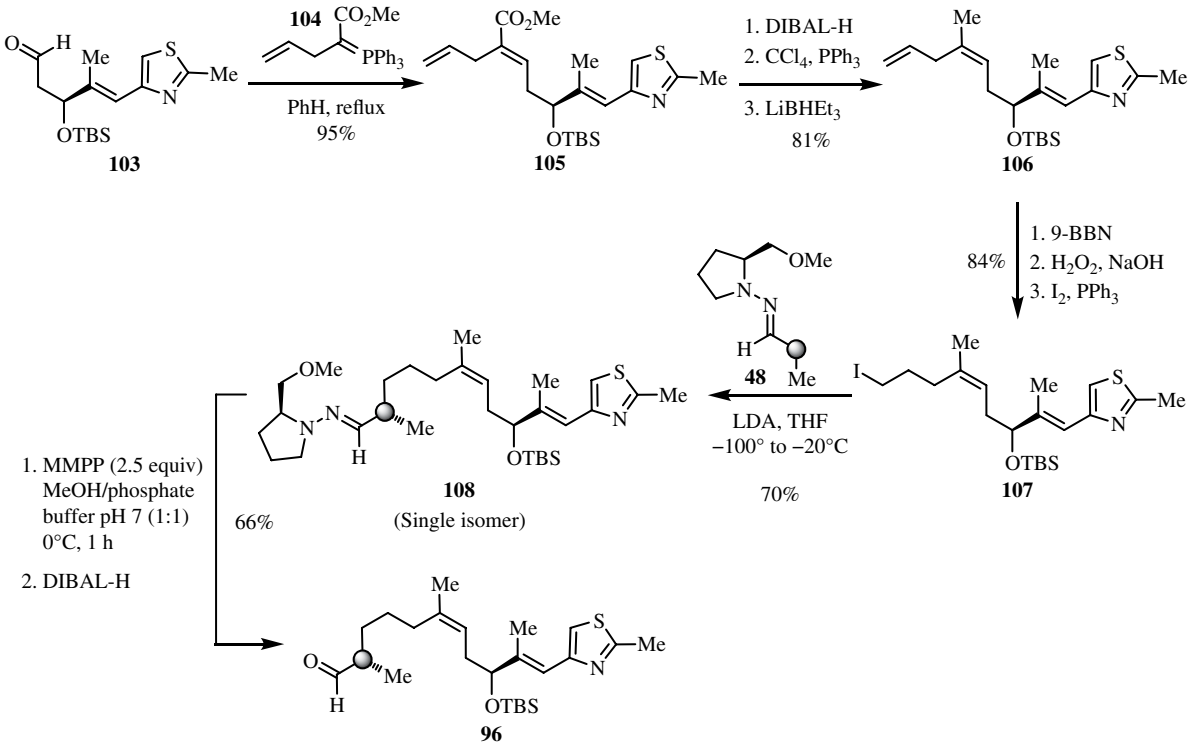



**SCHEME 2.61** Preparation of the C7–C21 fragment **102** of epothilone A by Nicolaou.

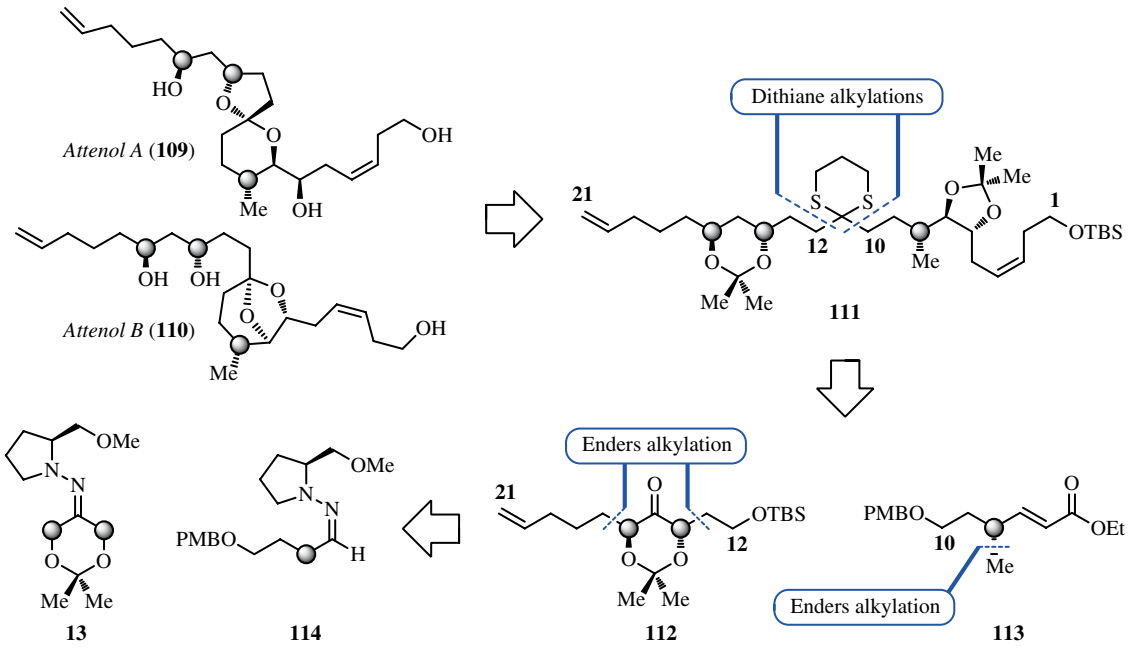
in an Enders alkylation with the enolate derived from hydrazine **48** to afford the corresponding alkylated product as a single isomer. Finally, cleavage of the chiral auxiliary in the presence of monoperoxyphthalic acid magnesium and reduction of the resulting aldehyde with DIBAL-H yielded the required C7–C21 fragment **96**.

*Attenols A and B* [83] In 2003, Enders and Lenzen reported the total syntheses of attenols A (**109**) and B (**110**) [83], two marine natural products isolated from a bivalve *Pinna attenuata* [84]. These two compounds, which are distinguishable by their mode of ketalization, both exhibit interesting cytotoxicity against cancer P388 cell lines at a micromolar level. The authors proposed a convergent approach based on the assembly of the two fragments **112** and **113** using a dithiane linchpin, while the control of the stereogenic centers would be ensured utilizing the SAMP methodology by employing hydrazones **13** and **114**, respectively (Scheme 2.63).

The first of the two key fragments bearing the C12–C21 carbon backbone was synthesized starting from 2,2-dimethyl-1,3-dioxan-5-one SAMP hydrazone **13**, which underwent two successive diastereoselective alkylations using (2-bromoethoxy)-*tert*-butyldimethylsilane and



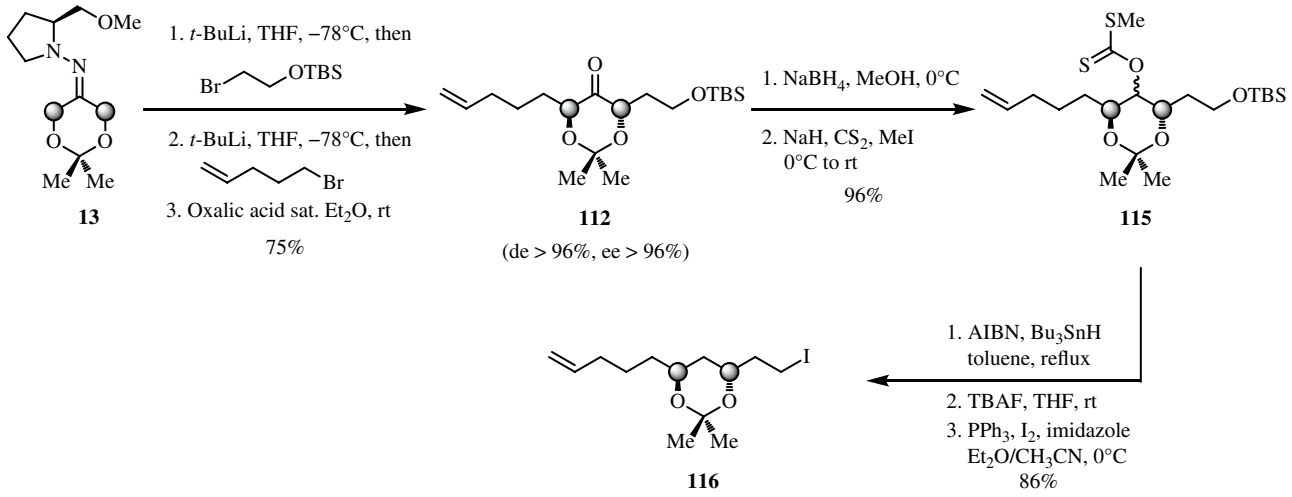

**SCHEME 2.62** Preparation of the C7–C21 fragment **96** of epothilone B by Nicolaou.



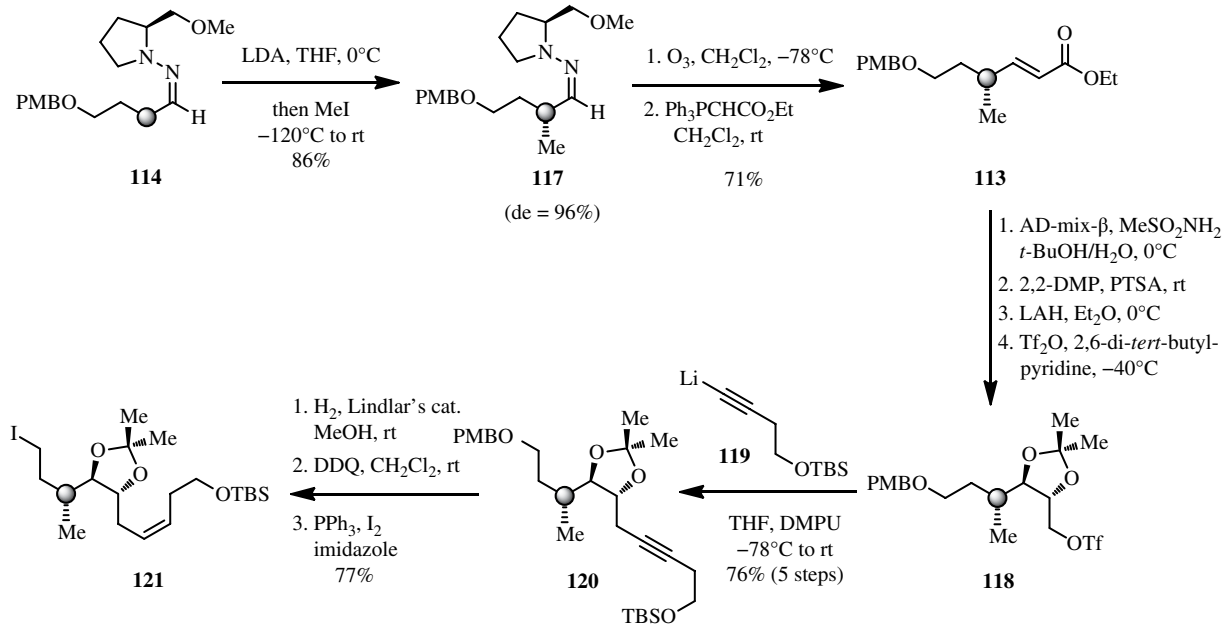

**SCHEME 2.63** Retrosynthetic analysis of attenols A (**109**) and B (**110**) by Enders.

5-bromopent-1-ene as electrophiles (Scheme 2.64). Cleavage of the chiral auxiliary in the presence of oxalic acid afforded ketone **112**, which was deoxygenated *via* a three-step sequence featuring a reduction of the carbonyl moiety, the formation of the corresponding xanthate, and a Barton–McCombie reaction. Finally, deprotection of the primary alcohol and subsequent iodination gave the desired coupling partner in eight steps and 62% overall yield.

The preparation of the other coupling partner **121** (structure not shown in Scheme 2.63) began with a



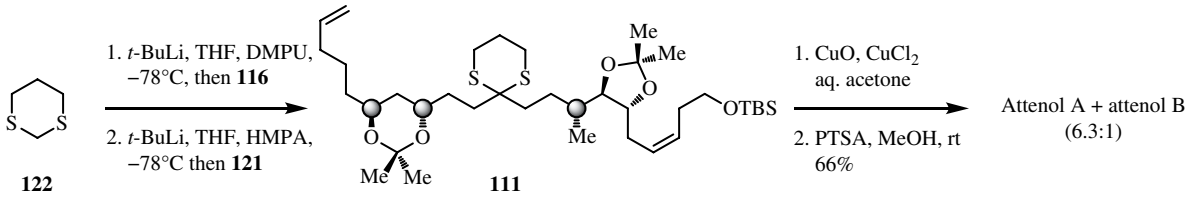

**SCHEME 2.64** Synthesis of the coupling partner **116** in the total synthesis of attenols A and B by Enders.



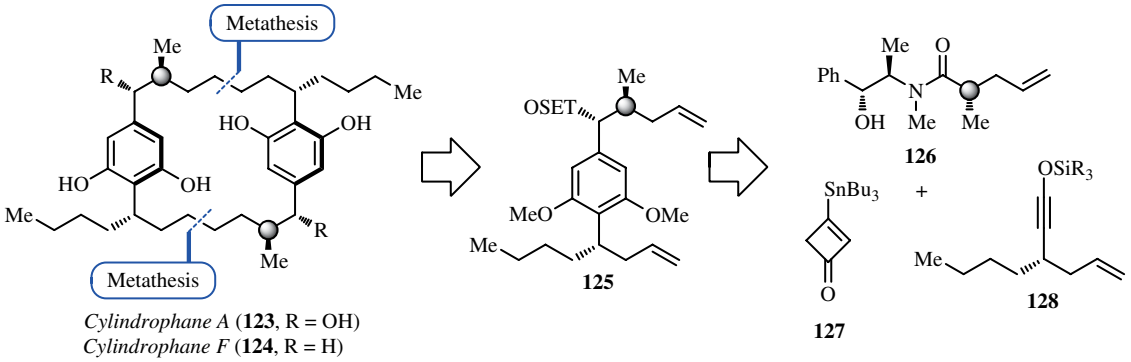

**SCHEME 2.65** Synthesis of the coupling partner **121** in the total synthesis of attenols A and B by Enders.

diastereoselective alkylation of hydrazone **114** with iodomethane (Scheme 2.65). The resulting methylated product **117**, which was obtained in 86% yield and an excellent diastereoselectivity (de = 96%), was subjected to ozonolysis conditions in order to remove the chiral auxiliary. The newly formed aldehyde was then engaged in a Wittig reaction to afford the α,β-unsaturated ester **113**, which was dihydroxylated under Sharpless conditions using AD-mix β. The resulting diol was then protected as an acetonide and the ester moiety converted to the corresponding alkyl triflate **118**. The latter was eventually coupled with the lithium acetylide **119** to afford alkyne **120**, which was partially reduced with Lindlar's catalyst and converted to the corresponding alkyl iodide **121**.

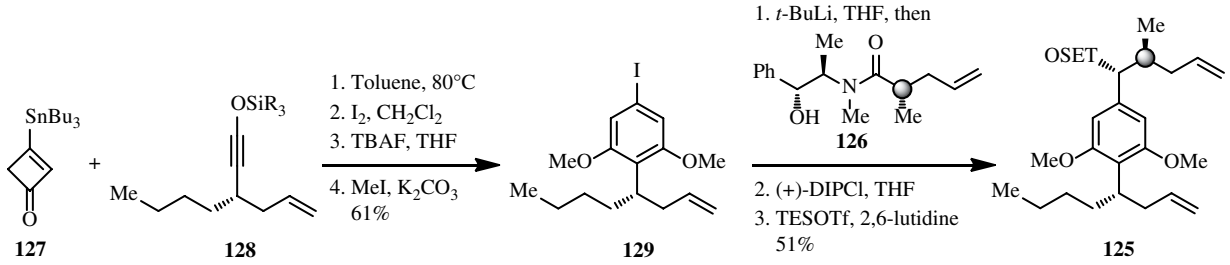
To complete the synthesis of attenols A and B, dithiane **122** was deprotonated with *t*-BuLi and treated with iodide **116** (Scheme 2.66). The resulting product was then engaged in a second alkylation reaction using iodide **121** to afford the attenol A and B precursor **111**. The ketone moiety and the two diols were eventually deprotected, which spontaneously triggered the ketalization leading to a mixture of attenols A and B in a 6.3:1 ratio.




**SCHEME 2.66** Final couplings and end game in the total syntheses of attenols A and B.




**SCHEME 2.67** Retrosynthetic analysis of cylindrocyclophane A (**123**) by Smith.




**SCHEME 2.68** Synthesis of monomer **125** by Smith.

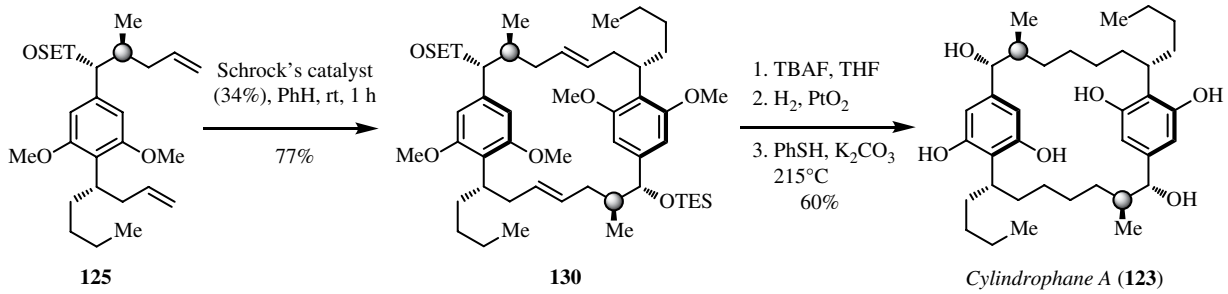
### *2.2.2.2 Applications of Myers' Alkylation Reaction*

*Cylindrocyclophane A [85]* In 2000, Smith and coworkers achieved the total synthesis of cylindrocyclophanes A (**123**) and F (**124**). Their strategy relied on a dimerization by metathesis (Scheme 2.67) [85]. This family of natural products presents an unusual 22-membered [7,7]-paracyclophane structure. Concerning the synthesis of cylindrocyclophane A, two stereogenic centers are controlled by a Myers' alkylation, while the monomer (**125**) is obtained from three different fragments, namely, the product of the Myers' alkylation **126**, cyclobutenone **127**, and the silylated ynol **128** bearing a stereogenic center controlled by an Evans alkylation.

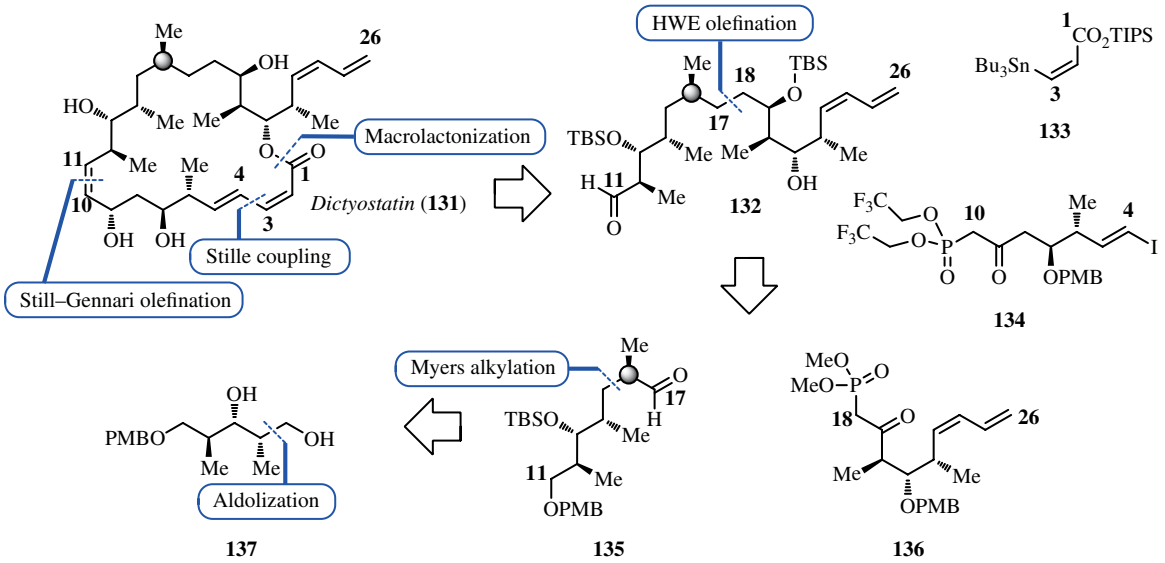
The Danheiser annulation [86] between cyclobutenone **127** and the silylated ynol **128** led to the formation of a resorcinol intermediate, which was converted to the tetrasubstituted aromatic derivative **129** after iododestannylation, desilylation, and etherification (Scheme 2.68). Lithium–iodine exchange followed by condensation with carboxamide **126** then led to a ketone intermediate, which was reduced in a diastereoselective fashion using (+)-DIPCl [87] (dr = 19:1). The resulting alcohol was finally protected to afford the silyl ether-protected monomer **125**.

The final steps of the synthesis of cylindrocyclophane A (**123**) involved the dimerization using Schrock's catalyst [88] followed by the deprotection of two secondary alcohols and a final hydrogenation (Scheme 2.69).

*Dictyostatin [90a]* Due to its exceptional biological profile as a promising anticancer agent at nanomolar concentrations, tremendous efforts have been devoted to the synthesis of dictyostatin (**131**). Indeed, this natural product that was extracted from a sponge from the Indian Ocean by Pettit et al.




**SCHEME 2.69** Completion of the synthesis of cylindrocyclophane A (**123**) by Smith.

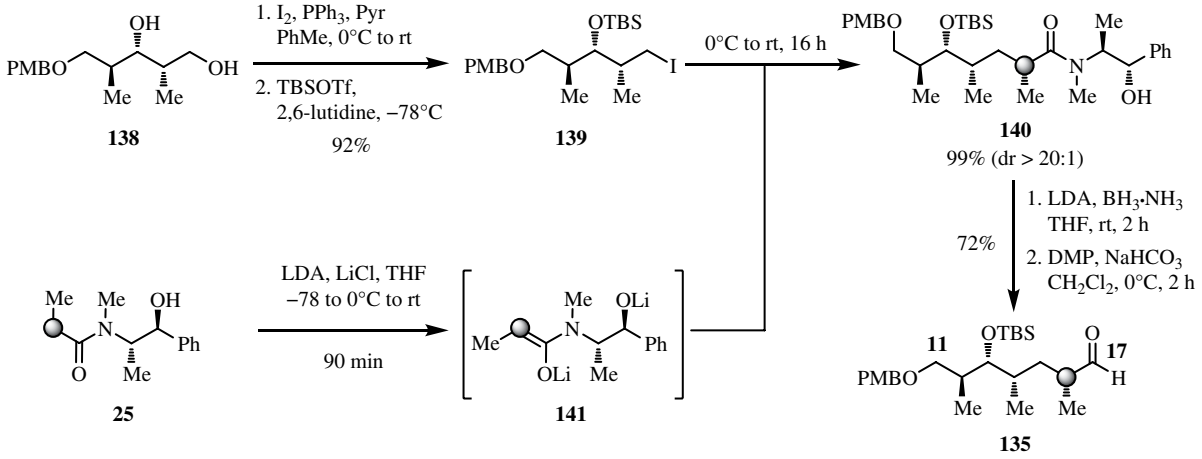



**SCHEME 2.70** Retrosynthetic analysis of dictyostatin by Paterson.

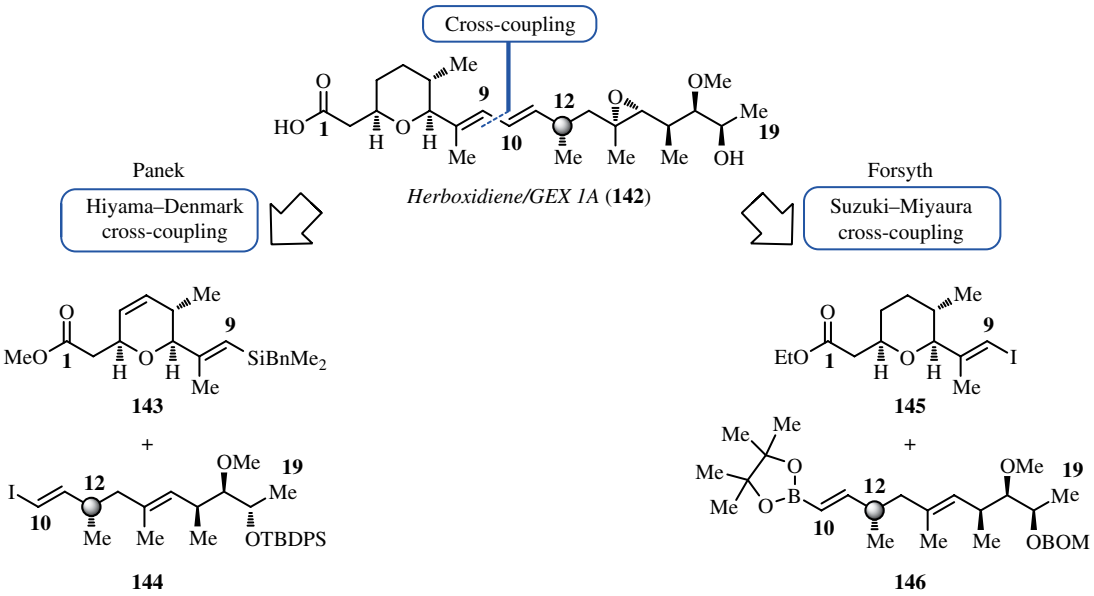
in 1994 [89] exhibits antimitotic activities against multidrug-resistant cell lines with a similar mode of action as Taxol. The group of Paterson described the first total synthesis of this macrolactone and assigned its absolute configuration [90]. The convergent strategy employed by Paterson and coworkers relied on a Yamaguchi macrolactonization, a Stille cross coupling to form the C3–C4 bond, and a Still–Gennari olefination to obtain the C10–C11 bond in a stereoselective fashion (Scheme 2.70). This disconnection led to three fragments including the C11–C26 fragment, which was obtained through a Horner–Wadsworth–Emmons olefination between aldehyde **132** and the β-ketophosphonate **134**. In this synthesis, a Myers' alkylation was used to control the stereochemistry of the stereogenic center at C16.

The preparation of the C11–C17 fragment involved a diastereoselective alkylation between pseudoephedrine carboxamide **25** and the elaborated primary alkyl iodide **139**, which was obtained in a few steps starting from Roche ester (Scheme 2.71) [91]. The alkylation product, which was obtained as a single diastereoisomer (>20:1 dr) in quantitative yield, was then reduced using a LDA/$BH_3{\cdot}NH_3$ mixture and reoxidation to the corresponding aldehyde with DMP.

*Herboxidiene/GEX 1A [93, 94]* Herboxidiene (**142**), also known as GEX 1A and TAN-1609, is a polyketide natural product isolated in 1992 from microorganisms by Isaac and coworkers [92]. This molecule exhibits various biological activities from herbicidal to antitumoral. In 2007 and 2008, the groups of Panek and Zhang [93] and Forsyth and Murray [94] reported two convergent syntheses of herboxidiene, both involving a cross coupling to form the C9–C10 bond (Scheme 2.72). Interestingly, the two syntheses relied on a Myers' alkylation to control the stereogenic center at C12.



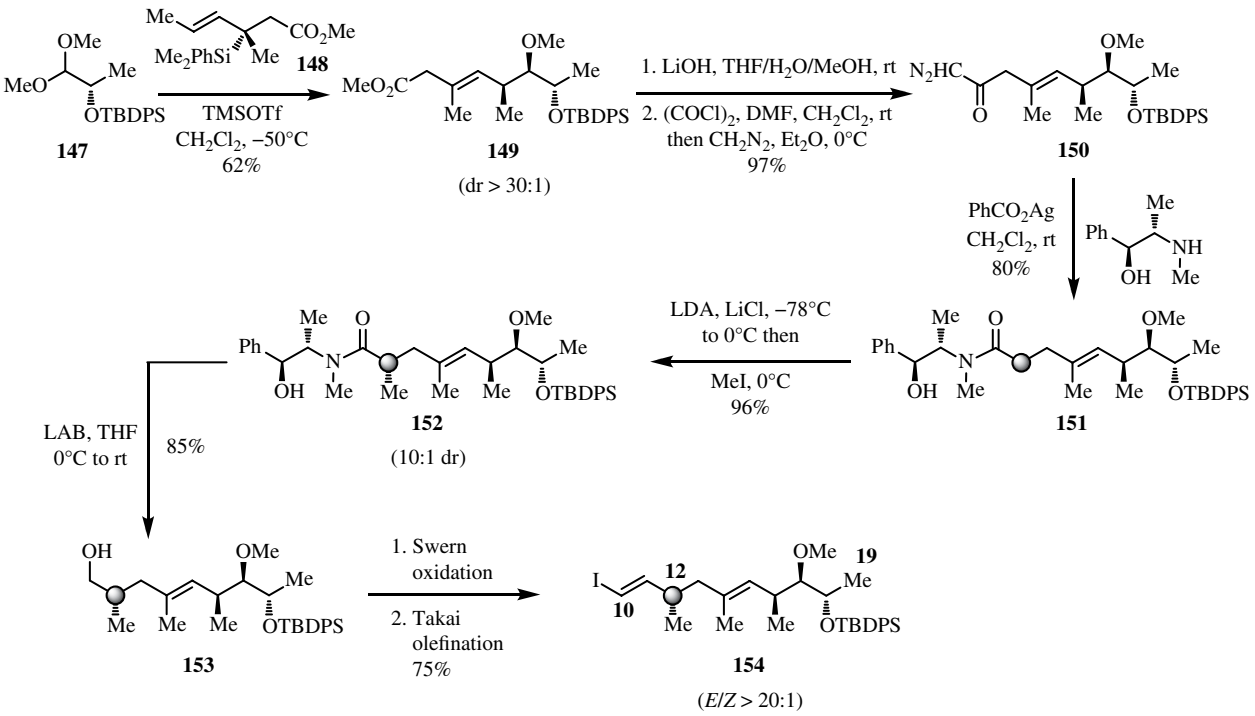

**SCHEME 2.71** Synthesis of the C11–C17 fragment **135** of dictyostatin by Paterson.



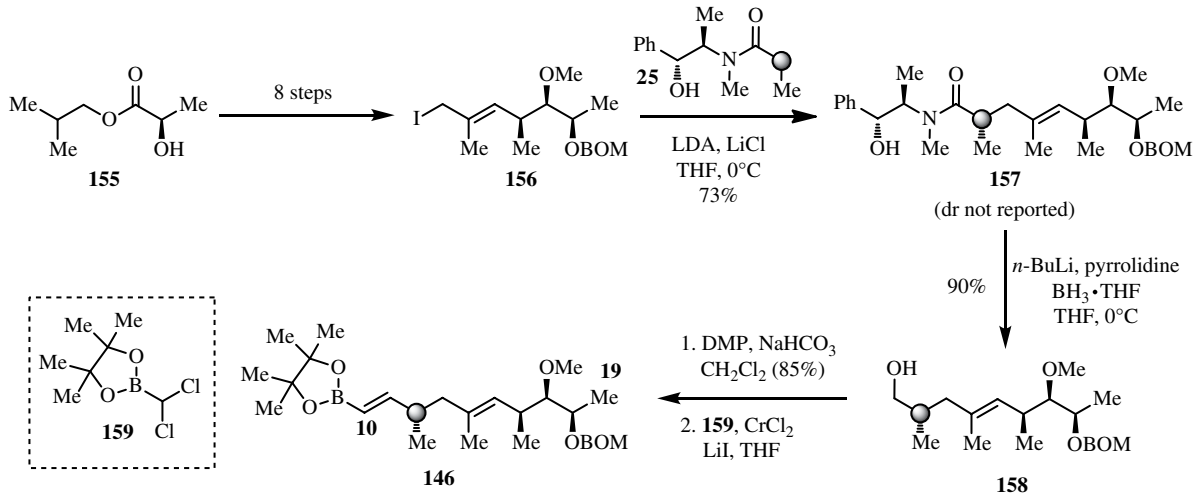

**SCHEME 2.72** Main retrosynthetic disconnections of Panek and Forsyth approaches.

Panek's synthesis of his C10–C19 fragment began by condensing acetal **147** with chiral allylsilane **148** in the presence of TMSOTf affording the ester **149** as a single diastereoisomer (Scheme 2.73). The formation of the ephedrine-derived carboxamide **151** was then conducted by first converting ester **149** to the diazo compound **150**. The latter was then engaged in an Arndt–Eistert rearrangement leading to a ketene intermediate, which was trapped by (+)-pseudoephedrine. The diastereoselective alkylation to introduce the C12 stereogenic center was then performed using iodomethane as the electrophile (dr = 10:1, measured after the removal of the chiral auxiliary). Finally, reduction using LAB followed by a Swern oxidation and a Takai olefination led to the desired C10–C19 vinyl iodide fragment **154**.

Forsyth's synthesis of his C10–C19 fragment of herboxidiene began by the alkylation of propionamide **25** with iodide **156**, initially obtained in eight steps starting from isobutyl lactate (**155**), to control the C12 stereogenic center at an early stage (Scheme 2.74). The efficient reduction of the carboxamide to the corresponding alcohol using *in situ* generated lithiopyrrolidide borane followed by a DMP-mediated oxidation and a Takai reaction with bis-chloroborolane **159** provided the desired C10–C19 vinylboronate fragment.

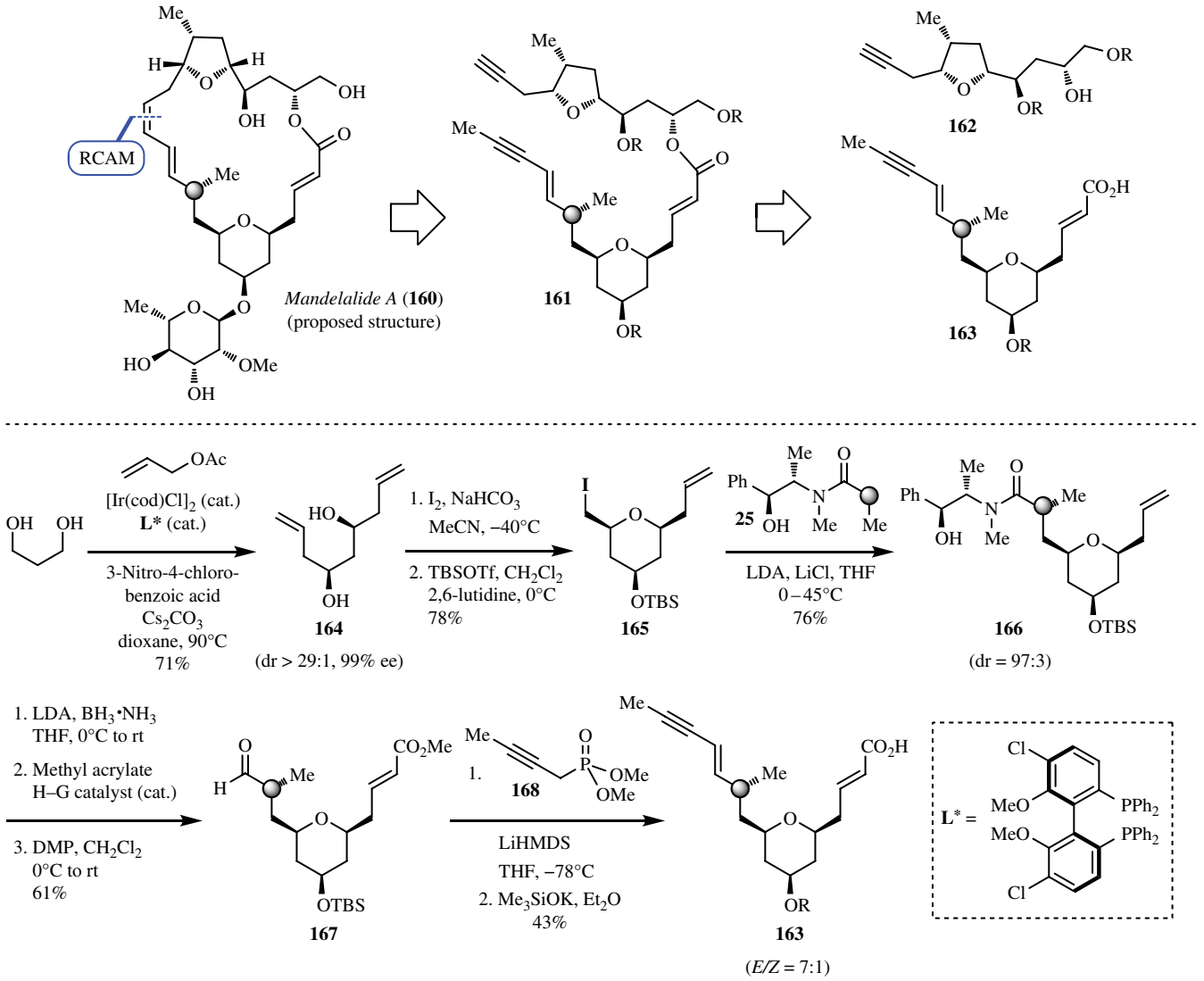



**SCHEME 2.73** Synthesis of C10–C19 fragment of Panek's approach.



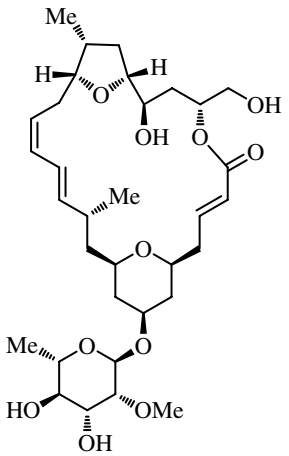

**SCHEME 2.74** Forsyth synthesis of the C10–C19 fragment **146** of herboxidiene.

*Mandelalide A [95]* In 2014, Willmacher and Fürstner reported the putative structure of mandelalide A (**160**) [95], a complex glycosylated macrolactone initially reported by McPhail and coworkers [96] bearing a 2,6-*cis*-tetrahydropyran and 2,5-*cis*-tetrahydrofuran. This molecule, which was isolated from a South African ascidian of the *Lissoclinum* genus, exhibits a strong cytotoxicity against several cancer cell lines. The authors proposed an approach where the macrolactone would be formed by a ring closing alkyne metathesis (RCAM) [97] of diyne **161**. This RCAM precursor would in turn be obtained by the reunion of the northern fragment **162** and the southern fragment **163**, for which a Myers' alkylation was envisioned to control one of the stereogenic centers (Scheme 2.75).

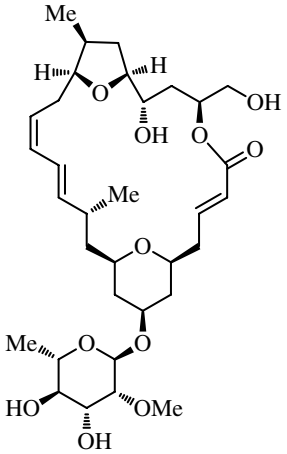



**SCHEME 2.75** Retrosynthetic analysis of putative mandelalide A by Fürstner and synthesis of its south fragment **163**.

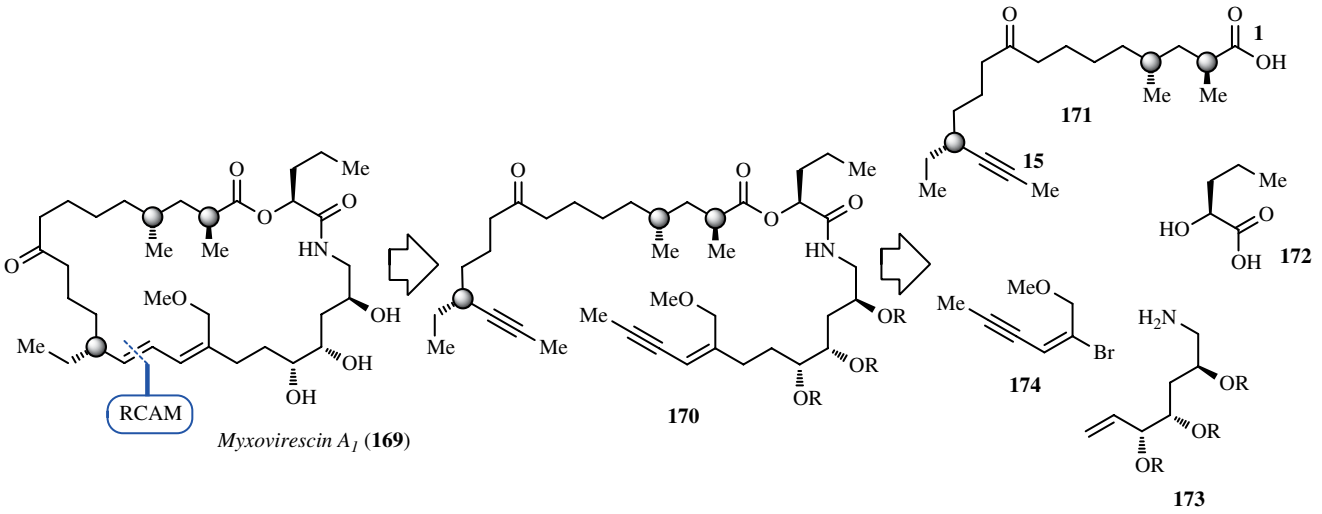
The synthesis of the southern fragment began with an enantioselective Krische bis-allylation of propane-1,3-diol [98] using a chiral iridium complex, which afforded the C2-symmetric diol **164** in 99% ee (Scheme 2.75). The THP **165** was then obtained after a diastereoselective iodo-etherification and the protection of the free hydroxyl group as a *tert*-butyldimethylsilylether. This intermediate was then engaged in a Myers' alkylation with propionamide **25** to form the corresponding alkylated product **166** with a high diastereoselectivity (dr = 97:3). Reductive cleavage of the chiral auxiliary, cross metathesis catalyzed by Hoveyda–Grubbs' catalyst (H–G catalyst), and oxidation of the primary alcohol afforded aldehyde **167**, which underwent olefination with phosphonate **168** and saponification under mild hydrolysis conditions to complete the synthesis of the southern fragment **163**.



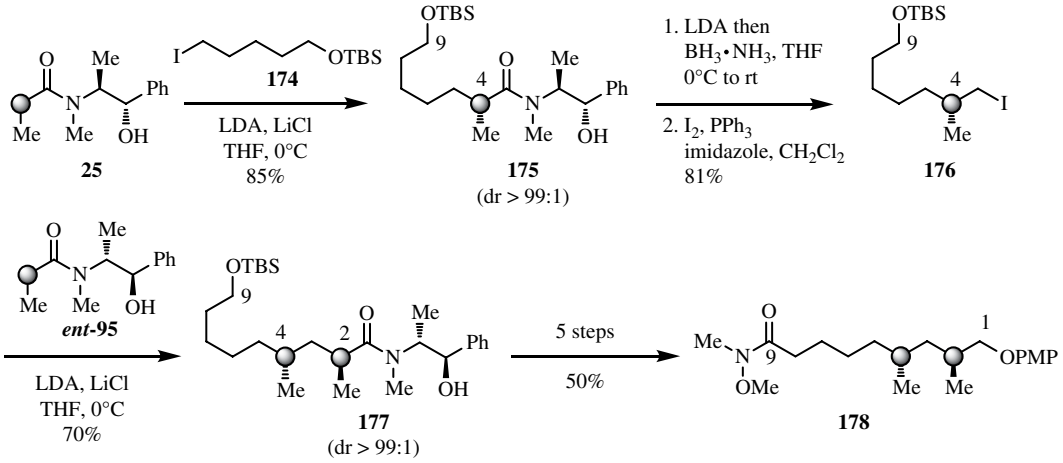
*Mandelalide A*
(proposed structure)



*Mandelalide A*
(revised structure)




**SCHEME 2.76** Retrosynthetic analysis of myxovirescin $A_1$ **169** by Fürstner.



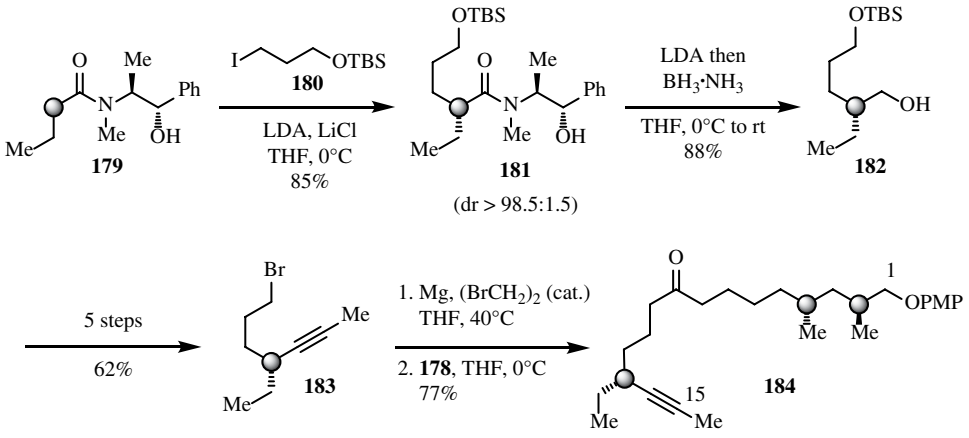

**SCHEME 2.77** Synthesis of C1–C9 fragment **178** of myxovirescin $A_1$ by Fürstner.

The same year, the group of Xu and Ye reassigned the structure of mandelalide A [99] based on the synthesis of the proposed structure and several of its diastereoisomers, one of which matched the $^1$H and $^{13}$C NMR analysis of the natural product.

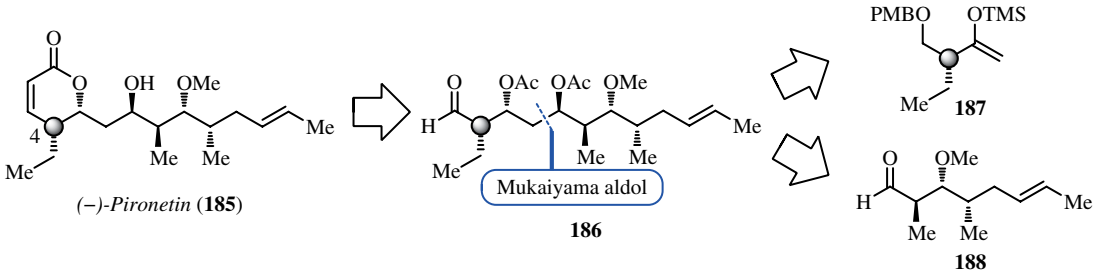
*Myxovirescin A$_1$ [100]* Isolated from *Myxococcus virescens*, the myxovirescins represent a family of 30 macrocyclic congeners exhibiting a broad spectrum of antibiotic activities particularly against Gram-negative bacteria. Myxovirescin $A_1$ (**169**) is a 28-membered macrolactam bearing seven stereogenic centers. As for mandelalide A, Fürstner's group envisioned its retrosynthesis based on the construction of the 28-membered ring through an RCAM [100] (Scheme 2.76). The RCAM precursor **170**, on the other hand, was disconnected into four key fragments, one of them bearing three stereogenic centers that would be controlled using three consecutive diastereoselective Myers' alkylations.

The synthesis began with a diastereoselective Myers' alkylation of the enolate derived from carboxamide **25** with iodide **174** affording the corresponding alkylated product **175** as a single diastereoisomer (de > 98%) (Scheme 2.77). Reductive cleavage of the chiral auxiliary followed by substitution of the hydroxyl group by iodine gave **176**, which was used in a second Myers' alkylation using propionamide **25** to install the stereogenic center at C2. Five additional steps led to the C1–C9 Weinreb amide fragment **178**.

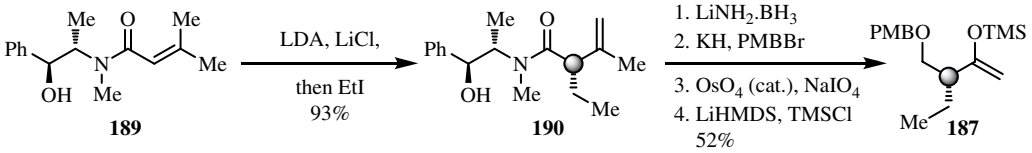
To introduce the third stereogenic center, an additional Myers' alkylation was performed using hydroxamide **179** and iodide **180** (Scheme 2.78). The resulting alkylated product **181**, obtained in high yield and excellent diastereoselectivity, was then converted to the corresponding alcohol **182** through a reductive cleavage of the chiral auxiliary.




**SCHEME 2.78** Synthesis of the C1–C15 fragment **184** of myxovirescin $A_1$ by Fürstner.




**SCHEME 2.79** Retrosynthetic analysis of (−)-pironetin by Keck.




**SCHEME 2.80** Synthesis of the C3–C6 fragment **187** of (−)-pironetin by Keck.

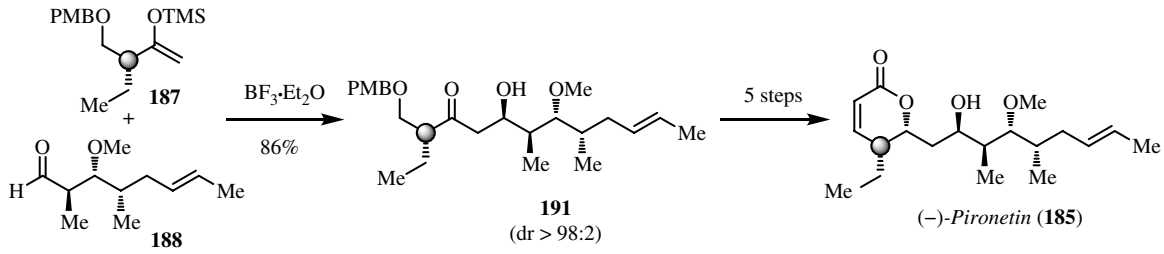
Five additional steps led to bromoalkyne **183**, which was metallated and condensed to the Weinreb amide **178** to afford the C1–C15 fragment **184** in 77% overall yield. Two additional steps eventually led to the required fragment that was used to complete the synthesis of myxovirescin $A_1$.

*(−)-Pironetin [101]* In 2001, Keck and coworkers described the total synthesis of (−)-pironetin **185** [101], an immunosuppressant natural product, which also exhibits a potent cytotoxicity due to the inhibition of the tubulin polymerization [102]. Their strategy relied on a late-stage construction of the δ-lactone and an aldolization between silyl enol ether **187** and aldehyde **188** to build the polypropionate side chain (Scheme 2.79). A Myers' alkylation was envisioned for the control of the C4 stereogenic center.

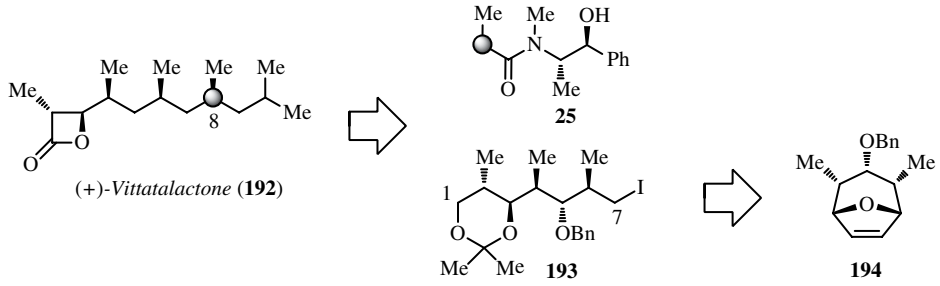
The synthesis of the C3–C6 fragment **186** started with a variant of the Myers' alkylation using acrylamide **189** (Scheme 2.80). Deprotonation under standard conditions (LDA, LiCl) afforded the dienolate intermediate, which was alkylated with iodoethane. Four additional steps including a reductive cleavage of the chiral auxiliary, the protection of the resulting primary alcohol, the oxidative cleavage of the double bond under Johnson–Lemieux conditions, and the formation of the silyl enol ether led to the desired fragment **187**.

The fragments **187** and **188** were coupled together through a diastereoselective Mukaiyama aldolization *via* a Felkin–Anh-type transition state to afford **191** as a single diastereoisomer in 86% yield (Scheme 2.81). Five additional steps eventually led to the completion of the synthesis.

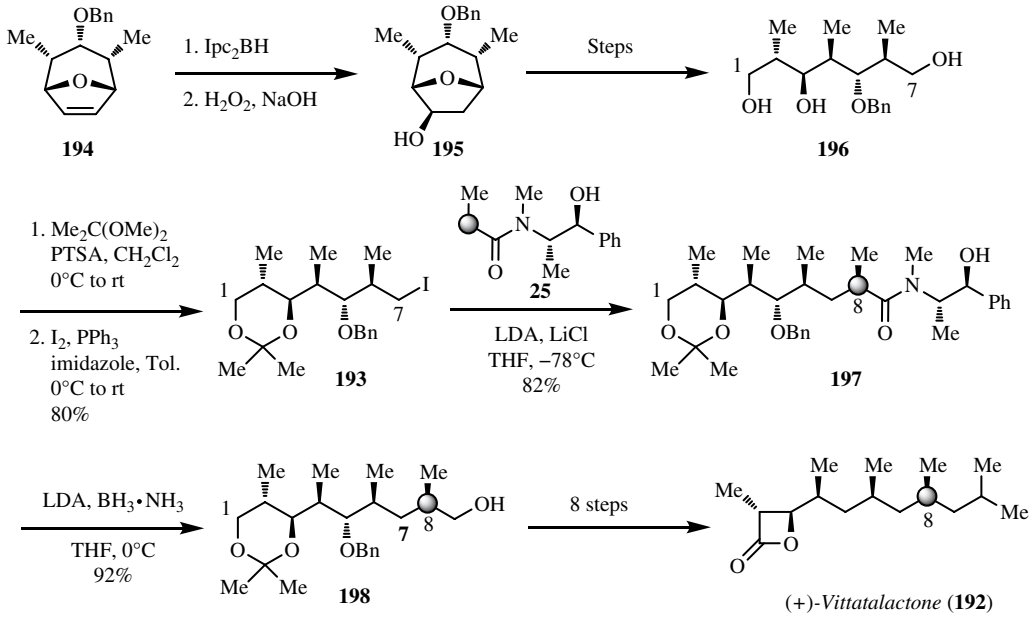
*(+)-Vittatalactone [105]* Vittatalactone (**192**) is a pheromone isolated in 2005 from the striped cucumber beetle *Acalymma vittatum* [103]. This natural product presents a unique structure bearing a *trans*-β-lactone and a deoxypropionate side chain. In 2009, Breit and coworkers assigned both its relative and absolute configurations [104].




**SCHEME 2.81** Completion of the synthesis of (−)-pironetin by Keck.



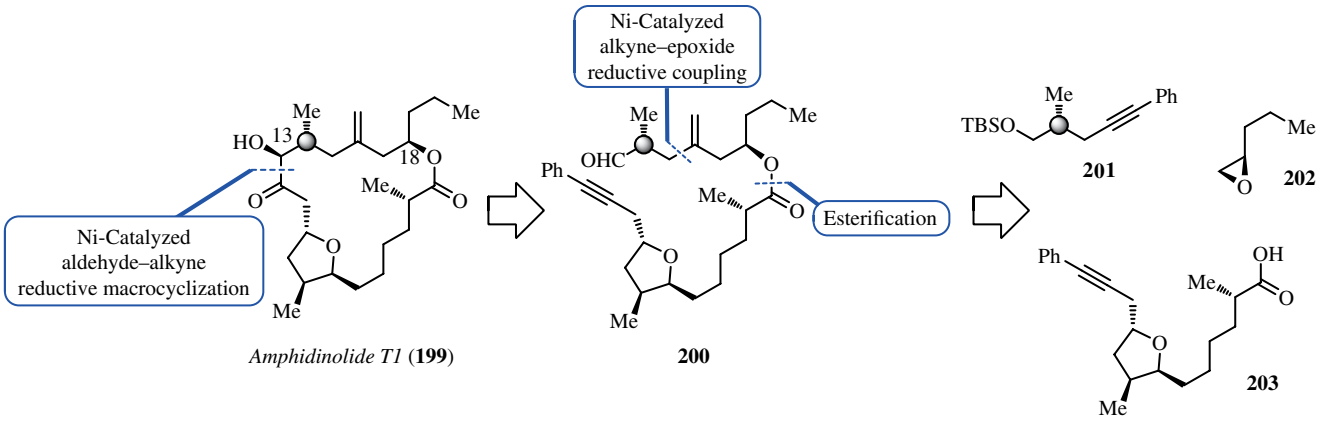

**SCHEME 2.82** Retrosynthetic analysis of (+)-vittatalactone **192** by Yadav.



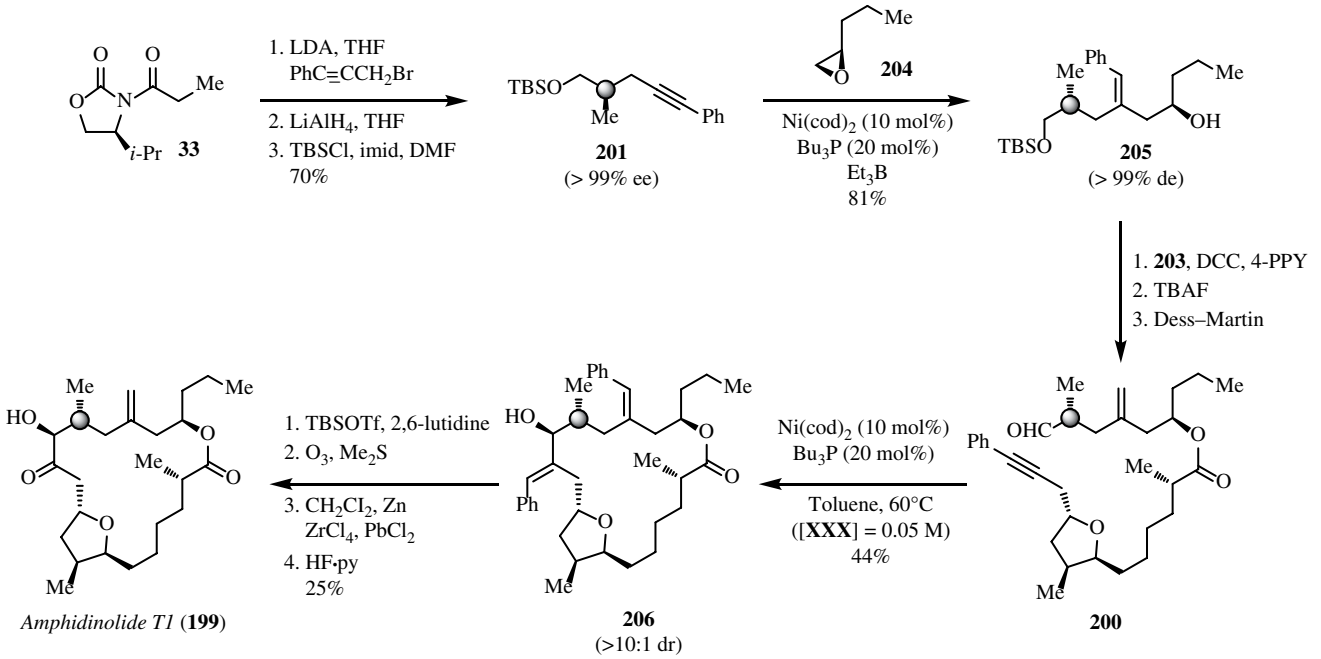

**SCHEME 2.83** Synthesis of (+)-vittatalactone (**192**) by Yadav.

The group of Yadav exploited the hidden symmetry included in a main portion of the natural product (Scheme 2.82) [105]. Their strategy revolved around a key Myers' alkylation between propionamide **25** and iodide **193** corresponding to the C1–C7 fragment of the natural product, which would in turn be obtained starting from *meso* oxabicycle **194**.

Hence, the oxabicycle was desymmetrized using a diastereoselective hydroboration with (+)-$Ipc_2BH$ affording, after oxidation, the alcohol **195** (Scheme 2.83) [106]. This latter intermediate was then converted in a few steps to the known acyclic triol **196**. The 1,3-diol moiety was then protected as a dimethyl acetonide, while the primary alcohol was converted to the corresponding iodide **193**, which was used in a subsequent Myers' alkylation using carboxamide **25** to afford **197** as a single diastereoisomer. A reductive cleavage of the chiral auxiliary using LAB led to alcohol **198**, while eight additional steps allowed to complete the synthesis of the natural product.




**SCHEME 2.84** Retrosynthetic analysis of amphidinolide T1 (**199**) by Jamison.

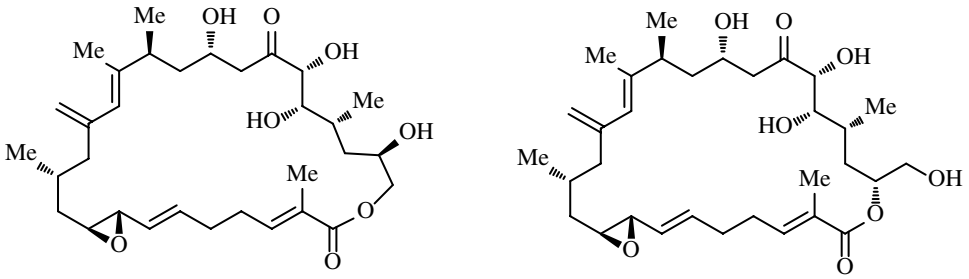



**SCHEME 2.85** Total synthesis of amphidinolide T1 by Jamison.

### *2.2.2.3 Applications of Evans' Alkylation Reaction*

*Amphidinolide T1 [111]* The amphidinolides are a unique family of macrolides isolated from the marine dinoflagellates *Amphidinium* sp. exhibiting antitumor activities against a variety of cancer cell lines [107]. Among them, amphidinolide T1 (**199**), a 19-membered macrocycle, has shown potent activity against murine lymphoma L1210 and human epidermoid carcinoma KB cell lines [108], thus stimulating considerable interest within the synthetic community [109]. In this context, Ghosh and Liu reported the first total synthesis of amphidinolide T1 in 2003 *via* a key oxocarbenium ion-mediated alkylation/macrolactonization sequence [110]. The next year, Jamison and coworkers also reported the total synthesis of amphidinolide T1 [111]. Their strategy (Scheme 2.84) revolved around an intramolecular nickel-catalyzed reductive alkyne–aldehyde coupling to generate the macrolactone core, an intermolecular nickel-catalyzed reductive alkyne–epoxide coupling to access the C13–C18 fragment of the molecule, and an Evans alkylation to control the stereogenic center at C14.

Jamison' synthesis of amphidinolide T1 started with the preparation of alkyne **201** *via* a diastereoselective propargylation using Evans' chiral oxazolidinone auxiliary and 3-bromo-1-phenyl-1-propyne [112] followed by the reduction of the diamide and protection of the resulting primary alcohol as a *tert*-butyldimethylsilylether (Scheme 2.85). The latter was then engaged in the first transition metal-catalyzed reductive coupling in the presence of chiral epoxide **204** to



*Amphidinolide G* (**207**) *Amphidinolide H* (**208**)

**SCHEME 2.86** Structures of amphidinolides G (**207**) and H (**208**).

complete the synthesis of the northern fragment of the molecule. Compound **205** was eventually coupled with **203** in the presence of DCC and 4-PPY, while conversion of the primary *tert*-butyldimethylsilylether to the corresponding aldehyde set the stage for the second nickel-catalyzed reductive coupling. The final steps of the synthesis involved the conversion of the C12 and C16 benzylidene moieties to the corresponding methylidenes through a sequential ozonolysis/selective methylenation using a modification of Takai's method [113] and a final HF-pyridine removal of the *tert*-butyldimethylsilyl protective group.

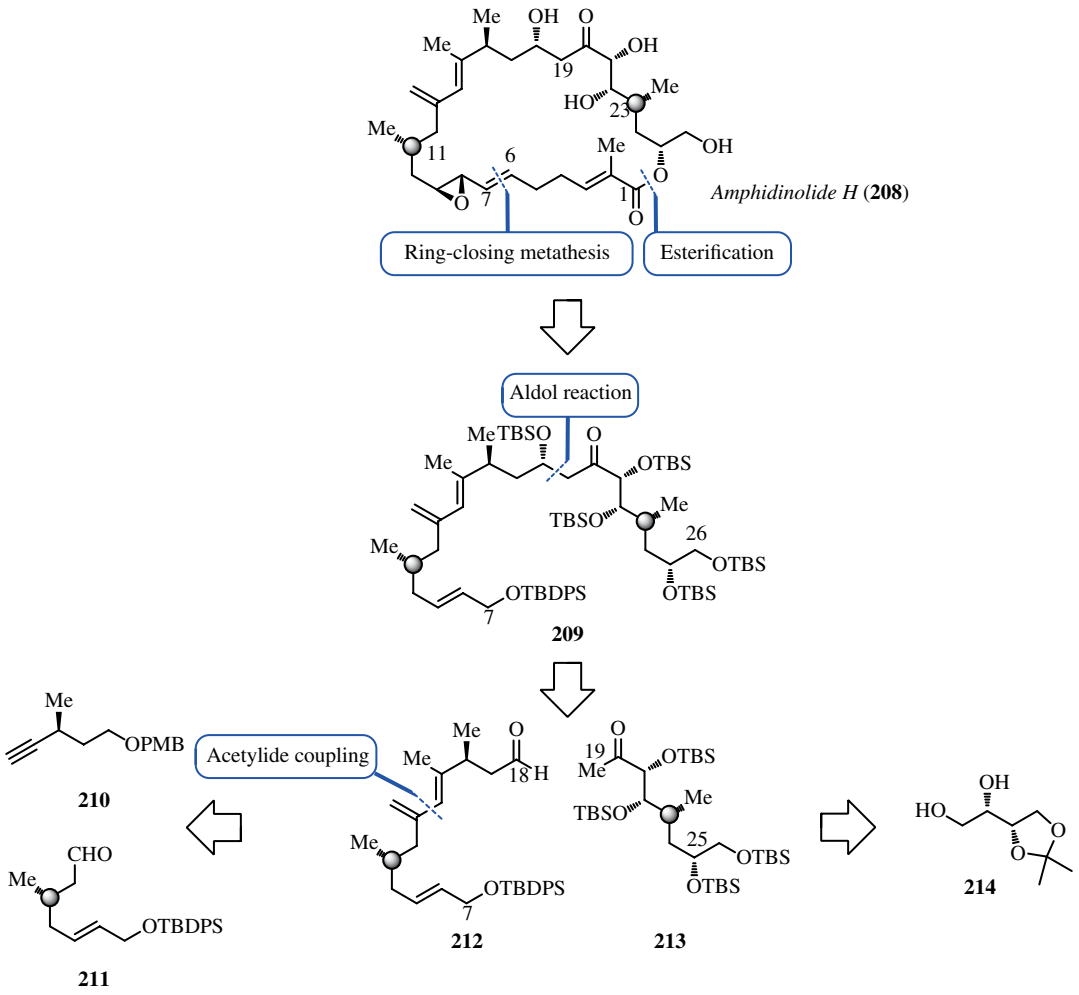
*Amphidinolide H [117]* Amphidinolides G (**207**) and H (**208**) are two other members of the amphidinolide family of natural products (Scheme 2.86). Isolated by Kobayashi and coworkers from the Okinawan flatworm *Amphiscolops* sp. [114], these two macrolides were found to exhibit a strong cytotoxicity against L1210 murine lymphoma ($IC_{50}$ = 5.4 ng/ml for **207** and 0.48 ng/ml for **208**) and KB human epidermoid ($IC_{50}$ = 5.9 ng/ml for **207** and 0.52 ng/ml for **208**) [115]. In addition, **208** was found to trigger actin polymerization by binding to the actin cytoskeleton in a covalent fashion [116].

In 2011, Nishiyama and coworkers [117] reported the synthesis of the common C7–C26 fragment of amphidinolides G and H. Their strategy relied on a key ring closing metathesis to construct the macrolactone core and two Evans alkylations to control the stereogenic centers at C11 and C23, while **209**, corresponding to the C7–C26 fragment, would be prepared through an aldol reaction between aldehyde **212** and methyl ketone **213**. Finally, an acetylide coupling between aldehyde **210** and acetylene **211** was envisioned to prepare C7–C18 aldehyde (Scheme 2.87).

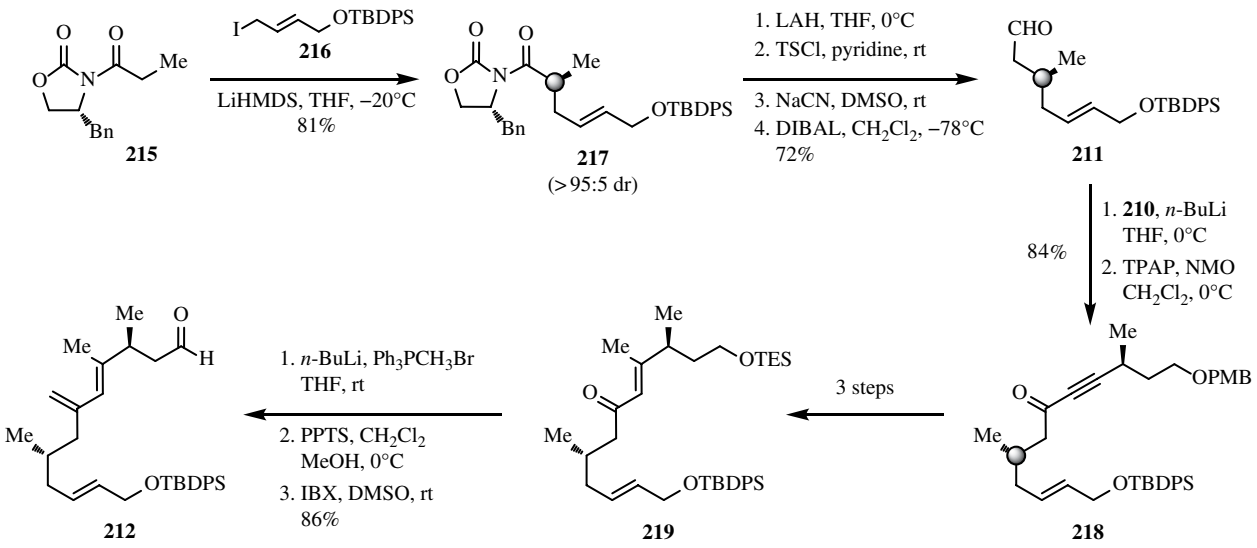
The synthesis of aldehyde **212** started with an Evans alkylation of the known acylated oxazolidinone **215** with allyl iodide **216** to form the corresponding alkylated product **217** as a single diastereoisomer in 81% yield (Scheme 2.88) [118]. Reductive removal of the chiral auxiliary followed by tosylation of the resulting primary alcohol, cyanide substitution, and reduction with DIBAL afforded aldehyde **211** in 72% overall yield. The latter was eventually coupled with the lithium acetylide derived from alkyne **210**, and the resulting propargylic alcohol underwent a TPAP/NMO-mediated oxidation to afford the corresponding α,β-unsaturated ketone **218** in 84% yield. Cleavage of the PMB group followed by protection of the resulting primary alcohol and treatment with Gilman's reagent led to the formation of the (*E*)-enone **219**, which was then converted to the corresponding conjugated diene through a Wittig olefination [119]. Finally, removal of the TES group followed by IBX oxidation of the resulting primary alcohol afforded the desired aldehyde **212**.

Ketone **226**, on the other hand, was prepared starting from known diol **214** [120], which was first converted to carboxylic acid **220** *via* a four-step sequence featuring an oxidative cleavage of the diol moiety, a Wittig olefination, a hydrogenation, and an ester hydrolysis (Scheme 2.89). Evans' chiral auxiliary was then introduced in order to promote the stereoselective methylation at C23 and removed under reductive conditions to afford the corresponding primary alcohol. This intermediate was then treated with PivCl, DMAP, and **221** to afford ester **222**, while removal of the acetonide, protection of the resulting diol as the bis-tributyldimethylsilyl ether, DIBAL reduction, TEMPO oxidation, and Wittig olefination gave the α,β-unsaturated ester **224**. The latter was then subjected to a Sharpless asymmetric dihydroxylation to afford the corresponding diol, which was treated with TBSOTf and 2,6-lutidine to produce the fully TBS-protected tetraol **225**. Four additional steps, which included a DIBAL reduction of the ester moiety, followed by a Parikh–Doering oxidation to the corresponding aldehyde, MeLi addition, and a TPAP-mediated oxidation, led to the desired methyl ketone **226**.

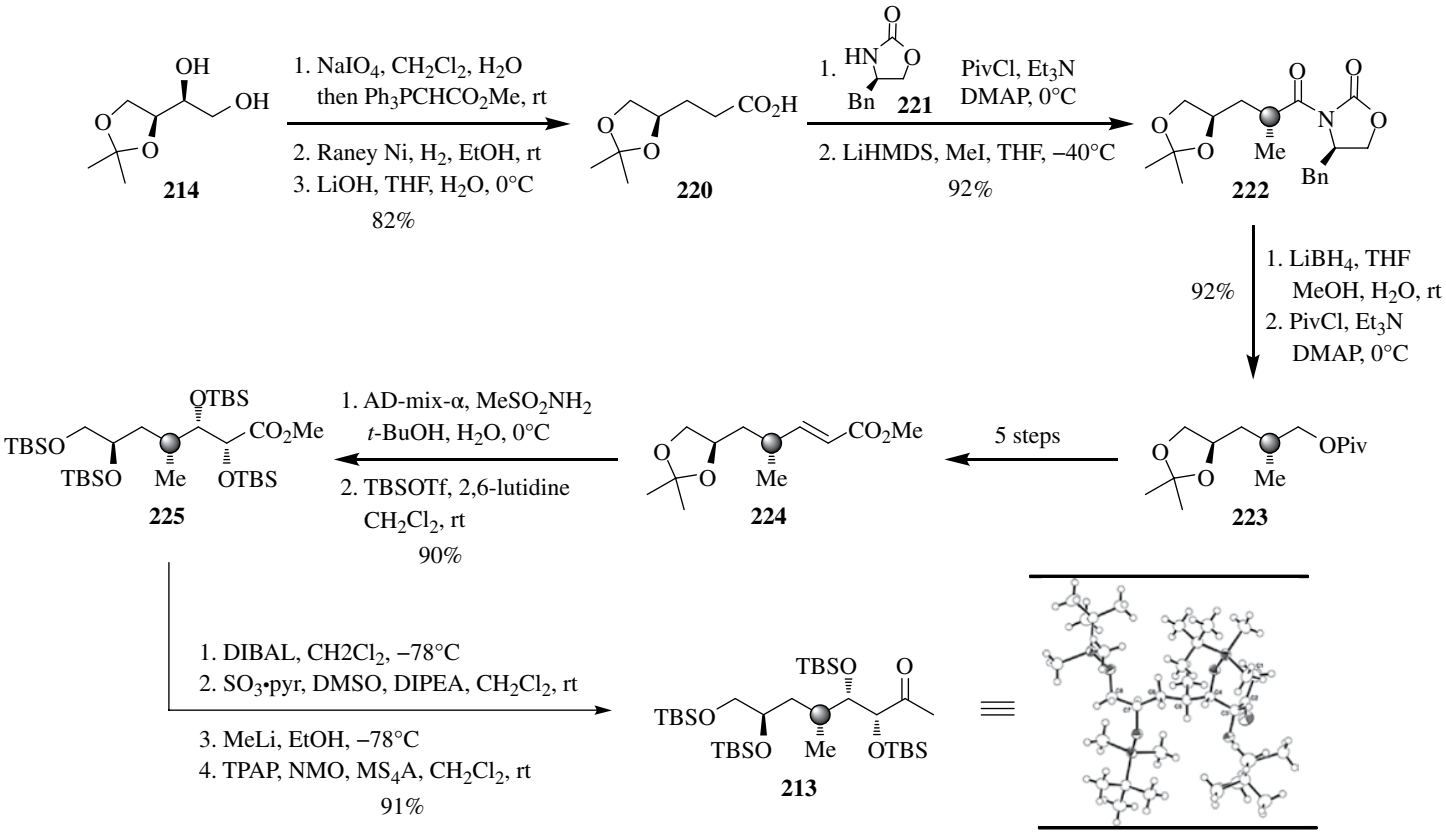
With the two aldol precursors in hand, the stage was set for the final coupling that would lead to the common C7–C26 fragment of both amphidinolides G and H (Scheme 2.90). Unfortunately, deprotonation of ketone **213** using LiHMDS and treatment of the resulting lithium enolate with aldehyde **212** at temperatures ranging from −78 to 0°C provided the desired diastereoisomer albeit in only moderate yield.



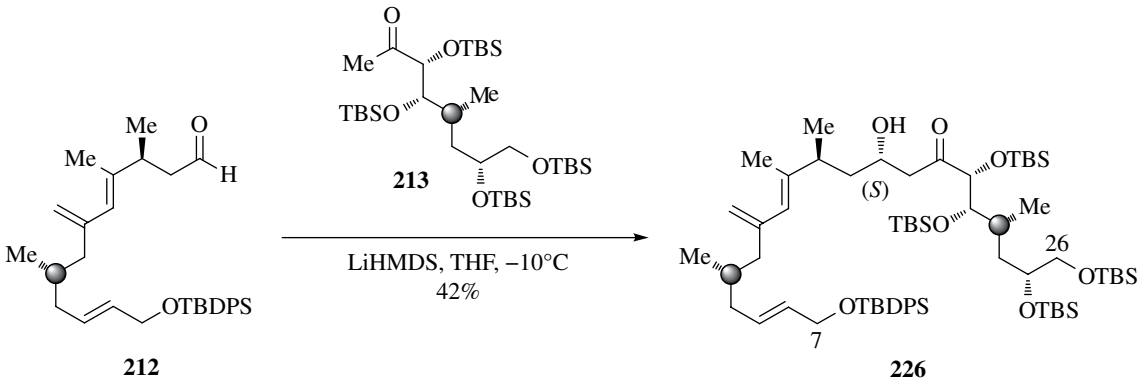

**SCHEME 2.87** Retrosynthetic analysis of amphidinolides G (**207**) and H (**208**) by Nishiyama.



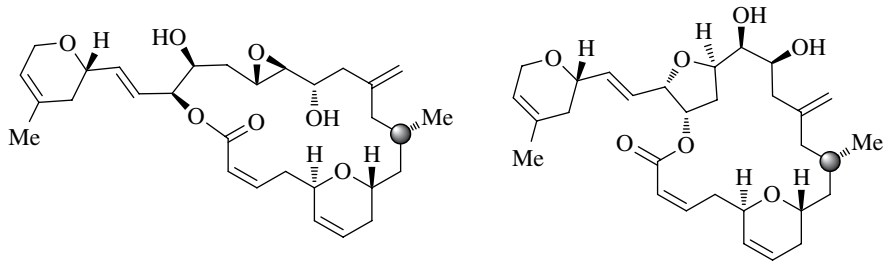

**SCHEME 2.88** Synthesis of the C7–C18 fragment **212**.



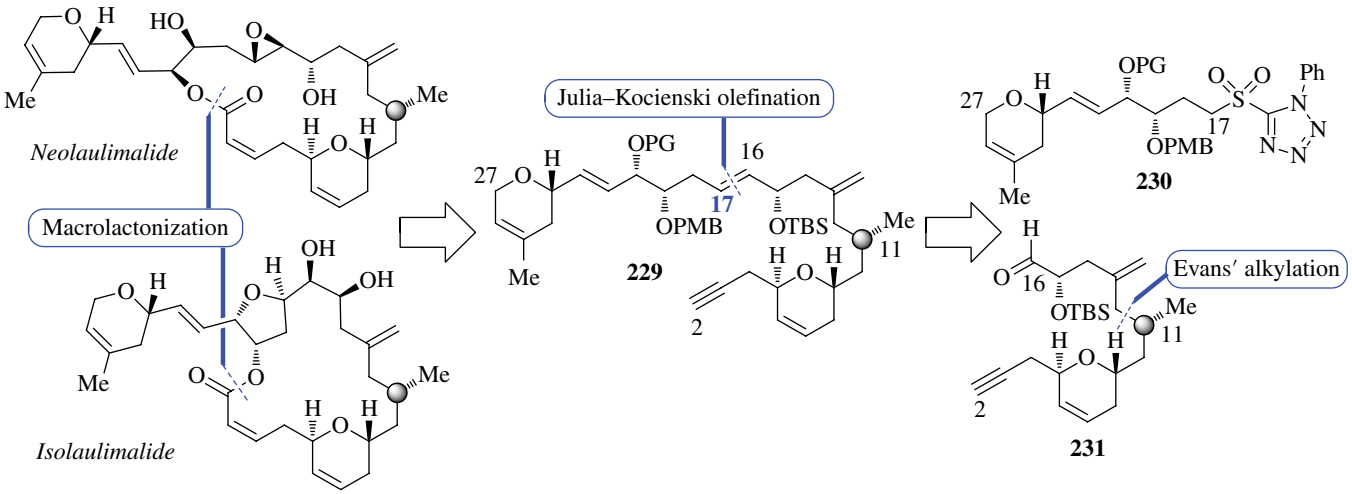

**SCHEME 2.89** Synthesis of the C19–C26 fragment **213**.




**SCHEME 2.90** Completion of the synthesis of the C7–C26 fragment of the amphidinolides G and H by Nishiyama.



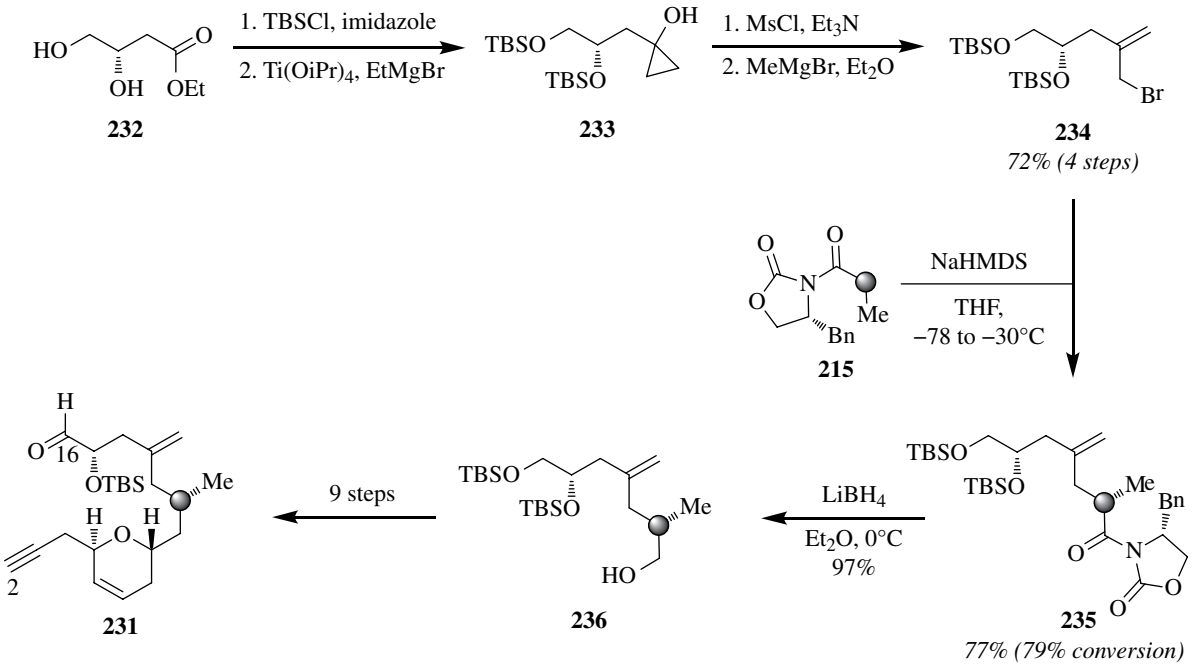

**SCHEME 2.91** Structures of neolaulimalide and isolaulimalide.



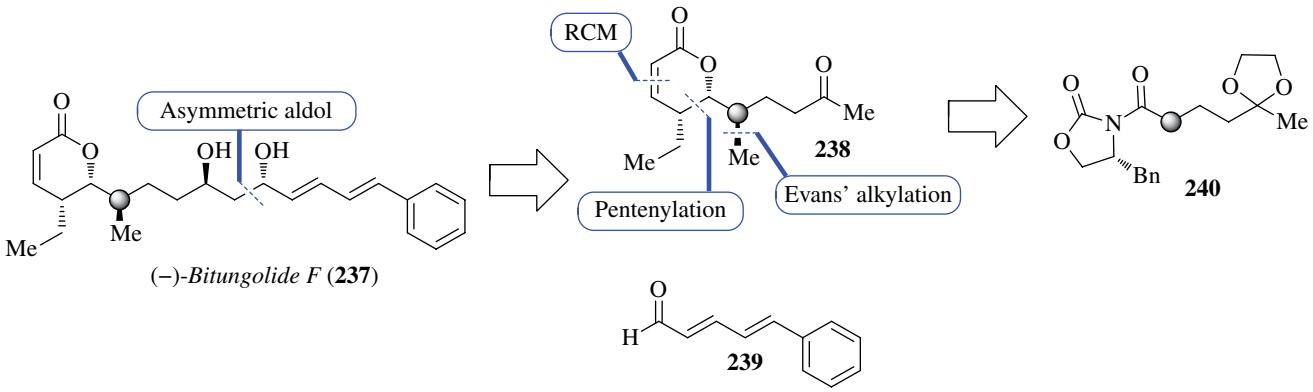

**SCHEME 2.92** Retrosynthetic analysis of neolaulimalide and isolaulimalide by Mulzer.

*Neolaulimalide and Isolaulimalide [122]* Neolaulimalide, isolaulimalide, and laulimalide are three natural products isolated from a marine sponge *Fasciospongia rimosa* (Scheme 2.91) [121]. These molecules are able to inhibit the proliferation of many tumor cell lines at a nanomolar level by stabilizing microtubules. Structurally, while laulimalide and neolaulimalide are distinguished be the size of their macrolactone, isolaulimalide results from an intramolecular ring opening of the epoxide and can be obtained by the treatment of laulimalide or neolaulimalide under acidic conditions.

In 2008, Gollner and Mulzer reported the first syntheses of neolaulimalide and isolaulimalide through a unified and convergent strategy (Scheme 2.92), which involved a late-stage Yamaguchi macrolactonization [122]. The common intermediate **229**, which was used to build the two natural products, was prepared through a Julia–Kocienski olefination between sulfone **230** and aldehyde **231**. The latter




**SCHEME 2.93** Synthesis of the fragment C2–C16 of neolaulimalide and isolaulimalide by Mulzer.

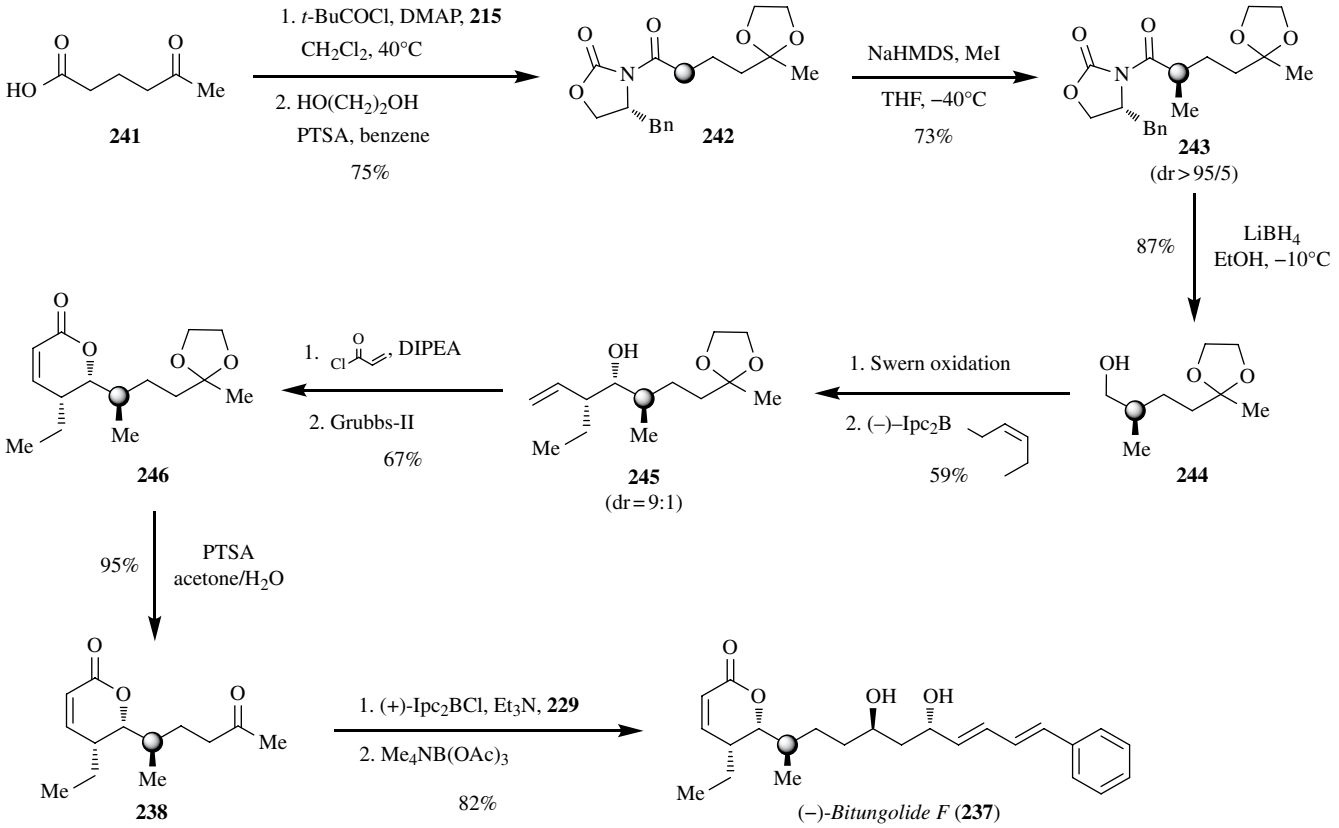



**SCHEME 2.94** Retrosynthetic analysis of (−)-bitungolide by Arseniyadis and Cossy.

was obtained through a 15-step sequence featuring an Evans alkylation to control the stereogenic center at C11.

The synthesis of the C2–C16 fragment began from commercially available dihydroxyester **232** derived from (*S*)-malic acid (Scheme 2.93). The two hydroxyl groups were first protected as *tert*-butyldimethylsilyl ethers before a Kulinkovich reaction was performed on the ester moiety to afford the corresponding cyclopropanol **233**. Mesylation of the free alcohol and treatment with $MgBr_2 \cdot OEt_2$ lead to the rearranged allylic bromide **234**, which was used as the electrophile in the subsequent Evans alkylation of the acylated oxazolidinone **215**. The alkylated product **235** was then reduced with $LiBH_4$, and the resulting alcohol **236** was converted to the desired C2–C16 fragment after nine additional steps.

*(−)-Bitungolide F [127]* Isolated in 2002 from the Indonesian sponge *Theonella cf. swinhoei* by Tanaka et al. [123], bitungolide F (**237**) incorporates a γ-ethyl substituted α,β-unsaturated δ-lactone common to a few other natural products such as the leustroducsins [124], the phoslactomycins [125], and pironetin [126], which have all attracted considerable attention over the past two decades due to their promising pharmacological properties. In this context, Arseniyadis, Cossy, and coworkers reported a particularly short synthesis [127] featuring a ring closing metathesis to build the α,β-unsaturated δ-lactone, a chiral boron-mediated aldol to control the C11 stereogenic center, a stereoselective pentenylation to introduce the ethyl side chain at C4, and an asymmetric Evans alkylation to install the C6 stereogenic center (Scheme 2.94).




**SCHEME 2.95** Synthesis of (−)-bitungolide by Arseniyadis and Cossy.

Their synthesis began by converting levulinic acid **241** to the corresponding chiral *N*-acyloxazolidinone and protecting the methyl ketone as a ketal (Scheme 2.95). The resulting product was then subjected to a highly diastereoselective alkylation following Evans' protocol to afford the corresponding methylated product **243** in 73% yield as a single diastereoisomer. Reductive removal of the chiral auxiliary [128] using $LiBH_4$ followed by the oxidation of the resulting allylic alcohol under Swern conditions led to the corresponding aldehyde, which was subjected to an asymmetric boron-mediated pentenylation reaction developed by the same group [129] and inspired by the asymmetric crotylation procedure reported by Brown et al. [130]. The resulting homoallylic alcohol **245** was then converted to the corresponding α,β-unsaturated δ-lactone using a two-step sequence featuring an acylation with acryloyl chloride and an RCM [131]. The ketone was eventually deprotected [132] and engaged in a chiral boron enolate-mediated asymmetric aldol reaction [133] with (*E*,*E*)-dienal **239** to afford the corresponding aldol adduct, which was converted to the natural product *via* a stereoselective *anti*-reduction.

## REFERENCES


1. For reviews, see: (a) A. Job, C. F. Janeck, W. Bettray, R. Peters, D. Enders, *Tetrahedron* 2002, **58**, 2253–2329; (b) M. C. Kohler, S. E. Wengryniuk, D. M. Coltart, Asymmetric α-alkylation of aldehydes, ketones and carboxylic acids, Chapter II, in *Stereoselective Synthesis of Drugs and Natural Products*, V. Andrushko and N. Andrushko Ed., John Wiley & Sons, Inc.: Hoboken, 2013; **1**, pp. 183–213.
2. G. Stork, R. Terrell, J. Szmuszkovicz, *J. Am. Chem. Soc.* 1954, **76**, 2029–2030.
3. G. Stork, S. R. Dowd, *J. Am. Chem. Soc.* 1963, **85**, 2178–2179.
4. A. I. Meyers, D. R. Williams, M. Druelinger, *J. Am. Chem. Soc.* 1976, **98**, 3032–3033.
5. D. Enders, H. Eichenauer, *Angew. Chem. Int. Ed. Engl.* 1976, **15**, 549–551.
6. D. Enders, H. Eichenauer, *Tetrahedron Lett.* 1977, **18**, 191–194.
7. (a) K. G. Davenport, H. Eichenauer, D. Enders, M. Newcomb, D. E. Bergbreiter, *J. Am. Chem. Soc.* 1979, **101**, 5654–5659; (b) D. Enders, M. Klatt, *Synthesis* 1996, 1403–1418.
8. D. Enders, H. Eichenauer, *Angew. Chem. Int. Ed. Engl.* 1976, **15**, 549–551.

9. D. Enders, A. Plant, *Synlett* 1990, 725–726.
10. D. Enders, A. Plant, *Synlett* 1994, 1054–1056.
11. A. B. Smith III, Z. Liu, V. Simov, *Synlett* 2009, 3131–3134.
12. D. Enders, T. Hundertmark, R. Lazny, *Synlett* 1998, 721–722 and references therein.
13. D. Enders, H. Schubert, *Angew. Chem. Int. Ed.* 1984, **96**, 366–369.
14. E. Diez, A. M. Lopez, C. Pareja, E. Martin, R. Fernandez, J. M. Lassaletta, *Tetrahedron Lett.* 1998, **39**, 7955–7958.
15. D. Enders, B. Bockstiegel, *Synthesis* 1989, 493–496.
16. For a review, see: D. Enders, M. Voight, A. Lenzen, *Angew. Chem. Int. Ed.* 2005, **44**, 1304–1325.
17. D. Enders, T. Hundertmark, *Tetrahedron Lett.* 1999, **40**, 4169–4172.
18. D. Enders, H. Kipphardt, P. Gerdes, L. J. Brena-Valle, V. Bhushan, *Bull. Soc. Chim. Belg.* 1988, **97**, 691–704.
19. J. Martens, S. Lübben, *Liebigs Ann. Chem.* 1990, 949–952.
20. D. Lim, D. M. Coltart, *Angew. Chem. Int. Ed.* 2008, **47**, 5207–5210.
21. X. Pan, Z. Liu, *Tetrahedron* 2014, **70**, 4602–4610.
22. H. Eichennauer, E. Friedrich, W. Lutz, D. Enders, *Angew. Chem. Int.* 1978, **17**, 206–207.
23. D. Enders, K. Papadopoulos, *Tetrahedron Lett.* 1983, **24**, 4967–4970.
24. D. Enders, C. F. Janeck, *Synlett* 2000, 641–643.
25. E. Nakamura, K. Kubota, G. Sakata, *J. Am. Chem. Soc.* 1997, **119**, 5457–5458.
26. F. A. Davis, L. C. Vishwakarma, J. G. Billmers, J. Finn, *J. Org. Chem.* 1984, **49**, 3241–3243.
27. D. Enders, T. Schäfer, O. Piva, A. Zamponi, *Tetrahedron* 1994, **50**, 3349–3362.
28. D. Enders, R. Joseph, C. Poiesz, *Tetrahedron* 1998, **54**, 10069–10078.
29. D. Enders, B. B. Lohray, *Angew. Chem. Int. Ed.* 1987, **26**, 351–352.
30. D. Enders, T. Berg, G. Raabe, J. Runsink, *Helv. Chim. Acta* 1996, **79**, 118–122.
31. M. Larchevêque, E. Ignatova, T. Cuvigny, *Tetrahedron Lett.* 1978, **41**, 3961–3964.
32. M. Larchevêque, E. Ignatova, T. Cuvigny, *J. Organomet. Chem.* 1979, **177**, 5–15.
33. A. G. Myers, B. H. Yang, H. Chen, J. L. Gleason, *J. Am. Chem. Soc.* 1994, **116**, 9361–9362.
34. A. G. Myers, B. H. Yang, H. Chen, L. McKinstry, D. J. Kopecky, J. L. Gleason, *J. Am. Chem. Soc.* 1997, **119**, 6496–6511.
35. D. A. Sandham, R. J. Taylor, J. S. Carey, A. Fässler, *Tetrahedron Lett.* 2000, **41**, 10091–10094.
36. A. G. Myers, B. H. Yang, H. Chen, L. McKinstry, D. J. Kopecky, J. L. Gleason, *J. Am. Chem. Soc.* 1997, **119**, 6496–6511.
37. W. J. Chain, A. G. Myers, *Org. Lett.* 2007, **9**, 355–357.
38. A. G. Myers, L. McKinstry, *J. Org. Chem.* 1996, **61**, 2428–2440.
39. J. L. Vicario, D. Badia, E. Dominguez, L. Carillo, *Tetrahedron Lett.* 1998, **39**, 9267–9270.
40. (a) J. L. Vicario, D. Badia, L. Carillo, *Org. Lett.* 2001, **3**, 773–776; (b) A. Iza, J. L. Vicario, L. Carillo, D. Badia, *Synthesis* 2006, 4065–4074.
41. J. H. Smitrovich, L. DiMichele, C. Qu, G. N. Boice, T. D. Nelson, M. A. Huffman, J. Murry, *J. Org. Chem.* 2004, **69**, 1903–1908.
42. R. B. Lettan II, C. V. Galliford, C. C. Woodward, K. A. Scheidt, *J. Am. Chem. Soc.* 2009, **131**, 8805–8814.
43. M. R. Morales, K. T. Mellem, A. G. Myers, *Angew. Chem. Int. Ed.* 2012, **51**, 4568–4571.
44. K. T. Mellem, A. G. Myers, *Org. Lett.* 2013, **15**, 5594–5597.
45. I. B. Seiple, J. A. M. Mercer, R. J. Sussman, Z. Zhang, A. G. Myers, *Angew. Chem. Int. Ed.* 2014, **53**, 4642–4647.
46. B. Peng, D. Geerdink, N. Maulide, *J. Am. Chem. Soc.* 2013, **135**, 14968–14971.
47. For review, see: (a) D. A. Evans, J. T. Shaw, *L'Actualité Chimique* 2003, 35–38; (b) D. A. Evans, *Aldrichimica Acta* 1982, **15**, 23–32; (c) D. J. Ager, I. Prakash, D. R. Schaad, *Chem. Rev.* 1996, **96**, 835–876.
48. D. A. Evans, M. D. Ennis, D. J. Mathre, *J. Am. Chem. Soc.* 1982, **104**, 1737–1340.
49. C. P. Decicco, P. Grover, *J. Org. Chem.* 1996, **61**, 3534–3541.
50. J. R. Gage, D. A. Evans *Org. Synth.* 1990, **68**, 77–82.
51. D. A. Evans, J. A. Ellman, R. L. Dorow, *Tetrahedron Lett.* 1987, **28**, 1123–1126.
52. D. A. Evans, T. C. Britton, J. A. Ellman *Tetrahedron Lett.* 1987, **28**, 6141–6144.
53. D. A. Evans, E. B. Sjogren, J. Bartoli, R. L. Dorow, *Tetrahedron Lett.* 1986, **27**, 4957–4960.
54. D. A. Evans, S. L. Bender *Tetrahedron Lett.* 1986, **27**, 799–802.
55. S. G. Davies, H. J. Sanganee, *Tetrahedron: Asymmetry* 1995, **6**, 671–674.
56. For an account pertaining to SuperQuat, see: S. D. Bull, S. G. Davies, A. C. Garner, D. Kruchinin, M.-S. Key, P. M. Roberts, E. D. Savory, A. D. Smith, J. E. Thomson, *Org. Biomol. Chem.* 2006, **4**, 2945–2964.
57. S. D. Bull, S. G. Davies, S. Jones, M. E. C. Polywka, R. S. Prasad, H. J. Sanganee, *Synlett* 1998, 519–521.
58. S. D. Bull, S. G. Davies, S. Jones, H. J. Sanganee, *J. Chem. Soc., Perkin Trans.* **1**, 1999, 387–398.
59. S. D. Bull, S. G. Davies, M.-S. Key, R. L. Nicholson, E. D. Savory, *Chem. Commun.* 2000, 1721–1722.
60. (a) S. D. Bull, S. G. Davies, R. L. Nicholson, H. J. Sanganee, A. D. Smith, *Tetrahedron: Asymmetry* 2000, **11**, 3475–3479; (b) S. D. Bull, S. G. Davies, R. L. Nicholson, H. J. Sanganee, A. D. Smith, *Org. Biomol. Chem.* 2003, **1**, 2886–2899.
61. A. Tessier, J. Pytkowicz, T. Brigaut, *Angew. Chem. Int. Ed.* 2006, **45**, 3677–3681.
62. G. Sini, A. Tessier, J. Pytkowicz, T. Brigaut, *Chem. Eur. J.* 2008, **14**, 3363–3370.
63. D. A. Evans, J. Bartroli, T. L. Shih, *J. Am. Chem. Soc.* 1981, **103**, 2127–2129.

64. D. A. Evans, F. Urpi, T. C. Somers, J. C. Clark, M. T. Bilodeau, *J. Am. Chem. Soc.* 1990, **112**, 8215–8216.
65. (a) D. A. Evans, M. D. Ennis, T. Le, *J. Am. Chem. Soc.* 1984, **106**, 1154–1156; (b) D. A. Evans, J. S. Clark, R. Metternich, V. J. Novak, G. S. Sheppard, *J. Am. Chem. Soc.* 1990, **112**, 866–868.
66. D. A. Evans, M. T. Bilodeau, T. C. Somers, J. Clardy, D. Cherry, Y. Kato, *J. Org. Chem.* 1991, **56**, 5750–5752.
67. D. A. Evans, M. M. Morissey, R. L. Dorow, *J. Am. Chem. Soc.* 1985, **107**, 4346–4348.
68. D. A. Evans, T. C. Britton, R. L. Dorow, J. F. Dellaria, *J. Am. Chem. Soc.* 1986, **108**, 6395–6397.
69. D. A. Evans, T. C. Britton, J. A. Ellman, R. L. Dorow, *J. Am. Chem. Soc.* 1990, **112**, 4011–4030.
70. D. A. Evans, J. A. Ellman, R. L. Dorow, *Tetrahedron Lett.* 1987, **11**, 1123–1126.
71. A. A. Birkbeck, D. Enders, *Tetrahedron Lett.* 1998, **39**, 7823–7826.
72. (a) J. E. Biskupiak, C. M. Ireland, *Tetrahedron Lett.* 1983, **24**, 3055–3058; (b) M. Norte, F. Cataldo, A. G. Gonzalez, M. L. Rodriguez, C. Ruiz-Perez, *Tetrahedron* 1990, **46**, 1669–1678; (c) M. J. Garson, C. J. Small, B. W. Skelton, P. Thinapong, A. H. White, *J. Chem. Soc. Perkin Trans.*, 1990, **1**, 805–807.
73. D. Enders, G. Geibel, S. Osborne, *Chem. Eur. J.* 2010, **6**, 1302–1309.
74. (a) G. Höfle, B. Kunze, C. Zorin, H. Reichenbach, *Liebigs Ann.* 1984, 1883–1904; (b) B. Kunze, G. Höfle, H. Reichenbach *J. Antibiotics* 1987, **40**, 258–265; (c) B. Kunze, T. Kemmer, G. Höfle, H. Reichenbach, *J. Antibiotics* 1984, **37**, 454–461.
75. (a) K. C. Nicolaou, K. Ajito, A. P. Patron, H. Khatuya, P. K. Richter, P. Bertinato, *J. Am. Chem. Soc.* 1996, **118**, 3059–3060; (b) K. C. Nicolaou, A. P. Patron, K. Ajito, P. K. Richter, H. Khatuya, P. Bertinato, R. A. Miller, M. J. Tomaszewski, *Chem. Eur. J.* 1996, **2**, 847–868.
76. (a) A. P. Patron, P. K. Richter, M. J. Tomaszewski, R. A. Miller, K. C. Nicolaou, *Chem. Commun.* 1994, 1147–1150; (b) P. K. Richter, M. J. Tomaszewski, R. A. Miller, A. P. Patron, K. C. Nicolaou, *Chem. Commun.* 1994, 1151–1152.
77. S. Carmely, Y. Kashman, *Tetrahedron Lett.* 1985, **26**, 511–514.
78. (a) M. Kobayashi, J. Tanaka, T. Katori, M. Matsura, I. Kitagawa, *Tetrahedron Lett.* 1989, **30**, 2963–2966; (b) M. Doi, T. Ishida, M. Kobayashi, I. Kitagawa, *J. Org. Chem.* 1991, **56**, 3629–3632; (c) I. Kitagawa, M. Kobayashi, T. Katori, M. Yamashita, *J. Am. Chem. Soc.* 1990, **112**, 3710–3712; (d) M. Kobayashi, J. Tanaka, T. Katori, M. Yamashita, M. Matsuura, I. Kitagawa, *Chem. Pharm. Bull.* 1990, **38**, 2409–2418; (e) M. Kobayashi, J. Tanaka, T. Katori, I. Kitagawa, *Chem. Pharm. Bull.* 1990, **38**, 2960–2966.
79. M. R. Bubb, I. Spector, A. D. Bershadsky, E. D. Korn, *J. Biol. Chem.* 1995, **270**, 3463–3466.
80. (a) H. Osada, H. Koshino, K. Isono, H. Takahashi, G. Kawanishi, *J. Antibiotics* 1991, **44**, 259–261; (b) H. Koshino, H. Takahashi, H. Osada, K. Isono, *J. Antibiotics* 1992, **45**, 1420–1427; (c) H. Takahashi, H. Osada, H. Koshino, T. Kuto, S. Amano, S. Shimizu, M. Yoshihama, K. Isono, *J. Antibiotics* 1992, **45**, 1409–1413.
81. (a) K. E. Drouet, E. A. Theodorakis, *J. Am. Chem. Soc.* 1999, **121**, 456–457; (b) K. E. Drouet, E. A. Theodorakis, *Chem. Eur. J.* 2000, **6**, 1987–2001.
82. K. C. Nicolaou, S. Ninkovic, F. Sarabia, D. Vourloumis, Y. He, H. Vallberg, M. R. V. Finlay, Z. Yang, *J. Am. Chem. Soc.* 1997, **119**, 7974–7991.
83. D. Enders, A. Lenzen, *Synlett* 2003, 2185–2187.
84. N. Takada, K. Suenaga, K. Yamada, S.-Z. Zheng, H.-S. Chen, D. Uemura, *Chem. Lett.* 1999, 1025–1026.
85. A. B. Smith III, S. A. Kozmin, C. M. Adams, D. V. Paone, *J. Am. Chem. Soc.* 2000, **122**, 4984–4985.
86. R. L. Danheiser, S. K. Gee, *J. Org. Chem.* 1984, **49**, 1672–1674.
87. H. C. Brown, J. Chandrasekharan, P. V. Ramachandran, *J. Am. Chem. Soc.* 1988, **110**, 1539–1546.
88. R. R. Schrock, J. S. Murdzek, G. C. Bazan, J. Robbins, M. DiMare, M. O'Regan, *J. Am. Chem. Soc.* 1990, **112**, 3875–3886.
89. G. R. Pettit, Z. A. Cichacz, F. Gao, M. R. Boyd, J. M. Schmidt, *J. Chem. Soc. Chem. Commun.* 1994, 1111–1112.
90. (a) I. Paterson, R. Britton, O. Delgado, A. Meyer, K. G. Poullennec, *Angew. Chem. Int. Ed.* 2004, **43**, 4629–4633; (b) I. Paterson, R. Britton, O. Delgado, N. M. Gardner, A. Meyer, G. J. Naylor, K. G. Poullennec, *Tetrahedron* 2010, **66**, 6534–6545.
91. I. Paterson, O. Delgado, G. J. Florence, I. Lyothier, J. P. Scott, N. Sereinig, *Org. Lett.* 2003, **5**, 35–38.
92. B. G. Isaac, S. W. Ayer, R. C. Elliott, R. J. Stonard, *J. Org. Chem.* 1992, **57**, 7220–7226.
93. Y. Zhang, J. S. Panek, *Org. Lett.* 2007, **9**, 3141–3143.
94. T. J. Murray, C. J. Forsyth, *Org. Lett.* 2008, **10**, 3429–3431.
95. J. Willmacher, A. Fürstner, *Angew. Chem. Int. Ed.* 2014, **53**, 4217–4221.
96. J. Sikorska, A. M. Hau, C. Anklin, S. Parker-Nance, M. T. Davies-Coleman, J. E. Ishmael, K. L. McPhail, *J. Org. Chem.* 2012, **77**, 6066–6075.
97. A. Fürstner, *Angew. Chem. Int. Ed.* 2013, **52**, 2794–2819.
98. X. Gao, H. Han, M. J. Krische, *J. Am. Chem. Soc.* 2011, **133**, 12795–12800.
99. H. Lei, J. Yan, J. Yu, Y. Liu, Z. Wang, Z. Xu, T. Ye, *Angew. Chem. Int. Ed.* 2014, **53**, 6533–6537.
100. A. Fürstner, M. Bonnekessel, J. T. Blank, K. Radkowski, G. Seidel, F. Lacombe, B. Gabor, R. Mynott, *Chem. Eur. J.* 2007, **13**, 8762–8783.
101. G. E. Keck, C. E. Knutson, S. A. Wiles, *Org. Lett.* 2001, **3**, 707–710.
102. (a) S. Kobayashi, K. Tsochia, T. Harada, M. Nishide, T. Kurokawa, T. Nakagawa, N. Shimada, K. Kobayashi, *J. Antibiot.* 1994, **47**, 697–702; (b) S. Kobayashi, K. Tsochia, T. Harada, M. Nishide, T. Kurokawa, T. Nakagawa, N. Shimada, T. Iitaka, *J. Antibiot.* 1994, **47**, 703–707.

103. B. D. Morris, R. Smyth, S. P. Foster, M. P. Hoffmann, W. L. Roelofs, W. Francke, *J. Nat. Prod.* 2005, **68**, 26–30.

104. (a) Y. Schmidt, B. Breit, *Org. Lett.* 2009, **11**, 4767–4769; (b) Y. Schmidt, K. Lehr, U. Breuninger, G. Brand, T. Reiss, B. Breit, *J. Org. Chem.* 2010, **75**, 4424–4433.

105. J. S. Yadav, E. Srinivas, C. K. S. Kumar, A. A. K. Al Ghamdi, *Synthesis* 2012, **44**, 628–634.

106. J. S. Yadav, C. Srinivas Rao, S. Chandrasekhar, A. V. Rama Rao, *Tetrahedron Lett.* 1995, **36**, 7717–7720.

107. J. Kobayashi, in *Comprehensive Natural Products Chemistry*, K. Mori Ed., Elsevier: New York, 1999; Vol. **8**, p 619–634.

108. M. Tsuda, T. Endo, J. Kobayashi, *J. Org. Chem.* 2001, **66**, 134–142.

109. For synthetic studies aimed at amphidinolides G and H, see: (a) A. F. Petri, J. S. Schneekloth, A. K. Mandal, C. M. Crews, *Org. Lett.* 2007, **9**, 3001–3004; (b) L. Deng, Z. Ma, Y. Zhang, G. Zhao, *Synlett* 2007, 87–90; (c) L. Deng, Z. Ma, G. Zhao, *Synlett* 2008, 728–732; (d) P. Formentin, J. Murga, M. Carda, J. A. Marco, *Tetrahedron: Asymmetry* 2006, **17**, 2938–2942; (e) F. P. Liesener, M. Kalesse, *Synlett* 2005, 2236–2238; (f) F. P. Liesener, U. Jannsen, M. Kalesse, *Synthesis* 2006, 2590–2602; (g) T. K. Chakraborty, V. R. Suresh *Tetrahedron Lett.* 1998, **39**, 7775–7778; (h) T. K. Chakraborty, V. R. Suresh, *Tetrahedron Lett.* 1998, **39**, 9109–9112.

110. A. K. Ghosh, C. Liu, *J. Am. Chem. Soc.* 2003, **125**, 2374–2375.

111. E. A. Colby, K. C. O'Brien, T. F. Jamison, *J. Am. Chem. Soc.* 2004, **126**, 998–999.

112. (a) D. A. Evans, M. D. Ennis, D. J. Mathre, *J. Am. Chem. Soc.* 1982, **104**, 1737–1739; (b) M. Savignac, J.-O. Durand, J.-P. Genêt, *Tetrahedron: Asymmetry* 1994, **5**, 717–722.

113. (a) K. Takai, T. Kakiuchi, Y. Kataoka, K. Utimoto, *J. Org. Chem.* 1994, **59**, 2668–2670; (b) F. W. Hartner, J. Schwartz, S. M. Clift, *J. Am. Chem. Soc.* 1983, **105**, 640–641.

114. J. Kobayashi, H. Shigemori, M. Ishibashi, T. Yamasu, H. Hirota, T. Sasaki, *J. Org. Chem.* 1991, **56**, 5221–5224.

115. J. Kobayashi, K. Shimbo, M. Sato, M. Tsuda, *J. Org. Chem.* 2002, **67**, 6585–6592.

116. T. Usui, S. Kazami, N. Dohmae, Y. Mashimo, H. Kondo, M. Tsuda, A. G. Terasaki, K. Ohashi, J. Kobayashi, H. Osada, *Chem. Biol.* 2004, **11**, 1269–1277.

117. A. Hara, R. Morimoto, Y. Ishikawa, S. Nishiyama, *Org. Lett.* 2011, **13**, 4036–4039.

118. M. Shindo, T. Sugioka, Y. Umaba, K. Shishido, *Tetrahedron Lett.* 2004, **45**, 8863–8866.

119. K. Ohi, S. Nishiyama, *Synlett* 1999, 571–572.

120. E. Abushanab, P. P. Raymond, *J. Org. Chem.* 1988, **53**, 2598–2602.

121. T. Higa, J.-I. Tanaga, G. Bernardinelli, C. W. Jefford, *Chem. Lett.* 1996, 255–256.

122. A. Gollner, J. Mulzer, *Org. Lett.* 2008, **10**, 4701–4704.

123. S. Sirirath, J. Tanaka, I. I. Ohtani, T. Ichiba, R. Rachmat, K. Ueda, T. Usui, H. Osada, T. Higa, *J. Nat. Prod.* 2002, **65**, 1820–1823.

124. (a) T. Kohama, R. Enokita, T. Okazaki, H. Miyaoka, A. Torikata, M. Inukai, I. Kaneko, T. Kagasaki, Y. Sakaida, A. Satoh, A. Shiraishi, *J. Antibiot.* 1993, **46**, 1503–1511; (b) T. Kohama, T. Nakamura, T. Kinoshita, L. Kaneko, A. Shiraishi, *J. Antibiot.* 1993, **46**, 1512–1519; (c) H. Matsuhashi, K. Shimada, *Tetrahedron* 2002, **58**, 5619–5626.

125. (a) S. Fushimi, S. Nishikawa, A. Shimazu, H. Seto, *J. Antibiot.* 1989, **42**, 1019–1025; (b) S. Fushimi, K. Furihata, H. Seto, *J. Antibiot.* 1989, **42**, 1026–1036; (c) T. Ozasa, K. Suzuki, M. Sasamata, K. Tanaka, M. Kobori, S. Kadota, K. Nagai, T. Saito, S. Watanabe, M. Iwanami, *J. Antibiot.* 1989, **42**, 1331–1338; (d) T. Ozasa, K. Tanaka, M. Sasamata, H. Kaniwa, M. Shimizu, H. Matsumoto, M. Iwanami, *J. Antibiot.* 1989, **42**, 1339–1343; (e) T. Shibata, S. Kurihara, K. Yoda, H. Haruyama *Tetrahedron* 1995, **51**, 11999–12012; (f) Y. Sekiyama, N. Palaniappan, K. A. Reynolds, H. Osada, *Tetrahedron* 2003, **59**, 7465–7471; (g) S. D. Choudhuri, S. Ayers, W. H. Soine, K. A. Reynolds, *J. Antibiot.* 2005, **58**, 573–582;(h)N. Mizuhara, Y. Usuki, M. Ogita, K. Fujita, M. Kuroda, M. Doe, H. Lio, T. Tanaka, *J. Antibiot.* 2007, **60**, 762–765.

126. (a) T. Yoshida, K. Koizumi, Y. Kawamura, K. Matsumoto, H. Itazaki, Japan Patent Kokai 5–310726, 1993; (b) T. Yoshida, K. Koizumi, Y. Kawamura, K. Matsumoto, H. Itazaki, European Patent 560389 A1, 1993; (c) K. Yasui, Y. Tamura, T. Nakatani, K. Kawada, M. Ohtani, *J. Org. Chem.* 1995, **60**, 7567–7574; (d) S. Kobayashi, K. Tsuchiya, T. Harada, M. Nishide, T. Kurokawa, T. Nakagawa, N. Shimada, K. Kobayashi, *J. Antibiot.* 1994, **47**, 697–702; (e) S. Kobayashi, K. Tsuchiya, T. Harada, M. Nishide, T. Kurokawa, T. Nakagawa, N. Shimada, T. Iitaka, *J. Antibiot.* 1994, **47**, 703–707.

127. A. ElMarrouni, S. R. Joolakanti, A. Colon, M. Heras, S. Arseniyadis, J. Cossy, *Org. Lett.* 2010, **12**, 4074–4077.

128. A. B. Smith III, D. Lee, *J. Am. Chem. Soc.* 2007, **129**, 10957–10962.

129. (a) R. P. Sonawane, S. R. Joolakanti, S. Arseniyadis, J. Cossy, *Synlett* 2009, 213–216. (b) For applications in natural product synthesis, see: C. Bressy, J.-P. Vors, S. Hillebrand, S. Arseniyadis, J. Cossy, *Angew. Chem. Int. Ed.* 2008, **47**, 10137–10140; (c) J. Moïse, R. P. Sonawane, C. Corsi, S. V. Wendeborn, S. Arseniyadis, J. Cossy, *Synlett* 2008, 2617–2620.

130. H. C. Brown, K. S. Bhat, *J. Am. Chem. Soc.* 1986, **108**, 293–294.

131. (a) A. Fürstner, K. Langemann, *J. Am. Chem. Soc.* 1997, **119**, 9130–9136; (b) A. K. Ghosh, J. Cappiello, D. Shin, *Tetrahedron Lett.* 1998, **39**, 4651–4654; (c) J. Cossy, D. Bauer, V. Bellosta, *Tetrahedron Lett.* 1999, **40**, 4187–4188; (d) V. Boucard, G. Broustal, J. M. Campagne, *Eur. J. Org. Chem.* 2007, 225–236.

132. R. S. Meissner, J. J. Perkins, L. T. Duong, G. D. Hartman, W. F. Hoffman, J. R. Huff, N. C. Ihle, C.-T. Leu, R. M. Nagy, A. Naylor-Olsen, G. A. Rodan, S. B. Rodan, D. B. Whitman, G. A. Wesolowski, M. E. Duggan, *Bioorg. Med. Chem. Lett.* 2002, **12**, 25–29.

133. (a) C. J. Cowden, I. Paterson, *Org. React.* 1997, **51**, 1–200; (b) I. Paterson, J. M. Goodman, *Tetrahedron Lett.* 1989, **30**, 997–1000; (c) I. Paterson, J. M. Goodman, M. A. Lister, R. C. Schumann, C. K. McClure, R. D. Norcross, *Tetrahedron* 1990, **46**, 4663–4684; (d) K. M. Cergol, M. J. Coster, *Nature Protocols* 2007, **10**, 2568–2573.

MARKUS KALESSE AND MARTIN CORDES

*Institute for Organic Chemistry and Center of Biomolecular Drug Research (BMWZ), Leibniz Universität Hannover, Hannover, Germany and Helmholtz Center for Infection Research (HZI), Hannover, Germany*

## 2.3 SYNTHESIS OF POLYKETIDES-FOCUS ON MACROLIDES

### 2.3.1 Introduction

The macrolides constitute a plethora of different structures exhibiting a large variety of biological activities. Naturally, strategies to construct these compounds and in particular to control their stereochemistry are of general interest in natural product synthesis and medicinal chemistry. Nature uses four basic transformations to generate polyketides from simple building blocks such as malonate and methyl malonate, which are the biosynthetic equivalents of acetate or propionate units. The KS performs an ester condensation to generate the β-keto ester motif, subsequent reduction of the keto carbonyl group by KR establishes a hydroxyl ester in an 1,3 functional group distance, and subsequent elimination induced by a DH can yield the α,β unsaturated ester [1]. In synthesis this transformation is often achieved through an aldol reaction that constructs both the new carbon–carbon bond and the chiral alcohol. The polyketides biosynthesis dissects these tasks and performs first the carbon–carbon bond formation and afterward a stereoselective reduction of the keto carbonyl group. Finally, the ER is able to remove the double bond (Scheme 2.96).

As a showcase the first steps in the biosynthesis of soraphen are depicted in Figure 2.1. In module 1 the intermediate β-keto ester is reduced stereoselectively to generate the chiral secondary alcohol.

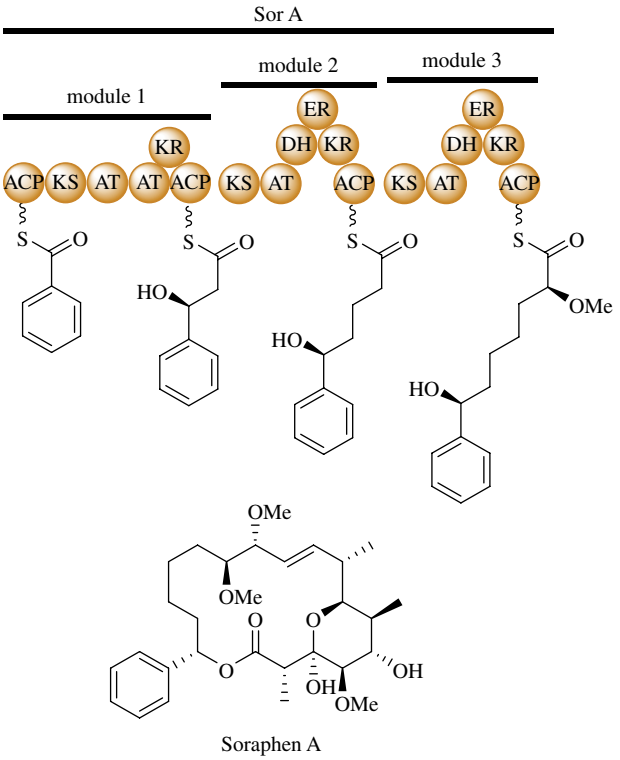
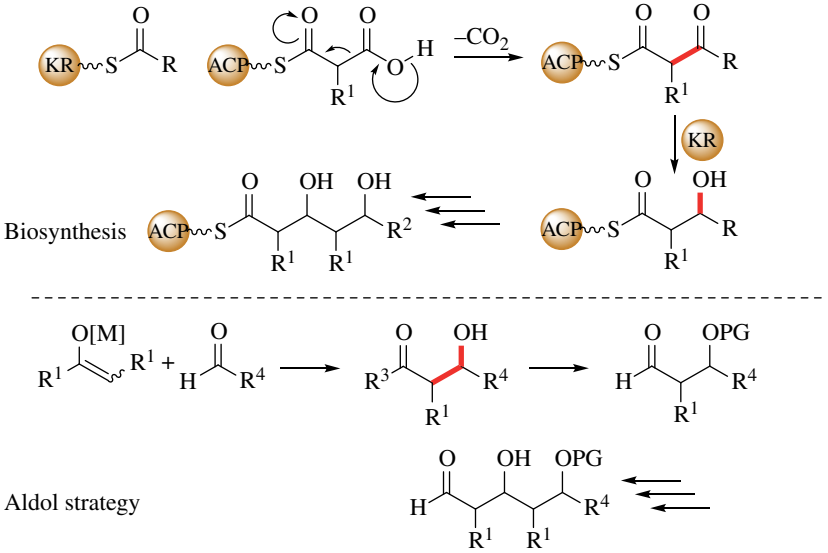



**FIGURE 2.1** First three modules of the biosynthesis of soraphen.




**SCHEME 2.96** Comparison of biosynthesis and chemical synthesis of polyketides.

In this chapter, we will cover both aspects, the aldol strategy and the selective reduction of carbonyl groups in the context of 1,3-diol formation. Additionally, nonaldol approaches will be covered as well.

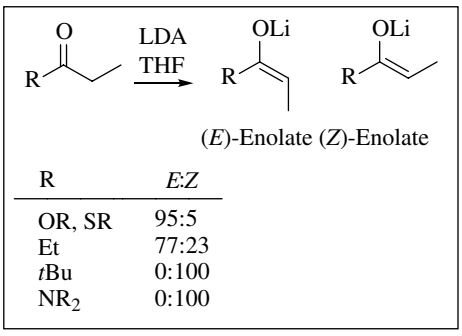
### 2.3.2 Stereoselective Synthesis of 1,3-Diols: Asymmetric Aldol Reactions

***2.3.2.1 Basic Models to Predict Stereoselection in Aldol Reactions*** In order to rationalize the stereochemical outcome of aldol reactions, two pivotal concepts are used, that is, the Zimmerman–Traxler transition state and the Felkin model, including its variations and refinements such as the Evans–Cornforth and Roush transition state. Even though not pivotal for the configuration at alcohols but for the configuration of contiguous methyl branches is the enolate geometry, which can be controlled and rationalized by the seminal work of Ireland (Scheme 2.97) [2]. The enolate geometry is controlled by steric effects, and ketones in general produce *Z*-enolates, whereas esters (in the absence of HMPA) generate the corresponding *E*-enolates.

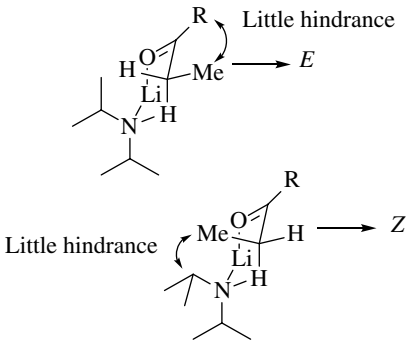
The so-obtained enolate geometry is translated during the aldol reaction, based on the Zimmerman transition state [3], to *anti*- or *syn*-aldol products (Scheme 2.98). The Zimmerman–Traxler model positions both the enolate and the aldehyde in a chair conformation with the R group at the aldehyde to adopt an equatorial position. The alkyl residue at the enolate, in most cases a methyl group, must be, depending on the enolate geometry, either axial or equatorial. This orientation finally distinguishes between *anti*- or *syn*-isomers. In general *E*-enolates perform not as selective as *Z*-enolates. This is a consequence from deviations from the ideal chair-like TS to a nonplanar or twisted transition state. If steric repulsion between the residues Bu und $R^2$ becomes more relevant, the transition state avoids this steric repulsion to adopt a *syn*-aldol TS. This has been taken into account as a rational explanation for the low selectivities (*syn*/*anti* = 1:3), which are observed when *E*-enolates are used. For small residues $R^1$ and $R^2$, the *syn*-TS becomes more favorable. The absence of these unfavorable interactions for *Z*-enolates has been taken as an explanation for the observed higher selectivities.

While the Zimmerman–Traxler transition state rationalizes the diastereoselectivity generated on both sides of the newly generated carbon–carbon bond during the aldol reaction, the Felkin–Anh, Evans–Cornforth, and polar Felkin transition states rationalize the diastereoselectivity between the newly generated chiral secondary alcohol and preexisting chiral centers at the α- or β-position of the reacting aldehyde. The Felkin transition state adopts a conformation at which the smallest substituent at the α-position and the aldehyde proton are located at the same half-sphere of the aldehyde. This is to provide the least steric hindrance for nucleophiles approaching along the Dunitz–Bürgi trajectory [4]. As the consequence, the newly generated alcohol and the alpha substituent exhibit *syn*-orientation. The Cram chelation transition state uses an equivalent explanation. Here, only the conformation is controlled by chelating Lewis acids between the aldehyde's carbonyl oxygen and an existing hetero substituent in the α- or β-position if present. Consequently, an *anti*-relationship is observed for such cases. Polar Felkin or Cornforth–Evans transition states are usually considered when heteroatoms are located at the α-position of the aldehyde. The polar Felkin model proposes an orientation at which the alpha substituent is oriented perpendicular to the carbonyl group, based on stereoelectronic considerations. Again, the smallest substituent is located in the same half-sphere, which is also occupied by the aldehyde proton, and attack occurs from the opposite side. The Cornforth–Evans model builds on electronic arguments and proposes a conformation that provides the smallest dipole moment for the aldehyde. As in the other models, nucleophilic attack occurs from the sterically least hindered side (Scheme 2.99).

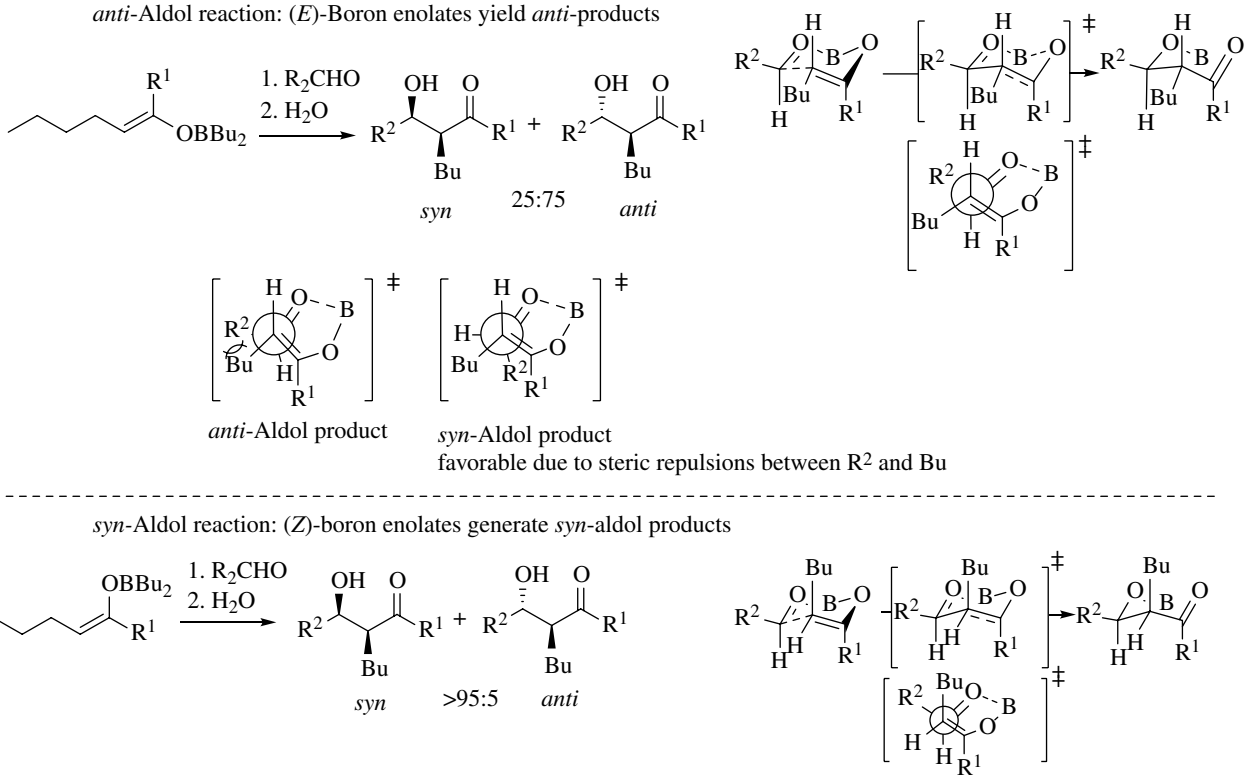
A slightly different situation is observed if Lewis acids are required for the nucleophilic attack. The Mukaiyama aldol reaction is such an example. Here silyl enol ethers or ketene acetals are used in combination with Lewis acids. Recently an excellent analysis for the observed selectivities and transition state models was proposed by Wiest and Helquist [5]. In addition to the *anti* transition state, they could




| R | *E*:*Z* |
|---|---|
| OR, SR | 95:5 |
| Et | 77:23 |
| *t*Bu | 0:100 |
| $NR_2$ | 0:100 |




**SCHEME 2.97** Ireland mechanism for the control of enolate formation.




**SCHEME 2.98** Zimmerman–Traxler transition state (substitution at boron atom has been removed for clarity).

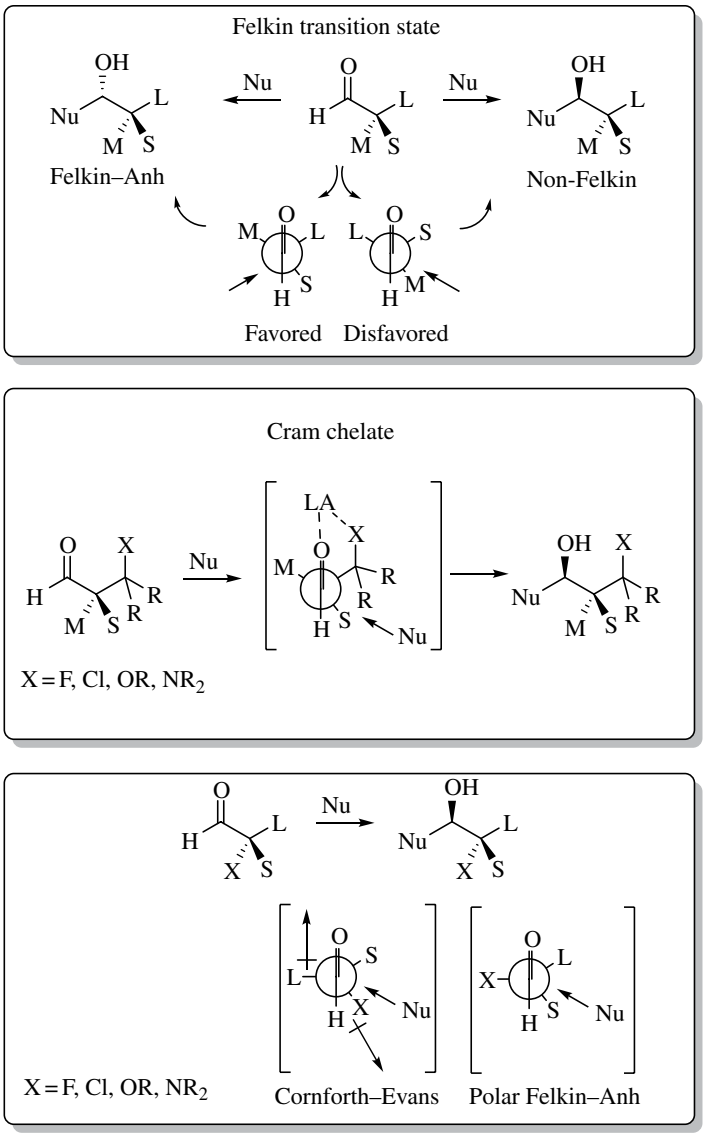
demonstrate that the *syn*-clinal transition state is also favored for large Lewis acids. In any case the enol ether's and the aldehyde's protons are positioned on the same half-sphere as the Lewis acid. The *syn*-clinal orientation generates a larger distance between the Lewis acid and the $R^2$ residue and is thus favored for sterically demanding Lewis acids and/or $R^2$ residues (Scheme 2.100).

***2.3.2.2 Aldols Based on Asymmetric Aldehydes*** The aforementioned transition state models are playing a crucial role when stereoselective addition to chiral aldehydes with α- and/or β-substituents needs to be predicted. For aldehydes with an *anti*-relationship, both the Felkin TS and the Cornforth–Evans TS predict the same face selectivity. Consequently, such aldehydes exhibit excellent stereoselectivities. On the other hand, 2,3-*syn* aldehydes provide Felkin and Cornforth–Evans opposing situations, which often results in poor selectivities (Scheme 2.101). At this point, we have to point out that the literature holds a vast amount of examples with excellent selectivities in contrast to the earlier predicted analysis.

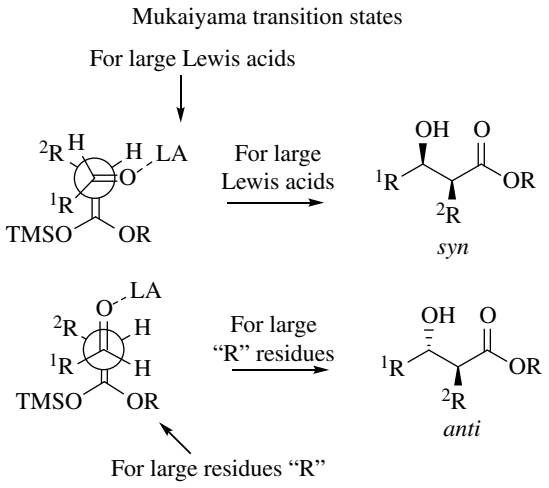
The opposite situation is observed if chelating aldehydes are involved. Then the 2,3-*anti*-situation is the opposing configuration, and the 2,3-*syn* case is the reinforcing one (Scheme 2.102).

The synergistic effects of all the described factors can even be slightly more complicated if the cyclic Zimmerman–Traxler transition state and the Felkin model are combined as it is the case when enolates are used as nucleophiles. Scheme 2.103 displays both analyses for *Z*- and *E*-enolates, respectively. For *E*-enolates, Felkin attack leads to a transition state, which does not impose unfavorable *syn*-pentane interactions. The opposite is true if the *anti*-Felkin transition state is adopted. On the other hand, *Z*-enolates impose such a *syn*-pentane interaction if a Felkin transition state is adopted. Consequently, not the α-proton but the methyl group is located in the half-sphere of the aldehyde's proton. This non-Felkin transition state is also called the Roush transition state and explains the unexpected facial selectivity for *Z*-enolates (Scheme 2.103).

An ample evidence that the earlier described models that are based on the full consideration of α- and β-substituents on the aldehyde are oversimplified can be evidenced by the reported synthesis of swinholide by Paterson et al. [6]. In their synthesis, a simple alteration in the configuration at γ-position changes completely the facial selectivity of the enol nucleophile. As shown in Scheme 2.104, equation **A**, Felkin control minimization of *syn*-pentane interactions and application of the Cornforth–Evans transition state lead to a reinforced Felkin attack. On the other side, just changing the aforementioned configuration (**B**) leads to *syn*-pentane interactions between the methyl groups at C4 and C2 and ultimately to a non-Felkin transition state (Scheme 2.104).



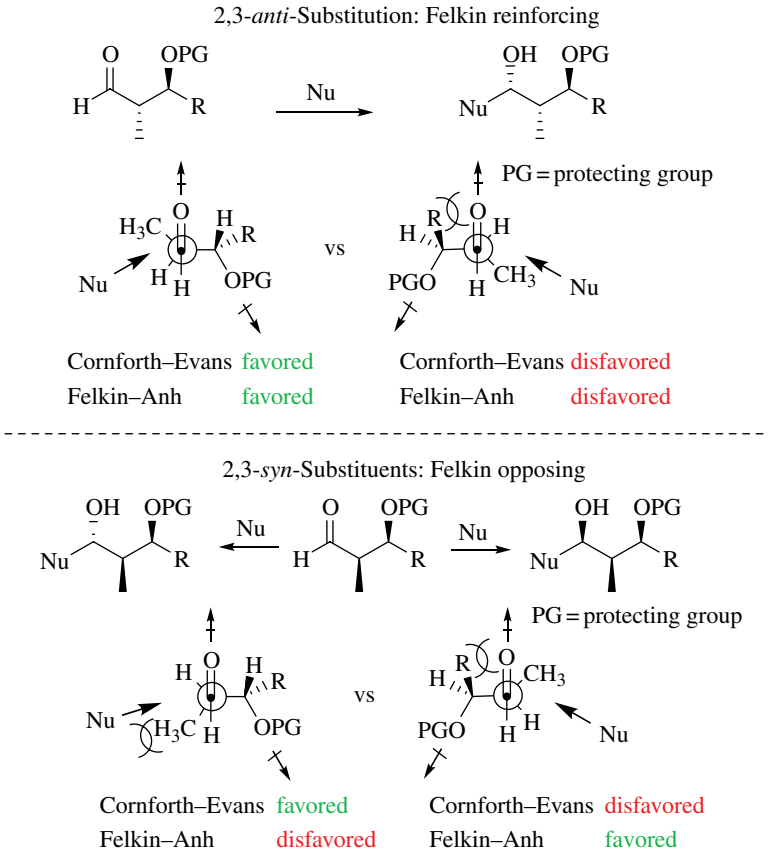

**SCHEME 2.99** Transition state models predicting nucleophilic attack at asymmetric carbonyl compounds.



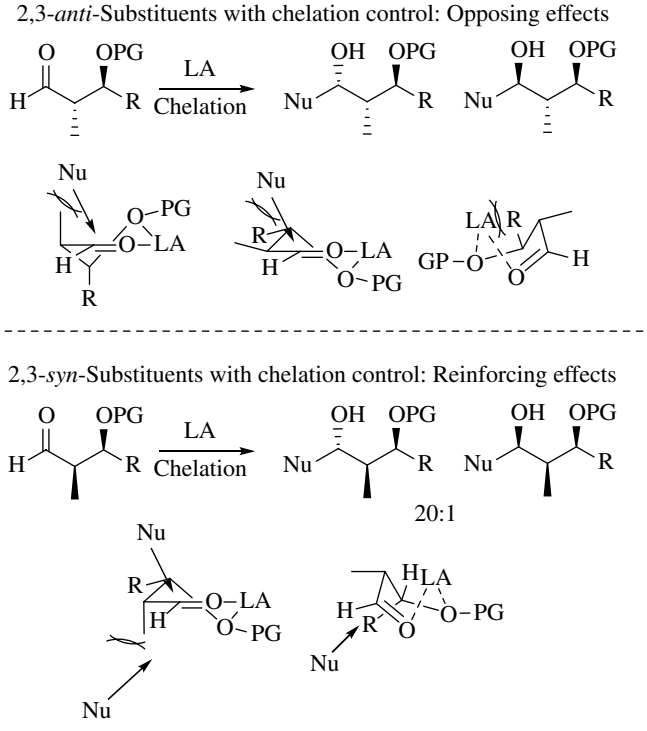

**SCHEME 2.100** Mukaiyama transition states.

***2.3.2.3 Aldols Based on Chiral Enolates*** Besides the predetermined selectivity observed in aldol reactions enforced by the earlier described factors, chiral auxiliaries on the enolate part can interfere and overrule the facial selection. One example is the use of isopinocampheyl ligands as introduced by Paterson. In both cases, the 2,3-*syn* and the 2,3-*anti*-aldehyde can be converted to their diastereoisomers in good to excellent selectivities (Scheme 2.105).

Similar to the stereocontrol executed by chiral centers at aldehydes, the α- and β-chiral centers of enolates can be used to control the stereochemical outcome of aldol reactions (Scheme 2.106) [7]. Both *Z*- and *E*-enolates with α-methyl branches transform under the influence of this chiral center to the corresponding *syn*- or *anti*-aldol products. If a β-alcohol capable of performing hydrogen bonding to the aldehyde's proton is present, an 1,5-*anti*-asymmetric induction can take place (Scheme 2.106).

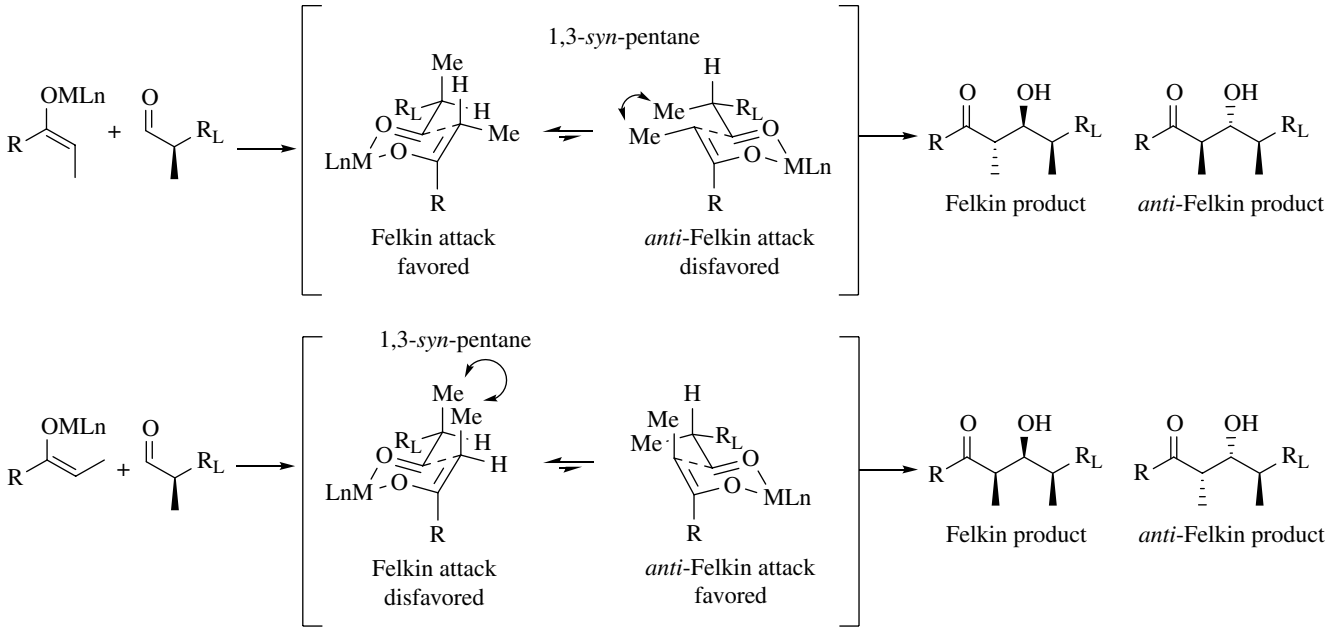



**SCHEME 2.101** Stereoselective nucleophilic attack rationalized on α- and β-substituents.

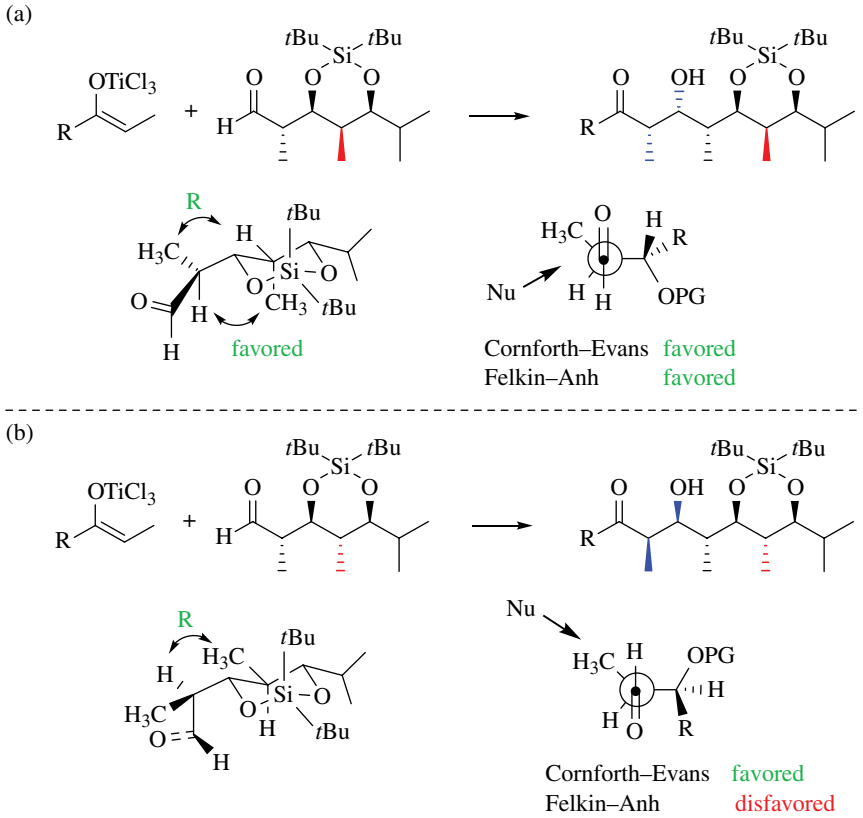



**SCHEME 2.102** Stereoselective nucleophilic attack rationalized on α- and β-substituents for chelation control.

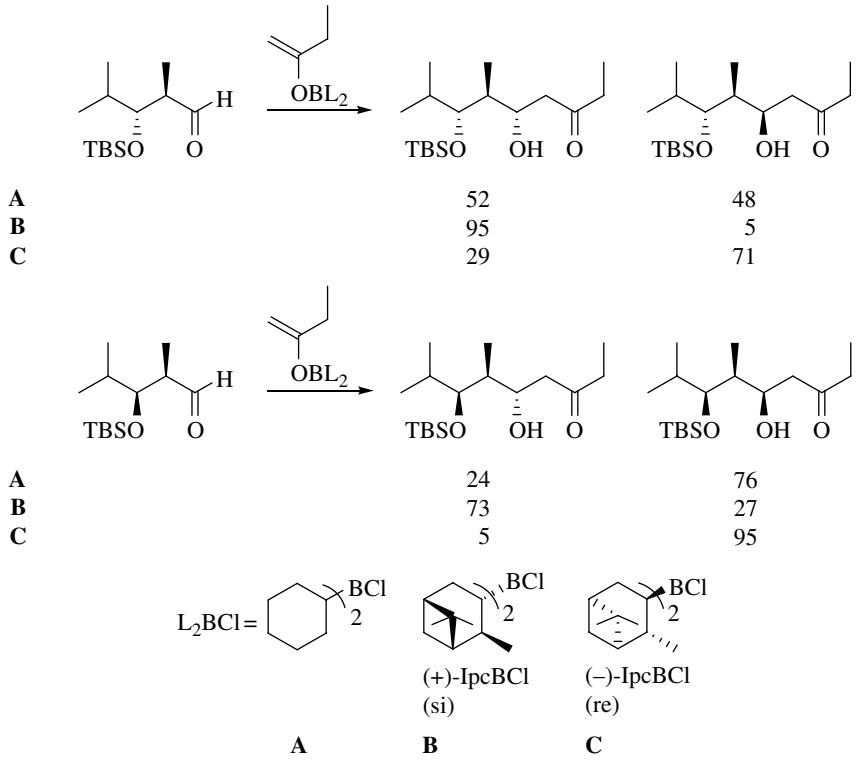
As in the analysis of stereocontrolling effects in 2,3-disubstituted aldehydes for 2,3-disubstituted ketones, a similar analysis can be performed (Scheme 2.107). Both the 2,3-*syn* and the 2,3-*anti*-ketones in Scheme 2.107 were transformed to their corresponding *Z*-enolates using $TiCl_4$ and $Et_3N$ as the base. Reaction with an achiral aldehyde generates in both cases the 2,2′ and 2′,3′ *syn*-product [8]. Here, obviously the β-substituent seems not to influence the stereochemical outcome of the reaction. Again, a chair transition state is proposed and the C2-hydrogen is oriented toward the metal's ligand in order to minimize steric repulsion. The sterically least hindered face of the enolate then adds to the carbonyl group. The 2′,3′-*syn* relationship follows the arguments of the aforementioned Zimmerman–Traxler transition state. The corresponding *E*-enolates were generated by using cyclohexyl boron chloride. Even though the enolate geometry had been changed, the product exhibits again *syn*-2,2′ relationship. However, the arguments for this selectivity are different. Since the *E*-enolate unfolds allylic strain between the enolate's methyl group and the proton at carbon C2, minimization of this interaction becomes more relevant and the proton is now oriented toward the enolate's substituent. As a consequence of the *E*-enolate geometry and the chair-like transition state, the 2′,3′ substituents are *anti*-configured.



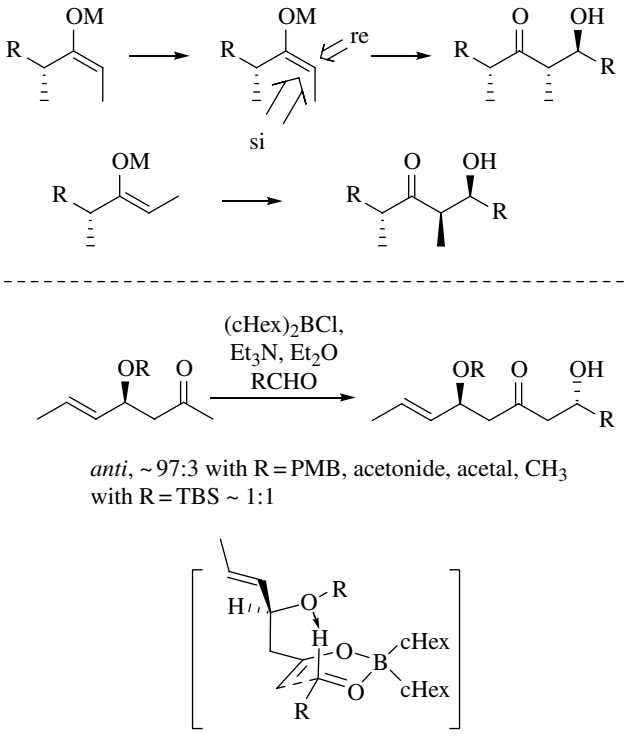

**SCHEME 2.103** Roush transition states describing the unexpected *Z*-enolate *anti*-Felkin attack.




**SCHEME 2.104** The determinant factor of γ-substituent positioned (a) *trans* or (b) *cis*, in swinholide synthesis.




**SCHEME 2.105** The use of isopinocampheyl enolates as a determining factor of facial selectivity.

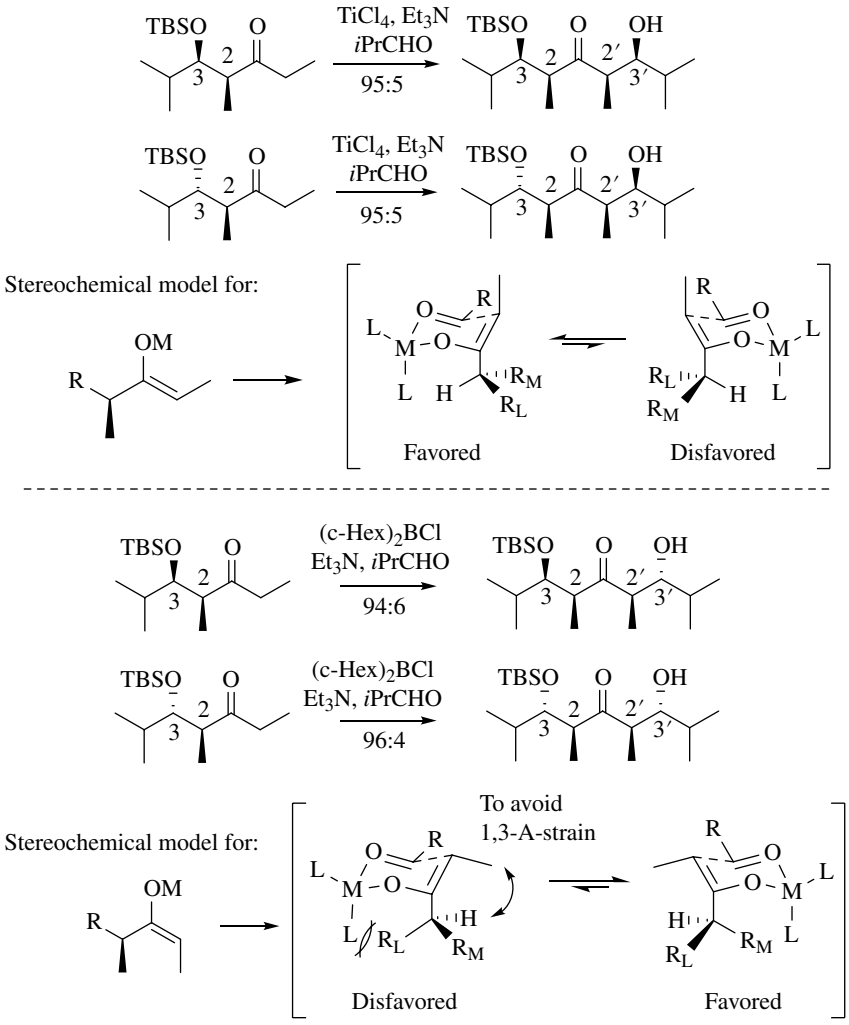



**SCHEME 2.106** Aldol reaction of α-chiral enolates.

Again, chiral ketones can be combined with Paterson's isopinocampheyl boron concept. The great advantage of Paterson's strategy is the fact that the Ipc ligands overrule the inherent selectivity and thus take over control of stereoselectivity (Scheme 2.108). A common subsequent step is the subsequent reduction to yield either the *anti*- or *syn*-diol. These strategies will be discussed in detail in the subsequent chapter.

*Chiral Auxiliaries in Aldol Reaction* Asymmetric aldol reactions utilizing chiral auxiliaries have emerged as one of the most reliable methods in organic synthesis. Both *syn*- and *anti*-selective aldol reactions have been developed over the years. The field of asymmetric *syn*-aldol reactions has been largely advanced by Evans since his development of dibutylboron enolate aldol chemistry based on amino acid-derived chiral oxazolidinones (Scheme 2.109) [9].

All these oxazolidinone-, oxazolidinethione-, and thiazolidinethione-based enolates react with aldehydes via the well-established six-membered Zimmerman–Traxler chair-like transition state. Due to the fact that the amino acid-derived chiral auxiliary is only readily available in one enantiomer and thus only provides one enantiomer of the *syn*-aldol, exhaustive studies by Crimmins established a method based on titanium enolates providing convenient




**SCHEME 2.107** Stereochemical analysis for the addition of aldehydes into 2,3-disubstituted ketones.

access to both "Evans" and "non-Evans" *syn*-aldol products (Scheme 2.110) [10]. The initial adaption of amino acid-derived oxazolidinone chiral auxiliaries to titanium enolate reactions was conducted by Thornton [11]. The "non-Evans" *syn*-aldol product can be rationalized by the second equivalent of $TiCl_4$, abstracting one additional chloride from the chelating Lewis acid and by doing so enabling coordination the chiral auxiliary. This trivalent coordination then leads to the opposite facial selectivity as observed when two equivalents of $TiCl_4$ are used.

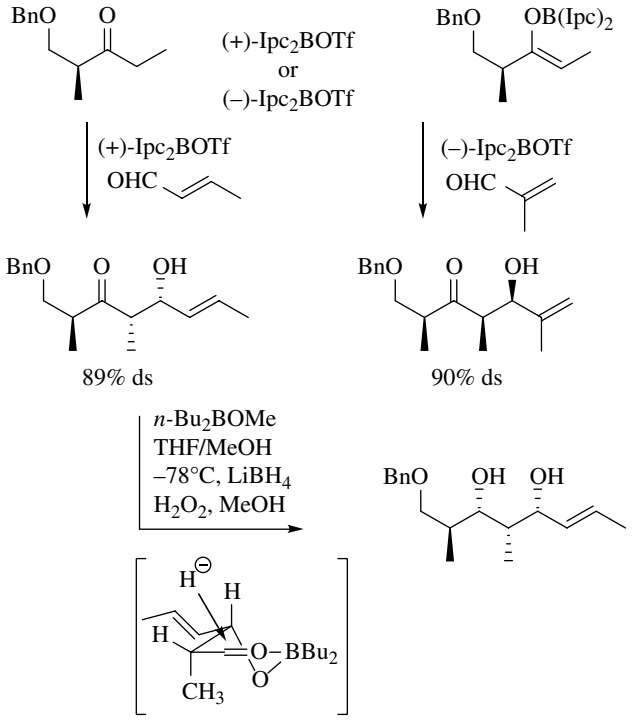
Another prominent example of a chiral auxiliary for highly diastereoselective synthesis of *syn*-aldol adducts was developed by Masamune utilizing (*R*)-mandelic acid (Scheme 2.111) [12]. This early example of chiral ethyl ketone takes advantage of the mandelic acid as the chiral source and liberation of the corresponding acid though oxidative cleavage.

The general applicability of the Oppolzer sultam as a practical chiral auxiliary in the preparation of enantiomerically pure *syn*-aldols compares very favorably with the aforementioned methods (Scheme 2.112) [13].

Oppolzer's application greatly benefits from the prospect of purifying the initially formed *syn*-aldol products by recrystallization. Additionally, the chiral auxiliary can be easily obtained from camphor and functionalization by Reychler's reaction [14].

A common example for auxiliary-controlled *anti*-aldol reactions is the Masamune–Abiko process since the procedure covers the synthesis of both enantiomers depending on the nature of the auxiliary, which is readily available in both enantiomeric forms [15]. This *anti*-selective aldol reaction has been performed by using enantiomerically pure carboxylic esters derived from (−)- or (+)-norephedrine. The method is applicable to a wide range of aldehydes with high selectivity (both *anti*/*syn* and diastereoselectivity of *anti*-isomer) [16]. A typical example of this aldol approach is depicted in Scheme 2.113. It is proposed that the reaction proceeds via a six-membered Zimmerman–Traxler transition state.

As an extension of the Evans' aldol reaction, the so-called Evans–Metternich variation [17] adds two polyketide units to the growing polyketide chain (Scheme 2.114). It should be pointed out that here not the chiral auxiliary controls the stereoselectivity but the α-chiral center, which in turn was previously generated by addition to the Evans propionate. Using different metals and reaction conditions, three out of four possible stereoisomers can be generated and subsequent reduction of the keto carbonyl group can construct an additional chiral alcohol (vide infra).

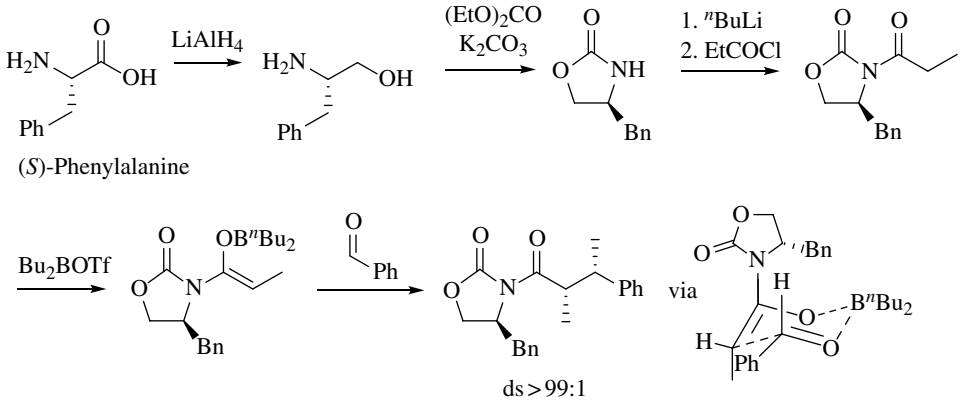



**SCHEME 2.108** Paterson's Ipc strategy on chiral ketones.

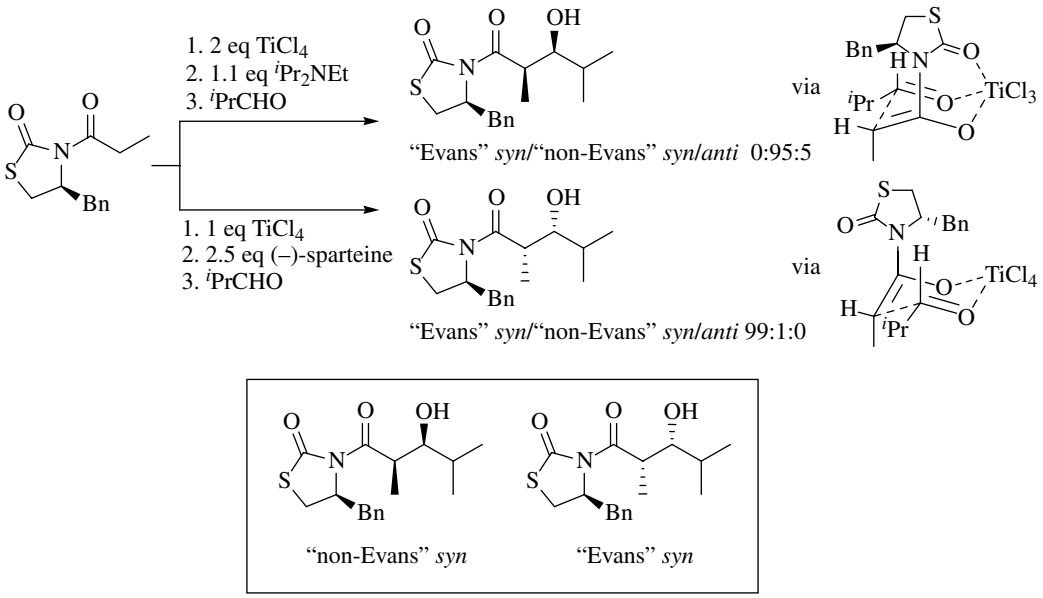
*Chiral Metal Enolates in Aldol Reaction* A general overview on common acetate aldol reaction using chiral metal enolates is given in Scheme 2.115. Both Masamune [18] and Corey [19] in their acetate aldol reaction use C2-symmetric boron complexes and as the acetate building block thio esters. Transformations with aldehydes usually provide enantiomeric ratios between 92:8 and 96:4 in good yields. More commonly used nowadays are Paterson's, Duthaler's, and Braun's acetate strategies.

Paterson's Ipc ligands [20] can be used for the aldol reaction of ethyl ketones and for methyl ketones. In both cases, good selectivities were observed. However, it should be pointed out here that for both ketones, different transition states are operative and that the Ipc ligands have opposite facial selectivities at methyl and ethyl ketones. When used with ethyl ketones, (–)-$Ipc_2$BOTf leads to *si*-attack, whereas with methyl ketones, (–)-$Ipc_2$BOTf leads to *re*-attack. The differences can be rationalized by changing from a chair transition state to a twist-boat transition state for methyl ketones, which do not longer suffer from unfavorable steric interactions between the chiral auxiliary and the substituent at the enolates terminal position. The great advantage over other reagents is the fact that ketones can be employed, which thus opens the possibility to use this aldol reaction as the pivotal step in convergent synthesis or as stitching reaction to add on both sides of the ketone aldehyde segments. Furthermore, recrystallization during the preparation of the reagent allows improving the enantiomeric purity of the chiral ligand, and this in turn leads to improved selectivities of the desired products.

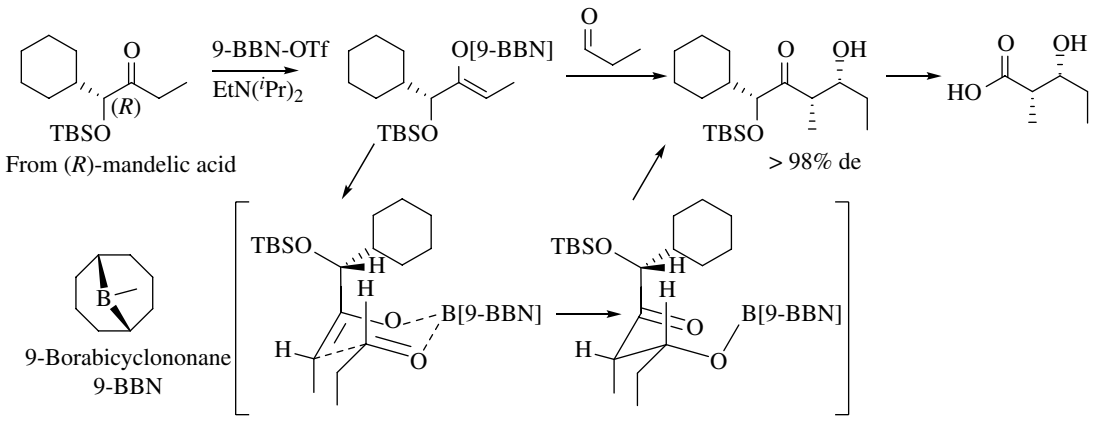
Braun's HYTRA reagent ((*R*)- or (*S*)-2-hydroxy-1,1,2-triphenyl acetate) is derived by simple transformations from inexpensive and enantiomerically pure methyl mandelate. Double deprotonation of the chiral acetate with LDA generates the enolate required for addition to aldehydes. The diastereomeric ratio observed ranges typically between 10:1 and 12:1. When the corresponding magnesium salts are



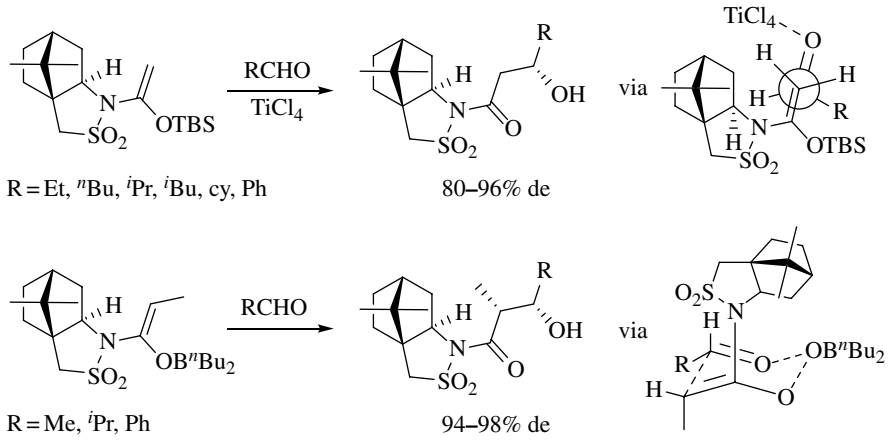

**SCHEME 2.109** Evans auxiliary performing highly *syn*-selective asymmetric boron aldol reaction.



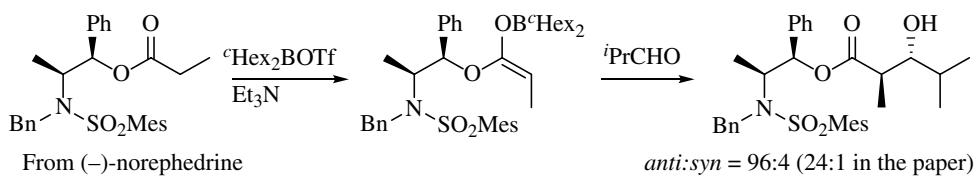

**SCHEME 2.110** Oxazolidinethione-based *syn*-Evans aldol reactions—"Evans" or "non-Evans" *syn*-aldol products.



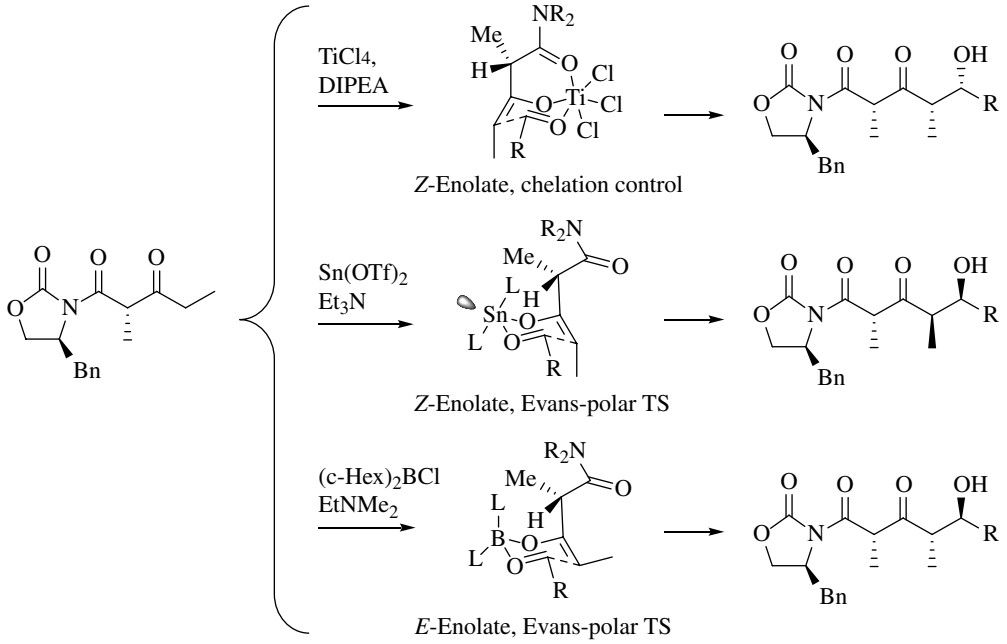

**SCHEME 2.111** *Syn*-selective aldol reaction using Masamune's (*R*)-mandelic acid-based auxiliary.



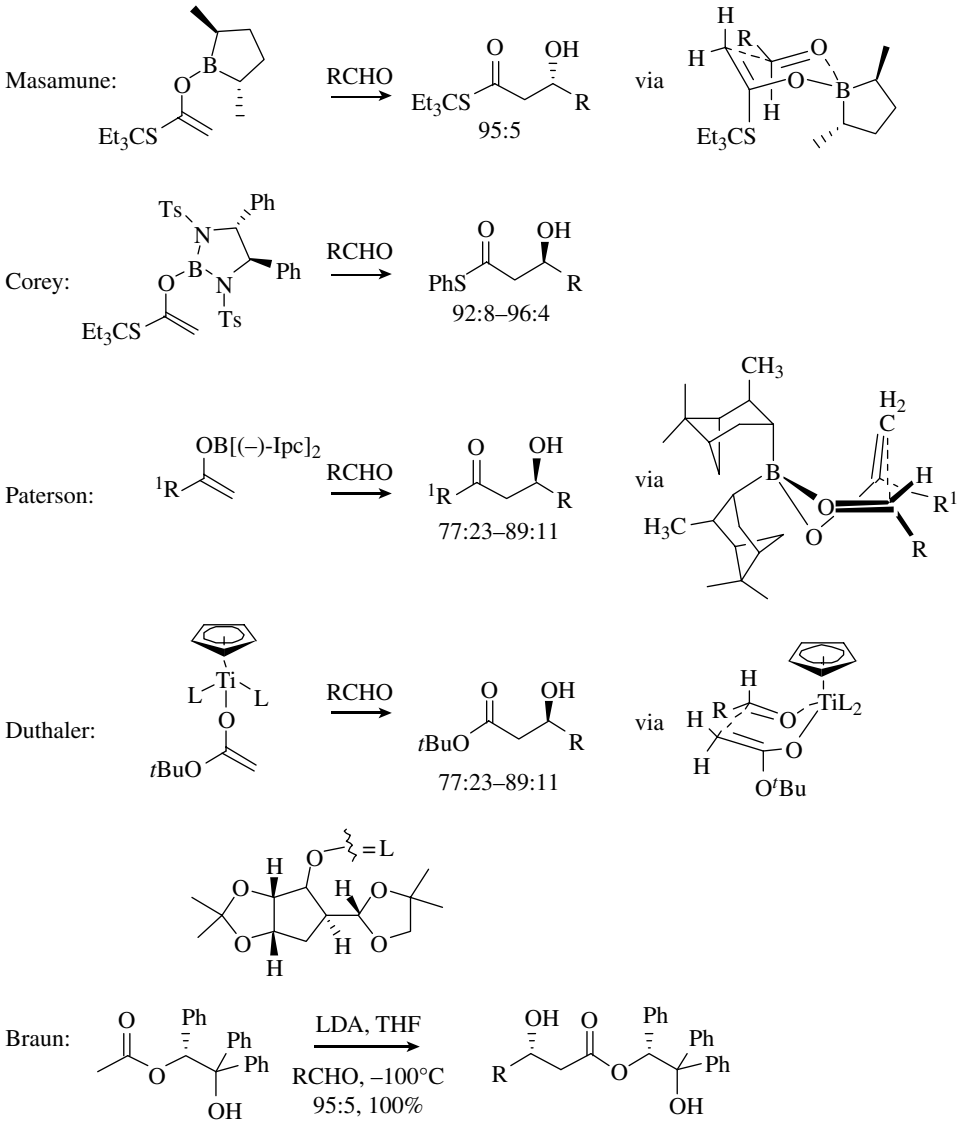

**SCHEME 2.112** Oppolzer sultam-directed asymmetric synthesis of *syn*-aldol products.



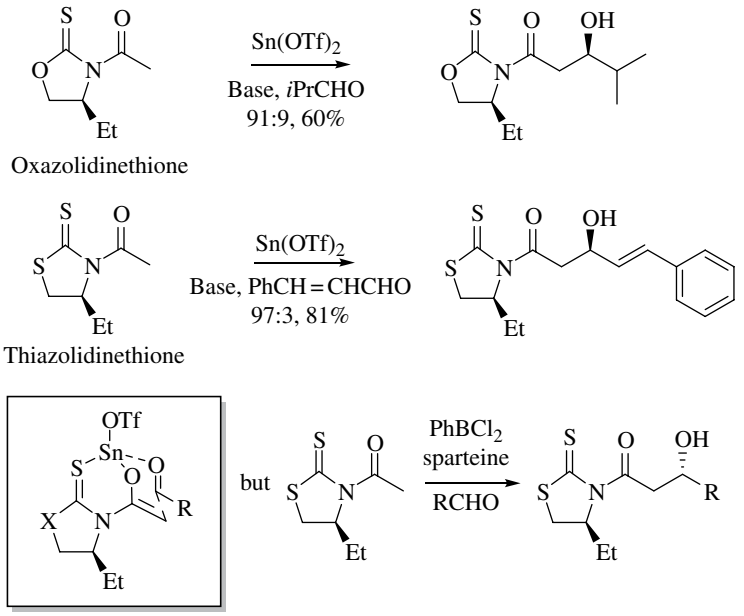

**SCHEME 2.113** Typical procedure for *anti*-selective Masamune–Abiko aldol reaction.




**SCHEME 2.114** Evans–Metternich aldol reaction.




**SCHEME 2.115** Aldol reaction using chiral enolates.




**SCHEME 2.116** Acetate aldol reactions using oxazolidinethione or thiazolidinethione.

used, the diastereomeric ratio increases up to 50:1. An additional advantage of this underexploited reagent lies in the fact that aldol products can be easily recrystallized and thus further improved with respect to their diastereoselectivity. After hydrolysis both the β-hydroxycarboxylic acid and triphenylglycol are easily separated.

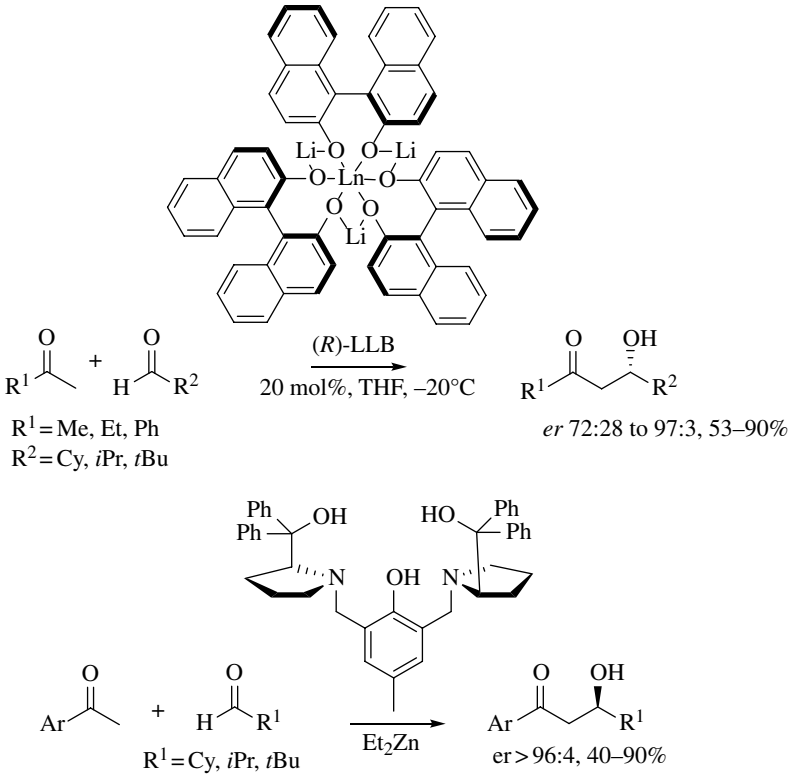
The Duthaler aldol reaction [21] utilizes the transmetalation of relatively stable lithium enolates of *tert*-butyl acetate with chloro(cyclopentadienyl)-bis(1,2:5,6-di-*O*-isopropylidene-α-D-glucofuranos-3-*O*-yl)titanate. The so-obtained titanium enolate adds to the *re*-side of aldehydes and can be converted under acid or basic conditions into its corresponding acid. As often performed for the Braun aldol reaction, recrystallization of the primary aldol product is used as a convenient way for purification and improvement of selectivities.

In contrast to Evans propionate methodology, the corresponding *N*-acetyl oxazolidinones yield aldol products only at an approximate 1:1 ratio [22]. Nagao and Fujita provided an extension of the original Evans strategy by taking advantage of the coordination capabilities of tin(II) to the sulfur atoms of *N*-acetyloxazolidinethione [23] and thiazolidinethione, respectively (Scheme 2.116) [24]. It turned out that oxazolidinethiones perform slightly less stereoselective than the corresponding thiazolidinethiones when α,β-unsaturated aldehydes are employed. An additional advantage of thiazolidinethione auxiliaries is the greater ease by which they are cleaved off the product. The observed selectivities can be explained by coordination of the exocyclic sulfur atom and the carbonyl oxygen to tin(II) generating a chair-like transition state. Sammakia and coworkers [25] reported on a variation of this protocol that uses boron enolates and dispenses tin(II) Lewis acids. Using instead sparteine provides a highly diastereoselective acetate aldol reaction (9.5:1 to 100:1), which is believed to operate through an open transition state.

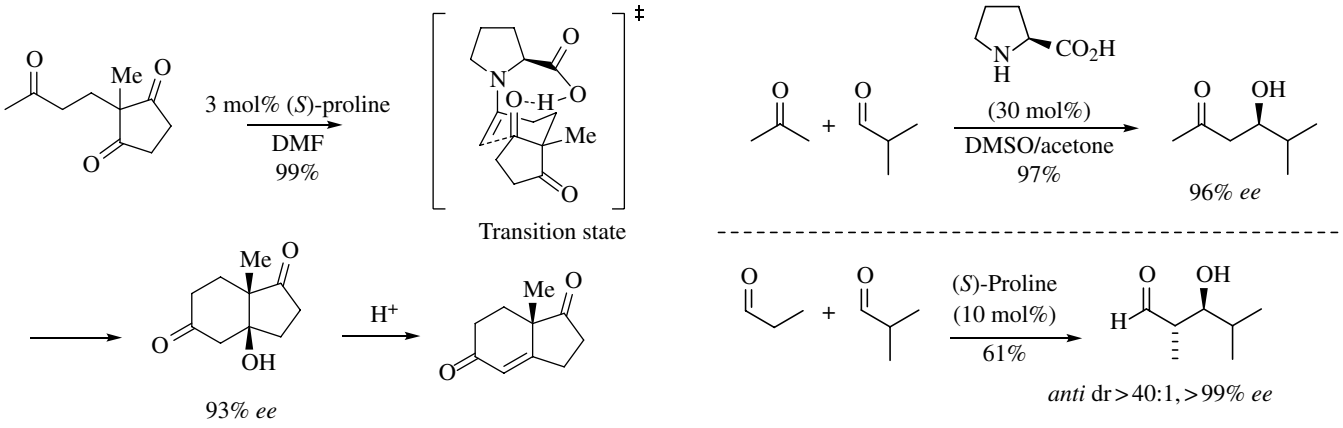
***2.3.2.4 Direct Aldol Reactions*** The most frequently applied direct aldol reactions in which unmodified achiral methyl ketones can be directly activated by catalysts were reported by Trost [26] and Shibasaki [27] (Scheme 2.117). Both used bimetallic catalysts as enzymatic mimetics for ketone activation. Shibasaki reported the use of $LnLi_3$tris (binaphthoxide) to perform aldol reactions between methyl ketones and branched aldehydes. The underlying notion was that this catalyst mimics enzymatic activity through Lewis acid activity based on the lanthanum ion and Brønsted basic activity due to the lithium binaphtoxide. The enantiomeric selectivity ranges from modest to excellent ratios.

On the other hand, Trost used zinc in his bimetallic catalyst. One zinc atom is believed to form the metal enolate, whereas the other acts as a Lewis acid for carbonyl activation. Aldol reactions between branched aldehydes and methyl ketones perform in good yields and excellent selectivities (Scheme 2.117). Besides aryl methyl ketones, simple acetone or methyl vinyl ketone could be used as well [28]. These extensions make this protocol a truly universal method for convergent natural product synthesis.

Even though the use of chiral amines and consequently the stereoselective reaction of enamines and aldehydes or ketones have been applied successfully as the Hajos–Parrish–Eder–Sauer–Wiechert reaction [29], it has been revived and applied to total synthesis starting in 2000 with the publication from Barbas and List (Scheme 2.118) [30].



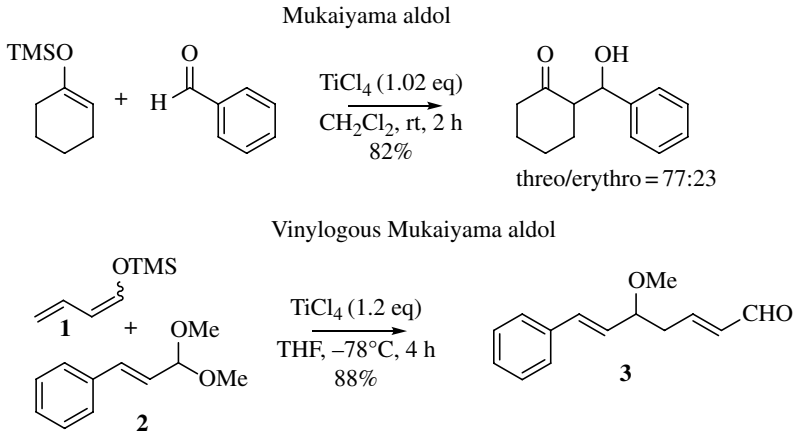

**SCHEME 2.117** Indicative chiral Lewis acid-catalyzed direct aldol reactions.




**SCHEME 2.118** Hajos–Parrish–Eder–Sauer–Wiechert reaction.

**SCHEME 2.119** Selected organocatalytic aldol reactions.

An important contribution to the field of direct aldol reaction was put forward by MacMillan who reported on the enantioselective direct cross aldol reaction (Scheme 2.119) [31]. Two aldehydes are brought to reaction with 10 mol% proline to produce selectively the *anti*-aldol product. If different aldehydes are used, the one that contains a sterically more crowded side chain acts as the carbonyl component, whereas simple aldehydes, in most cases acetaldehyde or even acetone, act as nucleophiles. The advantage of such organocatalytic aldol reactions is the fact that aldehydes can be used, which is practically prohibited if enolates or standard Lewis acids are used. Furthermore, the so-obtained aldol products can be used directly in subsequent transformations without the necessity to perform functional group transformations or oxidation state changes. Additionally,




**SCHEME 2.120** Mukaiyama aldol reaction.

in most cases, simple catalysts such as proline are sufficient and provide very good selectivities. The drawback is clearly that in most cases, such organocatalytic processes cannot be employed if the substrate contains a chiral position since the enamine formation would lead to epimerization at those centers. Scheme 2.119 exemplifies such a situation for both transformations. Starting from either acetone or acetaldehyde, proline leads to the required aldol product in excellent yields and selectivities. In general the proline-catalyzed aldol reaction with propionaldehyde generates the *anti*-aldol product. The product can be used directly in a subsequent aldol reaction without an additional oxidative stage to produce the requisite carbonyl group. However, even if in principle a second organocatalytic reaction would be possible, the second transformation uses a Lewis acid-catalyzed Mukaiyama aldol reaction that takes advantage of the Felkin-reinforcing *anti*-configuration.

### *2.3.2.5 Mukaiyama Aldol Reactions*

*Based on Chiral Coupling Partners* The first report on a new protocol for an aldol-type reaction using trimethylsilyl enol ethers was published in 1973 by Mukaiyama (Scheme 2.120). The reaction between trimethylsilyl enol ethers and ketones or aldehydes was performed in the presence of titanium tetrachloride as the Lewis acid [32]. It was immediately recognized that this was an important extension of established aldol protocols since addition to aldehydes would now take place through Lewis acid catalysis. An extension of their original work was achieved when Mukaiyama and Ishida applied Fuson's principle of vinylogy [33] to their new reaction. In their first vinylogous Mukaiyama aldol reaction (VMAR), the crotonaldehyde-derived silyl dienol ether (**1**) and cinnamaldehyde dimethyl acetal (**2**) were brought to reaction with $TiCl_4$ as the Lewis acid [34].

Different orbital coefficients and/or electrophilic susceptibility have been used to rationalize the fact that vinylogous ketene acetals unfold their nucleophilicity at the γ-position

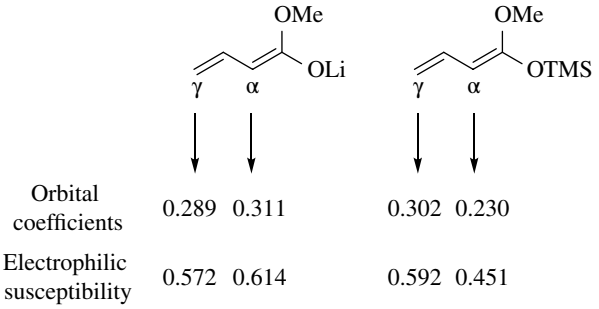
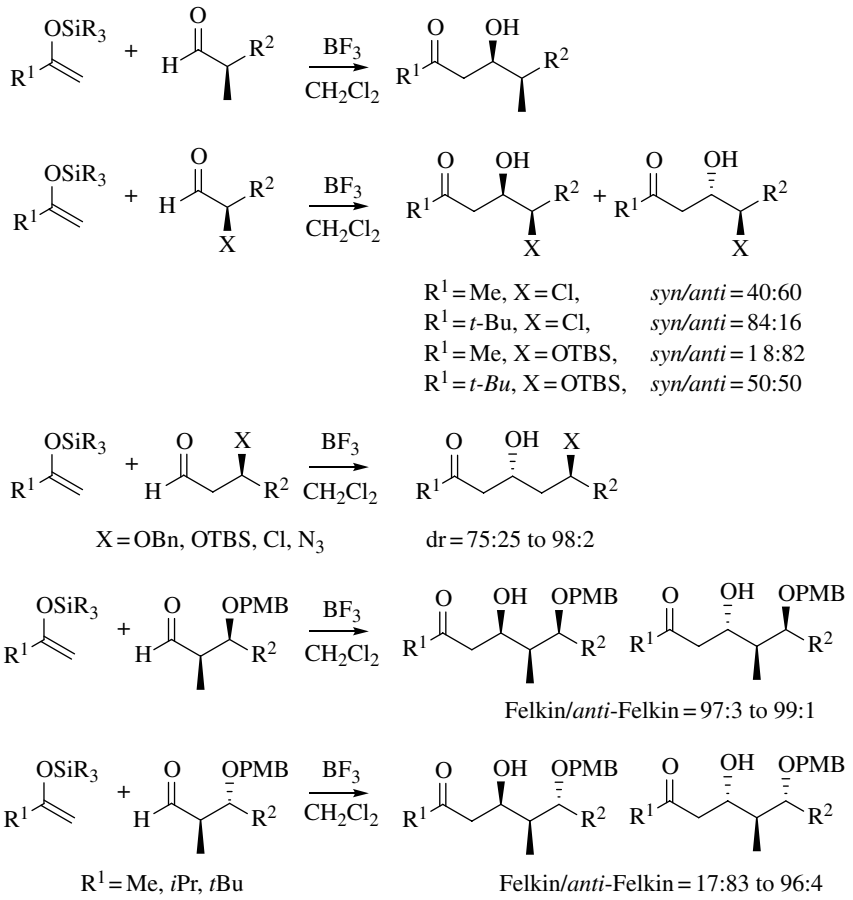



**FIGURE 2.2** Regioselectivity of the Mukaiyama aldol reaction.

in contrast to corresponding metal dienolates. Comparison of both values shows that for metal dienolates, both the orbital coefficients and electrophilic susceptibility are larger at the α-position, whereas for vinylogous silyl ketene acetals, the γ-position displays larger values (Fig. 2.2) [35].

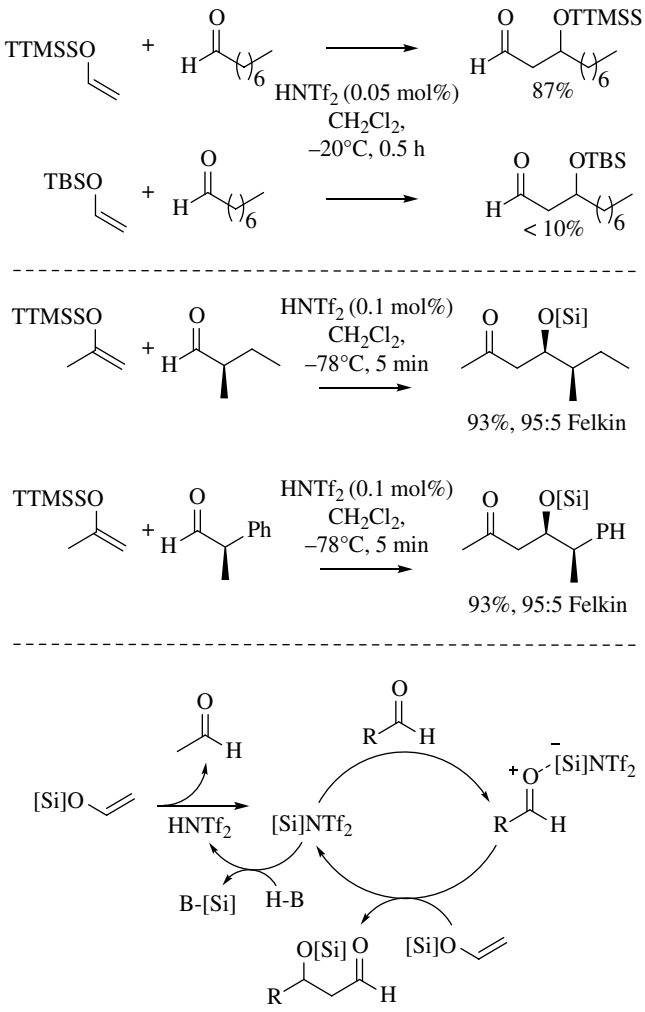
In contrast to aldol reaction, it is not a cyclic but an open transition state that is used for rationalizing the observed selectivities. First, valuable investigation of the Mukaiyama aldol reaction transition state was put forward by Heathcock [36] and later by Denmark [37] and others. In all their arguments, steric repulsion plays the pivotal role, and in presentations of the transition state using the Newman projection, both hydrogens at the reacting centers are located in the same half-sphere of the reacting molecule. At the same time, the Lewis acid adopts an orientation that locates itself on the same side as the aldehydes proton. Recently, excellent theoretical analysis of the Mukaiyama aldol transition states was put forward by Helquist and Wiest (vide supra). Taking all these arguments into consideration, one can nowadays rationalize the diastereoselectivity of Mukaiyama aldol reaction with good confidence. If silyl enol ethers of methyl ketones or acetates are used, the stereochemical analysis is simplified to just an assessment of Felkin and *anti*-Felkin products, and it follows the same arguments as discussed in




**SCHEME 2.121** Directing effects in Mukaiyama aldol reactions.

the preceding text. As shown in Scheme 2.121 a methyl branch controls the diastereoselective addition to produce the Felkin product with excellent selectivities. If a heteroatom is present at the α-position, the directing effect strongly depends on the nature of the heteroatom and the bulkiness of the residue R1 (Scheme 2.121). If small residues are present such as a methyl group, the stereoelectronic preferences favor the *anti*-product. If larger residues such as a *t*-butyl group are present, the steric arguments of the classical Felkin model favor the *syn*-product. The extent by which the individual effect governs the stereochemical outcome is mainly controlled by the nature of the hetero element and might be a reflection of the electronegative nature of these heteroatoms. Scheme 2.121 shows that in cases where the α-substituent is a chloride, large $R^1$ residues produce substantial amounts of the *syn*-product, whereas OTBS residues produce the *anti*-isomer as the major product with methyl as $R^1$ and basically a 1:1 mixture for *t*-butyl residues. As discussed in the preceding text, a heteroatom in β-position favors the *anti*-product due to either the polar Felkin or Cornforth–Evans transition state. Having both the α- and β-substituents present leads again to a situation at which Felkin-reinforcing (*anti*) and Felkin-opposing (*syn*) situations can be distinguished.

Based on the described logic, an innovative approach to 1,3-diols was put forward by Yamamoto and Yamaoka [38]. In their contribution, the super silyl group was introduced, which not served only as a unique protecting group but as a superior Lewis acid. Tris(triethylsilyl)silane ($(TES)_3Si$) and tris(trimethylsilyl)silane ($(TMS)_3Si$, TTMSS) can be easily prepared from trichlorosilane, chlorotriethylsilane, and chlorotrimethylsilane, respectively [39]. TTMSS ethers can be cleaved with photolysis (254 nm) or by the action of TBAF [40]. The convenient preparation of enol ethers from acetaldehyde and their conversion to the corresponding alcohols through nucleophilic addition to aldehydes allow transformations that were not as easily accessible under basic conditions. The same reaction when performed with the TBS ether of acetaldehyde yields only in less than 10% of the desired product. The addition to α-chiral aldehydes performs with excellent stereoselectivity in favor of the Felkin product. The putative mechanism involves the liberation of Lewis acidic silicon species from the enol ether using triflimide and the activation of an aldehyde with that. The addition of a TTMSS



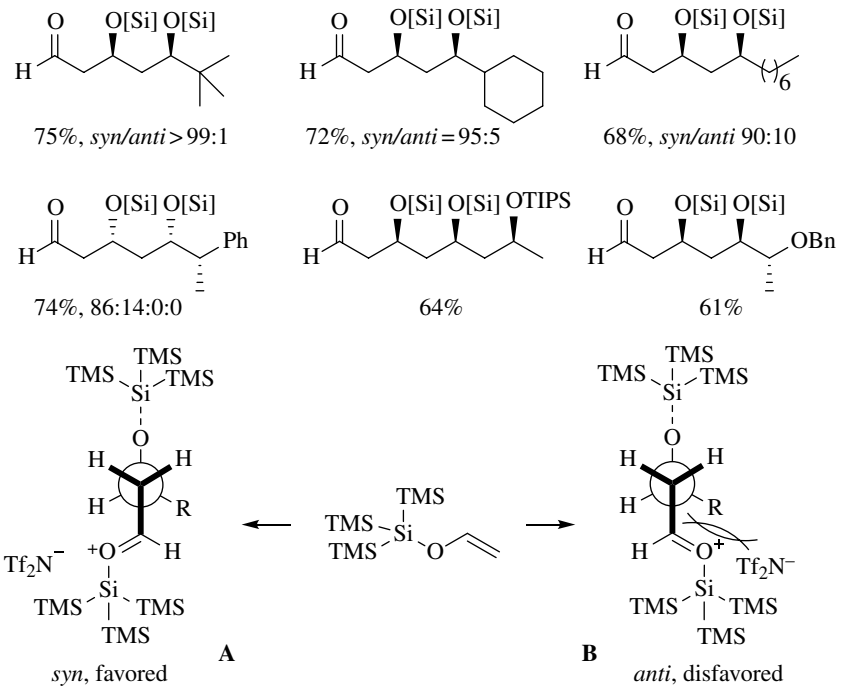

**SCHEME 2.122** Aldol reactions using Yamamoto's super silyl concept.

enol ether and concomitant protection of the resulting alcohol generate the aldol product and liberate a new silicon species to initiate the Mukaiyama aldol reaction. Catalyst loading of as little as 0.05 mol% is sufficient to generate full conversion. The observation that the same results could be obtained with $TTMSSN(Tf)_2$ as the catalyst supported the perception that this is indeed the true catalyst in what can be considered as a self-repairing catalytic system. It has to be pointed out that standard Mukaiyama aldol reaction would produce the *anti*-product on aldehydes with β-hydroxyl functionalities (Cornforth–Evans, polar Felkin), whereas enol ethers containing super silyl groups generate the corresponding *syn*-products with remarkably high selectivity (Scheme 2.122).

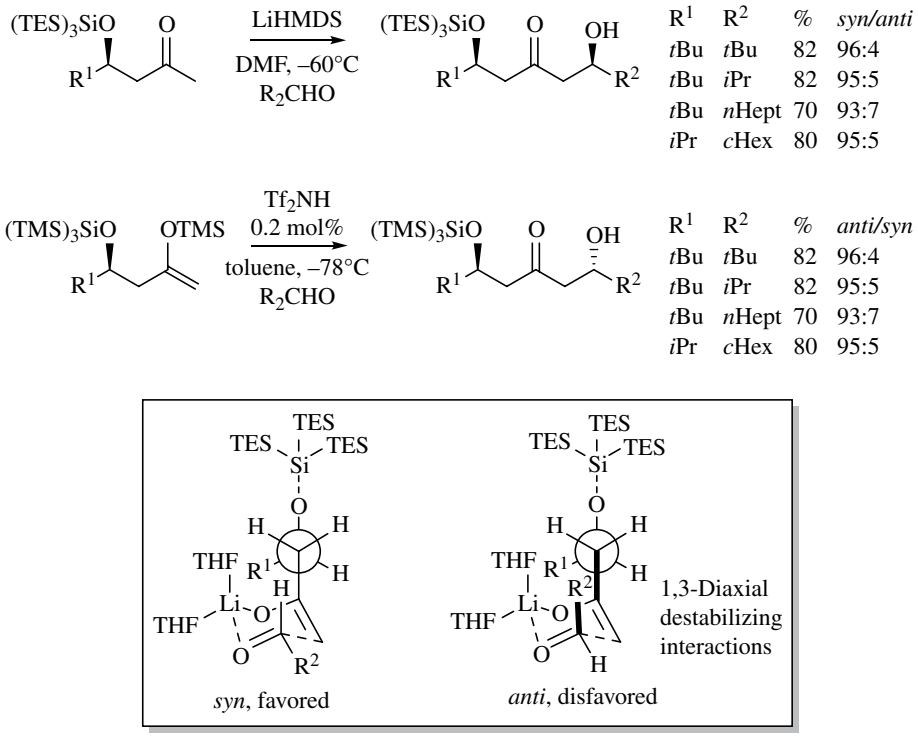
The earlier described concept can be turned into a practical protocol that would perform two consecutive additions to a given aldehyde. This can be achieved by using 2.2 equivalents of the silyl enol ether. The exceptional diastereoselectivity can be rationalized with steric arguments. First of all, the bulky TTMSS group shields the product and slows down the rate for the second conversion. This leads to complete consumption of the starting aldehyde due to its bulkiness, and the TTMSS group adopts an antiperiplanar orientation with respect to the carbonyl group. This in turn adopts an orientation away from the side chain at the β-position (Scheme 2.123). Transition state **A** reflects this behavior and exhibits no unfavorable steric interaction in contrast to transition state **B** [41].

Besides enol ethers of acetaldehyde, the corresponding enols from acetone can be also used performing comparable yields and selectivities [42]. The use of super silyl groups as protecting groups provides additional advantages for 1,5-inductions over established protecting groups. TTMSS-protected β-hydroxyl methyl ketone can be utilized in aldol reaction with other aldehydes under either basic (enolate) or acidic (Mukaiyama) conditions. As we had discussed earlier, the protected β-hydroxyl ketone motif can be used to establish a 1,5 *anti*-relationship, if protecting groups capable of coordinating to the aldehydes proton are used. By and large, this usually precludes silicon protecting group. Here however, the lithium enolate produces in good yields and selectivities the *syn*-product. On the other hand, if Mukaiyama conditions are employed, the *anti*-product is observed. The rationalization for the observed selectivity is considered to be based again on the antiperiplanar orientation of the TTMSS group. Essential to this logic is the fact that the enolate adopts an orientation that localizes the enolates oxygen on the same side as the side $R^1$ to minimize steric interactions. The aldehyde's side chain adopts an equatorial orientation to minimize gauche and 1,3 diaxial interactions. For enol ethers of methyl ketones, a similar picture is drawn. Again, the enol oxygen is located in proximity of the $R^1$ group. However, the aldehyde is attacked through an open transition state that leads to attack from the opposite face and consequently changes the selectivity from *syn* to *anti* (Scheme 2.124).

*Chiral Catalysis in Mukaiyama Reaction* The chiral (*S*,*S*)-bisoxazoline-copper (**4**, pybox) developed by Evans can be used in Mukaiyama reactions and VMARs. In particular, the use of bis(trimethylsilyl)dienol ether (**8**, Chan's diene) is of particular interest in the context of 1,3-diol formation since the keto carbonyl group can be reduced stereoselectively, as we will discuss in the succeeding text. The stereochemical outcome of these transformations was rationalized on the examination of the X-ray crystal structure of benzyloxyacetaldehyde (**5**) bound to the chiral (*S*,*S*)-bisoxazoline-copper complex (**4**). The X-ray data of the catalyst–substrate complex (**10**) indicates that the copper geometry is square pyramidal, with the carbonyl oxygen coordinated to the equatorial site in the ligand plane and the ether oxygen occupying an apical site (Scheme 2.125). This particular transformation provides excellent yields and selectivities; however bis-coordinating substrates such as benzyloxyacetaldehyde are required [43].



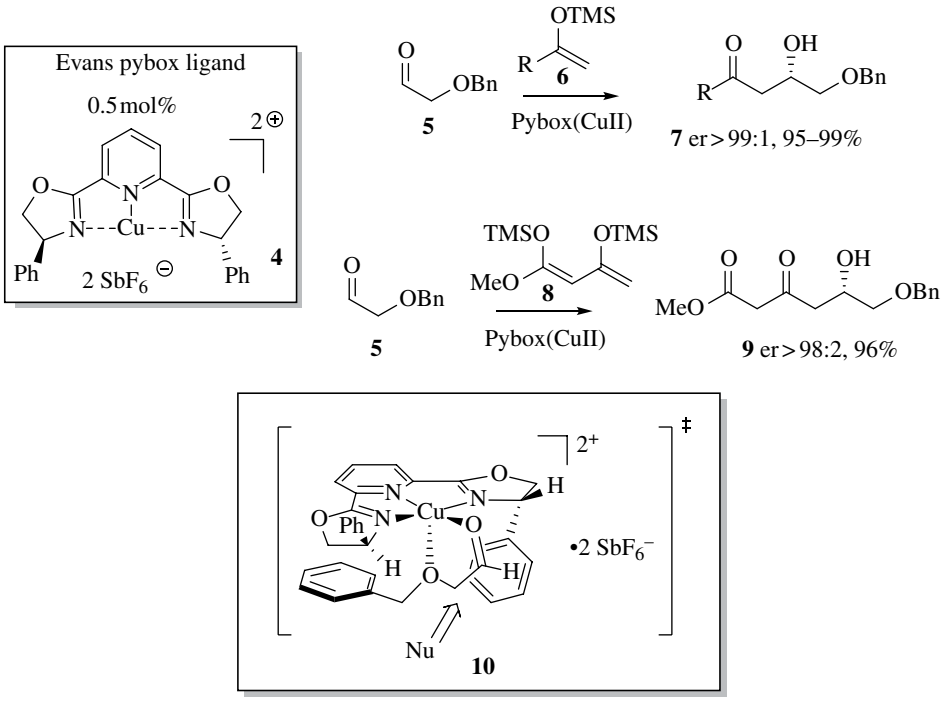

**SCHEME 2.123** Double Mukaiyama aldol reaction and transition states.




| $R^1$ | $R^2$ | % | *syn/anti* |
|---|---|---|---|
| *t*Bu | *t*Bu | 82 | 96:4 |
| *t*Bu | *i*Pr | 82 | 95:5 |
| *t*Bu | *n*Hept | 70 | 93:7 |
| *i*Pr | *c*Hex | 80 | 95:5 |

| $R^1$ | $R^2$ | % | *anti/syn* |
|---|---|---|---|
| *t*Bu | *t*Bu | 82 | 96:4 |
| *t*Bu | *i*Pr | 82 | 95:5 |
| *t*Bu | *n*Hept | 70 | 93:7 |
| *i*Pr | *c*Hex | 80 | 95:5 |

**SCHEME 2.124** Basic (enolate) vs. acidic (Mukaiyama) conditions changing 1,5-selectivity from *syn* to *anti*.



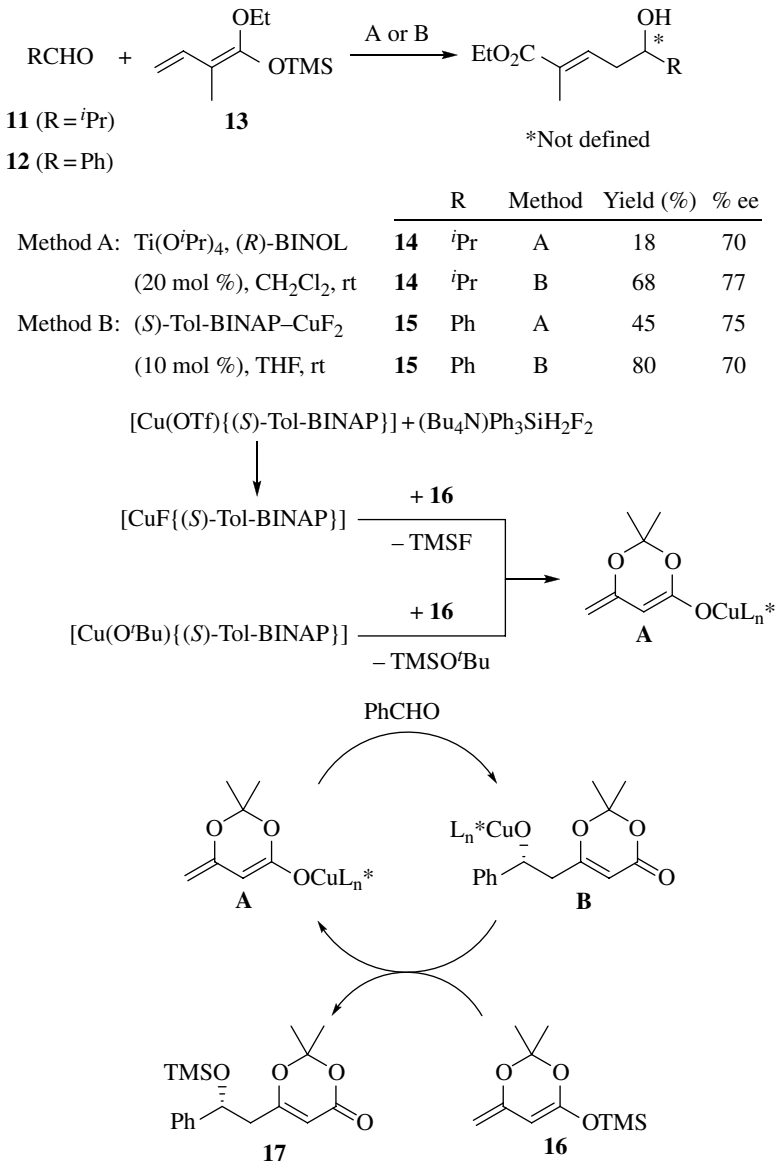

**SCHEME 2.125** Mukaiyama aldol reaction using Evans' pybox ligand.

In the course of developing catalytic asymmetric VMA reaction of ester-derived silyl dienol ethers enolates, activation through [$CuF_2$(*S*)-Tol-BINAP] became an alternative to Lewis acid activation by [(*R*)-BINOL-Ti(O*i*Pr)$_4$]. These two fundamentally different types of catalytic systems, Lewis acid activation and enolate activation, have been studied on simple aldehydes. Both catalysts provided comparable enantioselectivities but different yields (Scheme 2.126) [44]. During the mechanistic investigation of the reaction pathway, the involvement of Cu(I) species was investigated with Cu(I) alkoxide. When reaction was performed with 5 mol% of [Cu(O*t*Bu)((*S*)-Tol-BINAP)], approximately the same yields and enantioselectivities as with Cu(II) were observed, suggesting the involvement of a metal alkoxide within a catalytic cycle of Cu(I)/Cu(II) species [45]. This system was later applied in the syntheses of octalactin A [46] and (*S*)-(−)-goniothalamin [47]. The advantage of this catalytic system over Lewis acid-mediated transformations is the fact that also *Z*-configured double bond can be obtained. Using the same catalytic system, simple silyl ketene acetals can be added in excellent selectivities as well.

Chiral oxazaborolidinones (**20**, **22**, Scheme 2.127) can also promote Mukaiyama reactions and VMARs. It should be pointed out that the substitution on boron significantly alters the face selectivity of this process. If the boron atom is additionally substituted by alkyl groups (**20**), both this alkyl group and the residues on the amino acid adopt an *anti*-orientation. If the substituent is just hydrogen (**22**), then this becomes a *syn*-orientation and ultimately the face selectivity is altered.

The concept of Lewis base activation of Lewis acids was developed by Denmark, and it takes advantage of the fact that the Lewis acidity of silicon is increased when the coordination sphere is enlarged. If chiral Lewis bases are provided, here chiral phosphoramides and bisphosphoramide, $SiCl_4$ can be efficiently employed in asymmetric Mukaiyama aldol reactions. The Lewis base activation can be performed on trichlorosilyl enolates (**24**), which can be generated *in situ* by mercury-mediated trans-silylation of a TMS silyl enol ether (**18**) in the presence of $SiCl_4$. Generation of the hypervalent silicon species produces a more Lewis acidic silicon moiety, which acts to coordinate and activate the aldehyde that has to be brought to reaction (Scheme 2.128) [48].

Alternatively, $SiCl_4$ can also act as an external Lewis acid when chiral bisphosphoramide (**26**) is used. The nucleophilic oxygen atoms of the bisphosphoramide occupy an axial and an equatorial position around the hypervalent silicon atom, and coordination/activation of the reacting aldehyde occurs at the idle axial position *trans* to one of the phosphoramides (**34**). The exposure of the aldehyde's *re*-face is controlled by an interaction with the N-methyl group of the 1,1′-binaphthyl-2,2′-diamine backbone and the interactions with one of the naphthyl rings of the 1,1′-binaphthyl-2,2′-diamine. Originally, the N-methyl groups were believed to contribute only little to the observed selectivity. However, they protrude deep into the binding pocket and prevent any nucleophile from tackling the aldehyde's *si*-face (Scheme 2.129). The proposed transition state also suggests the possibility of a stabilizing, edge-to-face



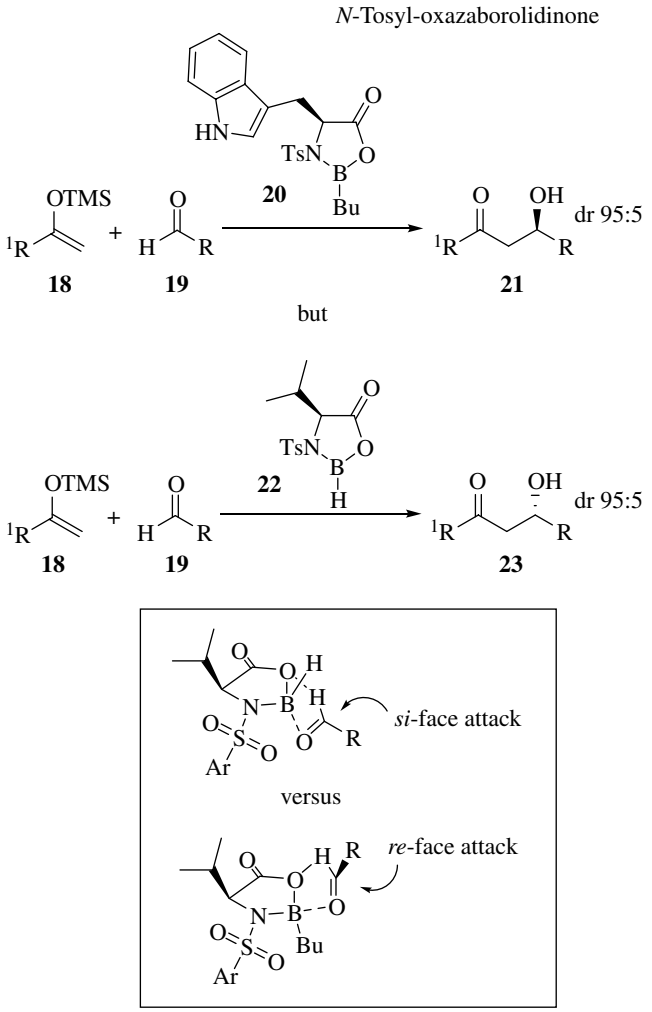

| | | | R | Method | Yield (%) | % ee |
|---|---|---|---|---|---|---|
| Method A: | $Ti(O^iPr)_4$, (*R*)-BINOL | **14** | $^i$Pr | A | 18 | 70 |
| | (20 mol %), $CH_2Cl_2$, rt | **14** | $^i$Pr | B | 68 | 77 |
| Method B: | (*S*)-Tol-BINAP–$CuF_2$ | **15** | Ph | A | 45 | 75 |
| | (10 mol %), THF, rt | **15** | Ph | B | 80 | 70 |

**SCHEME 2.126** Vinylogous Mukaiyama aldol reaction through enolate activation.

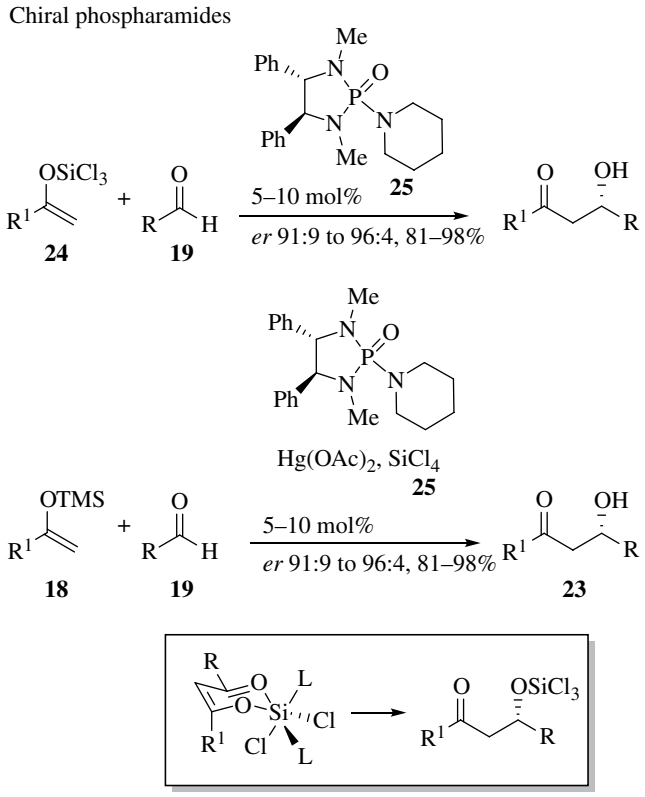
π–π interaction for this conformation, which adds to rationalize the remarkable selectivities observed for unsaturated aldehydes compared to that for aliphatic aldehydes (Scheme 2.129) [49].

A similar approach, even though initiated by a Brønsted acid, is the organocatalytic approach put forward by List et al. [50]. They used their chiral disulfonimide **36** to induce VMARs stereoselectively. With aromatic aldehydes as the substrates, selectivities up to 98:2 er can be obtained. Additionally, they were able to perform bis-VMARs with triene **40**. As mentioned earlier, even though a chiral Brønsted acid is used, the transition state also includes a hypervalent silicon species (**42**), which contains the disulfonimide anion and the coordinated aldehyde in a pentavalent, trigonal bipyramidal geometry (Scheme 2.130). Additionally, the authors propose a potential silatropic rearrangement to be involved. These mechanistic considerations were supported by crossover experiments that are consistent with silicon released from the nucleophile and formation of a new, chiral Lewis acid in combination with the employed Brønsted acid. Therefore, the active Lewis acid is generated *in situ* and is regenerated during the catalytic cycle.

An asymmetric protocol using a covalently attached chiral auxiliary was reported by Kobayashi [51]. They used the Evans auxiliary to generate vinylketene silyl *N*,*O*-acetal **43** (Scheme 2.131). This nucleophile performs in an efficient and highly selective 1,7 asymmetric induction. The stereochemical outcome was rationalized by transition state **45** in which the isopropyl group of the auxiliary shields the upper face of the dienol and the aldehyde approaches from the least




**SCHEME 2.127** Mukaiyama aldol reactions using oxazaborolidinones.



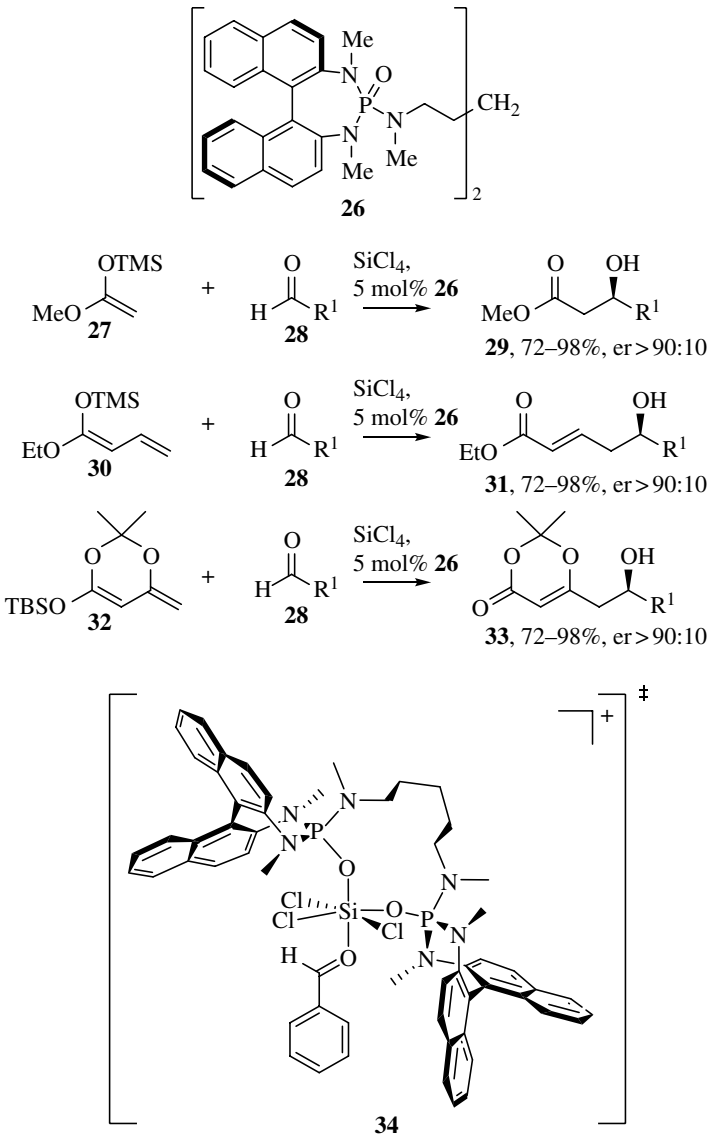

**SCHEME 2.128** Mukaiyama reaction through Lewis base activation.

hindered side. The established arguments for Mukaiyama aldol reactions make use of the Newman projection. The Lewis acid adopts again an orientation that locates itself on the same side as the aldehyde's proton and the R group on the opposite site compared to the α-methyl group of the nucleophile. The optimized protocol uses 1.0 equivalent of vinylketene silyl *N*,*O*-acetal **43** and $TiCl_4$ and 2.0 equivalents of the corresponding aldehyde in $CH_2Cl_2$ at −78°C. Under these conditions, VMAR products up to 97% yield and selectivities between 20:1 and 94:1 ds can be observed. This protocol was later utilized for the construction of a tertiary alcohol in the context of the synthesis of the convolutamydines B (**47**) and E (**48**) [52]. For initial studies and reaction optimizations, Kobayashi et al. used isatin (**49**) as the model compound. The use of an excess of isatin (**49**) (6.0 equiv) and stirring the reaction mixture at 0°C for 30 min before the addition of the vinylketene silyl *N*,*O*-acetal improved the yield to 69% with a diastereomeric ratio of 60:1. This result was then successfully transferred to the synthesis of convolutamydines B and E.

The authors propose a transition state for the pivotal Mukaiyama aldol reaction that puts the aromatic ring of the substrate in an *anti*-orientation to the α-methyl group of the vinylketene silyl *N*,*O*-acetal. Thus the rational for the transition state follows the basic concept for this structural motif, and once more, the α-methyl group plays a pivotal role for the stereo-directing effects.

### 2.3.3 Stereoselective Synthesis of 1,3-Diols: Asymmetric Reductions

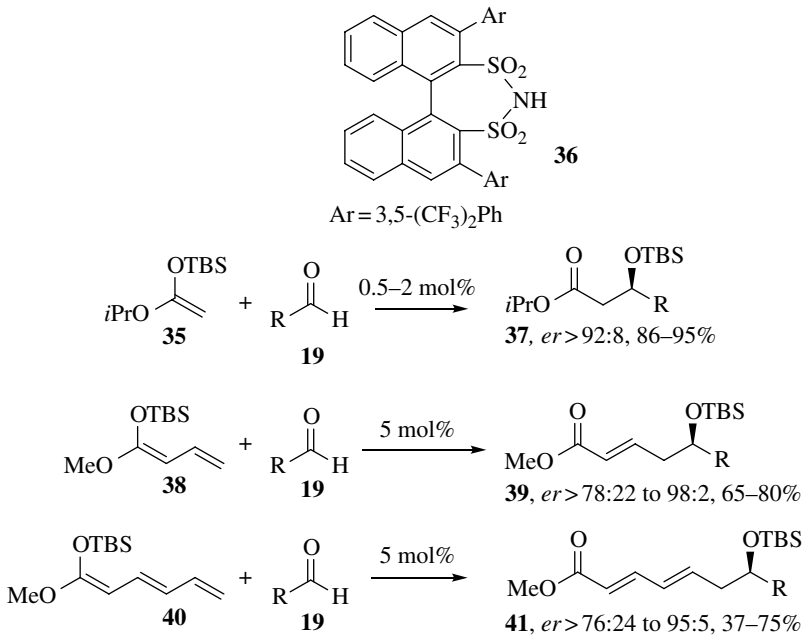
***2.3.3.1 Introduction*** As discussed in the introduction during the biosynthesis of polyketides, diols are generated by repetitive ester condensations and stereoselective reduction of β-keto esters. Synthetically, this biosynthetic strategy has been paralleled by classical ester condensation and as in its biosynthesis stereoselective reductions of the resulting β-keto ester. Already in 1887, Claisen and Lowman reported on the mechanism of the ester condensation and confirmed their hypothesis by providing experimental conditions that allowed the synthesis of ethyl benzoylacetate (**55**) from ethylbenzoate (**53**) and ethyl acetate (**54**) (Scheme 2.132) [53].




**SCHEME 2.129** Lewis base activation using chiral bisphosphoramide **34**.

A synthetically valuable variation of Claisen's ester condensation is the so-called Blaise reaction [54]. It is the zinc Reformatsky reaction [55] of an alpha halo ester (**56**) and a nitrile. A first improvement was put forward by Kagan [56] who reported the addition of a benzene solution of the α-bromo ester to a refluxing mixture of the nitrile and zinc. This protocol provides very good yields for α,α-disubstituted and α-mono-substituted products. In 1983, Kishi reported [57] the use of THF as the solvent and described the activation of zinc and the addition over 30–60 min to minimize self-condensation. These modifications improved the yield, but more importantly, they allowed the use of bromoacetates to generate α-unsubstituted products that could not be obtained by previous protocols. The Blaise reaction generates the β-keto esters that we have seen constructed previously through VMAR using Chan's diene (Scheme 2.133). These building blocks have been used by enzymatical and chemical strategies to establish chiral centers and, in the case of VMAR, to build reductively on the existing secondary alcohol in order to produce stereoselectively 1,3-diols.

***2.3.3.2 Enzymatic Reduction*** Reduction of β-keto ester can be achieved in very high enantio-, regio-, and chemoselectivities. One advantage of biocatalysts over chemical transformations is the general safety of the reactions. In particular, the absence of metal hydrides of $H_2$ is considered a substantial advantage for large-scale transformations. On the other side, enzymes are generally highly specific, and each transformation requires catalyst screening and optimization. Also, cofactor regeneration is an important issue, if enzymes are involved. One of the most prominent enzymatic β-keto ester reductions uses commercially available baker's

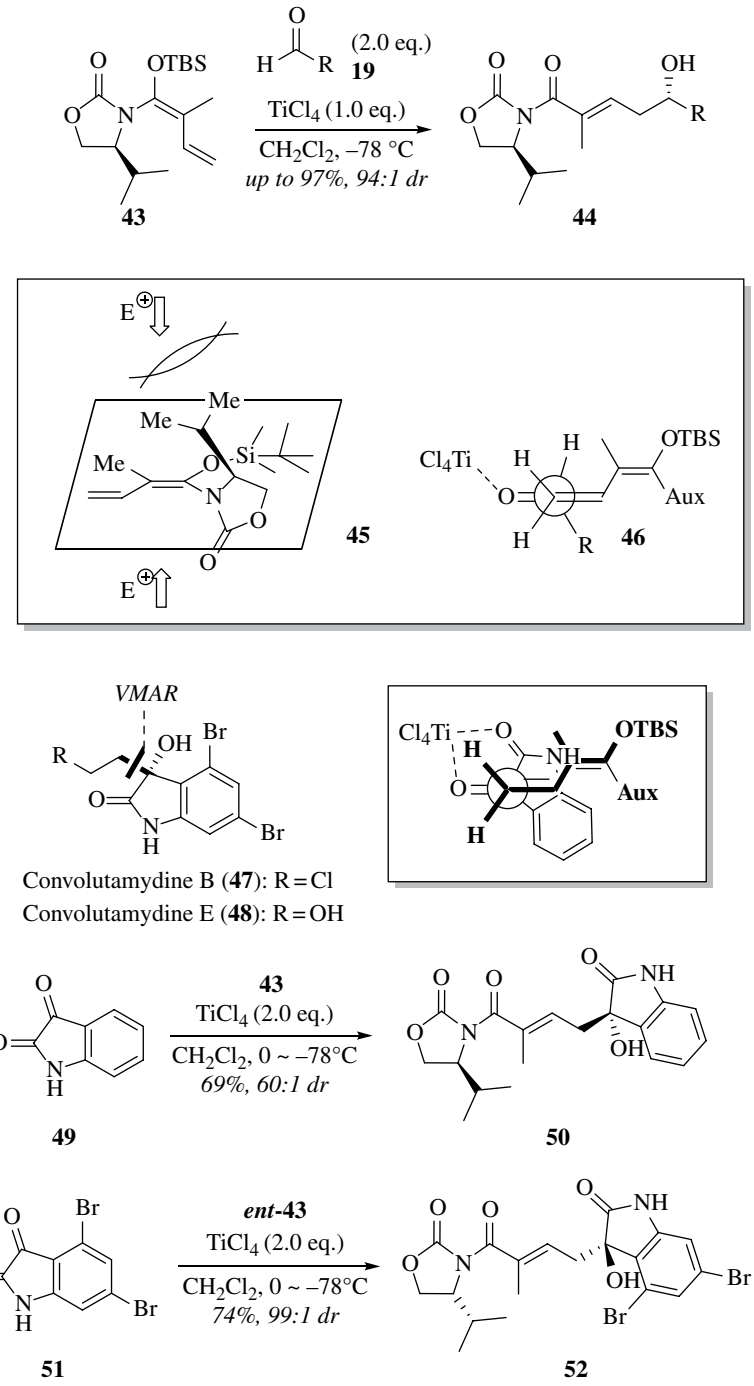



**SCHEME 2.130** Mukaiyama aldol reaction using a chiral Brønsted acid.

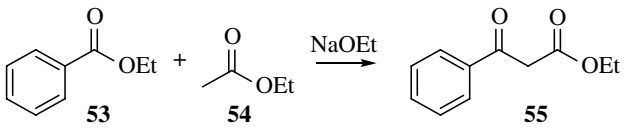
yeast. Already in the 1980s, Fráter [58] and Seebach [59] used the so-obtained β-hydroxy esters (e.g., **62**) for subsequent alkylations to produce *anti*-configured methyl branches (**63**) (Scheme 2.134). More recent contributions focused on using these biotransformations for large-scale productions of chiral β-hydroxyl esters [60]. As shown in Scheme 2.134, methyl-substituted (**64**) and halide functionalized starting materials (**66**) can be converted on large scale and with excellent yield and selectivities. Kula and Zelinski [61] focused on cofactor regeneration and reported their results in the context of starting materials that can be converted to drugs. Since the observed selectivities depend on the side chain differentiation on both sides of the to-be-reduced carbonyl group, it was not unexpected to realize that changing the alkyl chain length of the alcohol moiety of β-keto esters would also change the absolute configuration of the resulting alcohol (cf. **69** and **71**) (Scheme 2.134) [62].

***2.3.3.3 Chemical Reductions*** Enantioselective reduction of unsymmetric ketones to optically active alcohols is very important in organic synthesis. In the foreword to this section, we will summarize the best practical and useful methods and reagents.

*BINAL-H (Noyori)* Noyori has devised a chiral hydride reagent and its enantiomer by the modification of lithium aluminum hydride with equimolar amounts of either



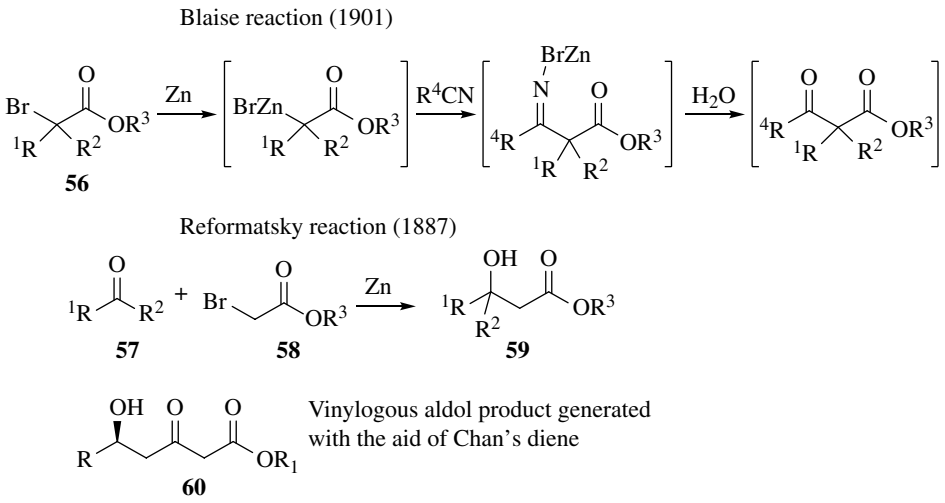

**SCHEME 2.131** Kobayashi aldol reaction.



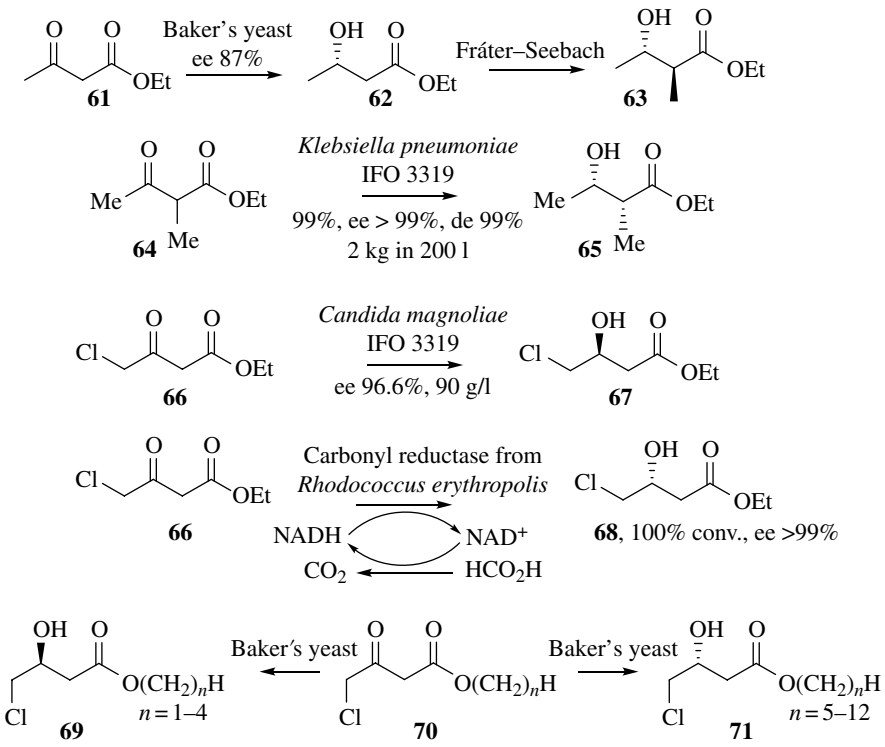

**SCHEME 2.132** Ester condensation.

(*R*)- (Scheme 2.135) or (*S*)-BINOL and a simple alcohol, usually methanol or ethanol [63].

The reducing agent exhibits exceptionally high enantioface-differentiating ability in the reduction of diverse unsaturated carbonyl compounds such as aromatic, alkynylic, and olefinic ketones.



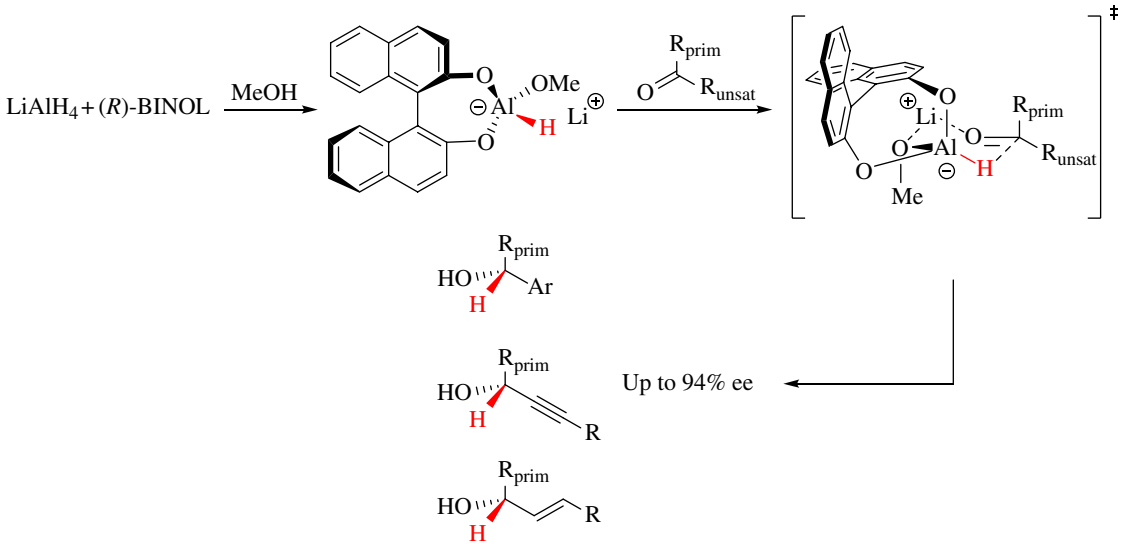

**SCHEME 2.133** Chemical synthesis of β-hydroxy esters and ketones.



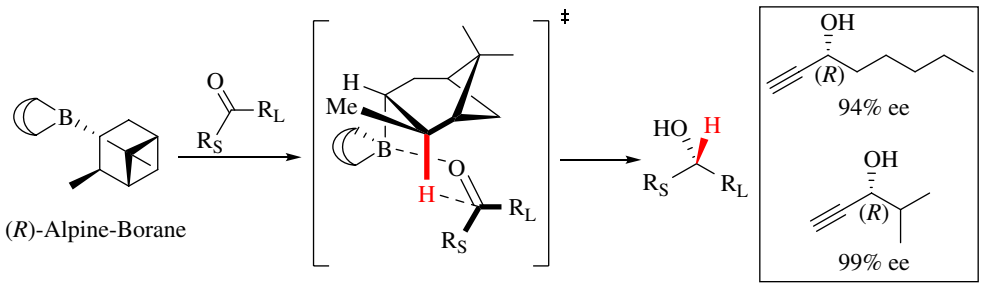

**SCHEME 2.134** Indicative examples of enzymatic reductions of β-keto esters.

*Alpine-Borane® (Midland)* Alpine-Borane is a trademark of Aldrich Chemical Company for *B*-3-pinanyl-9-borabicyclo[3.3.1]nonane. It is prepared by hydroboration of α-pinene with 9-borabicyclo[3.3.1]nonane (9-BBN). Synthesis of (*R*)-Alpine-Borane is prepared from (1*R*)-(+)-α-pinene, and since (+)- and (−)-α-pinenes are commercially available, both enantiomers of the reagent can easily be prepared. The reagent is only suitable for very reactive substrates, such as labeled aldehydes and acetylenic ketones (Scheme 2.136) [64]. With unreactive substrates, Alpine-Borane reacts slow and results in decreased enantioselectivities.

The cause for this poor selectivity in the reduction of simple and unreactive ketones with Alpine-Borane is presumed to be the dehydroboration of the reagent in these slow reductions followed by an achiral and very fast reduction of the carbonyl group by 9-BBN produced in the dehydroboration stage. This problem can be overcome by minimizing the unimolecular dissociation of Alpine-Borane by conducting




**SCHEME 2.135** Indicative examples of Noyori reduction.




**SCHEME 2.136** Significant examples of alpine-borane reduction.

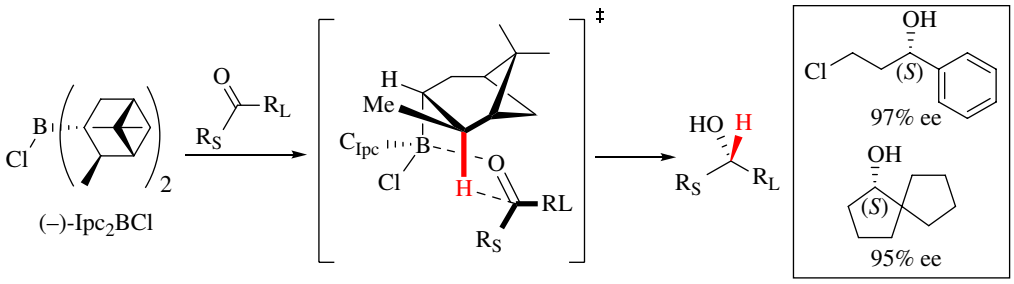
the reductions either in high concentrations or at elevated pressures. Even then the reagent is not really useful for the reduction of unactivated ketones.

*Brown's Chlorodiisopinocampheylborane ($Ipc_2BCl$)* Another method utilized for increasing the rate of reduction is by changing the electronic environment of the boron atom. In this regard, Brown has investigated a variety of dialkylhaloboranes, and among them, chlorodiisopinocampheylborane ($Ipc_2BCl$) has turned out to be the best. Placement of halogen on the boron makes it more Lewis acidic, resulting in an increase in its reactivity toward carbonyl compounds. The sterically more hindered $Ipc_2BCl$ derivative is also more stable toward dissociation.

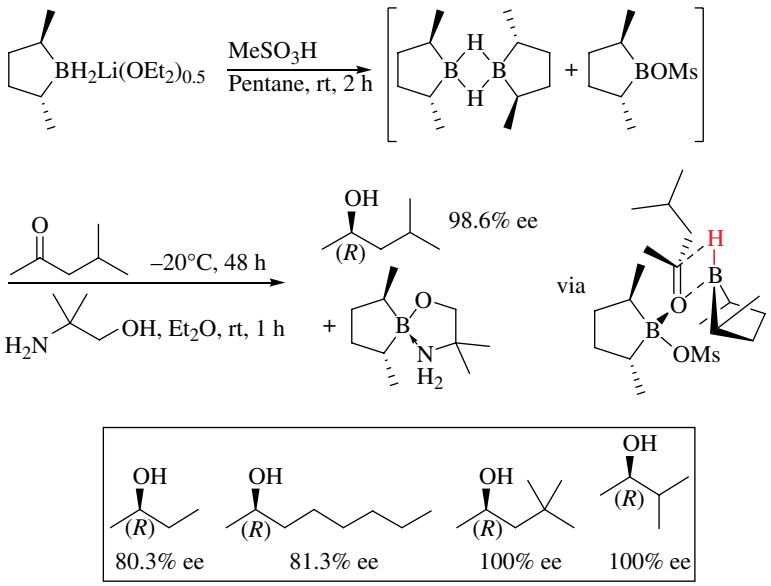
The reagent is a very good chiral reducing agent for aromatic alkyl and α-tertiary alkyl ketones (Scheme 2.137) [65]. Both the isomers of the reagent have been synthesized from commercially available (+)- and (−)-α-pinene. The reagent is not suitable for simple ketones like 2-butanone and enone types.

*Masamune's Chiral 2,5-Dimethylborolanes* Enantioselective reduction of aliphatic ketones like 2-butanone, 4-methyl-2-pentanone, and several others where both the appendages of the carbonyl group are sterically similar is very challenging. Masamune's dimeric ligand (*R*,*R*)- (Scheme 2.138) or (*S*,*S*)-2,5-dimethylborolane (not shown) is very efficient in reducing those types of ketones [66].

*CBS (Corey, Bakshi, and Shibata) Catalyst* Itsuno [67] paved the way for the discovery of oxazaborolidines as chiral catalysts for the borane-mediated enantioselective reduction of a wide variety of achiral ketones, the so-called CBS reduction. Scheme 2.139 summarizes some of these results and the proposed transition state [68]. These data show that the CBS reduction process results in excellent enantioselectivities and leads to a product whose absolute configuration can be predicted from the relative effective steric bulk of the two carbonyl appendages. It is noteworthy that the oxazaborolidine catalyst behaves like an enzyme in the sense that it binds with both ketone and borane and brings




**SCHEME 2.137** Brown's (–)-chlorodiisopinocampheylborane [(–)-$Ipc_2BCl$] and significant examples of reduction.




**SCHEME 2.138** Masamune's chiral 2,5-dimethylborolanes.

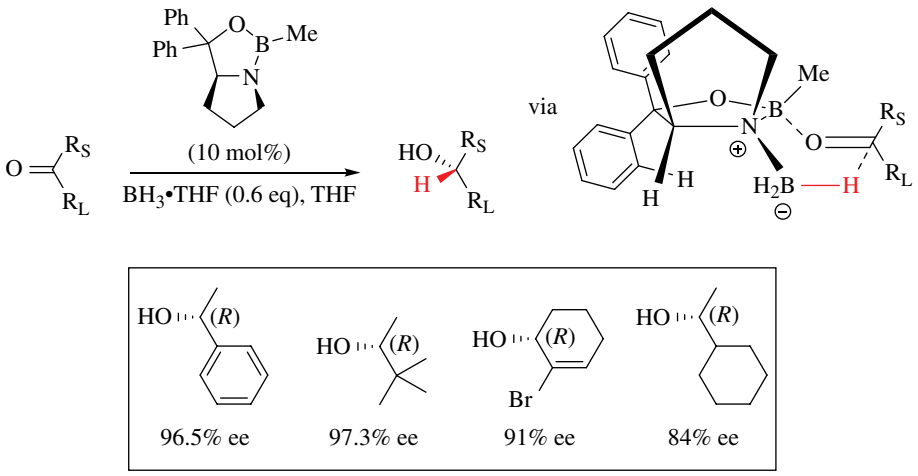
them closer (cf. transition state in Scheme 2.139). After the reaction is over, it releases them and it becomes free. Because of the enzyme-like catalytic activity, it has been named chemzyme.

*Noyori Asymmetric Transfer Hydrogenation* Noyori's well-designed chiral $Ru^{II}$–arene complexes catalyze the asymmetric transfer hydrogenation of ketones and imines (not shown) with stable organic hydrogen donors such as 2-propanol [69]. The reaction is reversible, and the involved chiral ruthenium species and the proposed transition state are depicted in Scheme 2.140.

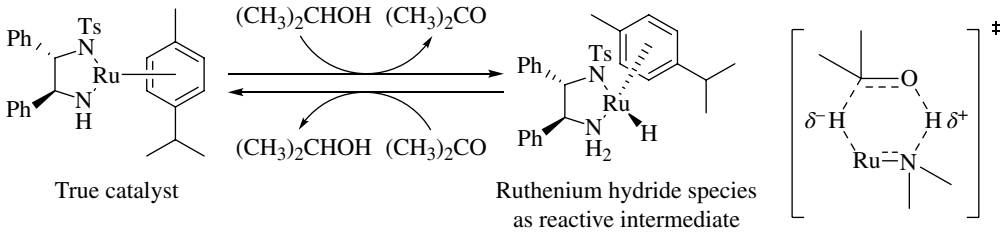
The Noyori transfer hydrogenation is operationally simple, and the achieved enantioselectivities are generally very high. For example, when a 0.1 M solution of acetophenone in 2-propanol containing $[\{RuCl_2(\eta^6\text{-}p\text{-cymene})\}_2]$, (1*S*,2*S*)-*N*-*p*-toluenesulfonyl-1,2-diphenylethylenediamine, and KOH (ketone : Ru : diamine : KOH = 200 : 1 : 1 : 2 molar ratio) was allowed to stand at 28°C for 10 h, (*S*)-1-phenylethanol was obtained in 97% ee and in 98% yield (Scheme 2.141) [70].

The stereochemical outcome of Noyori asymmetric transfer hydrogenation is predictable and depends on the particular diamine (*S*,*S* or *R*,*R*) used. Two other challenging examples of Noyori asymmetric transfer hydrogenation during the course of cytostatin total synthesis are depicted in Figure 2.3 [71].

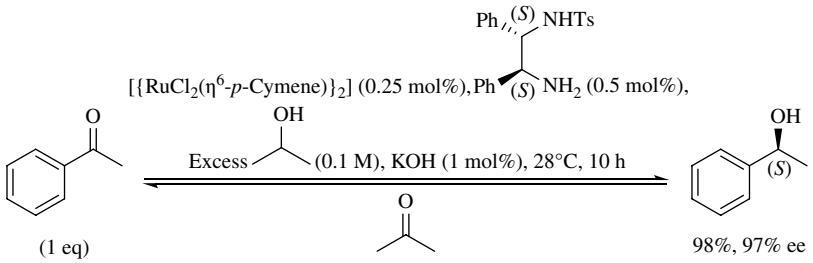
The reduction of the pre-fuctionalized, usually through the referred in the previous chapter aldols, asymmetric 5-hydroxy-3-ketoesters (**72**) can lead directly to functionalized 1,3-diols. This transformation can be achieved either by chemical reduction or by biotransformation. Since the Noyori reduction [72] is not only one of the most prominent and applied catalytic reductions but also highly applicable to β-keto esters, it was investigated by Shao et al. [73]. They used chiral ester **72** and performed Noyori reduction using both enantiomers of BINAP. It was realized that the chiral




**SCHEME 2.139** Indicative examples of CBS reduction of ketones.




**SCHEME 2.140** True catalyst, ruthenium hydride species as reactive intermediate and proposed six-membered cyclic transition state.




**SCHEME 2.141** Noyori asymmetric transfer hydrogenation.

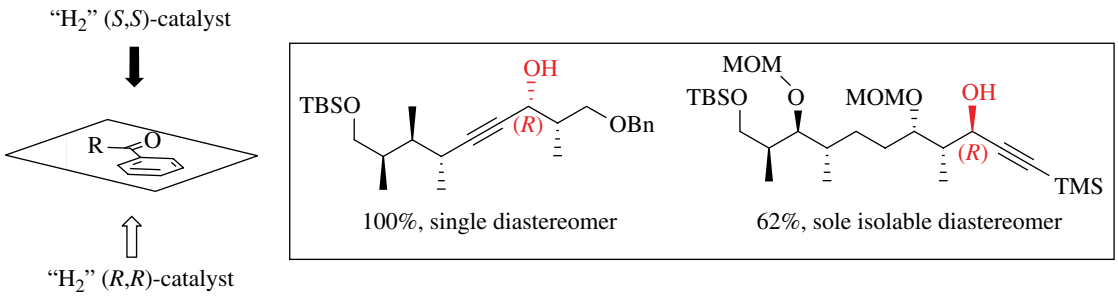
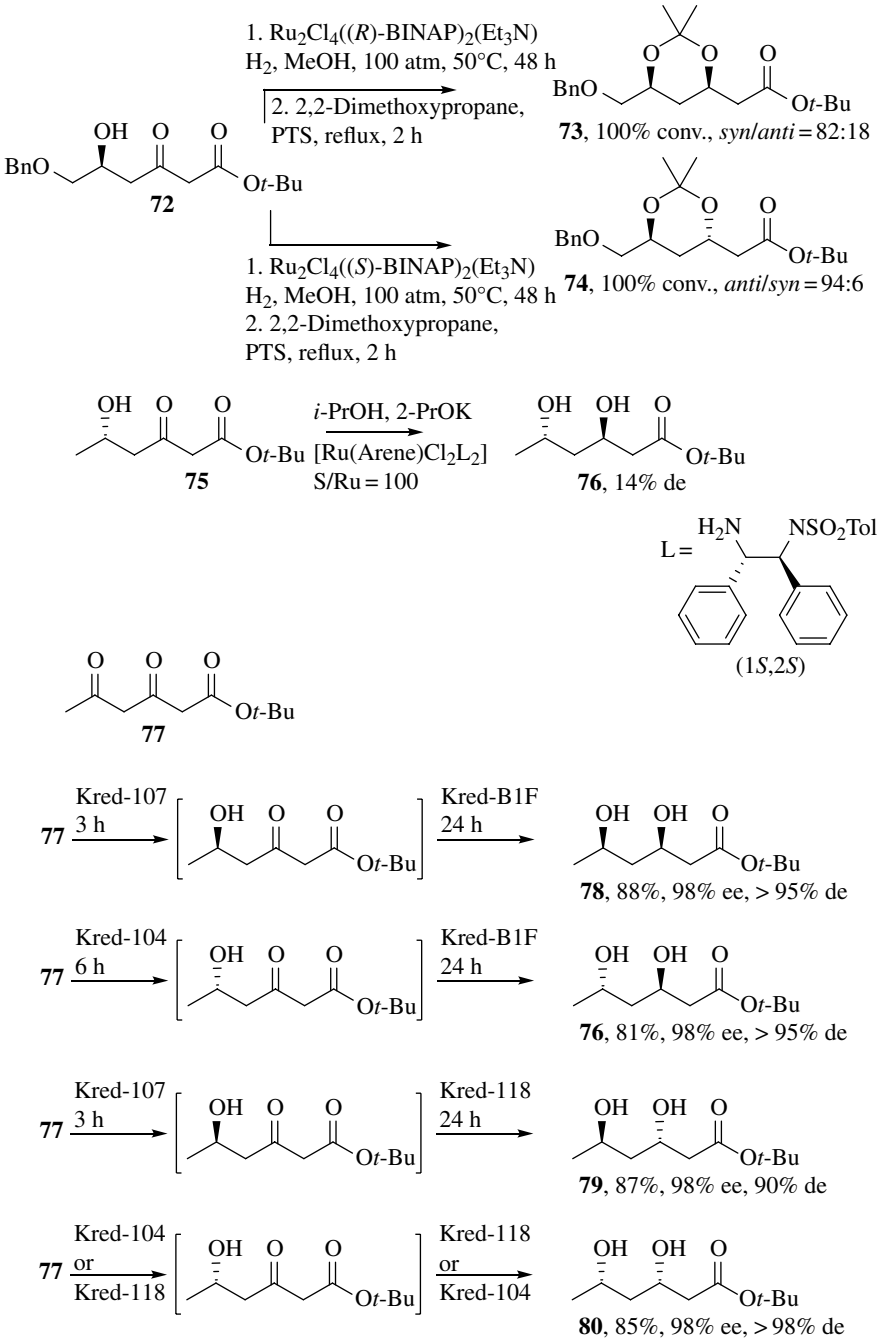


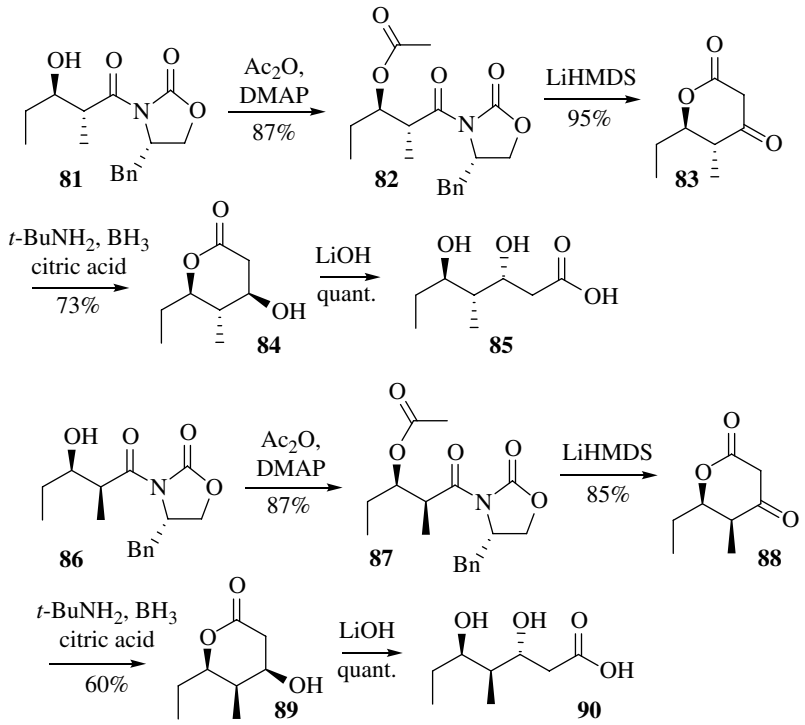

**FIGURE 2.3** General sense of asymmetric transfer hydrogenation and meaningful examples from cytostatin total synthesis.



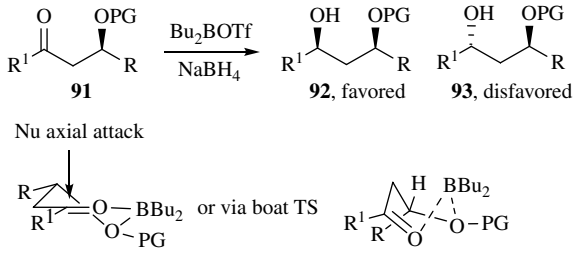

**SCHEME 2.142** Chemical and enzymatic reduction of carbonyl groups.

catalysts overrides the inherent selectivity and both the *syn*- and the *anti*-diastereomer can be obtained using both enantiomers of BINAP. Everaere and Carpentier used similar starting materials (**75**) but used the conditions of hydrogen transfer for this transformation (Scheme 2.142) [74]. More recently, Smonou et al. [75] reported on combinations of keto reductases to reduce both carbonyl groups of β,δ-diketo esters (**77**), a transformation that is usually difficult to obtain. Their strategy involves the utilization of two enzymes with different specificity for both carbonyl groups. A detailed investigation of the selectivities allowed them to combine the appropriate enzymatic activities and to perform both reductions in a one-pot protocol. Using this strategy, they were able to generate all four possible stereoisomers in excellent yields and selectivities (**78**, **76**, **79**, **80**).

In 2001, Hinterding and coworkers reported on a Claisen condensation/reduction sequence. They used an intramolecular Claisen-type reaction to cleave off the Evans




**SCHEME 2.143** Claisen-like condensation/reduction sequence.



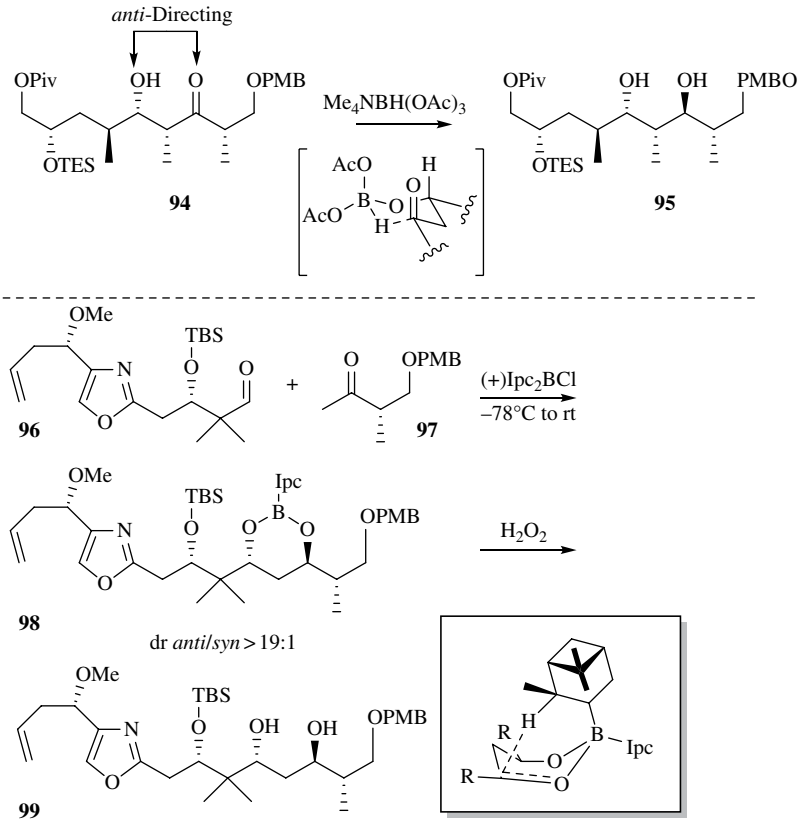

**SCHEME 2.144** Narasaka–Prasad reduction.

oxazolidinone (**81**). This was achieved by an acetate enolate that was generated by treatment with LiHMDS. The resulting ketone (**83**) was stereoselectively reduced by an amine–borane complex [76]. This protocol serves as a powerful alternative to standard acetate aldol transformation and uses a conformationally restricted β-keto ester as the target. As it can be seen in Scheme 2.143, the configuration of the originally established alcohol controls the stereochemical outcome of the borane reduction. Consequently, this protocol can be applied for *syn*- and *anti*-aldol products.

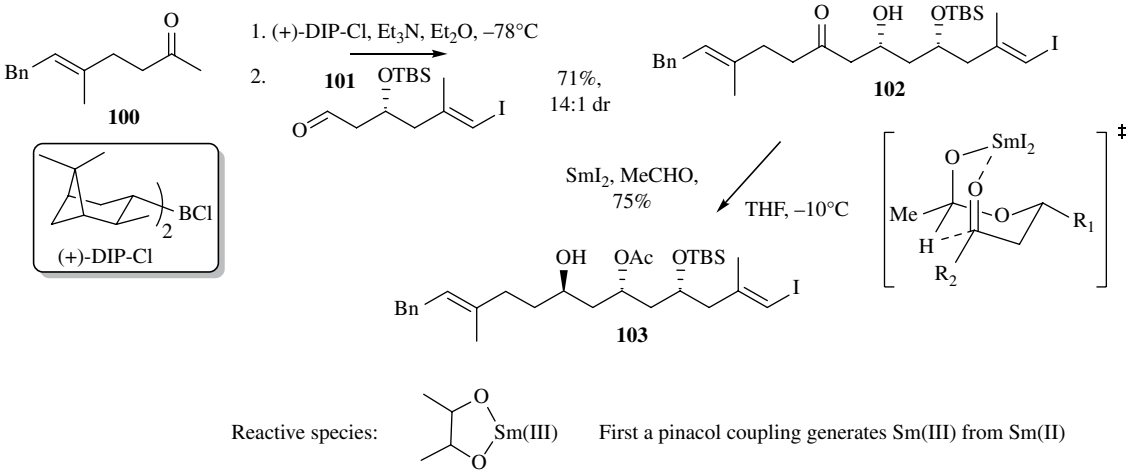
A more general approach to get access to 1,3-*syn*-diols is the *syn*-selective Narasaka–Prasad reduction [77]. It utilizes the chelating capabilities of boron reagents and delivers the hydride externally, usually from $NaBH_4$ (Scheme 2.144). Both a chair-like transition state and a boat transition state explain the observed *syn*-selective reduction. The incoming hydride approaches the keto carbonyl group in both cases from the least hindered side.

The corresponding *anti*-selective reduction takes advantage of internal hydride delivery (Scheme 2.145). Tetramethylammonium triacetoxyborohydride ($Me_4NBH(OAc)_3$) is the standard reagent employed for this reaction. This transformation was originally described by Saksena and Mangiaracina [78] for the stereoselective reduction of a carbonyl group at a steroid template. It was later further developed by Evans et al. [79] and is now one of the most established transformations in polyketide synthesis. A remarkable one-pot protocol of an Ipc-mediated aldol reaction with concomitant reduction was recently published by Menche and Dieckmann [80]. In the course of their rhizopodin synthesis, they discovered that upon warming up, the Paterson aldol reaction produced the corresponding *anti*-diol (**98**). They confirmed this one-pot protocol using various substrates and could show that this is a general method for the construction of 1,3-*anti*-diols. They rationalized the high stereoselectivity observed in the reduction step by a closed transition state, which transfers a hydride from the Ipc moiety to the carbonyl group (Scheme 2.145).

A similar strategy is employed when using the Evans–Tishchenko reaction [81]. The Tishchenko reaction that is first described in 1906 uses a Lewis acid-mediated disproportionation of two carbonyl moieties to form an ester. In 1990, Evans and Hoveyda reported on their variant, which involves a preformed β-hydroxy ketone and an aldehyde




**SCHEME 2.145** Saksena–Evans reduction and Menche one-pot *anti*-reduction.




**SCHEME 2.146** Evans–Tishchenko reduction.

undergoing a Lewis acid-catalyzed hemiacetal formation. The Lewis acid coordinates the hemiacetal oxygen and the carbonyl group to be reduced. Internal hydride delivery leads to ester formation and concomitant *anti*-selective reduction. The advantage of the Evans–Hoveyda protocol is the remarkable mild reaction conditions that allow this reaction to be performed in the presence of sensitive functional groups. The so-generated ester serves at the same time as a protecting group and renders the Evans–Tishchenko reaction a transformation in natural product syntheses. Scheme 2.146 shows a typical combination of Paterson aldol reaction followed by *anti*-selective reduction. The DIPCl-mediated aldol reaction sets the configuration at the new secondary alcohol (**102**). This configuration is then used for the

*anti*-selective Evans–Tishchenko reaction. At this point, it should be mentioned that prior to the reduction, Sm(II) performs a pinacol condensation with the aldehyde to generate a 1,2-diol Lewis acid. Only the chelate between Sm(III) and the 1,2 diol serves as the active species for the Evans–Tishchenko reduction.

### 2.3.4 Application of Stereoselective Synthesis of 1,3-Diols in the Total Synthesis of Macrolides

#### *2.3.4.1 Aldol Reactions Followed by Asymmetric Reduction*

*Spirangien A* The spirangiens A (**104**) and B (**105**) (Fig. 2.4) were isolated 2005 by Höfle et al. from the myxobacterium *Sorangium cellulosum* (Soce90) [82]. They exhibit antibiotic activity against yeast and fungi (diameter of inhibition zones: *Pichia membranaefaciens* 24 mm, *Rhodotorula glutins* 19 mm, *Botrytis cinerea* 11 mm), but even more importantly, they show high cytotoxicity against L929 mouse fibroblast cell line ($IC_{50} = 0.7$ ng/ml). Despite the fact that these compounds are representing some of the most active polyketides found in nature, their mode of action is still unknown and distinct from all the other polyketides isolated from gliding bacteria. Due to its high cytotoxicity and the fact that even a truncated spirangien exhibits high biological activity, several groups started programs to complete their total synthesis [83].

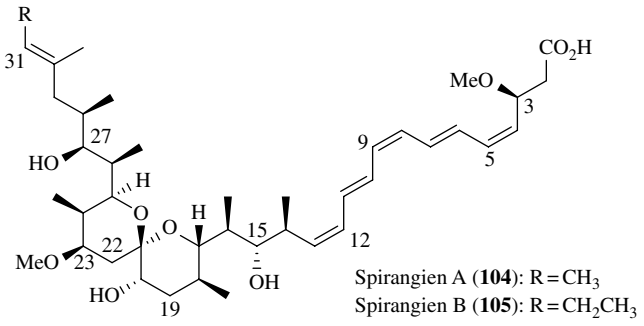
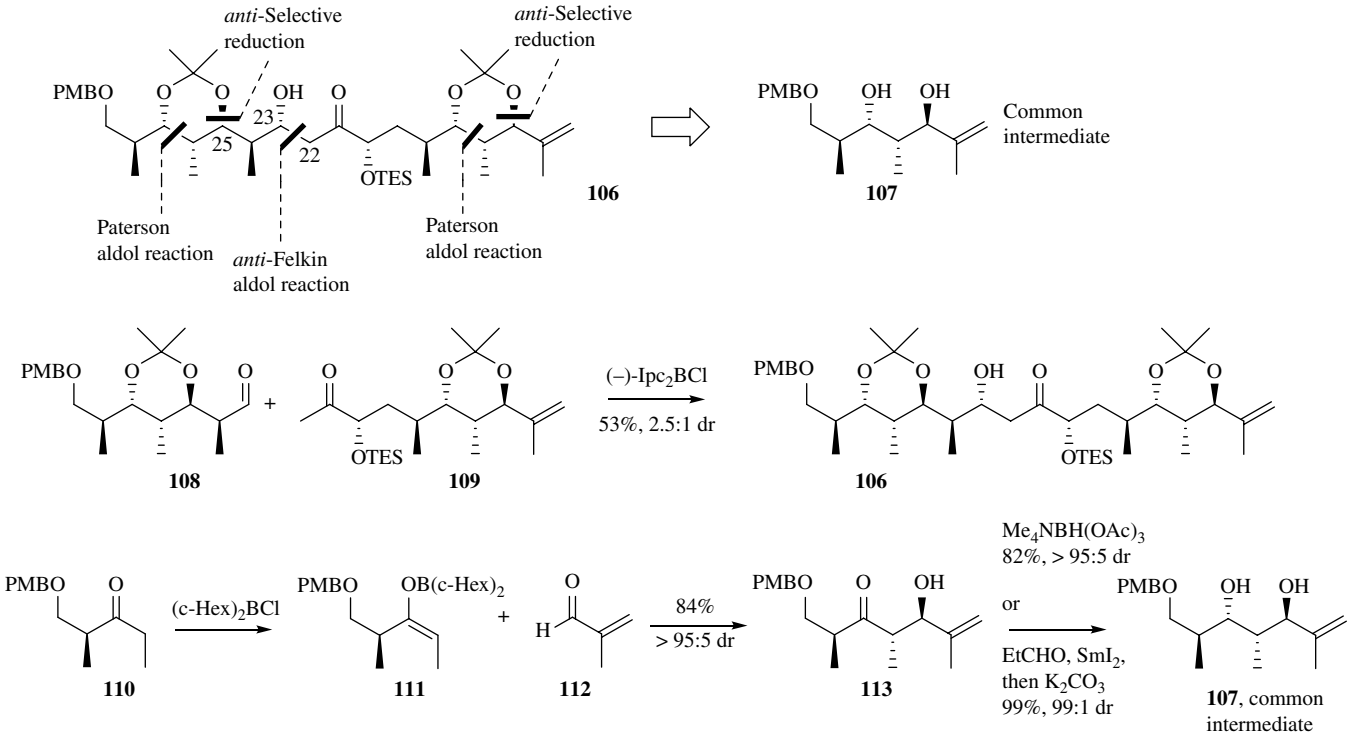
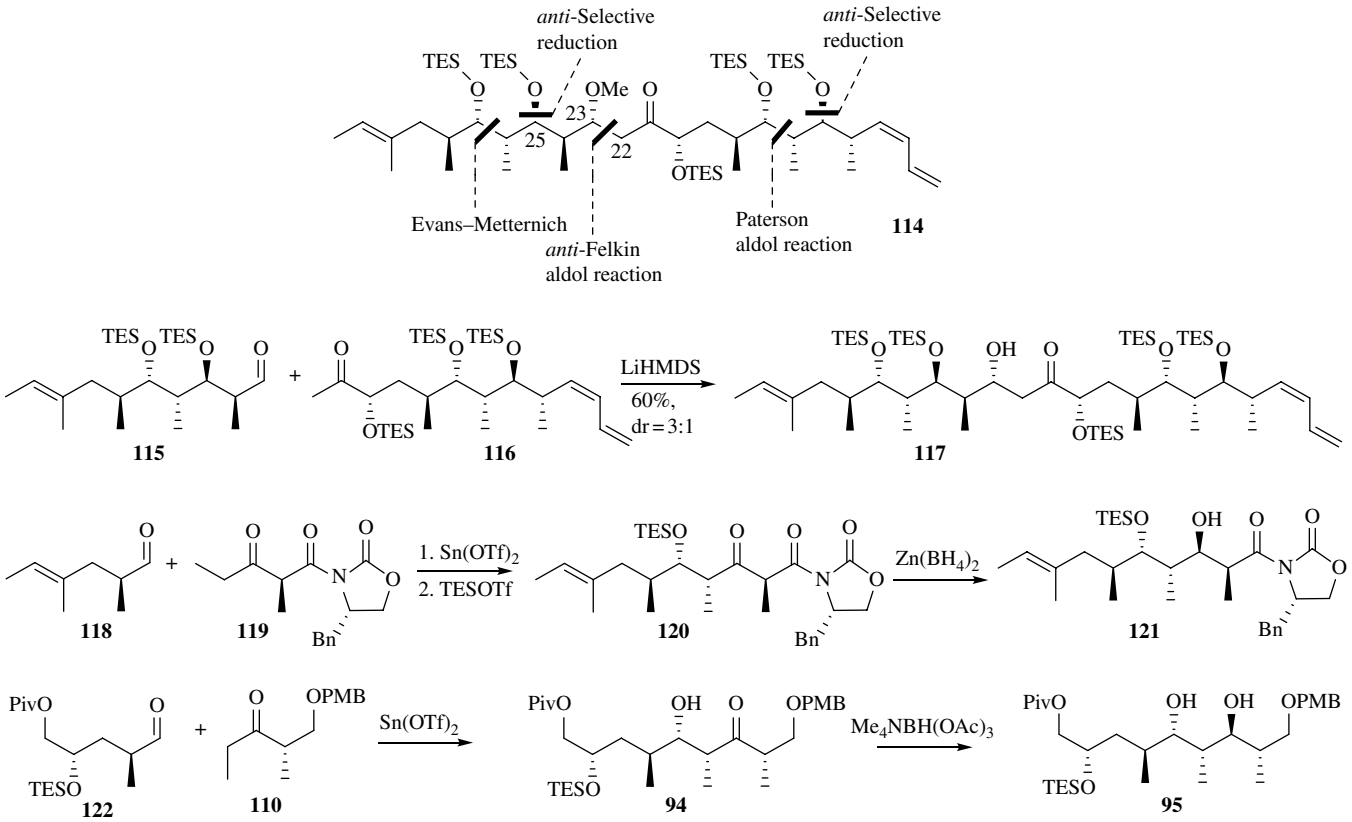



**FIGURE 2.4** Spirangienes.

The first total synthesis was accomplished by the Paterson group [84]. They used their Ipc-mediated aldol strategy to join both building blocks **108** and **109**. Since the *syn*-configuration at the aldehyde is Felkin opposing, it was not clear at the outset of the synthesis if good selectivities could be observed. Here, a moderate ratio of 2.5 : 1 for the desired compound was observed. Clue of their synthesis was the identification of a common intermediate **107**, accounting for the preparation of the two key building blocks **108** and **109**. This building block was obtained by an *anti*-selective aldol reaction of the *E*-enolate of the Roche ester-derived ethyl ketone **110**. Reaction of the *E*-boron enolate with methacrolein gave intermediate **113**, which was further reduced to the *anti*-diol either by an Evans–Saksena [85] or a samarium-catalyzed Evans–Tishchenko reaction [86]. This intermediate was then further elaborated to both pivotal building blocks (Scheme 2.147).




**SCHEME 2.147** Key steps toward Paterson total synthesis of spirangien A.

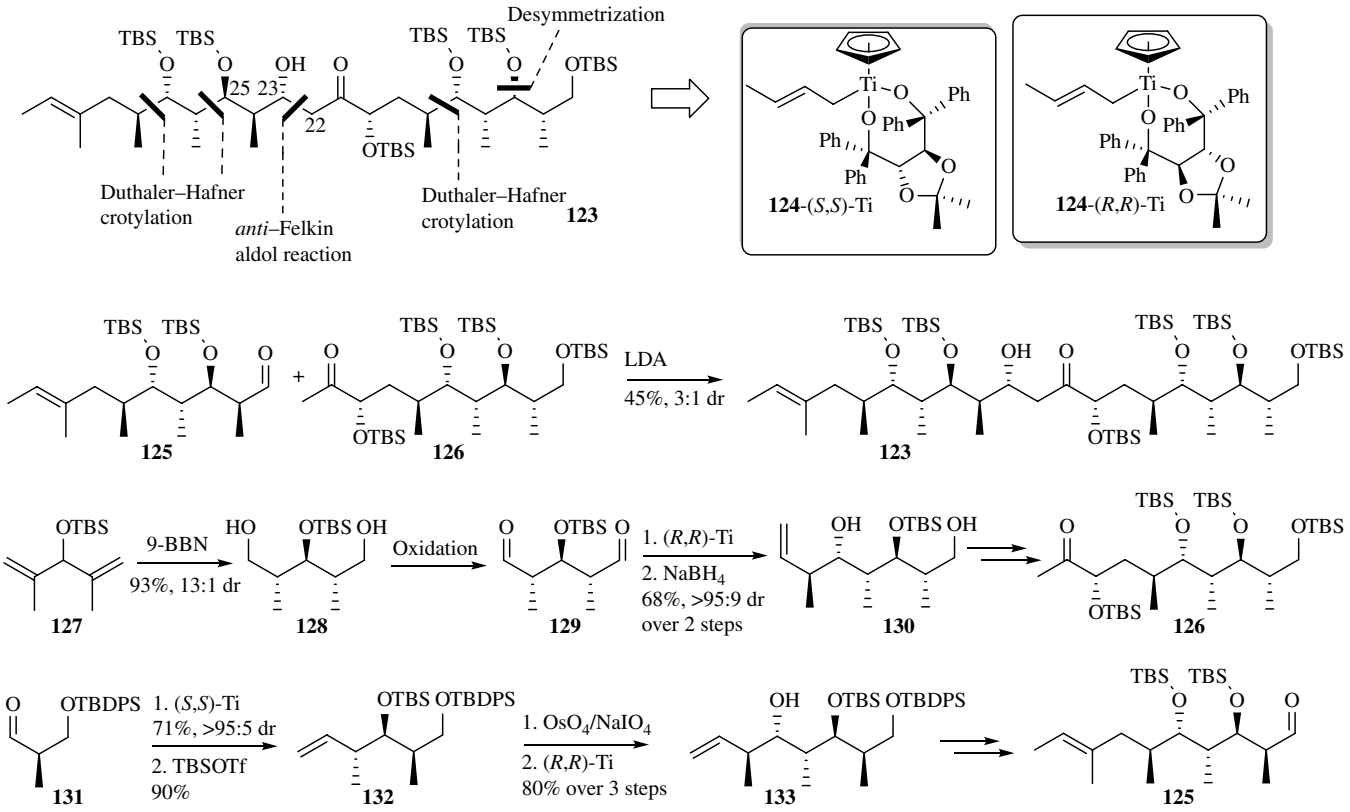



**SCHEME 2.148** Highlights from Kalesse total synthesis of spirangien A.

Toward the same endeavor, Kalesse group used an aldol disconnection in order to join fragments **115** and **116** (Scheme 2.148) [87]. This aldol reaction that performed with the lithium enolate of methyl ketone **115** provided the desired 23,25-*anti*-diol motif in 60% yield and as 3:1 diastereomeric mixture in favor of the desired isomer. The different selectivities obtained by Paterson and Kalesse on their routes are telling examples on how difficult it is with the current state of knowledge to precisely predict the selectivities in aldol disconnections. Here, unexpectedly the achiral metal enolate outperformed the chiral Ipc boron enolate and silicon protecting groups proofed to be superior over acetonides. In the Kalesse synthesis, the aldehyde **115** was obtained through an Evans–Metternich aldol reaction, which was reduced under chelating condition to provide the corresponding *anti*-diol (**121**). It is worth mentioning that the chiral auxiliary also directed the stereoselectivity of the reduction step. For the synthesis of methyl ketone **116**, a Peterson aldol reaction using the Roche ester-derived ethyl ketone **110** was performed as described earlier; the advantage of this aldol transformation is the fact that no further chiral auxiliary is required. The *anti*-diol was then established by an Evans–Saksena reduction [88].

Relied on our described aldol success, Cossy and her group utilized the same lithium enolate aldol strategy to obtain the same stereoselectivity (3 : 1) during their synthesis of spirangien A (Scheme 2.149) [89]. Their strategy to obtain the requisite building blocks **125** and **126** differs from the two previous routes. Utilization of a Duthaler–Hafner crotylation [90] was the reaction of choice for both the construction of aldehyde segment **125** and the desymmetrization of the *meso*-dialdehyde **129**. The dialdehyde was obtained by a two-step sequence of double hydroboration [91] and subsequent oxidation. The aldehyde **125** was obtained by two consecutive Duthaler–Hafner crotylations starting from Roche ester-derived aldehyde **131**. After the first crotylation, the required aldehyde was liberated by dihydroxylation and periodate cleavage.

*Rhizopodin* Rhizopodin (**134**) (Fig. 2.5) is a macrolide that was isolated from the myxobacterium *Myxococcus stipitatus* by Höfle et al. [92]. It exhibits significant antifungal activity and cytotoxicity against tumor cells with $IC_{50}$ values in the low nanomolar range [11]. Through an X-ray analysis of rhizopodin bound to two monomeric actin subunits, a detailed picture of its interaction with the target became available [93]. This led also to the revised structure of rhizopodin, which was originally proposed as a monomeric lactone. Due to its complex structure and remarkable biological activity, it became the target of several research groups [94].




**SCHEME 2.149** Key steps toward the Cossy total synthesis of spirangien A.

The Menche group was the only so far who completed the total synthesis of this natural product [95]. They dissected the target into three building blocks, which are joined by an HWE reaction, Suzuki cross coupling, and esterification. Two of these building blocks contain diol segments that were constructed during their synthesis. The synthesis of segment **138** started out from D-malic acid-derived ester **135**. Subsequent Claisen condensation with *tert*-butyl acetate provided β-keto ester **136**, which was subjected to asymmetric hydrogenation using Noyori's catalyst [96]. The alcohol was obtained in high diastereoselectivities (>20 : 1) with concomitant loss of the TBS group at the primary alcohol. Protection of both hydroxyl groups and selective removal of the primary alcohol, followed by Dess–Martin oxidation, provided the corresponding aldehyde, which was subjected to a Takai olefination [97]. Polyol **141** was planned to be assembled from aldehyde **96** and methyl ketone **97**. However, this aldol reaction proved to be nontrivial, and various boron aldol strategies and Mukaiyama conditions failed. Finally, only the lithium enolate of methyl ketone **97** provided excellent yields albeit with poor selectivities. Fortunately, both isomers could be separated and independently transformed to the desired product. The desired isomer was subjected to an *anti*-selective reduction, whereas the minor isomer was used in a *syn*-selective reduction and inversion of the C18 hydroxyl group (Scheme 2.150).

Paterson et al. [98] in their attempt used a similar disconnection for rhizopodin as described by Menche (fragments **144** and **149**) (Scheme 2.151). However, unlike Menche, they used silyl ketene acetal **16** in an asymmetric VMAR for the addition to (*E*)-iodoacrolein (**142**) to obtain dioxinone **143** in 94% ee. Methanolysis removed the acetonide, and the subsequent Narasaka reduction [99] provided the *syn*-diol **144** in 80% yield and a 10 : 1 selectivity for the desired isomer. The synthesis of segment **149** started with aldehyde **145**, which was ultimately derived from Roche ester. Carbon chain extension was achieved through a chelation-controlled Mukaiyama aldol reaction with silyl ketene acetal **146**, which installed the new chiral center with excellent stereocontrol (20 : 1 dr). For the installation of the third secondary alcohol, six-membered lactone **148** was obtained by treatment with $K_2CO_3$ in methanol. Subsequent borane reduction provided stereospecifically the desired alcohol, which was then further transformed to the desired acid (**149**).

Nicolaou et al. [100] on the other hand developed a route toward the synthesis of monorhizopodin (**150**) (Fig. 2.6), which relied on the utilization of a vinylogous Mukaiyama aldol approach for the construction of the C1–C7 fragment **156** (Fig. 2.6 and Scheme 2.152).

Using Denmark's [101] concept of Lewis base activation of Lewis acids, silyl ketene acetal **152** reacted with aldehyde **151** to provide **153** in 94% ee and 69% yield.

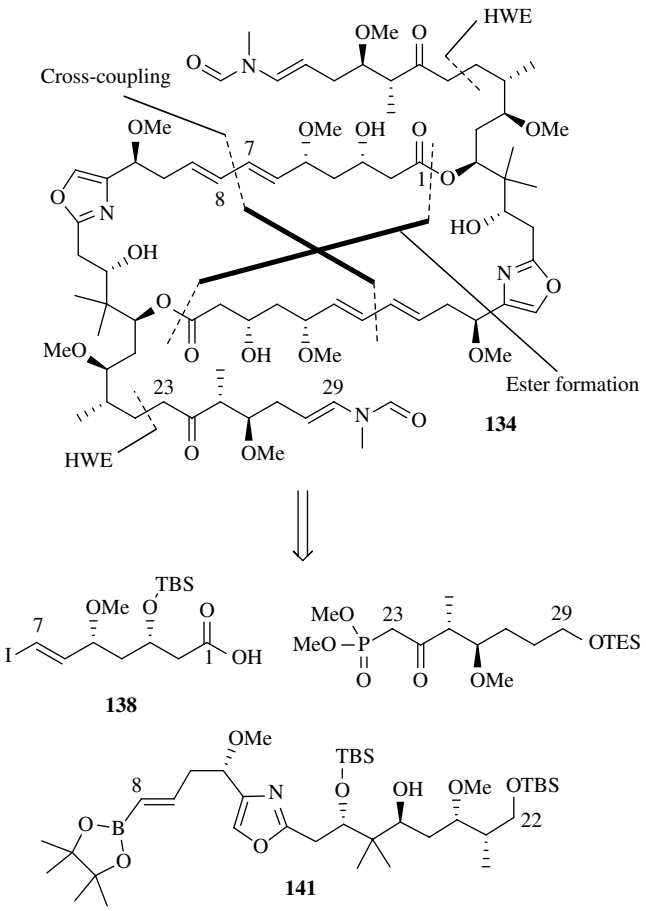
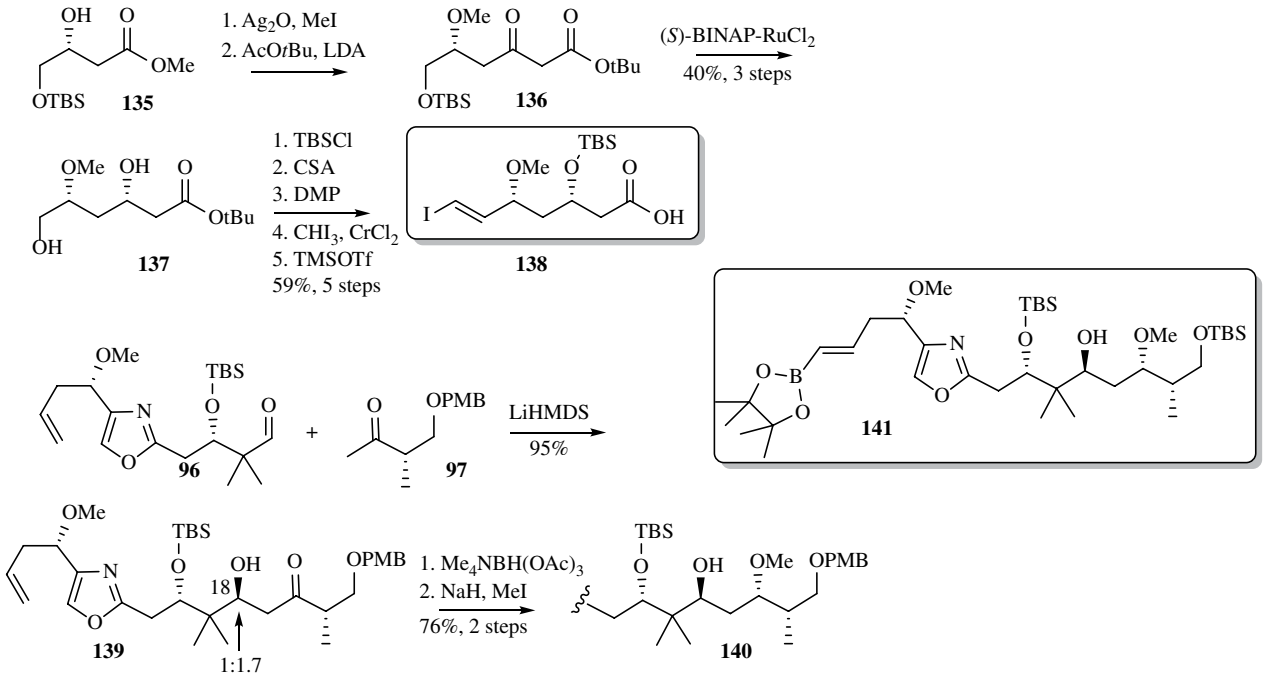



**FIGURE 2.5** Retrosynthetic analysis of rhizopodin.

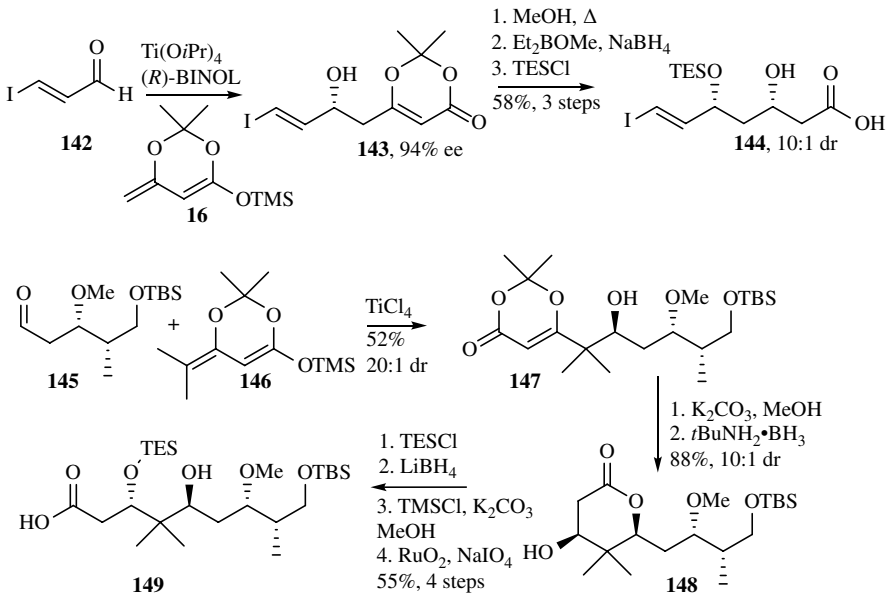
The 1,3-*syn*-diol **154** formation was achieved through treatment of **153** with KHMDS and benzaldehyde. For the discrimination of both hydroxyl groups, treatment with $K_2CO_3$ led to δ-lactone formation and subsequent TBS protection completed the hydroxyl group differentiation. Lactone saponification under basic conditions completed the synthesis of fragment **156**. On the other hand, the synthesis of fragment **163** started out from known diol **157** [102]. Acetonide formation was accomplished by treatment with 2,2-dimethoxy propane, and subsequent ozonolysis provided aldehyde **159** in 80% overall yield. The subsequent *syn*-crotylation using Brown Ipc borane established the desired *anti*-1,3-diol relationship. The final steps toward **163** were ozonolysis followed by reductive work-up, TBDPS protection of the primary hydroxyl group, acetal cleavage, and oxidation.

### *2.3.4.2 Different Approaches*

*Mycoticin [103]* Leighton developed an oxymercuration approach in order to generate 1,3-diols from allylation or crotylation products [104]. As in the concept of *syn*- or *anti*-reductions of β-hydroxyl ketones, the configuration of the chiral secondary alcohol is transferred to new hydroxyl group. Here, a double-bond activation using mercury salts initiates the oxidation process. In the presence of acetone and $Yb(OTf)_3$ as the Lewis acid, a hemiacetal is formed, which in turn adds to the mercury-activated double bond. This metal organic species can subsequently perform a




**SCHEME 2.150** Key steps on the Menche synthesis of rhizopodin.




**SCHEME 2.151** Synthesis of fragments during Paterson synthesis of rhizopodin.

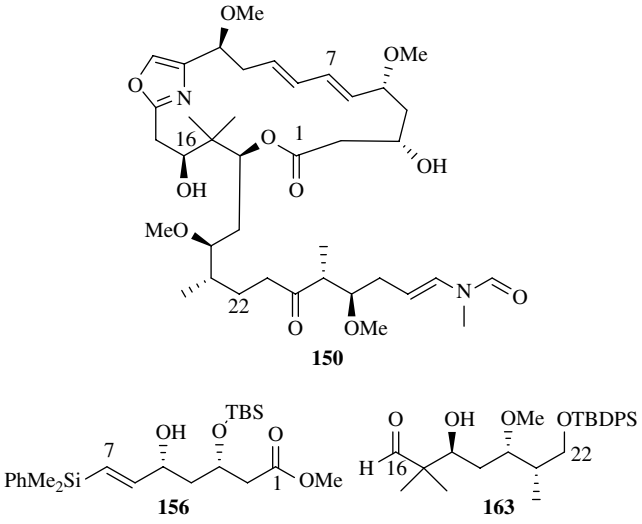


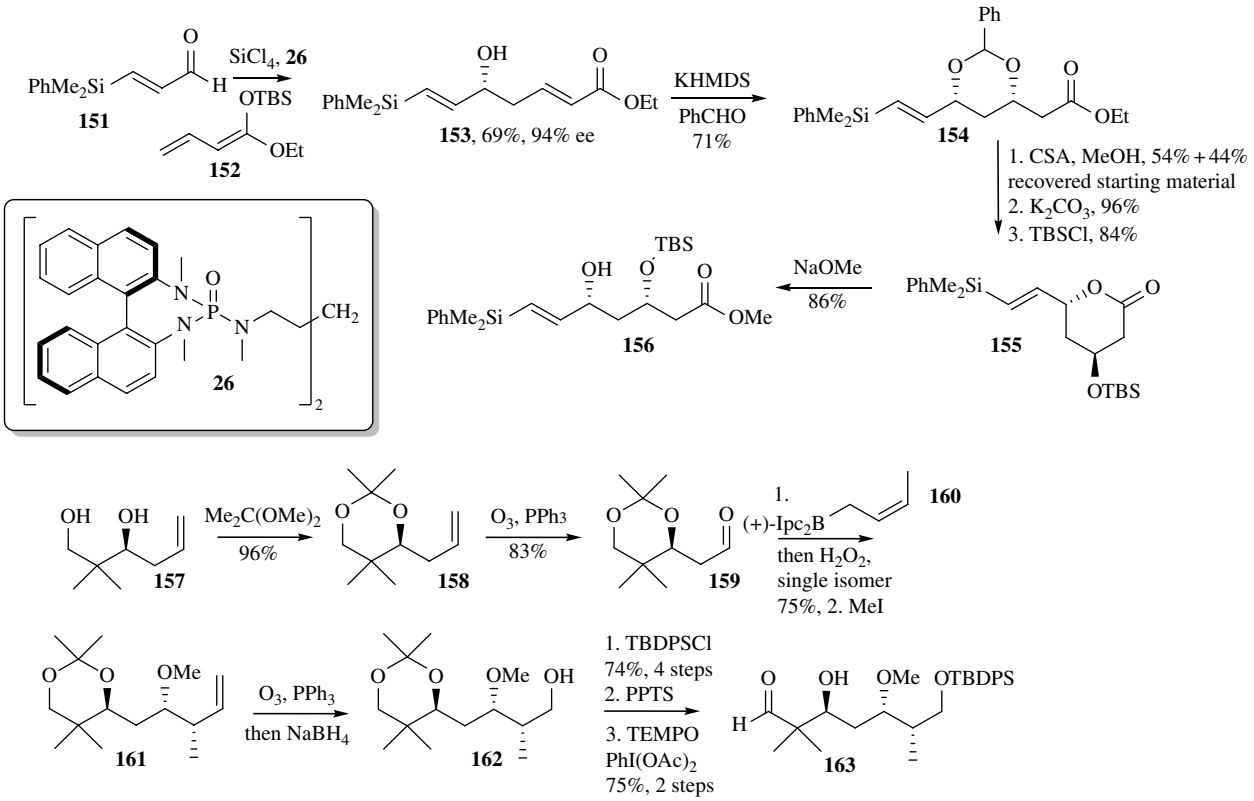

**FIGURE 2.6** Monorhizopodin and key fragments **156** and **163**.

hydroformylation in the presence of Rh(acac), CO, and hydrogen gas (Scheme 2.153). A similar, more direct way to access *syn*-diols with concomitant hydroformylation starts again from an allylation product but introduces a silyl hydride as the protecting group. Treatment with Rh(acac)$(CO)_2$ leads to Rh insertion into the Si–H bond and subsequent metal silylation of the olefin. As in the previous strategy, carbonylation with CO provides the hydroformylation product. The silicon–carbon bond serves as a protected hydroxyl group and can be transformed into the corresponding alcohol under oxidative conditions (Scheme 2.153) [105].

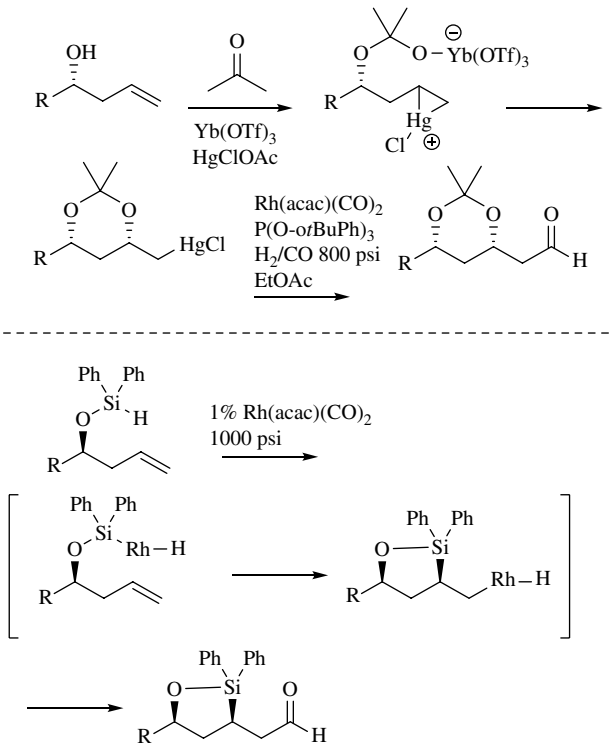
A further extension of this strategy uses bis-allyl silicon group as effective substituent for a subsequent intramolecular allylation reaction, providing polyols after oxidative conditions. The transition state that is depicted in Scheme 2.154 rationalizes the facial selectivity observed during the allylation step.

The same strategy when applied to propargylic ethers generates a vinyl silane during the hydrosilylation step, which is converted during the final oxidation to its enol and ultimately through tautomerization to the corresponding ketone (Scheme 2.155). Alternatively, the vinyl silane can be transformed to the disubstituted olefin by protodesilylation. It should be pointed out that when propargylic ethers are employed, a 1,5-*anti*-induction is observed in contrast to the 1,5-*syn* relationship for allyl ethers. Scheme 2.155 shows both possibilities, the formation of a ketone **165** with two hydroxyl groups in a 1,3 functional group distance from the carbonyl group and the formation of 1,5-*anti*-configured allyl–homoallyl diols **164**.

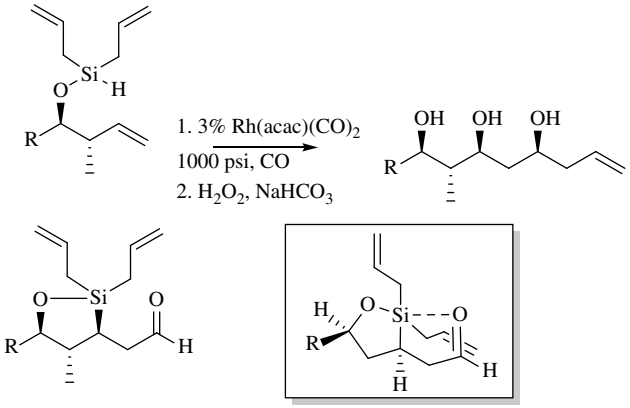
Leighton dissects in his mycoticin (**166**) synthesis the polyol fragment in two approximately equal size building blocks: ketone **167** and aldehyde **168**. Using the *anti*-directing effect of the β-oxygen, the methyl aldol reaction was expected to provide the desired 1,5-*anti*-product. An *anti*-selective reduction will then establish the correct configuration after reduction of the ketone. The synthesis of the ketone fragment commenced with cross metathesis reaction and liberation of the aldehyde by acidic acetal cleavage. Allylation provides the allyl–homoallyl alcohol, which is further transformed by the earlier described hydroformylation reaction. It is worth mentioning that only the homoallylic




**SCHEME 2.152** Highlighting the synthesis of fragments on Nicolaou synthesis of monorhizopodin.




**SCHEME 2.153** Seminal work of Leighton's group and its extension for the construction of 1,3-*syn*-diols.

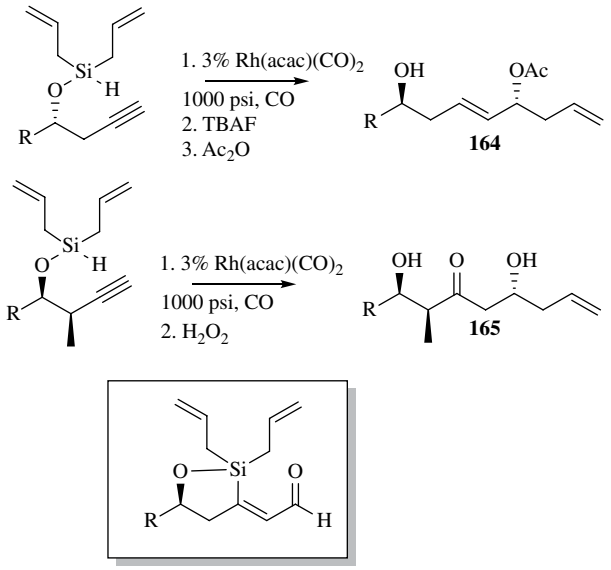



**SCHEME 2.154** Advancing Leighton protocol in polyol synthesis.

double bond undergoes reaction under these conditions. Treatment with $Y(OTf)_3$, HgCl(OAc), and acetone provides the acetonide-protected *syn*-1,3-diol, which is transformed to aldehyde **173**. The addition of MeMgBr and reoxidation completes the synthesis of the ketone segment (Scheme 2.156).

The hydroformylation–allylation sequence was also used by Leighton for the synthesis of the aldehyde segment (Scheme 2.157). The formation of bis-allyl silyl ether **175**

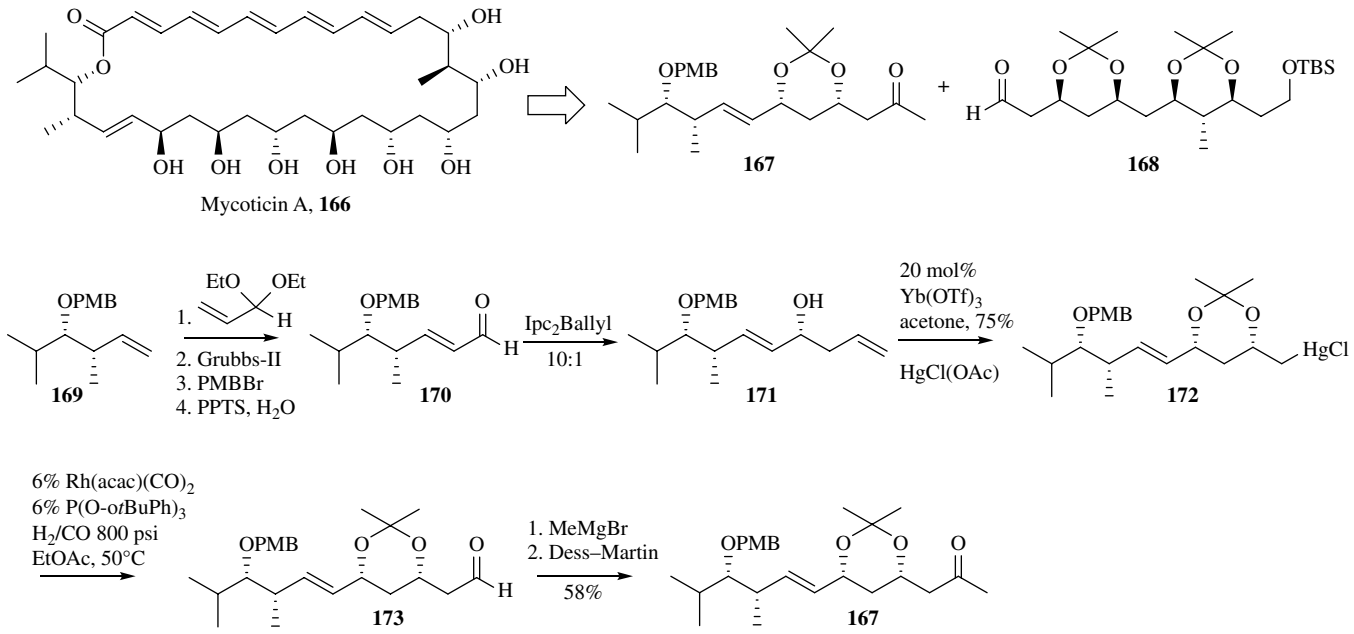
started out from alcohol **174**, obtained by an *anti*-selective crotylation. Deprotonation of the alcohol with butyl lithium and transformation with $HSiCl_3$ were directly followed by treatment with allyl magnesium bromide to generate the bis-allyl silane **175**. The subsequent hydroformylation–allylation process followed by oxidative work-up established tetraol **176** with three *syn*-configured alcohols. Protection of two OH groups as the acetonide allowed to conduct the mercury-induced hydroformylation step. As described in the preceding text, this transformation starts with the $Yb(OTf)_3$ formation of the hemiacetal, followed by the activation of the double bond by HgCl(OAc). Transmetalation and hydroformylation finally provided the bis-acetonide-protected pentaol aldehyde. With both fragments in hand, the methyl ketone was transformed to its silyl enol ether and reacted with aldehyde **168** using $BF_3$ as the Lewis acid to provide a 6 : 1 mixture in favor of the desired 1,5-*anti*-product. An *anti*-selective reduction using $Me_4NBH(OAc)_3$ completed the synthesis of the polyol segment.



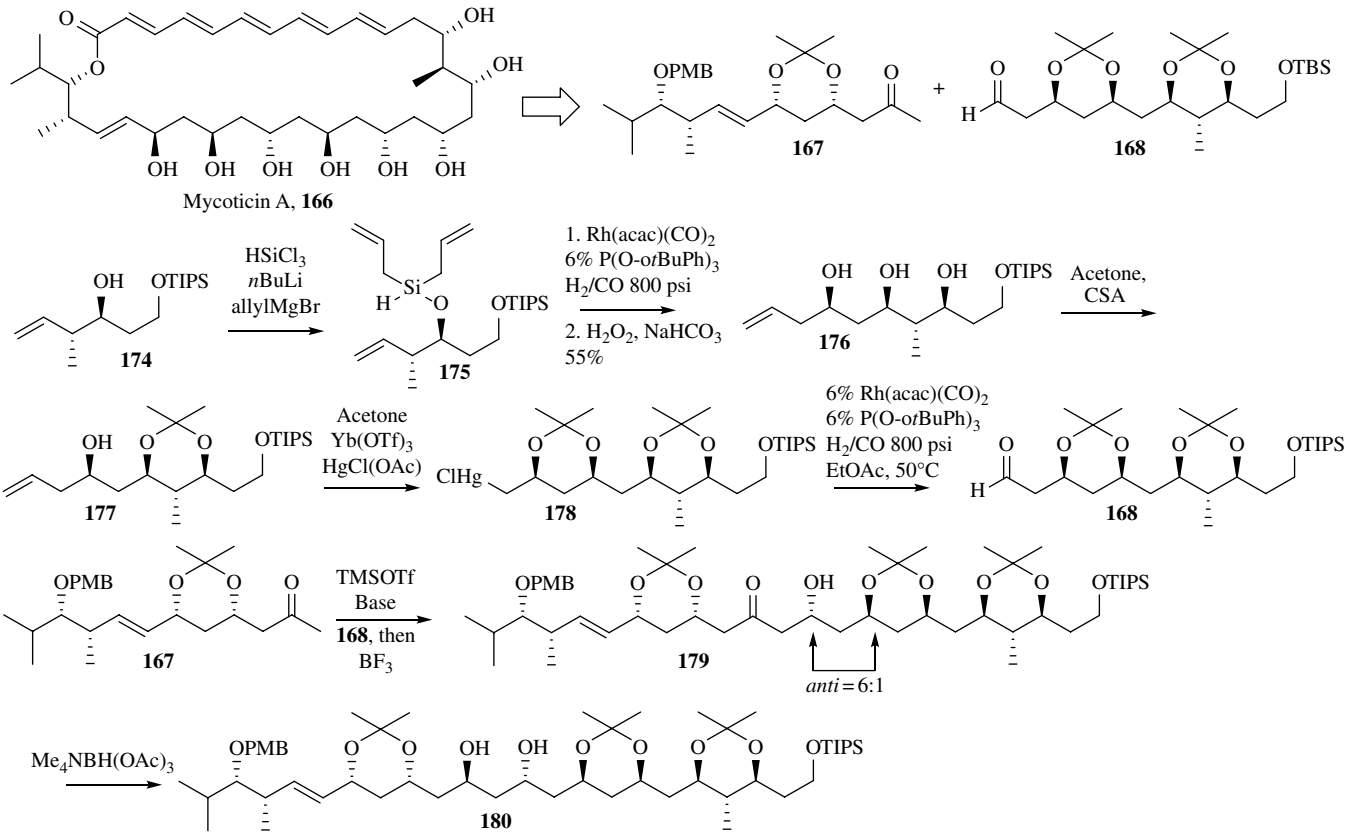

**SCHEME 2.155** Leighton oxymercuration.

*Roxaticin* A different approach for the construction of polyols was established by Rychnovsky. He envisioned that cyanohydrin acetonides can serve as conformationally restricted nucleophiles [106]. Using the umpolung strategy, these cyanohydrins can be deprotonated using a strong lithium base, and the so-generated nucleophile can be trapped with alkyl halides. The alkylation occurs predominantly at the equatorial position and generates a *syn*-1,3-diol substrate. Since the cyanide serves only as an umpolung reagent, it has to be removed under dissolving metal conditions. The so-generated anion can potentially exist as an equatorial or axial isomer. Mechanistic investigations have shown that the isomer with both side chains in an equatorial position is favored by 3.5 kcal/mol. This rational explains the high *syn*-selectivity observed for this protocol (Scheme 2.158).

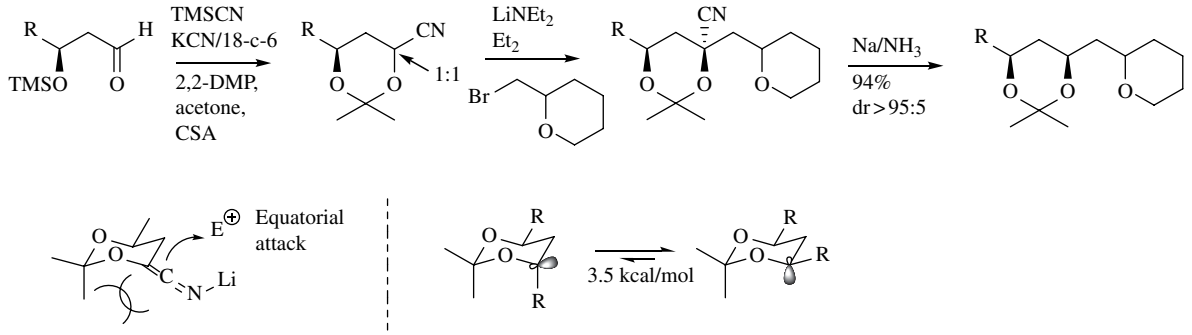
Rychnovsky's (−)-roxaticin retrosynthesis dissects the polyol segment into three pieces (Scheme 2.159) [107]: two cyanoacetonides and a C2-symmetric dibromide. The synthesis of the western part of the polyol segment uses a Blaise reaction for the synthesis of the β-keto ester. Using Noyori's




**SCHEME 2.156** Mycoticin A disconnection and the synthesis of fragment **167**.



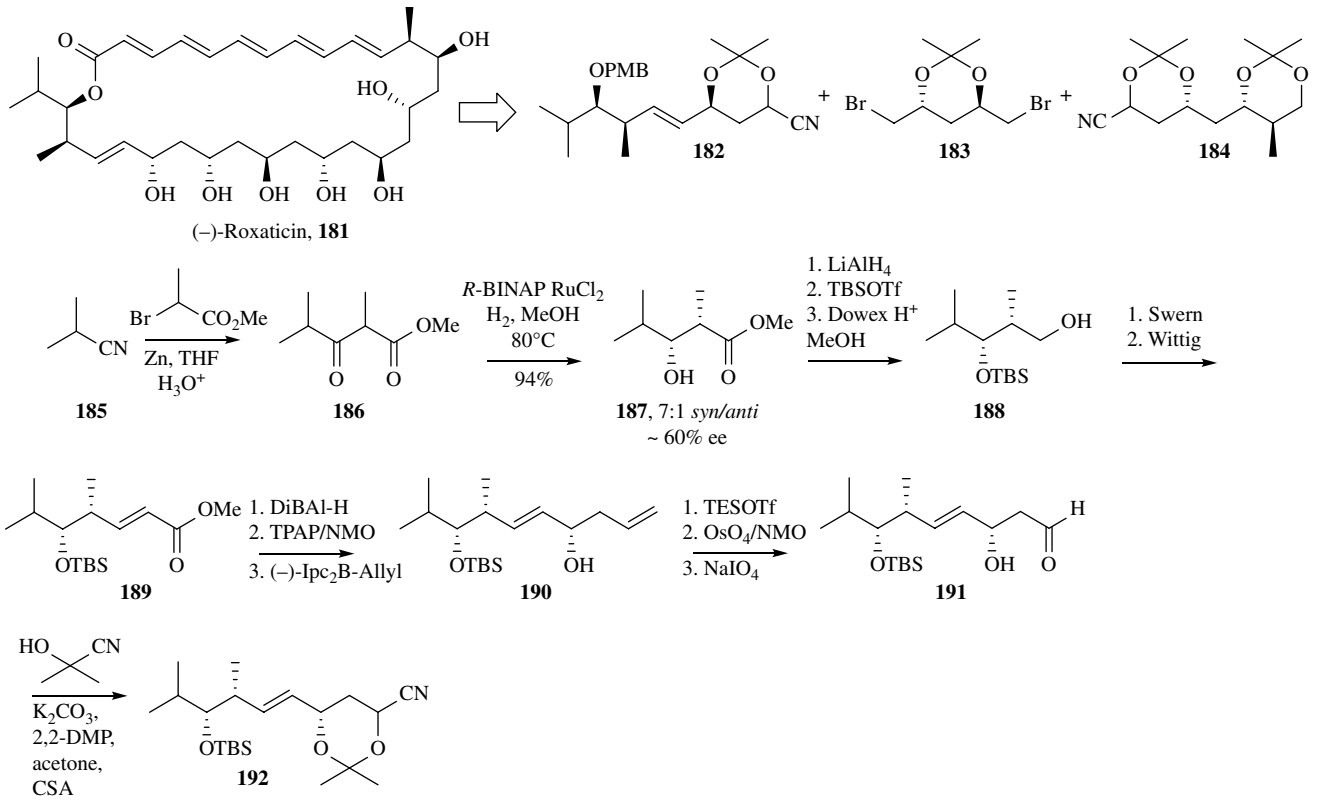

**SCHEME 2.157** Synthesis of fragment **168** and key aldol–reduction reactions.



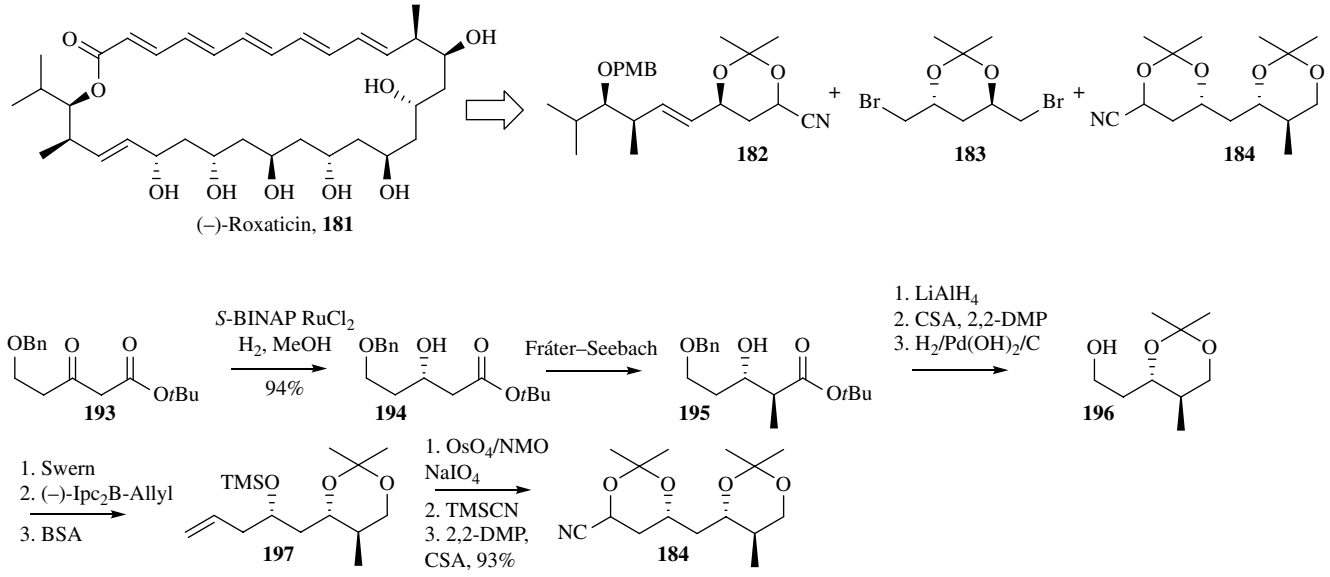

**SCHEME 2.158** Rychnovsky's acetonide strategy.

ruthenium/BINAP catalyst provides the desired β-hydroxy ester **187** in good yield and selectivities. Functional group manipulations provide primary alcohol, which is oxidized and extended by a Wittig reaction. Transformation of the ester to the aldehyde followed by allylation sets the stage for the cyanoacetonide formation. Oxidative cleavage of the double bond liberates the aldehyde, which is transformed to the cyanoacetonide **192**.

The eastern polyol segment starts from a β-keto ester **193**. Here the *t*-butyl ester was used to ease the separation of stereoisomers at a later stage. After stereoselective reduction, the Frater–Seebach protocol was applied and furnished the *anti*-β-hydroxy ester **195**. The subsequent steps are oxidation state changes, acetonide formation, and removal of the benzyl protecting group. The primary alcohol **196** was oxidized and a Brown allylation established the homoallylic alcohol **197**. From here the earlier described sequence of oxidative cleavage of the double bond and cyanoacetonide formation completed the synthesis of this building block (Scheme 2.160).

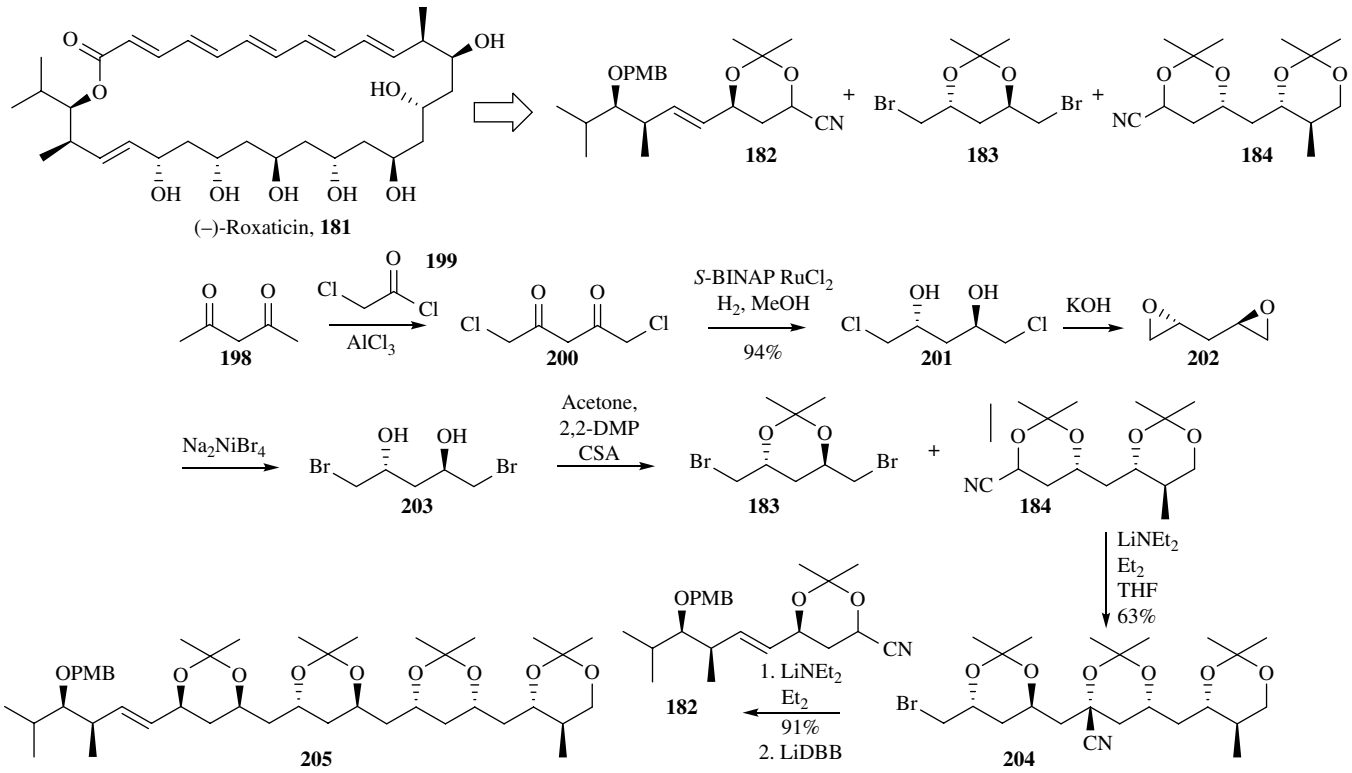



**SCHEME 2.159** Roxaticin disconnection by Rychnovsky and synthesis of fragment **182**.




**SCHEME 2.160** Synthesis of fragment **184** in the synthesis of roxaticin.

The pivotal dibromide was synthesized from acetyl acetone (**198**). An established protocol for chlorination at both methyl groups was followed by an *anti*-selective reduction of the diketone with Noyori's catalyst. Treatment with KOH generated the bis-epoxide, which was ring-opened with $Na_2NiBr_4$, which serves as an alternative to the Finkelstein protocol. The *anti*-diol **203** was protected as the acetonide and used in coupling reaction with both cyanoacetonides. The eastern segment was treated with base and trapped with the C2-symmetric dibromide **183**. Without any functional group manipulations, the second coupling reaction followed. The western cyanoacetonide was treated with base and




**SCHEME 2.161** Synthesis of dibromide fragment **183** and completion of the polyol fragment in the synthesis of roxaticin by Rychnovsky.

trapped with segment **182**. This transformation completed the polyol fragment of Rychnovsky's roxaticin synthesis (Scheme 2.161).

### 2.3.5 Conclusion

In summary, 1,3-diols are prominent motives in polyketides, and they can be constructed by various advanced methods. A practical access to 1,3-diols starts often with an aldol reaction. This aldol reaction can already construct a 1,3-diol if one hydroxyl group is already present in the starting material. Alternatively, *syn*- or *anti*-selective reductions of carbonyl groups offer an easy to predict stereoselective way to 1,3-diols. As we have seen in particular in the synthesis of roxaticin, direct reduction of diketones or β-keto esters proves an efficient entry into 1,3-diol segments.

## REFERENCES


1. (a) A. M. Hill, *Nat. Prod. Rep.* 2006, **23**, 256–320; (b) D. Schwarzer, M. A. Marahiel, *Nature* 2001, **88**, 93–101.
2. (a) R. E. Ireland, R. H. Mueller, A. K. Willard, *J. Am. Chem. Soc.* 1976, **98**, 2868–2877; (b) R. E. Ireland, P. Wipf, J. D. Armstrong, *J. Org. Chem.* 1991, **56**, 650–657.
3. H. E. Zimmerman, M. D. Traxler, *J. Am. Chem. Soc.* 1957, **79**, 1920–1923.
4. (a) H. B. Bürgi, J. D. Dunitz, E. Shefter, *J. Am. Chem. Soc.* 1973, **95**, 5065–5067; (b) H. B. Bürgi, J. D. Dunitz, J. M. Lehn, G. Wipff, *Tetrahedron* 1974, **30**, 1563–1572.
5. J. M. Lee, P. Helquist, O. Wiest, *J. Am. Chem. Soc.* 2012, **134**, 14973–14981.
6. (a) I. Paterson, J. D. Smith, R. D. Ward, *Tetrahedron* 1995, **51**, 9413–9436; (b) I. Paterson, R. D. Ward, J. D. Smith, *Tetrahedron* 1995, **51**, 9437–9466; (c) I. Paterson, K. S. Yeung, R. D. Ward, *Tetrahedron* 1995, **51**, 9467–9486; (d) I. Paterson, K. S. Yeung, R. D. Ward, J. G. Cumming, J. D. Smith, *J. Am. Chem. Soc.* 1994, **116**, 9391–9392; (e) I. Paterson, J. G. Cumming, J. D. Smith, R. D. Ward, K. S. Yeung, *Tetrahedron Lett.* 1994, **35**, 3405–3408; (f) I. Paterson, J. G. Cumming, J. D. Smith, R. D. Ward, *Tetrahedron Lett.* 1994, **35**, 441–444; (g) I. Paterson, J. D. Smith, *Tetrahedron Lett.* 1993, **34**, 5351–5354; (h) I. Paterson, J. D. Smith, *J. Org. Chem.* 1993, **57**, 3261–3264.
7. D. A. Evans, D. L. Rieger, M. T. Bilodeau, *J. Am. Chem. Soc.* 1991, **113**, 1047–1049.
8. D. A. Evans, D. L. Rieger, M. T. Bilodeau, F. Urpi, *J. Am. Chem. Soc.* 1991, **113**, 1047–1049.
9. D. A. Evans, J. Bartroli, T. L. Shih, *J. Am. Chem. Soc.* 1981, **103**, 2127–2129.
10. (a) M. T. Crimmins, B. W. King, E. A. Tabet, *J. Am. Chem. Soc.* 1997, **119**, 7883–7884; (b) M. T. Crimmins, K. Chaudhary, *Org. Lett.* 2000, **2**, 775–777.
11. (a) M. Nerz-Stormes, E. R. Thornton, *Tetrahedron Lett.* 1986, **27**, 897–900; (b) S. Shirodka, M. Nerz-Stormes, E. R. Thornton, *Tetrahedron Lett.* 1990, **31**, 4699–4702;

(c) M. Nerz-Stormes, E. R. Thornton, *J. Org. Chem.* 1991, **56**, 2489–2498.

12. S. Masamune, W. Choy, F. A. J. Kerdesky, B. Imperiali, *J. Am. Chem. Soc.* 1981, **103**, 1566–1568.
13. (a) W. Oppolzer, C. Starkemann, *Tetrahedron Lett.* 1992, **33**, 2439–2442; (b) W. Oppolzer, J. Blagg, I. Rodriguez, E. Walther, *J. Am. Chem. Soc.* 1990, **112**, 2767–2772.
14. A. Reychler, *Bull. Soc. Chim.* 1898, **19**, 120.
15. A. Abiko, J.-F. Liu, S. Masamune, *J. Am. Chem. Soc.* 1997, **119**, 2586–2587.
16. A. Abiko, *Org. Synth.* 2002, **79**, 116.
17. (a) D. A. Evans, A. S. Kim, R. Metternich, V. J. Novack, *J. Am. Chem. Soc.* 1998, **120**, 5921–5942; (b) D. A. Evans, J. S. Clark, R. Metternich, V. J. Novack, G. S. Sheppard, *J. Am. Chem. Soc.* 1990, **112**, 866–868
18. S. Masamune, T. Sato, B. M. Kim, *J. Am. Chem. Soc.* 1986, **108**, 8279–8281
19. E. J. Corey, R. Imwinkelried, S. Pikul, Y. B. Xiang, *J. Am. Chem. Soc.* 1989, **111**, 5493–5495.
20. (a) I. Paterson, J. M. Goodman, *Tetrahedron Lett.* 1989, **30**, 997–1000; (b) I. Paterson, J. M. Goodman, M. A. Lister, R. C. Schumann, C. K. McClure, R. D. Norcross, *Tetrahedron* 1990, **46**, 4663–4684.
21. R. O. Duthaler, P. Herold, W. Lottmhuch, K. Oertle, M. Riediker, *Angew. Chem. Int. Ed.* 1989, **28**, 495–497.
22. For recent examples, see: (a) V. Maggiotti, J.-B. Wong, R. Razet, A. R. Cowley, V. Gouverneur, *Tetrahedron Asymmetry* 2002, **13**, 1789–1798; (b) Q. Liang, J. Zhang, W. Quan, Y. Sun, X. She, X. Pan, *J. Org. Chem.* 2007, **72**, 2694–2697.
23. Y. Nagao, S. Yamada, T. Kumagai, M. Ochiai, E. Fujita, *J. Chem. Soc., Chem. Commun.* 1985, 1418–1419.
24. Y. Nagao, Y. Hagiwara, T. Kumagai, M. Ochiai, T. Inoue, K. Hashimoto, E. Fujita, *J. Org. Chem.* 1986, **51**, 2391–2393.
25. Y. Zhang, A. J. Phillips, T. Sammakia, *Org. Lett.* 2004, **6**, 23–25.
26. B. M. Trost, H. Ito, *J. Am. Chem. Soc.* 2000, **122**, 12003–12004.
27. N. Yoshikawa, Y. M. A. Das, J. Das, H. Sasai, M. Shibasaki, *J. Am. Chem. Soc.* 1999, **121**, 4168–4178.
28. (a) B. M. Trost, E. R. Silcoff, H. Ito, *Org. Lett.* 2001, **3**, 2497–2500; (b) B. M. Trost, S. H. Shin, J. A. Sclafani, *J. Am. Chem. Soc.* 2005, **127**, 8602–8603.
29. (a) Z. G. Hajos, D. R. Parrish *J. Org. Chem.* 1974, **39**, 1615–1621; (b) U. Eder, G. Sauer, R. Wiechert, *Angew. Chem. Int. Ed.* 1971, **10**, 496–497.
30. B. List, R. A. Lerner, C. F. Barbas III, *J. Am. Chem. Soc.* 2000, **122**, 2395–2396.
31. A. B. Northrup, D. W. C. MacMillan, *J. Am. Chem. Soc.* 2002, **124**, 6798–6799.
32. T. Mukaiyama, K. Narasaka, K. Banno, *Chem. Lett.* 1973, **9**, 1011–1014.
33. R. C. Fuson, *Chem. Rev.* 1935, **16**, 1–27.
34. T. Mukaiyama, A. Ishida, *Chem. Lett.* 1975, 319–322.
35. S. E. Denmark, J. R. Heemstra Jr., G. L. Beutner, *Angew. Chem. Int. Ed.* 2005, **44**, 4682–4698.
36. (a) C. H. Heathcock, K. Hug, L. A. Flippin, *Tetrahedron Lett.* 1984, **25**, 5973–5976; (b) C. H. Heathcock, S. Davidsen, K. Hug, L. A. Flippin, *J. Org. Chem.* 1986, **51**, 3027–3037; (c) C. H. Heathcock, L. Flippin, *J. Am. Chem. Soc.* 1983, **105**, 1667–1668.
37. (a) S. E. Denmark, W. Leehem, *Chem. Asian J.* 2008, **3**, 327–341; (b) S. E. Denmark, B. R. Henke, *J. Am. Chem. Soc.* 1991, **113**, 2177–2194; (c) S. E. Denmark, W. Lee, *Tetrahedron Lett.* 1992, **33**, 7729–7732; (d) S. E. Denmark, W. Lee, *J. Org. Chem.* 1994, **59**, 707–709.
38. Y. Yamaoka, H. Yamamoto, *J. Am. Chem. Soc.* 2010, **132**, 5354–5356.
39. H. Bürger, W. J. Kilian, *Organomet. Chem.* 1971, **26**, 47–55.
40. (a) M. A. Brook, C. Gottardo, S. Balduzzi, M. Mohamed, *Tetrahedron Lett.* 1997, **38**, 6997–7000; (b) M. A. Brook, S. Balduzzi, M. Mohamed, C. Gottardo, *Tetrahedron* 1999, **55**, 10027–10040.
41. M. B. Boxer, H. Yamamoto, *J. Am. Chem. Soc.* 2006, **128**, 48–49.
42. M. B. Boxer, M. Akakura, H. Yamamoto, *J. Am. Chem. Soc.* 2008, **130**, 1580–1582.
43. (a) D. A. Evans, J. D. Burch, E. Hu, G. Jaeschke, *Tetrahedron* 2008, **64**, 4671–4699; (b) D. L. Aubele, S. Wan, P. E. Floreancig, *Angew. Chem., Int. Ed.* 2005, **44**, 3485–3488; (c) D. A. Evans, M. C. Kozlowski, J. A. Murry, C. S. Burgey, K. R. Campos, B. T. Connell, R. J. Staples, *J. Am. Chem. Soc.* 1999, **121**, 669–685.
44. G. Bluet, J.-M. Campagne, *Tetrahedron Lett.* 1999, **40**, 5507–5509.
45. B. L. Pagenkopf, J. Krüger, A. Stojanovic, E. M. Carreira, *Angew. Chem., Int. Ed*. 1998, **37**, 3124–3126.
46. Bluet, G., Campagne, J.-M., *Synlett* 2000, **2**, 221–223.
47. B. Bazán-Tejeda, G. Bluet, G. Broustal, J.-M. Campagne, *Chem. Eur. J.* 2006, **12**, 8358–8366.
48. (a) G. Beutner, S. E. Denmark, *Angew, Chem Int. Ed.* 2013, **52**, 9086–9096; (b) S. E. Denmark, W. Lee, *Chem. Asian J.* 2008, **3**, 327–341; (c) G. Beutner, S. E. Denmark, *Angew, Chem Int. Ed.* 2008, **47**, 1560–1638; (d) S. E. Denmark, G. L. Beutner, T. Wynn, *J. Am. Chem. Soc.* 2005, **127**, 3774–3789.
49. (a) S. E. Denmark, S. Fujimori, *J. Am. Chem. Soc.* 2005, **127**, 8971–8973; (b) S. E. Denmark, G. L. Beutner, T. Wynn, M. D. Eastgate, *J. Am. Chem. Soc.* 2005, **127**, 3774–3789.
50. (a) L. Ratjen, P. Garcia-Garcia, F. Lay, M. Edmund Beck, B. List, *Angew. Chem. Int. Ed.* 2011, **50**, 754–758; (b) L. Ratjen, Organic Lewis acid catalysis-vinylogous aldol reactions and new catalysts. Dissertation, Universität Köln, 2012.
51. S.-I. Shirokawa, M. Kamiyama, T. Nakamura, M. Okada, A. Nakazaki, S. Hosokawa, S. Kobayashi, *J. Am. Chem. Soc.* 2004, **126**, 13604–13605.
52. T. Nakamura, S.-I. Shirokawa, S. Hosokawa, A. Nakazaki, S. Kobayashi, *Org. Lett.* 2006, **8**, 677–679.
53. L. Claisen, O. Lowman, *Chem. Ber.* 1887, **20**, 651–654.
54. E. E. Blaise, *C. R. Hebd. Seances Acad. Sci.* 1901, **132**, 478.
55. S. Reformatsky, *Chem. Ber.* 1887, **20**, 1210–1211.
56. H. B. Kagan, Y.-H. Suen, *Bull. Soc. Chim. Fr.* 1966, 1819.

57. S. M. Hannick, Y. Kishi, *J. Org. Chem.* 1983, **48**, 3833–3835.
58. G. Fráter, U. Müller, W. Günther, *Tetrahedron* 1984, **40**, 1269–1277.
59. D. Seebach, D. Wasmuth, *Helv. Chim. Acta* 1980, **63**, 197–200.
60. K. Nakamura, R. Yamanaka, T. Matsudab, T. Haradab, *Tetrahedron: Asymmetry* 2003, **14**, 2659–2681 and references cited therein.
61. T. Zelinski, M.-R. Kula, *Bioorg. Med. Chem. Lett.* 1994, **2**, 421–428.
62. (a) B.-N. Zhou, A. S. Gopalan, F. VanMiddlesworth, W.-R. Shieh, C. J. Sih, *J. Am. Chem. Soc.* 1983, **105**, 5925–5926; (b) C.-S. Chen, B.-N. Zhou, G. Girdaukas, W.-R. Shieh, F. VanMiddlesworth, A. S. Gopalan, C. Sih, *J. Bioorg. Chem.* 1984, **12**, 98–117; (c) W.-R. Shieh, A. S. Gopalan, C. J. Sih, *J. Am. Chem. Soc.* 1985, **107**, 2993–2994.
63. M. Nishizawa, M. Yamada, R. Noyori, *Tetrahedron Lett.* 1981, **22**, 247–250.
64. M. M. Midland, A. Tramontano, A. Kazubski, R. S. Graham, D. J. S. Tsai, D. B. Cardin, *Tetrahedron* 1984, **40**, 1371–1380.
65. H. C. Brown; P. V. Ramachandran, *Acc. Chem. Res.* 1992, **25**, 16–24.
66. (a) T. Imai, T. Tamura, A. Yamamuro, T. Sato, T. A. Wollmann, R. M. Kennedy, S. Masamune, *J. Am. Chem. Soc.* 1986, **108**, 7402–7404; (b) S. Masamune, R. M. Kennedy, J. S. Petersen, K. N. Houk, Y. Wu, *J. Am. Chem. Soc.* 1986, **108**, 7404–7405.
67. A. Hirao, S. Itsuno, S. Nakahama, N. Yamazaki, *Angew, Chem Int. J. Chem. Soc. Chem. Commun.* 1981, 315–317.
68. E. J. Corey, C. J. Helal, *Angew. Chemie Int. Ed.* 1998, **37**, 1986–2012 and references cited therein.
69. R. Noyori, S. Hashiguchi, *Acc. Chem. Res.* 1997, **30**, 97–102.
70. K.-J. Haack, S. Hashiguchi, A. Fujii, T. Ikariya, R. Noyori, *Angew. Chem. Int. Ed. Engl.* 1997, **36**, 285–288.
71. J. A. Marshall, K. Ellis, *Tetrahedron Lett.* 2004, **45**, 1351–1353.
72. K. Mashima, K.-H. Kusano, N. Sato, Y.-I. Matsumura, K. Nozaki, H. Kumobayashi, N. Sayo, Y. Hori, T. Ishizaki, *J. Org. Chem.* 1994, **59**, 3064–3076.
73. L. Shao, H. Kawano, M. Saburi, Y. Uchida, *Tetrahedron* 1993, **49**, 1997–2010.
74. K. Everaere, N. Franceschini, A. Mortreux, J.-F. Carpentier, *Tetrahedron Lett.* 2002, **43**, 2569–2571.
75. A. Bariotaki, D. Kalaitzakis, I. Smonou, *Org. Lett.* 2012, **14**, 1792–1795.
76. K. Hinterding, S. Singhanat, L. Oberer, *Tetrahedron Lett.* 2001, **42**, 8463–8465.
77. (a) K. Narasaka, F. C. Pai, *Tetrahedron* 1984, **40**, 2233–2238; (b) K. M. Chen, G. E. Hardtmann, K. Prasad, O. Repic, M. J. Shapiro, *Tetrahedron Lett.* 1987, **28**, 155–158.
78. A. K. Saksena, P. Mangiaracina, *Tetrahedron Lett.* 1983, **24**, 273–276.
79. D. A. Evans, K. T. Chapman, E. M. Carreira, *J. Am. Chem. Soc.* 1988, **110**, 3560–3578.
80. M. Dieckmann, D. Menche, *Org. Lett.* 2013, **15**, 228–231.
81. (a) V. Tishchenko, *Chem. Zentralbl.* 1906, **77**, 1309; (b) V. Tishchenko, *Chem. Zentralbl.* 1906, **77**, 1552; (c) D. A. Evans, A. H. Hoveyda, *J. Am. Chem. Soc.*1990, **112**, 6447–6449; (d) K. J. Ralston, A. N. Hulme, *Synthesis* 2012, **44**, 2310–2324.
82. (a) G. Höfle, N. Bedorf, K. Gerth, H. Reichenbach, Patent DE 42 11 056 C1, 1995; (b) J. Niggemann, N. Bedorf, U. Flörke, H. Steinmetz, K. Gerth, H. Reichenbach, G. Höfle, *Eur. J. Org. Chem.* 2005, **23**, 5013–5018.
83. (a) C. Gregg, M. V. Perkins, *Tetrahedron* 2013, **69**, 6845–6854; (b) C. Gregg, C. Gunawan, A. W. Y. Ng, S. Wimala, S. Wickremasinghe, M. A. Rizzacasa, *Org. Lett.* 2013, **15**, 516–519.
84. (a) I. Paterson, A. D. Findlay, E. A. Anderson, *Angew. Chem. Int. Ed.* 2007, **46**, 6699–6702; (b) I. Paterson, A. D. Findlay, C. Noti, *Chem. Commun.* 2008, 6408–6410; (c) I. Paterson, A. D. Findlay, C. Noti, *Chem. Eur. J.* 2009, **4**, 594–611.
85. D. A. Evans, K. T. Chapman, E. M. Carreira, *J. Am. Chem. Soc.* 1988, **110**, 3560–3578.
86. D. A. Evans, A. H. Hoveyda, *J. Am. Chem. Soc.*1990, **112**, 6447–6449.
87. (a) M. Lorenz, M. Kalesse, *Tetrahedron Lett.* 2007, **48**, 2905–2907; (b) M. Lorenz, M. Kalesse, *Org. Lett.* 2008, **10**, 4371–4374; (c) M. Lorenz, N. Bluhm, M. Kalesse, *Synthesis* 2009, 3061–3066.
88. D. A. Evans, K. T. Chapman, E. M. Carreira, *J. Am. Chem. Soc.* 1988, **110**, 3560–578.
89. A. Guerinot, G. Lepesqueux, S. Sable, S. Reymond, J. Cossy, *J. Org. Chem.* 2010, **75**, 5151–5163.
90. A. Hafner, R. O. Duthaler, R. Marti, G. Rib, P. Rothe-Streit, F. Schwarzenbach, *J. Am. Chem. Soc.* 1992, **114**, 2321–2336.
91. T. Harada, Y. Matsuda, L. Wada, J. Uchimura, A. Oku, *J. Chem. Soc., Chem. Commun.* 1990, 21–22.
92. F. Sasse, H. Steinmetz, G. Höfle, H. Reichenbach, *J. Antibiot.* 1993, **46**, 741.
93. G. Hagelüken, G. Albrecht, R. Jansen, H. Steinmetz, D. Heinz, M. Kalesse, F. Sasse, W.-D. Schubert, *Angew. Chem. Int. Ed.* 2009, **48**, 595–598.
94. (a) Z. Cheng, L. Song, Z. Xu, T. Ye, *Org. Lett.* 2010, **12**, 2036–2039; (b) T. K. Chakraborty, K. K. Pulukuri, M. Sreekanth, *Tetrahedron Lett.* 2010, **51**, 6444–6446; (c) T. K. Chakraborty, M. Sreekanth, K. K. Pulukuri, *Tetrahedron Lett.* 2011, **52**, 59–61; (d) M. Kretschmer, D. Menche, *Org. Lett.* 2012, **14**, 382–385; (e) L. K. Song, J. Y. Liu, H. G. Gui, C. G. Hui, J. J. Zhou, Y. Guo, P. P. Zhang, Z. S. Xu, T. Ye, *Chem.—Asian J.* 2013, **8**, 2955–2959; (f) H. G. Gui, J. Y. Liu, L. K. Song, C. G. Hui, J. M. Feng, Z. S. Xu, T. Ye, *Synlett* 2014, 138–142; (g) T. Bender, D. Loits, J. M. White, M. A. Rizzacasa, *Org. Lett.* 2014, **16**, 1450–1453; (h) K. K. Pulukuri, T. K. Chakraborty, *Org. Lett.* 2014, **16**, 2284–2287.
95. (a) M. Dieckmann, M. Kretschmer, P. Li, S. Rudolph, D. Herkommer, D. Menche, *Angew. Chem. Int. Ed.* 2012, **51**, 5667–5670; (b) M. Kretschmer, M. Dieckmann, P. F. Li, S. Rudolph, D. Herkommer, J. Troendlin, D. Menche, *Chem.–Eur. J.* 2013, **19**, 15993–16018; (c) M. Dieckmann, S. Rudolph,

C. Lang, W. Ahlbrecht, D. Menche, *Synthesis* 2013, 2305–2315.

96. (a) M. Kitamura, M. Tokunaga, T. Ohkuma, R. Noyori, *Org. Synth.* 1993, **71**, 1; (b) M. Kitamura, M. Tokunaga, T. Ohkuma, R. Noyori, *Tetrahedron Lett.* 1991, **32**, 4163–4166.
97. T. Okazoe, K. Takai, K. Utimoto, *J. Am. Chem. Soc.* 1987, **109**, 951–953.
98. S. M. Dalby, J. Goodwin-Tindall, I. Paterson, *Angew. Chem. Int. Ed.* 2013, **52**, 6517–6521
99. K. Narasaka, F.-C. Pai, *Tetrahedron* 1984, **40**, 2233.
100. K. C. Nicolaou, X. Jiang, P. J. Lindsay-Scott, A. Corbu, S. Yamashiro, A. Bacconi, V. M. Fowler, *Angew. Chem. Int. Ed.* 2011, **50**, 1139–1144.
101. (a) S. E. Denmark, G. L. Beutner, T. Wynn, M. D. Eastgate, *J. Am. Chem. Soc.* 2005, **127**, 3774–3789; (b) S. E. Denmark, S. Fujimori, *J. Am. Chem. Soc.* 2005, **127**, 8971–8973.
102. J. Bode, D. R. Gauthier, E. M. Carreira, *Chem. Commun.* 2001, 2560–2561.
103. S. D. Dreher, J. L. Leighton, *J. Am. Chem. Soc.* 2001, **123**, 341–342.
104. (a) S. D. Dreher, K. R. Hornberger, S. T. Sarraf, J. L. Leighton, *Org. Lett.* 2000, **2**, 3197–3199; (b) S. T. Sarraf, J. L. Leighton, *Org. Lett.* 2000, **2**, 403–405.
105. (a) I. J. Krauss, C. C.-Y. Wang, J. L. Leighton, *J. Am. Chem. Soc.* 2001, **123**, 11514–11515; (b) J. L. Leighton, D. N. O'Neil, *J. Am. Chem. Soc.* 1997, **119**, 11118–11119; (c) S. T. Sarraf, J. L. Leighton, *Org. Lett.* 2000, **2**, 403–405; (d) M. J. Zacuto, J. L. Leighton, *J. Am. Chem. Soc.* 2000, **122**, 8587–8588; (e) M. J. Zacuto, S. J. O'Malley, J. L. Leighton, *Tetrahedron* 2003, **59**, 8889–8900.
106. S. D. Rychnovsky, S. S. Swenson, *J. Org. Chem.* 1997, **62**, 1333–1340.
107. (a) S. D. Rychnovsky, R. C. Hoye, *J. Am. Chem. Soc.* 1994, **116**, 1753–1765; (b) S. D. Rychnovsky, C. Rodriguez, *J. Org. Chem.* 1992, **57**, 4793–4795.

# 3

# FATTY ACIDS AND THEIR DERIVATIVES

ANDERS VIK AND TROND VIDAR HANSEN
*School of Pharmacy, University of Oslo, Oslo, Norway*

## 3.1 INTRODUCTION

The natural products within the class of lipids constitute a wide range of compounds with diverse chemical structures. Traditionally, lipids have been defined as organic compounds that are soluble in a lipophilic solvent, such as chloroform or ether [1, 2]. Rather than using a physical property definition like solubility, a recent definition has been suggested where lipids have been defined as "hydrophobic or amphipathic small molecules that originate entirely or in part by carbanion-based condensations of thioesters and/or by carbocation-based condensations of isoprene units" [2]. Among the eight classes of naturally occurring compounds named as lipids according to this new definition, the class of fatty acyls or fatty acids is a central one [1]. Chemically, fatty acids are hydrocarbons attached to a carboxylic acid, which usually possess a long aliphatic chain that is either saturated or unsaturated [1].

## 3.2 BIOSYNTHESIS

The biosynthesis of saturated fatty acids has been extensively studied over the years. Already in 1907, Raper reported that fatty acids most likely were derived from a $C_2$ precursor [3]. In 1944, isotopically labeled compounds became available, and Rittenberg and Bloch fed rats with labeled acetate and concluded that fatty acids were indeed synthesized by successive condensation of $C_2$ units. They suspected that the actual metabolic intermediate was an activated form of acetate [4]. Finally, in 1948, Lipmann and Kaplan concluded that the activated form of acetate was acetyl-coenzyme A (Ac-CoA) [5].

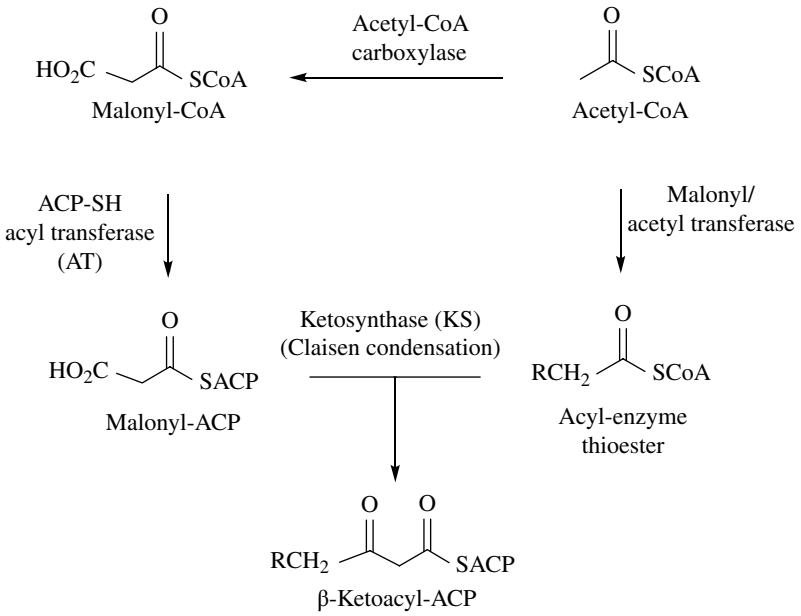
### 3.2.1 Fatty Acids and Lipids

Fatty acids are common in nature, but only trace amounts of their free, unesterified, form is found within living cells. However, they are of vital importance as building blocks for lipids, such as triglycerides, phosphoglycerides, phosphatides, sphingolipids, waxes, and steroidal alcohols, but also in combination with many other natural products. As triglycerides, fatty acids are components of cell membranes and are important for cell structure, but they are also functioning in protective coatings on leaves, furs, skins, and feathers. Moreover, fatty acids are also vital for energy storage.

Fatty acid biosynthesis *de novo* in a large variety of biological systems is catalyzed by two enzyme systems: acetyl-CoA carboxylase and the fatty acid synthase (FAS) enzyme systems.

***3.2.1.1 The Fatty Acid Synthase Enzyme Systems*** The FAS enzyme systems are central for the biosynthesis of saturated fatty acids [1] and share many similarities with the polyketide synthases (PKSs) involved in the biosynthesis of many polyketides [6]; see Section 2.1 for details. Common precursors, functional groups, and reactions are involved in each biosynthetic step. Saturated fatty acids, such as palmitic acid (**1**, Scheme 3.2), represent a rather small and structurally simple class of natural products produced by the FAS enzyme systems. The FAS enzyme system in animals is a large multifunctional protein with seven individual

*From Biosynthesis to Total Synthesis: Strategies and Tactics for Natural Products*, First Edition. Edited by Alexandros L. Zografos.
© 2016 John Wiley & Sons, Inc. Published 2016 by John Wiley & Sons, Inc.




**SCHEME 3.1** Outline of the first steps in the biosynthesis of saturated fatty acids.

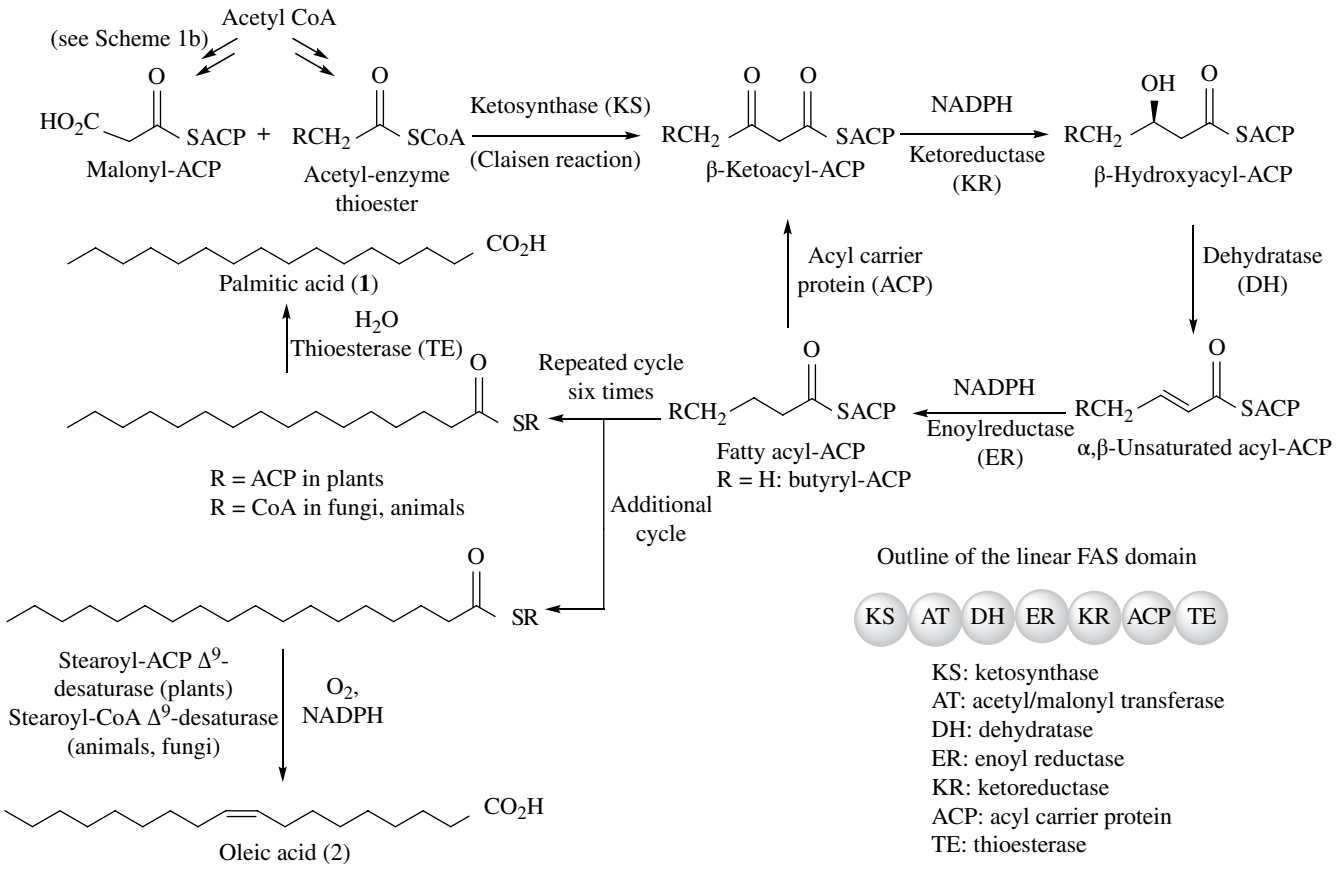
functional domains, where all of the catalytic components are present. All domains are on a single polypeptide that is encoded by a single gene, *FASN*. The enzyme exists as a homodimer and both units are needed for activity. In fungi, FAS is a multifunctional enzyme where the seven functional domains are spread out over two nonidentical polypeptides, named α and β. Fungal FAS exist as a $\alpha_6\beta_6$ dodecamer. The different FAS enzyme systems have been classified according to their different overall architecture. The multifunctional protein systems in animals and fungi are named type I FAS (FAS I) and are covalently connected in multifunctional megasynthases. The domain organization of the animal FAS I is linear and is responsible for loading both the starter and the chain-elongating substrates, whereas in modular PKSs, these substrates are loaded by separate acyl transferases (ATs), both in the loading and in the chain-extending modules. The type II FAS (FAS II) is expressed in bacteria and plants where the catalytic components are an assembly of free monofunctional polypeptide enzymes [6]. These separable enzymes are encoded by seven different genes.

For both FAS types, the catalytic domains include an AT, a ketosynthase (KS), a ketoreductase (KR), a dehydratase (DH), an enoylreductase (ER), an acyl carrier protein (ACP), and a thioesterase (TE). Both FAS I and FAS II utilize Ac-CoA and malonyl-CoA as substrates that are converted into enzyme-bound thioesters.

The animal FAS I polypeptides contain a single copy of all seven functional domains in a linear fashion. In contrast, the type I PKSs consist of multiple FAS-like "modules," each containing a KS, AT, and ACP with or without a full complement of the other catalytic domains; see Section 2.1 for details on the many PKS systems. The same set of enzymes is used iteratively for all steps in the chain elongation process in the FAS I system. The FAS II systems found in bacteria, chloroplasts, and mitochondria all utilize the free-standing enzymes in an iterative manner similar to the FAS I. The generic reaction scheme is shown in Schemes 3.1 and 3.2. It should be noted that the sequence of enzyme activities along the protein chain in the enzyme complex is not in accordance with the order of activity of the separate enzymes.

***3.2.1.2 Condensation Reactions*** First, Ac-CoA is converted into malonyl-CoA by acetyl-CoA carboxylase (Scheme 3.1). Acetyl-CoA carboxylase is at the point of control, by phosphorylation and/or by allosteric regulation, in the biosynthesis of saturated straight-chain fatty acids. Regulation by phosphorylation occurs mostly in mammals, while allosteric regulation occurs in most organisms. Allosteric control occurs due to feedback inhibition by palmitoyl-CoA, the final product of saturated fatty acid biosynthesis. When high levels of palmitoyl-CoA are biosynthesized, allosteric inactivation of acetyl-CoA carboxylase happens. This prevents a buildup of fatty acids in cells. Next, malonyl-CoA is converted by an acetyl transferase (AT) into the activated form, namely, malonyl-ACP; see Scheme 3.1. Then, a Claisen condensation reaction between malonyl-ACP and an activated fatty acid acyl-CoA unit gives a β-ketoacyl-ACP intermediate with the concurrent production of ACP and $CO_2$. This reaction is catalyzed by a β-KS.

In the first round, Ac-CoA is the activated fatty acid acyl-CoA unit. Surprisingly, both the primer acetyl and the chain-extender malonyl moiety are loaded onto the ACP–phosphopantetheine by the same AT. Thus, each substrate is




**SCHEME 3.2** Outline of the biosynthesis of the saturated fatty acid palmitic acid (**1**) and the monounsaturated fatty acid oleic acid (**2**) and a presentation of the linear domain organization of the animal FAS.

actually a competitive inhibitor of the other. The choice of which substrate to be loaded is entirely random. Therefore, a sorting process in which acetyl and malonyl moieties are rapidly exchanged between coenzyme A (CoA) and FAS I/FAS II is strictly needed. A productive reaction can only happen after the appropriate substrate is loaded; otherwise the inappropriately loaded substrate is transferred back to CoA. Hence, CoA must be present at all times during the FAS reaction to ensure efficient substrate sorting. The extremely rapid exchange of acetyl and malonyl moieties between CoA and FAS I/FAS II, catalyzed by the AT, ensures that this substrate sorting process is not rate limiting overall. Transfer of the primer moiety and the various saturated intermediates, from the ACP–phosphopantetheine to the active-site cysteine of the KS, is catalyzed by an innate transferase function of the KS. The vacant phosphopantetheine site is then filled by a malonyl moiety and the Claisen condensation reaction happens (Scheme 3.1). Then the β-ketoacyl-ACP intermediate is stereospecifically reduced by a β-KR to the corresponding β-hydroxy ester; see Scheme 3.2. The KR involved utilizes NADPH and involves the ubiquitous electron transport hemoprotein cytochrome $b_5$ in the redox step. The KR-catalyzed reduction of the 3-keto moiety to the 3*R*-alcohol happens by transfer of the pro-4*S*-hydride in NADPH. A dehydration reaction, catalyzed by a DH, then follows to afford an *E*-configured α,β-unsaturated thioester. This DH-catalyzed dehydration reaction to the *trans*-enoyl moiety occurs by a *syn* elimination of the 2*S*-hydrogen and the 3*R*-hydroxyl. Then reduction of the double bond is mediated by an ER in the presence of NADPH. In animals, the final reduction to a fully saturated acyl moiety proceeds by the transfer of the pro-4*R* hydride of NADPH to the pro-3*R* position with simultaneous addition of a water proton to the pro-2*S* position. Overall, this is a *syn* addition that also occurs in prokaryotes. Of notice, the yeast FAS appears to be an exception, since the pro-4*S* hydride of NADPH is transformed into the pro-3*S* position. Consequently, the water proton is incorporated at the pro-2*S* position. Hence, an *anti*-addition has occurred. Overall, after seven condensations, a saturated fatty acyl-ACP intermediate that is two carbon atoms longer than the starting material acetyl-CoA is produced. The saturated thioacyl intermediate is recycled to the active-site cysteine in preparation for the next condensation. Loading of acetyl groups is needed only for the first elongation reaction, when the four-carbon atom intermediate, that is, butyryl-ACP, is formed. In subsequent cycles, the product

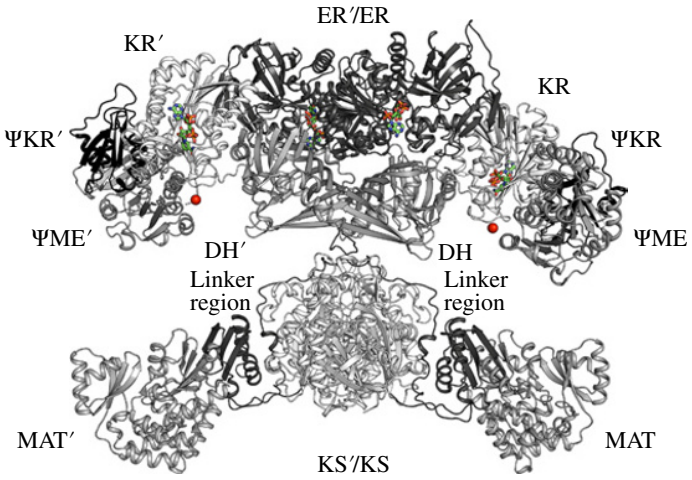



**FIGURE 3.1** An overview of the crystal structure of the multi-domain porcine fatty acid synthase (FAS) dimer with domain names, $NADP^+$ and ACP/TE anchoring points (PDB:2VZ9). Adapted from Maier et al. [10]. (*See insert for color representation of the figure.*)

of the ER action is transferred from ACP to the thiol of the cysteine present in the β-ketoacyl synthase (KS) active site. Alternatively, the resulting KS–thioester is attacked by malonyl-ACP to extend the chain by two carbons. Typically, after six turns of the cycle, when the saturated acyl chain length reaches 16 carbon atoms, the fatty acyl moiety is released from the ACP–phosphopantetheine complex through the action of the chain-terminating domain. Finally, the terminal TE domain catalyzes the hydrolysis of the thioester to the free acid (Scheme 3.2).

To summarize, all catalytic domains necessary for the biosynthesis of saturated fatty acid, such as palmitic acid (**1**), are distributed on two multidomain polypeptides in fungi, while in animals the domains are on a single polypeptide. These features ensure the efficient shuttle of substrates by ACP during the biosynthesis of fatty acids. Amazingly, the iterative animal FAS complex, involved in seven condensation reactions and 21 β-carbon processing steps, produces the C16 fatty acid **1** in less than a second.

***3.2.1.3 Structure Models of Fatty Acyl Synthases: Megasynthases*** The historical background and a thorough discussion of the many structural models reported of the fatty acyl synthases have in great detail been presented by Smith and Tsai in an exciting and thorough review article [6]. In both the FAS and the PKS systems, the same catalytic elements are covalently linked in the same order in the individual megasynthases. Megasynthase enzymes function in a manner analogous to an assembly line where multiple chemical building blocks are joined one after another into the final natural product. Since the 1950s, numerous attempts have been made to obtain high-quality structures of the different FAS systems using both X-ray and electron diffraction techniques. In 2006, Ban and colleagues obtained crystals of the full-length FAS that diffracted to 4.5 Å [7, 8]. Unfortunately, this level of resolution was not sufficient to identify the individual side chains. Moreover, the complete backbone of the two subunits proved impossible to assign. A major problem in obtaining high-resolution structures of proteins such as FAS is the inherent conformational flexibility, limiting the fidelity needed for a good three-dimensional reconstruction. The overall shape agreed well with the 15 Å resolution structure derived by electron microscopy [9] and revealed a large dimerization interface running across the body of the molecule. Unfortunately, all efforts to enhance the resolution of the structures were unsuccessful. Consequently, Ban and coworkers fitted high-resolution crystal structures of individual homologous type II bacterial proteins into their electron density maps. This allowed the assignment and location of the functional domains. Ban and colleagues characterized the FAS dimer as consisting of a central body composed of the ER, DH, and KS dimers that are flanked by a pair of arms and legs contributed by the monomeric KR domains and AT domains, respectively (Fig. 3.1). The ER domains are dimeric while the DH domains appear to be pseudodimeric. Each of the pseudosubunits, marked with an apostrophe, is derived from adjacent regions of the same polypeptide. The second of the two pseudosubunits of the DH domain occupied roughly 200 residues of an approximately 650-residue region of the FAS previously referred to as the central core. Both the AT and KR are apparently also monomeric. Thus, the oligomeric status of the KS, AT, DH, and ER domains turned out to be identical to that of their FAS II type counterparts. In Figure 3.1, the different domains and their pseudodimers are illustrated. The only exception appeared to be the monomeric KR domain, whose type II counterparts are tetramers. The ACP and TE domains were absent from the structure as no appropriate electron density could be identified. Gratifyingly, these were the only two domains for which high-resolution

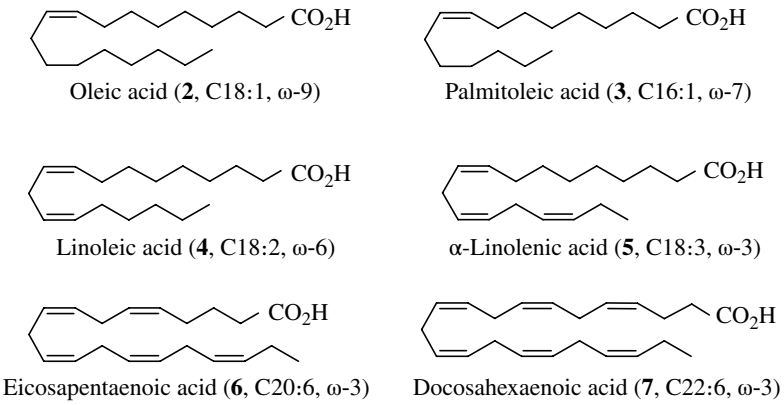



**FIGURE 3.2** Chemical structures of the unsaturated fatty acids, oleic acid (**2**), palmitoleic acid (**3**) linoleic acid (**4**), α-linolenic acid (**5**), eicosapentaenoic acid (**6**), and docosahexaenoic acid (**7**).

structures were available. The inherent mobility of these domains might be responsible for the lack of any clearly attributable electron density. Ban and colleagues then suggested that the most likely location of the ACP–TE region would be at the extremity of the arms, since in the linear sequence, the ACP is positioned directly following the KR domain.

The striking similarity of the overall topology of the KS–AT didomain of the PKS 6-deoxyerythronolide synthase, the most studied PKS, with its FAS counterpart, also contributes important information on the structure. Exciting new structural data on the FAS systems in mycobacteria, mammals, yeast, and fungi have recently been reported [10–13], and these efforts have been thoroughly reviewed [14].

### 3.2.2 Polyunsaturated Fatty Acids

Polyunsaturated fatty acids (PUFAs) are found in higher organisms and exhibits diverse and interesting biological effects [15]. Several beneficial health effects have been linked to the dietary intake of PUFAs. Most likely, derivatives and metabolites of the PUFAs are responsible for these health effects. Very often, the PUFA metabolites are available only in minute quantities from their natural sources. PUFAs are also important for energy storage and as structural building blocks, lipid mediators, messengers, hormones, and cofactors [15].

Chemically, PUFAs are fatty acids containing two or more methylene-interrupted double bonds in their structure. The configuration of the double bonds in many naturally occurring unsaturated fatty acids is *Z*. These compounds are also referred to as *cis*-fatty acids or "all-*cis*" fatty acids. PUFAs containing *E*-configured double bonds also occur naturally. These so-called *trans*-fatty acids have been isolated from bovine fat and the milk of cow, goat, and ewe [15]. There are four families of PUFAs, namely, the ω-9, ω-7, ω-6, and ω-3 PUFAs. Oleic acid (**2**) is the precursor for the ω-9 family, and palmitoleic acid (**3**) is the precursor for the ω-7 family (Fig. 3.2). These two monounsaturated fatty acids are nonessential fatty acids biosynthesized in the human body from their corresponding dietary and saturated precursors. In nature, linoleic acid (**4**) and α-linolenic acid (**5**) are the primary precursors for the ω-6 and ω-3 PUFAs, respectively.

The two marine ω-3 PUFAs, eicosapentaenoic acid (EPA, **6**) and docosahexaenoic acid (DHA, **7**), are depicted in Figure 3.2. Their biosynthesis and biological effects are outlined in the next chapter.

There are several biosynthetic pathways that unsaturated fatty acids can arise from. In most organisms, the common mechanism is by desaturation of the corresponding saturated fatty acid. Desaturation of fatty acids involves a process that requires molecular oxygen, NADH, and cytochrome $b_5$. The reaction, which occurs in the endoplasmic reticulum, results in the oxidation of both the fatty acid and NADH.

The stereospecific introduction of a *Z*-double bond occurs by the abstraction of two vicinal pro-*R* hydrogens atoms at C-9 and C-10 in a thioester (Fig. 3.3). In plants, R = ACP, while in animals and fungi, the thioester is activated as CoA. This reaction is catalyzed by stearoyl-ACP $\Delta^9$-desaturase in plants and stearoyl-CoA $\Delta^9$-desaturase in animals and fungi [1]. Oxygen and either NADPH or NADH as cofactors are required for both types of desaturases.

The $\Delta^9$-desaturase acts on fatty acyl-CoA, and C-14 to C-18 saturated fatty acyl chains are good substrates, with stearoyl-CoA being most active. A reduced pyridine nucleotide is required. The $\Delta^9$-desaturase is dependent on the presence of molecular oxygen, which acts as an electron acceptor for two pairs of hydrogens, one from NADH and the other from the fatty acyl-CoA.

The $\Delta^9$-desaturase system consists of three major proteins: (1) NADH–cytochrome $b_5$ reductase, (2) cytochrome $b_5$, and (3) a terminal desaturase component (Fig. 3.3). Under most circumstances, electron transport greatly exceeds the activity of the rate-limiting desaturase component. The $\Delta^9$-desaturase contains one atom of a nonheme.

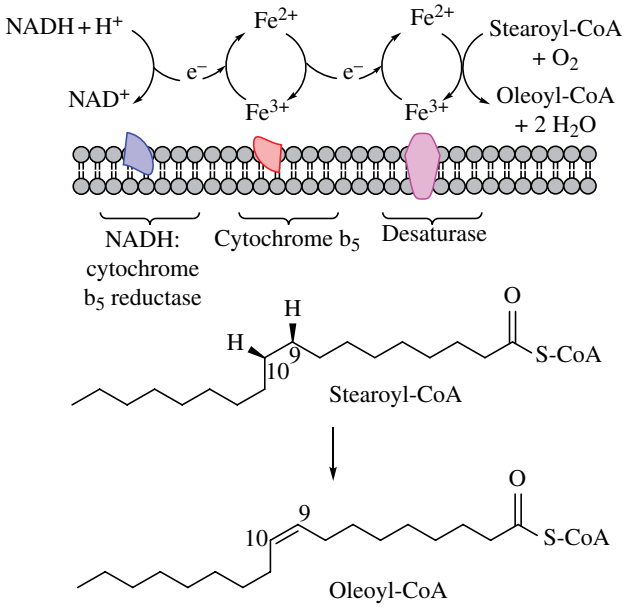



**FIGURE 3.3** An outline of the oxidation–reduction sequence in the $\Delta^9$-desaturase system.

NADH–cytochrome $b_5$ reductase is a flavoprotein of molecular weight 43 kDa, while cytochrome $b_5$ is a heme-containing protein of molecular weight 16.7 kDa. Cytochrome $b_5$ displays a catalytic hydrophilic region with 85-amino acid residues, including the $NH_2$-terminal, and the protein terminates in a hydrophobic COOH-terminal tail of approximately 40 amino acids. The latter connects the protein to the membrane.

Then further desaturation depends on the organism, as nonmammalian enzymes most often introduce additional double bonds between the existing double bond and the methyl end. Animals tend to introduce new double bonds toward the C-1 carboxylic acid since the $\Delta^{12}$- and $\Delta^{15}$-desaturase enzymes are not expressed in animals. Hence, animals must consume linoleic acid (**4**) and α-linolenic acid (**5**), since these fatty acids are not biosynthesized *in vivo*. Linoleic acid (**4**) and α-linolenic acid (**5**) are therefore termed essential fatty acids.

***3.2.2.1 Biosynthesis of ω-3 and ω-6 Polyunsaturated Fatty Acids*** Among the many unsaturated fatty acids found in nature, the ω-3 and ω-6 PUFAs have received a great interest from scientists in biology, medicine, and chemistry [15].

The two PUFAs, linoleic acid (**4**) and α-linolenic acid (**5**), depicted in Figure 3.2, are of plant origin [1, 15]. Some of the major sources of linoleic acid (**4**) are sunflower oil, soybean oil, and rapeseed oil, but the most important source is linseed oil. In plants and microorganisms, linoleic acid (**4**) and α-linolenic acid (**5**) are biosynthesized through the desaturation of oleic acid (**2**). In mammals, linoleic acid (**4**) and α-linolenic acid (**5**) are biosynthetic precursors for ω-3 and ω-6 PUFAs, respectively. As mentioned earlier, the desaturase enzymes required for the formation of linoleic acid (**4**) and α-linolenic acid (**5**) are absent in mammals, and these PUFAs must therefore be obtained from the diet [15]. In Scheme 3.3, the generally accepted biosynthetic pathways to EPA (**6**), DHA (**7**), and arachidonic acid (**8**) are outlined [16, 17]. As in Schemes 3.1 and 3.2, the thioesters are intermediates, but for simplicity, the free acids are drawn here.

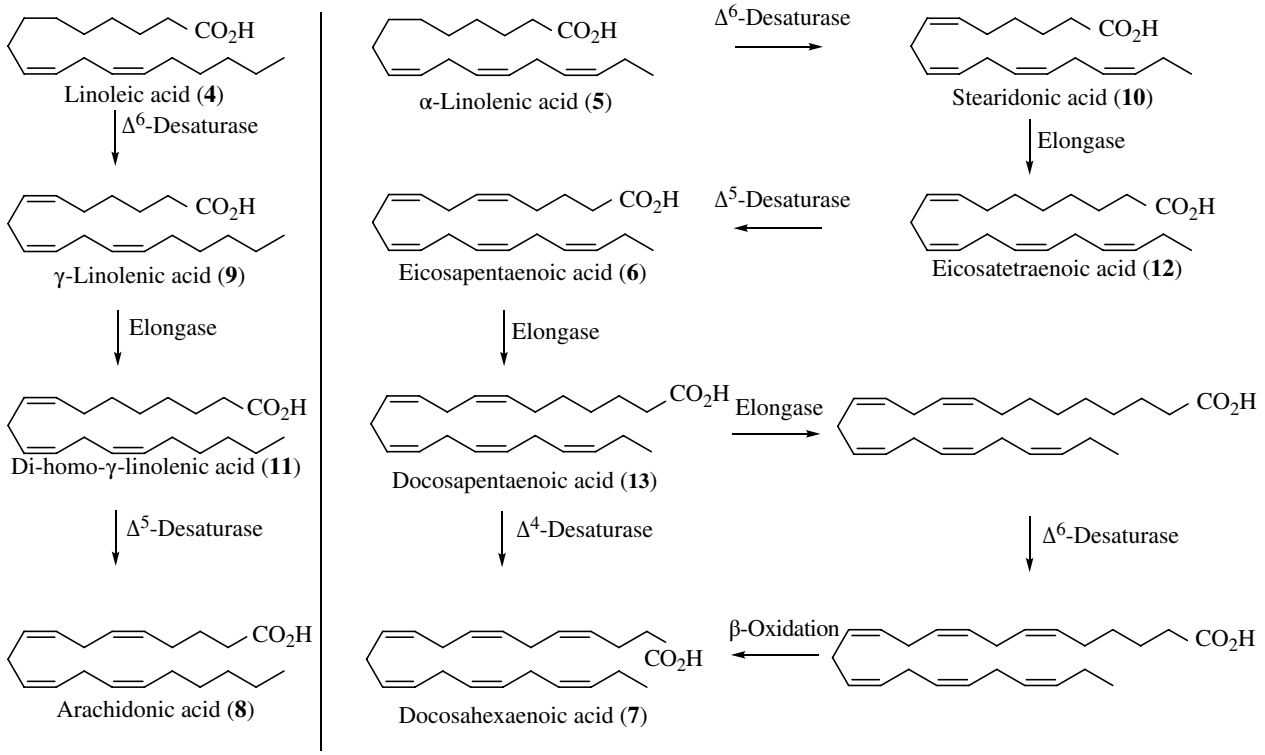
The enzymes involved in Scheme 3.3 are the same for the ω-3 and ω-6 PUFAs. The $\Delta^6$-desaturase enzyme installs a C6–C7 *cis* double bond on linoleic acid (**4**) and α-linolenic acid (**5**), which forms γ-linolenic acid (**9**) and stearidonic acid (**10**), respectively. Then an elongase transforms these two fatty acids to the two C20 fatty acids dihomo-γ-linoleic acid (**11**) and eicosatetraenoic acid (**12**), respectively. Claisen-type condensation reactions of thioesters are again involved. Desaturation on dihomo-γ-linoleic acid (**11**) by the $\Delta^5$-desaturase enzyme installs a C5–C6 *cis* double bond that leads to arachidonic acid (**8**). If the $\Delta^5$-desaturase enzyme uses eicosatetraenoic acid (**12**) as the substrate, EPA (**6**) is formed (Scheme 3.3).

From this point, the further biosynthetic route toward DHA (**7**) has been the subject of debate [18]. It has been demonstrated that in the microorganism *Thraustochytrium*, the biosynthesis toward DHA (**7**) from EPA (**6**) continues with an elongation to give docosapentaenoic acid (**13**). Then a $\Delta^4$-desaturase enzyme ensures the desaturation of the C4–C5 double bond to afford DHA (**7**) [19]. In mammals, it has been shown that the biosynthesis of DHA (**7**) occurs via elongation of docosapentaenoic acid (**13**) to a C24-PUFA, which undergoes desaturation at C6–C7 followed by a subsequent β-oxidation that produces DHA (**7**) (Scheme 3.3).

There are some controversy and discussions on the efficiency of the biosynthetic process from α-linolenic acid (**5**) to DHA (**7**) [18, 19]. Some studies have shown that plasma DHA (**7**) level does not increase with the addition of α-linolenic acid (**5**) [20], while others have shown that consumption of α-linolenic acid (**5**) leads to the enhanced formation of DHA (**7**) [21].

### 3.2.3 Mediated Oxidations of ω-3 and ω-6 Polyunsaturated Fatty Acids

The PUFAs are excellent substrates for enzymatically mediated oxidation reactions. These reactions lead to a plethora of biologically active natural products that have been isolated from plants, animals, and the marine environment. Very often EPA (**6**) and arachidonic acid (**8**) are substrates for these oxidations. One significant example is the eicosanoid class of natural products that constitute many pharmacologically active oxygenated PUFAs. Two such examples are the prostaglandins and the leukotrienes presented in more detail in the succeeding text. These two classes of




**SCHEME 3.3** Outline of the biosynthesis of eicosapentaenoic acid (**6**), docosahexaenoic acid (**7**), and arachidonic acid (**8**). For simplicity, the free acids are drawn.

natural products are biosynthesized by cyclooxygenases (COXs) and lipoxygenases (LOXs), respectively.

In the mid-1990s, the structures of two COX enzymes were reported, namely, COX-1 and COX-2 [22, 23]. COX-1, expressed in most tissues, is responsible for the physiological production of prostaglandins, while COX-2 is responsible for the biosynthesis of prostaglandins during inflammation. COX-2 is induced by cytokines, mitogens, and endotoxins in inflammatory cells. The two COX enzymes have two distinct active sites termed the COX active site and the peroxidase active site. Hamberg and Samuelsson outlined the mechanism of prostaglandin biosynthesis in 1967 [24]. This mechanism describes a biosynthetic process involving oxygenation, cyclization, and the generation of five stereogenic centers from achiral arachidonic acid (**8**). COX-1 and COX-2 have similar molecular weight, ca 70 and 72 kDa, respectively, with a 65% amino acid homology. The most important difference is the presence of the ILE-523 in COX-1, whereas in COX-2, a valine is present in this position. The smaller VAL-523 in COX-2 provides access to a hydrophobic side pocket. This minute difference in structure is most likely responsible for the different mode of actions that the two COX enzymes display, both biosynthetically and how they are inhibited by different NSAIDs. Both COX enzymes are homodimers that each contains one molecule of heme. Each COX subunit compromises an epidermal growth-factor domain, a membrane-binding domain, and a catalytic domain (Fig. 3.4).

In the resting enzyme, the iron is ferric and is most likely thermodynamically unable to oxidize the Tyr-385 phenol, which is central in the first radical hydrogen abstraction reaction. Apparently, a ferryl-oxo complex is first formed that is capable of abstracting a hydrogen radical from arachidonic acid (**8**) at the C-13 position (Scheme 3.4). Removal of the 13-pro-*S*-hydrogen radical occurs that is followed by reaction with oxygen. Then, the COX site cyclizes arachidonic acid (**8**), while a hydroperoxy group is formed at the C-15 position by the addition of another oxygen, resulting in prostaglandin $G_2$ ($PGG_2$, **14**); see Scheme 3.4. The separate peroxidase site of the same COX enzyme then reduces this hydroperoxy group to the hydroxy group to form prostaglandin $H_2$ ($PGH_2$, **15**) [26]. The Arg-120 is crucial for binding to the carboxylate group. When oxygen diffuses up the central channel, it can be trapped at C-11 and C-13, resulting in the formation of the endoperoxide. As mentioned, the Tyr-385 is necessary for the 13-pro-*S*-hydrogen abstraction, and this amino acid forms, together with Arg-120 and Glu-524, a hydrogen-bonding network. The ω-end most likely occupies the top of the enzyme active site close to the α-helix. COX-1 and COX-2 have similar enzymatic actions, and the biosynthesis of prostaglandin $H_2$ (**15**) is depending on the tissue where it is synthesized [27].

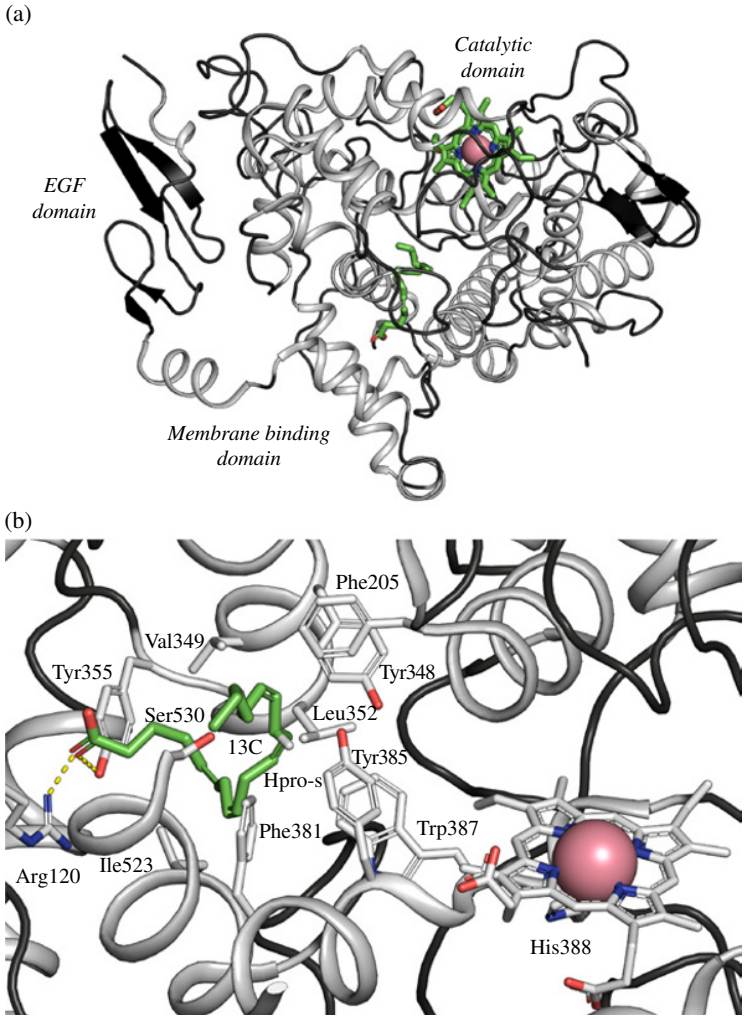
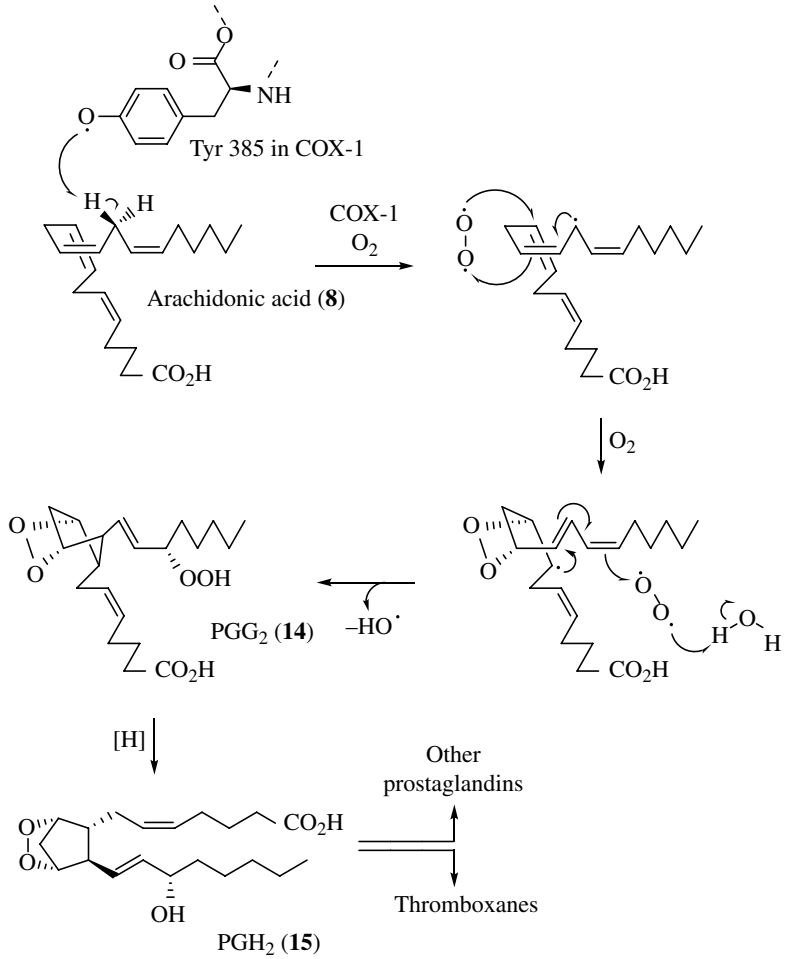



**FIGURE 3.4** The ovine $Co^{3+}$-COX-1 (PGHS-1) enzyme with arachidonic acid (**8**) in the COX channel (PDB: 1DIY). (a) Structural overview showing the domains of monomeric COX-1. (b) The peroxidase active site of COX-1 with arachidonic acid (**8**), important nearby residues, and the $Co^{3+}$-protoporphyrin IX. Phe209 has been omitted for clarity. Adapted from Malkowski et al. [25]. (*See insert for color representation of the figure.*)

Unlike the COXs, which are active in most body cells, LOX enzymes are primarily active in cells of the immune system. LOXs are enzymes that catalyze the stereospecific incorporation of molecular oxygen into PUFAs [23]. The LOXs are iron-containing enzymes, and so far five families of LOXs have been reported, namely, 5-, 8-, 12-, 13-, and 15-LOXs (Fig. 3.5).

The LOXs abstract a hydrogen radical from the C-3 of a *cis,cis*-1,4-pentadiene system present in PUFAs. So far, six distinct LOX enzymes have been reported in mammals. The overall shape of the LOXs is cylindrical and ca 100 Å in length and ca 45 Å in width. In 15-lipoxygenase (15-LOX), two $Ca^{2+}$-binding sites are present in its membrane-binding domain. The 15-LOX catalytic domain consists of approximately 20 helices. A high-resolution structure of human 15-LOX was reported very recently by Newcomer and coworkers [28]. They used the competitive inhibitor C8E4 as a substrate mimic of arachidonic acid (**8**) to obtain crystals at 2.65 Å resolution. This structure revealed that the substrate binding cavity in 15-LOX can easily accommodate arachidonic acid (**8**). Both the catalytic iron and an oxygen channel situated on the opposite face are present in this cavity. The inhibitor C8E4 and arachidonic acid (**8**) each fit with a U-shaped conformation in the 15-LOX binding cavity. This conformation of arachidonic acid (**8**) is stabilized by the presence of mostly hydrophobic residues. Close to the base of the U-shaped conformation of arachidonic acid (**8**) is the catalytic iron, held in place by histidines 373, 378, and 553, as well as the C-terminal carboxylate of Ile676. 15-LOX converts arachidonic acid (**8**) to 15-hydroperoxyeicosatetraenoic acid (15-HPETE, **16**) by attack at C-13, while 5-LOX abstracts the pro-*S*-hydrogen radical at C7 of




**SCHEME 3.4** Outline of the initial biosynthetic pathways of the prostaglandins.

arachidonic acid (**8**), forming 5-hydroperoxyeicosatetraenoic acid (5-HPETE, **17**). However, how the six different LOX enzymes are able to distinguish between the three *cis,cis*-1,4-pentadienes of arachidonic acid (**8**), to generate a specific hydroperoxyeicosatetraenoic acid isomer, is not yet established.

Leukotriene biosynthesis depends upon the availability of arachidonic acid (**8**) as the free carboxylic acid as the 5-LOX substrate, which typically requires the action of cytosolic phospholipase $A_2$ to release arachidonic acid (**8**) from membrane phospholipids [27]. The name leukotriene was conceived to capture two unique attributes of these molecules. The first relates to those white blood cells derived from the bone marrow that have the capacity to synthesize this class of eicosanoids, for example, the polymorph nuclear leukocyte. The last part of the name refers to the unique chemical structure, a conjugated triene retained within these eicosanoids [29, 30]. The first step for the leukotriene biosynthesis is the insertion of molecular oxygen at position 5 of arachidonic acid (**8**) to produce 5-HPETE (**17**) that can be converted to leukotriene $A_4$ (**18**) by the second catalytic activity of 5-lipoxygenase (Scheme 3.5) [31]. 5-HPETE (**17**) is also converted to 5-HETE (**23**).

Leukotriene $A_4$ (**18**) is the precursor of leukotriene $B_4$ (**19**); the latter is formed after enzymatic hydrolysis. The leukotrienes **20–22** are also formed from **18**. Leukotriene $B_4$ (**19**) displays many interesting biological effects, such as chemotactic and chemokinetic activity *in vivo* [32], while leukotriene $C_4$ (**20**) exhibits potent *smooth muscle* contracting activity and mediates leakage of vascular fluid in the process of edema [33].

The transformation of free arachidonic acid (**8**) to 12-HPETE (**24**) and 15-HPETE (**16**) is catalyzed by 12-LOX and 15-LOX, respectively (Scheme 3.6). These products are reduced to the corresponding hydroxy compounds 12-HETE (**25**) and 15-HETE (**26**) by cellular peroxidases. Arachidonic acid (**8**) is also transformed by 8-LOX into 8-HPETE (**27**). The first step of the biosynthesis of lipoxin $A_4$ ($LXA_4$, **29**) and lipoxin $B_4$ ($LXB_4$, **30**) is the formation of **16** by a 15-LOX. Subsequently, **16** is converted to form an epoxy intermediate, that is, 5*S*,6*S*-epoxy-15*S*-hydroxy-ETE (**28**). Then, depending on the cell type, specific hydrolases form

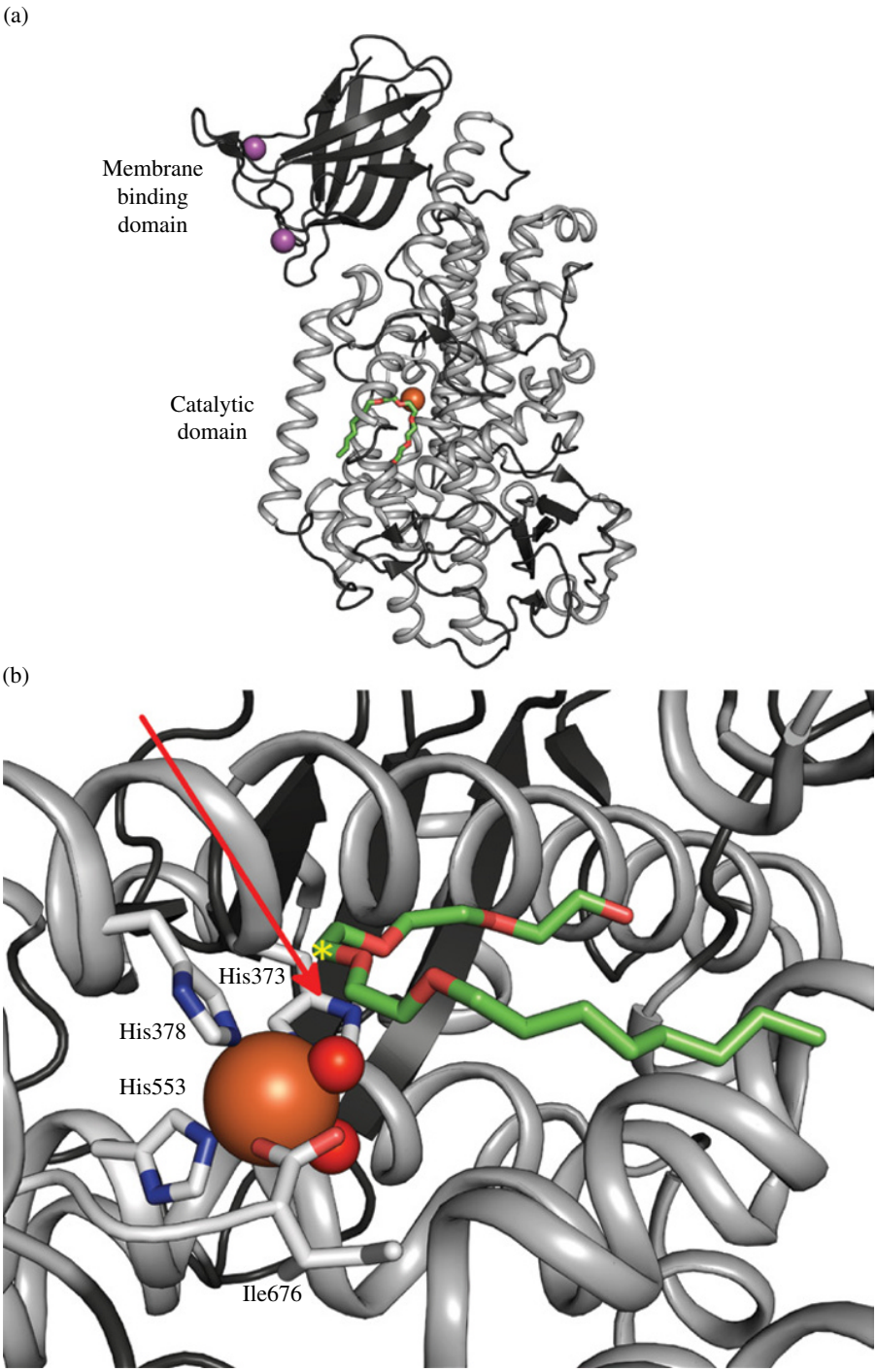
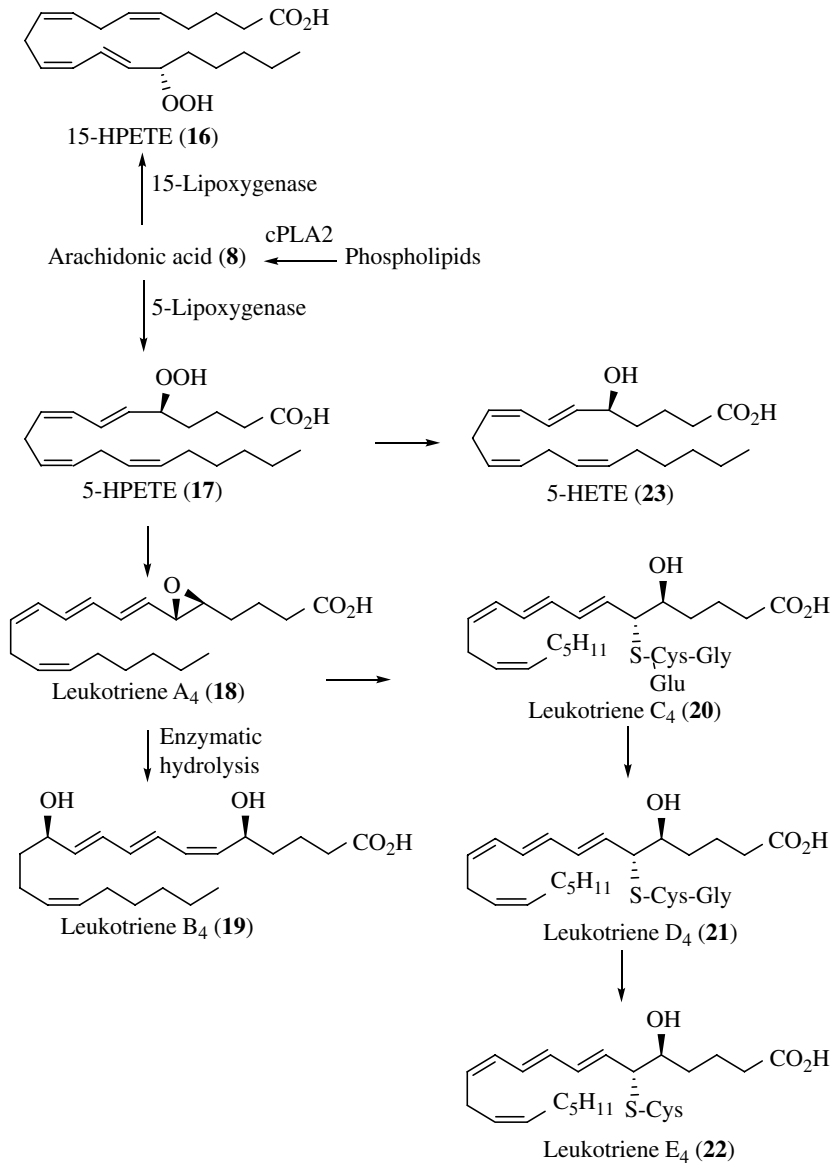



**FIGURE 3.5** The human LOX-15 enzyme bound to the substrate mimic octyl tetraethylene glycol ether (C8E4) (PDB: 4NRE). (a) Overview of the LOX-15 structure with domain names. (b) Structure of the LOX-15 active site showing the nonheme $Fe^{2+}$ coordinated by three histidines, the C-terminal carboxylate and two water molecules. The asterisk indicates the approximate position of the C13-carbon of arachidonic acid (**8**) when modeled into the C8E4 electron density. The arrow denotes the direction and opening of the $O_2$ channel toward the active site. Adapted from Kobe et al. [28]. (*See insert for color representation of the figure.*)




**SCHEME 3.5** An overview of the biosynthetic pathway of the different leukotrienes.

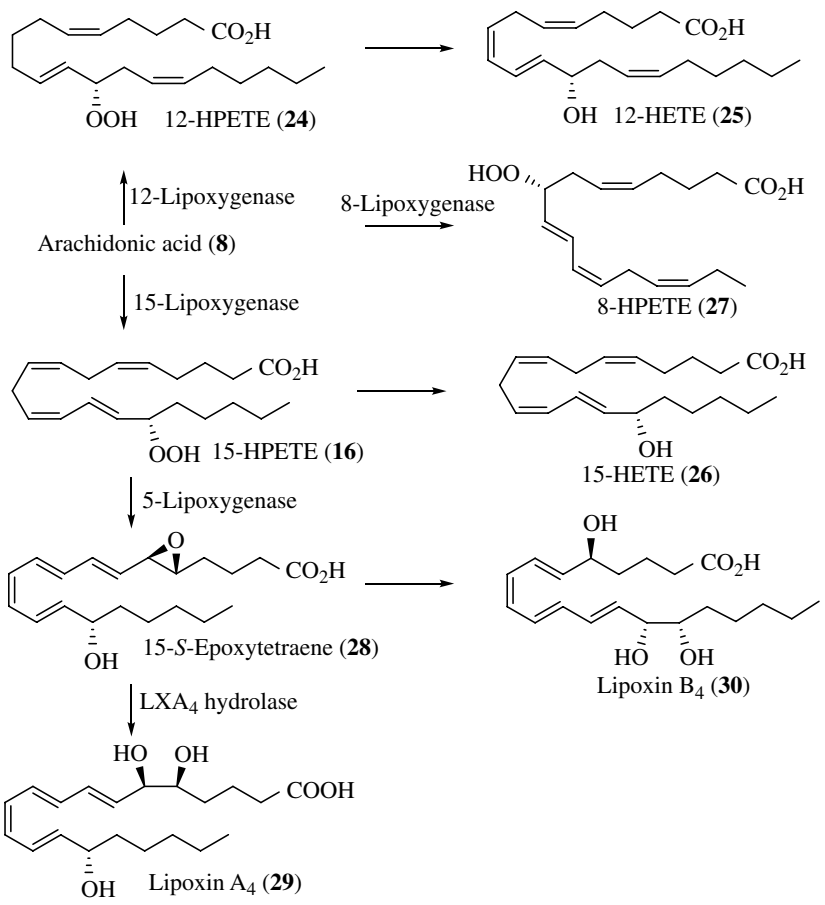
either lipoxin $A_4$ (**29**) or lipoxin $B_4$ (**30**); see Scheme 3.6 [33]. These bioactive trihydroxytetraene-containing lipid mediators appear to function as stop signals for inflammatory responses and to promote repair and wound healing [34, 35].

## 3.3 SYNTHESIS OF ω-3 AND ω-6 ALL-*Z* POLYUNSATURATED FATTY ACIDS

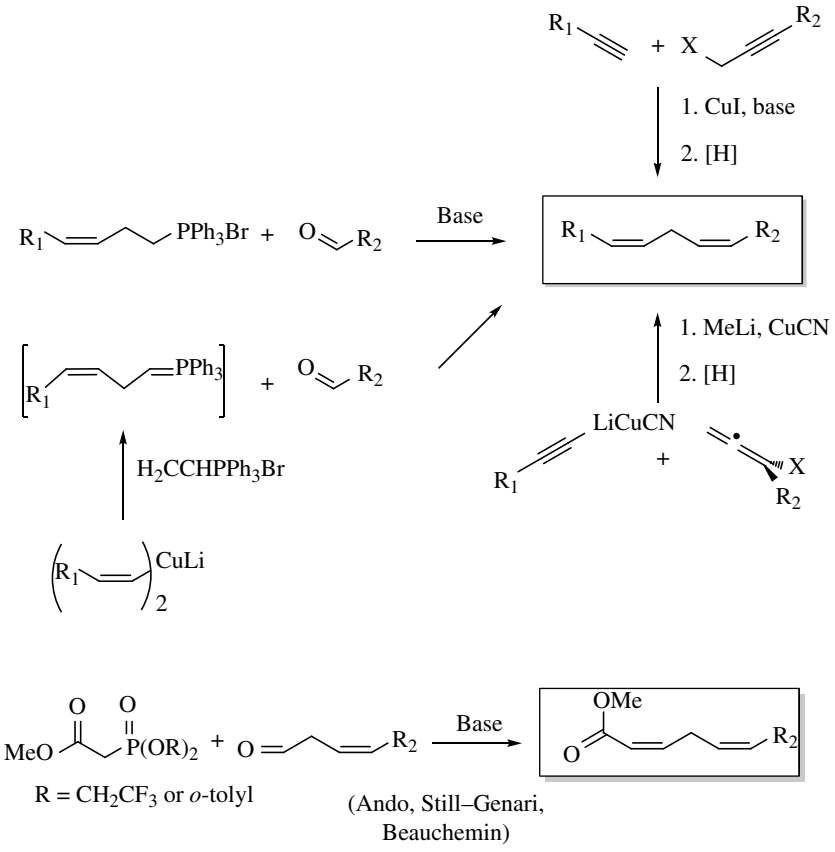
As mentioned in the previous chapters, the PUFAs and their metabolites have shown a plethora of interesting biological effects. Very often, the PUFA metabolites are available only in minute quantities from their natural sources. Hence, total organic synthesis is necessary not only to provide enough material for biological investigations but also to confirm the stereochemical structures of these natural products. This has attracted the attention and interest of many research groups in synthetic organic chemistry, leading to the development of several synthetic strategies toward PUFAs. In the succeeding text, some of the main strategies employed in the synthesis of ω-3 and ω-6 PUFAs are outlined.

### 3.3.1 Synthesis of Polyunsaturated Fatty Acids by the Wittig Reaction or by the Polyyne Semihydrogenation

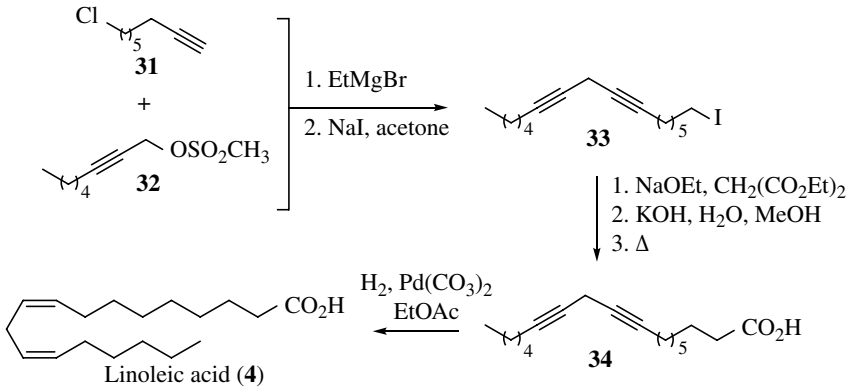
Among the methods outlined in Scheme 3.7, polyyne semihydrogenation and Wittig reactions are the two most common strategies to synthesize PUFAs and their metabolites [36, 37]. For the polyyne semihydrogenation sequence, numerous systems have been reported for the reduction of a



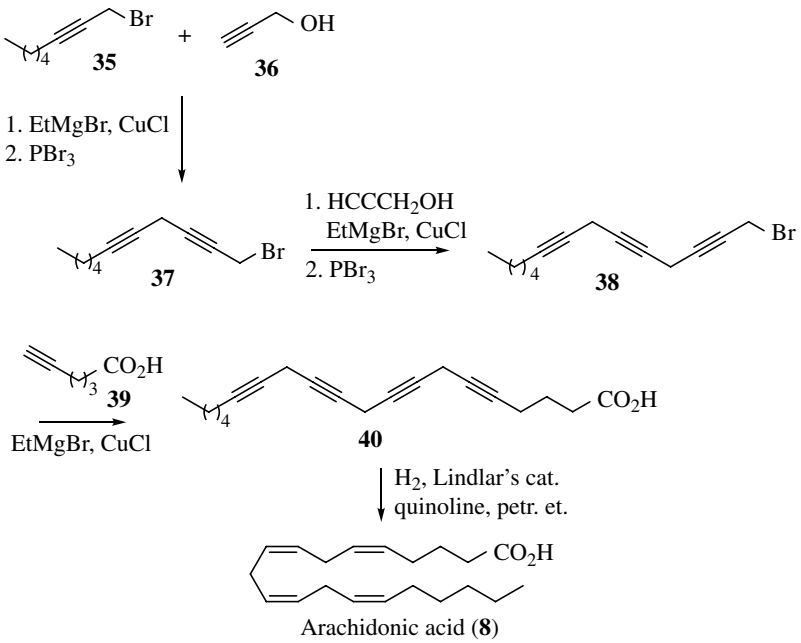

**SCHEME 3.6** Biosynthesis of lipoxins and catalytic actions of 12- and 15-LOX.




**SCHEME 3.7** Examples of the construction of the (*cis*,*cis*)-1,4-diene system.




**SCHEME 3.8** The first total synthesis of linoleic acid (**4**) by Raphael and Sondheimer [40].




**SCHEME 3.9** The first total synthesis of arachidonic acid (**8**) by Osbond [41].

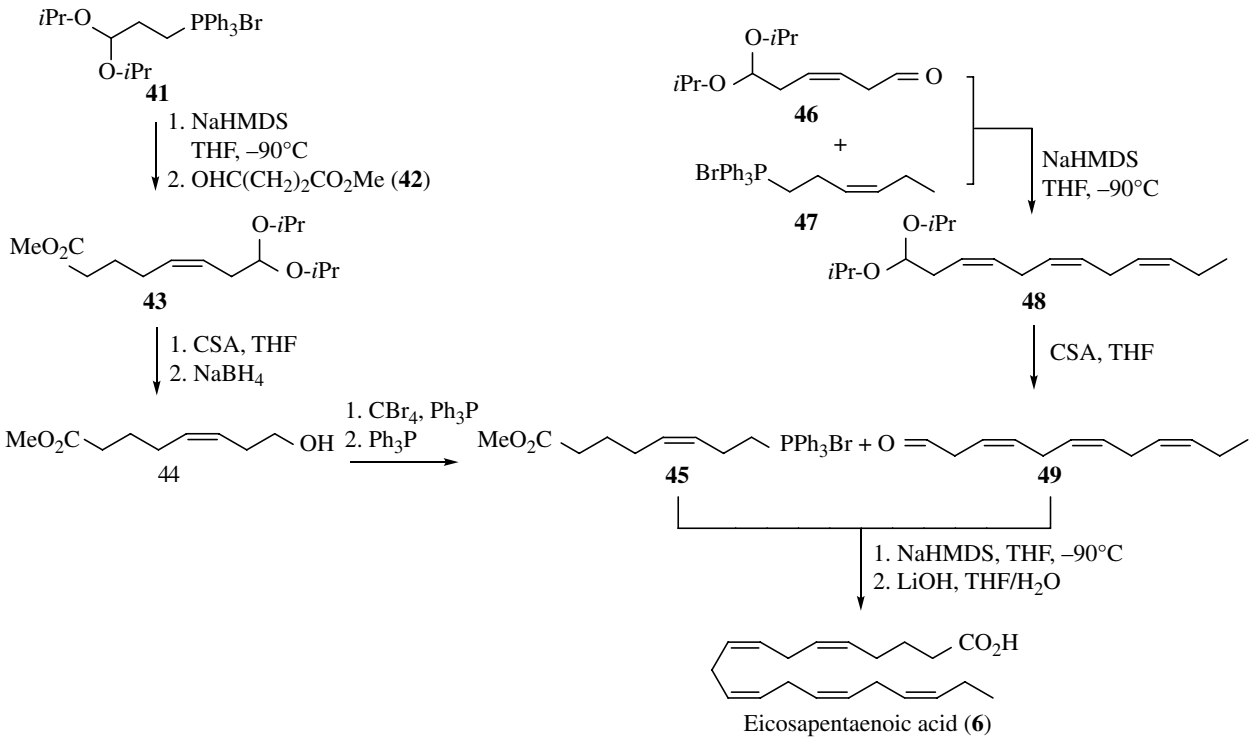
triple bond to a *Z*-double bond [37]. The *Z/E* selectivity is sometimes a challenge in the semireductions of alkynes, and very often the problem with overreduction of the double bonds is observed [37].

Also for the Wittig reaction, the product may be formed as a mixture of *Z*- and *E*-isomers, but each of these may be improved by applying appropriate reaction conditions. Studies on modifications on the Horner–Wadsworth–Emmons reaction done by Still and Gennari [38] and Ando [39] have resulted in improved *Z*-selective reactions. As of today, these reactions are limited to phosphonate esters.

Raphael and Sondheimer reported in 1950 the synthesis of linoleic acid (**4**) [40]. This was the first PUFA to be synthesized (Scheme 3.8). The acetylide of alkyne **31** was alkylated with mesylate **32**, which provided iodide **33** after a Finkelstein reaction. Iodide **33** was used to alkylate diethyl malonate and afford diyne acid **34** after hydrolysis and decarboxylation. Then, semi-reduction of the diyne provided linoleic acid (**4**).

In 1959, Osbond and coworkers synthesized arachidonic acid (**8**) based on iterative use of propargyl alcohol [41]. This synthetic protocol is considered as a general route to synthesize methylene-interrupted PUFAs (Scheme 3.9) [42]. Copper promoted acetylide alkylation of propargyl alcohol (**36**) with propargylic bromide **35** afforded diyne **37** after bromination of the resulting alcohol. Two more sequences of copper promoted alkylation gave tetrayne **40**, which was reduced with Lindlar's catalyst to give arachidonic acid (**8**).

EPA (**6**) was synthesized by Sandri and Viala by employing the acetal protected C-3 Wittig reagent **41** [43]; see Scheme 3.10. They also prepared DHA (**7**) by a similar strategy. A Wittig reaction between the C-3 homologating




**SCHEME 3.10** Synthesis of eicosapentaenoic acid (**6**) by Sandri and Viala [43].

agent **41** and aldehyde **42** afforded compound **43** that was deprotected and reduced by sodium borohydride to yield hydroxy ester **44**. Bromination and subsequent treatment with triphenylphosphine afforded the phosphonium salt **45**. The aldehyde **49** was synthesized by a Wittig reaction between aldehyde **46** and the ylide of phosphonium bromide **47**, followed by subsequent hydrolysis of the resulting acetal **48**. Finally, aldehyde **49** was converted in a Wittig reaction with phosphonium salt **45**, affording the methyl ester of EPA (**6**) with the correct all *Z*-double bonds. Saponification then produced EPA (**6**).

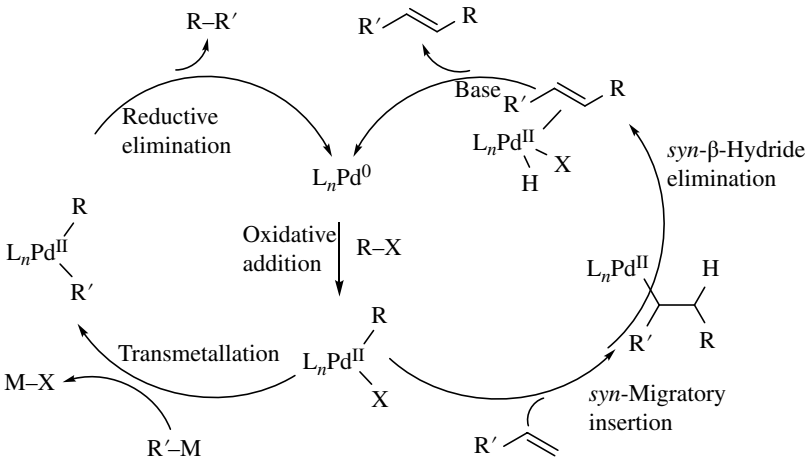
### 3.3.2 Synthesis of Polyunsaturated Fatty Acids via Cross Coupling Reactions

Palladium-catalyzed cross coupling of an organometallic compound with an organic electrophile for the formation of a C–C bond has emerged as one of the most general and selective methods for carbon–carbon bond formation. These reactions have become central tools for the synthesis of biologically active compounds both in academia [44] and in industry [45]. As a recognition of this, the Nobel Prize in Chemistry 2010 was jointly awarded to Professors Richard F. Heck, Ei-ichi Negishi, and Akira Suzuki "for palladium-catalyzed cross couplings in organic synthesis" [46]. Given the unsaturated nature of PUFAs and their derivatives, it should come as no surprise that cross coupling reactions often have been featured in their total synthesis.

The palladium-catalyzed cross coupling reactions can be divided into two general types depending on the nucleophilic coupling partner. Both types of the reactions employ an organohalide or pseudohalide as the electrophilic coupling partner. The accepted general mechanisms are depicted in Scheme 3.11 [47].

The oxidative addition of the organo halide (R–X) to the $Pd^0$ species is the first step in the catalytic cycle for both types of reactions. This step is often the rate-determining step. For reactions employing an organometal (R′–M) as the nucleophilic coupling partner, the oxidative addition is followed by transmetallation of the organometal (R′–M) to the $Pd^{II}$ intermediate containing both coupling partners. Subsequent reductive elimination provides the product (R–R′) and regeneration of the $Pd^0$ species. In reactions involving an alkene as the nucleophilic coupling partner, like in the Heck reaction, the oxidative addition is followed by the coordination of the alkene to the $Pd^{II}$ species, followed by *syn* migratory insertion. The formed organopalladium species then undergoes *syn*-β-hydride elimination to form the alkene and regenerate the $Pd^0$ species.

The catalytic $Pd^0$ species is often formed *in situ* using a palladium(II) source, such as $Pd(OAc)_2$ or $Pd(PPh_3)_2Cl_2$, and the necessary ligand. It can also be added as a preformed catalyst, like $Pd(PPh_3)_4$. Previously, most catalyst for cross coupling reactions employed triarylphosphine ligands. More recently, new bulky and electron-rich phosphine ligands that can improve the efficiency of sluggish cross coupling




**SCHEME 3.11** General catalytic cycles for palladium-catalyzed cross coupling reactions.

$$\text{R–X} \quad + \quad (\text{Y})_2\text{B–R}' \xrightarrow[\text{base}]{\text{Pd cat.}} \text{R–R}' \quad + \quad \text{X–B(Y)}_2$$

R = alkenyl, aryl, alkyl; R′ = alkyl, allyl, alkenyl, alkynyl, aryl

X = Cl, Br, I, OTf

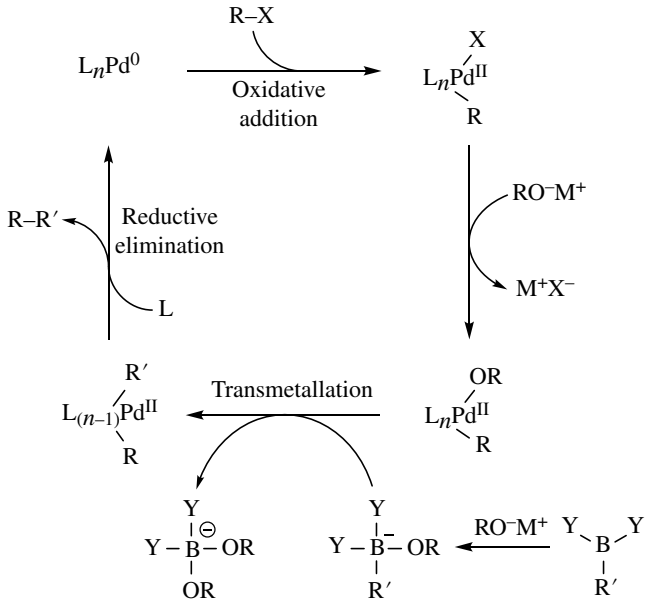
**FIGURE 3.6** The Suzuki cross coupling reaction.

reactions have been developed [48]. Many of these are now commercially available. Electron-donating ligands accelerate the oxidative addition step by increasing electron density around the metal. Bulky ligands may accelerate the elimination step. These new ligands have expanded the scope of substrates that can participate in cross coupling reactions.

The vast majority of the PUFA total synthesis employing palladium-catalyzed cross coupling reactions take advantage of either the Suzuki or the Sonogashira reactions. Therefore, the focus of this chapter will be on these two cross coupling reactions.

***3.3.2.1 The Suzuki Cross Coupling Reaction*** The Suzuki cross coupling reaction (Fig. 3.6) [49, 50], also known as the Suzuki–Miyaura cross coupling reaction, is an attractive strategy for PUFA synthesis as the coupling of alkenylboron compounds with alkenyl halides or triflates provides $sp^2$–$sp^2$ bonds stereoselectively.

The mild conditions of the reaction make it tolerant of a wide range of functional groups and can also be performed in the presence of water. Furthermore, many of the polar by-products are easily removed from the reaction mixture, and the boronic acids are substantially less toxic than organometallic reagents such as the organotin compounds used in the Stille cross coupling reaction. The boronic acids can be prepared by several approaches [51]. Most are based on the reaction of trialkylborates with Grignard or organolithium




**SCHEME 3.12** Mechanism of the Suzuki cross coupling reaction.

reagents, or by hydroboration of alkenes and alkynes. However, many boronic acids are today commercially available.

The mechanism for the Suzuki cross coupling reaction is believed to follow a sequence as depicted in Scheme 3.12 [52]. First, oxidative addition of the organohalide (R–X) generates a palladium(II) halide intermediate. Next, the anion attached to the palladium is exchanged for the anion of the base, followed by transmetallation with the alkylborate complex. The base will facilitate the otherwise slow transmetallation of the boronic acid by forming the more reactive negatively charged borate species. Finally, reductive elimination forms the C–C sigma bond and regenerates the $Pd^0$ species. No general rule for the selection of base has been

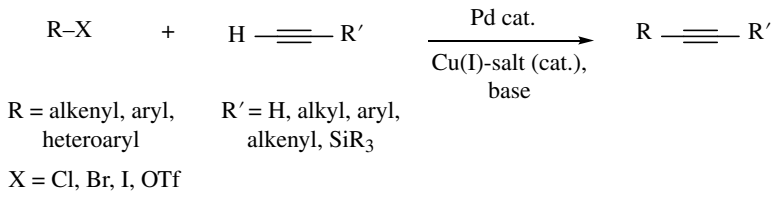
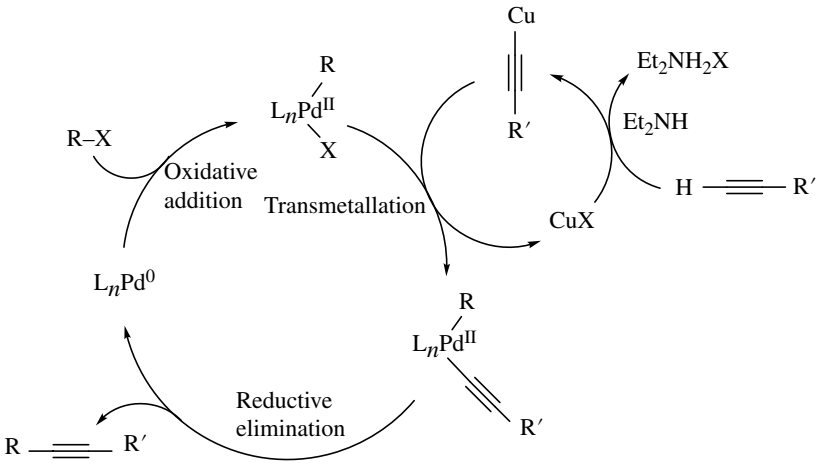



**FIGURE 3.7** The Sonogashira cross coupling reaction.




**SCHEME 3.13** Mechanism for the Sonogashira cross coupling reaction using diethylamine as base.

established, but the bases most commonly used are salts of carbonic acid or $K_3PO_4$.

In general, sterically hindered substrates and electron-rich aryl chlorides react sluggishly in the Suzuki cross coupling reaction. However, most of these problems can be overcome by taking advantage of the many new catalysts and ligands that have been developed for such Suzuki cross coupling reactions over the years [48, 53–55]. Suzuki cross coupling reactions where the halide is $sp^3$-hybridized are usually unsuccessful, most likely due to β-hydride elimination. But there have been some interesting developments in alkyl–alkyl Suzuki cross coupling reactions the last two decades [55, 56].

***3.3.2.2 The Sonogashira Cross Coupling Reaction*** The copper–palladium-catalyzed coupling of terminal alkynes with vinyl or aryl halides to give enynes is known as the Sonogashira cross coupling reaction (Fig. 3.7) [57]. Selective reduction of the conjugated triple bond in the resulting enyne provides an important alternative to the Suzuki reaction for the synthesis of polyene systems, and the Sonogashira reaction is therefore an attractive strategy in PUFA syntheses.

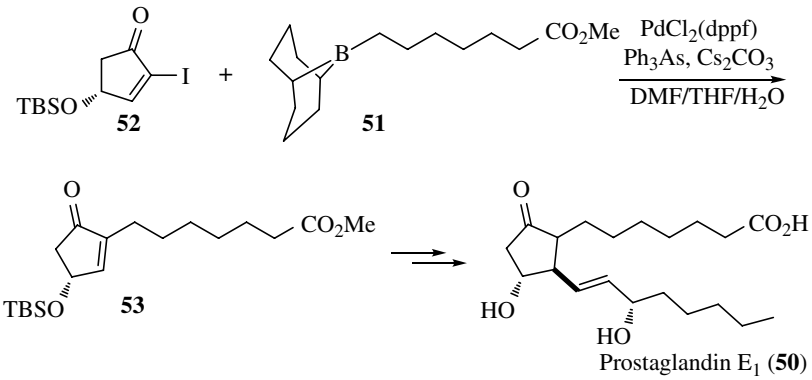
The Sonogashira reaction is believed to take place through two independent cycles: the palladium cycle and the copper cycle, as depicted in Scheme 3.13 [58, 59]. The Sonogashira reaction commences with the oxidative addition of the vinyl or aryl halide (R–X) to the $Pd^0$ species, followed by transmetallation by the copper(I) acetylide. Reductive elimination then affords the coupled product and regeneration of the catalyst.

The process is normally conducted at room temperature with the base serving as the solvent, but cosolvents are frequently used. The solvents and reagents do not need extensive drying, but deoxygenation of the solvent should be performed to avoid oxidation of Cu(I) to Cu(II), which will increase homocoupling of the alkyne. Usually, the base is a secondary or tertiary amine, like diethylamine or triethylamine, and the copper(I) catalyst is usually CuI added in 0.5–5 mol%. The most frequently encountered palladium catalysts in the Sonogashira reactions are $Pd(PPh_3)_2Cl_2$ and $Pd(PPh_3)_4$, but catalysts with bidentate ligands, like Pd(dppe)$Cl_2$, are sometimes also employed. A good functional group tolerance makes the Sonogashira reaction attractive in the later stages of total synthesis of sensitive PUFAs.

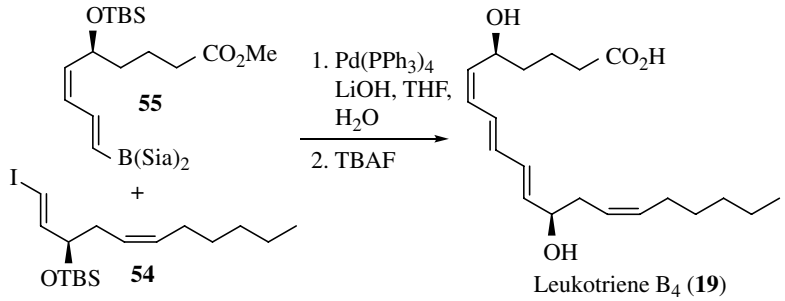
## 3.4 APPLICATIONS IN TOTAL SYNTHESIS OF POLYUNSATURATED FATTY ACIDS

### 3.4.1 Palladium-Catalyzed Cross Coupling Reactions

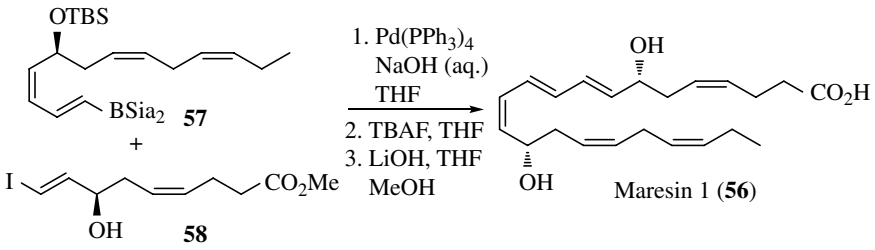
To the best of our knowledge, the first example of a Suzuki coupling reaction in the synthesis of a PUFA-derived natural product was disclosed in the synthesis of prostaglandin $E_1$




**SCHEME 3.14** Synthesis of prostaglandin $E_1$ (**50**) by Johnson and Braun [60].




**SCHEME 3.15** Synthesis of leukotriene $B_4$ (**19**) by Kobayashi and coworkers [61].



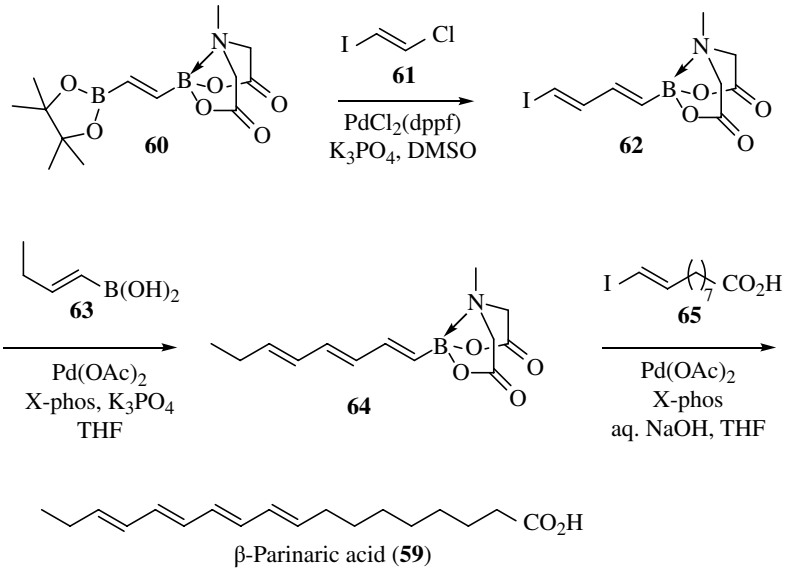

**SCHEME 3.16** Synthesis of maresin 1 (**56**) by Kobayashi and coworkers [62].

(**50**) by Johnson and Braun in 1993 (Scheme 3.14) [60]. Boron compound **51**, derived from hydroboration of methyl 6-heptanoate with 9-BBN, was coupled with vinyl iodide **52** to afford fragment **53** in good yield. Bis(diphenylphosphino) ferrocene palladium(II) chloride was used as precatalyst, with triphenylarsene serving as coligand. Interestingly, the presence of water was absolutely necessary for this cross coupling reaction to occur. The second side chain of prostaglandin $E_1$ (**50**) was introduced by conjugate addition chemistry using an *E*-vinylstannane.

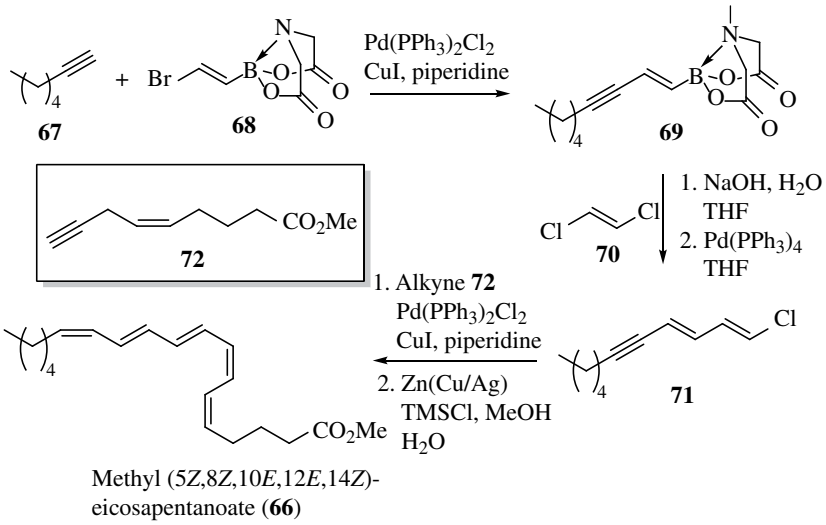
The Kobayashi group has frequently applied the Suzuki cross coupling reaction in several syntheses of oxygenated PUFAs. In their synthesis of leukotriene $B_4$ (**19**) [61], vinyliodide **54** was coupled with borane **55** under basic conditions to provide leukotriene $B_4$ (**19**) after deprotection of the silyl groups (Scheme 3.15).

The same group applied a very similar strategy for their synthesis of maresin 1 (**56**) (Scheme 3.16) [62]. Vinylborane **57** was reacted in a Suzuki cross coupling reaction with vinyliodide **58** to provide the complete carbon skeleton of maresin 1 (**56**). Deprotection and hydrolysis then produced maresin 1 (**56**). This DHA-derived natural product has been reported to exhibit several interesting biological effects *in vitro* and *in vivo*. For example, maresin 1 (**56**) regulates inflammation resolution and tissue regeneration and relieves lung injury in mice [63].

The MIDA-protected boronate esters developed by Burke and coworkers allow iterative Suzuki cross coupling reactions under mild conditions to give polyenes [64, 65]. The MIDA-protected boronate esters are stable and easily handled, and deprotection occurs readily at room temperature under mild basic conditions to provide the corresponding boronic acids.



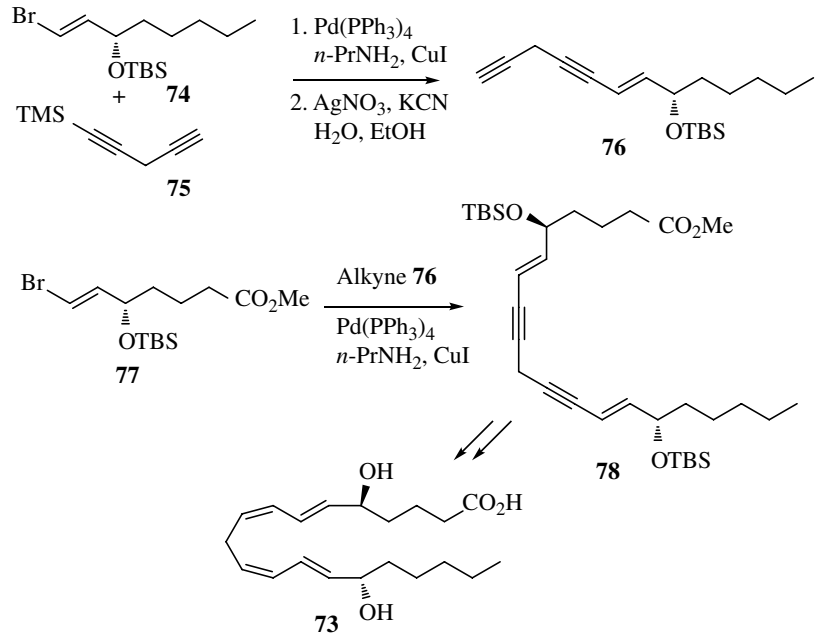

**SCHEME 3.17** Synthesis of β-parinaric acid (**59**) by Burke and coworkers[66].



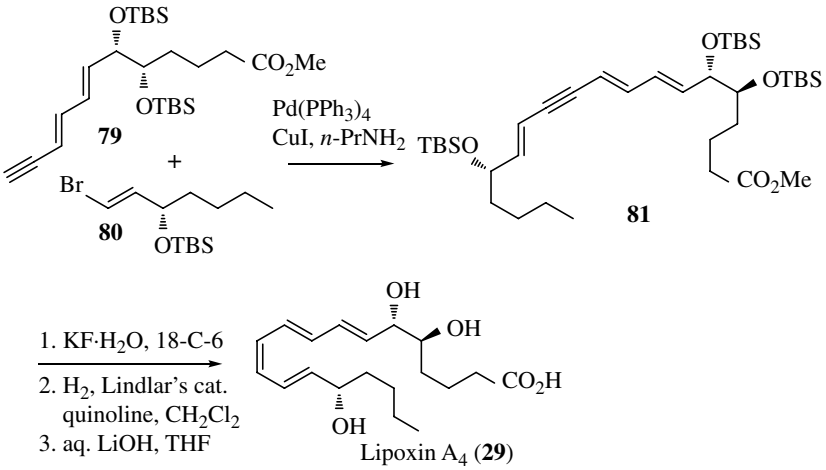

**SCHEME 3.18** Synthesis of methyl (5*Z*,8*Z*,10*E*,12*E*,14*Z*)-eicosapentanoate (**66**) by Hansen and Mohammed [67].

A large number of MIDA-protected boronate esters are now commercially available [66]. Burke and coworkers have demonstrated the use of the MIDA-protected boronates in modular syntheses of several polyene natural products, including the conjugated PUFA β-parinaric acid (**59**), which was synthesized in only three steps as shown in Scheme 3.17 [64]. The MIDA-protected boronate ester **60** was reacted in a Suzuki coupling reaction with vinyl chloride **61** to afford the conjugated vinyl iodide **62**. An additional Suzuki coupling with boronic acid **63** provided the MIDA-protected boronate ester **64**. This was hydrolyzed *in situ* and reacted in a final Suzuki coupling with vinyl iodide **65** to afford β-parinaric acid (**59**). This provided a highly stereoselective and efficient synthesis of β-parinaric acid (**59**).

Hansen and Mohammed prepared the natural product methyl (5*Z*,8*Z*,10*E*,12*E*,14*Z*)-eicosapentanoate (**66**) in seven steps using MIDA-boronate **48** as one of the key starting materials (Scheme 3.18) [67]. The terminal alkyne **67** was reacted with commercially available MIDA-protected boronate ester **68** in a Sonogashira cross coupling reaction to afford compound **69** in high yield. Then, basic aqueous hydrolysis of the MIDA-protected boronate ester in **69** afforded the corresponding boronic acid that, without isolation, reacted in a Suzuki cross coupling reaction with *trans*-1,2-dichloroethene (**70**) to afford vinyl chloride **71**. Finally, a Sonogashira cross coupling reaction of vinyl chloride **71** with alkyne **72** followed by a Boland reduction [68] of the internal alkyne provided the natural product **66**.



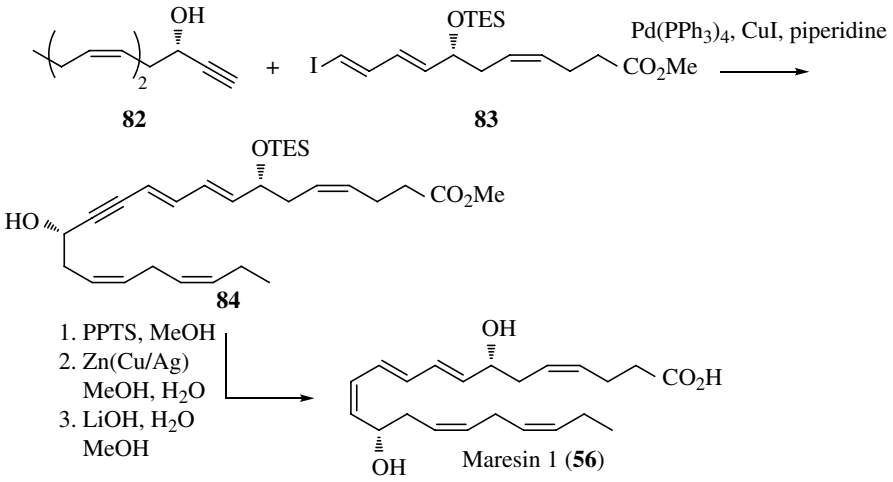

**SCHEME 3.19** Synthesis of (5*S*,15*S*)-dihydroxy-6,13-*trans*-8,11-*cis*-eicosatetraenoic acid (**73**) by Nicolaou and Webber [69].



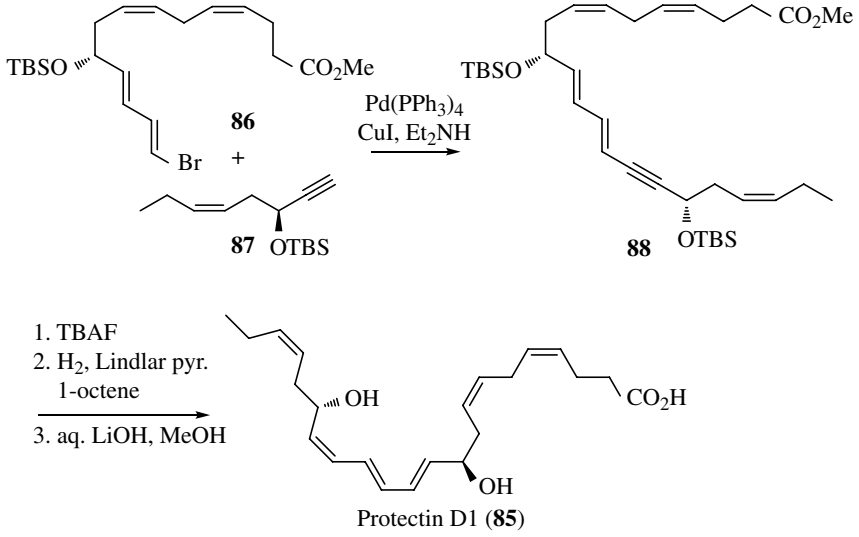

**SCHEME 3.20** Synthesis of lipoxin $A_4$ (**29**) by Nicolaou and coworkers [70].

Some of the first applications of the Sonogashira cross coupling reaction in total synthesis were indeed related to PUFA syntheses. One illustrative examples is Nicolaou and Webber's synthesis of (5*S*,15*S*)-dihydroxy-6,13-*trans*-8,11-*cis*-eicosatetraenoic acid (**73**) [69], an important oxygenated product of arachidonic acid (**8**), where two Sonogashira cross coupling reactions were featured (Scheme 3.19). In the first Sonogashira reaction, vinyl bromide **74** was coupled with terminal alkyne **75** to provide compound **76** after removal of the TMS group. Alkyne **76** was then reacted in a second Sonogashira cross coupling reaction with vinyl bromide **77**, affording ester **78** as a single geometric isomer in good yield. Then, desilylation, semireduction of the alkynes, and subsequent hydrolysis produced the target compound **73**.

Shortly after, Nicolaou and coworkers disclosed the first synthesis of lipoxin $A_4$ (**29**) along with several stereoisomers, where the two key fragments **79** and **80** were joined in a Sonogashira cross coupling reaction, furnishing compound **81**, containing the complete carbon skeleton of lipoxin $A_4$ (**29**), in excellent yield (Scheme 3.20) [70]. Removal of the silyl groups followed by a Lindlar reduction and subsequent hydrolysis produced lipoxin $A_4$ (**29**). At this time, the stereochemistry at the C-5 and C-6 atoms, as well as the configuration of the $\Delta^{11}$-double bond, had not been determined. With the synthesis of these isomers, the absolute configuration of




**SCHEME 3.21** Synthesis of maresin 1(**56**) by Spur and Rodriguez [72].




**SCHEME 3.22** Synthesis of protectin D1 (**85**) by Hansen and coworkers [73].

lipoxin $A_4$ (**29**) could be established by comparison with authentic material [71].

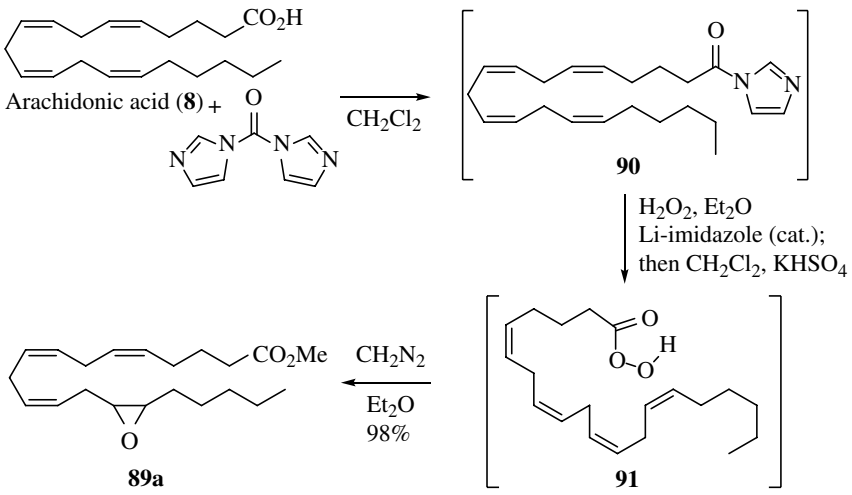
More recent applications of the Sonogashira reaction in PUFA synthesis include Spurs and Rodriguez's synthesis of maresin 1 (**56**) [72], a potent anti-inflammatory lipid mediator derived from DHA (**7**). As shown in Scheme 3.21, the Sonogashira cross coupling reaction of alkyne **82**, bearing an unprotected secondary alcohol, with vinyl iodide **83**, provided compound **84**. Then, removal of the TES group, Boland reduction of the triple bond, and subsequent hydrolysis of the methyl ester afforded maresin 1 (**56**).

In a synthesis of the anti-inflammatory lipid mediator protectin D1 (**85**) by Hansen and coworkers [73], the Sonogashira cross coupling reaction between vinyl bromide **86** and alkyne **87** played a crucial role in the late stage of this convergent total synthesis, affording compound **88** bearing the complete carbon skeleton of protectin D1 (**85**) (Scheme 3.22). Protectin D1 (**85**) was obtained after deprotection of the silyl groups, a modified Lidlar reduction [74] of the alkyne and subsequent hydrolysis. The synthetic material was matched with endogenously produced material.

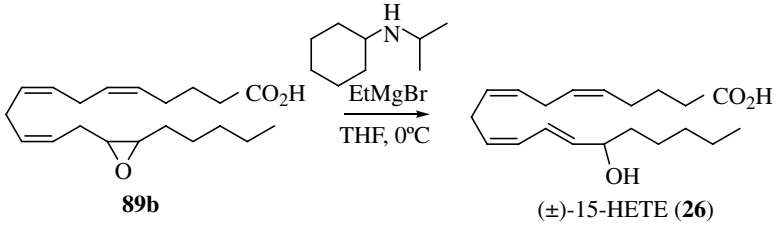
### 3.4.2 Biomimetic Transformations of Polyunsaturated Fatty Acids

PUFAs can be used in their own right as starting material for the semisynthesis of more complex members of the PUFA family. A particular advantage using this approach is the conservation of the methylene-interrupted double bonds throughout the synthesis and to be present in the final product.

Corey and coworkers devised a highly selective internal epoxidation of arachidonic acid (**8**) to afford epoxy methyl




**SCHEME 3.23** Corey's selective internal epoxidation of arachidonic acid (**8**) [75].



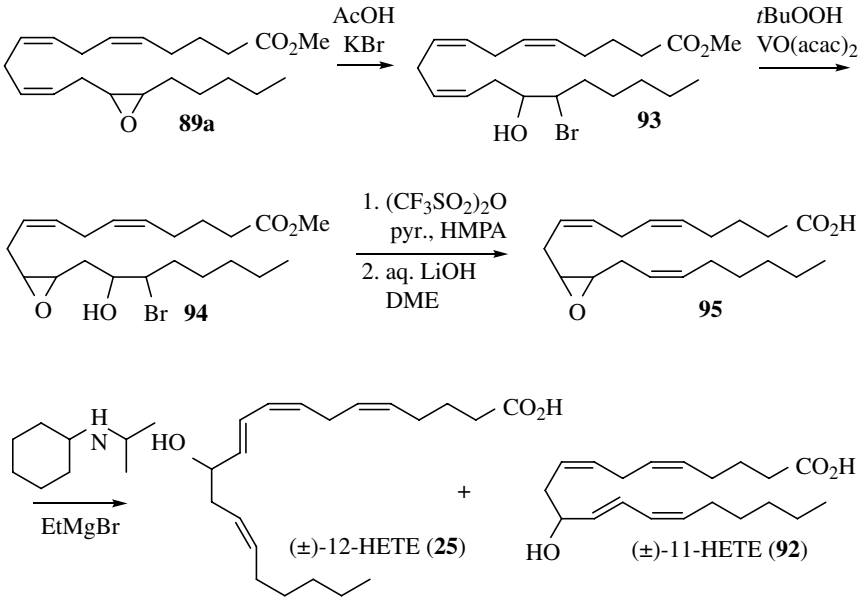

**SCHEME 3.24** Synthesis of (±)-15-HETE (**26**) [76].

ester **89**; see Scheme 3.23 [75]. Treatment of arachidonyl imidazole **90** with hydrogen peroxide in the presence of a base as catalyst provided the peroxy acid **91**, which upon standing gradually transformed into the $\Delta^{14,15}$ epoxy acid. Treatment with diazomethane provided the epoxy methyl ester **89a** in 98% yield from arachidonic acid (**8**). The remarkable selectivity was explained by an energetically favorable 15-membered cyclic structure, which allows the internal epoxidation to occur with high selectivity on the $\Delta^{14,15}$ position.

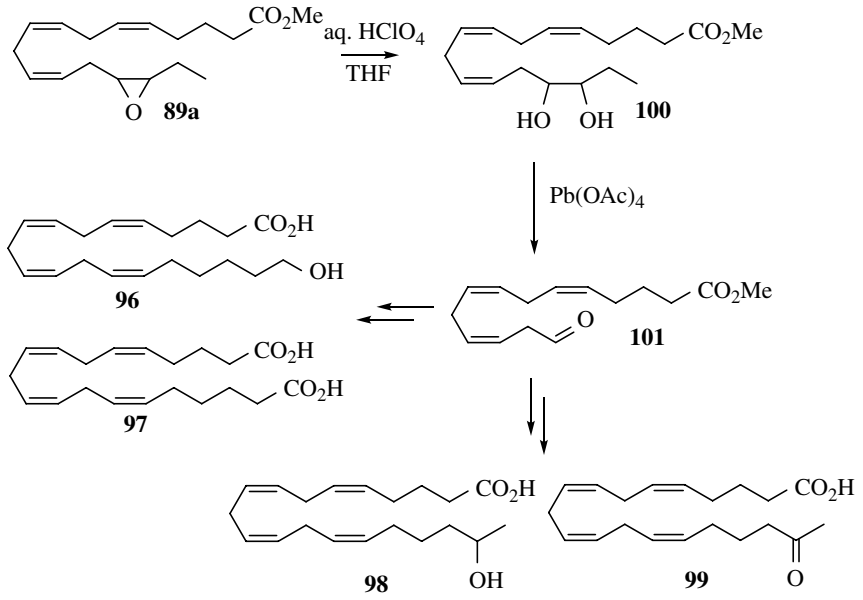
In the following years, epoxy ester **89a** was used as a key starting material for the synthesis of a number of metabolites of arachidonic acid (**8**) and analogs. Of particular interest is Corey's synthesis of (±)-11-HETE (**92**), (±)-12-HETE (**25**), (±)-15-HETE (**26**), and their corresponding peroxides published in 1980 [76]. (±)-15-HETE (**26**) was obtained in 70% yield in one step by reaction of the corresponding acid **89b** of epoxy methyl ester **89a** with excess of isopropyl cyclohexylamine and ethylmagnesium bromide (Scheme 3.24).

The synthesis of the (±)-11-HETE (**92**), (±)-12-HETE (**25**) began by treating epoxide **89b** with acetic acid and saturated aqueous KBr in THF to afford a mixture of bromohydrin **93** and its regioisomer (14-bromo, 15-hydroxy) in 95% yield in a 2:1 ratio, respectively (Scheme 3.25). Oxidation using *tert*-butyl hydroperoxide in the presence of vanadyl acetylacetonate afforded epoxy bromohydrin **94**, leaving the positional isomer mainly unchanged and easily separated by chromatography and recycled back to epoxy ester **89a** by base. The elimination of hydroxyl and bromine in **94** proved troublesome at first, but the issue was resolved using trifluoromethanesulfonic anhydride in a solution with bromohydrin **94** in pyridine/THF, followed by addition of HMPA. This provided epoxy acid **95** after saponification. The epoxy acid **95** was then treated with the reagent prepared from isopropyl cyclohexylamine and ethylmagnesium bromide to produce a mixture of (±)-11-HETE (**92**) and (±)-12-HETE (**25**) in a 1:1.5 ratio, respectively, which could be separated by chromatography. The corresponding hydroperoxy compounds were obtained by mesylation of the corresponding HETE esters followed by treatment with hydrogen peroxide at low temperature and subsequent saponification.

The compounds **96–99**, shown in Scheme 3.26, are all metabolites of arachidonic acid (**8**) produced in a NADPH-dependent cytochrome P-450-meditated oxidative pathways. Falck and coworkers [77] prepared these from Corey's epoxide methyl ester **89a** as shown in Scheme 3.26. Hydrolysis of the epoxide ester **89a** using perchloric acid, followed by oxidative cleavage of the resulting diol **100**, provided aldehyde **101**. Next, a Wittig reaction with aldehyde **101** followed by Jones oxidation and/or saponification



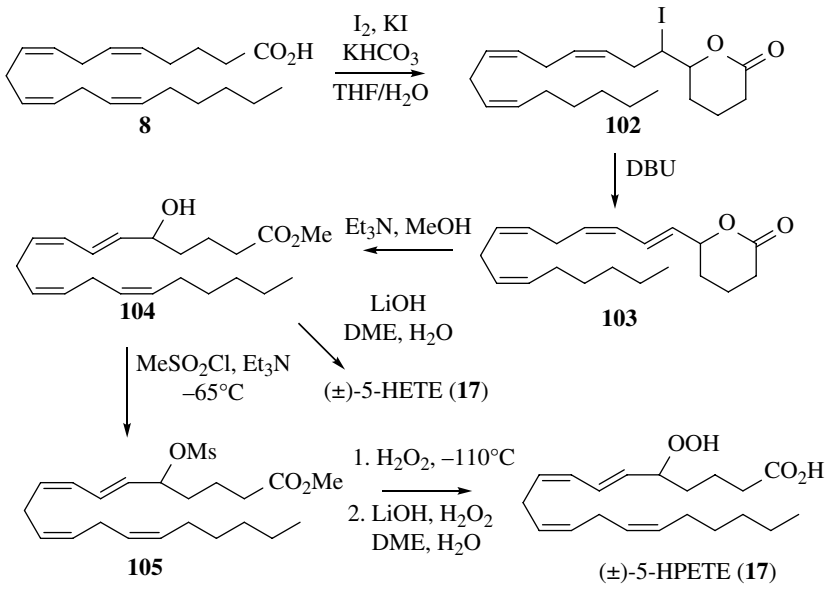

**SCHEME 3.25** Synthesis of (±)-12-HETE (**25**) (±)-11-HETE (**92**) [76].



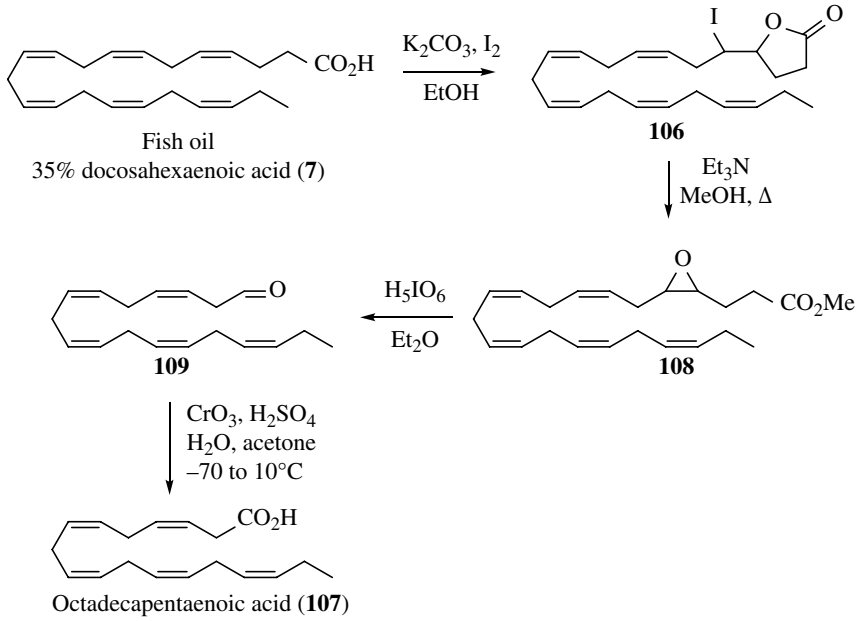

**SCHEME 3.26** Synthesis of the four metabolites **96–99** of arachidonic acid (**8**) [77].

provided the four metabolites **96–99**. Corey has also used aldehyde **101** in the syntheses of some dehydroarachidonic acid derivatives in order to study the mechanism of the formation of 15-HPETE (**16**, Scheme 3.5) [78] but also as the key building block in a synthesis of the macrolactone of 20-hydroxyarachidonic acid [79]. This enabled further studies of the conformational mobility of arachidonic acid (**8**).

In 1980, Corey and coworkers published a synthesis of racemic (±)-5-HETE (**23**) and (±)-5-HPETE (**17**) using arachidonic acid (**8**) as the starting material as shown in Scheme 3.27 [80]. Iodolactonization of arachidonic acid (**8**) provided iodolactone **102**, which upon treatment with the base 1,8-diazabicyclo[5.4.0]undec-7-ene (DBU) afforded the unsaturated lactone **103**. Basic methanolysis of lactone **103** produced hydroxy ester **104**, while aqueous hydrolysis provided the corresponding hydroxy acid, (±)-5-HETE (**23**). Mesylation of **104** afforded mesylate **105** that was treated with hydrogen peroxide at low temperature to afford (±)-5-HPETE (**17**) after hydrolysis. With a synthetic sample of racemic 5-HPETE (**17**) in hand as a reference, an enzymatic synthesis of (*S*)-5-HPETE (**17**) was achieved using a LOX from potato [80].



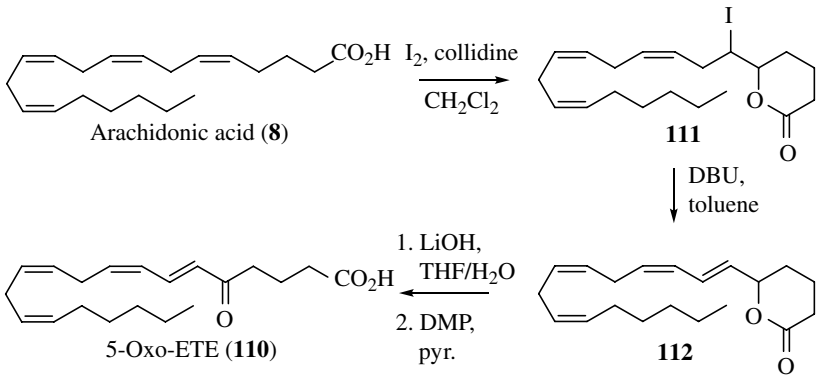

**SCHEME 3.27** Synthesis of 5-HPETE (**17**) [80].




**SCHEME 3.28** Kuklev and coworkers synthesis of all-*cis*-3,6,9,12,15-octadecapentaenoic acid (**107**) [82].

In 1987, Corey reported an effective process for the isolation of DHA (**7**) from fish oil containing a mixture of PUFAs by iodolactonization of **7**, forming the γ-lactone **106**, which could then be isolated and converted back to **7** [81]. Later, Kuklev and coworkers used fish oil containing 35% DHA (**7**) as the starting material for the synthesis of all-*cis*-3,6,9,12,15-octadecapentaenoic acid (**107**) [82], a PUFA isolated from the microalgae *Gymnodinium kowalevskii* (Scheme 3.28). Methanolysis of the iodolactone **106** under basic conditions afforded epoxy ester **108**, which could be cleaved with periodic acid to aldehyde **109**. Jones oxidation of aldehyde **109** then gave all-*cis*-3,6,9,12,15-octadecapentaenoic acid (**107**).

Ulven and coworkers reported a short synthesis of the anti-inflammatory mediator 5-oxo-ETE (**110**) from arachidonic acid (**8**) (Scheme 3.29) [83]. Iodolactonization on arachidonic acid (**8**) using $I_2$ and collidine in dichloromethane afforded iodolactone **111** in high and reproducible yields. Elimination of HI from iodolactone **111** with the base DBU afforded the conjugated lactone **112**. Hydrolysis and subsequent oxidation with Dess–Martin periodinane in the




**SCHEME 3.29** Synthesis of 5-oxo-ETE (**110**) by Ulven and coworkers [83].

presence of pyridine produced 5-oxo-ETE (**110**) in 70% overall yield from arachidonic acid (**8**).

### 3.4.3 Landmark Total Syntheses

Many of the free fatty acid-derived natural products are produced in microgram to nanogram amounts in biological systems. Hence, total synthesis becomes necessary for further biological studies. And, although an array of advanced spectroscopic methods today exist for the assignment of structures to molecules isolated from nature in submilligram quantities, chemical total synthesis still has important roles to play for structure elucidation [84].

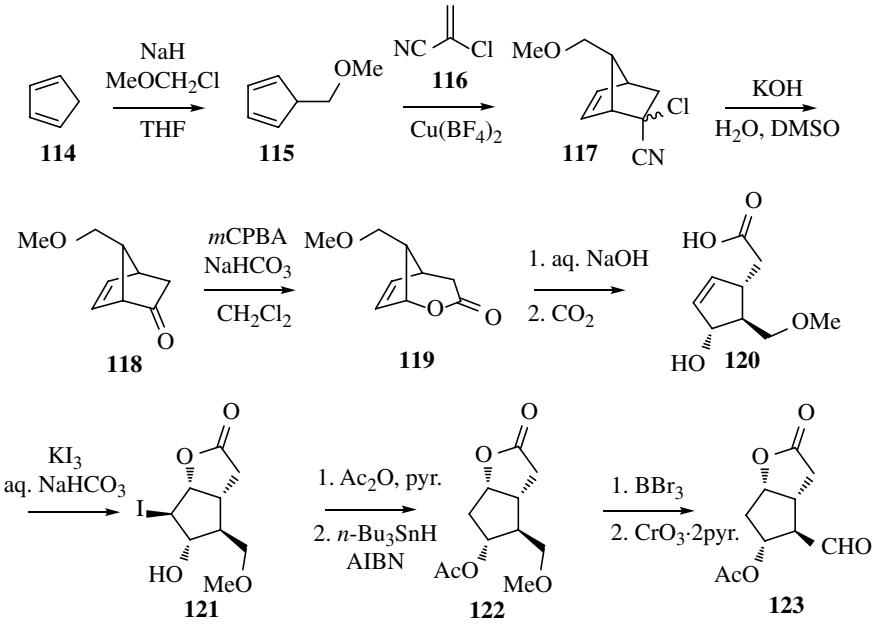
Of the syntheses already discussed in this chapter, the synthesis of linoleic acid (**4**) by Raphael and Sondheimer (Scheme 3.8) [40], and the synthesis of arachidonic acid (**8**) by Osbond (Scheme 3.8) [41], clearly stands out as landmark total syntheses of PUFAs. In the succeeding text, an outline of other total syntheses of PUFAs is given.

***3.4.3.1 Synthesis of Prostaglandins*** Von Euler and Goldblatt isolated independently in the 1930s prostanoic acid, which constitutes the common carbon skeleton found in the prostaglandins. These endogenous eicosanoids were coined prostaglandins to reflect their source of origin. After further research into this area, it soon became apparent that the prostaglandins were in fact a ubiquitous class of substances, found in nearly every nucleated cell, yet the misnomer has persisted. Further work was carried on by Bergström and Samuelsson in the 1960s. Together with Sir John R. Vane, who discovered aspirin's mode of action, these three scientists were jointly awarded the Nobel Prize in Physiology or Medicine in 1982 "for their discoveries concerning prostaglandins and related biologically active substances" [85]. It is now known that the prostaglandins are short-lived local lipid mediators synthesized from arachidonic acid (**8**) via COX enzymes. For a discussion of the biosynthesis of prostaglandins, see Section 3.2.3. Herein, we will limit our focus on four of several total synthesis of prostaglandin $F_{2\alpha}$ (**113**).

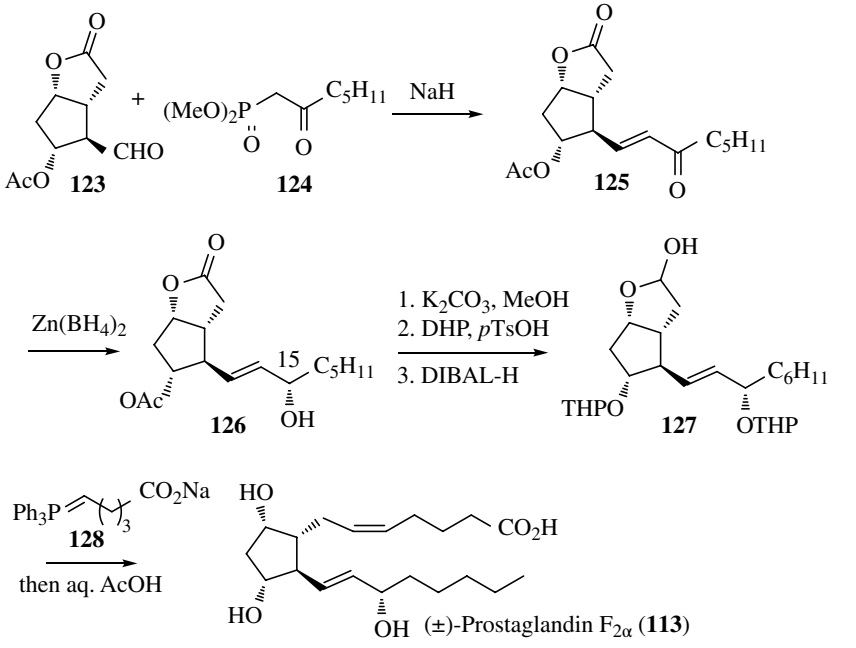
In 1969, Corey disclosed his landmark total synthesis of (±)-prostaglandin $F_{2\alpha}$ (**113**) [86]. Numerous improvements have since been disclosed, but here the original strategy will be discussed. Corey's diastereoselective synthesis of prostaglandin $F_{2\alpha}$ (**113**) begins with the alkylation of cyclopentadiene (**114**) with chloromethyl methyl ether to give the unstable diene **115**, which was immediately taken forward in a Diels–Alder reaction with ketene equivalent **116** in the presence of cupric tetrafluoroborate (Scheme 3.30). This yielded a racemic mixture of chloronitrile **117**. After treatment with potassium hydroxide on chloronitrile **117** in aqueous DMSO, hydrolysis of the chloronitrile moiety produced ketone **118** in high yields. Next, a regioselective Baeyer–Villiger oxidation provided lactone **119**. After saponification of the lactone and neutralization with carbon dioxide, the hydroxy acid **120** was obtained. The hydroxy acid **120** was then converted in an iodolactonization reaction with aqueous potassium triiodide to give iodolactone **121**. Acetylation of the hydroxyl group in **121**, followed by removal of the iodide using tri-*n*-butyltin hydride and a catalytic amount of AIBN, furnished the Corey lactone **122**. Cleavage of the methyl ether using boron tribromide and a subsequent Collins oxidation afforded aldehyde **123**.

Aldehyde **123** was then reacted in a stereoselective Horner–Wadsworth–Emmons reaction with the sodium salt of phosphonate **124** to produce enone **125** (Scheme 3.31). Chemo- and stereoselective reduction of enone **125** with zinc borohydride provided secondary alcohol **126** as a 1:1 mixture of C-15 epimers, which could be separated by chromatography. Next, solvolysis of the acetate in **126** with basic methanol was followed by protection of the two alcohols with dihydropyran in the presence of a catalytic amount of *para*-toluenesulfonic acid. Reduction with DIBAL-H then provided lactol **127**. Wittig reaction of **127** with the nonstabilized ylide **128** and subsequent deprotection produced (±)-prostaglandin $F_{2\alpha}$ (**113**).

Another noteworthy synthesis of prostaglandin $F_{2\alpha}$ (**113**) was reported by Stork and coworkers in 1986 [87]. The synthesis began with the conversion of cyclopentadiene (**114**) to



**SCHEME 3.30** The first steps in Corey's synthesis of (±)-prostaglandin $F_{2\alpha}$ (**113**) [86].

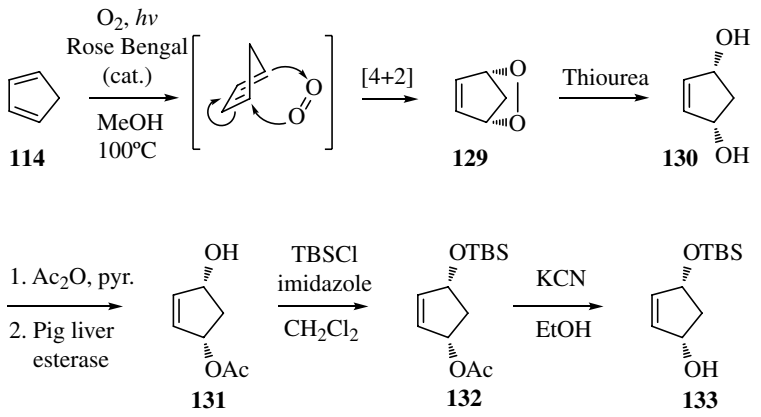


**SCHEME 3.31** The final steps in Corey's synthesis of (±)-prostaglandin $F_{2\alpha}$ (**113**) [86].

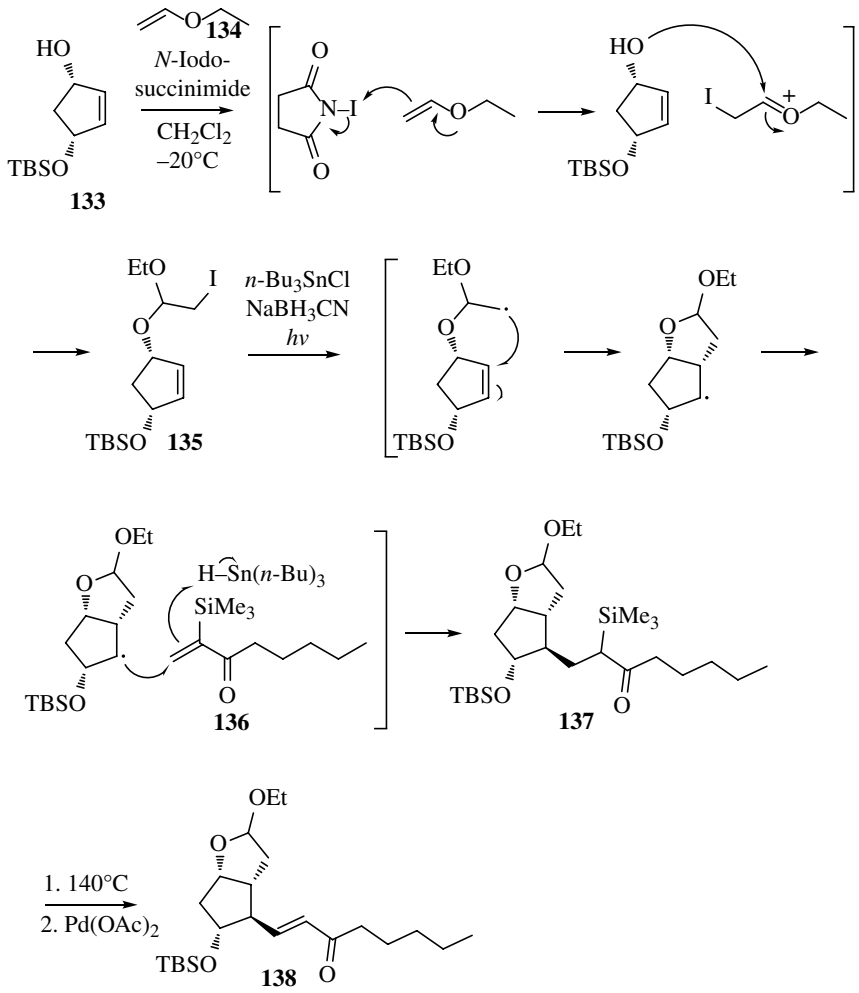
*cis*-4-cyclopentene-1,3-diol (**130**) by a photooxygen reduction using rose bengal as photosensitizer (Scheme 3.32). The diol **130** was converted into its corresponding diacetate, which was hydrolyzed into the monoacetate **131** using pig liver esterase. Then protection with TBS to **132** and subsequent cleavage of the remaining acetal provided alcohol **133**.

Next, alcohol **133** was treated with ethyl vinyl ether (**134**) and *N*-iodosuccinimide to yield the iodoacetal **135** as depicted in Scheme 3.33. The iodoacetal **135** was converted in an interesting radical cyclization–trapping reaction using light at 254 nm, tri-*n*-butyltin chloride, sodium cyanoborohydride, and a large excess of the conjugated ketone **136**. This provided the crude ketone **137**. Thermal rearrangement followed by Saegusa oxidation with palladium acetate led to key intermediate **138**.

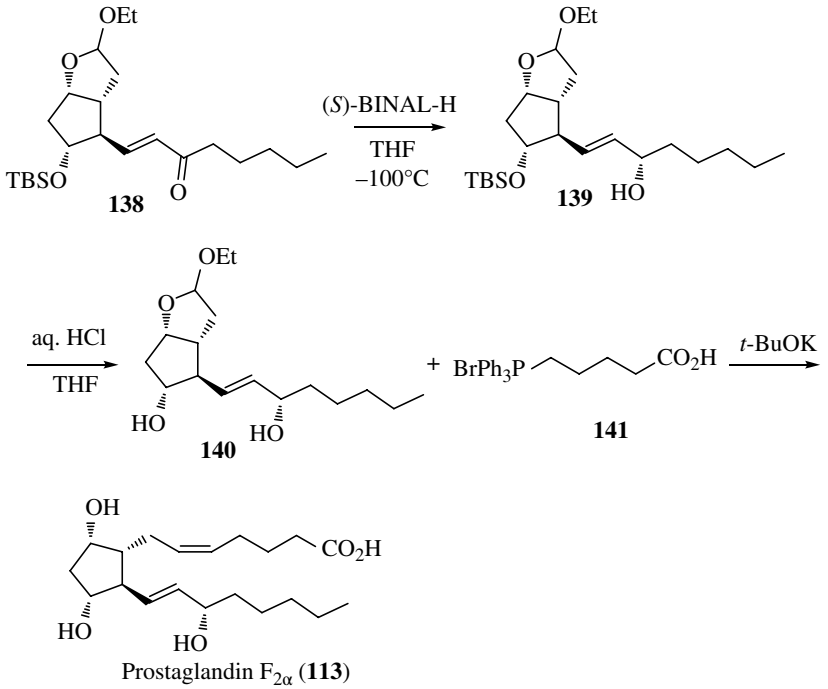
The conjugated ketone **138** was then reduced diastereoselectively with (*S*)-BINAL-H to the allylic alcohol **139** (Scheme 3.34). Hydrolysis with dilute aqueous hydrochloric acid in THF gave the lactone **140** that was converted in a



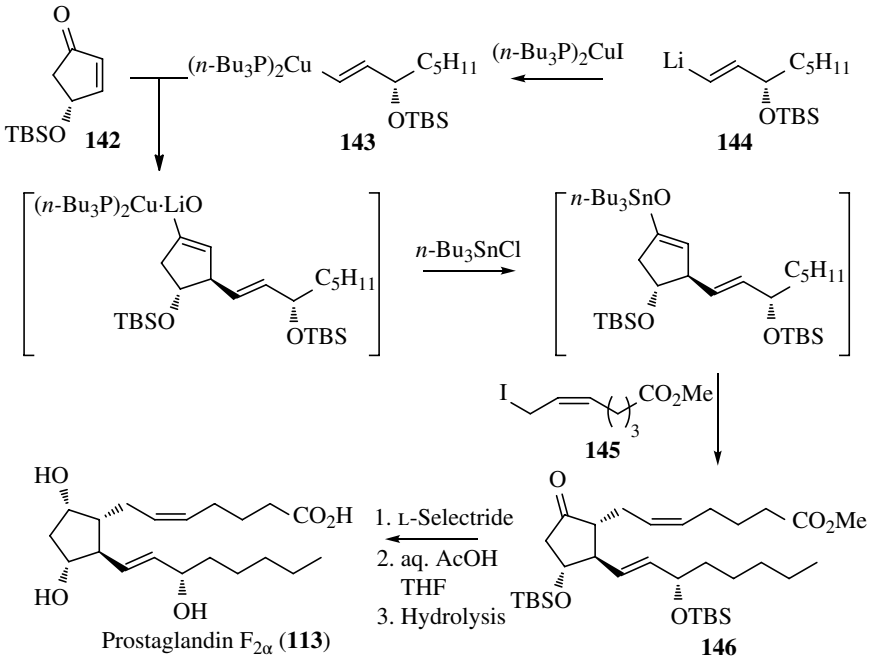

**SCHEME 3.32** Synthesis of alcohol **133** in Stork's synthesis of prostaglandin $F_{2\alpha}$ (**113**) [87].




**SCHEME 3.33** Synthesis of ketone **138** in the synthesis of prostaglandin $F_{2\alpha}$ (**113**) by Stork and coworkers [87].



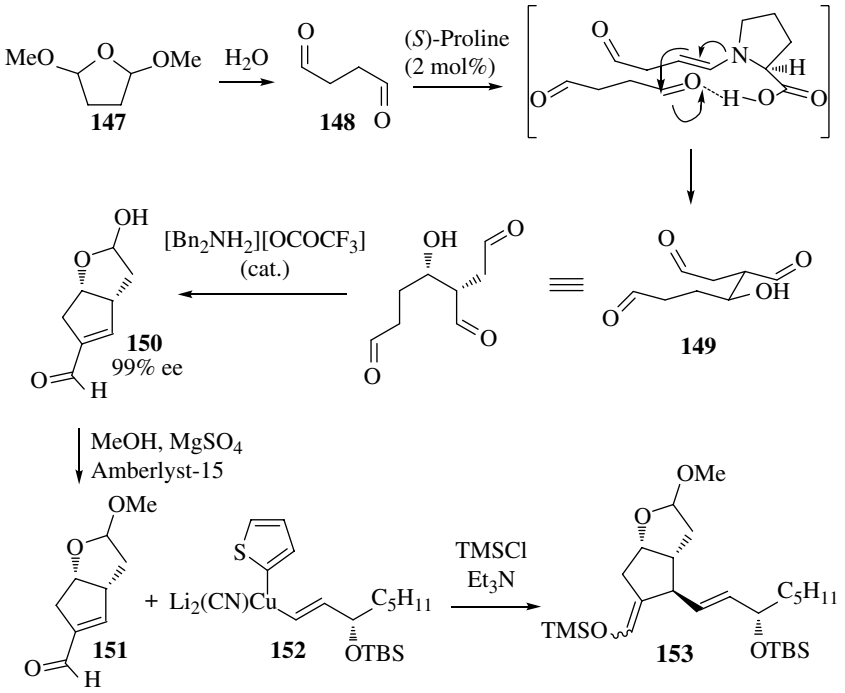

**SCHEME 3.34** The final steps in the synthesis of prostaglandin $F_{2\alpha}$ (**113**) by Stork and coworkers [87].



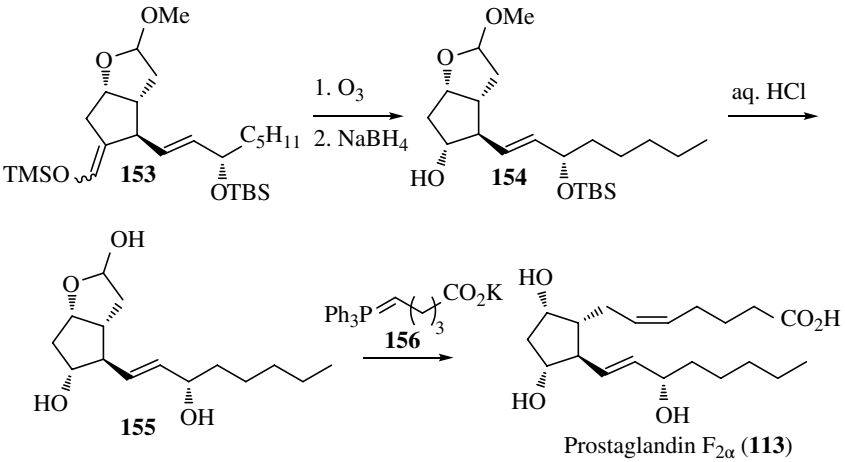

**SCHEME 3.35** The synthesis of prostaglandin $F_{2\alpha}$ (**113**) by Noyori and coworkers [88].

Wittig reaction with the ylide of phosphonium salt **141** to provide prostaglandin $F_{2\alpha}$ (**113**).

In 1988, Noyori and coworkers disclosed a convergent three-component coupling synthesis of prostaglandin $F_{2\alpha}$ (**113**) [88]. The whole prostaglandin framework was constructed in a one-pot reaction sequence (Scheme 3.35). An organocopper-mediated conjugate addition of **143** to protected cyclopentenone **142** was followed by trapping of the enolate species by alkyl halide **145** to afford compound **146**. Stereoselective reduction of the ketone in **146** using




**SCHEME 3.36** The first steps in the synthesis of prostaglandin $F_{2\alpha}$ (**113**) by Aggarwal and coworkers [89].

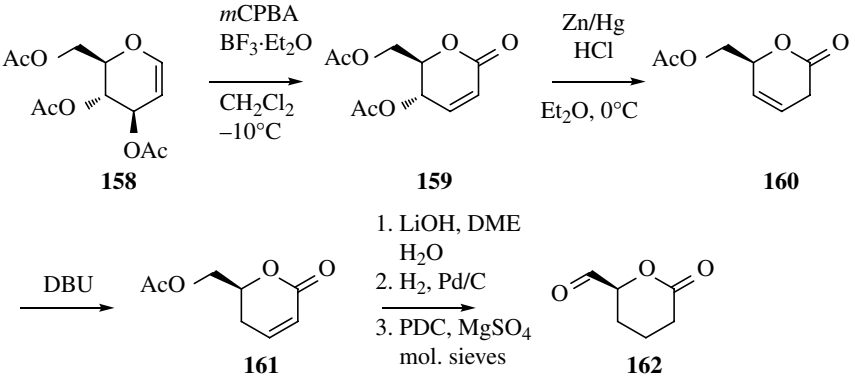



**SCHEME 3.37** The final steps in the synthesis of prostaglandin $F_{2\alpha}$ (**113**) by Aggarwal and coworkers [89].

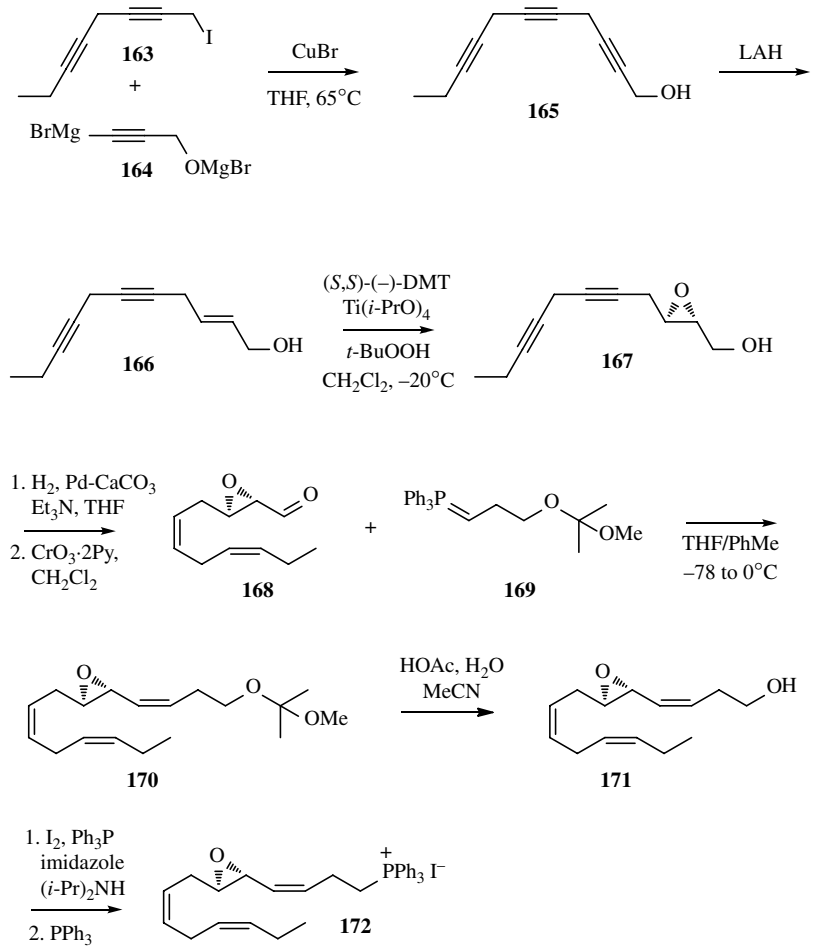
L-selectride established the secondary alcohol with the desired stereochemistry. Finally, deprotection and subsequent hydrolysis produced prostaglandin $F_{2\alpha}$ (**113**).

Even today, the prostaglandins remain interesting synthetic targets for organic chemists. The last major breakthrough in prostaglandin total synthesis was disclosed by Aggarwal and coworkers in 2012, where enantiomerically pure prostaglandin $F_{2\alpha}$ (**113**) was obtained in only seven steps (Scheme 3.36) [89]. Heating 2,5-dimethoxytetrahydrofuran (**147**) in water provided crude dialdehyde **148**, which was subjected to a cascade of two aldol reactions. The first aldol reaction was performed in the presence of a catalytic amount of (*S*)-proline. Then, subsequent addition of a second catalyst ($[Bn_2NH_2][OCOCF_3]$) achieved the second aldol reaction to afford the hemiacetal **150** in 99% ee and 14% yield from dialdehyde **148**. The hemiacetal **150** was then transformed to a diastereomeric mixture of methoxy acetals **151** using Amberlyst-15 and $MgSO_4$. Conjugate addition of the mixed vinyl cuprate **152** to methoxy acetal **151**, followed by trapping with trimethylsilyl chloride, furnished the silyl enol ether **153**.

The silyl enol ether **153** was then subjected to a controlled ozonolysis followed by a stereoselective reduction with sodium borohydride to give alcohol **154** (Scheme 3.37). Simultaneous cleavage of both protecting groups with aqueous HCl afforded diol **155**. Finally, a Wittig reaction with ylide **156** produced prostaglandin $F_{2\alpha}$ (**113**).




**SCHEME 3.38** Synthesis of aldehyde **162** in the synthesis of leukotriene $B_5$ (**157**) by Corey and coworkers [90].

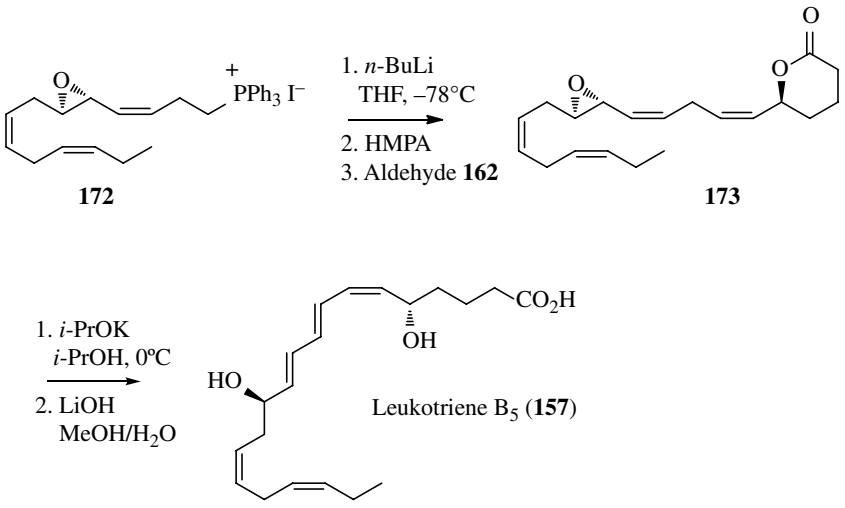



**SCHEME 3.39** Synthesis of phosphonium salt **172** in Corey's synthesis of leukotriene $B_5$ (**157**) [90].

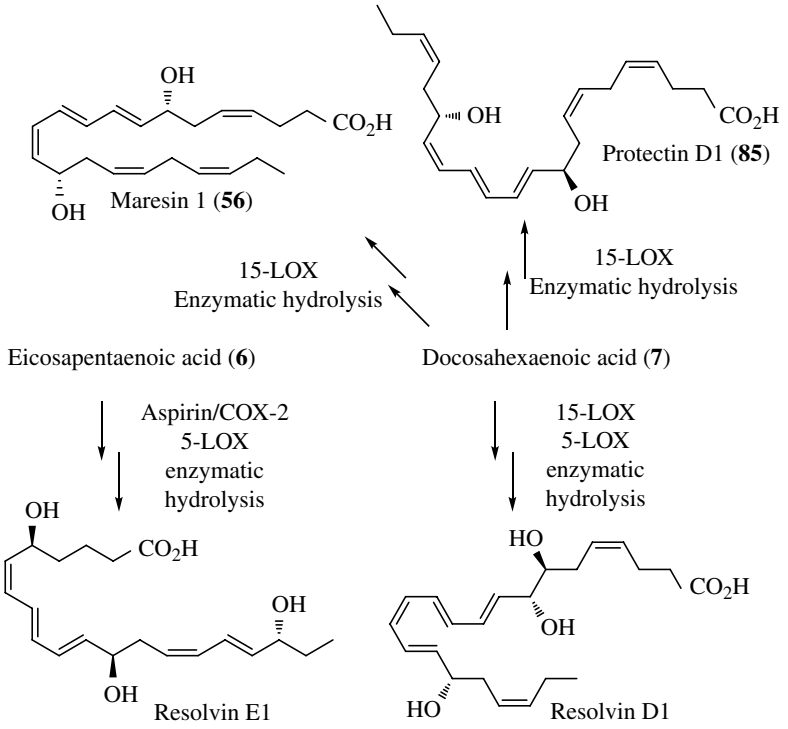
### 3.4.4 Synthesis of Leukotriene $B_5$

Leukotriene $B_5$ ($LTB_5$, **157**, Scheme 3.40) is formed in human neutrophils and is the 5-LOX product derived from EPA (**6**). Leukotriene $B_5$ (**157**) is less potent than leukotriene $B_4$ (**19**) as a chemotactic but also less active than leukotriene B4 (**19**) in increasing cytosolic free calcium ions.

In 1983, Corey and coworkers disclosed a stereocontrolled synthesis of $LTB_5$ (**157**) using commercial tri-*O*-acetyl-D-glucal (**158**) as a key starting material (Scheme 3.38) [90]. Oxidation of **158** with *meta*-chloroperoxybenzoic acid provided lactone **159**, which was converted into **160** using Zn(Hg) and HCl. Rearrangement of the double bond with 1,8-diazabicyclo[5.4.0]undec-7-ene (DBU) produced




**SCHEME 3.40** The final steps in the synthesis of leukotriene $B_5$ (**157**) by Corey and coworkers [90].




**SCHEME 3.41** A brief overview of the biosynthesis of the resolvins, maresins, and protectins [63].

conjugated lactone **161**. Hydrolysis of the acetate, reduction of the alkene, and subsequent oxidation of the resulting primary alcohol provided aldehyde **162**.

The second key building block, phosphonium salt **172**, was prepared as outlined in Scheme 3.39. Iodide **163** was reacted in a copper(I)-catalyzed alkylation with the bisbromomagnesium salt **164** to give triyne **165** in 90% yield. Reduction of the propargylic alcohol **165** to allylic alcohol **166** was achieved with lithium aluminum hydride (LAH), and then a Sharpless asymmetric epoxidation afforded epoxide **167** in 76% yield. Lindlar reduction, followed by oxidation with Collins reagent, yielded aldehyde **168**. A Wittig reaction of aldehyde **168** with the ylide **169** gave the homoallylic alcohol **171** after deprotection of **170** under acidic conditions. Alcohol **171** was converted into the corresponding iodide and reacted with triphenylphosphine to provide phosphonium salt **172**.

Wittig salt **172** was converted into the corresponding ylide with *n*-butyl lithium and reacted with aldehyde **162** in

THF/HMPA to give lactone **173**, along with minor amounts of the corresponding 6,7-*trans* isomer (Scheme 3.40). Exposure of **173** to potassium *iso*-propoxide in methanol followed by basic hydrolysis produced leukotriene $B_5$ (**157**) in 75% yield.

## 3.5 CONCLUSION

Advances in liquid chromatography and mass spectroscopy now enable analysis of more than 100 oxygenated fatty acid-derived natural products in one LC–MS/MS experiment [91]. These advances have provided us with new and biological interesting fatty acid-derived natural products. Some recent examples are resolvins, protectins, and maresins (Scheme 3.41), and the recent efforts by the Serhan group at Harvard Medical School, Brigham and Women's Hospital, have resulted in the identification of these oxygenated derivatives of EPA (**6**) and DHA (**7**) [92]. These derivatives have been named specialized proresolving mediators (SPMs). Among the many interesting biological effects reported for SPMs are that SPMs resolve inflammation, protect organs, stimulate homeostasis, and induce tissue regeneration [93]. These endogenously formed lipid products are biosynthesized mainly by LOXs but also by the action of COX-2. These classes of natural products have been covered in recent reviews [63, 92, 93].

These and other oxygenated fatty acid-derived natural products will provide opportunities in drug discovery for the development of new medicines for the benefit of mankind. Today, inhibitors targeting both the LOXs and the COXs exist. In the future, one can anticipate that new agonists toward these enzymes will also be developed, especially as agents involved in the resolution of inflammation. Such approaches have recently been highlighted [63].

## ACKNOWLEDGMENTS

Skillful technical assistance by Mr. Åsmund Kaupang, for the production of the protein structures, is sincerely acknowledged. We are grateful to the Research Council of Norway for financial support, and we want to thank Pronova BioPharma AS, and in particular Olav Thorstad, for generous donations of chemically pure EPA (**6**) and DHA (**7**).

## REFERENCES

1. F. D. Gunstone, *Fatty Acid and Lipid Chemistry*, Springer Verlag: New York (1996).
2. E. Fahy, S. Subramaniam, H. A. Brown, C. K. Glass, A. H. Merrill, Jr., R. C. Murphy, C. R. H. Raetz, D. W. Russell, Y. Seyama, W. Shaw, T. Shimizu, F. Spener, G. van Meer, M. S. VanNieuwenhze, S. H. White, J. L. Witztum, E. A. Dennis, *J. Lipid Res*. 2005, **46**, 839–861.
3. H. S. Raper, *J. Chem. Soc., Trans*. 1907, **91**, 1831–1838.
4. D. Rittenberg, K. Bloch, *J. Biol. Chem.* 1944, **154**, 311–312.
5. N. O. Kaplan, F. Lipmann, *J. Biol. Chem.* 1948, **174**, 37–44.
6. S. Smith, S. -C. Tsai, *Nat. Prod. Rep.* 2007, **24**, 1041–1072.
7. T. Maier, S. Jenni, N. Ban, *Science* 2006, **311**, 1258–1262.
8. S. Jenni, M. Leibundgut, T. Maier, N. Ban, *Science* 2006, **311**, 1263–1267.
9. F. J. Asturias, J. Z. Chadick, I. K. Cheung, H. Stark, A. Witkowski, A. K. Joshi, S. Smith, *Nat. Struct. Mol. Biol.* 2005, **12**, 225–232.
10. T. Maier, M. Leibundgut, N. Ban, *Science* 2008, **321**, 1315–1322.
11. D. Boehringer, N. Ban, M. Leibundgut, *J. Mol. Biol.* 2013, **425**, 841–849.
12. M. Leibundgut, S. Jenni, C. Frick, N. Ban, *Science* 2007, **316**, 288–290.
13. S. Jenni, M. Leibundgut, D. Boehringer, C. Frick, B. Mikolasek, N. Ban, *Science* 2007, **316**, 254–261.
14. T. Maier, M. Leibundgut, D. Boehringer, N. Ban, *Q. Rev. Biophys.* 2010, **43**, 373–422.
15. H. S. Hansen, *Dietary ω-3 and ω-6 Fatty Acids—Biological Effects and Nutritional Essentiality*, Plenum: New York (1989).
16. U. N. Das, *Biotechnol. J.* 2006, **1**, 420–439.
17. D. Meesapyodsuk, X. Qiu, *Lipids* 2012, **47**, 227–237.
18. X. Qiu, *Fatty Acids* 2003, **68**, 181–186.
19. H. Sprecher, D. L. Luthria, B. S. Mohammed, S. P. Baykousheva, *J. Lipid Res*. 1995, **36**, 2471–2477.
20. J. T. Brenna, N. Salem, A. J. Sinclair, S. C. Cunnane, *Fatty Acids* 2009, **80**, 85–91.
21. G. Barcelo-Coblijn, E. J. Murphy, *Prog. Lipid Res*. 2009, **48**, 355–374.
22. J. R. Vane, Y. S. Bakhle, R. M. Botting, *Annu. Rev. Pharmacol. Toxicol.* 1998, **38**, 97–120.
23. P. Needleman, J. Turk, B. A. Jakschik, A. R. Morrison, J. B. Lefkowith, *Annu. Rev. Biochem.* 1986, **55**, 69–102.
24. M. Hamberg, B. Samuelsson, *J. Biol. Chem.* 1967, **242**, 5336–5343.
25. M. G. Malkowski, S. L. Ginell, W. L. Smith, R. M. Garavito, *Science* 2000, **289**, 1933–1938.
26. O. P. Radmark, *Am. J. Respir Crit. Care Med.* 2000, **161**, S11–15.
27. E. A. Dennis, *J. Biol. Chem.* 1994, **269**, 13057–13060.
28. M. J. Kobe, D. B. Neau, C. E. Mitchell, S. G. Bartlett, M. E. Newcomer, *J. Biol. Chem.* 2014, **289**, 8562–8569.
29. P. Borgeat, B. Samuelsson, *J. Biol. Chem.* 1979, **254**, 2643–2646.
30. P. Borgeat, M. Hamberg, B. Samuelsson, *J. Biol. Chem.* 1976, **251**, 7816–7820.
31. M. Hamberg, B. Samuelsson, *Proc. Natl. Acad. Sci. U.S.A.* 1974, **71**, 3400–3404.
32. A. J. Wardlaw, R. Moqbel, O. Cromwell, A. B. Kay, *J. Clin. Invest.* 1986, **78**, 1701–1706.
33. B. Samuelsson, *Science* 1983, **220**, 568–575.
34. C. N. Serhan, M. Hamberg, B. Samuelsson, *Biochem. Biophys. Res. Commun.* 1984, **118**, 943–949.

35. C. N. Serhan, M. Hamberg, B. Samuelsson, *Proc. Natl. Acad. Sci. U.S.A.* 1984, **81**, 5335–5339.
36. S. Durand, J. -L. Parrain, M. Santelli, *J. Chem. Soc. Perkin* **1** 2000, 253–273.
37. C. Oger, L. Balas, T. Durand, J. -M. Galano, *Chem. Rev.* 2013, **113**, 1313–1350.
38. W. C. Still, C. Gennari, *Tetrahedron Lett.* 1983, **24**, 4405–4408.
39. K. Ando, *J. Org. Chem.* 1997, **62**, 1934–1939.
40. R. A. Raphael, F. Sondheimer, *J. Chem. Soc.* 1950, 2100–2103.
41. J. M. Osbond, J. C. Wickens, *Chem. Ind.* 1959, 1288.
42. J. M. Osbond, P. G. Philpott, J. C. Wickens, *J. Chem. Soc.* 1961, 2779–2787.
43. J. Sandri, J. Viala, *J. Org. Chem.* 1995, **60**, 6627–6630.
44. K. C. Nicolaou, P. G. Bulger, D. Sarlah, *Angew. Chem., Int. Ed*. 2005, **44**, 4442–4489.
45. C. Torborg, M. Beller, *Adv. Synth. Catal.* 2009, **351**, 3027–3043.
46. http://www.nobelprize.org/nobel_prizes/chemistry/laureates/2010/ (accessed September 29, 2015).
47. C. C. C. Johansson Seechurn, M. O. Kitching, T. J. Colacot, V. Snieckus, *Angew. Chem., Int. Ed*. 2012, **51** 5062–5085.
48. R. Martin, S.L. Buchwald, *Acc. Chem. Res.* 2008, **41**, 1461–1473.
49. N. Miyaura, A. Suzuki, *J. Chem. Soc., Chem. Commun.* 1979, 866–867.
50. A. Suzuki, *Angew. Chem., Int. Ed*. 2011, **50**, 6722–6737.
51. D. G. Hall, *Boronic Acids-Preparation, Applications in Organic Synthesis and Medicine*, Wiley-VCH, Weinheim, 2005, pp 31–73.
52. L. Kürti, B. Czakó, *Strategic Applications of Named Reactions in Organic Synthesis*, Elsevier, Dallas, 2005, pp 448–449.
53. J. P. Wolfe, R. A. Singer, B. H. Yang, S.L. Buchwald, *J. Am. Chem. Soc.* 1999, **121**, 9550–9561.
54. A. F. Littke, G. C. Fu, *Angew. Chem., Int. Ed*. 1999, **37**, 3387–3388.
55. C. J. O'Brien, E. A. B. Kantchev, C. Valente, N. Hadei, G. A. Chass, A. Lough, A. C. Hopkinson, M. G. Organ, *Chem.—Eur. J*. 2006, **12**, 4743–4748.
56. M. R. Netherton, C. Dai, K. Neuschuetz, G. C. Fu, *J. Am. Chem. Soc.* 2001, **123**, 10099–10100.
57. K. Sonogashira, Y. Tohda, N. Hagihara, *Tetrahedron Lett.* 1975, 4467–4470.
58. R. Chinchilla, C. Najera, *Chem. Rev.* 2007, **107**, 874–922.
59. L. Kürti, B. Czakó, *Strategic Applications of Named Reactions in Organic Synthesis*, Elsevier, Dallas, 2005, pp 424–425.
60. C. R. Johnson, M. P. Braun, *J. Am. Chem. Soc.* 1993, **115**, 11014–11015.
61. Y. Kobayashi, T. Shimazaki, H. Taguchi, F. Sato, *J. Org. Chem.* 1990, **55**, 5324–5335.
62. N. Ogawa, T. Tojo, Y. Kobayashi, *Tetrahedron Lett.* 2014, **55**, 2738–2741.
63. C. N. Serhan, *Nature* 2014, **510**, 92–101.
64. S. J. Lee, K. C. Gray, J. S. Paek, M. D. Burke, *J. Am. Chem. Soc.* 2008, **130**, 466–468.
65. E. M. Woerly, J. Roy, M. D. Burke, *Nat. Chem.* 2014, **6**, 484–491.
66. E. P. Gillis, M. D. Burke, *Aldrichimica Acta* 2009, **42**, 17–27.
67. Y. M. A. Mohamed, T. V. Hansen, *Tetrahedron Lett.* 2011, **52**, 1057–1059.
68. W. Boland, N. Schroer, C. Sieler, M. Feigel, *Helv. Chim. Acta*, 1987, **70**, 1025–1040.
69. K. C. Nicolaou, S. E. Webber, *J. Am. Chem. Soc.* 1984, **106**, 5734–5736.
70. K. C. Nicolaou, C. A. Veale, S. E. Webber, H. Katerinopoulos, *J. Am. Chem. Soc.* 1985, **107**, 7515–7518.
71. C. N. Serhan, K. C. Nicolaou, S. E. Webber, C. A. Veale, S. E. Dahlen, T. J. Puustinen, B. Samuelsson, *J. Biol. Chem.* 1986, **261**, 16340–16345.
72. A. R. Rodriguez, B. W. Spur, *Tetrahedron Lett.* 2012, **53**, 4169–4172.
73. M. Aursnes, J. E. Tungen, A. Vik, J. Dalli, T. V. Hansen, *Org. Biomol. Chem.* 2014, **12**, 432–437.
74. K. C. Nicolaou, T. Ladduwahetty, I. M. Taffer, R. E. Zipkin, *Synthesis* 1986, 344–347.
75. E. J. Corey, H. Niwa, J. R. Falck, *J. Am. Chem. Soc.* 1979, **101**, 1586–1587.
76. E. J. Corey, A. Marfat, J. R. Falck, J. O. Albright, *J. Am. Chem. Soc.* 1980, **102**, 1433–1435.
77. S. Manna, J. R. Falck, N. Chacos, J. Capdevila, *Tetrahedron Lett.* 1983, **24**, 33–36.
78. E. J. Corey, R. Nagata, *Tetrahedron Lett.* 1987, **28**, 5391–5394.
79. E. J. Corey, S. Iguchi, J. O. Albright, B. De, *Tetrahedron Lett.* 1983, **24**, 37–40.
80. E. J. Corey, J. O. Albright, A. E. Barton, S. Hashimoto, *J. Am. Chem. Soc.* 1980, **102**, 1435–1436.
81. S. W. Wright, E. Y. Kuo, E. J. Corey, *J. Org. Chem.* 1987, **52**, 4399–4401.
82. D. V. Kuklev, N. A. Aizdaicher, A. B. Imbs, V. V. Bezuglov, N. A. Latyshev, *Phytochemistry* 1992, **31**, 2401–2403.
83. R. Tyagi, B. Shimpukade, S. Blaettermann, E. Kostenis, T. Ulven, *MedChemComm* 2012, **3**, 195–198.
84. K. C. Nicolaou, S. A. Snyder, *Angew. Chem., Int. Ed*. 2005, **44**, 1012–1044.
85. http://www.nobelprize.org/nobel_prizes/medicine/laureates/1982/ (accessed September 29, 2015).
86. E. J. Corey, N. M. Weinshenker, T. K. Schaaf, W. Huber, *J. Am. Chem. Soc.* 1969, **91**, 5675–5677.
87. G. Stork, P. M. Sher, H. L. Chen, *J. Am. Chem. Soc.* 1986, **108**, 6384–6385.
88. M. Suzuki, A. Yanagisawa, R. Noyori, *J. Am. Chem. Soc.* 1988, **110**, 4718–4726.
89. G. Coulthard, W. Erb, V. K. Aggarwal, *Nature* 2012, **489**, 278–281.
90. E. J. Corey, S. G. Pyne, W. G. Su, *Tetrahedron Lett.* 1983, **24**, 4883–4886.
91. D. S. Dumlao, M. W. Buczynski, P. C. Norris, R. Harkewicz, E. A. Dennis, *Biochim. Biophys. Acta, Mol. Cell Biol. Lipids* 2011, **1811**, 724–736.
92. C. N. Serhan, N. A. Petasis, *Chem. Rev.* 2011, **111**, 5922–5943.
93. C. N. Serhan, N. Chiang, *Curr. Opin. Pharmacol.* 2013, **13**, 632–640.

# 4

# POLYETHERS

YOUWEI XIE[1] AND PAUL E. FLOREANCIG[2]

[1] *Max-Planck-Institut für Kohlenforschung, Mülheim, Germany*

[2] *Department of Chemistry, Chevron Science Center, University of Pittsburgh, Pittsburgh, PA, USA*

## 4.1 INTRODUCTION

Numerous attributes make epoxides impressively versatile functional groups in chemical synthesis. Ring strain of approximately 24 kcal/mol is present in these structures, making them considerably more prone toward reactions with nucleophiles than unstrained ethers. Strong nucleophiles generally react with the less substituted carbon of unsymmetrical epoxides with stereochemical inversion, consistent with an $S_N2$ mechanism. Reactions with weak nucleophiles are also possible in the presence of Brønsted or Lewis acids. These processes commonly occur at the more substituted carbon of unsymmetrical epoxides, consistent with $S_N1$ reactivity. However, stereochemical inversion is observed, indicating that the pathway has some $S_N2$ character, perhaps due to the presence of a tight ion pair resulting from the leaving group being tethered to the substrate. Significantly, the products of epoxide substitution reactions contain a hydroxyl group, in contrast to substitution reactions of conventional electrophiles in which no remnant of the leaving group is present.

Biological systems have evolved to exploit the reactivity of epoxides in the synthesis of a number of secondary metabolites (Fig. 4.1) [1], including ionophore antibiotics such as monensin (**1**) [2], terpene ethers, represented by thyrsiferol (**2**) [3], ladder toxins, represented by brevetoxin (**3**) [4], and annonaceous acetogenins, represented by murisolin (**4**) [5]. Chemical synthesis of cyclic ethers also frequently utilizes epoxides, often in the context of cascade cyclizations in which the hydroxyl group that is liberated acts as a nucleophile for a subsequent transformation. These processes have been the subject of recent reviews [6].

The purpose of this chapter is to describe the use of epoxides as biosynthetic precursors for cyclic ethers. The advances that allow for predictable chemical synthesis based on epoxide opening, including the development of models for regiocontrol in intramolecular ring-opening reactions and stereoselective synthesis, will be described. Numerous examples of epoxide cascade reactions in natural product synthesis will conclude the chapter.

## 4.2 BIOSYNTHESIS

### 4.2.1 Ionophore Antibiotics

Cane's studies on the biosynthesis of monensin A [7] showed that the core structure was derived from acetate, propionate, and butyrate through a classical polyketide synthase pathway. Elegant isotope-labeling studies showed that four oxygen atoms (labeled with an asterisk in Fig. 4.2) in the structure are not derived from the building blocks. This led to the speculation that these atoms were derived from $O_2$. This hypothesis was merged with Westley's hypothesis for polyether biosynthesis [8], leading to the proposal that triene **5** serves as the precursor to **1** via a sequence of alkene epoxidation reactions to yield **6** followed by intramolecular cascade ring opening.

These studies and observations on the stereochemical arrangements in related natural products led to the classic Cane–Celmer–Westley hypothesis [9]. This work formalized

*From Biosynthesis to Total Synthesis: Strategies and Tactics for Natural Products*, First Edition. Edited by Alexandros L. Zografos.
© 2016 John Wiley & Sons, Inc. Published 2016 by John Wiley & Sons, Inc.

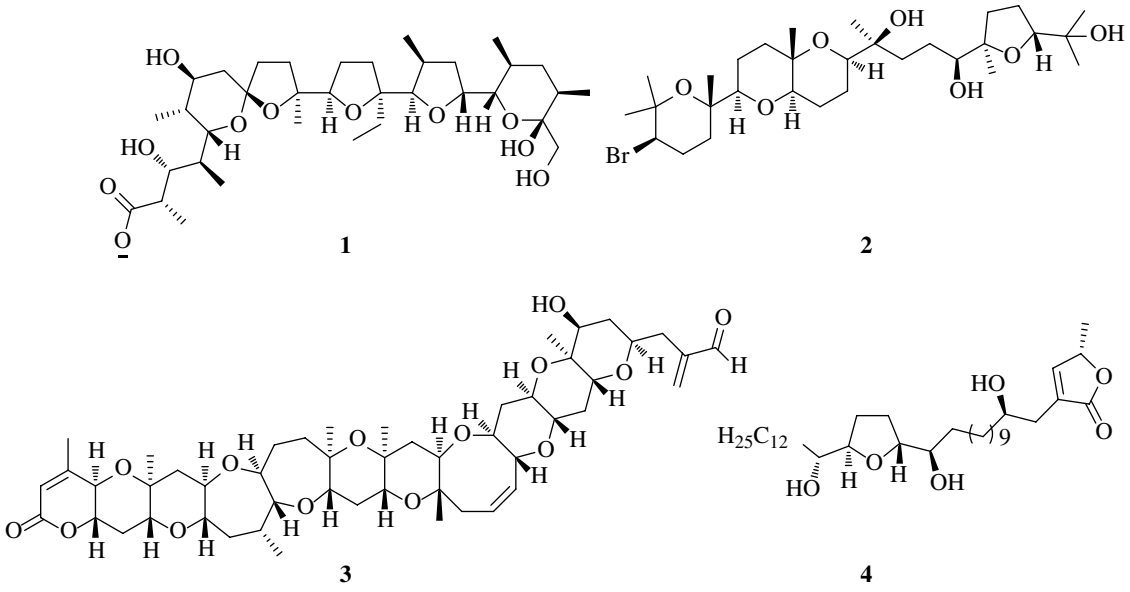



**FIGURE 4.1** Epoxide-derived secondary metabolites.

the postulate that epoxide cascades are involved in the formation of cyclic ethers. Additionally, the stereochemical homogeneity was proposed to arise from a conserved epoxidase subunit in the polyketide biosynthetic pathway reacting with *E*-alkenes. Molecular biology eventually provided validation for this hypothesis through Leadlay's discovery of MonCI [10]. This is a flavin-based epoxidase that is responsible for alkene oxidation of **5**. Deletion of *monCI*, the gene that encodes MonCI in the polyketide synthase cluster, resulted in the accumulation of **7**. The absence of the electrophilic epoxide groups allows for the formation of a lactone structure (Fig. 4.2). This work also confirmed the *E*-orientations of the alkenes in the triene precursor. This result was quite significant because the *E*-alkene geometry is essential to explain the stereochemical outcome of an epoxide cascade reaction in which the stereochemical orientation of the proximal carbon of a reactive epoxide is inverted while retention is observed at the distal carbon.

The epoxide-opening reactions in the monensin synthetic pathway lead to the formation of tetrahydrofuran structures through nucleophilic addition to the proximal carbon. An alternative pathway would proceed through nucleophilic addition to the distal carbon, which would provide a tetrahydropyran structure. The formation of tetrahydrofurans is preferred over the formation of tetrahydropyrans under mildly acidic conditions, as will be discussed later in this chapter. Therefore questions arose as to whether enzymes are involved with the epoxide cascade reaction. Enzymatic involvement was demonstrated during studies on the biosynthesis of lasalocid A (**8**). The precursor of **8** should be diepoxide **9** in accord with the Cane–Celmer–Westley hypothesis. However, the formation of the tetrahydropyran in the second structure differed from the normally observed tetrahydrofuran formation (Fig. 4.3).

The formation of the kinetically disfavored tetrahydropyran unit in lasalocid A implies enzymatic participation in ring formation. This was verified through the nearly simultaneous reports from Leadlay [11] and Oguri [12] of Lsd19 in the lasalocid polyketide synthase cluster. This unit shows structural homology with epoxide hydrolase enzymes, leading to speculation that it could participate in the cyclization reactions. Indeed exposing synthetic **9** to purified Lsd19 resulted in the formation of **8**. Further evidence for the ability of the enzyme to overcome the kinetic bias for tetrahydrofuran formation was obtained through the isolation of **10**, named isolasalocid A, upon exposing **9** to Brønsted acids (Scheme 4.1). Thus, enzyme control rather than substrate control leads to tetrahydropyran formation in the biosynthesis of **8**.

The manner in which Lsd19 promotes the cyclization was clarified through a beautiful combination of crystallography and computational analysis [13]. Oguri reported that Lsd19 does not promote the formation of both heterocycles in a single operation. Subunit Lsd19A catalyzes the formation of the tetrahydrofuran ring, while subunit Lsd19B catalyzes the formation of the tetrahydropyran ring. A crystal structure of Lsd19B with an unreactive substrate identified the binding pocket and suggested that the ring-closing reaction was promoted by nucleophilic activation of the hydroxyl group by an aspartate residue and electrophilic activation of the epoxide group by hydrogen bonding to a tyrosine residue (Scheme 4.2). Computational refinement of the reaction pathway by Houk using the theozyme model [14] showed that the placement of the activating residues leads to the barrier for the tetrahydropyran-forming pathway

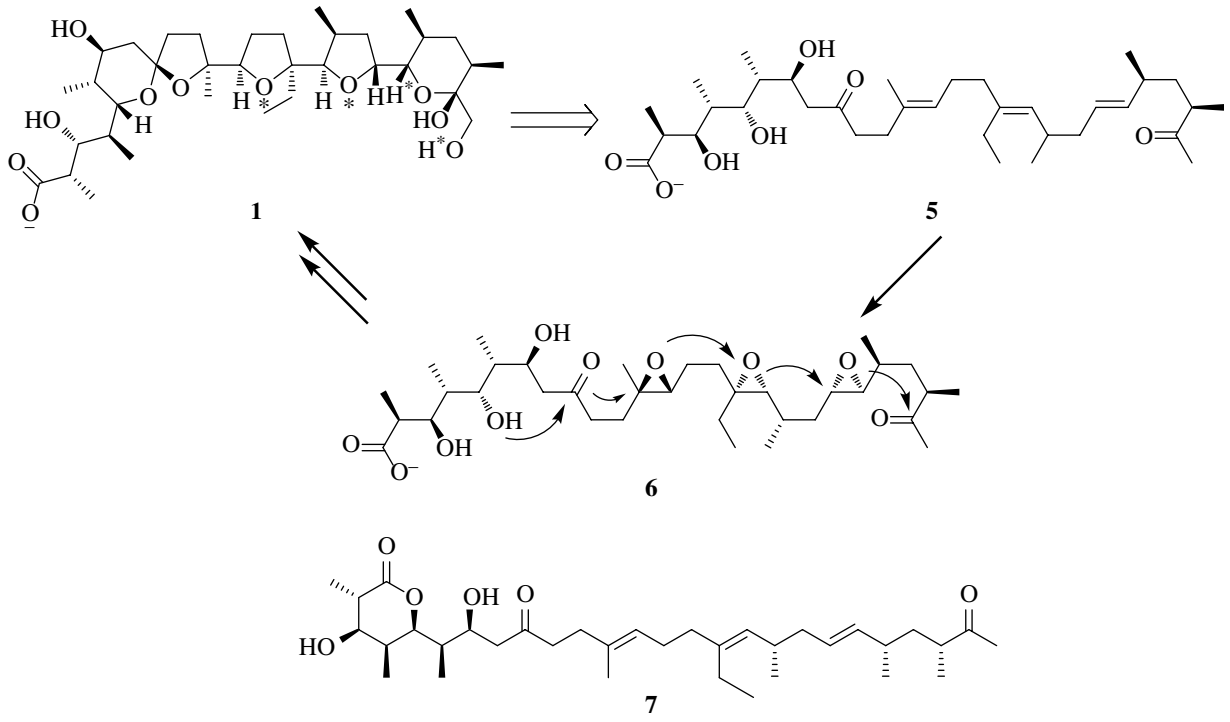



**FIGURE 4.2** Polyene precursor hypothesis for monensin A biosynthesis.

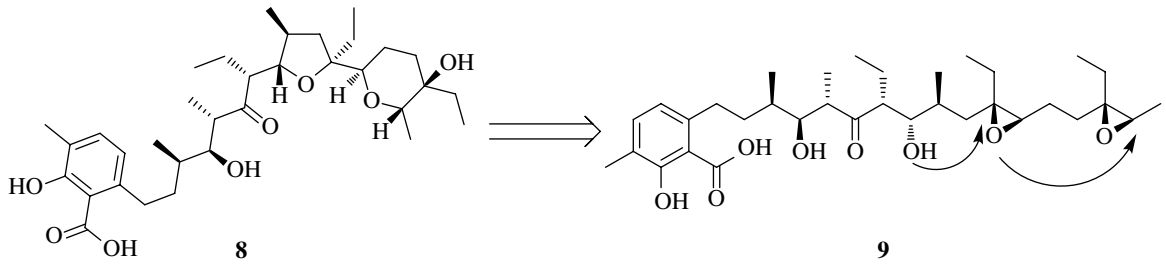
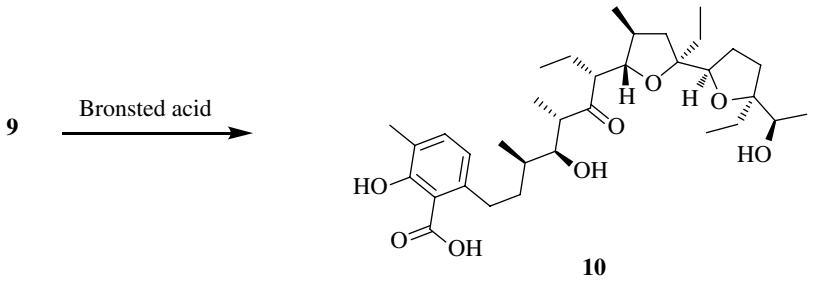
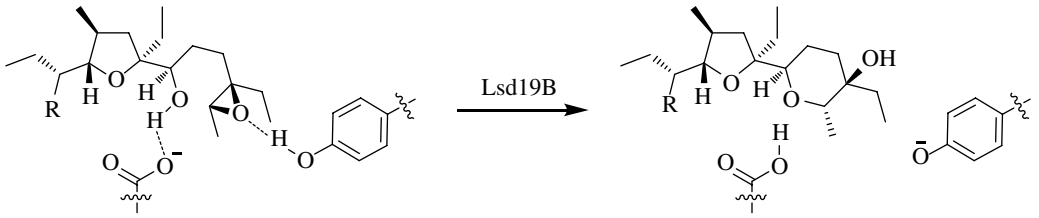



**FIGURE 4.3** Synthesis of lasalocid A through an epoxide cascade reaction.




**SCHEME 4.1** Nonenzymatic formation of isolasalocid A.




**SCHEME 4.2** Enzymatic tetrahydropyran formation.

being 2.5 kcal/mol lower in energy that the barrier for the tetrahydrofuran pathway.

### 4.2.2 Marine Ladder Toxins

The isolation of marine ladder toxins, represented by hemibrevetoxin (**11**) and brevetoxin (**12**), inspired significant speculation regarding their biological origins. Nakanishi [15] and Shimizu [16] proposed that these structures could arise from cascade reactions of polyepoxides such as **13** and **14** (Fig. 4.4). This notion has proven to be exceedingly influential for inspiring methodological studies relating to synthesizing these structures, despite Nakanishi's provision that the proposal should not be taken seriously [15b]. The attractive aspect of the hypothesis is the conserved stereochemical orientations of the epoxide groups in the precursor structures. The formation of fused polyethers through an epoxide cascade reaction, illustrated by the conversion of **14** to **12**, was unprecedented at the time of the postulates. Detailed studies of the biosynthesis of these structures have not advanced to the level that has been achieved in the polyether antibiotics area, and definitive evidence in favor or in opposition to the polyepoxide cascade pathway is not available.

### 4.2.3 Annonaceous Acetogenins and Terpene Polyethers

The acetogenins are characterized by the presence of one or more oxygen-containing heterocycles flanked by hydroxyalkyl groups. This structure strongly suggests a polyepoxide precursor in which an epoxide hydrolase initiates a cascade by opening one epoxide to form a diol that can continue the cascade by adding into a proximal epoxide, as shown by the conversion of **15** to **16** to **17** in Scheme 4.3. This notion

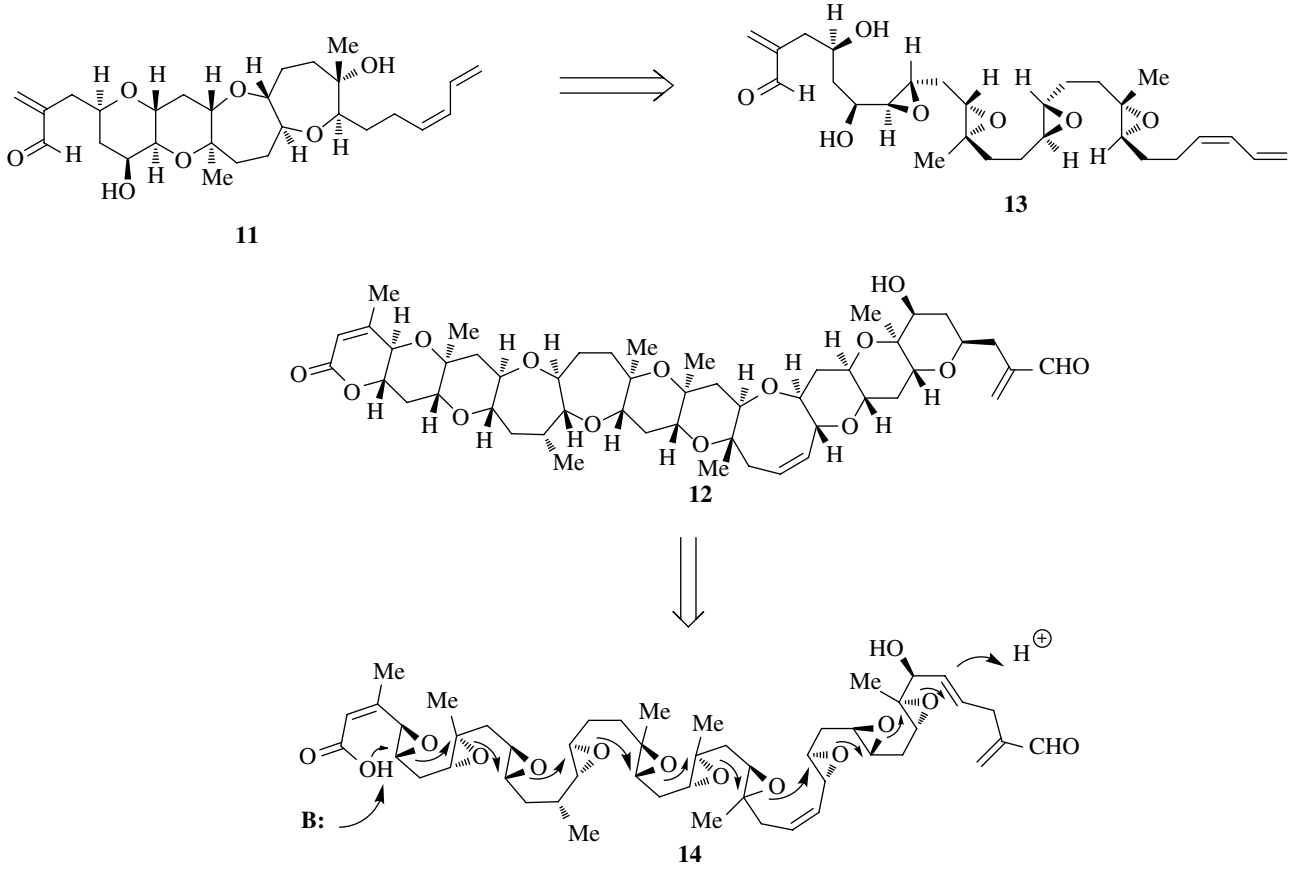
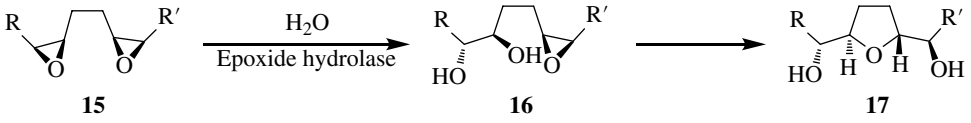



**FIGURE 4.4** Proposed polyepoxide-based routes to the ladder toxins.




**SCHEME 4.3** Epoxide hydrolase-based synthesis of an acetogenin tetrahydrofuran.

is supported by the observation that numerous epoxide hydrolases have been shown to promote the conversion of diepoxides into dihydroxytetrahydrofurans [17].

Terpene polyethers have also been proposed to arise through epoxide-opening cascade reactions. These structures are distinct from the other compound classes in this chapter because their carbon frameworks are not derived from polyketide synthase pathways. However, epoxide hydrolases are commonly encountered in terpene biosynthetic pathways [18], indicating that epoxides are viable intermediates in the construction of these compounds.

While the involvement of epoxides in the biosynthesis of the natural products in this section has been confirmed to different levels, the process of ring formation through intramolecular addition to epoxides is quite attractive for structures that contain an oxygen atom on a carbon that is adjacent to an annulation site. Significantly, the elegant hypotheses for the biosynthesis of these structures have inspired numerous efforts to design mimics for the processes that make many of the structures available through chemical synthesis.

## 4.3 EPOXIDE REACTIVITY AND STEREOSELECTIVE SYNTHESIS

The proposed biosyntheses of ether-containing natural products employ enzymes to introduce epoxide groups with complete stereocontrol and, in some cases, to dictate the regioselectivity of the nucleophilic addition reactions. Chemical mimicry of these pathways requires extensive understanding of the fundamental structural relationships for epoxide reactivity toward tethered nucleophiles. Additionally, diastereo- and enantioselectivity must be controlled to ensure that the products of these reactions are not mixtures of stereoisomers. This section will illustrate the development of models for understanding regiocontrol in epoxide-opening reactions and for controlling the stereochemical outcomes of epoxidation reactions.

### 4.3.1 Regiocontrol in Epoxide-Opening Reactions

Epoxide-opening reactions can proceed through *exo*-pathways, in which the nucleophile reacts with the proximal carbon of the epoxide to provide a product in which the resulting hydroxyl group is external to the newly formed ring. Alternatively the reactions can proceed through *endo*-pathways, in which the nucleophile reacts with the distal carbon of the epoxide to provide a product in which the resulting hydroxyl group is contained within the newly formed ring. These pathways are illustrated in Figure 4.5. Baldwin's rules [19] suggest that *exo*-pathways should be kinetically preferred based on the superior accessibility of the $\sigma^*$-orbital of the proximal C—O bond of the epoxide for the nucleophile. Houk calculated that the 5-*exo*-pathway for epoxide opening is preferred over the 6-*endo*-pathway by approximately 1.9 kcal/mol under either acidic or basic conditions [20]. However, differences in the substitution pattern and catalyst structure can lead to reversals in this selectivity.

Coxon illustrated (Scheme 4.4) the inherent preference for the 5-*exo*-pathway over the 6-*endo*-pathway under acidic conditions [21] through the conversion of hydroxy epoxide **18** to a greater than 5 : 1 mixture of tetrahydrofuran **19** and tetrahydropyran **20**. Kishi showed that the 5-*exo*-pathway is exclusively observed when the proximal carbon of the

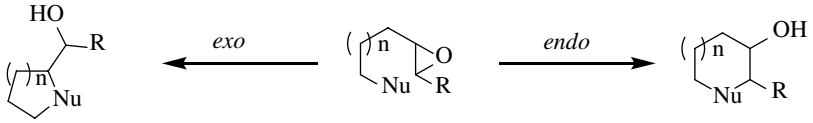
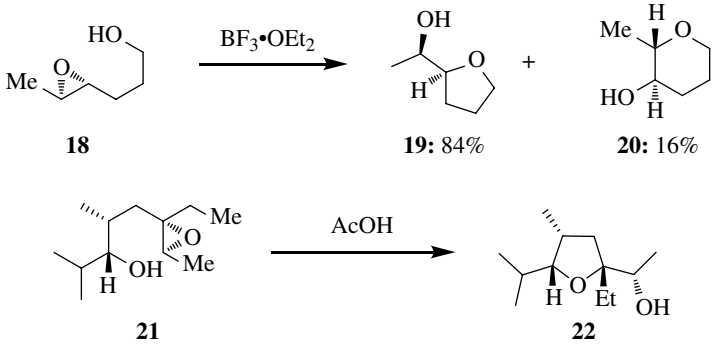
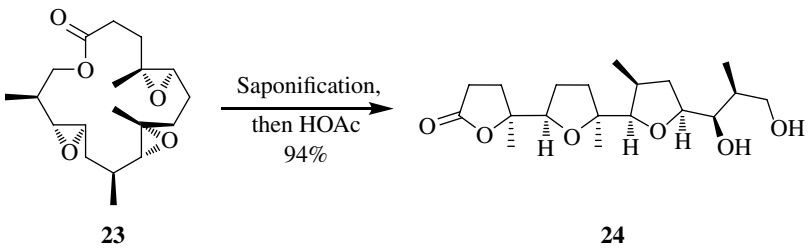



**FIGURE 4.5** *Exo*- and *endo*-epoxide-opening pathways.

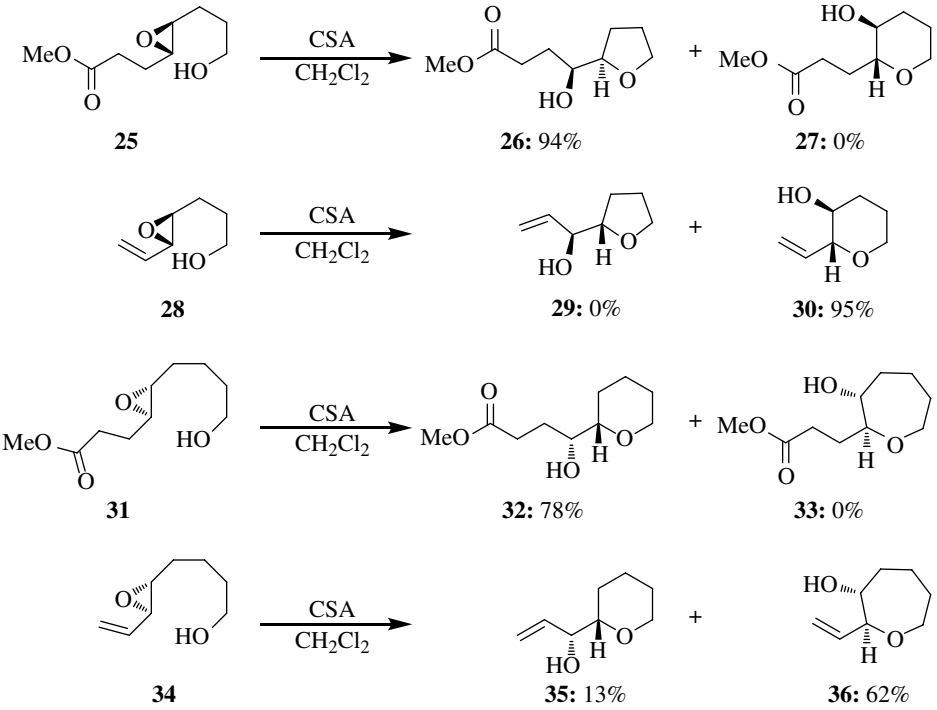



**SCHEME 4.4** *Exo*-preference for epoxide-opening reactions.




**23** **24**

**SCHEME 4.5** Cascade *exo*-cyclizations.

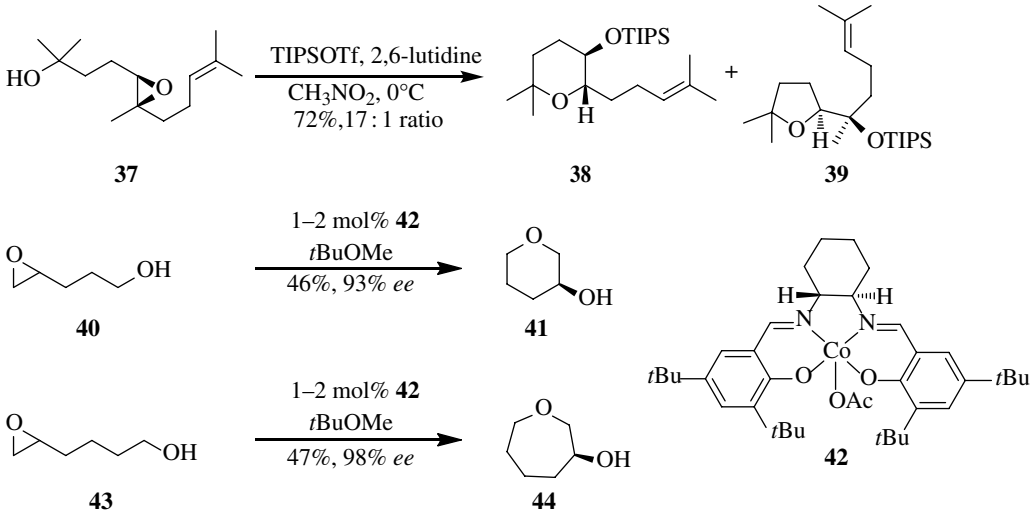



**SCHEME 4.6** Regiocontrol through rational substrate design.

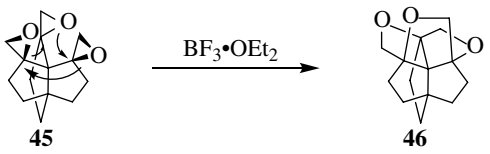
epoxide is more substituted than the distal carbon [22]. This is illustrated through the transformation of **21** to **22**. The enhanced selectivity can be attributed to the greater cationic character at the more substituted center of the protonated epoxide intermediate.

Excellent applications of these cyclizations were reported in consecutive papers from Still [23] and Schreiber [24]. The example from Still's group is shown in Scheme 4.5. Macrocyclic triepoxide **23** formed with high stereocontrol due to the conformational constraints of the macrocyclic architecture was saponified (conditions unspecified) and worked up with HOAc to generate tricycle **24** in high yield. The stereochemical outcome in this reaction implies that the cascade commences with the acid-mediated addition of the carboxylic acid into the proximal epoxide.

Nicolaou engaged in an effort to reverse the regioselectivity of these reactions in the context of synthesizing the ladder toxins. This study was based on the hypothesis that the *endo*-pathway should become competitive with the *exo*-pathway through rational stabilization of the cationic character on the distal carbon upon acidic activation of the epoxide. The principle was illustrated by the dramatic selectivity reversal shown in Scheme 4.6 [25]. Epoxide **25** cyclized in the presence of the Brønsted acid camphorsulfonic acid (CSA) to yield *exo*-product **26** in good yield and with no trace of *endo*-product **27**, consistent with Coxon's results albeit with higher selectivity. Epoxide **28**, in which the alkyl group was replaced with an alkenyl group, provided no trace of *exo*-product **29** and yielded *endo*-product **30** in excellent yield. These results can be attributed to the ability of the alkenyl group to stabilize the positive charge on the distal carbon of the protonated epoxide through conjugation. This strategy can also be used to dictate the selectivity between tetrahydropyran and oxepane formation [26]. Alkyl-substituted epoxide **31** cyclized in the presence of CSA to yield *exo*-product **32** while producing no




**SCHEME 4.7** *Endo*-cyclization through reagent control.




**SCHEME 4.8** Cascade cyclization through epoxonium ion intermediates.

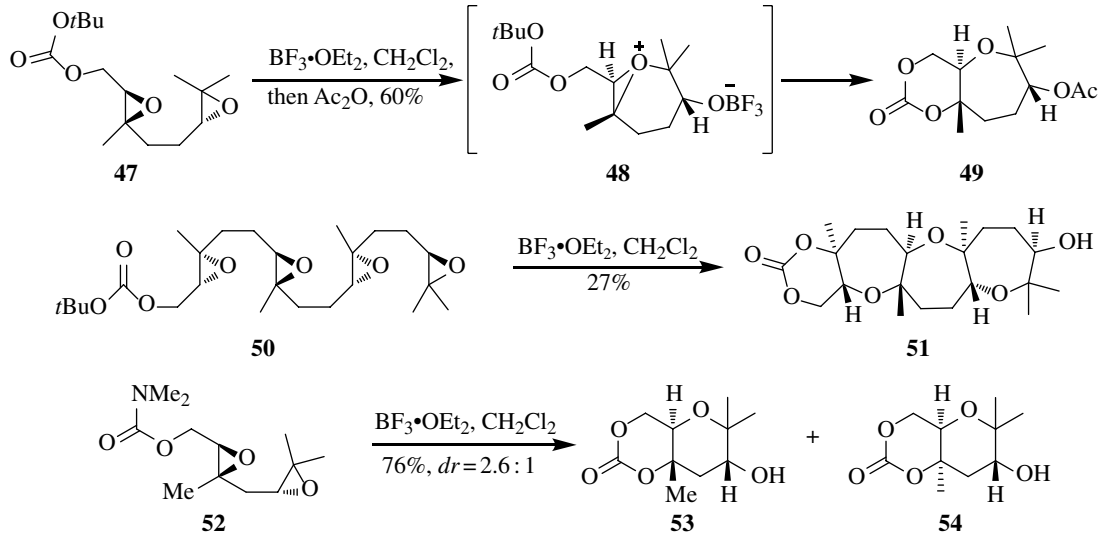
*endo*-product **33**. Alkenyl-substituted epoxide, however, yielded a minimal amount of **34** with oxepane **35** being formed as the major product.

Reagent control can also be exploited to alter the *exo*-/*endo*-preferences of these processes (Scheme 4.7). Morimoto showed that hydroxy epoxide **37** reacts with TIPSOTf to yield **38** and **39** in a 17 : 1 ratio [27]. Treatment of **37** with CSA leads to the expected strong preference (36 : 1) preference for the formation of **39**. This is explained by enhanced activation of the more substituted site through the greater steric repulsion of the silyl group with that center. Further evidence for this hypothesis is found in the observation that less bulky silyl triflates show diminished preference for the *endo*-pathway. Jacobsen showed that catalyst control can be exploited in the design of enantioselective *endo*-cyclization reactions [28]. Racemic hydroxy epoxide **40** yields tetrahydropyran **41** in the presence of chiral catalyst **42**. The catalyst serves to direct the hydroxyl group to the less substituted carbon of the epoxide while performing a very effective kinetic resolution. Oxepanes can also be formed in this manner as illustrated by the conversion of **43** to **44**.

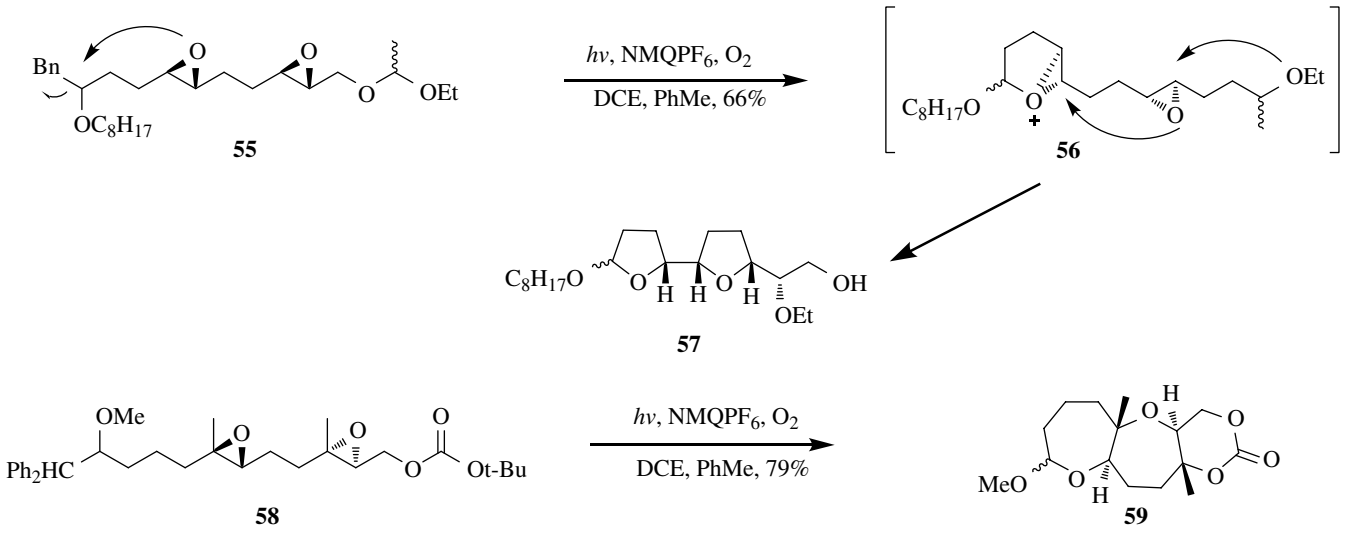
An alternate approach toward enhancing the electrophilicity of epoxides proceeds through the formation of bicyclic epoxonium ions. These species arise from intramolecular O-alkylation reactions of epoxides. An early example of this activation was reported by Paquette (Scheme 4.8). Propellane triepoxide **45** provided tris-tetrahydrofuran **46** upon exposure to $BF_3{\cdot}OEt_2$ [29]. Since no obvious external nucleophile was added to this reaction, the mechanism appears to be initiated through an intramolecular addition of one epoxide oxygen into the trisubstituted carbon of an activated adjacent epoxide. The resulting epoxonium ion is then sufficiently electrophilic to continue the annulation process until the stable final product is formed. A thermal variant of this transformation was reported simultaneously by Simmons [30].

McDonald extensively explored the use of Lewis acids to promote epoxonium ion formation (Scheme 4.9) [31]. This is illustrated by the reaction of diepoxide **47** with $BF_3{\cdot}OEt_2$. Nucleophilic addition into the activated epoxide generates epoxonium ion intermediate **48**, which can be opened by the carbonate group to form bicycle **49** in 60% yield upon hydroxyl acylation. Initiation of this reaction could be envisioned to arise from an initial addition of the carbonate group into the proximal epoxide. However, the strong *endo*-preference suggests that the epoxonium ion pathway, because the regioselectivity of the addition into the bicyclic epoxonium ion is different from that of a simple Lewis acid-coordinated epoxide. Multiple rings can be constructed in this manner, as shown by the conversion of **50** to **51**. The 27% isolated yield reflects a greater than 70% yield per ring-forming event. Tetrahydropyrans have also been formed through this approach. Exposing **52** to $BF_3{\cdot}OEt_2$ yields tetrahydropyrans **53** and **54** in good chemical yield. The 2.6 : 1 ratio of product diastereomers indicates that, in contrast to bicyclo[4.1.0] epoxonium ions, the bicyclo[3.1.0] epoxonium ion intermediate ionizes to form a carbocation that can react with stereochemical retention. Utilizing the dimethylcarbamate group as the terminal nucleophile proved to be essential for tetrahydropyran formation.

The potential for interconverting hydroxy oxepanes and hydroxyalkyl tetrahydropyrans via epoxonium ion

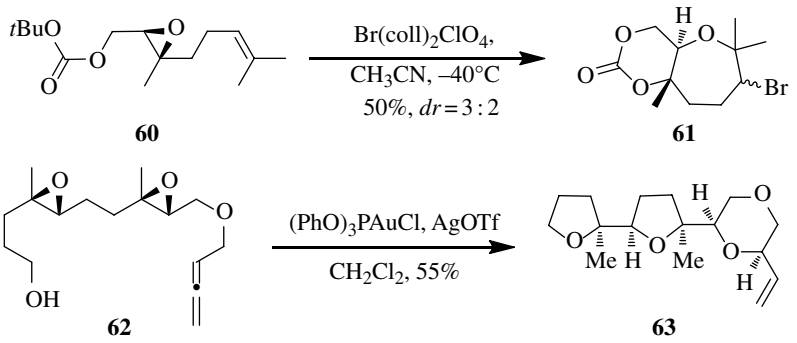



**SCHEME 4.9** Oxepane and tetrahydropyran formation through epoxonium ion intermediates.

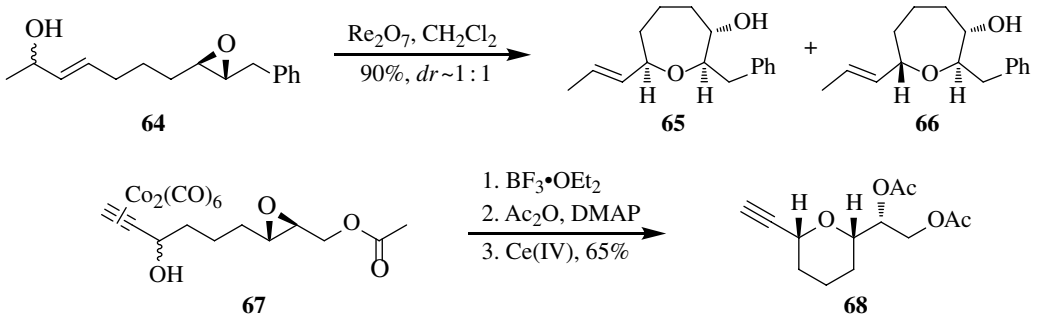



**SCHEME 4.10** Reactions through oxidatively generated epoxonium ions.

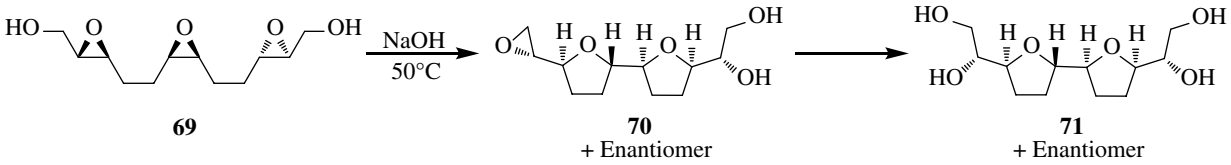
intermediates was demonstrated by Nakata [32], indicating that Lewis acid-mediated cascade reactions could yield the products of thermodynamic control rather than kinetic control. The Floreancig group devised a nonacidic method for initiating these processes to determine the kinetic preferences for related cascade reactions [33]. These transformations employ single-electron oxidation to initiate fragmentations of carbon─carbon bonds of homobenzylic ethers to generate oxocarbenium ions under neutral conditions. The oxocarbenium ions react with proximal epoxides to form epoxonium ions. Examples are shown in Scheme 4.10. Irradiating diepoxide **55** in the presence of catalytic *N*-methylquinolinium hexafluorophosphate ($NMQPF_6$) and $O_2$ as the terminal oxidant provided bis-tetrahydrofuran **57** in 66% yield via epoxonium ion **56**. This transformation proceeded through bicyclo[3.1.0] epoxonium ions that reacted exclusively through the *exo*-pathway. The mixed acetal group was used to deliver an ethoxy group as the cascade-terminating event. The conversion of **58** to **59**, however, proceeded exclusively through *endo*-cyclizations. Two differences can be noted between these processes. Bicyclo[4.1.0] epoxonium ions are the relevant reactive intermediates and trisubstituted epoxides rather than disubstituted epoxides are employed in the latter reaction. Computational studies from Houk [33c] showed that the transition state energy for the *endo*-opening in bicyclo[4.1.0] epoxonium ions is lower than *endo*-opening in bicyclo[3.1.0] ions because of better orbital overlap between the incoming nucleophile and the departing ether and




**SCHEME 4.11** Epoxonium ion-based cascades from alkene and allene precursors.




**SCHEME 4.12** Ionization-based methods for epoxonium ion formation and cyclization.



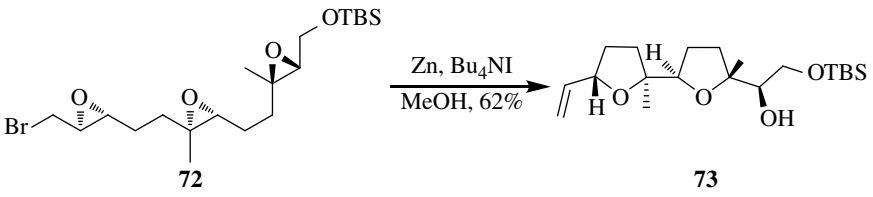

**SCHEME 4.13** Base-mediated *exo*-cyclizations.

that the added methyl group, as expected, enhances the capacity of the reactive carbon to stabilize positive charge.

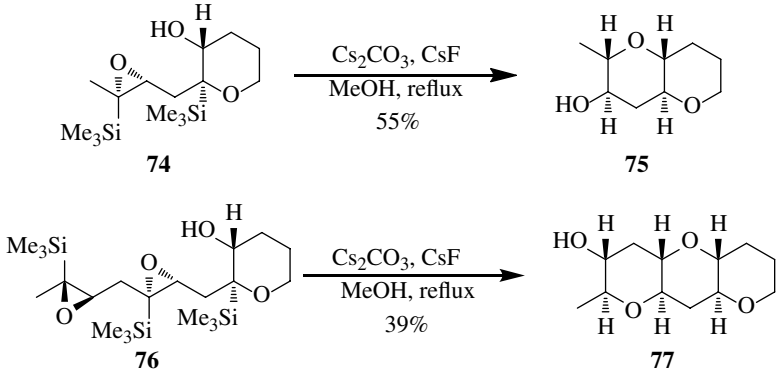
Other innovative methods have been useful for generating epoxonium ions under nonacidic conditions (Scheme 4.11). McDonald showed that alkenes could serve as electrophiles for these processes upon conversion to bromonium ions [34]. Thus, substrate **60** was exposed to biscollidine bromonium perchlorate ($Br(coll)_2ClO_4$) to yield diastereomeric bicycles **61**. These products formed through the addition of the epoxide group into diastereomeric bromonium ions to yield an epoxonium ion that was opened by the proximal carbonate with complete *endo*-selectivity. Gagné used gold activation of allenes to form electrophiles that react with pendent epoxide groups to generate epoxonium ions [35]. Thus, adding a cationic gold catalyst to allenyl diepoxide **62** provided tricycle **63** in 55% yield through the addition of the proximal epoxide group to the electrophilic gold-coordinated allene followed by a series of expected *exo*-cyclizations.

Solvolysis reactions have been effective processes for generating epoxonium ions through cationic intermediates (Scheme 4.12). Floreancig showed that exposing allylic alcohol **64** to $Re_2O_7$ resulted in the isolation of **65** and **66** in high yield [36]. Analysis of the absolute stereochemistry of products derived from enantiomerically enriched substrates conformed that the reaction proceeded through epoxonium ion formation from the intermediate allylic cation followed by bimolecular nucleophilic addition rather than through a direct *endo*-cyclization. Martín employed the Nicholas reaction to generate a carbocation to activate an appended epoxide group [37]. Cobalt complex **67** was ionized in the presence of $BF_3{\cdot}OEt_2$ to form an epoxonium ion that was opened with complete regiocontrol through anchimeric participation of the proximal acetate group. Acylation and oxidative cobalt cleavage provided tetrahydropyran **68** in good yield.

Hydroxy epoxides can also cyclize under basic conditions. This was demonstrated by Hoye (Scheme 4.13) through




**SCHEME 4.14** Initiation through reductive alkoxide formation.




**SCHEME 4.15** Vanishing silyl group strategy for *endo*-cyclizations.

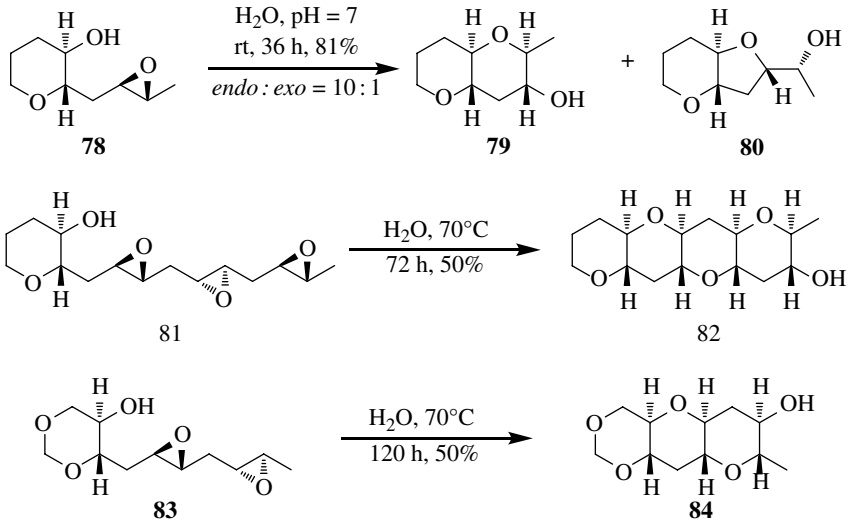
the treatment of triepoxy diol **69** with NaOH at 50°C [38]. The transformation proceeded through a Payne rearrangement to liberate an alkoxide that initiates cascade tetrahydrofuran formation to form **70** transiently followed by epoxide opening to yield **71**. The product was isolated as a nearly racemic mixture despite starting with enantioenriched substrate because different product enantiomers are formed through cascade initiation at the opposite termini. This work demonstrated that base-mediated intramolecular epoxide-opening reactions proceed through the 5-*exo*-pathway in preference to the 6-*endo*-pathway.

Marshall employed reductive conditions to form alkoxides that engaged in cascade cyclization reactions (Scheme 4.14) [39]. Exposing bromo epoxide **72** to Zn resulted in a reductive elimination to form a zinc alkoxide that initiated an *exo*-selective cascade reaction to form bis-tetrahydrofuran **73** in 65% yield.

Jamison showed that *endo*-cyclizations can occur under basic conditions through the clever "vanishing silyl group" strategy (Scheme 4.15) [40]. These reactions proceed through base-mediated additions of alcohols to silyl epoxides, as shown in the conversion of **74** to **75**. The hydroxyl group in the substrate appears to promote the cleavage of the trimethylsilyl group prior to cyclization, while the trimethylsilyl group on the epoxide enhances the electrophilicity of the appended carbon. The efficiency of this process is significantly heightened by using a tetrahydropyran unit to template the reactive groups. Cascade reactions can also be achieved through this approach, as seen in the conversion of **76** to **77**.

Jamison also showed that, remarkably, these cyclizations can be conducted under neutral conditions in water (Scheme 4.16) [41]. The reactions proceed most efficiently and selectively when a tetrahydropyran is used as a template, as seen in the conversion of **78** to *endo*-product **79**, with only a small amount of *exo*-product **80** being isolated. Notably, cascade variants of these reactions appear to become more *endo*-selective, with later cyclizations proceeding faster than the initial cyclization. This indicates that rigidity in the template promotes cyclization. The selective conversion of **81** to tetracycle **82** illustrates this observation. Dioxanes also serve as templates for these reactions. Heating **83** in water provides **84** with high selectivity. Although these reactions are somewhat slower than the corresponding reactions with tetrahydropyran template, the ability to cleave the dioxane group to liberate a diol is attractive from the perspective of further functionalization. Extensive mechanistic studies on these processes suggest that water forms an elaborate hydrogen-bonding network that is anchored by the cyclic template and creates for enhanced nucleophilicity for the hydroxyl group, enhanced electrophilicity for the epoxide group, and functional group orientation that promotes the *endo*-pathway [42].

These examples highlight the extensive opportunities that are available for utilizing epoxides as precursors to larger rings. Changes in substitution patterns and reaction mechanisms have a significant and rational impact on the regiochemical outcomes of these reactions. These studies have provided the basis for numerous successful applications in natural product synthesis.

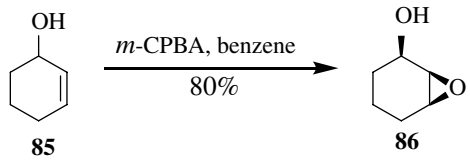



**SCHEME 4.16** Water-mediated *endo*-cyclizations.

### 4.3.2 Stereoselective Epoxide Synthesis

The ability to access stereochemically pure products from epoxide cascade reactions is critically dependent upon the capacity to prepare stereochemically pure epoxides. This section details the advances that make stereoselective synthesis through epoxide cascade reactions possible.

A key experiment for defining stereocontrol in epoxidation reactions was reported by Henbest in 1957 [43]. This manuscript showed (Scheme 4.17) that cyclohexenol (**85**) reacts with *m*-CPBA to provide epoxide **86**, where the oxygen was delivered from the same face as the hydroxyl group. This result was opposite to the stereochemical outcome of cyclohexenyl acetate epoxidation, leading the authors to postulate that hydrogen bonding can direct the facial approach of *m*-CPBA to alkenes.

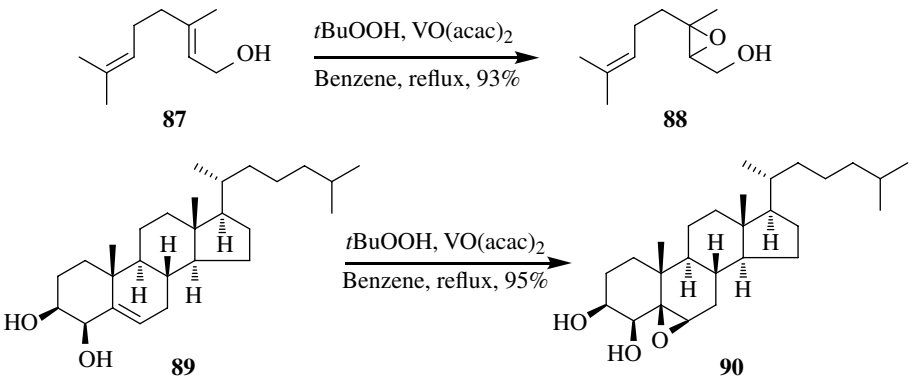



**SCHEME 4.17** Henbest's hydrogen-bonding directed epoxidation.

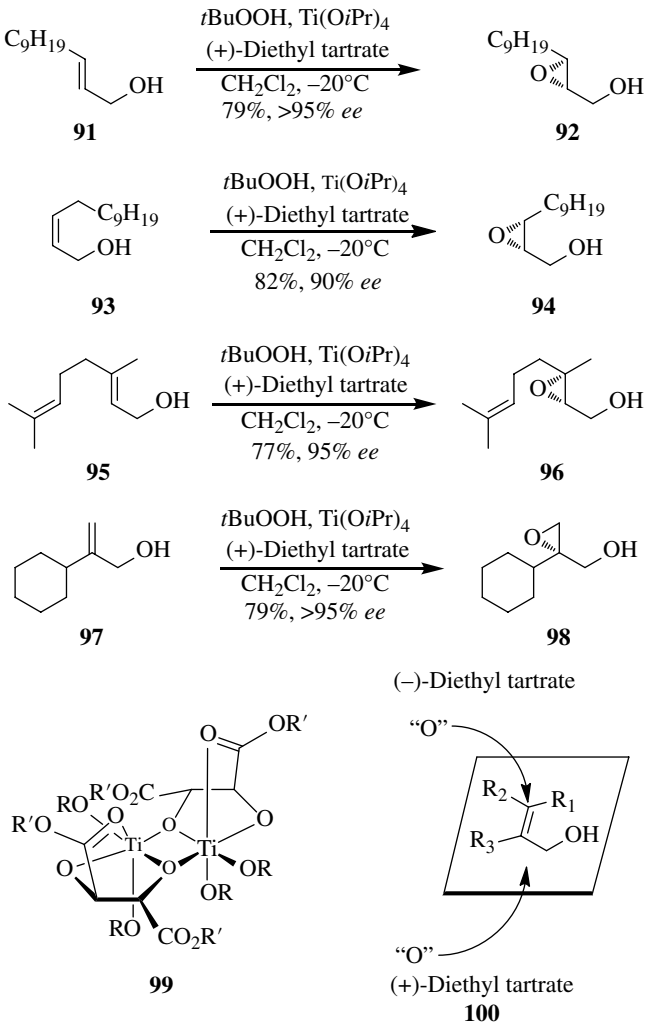
Sharpless advanced this notion through using a metal-based epoxidation catalyst (Scheme 4.18) [44]. This approach took advantage of the capacity of $VO(acac)_2$ to coordinate simultaneously to alcohols and peroxides and promote regioselective epoxidations of allylic and homoallylic alcohols with *t*BuOOH as the oxidant, as shown by the conversion of **87** to **88**. This approach also provides stereoselectivity, as shown by the transformation of **89** to **90** in which the hydroxyl group directs a *syn*-oxidation of the alkene. This procedure is selective because alkyl peroxides generally do not epoxidize alkenes but can be activated by coordination to the alcohol-coordinated vanadium Lewis acid.

This utility of this procedure was substantially enhanced by the observation that adding tartrate esters to the reaction mixture enhances the rate of the oxidation (ligand-accelerated catalysis) [45]. This also makes the oxidant chiral and enantiomerically pure, creating the possibility of directed asymmetric oxidation. This was realized by using $Ti(OiPr)_4$ as the Lewis acid, *t*BuOOH as the oxidant, and diethyl tartrate as the chiral ligand (Scheme 4.19). The Sharpless asymmetric epoxidation has proven to be one of the most versatile and efficacious reactions in organic synthesis because of its operational simplicity, impressive substrate scope, and valuable products. (*E*)- and (*Z*)-1,2-Disubstituted (**91** to **92** and **93** to **94**), trisubstituted (**95** to **96**), and 1,1-disubstituted (**97** to **98**) primary allylic alcohols react to provide products in high enantiomeric excess. Regioselectivity for allylic alcohols is high. The original protocol employed stoichiometric reagents, but subsequent studies showed that adding molecular sieves to the reaction mixture allowed for all reagents but the oxidant to be used in substoichiometric quantities [46]. Kinetic resolutions are also possible when using racemic secondary allylic alcohols as substrates. Despite extensive studies [47], no compelling model for the transition state of this reaction has emerged that accounts for all kinetic studies and observations of steric effects. However, the catalyst was shown to be dimeric structure **99** [48] and predictive capacity for the reaction can be realized through the use of mnemonic **100**.

Yamamoto took a similar approach for the epoxidation of allylic and homoallylic alcohols (Scheme 4.20). This process employed chiral hydroxamic acid ligand **101** to induce stereocontrol and $VO(OiPr)_3$ to serve as the Lewis acid [49]. (*E*)-Homoallylic alcohol **102** was converted to epoxide **103**




**SCHEME 4.18** Sharpless' regio- and diastereoselective epoxidation.

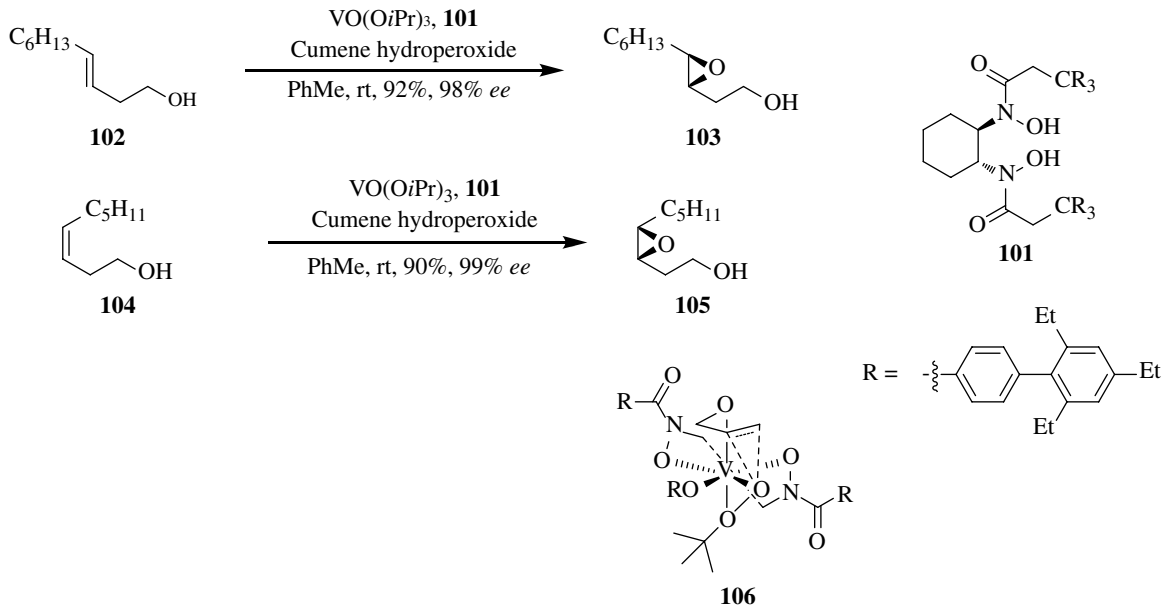



**SCHEME 4.19** The Sharpless asymmetric epoxidation.

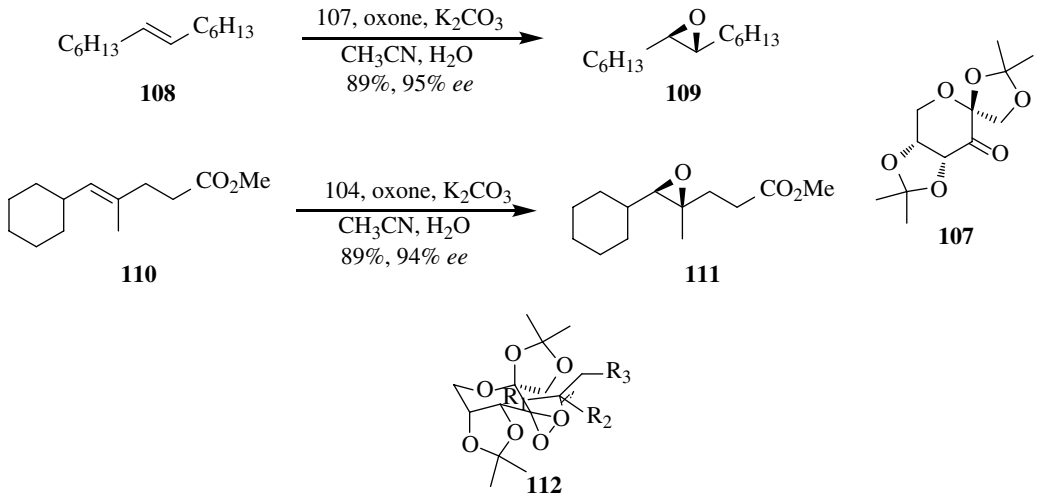
and (*Z*)-homoallylic alcohol **104** was converted to **105** in high yield and excellent enantiomeric excess. The proposed transition state for this process is depicted by **106**. This model is also consistent with results from kinetic resolution experiments. More recent work from the Yamamoto group showed that a similar ligand with a tungsten-based catalyst can also effect asymmetric epoxidation reactions on allylic and homoallylic alcohols [50].

Practical asymmetric epoxidation of a wide range of alkenes that lack a directing group became possible through Shi's carbohydrate-based epoxidation catalysts [51]. These catalysts are chiral ketones that react with $KHSO_5$ (Oxone®) to yield dioxirane intermediates that transfer an oxygen atom to alkenes with often very high facial control. Examples from the initial report are shown in Scheme 4.21. Ketone **107** is available from D-fructose in two steps. (*E*)-1,2-Disubstituted alkenes and trisubstituted alkenes are excellent substrates for this procedure, providing epoxides with predictable (*R*,*R*)-configurations in excellent yield and enantioselectivity. Although L-fructose is not readily available, the enantiomer of **107** can be accessed through a four-step sequence from easily accessible L-sorbose [52]. This expands the scope of products to include (*S*,*S*)-epoxides. Spirocyclic transition state **112**, in which facial approach is dictated by the avoidance of steric interactions with the acetonide group, was proposed to explain the stereochemical outcomes of these reactions.

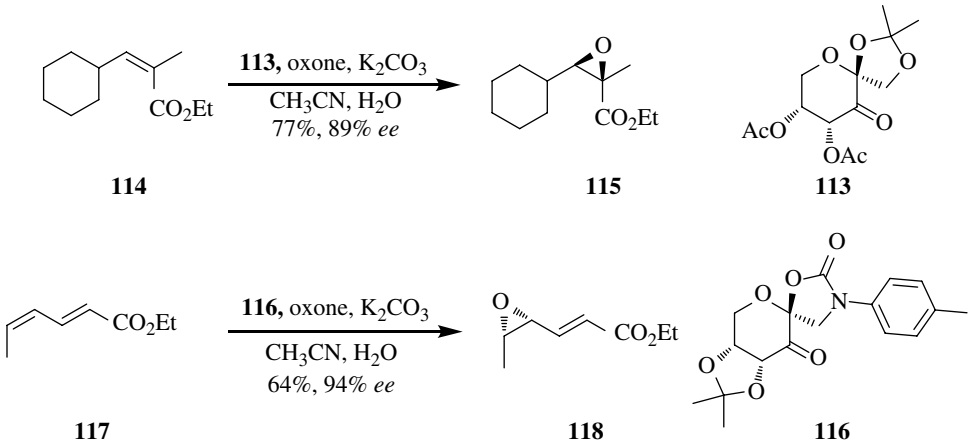
Dioxiranes are electron-deficient oxidants and, therefore, react with electron-deficient alkenes more slowly than electron-rich alkenes. Shi developed more reactive catalyst **113** to effect the epoxidation of alkenes that react sluggishly with dioxiranes formed from **107** (Scheme 4.22) [53]. Thus, even α,β-unsaturated esters such as **114** can be oxidized efficiently. Although the catalyst is slightly more difficult to make than **107**, it is more stable toward competitive decomposition via a Baeyer–Villiger reaction so catalyst loadings can be lowered. Epoxidizing (*Z*)-1,2-disubstituted alkenes that lack a directing group is a significant challenge in asymmetric synthesis. Shi's group partially solved this problem through the design of catalyst **116** [54]. This catalyst appears to be successful because of an attractive interaction between π-electrons in the substrate and the arene on the nitrogen, as seen in the oxidation of **117** to **118**.



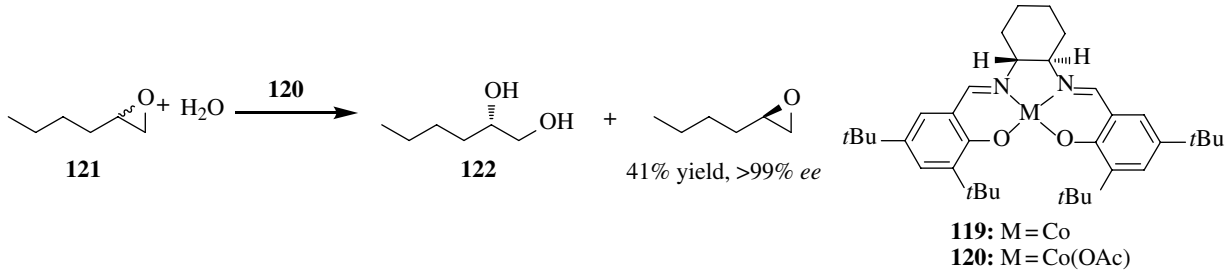

**SCHEME 4.20** Directed asymmetric homoallylic alcohol epoxidation.



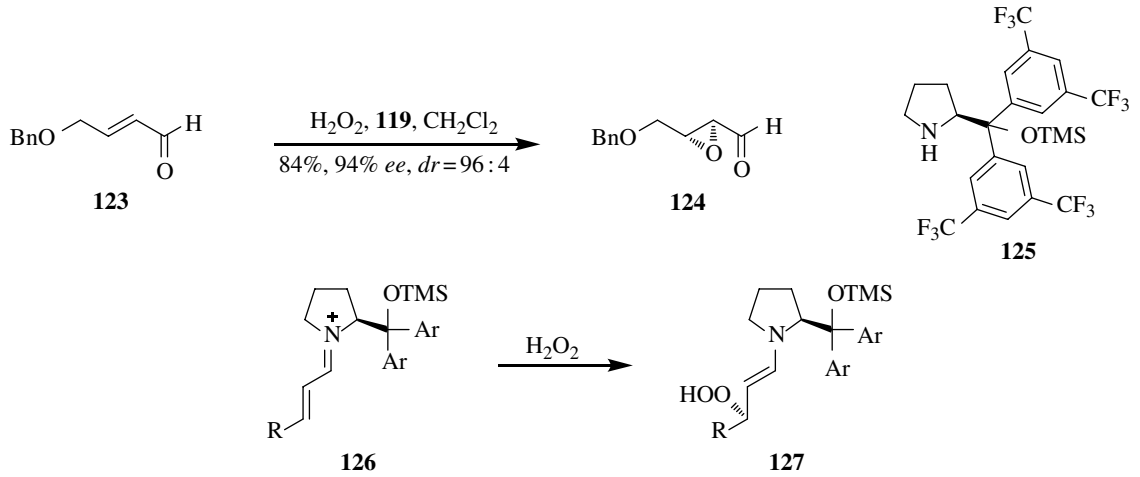

**SCHEME 4.21** The Shi asymmetric epoxidation.




**SCHEME 4.22** Scope expansion with second-generation Shi catalysts.




**SCHEME 4.23** The Jacobsen hydrolytic kinetic resolution.



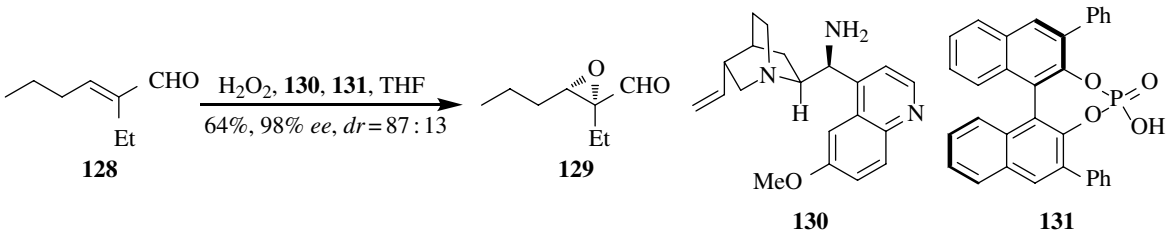

**SCHEME 4.24** Organocatalytic asymmetric epoxidation.

The direct formation of enantiomerically pure epoxides from terminal alkenes has yet to be achieved. Jacobsen, however, reasoned that racemic terminal epoxides are exceedingly easy to access and that kinetic resolution would be an effective strategy to form enantiomerically pure terminal epoxides [55]. This strategy is shown in Scheme 4.23. Exposing Co(II) precatalyst **119** to HOAc and air generates Co(III) catalyst **120**. Adding racemic terminal epoxide **121** and water to the catalyst leads to a selective hydrolysis reaction of the (*S*)-enantiomer to yield diol **122**. The (*R*)-enantiomer does not react and can be isolated in enantiomerically pure form through distillation. The chiral element in **119** is accessed in enantiomerically pure form through a resolution of racemic 1,2-cyclohexanediamine. Therefore both enantiomers of the catalyst are equally available. The reaction is generally run neat and catalyst loadings are low, making the protocol exceptionally practical.

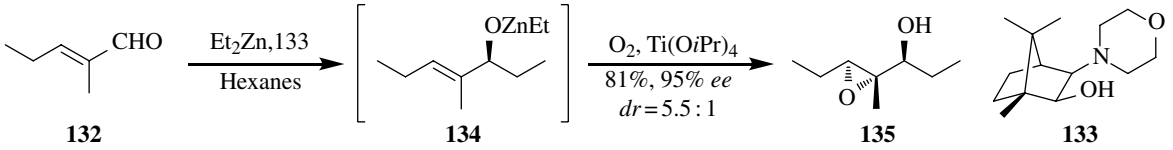
A common strategy for building complexity from the products of Sharpless epoxidation reactions is to oxidize the alcohol to an aldehyde and add a nucleophile. Therefore asymmetric epoxidation reactions of α,β-unsaturated aldehydes would be a redox economical strategy [56] for the preparation of useful precursors. This strategy requires the use of nucleophilic oxidants since even the reactive variants of the Shi catalyst are not sufficient for reactions with α,β-unsaturated aldehydes.

Jørgensen reported (Scheme 4.24) an organocatalytic route for α,β-unsaturated aldehyde epoxidation that utilizes hydrogen peroxide as the oxygen source [57]. Aldehyde **123** can be converted to epoxide **124** efficiently and stereoselectively in the presence of proline derivative **125** (10 mol%). The key to this process is that the iminium ion that forms from **123** and **125** is more electrophilic than **123**, thereby allowing for reaction with $H_2O_2$. Iminium ion formation is reversible, allowing for **125** to be used in substoichiometric quantities. The formation of small quantities of the *cis*-epoxide isomer indicates that the epoxidation is stepwise, as would be expected for a nucleophilic process. The stereochemical outcome is explained by the front face of iminium ion **126** being blocked, forcing peroxide to approach from the backside to yield **127**. MacMillan subsequently reported a related reaction that utilizes PhIO as the oxidant [58].

List showed that iminium ion catalysis can be coupled with chiral Brønsted acid catalysis in the epoxidation of α-alkyl-α,β-unsaturated aldehydes (Scheme 4.25) [59]. Substrates with the α-alkyl group are less reactive than those that contain a hydrogen at the α-position, making their nucleophilic epoxidation more challenging. The List protocol allows for the conversion of aldehyde **128** to epoxide




**SCHEME 4.25** Dual catalysis for epoxidizing hindered aldehydes.




**SCHEME 4.26** Diastereoselective epoxidation following asymmetric addition.

**129** with outstanding enantioselectivity and good diastereoselectivity in the presence of hydrogen peroxide, cinchona alkaloid-derived amine catalyst **130**, and chiral phosphoric acid **131**. The absolute configurations of the amine and acid are matched in this process, showing that chiral variants of both catalyst components are necessary for success.

Walsh approached the formation of epoxides with adjacent secondary alcohols through the asymmetric addition of alkylzinc reagents to α,β-unsaturated aldehydes followed by diastereoselective epoxidation (Scheme 4.26) [60]. Aldehyde **132** reacted with $Et_2Zn$ in the presence of catalyst **133** to yield zinc alkoxide **134**. Introducing $O_2$ to the system followed by $Ti(OiPr)_4$ led to the isolation of epoxy alcohol **135** in high yield and enantiomeric excess and with good diastereocontrol. This one-pot process was proposed to occur through the intermediacy of a zinc peroxide that forms upon the addition of $O_2$ to the system.

The results in this section clearly demonstrate that virtually any epoxide can be accessed in enantio- and diastereomerically pure form from alkene precursors. The Sharpless and Shi epoxidation methods have dominated the recent applications to cascade reactions in synthesis. However, new protocols offer experimental facility and substrate scope that will lead to future applications in complex molecule construction.

## 4.4 APPLICATIONS TO TOTAL SYNTHESIS

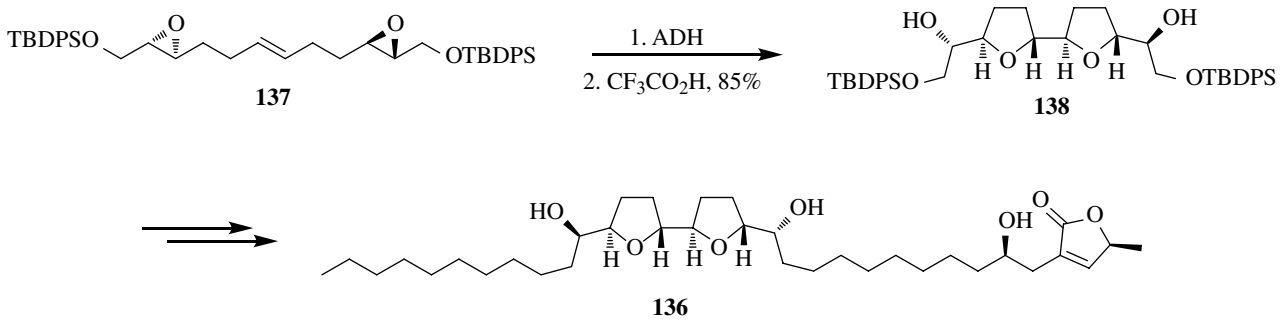
The numerous methods for stereoselective epoxide synthesis and the extensive base of knowledge regarding regiocontrol in intramolecular opening reactions combine to create numerous opportunities for natural product synthesis. This section will illustrate many of the routes that have exploited this approach. These routes are often called biomimetic syntheses due to their similarities to the proposed biosynthetic pathways to the target molecules, though no enzymes are involved in these approaches.

### 4.4.1 Acid-Mediated Transformations

Hoye applied a bidirectional acid-mediated epoxide-opening sequence to the total synthesis of the annonaceous acetogenin parviflorin (**136**; Scheme 4.27) [61]. This reaction employed a Sharpless asymmetric dihydroxylation (ADH) reaction of **137**, in which the epoxides were introduced by a double Sharpless epoxidation to yield a diol intermediate that was immediately treated with $CF_3CO_2H$ to yield **138** in 85% yield. No competition from 6-*exo*-pathways was reported, showing the kinetic preference for tetrahydrofuran formation over tetrahydropyran formation. The natural product was accessed through a multistep route from **138** that inverted the configurations of the two alcohol centers.

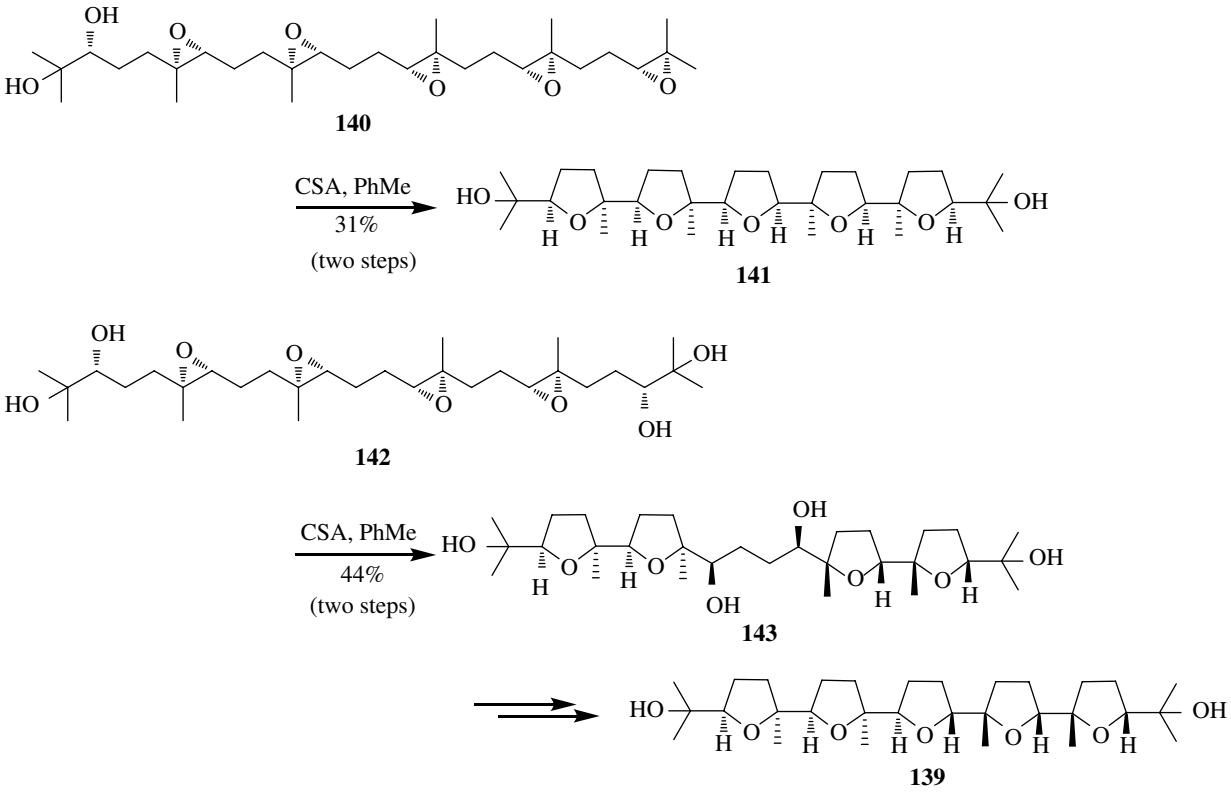
Corey applied a cascade approach to the synthesis of the proposed structure of the terpene polyether glabrescol (**139**; Scheme 4.28) [62]. Pentaepoxide **140** was prepared through a Shi epoxidation of the pentaene precursor. Treating **140** with CSA yielded **141**, which was the proposed structure of glabrescol, in 31% yield for the epoxidation and cyclization steps. Spectroscopic analysis revealed differences between synthetic and natural materials, suggesting that glabrescol is actually a stereoisomer of the proposed structure. The natural product was eventually prepared through a variation on the strategy in which tetraepoxide **142** cyclized under acidic conditions to form tetraol **143** [63]. Closure of the central diol to form the final tetrahydrofuran ring confirmed that glabrescol is a stereoisomer of the initially proposed structure.

Morimoto employed a bidirectional epoxidation/ring-opening sequence in the total synthesis of longilene peroxide (**144**; Scheme 4.29) [64]. Diepoxide **145** was prepared




**137** **138** **136**

**SCHEME 4.27** Hoye's synthesis of parviflorin.



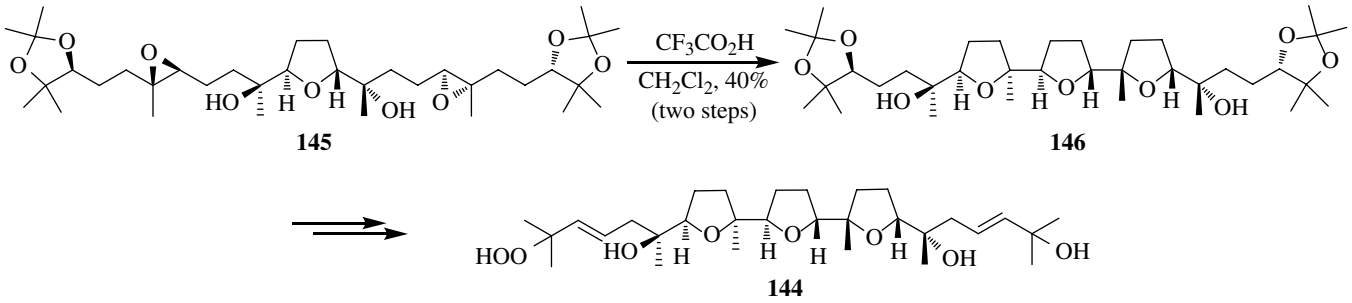

**140** **141** **142** **143** **139**

**SCHEME 4.28** Corey's total synthesis of glabrescol.

through a Shi epoxidation. Treatment with $CF_3CO_2H$ completed the formation of the tris-tetrahydrofuran core (**146**) of the molecule in 40% yield from the diene precursor. Longilene peroxide was prepared in five steps from **146**.

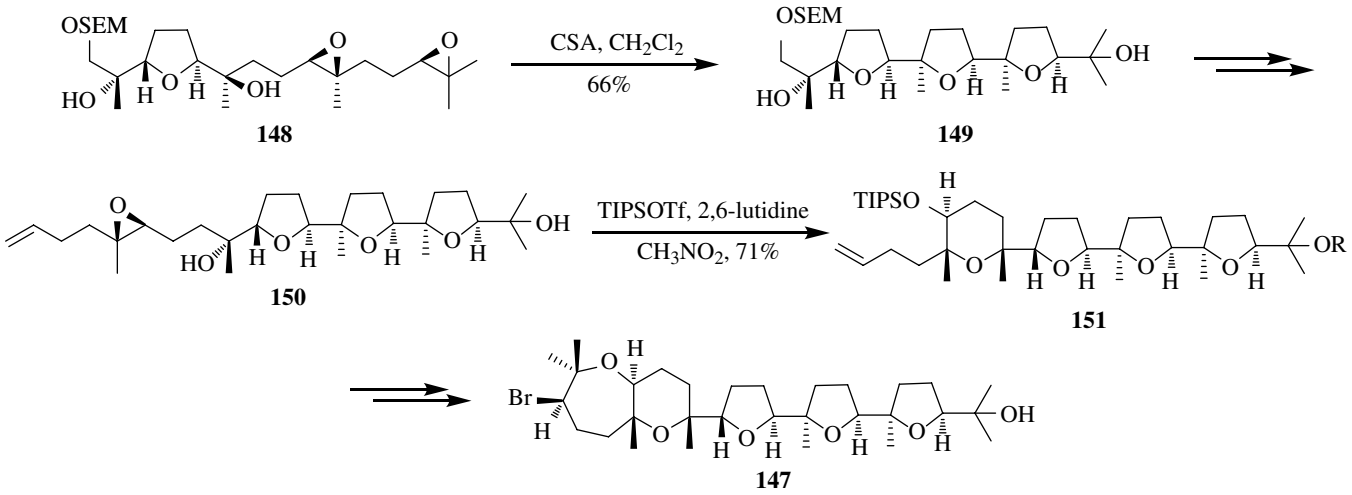
Morimoto used two epoxide-opening strategies for the total synthesis of enshuol (**147**; Scheme 4.30) [65]. An efficient acid-mediated *exo*-cascade was utilized to convert **148** to **149**. A six-step sequence was used to prepare epoxide **150** from **149**. An *endo*-cyclization was achieved to provide **151** through the use of the bulky Lewis acid TIPSOTf, in accordance with this group's previous studies. A two-step sequence was employed to complete the natural product synthesis.

Xiong used an acid-mediated epoxide-opening cascade to prepare a penta-tetrahydrofuran structure for the synthesis of the tetra-tetrahydrofuran natural product omaezakianol (**152**; Scheme 4.31) [66]. This allowed for the synthesis of cyclization precursor **153** from squalene. Exposing **153** to CSA provided pentacycle **154** in a 21% yield that includes the formation of the epoxides. Reductive opening resulted in



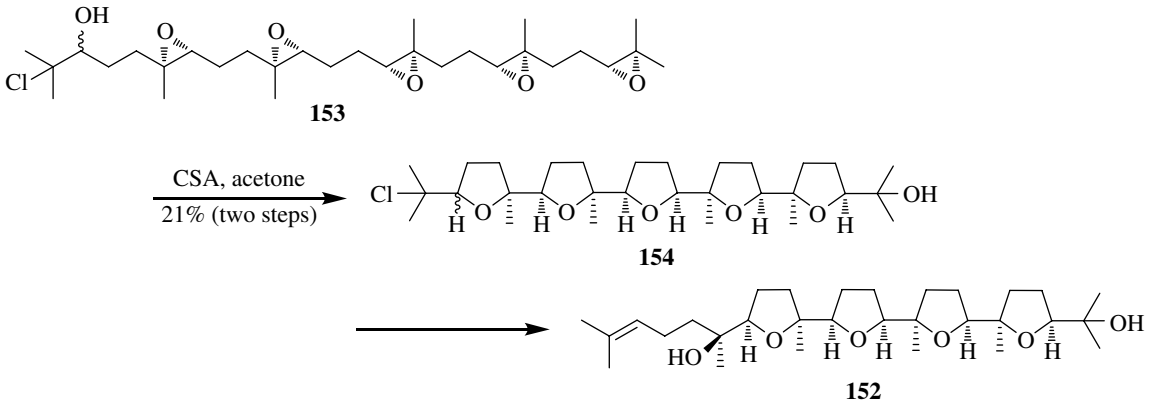

145 146 144

**SCHEME 4.29** Morimoto's total synthesis of longilene peroxide.




148 149 150 151 147

**SCHEME 4.30** Morimoto's total synthesis of enshuol.

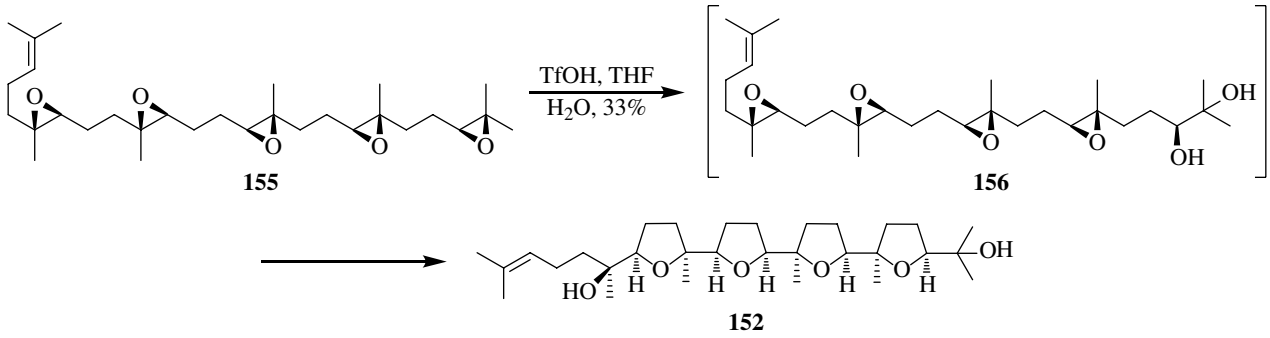



153 154 152

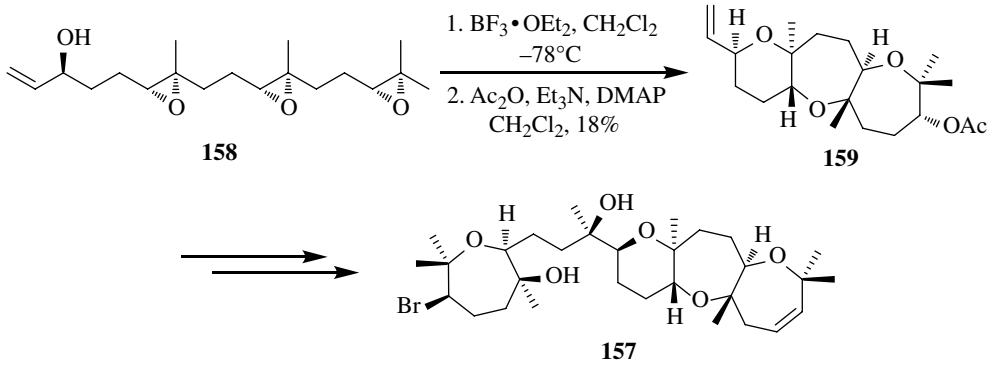
**SCHEME 4.31** Xiong's synthesis of omaezakianol.

the formation of the natural product through an impressive five-step sequence.

Morimoto reported the synthesis of omaezakianol through a pathway that was designed to mimic the epoxide hydrolase-based initiation step that was proposed for the biosynthesis of these structures (**155**; Scheme 4.32) [67]. Thus, epoxide **155** was treated with TfOH in aqueous THF. The authors propose that acid-mediated hydrolysis occurs at the dimethyl center of the epoxide to form diol **156** transiently. This proceeds through the cascade to yield the natural product in




**SCHEME 4.32** Epoxide hydrolase mimicry for the synthesis of omaezakianol.




**SCHEME 4.33** Jamison's synthesis of armatol A.

33% yield. Hydrolysis at the opposite terminus would yield the enantiomer of the natural product, so the observation of high enantiocontrol for product formation supports the authors' mechanistic hypothesis although the reason for the selectivity is not clear.

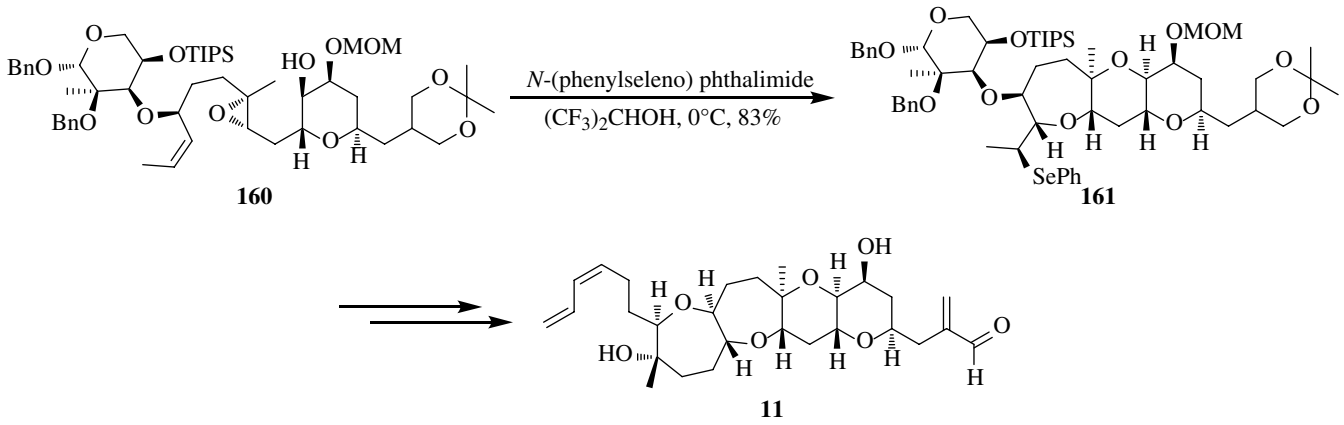
Jamison employed an *endo*-selective Lewis acid-mediated epoxide cascade reaction in the total synthesis of armatol A (**157**; Scheme 4.33) [68]. The key transformation was the $BF_3{\cdot}OEt_2$-mediated isomerization of triepoxide **158**. This resulted, upon acylation, in the formation of fused tricycle **159**. Also of note, a bromonium ion-mediated epoxonium ion-forming reaction was used to form the isolated oxepane unit en route to the completion of the synthesis of the natural product.

### 4.4.2 Cascades via Epoxonium Ion Formation

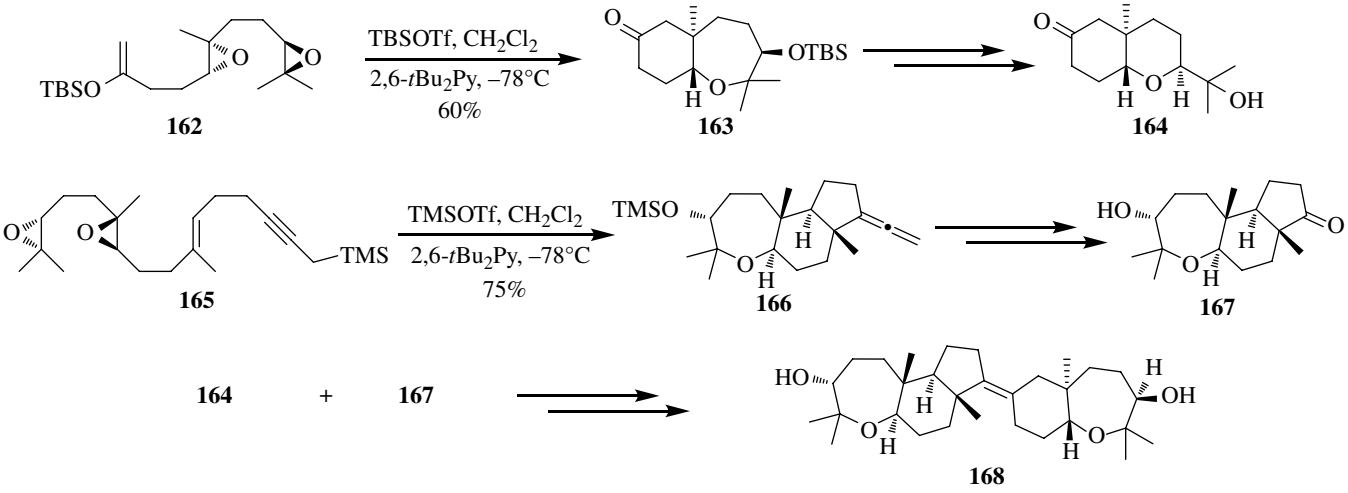
Holton reported an influential application of epoxonium ions as intermediates in cascade reactions through the total synthesis of hemibrevetoxin B (**11**; Scheme 4.34) [69]. This process utilized *N*-(phenylseleno)phthalimide to form a selenonium ion from alkenyl epoxide **160**. *Exo*-opening of the selenonium ion by the epoxide followed by *endo*-opening of the resulting epoxonium ion provided **161** in an impressive 83% yield. This structure was converted to the natural product through a multistep sequence.

McDonald employed π-nucleophiles to open epoxonium ions in the synthesis of several natural products (Scheme 4.35) [70]. Activating diepoxide **162** with TBSOTf provided bicycle **164** through the addition of the enolsilane into the intermediate epoxonium ion. Durgamone (**164**) was prepared through a pathway that proceeded via a solvolytic ring contraction. A second natural product synthesis was initiated by treating **165** with TMSOTf to provide tricycle **166** in 75% yield, whereby the addition of the trisubstituted alkene initiated a π-bond cascade that terminated with the formation of the allene group from the propargylsilane. The natural product nakorone (**167**) was accessed from **166** through a sequence of ozonolysis and deprotection. Vinyl triflate derivatives of **164** and **167** were united through a reductive cross-coupling process en route to abudinol B (**168**). These structures were prepared as the antipodes of the natural products due to the greater accessibility of the fructose-derived enantiomer of the Shi catalyst.

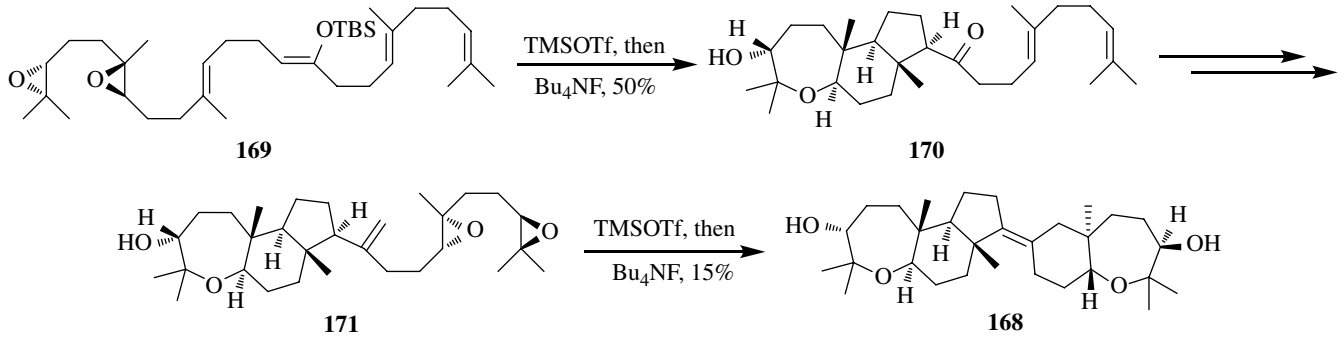
The McDonald group reported a second generation of abudinol B that employed two cascade reactions in a linear sequence (Scheme 4.36) [71]. The left tricycle was formed from diepoxide **169** through the use of an enolsilane as the




**SCHEME 4.34** Holton's synthesis of hemibrevetoxin B.



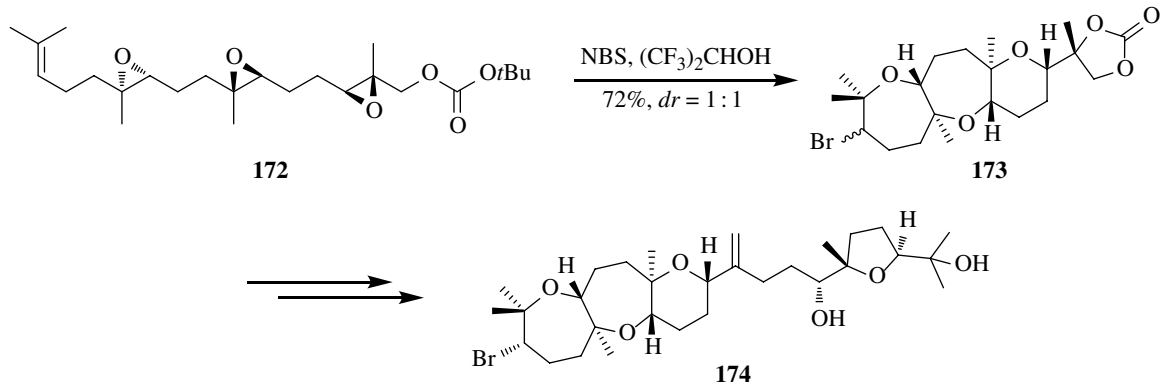

**SCHEME 4.35** π-Nucleophiles in epoxonium ion cascade reactions.




**SCHEME 4.36** McDonald's second-generation synthesis of abudinol B.

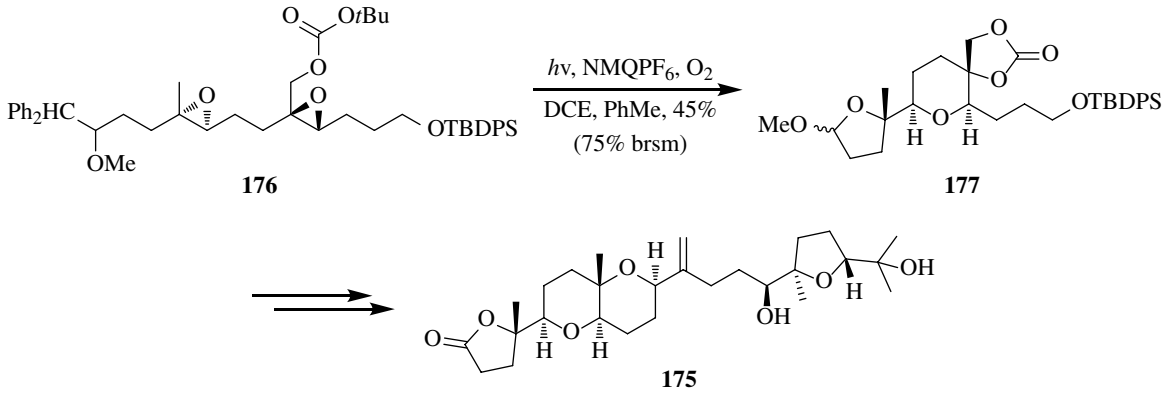
terminating nucleophile in the cascade reaction. Converting the resulting tricycle **170** to diepoxide **171** allowed for the second cascade in which an ene-type reaction was utilized to terminate the cascade. While this step proceeded in low yield, the overall strategy allowed for a shorter sequence to prepare the natural product.

As illustrated in Scheme 4.37, Jamison showed that multiple oxepanes can be formed through alkene activation with *N*-bromosuccinimide (NBS) [72]. Treating alkenyl triepoxide **172** with NBS produced **173**, containing the fused tricyclic core of dioxepandehydrothyrsiferol (**174**), in an excellent 72% yield. The cyclic carbonate group arose from the *exo*-ring




172 173 174

**SCHEME 4.37** Jamison's dioxepanethyrsiferol synthesis.




176 177 175

**SCHEME 4.38** Oxidative synthesis of lactodehydrothyrsiferol.

closure of the *tert*-butyl carbonate into an epoxonium ion intermediate. The diastereomeric products resulted from a nonselective bromonium ion formation but were separable, and the undesired stereoisomer could be converted to the diastereomer through reductive ring opening followed by reclosure.

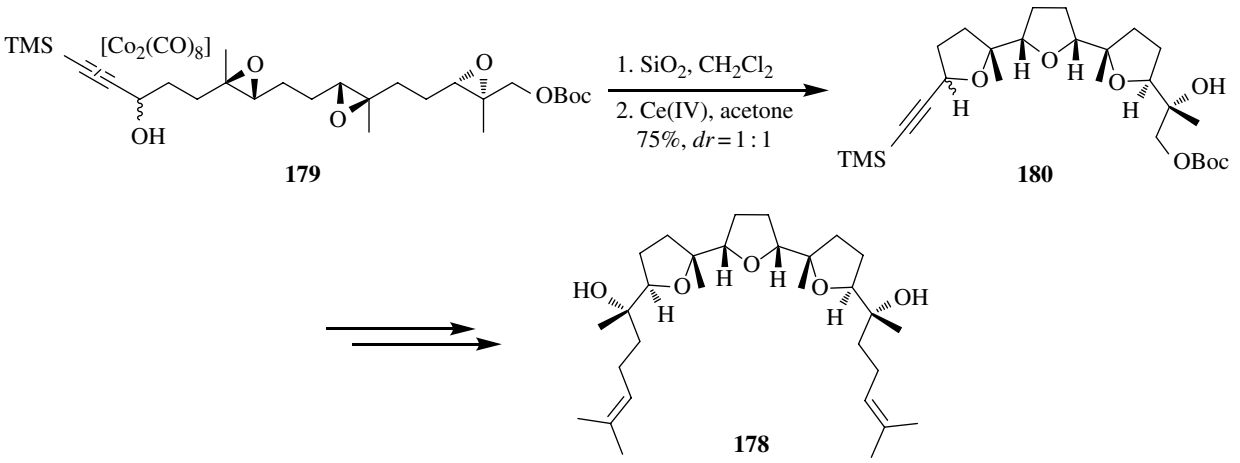
The Floreancig group employed an oxidatively initiated cascade cyclization for the synthesis of lactodehydrothyrsiferol (**175**; Scheme 4.38) [73]. The synthesis of substrate **176** employed a one-pot double epoxidation in which oxidizing the more reactive alkene in the diene precursor was achieved with the standard sorbose-derived Shi catalyst and the less reactive allylic carbonate was epoxidized in the same pot by a more reactive pseudoenantiomeric catalyst **113**. The cyclization proceeded smoothly initially but subsequently stalled, giving a 45% isolated yield of tricycle **177** and a 75% yield based on recovered starting material. The tricycle was converted to the natural product through a multistep sequence, where the generation of the acetal in the cascade cyclization facilitated the formation of the lactone group.

Martín showed that a Nicholas reaction could be applied to initiate a cascade reaction to form the natural product teurilene (**178**; Scheme 4.39) [74]. This procedure employed cobalt complex **179**, in which the epoxides were introduced through Sharpless and Shi protocols. Exposing **179** to silica gel led to ionization and epoxonium ion formation, initiating a cascade reaction that yielded tricycle **180** in 75% yield as a 1 : 1 mixture of diastereomers at the propargylic position after oxidative cobalt release. Interestingly the carbonate group in the substrate did not convert to a cyclic carbonate group, as has been often seen in related reactions. This mixture proved to be inconsequential since equilibration at that site could be achieved subsequently. The natural product was formed from **180** through a multistep sequence.

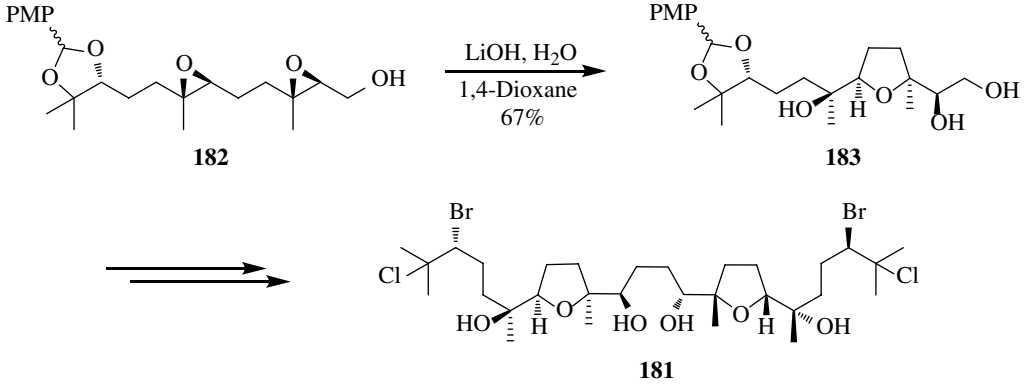
### 4.4.3 Cyclizations under Basic Conditions

Morimoto employed Hoye's strategy of promoting cascade cyclization reactions through a base-mediated Payne rearrangement in the total synthesis of intricatetraol (**181**; Scheme 4.40) [75]. Diepoxide **182** reacts with LiOH to initiate a Payne rearrangement that results in an *exo*-cyclization. The resulting epoxide opens to form the diol in **183** in the same transformation. Functional group interconversions and dimerization provided the natural product.

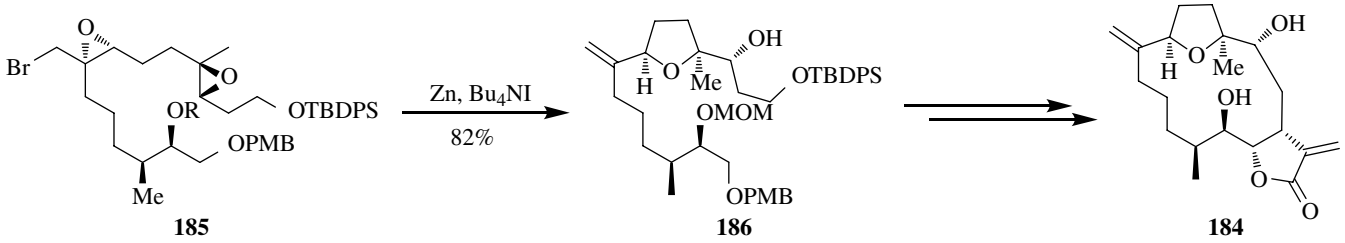
Marshall used reductive ring opening to generate an alkoxide that engaged in an epoxide-opening reaction toward the synthesis of compound **184**, a diastereomer of the natural product uprolide D (Scheme 4.41) [76]. Bromo epoxide **185**,




**SCHEME 4.39** Martín's synthesis of teurilene.




**SCHEME 4.40** Payne rearrangement approach to intricatetraol.



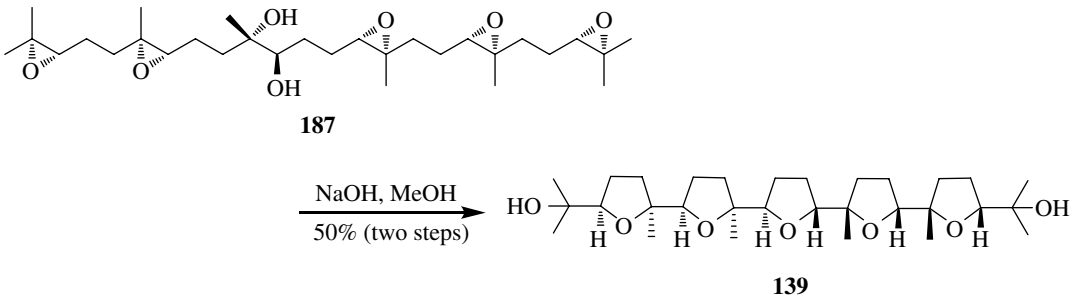

**SCHEME 4.41** Marshall's reductive approach to uprolide.

in which the epoxides were introduced by Sharpless and Shi epoxidations, was reduced with Zn in the presence of $Bu_4NI$ to form a zinc alkoxide that proceeded through an *exo*-cyclization pathway leading to **186**. This product was converted to **185** through a multistep sequence.

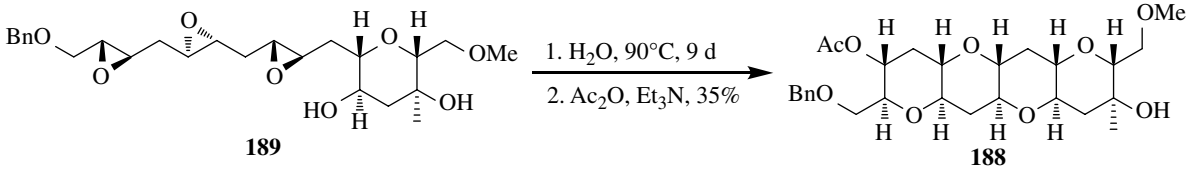
Qu employed a bidirectional approach to the synthesis of glabrescol (**139**; Scheme 4.42) [77]. Pentaepoxide **187**, formed through a Shi oxidation, was subjected to NaOH to deliver the natural product directly.

### 4.4.4 Cyclization in Water

Although no natural product synthesis has yet to be completed by a cascade in water under neutral conditions, the Jamison group has used the protocol to prepare the impressively complex tetra-tetrahydropyran core of the ladder toxin gymnocin (**188**; Scheme 4.43) [78]. Triepoxide **189** was heated to 80°C in water for 9 days to yield **188** in 35% yield. The reaction rate was slower than previously observed rates because the final cyclization step was sluggish. The authors




**SCHEME 4.42** Bidirectional approach to glabrescol.




**SCHEME 4.43** Jamison's approach to the gymnocin tetrahydropyran core.

attributed this observation to the presence of the inductively electron-withdrawing benzyl ether group, which had not been incorporated into previous substrates.

The examples in this section clearly highlight that a wide range of natural products and their subunits can be prepared through epoxide cascade reactions. The transformations do not result in a net increase of ring structures, since the substrates contain the same number of rings as the products. However, the strategy is desirable because of the accessibility of epoxides from simple alkene precursors and the facile conversion of epoxides to larger rings. As strategies for stereoselective epoxidation, innovations in substrate design, and mechanisms for cascade initiation evolve, the practicality of complex polyether synthesis will continue to improve, making useful quantities of these medicinally relevant compounds available for further study and function optimization.

## 4.5 CONCLUSIONS

Polyether natural products exhibit complex and aesthetically appealing molecular architectures and effect a wide range of biological responses. This merger has predictably drawn the interest of many in the scientific community with an interest in natural products. Early studies on the biosyntheses of these natural products implicated epoxides as key intermediates in the synthesis of polyether natural products. The logic of this process is exceptional. Alkenes are readily synthesized by biological synthesis, epoxides are easily accessed from alkenes through oxidative enzymes, nucleophilic additions into epoxides are facile due to strain release, and the products of the additions contain a hydroxyl group that can engage in additional reactions. Molecular biology, crystallography, and computational chemistry have played essential roles in strengthening these biosynthetic hypotheses.

The insights from the biosynthetic studies have inspired numerous methodological investigations into the use of epoxides to form larger cyclic ethers. Since epoxides contain two reactive sites, critical elements in these studies are controlling the regioselectivity of intramolecular nucleophilic additions. Base-promoted reactions should favor nucleophilic attack at the less substituted site, while acid-promoted reactions should favor nucleophilic attack at the more substituted site, though orbital overlap is an additional complication. Numerous strategies have been developed for controlling ring sizes through these pathways and have been employed in the design of cascade processes in which polyepoxides react to form multiple rings in a single transformation.

Advances in applying these studies to stereoselective oxacycle synthesis have been critically dependent upon the development of enantioselective epoxidation methods. Extensive research into designing these reactions has resulted in a wide range of structurally distinct epoxides being available in enantiomerically pure form through experimentally facile methods that utilize easily accessible catalysts. These enabling methods assure that substrate synthesis will not limit further exploration in epoxide-based cyclization reaction development.

The understanding of epoxide reactivity patterns and the availability of stereochemically defined epoxides has made complex natural products accessible through often shockingly short sequences. These efforts have resulted in the capacity to prepare analogs and probes that provide greater insight into the biological activities that these compounds effect.

Challenges still remain in this area despite the dramatic advances that have been detailed. Definitive proof of the epoxide cascade route to the marine ladder toxins has yet to be

found. Understanding the pathways by which organisms control the formation of the various sized rings in these compounds could prove to be exceedingly valuable in future synthesis efforts since versatile approaches to *endo*-cyclizations are still rare. Greater regiocontrol in selective epoxidation reactions of polyenes would facilitate substrate syntheses where polyepoxides are not configurationally homogeneous. Syntheses that utilize cascade reactions for the constructions of multiple rings of different size will certainly improve access to more complex ladder ethers. The continued interest in these pathways and targets and the creativity that their structures have inspired provide ample reason for optimism that these issues will be addressed in due course.

## REFERENCES


1. B. T. Ueberbacher, M. Hall, K. Faber, *Nat. Prod. Rep.* 2012, **29**, 337–350.
2. (a) M. M. Faul, B. E. Huff, *Chem. Rev.* 2000, **100**, 2407–2473; (b) K. A. Dion, II, D. A. F. Muejo, M. T. Hamann, *Expert Opin. Drug Discov.* 2009, **4**, 109–146.
3. J. J. Fernández, M. L. Souto, M. Norte, *Nat. Prod. Rep.* 2000, **17**, 235–246.
4. (a) K. C. Nicolaou, M. O. Frederick, R. J. Aversa, *Angew. Chem. Int. Ed.* 2000, **47**, 7182–7225; (b) T. Yasumoto, *Chem. Rec.* 2001, **1**, 228–242; (c) T. Yasumoto, M. Murata, *Chem. Rev.* 1993, **93**, 1897–1909.
5. L. Zeng, Q. Ye, N. H. Oberlies, G. Shi, Z.-M. Gu, K. He, J. L. McLaughlin, *Nat. Prod. Rep.* 1996, **13**, 275–306.
6. (a) I. Vilotijevic, T. F. Jamison, *Angew. Chem. Int. Ed.* 2009, **48**, 5250–5281; (b) I. Vilotijevic, T. F. Jamison, *Mar. Drugs* 2010, **8**, 763–809; (c) Y. Zhu, Q. Wang, R. G. Cornwall, Y. Shi, *Chem. Rev.* 2014, **114**, 8199–8256.
7. D. E. Cane, T. C. Liang, H. Hasler, *J. Am. Chem. Soc.* 1981, **103**, 5962–5965.
8. J. W. Westley, J. F. Blount, R. H., Evans, Jr., A. Stempel, J. Berger, *J. Antibiot.* 1974, **27**, 597–604.
9. D. E. Cane, W. D. Celmer, J. W. Westley, *J. Am. Chem. Soc.* 1983, **105**, 3594–3600.
10. A. Bhatt, C. B. W. Stark, B. M. Harvey, A. R. Gallimore, Y. A. Demydchuk, J. B. Spencer, J. Staunton, P. F. Leadlay, *Angew. Chem. Int. Ed.* 2005, **44**, 7075–7078.
11. L. Smith, H. Hong, J. B. Spencer, P. F. Leadlay, *Chembiochem* 2008, **9**, 2967–2975.
12. Y. Shichijo, A. Migita, H. Oguri, M. Watanabe, T. Tokiwano, K. Watanabe, H. Oikawa, *J. Am. Chem. Soc.* 2008, **130**, 12230–12231.
13. K. Hotta, X. Chem, R. S. Paton, A. Minami, H. Li, K. Swaminathan, I. I. Mathews, K. Watanabe, H. Oikawa, K. N. Houk, C.-Y. Kim, *Nature* 2012, **483**, 355–359.
14. (a) D. J. Tantillo, J. G. Chen, K. N. Houk, *Curr. Opin. Chem. Biol.* 1998, **2**, 743–750; (b) G. Kiss, N. Celebi-Olcum, R. Moretti, D. Baker, K. N. Houk, *Angew. Chem. Int. Ed.* 2013, **52**, 5700–5725.
15. (a) K. Nakanishi, *Toxicon* 1984, **23**, 473–479; (b) M. S. Lee, D. J. Repeta, K. Nakanishi, *J. Am. Chem. Soc.* 1986, **108**, 7855–7856.
16. (a) H.-N. Chou, Y. Shimizu, *J. Am. Chem. Soc.* 1987, **109**, 2184–2185; (b) A. V. Krishna Prasad, Y. Shimizu, *J. Am. Chem. Soc.* 1989, **111**, 6476–6477.
17. B. T. Ueberbacher, G. Oberdorfer, K. Gruber, K. Faber, *Chembiochem* 2009, **10**, 1697–1704.
18. M. Arand, B. M. Hallberg, J. Zou, T. Bergfors, F. Oesch, M. J. van der Werf, J. A. M. de Bont, T. A. Jones, S. L. Mowbray, *EMBO J.* 2003, **22**, 2583–2592.
19. (a) J. E. Baldwin, *J. Chem. Soc., Chem. Commun.* 1976, 734–736; (b) J. E. Baldwin, J. Cutting, W. Dupont, L. Kruse, L. Silberman, R. C. Thomas, *J. Chem. Soc., Chem. Commun.* 1976, 736–738; (c) J. E. Baldwin, T. C. Thomas, L. I. Kruse, L. Silberman, *J. Org. Chem.* 1977, **42**, 3846–3852; (d) J. E. Baldwin, M. J. Lusch, *Tetrahedron* 1982, **38**, 2939–2947.
20. J. Na, K. N. Houk, C. G. Shevlin, K. D. Janda, R. A. Lerner, *J. Am. Chem. Soc.* 1993, **115**, 8453–8454.
21. J. M. Coxon, M. P. Hartshorn, W. H. Swallow, *Aus. J. Chem.* 1973, **26**, 2521–2526.
22. T. Fukuyama, B. Vranesic, D. P. Degri, Y. Kishi, *Tetrahedron Lett.* 1978, **31**, 2741–2744.
23. W. C. Still, A. G. Romero, *J. Am. Chem. Soc.* 1986, **108**, 2105–2106.
24. S. L. Schreiber, T. Sammakia, B. Hulin, G. Shulte, *J. Am. Chem. Soc.* 1986, **108**, 2106–2108.
25. (a) K. C. Nicolaou, M. E. Duggan, C.-K. Hwang, P. K. Somers, *J. Chem. Soc., Chem. Commun.* 1985, 1359–1362; (b) K. C. Nicolaou, C. V. C. Prasad, P. K. Somers, C.-K. Hwang, *J. Am. Chem. Soc.* 1989, **111**, 5330–5334.
26. K. C. Nicolaou, C. V. C. Prasad, P. K. Somers, C.-K. Hwang, *J. Am. Chem. Soc.* 1989, **111**, 5335–5340.
27. Y. Morimoto, Y. Nishikawa, C. Ueba, T. Tanaka, *Angew. Chem. Int. Ed.* 2006, **45**, 810–812.
28. M. H. Wu, K. B. Kansen, E. N. Jacobsen, *Angew. Chem. Int. Ed.* 1999, **38**, 2012–2014.
29. L. A. Paquette, M. Vazeux, *Tetrahedron Lett.* 1981, **22**, 291–294.
30. H. E. Simmons, III, J. E. Maggio, *Tetrahedron Lett.* 1981, **22**, 287–290.
31. (a) F. E. McDonald, X. Wang, B. Do, K. I. Hardcastle, *Org. Lett.* 2000, **2**, 2917–2919; (b) F. E. McDonald, F. Bravo, X. Wang, X. Wei, M. Toganoh, J. R. Rodríguez, B. Do, W. A. Neiwert, K. I. Hardcastle, *J. Org. Chem.* 2002, 2515–2523; (c) F. Bravo, F. E. McDonald, W. A. Neiwert, B. Do, K. I. Hardcastle, *Org. Lett.* 2003, **5**, 2123–2126.
32. T. Nakata, S. Nomura, H. Matsukura, *Tetrahedron Lett.* 1996, **38**, 5545–5548.
33. (a) V. S. Kumar, D. L. Aubele, P. E. Floreancig, *Org. Lett.* 2002, **4**, 2489–2492; (b) V. S. Kumar, S. Wan, D. L. Aubele, P. E. Floreancig, *Tetrahedron Asymmetry* 2005, **16**, 3570–3578; (c) S. Wan, H. Gunaydin, K. N. Houk, P. E. Floreancig, *J. Am. Chem. Soc.* 2007, **129**, 7915–7923.
34. F. Bravo, F. E. McDonald, W. A. Neiwert, K. I. Hardcastle, *Org. Lett.* 2004, **6**, 4487–4489.

35. M. A. Tarselli, J. L. Zuccarello, S. J. Lee, M. R. Gagné, *Org. Lett.* 2009, **11**, 3490–3492.
36. Y. Xie, P. E. Floreancig, *Angew. Chem. Int. Ed.* 2003, **52**, 625–628.
37. F. R. P. Crisóstomo, T. Martín, V. S. Martín, *Org. Lett.* 2004, **6**, 565–568.
38. (a) T. R. Hoye, J. C. Suhadolnik, *J. Am. Chem. Soc.* 1985, **107**, 5312–5313; (b) T. R. Hoye, S. A. Jenkins, *J. Am. Chem. Soc.* 1987, **109**, 6196–6198.
39. J. A. Marshall, R. K. Hann, *J. Org. Chem.* 2008, **73**, 6753–6757.
40. (a) T. P. Heffron, T. F. Jamison, *Org. Lett.* 2003, **5**, 2339–2342; (b) G. L. Simpson, T. P. Heffron, E. Merino, T. F. Jamison, *J. Am. Chem. Soc.* 2006, **128**, 1056–1057.
41. (a) I. Vilotijevic, T. F. Jamison, *Science* 2007, **317**, 1189–1192; (b) C. J. Morten, T. F. Jamison, *J. Am. Chem. Soc.* 2009, **131**, 6678–6679; (c) J. J. Mousseau, C. J. Morten, T. F. Jamison, *Chem. Eur. J.* 2013, **19**, 10004–10016.
42. (a) J. A. Byers, T. F. Jamison, *J. Am. Chem. Soc.* 2009, **131**, 6383–6385; (b) C. J. Morten, J. A. Byers, T. F. Jamison, *J. Am. Chem. Soc.* 2011, **133**, 1902–1908; (c) J. A. Byers, T. F. Jamison, *Proc. Natl. Acad. Sci. U. S. A.* 2013, **110**, 16724–16729.
43. H. B. Henbest, R. A. L. Wilson, *J. Chem. Soc.* 1957, 1958–1965.
44. (a) K. B. Sharpless, R. C. Michaelson, *J. Am. Chem. Soc.* 1973, **95**, 6136–6137; (b) S. Tanaka, H. Yamamoto, H. Nozaki, K. B. Sharpless, R. C. Michaelson, J. D. Cutting, *J. Am. Chem. Soc.* 1974, **96**, 5254–5255; (c) A. O. Chong, K. B. Sharpless, *J. Org. Chem.* 1977, **42**, 1587–1590.
45. (a) T. Katsuki, K. B. Sharpless, *J. Am. Chem. Soc.* 1980, **102**, 5974–5976; (b) B. E. Rossiter, T. Katsuki, K. B. Sharpless, *J. Am. Chem. Soc.* 1981, **103**, 464–465; (c) V. S. Martin, S. S. Woodard, T. Katsuki, Y. Yamada, M. Ikeda, K. B. Sharpless, *J. Am. Chem. Soc.* 1981, **103**, 6237–6240.
46. (a) Y. Gao, R. M. Hanson, J. M. Klunder, S. Y. Ko, H. Masamune, K. B. Sharpless, *J. Am. Chem. Soc.* 1987, **109**, 5765–5780; (b) M. G. Finn, K. B. Sharpless, *J. Am. Chem. Soc.* 1991, **113**, 113–126.
47. (a) K. B. Sharpless, S. S. Woodard, M. G. Finn, *Pure Appl. Chem.* 1983, **55**, 1823–1836; (b) S. S. Woodard, M. G. Finn, K. B. Sharpless, *J. Am. Chem. Soc.* 1991, **113**, 106–113; (c) E. J. Corey, *J. Org. Chem.* 1990, **55**, 1693–1694; (d) K. A. Jørgensen, R. A. Wheeler, R. Hoffmann, *J. Am. Chem. Soc.* 1987, **109**, 3240–3246; (e) R. D. Bach, G. J. Wolber, B. A. Coddens, *J. Am. Chem. Soc.* 1984, **106**, 6098–6099.
48. M. G. Finn, K. B. Sharpless, *J. Am. Chem. Soc.* 1991, **113**, 113–126.
49. (a) W. Zhang, A. Basak, Y. Kosugi, Y. Hoshino, H. Yamamoto, *Angew. Chem. Int. Ed.* 2005, **44**, 4389–4391; (b) W. Zhang, H. Yamamoto, *J. Am. Chem. Soc.* 2006, **129**, 286–287.
50. C. Wang, H. Yamamoto, *J. Am. Chem. Soc.* 2014, **136**, 1222–1225.
51. Z.-X. Wang, Y. Tu, M. Frohn, J.-R. Zhang, Y. Shi, *J. Am. Chem. Soc.* 1997, **119**, 11224–11235.
52. M.-X. Zhao, Y. Shi, *J. Org. Chem.* 2006, **71**, 5377–5379.
53. X.-Y. Wu, X. She, Y. Shi, *J. Am. Chem. Soc.* 2002, **124**, 8792–8793.
54. H. Tian, X. She, L. Shu, H. Yu, Y. Shi, *J. Am. Chem. Soc.* 2002, **122**, 11551–11552.
55. S. E. Schaus, B. D. Brandes, J. F. Larrow, M. Tokunaga, K. B. Hansen, A. E. Gould, M. E. Furrow, E. N. Jacobsen, *J. Am. Chem. Soc.* 2002, **124**, 1307–1315.
56. N. Z. Burns, P. S. Baran, R. W. Hoffmann, *Angew. Chem. Int. Ed.* 2009, **48**, 2854–2867.
57. M. Marigo, J. Franzén, T. B. Poulsen, W. Zhuang, K. A. Jørgensen, *J. Am. Chem. Soc.* 2005, **127**, 6964–6965.
58. S. Lee, D. W. C. MacMillan, *Tetrahedron* 2006, **62**, 11413–11424.
59. O. Lifchits, M. Mahlau, C. M. Reisinger, A. Lee, C. Farès, I. Polyak, G. Gopakumar, W. Thiel, B. List, *J. Am. Chem. Soc.* 2013, **135**, 6677–6693.
60. (a) S.-J. Jeon, P. J. Walsh, *J. Am. Chem. Soc.* 2003, **125**, 9544–9545; (b) A. E. Lurain, A. Maestri, A. R. Kelly, P. J. Carroll, P. J. Walsh, *J. Am. Chem. Soc.* 2004, **126**, 13608–13609; (c) S.-J. Jeon, H. Li, P. J. Walsh, *J. Am. Chem. Soc.* 2005, **127**, 16416–16425.
61. T. R. Hoye, Z. Ye, *J. Am. Chem. Soc.* 1996, **118**, 1801–1802.
62. Z. Xu, E. J. Corey, *J. Am. Chem. Soc.* 2000, **122**, 4831–4832.
63. Z. Xu, E. J. Corey, *J. Am. Chem. Soc.* 2000, **122**, 9328–9329.
64. Y. Morimoto, T. Iwai, T. Kinoshita, *Tetrahedron Lett.* 2001, **42**, 6307–6309.
65. Y. Morimoto, H. Yata, Y. Nishikawa, *Angew. Chem. Int. Ed.* 2007, **46**, 6481–6484.
66. Z. Xiong, R. Busch, E. J. Corey, *Org. Lett.* 2010, **12**, 1512–1514.
67. Y. Morimoto, T. Okita, H. Kambara, *Angew. Chem. Int. Ed.* 2009, **48**, 2538–2541.
68. B. S. Underwood, J. Tanuwidjaja, S.-S. Ng, T. F. Jamison, *Tetrahedron* 2013, **69**, 5205–5220.
69. A. Zakarian, A. Batch, R. A. Holton, *J. Am. Chem. Soc.* 2003, **125**, 7822–7824.
70. R. Tong, J. C. Valentine, F. E. McDonald, R. Cao, X. Fang, K. I. Hardcastle, *J. Am. Chem. Soc.* 2007, **129**, 1050–1051.
71. (a) R. Tong, F. E. McDonald, *Angew. Chem. Int. Ed.* 2008, **47**, 4377–4379; (b) M. A. Boone, R. Tong, F. E. McDonald, S. Lense, R. Cao, K. I. Hardcastle, *J. Am. Chem. Soc.* 2010, **132**, 5300–5308.
72. J. Tanuwidjaja, S.-S. Ng, T. F. Jamison, *J. Am. Chem. Soc.* 2009, **131**, 12084–12085.
73. D. J. Clausen, S. Wan, P. E. Floreancig, *Angew. Chem. Int. Ed.* 2011, **50**, 5178–5181.
74. J. Rodríguez-López, F. P. Crisóstomo, N. Ortega, M. López-Rodríguez, V. S. Martín, T. Martín, *Angew. Chem. Int. Ed.* 2013, **52**, 3659–3662.
75. Y. Morimoto, T. Okita, M. Takaishi, T. Tanaka, *Angew. Chem. Int. Ed.* 2007, **46**, 1132–1135.
76. J. A. Marshall, C. A. Griot, H. R. Chobanian, W. H. Myers, *Org. Lett.* 2010, **12**, 4328–4331.
77. P. Yang, P.-F. Li, J. Qu, L.-F. Tang, *Org. Lett.* 2012, **14**, 3932–3935.
78. A. R. Van Dyke, T. F. Jamison, *Angew. Chem. Int. Ed.* 2009, **48**, 4430–4432.

# SECTION II

# MEVALONATE BIOSYNTHETIC PATHWAY

# 5

# FROM ACETATE TO MEVALONATE AND DEOXYXYLULOSE PHOSPHATE BIOSYNTHETIC PATHWAYS: AN INTRODUCTION TO TERPENOIDS

Alexandros L. Zografos[1] and Elissavet E. Anagnostaki[1,2]

[1] *Department of Chemistry, Laboratory of Organic Chemistry, Aristotle University of Thessaloniki, Thessaloniki, Greece*
[2] *Research and Development Department, Pharmathen S.A., Thessaloniki, Greece*

## 5.1 INTRODUCTION

Terpenes and their oxidized members, terpenoids, constitute the largest and most diverse family of natural products in nature [1]. Terpene structures contain $(C_5)_n$ diverse carbon skeletons derived from the chemical connection of $C_5$ isoprene units in a head-to-tail fashion. Typical terpenes are classified to subgroups of five-carbon atoms chains, independently of their diverse connectivities. Thus, taxonomically, terpenes are subdivided to hemiterpenes ($C_5$), monoterpenes ($C_{10}$), sesquiterpenes ($C_{15}$), diterpenes ($C_{20}$), sesterterpenes ($C_{25}$), triterpenes ($C_{30}$), and tetraterpenes ($C_{40}$), whereas in some cases higher polymers can be encountered in materials like natural rubber (Fig. 5.1) [2].

Biosynthetically, all terpenoids are traced back to a common synthon of biochemically active isoprene unit found in the forms of pyrophosphate esters either as dimethylallyl diphosphate (DMAPP) or isopentenyl diphosphate (IPP) (Fig. 5.1). In turn, DMAPP and IPP are derived by two distinct biosynthetic pathways, *the mevalonate pathway* (MVA pathway) and the *mevalonate-independent pathway* or *pathway of deoxyxylulose phosphate* (DXP pathway), which are considered to be the major "natural synthetic routes" for the synthesis of terpenoids (Fig. 5.2).

The *mevalonate pathway* [3] is an important primary, cellular, metabolic pathway, which is present in all higher eukaryotes and many bacteria. It serves, as the basis for the biosynthesis of DMAPP and IPP, not only for the production of useful for the defense of the organism secondary metabolites but also for protein prenylation [4], cell membrane maintenance, protein anchoring, etc. In contrast to the classical mevalonate pathway, apicomplexan protozoa, such as malaria parasites, and most of the bacteria are producing terpenoids by an alternative pathway, the *mevalonate-independent pathway or pathway of deoxyxylulose phosphate* [5]. Plants, on the other hand, have the ability to use both the MVA pathway and the DXP pathways for isoprenoid synthesis. The accurate compartmentations of these metabolic processes in the cells of the plants have not been yet firmly elucidated. It is believed that the mevalonate pathway is running in the cytosol, while the deoxyxylulose phosphate pathway is producing "active isoprene units" in their plastids (Fig. 5.3) [6]. Substrate exchanges between the plastids and the cytosolic pathways could occur at the level of IPP production, which is highly resistant to endemic phosphatases [7]. Further biosynthetic transformations concerning the final oxidative state of the terpenoids are usually taken place in the endoplasmic reticulum of the cell. Usually, sesquiterpenoids, triterpenoids, and higher terpenoids are cytosolic products, while monoterpenoids and diterpenoids are formed in the plastids. Mitochondria also participate in isoprenoid biosynthesis [8].

*From Biosynthesis to Total Synthesis: Strategies and Tactics for Natural Products*, First Edition. Edited by Alexandros L. Zografos.
© 2016 John Wiley & Sons, Inc. Published 2016 by John Wiley & Sons, Inc.

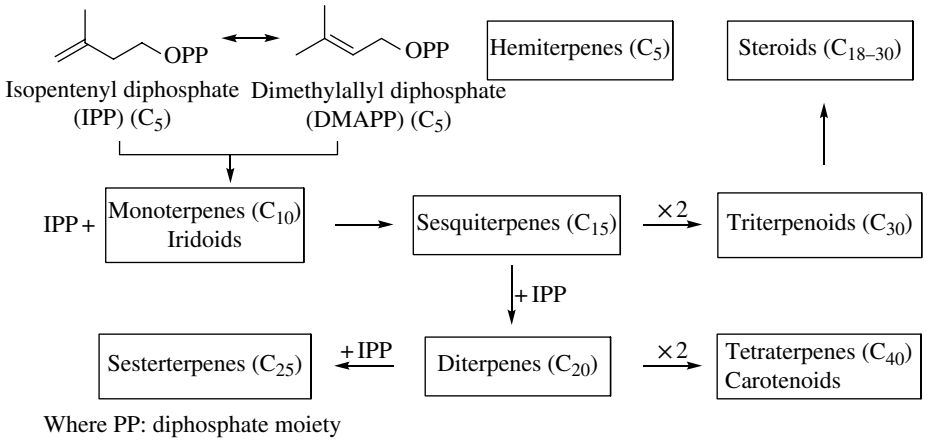



**FIGURE 5.1** Classification of terpenoids based on isoprene units.

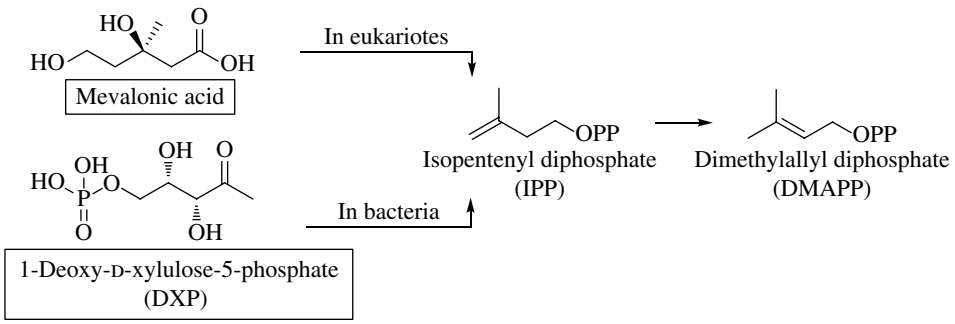



**FIGURE 5.2** The two basic biosynthetic pathways to IPP and DMAPP scaffolds.

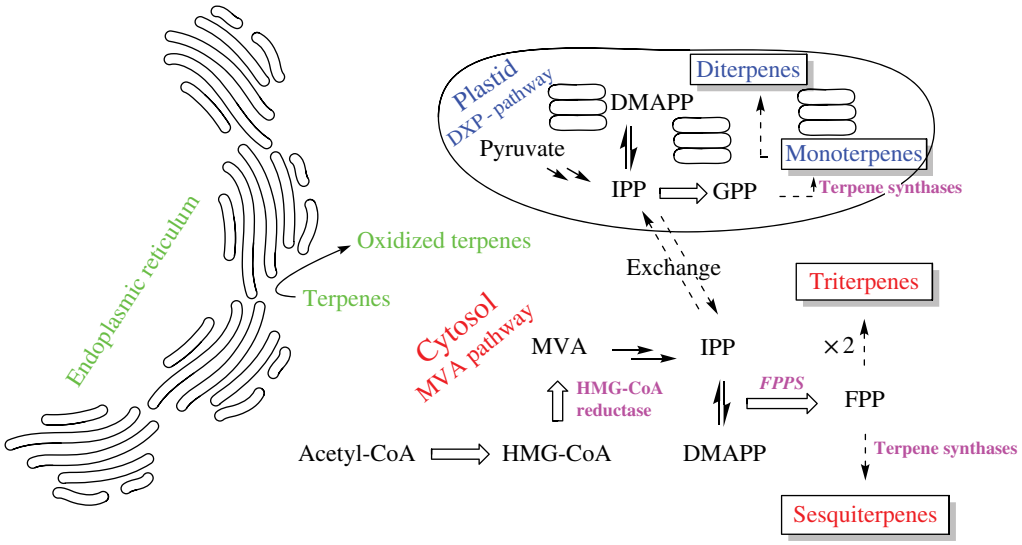



**FIGURE 5.3** Subcellular compartmentation of terpenoid biosynthesis in plants.

## 5.2 MEVALONIC ACID PATHWAY

Mevalonic acid itself is a product of acetate metabolism. Three molecules of acetate coenzyme A, produced by the citric acid cycle, are used to form mevalonic acid (Scheme 5.1). Two molecules undergo a Claisen condensation *via* acetyl-CoA–acetyltransferase enzyme [EC 2.3.1.9] to produce acetoacetyl-CoA, and a third is incorporated in a stereospecific aldol addition to the formation of β-hydroxy-β-methylglutaryl-CoA (HMG-CoA) by the aid of HMG-CoA synthase [EC 2.3.3.10]. The first Claisen reaction was found to involve formation of Cys-89 acetyl-*S*-enzyme reaction intermediate [9]. Then, Cys-378 residue on the active site of the enzyme activates a second molecule of acetyl-CoA to initiate the condensation reaction (Fig. 5.4) [11]. Similarly, in HMG-CoA synthases (*S. aureus* HMG-CoA synthase), Cys111/129 are the crucial residues of covalent attach to acetyl-CoA to produce acetyl-enzyme thioester with the subsequent loss of coenzyme A (Fig. 5.4). Glu79/95 residues are responsible for the enolization of acetyl-enzyme intermediate in order to react with acetoacetyl-CoA, which is bound to His233/264 residues [12].

In contrast to this context, in the acetate pathway (please refer to biosynthetic parts of Chapters 2–4), an acetoacetic acid thioester in an acyl carrier protein (ACP) would have been formed by the use of the more nucleophilic malonic acid thioester. This crucial difference of reactant selection distinguishes the two biosynthetic pathways from the very first step.

Next to the mevalonate biosynthesis is the reduction of HMG-CoA to mevalonic acid by HMG-CoA reductase [EC 1.1.1.34] (Scheme 5.1). The enzyme is found in eukaryotes, archaebacteria, and some eubacteria. The conversion of the thioesterified HMG-CoA carboxyl to alcohol represents a two-step reaction. The reaction proceeds through the successive reduction to first produce bound mevaldyl-CoA, collapse of the thiohemiacetal to release CoASH and form mevaldehyde, and further reduced to produce mevalonic acid. Investigations on the structures of the soluble catalytic domain of human HMG-CoA enzyme liganded to substrates or products revealed three residues (Asp767, Lys691, and Glu559) to be implicated in the enzyme function [13].

As soon as mevalonate acid has formed, a series of enzymes are involved in order to transform MVA to IPP. Mevalonate kinase [EC 2.7.1.36] phosphorylates the primary alcohol to mevalonate 5-phosphate, whereas phosphomevalonate kinase [EC 2.7.4.2] produces 5-pyrophosphomevalonate

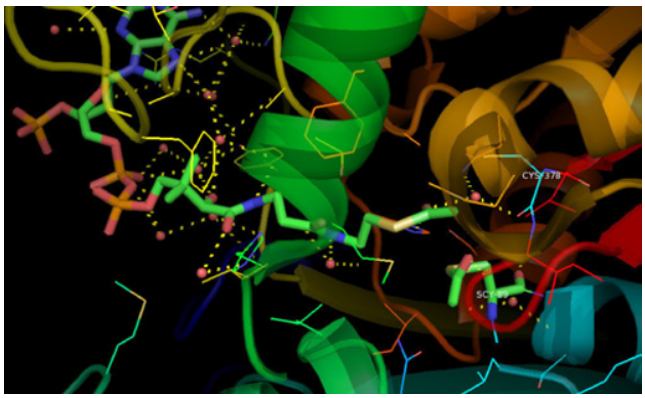
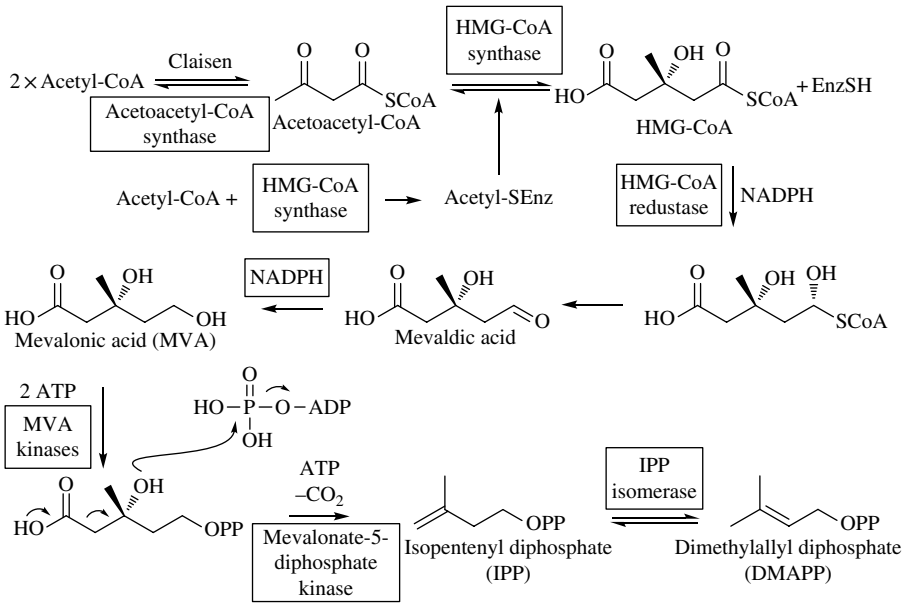


**FIGURE 5.4** Acetylated crystal structure of acetoacetyl-CoA transferase from *Zoogloea ramigera* cocrystallized with acetyl-CoA based on structural coordinates PDB: 1DM3 [10]. (*See insert for color representation of the figure.*)




**SCHEME 5.1** Mevalonate biosynthetic pathway.

(Scheme 5.1). Both kinases are utilizing a Mg-ATP binding site, which promotes the reversible phosphorylation in the appropriate sides of mevalonate [14, 15].

Mevalonate-5-pyrophosphate decarboxylase [EC 4.1.1.33] catalyzes the ATP-dependent decarboxylation of 5-pyrophosphate mevalonate to form IPP. While a third molecule of ATP is essential for this decarboxylation, there is no evidence for the direct phosphorylation of the free hydroxyl group. Probably ATP acts synergistically for the loss of the hydroxyl group by triggering a concerted rather than a dissociative decarboxylation process to produce IPP [16]. Finally, IPP isomerase [EC 5.3.3.2] promotes the allylic isomerization of IPP to the more stable isomer DMAPP. This reaction was found to be stereospecific removing the *pro*-R proton from C-2 of IPP and incorporating a proton from water to C-4 of DMAPP. The antarafacial stereochemistry of the isomerization is consistent with an active site containing two residues (Cys87, Glu 149 in humans) located in the opposite faces of the allyl moiety in IPP to assist the addition and elimination of protons [17].

Mevalonic acid pathway represents a primary metabolic pathway in all eukaryotes producing all the essential steroids in the organism and therefore it controls major metabolic pathways for its survival. The rate-determining step of this metabolic process is found to be the formation of mevalonic acid by HMG-CoA reductase in cytosol. Normally in mammalian cells this enzyme is suppressed by cholesterol derived from the internalization and degradation of low-density lipoprotein (LDL) *via* the LDL receptor, as well as oxidized species of cholesterol. It is worth mentioning that inhibition of the active center of HMG-CoA reductase accounts for the strong efficacy of statin drugs (e.g., rosuvastatin (CRESTOR), atorvastatin (Lipitor), etc.) in regulation of human cholesterol [18]. These drugs are used to lower serum cholesterol as a means of reducing the risk for cardiovascular disease.

## 5.3 MEVALONATE-INDEPENDENT PATHWAY

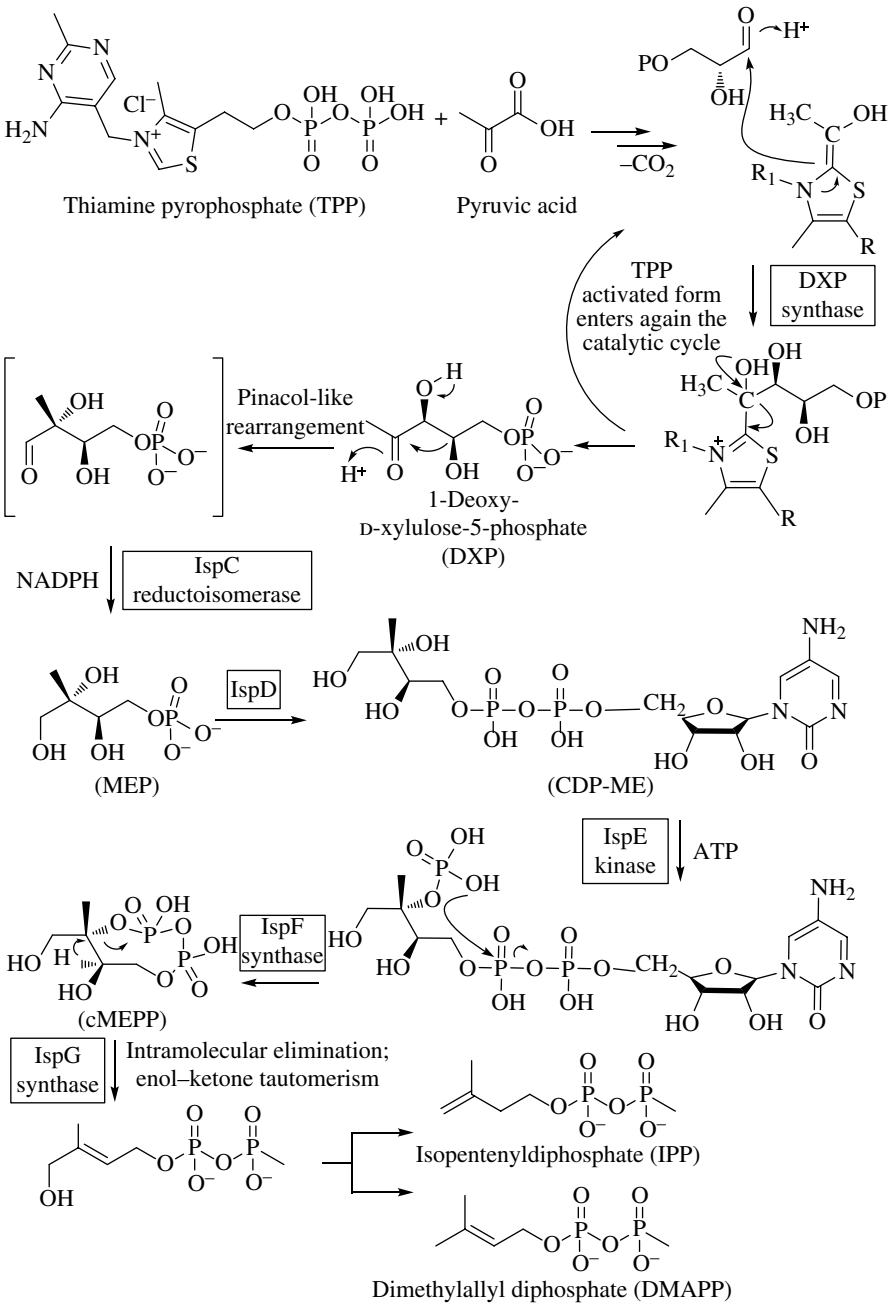
1-Deoxy-D-xylulose-5-phosphate (DXP) is the key intermediate used from protozoa, bacteria, and some plants to produce IPP and DMAPP scaffolds through the mevalonate-independent pathway. DXP is produced by pyruvic acid and glyceraldehyde 3-phosphate (Scheme 5.2), both products of glycolysis, catalyzed by DXP synthase [EC 2.2.1.7], with thiamine pyrophosphate (TPP) acting as a cofactor. In the first step of this sequence, pyruvic acid is decarboxylated and activated forming the activated enamine form of acetaldehyde with TPP. Nucleophilic attack of the enamine to glyceraldehyde 3-phosphate, catalyzed by DXP synthase, produces DXP after subsequent loss of TPP carrier, which is regenerated (Fig. 5.5). Several key interactions have been identified following the cocrystallization of DXP synthase from *Deinococcus radiodurans* with TPP [19]. The pyrophosphate moiety of TPP is divalently coordinated to a $Mg^{2+}$ ion, which is also coordinated by two acidic residues (Fig. 5.5). Pyruvate covalently binds to TPP *via* the C-2 atom of the thiazolium ring. Glyceraldehyde 3-phosphate is predicted to interact with His51, His304, Tyr395, and Arg480, which form the binding pocket.

Following the DXP pathway, a pinacol-like rearrangement of DXP, followed by NAPDH-dependent reduction, which is realized by 1-deoxy-D-xylulose-5-phosphate reductoisomerase (IspC) [1.1.1.267] [20], provides 2-C-methyl-D-erythritol-4-phosphate (MEP) (Scheme 5.2). More than 30 crystal structures have been published for this enzyme, mostly from *Escherichia coli*, *Mycobacterium tuberculosis*, and *Plasmodium falciparum*. NADPH, which acts as a cofactor, is located in the *N*-terminal domain, which includes the majority of the active site residues. $Mg^{2+}$ ion is indispensable for the catalytic activity of the enzyme. DXP is binding to Lys125, Glu231, Glu152, Asn227, and Lys 228 residues consisting the active site of the enzyme. IspC is perhaps the most widely cited therapeutic target in DXP pathway. Fosmidomycin, one of the most potent inhibitors of DXP pathway to date, inhibits this IspC from multiple organisms [21].

From this point, MEP is coupled to cytidine triphosphate to produce 4-diphosphocytidyl-2*C*-methyl-D-erythritol (CDP-ME) in a reaction, which is catalyzed by 4-diphosphocytidyl-2C-methyl-D-erythritol transferase (IspD) [2.7.7.60] (Scheme 5.2). IspD structure–mechanism analysis showed that a sequential mechanism applies with a $Mg^{2+}$ ion coordinating first, followed by CTP binding and then MEP [22]. The cytosine base portion of the substrate or the product is hydrogen bonded to Ala14, Ala15, Gly82, Asp 83, and Sep88 based on studies conducted on product-bound cocrystal of IspD from *E. coli* [23].

CDP-ME undergoes phosphorylation by an ATP-dependent kinase, 4-diphosphocytidyl-2C-methyl-D-erythritol kinase (IspE) [2.7.1.148] (Scheme 5.2). Examination of the *E. coli* IspE crystal structure cocrystallized with CDP-ME, and the nonfunctional analog of ATP/ATP-PNP reveals that the active site of the enzyme is positioned at the interphase of N-terminal and C-terminal domains [24]. The CDP-ME binding site is adjacent to the ATP/ATP-PNP binding pocket interacting majorly with Tyr25, Phe185, and His26 residues.

The phosphorylated CDP-ME substrate is then cyclized to the cyclic phosphoanhydride cMEPP, with the aid of 2C-methyl-D-erythritol-2, 4-cyclodiphosphate (MECP) synthase (IspF) [4.6.1.12], and subsequent loss of a CTP molecule (Scheme 5.2). IspF is arranged in a bell-shaped homotrimer with each active site located at the interphase of two monomeric units, thereby providing three active sites per trimer [25]. Each active sites accommodate phosphorylated CDP-ME and two cations $Zn^{+2}$ and $Mn^{+2}$, both of which are required for catalysis. These metal ions act to position and polarize the substrate for the intramolecular cyclization.




**SCHEME 5.2** Deoxyxylulose phosphate pathway or mevalonate-independent pathway.

Substrate binding pocket of IspF from *E. coli* consists of Ile57, Leu76, Ser35, Ser73, and Asp63 residues.

Finally, a two electron reduction of cMEPP forms 2-methyl-2-(*E*)-butenyl diphosphate followed by conversion to IPP and DMAPP. These steps are catalyzed by 1-hydroxy-2-methyl-2-(*E*)-butenyl-4-diphosphate synthase (IspG) [26] and 4-hydroxy-3-methyl-2-(*E*)-butenyl-4-diphosphate reductase (IspH) [27], respectively. IspG and IspH enzymes possess [4Fe–4S] iron–sulfur redox cluster in their C-terminal domains, which represents the active center of the enzymes. The newest cocrystal structures of IspH from *E. coli* revealed the presence of a [4Fe–4S] cluster when the substrate is bound and a [3Fe–4S] cluster when the products are bound.

Animals appears to lack DXP pathway completely, thus formation of terpenes is exclusively produced by mevalonate pathway. It has to be pointed out that inhibitors of mevalonate pathway enzyme HMG-CoA reductase, like statins, do not affect the production of terpenoids by DXP pathway due to the absence of the particular enzyme in this metabolic pathway. On the other hand, it is possible to inhibit terpenoid production without affecting steroid formation by selectively inhibit DXP pathway in plants (e.g., fosmidomycin antibiotic) [5b, 28].

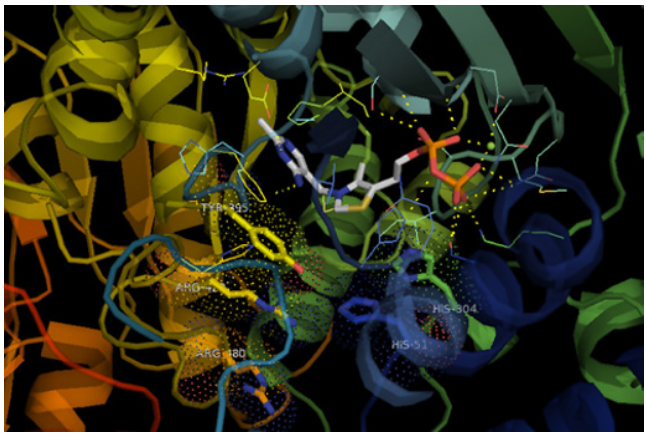



**FIGURE 5.5** Active site of DXP synthase from *D. radiodurans* based on structural coordinates PDB: 2O1X. TPP-cofactor is shown in stick colored by element, magnesium atom is shown in stick colored in grey-scale by element, active binding site of glyceraldehyde-3-phosphate is highlighted by dots [10a]. (*See insert for color representation of the figure*.)

## 5.4 CONCLUSION

MVA and DXP biosynthetic pathways provide the essential "active isopropene units" in the form of IPP and DMAPP for the construction of natural terpenoids. Following this introduction, terpenoids have been organized in accordance to their major classifications into four subchapters, monoterpenes, sesquiterpenes, diterpenes, and higher terpenes. In each of these chapters, a detailed biosynthetic analysis is attempted. Thus, the current chapter serves only as an introduction and by any mean does not serve as an exhaustive review on the topic of mevalonic and deoxyxylulose biosynthetic pathways.

## REFERENCES

1. (a) C. Sacchettini, C. D. Poulter, *Science* 1997, **277**, 1788–1789; (b) For a review on modern synthetic efforts towards some of the most classical biological active terpenes: T. J. Maimone, P. S. Baran, *Nat. Chem. Biol.* 2007, **3**, 396–407.
2. (a) P. M. Dewick, *Medicinal Natural Products: A Biosynthetic Approach*, 2nd Edition, John Wiley & Sons, Inc., New York (2002): refer to Chapter 5, pp. 167–285; (b) J. S. Dickchat, *Nat. Prod. Rep.* 2011, **28**, 1917–1936.
3. (a) K. Bloch, *Science* 1965, **150**, 19–28; (b) H. M. Miziorko, *Arch. Biochem. Biophys.* 2011, **505**, 131–143.
4. (a) C. C. Palsuledasai, M. D. Distefano, *ACS Chem. Biol.* 2015, **10**, 51–62; (b) X. Na, S. Ning, W. XiuXing, J. Shan, X. Bin, L. ChaoJun, *Sci. China Life Sci.* 2015, **58**, 328–335.
5. (a) T. Gräwert, M. Groll, F. Rohdich, A. Bacher, W. Eisenreich, *Cell. Mol. Life Sci.* 2011, **68**, 3797–3814; (b) I. Hale, P. M. O'Neill, A. Odom, R. Sharma, *Med. Chem. Commun.* 2012, **3**, 418–433; (c) L. Zhao, W.-C. Chang, Y. Xiao, H.-W. Liu, P. Liu, *Annu. Rev. Biochem.* 2013, **82**, 497–530.
6. (a) W. Eisenreich, A. Bacher, D. Arigoni, F. Rohdich, *Cell. Mol. Life Sci.* 2004, **61**, 1401–1426; (b) W. N. Hunter, *J. Biol. Chem.* 2007, **282**, 21573–21577 (c) J. Joyard, M. Ferro, C. Masselon, D. Seigneurin-Berny, D. Dalvi, J. Garin, N. Rolland, *Mol. Plant* 2009, **2**, 1154–1180.
7. F. Bouvier, C. Suire, A. d'Harlingue, R. A. Backhaus, B. Camara, *Plant J.* 2000, **24**, 241–252.
8. F. Bouvier, A. Rahier, B. Camara, *Prog. Lipid Res.* 2005, **44**, 357–429.
9. S. Thompson, F. Mayerl, O. P. Peoples, S. Masamune, A. J. Sinkey, C. T. Walsh, *Biochemistry* 1989, **28**, 5735–5742.
10. (a) Image created with PyMol: LLC Schrodinger, *The PyMOL Molecular Graphic System*, Version 1,3r1; 2010; (b) Y. Modis, R. K. Wierenga, *J. Mol. Biol.* 2000, **297**, 1171–1182.
11. M. A. J. Palmer, R. Gamboni, S. F. Williams, O. P. Peoples, C. T. Walsh, A. J. Sinskey, S. Masamune, *J. Biol. Chem.* 1991, **266**, 8369–8375.
12. M. J. Theisen, I. Misra, D. Saadat, N. Campobasso, H. M. Miziorko, D. H. Harrison, *Proc. Natl. Acad. Sci. U. S. A.* 2004, **101**, 16442–16447.
13. (a) C. M. Lawrence, V. W. Rodwell, C. V. Stauffacher, *Science* 1995, **268**, 1758–1762; (b) L. Tabernero, D. A. Bochar, V. W. Rodwell, C. V. Stauffacher, *Proc. Natl. Acad. Sci. U. S. A.* 1999, **96**, 7167–7171.
14. Z. Fu, M. Wang, D. Potter, H. M. Miziorko, J. J. Kim, *J. Biol. Chem.* 2002, **277**, 18134–18142.
15. (a) H. Hellig, G. Popjak, *J. Lipid Res.* 1961, **2**, 235–243; (b) S. Bazaes, E. Beytia, A. M. Jabalquinto, F. Solis de Ovando, I. Gomez, J. Eyzaguirre, *Biochemistry* 1980, **19**, 2300–2304.
16. S. T. Lefurgy, S. B. Rodriguez, C. S. Park, S. Cahill, R. B. Silverman, T. S. Leyh, *J. Biol.Chem.* 2010, **285**, 20654–20663.
17. W. Zheng, F. Sun, M. Bartlam, X. Li, R. Li, Z. Rao, *J. Mol. Biol.* 2007, **366**, 1447–1458.
18. E. S. Istvan, J. Deisenhofer, *Science* 2001, **292**, 1160–1164.
19. S. Xiang, G. Usunow, G. Lange, M. Busch, L. Tong, *J. Biol. Chem.* 2007, **282**, 2676–2682.
20. P. J. Proteau, *Bioorg. Chem.* 2004, **32**, 483–493.
21. A. Mac Sweeney, R. Lange, R. P. M. Fernandes, H. Schulz, G. E. Dale, A. Douangamath, P. J. Proteau, C. Oefner, *J. Mol. Biol.* 2005, **345**, 115–127.
22. S. Richard, A. M. Lillo, C. Tetzlaff, M. E. Bowman, J. P. Noel, D. E. Cane, *Biochemistry* 2004, **43**, 12189–12197.
23. S. B. Richard, M. E. Bowman, W. Kwiatkowski, I. Kang, C. Chow, M. A. Lillo, D. E. Cane, J. P. Noel, *Nat. Struct. Biol.* 2001, **8**, 641–648.
24. L. Miallau, M. S. Alphey, L. E. Kemp, G. A. Leonard, S. M. McSweeney, S. Hecht, A. Bacher, W. Eisenreich, F. Rohdich, W. N. Hunter, *Proc. Natl. Acad. Sci. U. S. A.* 2003, **100**, 9173–9178.
25. S. Steinbacher, J. Kaiser, J. Wungsintaweekul, S. Hecht, W. Eisenreich, S. Gerhardt, A. Bacher, F. Rohdich, *J. Mol. Biol.* 2002, **316**, 79–88.

26. M. Lee, T. Gräwert, F. Quitterer, F. Rohdich, J. Eppinger, W. Eisenreich, A. Bacher, M. Groll, *J. Mol. Biol.* 2010, **404**, 600–610.

27. T. Gräwert, F. Rohdich, I. Span, A. Bacher, W. Eisenreich, J. Eppinger, M. Groll, *Angew. Chem. Int. Ed.* 2009, **48**, 5756–5759.

28. H. Jomaa, J. Wiesner, S. Sanderbrand, B. Altincicek, C. Weidemeyer, M. Hintz, I. Turbachova, M. Eberl, J. Zeidler, H. K. Lichtenthaler, D. Soldati, E. Beck, *Science* 1999, **285**, 1573–1576.

# 6

# MONOTERPENES AND IRIDOIDS

Mario Waser[1] and Uwe Rinner[1,2]

[1] *Institute of Organic Chemistry, Johannes Kepler University Linz, Linz, Austria*
[2] *Department of Chemistry, College of Science, Sultan Qaboos University, Muscat, Oman*

## 6.1 INTRODUCTION

Monoterpenes and iridoids are important classes of secondary metabolites, and their biosynthesis as well as total synthesis approaches to access these compounds has attracted the interest of chemists for a long time. This overview will summarize the most important biosynthesis pathways and in addition will illustrate how one of the most important recent developments in organic chemistry, asymmetric organocatalysis, contributed in the development of total synthesis approaches toward these compounds. Therefore, a comprehensive introduction to asymmetric organocatalysis will be given as well. However, it should be noted that the applicability of this methodology to the synthesis of natural products is of course not only limited to monoterpenes and iridoids but holds much promise for other classes of primary and secondary metabolites as well.

## 6.2 BIOSYNTHESIS

The biosynthetic pathways leading to the formation of (mono)terpenes by different organisms have been systematically investigated in the past [1–4]. As already discussed in the preceding chapter, the biosynthesis sequence commences with formation of the two key building blocks isopentenyl diphosphate (IPP, **1**) and dimethylallyl diphosphate (DMAPP, **2**) either via the mevalonate or the mevalonate-independent pathway [1, 3, 4]. These two compounds represent the "activated isoprene units" that can be assembled and further modified in different ways to access an impressively broad and diverse number of structurally different higher terpenes with different (biological) properties. Whereas DMAPP is a highly electrophilic species, which upon liberation of diphosphate can ionize readily to give a stabilized allylic cation, IPP represents the nucleophilic isoprene unit, and usually these two groups assemble in a so-called head-to-tail fashion (Scheme 6.1). Mechanistically, terpenoid formation is thus mainly based on the reactivity of carbocations, and a lot of the reactions that are usually associated with carbocations (e.g., nucleophile additions, Wagner–Meerwein rearrangements, hydride shifts, etc.) play a very important role in the biosynthesis of terpenes. However, it should also be pointed out that in nature these cations may not exist as such discrete species as drawn in the following simplified schemes but more reasonably they exist as ion pairs with an appropriate counter anion (e.g., a diphosphate group) in the presence of the relevant enzymes.

A class of enzymes called prenyltransferases efficiently catalyzes the addition of IPP to DMAPP to form the parent monoterpene skeleton. Most commonly this addition gives access to the (*E*)-configured geranyl diphosphate (GPP, **3**) by a stereoselective abstraction of the $H_R$ proton as depicted in Scheme 6.1.

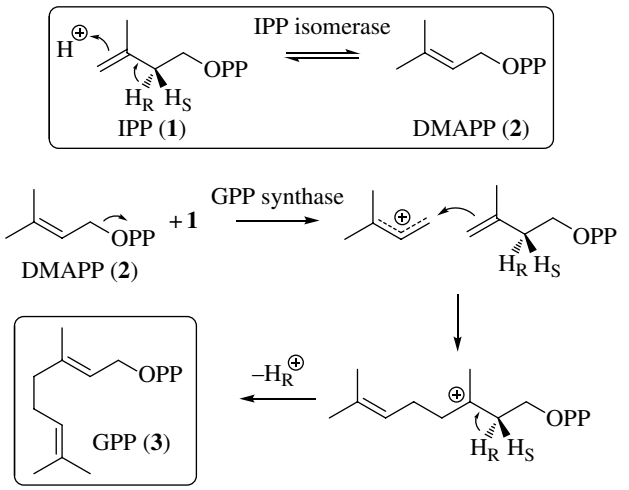
The (*E*)-olefin GPP (**3**) can then be easily isomerized to the (*Z*)-configured neryl diphosphate (NPP, **4**). This isomerization most reasonably proceeds via carbocation formation and diphosphate addition to the tertiary carbon to give the conformationally flexible linalyl diphosphate (LPP, **5**) (Scheme 6.2). In addition there are also enzymes known that

*From Biosynthesis to Total Synthesis: Strategies and Tactics for Natural Products*, First Edition. Edited by Alexandros L. Zografos.
© 2016 John Wiley & Sons, Inc. Published 2016 by John Wiley & Sons, Inc.

directly favor the formation of **4** from IPP and DMAPP due to a stereospecifically alternative deprotonation pathway [5, 6]. Independent of the pathway by which compounds **3**, **4**, and **5** are accessed, these three highly reactive diphosphates are the parent intermediates for either higher terpenes (upon further addition of IPP) [5] or can be subsequently transformed and modified to access acyclic, monocyclic, or polycyclic monoterpenes and iridoids.

### 6.2.1 Acyclic Monoterpenes

The biosyntheses of terpenes belong to the most diverse strategies developed by nature. As mentioned earlier at Chapter 5, just two simple building blocks (compounds **1** and **2**) are necessary to generate a fascinating diversity of different (biologically relevant) molecules. With respect to the syntheses of monoterpenes, the three isomeric diphosphates **3–5** are the structural key intermediates. By rather subtle modifications and changes only, a variety of different acyclic monoterpenes can be generated (Scheme 6.3). Depending on the formation of either the geranyl cation intermediate **A** or the neryl/linalyl cation **B** and subsequent addition of $H_2O$, followed by further simple functional group manipulations, either terpenoid hydrocarbons, alcohols, aldehydes, or even esters can be generated. These volatile compounds are often utilized as odorants in perfumes or for other flavoring purposes [1, 7]. Mechanistically, it was shown that these enzyme-catalyzed reactions do proceed via the formation of the carbocation intermediates (which are then trapped by $H_2O$) rather than by a simple hydrolysis of the diphosphate (e.g., LPP would give linalool by such a seemingly reasonable transformation) [1].

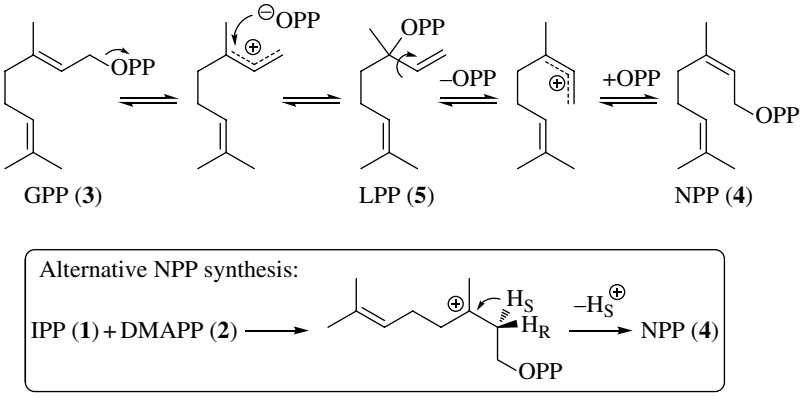



**SCHEME 6.1** Biosynthesis of the monoterpene key intermediate GPP (**3**) by addition of IPP (**1**) to DMAPP (**2**).

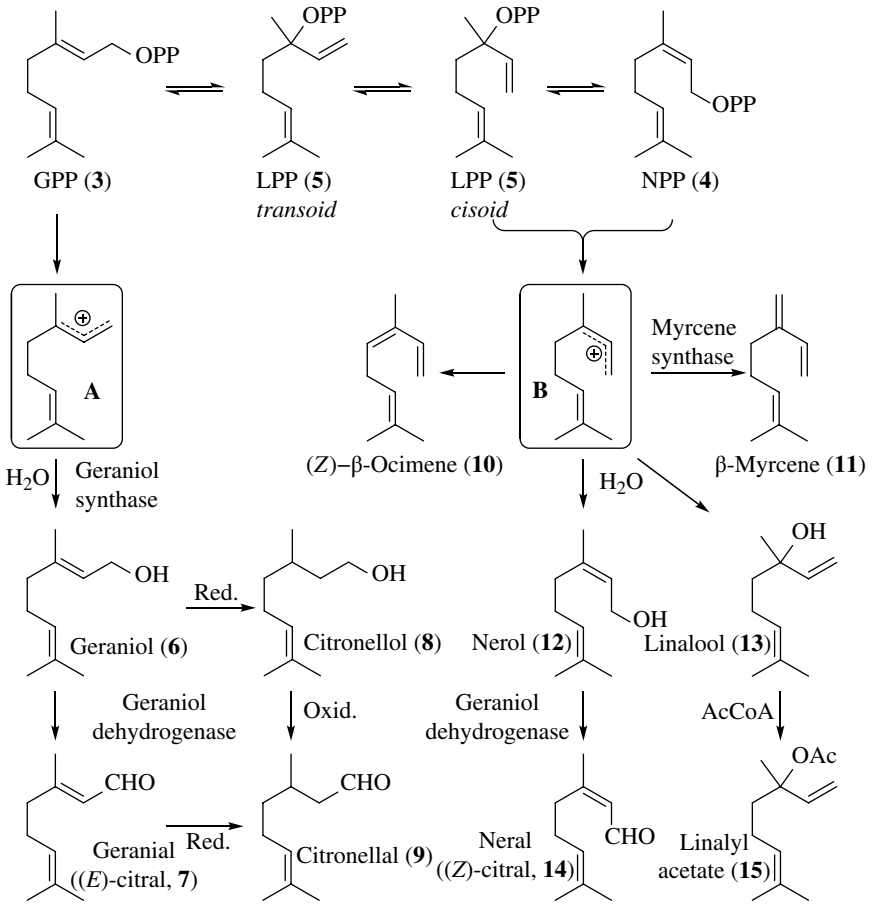
### 6.2.2 Cyclic Monoterpenes

Besides the direct addition of $H_2O$ to the linear allylic cations generated from diphosphates **3–5** or a deprotonation leading to double bond formation (both transformations give acyclic monoterpenes), cyclization reactions of the intermediates and further transformations give access to a large number of different mono- and bicyclic monoterpenes [8]. The key step hereby is the formation of the menthyl or α-terpinyl cation **C**, with LPP (**5**) being the preferred substrate for such monoterpene cyclases (it is worth to note that also compounds **3** and **4** can be accepted by these enzymes). The resulting cationic intermediate **C** can then undergo a series of cyclizations, hydride shifts, or Wagner–Meerwein rearrangements until a final deprotonation or addition of a nucleophile takes place [1]. These remarkably diverse reaction cascades enable the biosyntheses of a broad variety of mono- and bicyclic monoterpenes with the important parent skeletons shown in Scheme 6.4.

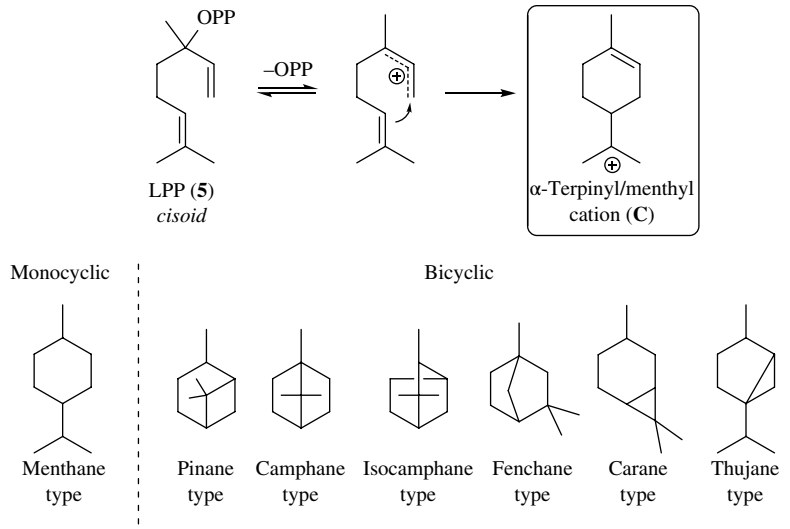
With respect to the biosyntheses of menthane-type monoterpenes, the menthyl cation **C** can either lose a proton resulting in the formation of limonene (**16**), or it may be directly attacked by $H_2O$ to give α-terpineol (**17**), which can




**SCHEME 6.2** Isomerization between GPP (**3**), LPP (**5**), and NPP (**4**) and an alternative enzymatic pathway toward NPP (**4**).

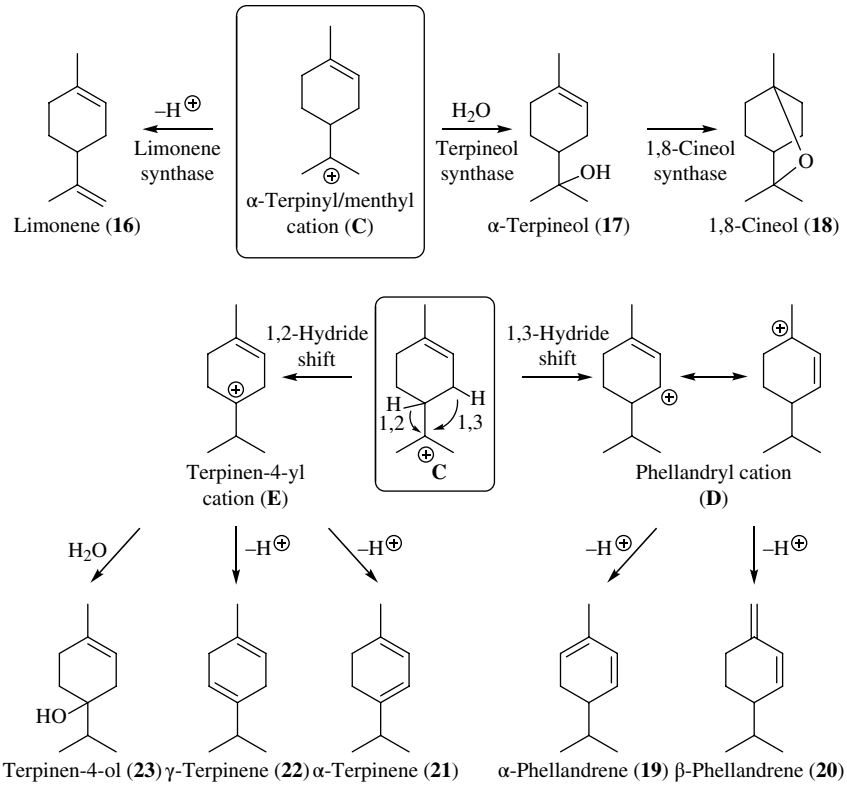



**SCHEME 6.3** Biosynthesis pathways toward different prominent acyclic monoterpenes.




**SCHEME 6.4** Formation of the linchpin intermediate **C** and parent skeletons of different cyclic monoterpenes.

then undergo an etherification reaction to yield 1,8-cineole (**18**) (Scheme 6.5). In addition, **C** can also either undergo a 1,3-hydride shift to furnish the phellandryl cation **D** or a 1,2-hydride shift to obtain the terpinen-4-yl cation **E**. Both intermediates can then liberate a proton to obtain the isomeric monocyclic terpenes **19–22** or can be trapped by addition of $H_2O$, which, for example, can result in the formation of terpinen-4-ol (**23**).

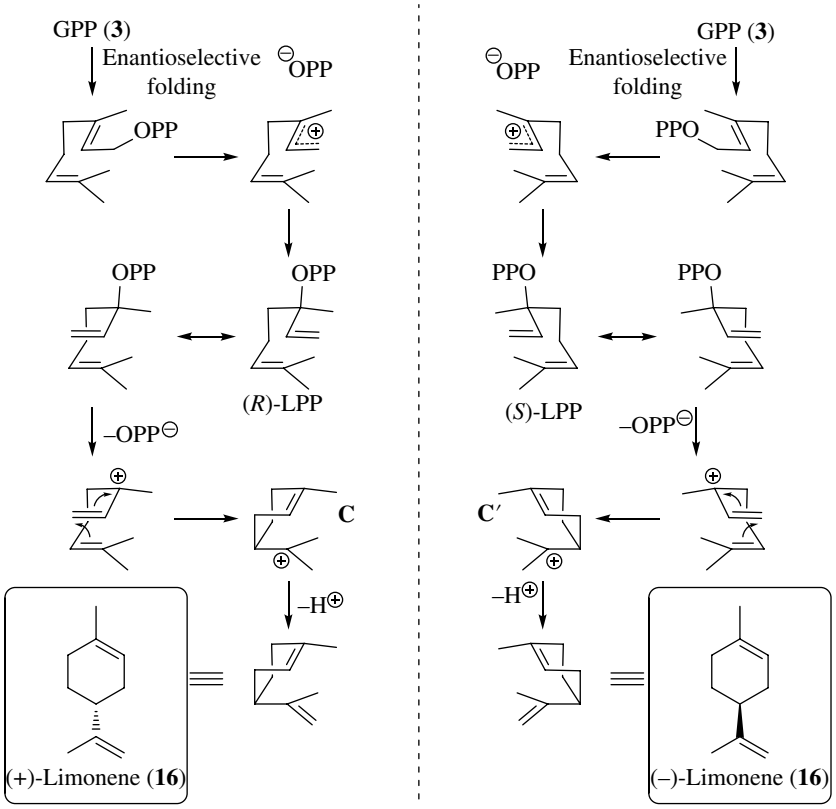



**SCHEME 6.5** Exemplified biosynthetic pathways toward monocyclic monoterpenes and advanced (bicyclic) derivatives thereof.

In all the Schemes shown so far, the structures have been given without any information regarding the stereochemistry of these compounds. However, most readers will be aware of the fact that the two enantiomers of a certain monoterpene often do have very different (e.g., olfactory) properties [9]. For example, both enantiomers of the monocyclic limonene (**16**) have a very characteristic odor. Whereas (+)-**16** smells like oranges, (–)-**16** has a lemonlike smell, and analogous examples can be given for other (mono)terpenes. With respect to the high enantioselectivities observed in the biosynthesis of different terpenes, the question how the specific enzymes can control the stereochemistry of the target molecules arises. The biosynthesis of the enantiomers of limonene (**16**) serves as a well-understood example to illustrate how enzymes are able to control the absolute configuration in monoterpene synthesis (Scheme 6.6) [1]. Thus, the enzyme controls the folding of GPP early in the sequence, and the corresponding enantiomeric conformations are then further transferred through the whole sequence via (*R*)- or (*S*)-LPP, and the two enantiomeric α-terpinyl cations **C** or **C′** do give either (+)- or (–)-**16**. Advanced transformations of the intermediate cations can also give access to other (bicyclic) monoterpenes (e.g., see the formation of pinene in Scheme 6.9) with excellent stereocontrol. Noteworthy, there are examples where both enantiomers of a certain terpene are present in a single organism and others where different organisms produce different enantiomers. It is now commonly assumed that in those cases where both enantiomers are present in, for example, a single plant, two separate enzymes are responsible for the synthesis of either enantiomer [1].

Limonene (**16**) can also serve as the starting material for a series of further transformations to obtain such important oxygenated monocyclic monoterpenes like menthol (**38**) or others as shown in Scheme 6.7. These are further impressive examples how nature can employ rather simple molecules like **16** that contain at least two activated sites for further enzyme-catalyzed transformations to get access to a very diverse assembly of different metabolites. Hereby, allylic oxidations and subsequent (stereoselective) redox state manipulations as well as isomerization reactions are the main chemical transformations. Further dehydrogenation reactions of either limonene or advanced oxygenated monocyclic terpenes can also lead to an aromatization giving access to a small group of aromatic compounds (e.g., *p*-cymene (**39**) or thymol (**40**)) that are not biosynthesized by more common pathways like the shikimic acid pathway [1, 3].

With respect to the biosynthesis of bicyclic monoterpenes, several pathways are known. For example, the menthyl cation **C** can undergo a deprotonation in position 5 of the ring followed by an immediate cyclopropane formation to access the carane-type bicyclic compound **41**.




**SCHEME 6.6** Stereoselective limonene biosynthesis.

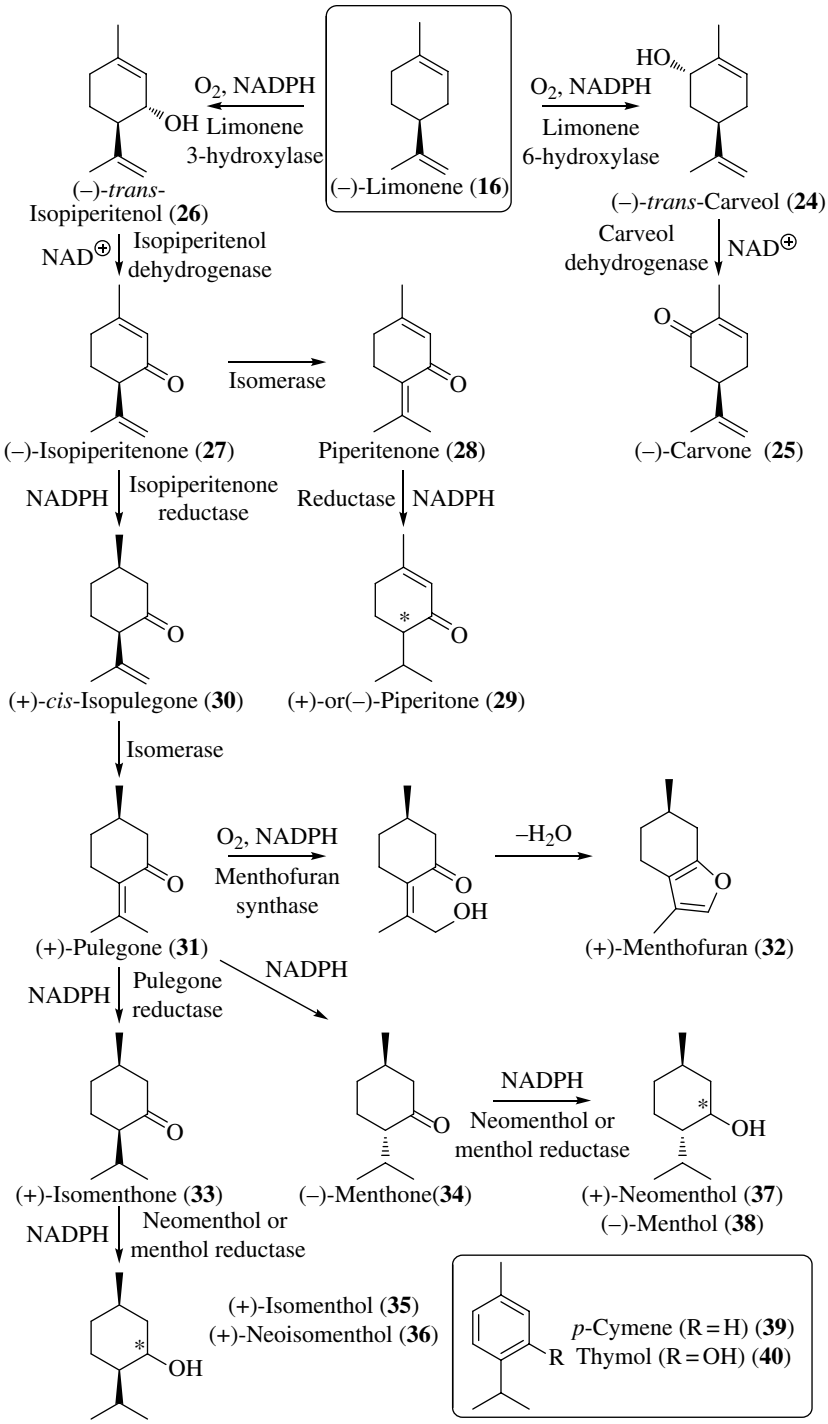
Alternatively, the pathway toward the cyclopropane-containing thujane-type monoterpenes utilizes the terpinen-4-yl cation **E**, which can form the thujyl cation **F** via a π-cation cyclization. Subsequent deprotonation then gives the bicyclic sabinene (**42**), which can also be further metabolized to thujone (**43**) (Scheme 6.8).

Alternatively, another π-cation cyclization of **C** can result either in the formation of the pinyl cation **G** or the bornyl cation **H** (Scheme 6.9). Cation **G** may then be selectively deprotonated to obtain α- or β-pinene (**44**, **45**). Again different enzymes favor the formation of either the (+)- or (–)-enantiomers of these compounds due to a selective folding of the precursor as already illustrated in Scheme 6.6. In addition, the tertiary carbocation **G** can undergo a strain releasing 1,2-alkyl shift resulting in the formation of the secondary fenchyl cation **I**, which is then trapped by $H_2O$ to give fenchol (**50**) and subsequently fenchone (**51**) upon oxidation. The bornyl cation **H** can either be trapped by a diphosphate anion and further hydrolyzed to borneol (**47**), which also serves as a precursor of camphor (**48**), or **H** can also undergo a 1,2-alkyl shift to generate the more stable tertiary carbocation **J**, which then allows for the biosynthesis of camphene (**49**), illustrating again the impressively diverse pathways nature utilizes starting from just one simple key intermediate.

### 6.2.3 Iridoids

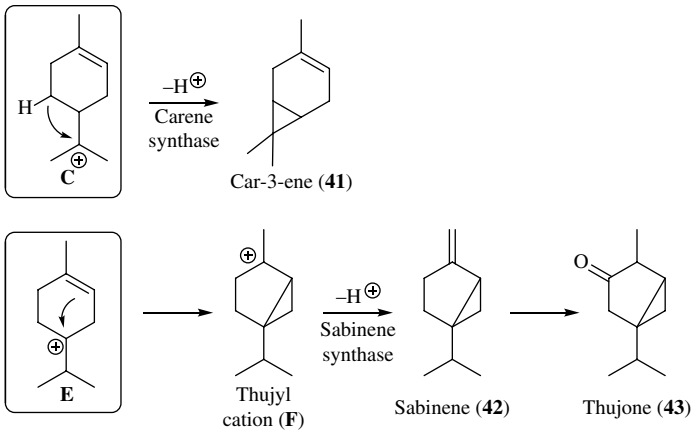
Iridoids are a large and structurally diverse class of secondary metabolites of monoterpenoid origin [10, 11]. Their structural parent system is the iridane skeleton, which is derived from geraniol (**6**) by a cyclization pathway that is mechanistically different to the cyclization reactions that are usually found in classical terpene chemistry [1, 12]. Further enzymatic transformations then give the fundamental iridoid skeleton or the thereof derived secoiridoid motive (with an alternative connectivity as shown in Scheme 6.10), which often serves as a building block for the synthesis of more complex monoterpenoid indole alkaloids [1]. Noteworthy, hereby the isoprene rule is often not fulfilled anymore as the terpenoid parts of such compounds sometimes contain nine carbon atoms only due to a decarboxylation step somewhere in the sequence. Very often iridoids and secoiridoids are present as glycosides in nature.

The first step in the biosynthesis is an allylic oxidation of geraniol (**6**) to give 10-hydroxygeraniol (**52**), which is then further oxidized to **53**. This dialdehyde serves as the substrate for the key cyclization step to iridodial (**54**). Mechanistically this reaction is supposed to proceed via a substrate–enzyme iminium species (please see the mechanism in Scheme 6.11), a type of activation that we will see

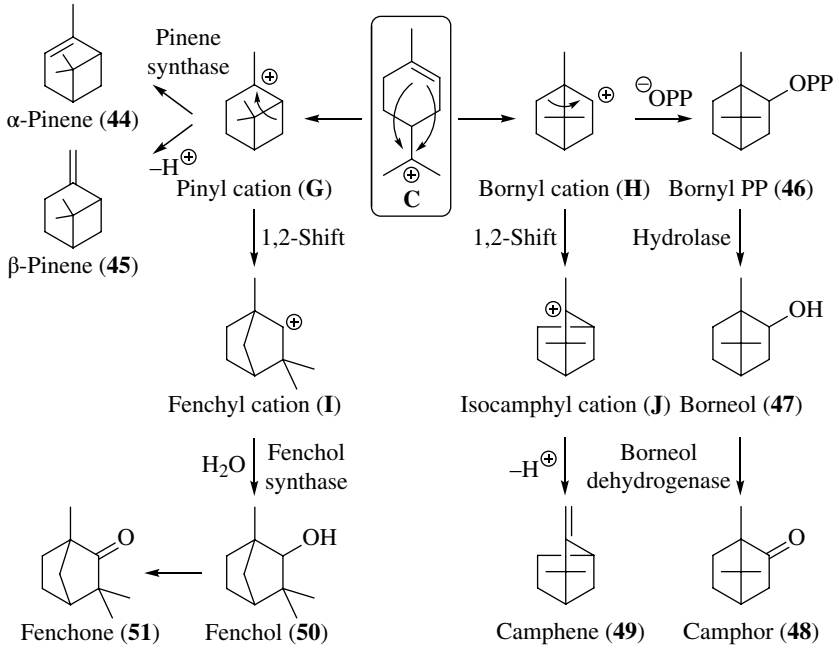



**SCHEME 6.7** Limonene (**16**) as a precursor for different oxygenated monoterpenes.

again later in the organocatalysis chapter (i.e., iminium catalysis). Iridodial is in equilibrium with its enol tautomer and the cyclic hemiacetal form. A further oxidation then gives the trialdehyde iridotrial (**55**) that is again in equilibrium with its hemiacetal form, which already represents the parent bicyclic iridoid skeleton. Subsequent oxidation and glycosylation followed by a site-selective hydroxylation then gives loganic acid (**57**), and an SAM-mediated methylation yields loganin (**58**), which is the key intermediate toward secologanin (**59**) and advanced terpenoid indole alkaloids. Whereas the parent monoterpenoid iridane skeleton is still present in **58**, an oxidative cleavage




**SCHEME 6.8** Biosynthetic pathways toward carane- and thujane-type monoterpenes.



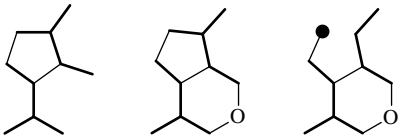

**SCHEME 6.9** Biosynthetic pathways toward important bicyclic monoterpenes.

catalyzed by a cytochrome P450-dependent monooxygenase following a radical mechanism [1, 3] leads to the formation of the parent secoiridoid skeleton. As already mentioned, an amazingly broad diversity of different natural iridoids or secoiridoids are found in a variety of organisms, and the main structural variations are a result of (stereoselective) hydroxylations, esterifications, or also epimerization reactions. In addition these compounds can lose a carbon atom because of decarboxylation, and very often they are key building blocks to achieve further structural diversity by means of coupling reactions with other motives like amino acids [10, 11].

### 6.2.4 Irregular Monoterpenes

Besides classical monoterpenes that are formed via a head-to-tail addition of IPP to DMAPP (and the analogous addition of IPP to advanced intermediates toward higher terpenes), there are also monoterpenes known where the C10 skeleton cannot be rationalized by this standard coupling of the two activated isoprene units. Two important examples are chrysanthemic acid (**60**) and pyrethric acid (**61**), which are the main (ester bound) building blocks for the well-known family of the pyrethrins [1, 13]. In this case, an enzyme-catalyzed

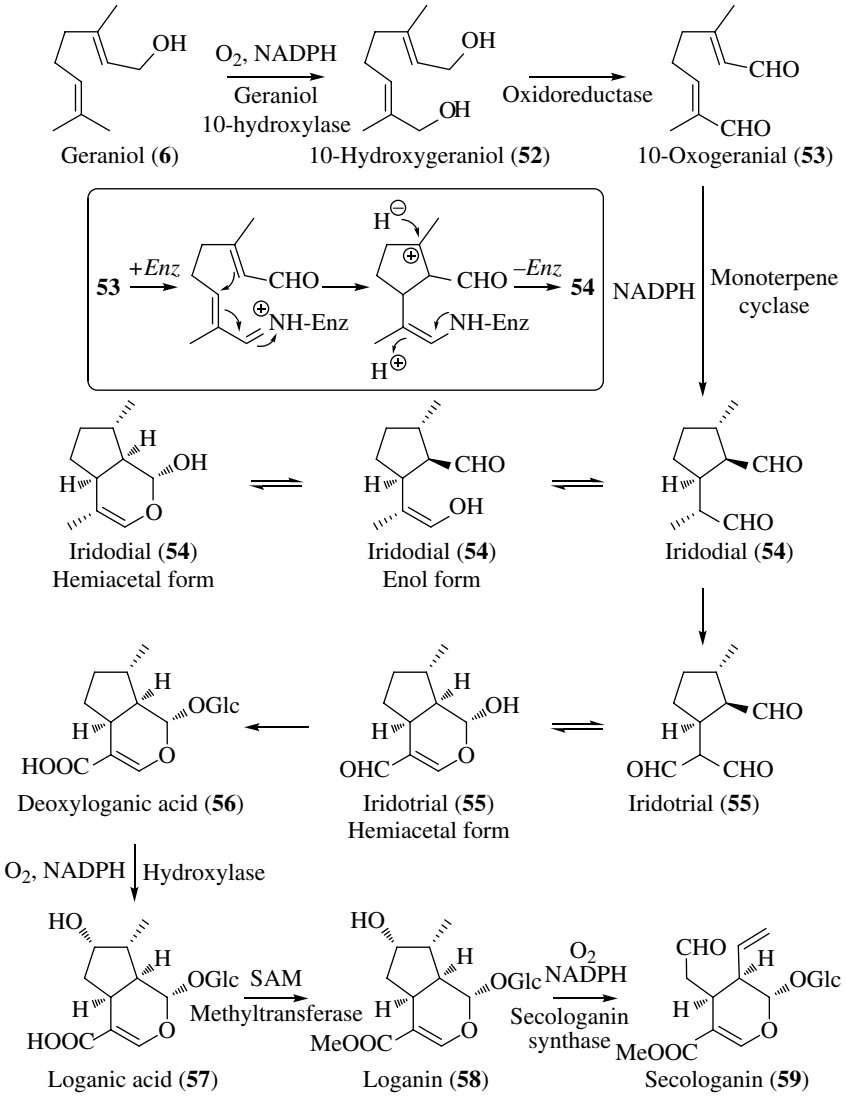
dimerization of DMAPP (**2**) takes place first. After deprotonation and carbocation trapping, the cyclopropane-containing chrysanthemyl diphosphate (**62**) is formed, which can then be further transferred into **60** or **61** (Scheme 6.12).



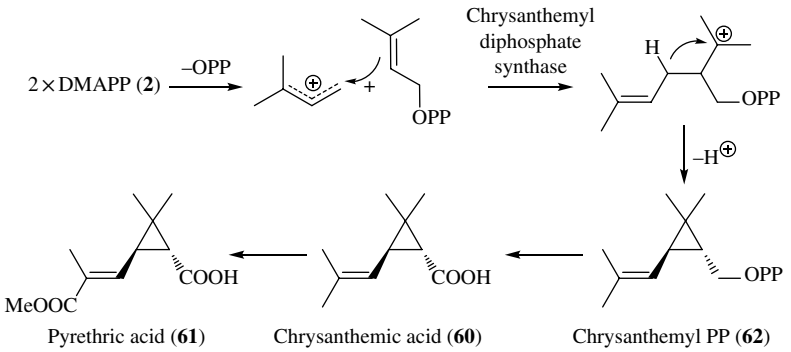

**SCHEME 6.10** Illustration of the monoterpenoid-derived iridoid and secoiridoid parent skeletons.

## 6.3 ASYMMETRIC ORGANOCATALYSIS

The importance to control the three-dimensional structure of organic molecules does not require any further explanation, and it was already discussed before that nature has developed an impressively effective catalytic machinery to obtain single stereoisomers with full control of their absolute configuration (e.g., see Scheme 6.6). Synthesis-oriented (organic) chemists have for decades been working on the development of novel strategies to carry out (complex) transformations with high enantio- and diastereoselectivities. Besides enzymatic and metal-catalyzed asymmetric transformations, the use of small organic molecule-based catalysts (so-called organocatalysts) has proven to possess an enormous potential for the catalysis of stereoselective reactions [14].




**SCHEME 6.11** Biosynthetic pathways toward iridoids and secoiridoids.




**SCHEME 6.12** Tail-to-middle combination of two molecules of DMAPP in the biosynthesis of irregular monoterpenes like chrysanthemic acid (**60**) and pyrethric acid (**61**).

### 6.3.1 Introduction and Historical Background

Although the use of organic compounds for the catalysis of a variety of organic reactions has been known for decades [14–24], it was only just one and a half decades ago when the seminal publications of MacMillan et al. [25] and List, Barbas, and Lerner [26] set the stage for a new trend in organic synthesis. It is also due to David MacMillan that the term "organocatalysis" has become a catchword for a whole field of research in (organic) chemistry [25]. Although these two publications from 2000 are often considered to represent the genesis of modern organocatalysis, several very important contributions appeared long before, but have not been considered to belong to the field of organocatalysis, simply because this classification did not exist at the time of their appearance.

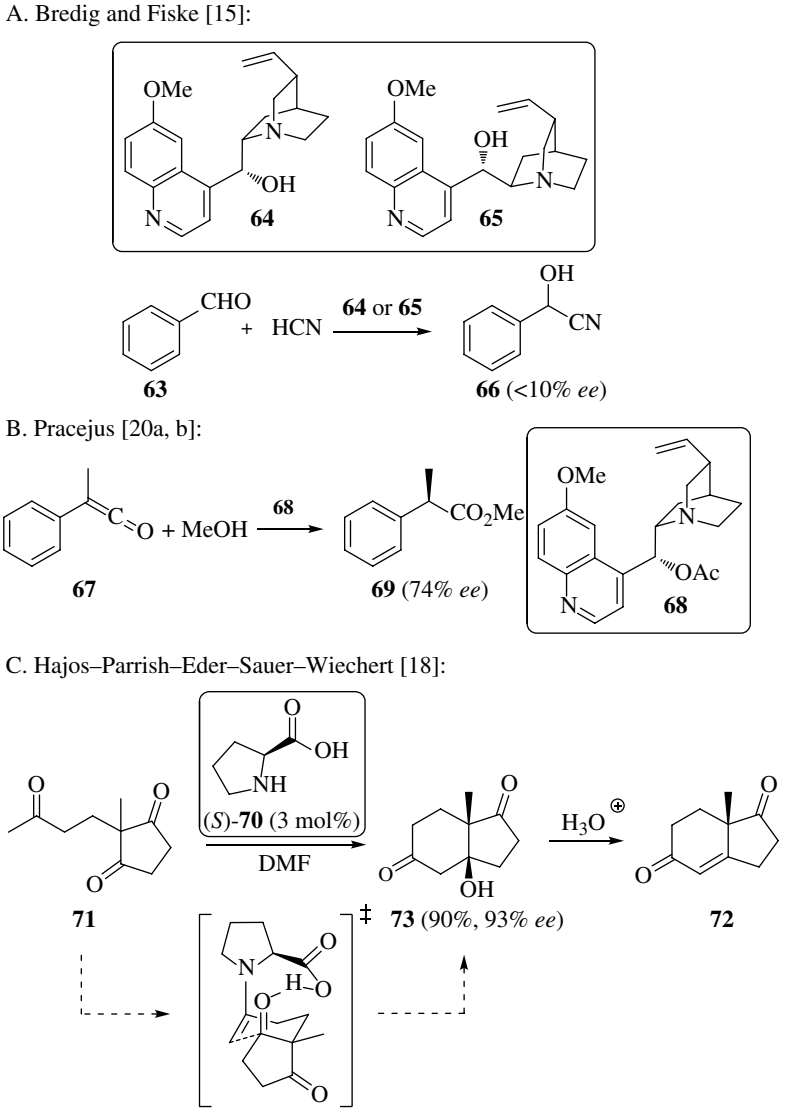
Organic molecules have been used as catalysts since the days of Justus von Liebig who found that dicyan is transformed into oxamide in the presence of an aqueous solution of acetaldehyde [27]. Asymmetric organocatalysis can be dated back to the beginning of the last century when Bredig performed the addition of HCN to benzaldehyde (**63**) in the presence of quinine (**64**) or quinidine (**65**) (Scheme 6.13A) [15]. With an enantiomeric excess of slightly less than 10%, this was one of the conceptually groundbreaking investigations in this field. Later on, in the 1950s, Prelog reinvestigated this reaction [19], and in the late 1950s Pracejus reported one of the first highly enantioselective reactions ever by adding methanol to methyl phenyl ketene (**67**) in the presence of *O*-acetylquinine (**68**) (Scheme 6.13B) [20].

Two milestone reports that significantly influenced modern asymmetric (organo)catalysis appeared in the early 1970s when Eder, Sauer, and Wiechert at Schering [17] and Hajos and Parrish at Hoffmann-La Roche [18] independently reported the proline (**70**)-catalyzed intramolecular aldol reaction of the triketone **71** as the key step in the synthesis of the diketone **72**, a highly important building block in steroid synthesis [28]. Remarkably, Hajos and Parrish obtained intermediate **73** in excellent yield and enantioselectivity with only 3 mol% of catalyst (Scheme 6.13C).

It is worth noting that although Hajos and Parrish considered this reaction to be "a simplified model of a biological system in which (*S*)-proline plays the role of an enzyme," which represented a unique and groundbreaking approach for the introduction of stereogenic centers, this methodology was not developed further for almost 30 years until List, Barbas, and Lerner published their breakthrough report on the intermolecular proline-catalyzed aldol reaction proceeding via the nowadays well-accepted enamine activation mechanism (Scheme 6.14A) [26]. Despite several other (mechanistically different) breakthrough reports in the late 1970s, especially by Wynberg's group, and in the early 1980s [22–24], it is due to this report by List et al. in 2000 and MacMillan's simultaneous report on asymmetric Diels–Alder reactions proceeding via formation of an chiral iminium ion (Scheme 6.14B) [25] that asymmetric organocatalysis became one of the most extensively investigated and most competitive fields over the last years. This trend can also be well documented by the annual number of scientific publications covering the topic organocatalysis (Scheme 6.15), which has increased significantly since these seminal reports in 2000.

Several ways how (asymmetric) organocatalysts can be classified have been reported [14]. One general strategy is a classification according to Lewis acids/Lewis bases and Brønsted acids/Brønsted bases with the general simplified activation modes depicted in Scheme 6.16.

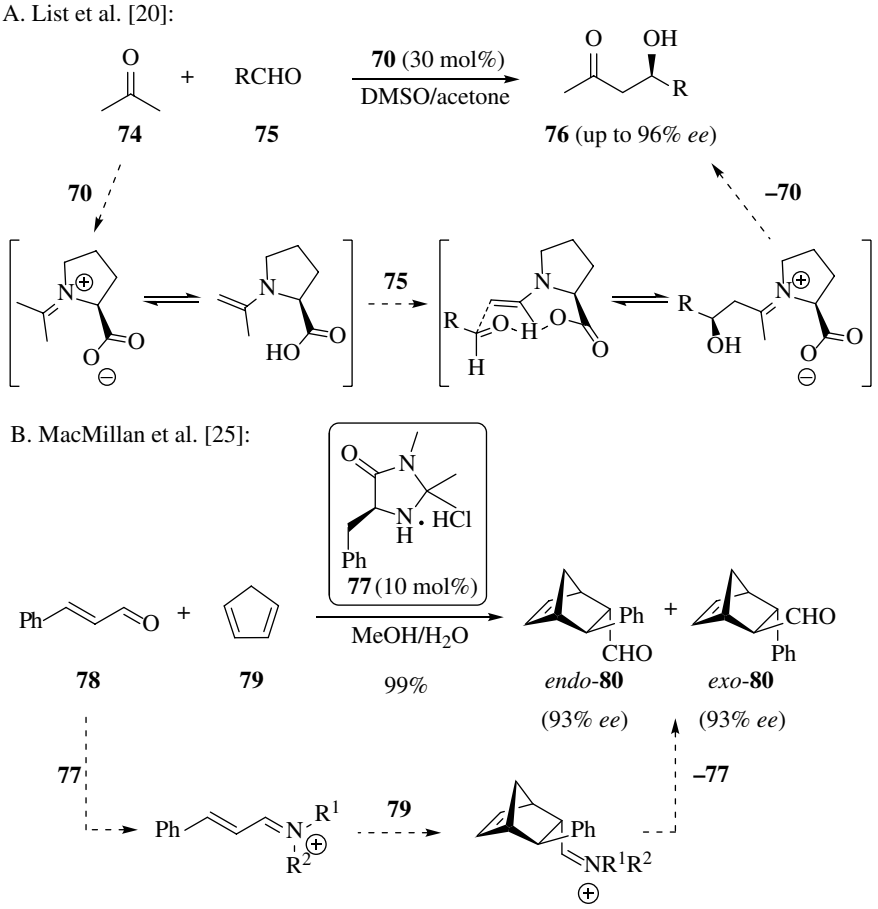
An alternative possibility is a classification according to the activation modes of the catalysts, for example, the iminium or enamine catalysis, H-bonding catalysis, or ion-pairing catalysis or more generally to differentiate between covalent or noncovalent activation modes (Scheme 6.17) [14, 29]. Looking at these different types of (complementary) activation modes that are feasible using organocatalysts, it is obvious that the possible application scope of these catalysts is rather diverse and therefore, depending on



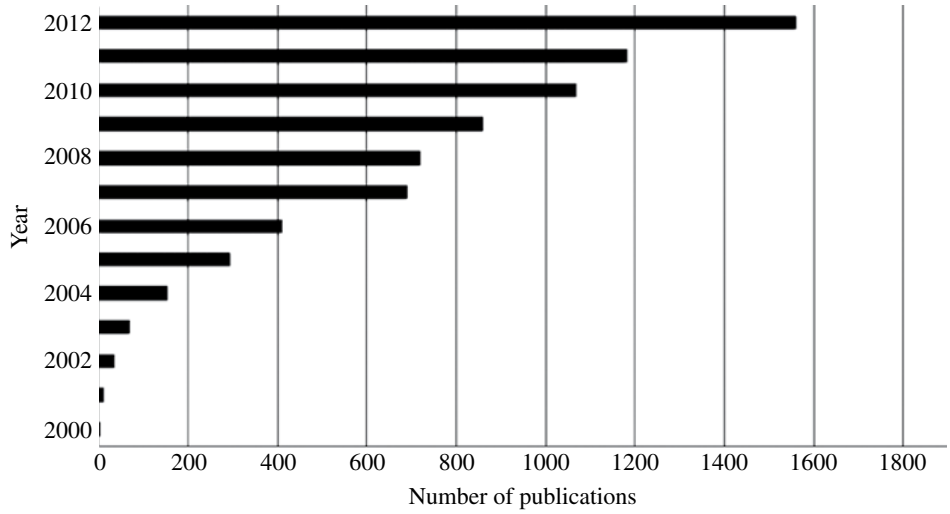

**SCHEME 6.13** Seminal early reports in the field of asymmetric (organo)catalysis.

the type of catalyst, a variety of different complex transformations can be facilitated. Thus it also comes as no surprise that asymmetric organocatalysis has become a powerful tool in natural product synthesis [30]. Obviously, asymmetric organocatalysis cannot only be associated with a single class of natural products that can be accessed thereby. In contrast, by looking at the recent literature, it has been well documented that, depending on the used catalyst type and the chosen retrosynthetic strategy, organocatalysts can be powerful tools in the synthesis of a broad variety of either primary or secondary metabolites [30].

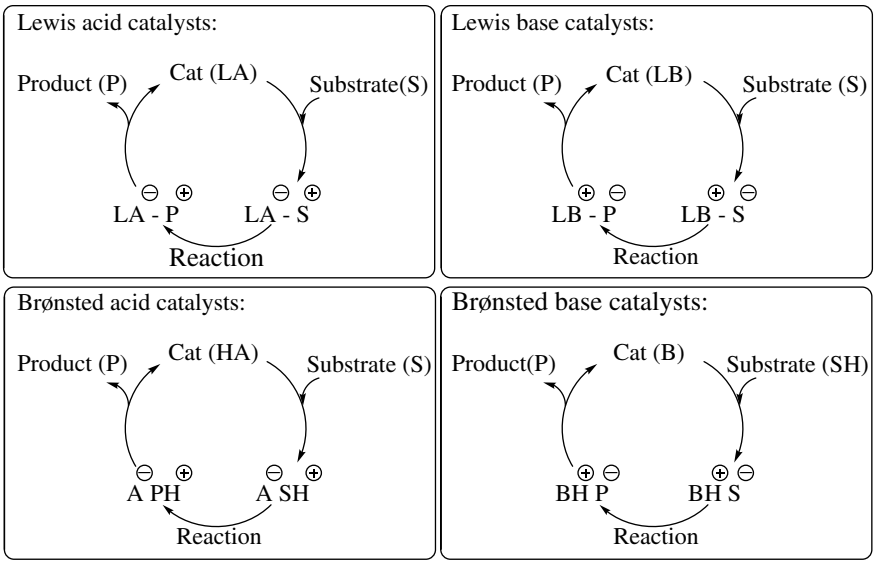
The following parts of this chapter will be mainly divided according to the used catalyst classes and the commonly accepted activation mechanisms. However, some caution is necessary. As already shown in the case of the proline-catalyzed intermolecular aldol reaction by List et al. (Scheme 6.14), proline (**70**) can be considered to act as a bifunctional catalyst. In addition, it is often not so easy to define exactly the actual activation mechanism as, for example, it is sometimes difficult to differentiate if a Brønsted acid catalyst either activates the substrate by a full protonation and ion-pair formation or via H-bonding. Accordingly, a strict classification according to just one single activation mechanism will not always be possible, and very often activation modes like enamine formation are accompanied with additional interactions, such as hydrogen bonding. It is also not the intention to give an encyclopedic overview about the field (for more details, the interested reader is referred to much more detailed and excellent reviews by others [14]), but to provide an illustrative introduction to some of the most important strategies and applications in asymmetric organocatalysis by highlighting the



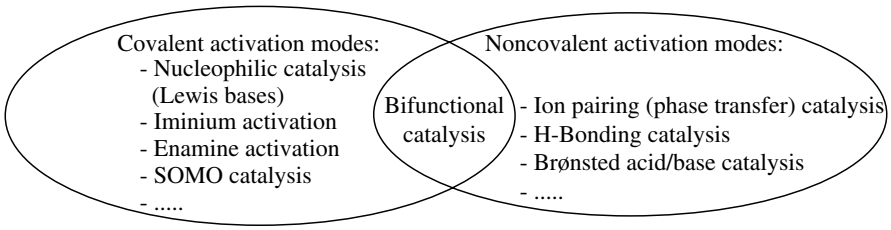

**SCHEME 6.14** Breakthrough reports by List et al. and MacMillan et al. introducing the concepts of enamine and iminium activation in 2000.




**SCHEME 6.15** Annual number of publications covering the topic organocatalysis (Data from SciFinder®, Chemical Abstracts Service, Columbus, OH, U.S.A.)




**SCHEME 6.16** Classification of organocatalysts according to their acid–base properties.




**SCHEME 6.17** Classification of organocatalysts according to their activation modes.

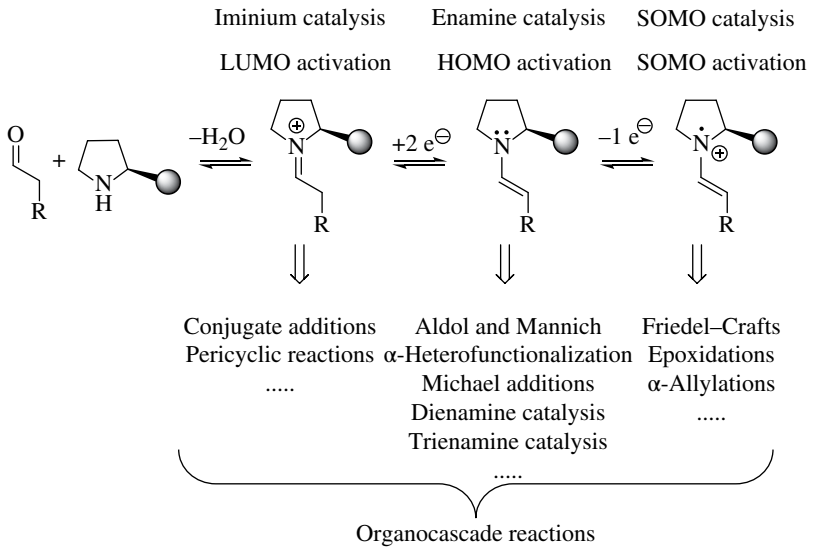
seminal contributions as well as some of the most impressive recent examples. Finally, selected examples about the successful application of asymmetric organocatalysis in the synthesis of iridoids and some monoterpenoid indole alkaloids will be discussed to demonstrate the high synthetic potential of these unique catalysts in natural product synthesis.

### 6.3.2 Enamine, Iminium, and Singly Occupied Molecular Orbital Activation

The use of chiral primary or secondary amines as covalent catalysts allows for the activation of carbonyl compounds for different reactions. Either the initially formed iminium species are the reactive intermediate (LUMO lowering), which is mainly the case when using α,β-unsaturated carbonyl compounds, or the derived enamine can be utilized for enolate-type reactions (HOMO activation), or, after a single electron oxidation of the enamine, a singly occupied molecular orbital (SOMO) activation is possible (Scheme 6.18) [14, 31, 32]. In addition, by combining these complementary activation modes, it has been possible to carry out organocascade reactions with excellent control of the absolute and relative configuration of the newly formed stereogenic centers.

Utilization of carbonyl groups by steering and controlling their reactions via enamine derivatives (HOMO activation) plays a fundamental role in organic synthesis [14, 32]. As enamine catalysis can be viewed as reducing the function and activation mode of aldolase enzymes to small organic molecules, it can be stated beyond doubt that this methodology represents one of the most powerful methods for the stereoselective α-functionalization of aldehydes and ketones currently known. In addition, this strategy can nowadays also be expanded toward the γ- and ε-functionalization of conjugated carbonyl compounds via dienamine [33] or trienamine activation [34]. As mentioned before, the seminal investigations in this field date back to the 1970s, with the Hajos–Parrish–Eder–Sauer–Wiechert reaction [17, 18] (Scheme 6.13) as the conceptually groundbreaking report for the development of new methods for asymmetric catalysis. Following the publication of List, Barbas, and Lerner in 2000 (Scheme 6.14A), a large variety of different applications and different catalysts have been reported over the last years.

The classical reactions that are usually associated with asymmetric enamine catalysis are aldol and Mannich-type

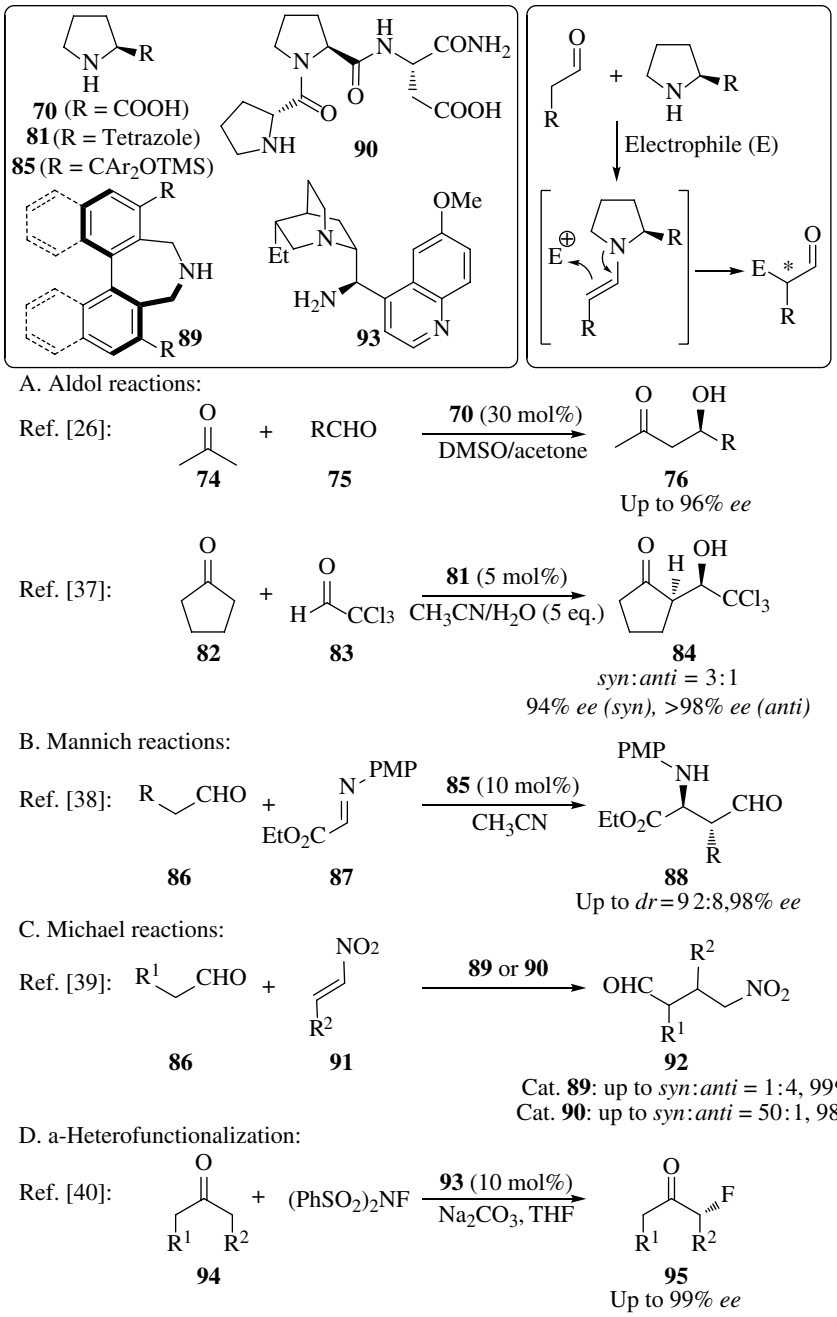



**SCHEME 6.18** Complementary covalent activation modes that can be achieved using chiral amine catalysts.

reactions, Michael additions, and α-heterofunctionalization (e.g., fluorination, amination, oxygenation, etc.) reactions. With respect to the catalysts of choice, the initially and most commonly employed chiral amine is definitely proline (**70**). However, significant efforts have been made in designing alternative (systematically fine-tuned) catalysts derived from proline, as demonstrated by Hayashi and Jørgensen (catalysts **85**) to mention the most prominent example [31d]. This catalyst was also very recently successfully used in a very impressive one-pot synthesis of (–)-oseltamivir phosphate (Tamiflu) by Hayashi's group, thus highlighting the outstanding catalytic potential of this easily available compound [35]. Noteworthy, whereas proline is supposed to transfer the stereochemical information in, for example, aldol reactions via a bifunctional activation mode (see Scheme 6.14) [36], the Hayashi–Jørgensen catalyst is supposed to control the stereoselectivity by shielding one face of the enamine because of its bulky substituents. Besides proline-derived catalysts, also biphenyl- and binaphthyl-based secondary amines **89** [32d] and peptides like compound **90** [31f] have been successfully used for enamine and iminium catalysis. In addition, primary chiral amines (e.g., compound **93** derived from cinchona alkaloids) have shown their potential as chiral enamine-activating catalysts [31g]. Accordingly, looking at the wealth of highly selective protocols that have been developed in this field over the last years, it is without doubt that this type of activation mode nowadays belongs to the most powerful strategies to control the absolute and relative configuration in reactions of carbonyl nucleophiles with different electrophiles. Scheme 6.19 gives an overview of selected examples of important reactions that can be facilitated via enamine activation [26, 37–40] and of some of the most interesting and powerful catalysts introduced in the past. However, for a detailed overview, the reader is referred to more comprehensive reviews and the primary literature cited therein [14, 31, 32].

The use of an amine catalyst for the activation of an α,β-unsaturated carbonyl group as a nucleophile represents a very useful extension of the concept of enamine activation (dienamine catalysis) [33]. By transmission of the nucleophilic properties of an enamine to an adjacent olefin (vinylogy), the γ-position can be rendered nucleophilic, and furthermore, it can react as an electron-rich diene in [4+2] cycloadditions. In 1998 already, Serebryakov et al. reported the prolinol **96**-catalyzed [4+2] cycloaddition of the α,β-unsaturated aldehyde **97** with acceptor **98** [41] (Scheme 6.20A). In 2006 Jørgensen et al. successfully applied this activation strategy to the stereoselective γ-amination of α,β-unsaturated carbonyl compounds [42] (Scheme 6.20B), and over the last years this concept become a powerful tool to make the γ-position of α,β-unsaturated carbonyl compounds nucleophilic and control the absolute configuration in different transformations using different chiral amine catalysts [33]. Barbas III et al. introduced an alternative strategy for dienamine activation by using α,β-unsaturated ketones as the starting materials that, in the presence of a chiral amine catalyst, form highly reactive dienes *in situ*, which can undergo stereoselective Diels–Alder reactions [43]. In 2003, this group reported a Knoevenagel/Diels–Alder cascade of enones **104** with different aldehydes **75** and Meldrum's acid **105**, which is supposed to involve formation of the enamine-activated diene first, followed by a [4+2] cyclization with the Knoevenagel product of **75** and **105** (Scheme 6.20C) [44].

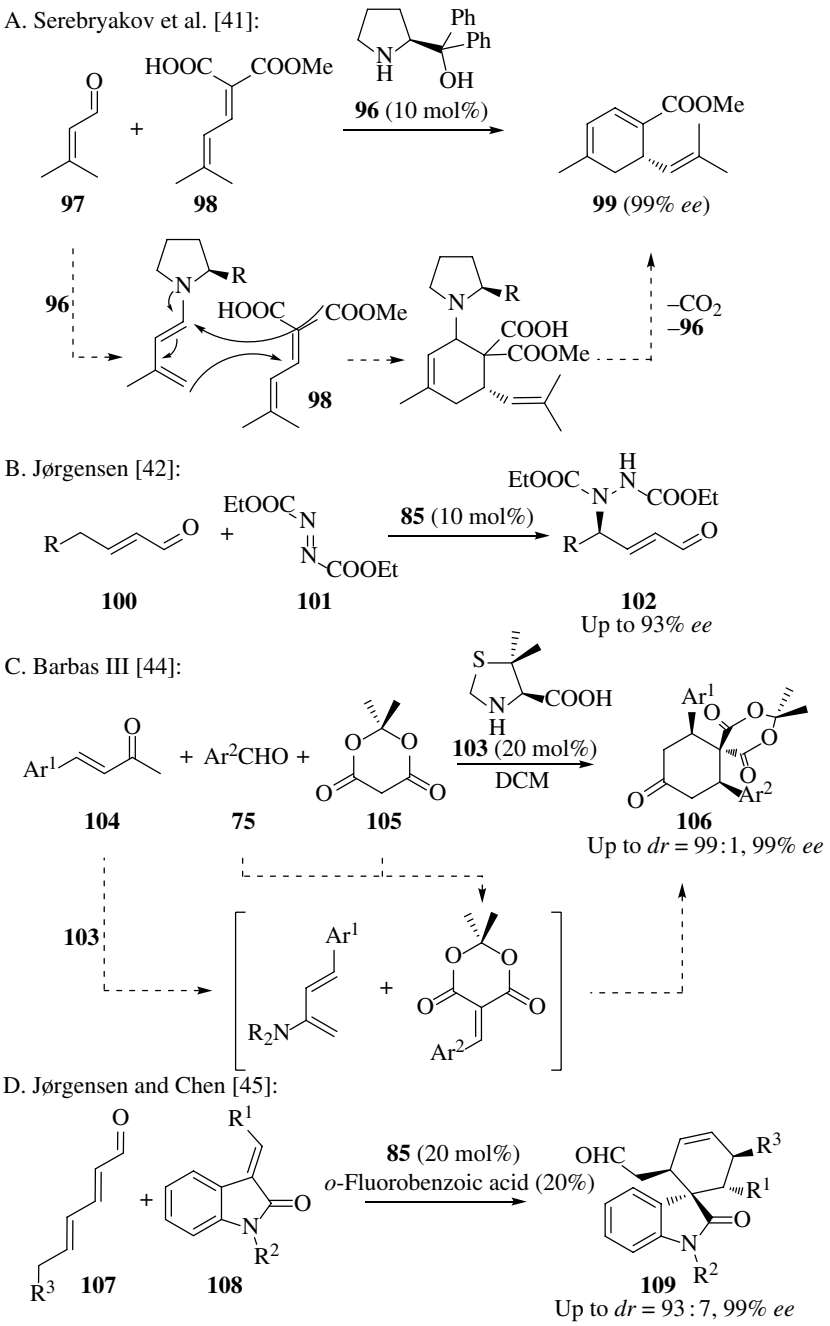
More recently, by using 2,4-dienals also the ε-position can be rendered nucleophilic and controlled in stereoselective addition reactions to Michael acceptors mainly (trienamine catalysis) [34]. This concept was introduced in 2011




**SCHEME 6.19** Selected examples about the use of chiral amine catalysts for the enamine activation of carbonyl compounds.

by Chen and Jørgensen [45] and could be successfully employed for [4+2] cycloaddition reactions between dienals **107** and Michael acceptors **108** (Scheme 6.20D). Over the last 2 years, this strategy became one of the emerging areas of interest in asymmetric organocatalysis and was already successfully employed by several research groups for different target reactions [34].

Besides the use of chiral amines to activate carbonyls to act as nucleophiles via enamine formation, their use as acceptor-activating catalysts via iminium formation has resulted in the development of numerous impressive applications over the last decade. The concept of iminium activation of conjugated enones has been postulated to play a pivotal role in the biogenesis of natural products as proposed by Baldwin et al. in, for example, the key Diels–Alder step in the biosynthesis of himgravine [46]. MacMillan's seminal report on the use of chiral imidazolidinone catalysts for Diels–Alder reactions in 2000 (Scheme 6.14) [25] introduced a highly useful and generalized strategy for asymmetric catalysis by activating an α,β-unsaturated carbonyl compound



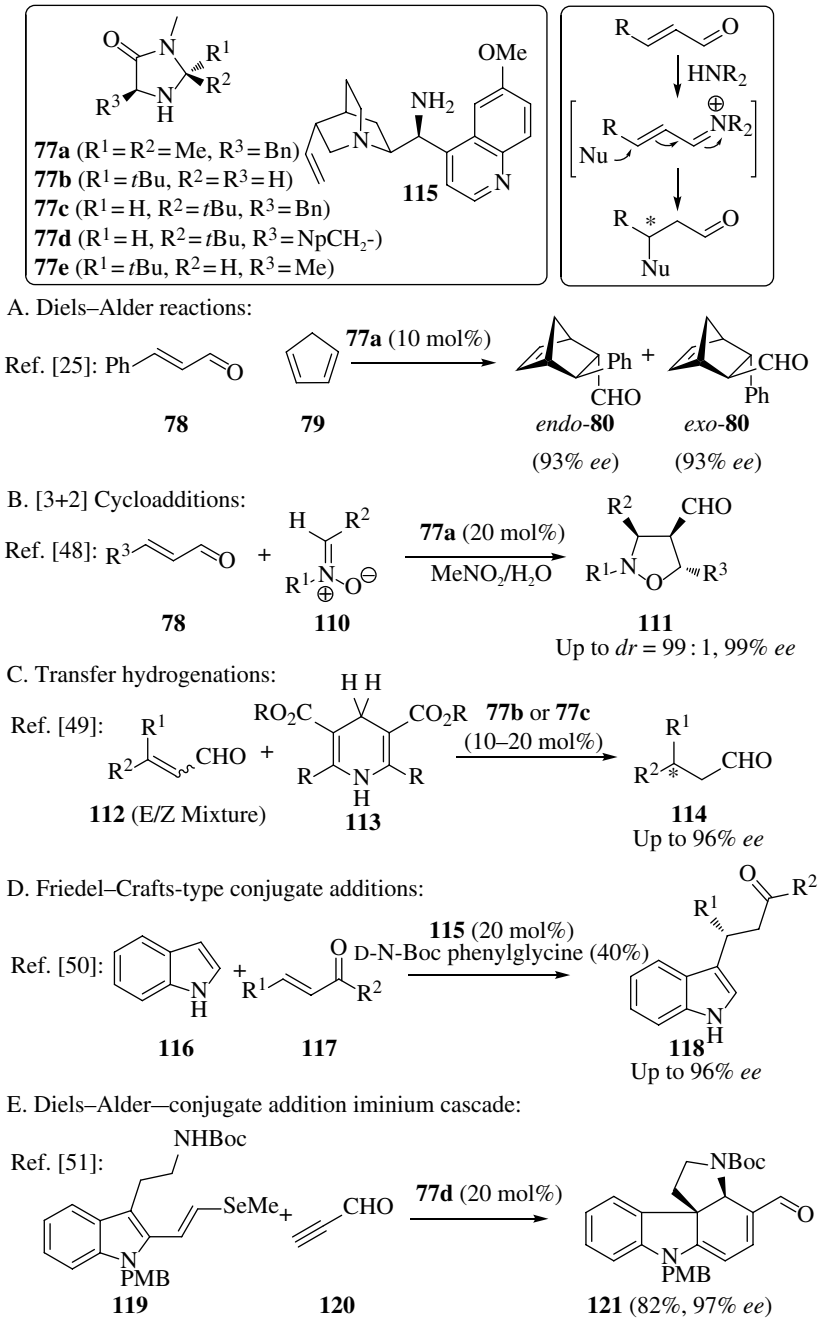

**SCHEME 6.20** Seminal reports to activate (di)enals via asymmetric dienamine and trienamine catalysis.

with catalytic amounts of a chiral secondary amine. The conceptual breakthrough was the realization that the *in situ* iminium formation between the catalyst and the enone results in a significant LUMO lowering of the electrophile by analogy with the LUMO-lowering effect of commonly employed Lewis acid catalysts. Moreover, in contrast to Lewis acids, the chiral information is much closer to the reactive site when a chiral amine forms the iminium intermediate, thus resulting in a significant discrimination of the two faces of the acceptor molecule. Therefore, the concept of iminium activation allowed for the development of some of the most useful organocatalytic transformations known today like cycloadditions or conjugate additions as well as different organocascade reactions [47]. As exemplified in Scheme 6.21, these can be [4+2] or [3+2] cycloadditions [25, 48], conjugate additions of heteroatoms (e.g., aminations or transfer hydrogenations using Hantzsch esters as the hydride source) [49], as well as conjugate additions of carbon nucleophiles like Friedel–Crafts-type reactions of indoles [50], to mention only a few of the relevant examples

(again detailed overviews can be found in more focused reviews [14, 31, 47]). Furthermore, this methodology also works extremely well in iminium-activated cascade approaches with, for example, an initial cycloaddition followed by a conjugated addition reaction as demonstrated by MacMillan et al. in their synthesis of compound **121** (a key intermediate to access *Strychnos*, *Aspidosperma*, and *Kopsia* alkaloids; please refer to the final chapter about the use of organocatalysis in total syntheses for more details about this transformation) [51].

With respect to the catalysts of choice, the MacMillan imidazolidinones **77** emerged as the most commonly used ones in iminium catalysis, but also cinchona alkaloid-based amines like **115** as well as the Hayashi–Jørgensen catalysts **85** have been highly successful in this field [31, 47].

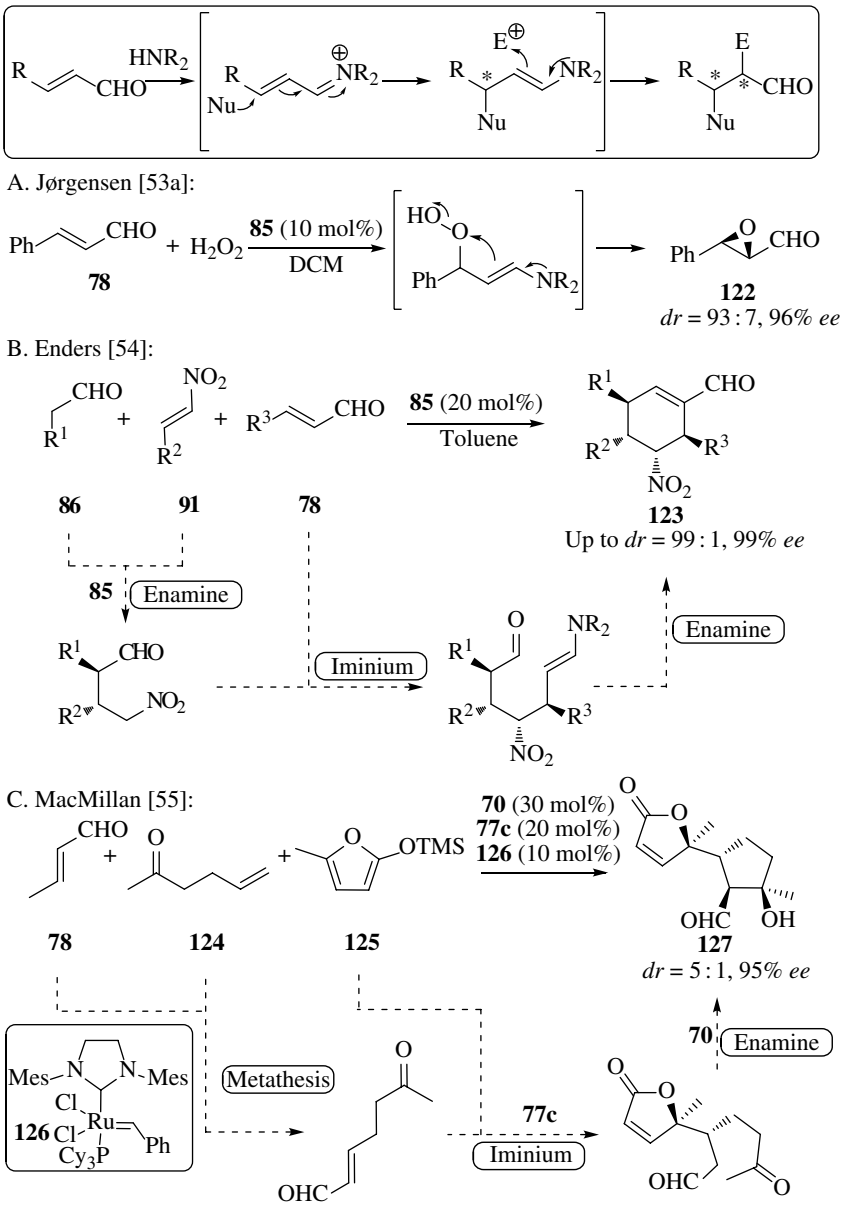
The use of chiral amine catalysts also allows for the combination of alternative activation modes, that is, enamine/iminium activation in operationally simple one-pot cascade reactions, either with a single catalyst or using multiple catalysts [52]. A broad variety of the organocascade approaches



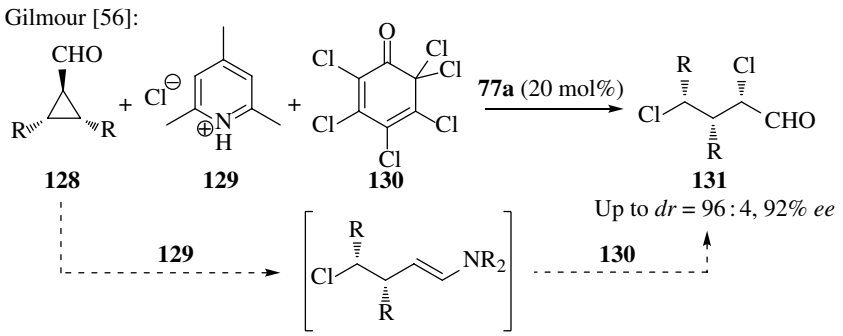

**SCHEME 6.21** Selected examples in the use of chiral amine catalysts for the iminium activation of α,β-unsaturated carbonyl compounds.

that have been developed over the last years are based on an initial iminium-activated conjugated addition (either using carbon nucleophiles or heteroatoms) to give an enamine species, which can then react further with an electrophile (Scheme 6.22). Several strategies that make use of this powerful approach have been introduced in the past [14, 52], and Scheme 6.22 highlights how diverse this strategy can be with respect to the reactions that can be facilitated and the products that can be obtained. For example, the *sec*-amine-catalyzed epoxidation of enals **78** was introduced by Jørgensen et al. in 2005 [53]. Thus, the peroxide is supposed to be added to the iminium-activated Michael acceptor first, followed by a nucleophilic addition of the enamine intermediate to the electrophilic peroxygen. In 2006, the Enders group published one of the milestone reports in the field of asymmetric organocatalysis [54]. By using the amine catalyst **85**, they were able to carry out an organocatalytic triple cascade reaction of aldehydes **86** with the Michael acceptors **78** and **91** with full control of four stereogenic centers (Scheme 6.22B). Following this impressive report, different research groups developed a variety of other highly selective enamine/iminium-catalyzed cascade reactions that belong to some of the most powerful applications of chiral secondary amine catalysis known yet [52].

In addition, also the combination of *sec*-amine catalysis with transition metal catalysis in cascade approaches has




**SCHEME 6.22** Selected organocascade approaches involving asymmetric enamine and iminium activation.




**SCHEME 6.23** Amine-catalyzed cyclopropane activation developed by Gilmour et al.

been very successfully introduced over the last years. A remarkable multicatalyst cascade approach was published in 2009 by MacMillan's group [55]. By using a combination of (*S*)-proline (**70**), imidazolidinone **77c**, and Grubbs' second-generation catalyst **126** in the same reaction, compound **127** could be obtained with excellent selectivity in a one-pot triple cascade sequence by adding the correct catalysts and reagents stepwise (**127** is the key intermediate in the total synthesis of (–)-aromadendranediol). The successful sequence commenced with a cross-metathesis reaction between crotonaldehyde (**78**) and ketone **124**, followed by subsequent addition of silyloxyfuran **125** and imidazolidinone **77c** and a final addition of **70** (Scheme 6.22C).

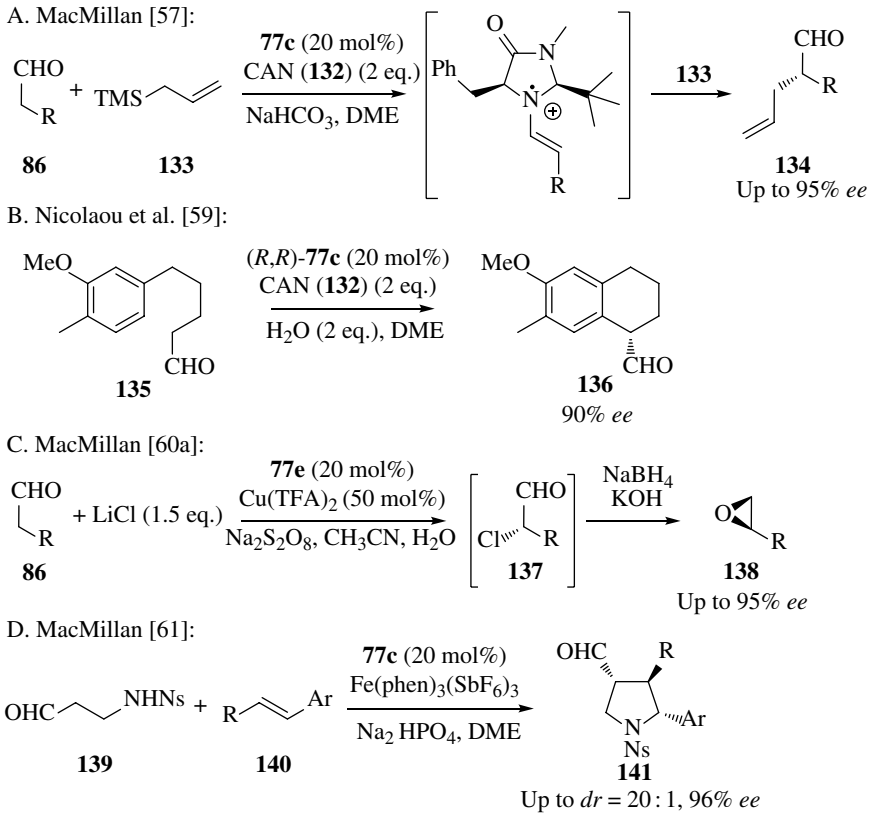
In 2011, the Gilmour group expanded the application scope of chiral iminium catalysis significantly by introducing a new concept for the activation and Umpolung of cyclopropane carbaldehydes **128** [56]. It was found that in the presence of MacMillan's catalyst **77a** the γ-position of the cyclopropane ring can be activated toward a nucleophilic attacked by a chloride source like pyridinium salt **129** first. This results in the formation of a ring-opened enamine intermediate that can then react further with an electrophilic chlorine species, like compound **130**, to furnish the α,γ-dichlorinated carbaldehydes **131** with high stereoselectivities (Scheme 6.23) [56].

In 2007, MacMillan and coworkers succeeded in interrupting the rapid two-electron redox process interconversion between iminium and enamine species (proton abstraction of an iminium species results in an enamine; see Scheme 6.18) by carrying out a one-electron oxidation of an enamine. This generates a three-π-electron radical cation with a SOMO that is activated toward catalytic transformations (racemic or asymmetric) that are not possible using classical enamine or iminium activation [57–61]. In their seminal studies, MacMillan et al. found that SOMO activation of different aldehydes in the presence of the amine catalyst **77c** is possible by using ceric ammonium nitrate (CAN, **132**) as the stoichiometric oxidant. The SOMO-activated intermediate reacted with allyltrimethylsilane (**133**) to give the corresponding α-allylated aldehydes **134** in high yields and enantioselectivities (Scheme 6.24A). Other selected impressive applications using this methodology are depicted in Scheme 6.24. For example, the Nicolaou group successfully employed SOMO activation for the enantioselective intramolecular Friedel–Crafts-type α-arylation of aldehyde **135** en route to the total synthesis of the naturally occurring cytotoxic agent demethyl calamenene [59]. MacMillan's group developed an α-chlorination protocol of aldehydes where the chiral products **137** can be directly transferred into the terminal epoxides **138** [60a], a strategy that was recently successfully used by the Christmann group to convert terpene feedstock into polyketides [60b]. MacMillan et al. also succeeded in carrying out a [3+2] cycloaddition between γ-aminated aldehydes and styrene derivatives to obtain highly functionalized pyrrolidines **141** with high dia- and enantioselectivities (Scheme 6.24D) [61]. By looking at all these examples, it becomes obvious that this methodology unites the unique reactivity of radicals with the high stereoselectivities that can be achieved using chiral secondary amine-based organocatalysts, thus making organocatalysis using SOMO activation a powerful methodology for asymmetric catalysis.

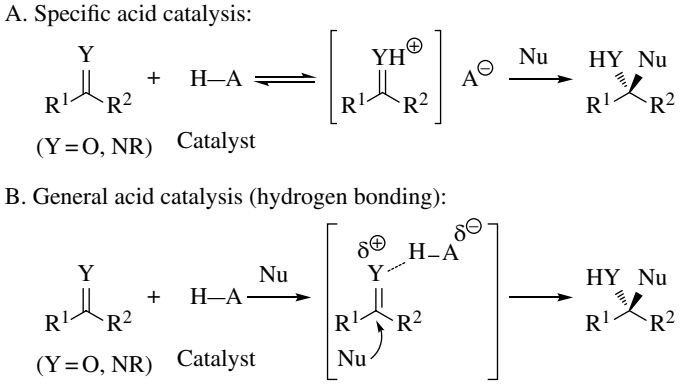
### 6.3.3 Chiral (Brønsted) Acids and H-Bonding Donors

Hydrogen bonding is one of the most important attractive forces in nature. In addition to its importance as a structural determinant, hydrogen bonding also plays a crucial role in catalysis. As hydrogen bonding to an electrophile decreases the electron density of this species, activation toward a nucleophilic attack is achieved. This strategy is successfully employed by nature's catalysts, the enzymes, for the acceleration of a wide range of chemical processes. Mimicking this strategy, organic chemists have begun only recently to appreciate the tremendous potential offered by hydrogen bonding as a catalytic principle for electrophile activation using small-molecule catalysts [62].

From a historical point of view, it is surprising that organic chemists did not start investigating this mode of catalysis until the 1990s, because the first report of Wassermann discussing the beneficial effect of protic additives such as carboxylic acids and phenols to accelerate the cycloaddition of cyclopentadiene with benzoquinone appeared as long ago as 1942 [63]. Looking at the mode of activation, one should



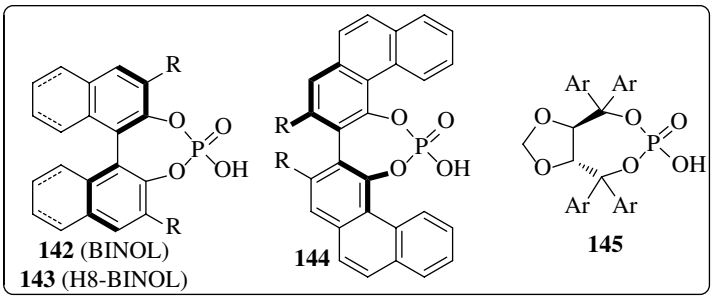

**SCHEME 6.24** Selected reports of asymmetric organocatalysis using SOMO activation.




**SCHEME 6.25** Simplified mechanistic differences between specific and general acid catalysis.

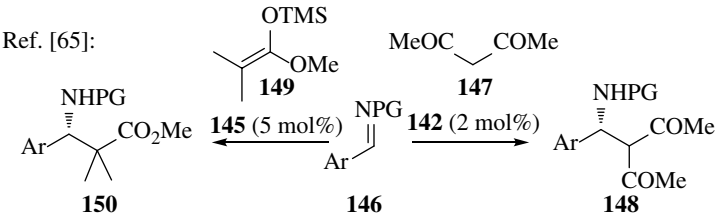
consider two commonly accepted mechanisms: (i) specific acid catalysis and (ii) general acid catalysis. While specific acid catalysis refers to the reversible protonation of the electrophile with a strong acid in a preequilibrium step prior to nucleophilic attack, general acid catalysis involves the proton transfer or hydrogen-bonding activation to the transition state in the rate-determining step (e.g., nucleophilic attack), usually under weakly acidic or neutral conditions (Scheme 6.25) [62]. Realizing the high potential of both, strong Brønsted acids and weaker hydrogen bond donors as (chiral or achiral) small-molecule catalysts to activate electrophiles to facilitate different transformations, a variety of catalysts have been introduced successfully over the last few years [62].

Protons are the simplest and most easily available Lewis acids available to catalyze organic transformations, and the use of a chiral Brønsted acid combines the potential of proton catalysis with asymmetric induction achieved through the choice of the proper counteranion. It is without doubt that chiral phosphoric acids have been the most successfully used chiral Brønsted acids so far [62, 64] and a variety of different applications have been reported over the last years. Scheme 6.26 gives a summarizing overview about only a few



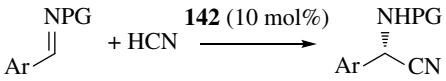

A. Mannich reactions:

Ref. [65]:




B. Strecker reactions:

Ref. [66]:

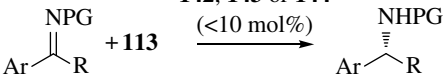



146 151

Up to 99% *ee*

C. Transfer hydrogenations:

Ref. [67]:

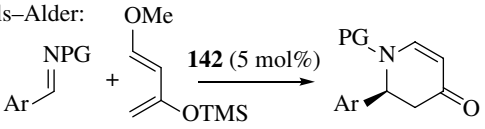



152 153

Up to 99% *ee*

D. (Hetero)-Diels–Alder:

Ref. [68]:

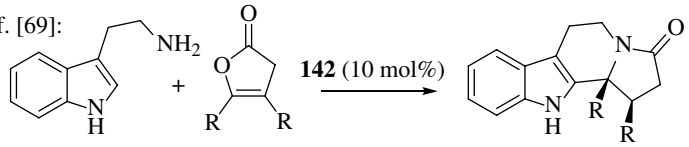



146 154 155

Up to 91% *ee*

E. Cyclization cascades:

Ref. [69]:

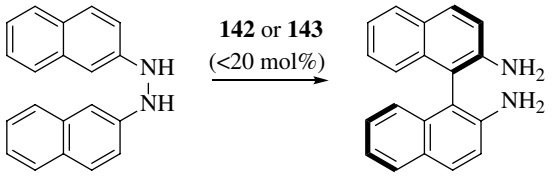



156 157 158

Up to 99% *ee*

F. [3,3]-Rearrangements:

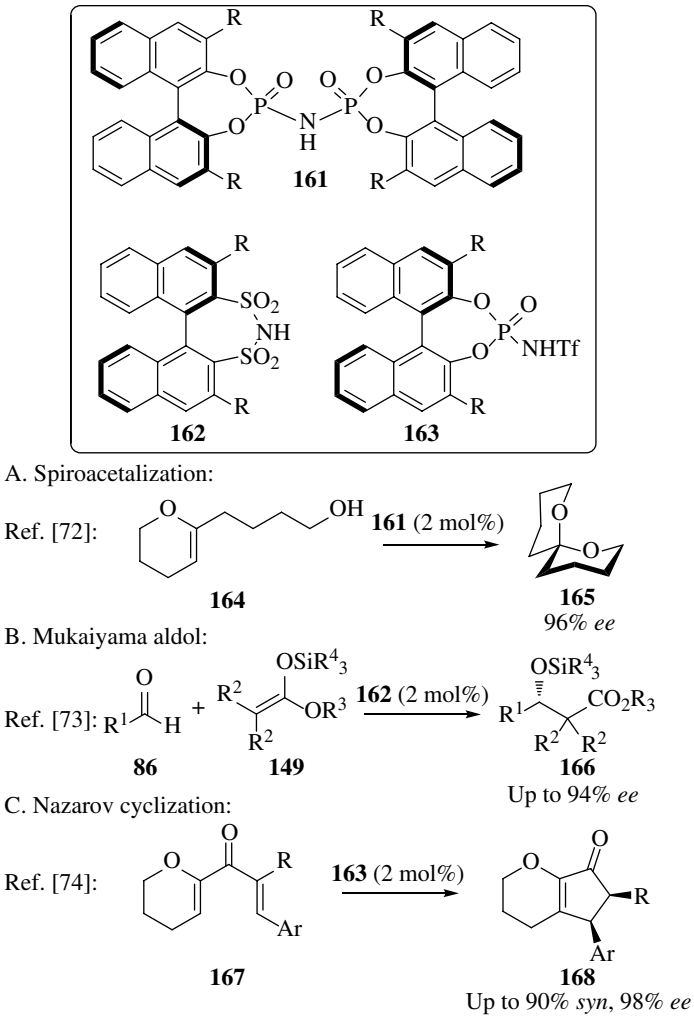
Ref. [70]:




159 160

Up to 92% *ee*

**SCHEME 6.26** Selected applications using chiral phosphoric acid catalysts.

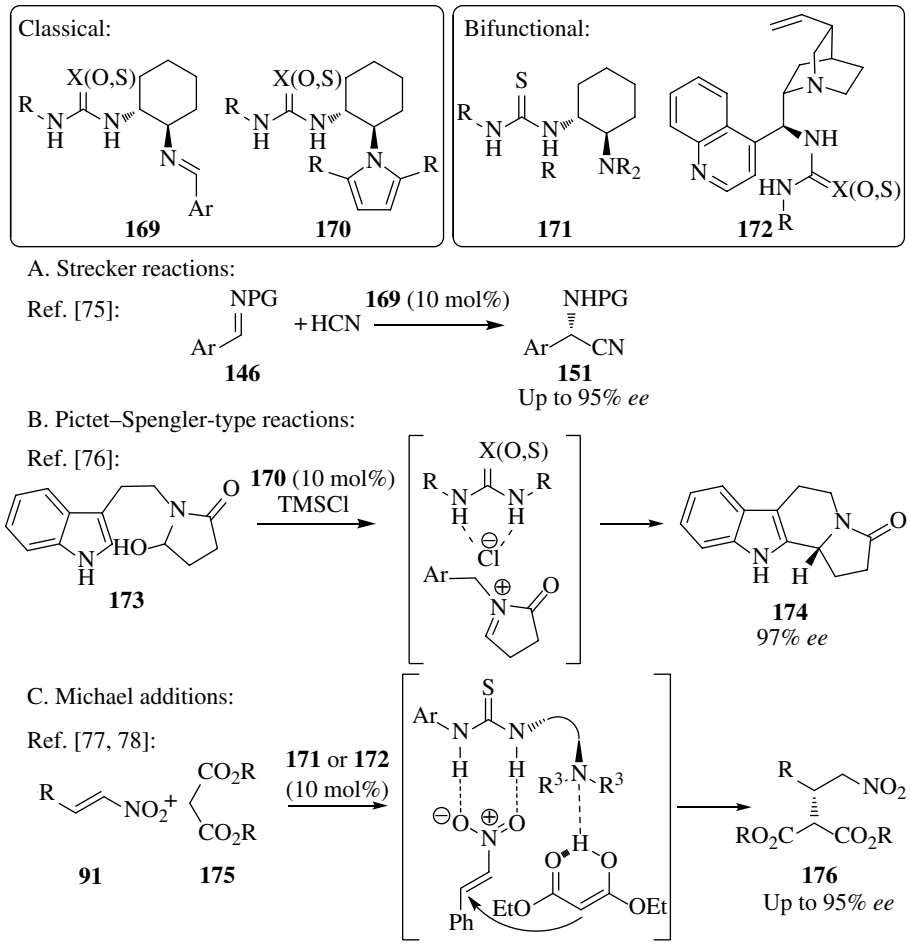



**SCHEME 6.27** Alternative powerful chiral acid organocatalysts and their applications in highly challenging transformations.

of the important reactions [65–70] that can be facilitated and controlled by these catalysts (much more examples and details are discussed in reviews by others [62, 64]). With respect to the catalysts employed therein, binaphthyls have been found to be the most promising chiral backbones for this purpose. However, also other easily available chiral sources like tetraaryl-1,3-dioxolan-4,5-dimethanol (TADDOLs) have been successfully used to access highly efficient catalysts. It should also be noted that recently chiral phosphoric acids have become increasingly important as chiral ligands in metal catalysis and as chiral anionic phase-transfer catalysts (PTCs) [71].

Besides chiral phosphoric acids, also chiral imidodiphosphoric acids **161** [72], disulfonimides **162** [73], or triflylimides **163** [74] have emerged as powerful (Brønsted or Lewis) acid organocatalysts for challenging asymmetric transformations like spiroacetalizations, Mukaiyama aldol reactions, or Nazarov cyclizations (Scheme 6.27).

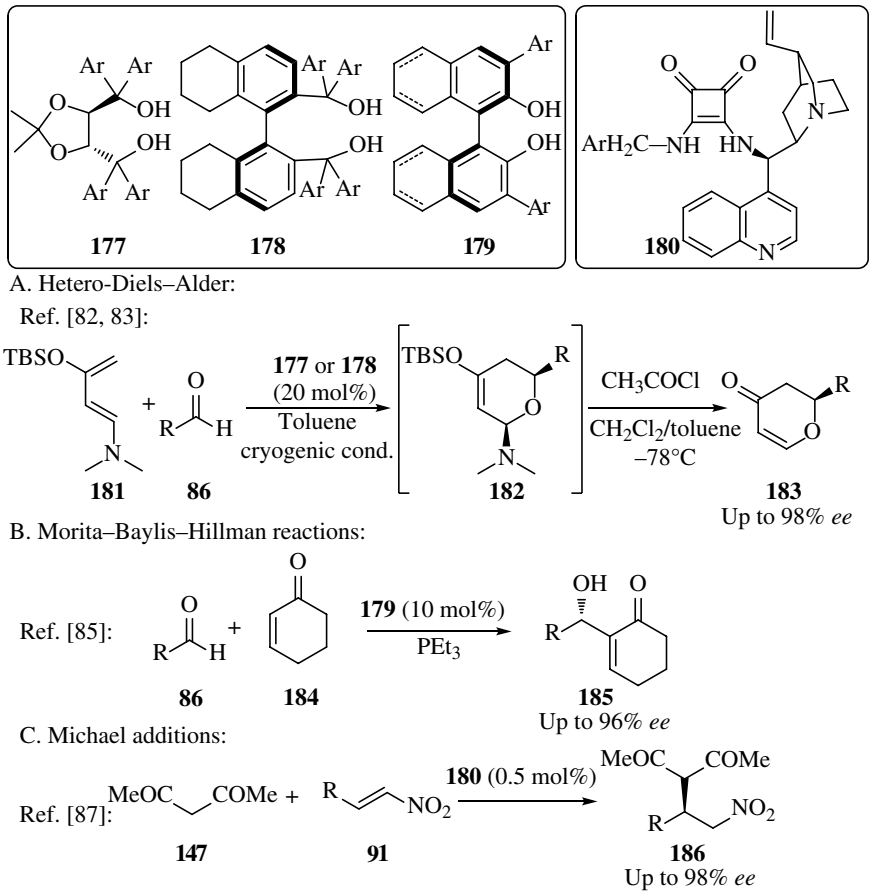
With respect to less acidic chiral hydrogen-bonding catalysts, the most commonly used classes are (thio)ureas, squaramides, (di)alcohols, and guanidinium salts [62]. Significant progress has been made in this field over the last decades, especially when using (thio)ureas. However, concerning the exact activation mode, some caution is necessary. Very often, these chiral thiourea catalysts contain an additional catalytically active motif (bifunctional catalysts) like a basic nitrogen or an additional H-bonding donor, and sometimes it is not that obvious whether a proper bifunctional activation mode is predominant or not. As can be seen by the seminal early examples illustrated in Scheme 6.28, different reactions can be controlled by such bi- or monofunctional catalysts [62, 75–78]. Jacobsen's early landmark reports describing H-bonding-catalyzed Strecker reactions, accompanied by further mechanistic studies that revealed that the (thio)urea is supposed to activate the electrophile in such reactions [75], set the stage for a broad variety of different target reactions that can be successfully controlled by mainly *trans*-1,2-cyclohexanediamine or cinchona alkaloid-based catalysts. One example of a very powerful application




**SCHEME 6.28** Early landmark reports describing the use of chiral (thio)urea organocatalysts.

of these catalysts are asymmetric Pictet–Spengler-type reactions [76]. The cyclization of compound **173** in the presence of catalyst **170** and TMSCl is supposed to proceed through an $S_N1$-type pathway by formation of a chiral ion pair between the catalyst and the substrate [79]. Bifunctional activation using chiral (thio)ureas has obtained a prominent position in asymmetric organocatalysis, and most commonly the second activation site is a tertiary amine group. In 2003, the Takemoto group has introduced the conjugate addition of Michael donors like compound **175** to acceptors **91** catalyzed by bifunctional catalysts **171** [77]. This bifunctional coordination mode is well accepted nowadays and is also supposed to be one of the main reasons for the impressive catalytic potential of bifunctional (thio)urea-containing cinchona alkaloid catalysts like compound **172** in a number of different applications (also in a synergistic fashion with complementary catalysts and activation modes [80, 81]). As already mentioned before, this article cannot give a full overview about the field, and asymmetric organocatalysis with chiral (thio)ureas has been one of the most heavily investigated topics over the last years. Thus, Scheme 6.28 only gives a very condensed introduction to some of the seminal reports, and for further examples and details, the reader is referred to other reviews and the original literature cited therein [62].

In 2003, Rawal reported the use of TADDOLs **177** as chiral H-bonding catalysts to facilitate highly enantioselective hetero-Diels–Alder reactions between dienes **181** and different aldehydes **86** (Scheme 6.29A) [82], and also BINOL-based catalysts **178** were found to facilitate this reaction with excellent selectivities [83]. TADDOLs were also successfully used as organocatalysts for other asymmetric transformations like Mukaiyama aldol reactions, nitroso aldol reactions, or Strecker reactions to mention a few examples only [84]. In addition, also BINOL derivatives have been employed as efficient chiral H-bonding activators as exemplified in the Morita–Baylis–Hillman reaction of enone **184** with different carbaldehydes **86** [85]. The use of chiral squaramides for asymmetric reactions dates back to 2005 when Xie et al. first used camphor-derived squaric amino alcohols as ligands in borane reductions [86]. The first truly organocatalytic application was described by Rawal et al. in 2008 who found that minute amounts of the bifunctional cinchona alkaloid-based squaramide **180** are



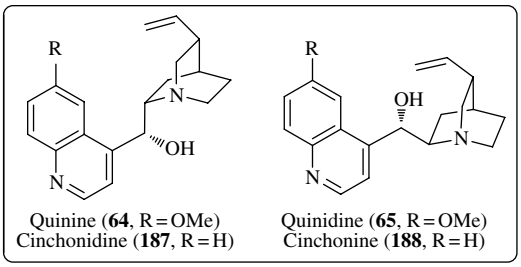

**SCHEME 6.29** Seminal reports describing the use of chiral diol and squaramide organocatalysts.

sufficient to promote the Michael addition of **147** to nitroolefins **91** with excellent selectivities (Scheme 6.29C) [87]. Besides (thio)ureas, diols, and squaramides, also chiral guanidinium salts or amidinium salts as well as other weakly acidic Brønsted acids have been successfully utilized as asymmetric H-bonding organocatalysts, and further details can be found in comprehensive reviews by others [62].

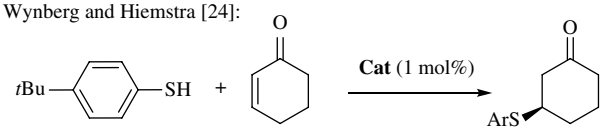
### 6.3.4 Chiral Brønsted/Lewis Bases and Nucleophilic Catalysis

The majority of the organocatalysts that are commonly employed are chiral Lewis or Brønsted bases, and the catalytic potential of base functionalities has been referred to in previous chapters to some extent already. As discussed before, the use of chiral primary or secondary amines for enamine or iminium activation belongs to the most important applications of asymmetric organocatalysts nowadays. In addition, also the interplay between an acidic (thio)urea and a basic amine separated by a chiral linker was shown to enable the simultaneous activation of both the electrophile and nucleophile. In addition to such bifunctional thiourea-containing acid–base catalysts, chiral catalysts containing a (Lewis or Brønsted) base functionality as the sole catalytically active group as well as those having an alternative H-bond donor like a hydroxy group (e.g., cinchona alkaloids) have found widespread applications in asymmetric catalysis [88]. The potential of these catalysts is due to the fact that a variety of different activation modes are possible, thus facilitating their application for different types of reactions. On the one hand, chiral (Brønsted) bases can be used to carry out face-selective deprotonations and the formation of chiral ion pairs, but, on the other hand, chiral (Lewis) bases can also be used as nucleophilic catalysts, which represent a very important application field of chiral base catalysts.

Chiral tertiary amines have found to be among the most useful bases used in modern asymmetric catalysis. With respect to the chiral backbone of these catalysts, cinchona alkaloids have emerged as the most commonly employed representatives and have proven their potential in numerous demanding applications [14, 88]. As mentioned in the introductory chapter, historically one of the first asymmetric organocatalytic reactions can be dated back to Bredig's quinine (**64**)- or quinidine (**65**)-mediated addition of HCN to benzaldehyde (**63**) at the beginning of the last century (Scheme 6.13) [15], a reaction that was later on reinvestigated




Wynberg and Hiemstra [24]:



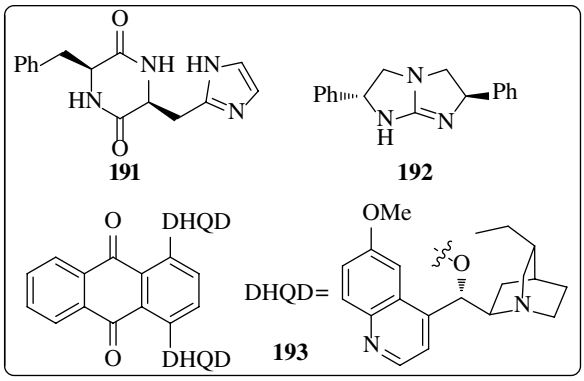

**SCHEME 6.30** Wynberg's and Hiemstra's seminal report describing the use of cinchona alkaloids for asymmetric conjugate additions.

by Prelog [19]. In addition, one of the first highly enantioselective reactions ever was reported by Pracejus in the 1950s, who carried out the addition of methanol to methyl phenyl ketene (**67**) in the presence of *O*-acetylquinine (**68**) (Scheme 6.13) [20]. Thus, cinchona alkaloids are among the most important and versatile chiral natural products available with respect to their application in asymmetric catalysis.

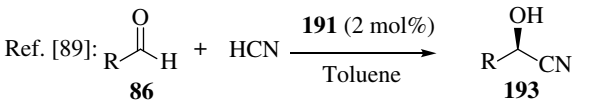
In 1981, Hiemstra and Wynberg reported a thorough investigation of the cinchona alkaloid-catalyzed addition of thiols to α,β-unsaturated enones [24] (Scheme 6.30). Mechanistic studies revealed that the free OH group is crucial in this reaction and thus cinchona alkaloids most likely act as bifunctional catalysts herein. This report may now be considered as one of the major breakthroughs in asymmetric organocatalysis and has inspired a lot of further research toward the development of asymmetric Lewis or Brønsted base catalysts.

Typical other trademark applications of asymmetric Brønsted base catalysis include hydrocyanation reactions, Strecker reactions, or also desymmetrizing esterifications, to mention a few examples only (see Scheme 6.31 for selected seminal reports and Brønsted base catalysts used therein) [89–91].

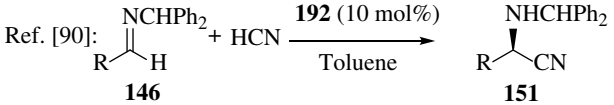
Besides their use as Brønsted bases, chiral tertiary amines have very successfully been used as asymmetric nucleophilic catalysts. Their catalytic potential has been known for decades, and systematic investigations have led to the development of a variety of powerful (a)chiral methodologies [88, 92]. Some of the most prominent applications involve the *in situ* generation of chiral ammonium enolates, which can then be employed for an impressively diverse variety of reactions as illustrated in Scheme 6.32 (for a detailed overview of this rather broad application field of chiral tertiary amines, please see more focused reviews and the literature cited therein [92]). Besides the good



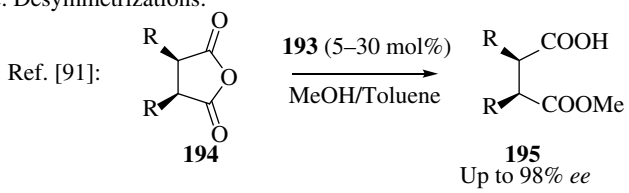

A. Hydrocyanations:




B. Strecker reactions:




C. Desymmetrizations:




**SCHEME 6.31** Early reports describing the use of chiral Brønsted base catalysis.

nucleophilicity of these catalysts (giving the reactive chiral intermediates), this methodology also benefits from the good leaving group ability of the *tert*-amine group, thus resulting in a powerful catalytic principle for demanding applications. This opened the stage for approaches where common (weaker) achiral leaving groups like halides can be replaced by chiral *tert*-amines *in situ* and the corresponding chiral enolates then undergo different [*n*+1] or [*n*+2] cyclization reactions (types 1 and 2). In addition nonnucleophilic starting materials like enones or allenoates can be activated *in situ* and used as nucleophiles for Morita–Baylis–Hillman-type reactions or cycloaddition reactions (type 3) [92] (Scheme 6.32). The most commonly employed classes of catalysts for these approaches are cinchona alkaloids and various fine-tuned derivatives thereof as well as planar-chiral DMAP analogous [93].

Besides chiral amines, also phosphines, sulfides, *N*-heterocyclic carbenes (NHCs), phosphoramides, and formamides have been impressively utilized as chiral Lewis base catalysts in numerous case studies [14, 88]. Chiral phosphines have been mainly used for Baylis–Hillman-type reactions and allenoate activations in this context [88, 94].

For example, the first chiral phosphine-catalyzed [3+2] cycloaddition has been reported in 1997 by Zhang's group [95] (Scheme 6.33A), and a variety of different chiral phosphine catalysts and applications thereof have been reported over the last years [94]. Besides monofunctional catalysts, also bifunctional phosphines like the amino acid-derived **197** have been successfully designed and applied for challenging reactions recently [96], and this additional noncovalent coordination site turned out to be highly beneficial to obtain good selectivities in these transformations. Chiral sulfides have emerged as powerful catalysts to facilitate catalytic stereoselective Corey–Chaykovsky-type epoxidation, cyclopropanation, or aziridination reactions (for an early example in this field, see Scheme 6.33C) [97, 98].

Like (chiral) phosphines that have primarily been used as ligands in (transition) metal catalysis or as achiral nucleophilic catalysts before evolving as powerful asymmetric organocatalysts more recently, also carbenes have for a long time mainly been employed either as ligands or as achiral Umpolung catalysts. The latter has been systematically investigated since Breslow's pioneering studies on the activation mechanism of thiamine in the Umpolung of aldehydes (proceeding via the so-called Breslow intermediate) in the 1950s [99]. The use of chiral carbenes as asymmetric organocatalysts has attracted the interest of more and more research groups over the last years [88, 100]. Noteworthy, the use of chiral heterocyclic carbenes for asymmetric benzoin condensations dates back to 1966 when Sheehan et al. used the thiazolium salt **206** to obtain benzoin **207** with an optical purity of around 20% [101] (Scheme 6.34A), and other groups introduced more powerful chiral thiazolium catalysts later [100]. The Enders group introduced chiral triazolium catalysts like compound **208** for asymmetric benzoin and Stetter reactions in 1996 [102], and this catalyst class was then systematically developed further [100]. For example, the Rovis group used triazolium salts **209** for highly asymmetric intramolecular Stetter reactions [103]. In 2008, She et al. first reported the intramolecular racemic hydroacylation of electron-rich enol ethers [104], and in 2011 the Glorius group carried out the highly enantioselective hydroacylation of electron-neutral olefins like **213** under NHC catalysis [105].

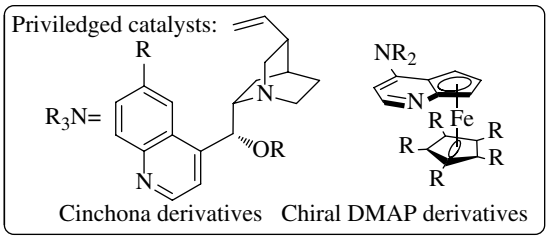
One of the most versatile applications of NHC catalysis is the conjugate Umpolung of α,β-unsaturated aldehydes, thus making the β-position nucleophilic (homoenolate equivalents) [106]. This concept was first introduced by the groups of Bode and Glorius using achiral NHC catalysts in 2004 [107]. In addition, the homoenolate intermediate can also undergo a β-protonation to obtain an enol or enolate species with the characteristic nucleophilic α-position or the tautomeric activated carboxylate species (see Scheme 6.34E) [106]. The Scheidt group demonstrated that it is possible to control the generation of these reactive intermediates by carefully chosen reaction conditions and carry out subsequent reactions like the intramolecular Michael reaction/lactone formation cascade of compound **216** with excellent enantioselectivities (Scheme 6.34E) [108]. Over the last years, this unique methodology was significantly developed further and resulted in the implementation of a variety of highly versatile enantioselective organocatalytic protocols by different research groups [106].

Chiral formamides and chiral phosphoramides have proven to be useful Lewis base catalysts for the activation of Lewis acids, especially organosilicon nucleophiles [88d]. The activation is normally considered to be due to a Lewis base–Lewis acid interaction between the catalyst and the silicon of the nucleophile, forming a hypervalent highly reactive silicon intermediate, which then activates the carbonyl group. This concept of Lewis base activation of a Lewis acid was thoroughly investigated especially by the Denmark group in the past [88d]. In 1994, Denmark et al. first reported the chiral phosphoramide **218**-catalyzed allylation of aromatic aldehydes using allyltrichlorosilane as the nucleophile (Scheme 6.35A) [109]. The same group subsequently carried out very detailed investigations concerning the mechanism and activation mode of these catalysts and found dimeric catalysts like compound **219** to be superior for this important reaction and also highly versatile for asymmetric crotylation reactions [110]. In 1998, Iseki et al. reported the use of chiral formamide **220** for this transformation [111]. A third class of chiral Lewis base activators capable of rendering this transformation stereoselective are chiral *N*-oxides like compound **221**, which was implemented by Nakajima's group in 1998 [112] (Scheme 6.35A).

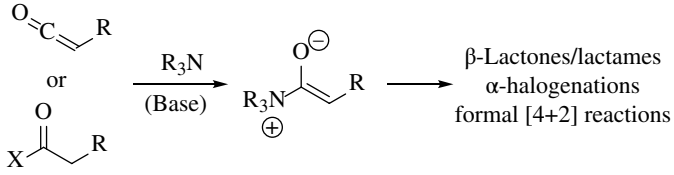
Over the years the chiral Lewis base activation of group 14 Lewis acids has resulted in the development of a variety of asymmetric protocols for challenging target reactions like asymmetric Mukaiyama aldol reactions or reductions of imines using trichlorosilane as the reducing agent (for a detailed overview, please see two very comprehensive reviews by Denmark's group and the primary literature cited therein [88d, 113]). Besides the stereoselective activation of group 14 Lewis acids, also the reactivity of reagents containing group 16 or group 17 Lewis acids can be controlled in a stereoselective fashion using chiral Lewis base catalysts. For example, very recently the Denmark group succeeded in carrying out the enantioselective intramolecular carbosulfenylation of olefins **225** using the selenophosphoramide **222** as a chiral Lewis base activator (Scheme 6.35B) [114]. The potential of chiral Lewis bases in asymmetric halofunctionalization reactions has also recently be reviewed and compared with other activation modes by Denmark et al., and the interested reader is referred to this excellent overview [115].

### 6.3.5 Asymmetric Phase-Transfer Catalysis

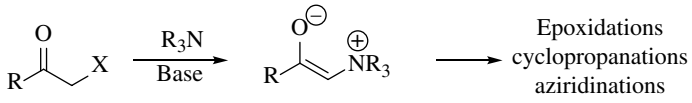
The term "phase-transfer catalysis" was introduced in 1971 by Starks, explaining the critical role of tetraalkylammonium or phosphonium salts to promote reactions between two



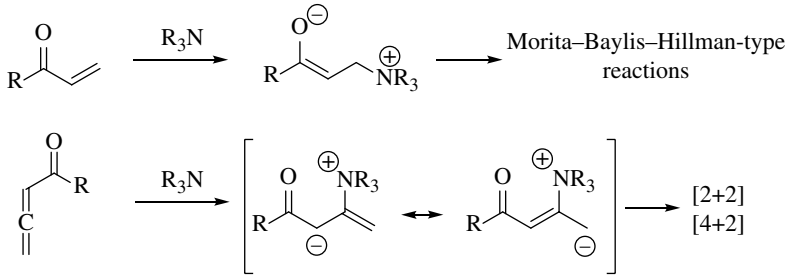

A. TYPE 1 (C2 building block for [n+2] cyclizations):



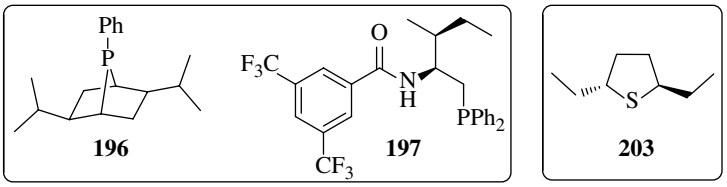

B. TYPE 2 (C1 building block for [n+1] cyclizations):



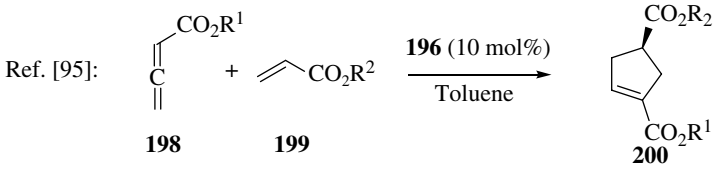

C. TYPE 3 (Activation of enones and allenoates):



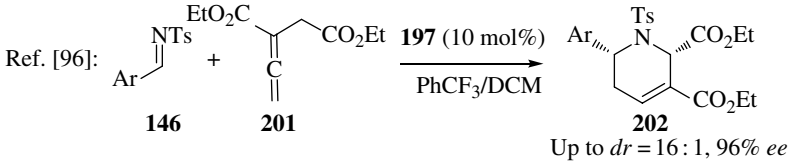

**SCHEME 6.32** General overview about the possible applications of chiral tertiary amine-based nucleophilic catalysts.



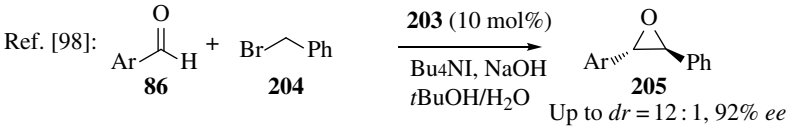

A. [3+2] Cycloaddition:



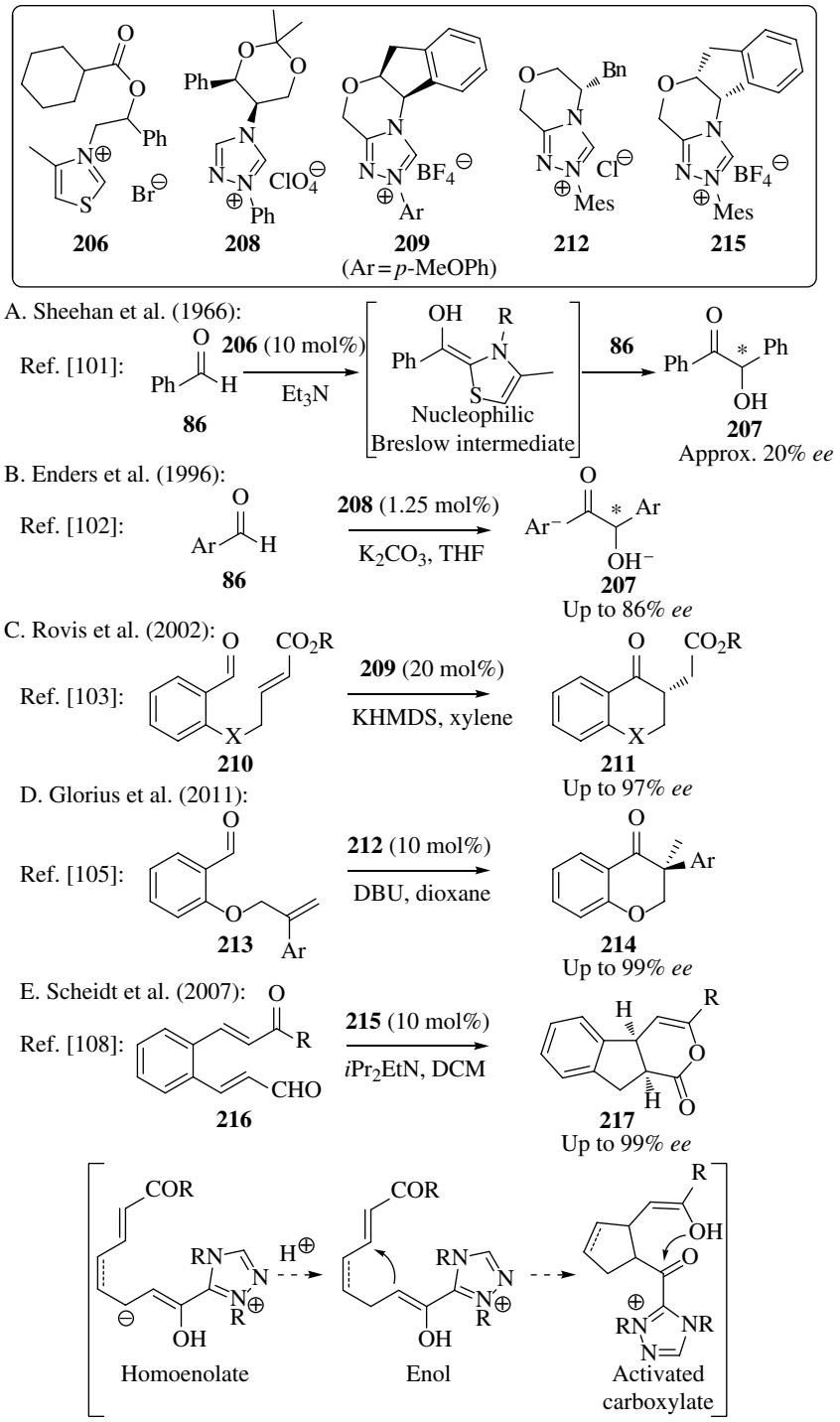

B. [4+2] Cycloaddition:




C. Catalytic stereoselective Corey–Chaykovsky epoxidations:

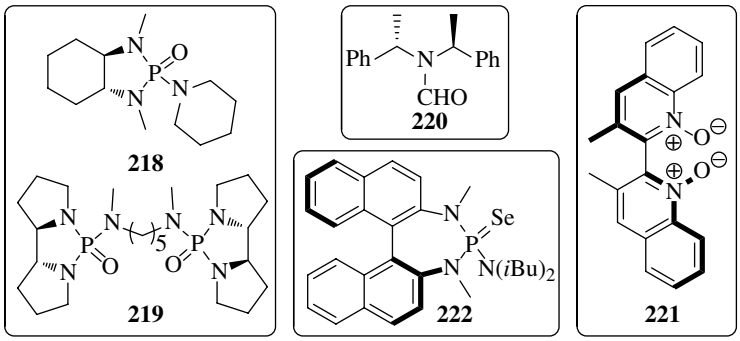



**SCHEME 6.33** Selected landmark reports in the field of chiral phosphine- or sulfide-based Lewis base catalysis.

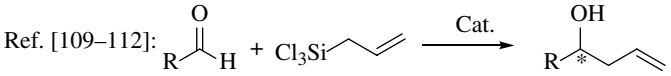



**SCHEME 6.34** Selected milestone reports in the field of asymmetric NHC catalysis.

substances located in different immiscible phases [116]. Subsequently, the use of achiral quaternary ammonium salts as PTCs has attracted widespread interest not only in academia but also for industrial applications soon after the first reports in the 1970s [117]. On the other hand, the development of asymmetric phase-transfer catalysis has progressed significantly more slowly [79, 118]. From a historical point of view, this is rather surprising as the first example by Wynberg reporting the use of cinchona alkaloid-derived quaternary ammonium salts for asymmetric epoxidation reactions dates back to 1976 [23] (Scheme 6.36A) and the first highly enantioselective application was reported back in



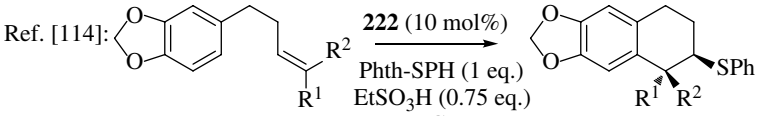

A. Activation of group 14 Lewis acids (e.g., allylation reactions):




**86** **223** **224**

Cat. **218** (25 mol%) : up to 60% *ee*
Cat. **219** (5 mol%) : up to 88% *ee*
Cat. **220** (20 mol%) : up to 93% *ee*
Cat. **221** (10 mol%) : up to 92% *ee*

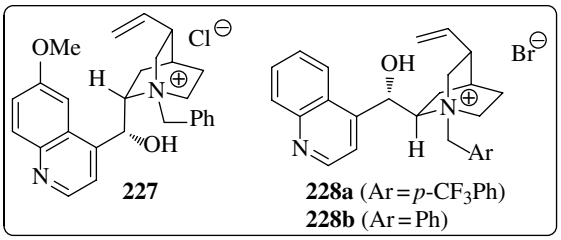
B. Activation of group 16 Lewis acids (e.g., carbosulfenylation of olefins):



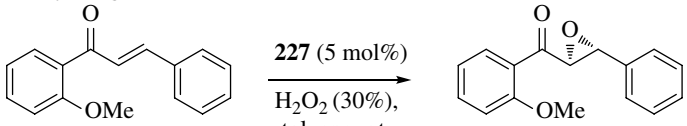

**225** **226**

Up to *dr* = 100 : 1 and 94% *ee*

**SCHEME 6.35** Exemplified reports illustrating the use of chiral Lewis base catalysts for the activation of Lewis acids.

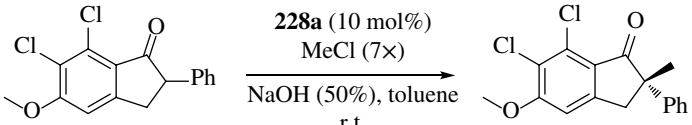



A. Wynberg et al. [23]:



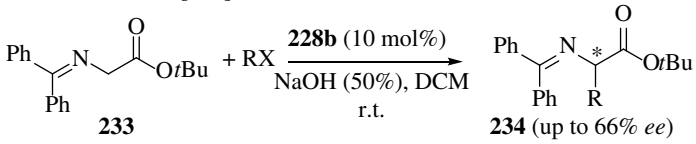

**229** **230** (98%, 25% *ee*)

B. Dolling et al. [22]:



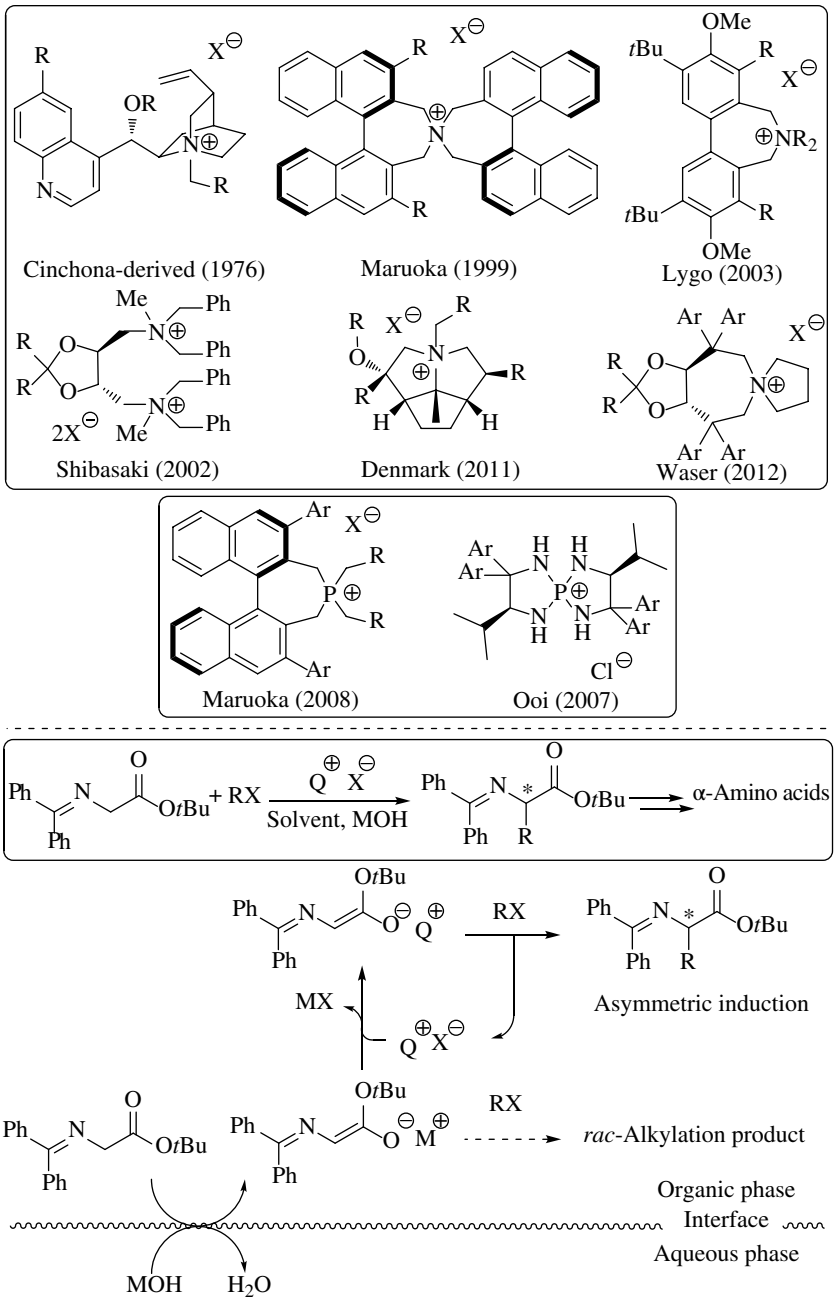

**231** **232** (95%, 92% *ee*)

C. O' Donnell et al. [119]:




**233** **234** (up to 66% *ee*)

**SCHEME 6.36** Seminal reports describing the use of chiral ammonium salt PTCs.




**SCHEME 6.37** Structures of different classes of chiral PTCs and illustration of their ion-pairing activation mechanism.

1984 by Dolling's group at Merck Research Laboratories who succeeded in carrying out the α-methylation of phenylindanone **231** with high selectivities (Scheme 6.36B) [22]. In 1989, O'Donnell et al. first reported the use of chiral ammonium salt catalysts for the asymmetric α-alkylation of glycine Schiff base **233** giving access to chiral (non)natural amino acid derivatives in a so far unprecedented way (Scheme 6.36C) [119].

The α-alkylation of glycine Schiff base **233** has become one of the most important applications of chiral PTCs, and over the years a variety of structurally different chiral ammonium and phosphonium salt catalysts have been developed by different groups [118]. Scheme 6.37 gives an overview of representative catalysts and the commonly accepted chiral ion-pairing mechanism of such catalysts ($Q^+X^-$) in the benchmark alkylation of **233**. In analogy, also the addition of **233** to Michael acceptors can be controlled very efficiently by using these catalysts [118]. With respect to the privileged catalyst motives that are commonly used, the cinchona-derived salts and the Maruoka-type ammonium salt catalysts

have emerged as the most thoroughly investigated and routinely used chiral PTCs in the past [118].

Compared to other commonly employed activation modes, the use of chiral ion-pairing catalysts is a complementary strategy that allows to stereoselectively activate important prochiral nucleophiles like enolates in a noncovalent fashion. Accordingly, a broad variety of fundamental enolate reactions can be controlled by using these catalysts, and a number of excellent reviews covering this topic have been published in the past [118].

Besides classical monofunctional onium salts, also catalysts containing a complementary second activation site (e.g., a free OH group; see Scheme 6.36—catalysts **227** and **228** for early examples) have been systematically developed and applied for challenging target reactions over the last decades [120]. Hereby, the mode of action of the second functionality can either be an additional coordination of the nucleophile (thus achieving a better control of the orientation of the nucleophile) or an activation/coordination of the electrophile, thus resulting in a highly ordered transition state. Besides additional free OH groups, also alternative catalytically powerful functional groups like (thio)ureas or Lewis acids have been successfully implemented recently [120].

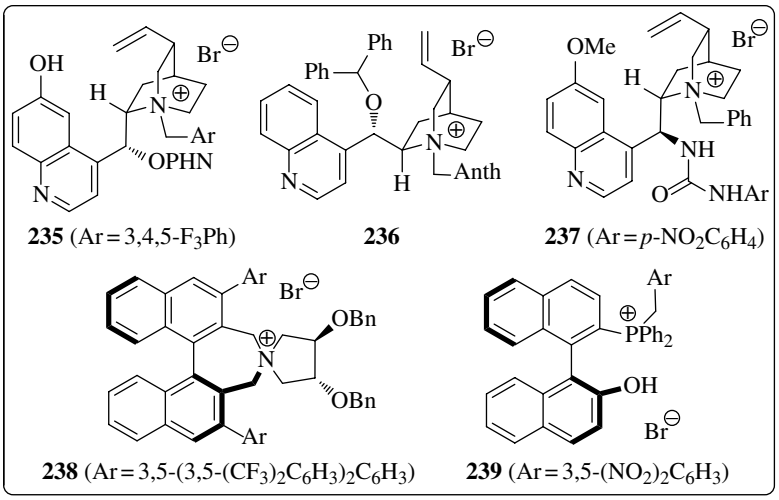
Scheme 6.38 highlights some chosen more recent impressive reports [121–125] using chiral mono- and bifunctional onium salt catalysts to illustrate the high potential of this catalytic principle for asymmetric catalysis (for more examples and further details, the interested reader is referred to detailed reviews and the primary literature cited therein [118, 120]). As can be seen in these selected examples, the possible application scope of chiral cationic PTCs is a very broad one facilitating such important transformations like Darzens reactions [121], diaziridinations [122], 5-endo-dig cyclizations [123], or even functionalizations of allenes [124]. In addition, as illustrated in the base-free Michael addition protocol developed by Maruoka's group (Scheme 6.38E), in some cases exceptionally low catalyst loadings still gave very high selectivities [125].

Besides chiral cations, also chiral anion PTCs have recently been successfully implemented for challenging asymmetric transformations [71, 126]. However, this strategy was much less thoroughly investigated in the past than the use of chiral cation catalysts. One fact that should be emphasized is that an exact classification of the real activation mode is not always trivial in this field. To illustrate the difficulties associated with respect to the classification of chiral anion PTCs and the exact activation mechanism, the use of asymmetric phosphoric acid catalysts should be briefly mentioned. Hereby different modes of activation are possible in principle (see also the previous chapter on chiral acids). One extreme case involves complete protonation of the substrate and formation of a chiral ion pair with the conjugated base of the catalyst. On the other hand, such catalysts might also activate the substrate via H-bonding, and therefore, it is also a question of definition and a matter of understanding of the exact mechanism of such reactions whether a catalyst is considered to be an ion-pairing PTC or an H-bonding activator (for a very detailed discussion of this matter please, see a recent review by Toste et al. [71]). In addition, it was already shown before (see Scheme 6.28; Pictet–Spengler reaction) that chiral (thio)ureas are capable of forming chiral ion pairs during the catalytic cycle [76], thus illustrating that the concept of chiral ion-pairing catalysis is not only limited to classical phase-transfer catalysis.

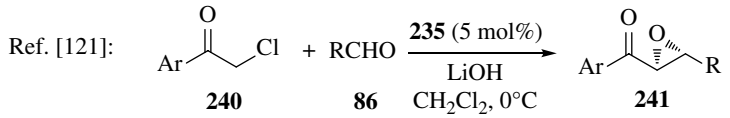
Scheme 6.39 shows two recent examples of Toste's group using chiral anion ion-pairing catalysts [127, 128]. In 2008, they succeeded in using chiral silver phosphates (generated *in situ* from an achiral sparingly soluble silver source and compound **250**) to catalyze the highly stereoselective ring opening of *in situ* formed *meso*-aziridinium or episulfonium compounds [127]. Thus, the silver ion first facilitates aziridinium formation by abstraction of the chloride of **251**, and the aziridinium intermediate then forms a chiral ion pair with the chiral phosphate, which then undergoes highly enantioselective ring-opening reactions with different alcohols (Scheme 6.39A). More recently, Toste et al. described the use of chiral anionic PTCs for asymmetric fluorination reactions [128]. In this inspiring approach Selectfluor (**253**) was used as a cationic fluorinating agent, which is normally insoluble in nonpolar organic solvents. It was hypothesized that lipophilic chiral phosphate anions like the base of **250b** will undergo an anion exchange with the tetrafluoroborate anions of Selectfluor to bring the reagent into solution. The resulting chiral ion pair can then facilitate an asymmetric fluorination of different organic substrates (Scheme 6.39B) [128].

## 6.4 ORGANOCATALYSIS IN THE TOTAL SYNTHESIS OF IRIDOIDS AND MONOTERPENOID INDOLE ALKALOIDS

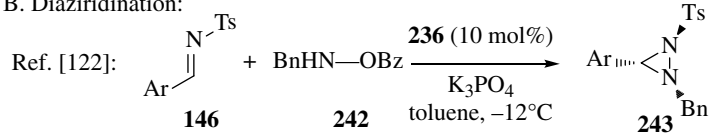
Over the last 15 years, asymmetric organocatalysis has become a powerful tool in natural product synthesis [30]. This chapter will cover some selected examples with the aid of organocatalysts for the synthesis of iridoids and the terpenoid parts of monoterpenoid indole alkaloids. However, looking at the different types of activation modes that are possible using organocatalysts and their diverse application scope, it becomes obvious that asymmetric organocatalysis cannot only be associated with a single class of natural products that can be accessed thereby. In contrast, it turned out that organocatalysts can be powerful tools in the synthesis of a very broad variety of primary or secondary metabolites, and the interested reader is referred to comprehensive reviews about this topic for further details [30]. In addition, it is also not only one single class of organocatalysts that has



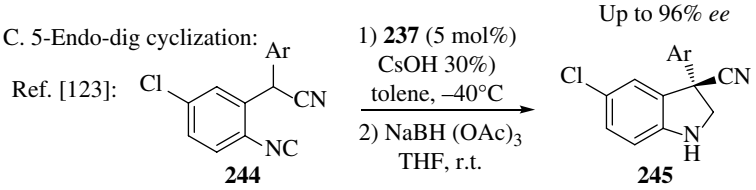

A. Darzens reaction:



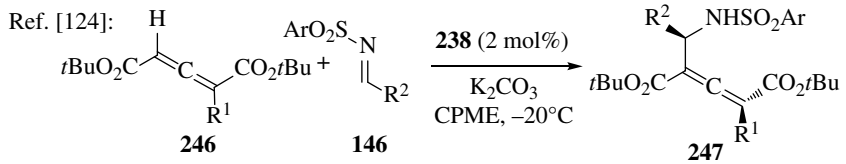

B. Diaziridination:



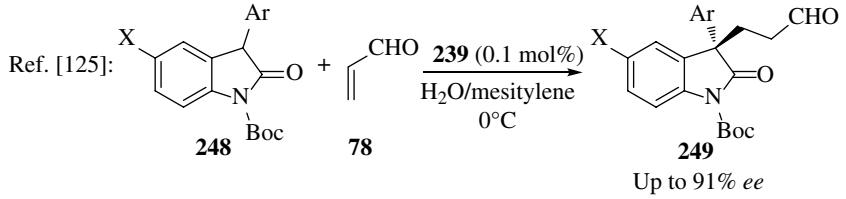

C. 5-Endo-dig cyclization:




D. Alleno–Mannich reaction:




E. Base-free Michael addition:

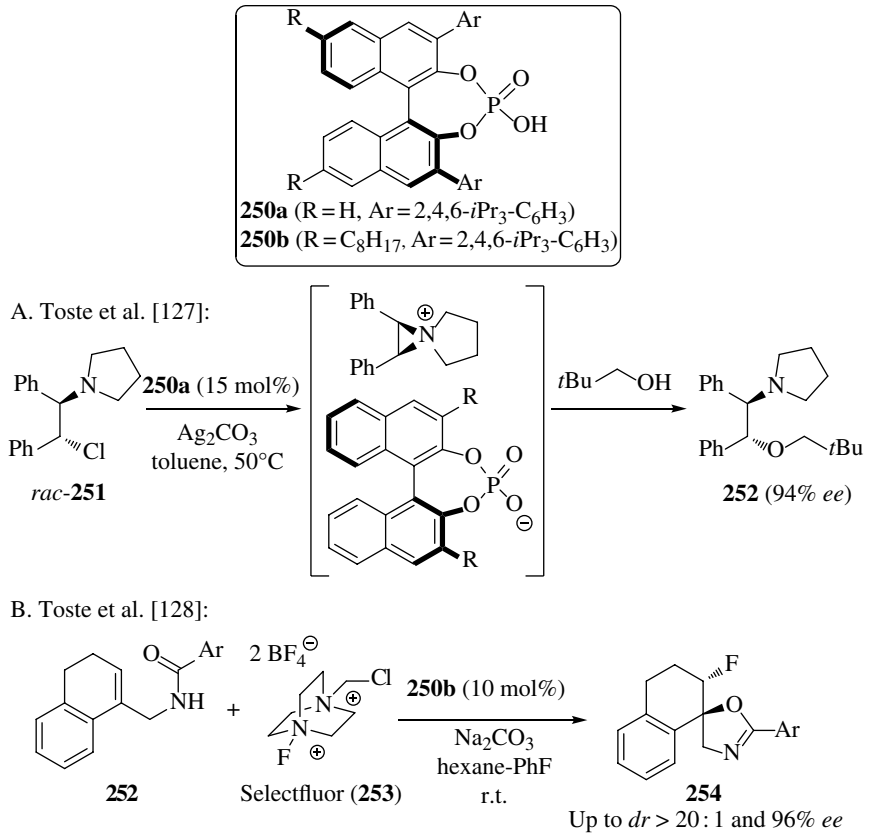



**SCHEME 6.38** Selected recent examples using chiral cationic PTCs.

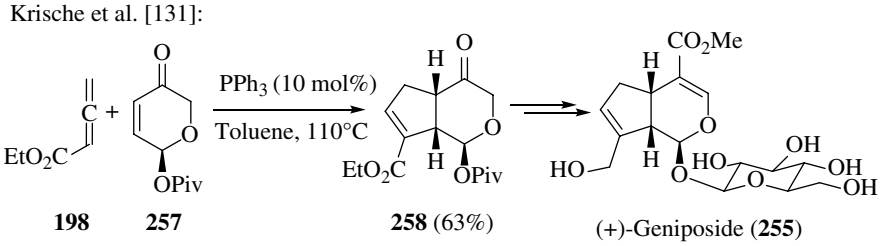
been primarily used herein. In contrast, because of different retrosynthetic strategies and disconnection approaches, different classes of organocatalysts, either chiral or achiral, have been successfully employed for the total synthesis of iridoids and monoterpenoid indole alkaloids.

### 6.4.1 (+)-Geniposide and 7-Deoxyloganin

The total syntheses of the iridoids (+)-geniposide (**255**) and 7-deoxyloganin (**256**) are two illustrative cases where achiral nucleophilic organocatalysts have been successfully used to facilitate cyclization reactions of chiral starting materials.




**SCHEME 6.39** Selected recent examples using chiral anionic ion-pairing catalysts.




**SCHEME 6.40** Phosphine-catalyzed [3+2] cycloaddition in the total synthesis of the iridoid β-glucoside (+)-geniposide (**255**).

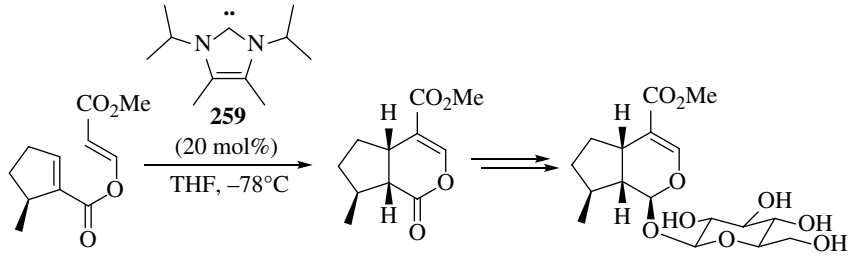
The iridoid β-glucoside (+)-geniposide (**255**) was isolated from *Gardenia jasminoides* [129] and displays potential antitumor and anti-inflammatory activities [130]. A triphenylphosphine-catalyzed [3+2] cycloaddition (please compare with Scheme 6.33) between allene **198** and the chiral enone **257** was the key step in a recent synthesis of (+)-geniposide (**255**) by the Krische group [131]. By carrying out the cycloaddition at elevated temperature (110°C), the bicyclic key intermediate **258** could be obtained in 63% yield as a single regio- and stereoisomer (Scheme 6.40).

The Lupton group has reported the total synthesis of 7-deoxyloganin (**256**; compare with Scheme 6.11) [132]. Hereby, the synthesis of the bicyclic core was accomplished by an achiral NHC (**259**)-catalyzed rearrangement of the chiral enol ester **260** (Scheme 6.41). This furnished the lactone **261** in reasonable yield and with full transfer of stereoinformation, giving access to **256** after just three further steps.

### 6.4.2 (–)-Brasoside and (–)-Littoralisone

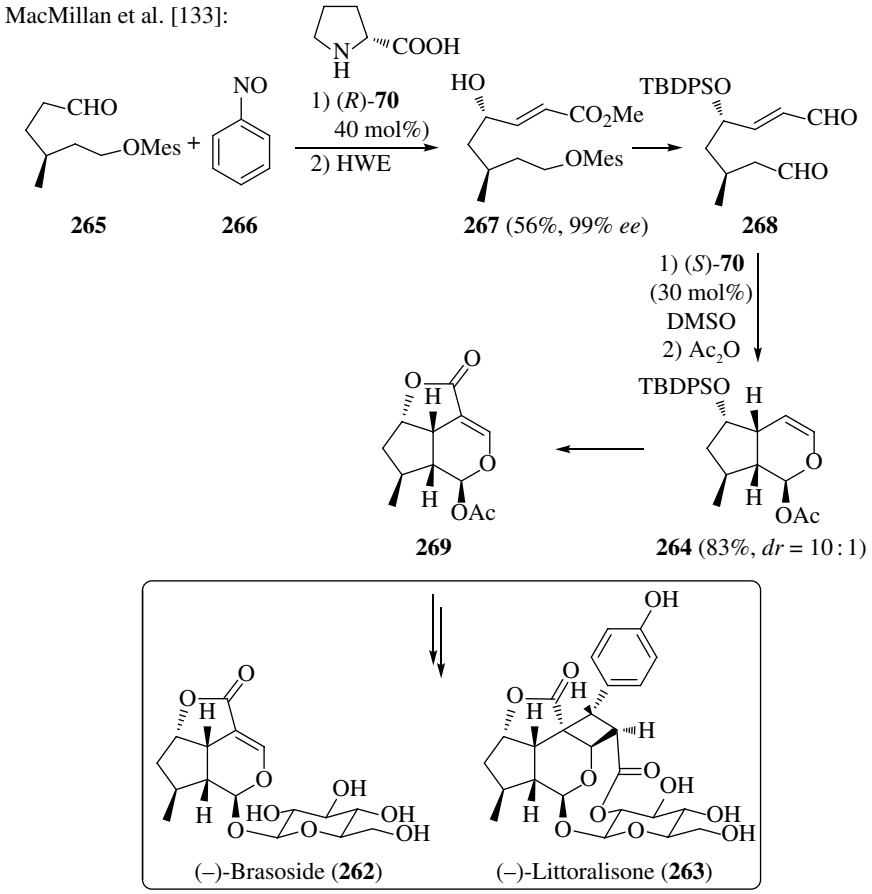
The first stereoselective total syntheses of the two complex natural products brasoside (**262**) and littoralisone (**263**) were reported by MacMillan's group in 2005 [133] (Scheme 6.42). Littoralisone (**263**) is the active ingredient of extracts of *Verbena litoralis* for increased nerve growth factor (NGF)-induced neurite outgrowth in PC12D cells [134] and is presumed to be derived biochemically from brasoside (**262**)

Lupton et al. [132]:



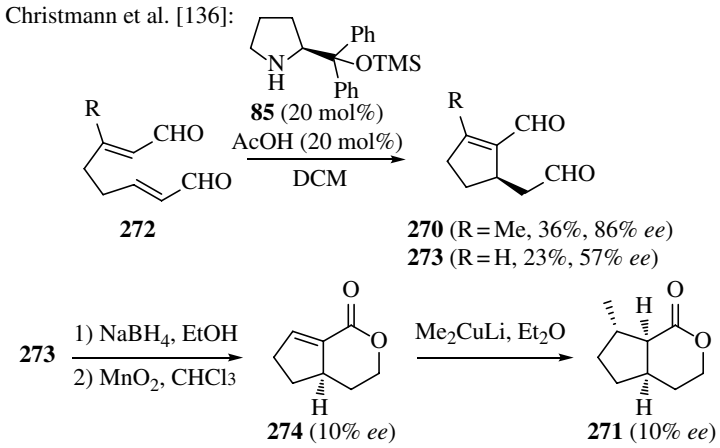

**SCHEME 6.41** NHC-catalyzed cyclization in the synthesis of 7-deoxyloganin (**256**).

MacMillan et al. [133]:




**SCHEME 6.42** Proline-catalyzed transformations in the total syntheses of (–)-brasoside (**262**) and (–)-littoralisone (**263**) proceeding via the iridoid **264**.

[135]. Retrosynthetically, the syntheses of both compounds build on the iridoid **264** as the key intermediate. The required *cis*-bicyclic skeleton was obtained successfully starting from the (–)-citronellol-derived aldehyde **265**. First, an asymmetric enamine-activated α-oxygenation catalyzed by (*R*)-proline (**70**) followed by a Horner–Wadsworth–Emmons (HWE) olefination gave compound **267**. Redox state manipulations and O-protection then result in the formation of the dialdehyde **268**. This formyl-enal Michael acceptor was submitted further to a (*S*)-**70**-catalyzed intramolecular conjugate addition (please compare also with Scheme 6.19—enamine activation). The crucial part hereby was the choice of solvent. While $CHCl_3$ resulted in the formation of the *trans*-isomer, the use of DMSO gave the kinetic *cis*-product **264** in good yield and selectivity upon *in situ* O-acylation of the intermediate lactol. The iridoid **264** was then converted into




**SCHEME 6.43** Chiral amine-catalyzed Rauhut–Currier-type cyclization in the synthesis of the iridoid (+)-mitsugashiwalactone (**271**).

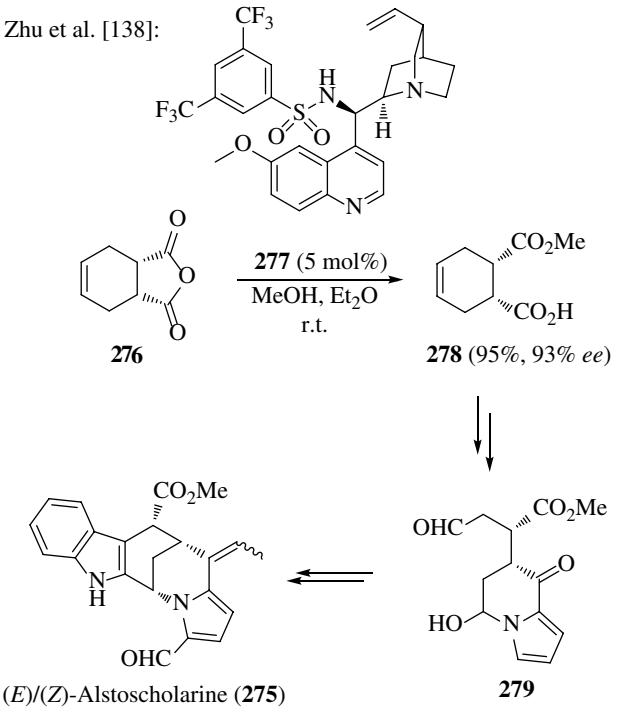
the lactone **269** by standard methods (Scheme 6.42). This advanced intermediate was then successfully used to accomplish the total syntheses of (–)-brasoside (**262**) and (–)-littoralisone (**263**) (for further details on these impressive total syntheses, please see MacMillan's original report [133]).

### 6.4.3 (+)-Mitsugashiwalactone

The Christmann group reported the application of dienamine intermediates for Rauhut–Currier-type reactions [136]. In this case, the α-position of an *in situ* formed dienamine acts as the nucleophile in an intramolecular cyclization reaction, giving access to functionalized monocyclic compounds that can be used to access different natural products. The applicability of this strategy was first tested in the synthesis of the mosquito repellent (*R*)-rotundial (**270**) [136a] and then for the synthesis of the iridoid mitsugashiwalactone (**271**) [136b] (Scheme 6.43). The sequence started with the open-chain precursor **272**. Rauhut–Currier-type cyclization using catalyst **85** then gave the dialdehyde **273** with moderate enantioselectivity (Scheme 6.43; the selectivity is strongly dependent on the substituents of the precursor **272**). Unfortunately, after reduction to the corresponding diol and oxidation to lactone **274**, the enantiopurity dropped significantly. Thus, the final product **271** could be obtained with a rather low *ee* of 10% only. Despite of this low selectivity, this report still illustrates the potential of chiral amine catalysts to access functionalized chiral cyclic molecules in a straightforward manner, and the encouraging results obtained so far still leave space for improvement with respect to future applications.

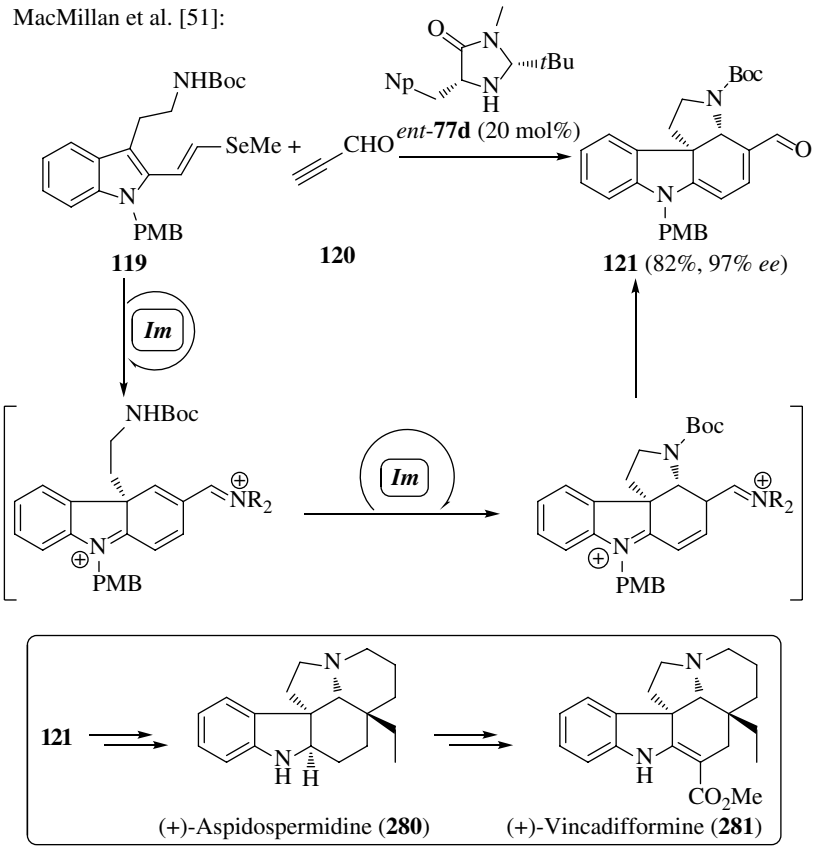
### 6.4.4 Alstoscholarine

The complex monoterpenoid indole alkaloids (*E*)- and (*Z*)-alstoscholarine (**275**) were isolated from the leaves of *Alstonia scholaris*, a plant used in traditional medicine in South and Southeast Asia [137]. An organocatalytic




**SCHEME 6.44** Organocatalytic desymmetrization of the *meso*-anhydride **276** in the syntheses of the monoterpenoid indole alkaloids (*E*)- and (*Z*)-alstoscholarine (**275**).

desymmetrization of the *meso*-anhydride **276** was the starting point in a recent efficient protecting group-free total synthesis of these natural products by the group of Zhu [138]. The desymmetrization of **276** could be achieved by using the bifunctional catalyst **277** to give the hemiester **278** in nearly perfect yield (95%) and high enantioselectivity (93% *ee*) (Scheme 6.44). The advanced intermediate **279** could then be obtained in just three more steps, thus paving the way for the remarkably short and efficient total syntheses of (*E*)- and (*Z*)-alstoscholarine (**275**) [138].



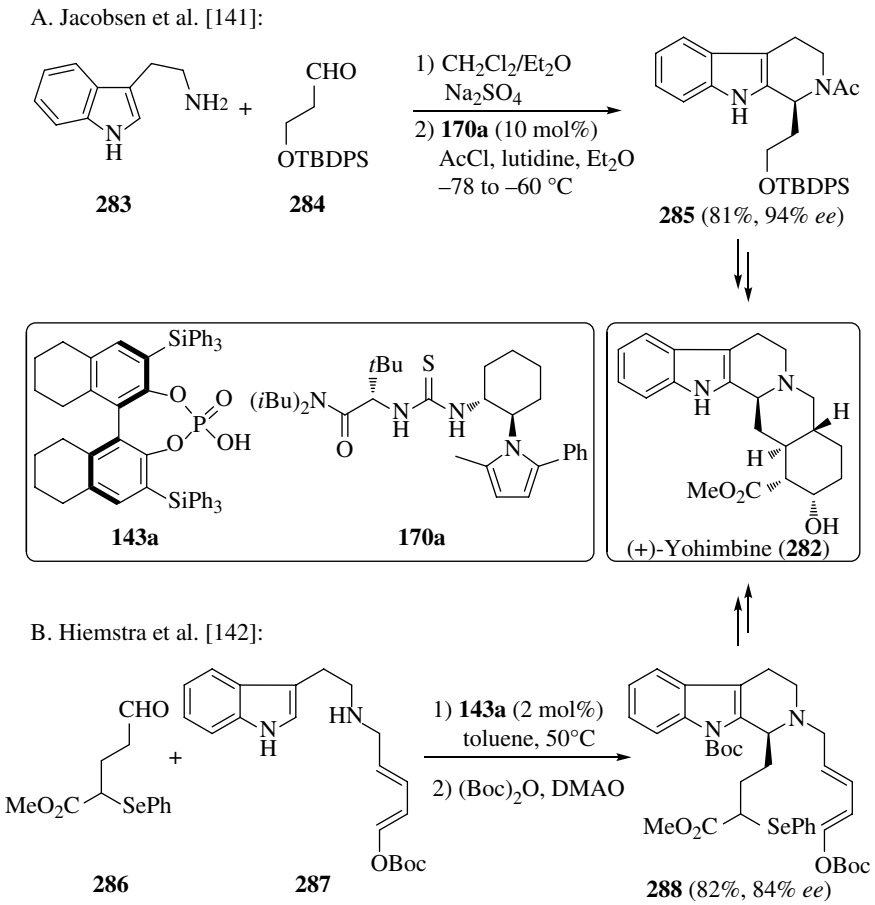

**SCHEME 6.45** Organocatalytic iminium-catalyzed cascade reaction in the total syntheses of (+)-aspidospermidine (**280**) and (+)-vincadifformine (**281**).

### 6.4.5 (+)-Aspidospermidine and (+)-Vincadifformine

As depicted in Scheme 6.21 already (lower reaction), MacMillan et al. have recently developed an impressive iminium-catalyzed organocascade approach to access the highly functionalized indole derivative **121** straightforwardly (Scheme 6.45). Compound **121** is a well-chosen key intermediate for the generation of structurally diverse natural products from simple starting materials, which was demonstrated in the synthesis of six different *Strychnos*, *Aspidosperma*, and *Kopsia* alkaloids [51]. This elegant strategy was of course inspired by the fact that several *Strychnos*, *Aspidosperma*, and *Kopsia* alkaloids share a common biosynthetic intermediate that arises biosynthetically through an enzymatic cascade reaction starting from tryptamine and secologanin [139]. Employing catalyst **77d**, MacMillan and coworkers were able to directly access the key intermediate **121** in a single operation cascade reaction between the tryptamine-derived indole derivate **119** and propynal (**120**). As illustrated in Scheme 6.45, the reaction is assumed to proceed via two iminium catalysis cycles (Diels–Alder cyclization first, followed by conjugate addition). The bioinspired intermediate **121** then served as the starting material to access six structurally different alkaloids in high yields, among them (+)-aspidospermidine (**280**) (24% overall yield) and (+)-vincadifformine (**281**) (8.9% overall yield), two members of the *Aspidosperma* family of monoterpenoid indole alkaloids. These syntheses are by far the shortest and the highest yielding ones published so far for these important biologically active compounds, and further details can be found in the original report by MacMillan et al. [51].

### 6.4.6 (+)-Yohimbine

The final natural product that will be discussed herein to demonstrate the applicability of asymmetric organocatalysis to assemble the monoterpenoid part of indole alkaloids is (+)-yohimbine (**282**) (Scheme 6.46). Yohimbine is a well-known monoterpenoid indole alkaloid that has been isolated from several natural sources and for which the first total synthesis dates back to the 1950s [140]. Two organocatalytic total syntheses of this important natural product have been reported recently by the groups of Jacobsen and Hiemstra [141, 142]. Jacobsen's synthesis of **282** commenced with the thiourea **170a**-catalyzed acyl-Pictet–Spengler reaction between tryptamine **283** and the protected hydroxyaldehyde




**SCHEME 6.46** Organocatalytic Pictet–Spengler reactions in the total synthesis of (+)-yohimbine (**282**).

**284**. Intermediate **285** was then employed successfully to access (+)-yohimbine (**282**) (Scheme 6.46A) [141]. Hiemstra's synthesis of this challenging target employed the phosphoric acid **143a**-catalyzed Pictet–Spengler reaction of aldehyde **286** and tryptamine derivative **287** to install the tertiary stereogenic center in 84% *ee* (Scheme 6.46B). Intermediate **288** was then converted to yohimbine (**282**) by analogy to Jacobsen's report [142].

## 6.5 CONCLUSION

Monoterpenes and iridoids are very important natural products, and the biosynthetic pathways toward these compounds are nowadays well understood. We choose this class of secondary metabolites to highlight the potential of asymmetric organocatalysis for the total synthesis of complex natural products. Asymmetric organocatalysis has been one of the most exciting fields in organic chemistry over the last decades, and we hope that we have been able to illustrate how diverse and powerful this methodology can be with respect to different activation modes that are possible and different substance classes that can be easily accessed thereby.

## REFERENCES

1. P. M. Dewick, *Medicinal Natural Products*, 3rd ed., John Wiley & Sons, Ltd, Chichester, (2009), pp. 187–310.
2. L. Ruzicka, A. Eschenmoser, H. Heusser, *Experientia* 1953, **9**, 357–396.
3. For selected illustrative reviews and further references, see (a) D. W. Christianson, *Chem. Rev.* 2006, **106**, 3412–3442; (b) P. M. Dewick, *Nat. Prod. Rep.* 2002, **19**, 181–222; (c) P. M. Dewick, *Nat. Prod. Rep.* 1999, **16**, 97–130; (d) P. M. Dewick, *Nat. Prod. Rep.* 1997, **14**, 111–144; (e) R. Croteau, *Chem. Rev.* 1987, **87**, 929–954; (f) D. V. Banthorpe, B. V. Charlwood, M. J. O. Francis, *Chem. Rev.* 1972, **72**, 115–155; (g) T. Kuzuyama, H. Seto, *Nat. Prod. Rep.* 2003, **20**, 171–183; (h) J. Bohlmann, G. Meyer-Gauen, R. Croteau, *Proc. Natl. Acad. Sci. U. S. A.* 1998, **95**, 4126–4133.
4. (a) W. N. Hunter, *J. Biol. Chem.* 2007, **282**, 21573–21577; (b) W. Eisenreich, A. Bacher, D. Arigoni, F. Rohdich, *Cell. Mol. Life Sci.* 2004, **61**, 1401–1426; (c) V. S. Dubey, R. Bhalla, R. Luthra, *J. Biosci.* 2003, **28**, 637–646; (d) M. Rodriguez-Concepcion, A. Boronat, *Plant Physiol.* 2002, **130**, 1079–1089.
5. K. Ogura, T. Koyama, *Chem. Rev.* 1998, **98**, 1263–1276.
6. A. L. Schilmiller, I. Schauvinhold, M. Larson, R. Xu, A. L. Charbonneau, A. Schmidt, C. Wilkerson, R. L. Lasta,

E. Pichersky, *Proc. Natl. Acad. Sci. U. S. A.* 2009, **106**, 10865–10870.

7. (a) A. E. Edris, *Phytother. Res.* 2007, **21**, 308–323; (b) N. Dudareva, E. Pichersky, J. Gershenzon, *Plant Physiol.* 2004, **135**, 1893–1902.
8. J. Degenhardt, T. G. Köllner, J. Gershenzon, *Phytochemistry* 2009, **70**, 1621–1637.
9. R. Bentley, *Chem. Rev.* 2006, **106**, 4099–4112.
10. (a) B. Dinda, S. Debnath, Y. Harigaya, *Chem. Pharm. Bull.* 2007, **55**, 159–222; (b) B. Dinda, S. Debnath, Y. Harigaya, *Chem. Pharm. Bull.* 2007, **55**, 689–728; (c) L. J. El-Naggar, J. L. Beal, *J. Nat. Prod.* 1980, **43**, 649–707; (d) C. A. Boros, F. R. Stermitz, *J. Nat. Prod.* 1990, **53**, 1055–1147;(e) C. A. Boros, F. R. Stermitz, *J. Nat. Prod.* 1991, **54**, 1173–1246.
11. R. Tundis, M. R. Loizzo, F. Menichini, G. A. Statti, F. Menichini, *Mini Rev. Med. Chem.* 2008, **8**, 399–420.
12. A. Oudin, M. Courtois, M. Rideau, M. Clastre, *Phytochem. Rev.* 2007, **6**, 259–276.
13. (a) B. P. S. Khambay, *Pestic. Outlook* 2002, **13**, 49–54; (b) L. Crombie, *Pestic. Sci.* 1980, **11**, 102–118.
14. For selected books and reviews, see (a) A. Berkessel, H. Gröger, *Asymmetric Organocatalysis: From Biomimetic Concepts to Applications in Asymmetric Synthesis*, Wiley-VCH, Weinheim, (2005); (b) I. Dalko, *Enantioselective Organocatalysis*, Wiley-VCH, Weinheim, (2007); (c) M. J. Gaunt, C. C. C. Johansson, A. McNally, N. T. Vo, *Drug Discov. Today* 2007, **12**, 8–27; (d) J. Seayad, B. List, *Org. Biomol. Chem.* 2005, **3**, 719–724; (e) S. Bertelsen, K. A. Jørgensen, *Chem. Soc. Rev.* 2009, **38**, 2178–2189; (f) D. W. C MacMillan, *Nature* 2008, **455**, 304–308; (g) A. Dondoni, A. Massi, *Angew. Chem. Int. Ed.* 2008, **47**, 4638–4660; (h) B. List, K. Maruoka, *Asymmetric Organocatalysis*, Thieme, Stuttgart, (2012); (i) H. Pellissier, *Tetrahedron* 2007, **63**, 9267–9331.
15. G. Bredig, P. S. Fiske, *Biochem. Z.* 1912, **46**, 7–23.
16. W. Langenbeck, *Angew. Chem.* 1932, **45**, 97–99.
17. U. Eder, G. Sauer, R. Wiechert, *Angew. Chem. Int. Ed.* 1971, **10**, 496–497.
18. (a) Z. G. Hajos, D. R. Parrish, *J. Org. Chem.* 1974, **39**, 1615–1621; (b) Z. G. Hajos, D. R. Parrish, (1971) German Patent DE 2102623.
19. V. Prelog, M. Wilhelm, *Helv. Chim. Acta* 1954, **37**, 1634–1660.
20. (a) H. Pracejus, *Justus Liebigs Ann. Chem.* 1960, **634**, 9–22; (b) H. Pracejus, *Justus Liebigs Ann. Chem.* 1960, **634**, 23–29.
21. G. Stork, R. Terrell, J. Szmuszkovicz, *J. Am. Chem. Soc.* 1954, **76**, 2029–2030.
22. U. H. Dolling, P. Davis, E. J. J. Grabowski, *J. Am. Chem. Soc.* 1984, **106**, 446–447.
23. R. Helder, J. C. Hummelen, R. W. P. M. Laane, J. S. Wiering, H. Wynberg, *Tetrahedron Lett.* 1976, **17**, 1831–1834.
24. H. Hiemstra, H. Wynberg, *J. Am. Chem. Soc.* 1981, **103**, 417–430.
25. K. A. Ahrendt, C. J. Borths, D. W. C. MacMillan, *J. Am. Chem. Soc.* 2000, **122**, 4243–4244.
26. B. List, R. A. Lerner, C. F. Barbas, III, *J. Am. Chem. Soc.* 2000, **122**, 2395–2396.
27. J. von Liebig, *Justus Liebigs Ann. Chem.* 1860, **113**, 246–247.
28. For mechanistic investigations, see L. Hoang, S. Bahmanyar, K. N. Houk, B. List, *J. Am. Chem. Soc.* 2003, **125**, 16–17.
29. J.-F. Briere, S. Oudeyer, V. Dalla, V. Levacher, *Chem. Soc. Rev.* 2012, **41**, 1696–1707.
30. (a) R. M. de Figueiredo, M. Christmann, *Eur. J. Org. Chem.* 2007, 2575–2600; (b) E. Marques-Lopez, R. P. Herrera, M. Christmann, *Nat. Prod. Rep.* 2010, **27**, 1138–1167; (c) M. Waser, Asymmetric organocatalysis in natural product synthesis, in: Kinghorn A. D., Falk H., Kobayashi J. (eds), *Progress in the Chemistry of Organic Natural Products*, **96**, Springer, Berlin, (2012).
31. (a) B. List, *Synlett* 2001, **11**,1675–1686; (b) E. R. Jarvo, S. Miller, *Tetrahedron* 2002, **58**, 2481–2495; (c) T. Kano, K. Maruoka, *Bull. Chem. Soc. Jpn.* 2010, **83**, 1421–1438; (d) K. L. Jensen, G. Dickmeiss, H. Jiang, L. Albrecht, K. A. Jørgensen, *Acc. Chem. Res.* 2012, **45**, 248–264; (e) S. Meninno, A. Lattanzi, *Chem. Commun.* 2013, **49**, 3821–3832; (f) H. Wennemers, *Chem. Commun.* 2011, **47**, 12036–12041; (g) P. Melchiorre, *Angew. Chem. Int. Ed.* 2012, **51**, 9748–9770; (h) E. A. Colby Davie, S. M. Mennen, Y. Xu, S. J. Miller, *Chem. Rev.* 2007, **107**, 5759–5812.
32. (a) B. List, *Acc. Chem. Res.* 2004, **37**, 548–557; (b) S. Mukherjee, J. W. Yang, S. Hoffmann, B. List, *Chem. Rev.* 2007, **107**, 5471–5569; (c) W. Notz, F. Tanaka, C. F. Barbas, III, *Acc. Chem. Res.* 2004, **37**, 580–591; (d) T. Kano, K. Maruoka, *Chem. Sci.* 2013, **4**, 907–915.
33. D. B. Ramachary, Y. V. Reddy, *Eur. J. Org. Chem.* 2012, 865–887.
34. I. Kumar, P. Ramaraju, N. A. Mir, *Org. Biomol. Chem.* 2013, **11**, 709–716.
35. T. Mukaiyama, H. Ishikawa, H. Koshino, Y. Hayashi, *Chem. Eur. J.* 2013, **19**, 17789–17800.
36. For a discussion of this concept, see also L. Albrecht, H. Jiang, K. A. Jørgensen, *Chem. Eur. J.* 2014, **20**, 358–368.
37. H. Torii, M. Nakadai, K. Ishihara, S. Saito, H. Yamamoto, *Angew. Chem. Int. Ed.* 2004, **43**, 1983–1986.
38. J. Franzen, M. Marigo, D. Fielenbach, T. C. Wabnitz, A. Kjaersgaard, K. A. Jørgensen, *J. Am. Chem. Soc.* 2005, **127**, 18296–18304.
39. (a) T. Kano, H. Sugimoto, O. Tokuda, K. Maruoka, *Chem. Commun.* 2013, **49**, 7028–7030; (b) M. Wiesner, M. Neuburger, H. Wennemers, *Chem. Eur. J.* 2009, **15**, 10103–10109.
40. P. Kwiatkowski, T. D. Beeson, J. C. Conrad, D. W. C. MacMillan, *J. Am. Chem. Soc.* 2011, **133**, 1738–1741.
41. E. P. Serebryakov, A. G. Nigmatov, M. A. Shcherbakov, M. I. Struchkova, *Russ. Chem. Bull.* 1998, **47**, 82–90.
42. S. Bertelsen, M. Marigo, S. Brandes, P. Diner, K. A. Jørgensen, *J. Am. Chem. Soc.* 2006, **128**, 12973–12980.
43. R. Thayumanavan, B. Dhevalapally, K. Sakthivel, F. Tanaka, C. F. Barbas, III, *Tetrahedron Lett.* 2002, **43**, 3817–3820.
44. D. B. Ramachary, N. S. Chowdari, C. F. Barbas, III, *Angew. Chem. Int. Ed.* 2003, **42**, 4233–4237.

45. Z.-J. Jia, H. Jiang, J.-L. Li, B. Gschwend, Q.-Z. Li, X. Yin, J. Grouleff, Y. C. Chen, K. A. Jørgensen, *J. Am. Chem. Soc.* 2011, **133**, 5053–5061.
46. J. E. Baldwin, R. Chesworth, J. S. Parker, A. T. Russell, *Tetrahedron Lett.* 1995, **36**, 9551–9554.
47. A. Erkkila, I. Majander, P. M. Pihko, *Chem. Rev.* 2007, **107**, 5416–5470.
48. W. S. Jen, J. J. M. Wiener, D. W. C. MacMillan, *J. Am. Chem. Soc.* 2000, **121**, 9874–9875.
49. (a) J. W. Yang, M. T. H. Fonseca, B. List, *Angew. Chem. Int. Ed.* 2004, **43**, 6660–6662; (b) J. W. Yang, M. T. H. Fonseca, N. Vignola, B. List, *Angew. Chem. Int. Ed.* 2005, **44**,108–110; (c) S. G. Ouellet, J. B. Tuttle, D. W. C. MacMillan, *J. Am. Chem. Soc.* 2005, **127**, 32–33.
50. (a) W. Chen, W. Du, L. Yue, R. Li, Y. Wu, L.-S. Ding, Y.-C. Chen, *Org. Biomol. Chem.* 2007, **5**, 816–821; (b) G. Bartoli, A. Carlone, F. Pesciaioli, L. Sambri, P. Melchiorre, *Org. Lett.* 2007, **9**, 1403−1405; (c) A. Moran, A. Hamilton, C. Bo, P. Melchiorre, *J. Am. Chem. Soc.* 2013, **135**, 9091–9098.
51. S. B. Jones, B. Simmons, A. Mastracchio, D. W. C. MacMillan, *Nature* 2011, **475**, 183–188.
52. (a) D. Enders, C. Grondal, M. R. M. Hüttl, *Angew. Chem. Int. Ed.* 2007, **46**, 1570–1581; (b) C. Grondal, M. Jeanty, D. Enders, *Nat. Chem.* 2010, **2**, 167–178.
53. (a) M. Marigo, J. Franzen, T. B. Poulsen, W. Zhuang, K. A. Jørgensen, *J. Am. Chem. Soc.* 2005, **127**, 6964–6965; (b) R. L. Davis, K. L. Jensen, B. Gschwend, K. A. Jørgensen, *Chem. Eur. J.* 2014, **20**, 64–67.
54. H. Enders, M. R. M. Hüttl, C. Grondal, G. Raabe, *Nature* 2006, **441**, 861–863.
55. B. Simmons, A. M. Walji, D. W. C. MacMillan, *Angew. Chem. Int. Ed.* 2009, **48**, 4349–4353.
56. C. Sparr, R. Gilmour, *Angew. Chem. Int. Ed.* 2011, **50**, 8391–8395.
57. T. D. Beeson, A. Mastracchio, J. B. Hong, K. Ashton, D. W. C. MacMillan, *Science* 2007, **316**, 582–585.
58. (a) H. Kim, D. W. C. MacMillan, *J. Am. Chem. Soc.* 2008, **130**, 398–399; (b) T. H. Graham, C. M. Jones, N. T. Jui, D. W. C. MacMillan, *J. Am. Chem. Soc.* 2008, **130**, 16494–16495; (c) N. T. Jui, E. C. Y. Lee, D. W. C. MacMillan, *J. Am. Chem. Soc.* 2010, **132**, 10015–10017.
59. K. C. Nicolaou, R. Reingruber, D. Sarlah, S. Bräse, *J. Am. Chem. Soc.* 2009, **131**, 2086–2087.
60. (a) M. Amatore, T. D. Beeson, S. P. Brown, D. W. C. MacMillan, *Angew. Chem. Int. Ed.* 2009, **48**, 5121–5124; (b) P. Winter, C. Vaxelaire, C. Heinz, M. Christmann, *Chem. Commun.* 2011, **47**, 394–396.
61. N. T. Jui, J. A. O. Garber, F. G. Finelli, D. W. C. MacMillan, *J. Am. Chem. Soc.* 2012, **134**, 11400–11403.
62. For selected reviews about H-bonding and Brønsted acid catalysis, see (a) M. S. Taylor, E. N. Jacobsen, *Angew. Chem. Int. Ed.* 2006, **45**, 1520–1543; (b) A. G. Doyle, E. N. Jacobsen, *Chem. Rev.* 2007, **107**, 5713–5743; (c) X. H. Yu, W. Wang, *Chem. Asian. J.* 2008, **3**, 516–532; (d) T. Akiyama, J. Itoh, K. Fuchibe, *Adv. Synth. Catal.* 2006, **348**, 999–1010; (e) C. H. Cheon, H. Yamamoto, *Chem. Commun.* 2011, **47**, 3043–3056; (f) M. Rueping, A. Kuenkel, I. Atodiresei, *Chem. Soc. Rev.* 2011, **40**, 4539–4549; (g) J. Aleman, A. Parra, H. Jiang, K. A. Jørgensen, *Chem. Eur. J.* 2011, **17**, 6890–6899; (h) P. Selig, *Synthesis* 2003, 703–718.
63. A. Wassermann, *J. Chem. Soc.* 1942, 618–621.
64. (a) M. Terada, *Synthesis* 2010, 1929–1982; (b) A. Zamfir, S. Schenker, M. Freund, S. B. Tsogoeva, *Org. Biomol. Chem.* 2010, **8**, 5262–5276.
65. (a) D. Uraguchi, M. Terada, *J. Am. Chem. Soc.* 2004, **126**, 5356–5357; (b) T. Akiyama, J. Itoh, K. Yokota, K. Fuchibe, *Angew. Chem. Int. Ed.* 2004, **43**, 1566–1568; (c) T. Akiyama, Y. Saitoh, H. Morita, K. Fuchibe, *Adv. Synth. Catal.* 2005, **347**, 1523–1526.
66. M. Rueping, E. Sugiono, C. Azap, *Angew. Chem. Int. Ed.* 2006, **45**, 2617–2619.
67. For a review and further examples, see M. Rueping, E. Sugiono, F. R. Schoepke, *Synlett* 2010, **6**, 852–865.
68. T. Akiyama, Y. Tamura, J. Itoh, H. Morita, K. Fuchibe, *Synlett* 2006, 141–143.
69. M. E. Muratore, C. A. Holloway, A. W. Pilling, R. A. Storer, G. Trevitt, D. J. Dixon, *J. Am. Chem. Soc.* 2009, **131**, 10796–10797.
70. (a) G.-Q. Li, H. Gao, C. Keene, M. Devonas, D. H. Ess, L. Kürti, *J. Am. Chem. Soc.* 2013, **135**, 7414–7417; (b) C. K. De, F. Pesciaioli, B. List, *Angew. Chem. Int. Ed.* 2013, **52**, 9293–9295.
71. R. J. Phipps, G. L. Hamilton, F. D. Toste, *Nat. Chem.* 2012, **4**, 603–614.
72. I. Coric, B. List, *Nature* 2012, **483**, 315–319.
73. P. Garcia-Garcia, F. Lay, P. Garcia-Garcia, C. Rabalakos, B. List, *Angew. Chem. Int. Ed.* 2009, **48**, 4363–4366.
74. M. Rueping, W. Ieawsuwan, A. P. Antonchick, B. J. Nachtsheim, *Angew. Chem. Int. Ed.* 2007, **46**, 2097–2100.
75. (a) M. S. Sigman, E. N. Jacobsen, *J. Am. Chem. Soc.* 1998, **120**, 4901–4902; (b) P. Vachal, E. N. Jacobsen, *Org. Lett.* 2000, **2**, 867–870; (c) P. Vachal, E. N. Jacobsen, *J. Am. Chem. Soc.* 2002, **124**, 10012–10014.
76. M. S. Taylor, E. N. Jacobsen, *J. Am. Chem. Soc.* 2004, **126**, 10558–10559.
77. (a) T. Okino, Y. Hoashi, Y. Takemoto, *J. Am. Chem. Soc.* 2003, **125**, 12672–12673; (b) T. Inokuma, Y. Hoashi, Y. Takemoto, *J. Am. Chem. Soc.* 2006, **128**, 9413–9419.
78. (a) S. H. McCooey, S. J. Connon, *Angew. Chem. Int. Ed.* 2005, **44**, 6367–6370; (b) J. Ye, D. J. Dixon, P. S. Hynes, *Chem. Commun.* 2005, 4481–4483.
79. For a recent review about chiral ion pairs in catalysis, see K. Brak, E. N. Jacobsen, *Angew. Chem. Int. Ed.* 2013, **125**, 558–588.
80. For an overview, see S. J. Connon, *Chem. Commun.* 2008, **44**, 2499–2510.
81. For a very recent example about the combination of photoredox activation and anion binding catalysis, see G. Bergonzini, C. S. Schindler, C.-J. Wallentin, E. N. Jacobsen, C. R. J. Stephenson, *Chem. Sci.* 2014, **5**, 112–116.

82. Y. Huang, A. K. Unni, A. N. Thadani, V. H. Rawal, *Nature* 2003, **424**, 146.
83. A. K. Unni, N. Takenaka, H. Yamamoto, V. H. Rawal, *J. Am. Chem. Soc.* 2005, **127**, 1336–1337.
84. For a review on tartaric acid-derived organocatalysts, see K. Gratzer, G. N. Gururaja, M. Waser, *Eur. J. Org. Chem.* 2013, 4471–4482.
85. N. T. McDougal, S. E. Schaus, *J. Am. Chem. Soc.* 2003, **125**, 12094–12095.
86. H.-H. Zou, J. Hu, J. Zhang, J.-S. You, D. Ma, D. Lü, R.-G. Xie, *J. Mol. Catal. A* 2005, **242**, 57–61.
87. J. P. Malerich, K. Hagihara, V. H. Rawal, *J. Am. Chem. Soc.* 2008, **130**, 14416–14417.
88. For selected reviews, see (a) S. K. Tian, Y. G. Chen, J. F. Hang, L. Tang, P. McDaid, L. Deng, *Acc. Chem. Res.* 2004, **37**, 621–631; (b) S. France, D. J. Guerin, S. J. Miller, T. Lectka, *Chem. Rev.* 2003, **103**, 2985–3012; (c) D. Enders, O. Niemeier, A. Henseler, *Chem. Rev.* 2007, **107**, 5606–5655; (d) S. E. Denmark, G. L. Beutner, *Angew. Chem. Int. Ed.* 2008, **47**, 1560–1638.
89. K. Tanaka, A. Mori, S. Inoue, *J. Org. Chem.* 1990, **55**, 181–185.
90. E. J. Corey, M. J. Grogan, *Org. Lett.* 1999, **1**, 157–160.
91. Y. Chen, S.-K. Tian, L. Deng, *J. Am. Chem. Soc.* 2000, **122**, 9542–9543.
92. (a) M. J. Gaunt, C. C. C. Johansson, *Chem. Rev.* 2007, **107**, 5596–5605; (b) C.-K. Pei, M. Shi, *Chem. Eur. J.* 2012, **18**, 6712–6716.
93. (a) G. C. Fu, *Acc. Chem. Res.* 2004, **37**, 542–547; (b) G. C. Fu, *Acc. Chem. Res.* 2000, **33**, 412–420.
94. (a) A. Marinetti, A. Voituriez, *Synlett* 2010, 174–194; (b) L.-W. Xu, *ChemCatChem* 2013, **5**, 2775–2784; (c) C. Gomez, J.-F. Betzer, A. Voituriez, A. Marinetti, *ChemCatChem* 2013, **5**, 1055–1065.
95. G. Zhu, Z. Chen, Q. Jiang, D. Xiao, P. Cao, X. Zhang, *J. Am. Chem. Soc.* 1997, **119**, 3836–3837.
96. H. Xiao, Z. Chai, H. F. Wang, X. W. Wang, D. D. Cao, W. Liu, Y. P. Liu, Y. Q. Yang, G. Zhao, *Chem. Eur. J.* 2011, **17**, 10562–10565.
97. E. M. McGarrigle, E. L. Myers, O. Illa, M. A. Shaw, S. L. Riches, V. K. Aggarwal, *Chem. Rev.* 2007, **107**, 5841–5883.
98. J. Zanardi, C. Leriverend, D. Aubert, K. Julienne, P. Metzner, *J. Org. Chem.* 2001, **66**, 5620–5623.
99. R. Breslow, *J. Am. Chem. Soc.* 1958, **80**, 3719–3726.
100. (a) D. Enders, T. Balensiefer, *Acc. Chem. Res.* 2004, **37**, 534–541; (b) K. Zeitler, *Angew. Chem. Int. Ed.* 2005, **44**, 7506–7510; (c) N. Marion, S. Diez-Gonzalez, S. P. Nolan, *Angew. Chem. Int. Ed.* 2007, **46**, 2988–3000; (d) X. Bugaut, F. Glorius, *Chem. Soc. Rev.* 2012, **41**, 3511–3522.
101. J. C. Sheehan, D. H. Hunneman, *J. Am. Chem. Soc.* 1966, **88**, 3666–3667.
102. (a) D. Enders, K. Breuer, J. H. Teles, *Helv. Chim. Acta* 1996, **79**, 1217–1221; (b) D. Enders, K. Breuer, J. Runsink, J. H. Teles, *Helv. Chim. Acta* 1996, **79**, 1899–1902.
103. M. S. Kerr, J. Read de Alaniz, T. A. Rovis, *J. Am. Chem. Soc.* 2002, **124**, 10298–10299.
104. J. He, S. Tang, J. Liu, Y. Su, X. Pan, X. She, *Tetrahedron* 2008, **64**, 8797–8800.
105. I. Piel, M. Steinmetz, K. Hirano, K. Fröhlich, S. Grimme, F. Glorius, *Angew. Chem. Int. Ed.* 2011, **50**, 4983–4987.
106. V. Nair, R. S. Menon, A. T. Biju, C. R. Sinu, R. R. Paul, A. Jose, V. Sreekumar, *Chem. Soc. Rev.* 2011, **40**, 5336–5346.
107. (a) S. S. Sohn, E. L. Rosen, J. W. Bode, *J. Am. Chem. Soc.* 2004, **126**, 14370–14371; (b) C. Burstein, F. Glorius, *Angew. Chem. Int. Ed.* 2004, **43**, 6205–6208.
108. E. M. Phillips, M. Wadamoto, A. Chan, K. A. Scheidt, *Angew. Chem. Int. Ed.* 2007, **46**, 3107–3110.
109. S. E. Denmark, D. M. Coe, N. E. Pratt, B. D. Griedel, *J. Org. Chem.* 1994, **59**, 6161–6163.
110. (a) S. E. Denmark, J. Fu, *J. Am. Chem. Soc.* 2001, **123**, 9488–9489; (b) S. E. Denmark, J. Fu, *J. Am. Chem. Soc.* 2003, **125**, 2208–2216.
111. K. Iseki, S. Mizuno, Y. Kuroki, Y. Kobayashi, *Tetrahedron Lett.* 1998, **39**, 2767–2770.
112. M. Nakajima, M. Saito, M. Shiro, S. Hashimoto, *J. Am. Chem. Soc.* 1998, **120**, 6419–6420.
113. G. L. Beutner, S. E. Denmark, *Angew. Chem. Int. Ed.* 2013, **52**, 9086–9096.
114. S. E. Denmark, A. Jaunet, *J. Am. Chem. Soc.* 2013, **135**, 6419–6422.
115. S. E. Denmark, W. E. Kuester, M. T. Burk, *Angew. Chem. Int. Ed.* 2012, **51**, 10938–10953.
116. C. M. Starks, *J. Am. Chem. Soc.* 1971, **93**, 195–199.
117. (a) E. W. Dehmlow, S. S. Dehmlow, *Phase Transfer Catalysis*, 3rd ed., Wiley-VCH, Weinheim (1993); (b) C. M. Starks, C. L. Liotta, M. E. Halpern, *Phase-Transfer Catalysis*, Chapman & Hall, New York, (1994).
118. For selected reviews, see (a) M. J. O'Donnell, Asymmetric phase-transfer reactions. In: Ojima I. (ed), *Catalytic Asymmetric Syntheses*, 2nd ed., Wiley-VCH, New York (2000), pp 727; (b) K. Maruoka, *Asymmetric Phase Transfer Catalysis*, Wiley-VCH, Weinheim, (2008); (c) M. J. O'Donnell, *Acc. Chem. Res.* 2004, **37**, 506–517; (d) K. Maruoka, T. Hashimoto, *Chem. Rev.* 2007, **107**, 5656–5682; (e) S. Shirakawa, K. Maruoka, *Angew. Chem. Int. Ed.* 2013, **52**, 4312–4348.
119. M. J. O'Donnell, W. D. Bennett, S. Wu, *J. Am. Chem. Soc.* 1989, **111**, 2353–2355.
120. For a review on bifunctional ammonium salt catalysts, see J. Novacek, M. Waser, *Eur. J. Org. Chem.* 2013, 637–648.
121. Y. Liu, B. A. Provencher, K. J. Bartelson, L. Deng, *Chem. Sci.* 2011, **2**, 1301–1304.
122. L. Lykke, K. S. Halskov, B. D. Carlsen, V. X. Chen, K. A. Jørgensen, *J. Am. Chem. Soc.* 2013, **135**, 4692–4695.
123. M. Li, P. A. Woods, M. D. Smith, *Chem. Sci.* 2013, **4**, 2907–2911.
124. T. Hashimoto, K. Sakata, F. Tamakuni, M. J. Dutton, K. Maruoka, *Nat. Chem.* 2013, **5**, 240–244.

125. S. Shirakawa, A. Kasai, T. Tokuda, K. Maruoka, *Chem. Sci.* 2013, **4**, 2248–2252.

126. For reviews see (a) J. Lacour, D. Moraleda, *Chem. Commun.* 2009, **5**, 7073–7089; (b) R. J. Phipps, G. L. Hamilton, F. D. Toste, *Nat. Chem.* 2012, **4**, 603–614.

127. G. L. Hamilton, T. Kanai, F. D. Toste, *J. Am. Chem. Soc.* 2008, **130**, 14984–14986.

128. V. Rauniyar, A. D. Lackner, G. L. Hamilton, F. D. Toste, *Science* 2011, **334**, 1681–1684.

129. H. Inouye, S. Saito, H. Taguchi, T. Endo, *Tetrahedron Lett.* 1969, **10**, 2347–2350.

130. (a) S. Ueda, Y. Iwahashi, H. Tokuda, *J. Nat. Prod.* 1991, **54**, 1677–1680; (b) M. J. Lee, J. D. Hsu, C. J. Wang, *Anticancer Res.* 1995, **15**, 411–416.

131. R. A. Jones, M. J. Krische, *Org. Lett.* 2009, **11**, 1849–1851.

132. L. Candish, D. W. Lupton, *Org. Lett.* 2010, **12**, 4836–4839.

133. I. K. Mangion, D. W. C. MacMillan, *J. Am. Chem. Soc.* 2005, **127**, 3696–3697.

134. Y. S. Li, K. Matsunaga, M. Ishibashi, Y. Ohizumi, *J. Org. Chem.* 2001, **66**, 2165–2167.

135. (a) H. Rimpler, B. Schafer, *Z. Naturforsch.* 1979, **34**, 311–318; (b) A. Franke, H. Rimpler, *Phytochemistry* 1987, **26**, 3015–3020.

136. (a) E. Marques-Lopez, R. P. Herrera, T. Marks, W. C. Jacobs, D. Konning, R. M. de Figueiredo, M. Christmann, *Org. Lett.* 2009, **11**, 4116–4119; (b) E. Marques-Lopez, R. P. Herrera, T. Marks, W. C. Jacobs, M. Christmann, *Synthesis* 2013, 1016–1028.

137. X. H. Cai, Z. Z. Du, X. D. Luo, *Org. Lett.* 2007, **9**, 1817–1820.

138. T. Gerfaud, C. S. Xie, L. Neuville, J. P. Zhu, *Angew. Chem. Int. Ed.* 2011, **50**, 3954–3957.

139. T. Hudlicky, J. W. Reed, *The Way of Synthesis: Evolution of Design and Methods for Natural Products*, Wiley-VCH, Weinheim (2007).

140. E. E. V. Tamelen, M. Shamma, A. W. Burgstahler, J. Wolinsky, R. Tamm, P. E. Aldrich, *J. Am. Chem. Soc.* 1958, **80**, 5006–5007.

141. D. J. Mergott, S. J. Zuend, E. N. Jacobsen, *Org. Lett.* 2008, **10**, 745–748.

142. B. Herle, M. J. Wanner, J. H. van Maarseveen, H. Hiemstra, *J. Org. Chem.* 2011, **76**, 8907–8912.

# 7

# SESQUITERPENES

Alexandros L. Zografos[1] and Elissavet E. Anagnostaki[1,2]

[1]*Department of Chemistry, Laboratory of Organic Chemistry, Aristotle University of Thessaloniki, Thessaloniki, Greece*
[2]*Research and Development Department, Pharmathen S.A., Thessaloniki, Greece*

## 7.1 BIOSYNTHESIS

Sesquiterpenes are a major class of terpenes consisting of three isoprene units, providing the formula of $C_{15}H_{24}$ to their molecular structures (Fig. 7.1) [1]. Like all terpenes, their carbon skeletons are derived from the sequential addition of the "active isoprene unit" isopentenyl diphosphate (IDP or IPP) to other active diphosphates. In the case of sesquiterpenes, addition of a further IDP unit to geranyl diphosphate (GDP or GPP) (the essential precursor of all monoterpenes, please see Chapter 6) provides the fundamental sesquiterpene precursor farnesyl diphosphate (FDP or FPP).

Following the biosynthetic mechanism, initial ionization of GDP to the cation followed by the subsequent addition of the IDP unit forms the FDP cation in a reaction that is catalyzed by FPPS prenyltransferase (Scheme 7.1) [2]. The mechanism is based on the findings that the enzyme, which normally catalyzes the addition of GDP to IDP, is also able to catalyze the hydrolysis of GDP [3]. Deuterium experiments of this hydrolysis process either with $D_2O$ or with (1*S*)-[1-$^3$H] GDP indicated that C—O bond was broken and the chirality of the C-1 carbon of GDP was inverted in this process. In addition, when trifluoromethyl group was present at the C-3 position or fluoro atom at the C-2 position of the allylic substrate, destabilization of the cation has been witnessed as observed on the retard of enzyme reaction [4]. In the elimination step (Scheme 7.1) hydrogen is removed from C-2 of IDP part with simultaneous formation of a double bond. The formation of a *trans* or *cis* double bond during the FPPS reaction depends on the spatial orientation of IDP relative to the elongating FDP. In the *trans*-prenyltransferases, the GDP is added to the *si* face of the double bond of IDP, and the *pro*-R proton is removed to form the new *trans* double bond. The amino acid involved in the removal of the proton has not yet been determined in this process [4].

Prenyltransferases are commonly divided into two classes' *cis*- and *trans*-prenyltransferases depending upon the stereochemistry of the resulting products. The first crystal structure reported for a *trans*-prenyltransferase was that of avian *trans*-farnesyl pyrophosphate synthase (FPPS) (Fig. 7.2) [5].

As shown in Figure 7.2, FPPS is consisting of 13α helices, 10 of them surrounding the large central cavity of the enzyme. Two conserved DDxxD sequences are located in this deep cleft, which forms the substrate binding pocket. Cocrystal structure of evian *trans*-FPPS with IDP and GDP clearly showed that the first DDxxD of the two sequences is bound to the allylic substrate GDP while the other to the IDP [6]. Reaction catalysis between the two bounded substrates is catalyzed by a $Mg^{+2}$ cofactor, which is essential for the enzyme activity. Elongation of the side chain is determined by a large Phe amino acid residue located at the fifth position before the first DDxxD (Phe112 residue). This amino acid can block further elongation of the product and represents the mechanism to control the chain length. Mutations expressed by the replacement of aromatic Phe112 and Phe113 residues with smaller amino acids resulted in the product specificity shifting from $C_{15}$ (FDP) to $C_{20}$ (GGPP) (F112A), $C_{25}$ (geranylfarnesyldiphosphate) (F113S), and longer products (F112A/F113S double mutant) (Fig. 7.3) [6].

Interestingly, *cis*-prenyltransferases show no amino acid sequence similarity to *trans*-enzymes. *Cis*-enzymes lack

*From Biosynthesis to Total Synthesis: Strategies and Tactics for Natural Products*, First Edition. Edited by Alexandros L. Zografos.
© 2016 John Wiley & Sons, Inc. Published 2016 by John Wiley & Sons, Inc.

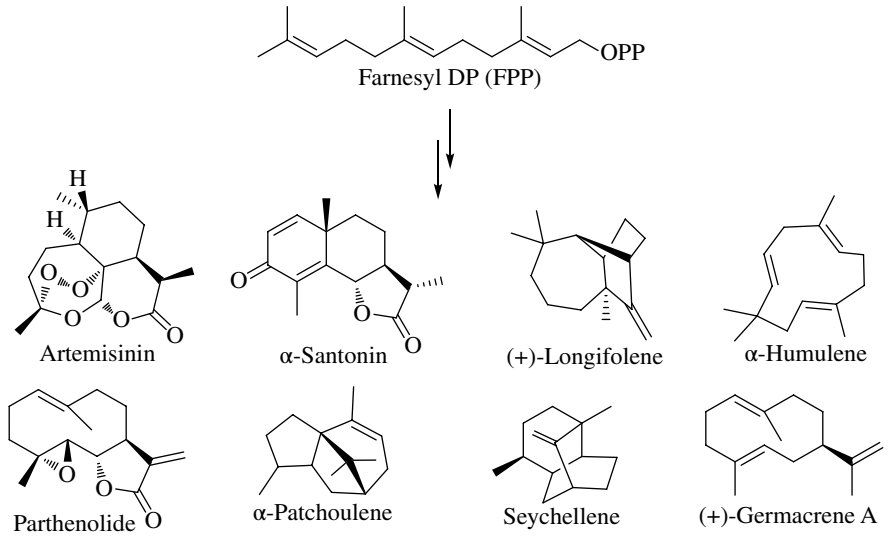
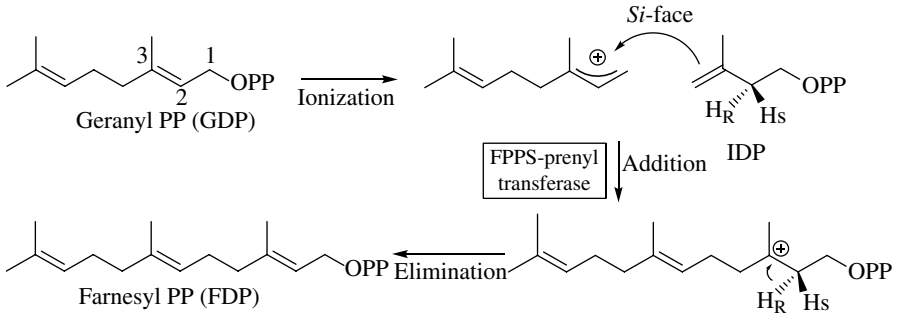



**FIGURE 7.1** Farnesyl diphosphate and selected diverse sesquiterpene motifs.




**SCHEME 7.1** Formation of farnesyl diphosphate (FDP).

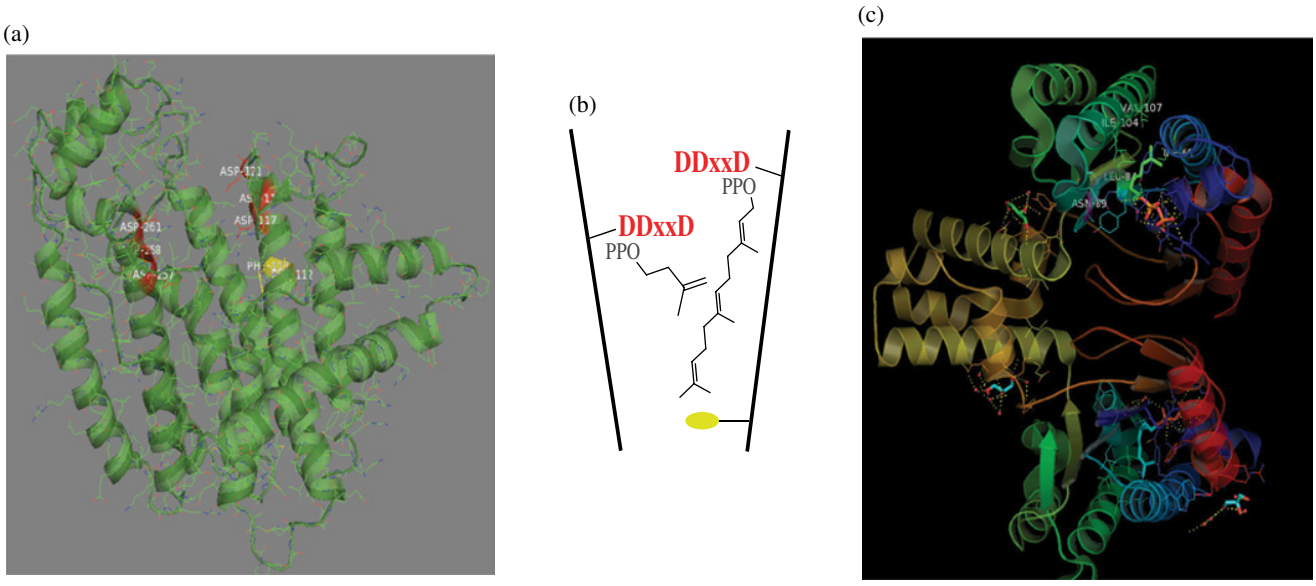



**FIGURE 7.2** (a) Crystal structure of avian *trans*-FPPS, where indicative residues for the conserved DDxxD areas and terminating FF residues are presented and (b) graphic animation of the active center of synthase enzymes; (c) crystal structure of cis-prenyltransferase Rv1086 producing *Z,E*-farnesyl diphosphate. Images created with PyMOL. (*See insert for color representation of the figure*.)

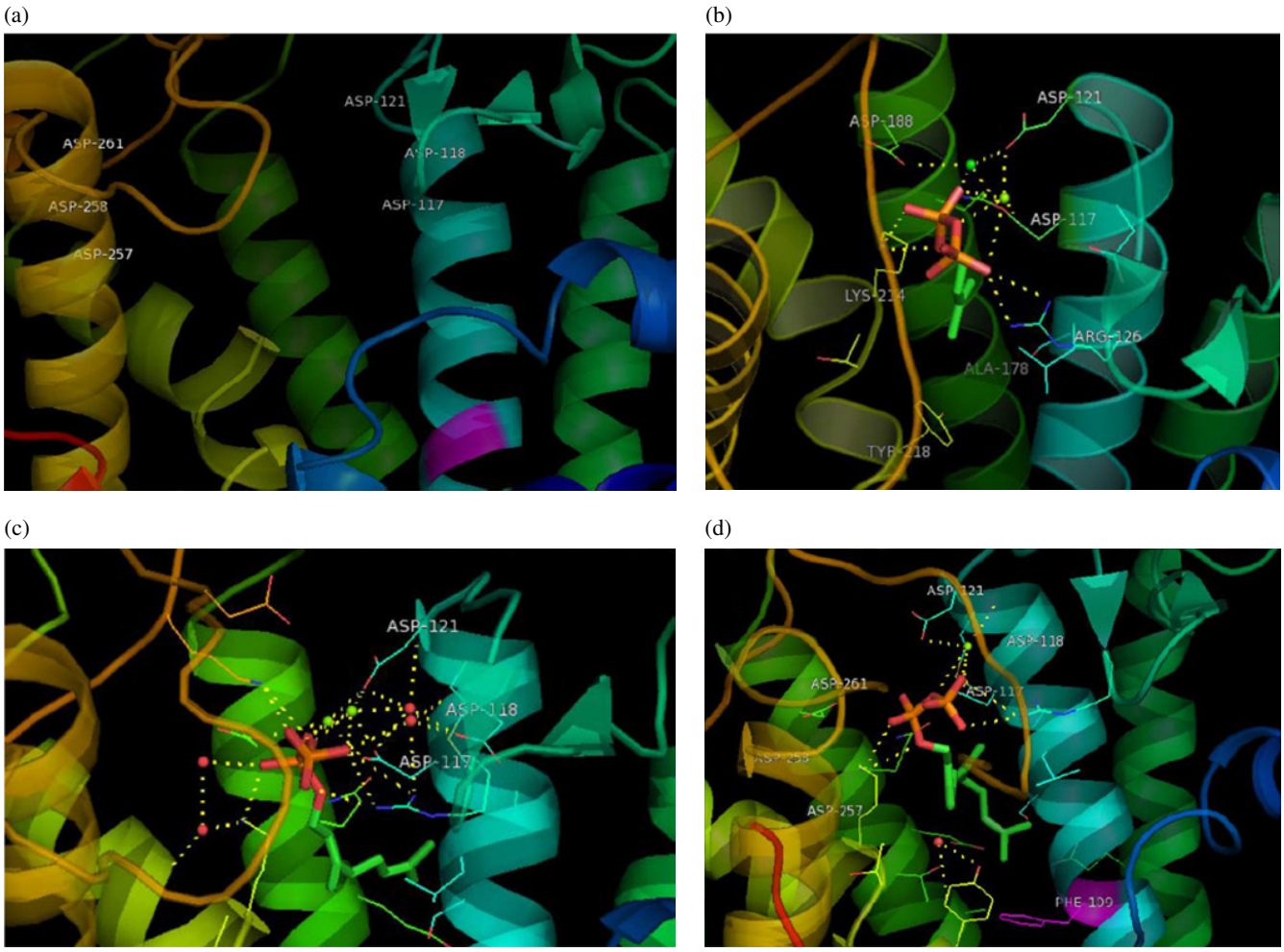
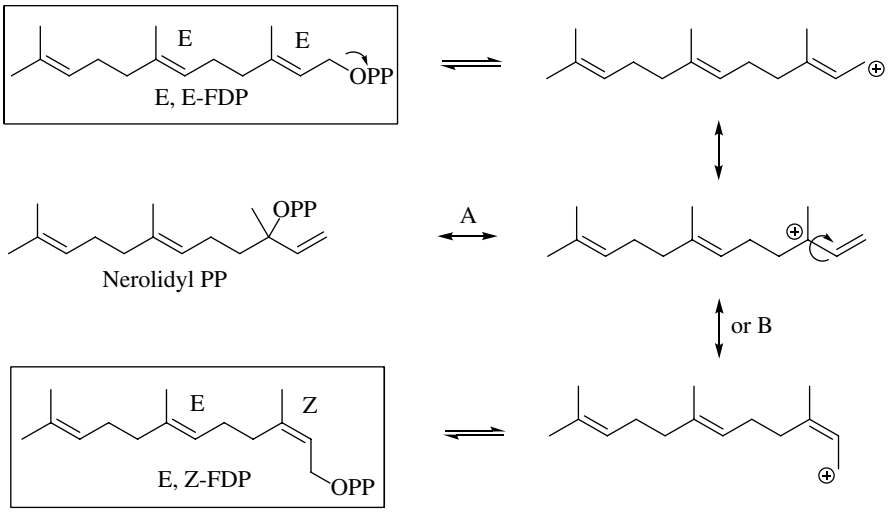



**FIGURE 7.3** Crystal structures of (a) *trans*-farnesyl diphosphate synthase; cocrystallized with (b) IDP, (c) GDP, (d) FDP (metal coordination and hydrogen bonds are shown as dashed lines; magnesium ions and water molecules are shown spheres, terminating residue Phe109 is indicated); Images created with PyMOL. (*See insert for color representation of the figure*.)

the DDxxD motifs, although they still require magnesium ions for their activity. All *cis*-prenyltransferases so far identified have products of chain length at least of 55 carbon atoms, except of a short-chain FDP synthesizing enzyme Rv1086, identified from *Mycobacterium tuberculosis* (Fig. 7.2c) [7]. In this enzyme, residue N89 (shown in purple in Fig. 7.2c insert) was accounted to act as the catalytic base for the abstraction of *pro*-S proton, required for the formation of the Z-conformed double bond (Scheme 7.1). Also, residue L84 is hypothesized to provide the requisite bulky side chain for limiting chain length to $C_{15}$ [7].

Like GDP in monoterpenes, FDP in sesquiterpenes can give rise to linear or cyclic compounds. Due to the increased complexity of FDP translated to the length of the side chain and the multiple unsaturation compared to GDP, the number of possible cyclization modes is also increased and a large number of mono-, bi-, and tricyclic diverse structures can be formed catalyzed by specific enzymes collectively termed as *sesquiterpene synthases*. As in the case of GDP, the additional stereochemical element of double-bond geometry nearest to diphosphate can also be present in the case of FDP (Scheme 7.2). In some natural products, the rearranged product nerolidyl diphosphate (NDP) has been biosynthetically implicated as a more immediate precursor than FDP. This further expands the folding possibilities of these precursors to maximize the diversity within the family.

Several sesquiterpene synthases have been isolated, crystallized, and cocrystallized with various substrates (until 2012, protein data bank contained the crystal structure of seven distinct sesquiterpene synthases that have been solved in 42 forms). Sesquiterpene synthase catalyze, within a shared three-dimensional fold, the conversion of FDP (and in some cases NDP) into more than 300 different sesquiterpenes [8]. Their catalytic mechanism can be divided into three phases: (i) ionization of FDP to the corresponding cation, which acts as the electrophile for the intramolecular




**SCHEME 7.2** Isomerization of FDP to NDP.

addition into a double bond; (ii) relocalization of the carbocation by hydride shift and Wagner–Meerwein rearrangements; and (iii) either appropriate deprotonation to form unsaturation or quench of the carbocation by an exogenous nucleophile.

Most of cyclases isolated have common structural features highlighted by their rich Asp motifs and the existence of metal atoms on the active centers, suggesting their similarity in activating the FDP substrate. The formation of sesquiterpenes is initiated by a divalent metal (usually $Mg^{+2}$)-dependent cleavage of diphosphate unit (PPi) from FDP. To succeed that, three metal ions are bound at the top of the active site and coordinate diphosphate prior its cleavage (Fig. 7.4). From a structural point of view, all sesquiterpene synthases contain the class I terpene synthase fold referred as *terpenoid synthase fold* containing 10–12 mostly antiparallel α-helices in their active centers [9–11]. Plant sesquiterpene synthase also contain a catalytically silent class II terpene synthase fold [12]. The most conserved motifs in *terpenoid synthase fold* are, as in the case of FPPS prenyltransferase, a DDxxD/E motif located in helix D, which binds two of the magnesium ions contained in the active center and a DTE/NSE or a second DDxxD motif on helix H, which binds the third magnesium atom. These two metal ion binding sites are responsible in all sesquiterpene synthase for the coordination of diphosphate unit of FDP and finally for its cleavage. The binding of the three magnesium ions is highly ordered and triggers the closure of the active site in which active farnesyl is sheltered from water.

Crystallographic analysis of several sesquiterpene synthases on the absence or presence of FDP substrate and magnesium ions revealed the conformational changes upon the binding of ligands and led to the prediction of binding events upon catalysis [13,14]. Thus, binding of the substrate to the open form of the enzyme in the absence of metal ions is followed by coordination of the two magnesium ions and active site closure. The reactive conformation of FDP is formed after the third metal ion binds to initiate the reaction cascade. Product and two magnesium atoms release are accompanied by active site opening followed by release of the third magnesium ion and diphosphate to complete the reaction cycle (Fig. 7.4).

Following diphosphate cleavage and generation of the initial carbocation (*trans*-farnesyl cation; Scheme 7.3), sesquiterpene synthases lead the reaction to often complex carbocationic cascades producing diverse cyclization modes through Wagner–Meerwein rearrangements till the final consumption of cation charge. Directing the reaction along a specific pathway is largely achieved by spatial orientation and stabilization of the active cationic substrate within the active site of the enzyme as this was evidenced by site-directed mutagenesis studies [8].

As with monoterpenes, standard reactions of carbocations explain most of the structural core structures encountered for sesquiterpenes. A representative selection of these is given in Scheme 7.3.

Following the logic behind the diverse production of sesquiterpene structures, one can find the initial formation of farnesyl cation in either of its geometrical forms (E,E (**1**) or E,Z (**3**)). Both farnesyl cations provide with their direct cyclization either the ten-membered *cis*- (**7**) or *trans*-germacrane (**5**) cations or the eleven-membered *cis*- (**6**) or *trans*-humulyl (**4**) cations. What is more, (**3**) cation can also collapse, due to its *cis*-orientation, to an alternative cyclization mode in order to provide bisabolyl (**8**) and carotyl (**12**) cations. Next, each of the cations formed can either produce the corresponding unsaturated core by abolishing a proton or further rearrange through Wagner–Meerwein reactions to provide further diversity like the production of caryophilyl (**9**) cation from humulyl-type intermediates and artemisinyl

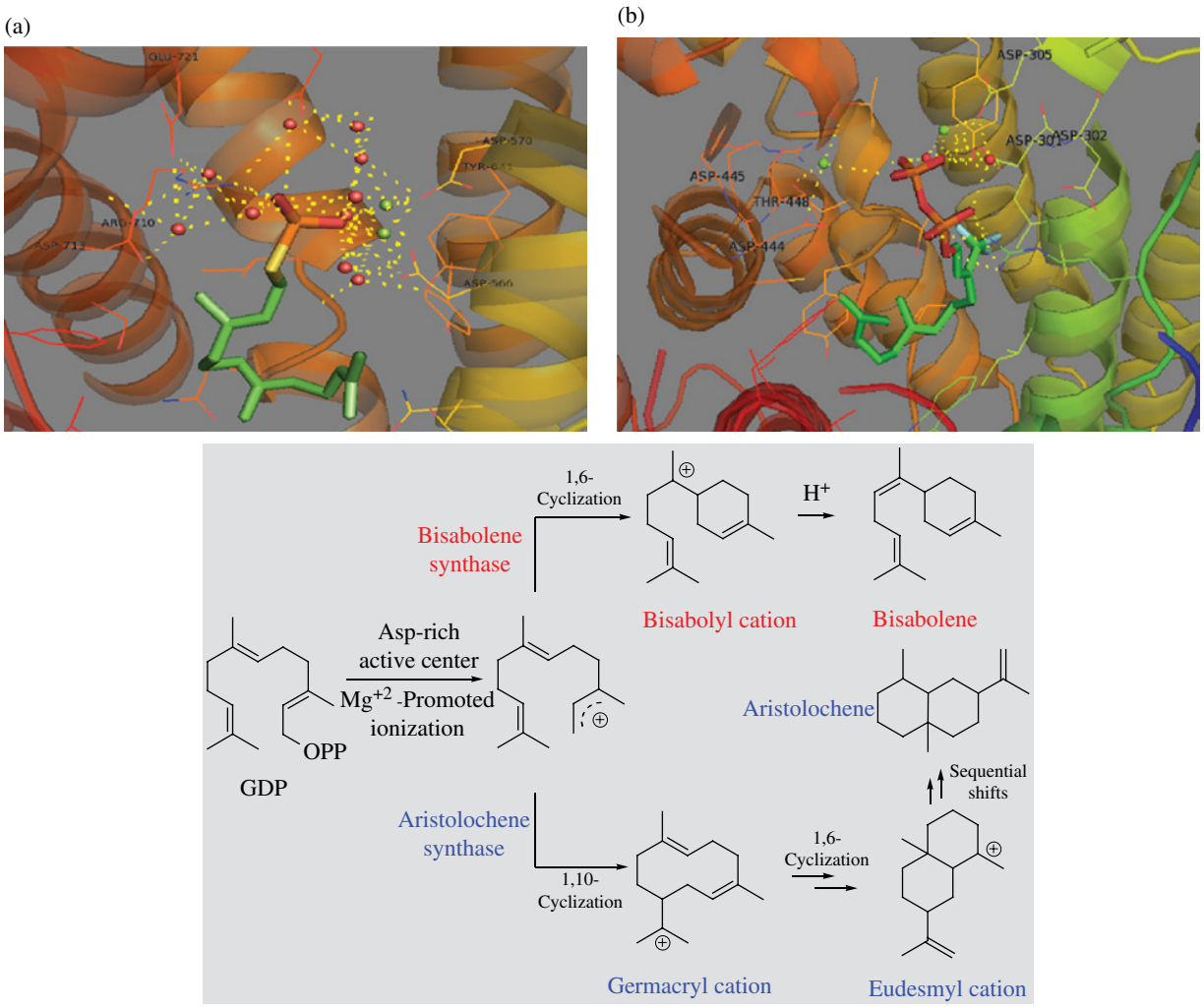
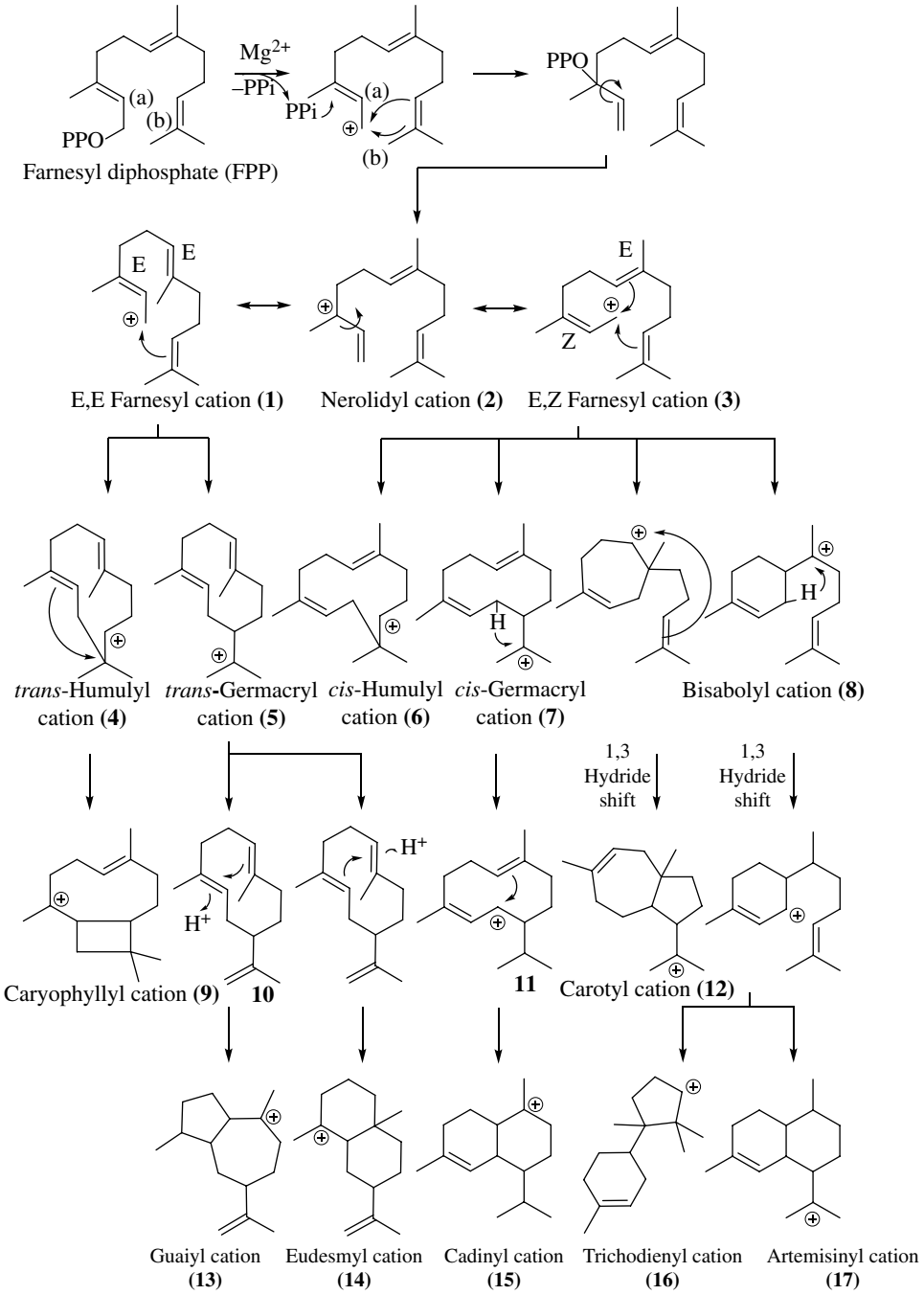



**FIGURE 7.4** Crystal structure of (a) bisabolene synthase active center bound to farnesyl diphosphate inhibitor; (b) aristolochene synthase cocrystallized with FDP (metal coordination and hydrogen bonds are shown as dashed lines; magnesium anions and water molecules are shown as spheres) and the proposed catalytic mechanisms for each cyclization; Images created with PyMOL. (*See insert for color representation of the figure*.)

(**17**) cation from bisabolyl intermediates. On the other hand, the neutral products such as germacranes (**10**) can be further excited in their cationic form through enzymic protonation to create a new series of cationic cores like guaiyl (**13**), eudesmyl (**14**), and cadinyl (**15**) cations (Scheme 7.3).

Apart from the diversity presented by their core structures, sesquiterpenes are commonly decorated with lactone moieties and hydroxyls throughout the basic core. Thus, usually isolated biologically active natural sesquiterpenes are highly oxidized, referred in the literature as *sesquiterpenoids*. The α,β-unsaturated lactone functionality is a common feature of many cytotoxic sesquiterpenoids accounting as a powerful alkylating side through a Michael-type addition to suitable biomolecules as the cysteine residues on proteins and enzymes. Thus, several biological active sesquiterpenoids have been isolated and used in traditional and modern medicine with exemplified examples those of parthenolide, santonin, artemisinin, thapsigargin, trichothecenes, and so on, shown in Figure 7.5.

Parthenolide (**18**) (Fig. 7.5), a traditional antimigraine agent isolated from *Tanacetum parthenium* (feverfew), has recently been correlated with important biological activities as the modulation of NF-kB mediated inflammatory response [15], the selective induced apoptosis of acute myelogenic leukemia (AML) cells [16], and the lately discovered selective cytotoxic activity against an array of cancer stem cells [17]. Parthenolide is classified as a lactone germacrane (germacranolide) with its biosynthesis being obviously derived from germacryl cation (**5**). The proposed biosynthesis begins with FDP cyclization to germacrane A by sesquiterpene synthase. (+) Germacrane A hydroxylase then hydroxylates the isopropenyl side chain to the alcohol and then




**SCHEME 7.3** Selected cyclization modes in sesquiterpene family.

$NADP^+$-dependent hydrogenase to the corresponding acid. Germacratrien-12-oic acid is finally hydroxylated at C-6 position followed by intramolecular lactonization to produce costunolide (**23**), an established precursor of parthenolide after the chemoselective epoxidation of the more electron-rich alkene (Scheme 7.4) [18].

The same biosynthetic pathway has also been proposed for the production of α-santonin. α-Santonin isolated from *Artemisia maritima* is a drug that was widely used in the past as anthelmintic and was later removed based on its severe side effects. Its biosynthesis is based on the methylene reduction of costunolide (**23**) and its proton activation and cyclization of germacrane core to provide eudesmyl cation (**14**). Sequential oxidative steps at C-1 and C-3 positions, followed by elimination of water, complete the route to α-santonin [19].

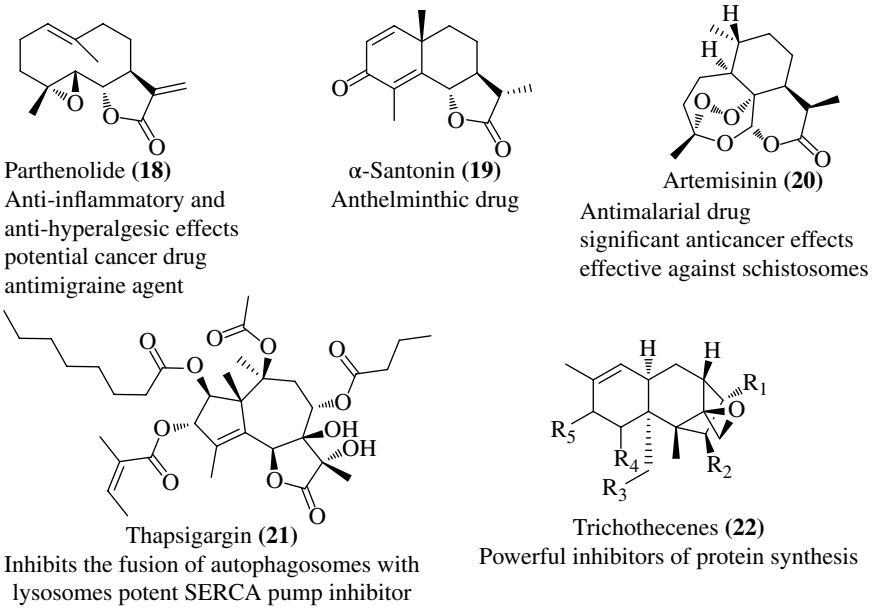
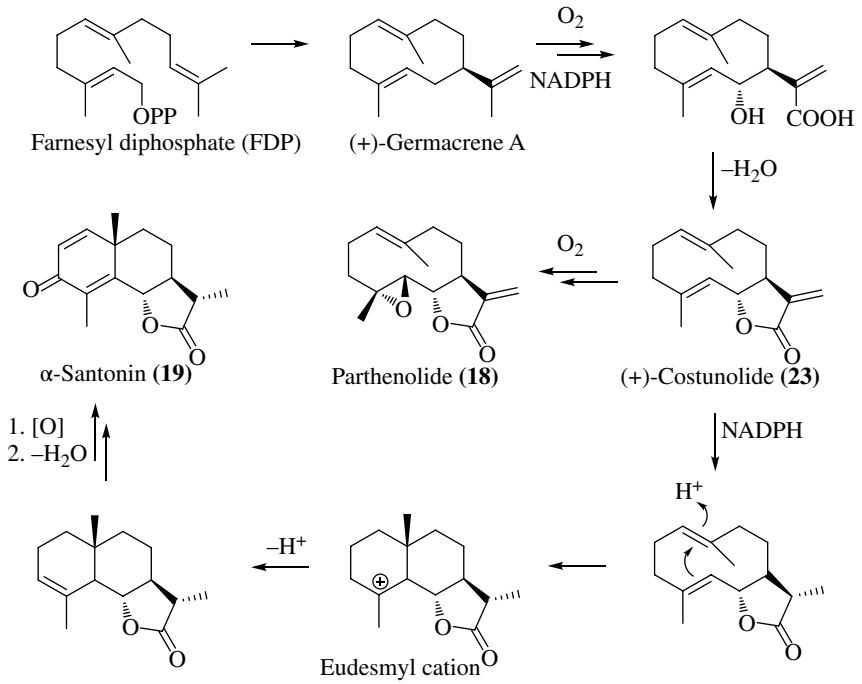
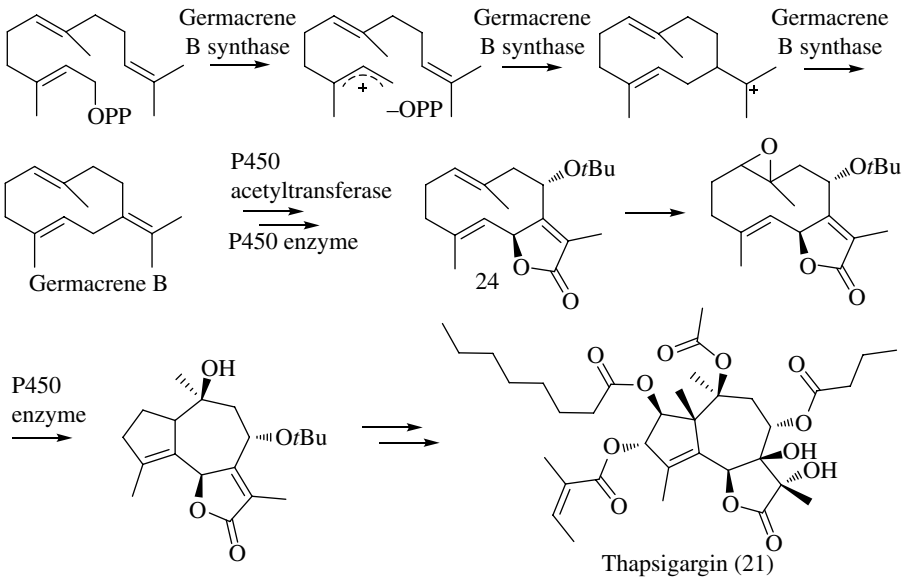



**FIGURE 7.5** Biological intriguing sesquiterpenoids.

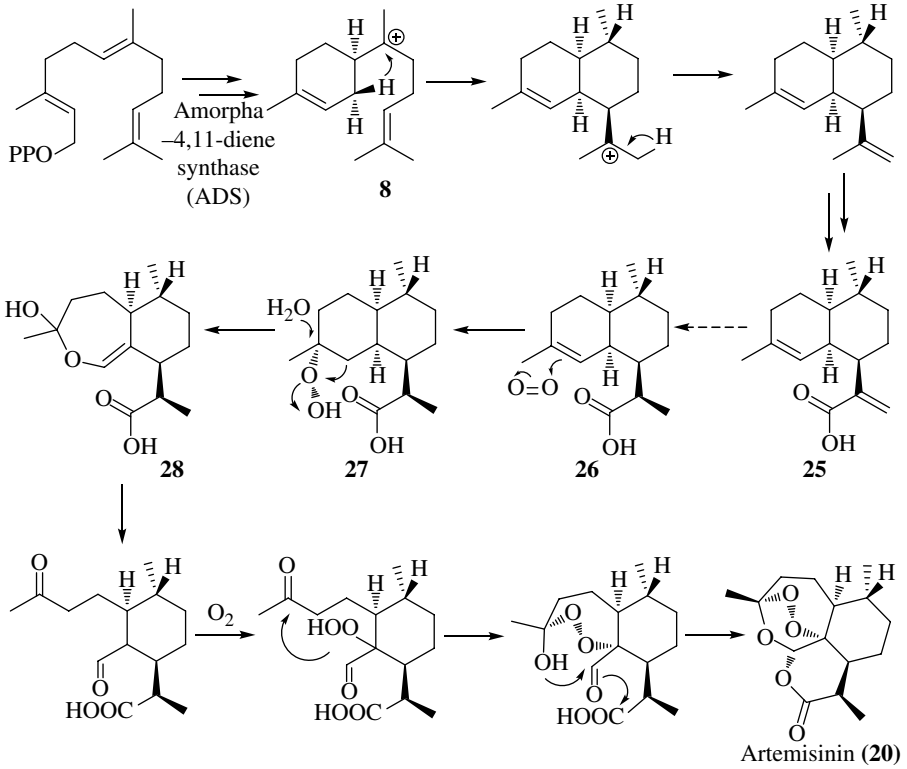



**SCHEME 7.4** Biosynthesis of α-santonin (**19**), parthenolide (**18**), and costunolide (**23**).

Thapsigargin, a highly oxidized sesquiterpenoid, is a potent SERCA pump inhibitor [20] isolated from Mediterranean plant *Thapsia garganica* [21]. This compound is of considerable pharmacological interest as a tumor promoter and as a potent activator of cells involved in the inflammatory response. Its biosynthesis has not yet fully elucidated but it is proposed to invoke FDP cyclization to germacrane B through a germacrane synthase, C-6 allylic oxidation, and an acyloxy addition by P450 acetyltransferase to **24**. Next, lactone ring is formed by a cytochrome P450 enzyme using $NADP^+$, providing only the 6,12-lactone ring. Selective epoxidation is promoting the intramolecular ring formation of guaianolide. Although it is not known whether the secondary modifications to the guaianolide occur prior



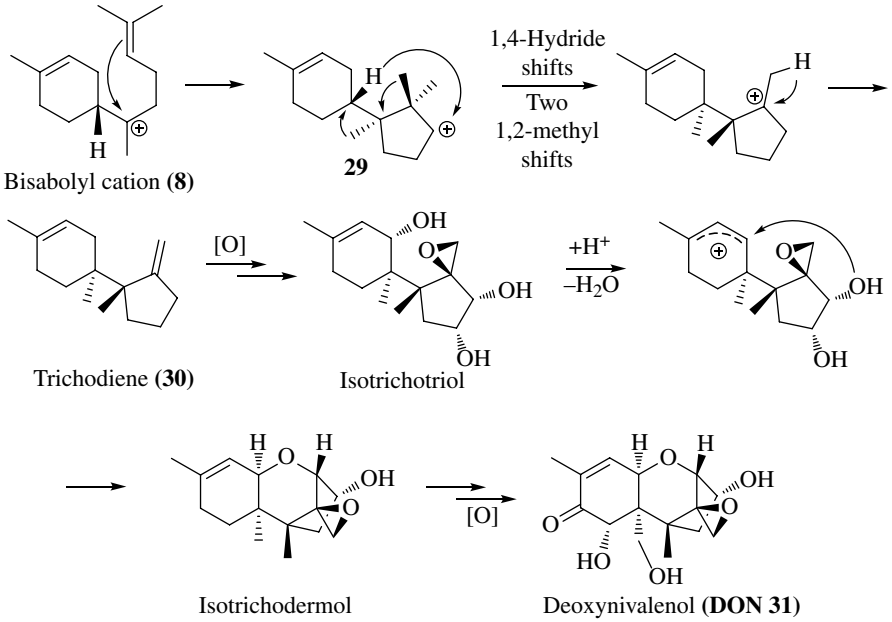

**SCHEME 7.5** Biosynthesis of thapsigargin (**21**).




**SCHEME 7.6** Proposed biosynthesis of artemisinin (**20**).

or after the formation of the basic core, the essential transformation of germacrane to guainyl cation is present (Scheme 7.5).

Artemisinin (**20**) (Scheme 7.6) is another biological important molecule, which possesses the most rapid action of all current drugs against *Plasmodium falciparum* malaria. Treatments containing artemisinin combination treatment are now standard treatment worldwide [22]. Artemisinin is isolated from *Artemisia annua* [23] and is structurally characterized as a sesquiterpene lactone containing an unusual




**SCHEME 7.7** Proposed biosynthesis of deoxynivalenol.

peroxide bridge. Its biosynthesis is proposed to be based on the formation of bisabolyl cation (**8**) either by E, Z-farnesyl cation (**3**) or nerodyl cation (**2**) rearrangement. Next bisabolyl cation further cyclizes to the condensed 6–6 ring system of artemisinic acid. From this point sequential oxidation steps are taking place to isopropenyl side chain leading to artemisinic acid. Chemoselective reduction of the unsaturation provides dehydroartemisinic acid (**26**), an established biosynthetic precursor of artemisinin through a photooxidative cascade under conditions that might normally be present in the plant suggesting that all further transformations may in fact be nonenzymic. The cascade initiates a singlet oxygen ene reaction to (**27**), a Hock cleavage for the ring opening of oxidized six-member ring (**28**) and a triple oxygen addition of hydroperoxide moiety, which is finally intramolecularly cyclizes to produce artemisinin (**20**).

The trichothecenes (**22**) are a group of fungal toxins found typically in affected grain foods [24]. The trichothecenes have their biosynthetic origins in NDP cyclization to bisabolyl cation (**8**) (Scheme 7.7). The latter further cyclizes to (**29**), providing the opportunity for Wagner–Meerwein rearrangements to initiate, producing finally trichodiene core structure (**30**). Oxidation of this main core prepares deoxynivalenol (vomitoxin) (**31**), a particular prominent trichothecene contaminant (Scheme 7.7) [25].

These biosyntheses are only indicative examples of the structural diversity that can be achieved by sesquiterpene synthases on the synthesis of sesquiterpenoids. Summarizing this multistage process, the biosynthesis begins by the synthesis of FDP, the major precursor of all sesquiterpenoids, through prenyltransferase. Sesquiterpene synthases are then catalyze the cyclization of FDP to produce the basic cationic forms for the core structures of sesquiterpenes. Various C–H allylic oxidations introduce functionality in the molecule and set the stage for cationic cyclization rearrangements to further expand their diversity decorated usually by a last stage of oxidation process.

## 7.2 CYCLOISOMERIZATION REACTIONS IN ORGANIC SYNTHESIS

As simplified as it was presented in Section 7.1, biosynthesis of sesquiterpenoids is regarded probably as the most engineered process in nature, earning its major strength from the evolutionary advance of sesquiterpenoid synthase in providing selectively a variety of cyclized modes for the synthesis of sesquiterpenoids (Fig. 7.6). This powerful diversity-oriented biosynthetic machinery is well suited to produce variations so as to optimize the function of these secondary metabolites. Sesquiterpene synthases that catalyze these diverse modes of cyclization by the involvement of an intricate series of carbocation intermediates (please refer to Section **7.1**), are difficult to be controlled control even in modern synthetic chemistry. However, the same logic of common acyclic carbon chains containing multiple unsaturation in analogy to farnesyl diphosphate and leading to controlled cyclization modes have intrigued scientific community in advancing cycloisomerization reactions [26].

Cycloisomerization is described, the intramolecular reaction of a polyunsaturated substrate for the formation of

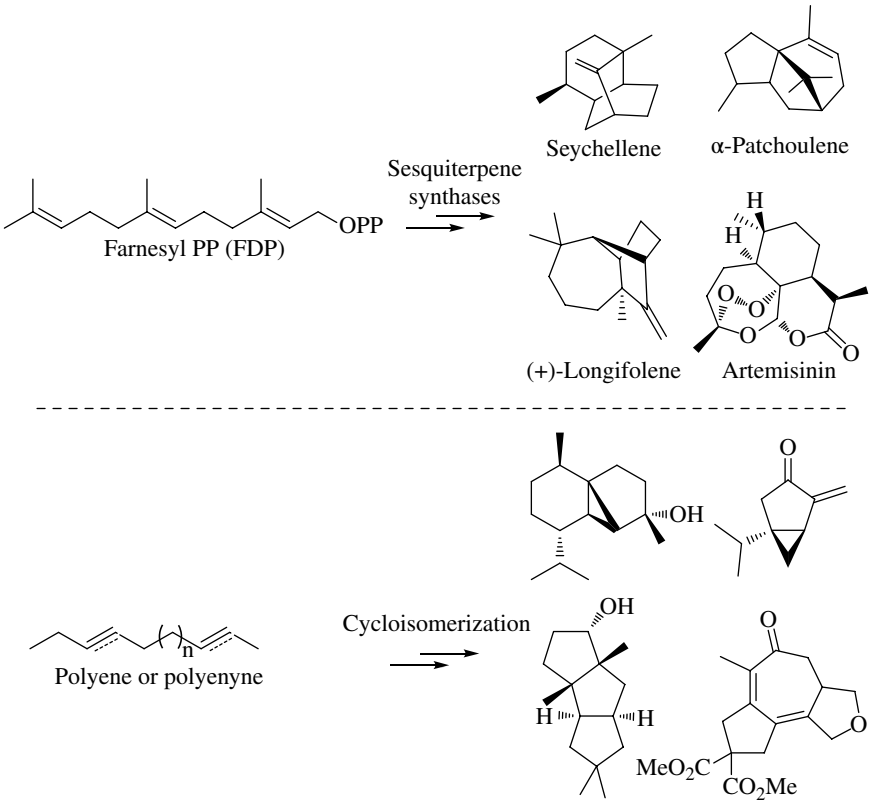



**FIGURE 7.6** Cycloisomerization reactions and their biosynthetic correlation with sesquiterpene synthases.

new C−C bonds, after the typical reorganization of its π-derived electron density. Cycloisomerizations are performed commonly in the presence of a metal catalyst falling into the class of C–H cross-coupling reactions [27]. Within the compendium of chemical reactions, a number of well-known cycloisomerization reactions exist that usually are not classified in this category, as the intramolecular versions of Michael, Stetter, and Diels–Alder reactions, which will not be covered in this chapter, focusing mainly on the biocorrelated diene and enyne counterparts.

Transition metal-catalyzed cycloisomerizations have been the subject of particular attention as atom-efficient methods for the construction of carbo- and heterocyclic molecules, which are fundamental constituents of natural products, pharmaceutical compounds, and functional materials. In view of their importance, several studies concerning their metal-catalyzed cyclization mechanisms have been undertaken in α,ω-bifunctional substrates such as dienes, enynes, and diynes.

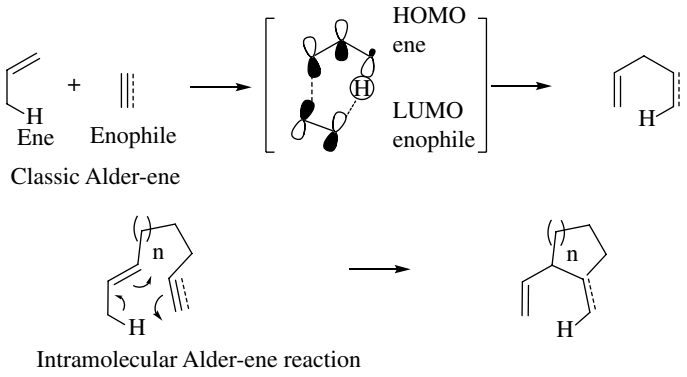
### 7.2.1 Enyne Cycloisomerization

Alder-ene reaction of 1,n-enynes can be regarded as the archetypal of cycloisomerization reaction known for over 60 years in its uncatalyzed thermal form [28]. From mechanistic point of view, the reaction involves a six-electron pericyclic rearrangement between an allylic hydrogen (the ene) and an alkyne (the enophile), causing the formation of two new σ-bonds (Scheme 7.8). The uncatalyzed thermal reaction has had few applications in organic synthesis presumably due to the high temperatures required.

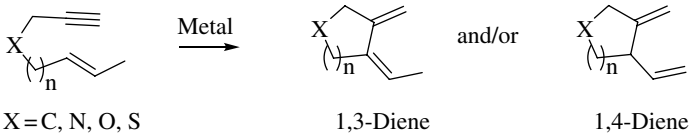
In 1985, Trost et al. [29] discovered the palladium-catalyzed variation of the reaction and since then a multitude of other metals (Ti, Co, Rh, Fe, Pt, Au, etc.) have been successfully incorporated in this process. In contrast to the thermal variant of this process that produces only 1,4-dienes, metal-catalyzed reactions succeeded to provide either 1,3- or 1,4-dienes often with high selectivities (Scheme 7.9). Soon, this reaction developed into a powerful method for the construction of complex molecular frameworks in a highly chemo-, regio-, and diastereoselective manner.

***7.2.1.1 Proposed Mechanisms*** Different mechanistic pathways have been proposed for the metal-catalyzed cycloisomerization reactions. In the case of enynes, these are highlighted as (i) the metallocyclopentene pathway, (ii) the $n^2$-metal pathway, and (iii) the vinylmetal pathway (Scheme 7.10) [30].

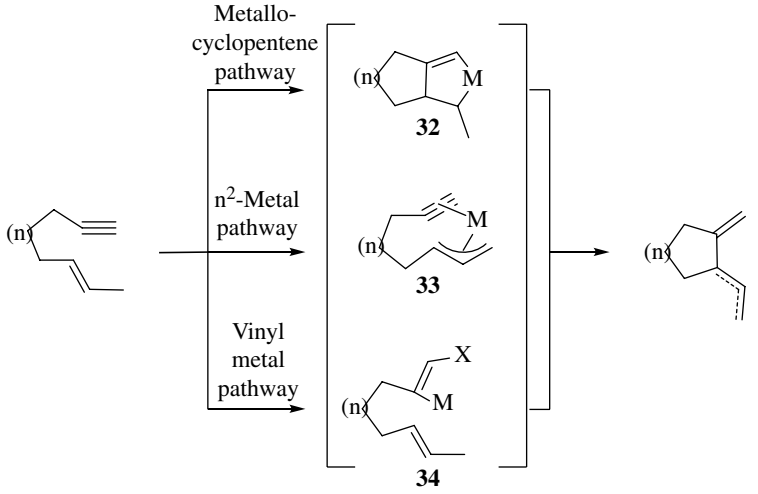
In metallocyclopentene pathway, simultaneous activation of alkyne and alkene moieties leads preferentially to the formation of metallacycle intermediate (**32**). Almost all transition metals could react to generate such intermediates; however their reactivity can be quite different as will be




**SCHEME 7.8** The Alder-ene reaction.




**SCHEME 7.9** Metal-catalyzed enyne reactions.

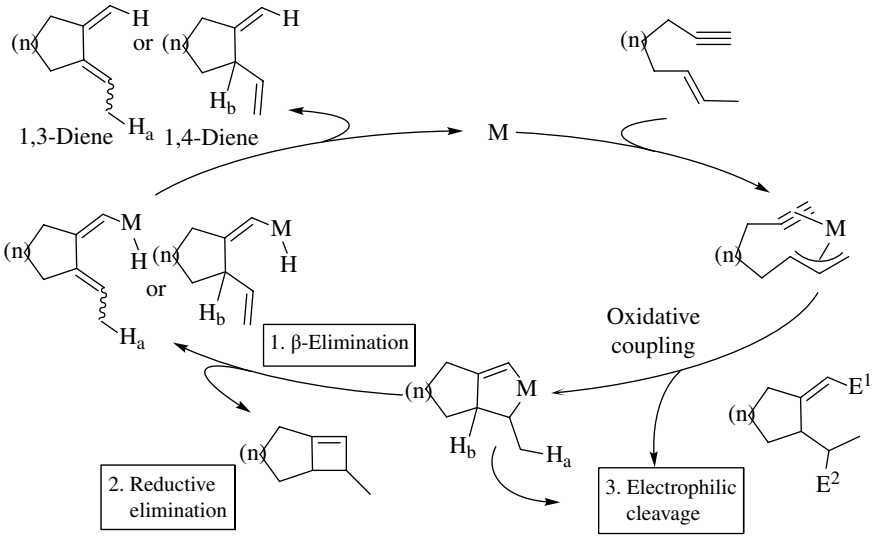



**SCHEME 7.10** Proposed mechanistic pathways for metal-catalyzed cycloisomerization of enynes.

discussed further in this chapter. On the other hand, the presence of functional group in the allylic position promotes the formation of π-allyl complexes (**33**), which could further react with alkynes in the $n^2$-metal pathway. Alternatively, hydrometallation of the alkyne may instead lead to vinylmetal species (**34**) that may carbometalate the olefin in the so-called vinylmetal pathway.

The formation of metallacyclopentenes is very general and occurs with almost all the coordinatively unsaturated transition metals and with great variety of unsaturated partners. The main steps of the catalytic cycle are described in Scheme 7.11. The cycle starts with the complexation of enyne to the metallic moiety followed by its oxidative coupling, which leads to the metallocyclopentene. The formation of metallacycle can then follow three distinct reaction pathways containing its (i) β-elimination, (ii) reductive elimination, and (iii) electrophilic cleavage [30].

The β-elimination pathway is the fastest process and the most usual, leading, after the reductive elimination of the metal, to the formation of 1,3- and/or 1,4-dienes. The β-elimination requires a vacant coordination site on the metal and a *cis* relationship between carbon—metal and carbon—hydrogen




**SCHEME 7.11** Catalytic cycle of cycloisomerization and mechanistic fate following the metallacycle formation; β-elimination process on the metallacycle leading either to 1,3 or 1,4-dienes.

bonds, which have to be aligned to optimize the orbital overlap. Whenever two hydrogens are β-positioned to the metal, both can be eliminated leading to the observed 1,3- or 1,4-diene products (Scheme 7.11). Although, someone would notice that C—$H_a$ bond energy is higher than this of allylic C—$H_b$ bond, its spatial orientation (the dihedral angle almost 0° to the metal compared to the nonideal dihedral angle of C—$H_b$) promotes its elimination in numerous cases. Several transition metal catalysts have been employed in this process with most usual those of palladium, ruthenium, cobalt, and rhodium.

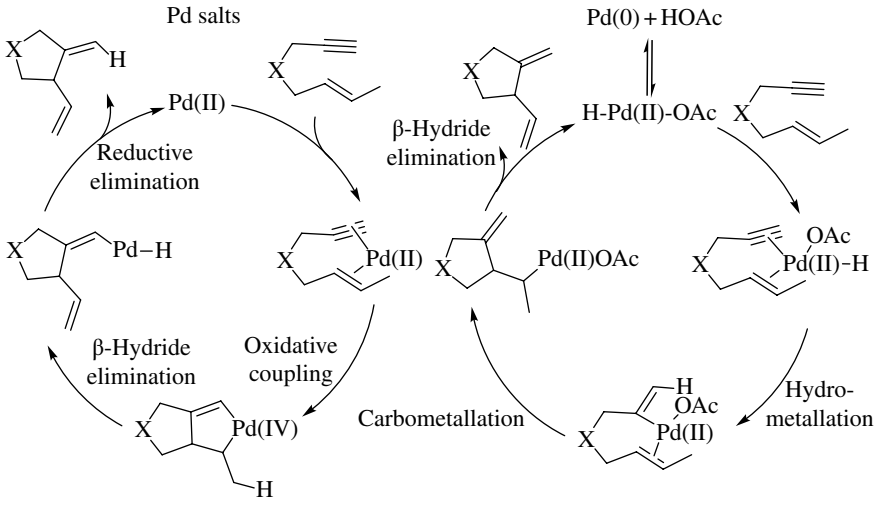
On the other hand, when the rate of β-elimination slows down for geometrical, steric, or even electronic reasons, the reductive elimination of metallocyclopentene intermediate is feasible leading to formal [2+2] products, which usually collapse to 1,3-dienes. Catalysts capable to mediate such transformations are palladium, platinum, gold, and ruthenium.

Although elimination pathways are favored in metallacyclopentenes from the group 8, 9, and 10 metals, when metallacycles derived from coordinatively saturated metals (such as titanium, cobalt, and zirconium) are involved in the presence of electrophiles, the electrophilic cleavage of metallacycles can be predominated. Consequence of electrophilic cleavage is the reaction of an electrophile to either one of the two carbon metal bonds existing in the metallacycle. Several electrophiles have been used in these processes like carbon monoxide, halogens, etc. with most known and widely used the Pauson–Khand reaction. Cycloisomerization involving electrophilic cleavage of the metallacycle is above the scope of this chapter [30].

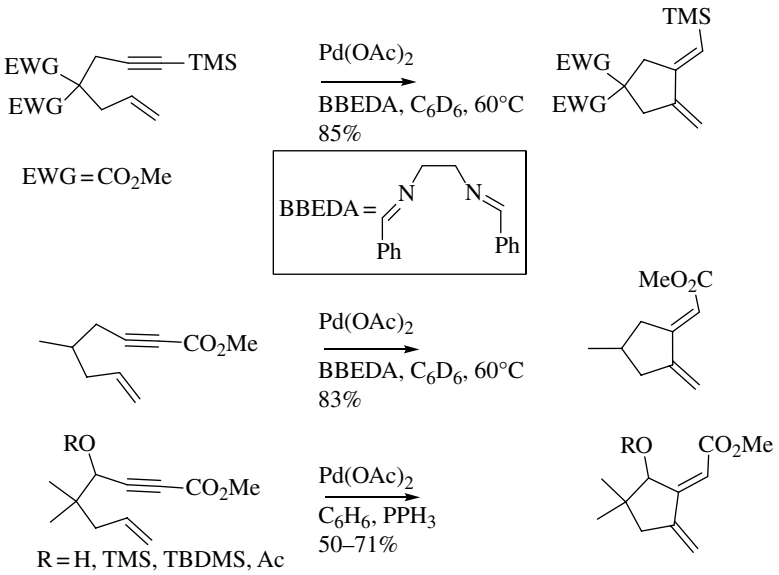
***7.2.1.2 β-Elimination Pathway*** Among the catalysts following β-elimination pathway, palladium catalysis has received the higher attention. Trost and Lautens disclosed the discovery of palladium-catalyzed cycloisomerization of enynes in 1985 [29]. The reaction is thought to proceed through one of two possible catalytic cycles employing either Pd(II)–Pd(IV) or Pd(0)–Pd(II) catalysis, depending on the reaction conditions or the choice of the precatalyst and following the catalytic cycles of Scheme 7.12. Use of palladium(II) salts such as palladium acetate, in the absence of any reducing agent, favors the palladium(II)–palladium(IV) cycle through the formation of a metallocyclopentene intermediate. On the other hand, if a palladium(0) catalyst is used in the presence of an acid, the oxidative addition of palladium(0) to the acid takes place to generate a palladium(II) hydride species. After complexation to the enyne, hydrometallation of the alkyne follows according to the vinylmetal pathway (Scheme 7.10) [30,31].

Since its initial discovery, Trost and his coworkers contributed majorly in this field by publishing an array of elegant papers compiling the factors governing the kinetics and stereoselectivity of palladium-mediated cycloisomerization of enynes [32]. Based on these studies, it was concluded that:

- The presence of geminal electron-withdrawing groups or alkyl groups on the tether facilitates the cycloisomerization but is not required (Scheme 7.13) [33].
- Steric factors influence the regioselectivity of the reaction. Higher substituted allylic positions at ene-end tend to provide 1,3-dienes in contrast to unsubstituted allylic methylene moieties, which afford 1,4-dienes (Reactions A and B; Scheme 7.14) [33a].
- High regioselectivities can be attained when allylic oxygen is present in ene-end for the formation of 1,3-dienes, whereas homoallylic oxygen promoted the production of 1,4-dienes (Reactions C and D; Scheme 7.14) [32a].




**SCHEME 7.12** Two distinct catalytic cycles for palladium cycloisomerization.

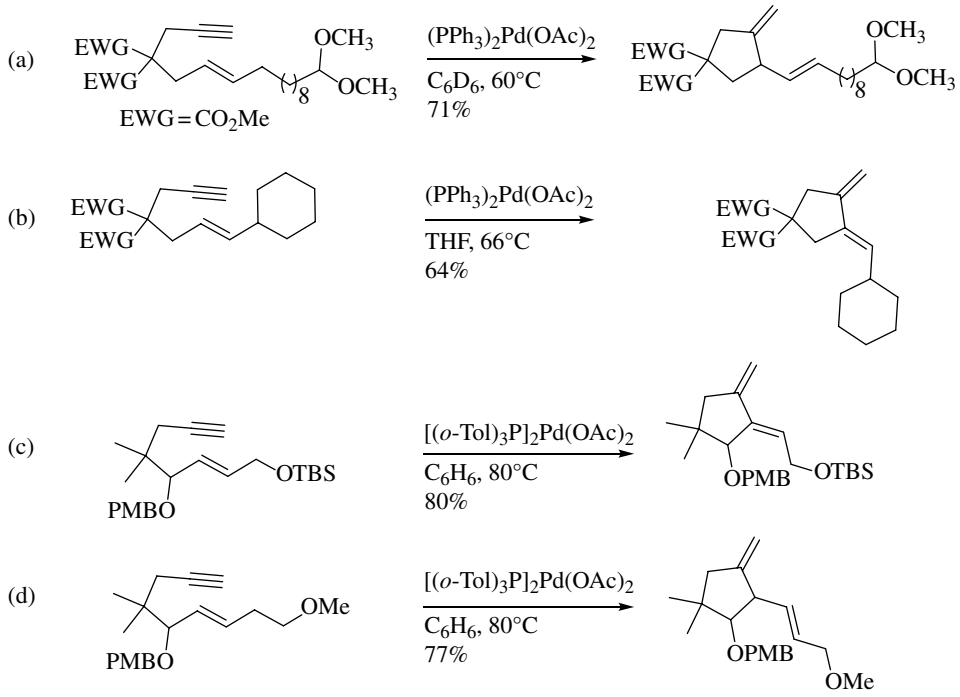



**SCHEME 7.13** The influence of substituents positioned in the tether in cycloisomerization of enynes.

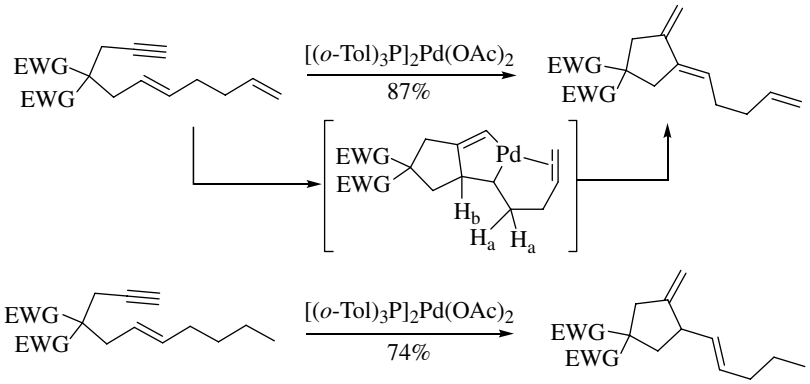
- A remote alkene moiety on enyne provides the regioselective formation of 1,3-dienes due to remote binding to the metal (Scheme 7.15) [32a,33a].

Although palladium cycloisomerization chemistry has been advanced during the previous 20 years, still the creation of larger rings can be overlooked as problematic. The difficulty for that is ascribed to the poorer ability of larger 1,n-enynes to function as bidentate ligands. This problem can be partially circumvented by introducing appropriate functional groups to the ene in order to enhance the coordination ability of chains to the metal (Scheme 7.16) [34].

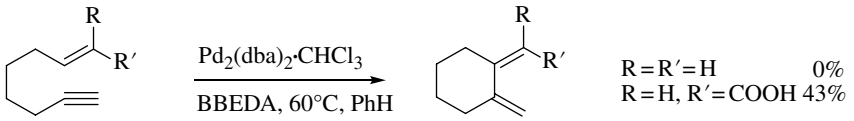
*7.2.1.3 Inducing Asymmetry in β-Elimination Pathway*
Apart from its racemic variants, cycloisomerization of enynes has been successfully employed in asymmetric synthesis. In the first example of an asymmetric cycloisomerization reaction, Trost et al. used a combination of palladium(0) and a chiral acid to catalyze the cycloisomerization of 1,6-enynes resulting in a rather low enantioselectivity of 33% ee for the formation of 1,4-diene (**35**) (Scheme 7.17(a)) [35]. Modern development of chiral phosphoric acids has allowed the reexamination of this approach. Thus, when palladium(0) and chiral (*S*)-TRIP were used with enyne **36** a 71% yield of diene **37** was isolated in 88% ee [36]. Under the same concept, Mikami and coworkers found that cationic palladium




**SCHEME 7.14** Regioselectivity of cycloisomerization reaction based on allylic substitution.




**SCHEME 7.15** Remote alkene as factor to influence regioselectivity of cycloisomerization reaction.

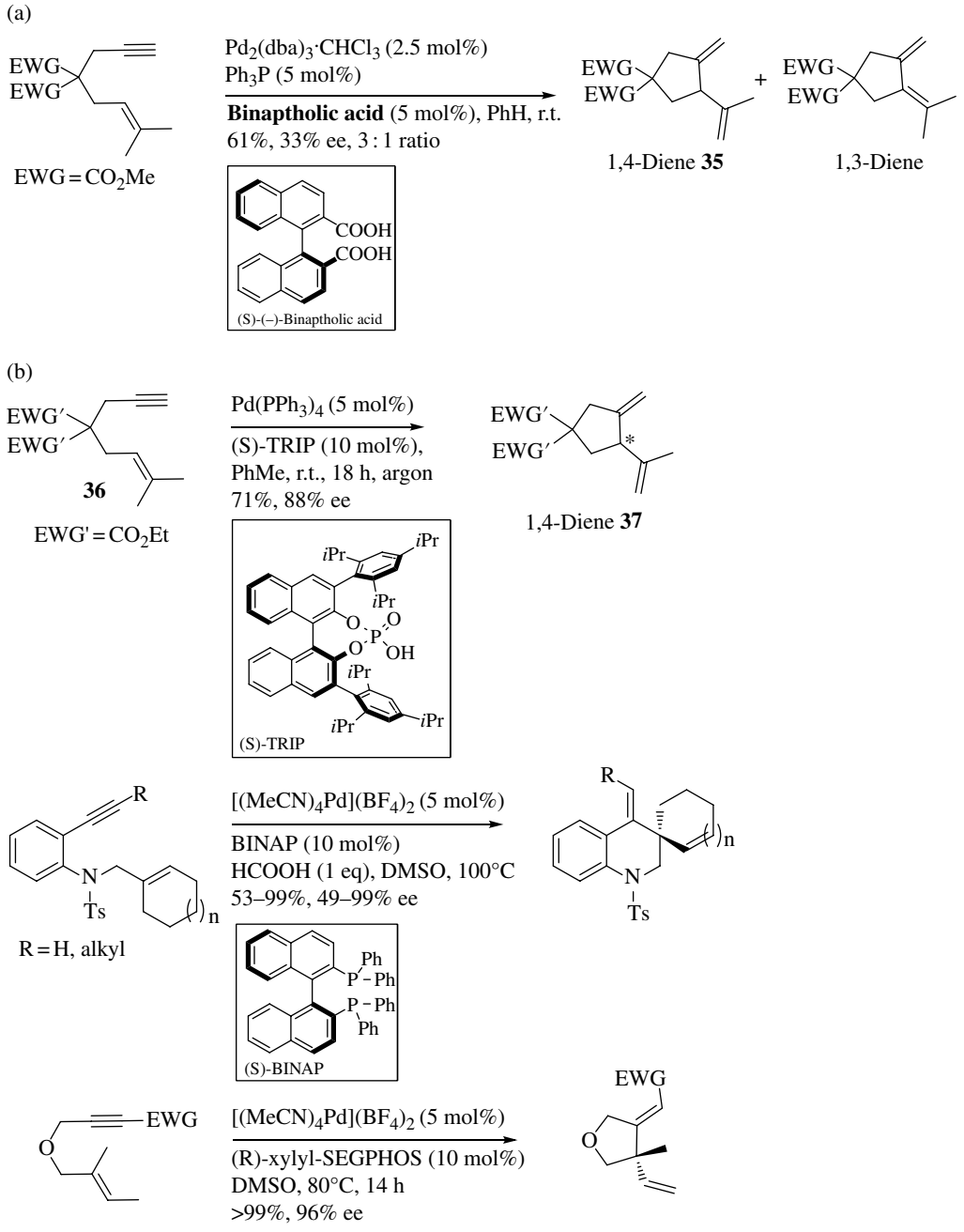



**SCHEME 7.16** Cycloisomerization of 1,7-enynes.

complexes along with chiral BINAP phosphines or related ligands can further improve the enantioselectivity of cycloisomerization either of 1,6- or 1,7-enynes [37,38].

Expansion of the substrate scope on asymmetric cycloisomerization came from the advancement of rhodium catalysis. Following the same catalytic cycle, rhodium(I) complexes coordinate enynes followed by oxidative cyclization to form a rhodium(III) metallocyclopentene. This intermediate usually undergoes regiospecific β-hydride elimination to give E-olefin geometry followed by reductive elimination to generate the 1,4-diene product (Scheme 7.18).

Lean into this process, Zhang and coworkers managed to produce high enantioselectivities of 1,4-dienes from enynes in the presence of rhodium complexes and chiral

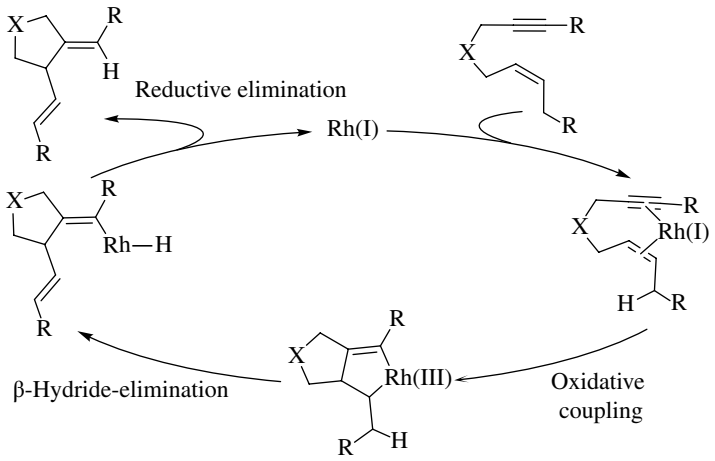



**SCHEME 7.17** (a) Seminal first enantioselective cycloisomerization of 1,6-enynes and (b) modern enantioselective variants.

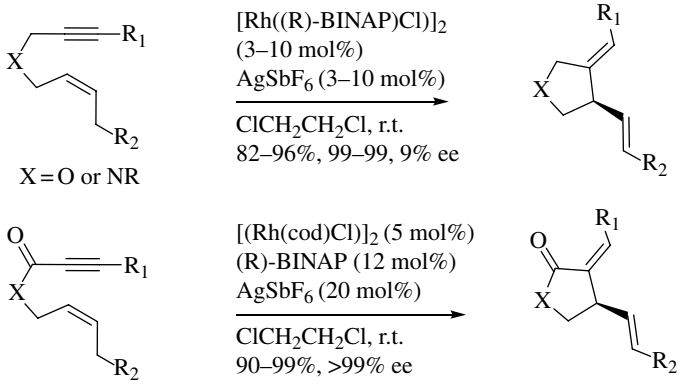
bidentate phosphines such as MeDuPhos, BINAP, BICP, and so on (Scheme 7.19) [39].

Several other groups extended the scope of the reaction to terminal alkynes [40], to cycloisomerization–hydrosilylation protocols [41], or even to hydrogen-mediated reductive cyclizations [42] to produce nowadays a convenient asymmetric method.

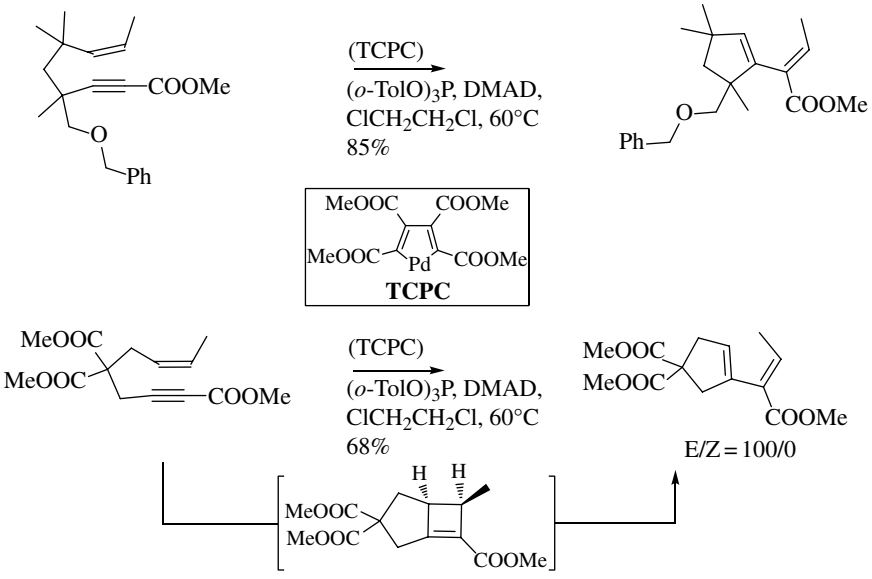
***7.2.1.4 Reductive Elimination Pathway*** On the other hand, interesting cycloisomerizations promoted by palladium complexes that follow the reductive elimination pathway of a metallocyclopentene (Scheme 7.10; pathway 2) provide formal metathesis products through the ring opening of cyclobutenes (Scheme 7.20) [43]. Stereoelectronic features of the substrates are influencing the competition between metathesis and cycloisomerization reaction. Among the most crucial is the presence of an electron-withdrawing group on the alkyne and the disubstitution of allylic position on the substrate. In general severe steric congestion promotes the effectiveness of metathesis reaction.



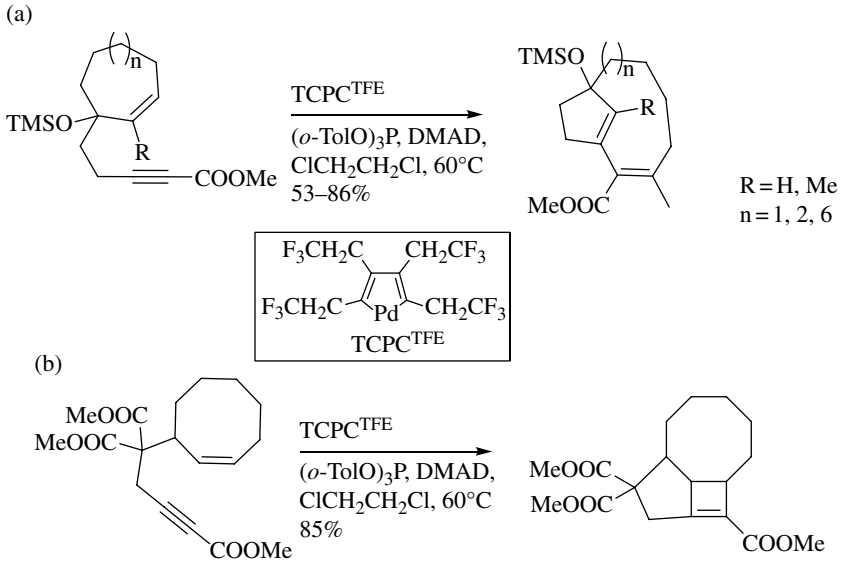

**SCHEME 7.18** Rhodium catalytic cycle.



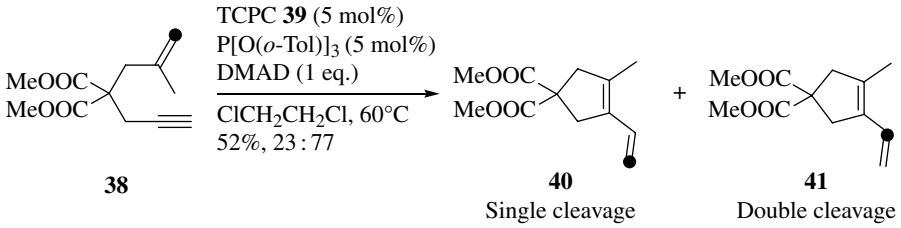

**SCHEME 7.19** Rhodium-catalyzed enantioselective cycloisomerizations.




**SCHEME 7.20** Palladium-mediated formal metathesis of 1,6-enynes.




**SCHEME 7.21** Examples of "metathesis reaction" from alkene endocyclic bonds (a) to form bridged compounds or (b) strained cyclobutenes.




**SCHEME 7.22** Labeling experiments for the cyclization of enynes.

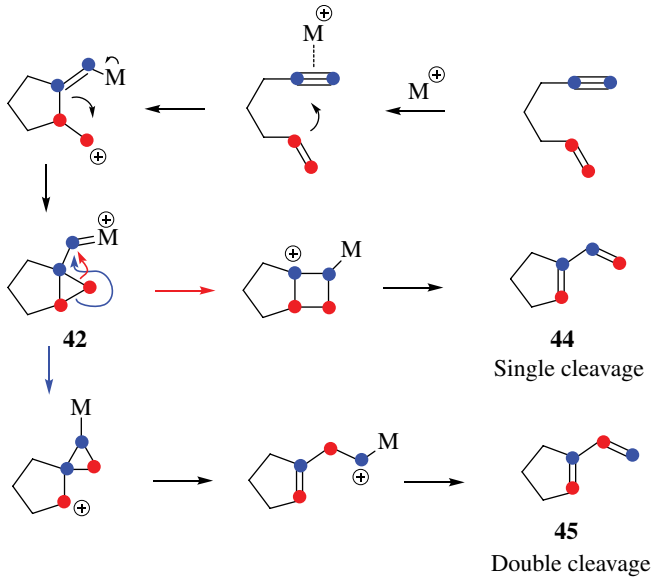
Under the same mechanistic concept, when endocyclic double bonds are present, the metathesis allows the ring expansion to bridged bicycles (Reaction a; Scheme 7.21) [44]. Although cyclobutane mechanistic pathway has been debated for several years, it was rarely supported by the isolation of cyclobutanes or isomerized cyclobutanes formed from the cyclization of 1,6-, 1,7-, or 1,8-enynes (Reaction b; Scheme 7.21) [45,46].

However further studying of reaction mechanism by $^{2}H$ and $^{13}C$-labeling experiments [47] have shown that two kinds of metathesis dienes are obtained. Treatment of labeled enyne **38** with palladacycle complex **39** led to a mixture of 1,3-dienes **40** and **41**, which were designated as "single cleavage" and "double cleavage" products, respectively (Scheme 7.22).

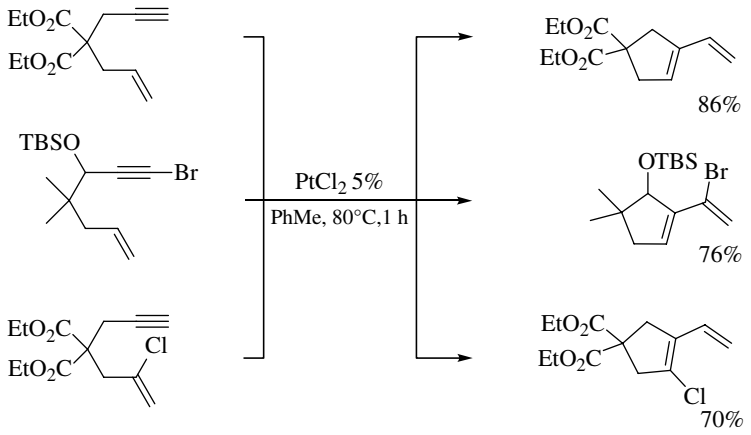
In order to take these results into account, a different mechanistic pathway was proposed relying on the generation of a (cyclopropylcarbene)palladium intermediate **42**. Successive [2+2] and retro-[2+2] rearrangements lead to the formation of carbene **43**. A 1,2-hydride shift and elimination complete the catalytic cycle to produce the dienes **44** and **45** (Scheme 7.23).

***7.2.1.5 Platinum and Gold in Metathesis*** In connection with the palladium-mediated metathesis, Trost has also shown that platinum complexes like $(PPh_3)_2Pt(OAc)_2$ are able to catalyze this reaction [43]. Murai and coworkers expanded the scope of the reaction utilizing the versatile $PtCl_2$ catalyst with a broad range of substrates (Scheme 7.24) [48].

Pursuing further results on this topic Murai et al. also recognized the anomalous carbon–carbon bond formation behavior on several platinum cycloisomerizations, based on deuterium experiments [48], suggesting the intervention of a carbenoid intermediate [49]. Today, after several studies concerning majorly platinum but also gold cycloisomerizations, it is believed that these transformations proceed via the formation of a cyclopropylcarbene complex analogous to **42**, Scheme 7.23, which is triggered by the initial metal coordination on the alkyne (Scheme 7.25). The bonding in late transition metal complexes with alkynes and olefins is described by a combination of the interaction of the occupied ligand π-orbital to the metal vacant *dsp* and donation of the metal *d* electrons to olefin or acetylene empty π*. As such zwitterionic complexes as well as carbenes are implicated in the cyclopropanation reaction observed by these metals.



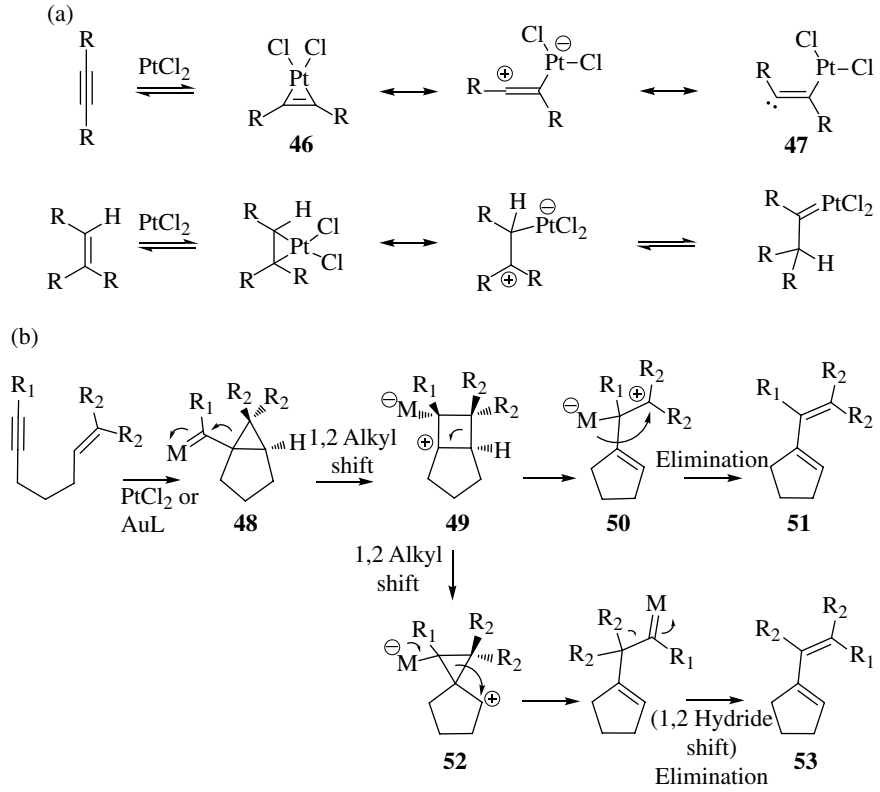

**SCHEME 7.23** Single and double cleavage rearrangement products and a more detailed description of double cleavage product highlighted by the collapse of a metallocyclopentene. (*See insert for color representation of the figure*.)



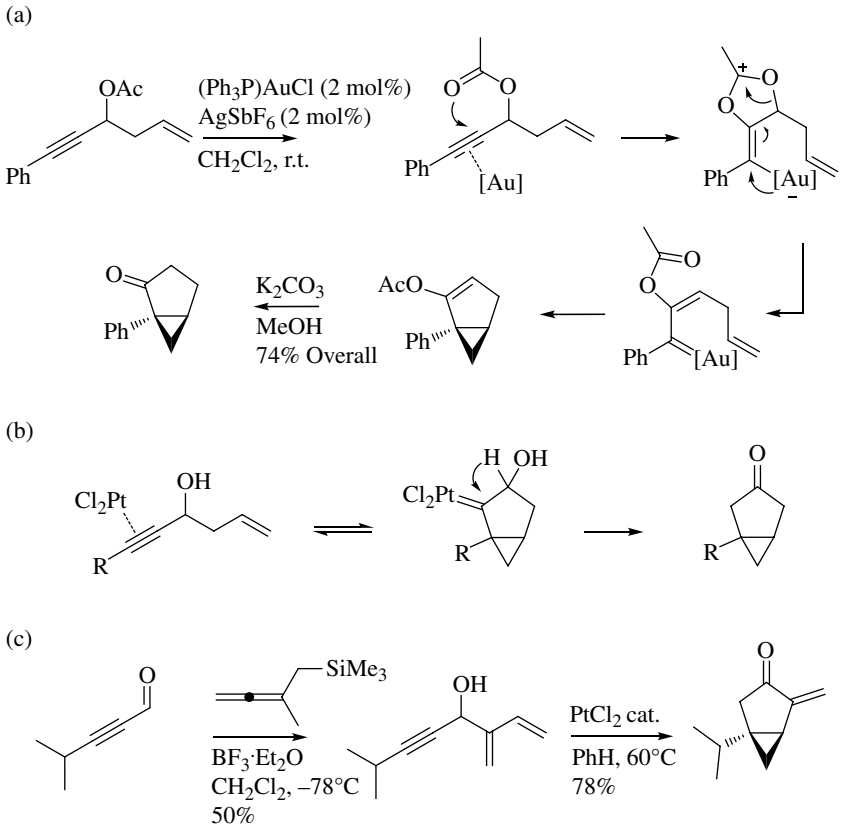

**SCHEME 7.24** Enyne metathesis catalyzed by platinum chloride.

The process is believed to begin by the chemoselective metal complexation to the alkyne followed by cyclopropanation of the proximate alkene to produce cyclopropyl metal carbene (**48**) through the direct incorporation of the carbene intermediate **47** [50]. In the absence of external nucleophiles, carbene **48** collapses to zwitterion **49**, which, as previously, depending on the substituent $R_2$, follows one or two fragmentations to produce both observed dienes. Based on the mechanism provided, trisubstituted alkenes favor the formation of dienes **51**, through the stabilization of intermediate **50**, whereas terminal alkenes destabilize the carbocation **50** forcing the reaction to proceed through intermediate **52** to produce product **53**.

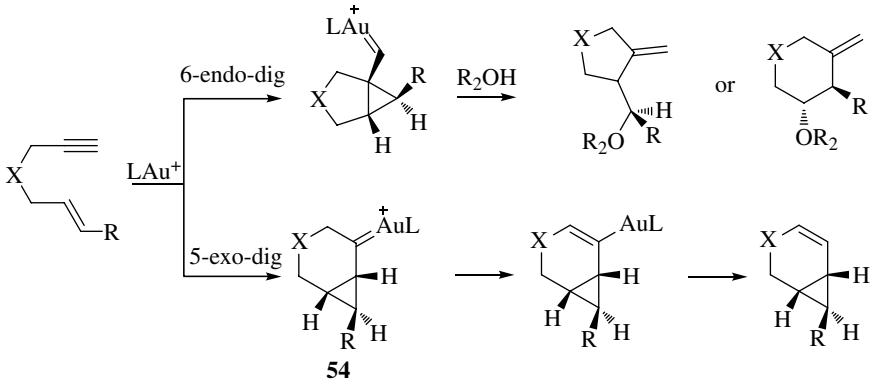
The unique propensity of platinum(II) but especially gold(I) to activate alkynes, coupled with their ability to stabilize carbocation intermediates, make them particularly useful catalyst in cycloisomerization reactions. Unlike the Alder-ene-type reactions that are usually observed with palladium and rhodium catalysts as presented previously, in the presence of gold or platinum catalysts, 1,n-enynes are likely to undergo skeletal rearrangements following the formation of metal carbenes as described in Scheme 7.25. Cationic gold(I)-catalyzed cycloisomerizations was first reported in 2004 to produce either bicyclic cyclopropane products (Scheme 7.26) [51] or intermolecularly cleaved by nucleophiles to yield cyclopentane or cyclohexane compounds (Scheme 7.27) [50a]. As it is pointed out in Scheme 7.27, the cyclization onto the activated alkyne may occur in either a 5-exo-dig or 6-endo-dig manner. Products derived from intermediate **54** after β-hydride elimination have been found only for substrates containing ethereal or tosylamine substituents.



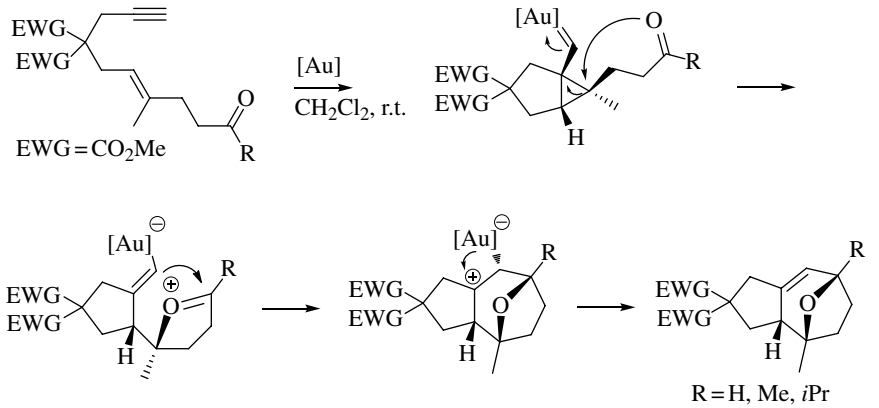

**SCHEME 7.25** (a) Zwitterions between metals and alkynes or alkenes and (b) proposed mechanism for the cycloisomerization of enynes with platinum and gold complexes.




**SCHEME 7.26** Platinum and gold cycloisomerization of 1,5-enynes with subsequent (a) migration of an acetyl group; or (b) and (c) oxidation of a hydroxy group.




**SCHEME 7.27** Gold-catalyzed cycloisomerization of 1,6-enynes.




**SCHEME 7.28** Cycloisomerization of 1,6-enynes-Prins cascade catalyzed by gold complexes.

The remarkable ability of these catalysts to cycloisomerize 1,n-enynes has been exemplified in reaction cascades for the straightforward induction of molecular complexity (Scheme 7.28).

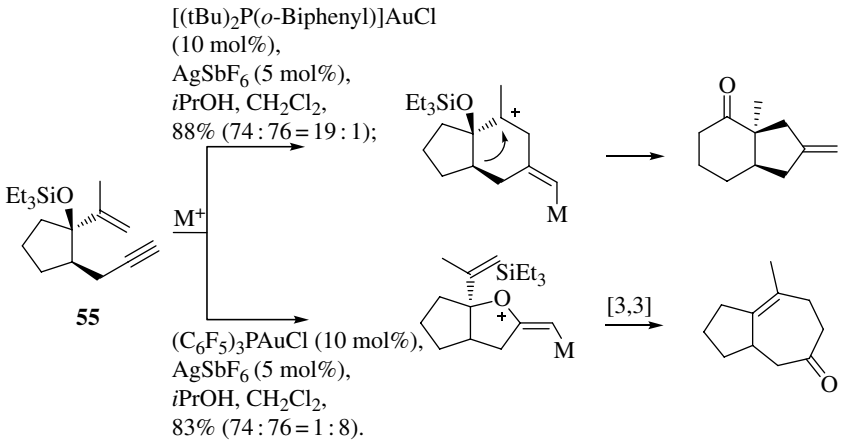
The putative metal cationic intermediates can be interconnected into a series of cationic processes such as Friedel–Crafts, pinacol, Nazarov, Prins-type reactions. In Scheme 7.28, the gold-catalyzed cycloisomerization of 1,6-enynes is followed by an intramolecular nucleophilic attack by the proximate carbonyl to generate the tetrahydropyranyl cation, which participate in a Prins-type reaction to produce tricyclic compounds resembling the core structures of several terpenoids [52].

In another cascade sequence Kisrch and coworkers utilized substrate **55** as a common intermediate to produce two different carbocycles, relying either on the subsequent pinacol or a [3+3] rearrangement of two different, depending on the conditions, carbocations (Scheme 7.29).

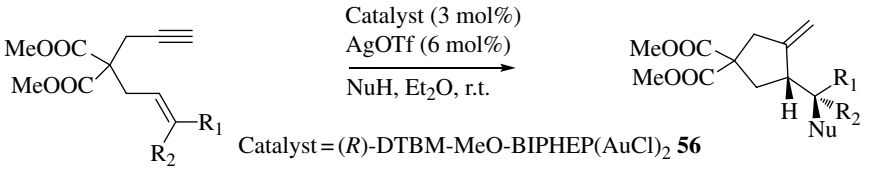
Chiral bisphosphine gold(I) complexes have been employed in the asymmetric variants of a number of gold-catalyzed transformations. Michelet and coworkers reported an asymmetric cycloisomerization of 1,6-enynes trapped by external nucleophiles to afford a variety of functionalized hydroaryl–cyclopentane products in excellent yields and ee's (Scheme 7.30) [53]. The optimal catalyst for this transformation was found to be (*R*)-DTBM-MeO-BIPHEP$(AuCl)_2$ complex with AgOTf. The same catalyst was also found to be effective for the intramolecular cyclopropanation of 1,6-enynes providing bicyclo[4.1.0]heptane in high enantioselectivities [54]. This concept has also been expanded to the asymmetric synthesis of antidepressant drug GSK1360707 (Scheme 7.31) [55].

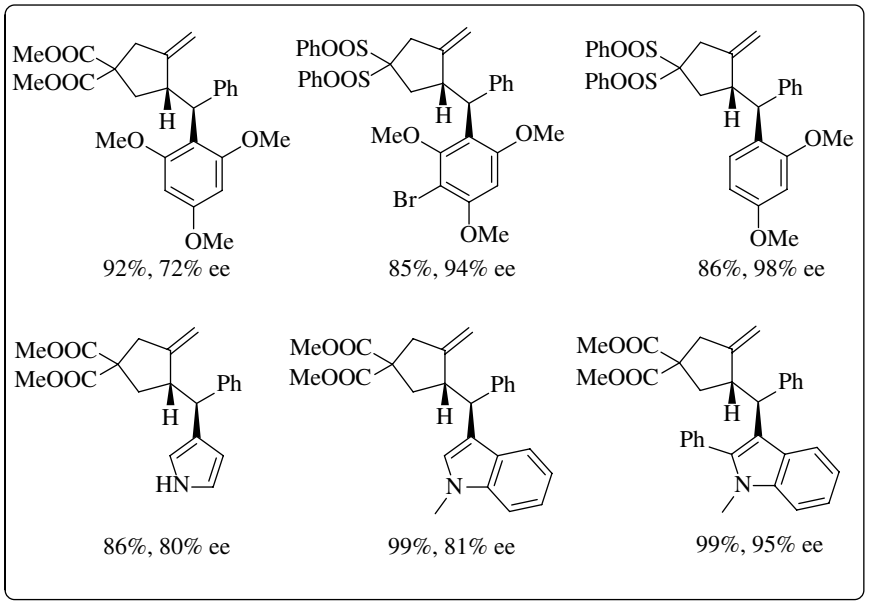
More complicated cascades has also been achieved by the use of (*R*)-DTBM-MeO-BIPHEP$(AuCl)_2$ catalyst when fully functionalized with internal nucleophiles enynes have been utilized as starting components (Scheme 7.32) [26b].

Toste and coworkers have developed an efficient method for the asymmetric gold(I)-catalyzed preparation of medium-size rings. The reaction involves the coordination of the cationic gold(I) complex to the alkyne followed by a 1,2-shift of an acetate to generate the corresponding vinyl carbenoid (Scheme 7.33) [56].

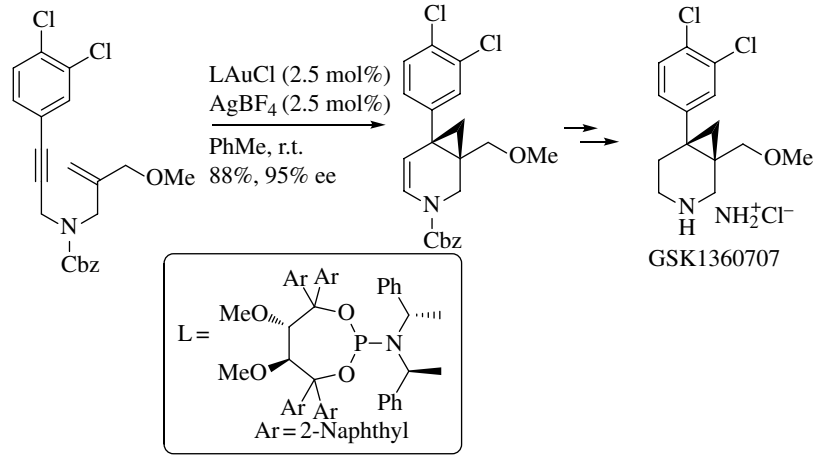



**SCHEME 7.29** Pinacol and [3+3] cascades after the cycloisomerization of 1,6-enynes.

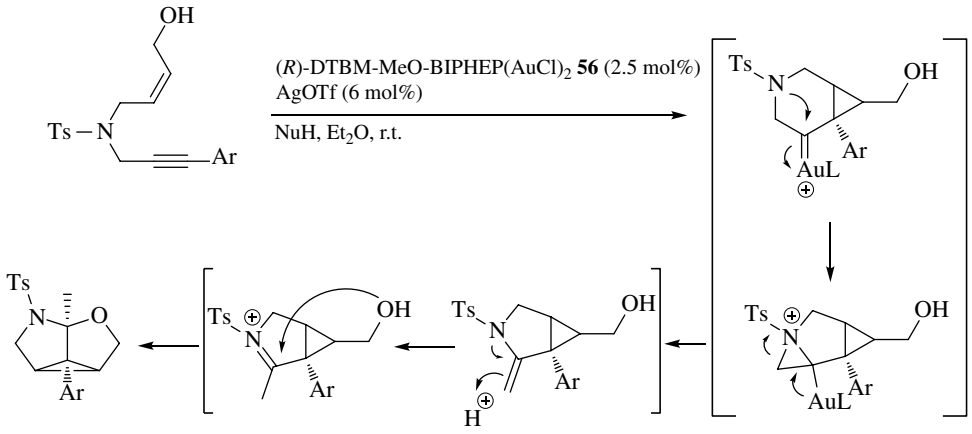


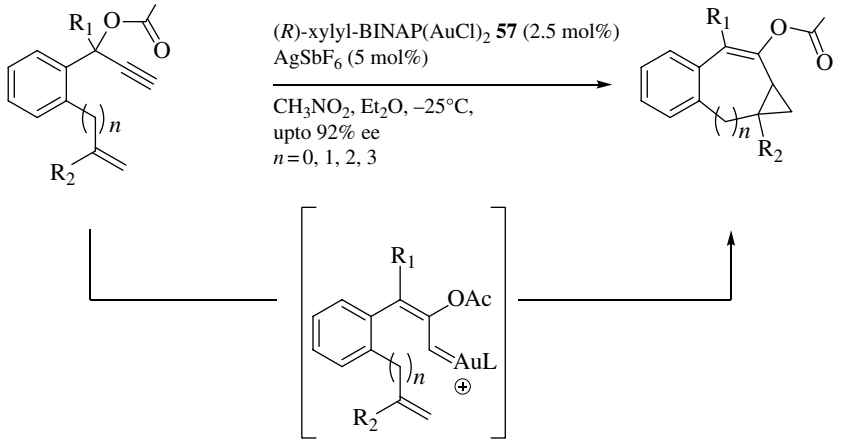

**SCHEME 7.30** Asymmetric cycloisomerization trapped with external nucleophiles.




**SCHEME 7.31** Asymmetric cyclopropanation of 1,6-enynes.




**SCHEME 7.32** Indicative asymmetric cycloisomerization cascades.



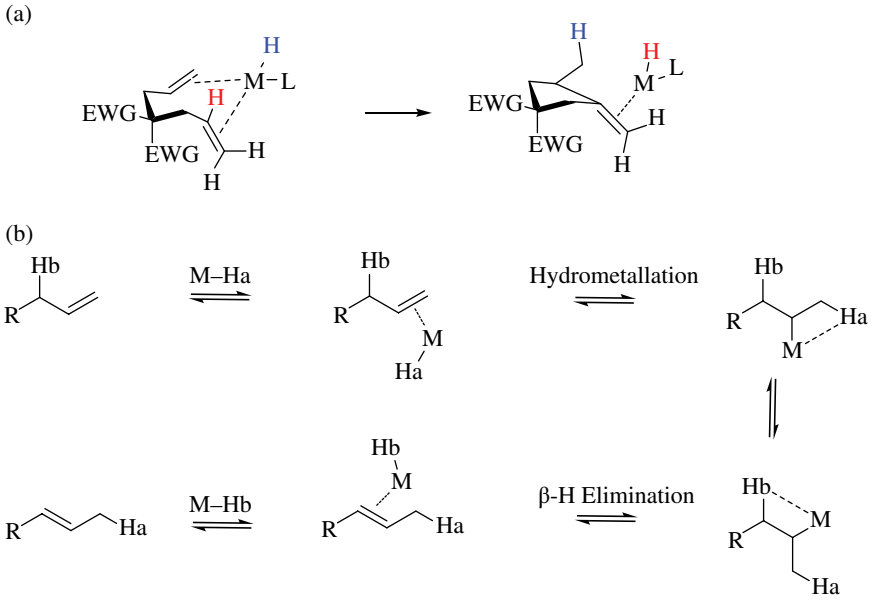

**SCHEME 7.33** Asymmetric preparation of medium-size cyclopropane derivatives.

### 7.2.2 Diene Cycloisomerization

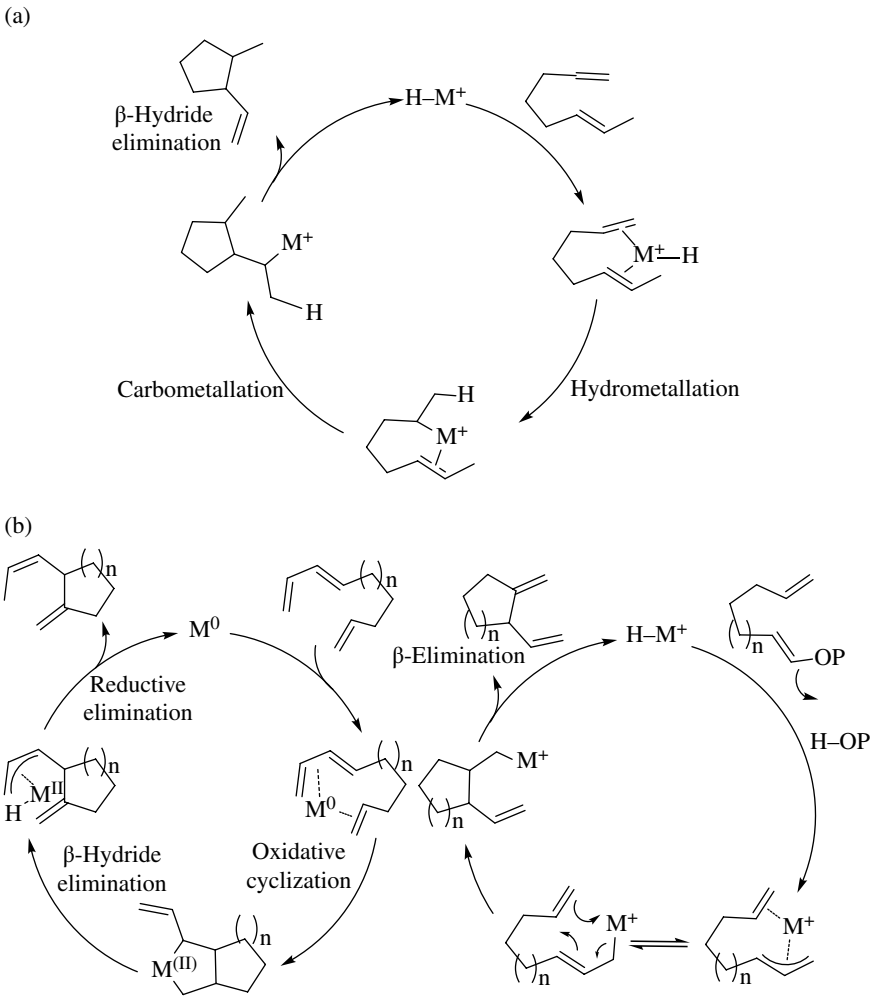
Apart from the formation of vinylmetals and metallacycles and all the possible pathways deriving from them, π-allyl metal pathway ($n^2$-metal pathway; Scheme 7.10) are quite rare in the cycloisomerization of enynes. On the other hand, cycloisomerizations of dienes are common to be performed either through the generation π-allyl complexes or through hydrometallation of alkenes [26a].

The major drawbacks concerning the use of dienes in cycloisomerization reactions usually rely on the poor control of the regiochemical outcome, based on the lack of significant reactivity difference between the reacting alkenes. What is more, olefinic positional isomers are commonly obtained due to the facile transposition of alkenes via the reversible hydrometallation/β-hydride elimination, which is usually feasible during the standard cycloisomerization conditions (Scheme 7.34). To address these issues, considerable efforts have been directed toward the identification of catalytic systems and reaction conditions to realize isomer selective cycloisomerization of dienes.

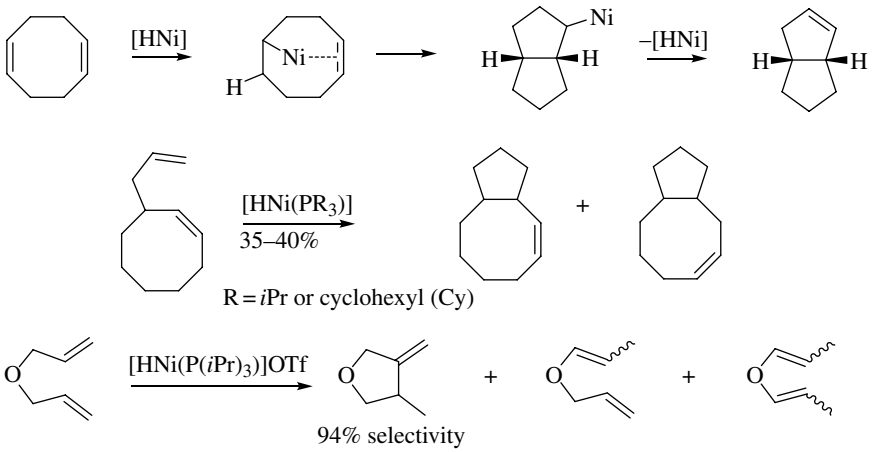
Based on the diene substrates and the reaction conditions, two distinct mechanisms can be followed to induce alkene activation and consequent cycloisomerization. The first mechanism invokes the hydrometallation of an alkene, followed by its subsequent carbometallation into the second one, terminated by a β-hydride elimination. The second mechanism implies the formation of a π-allylic complex either by its prior or later to the cycloisomerization formation (Scheme 7.35). Dienes possessing heteroatom functionality in the allylic position is able to provide π-allylic complex with a metal prior its cyclization. On the other hand, polyenes bearing 1,3-dienes in their system are commonly producing a 1,3-metal complex, which is readily cycloisomerize to give a π-allyl metal complex after the formation of the new carbon─carbon bonds.



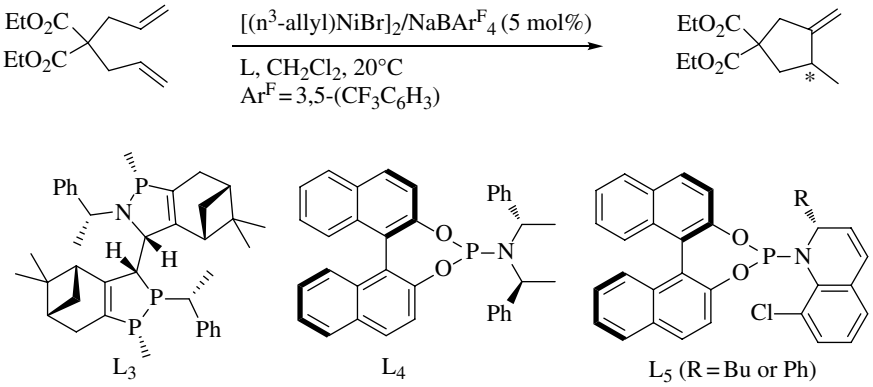

**SCHEME 7.34** (a) The basic concept of diene cycloisomerization and (b) general mechanism for alkene transposition.




**SCHEME 7.35** (a) Hydrometalation of dienes and (b) π-allyl metal pathways.




**SCHEME 7.36** Seminal study on nickel-catalyzed cycloisomerization of dienes.




**SCHEME 7.37** Variations of asymmetric cycloisomerization of 1,6 dienes under nickel catalysis.

Several metals have been applied in the hydrometallation of dienes with more prevalent those of palladium, rhodium, nickel, and platinum. One of the earliest examples of transition metal-catalyzed cycloisomerization was realized by nickel complexes [57]. In this seminal article, Bogdanovic and coworkers prepared active hydride nickel species *in situ* by reacting π-allyl nickel precursors $[(n^3\text{-allyl})NiX]_2$ with alkyl aluminum reagents (i.e., $R_nAlX_{3-n}$) in the presence or absence of phosphine ligands. Alternatively, nickel hydride species can be prepared, in analogy to palladium-hydride species (please refer to Scheme 7.12), by treatment of precursors $Ni(PR_3)_4$ or $Ni(cod)_2$ with strong acids like $CF_3COOH$ and $HBF_4$. Under these catalysts an array of 1,5- and 1,6-dienes can be cycloisomerize efficiently to produce the corresponding cyclopentenes (Scheme 7.36) [58].

The reaction was considered to proceed via hydrometallation/carbometallation/β-hydride elimination sequence followed in some cases by alkene transposition. Asymmetric variants of the reaction have been developed by the same group [59] and others [60], utilizing chiral phosphine ligands (Scheme 7.37), and concluded that the isomer ratios, ee's, and catalytic activity observed are dependent on the combination of phosphine ligand and the counteranions of the catalysts (Table 7.1).

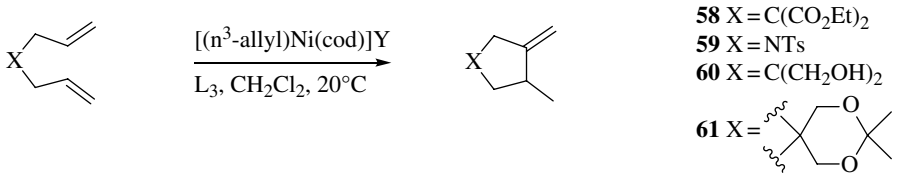
Early discoveries on the cycloisomerization of dienes were also achieved by utilizing rhodium complexes. Malone and coworkers in 1971 discovered that heating diallyl ether with $RhCl_3 \cdot 3H_2O$ resulted in the formation of exo-methylene tetrahydrofuran (Scheme 7.38) [61].

Rhodium catalysts as in the case of nickel favors electronically neutral alkenes for cyclization producing exo-methylene derivatives as the major products. This selectivity is clearly demonstrated in cycloisomerization of amides **62** and **63** (Scheme 7.39) [58].

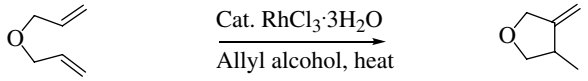
Although the mechanism in rhodium catalysis is still unclear, it is believed that the reaction initiates through an oxidative cyclization of a diene with a low-valent rhodium species to produce a rhodacycle, which undergoes β-hydride elimination to form the common intermediate for both exo- and endo-observed products (Scheme 7.40) [59].

In contrast to nickel- and rhodium-catalyzed reactions, palladium cycloisomerizations of 1,6-dienes produce different isomers as the major products [62,63]. Palladium catalysts show a preference on electron-deficient alkenes for the

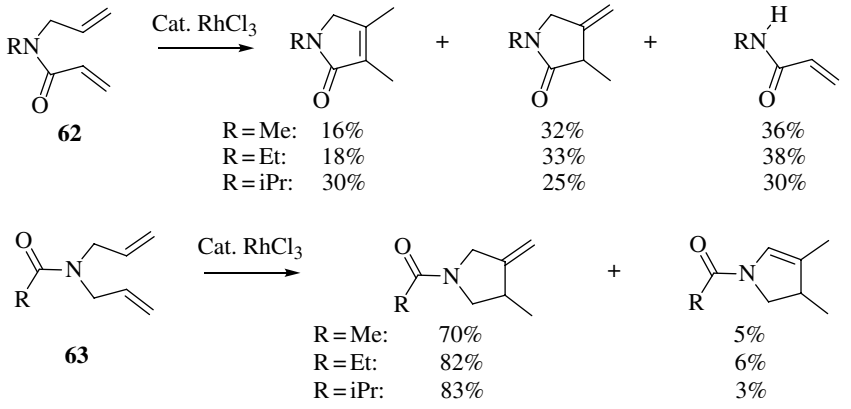
**TABLE 7.1 Dependence of Counteranions of the Catalyst on the Asymmetric Cycloisomerization of 1,6-Dienes**



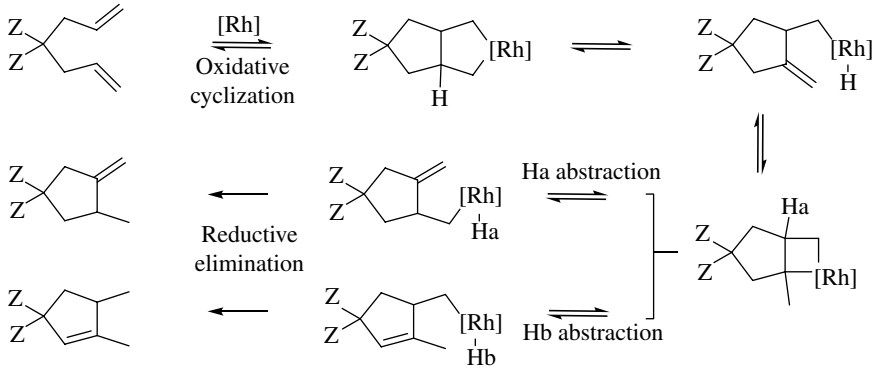

| Y (cat./% mol) | Diene | Time (h) | Conversion (%) | Isomer Selectivity (%) | *ee* (%) |
|---|---|---|---|---|---|
| BArF (5) | **58** | 0.5 | 96 | 91 | 71 |
| $SbF_6$ (5) | **58** | 0.5 | 92 | 91 | 72 |
| $AsF_6$(5) | **58** | 0.5 | 88 | 94 | 74 |
| $PF_6$ (5) | **58** | 0.5 | 57 | 84 | 74 |
| BArF (0.5) | **58** | 1 | 72 | 91 | 72 |
| Al(pftb)$_4$ (0.5) | **58** | 1 | 79 | 97 | 73 |
| Al(hfpp)$_4$ (0.5) | **58** | 1 | 55 | 91 | 73 |
| BArF (0.5) | **59** | 1 | 64 | 95 | 33 |
| Al(pftb)$_4$ (0.5) | **59** | 1 | 11 | 99 | 54 |
| Al(hfpp)$_4$ (0.5) | **59** | 1 | 34 | 99 | 48 |
| BArF (5) | **60** | 1 | 39 | >99 | 91 |
| BArF (5) | **61** | 1 | >99 | 87 | 86 |



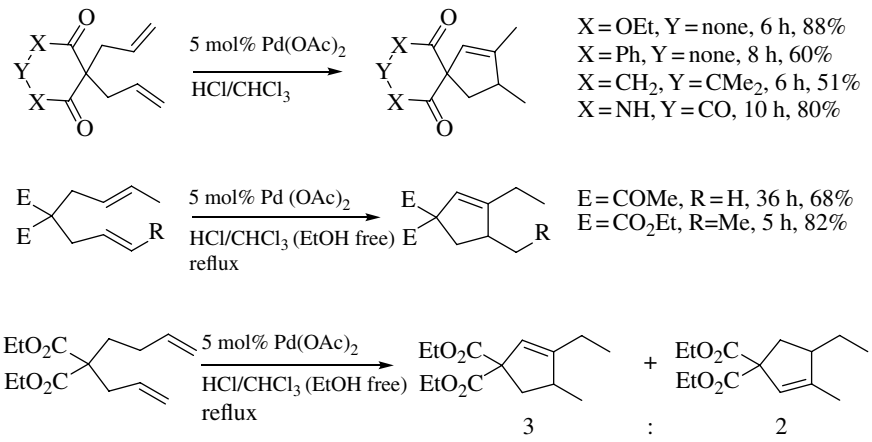

**SCHEME 7.38** Seminal publication on rhodium-catalyzed cycloisomerization of 1,6-dienes.



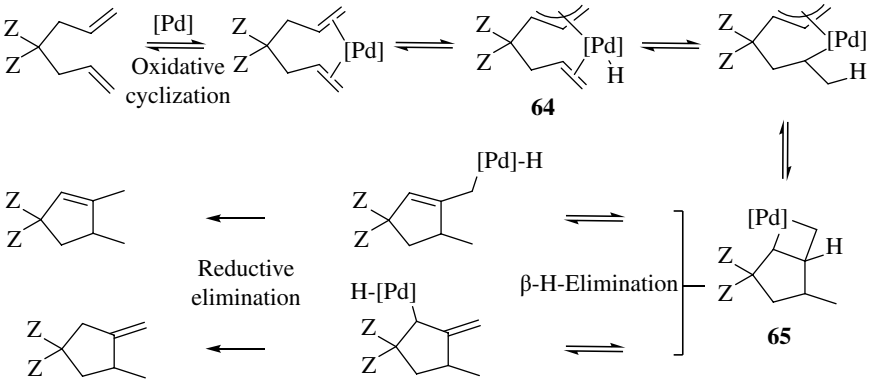

**SCHEME 7.39** Selectivity of rhodium-catalyzed cycloisomerization of dienes.




**SCHEME 7.40** Postulated mechanism for rhodium-catalyzed cycloisomerizations.




**SCHEME 7.41** Examples of palladium-catalyzed cycloisomerization of dienes.




**SCHEME 7.42** Postulated reaction mechanism for palladium-catalyzed cycloisomerization of dienes.

cyclization and produce the more highly substituted olefinic isomers (Scheme 7.41). Concerning its mechanism, the fact that deuterium was not incorporated into the product during the $Pd(OAc)_2$-catalyzed reaction in the presence of DCl outlined the absence of palladium-hydride species during the reaction (Scheme 7.42). The reaction is considered to be initiated by allylic C–H activation producing π-allyl complex **64**. Hydrometallation onto the second alkene, followed by intramolecular attack of the resulting complex at the central carbon of the π-allyl group, affords metallacyclobutane **65**. Sequential β-hydride elimination/reductive elimination reactions produce the usually observed isomeric partners.

On the other hand, when hydrosilane additives were introduced in the reaction mixture, a significant improvement of the cycloisomerization reaction was observed (Scheme 7.43) [64].

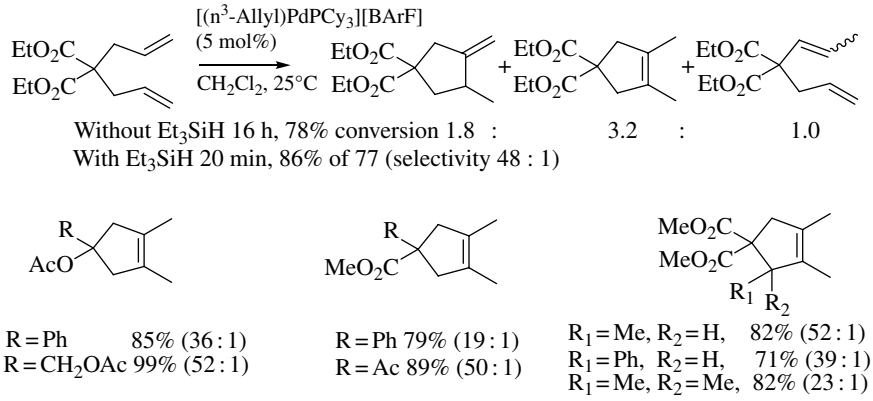
Deuterium experiments with $DSiEt_3$ revealed a direct incorporation of deuterium into the product, indicating the initial formation of palladium-hydride species. The reaction mechanism proceeds through a hydrometallation of the first alkene, insertion into the second alkene, and β-hydride elimination to **66**. Isomerization of the later by reinsertion and re-β-hydride elimination leads to the major isomer **67** (Scheme 7.44) [65].

Further studies enriched the field with several palladium precatalyst as [(phen)PdMe(MeCN)]BarF [62], [($\eta^3$-allyl) $Pd(MeCN)_2$][OTf] [63], and so on, acting as palladium-hydride species under the reaction conditions. Thus, those are providing good to excellent yields of cyclized products in a high ratio between the major regioisomers and without the need of hydrosilane additives (Scheme 7.45).

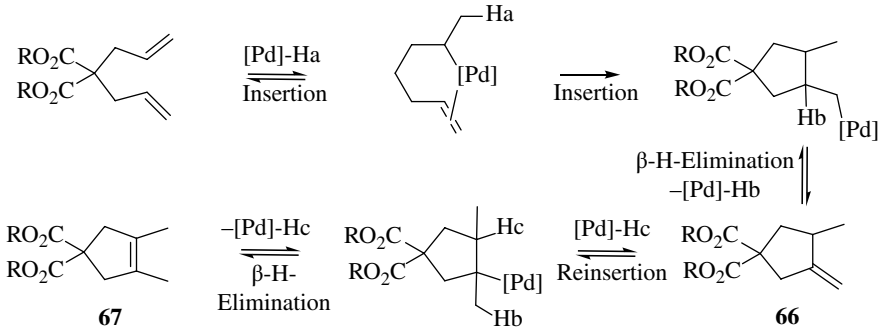
Palladium-catalyzed cycloisomerization providing the thermodynamically less-favored exo-alkylidene compounds has been elusive. However, lately this unique selectivity has also been accessed by utilizing N-heterocyclic carbene and 1,5-cyclooctadiene-derived catalysts [65].

Concerning the asymmetric variants of palladium catalysis, still the examples are very few reporting only moderate ee's (Scheme 7.46) [66].

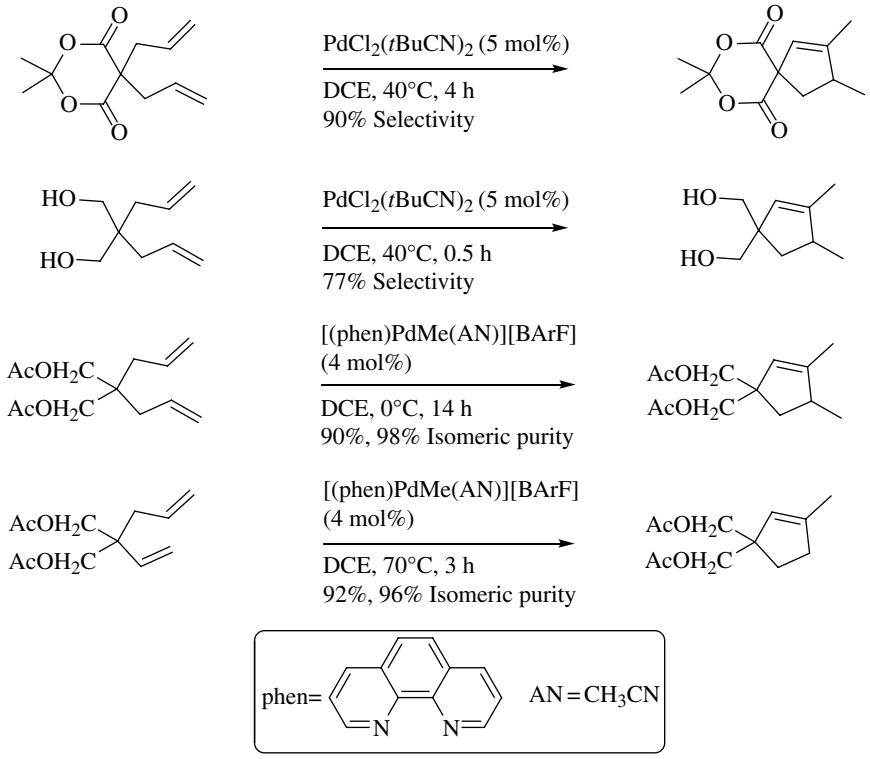
The activation of alkenes by carbophilic Lewis acids is another way to induce cycloisomerization of dienes through a cation cyclization mechanism, provided that undesirable



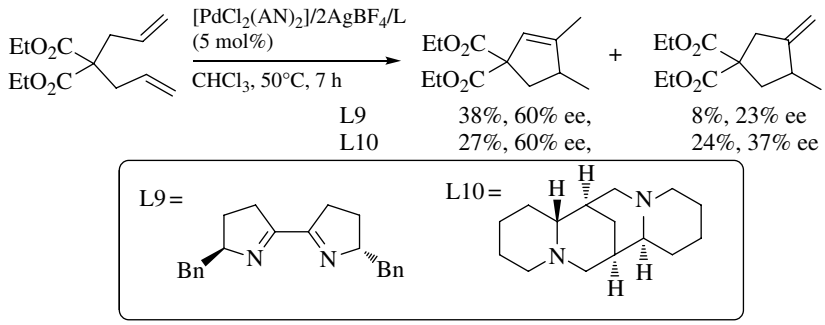

**SCHEME 7.43** Improvement of diene cycloisomerization with hydrosilane additives under palladium catalysis.



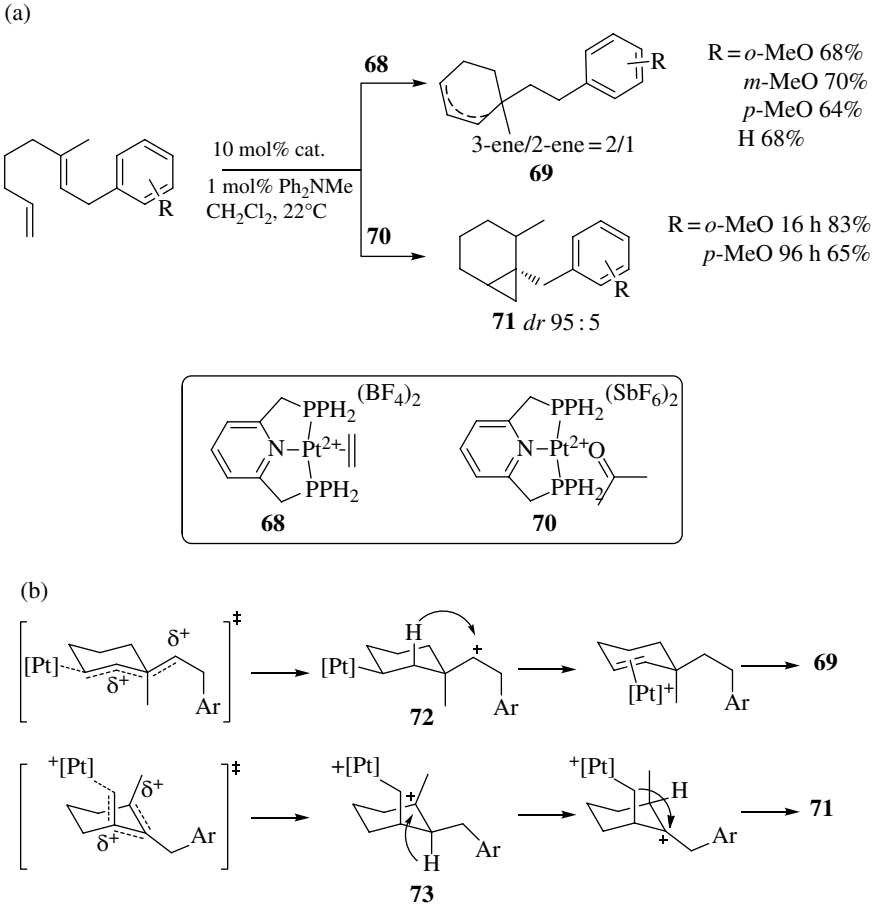

**SCHEME 7.44** Mechanism promoted by hydrosilane additives.




**SCHEME 7.45** Examples employing different precatalysts for the cycloisomerization of 1,6-dienes.



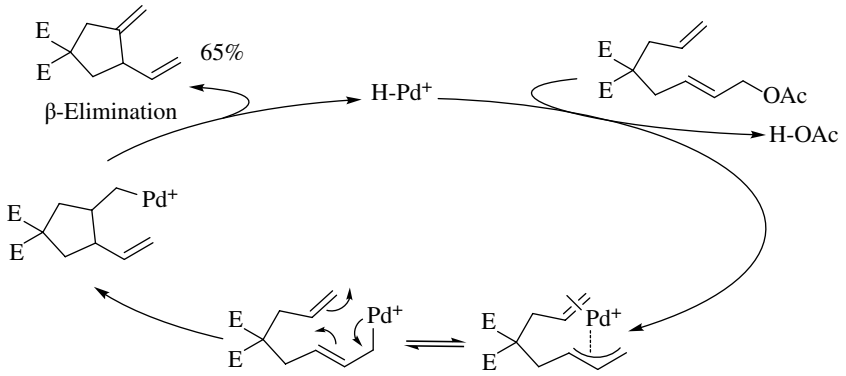

**SCHEME 7.46** Moderate enantioselectivities in palladium-catalyzed cycloisomerization of dienes.



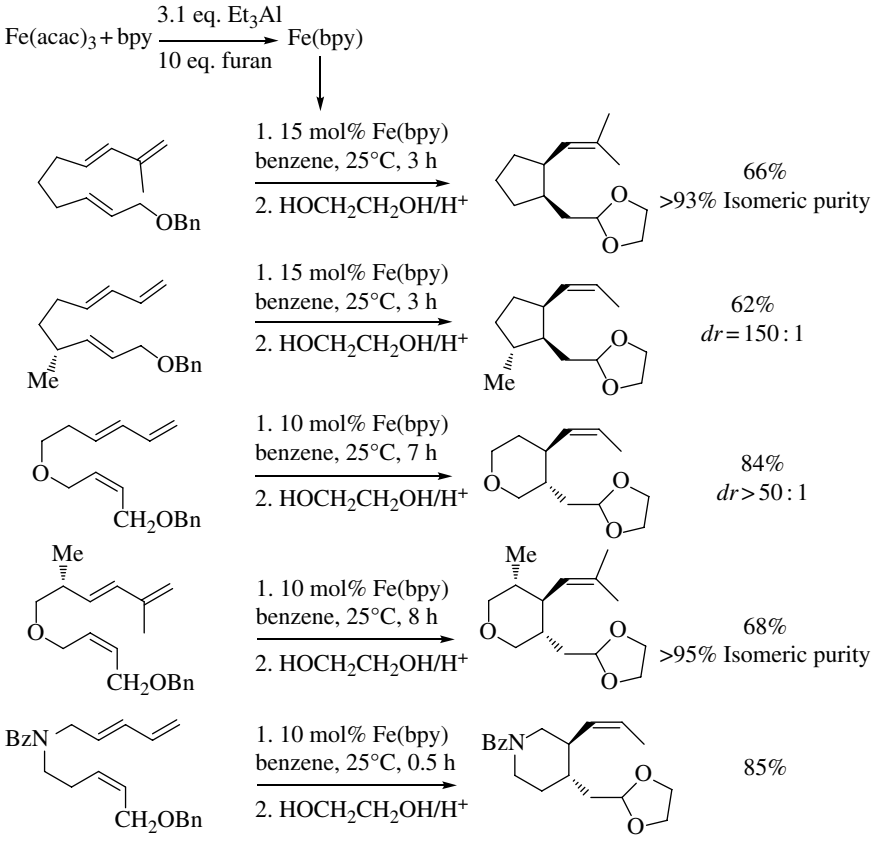

**SCHEME 7.47** (a) Cycloisomerization of 1,6-dienes using cationic platinum pincer complexes and (b) mechanism of platinum pincer complexes.

β-elimination of metal alkyl intermediates can be inhibited. Gagne and coworkers invented a pincer-type platinum complex bearing tridentate ligands, which effectively suppress the problematic β-hydride elimination [67]. Extensive studies of the same group led to effective cycloisomerization of 1,6-dienes to cyclohexene derivatives or bicycle[4.1.0] heptanes depending on the catalytic platinum species (Scheme 7.47). The formation of the two compounds is rationalized through the electrophilic activation of terminal alkene, which triggers cation cyclizations via two distinct transition states **72** and **73**.

In sharp contrast to simple dienes, where slow kinetics and regioselectivity issues are present, polyenes bearing a conjugated 1,3-diene system or dienes with heteroatoms positioned in the allylic position of one of the two alkenes are generally more reactive toward cycloisomerization reactions. What is more, the existence of allylic or conjugated diene moiety in these substrates resolves the regiochemical issues of alkene




**SCHEME 7.48** Cycloisomerization of dienes bearing allylic substitution.



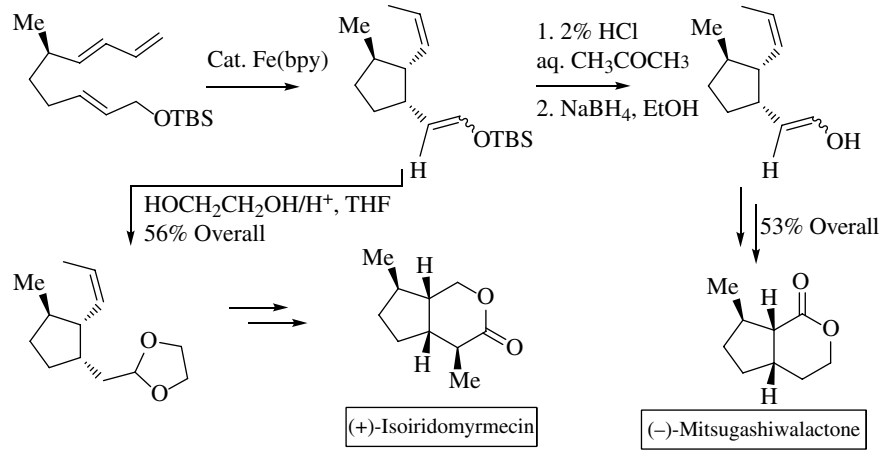

**SCHEME 7.49** Iron-catalyzed cycloisomerization of trienes.

activation and provides usually a much cleaner reaction. In both cases, reactions proceed through the formation of π-allylic complex as it was presented in Scheme 7.35.

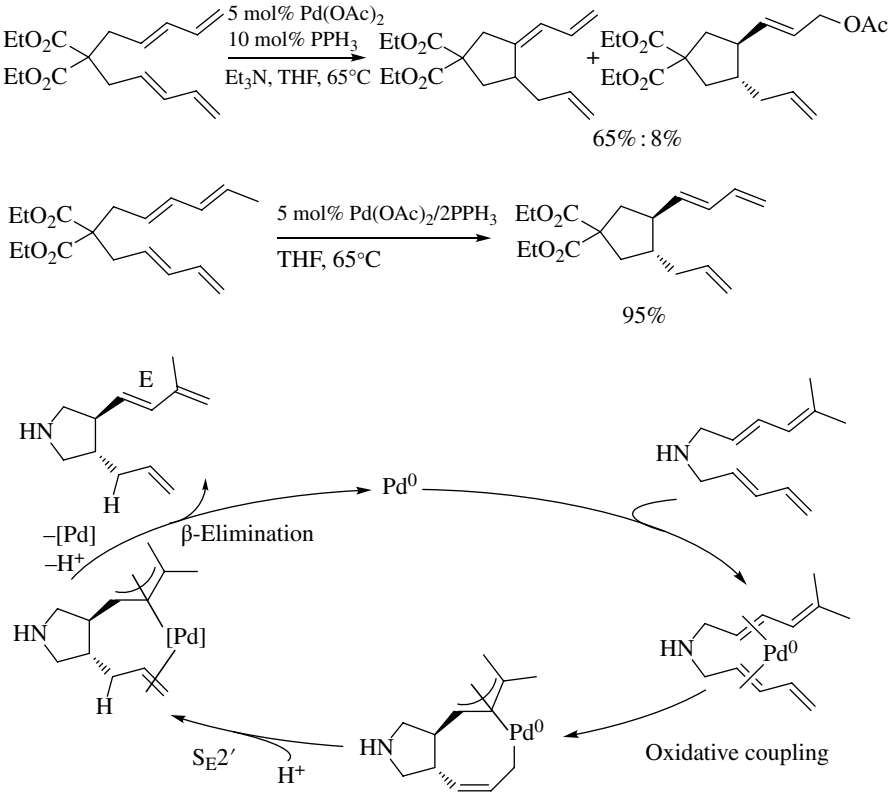
The palladium-catalyzed carbocyclization of allylic acetates with alkenes is a powerful method for the formation of five- and six-member rings. The reaction initiates through the formation of a π-allyl palladium complex followed by carbometallation of the second double bond. The formed palladium complex is then eliminated to produce commonly the cyclized 1,4-dienes (Scheme 7.48).

The earliest example of cycloisomerization in conjugated dienes was reported by Takacs et al. in 1980 [68]. In their study a low-valent iron bipyridine complex was prepared by reducing $Fe(acac)_3$ with $Et_3Al$ and used for the cycloisomerization of trienes (Scheme 7.49).

Notably the reaction works equally well for the formation of cyclopentanes and cyclohexanes [69] in high diastereoselectivity, which can be translated to optical purity whenever a substituent with absolute stereochemistry is present in an allylic position of either diene or isolated




**SCHEME 7.50** Application of cycloisomerization of trienes in the total synthesis of iridoids.




**SCHEME 7.51** Cycloisomerization of 1,3,8,10-tetraenes.

alkene. In all of these catalyzed triene cycloisomerizations, benzyl ether moieties were critical for the high efficiency and diastereoselectivity of the reaction. The same reaction was successfully applied in the asymmetric total synthesis of iridoids natural products by the same group (Scheme 7.50) [70].

The scope of cycloisomerization on polyenes was further extended by utilizing 1,3,8,10-tetraenes under palladium catalysis (Scheme 7.51). The reaction provides cyclopentanes in high yields depending on the substrates. Elucidation of reaction mechanism by deuterium experiments revealed the incorporation of a σ,π-bisallyl complex.

In summary, cycloisomerizations of enynes and dienes represent a powerful tool in the hand of organic chemists. Although in the past 20 years, the field has witnessed remarkable advances especially in their asymmetric variants; in the years to come, cycloisomerizations will continue to enrich our knowledge with atom-economical

routes and impressive cascades to reach more complex substrates. The subchapter that follows highlights only a part of cycloisomerization power to some selected total syntheses of sesquiterpenoids.

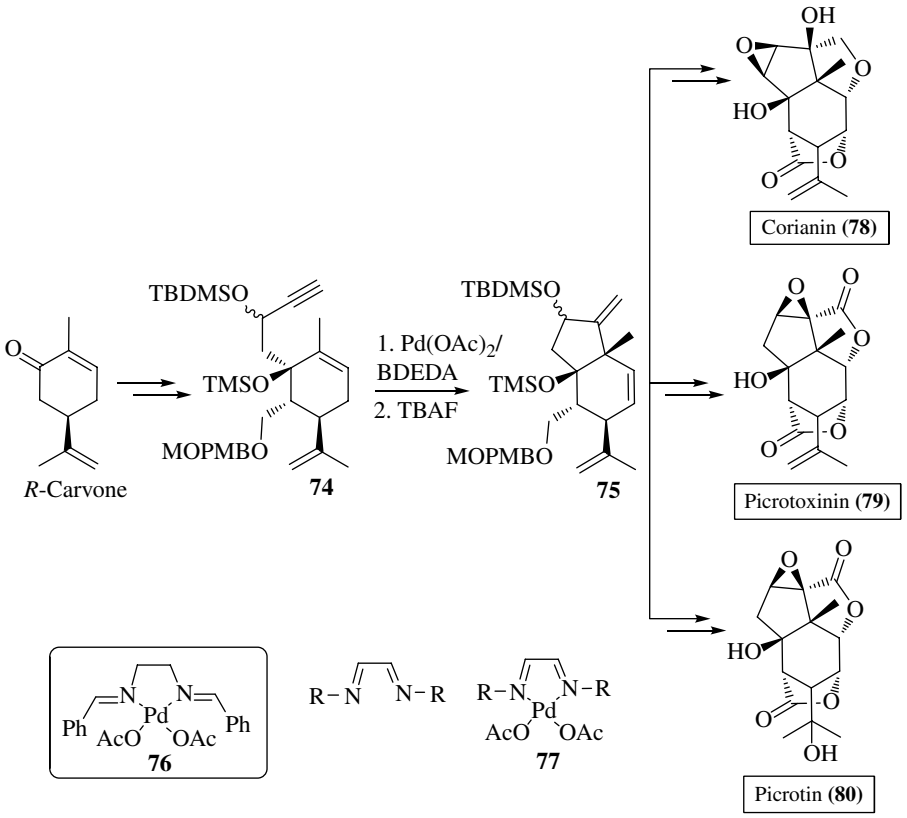
## 7.3 APPLICATION OF CYCLOISOMERIZATIONS IN THE TOTAL SYNTHESIS OF SESQUITERPENOIDS

The close relationship of cyclization modes existed in sesquiterpene biosynthetic machinery, with those presented by the metal-catalyzed cycloisomerizations, justify the vast amount of reports on total synthesis of sesquiterpenes, in which the utilization of enyne or diene cycloisomerizations are the key components of their synthetic strategy. This chapter is intended to cover only selected examples on the topic. Special concern is given on covering catalyzed reactions, which are triggering different cyclization modes, only for the construction of sesquiterpene core structures. Assuredly, cycloisomerization reactions are powerful tools in providing also other classes of secondary metabolites, as complex terpenoids and alkaloids, in which the readers are referred to more general reviews on the topic [26,30].

### 7.3.1 Picrotoxane Sesquiterpenes

Pioneering the field of metal-catalyzed cycloisomerizations, Trost and his group was also the first to discover the power of cycloisomerizations in the total synthesis of complex natural structures. In 1999, he reported the first-and second-generation strategy for the synthesis of picrotoxane core structure through a palladium-catalyzed cycloisomerization [71].

The picrotoxane sesquiterpenes is a large family of natural products with a chemical history extending back to 1600s where there exist the first written accounts of Indian natives using the poisonous berries of *Menispermum cocculus*. Probably the most known component of the family is picrotoxinin [72], a highly toxic compound which was found to be potent and specific antagonist against the neurotransmitter suppressor γ-aminobutyric acid (GABA) [73] inhibiting the opening of chloride ion *in vivo* [74]. To date, over 50 picrotoxane-related compounds possessing similar biological activity have been isolated not only from plants but also from marine and terrestrial animal as well. Trost's synthetic design of picrotoxane core was relied on a palladium-catalyzed cycloisomerization of enyne **74**, which was readily prepared from *R*-carvone through sequential alkylation events (Scheme 7.52). Although enyne **74** bears a sensitive tertiary alcohol to any Lewis acid catalysts, the appropriate selection of a ligand that can be reasonable acceptor as well as donor to a π-coordinative




**SCHEME 7.52** Total synthesis of picrotoxane sesquiterpenes.

transition metal allows the smooth balance between its coordinative reactivity to the alkyne and the inhibition of its Lewis acid activity. The synthesis highlights for the first time the rational design of a catalytic system in order to promote a cycloisomerization reaction. Simple amines and pyridines failed to react due to their strong σ-donor characters that inhibit enyne coordination. On the other hand, the bisimine ligand **77**, which also failed to initiate the cycloisomerization reaction, is a weak σ-donor but a very good π-acceptor that might not stabilize adequately the palladium (+4) species in catalytic cycle. In sharp contrast, imines derived from ethylenediamine and carboxaldehydes including benzaldehyde, furfural, and isobutyraldehyde were proved to be effective ligands for this transformation, attributed to its stronger σ-donation character compared to complex **76**. Thus, reaction of **74** with palladium catalyst **76** provided the 1,4-diene product **75** in 79% yield after cycloisomerization/β-elimination sequence according to the mechanism discussed in Scheme 7.12.

Further elaboration on the oxidation states of diene bicycle **75** provided the divergent total synthesis of corianin (**78**), picrotoxinin (**79**), and picrotin (**80**) in less than half the number of steps previously reported.

### 7.3.2 Aromadendrane Sesquiterpenes: Epiglobulol

Aromadendranes are dimethylcyclopropane azulenes collectively named after the first isolated molecule of the family (+)-aromadendrane, found as a constituent of the essential oil of *Eucalyptus trees*. The occurrence of these sesquiterpenes in nature is high, with the higher plants essential oils to be their major sources. Some of the biological properties that have been reported for isolated aromadendranes include antifungal, antibacterial, antifeedant, and cytotoxic activities [75].

In 2006, Sato and coworkers discovered an efficient cycloisomerization of polyene aldehydes leading to the construction of 5–7 condensed carbocyclic systems resembling to natural aromadendrane motifs [76]. During their research on hydroacylation of dienals by Rh(I) catalysis, they found that the same catalyst was able to cycloisomerize 1,3-dienes and tethered alkenes to produce cyclopentene derivatives in good yields. Following their discovery, a cascade sequence combining both reaction was designed. Thus, when the appropriate 4,6,10,12-tetraeneal **81**, bearing gem disubstitution at position 9, was used as the starting material in reaction with $[Rh(dppe)]ClO_4$ catalyst, a sole product **82** was isolated in 44% yield (Scheme 7.53). Functional manipulations completed the total synthesis of *rac*-epiglobulol (**84**) from apoaromadendrone (**83**).

The reaction mechanism leading to advanced intermediate **85** starts with rhodium insertion into the aldehyde moiety. Rhodacycle formation follows to promote hydroacylation into the 4,6-diene providing cycloheptene compound **86**. Then, rhodium catalyze a highly regioselective cycloisomerization reaction on the resulting triene to produce the final product **87** (Scheme 7.54; please refer also to Scheme 7.51).

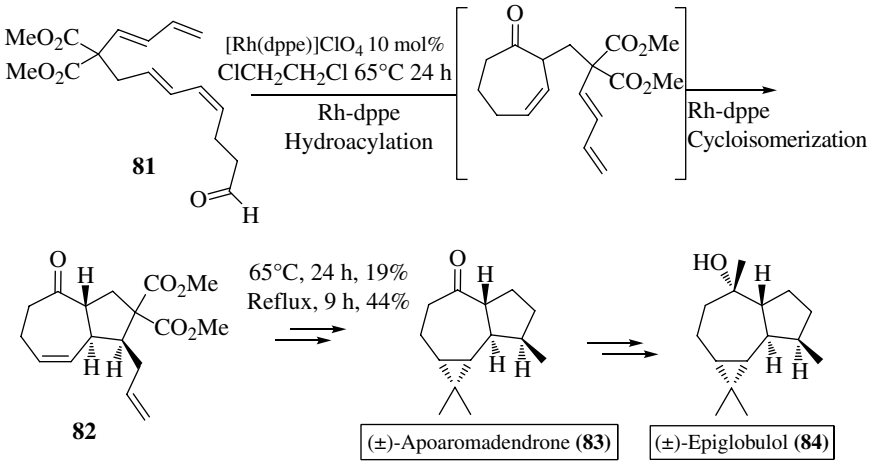
Interestingly, the reaction cascade fails to provide cycloisomerized products in the absence of the gem disubstitution in accordance with Trost's observations on Thorpe–Ingold effect as discussed in the previous subchapter.

Related tricyclic systems of guaiane sesquiterpenoids resembling the structure of globulol and epiglobulol have also been reported by Echavarren [77,78]. In his report, polyene propargylic alcohols are utilized to produce guaiane cores under gold catalysis (Scheme 7.55).

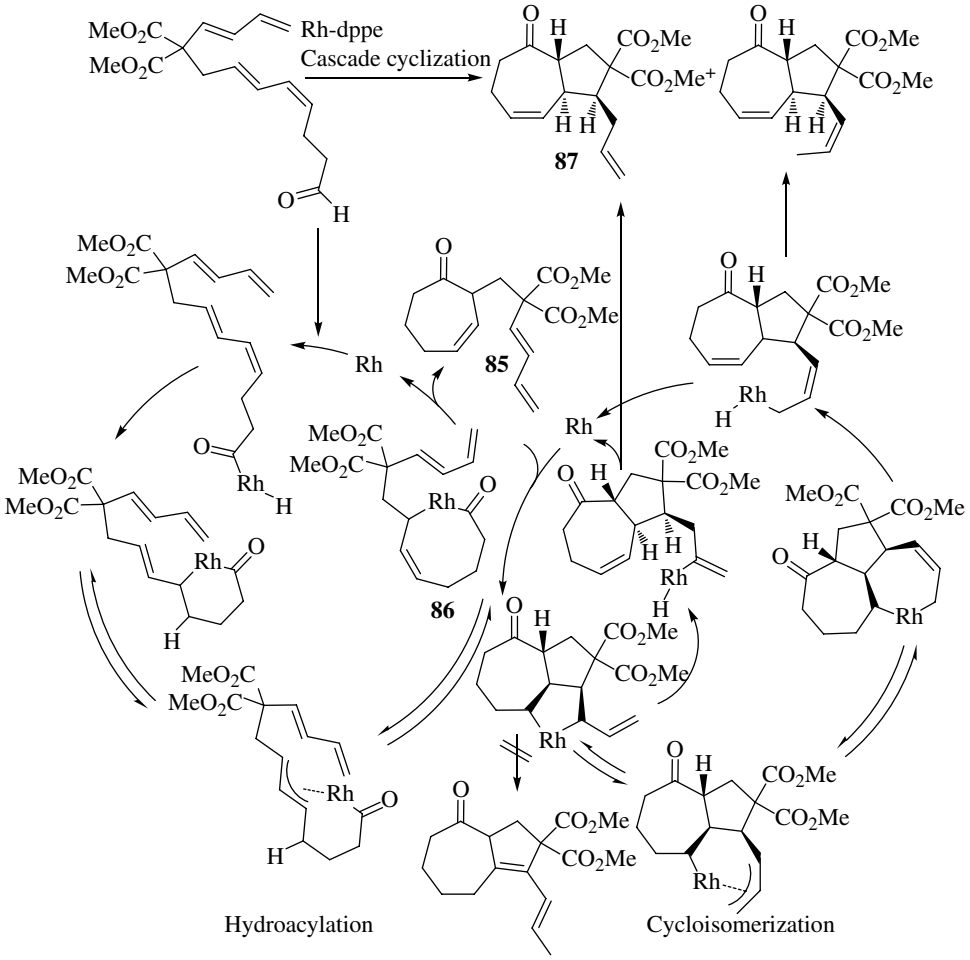
The reaction is believed to proceed through an initial cyclopropylcarbene intermediate **88**, followed by an intramolecular 1,5-migration of the –OR group according to Scheme 7.56.

### 7.3.3 Cubebol–Cubebenes Sesquiterpenes

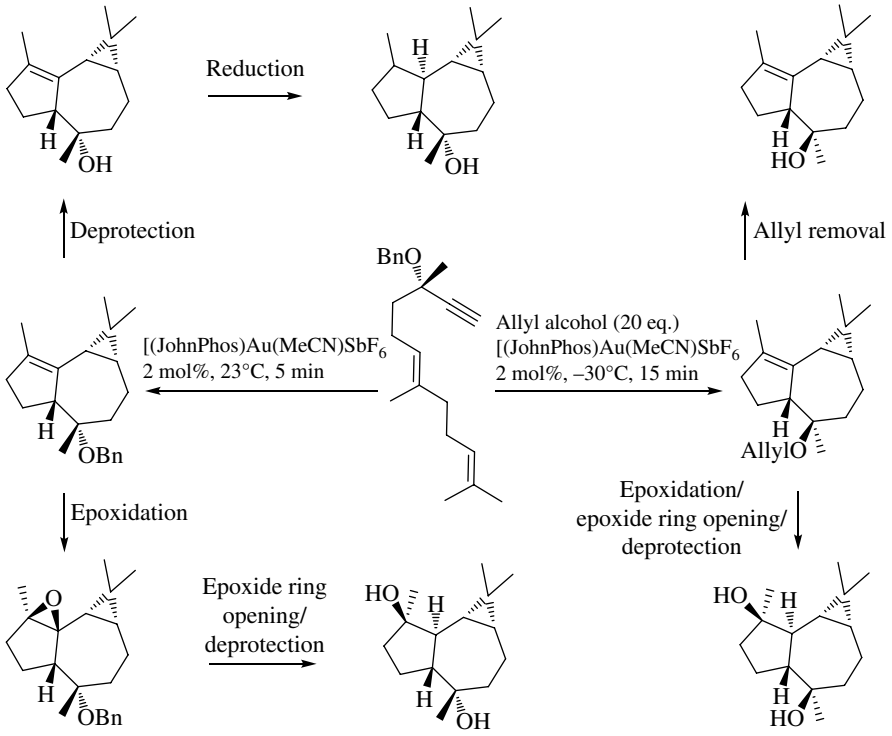
Cubebol (**91**), α-cubebene (**92**), and β-cubebene (**93**) are isolated from the berries of *Piper cubeba* [79]. Due to its pronounced cooling effects, cubebol was patented in 2001 as a refreshing agent for applications in various products ranging



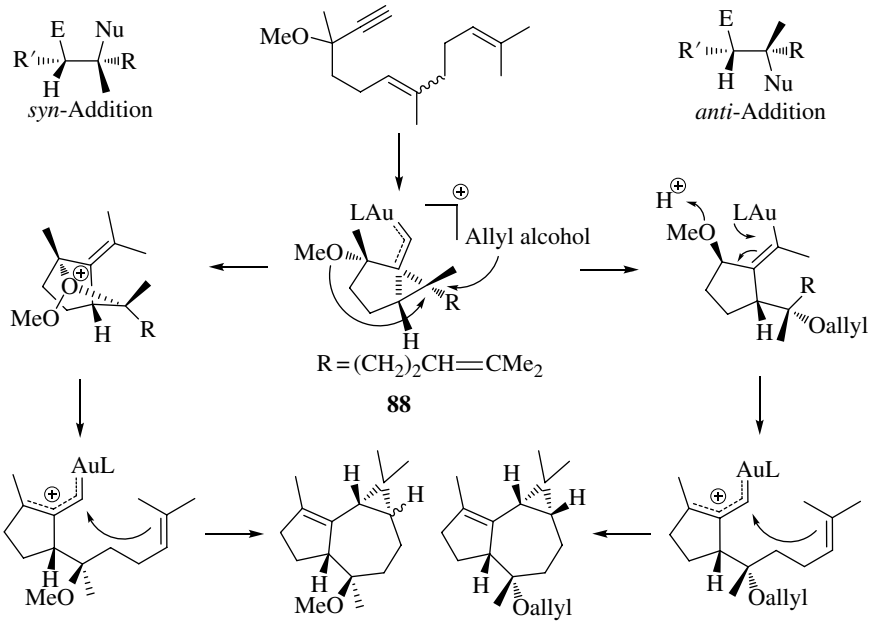

**SCHEME 7.53** Total synthesis of apoaromadendrone and epiglobulol.



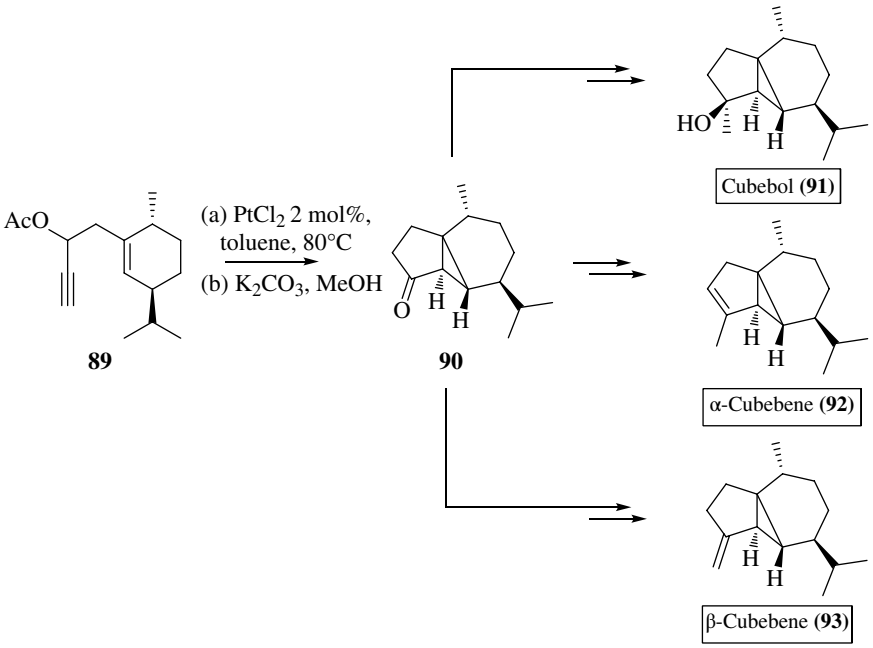

**SCHEME 7.54** Reaction mechanism of hydroacylation cycloisomerization of tetraenes.




**SCHEME 7.55** Cycloisomerization of polyene propargylic alcohols under gold catalysis.

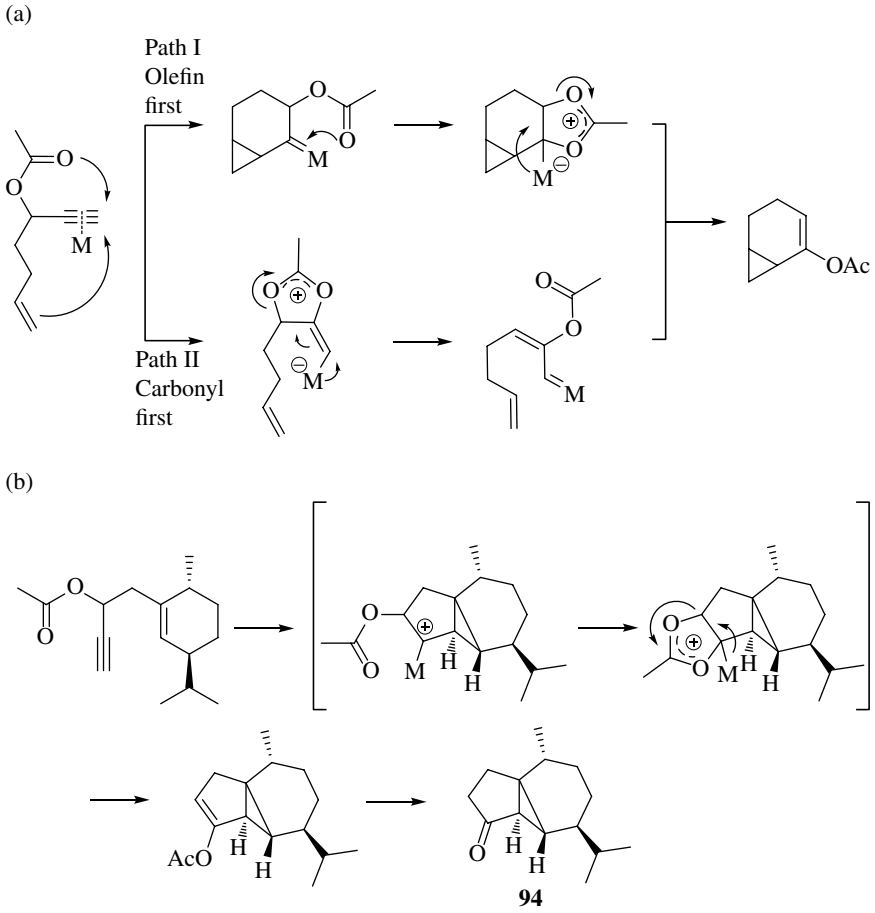



**SCHEME 7.56** Mechanism for the cycloisomerization of **88**.




**SCHEME 7.57** Key cycloisomerization reaction for the total synthesis of "cubebol natural products."

from chewing gum to sorbets, toothpastes, and so on [80]. In 2006, two groups were reported, independently, the total synthesis of cubebol and related natural products through the cycloisomerization of acetylenic esters by platinum, gold, and copper catalysis (Scheme 7.57) [81]. During their studies they found that compound **89** is able to cycloisomerize to **90**, an advanced common intermediate for the synthesis of an array of sesquiterpenoid natural products. Mechanistically the reaction invokes a metal alkyne activation/cyclopropanation reaction with a concomitant transposition of the acetyl ester. Such events are likely to take place through the two possible reaction pathways shown in Scheme 7.64. Although both of them retain the same propensity to form the cyclized product in computational studies [82], Fürstner and coworkers provided ample evidence for a prior cyclopropanation, later transposition sequence (Scheme 7.58b). His suggestion was based on the observed direct dependence of acetyl group absolute configuration to the diastereoselection of the



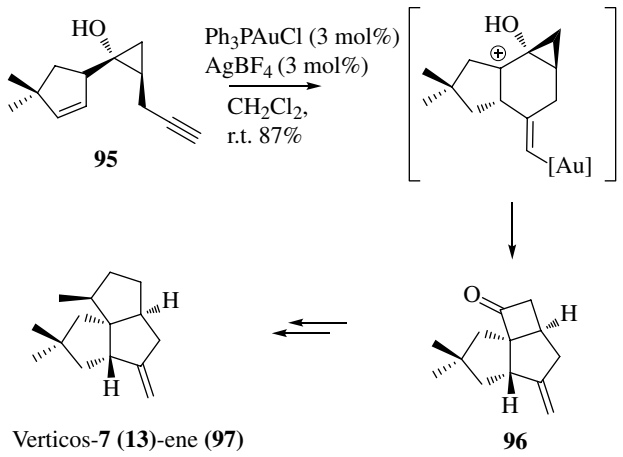

**SCHEME 7.58** (a) Mechanistic pathways for cycloisomerization reaction of acetylenic esters and (b) proposed mechanism for the synthesis of product **94**.

cycloisomerization reaction. A pathway involving prior transposition of the acetyl group would eventually loose chiral information leading to planar transition states implying that both isomers would lead to the same product distribution.

### 7.3.4 Ventricos-7(13)-ene

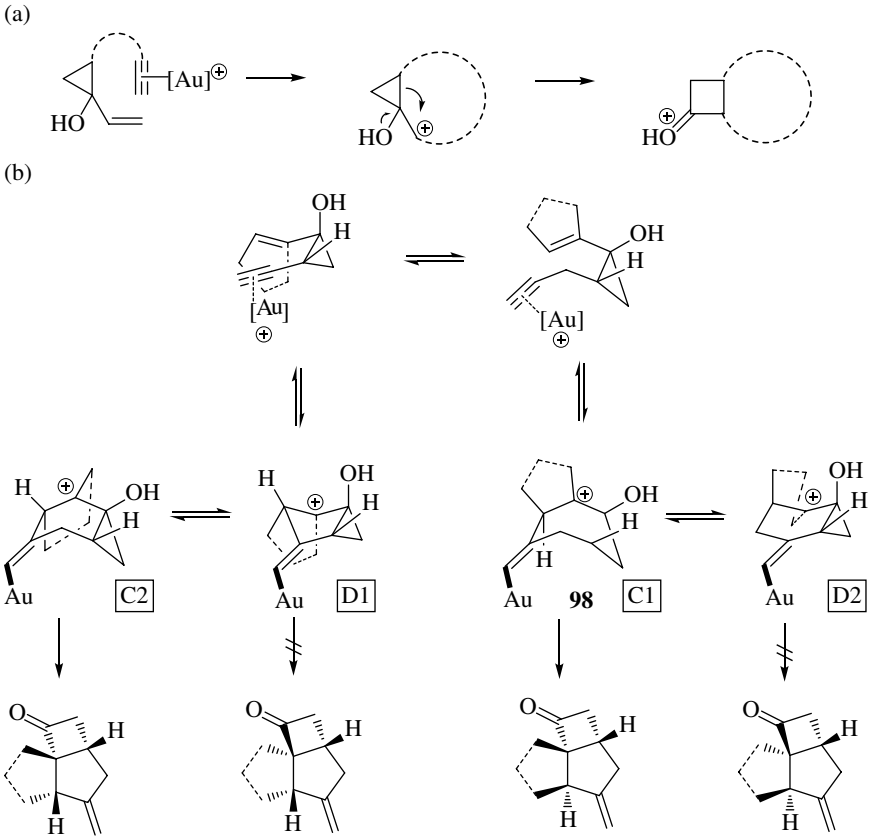
An intriguing cycloisomerization of an enyne bearing a cyclopropanol moiety was chosen by Toste and his group for the synthesis of ventricos-7(13)-ene sesquiterpene [83]. Ventricos-7(13)-ene belongs to the family of angular triquinane natural products and contains an unpresented rearranged pentalenene skeleton [84]. Toste relied his synthesis on the late expansion of a tricyclic condensed cyclobutane ring **96** to the corresponding triquinane skeleton of ventricosene (Scheme 7.59).

Key reaction for the production of cyclobutane **96** was the cycloisomerization of cyclopropyl enyne **95**. When **95** was allowed to react with catalytic amounts of $Ph_3PAuCl$ and $AgBF_4$, an 87% yield was isolated as a sole product. The reaction proceeds through a gold alkyne activation/cycloisomerization sequence followed by the ring expansion of the




**SCHEME 7.59** Synthetic route for the total synthesis of ventricos-7(13)-ene.

cyclopropane to provide cyclobutanone core (Scheme 7.60). Stereochemical rationalization allows the assumption of an initial cyclization through a two-boat conformers that leads to intermediates C1 or D1 (Scheme 7.60). A semipinacol shift




**SCHEME 7.60** (a) Mechanism and (b) stereochemical analysis of cyclopropanol cycloisomerization.

through conformer D1 and D2 does not occur due to the production of highly constrained *trans*-cyclobutanones. On the other hand, conformer C2 is also disfavored as the transition state would lead to high-energy *trans*-diquinane core. Thus, the high selectivity observed in the production of **97** is attributed to a selective semipinacol derived from intermediate **98**.

### 7.3.5 Englerins

Since the discovery of gold cycloisomerizations, Echavarren and his group are pioneering the field with an array of elegant studies (please refer to subchapter 7.2). In an attempt to utilize their gathered experience in the field, they reported the total synthesis of several tricyclic guaiane sesquiterpenoids. Among them, the synthesis of (+)-orientalol F, *rac*-pubinernoid B [85], and (-)-englerins A and B [86]. All of them were based on gold(I)-catalyzed [2+2+2] alkyne–alkene–carbonyl cycloaddition of 1,6-enynes bearing a carbonyl group.

Englerins A and B were isolated from the stem bark of the east African plant *Phyllanthus engleri* and have been shown to selectively inhibit the growth of renal cancer cell lines at the nanomolar level [87]. According to their synthesis, the unprotected enyne compound **99**, derived from geraniol, was allowed to react with catalyst $[IPrAuNCPh]SbF_6$ (3 mol %) at room temperature to produce the advanced intermediate **100** in 58% yield as a single diastereoisomer (Scheme 7.61). The cycloisomerization invokes the initial formation of a cyclopropyl carbene intermediate **101** followed by its intramolecular attack from the proximal carbonyl group to provide intermediate **102**. Further cyclization furnishes the core structure of englerins in a highly stereoselective fashion.

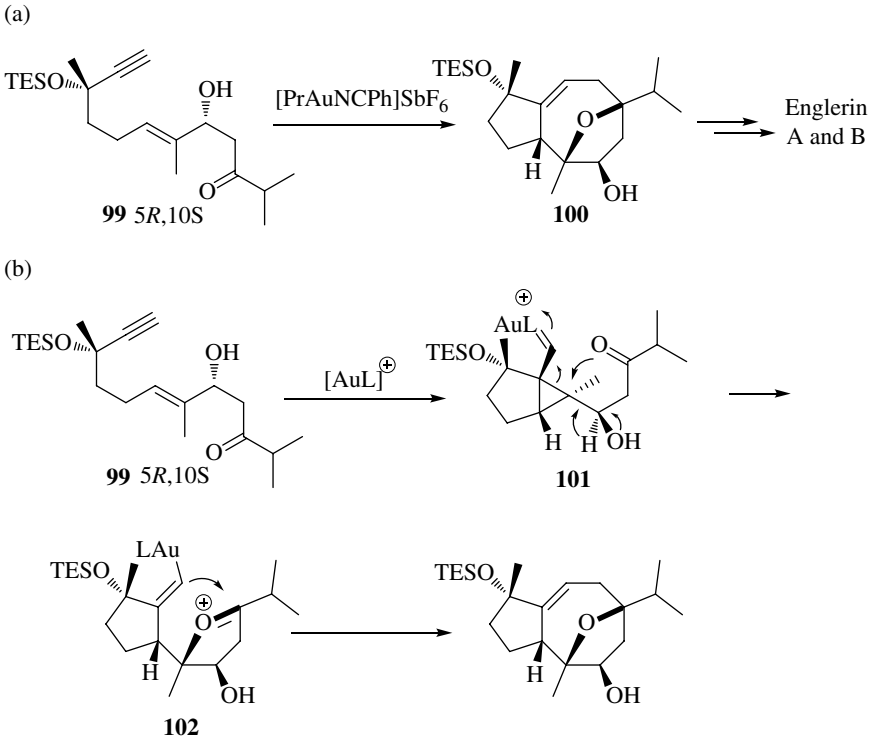
Interestingly, at the same period a closely related enyne has also been utilized by Prof. Ma's group to complete also the total synthesis of (−)-englerin A [88].

### 7.3.6 Echinopines

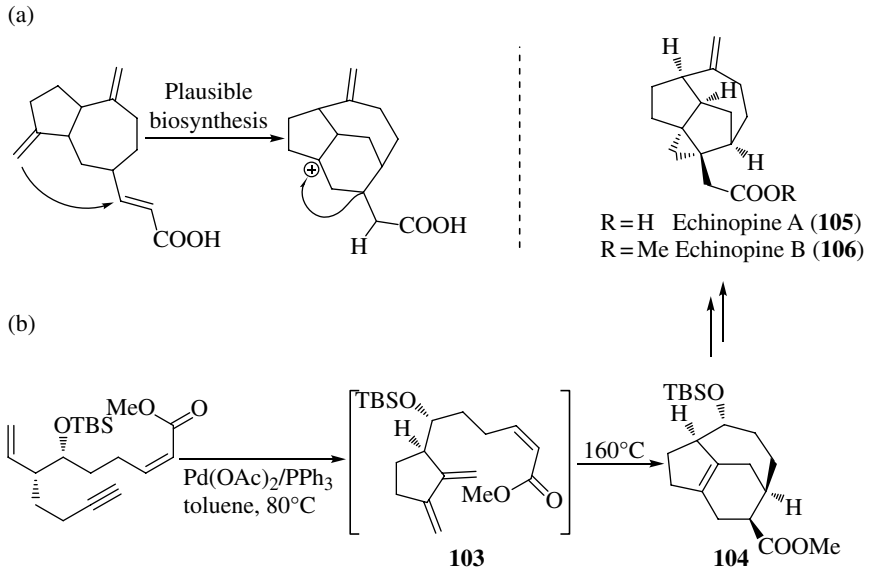
In 2008, Shi and coworkers reported the isolation and characterization of two unique sesquiterpenes, namely, echinopines A and B (**105** and **106**), with an unpresented structural core from the roots of *Echinops spinosus* [89]. Although not noted for their biological activity, their challenging molecular architectures provoked the interest of synthetic community and provided the ground for the development of unique cycloisomerization cascades.

Chen and coworkers [90] was the first to utilize a cycloisomerization reaction in order to access the postulated biosynthetically related intermediate **103**, which was later transformed to, the known by prior total syntheses [91], echnopines precursor **104** (Scheme 7.62)

With a cascade process in mind, Chen envisaged a transition metal-catalyzed cycloisomerization reaction,



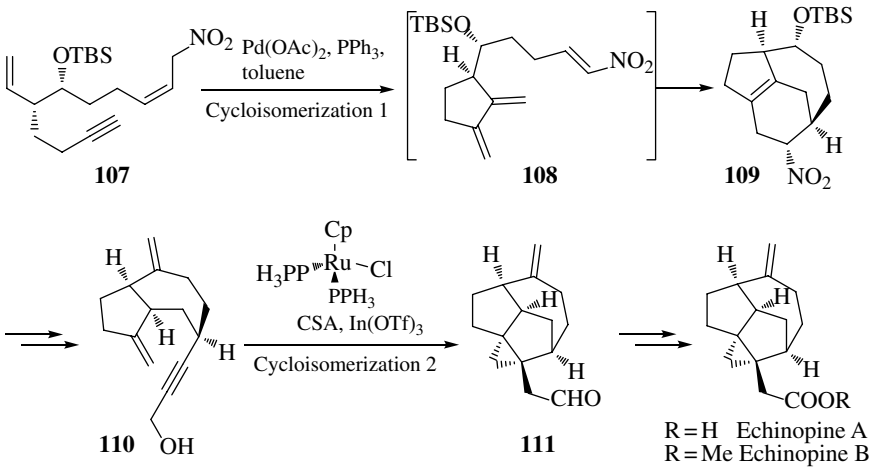

**SCHEME 7.61** (a) Key cycloisomerization of enyne **99** and (b) the postulated mechanism.



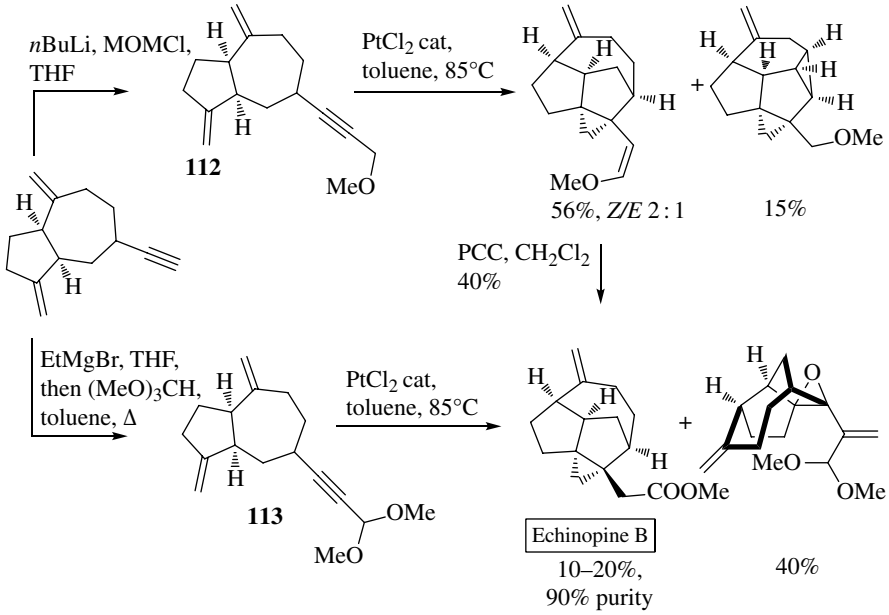

**SCHEME 7.62** (a) Proposed biosynthesis and (b) key reaction to the formal synthesis of echinopines A and B.

which would be followed by an intramolecular Diels–Alder reaction in the presence of the proximal dienophile upon generation of the transient diene **108**. Preparation of the acyclic substrate **107** was obtained through an asymmetric aldol reaction and functional group manipulation. Advanced intermediate **107** was subjected to $Pd(OAc)_2/PPh_3$-catalyzed cycloisomerization (toluene-80 °C) to provide cleanly diene **108**. Prolonged reaction times and higher temperature of the reaction (160 °C) led also to a subsequent intramolecular Diels–Alder reaction to furnish the designed tricycle **109** in 75% overall yield.

Few months later, the same group reported an optimized reaction sequence for the synthesis of echinopines A and B based on a related cascade transformation to **110**. Cascade product **110** was further elaborated into the postulated biosynthetic guaiane-type intermediate **111**, followed by a ruthenium-catalyzed cycloisomerization reaction to provide echinopines core (Scheme 7.63).




**SCHEME 7.63** Second-generation total synthesis of echinopines A and B by Chen et al.

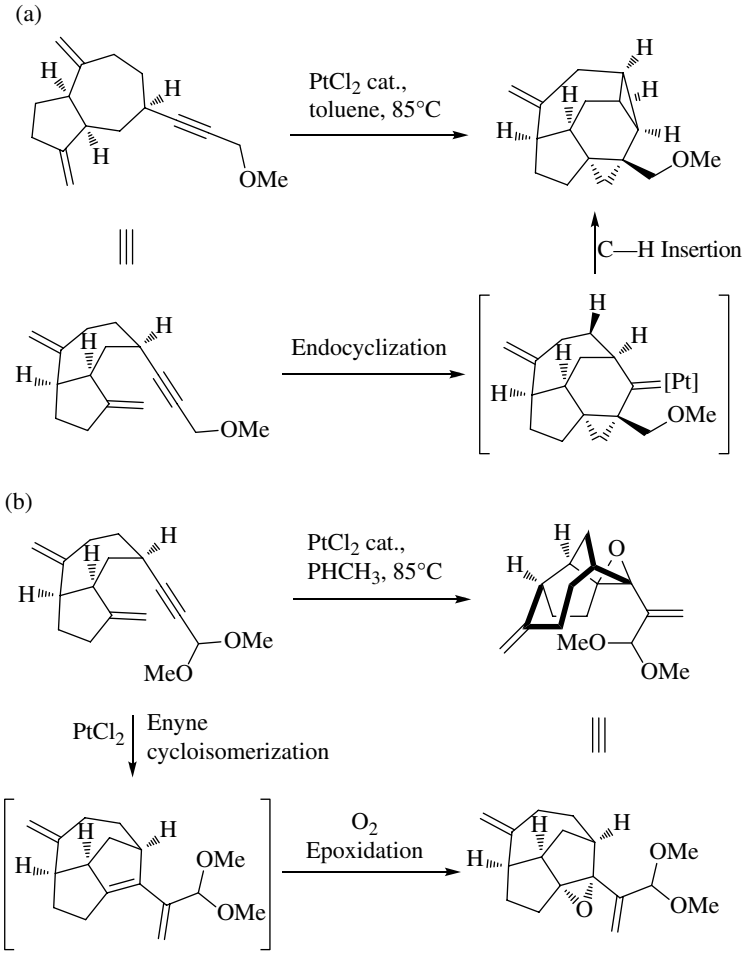



**SCHEME 7.64** Key stages for the first- and second-generation strategy for the total synthesis of echinopine B by Vanderwal et al.

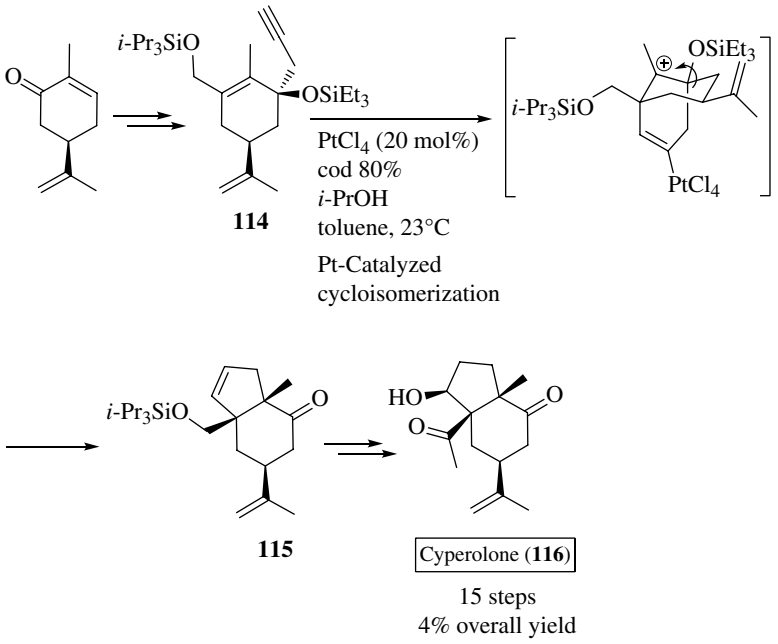
In 2012, Vanderwal group reported two strategies for the short synthesis of echinopine B, both relying on platinum-catalyzed cycloisomerization closely related to Chen synthesis enynes **112** and **113** (Scheme 7.64) [92]. In each case, the group isolated fair amounts of by-products attributed to the different cycloisomerization modes of platinum chloride reaction (Scheme 7.65).

### 7.3.7 Cyperolone

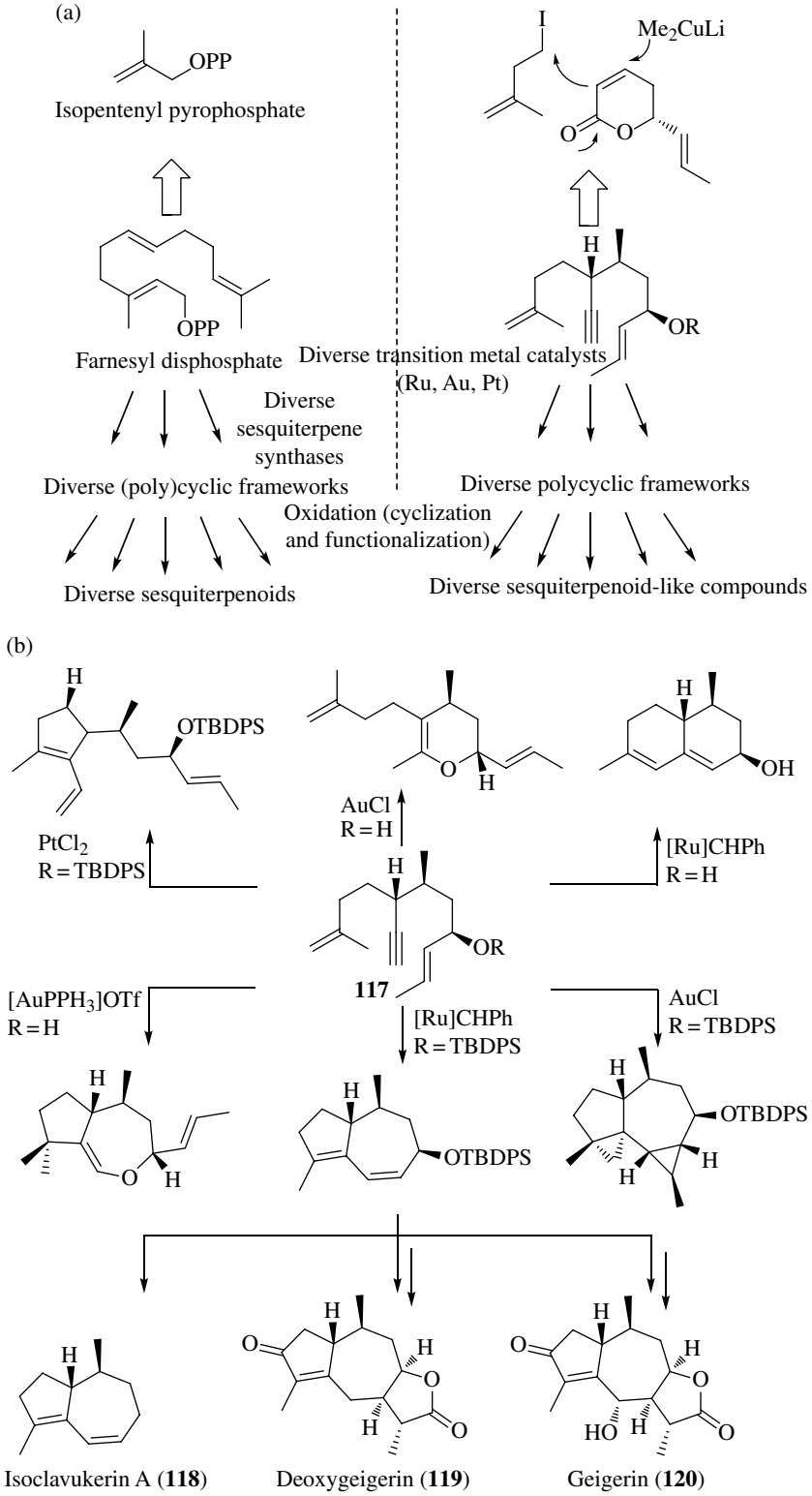
Cyperolone (**116**) was isolated from *Cyperus rotundus* and belongs to the rather abandoned class of cyperanes [93]. Cyperolone possess properties of plant growth inhibition [94] but its biological activity has not yet fully evaluated. The congested structure of cyperolone, which is characterized by a cis-fused bicyclo[4.3]nonane, was able to be prepared through a platinum-catalyzed cycloisomerization reaction of substrate **114**, followed by a pinacol-type shift [95]. Starting from (*R*)-carvone, Kirsch and his group reported the cycloisomerization of advanced intermediate **115**, either by $PtCl_2$ or $PtCl_4$ as precatalysts in the presence of substoichiometric amounts of cyclooctadiene, to provide up to 90% yield of compound **116**. The latter was readily transformed to the desired natural substances (Scheme 7.66).




**SCHEME 7.65** Reaction mechanism and formation of by-products in the synthesis of echinopines by Vanderwal et al. (a) for enyne **112** and (b) enyne **113**.




**SCHEME 7.66** Cycloisomerization/pinacol shift for the total synthesis of cyperolone.




**SCHEME 7.67** (a) The biomimetic logic for the production of diverse sesquiterpene scaffolds and (b) diversity in cycloisomerization reaction of enyne **117**.

### 7.3.8 Diverse Sesquiterpenoids

In 2012, Winssinger and coworkers presented an elegant approach for the synthesis of diverse structures of sesquiterpenoids based on catalyzed cycloisomerization of enynes [96]. Their concept is inspired by the logic of sesquiterpene biosynthesis and utilizes the cycloisomerization reaction as the point to induce the desired diversity. The appropriate enyne substrates are readily prepared by sequential alkylation events and subjected in various metal-catalyzed reactions. Depending on the metal an array of polycyclized products was selectively delivered as shown in Scheme 7.67. Still, although most of the prepared structures does not correspond to natural motifs, the group managed to synthesize by ruthenium catalysis compound **117**, which has been transformed to natural products isoclavukerin A (**118**), deoxygeigerin (**119**), and geigerin (**120**) after the appropriate adjustion of oxidation states.

## 7.4 CONCLUSION

The examples presented in this subchapter represent only a selected portion of the vast amount of literature publications highlighting the ability of cycloisomerization reactions to built structural diversity within the class of sesquiterpenoids. As the reaction mechanisms are refined and more things are currently known not only from palladium cycloisomerization chemistry but also from other unique pi-metals like gold and platinum, more impressive cascades are expected to flourish the chemical literature. Although cycloisomerization reaction is counting more than four decades from its concept discovery, we are convinced that it will still remain one of the best atom-economical methods for the construction of structurally complicated natural products as those contained in the unlimited sesquiterpene family.

## REFERENCES


1. Series of annual reviews by: B. M. Fraga, *Nat. Prod. Rep.* 2013, **30**, 1226–1264.
2. P.-H. Liang, T.-P. Ko, A. H.-J. Wang, *Eur. J. Biochem.* 2002, **269**, 3339–3354.
3. C. D. Poulter, H. C. Rilling, *Biochemistry* 1976, **15**, 1079–1083.
4. C. D. Poulter, H. C. Rilling, *Acc.Chem. Res.* 1978, **11**, 307–311.
5. L. C. Tarshis, M. Yan, C. D. Poulter, J. C. Sacchettini, *Biochemistry* 1994, **33**, 10871–10877.
6. L. C. Tarshis, P. J. Proteau, B. A. Kellogg, J. C. Sacchettini, C. D. Poulter, *Proc. Natl. Acad. Sci. U. S. A.* 1996, **93**, 15018–15023.
7. (a) M. C. Schulbach, P. J. Brennan, D. C. Crick, *J. Biol. Chem.* 2000, **275**, 22876–22881; (b) W. Wang, C. Dong, M. McNeil, D. Kaur, S. Mahapatra, D. C. Crick, J. H. Naismith, *J. Mol. Biol.* 2008, **381**, 129–240.
8. D. J. Millet, R. K. Allemann, *Nat. Prod. Rep.* 2012, **29**, 60–71.
9. C. M. Starks, K. Back, J. Chappel, J. P. Noel, *Science* 1997, **277**, 1815–1820.
10. C. A. Lesburg, G. Zhai, D. E. Cane, D. W. Christianson, *Science* 1997, **277**, 1820–1822.
11. M. J. Rynkiewicz, D. E. Cane, D. W. Christianson, *Proc. Natl. Acad. Sci. U. S. A.* 2001, **98**, 13543–13548.
12. D. W. Christianson, *Chem. Rev.* 2006, **106**, 3412–3442.
13. E. Y. Shishova, F. L. Yu, D. J. Miller, J. A. Faraldos, Y. X. Zhao, R. M. Coates, R. K. Allemann, D. E. Cane, D. W. Christianson, *J. Biol. Chem.* 2008, **283**, 15431–15439.
14. J. A. Aaron, X. Lin, D. E. Cane, D. W. Christianson, *Biochemistry* 2010, **49**, 1787–1797.
15. (a) B. H. B. Kwok, B. Koh, M. I. Ndubuisi, M. Elofsson, C. M. Crews, *Chem. Biol.* 2001, **8**, 759–766; (b) M. Li-Weber, K. Palfi, M. Giaisi, P. Krammer, *Cell Death Differ.* 2005, **12**, 408–409.
16. A. J. Steele, D. T. Jones, K. Ganeshaguru, V. M. Duke, B. C. Yogashangary, J. M. North, M. W. Lowdell, P. D. Kottaridis, A. B. Mehta, A. G. Prentice, A. V. Hoffbrand, R. G. Wickremasinghe, *Leukemia* 2006, **20**, 1073–1079.
17. A. Ghantous, H. Gali-Muhtasib, H. Vuorela, N. A. Saliba, N. Darwiche, *Drug Discov. Today* 2010, **15**, 668–678.
18. (a) M. Majdi, Q. Liu, G. Karimzadeh, M. A. Malboobi, J. Beekwilder, K. Cancar, R. de Vos, S. Todorovic, A. Simonovic, H. Bouwmeester, *Phytochemistry* 2011, **72**, 1739–1750; (b) J.-W. De Kraker, M. C. R. Franssen, M. C. Dalm, A. de Groot, H. J. Bouwmeester, *Plant Physiol.* 2001, **125**, 1930–1940; (c) J.-W. De Kraker, M. C. R. Franssen, M. C. Dalm, M. Joerink, A. de Groot, H. J. Bouwmeester, *Plant Physiol.* 2002, **129**, 257–268.
19. D. H. R. Barton, G. P. Moss, J. A. Whittle, *J. Chem. Soc.* 1968, **338**, 1813–1818.
20. (a) Y. Kijima, E. Ogunbunmni, S. Fleischer, *J. Biol. Chem.* 1991, **266**, 22912–22918; (b) J. Lytton, M. Westlin, M. R. Hanley, *J. Biol. Chem.* 1991, **266**, 17067–17071; (c) Y. Sagara, G. Inesi, *J. Biol. Chem.* 1991, **266**, 13503–13506.
21. (a) S. B. Christensen, I. K. Larsen, U. Rasmussen, *J. Org. Chem.* 1982, **47**, 649–652; (b) U. Rasmussen, S. B. Christensen, F. Sandberg, *Acta Pharm. Suec.* 1978, **15**, 133–140.
22. (a) T. Kuhn, Y. Wang, *Prog. Drug Res.* 2007, **65**, 385–422; (b) D. Chaturvedi, S. Goswami, P. P. Saikia, N. C. Barua, P. G. Rao, *Chem. Soc. Rev.* 2010, **39**, 435–454.
23. (a) H. N. ElSohly, E. M. Groom, F. S. El-Feraly, M. M. El-Sherei, *J. Nat. Prod.* 1990, **53**, 1560–1564; (b) A. Lapkin, P. Plucinski, M. Cutler, *J. Nat. Prod.* 2006, **69**, 1653–1664.
24. O. Rocha, K. Ansari, F. M. Doohan, *Food Addit. Contam.* 2005, **22**, 369–378.
25. C. H. Tam, W. Breitenstein, *The Biosynthesis of Mycotoxins: A study of secondary metabolism* P. S. Steyn (ed.), "The Biosynthesis of Trichothecene Mycotoxins" Academic Press (London), 1980, pp. 69–101.
26. For comprehensive reviews on cycloisomerization reactions please refer to: (a) Y. Yamamoto, *Chem. Rev.* 2012, **112**, 4736–4769; (b) I. D. G. Watson, F. D. Toste, *Chem. Sci.* 2012, **3**,

2899–2919; (c) V. Michelet, P. Y. Toullec, J.-P. Genet, *Angew. Chem. Int. Ed.* 2008, **47**, 4268–4315; (d) A. Fürstner, *Chem. Soc. Rev.* 2009, **38**, 3208–3221.

27. (a) X. Chen, K. M. Eagle, D. H. Wang, J. Q. Yu, *Angew. Chem. Int. Ed.* 2009, **48**, 5094–5115; (b) J. Yamaguchi, A. D. Yamaguchi, K. Itami, *Angew. Chem. Int. Ed.* 2012, **51**, 8960–9009.
28. K. Alder, F. Pascher, A. Schmitz, *Ber. Dtsch. Chem. Ges. B* 1943, **76**, 27–53.
29. B. M. Trost, M. Lautens, *J. Am. Chem. Soc.* 1985, **107**, 1781–1783.
30. C. Aubert, O. Buisine, M. Malacria *Chem. Rev.* 2002, **102**, 813–834.
31. B. M. Trost, D. L. Romero, F. Rise, *J. Am. Chem. Soc.* 1994, **116**, 4268–4278.
32. (a) B. M. Trost, G. J. Tanoury, M. Lautens, C. Chan, D. T. MacPherson, *J. Am. Chem. Soc.* 1994, **116**, 4255–4267; (b) B. M. Trost, D. L. Romero, F. Rise, *J. Am. Chem. Soc.* 1994, **116**, 4268–4278.
33. (a) B. M. Trost, M. Lautens, C. Chan, D. J. Jebaratnam, T. Mueller, *J. Am. Chem. Soc.* 1991, **113**, 636–644; (b) B. M. Trost, P. A. Hipskind, J. Y. L. Chung, C. Chan, *Angew. Chem. Int. Ed. Engl.*. 1989, **28**, 1502–1504.
34. B. M. Trost, O. J. Gelling, *Tetrahedron Lett.* 1993, **34**, 8233–8236.
35. B. M. Trost, D. C. Lee, F. Rise, *Tetrahedron Lett.* 1989, **30**, 651–654.
36. G. L. Hamilton, E. J. Kang, M. Mba, F. D. Toste, *Science* 2007, **317**, 496–499.
37. (a) M. Hatano, M. Terada, K. Mikami, *Angew. Chem. Int. Ed.* 2001, **40**, 249–253; (b) K. Mikami, M. Hatano, *Proc. Natl. Acad. Sci. U. S. A.* 2004, **101**, 5767–5769.
38. M. Hatano, K. Mikami, *J. Am. Chem. Soc.* 2003, **125**, 4704–4705.
39. (a) P. Cao, X. Zhang, *Angew. Chem. Int. Ed.* 2000, **39**, 4104–4106; (b) A. Lei, M. He, S. Wu, X. Zhang, *Angew. Chem. Int. Ed.* 2002, **41**, 3457–3459; (c) E. G. Corkum, M. J. Hass, A. D. Sullivan, S. H. Bergens, *Org. Lett.* 2011, **13**, 3522–3525; (d) K. Mikami, S. Kataoka, K. Aikawa, *Org. Lett.* 2005, **7**, 5777–5780; (e) K. Mikami, S. Kataoka, Y. Yusa, K. Aikawa, *Org. Lett.* 2004, **6**, 3699–3701; (f) R. Okamoto, E. Okazaki, K. Noguchi, K. Tanaka, *Org. Lett.* 2011, **13**, 4894–4897; (g) A. Lei, M. He, X. Zhang, *J. Am. Chem. Soc.* 2002, **124**, 8198–8199.
40. (a) K. C. Nicolaou, A. Li, S. P. Ellery, D. J. Edmonds, *Angew. Chem. Int. Ed.* 2009, **48**, 6293–6295; (b) K. C. Nicolaou, D. J. Edmonds, A. Li, G. S. Tria, *Angew. Chem. Int. Ed.* 2007, **46**, 3942–3945; (c) K. C. Nicolaou, A. Li, D. J. Edmonds, *Angew. Chem. Int. Ed.* 2006, **45**, 7086–7090.
41. H. Chakrapani, C. Liu, R. A. Widenhoefer, *Org. Lett.* 2003, **5**, 157–159.
42. H.-Y. Jang, M. J. Krische, *J. Am. Chem. Soc.* 2004, **126**, 7875–7880.
43. B. M. Trost, V. K. Chang, *Synthesis* 1993, 824–832.
44. B. M. Trost, M. K. Trost, *J. Am. Chem. Soc.* 1991, **113**, 1850–1852.
45. B. M. Trost, M. Yanai, K. Hoogsteen, *J. Am. Chem. Soc.* 1993, **115**, 5294–5295.
46. B. M. Trost, M. K. Trost, *Tetrahedron Lett.* 1991, **32**, 3647–3650.
47. M. Trost, B. A. Czeskis, *Tetrahedron Lett.* 1994, **35**, 211–214.
48. N. Chatani, N. Furukawa, H. Sakurai, S. Murai, *Organometallics* 1996, **15**, 901–903.
49. N. Chatani, K. Kataoka, S. Murai, N. Furukawa, Y. Seki, *J. Am. Chem. Soc.* 1998, **120**, 9104–9105.
50. (a) C. Nieto-Oberhuber, M. P. Muñoz, E. Buñuel, C. Nevado, D. J. Cardenas, A. M. Echavarren, *Angew. Chem. Int. Ed.* 2004, **43**, 2402–2406; (b) C. Nevado, C. Ferrer, A. M. Echavarren, *Org. Lett.* 2004, **6**, 3191–3194.
51. (a) V. Mamane, T. Gress, H. Krause, A. Furstner, *J. Am. Chem. Soc.* 2004, **126**, 8654–8655; (b) M. R. Luzung, J. P. Markham, F. D. Toste, *J. Am. Chem. Soc.* 2004, **126**, 10858–10859.
52. E. Jiménez-Nuñez, C. K. Claverie, C. Nieto-Oberhuber, A. M. Echavarren, *Angew. Chem. Int. Ed.* 2006, **45**, 5452–5455.
53. C.-M. Chao, M. R. Vitale, P. Y. Toullec, J.-P. Genêt, V. Michelet, *Chem. Eur. J.* 2009, **15**, 1319–1323.
54. C.-M. Chao, D. Beltrami, P. Y. Toullec, V. Michelet, *Chem. Commun.* 2009, 6988–6990.
55. (a) H. Teller, A. Fürstner, *Chem. Eur. J.* 2011, **17**, 7764–7767; (b) N. M. Deschamps, V. I. Elitzin, B. Liu, M. B. Mitchell, M. J. Sharp, E. A. Tabet, *J. Org. Chem.* 2011, **76**, 712–715.
56. I. D. G. Watson, S. Ritter, F. D. Toste, *J. Am. Chem. Soc.* 2009, **131**, 2056–2057.
57. (a) B. Bogdanović, B. Henc, H.-G. Karmann, H.-G. Nüssel, D. Walter, G. Wilke, *Ind. Eng. Chem.* 1970, **62**, 34–41; (b) B. Bogdanović, *Adv. Organomet. Chem.* 1979, **17**, 105.
58. E. Schmitz, U. Heuck, D. Habisch, *J. Prakt. Chem.* 1976, **318**, 471.
59. R. Grigg, J. F. Malone, T. R. B. Mitchell, A. Ramasubbu, R. M. Scott, *J. Chem. Soc. Perkin Trans.* 1984, **1**, 1745–1750.
60. (a) C. Böing, G. Franciò, W. Leitner, *Chem. Commun.* 2005, 1456–1458; (b) C. J. Diez-Holz, C. Böing, G. Franciò, M. Hölscher, W. Leitner, *Eur. J. Org. Chem.* 2007, 2995–3002.
61. A. Bright, J. F. Malone, J. K. Nicholson, J. Powell, B. L. Shaw, *J. Chem. Soc. Chem. Commun.* 1971, 712–714.
62. (a) P. Kisanga, L. A. Goj, R. A. Widenhoefer, *J. Org. Chem.* 2001, **66**, 635–637; (b) L. A. Goj, R. A. Widenhoefer, *J. Am. Chem. Soc.* 2001, **123**, 11133–11147; (c) L. A. Goj, G. A. Cisneros, W. Yang, R. A. Widenhoefer, *J. Organomet. Chem.* 2003, **687**, 498–507; (d) L. A. Goj, G. A. Cisneros, W. Yang, R. A. Widenhoefer, *J. Organomet. Chem.* 2004, **689**, 2845–2849.
63. (a) K. L. Bray, J. P. H. Charmant, I. J. S. Fairlamb, G. C. Lloyd-Jones, *Chem. Eur. J.* 2001, **7**, 4205–4215; (b) K. L. Bray, G. C. Lloyd-Jones, *Eur. J. Org. Chem.* 2001, 1635–1642.
64. (a) R. A. Widenhoefer, N. S. Perch, *Org. Lett.* 1999, **1**, 1103–1105; (b) P. Kisanga, R. A. Widenhoefer, *J. Am. Chem. Soc.* 2000, **122**, 10017–10026.
65. (a) C. H. Oh, J. D. Kim, J. W. Han, *Chem. Lett.* 2001, 1290–1291; (b) Y.-J. Song, I. G. Jung, H. Lee, Y. T. Lee, Y. K. Chung, H.-Y. Jang, *Tetrahedron Lett.* 2007, **48**, 6142–6146.

66. A. Heumann, M. Moukhliss, *Synlett* 1998, 1211–1213.
67. W. D. Kerber, J. H. Koh, M. R. Gagné, *Org. Lett.* 2004, **6**, 3013–3015.
68. (a) J. M. Takacs, L. G. Anderson, *J. Am. Chem. Soc.* 1987, **109**, 2200–2202; (b) J. M. Takacs, Y.-C. Myoung, L. G. Anderson, *J. Org. Chem.* 1994, **59**, 6928–6942.
69. (a) J. M. Takacs, L. G. Anderson, M. W. Creswell, B. E. Takacs, *Tetrahedron Lett.* 1987, **28**, 5627–5630; (b) B. E. Takacs, J. M. Takacs, *Tetrahedron Lett.* 1990, **31**, 2865–2868.
70. (a) J. M. Takacs, Y. C. Myoung, *Tetrahedron Lett.* 1992, **33**, 317–320; (b) J. M. Takacs, S. C. Boito, *Tetrahedron Lett.* 1995, **36**, 2941–2944; (c) J. M. Takacs, S. Vayalakkada, S. J. Mehrman, C. L. Kingsbury, *Tetrahedron Lett.* 2002, **43**, 8417–8420.
71. (a) B. M. Trost, C. D. Haffner, D. J. Jebaratnam, M. J. Krische, A. P. Thomas, *J. Am. Chem. Soc.* 1999, **121**, 6183–6192; (b) B. M. Trost, M. J. Krische, *J. Am. Chem. Soc.* 1999, **121**, 6131–6141.
72. (a) H. Conroy, *J. Am. Chem. Soc*. 1951, **73**, 1889–1891; (b) H. Conroy, *J. Am. Chem. Soc.* 1952, **74**, 491–498; (c) H. Conroy, *J. Am. Chem. Soc*. 1952, **74**, 3046–3051; (d) H. Conroy, *J. Am. Chem. Soc*. 1957, **79**, 1726–1733; (e) H. Conroy, *J. Am. Chem. Soc.* 1957, **79**, 5550–5553.
73. M. K. Ticku, T. P. Burch, W. Davis, *Adv. Biochem. Psychopharmacol.* 1981, **29**, 411–414.
74. A. Nistri, A. Constanti, *Progress in Neurobiology*; Pergamon: New York, 1979; Vol. **13**, 117–235.
75. (a) I. C. Moreira, G. J. H. Lago, M. M. C. Young, F. N. Roque, *J. Braz. Chem. Soc.* 2003, **14**, 828–831; (b) C. Gaspar-Marques, M. F. Simoes, B. Rodriguez, *J. Nat. Prod.* 2004, **67**, 614–621; (c) A. Messer, K. McCormick, H. Sunjaya, H. H. Hagedorn, F. J. Tumbel, Meinwald, J., *J. Chem. Ecol.* 1990, **16**, 3333–3352; (d) Z. Su, S. Yin, Z. Zhou, Y. Wu, J. Ding, J. Yue, *J. Nat. Prod.* 2008, **71**, 1410–1413.
76. Y. Oonishi, A. Taniuchi, M. Mori, Y. Sato, *Tetrahedron Lett.* 2006, **47**, 5617–5621.
77. E. Jiménez-Nunez, M. Raducan, T. Lauterbach, K. Molawi, C. R. Solorio, A. M. Echavarren, *Angew. Chem. Int. Ed.* 2009, **48**, 6152–6155.
78. J. Carreras, M. Livendahl, P. R. McGonical, A. M. Echavarren, *Angew. Chem. Int. Ed.* 2014, **53**, 4896–4899.
79. (a) F. Vanasek, V. Herout, F. Sorm, *Collect. Czechoslov. Chem. Commun.* 1960, **56**, 919–923; (b) Y. Ohta, K. Ohara, Y. Hirose, *Tetrahedron Lett.* 1968, **9**, 4181–4184 and references therein.
80. M. I. Velazco, L. Wuensche, P. Deladoey (Firmenich SA), US 6214788 (prior. March 31, 1999), 1999; [Chem. Abstr. 2000, 133, 265959].
81. (a) A. Fürstner, P. Hannen, *Chem. Eur. J.* 2006, **12**, 3006–3019; (b) C. Fehr, J. Galindo, *Angew. Chem. Int. Ed.* 2006, **45**, 2901–2904.
82. E. Soriano, P. Ballesteros, J. Marco-Contelles, *Organometallics* 2005, **24**, 3182–3191.
83. S. G. Sethofer, S. T. Staben, O. Y. Hung, F. D. Toste, *Org. Lett.* 2008, **10**, 4315–4318.
84. R. Lu, C. Paul, S. Basar, W. A. König, *Tetrahedron Asymmetry* 2005, **16**, 883–887.
85. E. Jiménez-Nunez, K. Molawi, A. M. Echavarren, *Chem. Commun.* 2009, 7327–7329.
86. K. Molawi, N. Delpont, A. M. Echavarren, *Angew. Chem. Int. Ed.* 2010, **49**, 3517–3519.
87. R. Ratnayake, D. Covell, T. T. Ransom, K. R. Gustafson, J. A. Beutler, *Org. Lett.* 2009, **11**, 57–60.
88. Q. Zhou, X. Chen, D. Ma, *Angew. Chem. Int. Ed.* 2010, **49**, 3513–3516.
89. M. Dong, B. Cong, S.-H. Yu, F. Sauriol, C.-H. Huo, Q.-W. Shi, Y.-C. Gu, L. O. Zamir, H. Kiyota, *Org. Lett.* 2008, **10**, 701–704.
90. P. A. Peixoto, R. Severin, C.-C. Tseng, D. Y.-K. Chen, *Angew. Chem. Int. Ed.* 2011, **50**, 3013–3016.
91. (a) T. Magauer, J. Mulzer, K. Tiefenbacher, *Org. Lett.* 2009, **11**, 5306–5309; (b) K. C. Nicolaou, H. Ding, J.-A. Richard, D. Y.-K. Chen, *J. Am. Chem. Soc.* 2010, **132**, 3815–3818.
92. T. D. Michels, M. S. Dowling, C. D. Vanderwal, *Angew. Chem. Int. Ed.* 2012, **51**, 7572–7576.
93. (a) H. Hikino, K. Aota, Y. Maebayashi; T. Takemoto, *Chem. Pharm. Bull.* 1966, **14**, 1439–1441.
94. K. Komai, N. Seto, K. Matsubayashi, M. Hamada, *Zasso Kenkyu (Weed Res. Jp.)* 1990, **35**, 164–168.
95. P. Klahn, A. Duschek, C. Liébert S. F. Kirsch, *Org. Lett.* 2012, **14**, 1250–1253.
96. G. Valot, J. Garcia, V. Duplan, C. Serba, S. Barluenga, N. Winssinger, *Angew. Chem. Int. Ed.* 2012, **51**, 5391–5394.

# 8

# DITERPENES

LOUIS BARRIAULT
*Department of Chemistry, University of Ottawa, Ottawa, Ontario, Canada*

## 8.1 INTRODUCTION

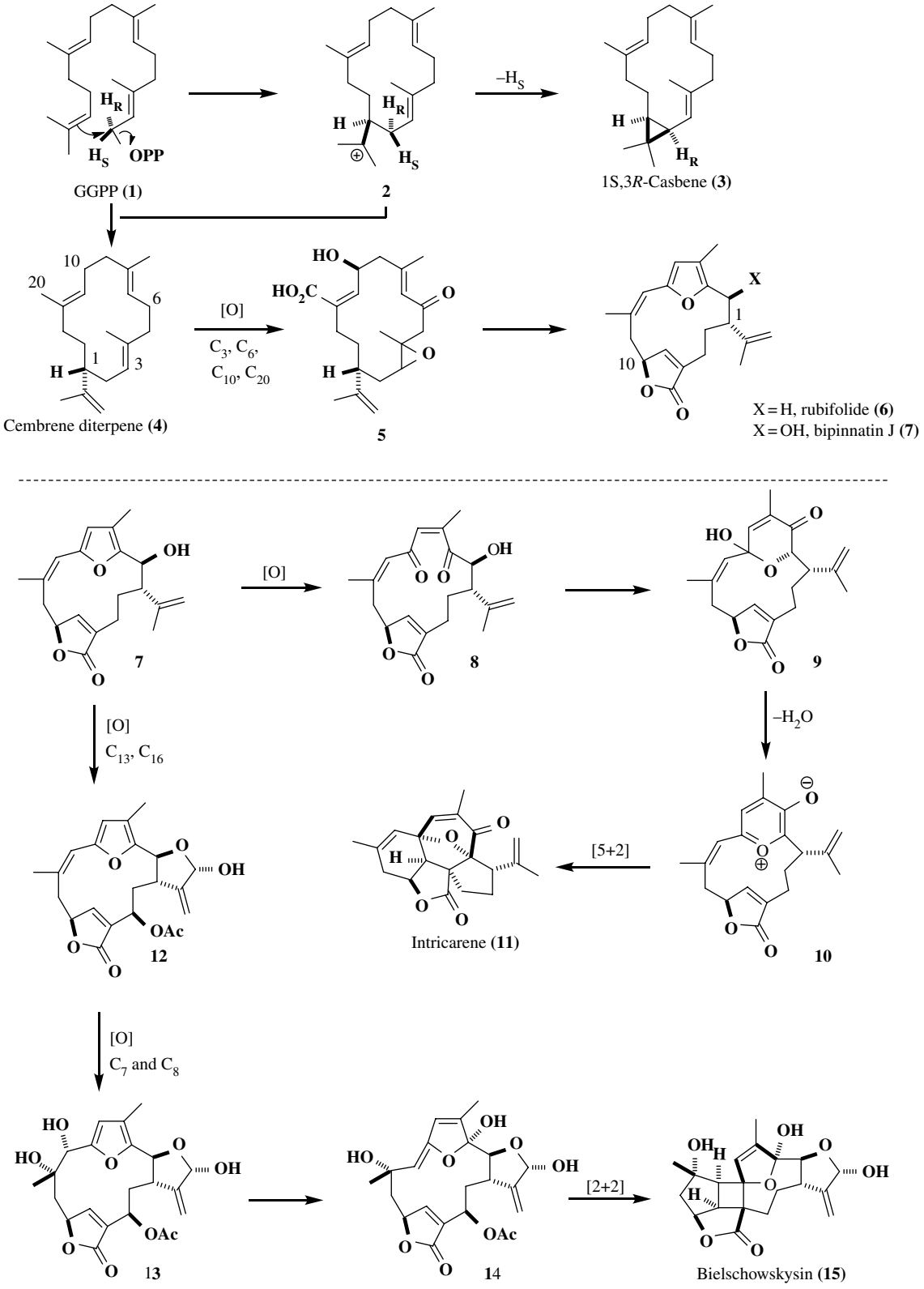
Diterpenes are among the most abundant terpenoids on the planet. Although significant advancements have been made, the biosynthesis of diterpenes is not fully elucidated. In this chapter, a general overview of the biosynthesis of diterpenes and selected applications of pericyclic reactions for the synthesis of complex diterpenes will be presented.

## 8.2 BIOSYNTHESIS OF DITERPENES BASED ON CATIONIC CYCLIZATIONS, 1,2-SHIFTS, AND TRANSANNULAR PROCESSES

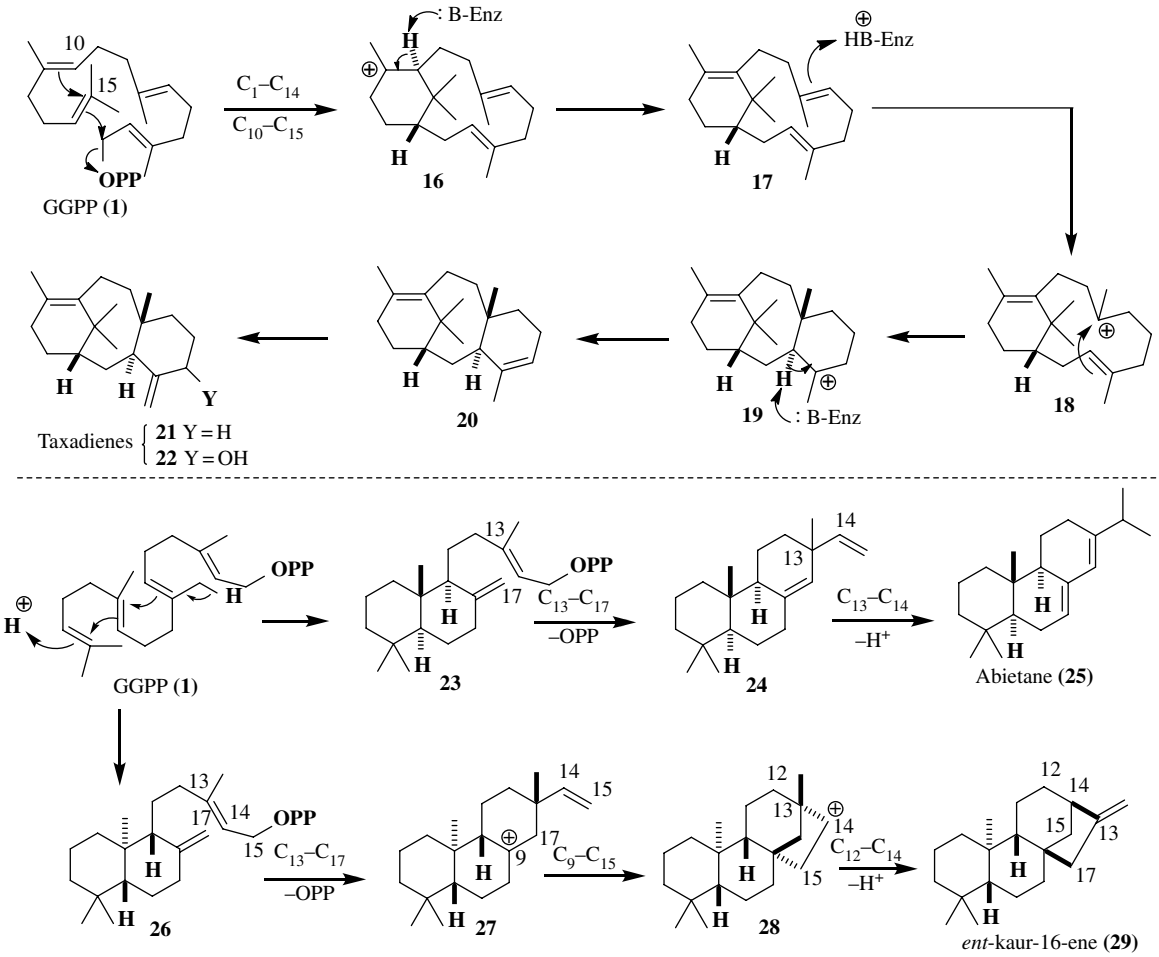
Natural diterpenes are a great basin of compounds having significant biological activities where many of these compounds found useful applications in pharmaceutical and agrochemical sectors. Diterpenoid frameworks contain four isoprene units, which are stitched together to generate a wide array of polycyclic structures. Their formation can be rationalized through the different types of cyclization of geranylgeranyl diphosphate (GGPP) catalyzed by enzymes (cyclase) (Scheme 8.1) [1]. To date, four cyclase enzymes such as casbene, taxadiene, *ent*-copalyl diphosphate, and abietane synthases have been identified, sequenced, and cloned. The formation of (1*S*,3*R*)-casbene **3** is the product of a casbene synthase-catalyzed cyclization of GGPP **1** via an ionization process [2]. One can also envisage the formation of cembranoid **4** through a common cationic cyclic intermediate **2**. Cembranoids are 14-membered macrocyle ring, which are adorned with a variety of oxidation patterns. Probably the most abundant cembranoids possess furan and butenolide moieties such as rubifolide (**6**) and bipinnatin J (**7**). These natural products are the results of site-specific enzymatic oxidation on the cembranoid framework [3]. One can suggest that a higher oxidation state macrocycle such as 5 could be derived into **6** and **7**. It is believed that more complex diterpenes could be obtained from these cembranoids via *in vivo* transannular processes. Independent work from Trauner [4] and Pattenden [5] shows intricarene (**11**) could be biogenetically linked to **7**. Their premises involve the oxidation of furan moiety in **7** to give dienone **8**, which is then converted to hemiketal **9**. After elimination of water, oxidopyrylium **10** undergoes a spontaneous transannular [5+2] reaction to provide intricarene **11**. Other diterpenes, such as bielschowskysin (**15**), could be obtained from a series of oxidations at **7** to give **14**, which can undergo a light-mediated [2+2] transannular cycloaddition to deliver **15** [2, 6]. Clearly, the idea of transannular cycloadditions in the biogenesis of diterpenes is an exciting one and will be discussed later in the chapter.

A series of ionization and proton-induced cyclizations **16** → **20** catalyzed by the taxadiene synthase convert GGPP **1** into the taxadienes **21** and **22** for *en route* synthesis of biological important natural products such as taxol and analogs (Scheme 8.2) [7]. Abietanes and kauranes are important classes of diterpenes. In the presence of abietadiene synthase, **1** undergoes a proton-induced cascade cyclization to produce the copalyl diphosphate intermediate **23** (Scheme 8.2) [8]. The latter is converted to **24** via an ionic cyclization and then to **25** through a methyl 1,2-shift between C13 and C14 [9]. In contrast, diterpene *ent*-kaur-16-ene **29** is not formed via the same cyclase enzyme. Consequently, it was proposed that two enzymes, *ent*-copalyl diphosphate and *ent*-kaurene

*From Biosynthesis to Total Synthesis: Strategies and Tactics for Natural Products*, First Edition. Edited by Alexandros L. Zografos.
© 2016 John Wiley & Sons, Inc. Published 2016 by John Wiley & Sons, Inc.




**SCHEME 8.1** Biosyntheses of casbene and cembrane and postulated biosyntheses of some complex members of deterpenoids.

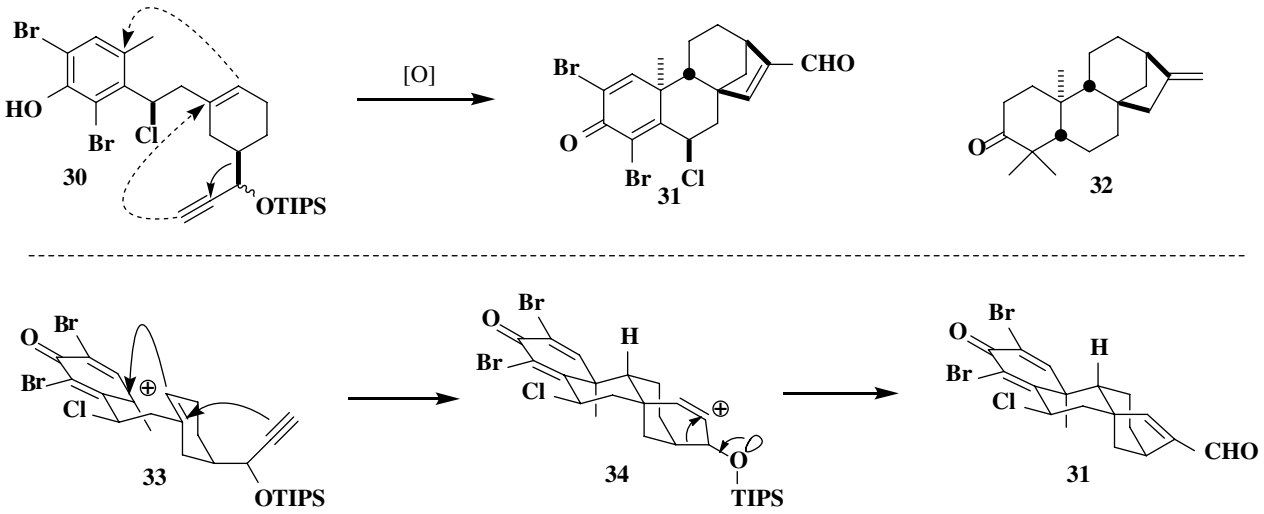



**SCHEME 8.2** Biosyntheses of taxadienes, abietanes, and *ent*-kaurane diterpene motifs.

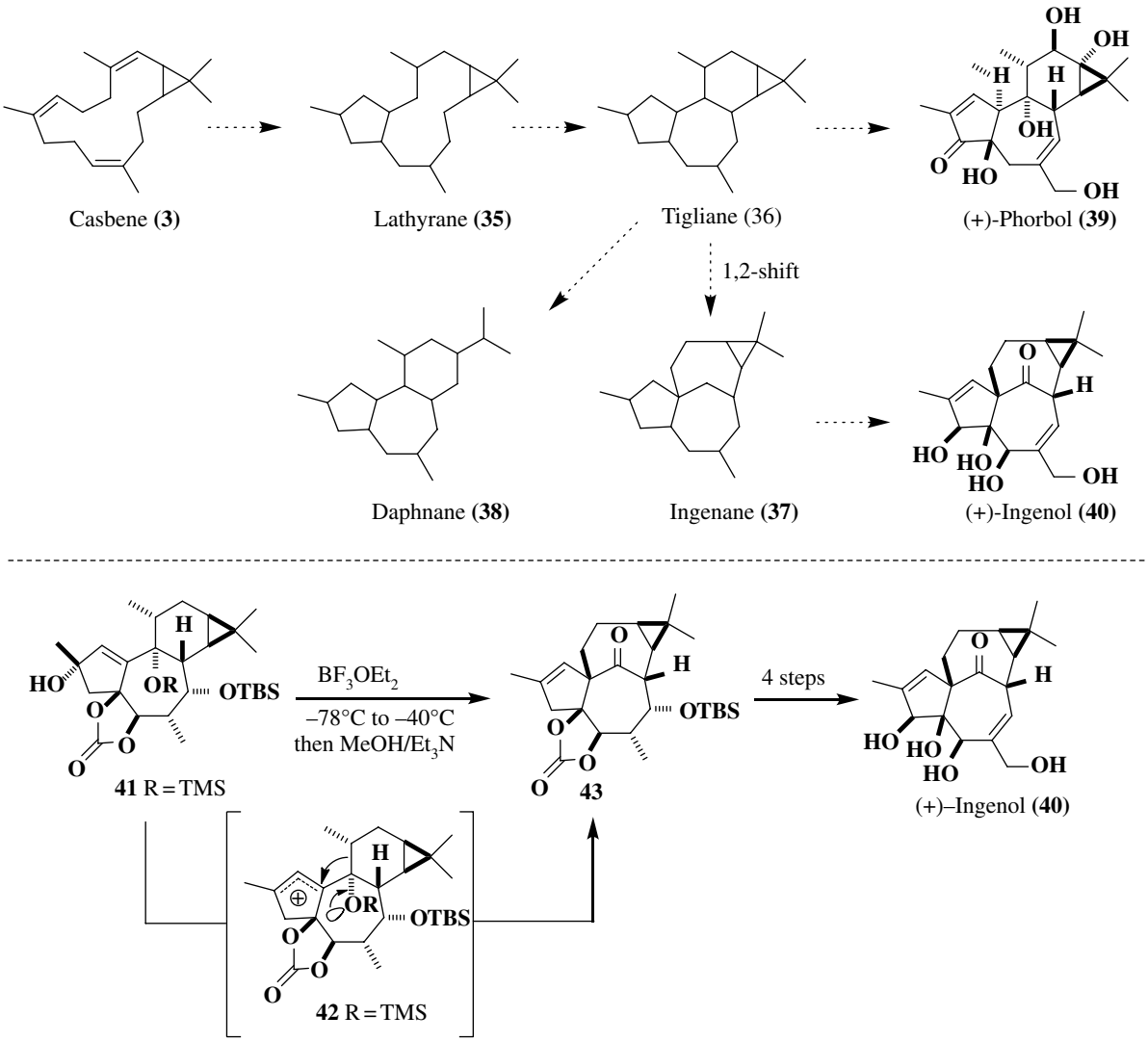
synthase, are involved in two specific processes, **1** → **26** and **27** → **29**, respectively [10]. However, it was shown that the enzyme *ent*-CPP found in the fungus *Phaeosphaeria* sp. L487 converts GGPP (**1**) into **29** in a single process [11].

As it will be discussed in the next chapter, the cationic cyclization of squalenes represents a powerful method to generate polycyclic compounds in a high diastereoselective manner. Organic chemists have been mimicking Nature by accomplishing the synthesis of high-order cyclic terpenes by cationic cyclization of polyunsaturated carbon chain (Chapter 9 for more details). Canesi et al. reported an elegant domino stereoselective oxidative cationic cyclization for the synthesis of kaurane diterpene frameworks such as **32** (Scheme 8.3) [12]. Oxidative dearomatization of **30** using phenyliodine bis (trifluoroacetate) (PIFA) produces a phenoxionium intermediate **33**, which triggers an intramolecular cationic cyclization to give intermediate **34**. The latter is poised to undergo a 1,2-shift (pinacol rearrangement) to afford the kaurane scaffold **31**. The high diastereoselectivity of the process can rationalized as follows. Assuming that the cyclization proceeds through a chair-like transition state, one can imagine that the chlorine substituent is oriented in the equatorial position minimizing the steric interaction thus favoring the formation of **31**.

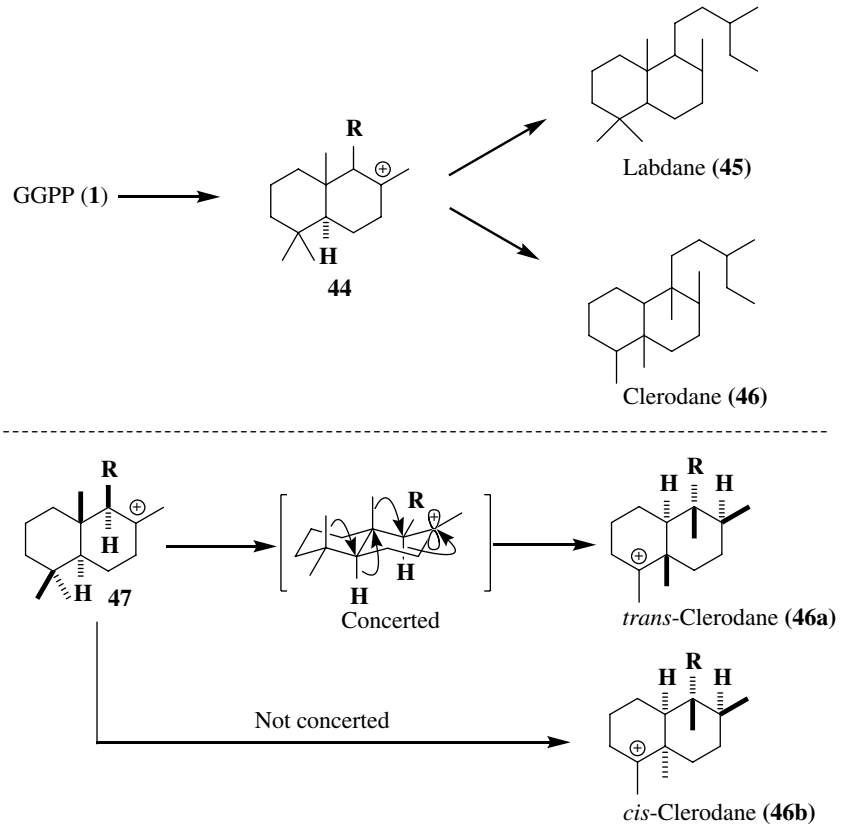
Various diterpenoids having lathyrane (**35**), tigliane (**36**), ingenane (**37**), and daphnane (**38**) scaffolds have been isolated from *Euphorbia genus* (Scheme 8.4). It has been proposed that the biosynthesis of these diterpenes is originated from casbene **3**. Although their biogenesis has not been disclosed in detail, one can speculate that a sequence of stepwise cyclizations starting from casbene **3** is involved for the formation of new sigma bonds [14]. Among these diterpenes, ingenol (**40**) (ingenane type) and phorbol (**39**) (tigliane type) are the most notable members of these families. Owing to their structures and impressive therapeutic profile, **39** and **40** have generated significant interest from synthetic organic chemists [15]. Baran and coworkers have disclosed a short and efficient synthesis of (+)-ingenol (**40**) starting from the readily available (+)-carene [13]. They took advantage of a pinacol rearrangement of **41** via intermediate **42** to form the *in*/*out* bicyclic scaffold of **43**. One can argue that the efficiency of their synthesis could support a proposal for




**SCHEME 8.3** Biomimetic cyclization to kaurane scaffolds.




**SCHEME 8.4** Postulated biosynthesis of complex casbene diterpene families and biomimetic synthesis of ingenol by Baran et al. [13].

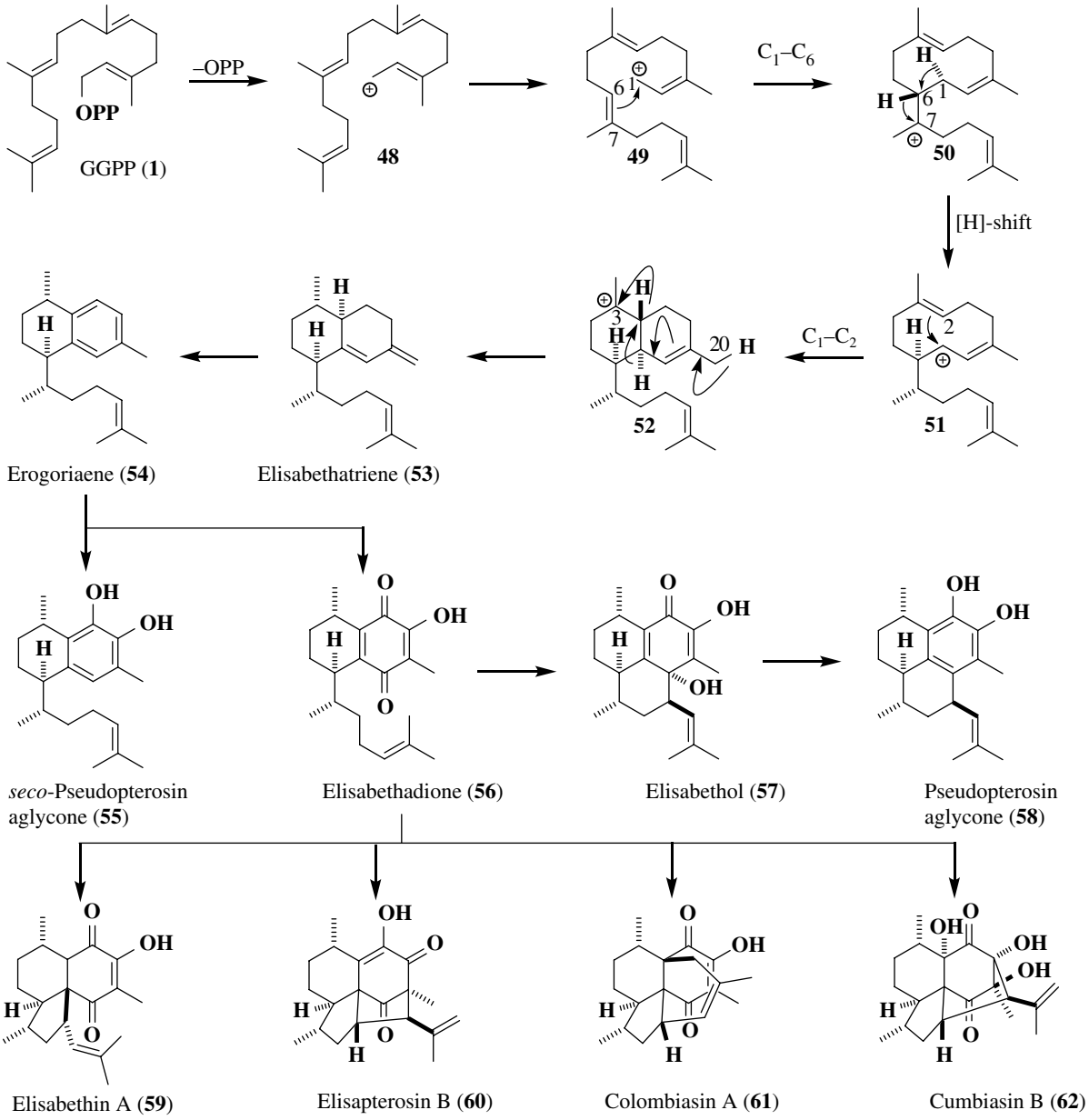



**SCHEME 8.5** Biosyntheses of labdane and clerodane diterpenes.

the biosynthesis of ingenane **37** via a cationic 1,2-shift of tigliane diterpene **36**.

Although labdane and clerodane diterpenoids **45** and **46** are frequently encountered in Nature, few biosyntheses have been reported, and it has been suggested that these diterpenes are originated from GGPP (**1**) via a two-step process (Scheme 8.5) [16]. In the case of clerodane diterpenes, it has been proposed that the *trans*- and *cis*-clerodanes **46a** and **46b** are the result of a series of migrations from a common cationic intermediate **47** [17]. A closer look at the biogenesis suggests that the methyl and hydrogen 1,2-shifts operate in a concerted manner. However, if one takes into consideration the stereoelectronic effects, one could suggest that the process to obtain *cis*-clerodanes **46b** is not concerted, and the formation of cationic intermediate could be envisaged.

A large number diterpenes including serrulatane, amphilectane, elisabethane, colombiane, cumbiane, and elisapterane have been isolated from a gorgonian octocoral, *Pseudopterogorgia elisabethae* [18]. These diterpenes possess a remarkable array of structural diversity along with interesting medicinally important properties. An overview of their biosynthetic pathways is presented in Scheme 8.6. It was shown that the formation of serrulatane diterpene such as elisabethatriene (**53**) is catalyzed by the pseudopterosin diterpene cyclase [19]. The cyclization is triggered by the loss of the pyrophosphate group (OPP) generating an allylic carbocation, which undergoes an isomerization *E*/*Z* (**48** → **49**). Formation of the C1–C6 bond **49** → **50** followed by a hydride [1,2]-shift delivers intermediate **51**, which is poised to undergo C1–C2 bond formation **51** → **52** followed by sequential hydride shifts to give elisabethatriene (**53**). The latter is converted to erogoriaene (**54**), which serves as a pivotal intermediate to access to other diterpenes. At this point, one can imagine a series of oxidation to generate the *seco*-pseudopterosin aglycone (**55**) and elisabethadione (**56**). The latter is converted to elisabethol (**57**) via a ring closure, and then aromatization gives the pseudopterosin aglycone (**58**). The fact that the pseudopterosins were isolated with the *seco*-pseudopterosin aglycones (**58**) implies that these two classes of diterpenes arise from **53**. Although the biosyntheses of elisabethin A (**59**), elisapterosin B (**60**), colombiasin A (**61**), cumbiasin B (**62**), and other elisapteranes are still elusive, one can suggest that these compounds originated from elisabethadione (**56**) via intramolecular cyclizations. Furthermore, the fact that these compounds were isolated from the same coral species, *P. elisabethae*, strongly suggests that these share a common biosynthetic pathway [17].



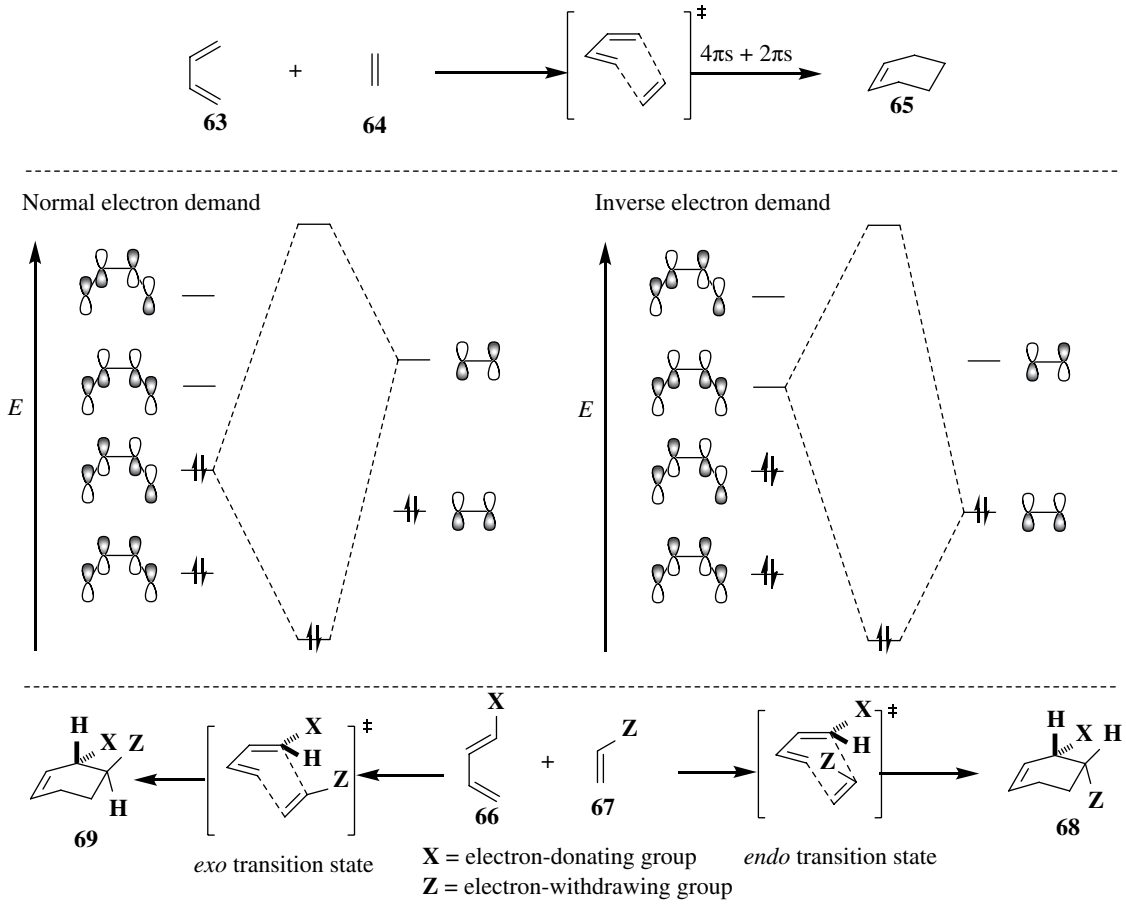

**SCHEME 8.6** Correlation of an array of diterpene scaffolds on common biosynthetic routes.

## 8.3 PERICYCLIC REACTIONS AND THEIR APPLICATION IN THE SYNTHESIS OF SELECTED DITERPENOIDS

Pericyclic reactions such as cycloaddition, sigmatropic, electrocyclic, and ene reactions are characterized by a concerted series of bond-breaking and bond-forming events through a single cyclic transition state without the formation of a charged intermediate. These reactions are not affected by the solvent or by radical initiators and scavenger reagents. The application of some pericyclic reactions in the synthesis of complex diterpenes will be detailed in the following sections.

### 8.3.1 Diels–Alder Reaction and Its Application in the Total Synthesis of Diterpenes

The Diels–Alder reaction is cycloaddition of a 1,3-diene and a substituted alkene, alkyne, benzene, or allene (dienophile) to generate a six-membered ring having up to four stereocenters, which are often formed with high regio- and stereoselectivity (Scheme 8.7) [20]. The early reports of this reaction involved the mixing and heating of a diene **63** and a dienophile **64** in a nonpolar solvent to produce the corresponding cycloadduct **65**. However, the general applicability of this reaction in the context of synthesis has been greatly enhanced through the development of a wide array of conditions,



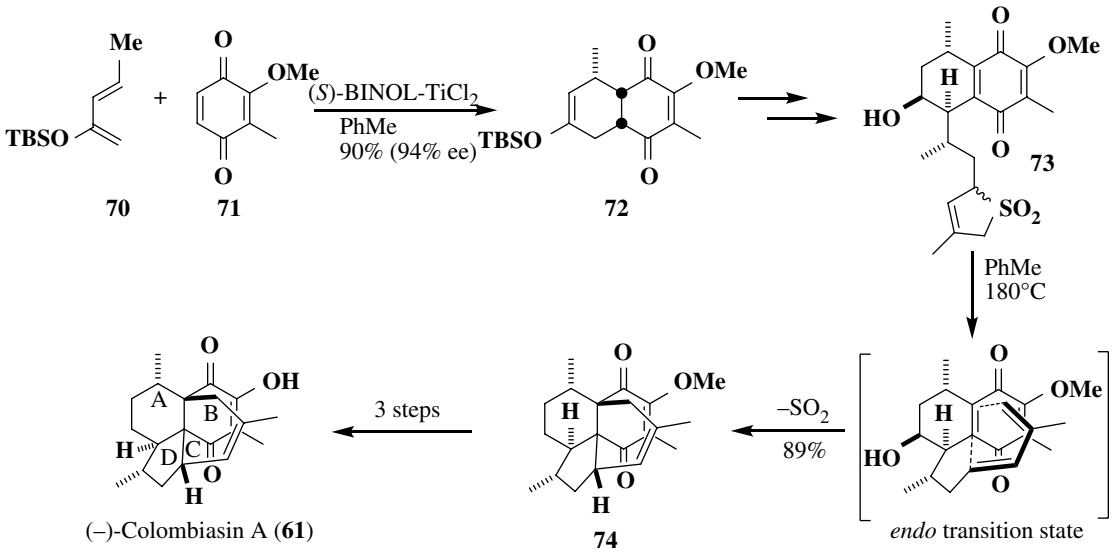

**SCHEME 8.7** Diels–Alder reaction.

including Lewis acid catalyzed, high pressure, inverse electron demand, and *hetero*-variants. One of the major assets of the Diels–Alder reaction resides in its predictability. The Woodward–Hoffmann rules are used to predict the stereochemical outcome of pericyclic reactions based on their molecular orbitals [21]. In this case, the Diels–Alder reaction is described as being a *symmetry-allowed* [π4s+π2s] process operating in a concerted manner via a highly organized transition state but not necessarily in a symmetrically synchronous fashion. The electronic nature of the substituent directly influences the size the molecular orbital coefficient of the diene **66** and dienophile **67**, which is linked to the regio- and stereoselectivity outcome of the Diels–Alder reaction. It has been proposed that the interactions between nonbonding atomic orbitals, namely, secondary orbital interactions, could account for the preferential formation of the *endo* product **68** over the *exo* product **69** [22]. However, it has been recently proposed that steric interactions, solvent effect, hydrogen bonds, and electrostatic interactions can explain the selectivity of Diels–Alder reaction without relying on the secondary orbital interactions [23].

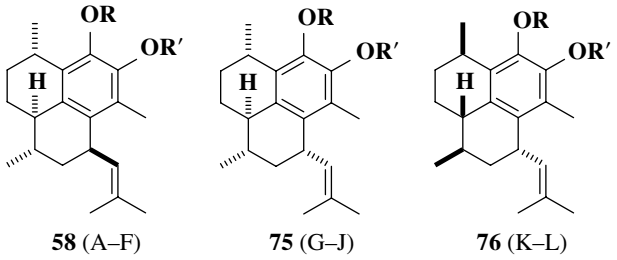
Since its discovery by Otto Diels and Kurt Alder in 1928, this pericyclic reaction is probably the most powerful and versatile reaction for the formation of C–C bonds and has profoundly shaped the art of total synthesis as it is [24]. Looking over the years, we see that the Diels–Alder reaction continues to be used in attaining some very complex natural products.

In 2001, Nicolaou and coworkers disclosed an elegant total synthesis of (−)-colombiasin A (**61**) using two Diels–Alder reactions as key steps to construct the core of the molecule (Scheme 8.8) [25]. This compound isolated from *P. elisabethae* has shown potent inhibitory activity against tuberculosis (Scheme 8.6) [26]. The first cycloaddition was performed enantioselectively using Mikami's catalytic system to afford a single product **72** (*endo* product) in 90% yield and 94% of enantiomeric excess. Cycloadduct **72** was converted into intermediate **73**, containing a sulfone-masked diene, which was then subjected to refluxing toluene to unveil the diene unit, which was poised to undergo an intramolecular Diels–Alder (IMDA) reaction to give intermediate **74** in 89% yield. The latter was converted to (−)-colombiasin A (**61**). Other groups have also utilized a similar IMDA strategy to construct the C and D rings of **61** [27].

Other interesting diterpenes such as pseudopterosins A–L have been isolated from the same organism [28]. All of these




**SCHEME 8.8** Total synthesis of colombiasin A by Nicolaou et al. [25].



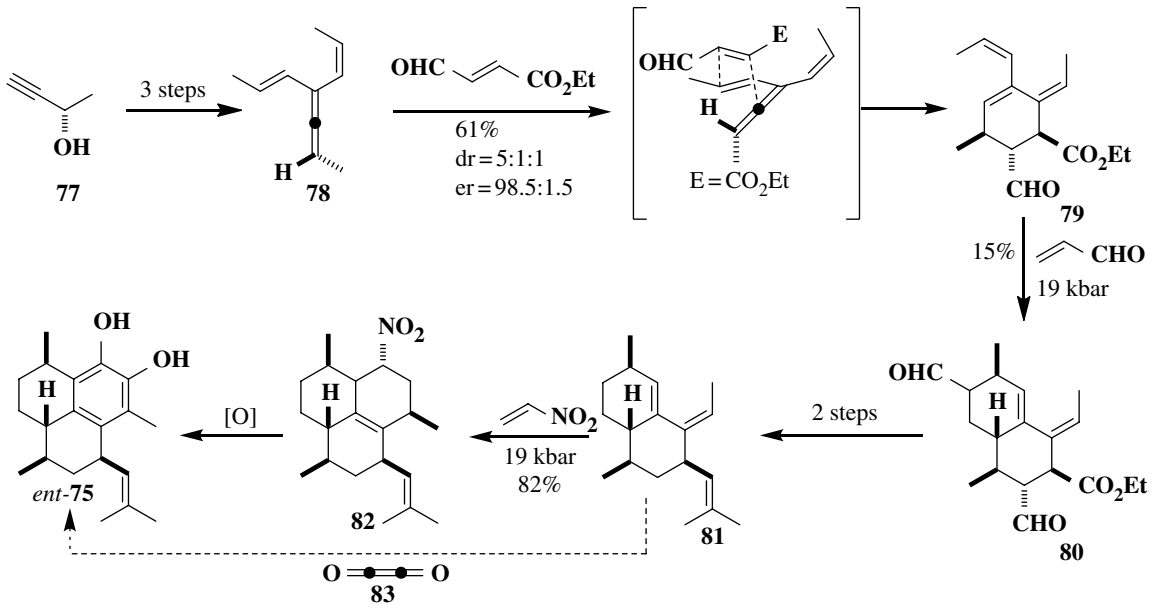

**SCHEME 8.9** Pseudopterosin natural motifs.

diterpenes belong to the family of amphilectane and are derived from three stereoisomeric aglycones **58**, **75**, and **76** (Scheme 8.9). The nature of the glycoside unit and the glycosidation site accounts for the remaining structural difference. Several members of the pseudopterosin family show a wide array of biological activities including anticancer, anti-inflammatory, and antimalarial properties [28]. The challenging structure and the therapeutic profile of these compounds have attracted the attention of the organic synthetic practitioners. To date, 15 total and formal syntheses of pseudopterosin aglycones have been reported [29].

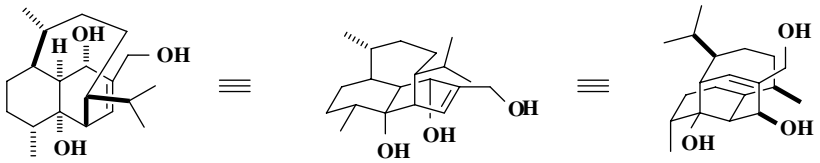
In 2014, Sherburn and coworkers disclosed a short synthesis of (–)-pseudopterosins (G–J) aglycone **75** (Scheme 8.10) [30]. To build the carbocyclic scaffold, they delineated an unconventional strategy, which relies upon the use of a diene-transmissive triple Diels–Alder reaction. The enantioenriched 1,1-divinylallene **78** was prepared in three steps from the chiral propargyl alcohol **77** (chiral pool). This unusual diene was then subjected to a Diels–Alder reaction to provide the cycloadduct **79** in 61% yield and in good diastereomeric ratio. A second [4+2] cycloaddition of **79** with acrolein using high-pressure conditions took place to afford the expected cycloadduct **80** in 15% yield. Although a low conversion was observed, the reaction reveals to be highly regio- and stereoselective. The two now unneeded formyl groups were removed in a single operation employing the Wilkinson's complex. The conversion of ester **80** into **81** containing the prenyl group sets the stage for the third cycloaddition, which generated the catechol portion of the molecule. One can conceive that ethylene dione **82** could be the ideal dienophile but highly impractical. Thus, nitroethylene was used as a surrogate for the high-pressure Diels–Alder reaction to provide **82** in 82% yield. The latter was readily converted to the desired *ent*-pseudopterosin aglycone **75** in three steps through a series of oxidative processes.

Vinigrol (**84**) is a novel diterpenoid first isolated in 1987 by Ando and coworkers from *Virgaria nigra* F-5408, a fungus strain found at the foot of Mount Aso, in Kumamoto Prefecture in Japan (Scheme 8.11) [31]. Its tricyclic core contains an unusual *cis*-fused [4.4.0] system bridged by an eight-membered ring and features eight contiguous stereocenters. Vinigrol possesses a wide array of biological activity including antihypertensive and platelet aggregation inhibitory activity. Also, it was found that **84** is powerful tumor necrosis factor (TNF) antagonist [32].

As discussed previously, serrulatane can lead to various diterpenes such as amphilectane (pseudopterosins), colombiane, elisabethane, and elisapterane. Although the biosynthesis of vinigrol (**84**) is still not elucidated, Goodman a Corey's laboratory proposed a biosynthetic pathway inspired by the biogenesis of pseudopterosins (Scheme 8.12) [33]. From erogorgiaene (**54**), they postulate a series of oxidation leading to the phenoxy radical **85**, which could undergo a radical cyclization to give the unprecedented core of vinigrol **86**. Finally, successive enzymatic oxidation could provide vinigrol (**84**). Although this proposal seems promising, the highly strained structure of **86** may thwart the ability of

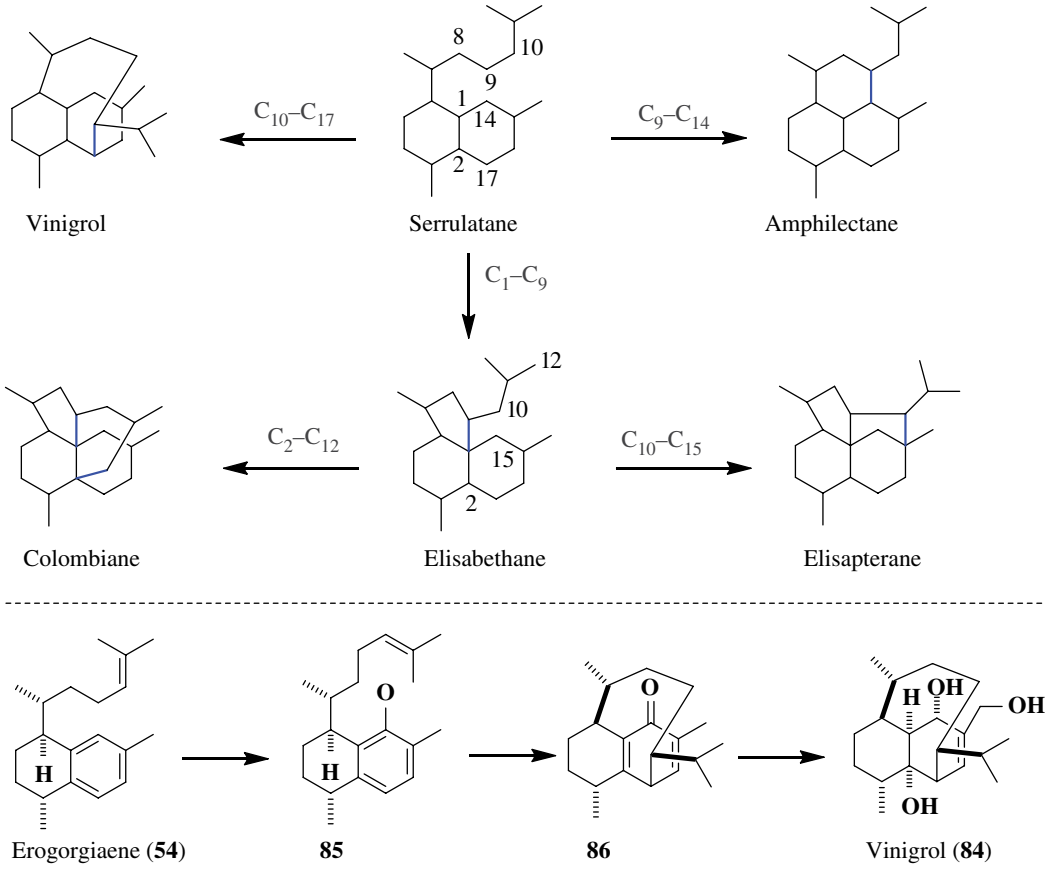



**SCHEME 8.10** Total synthesis of pseudopterosin (G–J) aglycon by Sherburn et al. [30].

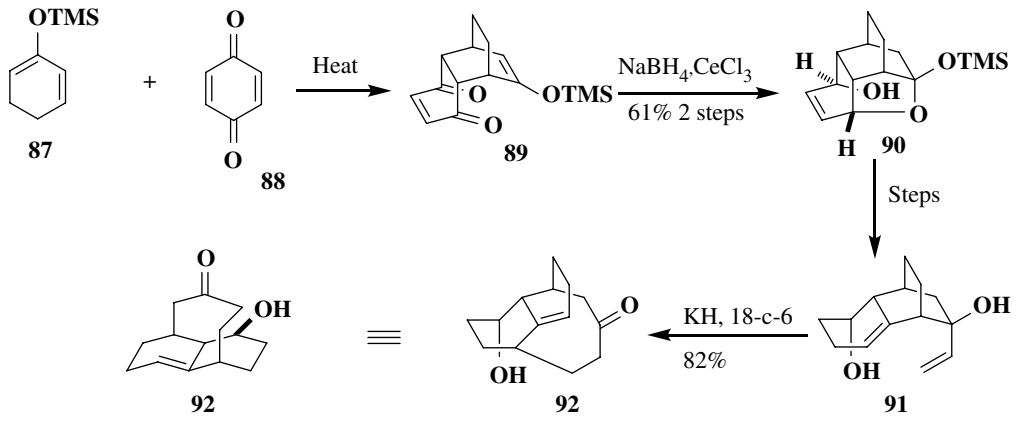



Vinigrol (**84**)

**SCHEME 8.11** Molecular structure of vinigrol.




**SCHEME 8.12** Proposed biosynthesis of vinigrol.




**SCHEME 8.13** Synthetic approach to vinigrol core **92** by Hanna et al. [35].

the cyclization to occur. Not surprisingly, the challenging structure of vinigrol combined with its impressive therapeutic profile has resulted in considerable attention from the synthetic community [34].

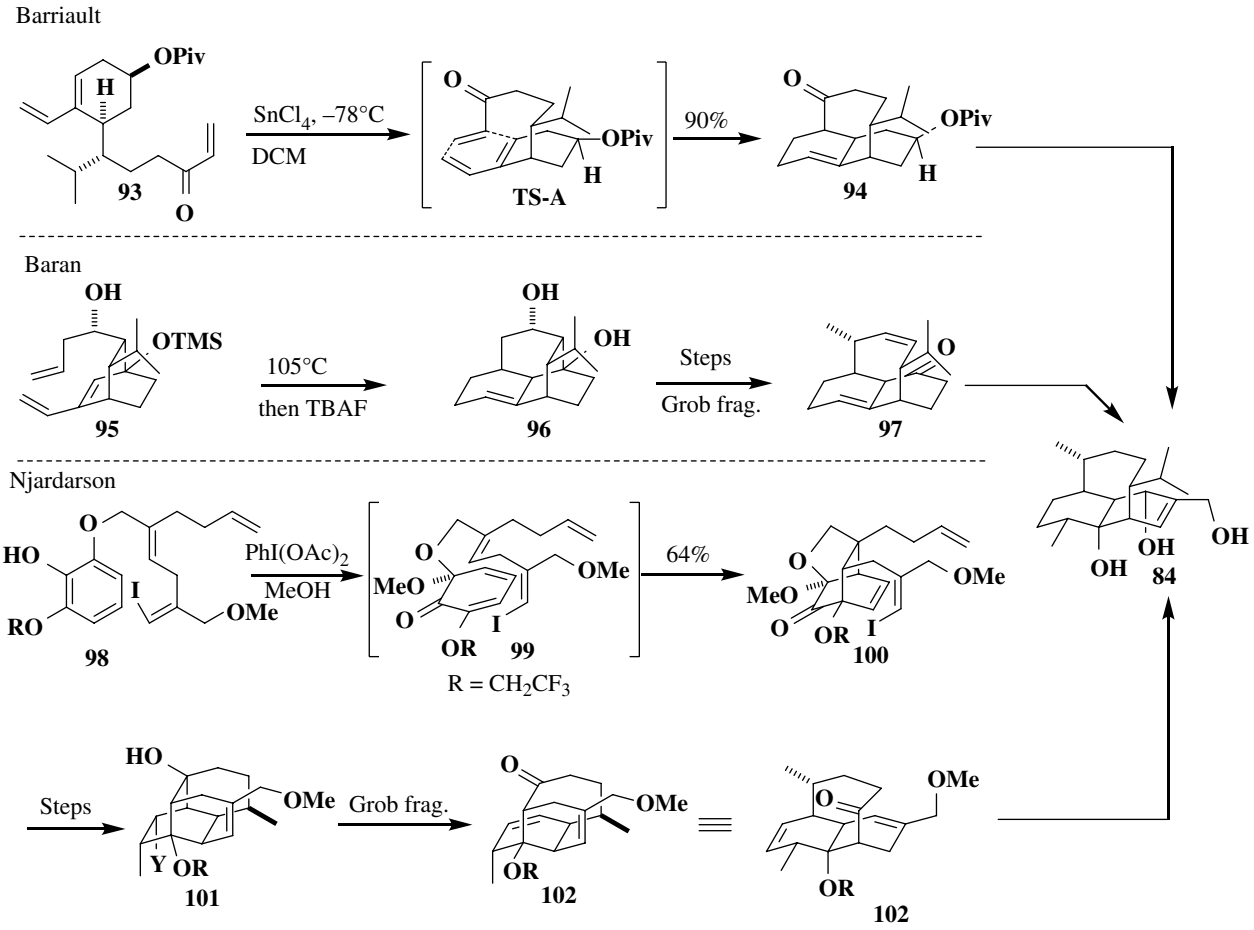
To date, the stereocontrolled synthesis of *the tricyclic vinigrol core was only achieved through the use of pericyclic reactions*. In 1993, Hanna et al. disclosed the first synthesis of the tricyclic core of vinigrol **92** (Scheme 8.13) [35]. Their approach features an intermolecular Diels–Alder reaction between cyclic diene **87** and 1,4-benzoquinone **88** to give tricycle **89**, which upon treatment with $NaBH_4$ afforded **90** in 62% over two steps. After functional group manipulations, compound **91** underwent an anionic oxy-Cope rearrangement to deliver **92** in 82% yield.

Recently, Baran, Barriault, and Njardarson have completed the total synthesis of vinigrol (Scheme 8.14) [36]. In all of these cases, an IMDA reaction features as the key to generate the tricyclic core of vinigrol. The strategy deployed by Barriault revealed an audacious Lewis acid-catalyzed IMDA reaction of triene **93** to generate the 8- and 6-membered rings of the vinigrol core in a single operation [36b, 37]. This highly regio- and stereoselective transformation proceeded through transition state **TS-A** to produce **94** in 90% yield as a sole isomer. The effectiveness of the IMDA approach was subsequently established by Baran and coworkers, in which, triene **95** was converted to tetracycle **96** in 75% yield [36a, 38]. The latter was then converted into the core of vinigrol **97** via a Grob fragmentation. Finally, Njardarson et al. used an oxidative dearomatization/IMDA and Grob fragmentation as key step to construct the core of vinigrol [36c, 39]. Exposure of **98** to $PhI(OAc)_2$ gave a mix acetal **99**, which upon heating underwent IMDA to give **100** in 64% yield. After a series of functional group manipulations, compound **101** was obtained ready to go through a Wharton–Grob fragmentation to provide the core of vinigrol **102**.

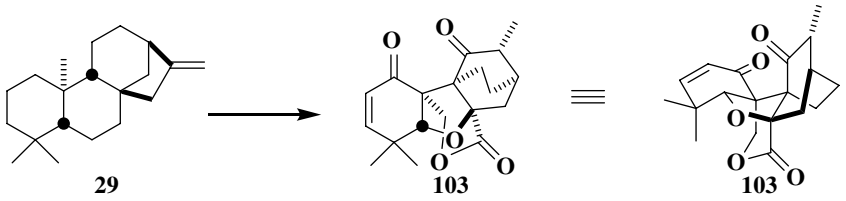
In 2004, Sun and coworkers isolated from *Isodon eriocalyx* a unique and architecturally complex diterpene named maoecrystal V (**103**) (Scheme 8.15) [40]. It has been proposed that this natural product is biosynthetically derived from the common *ent*-kaurene scaffold via bond reorganization and oxidation processes. Maoecrystal V displays potent and selective inhibitory activity against HeLa cells ($IC_{50}$) (60 nM). Its unusual structure comprises two vicinal quaternary stereocenters at C9 and C10, a highly strained cyclic ether between C5 and C8, a spirocyclic lactone, and a bicyclo[2.2.2]octane ring system. One could suggest that bicyclo[2.2.2]octane ring unit could be prepared via a Diels–Alder reaction. The groups of Yang, Danishefsky, Zakarian, and Thomson have included this disconnection strategy in their syntheses of **103** [41].

In 2010, Yang and coworkers reported the first total synthesis of **103** by an oxidative dearomatization/IMDA reaction of **104** to generate the cyclic ether, lactone, and bicyclo[2.2.2]octane units of **105** in a single operation (Scheme 8.16, eq. 1) [42]. Baran reported a similar disconnection in the synthesis toward **103** [43]. Later, Danishefsky and Peng's strategy reported of an IMDA reaction of ester **106** followed by a subsequent arylsulfone elimination to construct the bicyclo[2.2.2]octane ring system **107** (eq. 2) [44]. As shown in eq. 3, Zakarian and coworkers prepared the bicyclo[2.2.2]octane core **109** through a silicon-tethered IMDA reaction of vinyl silane **108** [45]. Lastly, Thomson and coworkers reported an alternative strategy employing an intermolecular Diels–Alder reaction between diene **110** and nitroethylene to construct the bicyclo[2.2.2]octane ring **111** (eq. 4) [46]. Their synthetic efforts culminated in the enantioselective synthesis (−)-maoecrystal V (**103**).

In a screening to identify new platelet-activating factor antagonist from sea coral, chatancin (**112**) was isolated and characterized by Sato and coworkers from a soft coral (*Sarcophyton* sp.) (Scheme 8.17) [47]. This new diterpene shows moderate inhibition for both PAF-induced platelet aggregation ($IC_{50} = 2.2$ mm) and PAF receptor binding ($IC_{50} = 0.32$ mm). A cursory inspection of the structure reveals that chatancin possesses a rigid tricyclo[8.4.4.0] tetradecane skeleton by virtue of a hemiketal bridge




**SCHEME 8.14** Key steps to the total synthesis of vinigrol.

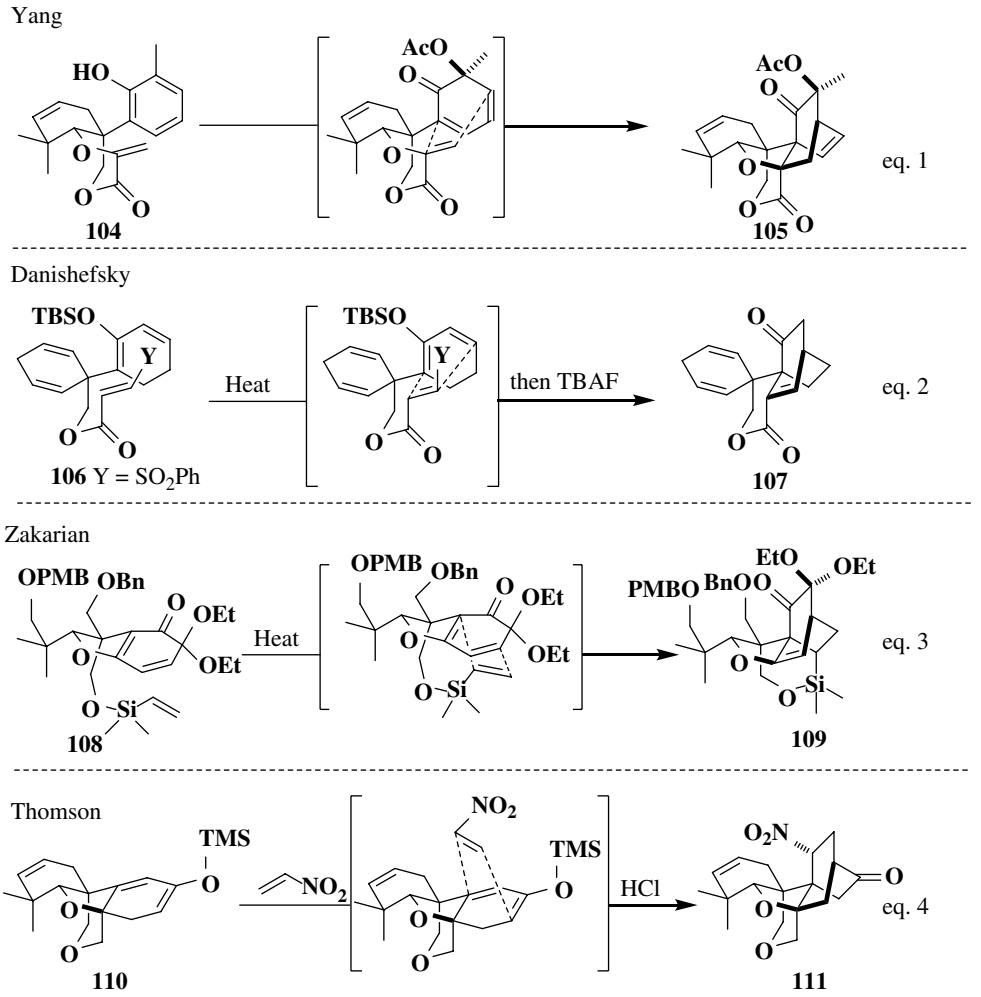



**SCHEME 8.15** Molecular structure of maoecrystal V.

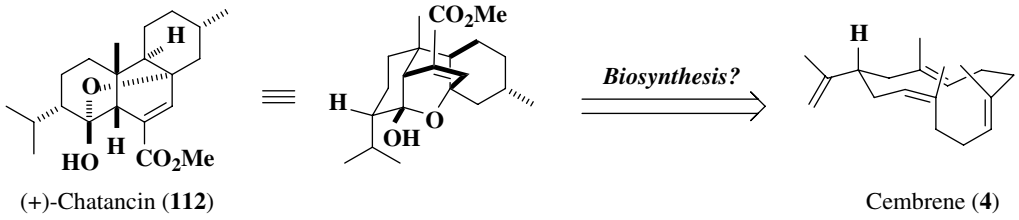
featuring a *cis–anti–cis* stereochemistry at ring junction. As discussed in Section 8.2, 14-membered macrocyle cembrane diterpenoids such as **4** are probably precursors for the biogenesis of a variety of polycyclic diterpenes [3]. Thus, one can draw a parallel with a plausible biosynthesis of chatancin via transannular processes from **4**.

In 2003, Deslongchamps and coworkers reported an elegant synthesis of (+)-chatancin (**112**) in 17 steps involving a biomimetic transannular cycloaddition (Scheme 8.18) [48]. Although there are no evidences of *in vivo* transannular Diels–Alder (TADA) reaction in cembranoids, Deslongchamps hypothesized that **112** could be obtained from a macrocyclic pyranophane such as **116a**. To verify their hypothesis, the macrocycle **115** was assembled in 16 steps from (+)-citronellol **113** and sulfone **114**. Four different pyranophanes **116a–d** can be obtained from macrocycle **115**, which upon TADA reaction can produce four possible diterpenes including chatancin. Gratifyingly, heating of **115** (as a mixture of isomers) gave exclusively (+)-**112** in 70–75% yields suggesting that the TADA reaction process through a highly organized transition state such as **TS-A**. Based on this result, one can propose that chatancin could be biogenetically linked to cembranoids.

Twelve years later, Maimone and Zhao reported a concise seven-step enantiospecific synthesis of (+)-chatancin [49]. They identified a synthetic route, in which the




**SCHEME 8.16** Synthetic approaches to the total synthesis of maoecrystal V.

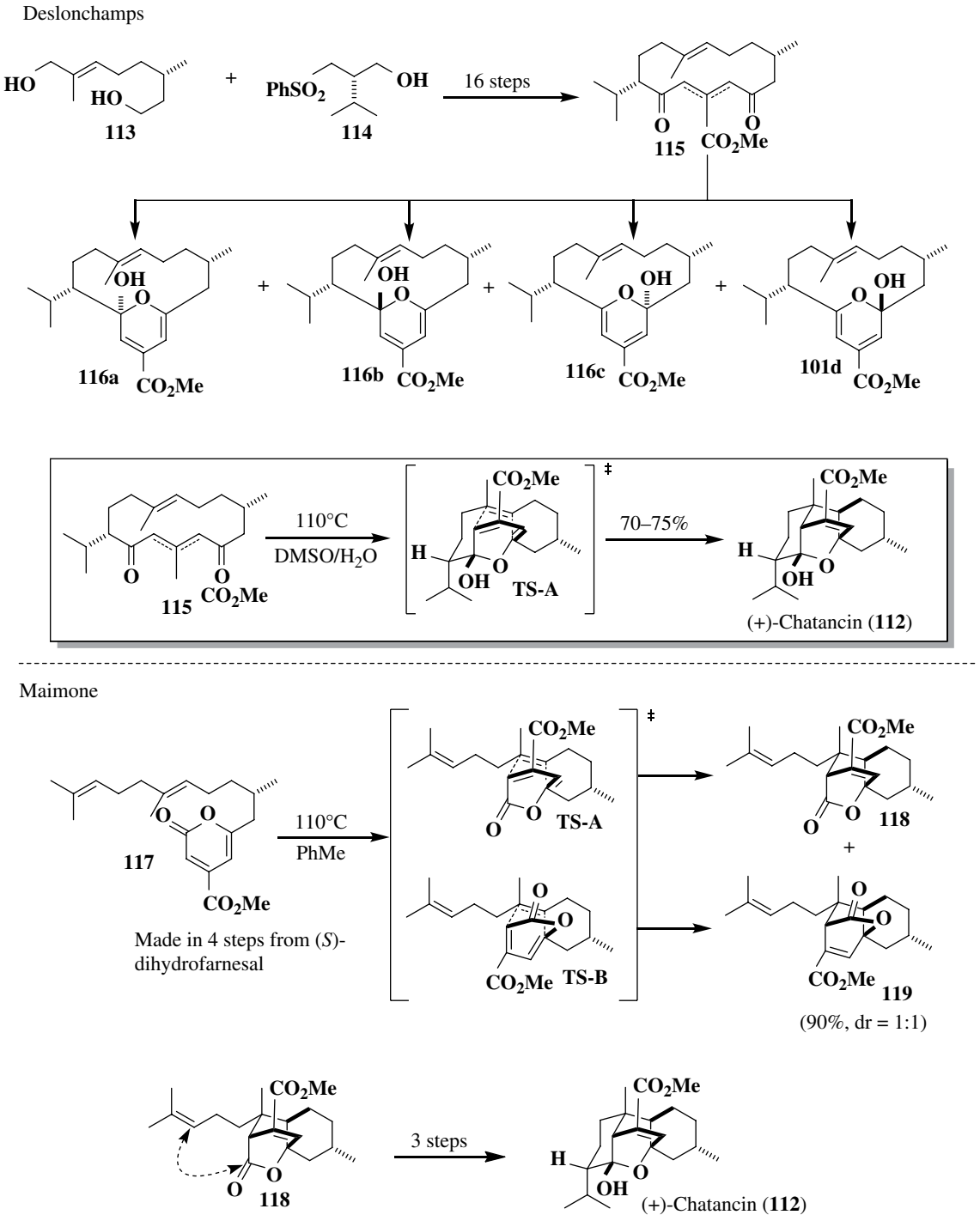



(+)-Chatancin (**112**) Cembrene (**4**)

**SCHEME 8.17** Structure of chatancin and its potential biosynthetic correlation to cembrane.

macrocyclization approach is circumvented, opting for an IMDA reaction to construct the chatancin scaffold. Starting from (*S*)-dihydrofarnesal, tetraene **117** was prepared in four steps and then heated at 100°C in toluene for 4 days to give cycloadducts **118** and **119** in 90% yield as an equal mixture of diastereomers. According to these results, one can propose that the IMDA reaction of **117** proceeds through two energetically equivalent transition states (**TS-A** and **TS-B**). Although a poor diastereoselectivity was obtained, **118** was readily converted to (+)-chatancin in three steps.

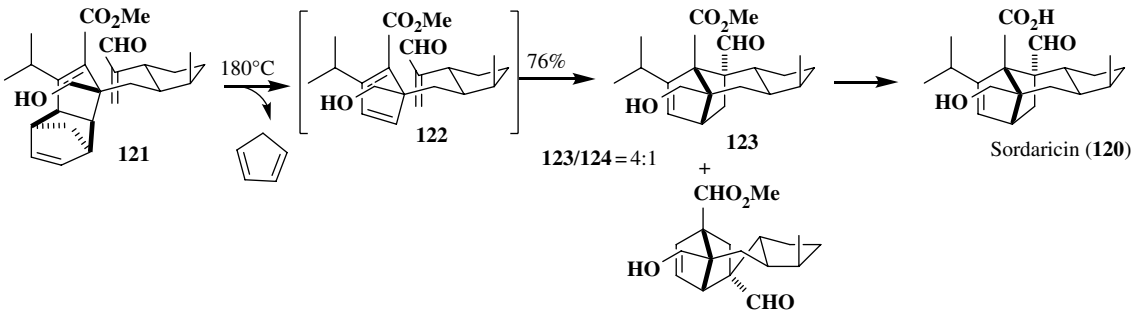
Right from the discovery of the Diels–Alder reaction in 1928, its importance in the synthesis of natural products was recognized. From early syntheses (such as cortisone) to more contemporary examples highlighted previously, the Diels–Alder reaction continues to play a prominent role in the synthesis of complex natural products.



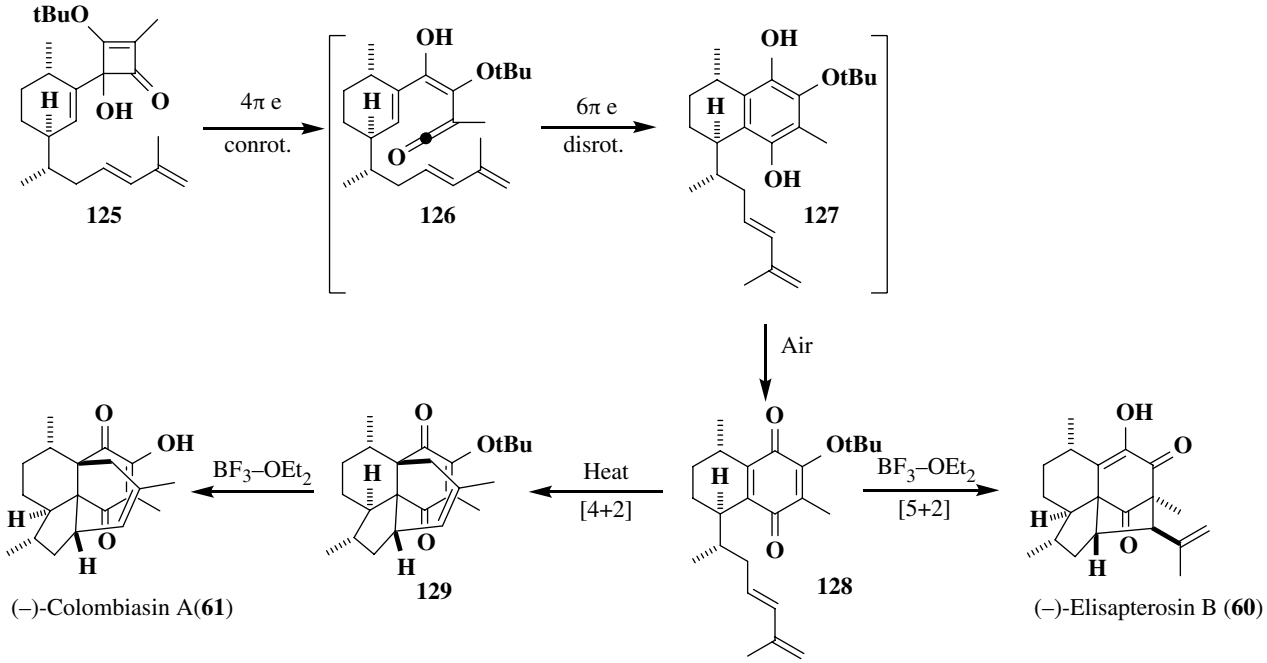

**SCHEME 8.18** Key steps of the total syntheses of chatancin natural diterpenoid.

### 8.3.2 Cascade Pericyclic Reactions and Their Application in the Total Synthesis of Diterpenes

Recent years have seen the emergence of reactions occurring in cascade as a powerful tool to construct complicated molecular scaffolds. One can define domino or cascade reactions as two or more distinct chemical transformations that happen in quick succession in the same reaction vessel. The use of domino reactions in organic chemistry is not a new concept, and many excellent reviews have been published on the subject [50]. The concerted nature of pericyclic reactions renders these transformations particularly attractive due to the relative ease of predicting the stereochemical outcome of the final product. In other words, domino




**SCHEME 8.19** Total synthesis of sordaricin by Mander and Thomson [51].



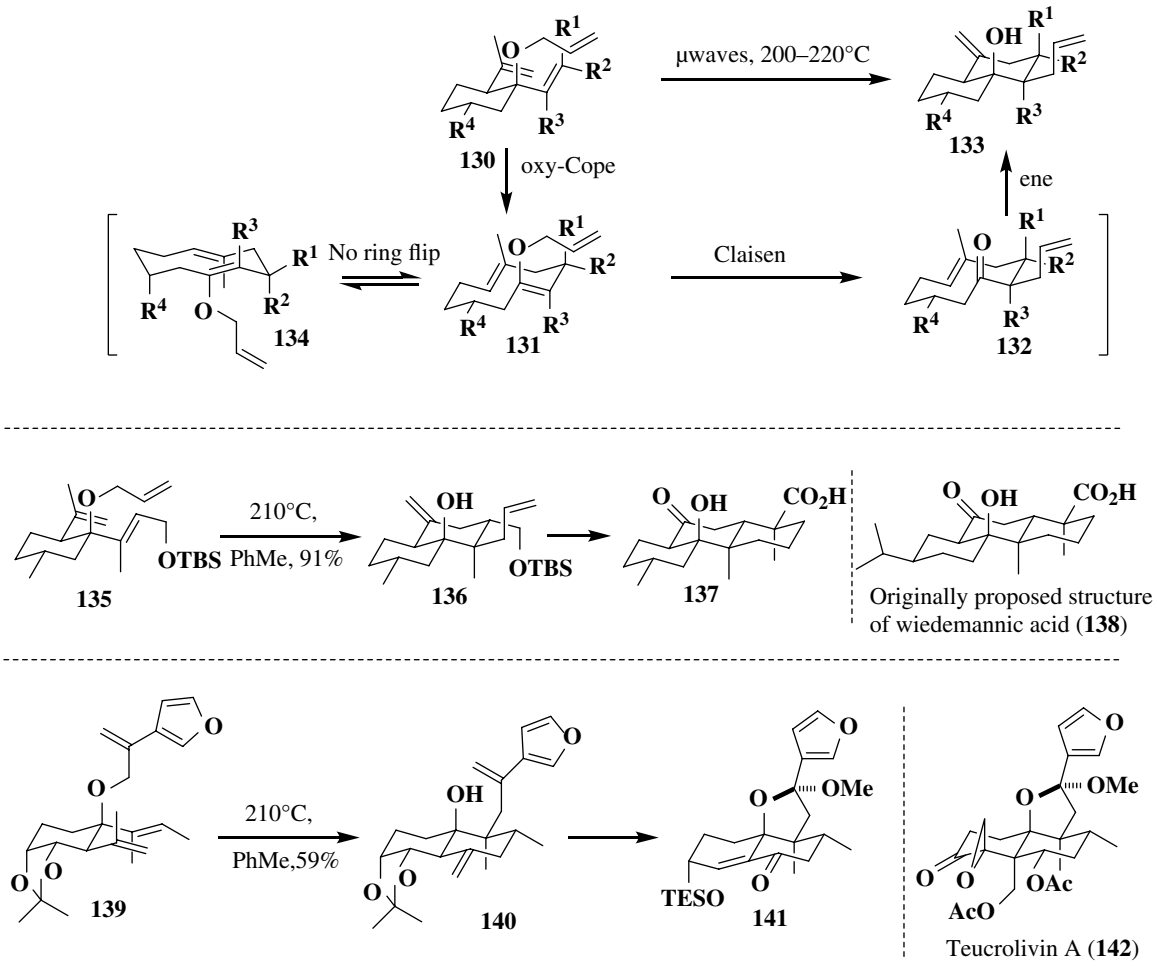

**SCHEME 8.20** Total syntheses of colombiasin A and elisapterosin B through a common intermediate **127**.

reactions can represent a real advantage when elaborating a blueprint for the synthesis of architecturally complex molecules possessing multiple stereogenic centers.

Mander and Thomson reported the total synthesis of sordaricin (**120**), a diterpene isolated from the ascomycete *Sordaria araneosa* Cain (Scheme 8.19) [51]. Inspired by its biogenesis, they devised a synthetic plan involving a domino retro Diels–Alder/IMDA reaction of a mask cyclopentene **121**. Upon liberation of cyclopentene, intermediate **122** underwent an IMDA reaction to give the desired sordaricin analog **123** along with a minor cycloadduct regioadduct **124**.

Harrowven and coworkers disclosed a short synthesis of (–)-elisapterosin B (**60**) and (–)-colombiasin (**61**) combining the Moore rearrangement and intramolecular cycloaddition reactions (Scheme 8.20) [27b]. The bicyclic quinone **126** was generated from **125** via a domino 4π-e conrotatory ring opening **125** → **126**/6π-e disrotatory electrocyclization **126** → **127** (Moore rearrangement). This intermediate can be converted in both natural products **60** and **61** via an intramolecular [5+2] and [4+2] cycloaddition, respectively.

One of the problems encountered in the synthesis of polycyclic compounds is the stereoselective formation of quaternary carbon centers. Barriault and coworkers reported the development of domino oxy-Cope/Claisen/ene reaction of divinyl cyclohexanol **130** as an efficient method for the assembly of decalin system possessing contiguous quaternary centers such as **133** (Scheme 8.21) [54]. Heating of alcohol **130** triggers an oxy-Cope reaction to provide the 10-membered ring macrocyle **131**, which is poised to undergo a Claisen rearrangement. The resulting ketone **132** is converted to the decalin **133** via a transannular carbonyl-ene reaction. An extensive mechanistic study demonstrated that (i) there is no ring flip of the tetrasubstituted enol ether **131** → **134** and (ii) macrocyclic ketone **132** undergoes a fast




**SCHEME 8.21** Cascade of an oxy-Cope/Claisen/ene reaction for the construction of complex diterpene core structures by Barriault et al. [52, 53].

and facile ring flip. As a result, the ratio of the ene product reaction is governed by the Curtin–Hammett principle. Barriault applied of this domino process in the synthesis of wiedemannic acid (**138**) an abietane diterpene isolated from *Salvia wiedemanni* [52]. A close inspection of the structure reveals five contiguous stereogenic centers based around a trans-decalin core. Heating of **135** gave intermediate **136** in 90% yield as the sole isomer. The latter was converted to **137**, which possesses several architectural features of wiedemannic acid (**138**). Unfortunately, the comparison of $^{1}$H and $^{13}$C NMR data of **137** and the reported structure of wiedemannic acid showed significant difference in the chemical shift and *J* coupling constant. These differences strongly suggest that the structure of **138** was incorrect.

Taking advantage of the predictability of the domino oxy-Cope/Claisen/ene reaction, the same group reported the highly diastereoselective synthesis of a carbocycle **140** from **139** in 59% yield in a single operation [53]. The latter was converted in a few steps to **141**, which represents an advanced intermediate *en route* toward the synthesis of teucrolivin A (**142**), a neoclerodane diterpenoid isolated from *Teucrium oliverianum*.

## 8.4 CONCLUSION

The wide diversity of diterpenes has spurred organic chemists to develop new reactions and innovative tactics. Among them, the pericyclic reactions stood as one the most efficient transformations to generate a wide array of structural diversity. Although the biosyntheses of several diterpenes are not fully elucidated, one can propose that some pericyclic reactions, notably the Diels–Alder reaction, could be involved in these processes. The selected examples in this chapter demonstrate the importance of these transformations in the context of complex diterpene synthesis. Although pericyclic reactions were discovered almost 100 years ago, their use in synthesis is still in its infancy.

## REFERENCES


1. T. Toyomasu, T. Sassa, *Comprehensive Natural Product II*, vol. **1**, Elsevier: Oxford, 2010, p. 643.
2. (a) C. J. D. Mau, C. A. West, *Proc. Natl. Acad. Sci. U. S. A.* 1994, **91**, 8497; (b) M. T. Dueber, W. Adolf, C. A. West, *Plant Physiol.* 1978, **62**, 598; (c) P. Moesta, C. A. West, *Arch. Biochem. Biophys.* 1985, **238**, 325.
3. For recent reviews, see: (a) Y. Li, G. Pattenden, *Nat. Prod. Rep.* 2011, **28**, 1269; (b) P. A. Roesthle, D. Trauner, *Nat. Prod. Rep.* 2007, **25**, 298.
4. (a) P. A. Roethle, P. T. Hernandez, D. Trauner, *Org. Lett.* 2006, **8**, 5901; (b) P. A. Roethle, D. Trauner, *Org. Lett.* 2006, **8**, 345.
5. B. Tang, C. D. Bray, G. Pattenden, *Tetrahedron Lett.* 2006, **47**, 6401.
6. For model study using transannular cycloaddition, see: K. C. Nicolaou, V. A. Adsool, C. R. H. Hale. *Angew. Chem. Int. Ed.* 2011, **50**, 5149.
7. (a) M. R. Wildung, R. Croteau, *J. Biol. Chem.* 1996, **271**, 9201; (b) M. Hezari, N. G. Lewis, R. Croteau, *Arch. Biochem. Biophys.* 1995, **322**, 437.
8. (a) T.-P. Sun, H. M. *Cell* 1992, **4**, 119; (b) T.-P. Sun, Y. Kamiya, *Plant Cell* 1994, **6**, 1509.
9. (a) B. Stofer Vogel, M. R. Wildung, G. Vogel, R. Croteau, *J. Biol. Chem.* 1966, **271**, 23262; (b) R. E. LaFever, B. Stofer Vogel, R. Croteau, *Arch. Biochem. Biophys.* 1994, **313**, 139.
10. (a) T. Saito, H. Abe, H. Yamane, A. Sakurai, N. Murofushi, K. Takio, N. Takahashi, Y. Kamiya, *Plant Physiol.* 1995, **109**, 1239; (b) S. Yamaguchi, T. Saito, H. Abe, H. Yamane, N. Murofushi, Y. Kamiya, *Plant J.* 1996, **10**, 203.
11. H. Kawaide, R. Imai, T. Sassa, Y. Kamiya, *J. Biol. Chem.* 1997, **272**, 21706.
12. S. Desjardins, G. Maertens, S. Canesi, *Org. Lett.* 2014, **16**, 4928.
13. (a) L. Jørgensen, S. J. McKerrall, C. A. Kuttruff, F. Ungeheuer, J. Felding, P. S. Baran, *Science* 2013, **341**, 878; (b) S. J. McKerrall, L. Jørgensen, C. A. Kuttruff, F. Ungeheuer, P. S. Baran, *J. Am. Chem. Soc.* 2014, **136**, 5799.
14. (a) E. Hecker, *Pure Appl. Chem.* 1977, **49**, 1423; (b) W. Adolf, E. Hecker, *Isr. J. Chem.* 1977, **16**, 75; (c) R. Schmidt, *Bot. J. Linn. Soc.* 1987, **94**, 221; (d) J. Kirby, M. Nishimoto, J. G. Park, S. T. Withers, F. Nowroozi, D. Behrendt, E. J. Garcia Rutledge, J. L. Fortman, H. E. Johnson, J. V. Anderson, J. D. Keasling, *Phytochemistry* 2010, **71**, 1466.
15. For reviews, see: (a) S. Kim, J. D. Winkler, *Chem. Soc. Rev.* 1997, **26**, 387; (b) I. Kuwajima, K. Tanino, *Chem. Rev.* 2005, **105**, 4661; (c) J. K. Cha, O. L. Epstein, *Tetrahedron* 2006, **62**, 1329.
16. A. F. Barrero, J. F. Sanchez, F. G. Cuenca, *Phytochemistry* 1988, **27**, 3676.
17. (a) A. T. Merritt, S. V. Ley, *Nat. Prod. Rep.* 1992, **9**, 243; (b) A. Akhila, K. Rani, R. S. Thakur, *Phytochemistry* 1991, **30**, 2573; (c) K. Nabeta, T. Ishikawa, H. Okuyama, *J. Chem. Soc. Perkin Trans.* 1995, 3111.
18. T. J. Heckrodt, J. Mulzer, *Top. Curr. Chem.* 2005, **244**, 1 and references cited therein.
19. (a) A. C. Kohl, A. Ata, R. G. Kerr, *J. Ind. Microbiol. Biotechnol.* 2003, **30**, 495; (b) A. C. Coleman, R. G. Kerr, *Tetrahedron* 2000, **56**, 9569.
20. (a) O. Diels, K. Alder, *Justus Liebigs Ann. Chem.* 1928, **460**, 98; (b) O. Diels, K. Alder, *Chem. Ber.* 1929, **62**, 2081
21. R. B. Woodward, R. Hoffmann, *The Conservation of Orbital Symmetry*; Academic Press: New York, 1970.
22. (a) K. Alder, G. Stein, *Angew. Chem.* 1937, **50**, 510; (b) R. Hoffmann, R. B. Woodward, *J. Am. Chem. Soc.* 1965, **87**, 4388; (c) R. Hoffmann, R. B. Woodward, *J. Am. Chem. Soc.* 1965, **87**, 4389; (d) D. Ginsburg, *Tetrahedron* 1983, **39**, 2095; (e) R. Gleiter, M. C. Böhm, *Pure Appl. Chem.* 1983, **55**, 237.
23. J. I. Garcia, J. A. Mayoral, L. Salvatella, *Acc. Chem. Res.* 2000, **33**, 658.
24. For recent reviews see: (a) K. C. Nicolaou, S. A. Snyder, T. Montagnon, G. Vassilikogiannakis, *Angew. Chem. Int. Ed.* 2002, **41**, 1668; (b) E. G. Mackay, M. S. Sherburn, *Synthesis* 2014, **47**, 1.
25. (a) K. C. Nicolaou, G. Vassilikogiannakis, W. Magerlein, R. Kranich, *Angew. Chem. Int. Ed.* 2001, **40**, 2482; (b) K. C. Nicolaou, G. Vassilikogiannakis, W. Magerlein, R. Kranich, *Chem. Eur. J.* 2001, **7**, 5359.
26. A. D. Rodrigez, C. Ramirez, *Org. Lett.* 2000, **2**, 507.
27. (a) A. I. Kim, S. D. Rychnovsky, *Angew. Chem. Int. Ed.* 2003, **42**, 1267; (b) D. C. Harrowven, D. D. Pascoe, D. Demurtas, H. O. Bourne, *Angew. Chem. Int. Ed.* 2005, **44**, 1221; (c) A. A. Boezio, E. R. Jarvo, B. M. Lawrence, E. N. Jacobsen, *Angew. Chem. Int. Ed.* 2005, **44**, 6046; (d) H. M. L. Davies, X. Dai, M. S. Long, *J. Am. Chem. Soc.* 2006, **128**, 2485.
28. (a) S. A. Look, W. Fenical, G. K. Matsumoto, J. Clardy, *J. Org. Chem.* 1986, **51**, 5140; (b) S. A. Look, W. Fenical, R. S. Jacobs, J. Clardy, *Proc. Natl. Acad. Sci. U. S. A.* 1986, **83**, 6238; (c) F. Berrué, M. W. B. McCulloch, R. G. Kerr, *Bioorg. Med. Chem.* 2011, **19**, 6702.
29. For a review of the syntheses, see: C. G. Newton, M. S. Sherburn, *Nat. Prod. Rep.* 2015, **32**, 865.
30. C. G. Newton, S. L. Drew, A. L. Lawrence, A. C. Willis, M. N. Paddon-Row, M. S. Sherburn, *Nat. Chem.*, 2015, **7**, 82.
31. I. Uchida, T. Ando, N. Fukami, K. Yoshida, M. Hashimoto, T. Tada, S. Koda, Y. Morimoto, *J. Org. Chem.* 1987, **52**, 5292.
32. (a) T. Ando, Y. Tsurumi, N. Ohata, I. Uchida, K. Yoshida, M. Okuhara, *J. Antibiot.* 1988, **41**, 25; (b) T. Ando, K. Yoshida, M. Okuhara, *J. Antibiot.* 1988, **41**, 31; (c) D. B. Norris, P. Depledge, A. P. Jackson, PCT Int. Appl. WO 9107 953, 1991; (d) J. T. Keane, PCT Int. Appl. WO 01 00 229, 2001.
33. S. N. Goodman, Ph.D. Thesis, Harvard University, 2000.
34. For reviews, see: (a) C. Draghici, J. T. Njardarson, *Tetrahedron*, 2015, **71**, 3775; (b) G. Tessier, L. Barriault, *Org. Prep. Proced. Int.* 2007, **37**, 313; (c) M. Harmata, N. L. Calkins, *Chemtracts* 2009, **22**, 205; (d) J.-Y. Lu, D. G. Hall, *Angew. Chem. Int. Ed.* 2010, **49**, 2286; (e) A. D. Huters, N. K. Garg, *Chem. Eur. J.* 2010, **16**, 8586.

35. (a) J.-F. Devaux, I. Hanna, J.-Y. Lallemand, *J. Org. Chem.* 1993, **58**, 2349; (b) J.-F. Devaux, I. Hanna, P. Fraisse, J.-Y. Lallemand, *Tetrahedron Lett.* 1995, **36**, 9471; (c) J.-F. Devaux, I. Hanna, J.-Y. Lallemand, *J. Org. Chem.* 1997, **62**, 5062; (d) L. Gentric, I. Hanna, A. Huboux, R. Zaghdoudi, *Org. Lett.* 2003, **5**, 363; (e) L. Gentric, X. Le Goff, L. Ricard, I. Hanna, *J. Org. Chem.* 2009, **74**, 9337.
36. (a) T. J. Maimone, J. Shi, S. Ashida, P. S. Baran, *J. Am. Chem. Soc*. 2009, **131**, 17066; (b) J. Poulin, G. M. Grisé-Bard, L. Barriault, *Angew. Chem. Int. Ed.* 2012, **51**, 2111; (c) Q. Yang, J. T. Njardarson, C. Draghici, *Angew. Chem. Int. Ed.* 2013, **52**, 8648.
37. G. Tessier, C. M. Grisé, L. Barriault, *Org. Lett.* 2007, **9**, 1545.
38. P. S. Baran, T. J. Maimone, A.-F. Voica, *Angew. Chem. Int. Ed.* 2008, **47**, 3054.
39. (a) J. G. M. Morton, L. D. Kwon, J. D. Freeman, J. T. Njardarson, *Synlett* 2009, 23; (b) J. G. M. Morton, L. D. Kwon, J. D. Freeman, J. T. Njardarson, *Tetrahedron Lett.* 2009, **50**, 1684; (c) J. G. M. Morton, C. Draghici, L. D. Kwon, J. T. Njardarson, *Org. Lett.* 2009, **11**, 4492.
40. S. H. Li, J. Wang, X. M. Niu, Y. H. Shen, H. J. Zhang, H. D. Sun, M. L. Li, Q. E. Tian, Y. Lu, P. Cao, Q. T. Zheng, *Org. Lett.* 2004, **6**, 4327.
41. For recent reviews on the synthesis of maoecrystal V, see: (a) T. K. Behara, S. N. Islam, V. J. Singh, *Chem. Sci.* 2013, **125**, 1301; (b) K. E. Lazarski, B. J. Moritz, R. J. Thomson, *Angew. Chem. Int. Ed.* 2014, **53**, 10588; (c) Y. Zhang, J. Gong, Z. Yang, *Chem. Rec.* 2014, **14**, 606.
42. J. Gong, G. Lin, W. Sun, C.-C. Li, Z. Yang, *J. Am. Chem. Soc.* 2010, **132**, 16745.
43. P. J. Krawczuk, N. Schöne, P. S. Baran, *Org. Lett.* 2009, **11**, 4774.
44. F. Peng, S. J. Danishefsky, *J. Am. Chem. Soc.* 2012, **134**, 18860.
45. (a) P. Lu, Z. Gu, A. Zakarian, *J. Am. Chem. Soc.* 2013, **135**, 14552; (b) P. Lu, A. Mailyan, D. M. Guptil, H. Wang, H. M. L. Davies, A. Zakarian, *J. Am. Chem. Soc.* 2014, **136**, 17738.
46. C. Zheng, I. Dubovyk, K. E. Lazarski, R. J. Thomson, *J. Am. Chem. Soc.* 2014, **136**, 17750.
47. M. Sugano, T. Shindo, A. Sato, Y. Iijima, T. Oshima, H. Kuwano, T. Hata, *J. Org. Chem.* 1990, **55**, 5803.
48. P. Soucy, A. L'heureux, A. Toro, P. Deslongchamps, *J. Org. Chem.* 2003, **68**, 9983.
49. Y.-M. Zhao, T. J. Maimone, *Angew. Chem. Int. Ed.* 2015, **54**, 1223.
50. K. C. Nicolaou, D. J. Edmonds, P. G. Bulger, *Angew. Chem. Int. Ed.* 2006, **45**, 7134.
51. L. N. Mander, R. J. Thomson, *J. Org. Chem.* 2005, **70**, 1654.
52. E. L. O. Sauer, L. Barriault, *Org. Lett.* 2004, **6**, 3329.
53. S. Arns, L. Barriault, *J. Org. Chem.* 2006, **71**, 1809.
54. (a) S. Arns, L. Barriault, *Chem. Commun.* 2007, 2211; (b) E. L. O. Sauer, L. Barriault, *J. Am. Chem. Soc.* 2004, **126**, 8569; (c) E. L. O. Sauer, J. H. Hooper, T. Woo, L. Barriault, *J. Am. Chem. Soc.* 2007, **129**, 2112.

# 9

# HIGHER TERPENES AND STEROIDS

Kazuaki Ishihara

*Department of Biotechnology, Graduate School of Engineering, Nagoya University, Nagoya, Japan*

## 9.1 INTRODUCTION

Conventional multistep synthesis of natural products reduces the overall yield of the target molecules. In contrast, biomimetic enantioselective domino reactions, promoted by small-molecule artificial enzymes, are more useful for the practical synthesis of natural products and related compounds. The stereoselective formation of polycyclic isoprenoids by the cyclase-induced cyclization of polyprenoids is one of the most remarkable steps in biosynthesis because this reaction results in the formation of several new quaternary and tertiary stereocenters and new rings in a single step. The use of biomimetic polycyclization with artificial cyclase is the most ideal chemical method for the synthesis of these polycyclic terpenoids. In this chapter, biosynthesis of polycyclic terpenoids, biomimetic stereoselective polyene cyclization induced by artificial cyclases, and total synthesis of bioactive natural products using stereoselective polyene cyclization as a key step will be discussed.

## 9.2 BIOSYNTHESIS

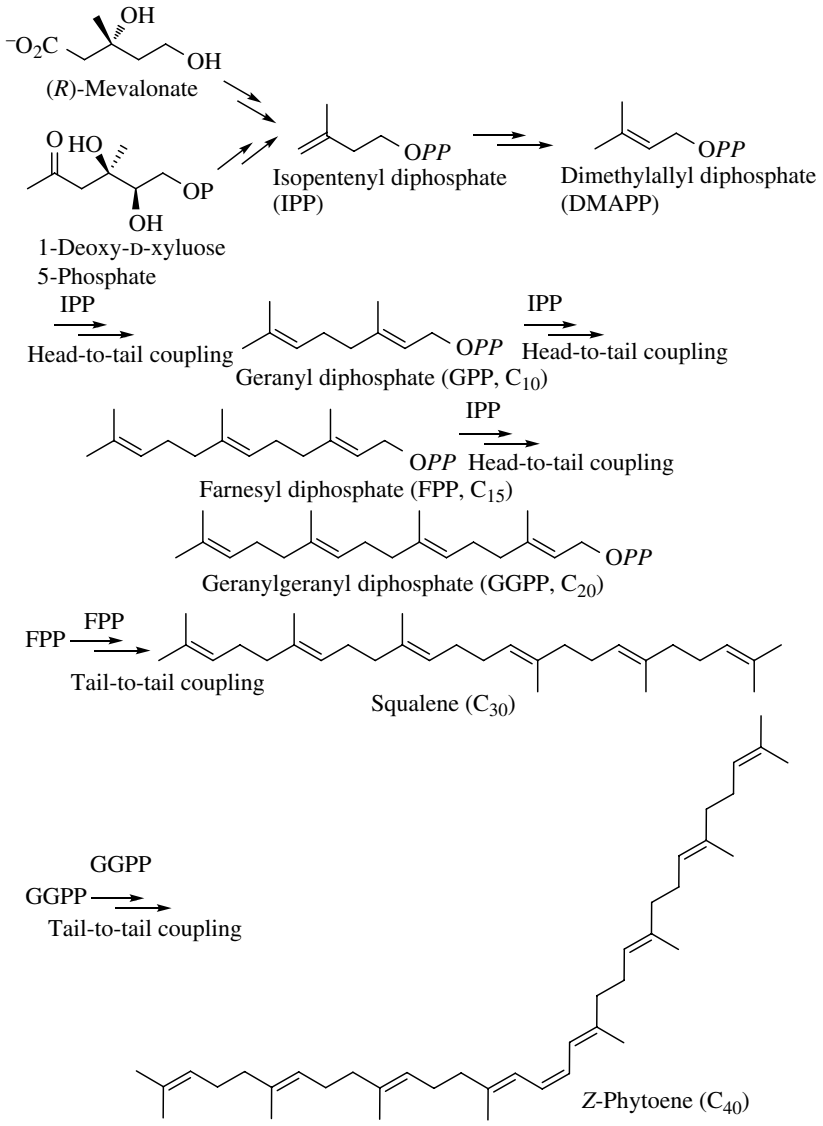
Terpenoids are a large group of substances found primarily in plants, bacteria, archaea, and fungi, as well as in animals [1]. More than 22,000 terpenoids with a vast diversity of structure are known. Although they appear structurally unrelated, all contain a multiple of five-carbon atoms. Terpenoids have multiples of five-carbon atoms because they arise biosynthetically from the five-carbon precursor isopentenyl diphosphate (IPP) (Scheme 9.1). IPP is biosynthesized by two different pathways depending on the organism and the structure of the final terpenoid (Chapter 5 for more details).

In animals and higher plants, sesquiterpenes (containing 15 carbons) and triterpenes (containing 30 carbons) arise primarily from (*R*)-mevalonate, while monoterpenes (containing 10 carbons), diterpenes (containing 20 carbons), and tetraterpenes (containing 40 carbons) are biosynthesized from 1-deozy-D-xylulose 5-phosphate. In bacteria, both pathways are used. The conversion of IPP to terpenoids begins with isomerization to dimethylallyl diphosphate (DMAPP). These two $C_5$ building blocks then combine to give $C_{10}$ unit geranyl diphosphate (GPP), which combines with another IPP to give the $C_{15}$ unit farnesyl diphosphate (FPP), and so on up to $C_{25}$. Terpenoids with more than 25 carbons such as squalene ($C_{30}$) and *Z*-phytoene ($C_{40}$) are biosynthesized by dimerization of $C_{15}$ and $C_{20}$ units, respectively.

Polycyclic terpenoids are metabolite products that are commonly found in nature and have a variety of biological activities. According to the Stork–Eschenmoser hypothesis, many polycyclic isoprenoids are biosynthesized from simple linear polyprenoids such as geraniol, farnesol, geranylgeraniol, and squalene via cationic polycyclization, which is considered to one of the most complex carbon–carbon bond-forming reactions in nature [1]. The complicated polycyclic structures of isoprenoids, which have many chiral centers including quaternary carbons, are stereoselectively constructed by cyclases in an impressive key step (Schemes 9.2 and 9.3) [2].

Bacterial membranes frequently contain hopanoids (Scheme 9.2), triterpenoids that appear to take the place of the sterols that are typically found in the membranes of

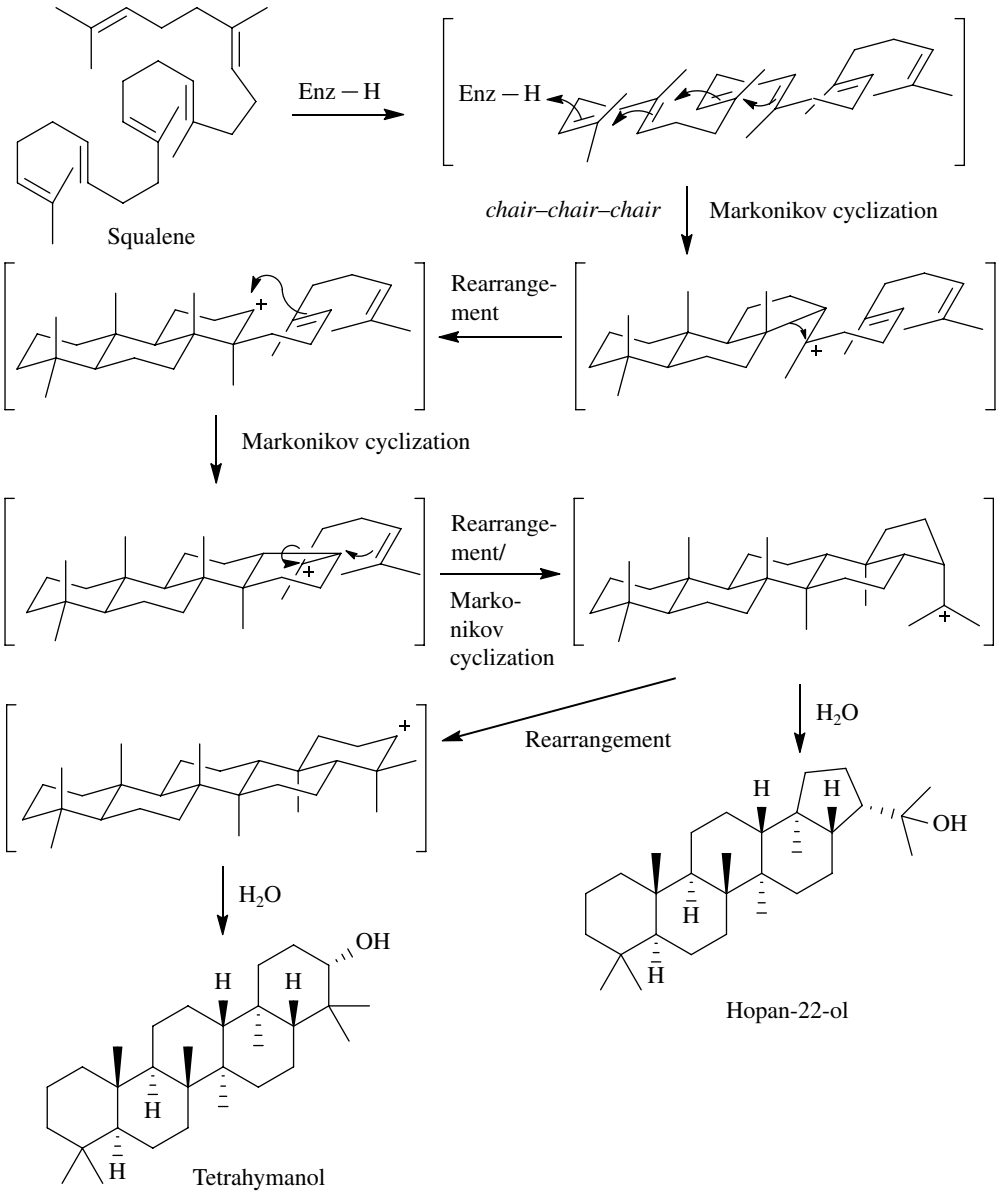
*From Biosynthesis to Total Synthesis: Strategies and Tactics for Natural Products*, First Edition. Edited by Alexandros L. Zografos.
© 2016 John Wiley & Sons, Inc. Published 2016 by John Wiley & Sons, Inc.




**SCHEME 9.1** Biosynthesis of linear terpenoids.

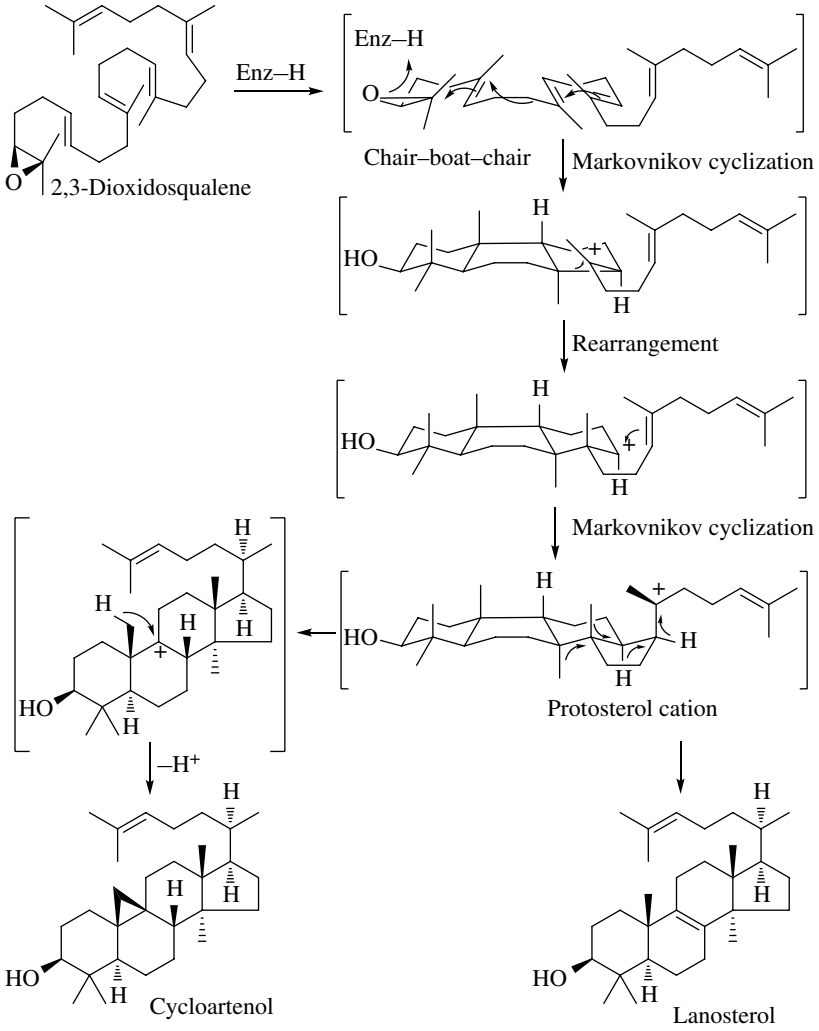
higher organisms, helping to maintain the structural integrity and to control permeability [1]. Hopanoids arise from squalene by a carbocation cyclization mechanism and do not involve an initial epoxidation to squalene oxide. Instead, the carbocation is produced by protonation, and the resultant compounds tend to lack the characteristic of 3-hydroxy group, for example, hopan-22-ol. On the other hand, tetrahymanol in which a 3-hydroxy group is present, this hydroxyl is derived from water and not molecular oxygen as would be the case, if squalene oxide was involved. As in the formation of the protesteryl cation, Wagner–Meerwein ring expansions occur during the cyclization sequence as shown in Scheme 9.2 so that the first-formed tertiary carbocation/five-membered ring (Markovnikov cyclization) becomes a secondary carbocation/six-membered ring.

In sharp contrast, in biosynthesis of sterols, cyclization of squalene is initiated by the intermediate squalene-2,3-oxide, produced in a reaction catalyzed by a flavoprotein requiring $O_2$ and NADPH cofactors (Scheme 9.3) [1]. If squalene oxide is suitably positioned and folded on the enzyme surface, the polycyclic triterpene structures formed can be rationalized in terms of a series of cyclizations, followed by a sequence of concerted Wagner–Meerwein migration of methyls and hydrides. The cyclizations are carbocation mediated and proceed in a stepwise sequence. Thus, protonation of the epoxide group will allow opening of this ring and generation of the preferred tertiary carbocation, suitably placed to allow electrophilic addition to a double bond, formation of a six-membered ring, and production of a new tertiary carbocation. This process continues twice more, generating the




**SCHEME 9.2** Biosynthesis of pentacyclic triterpenoids via nonsterol folding.

preferred tertiary carbocation (Markovnikov cyclization) after each ring formation. We have to point out that although the third ring closure formed through this process initially provides a cyclopentane carbocation, it is later rearranges through a Wagner–Meerwein 1,2-alkyl shift to the six member carbocycle shown in Scheme 9.3. A further electrophilic addition generates the tertiary protosteryl cation. The stereochemistries in this cation are controlled by the type of folding achieved on the enzyme surface, and this probably also limits the extent of the cyclization process. Thus, if the folded squalene oxide approximates to a chair–boat–chair conformation, the transient protosteryl cation will be produced with these conformational characteristics. This cation then undergoes a series of Wagner–Meerwein 1,2-shifts, firstly migrating a hydride and generating a new cation, migrating the next hydride, then a methyl and so on until a proton is lost forming a double bond and thus creating lanosterol. The stereochemistry of the protosteryl cation is crucial for the described migration sequence. Close inspection reveals that the migrating groups are positioned *anti* to each other. Thus, when one group enters, the other leaves from the opposite side, inverting the configuration at each carbon atom. Absence of an appropriate *anti*-positioned substituent terminates this migration cascade as in the case of C-9 position (steroid numbering), in which the *syn* configuration of the substituent force the loss of proton H-9 to produce lanosterol. Lanosterol is a typical animal triterpenoid and the precursor for cholesterol and other sterols in animals and fungi.




**SCHEME 9.3** Biosynthesis of pentacyclic triterpenoids via sterol folding.

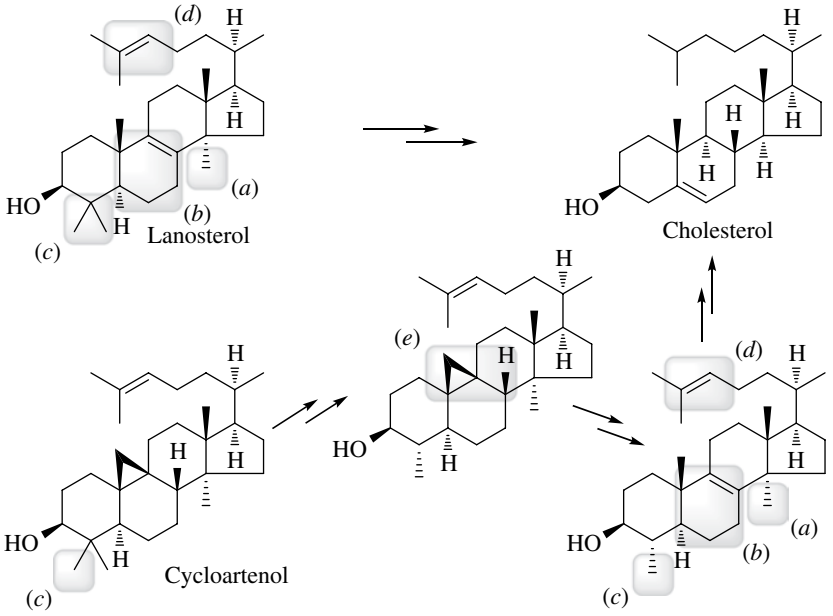
In plants, its role is taken by cycloartenol, which contains a cyclopropane ring, generated by the intramolecular quenching of produced cation from the methyl group at C-10. For many plant steroids, this cyclopropane ring has then to be reopened. Most natural triterpenoids and steroids contain a 3-hydroxy group, representing the original epoxide oxygen from squalene oxide.

In animals, lanosterol is converted into cholesterol, a process that requires the loss of three methyl groups (*a* and *c*), reduction of the side-chain double bond (*d*), and generation of a $\Delta^{5,6}$ double bond in place of the $\Delta^{8,9}$ double bond (*b*) (Scheme 9.4) [1]. The sequence of these steps is to some extent variable and dependent on the organism involved.

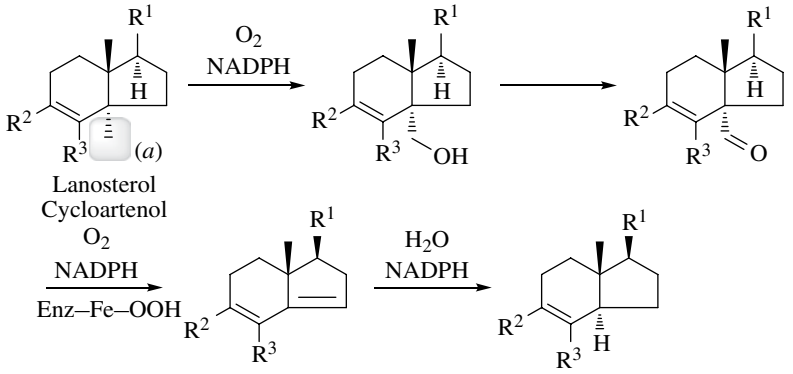
The (*a*) methyl at C-14 is usually the one lost first, as a formic acid (Scheme 9.5) [1]. The reaction is catalyzed by a cytochrome P-450 monooxygenase, which achieves two oxidation reactions to give the 14α-formyl derivative. Loss of this formyl group provides the $\Delta^{8,14}$ diene, most probably via homolytic cleavage of its peroxy adduct. The 14-demethyl sterol is then obtained by an NADPH-dependent reduction step, in which the 15-proton is derived from a molecule of water.

Loss of the C-4 methyl groups occurs sequentially, usually after removal of the 14α-methyl, with both carbons being cleaved off via a decarboxylation mechanism (Scheme 9.6) [1]. This is facilitated by oxidizing the 3-hydroxyl to a ketone, thus generating intermediate β-keto acids. In this sequence, the enolate is restored to a ketone, in which the remaining C-4 methyl takes up the more favorable equatorial (4α) orientation.

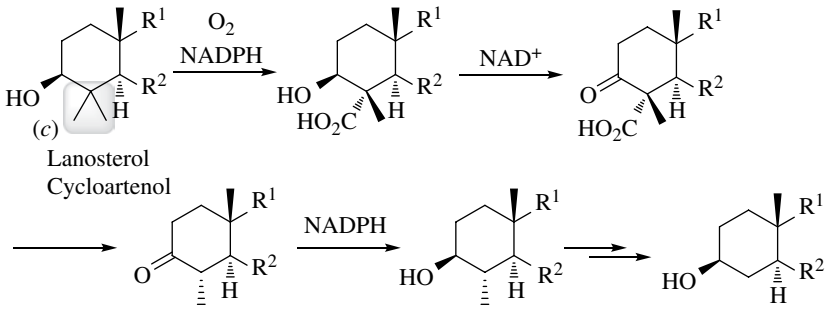
Finally, the double bond modifications include the reduction of the side-chain $\Delta^{24}$ double bond (*d*) by an NADPH-dependent reductase, in which the hydride from the coenzyme is being added at C-25, with H-24 being derived from water (Scheme 9.7) [1] and the migration of $\Delta^{8}$ double bond (*b*) to $\Delta^{5}$ via $\Delta^{7}$ and the $\Delta^{5,7}$ diene (Scheme 9.7) [1].



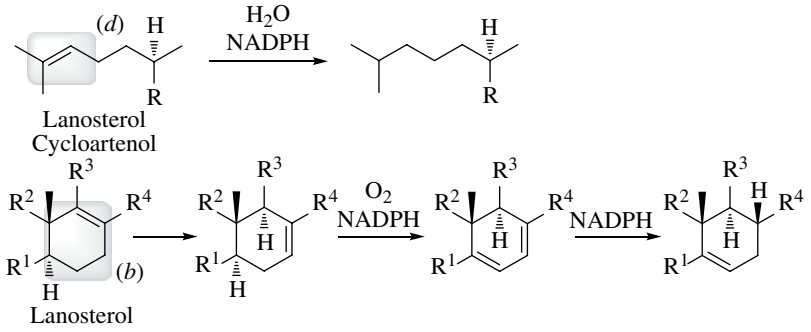

**SCHEME 9.4** Biosynthesis of cholesterol from lanosterol and cycloartenol.




**SCHEME 9.5** The loss of the methyl group (*a*) at C-14 of lanosterol and cycloartenol.




**SCHEME 9.6** The loss of the methyl groups (*c*) at C-4 of lanosterol and cycloartenol.




**SCHEME 9.7** The reduction of $\Delta^{24}$ double bond (*d*) and migration of $\Delta^{8}$ double bond (*b*) at C-4 of lanosterol and cycloartenol.

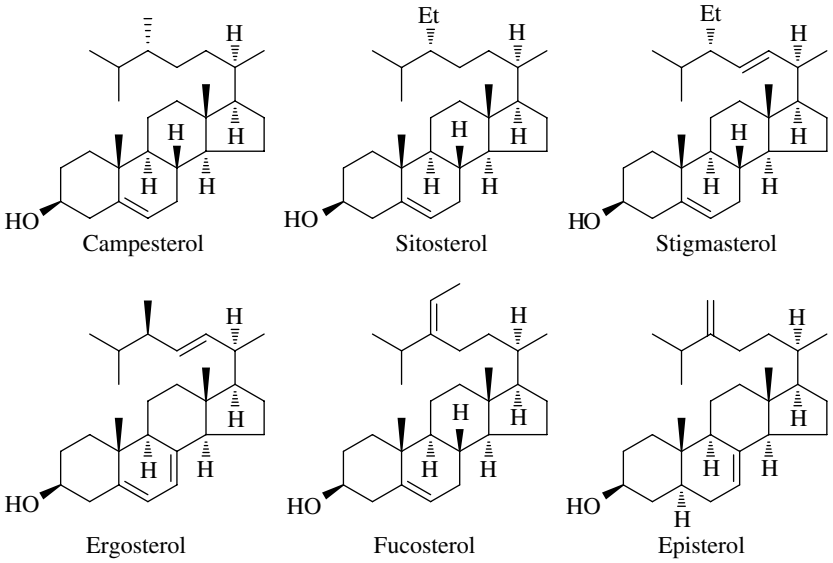



**FIGURE 9.1** Phytosterols.

The latter sequence involves an allylic isomerization, a dehydrogenation and a reduction. Newly introduced protons at C-9 and C-8 originate from water and that at C-7 from NADPH.

The role of lanosterol in nonphotosynthetic organisms (animals, fungi) is taken in photosynthetic organisms (plants, algae) by its cyclopropane triterpenoid counterpart cycloartenol (Scheme 9.4) [1]. This cyclopropane moiety is found in a number of plant sterols, but majority steroids contain the normal methyl at C-10. Thus, additional biosynthetic mechanisms exist to reopen the cyclopropane ring when necessary. The observed stereochemistry at C-8 (Hβ) in these compounds is unfavorable for a concerted mechanism involving the loss of H-8 with concomitant cyclopropane ring opening. To address this observation, an enzymic nucleophilic cyclopropane opening is suggested followed by the incorporation of a proton from water. A *trans* elimination then generates the $\Delta^8$ double bond. The high specificity of the cyclopropane ring-opening enzyme concludes the inability of cycloartenol to be converted into lanosterol, and lanosterol is thus absent from virtually all plant tissues. Although cholesterol is almost always present in plants, though often in trace amounts, its formation is attributed via the transformation of cycloartenol (Scheme 9.4).

On the other hand, the major sterol found in mammals is cholesterol, which acts as a precursor for other steroid structures such as sex hormones and corticosteroids. The main sterols in plants, fungi, and algae are characterized by extra one-carbon or two-carbon substituents on the side chain, attached at C-24 as shown in Figure 9.1. The source of this extra methyl or ethyl side-chain carbons in both cases is *S*-adenosylmethionine (SAM) and to achieve alkylation the side chain must have a $\Delta^{24}$ double bond, that is, the side chains seen in lanosterol and cycloartenol.

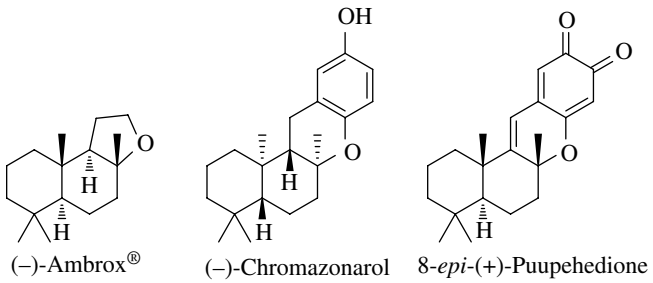



**FIGURE 9.2** Polycyclic terpenoids.

Optically active polycyclic compounds have broad range of useful properties, which makes them valuable for industrial and pharmacological applications. For example, (−)-Ambrox® has a strong amber-like aroma. It is used in place of one of the constituents of ambergris, which is a metabolic product found in the gut of sperm whale [3]. Some marine natural secondary metabolites, such as (−)-chromazonarol [4], 8-*epi*-(+)-puupehedione [5], and their derivatives, are also known to show a wide range of potent biological activities, including cytotoxic, antiviral, antifungal, and immunomodulatory properties (Fig. 9.2) [6].

Many polycyclic natural compounds that contain bromine atoms have been isolated from several different marine organisms (Fig. 9.3) [7, 8]. Most of them possess bioactivities of pharmacological interest such as antibacterial, anticancer, antifungal, anti-inflammatory, and antiviral activities. Natural products that have an α-bromo-β,β-dimethylcyclohexane structure are also bioactive compounds. Their biosynthesis

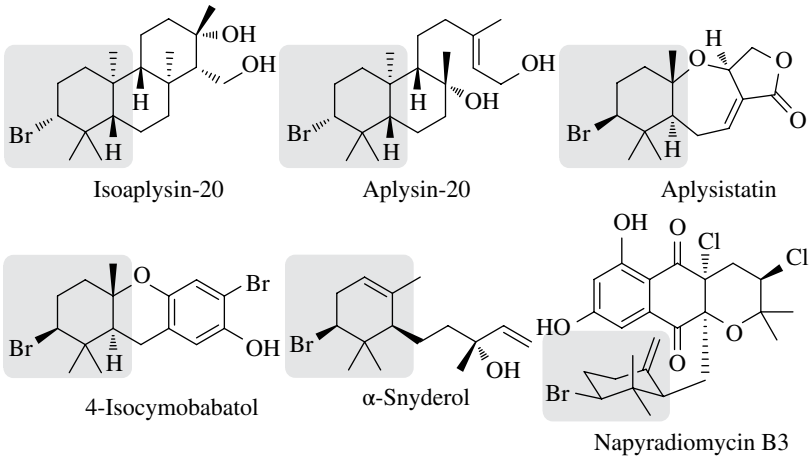
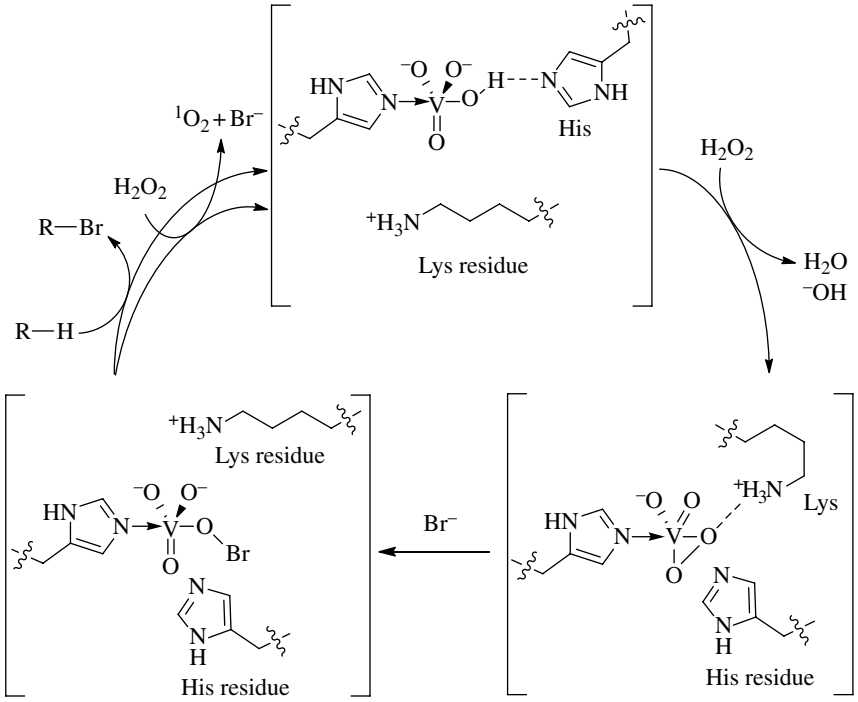



**FIGURE 9.3** Bromine-containing natural products.




**SCHEME 9.8** Proposed catalytic mechanism for V-BPO.

appears to be initiated by electrophilic bromination at the terminal olefin of polyprenoids in the chiral cavity of enzymes [9, 10]. Subsequent diastereoselective polycyclization gives bromine-containing natural products. Since several new quaternary and tertiary stereocenters and new rings are formed in one step, bromonium ion-induced polyene cyclization can be envisaged as one of the most efficient biosynthetic polycyclization reactions.

Vanadium haloperoxidases (V-HPO) promote the oxidation of halides (chloride, bromide, and iodide) and the electrophilic halogenation of organic compounds. Vanadium bromoperoxidases (V-BPO) have been considered to be the predominant enzymes for the bromocyclization of polyprenoids. The vanadium active center of V-BPO acts as a Lewis acid and oxidizes a halide with $H_2O_2$. A proposed catalytic mechanism for V-BPO is shown in Scheme 9.8 [9, 10b].

In the first stage, one equivalent of $H_2O_2$ coordinates to the resting vanadium(V) state to form the oxoperoxovanadium(V) intermediate. The oxoperoxovanadium(V) intermediate is proposed to oxidize the bromide ($Br^-$) by two electrons and generate a bromonium ion ($Br^+$)-type intermediate. A Lys side chain is proposed to play a crucial role in the catalytic reaction because it would increase the potential of the oxoperoxovanadium(V) intermediate for the

oxidation of bromides. The electrophilic halogenation of organic substrates with a bromonium ion-type intermediate affords the brominated compounds. In the absence of organic substrates, the electrophilic halogenation of a second equivalent of $H_2O_2$ gives the singlet oxygen and the bromide anion. While an extra His residue does not interact directly with the vanadium center, it has been proposed that the His side chain participates as a proton donor and acceptor during the catalytic cycle and could affect the overall oxidation potential of the oxoperoxovanadium(V) intermediate.

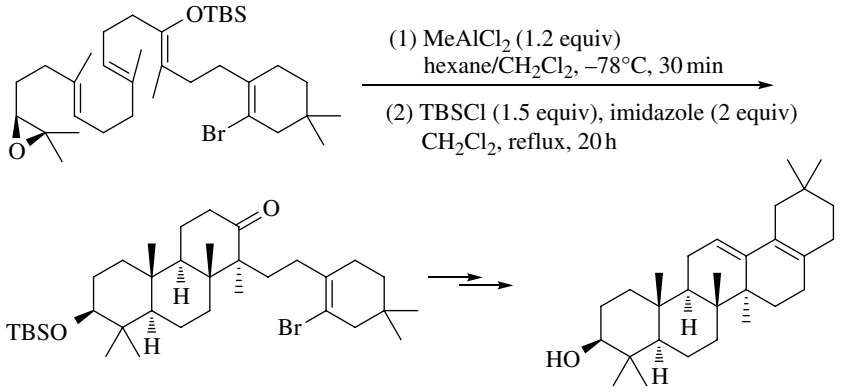
## 9.3 CASCADE POLYENE CYCLIZATIONS

The chemical simulation of this biosynthetic process has been developed as an important methodology in organic synthesis. Van Tamelen reported the acid-catalyzed cyclization of chiral terminal epoxides of polyprenoids [11]. In contrast, Johnson adopted the acid-catalyzed cyclization of polyprenic acetals derived from chiral diols [12]. In addition to these pioneering studies, the biomimetic polyene cyclizations of polyprenoids, which are induced by a variety of electrophiles such as proton, oxonium ion, halonium ion [13], or metal ion [14], have also been developed. Despite extensive studies on these diastereoselective olefin cyclizations, enantioselective processes using synthetic chiral catalysts had not been developed for a long time. In 1999, Yamamoto's group reported the first enantioselective biomimetic polycyclization of polyprenoids using a tin(IV) chloride-chelated chiral binaphthol derivative, which is called a Lewis acid-assisted chiral Brønsted acid (chiral LBA) [15a]. Since then, the enantioselective biomimetic olefin cyclization has received great attention, and several methods have been developed. In this section, recent progress on the stereoselective polyene cyclizations is overviewed.

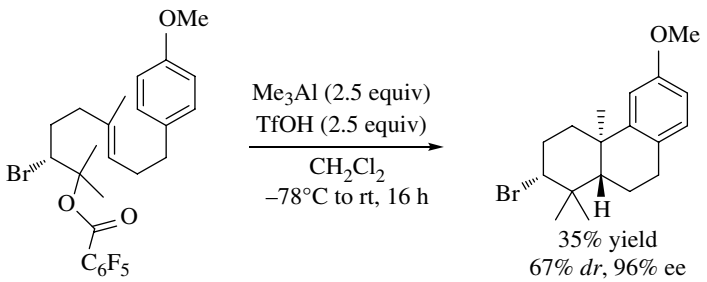
### 9.3.1 Diastereoselective Polyene Cyclizations

According to the Stork–Eschenmoser hypothesis [1b, c], many polycyclic terpenoids such as hopene and lanosterol are biosynthesized via the site- and enantioselective protonation or epoxidation of a terminal olefin followed by diastereoselective π-cation cyclization [16]. Corey's group performed pioneering work on the cation-induced diastereoselective polycyclization of enantiopure epoxides [17]. For example, a very direct enantioselective total synthesis of members of the β-amyrin family of pentacyclic triterpenes has been developed by diastereoselective π–cation tricyclization reaction as a key step (Scheme 9.9) [17g].

In 2013, Braddock's group reported that enantiospecific polyene cyclization was initiated by the formation of an enantiopure bromiranium ion (Scheme 9.10) [18]. Enantiopure bromohydrin esters were synthesized from the corresponding olefins in a three-step sequential reaction. The reaction gave




**SCHEME 9.9** Diastereoselective polycyclization of enantiopure epoxide.



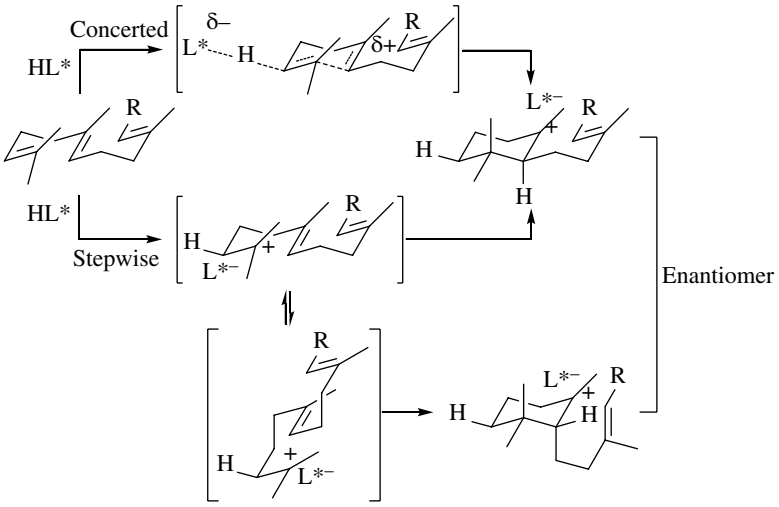

**SCHEME 9.10** Diastereoselective polycyclization.

the dicyclized products when treated with a mixture of Lewis and protic acids without a loss of enantiomeric excess despite the low yield and diastereoselectivity.

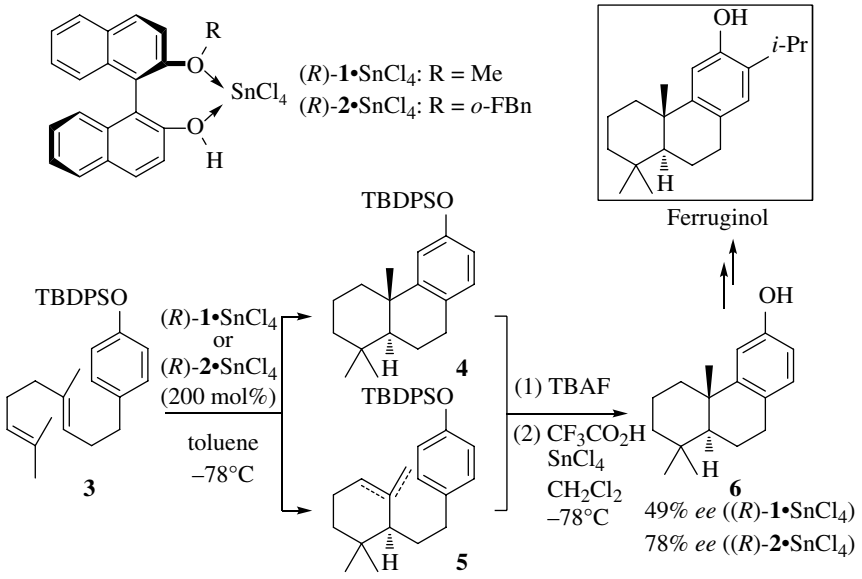
### 9.3.2 "Chiral proton ($H^+$)"-Induced Polyene Cyclizations

Well-designed chiral Brønsted acid ($HL^*$) were found to adequately discriminate the enantioface of the terminal isoprenyl group of linear polyprenoids, leading to high enantioselective protocyclizations when concerted reactions were occurred. On the other hand, when stepwise pathway is thermodynamically preferred, the enantioselectivity is amenable to lower *ee*'s (Scheme 9.11).

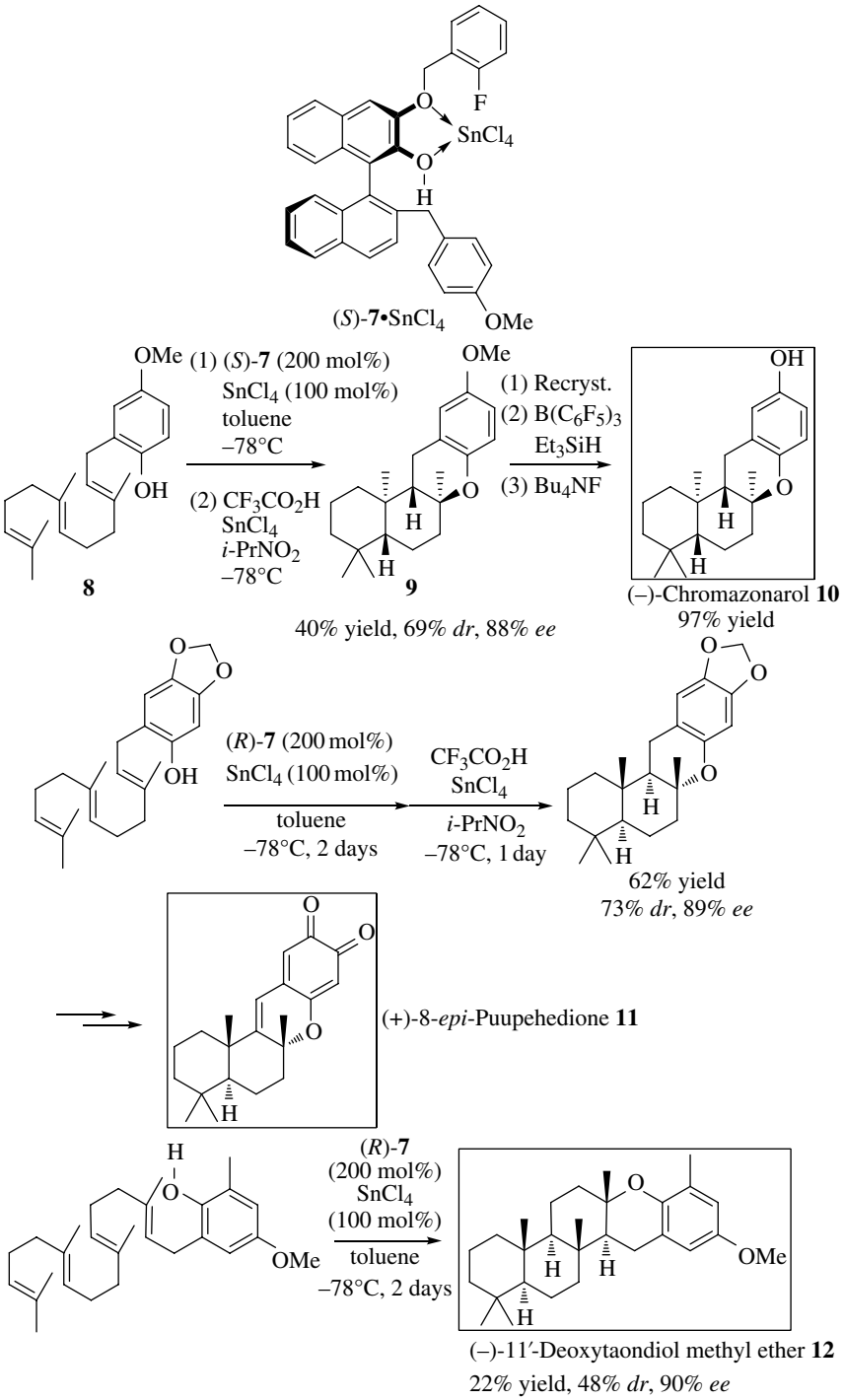
Yamamoto's group developed the first enantioselective biomimetic polyene cyclization in 1999 [15a]. In this pioneering study, Lewis acid-assisted chiral Brønsted acid (chiral LBA) **1**·$SnCl_4$ was used as an artificial cyclase of an array of linear polyprenoids (Scheme 9.12). The enantioselectivity of this cyclization was further improved in 2002 by using chiral LBA **2**·$SnCl_4$, as highlighted by the synthesis of (−)-Ambrox®, which was synthesized from (*E*,*E*)-homofarnesyl triethylsilyl ether in 54% yield with 75% *ee* and 76% *ds*. Furthermore, the same group applied **2**·$SnCl_4$ to the enantio- and diastereoselective stepwise cyclization of polyprenoids with an aromatic ring as the terminating group instead of a hydroxyl terminator. Thus, **2**·$SnCl_4$ is effective for achieving absolute stereocontrol in




**SCHEME 9.11** Enantioselective protocyclization of a linear polyprenoid with chiral Brønsted acid.



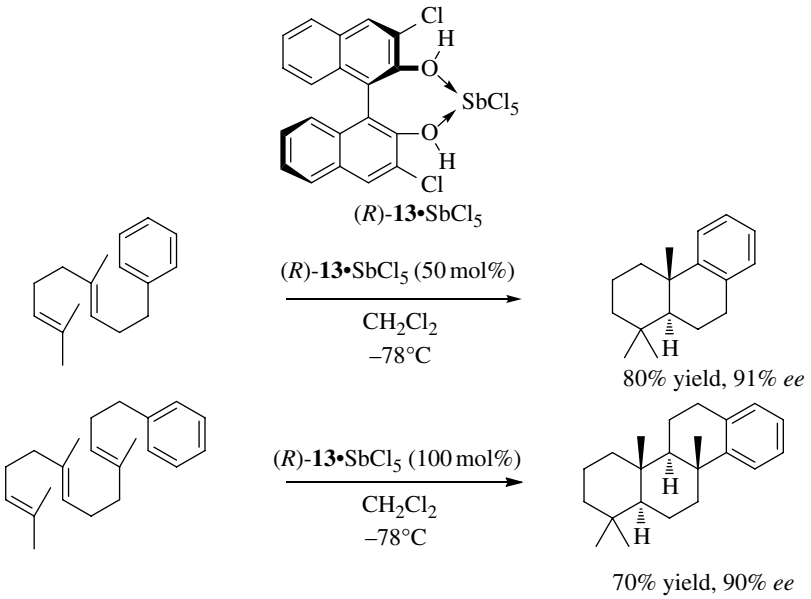

**SCHEME 9.12** Enantioselective polyene cyclization promoted by LBA.



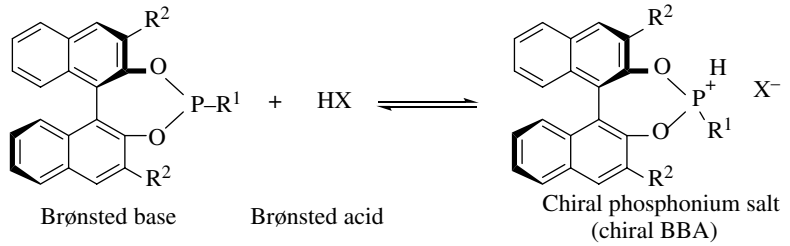

**SCHEME 9.13** Enantioselective polyene cyclization promoted by LBA **7**·$SnCl_4$.

the initial cyclization of 4-(homogeranyl)phenol derivative **3** to produce AB-ring product **4** together with *endo*- and *exo*-isomeric A-ring products **5**. After the TBDPS group was removed from the mixture of **4** and **5**, the treatment with achiral LBA ($CF_3CO_2H$, $SnCl_4$) promoted diastereoselective cyclization of the B-ring and gave the desired AB-ring product **6** (R′ = H) in 94% yield (three steps from **3**) with 78% *ee*. This method provides the first route to enantioenriched ferruginol (R′ = *i*-Pr), since (±)-**6** (R′ = H) has already been converted into racemic ferruginol by King's [19] and Ghatak's group [20].

In 2004, Yamamoto–Ishihara's group designed a new artificial cyclase **7** and used it for the efficient synthesis of (–)-chromazonarol (**10**) (Scheme 9.13) [15g]. The five-membered




**SCHEME 9.14** Enantioselective polyene cyclization promoted by LBA **13**·$SbCl_5$.



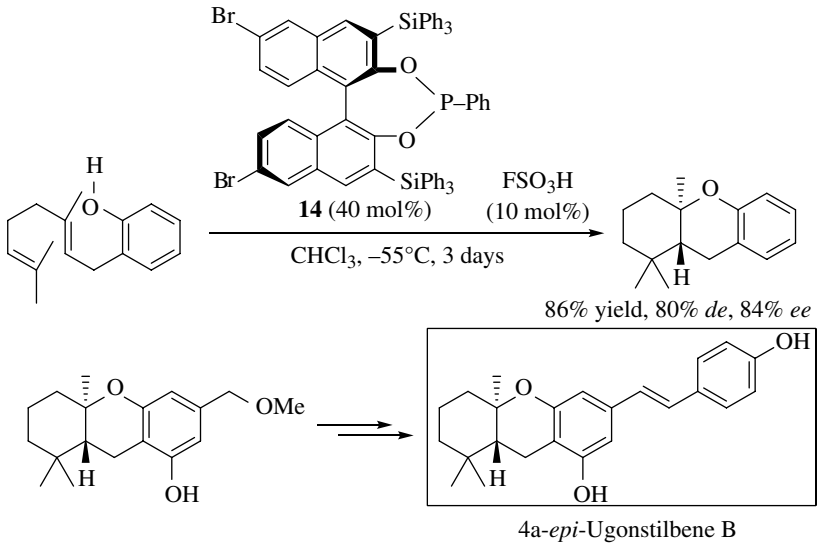

**SCHEME 9.15** Design of chiral Brønsted base-assisted Brønsted acids (chiral BBAs).

chelation structure formed by 2-alkoxyphenol and $SnCl_4$ was found suitable for its use as an LBA. Reaction of **8** with **7** and the subsequent treatment with $CF_3CO_2H$ and $SnCl_4$ gave tetracyclic compound **9** in 40% yield with 69% *dr* and 88% *ee*, while the use of catalyst **2** instead gave **9** in 25% yield with 55% *dr* and 40% *ee*. Compound **9** was converted to (−)-**10** in 97% yield with 83% *dr* and 91% *ee* after recrystallization and reductive removal of the methyl protection. The same logic was further demonstrated by the same group in the syntheses of (+)-8-*epi*-puupehedione (**11**), a key synthetic intermediate of (+)-wiedendiol, and (−)-11′-deoxytaondiol methyl ether (**12**).

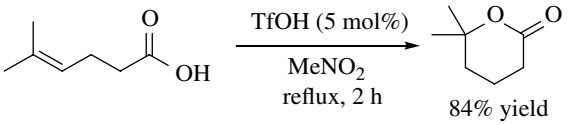
In 2012, LBA system was improved by the combined use of $SbCl_5$, which was a stronger Lewis acid than $SnCl_4$ and (*R*)-3,3′-dichlorobinaphthol **13** by Corey's group (Scheme 9.14) [21]. The enantioselective polycyclization of homogeranylarenes and homofarnesylarenes proceeded at −78°C in $CH_2Cl_2$ with reaction times in the range of 4–6 h and provided the polycyclic products with remarkable enantioselectivity, generally in the range 20–50 : 1. In all cases 50–100 mol% of catalyst was used. Further studies revealed that $SbCl_5$ was far superior to $InCl_3$, $AlCl_3$, and $TiCl_4$ in terms of reaction rate and enantioselectivity.

Ishihara's group designed chiral Brønsted base-assisted Brønsted acids (chiral BBAs), phosphonium salts [22], which were prepared from a chiral phosphorus(III) compound with an achiral Brønsted acid (HX) (Scheme 9.15) [23a]. The chiral phosphorus(III) compound as a Brønsted base could coordinate to the proton of the achiral Brønsted acid to provide phosphonium salts. Since the active proton of that phosphonium salt is surrounded by the chiral environment of the chiral phosphorus(III) compound, they envisioned that this catalytic system might facilitate a highly enantioselective transformation. Notably, the Brønsted acidity of chiral BBAs should strongly depend on the structure of the chiral phosphorus(III) compound. Therefore, chiral BBAs with suitable acidity should appropriately control asymmetric induction in the protonation of the isoprenyl group through the biomimetic cyclization of simple isoprenoids.

Ishihara's group explored the enantioselective cyclization of simple isoprenoids catalyzed by chiral Brønsted acids and sought to achieve a short-step synthesis of natural compounds using chiral cyclization products. First, they designed chiral BBAs as new chiral Brønsted acid catalysts for enantioselective cyclization. As a result of this investigation, they




**SCHEME 9.16** Enantioselective cyclization of 2-geranylphenols catalyzed by chiral BBA **14**·$FOSO_3H$ and synthesis of 4a-*epi*-ugonstilbene B.



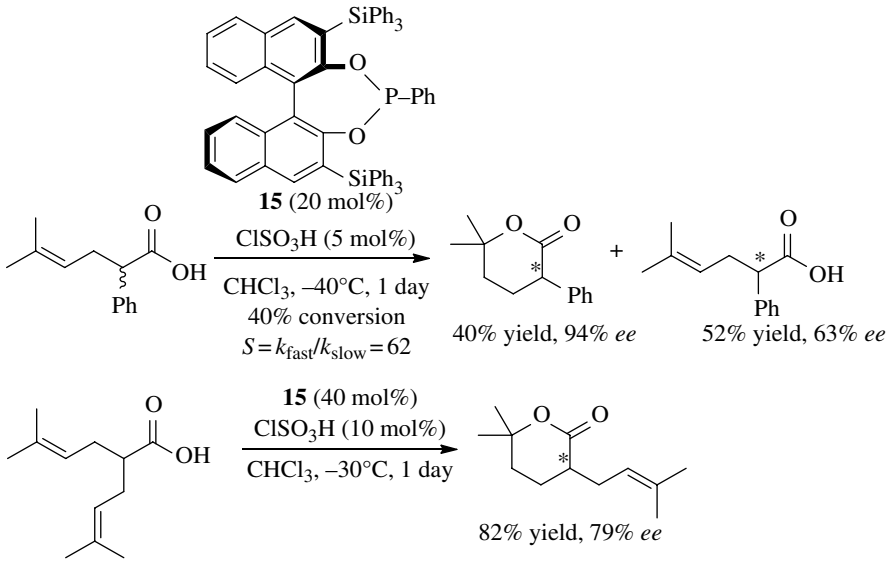

**SCHEME 9.17** Cyclization of unsaturated carboxylic acids catalyzed by TfOH.

found that chiral phosphonium salt **14**·$FOSO_3H$, which was prepared from a chiral phosphorus(III) compound **14** and an achiral Brønsted acid $FSO_3H$, catalyzed the enantioselective cyclization of 2-geranylphenols (Scheme 9.16) [23a]. Next, they conducted a short-step synthesis of natural compounds using this BBA-catalyzed cyclization system. Cyclized products were useful chiral building blocks for the synthesis of various bioactive natural compounds [24]. The four-step conversion of chiral cyclized products gave 4a-*epi*-ugonstilbene B [25].

The intramolecular cyclization of unsaturated carboxylic acids is one of the most straightforward routes to the synthesis of lactones, which leads directly to the desired products. In general, electrophilic reagents such as iodine, phenylselenium chloride, and mercuric or palladium salts promote this cyclization [26]. However, a second step is necessary to remove the reagent. Although the cyclization of unsaturated carboxylic acids promoted by a Brønsted acid is a well-known reaction, it occurs mostly with more than stoichiometric quantities of a Brønsted acid [27]. On the other hand, it was reported that a variety of substituted γ- and δ-lactones could be easily prepared from unsaturated carboxylic acids in excellent yields using trifluoromethanesulfonic acid (TfOH) as a catalyst (Scheme 9.17) [28]. However, applications of this method, such as an asymmetric version, are limited because these reactions require harsh conditions. While there is a growing number of chiral Brønsted acid catalysts, the chiral proton-induced lactonization of unsaturated carboxylic acids is still rare [29]. This is mainly due to the low nucleophilicity of the carboxyl group and the higher proton affinity of a carboxyl group compared to unactivated alkenes.

Some chiral resolving agents have been developed for the derivatization of racemic carboxylic acids to form pairs of diastereomers, which can be separated by conventional methods such as recrystallization. However, in some cases, this process requires several repetitions of salt formation between a carboxylic acid and an amine followed by recrystallization and subsequent separation of the chiral auxiliaries from the acid component to obtain a pure enantiomer. On the other hand, the conversion of a racemic substrate to enantioenriched products, commonly referred to as a kinetic resolution, is also an established method with broad applications [30, 31].

Ishihara's group explored the enantioselective reaction catalyzed by a chiral BBA, which could recognize an enantioface of a terminal isoprenyl group [23]. With regard to asymmetric protocyclization reactions, they envisioned that the chiral BBA-promoted method could be applied to the kinetic resolution of racemic unsaturated carboxylic acids via asymmetric protolactonization. Such a reaction system could lead to a novel and effective approach for providing optically active carboxylic acids and lactones without the generation of by-products derived from activating reagents. As a result of this investigation, Ishihara's group found that chiral BBA **15**·$ClSO_3H$ promoted the kinetic resolution of racemic α-substituted carboxylic acids through asymmetric protolactonization (Scheme 9.18) [23b]. This reaction gave




**SCHEME 9.18** Kinetic resolution and desymmetrization catalyzed by chiral BBA **15**·$ClSO_3H$.

cyclization products (lactones) and the recovered starting materials (carboxylic acids) with high selectivities and high *S* values. This method was applied to the desymmetrization of unsaturated carboxylic acids. The desymmetrization of carboxylic acids catalyzed by chiral BBA **15**·$ClSO_3H$ through asymmetric protolactonization gave the desired lactones in good yield with good enantioselectivity (Scheme 9.18) [23b].

### 9.3.3 "Chiral Metal Ion"-Induced Polyene Cyclizations

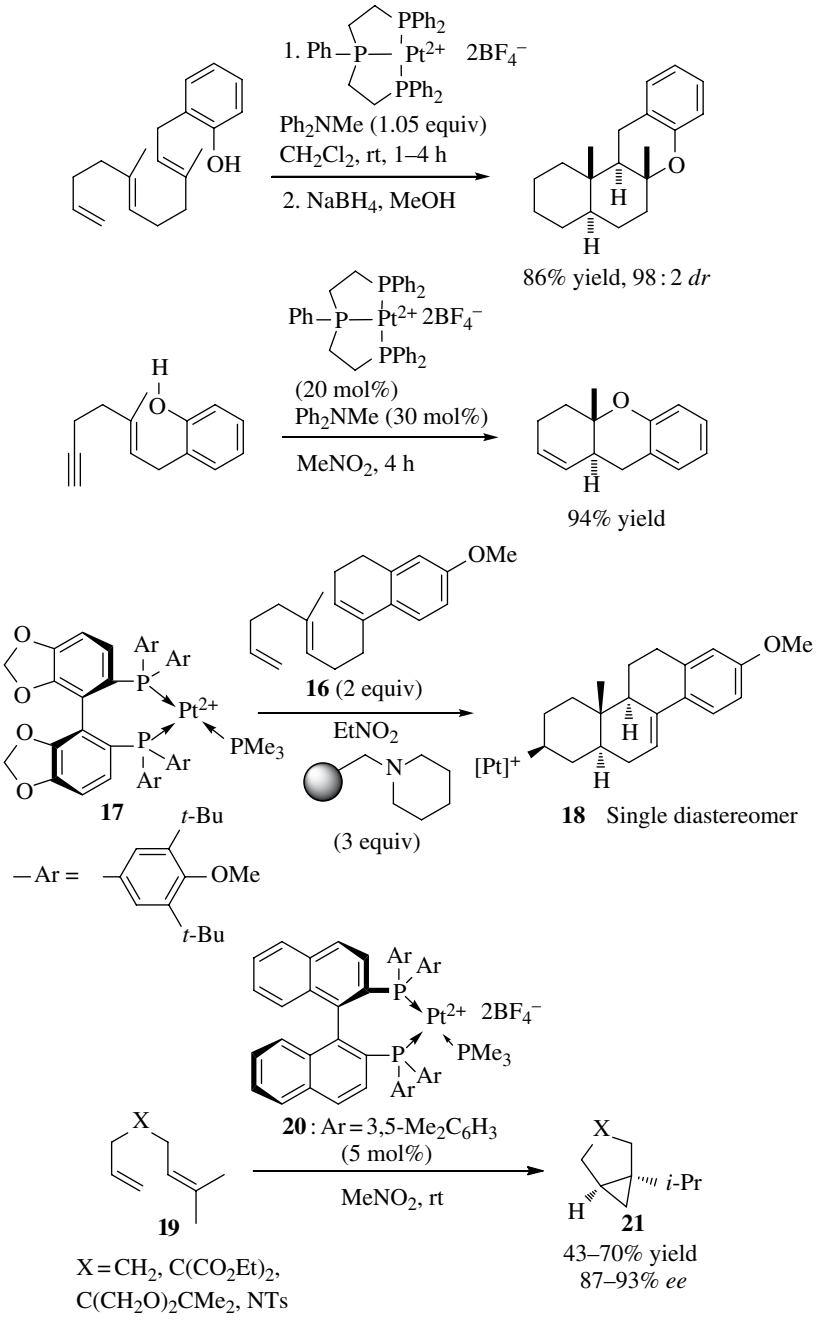
Gagné's group developed an electrophilic polycyclization of *o*-(homogeranyl)phenol and *o*-(homofarnesyl)phenol, using [(PPP)Pt]$(BF)_2$, a dicationic Pt(II) complex with tridentate phosphine ligand (PPP = triphos), to give dicyclized and tricyclized products with high diastereoselectivities (>98% *ds*) (Scheme 9.13) [32a–c]. In contrast, 20 mol% of [(PPP)Pt]$(BF)_2$ catalyzed the cycloisomerization of 1,5-enyne-ols by initiative π-activation of the alkyne moiety (Scheme 9.19) [32d]. In the cyclization of **16** with chiral Pt(II) complex **17**, polycyclic product **18** was obtained as a single diastereomer (Scheme 9.19) [32e]. They also reported the diastereoselective cycloisomerization of 1,6- and 1,7-dienes to give bicyclic cyclopropanes [32f, g]. In a recent study, they designed new dicationic Pt(II) catalysts that contained diphosphine/monophosphine combinations as ligands to improve the catalytic activities. Furthermore, they achieved the enantioselective cycloisomerization of 1,6-dienes **19** using chiral complex **20** to give bicyclic products **21** with 87–93% *ee* (Scheme 9.19) [32h].

Bromine-containing polycyclic terpenoids are also considered to be biosynthesized via the site- and enantioselective bromination of a carbon–carbon double bond followed by diastereoselective π-cation cyclization. While several cation-induced enantioselective polyene cyclizations have been reported, the bromonium ion-induced polyene cyclization is very rare, since, in addition to the primary difficulty of polyene cyclization, which involves low reactivity and low stereoselectivity, the racemization of enantiopure bromiranium ion via inter- or intramolecular bromiranium ion-to-olefin transfer must be avoided. To overcome these problems, stepwise methods that require more than two steps have been reported by some groups.

In 2010, Snyder's group reported the Hg(II)-induced polyene cyclization and bromination of polyprenoids (Scheme 9.20) [33], which has a reaction mechanism similar to that in Gagné's polyene cyclization/fluorination reaction (Scheme 9.21). The combination of 1.2 equiv of chiral bis(oxazoline) ligand (Box) and 1.1 equiv of $Hg(OTf)_2$ followed by treatment with aqueous sodium bromide generated the organomercury bromide. Subsequent treatment with $Br_2$ in oxygenated pyridine gave bromine-containing polycyclic products in high yield with high enantioselectivity.

In 2007, Gagné's group succeeded in a regio- and diastereoselective oxidative polycyclization of di- and trienols catalyzed achiral [(dppe)Pt] dications, wherein turnover was achieved by the trityl cation abstracting a hydride from a putative $[(dppe)Pt\text{-}H]^+$ intermediate [32i]. One year later, Gagné's group developed the catalytic enantioselective polyene cyclization induced by [(*S*)-(xylyl-PHANEPHOS)Pt][$(BF_4)_2$] catalyst, which was prepared from (*S*)-(xylyl-PHANEPHOS)$PtI_2$ and $AgBF_4$ *in situ* (Scheme 9.21) [32j]. This asymmetric catalysis enables the oxidative cascade cyclization of polyalkene substrates [32k] (Scheme 9.15).

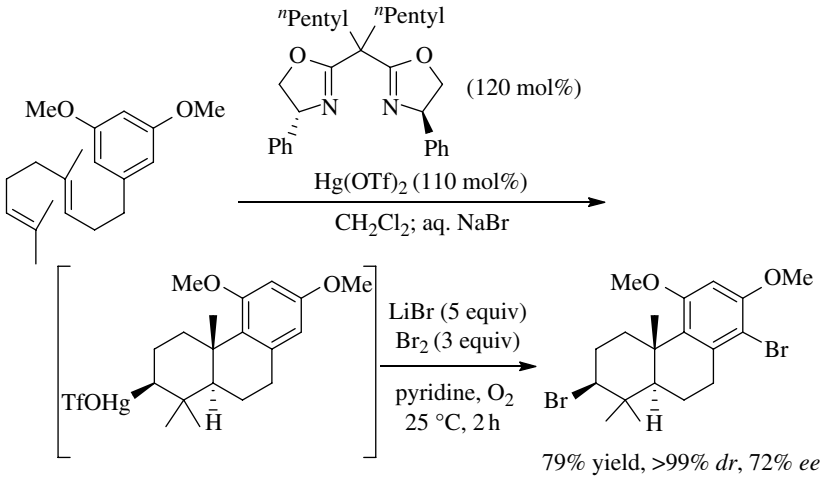
In 2013, Gagné's group demonstrated catalytic enantioselective polyene cyclization and C3-fluorination for



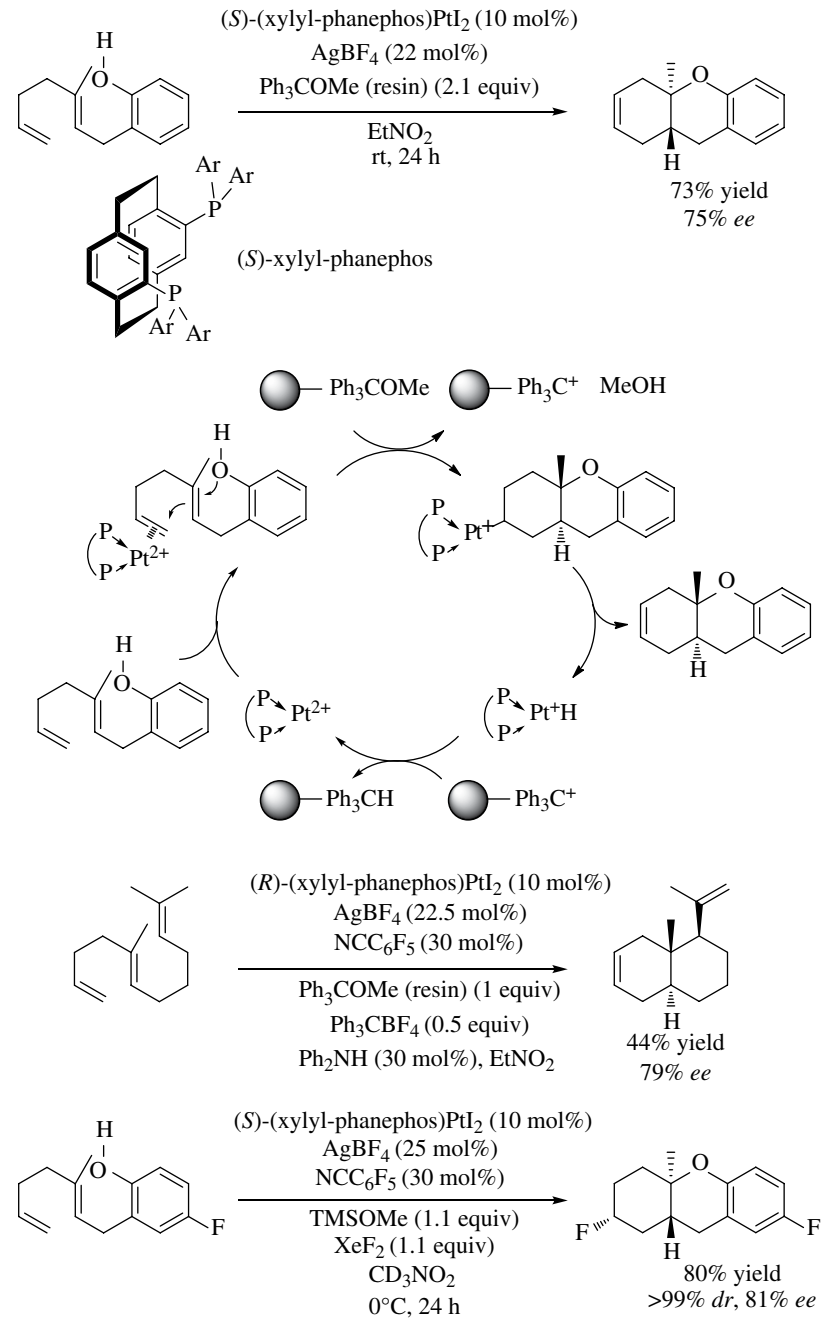

**SCHEME 9.19** Enantioselective polyene cyclizations promoted by dicationic Pt(II) complexes.

fluorine-containing polycyclic products [32l, m]. The combination of (*S*)-(xylyl-PHANEPHOS)$PtI_2$, $AgBF_4$, and $NCC_6F_5$ generated the active [(*S*)-(xylyl-PHANEPHOS)$Pt(NCC_6F_5)_2$] [$(BF_4)_2$] catalyst. This active catalyst induced enantioselective polyene cyclization and the organoplatinum intermediates were formed. Subsequent reaction of the organoplatinum intermediates with $XeF_2$ generated the fluorine-containing polycyclic products (Scheme 9.21).

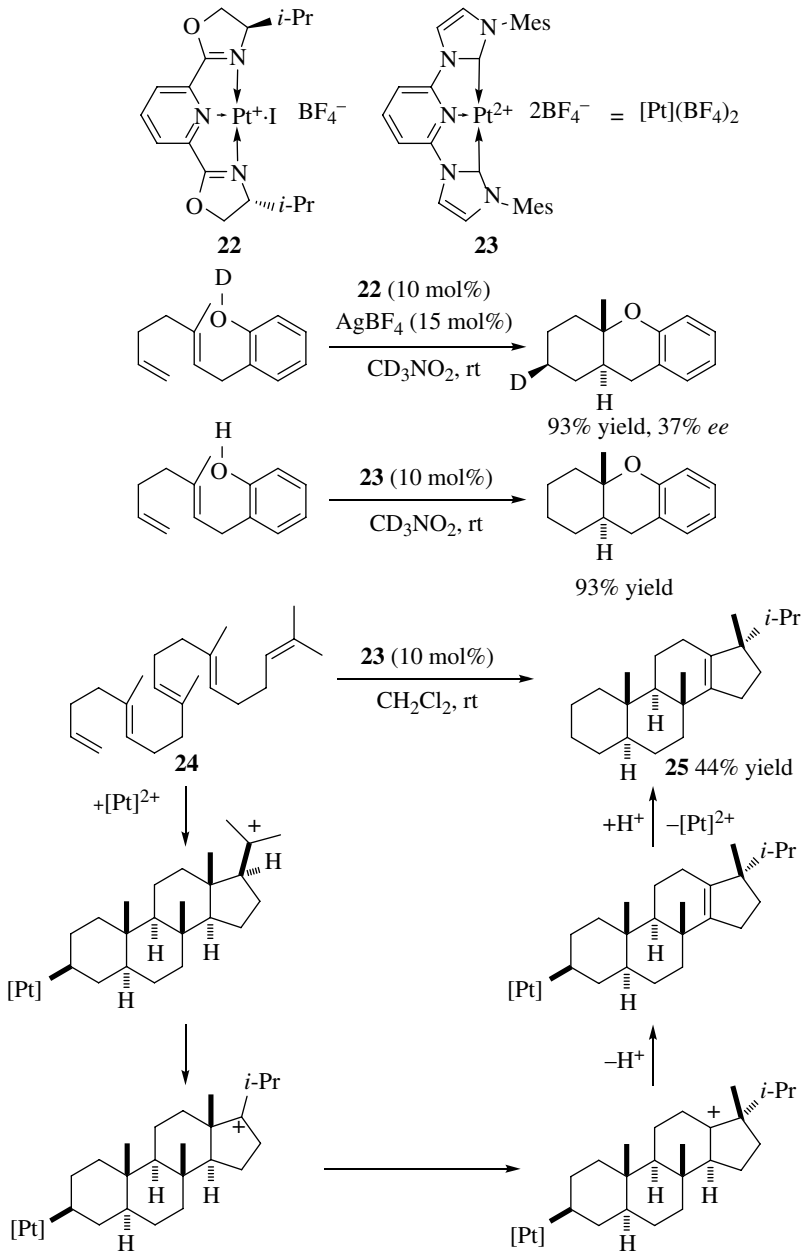
Gagné's group also has developed chiral platinum–pybox complex **22** that is capable of the cyclization/protonation of polyenes to polycyclic structures with good yield, high diastereoselectivity, and moderate enantioselectivity (Scheme 9.22) [32n]. This study suggests that changes in the hard/soft character of the ligands can significantly increase the tendency for (oxidatively induced) protodemetalative reactions at a cationic Pt(II) center. Furthermore, platinum–tridentate NHC containing pincer ligand complex **23** is more effective than **22** for the catalytic, diastereoselective cycloisomerization of biogenic alkene terminated substrates to the polycyclic counterparts (Scheme 9.22) [32o]. Cyclization of **24**




**SCHEME 9.20** Stepwise enantioselective bromocyclization.




**SCHEME 9.21** Chiral Pt(II)-induced enantioselective polyene cyclizations.

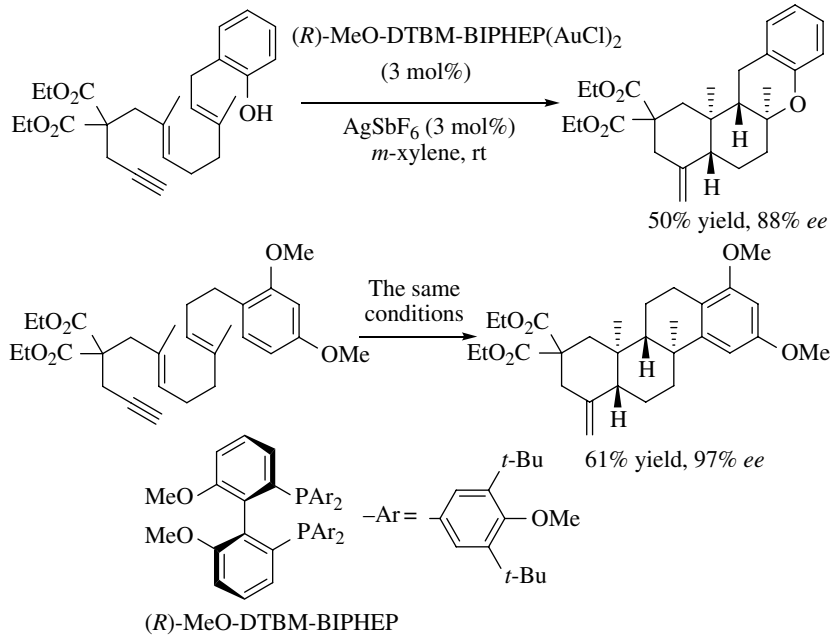



**SCHEME 9.22** Chiral Pt(II)-induced stereoselective polycyclization/protodemetalation.

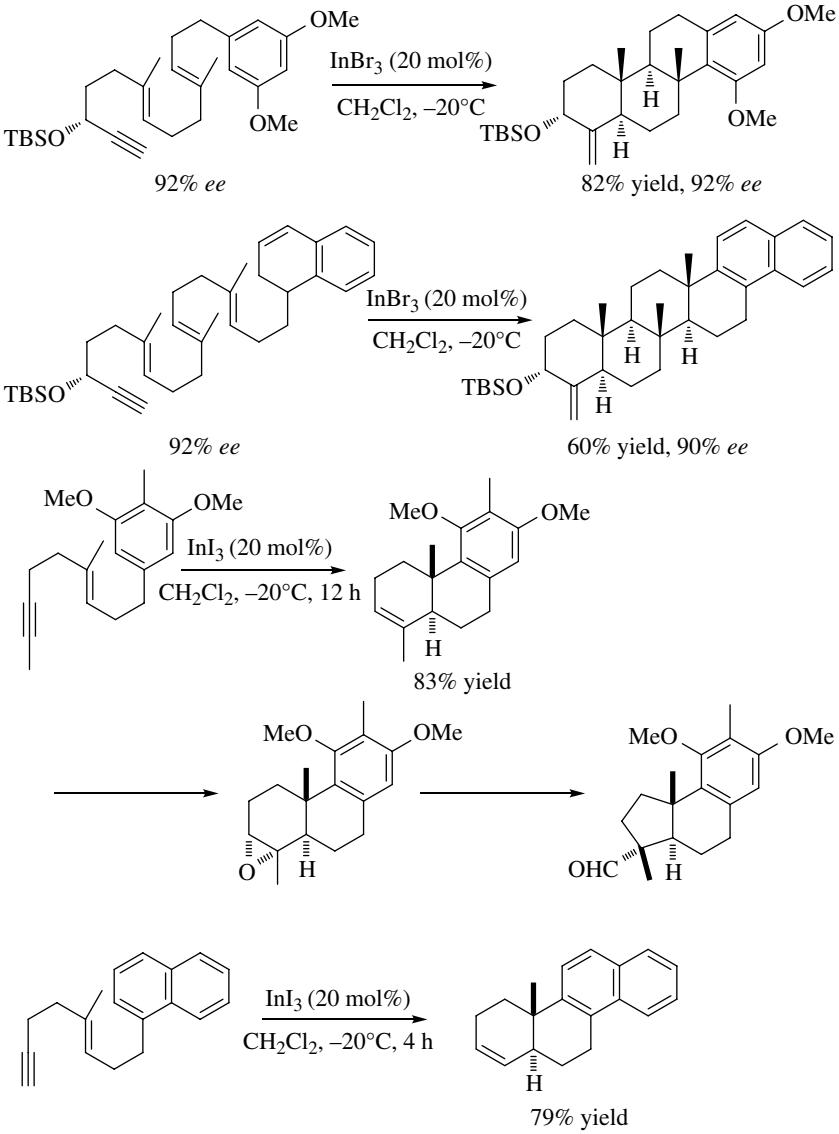
provided the tetracycle **25** in 44% yield, forming five stereocenters and providing the 6–6–6–5 sterol framework in a single step. Initial cyclization terminates the D-ring in a 5-exo manner to generate an exocyclic tertiary cation akin to the protosterol cation observed in the conversion of 2,3-oxidosqualene to lanosterol.

In 2010, Toste's group reported the first example of a highly enantioselective polyene cyclization reaction in which transition metal-promoted alkyne activation serves as the cyclization initiating event [34]. The (MeO-DTBM-BIPHEP)gold(I)-catalyzed reaction offers an efficient method for the stereoselective synthesis of polycyclic compounds whose stereochemistry is consistent with the Stork–Eschenmoser postulate for polyene cyclization (Scheme 9.23). In this context, a number of nucleophile can be used to terminate the reaction and therefore carbo- and heterocyclic structures can be accessed.

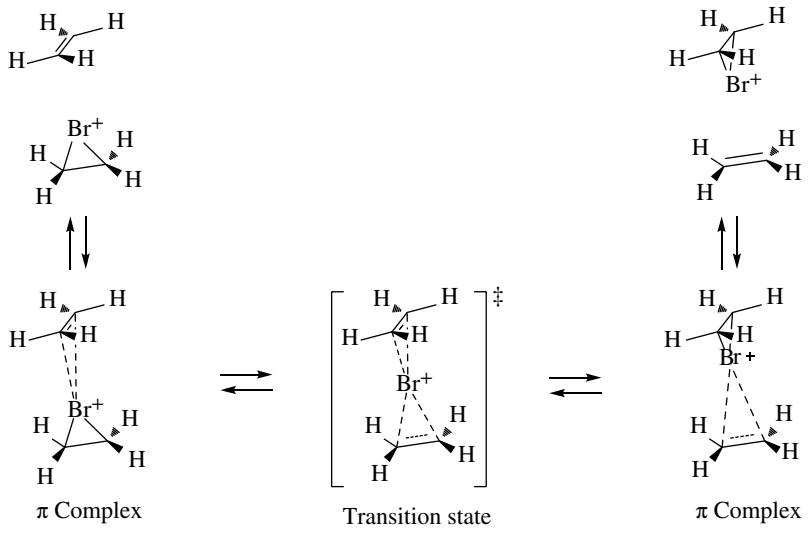
In 2011, Corey's group found that $InI_3$ and $InBr_3$ were effective catalysts for the π activation of C≡C triple bonds to initiate the conversion of chiral propargylic alcohols or silyl ethers to polycyclic products in excellent yields with high stereoselectivity (Scheme 9.24) [35]. The method was applied to the synthesis of chiral fused hexacyclic ring systems with the creation of multiple new stereocenters.




**SCHEME 9.23** Chiral Au(I)-induced enantioselective polyene cyclizations.




**SCHEME 9.24** Diastereoselective polycyclization catalyzed by In(III).




**SCHEME 9.25** Mechanism of bromiranium ion transfer between two ethylenes.

The power and scope of the method have been illustrated by a variety of examples. Obviously, In(III) catalysis is far superior to the use of heavy metals such as Ag(I), Hg(II), Au(I) in terms of cost, lack of toxicity, and intrinsic effectiveness.

### 9.3.4 "Chiral Halonium Ion ($X^+$)"-Induced Polyene Cyclizations

A variety of polycyclic bioactive natural products that contain halogen atoms have been isolated from different marine organisms [36]. The biosynthesis of these natural products appears to be initiated by an electrophilic halogenation reaction at a carbon–carbon double bond via a mechanism that is similar to a proton-induced olefin polycyclization [10]. Enzymes such as haloperoxidases generate an electrophilic halonium ion (or its equivalent), which enantioselectively reacts with the terminal carbon–carbon double bond of the polyprenoid, diastereoselectively inducing a cyclization reaction that produces a halogenated polycyclic terpenoid. The use of an enantioselective halocyclization reaction is one possible way to chemically synthesize these halogenated cyclic terpenoids. Although, several brominated cyclic terpenoids have been synthesized via a diastereoselective halocyclization reaction that uses stoichiometric quantities of a brominating reagent [13], the enantioselective halocyclization of polyprenoids induced by a chiral promoter has not yet been reported. Recently, Ishihara's group developed the enantioselective iodocyclization of simple polyprenoids using a nucleophilic promoter [37a]. This is the first successful example of the enantioselective iodopolycyclization of simple polyprenoids. In 2003, Kang's group reported the catalytic enantioselective intramolecular iodoetherification of γ-hydroxy-*cis*-alkenes [38]. The electrophilic iodination of a *cis*-olefin with iodine promoted by a chiral Lewis acid catalyst induced the cyclic ether formation to give 2-substituted tetrahydrofurans with high enantioselectivities.

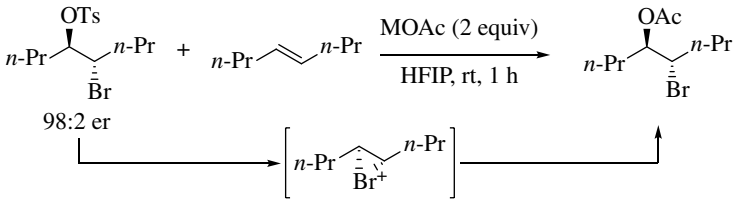
The electrophilic addition of a halogen to an olefin usually proceeds via cyclic halonium (haliranium) ion intermediates [39]. Brown's group investigated the reaction mechanism of halocyclization. They demonstrated that $Br^+$ and $I^+$ transfer rapidly from the haliranium ions of adamantylidene adamantine to other olefins [40]. Calculations of bromiranium ion transfer between two ethylenes revealed the reaction mechanism illustrated in Scheme 9.25.

In 2010, Denmark's group demonstrated racemization of the enantiopure (4*R*,5*S*)-5-bromo-4-octyl tosylate via bromiranium ion-to-olefin transfer in acetolysis [41]. While no decrease in enantiospecificity was observed in the absence of the (*E*)-4-octene, in the presence of the (*E*)-4-octene, the enantiopure bromiranium ion generated from the (4*R*,5*S*)-5-bromo-4-octyl tosylate transferred to the (*E*)-4-octene, and enantiospecificity was lost at the same time (Table 9.1). Based on these reports, suppression of haliranium ion transfer from the *in situ*-generated enantiopure haliranium ion to an unreacted substrate is crucial for the successful catalytic asymmetric halocyclization.

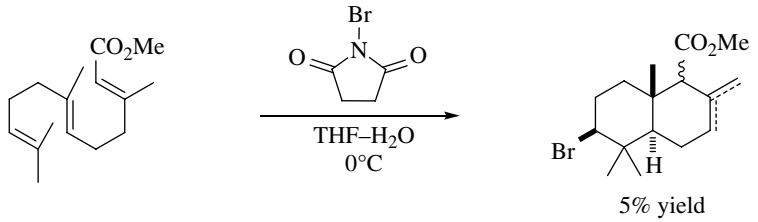
Chemical syntheses of brominated polycyclic compounds have been developed over the past 50 years [42]. In 1966, the first bromonium ion-induced polyene cyclization was demonstrated by van Tamelen's group [43]. The reaction of methyl farnesoate with *N*-bromosuccinimide (NBS) in a mixture of THF and $H_2O$ at 0°C gave an isomeric mixture of brominated bicyclic esters, although the yield was very low. This may has been due to the low site selectivity of the reaction of the brominating reagent with terminal or internal olefins (Scheme 9.26).

Kato's group greatly advanced bromonium ion-induced polyene cyclization [44]. In 1986, they developed 2,4,4,6-tetrabromocyclohexa-2,5-diene (TBCO) as a brominating

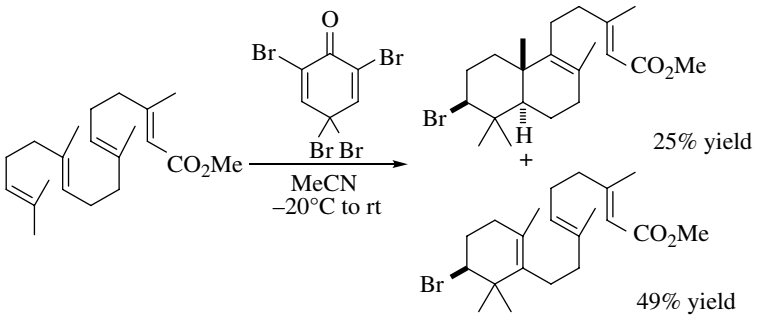
**TABLE 9.1 Decrease in Enantiospecificity in Acetolysis from Bromiranium Ion-to-Olefin Transfer**



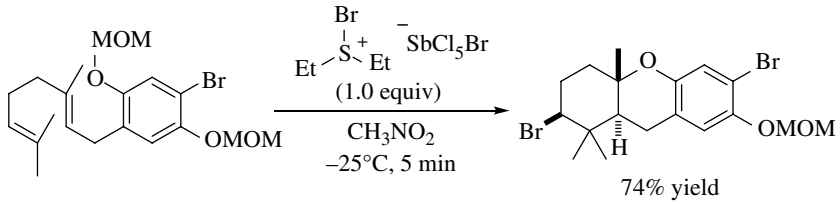

| MOAc | (*E*)-4-Octene (equiv) | Yield (%) | Er |
|---|---|---|---|
| NaOAc | 0 | 79 | 97:3 |
| NaOAc | 1.0 | 75 | 62:38 |
| $Bu_4NOAc$ | 0 | 77 | 98:2 |
| $Bu_4NOAc$ | 1.0 | 73 | 88:12 |




**SCHEME 9.26** First electrophilic bromocyclization of polyprenoids.




**SCHEME 9.27** Bromocyclization of methyl geranyl geranate with TBCO.

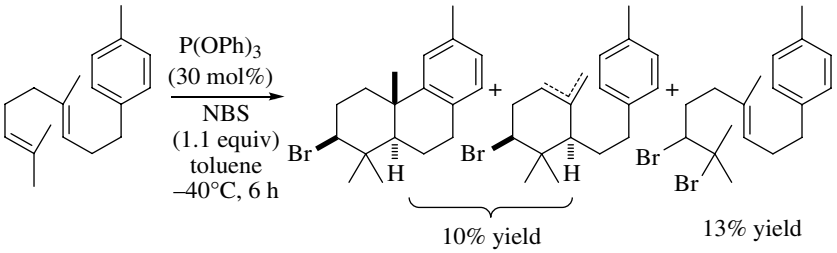



**SCHEME 9.28** BDSB-promoted bromonium ion-induced polyene cyclization.

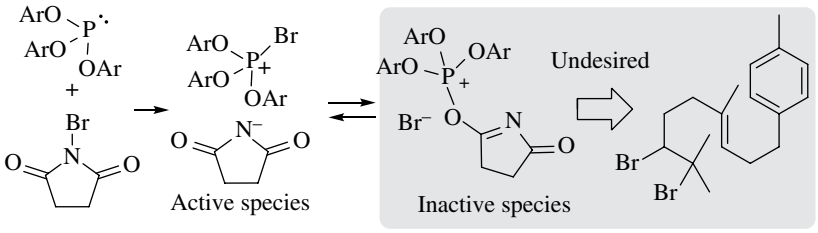
reagent and reported that the bromocyclization of methyl geranyl geranate with TBCO afforded brominated bi- or monocyclic compounds (Scheme 9.27) [44f]. While TBCO was used in several bromocyclizations, in many cases the yields were low to moderate.

In 2009, Snyder's group demonstrated that bromodiethylsulfonium bromopentachloroantimonate (BDSB) was an efficient brominating reagent [45]. Several brominated compounds were obtained in good yield with the use of BDSB (Scheme 9.28).

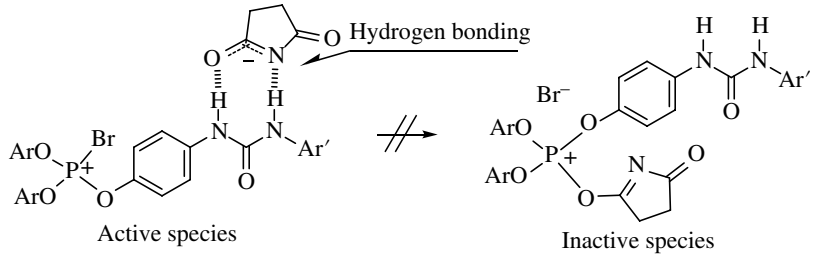
While several brominating reagents have been developed for the bromocyclization of polyprenoids, catalysts for this reaction have not been developed for many years. Ishihara's group developed new nucleophilic phosphorous




**SCHEME 9.29** $P(OPh)_3$-catalyzed bromocyclization of homogeranyltoluene.




**SCHEME 9.30** Proposed mechanism for the generation of dibrominated by-product.




**SCHEME 9.31** Capture of succinimide anion via hydrogen bonding.

catalysts [37d, 46]. First, they examined the triphenyl phosphite $P(OPh)_3$-catalyzed bromocyclization of homogeranyltoluene (Scheme 9.29). Bromocyclization with 30 mol% of $P(OPh)_3$ and 1.1 equiv of NBS gave the desired cyclic products (10% yield) along with the undesired dibrominated by-product (13% yield).

Through several experiments, Ishihara's group found that $P(OPh)_3$ was inactivated during generation of the dibrominated by-product. In other words, $P(OPh)_3$ was inactivated by nucleophilic attack of the succinimide anion to the bromophosphonium salt, which is the active species [47]. The bromide anion was generated at the same time, which led to formation of the dibrominated by-product (Scheme 9.30). Therefore, the nucleophilic attack of the succinimide anion to the bromophosphonium salt must be avoided if this reaction is to be successful.

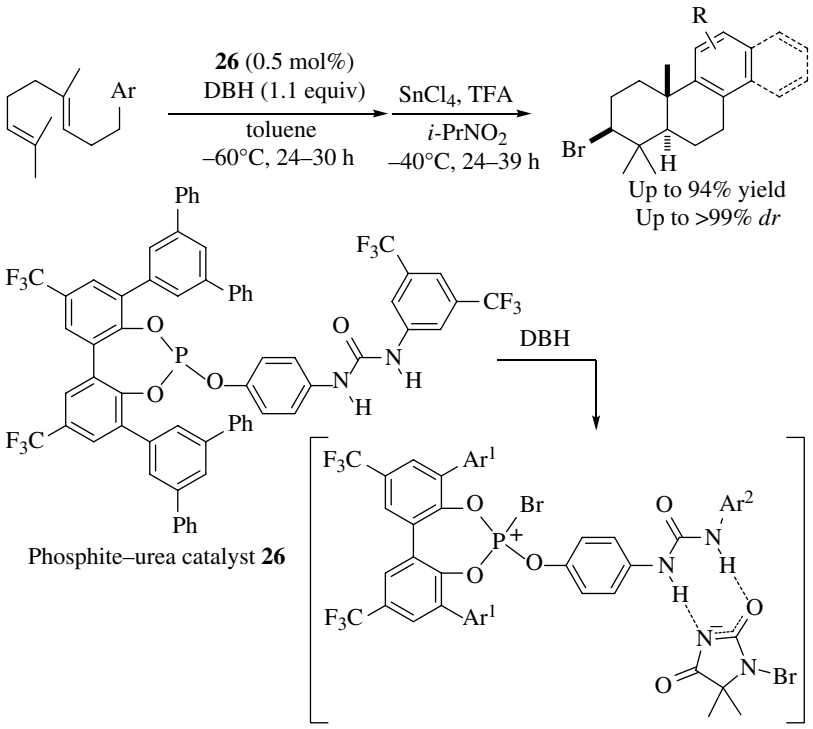
It was proposed that urea groups could capture the succinimide anion via hydrogen bonding, and inactivation of the catalyst could be suppressed (Scheme 9.31).

As a result, Ishihara's group found that phosphite–urea cooperative catalyst **26** was efficient for the highly site- and diastereoselective bromocyclization of homogeranylarenes (Scheme 9.32) [46a]. Moreover, they found that 1,3-dibromo-5,5-dimethylhydantoin (DBH) was a highly reactive brominating reagent. Only 0.5 mol% of **26** was sufficient to give the desired product in quantitative yield when the reaction of homogeranyltoluene was conducted with DBH. The *cis*-fused products were generated in the second acid-treatment step, while the first bromonium ion-induced cyclization step gave only *trans*-diastereomers.

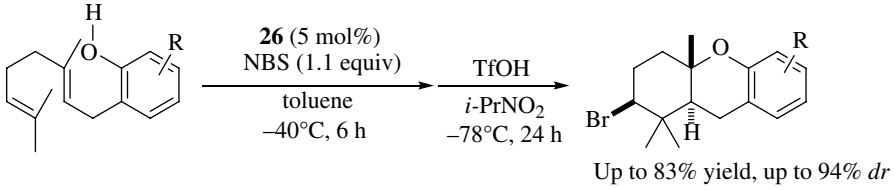
This method could also be applied to the bromocyclization of 2-geranylphenols (Scheme 9.33) [46b]. NBS (1.1 equiv) was used as the brominating reagent, since bromination at the *ortho*- and *para*-positions of phenol occurred when DBH was used as a brominating reagent. The reactions were conducted using 5 mol% of **26**, and the desired tricyclic compounds were obtained in good yields.

Recently, McErlean's group reported bromocyclization for the synthesis of (+)-luzofuran [48]. 2,4,5-Trichlorophenyltriazole-flanked phosphoramidite (TCPT) was used as a catalyst. Triazole groups were introduced at the 3,3′-positions of BINOL, inspired by V-BPO which has several histidines at the active site. The reaction was promoted with 20 mol% of TCPT and 1.0 equiv of NBS, although the yield and the diastereoselectivity were moderate (Scheme 9.34).

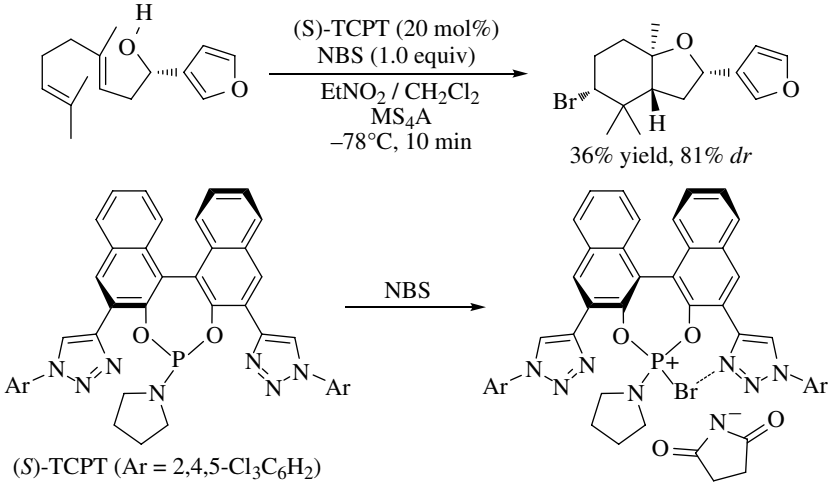
To achieve high enantioselectivity in the electrophilic halocyclization of simple polyprenoids, Ishihara's group



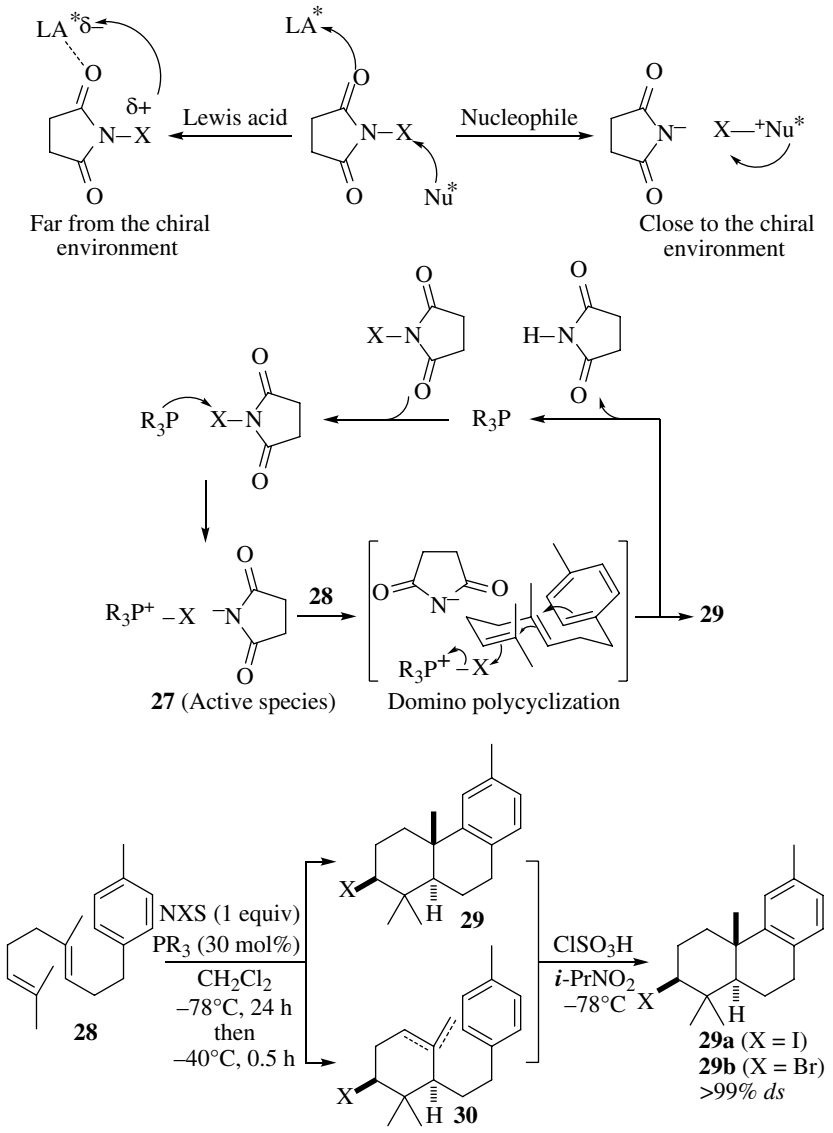

**SCHEME 9.32** Phosphite–urea cooperative catalysis for the site- and diastereoselective bromocyclization of homogeranylarenes.




**SCHEME 9.33** Bromocyclization of 2-geranylphenols.

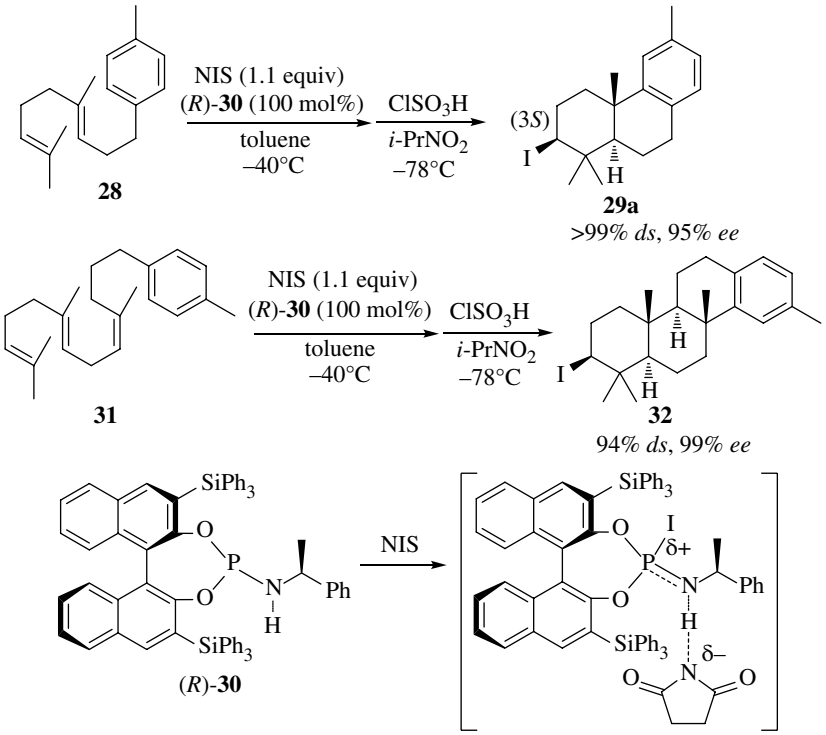



**SCHEME 9.34** Synthesis of (+)-luzofuran with (*S*)-TCPT.




**SCHEME 9.35** Diastereoselective halopolycyclization of polyprenoids promoted by nucleophilic phosphorus compounds.

focused on the method used to activate the halogenating reagents by chiral nucleophilic promoters [37]. The concept of this nucleophilic approach is illustrated in Scheme 9.35. If chiral nucleophilic promoters (*Nu**) can activate the halogenating reagents such as with *N*-halosuccinimides, the activated halogen atom could be placed close to the chiral environment of the nucleophilic promoter in the active species such as **27** and the halogenated products would be obtained with high enantioselectivity. In contrast, a Lewis acid (*LA**) activates a halogenating reagent by coordinating to the carbonyl group, the activated halogen atom is placed far from the chiral environment of the Lewis acid. However, no successful methods for the enantioselective halocyclization of polyprenoids induced by nucleophilic promoters have been reported until very recently, although there have been several examples of halocyclizations using chiral amine promoters, albeit with quite low enantioselectivity [49]. Therefore, they initially investigated nucleophilic promoters for the activation of halogenating reagents. First, they examined the activities of various achiral nucleophiles that promoted the halocyclization of 4-(homogeranyl)toluene (**28**) with NIS. The reaction was catalytically conducted with NIS (1 equiv) in the presence of nucleophilic promoter (30 mol%) in $CH_2Cl_2$ to give the desired AB-ring product **29a** together with *endo*- and *exo*-isomeric A-ring products **30a**. After the mixture was treated with $ClSO_3H$ in *i*-$PrNO_2$, the desired iodocyclization product **29a** was obtained as a single *trans*-diastereomer. By screening nucleophilic promoters, they found that several nucleophilic phosphorus compounds such as tributylphosphine ($PBu_3$), triphenylphosphine ($PPh_3$), tris(*p*-methoxyphenyl)phosphine ($P[C_6H_4(p\text{-OMe})]_3$), and triphenyl phosphite [$P(OPh)_3$] showed good catalytic



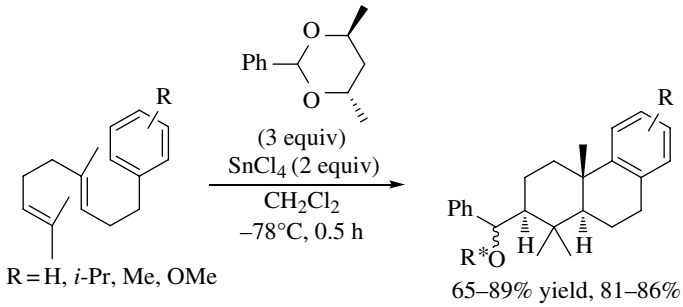

**SCHEME 9.36** Enantioselective iodopolycyclization of polyprenoids promoted by nucleophilic phosphoramidites.

activities, and **29a** was obtained in yields of 51–99%. In particular, the use of highly nucleophilic tributylphosphine gave the best results (99% yield). When the reaction was conducted in toluene, the catalytic activity of triphenylphosphine unexpectedly decreased (ca. 0% yield). NBS showed reactivity comparable to NIS in the present reaction. In contrast, unexpectedly, nucleophilic amines such as 1,4-diazabicyclo [2.2.2]octane (DABCO) and 4-(*N,N*-dimethylamino)pyridine (DMAP) were completely inert. Thus, nucleophilic phosphorus compounds catalyzed the electrophilic iodination/bromination of the terminal olefin of **28**, and this efficiently induced diastereoselective cyclization to give the halogenated tricyclic product **29** as a single diastereomer.

Encouraged by these results, Ishihara's group next investigated the enantioselective iodocyclization of **28** with NIS using chiral nucleophilic promoters [37]. After an extensive investigation into chiral nucleophilic phosphorus compounds, they designed the chiral promoter **30**, which is a phosphoramidite of (*S*)-phenethylamine and has two triphenylsilyl groups at the 3 and 3′ positions of the binaphthyl moiety (Scheme 9.36). Despite the bulkiness of the triphenylsilyl groups, **30** showed high activity (95% yield) for the iodocyclization of **28** in $CH_2Cl_2$. However, the resulting **29a** was racemic. Very surprisingly, the reaction conducted with **30** (100 mol%) in toluene gave (+)-**29a** with a remarkably high enantioselectivity (95% *ee*), although the yield of (+)-**29a** was moderate (57% yield). Since the P—N bond of the phosphoramidites might be weak, the phosphoramidites might have partially decomposed under these reaction conditions. Thus, they succeeded in the enantioselective iodocyclization of 3-(homogeranyl)toluene **28**, 4-(homogeranyl)anisole, and 4-(homofarnesyl)toluene **31** (91–99% *ee*). In principle, the iodopolycyclization of **31** may provide 32 ($=2^5$) diastereomers and enantiomers of the tetracyclic 3-iodoterpenoid **32**. Surprisingly, the present method gave the desired product **32** with 99% *ee* and 94% *ds*.

Enantioselective bromo- and chlorocyclizations are very valuable because there are many marine natural products that contain bromo and/or chloro substituents. Unfortunately, however, the previously described methodology provides low enantioselectivity for bromo- and chlorocyclization using NBS and NCS. For example, the bromocyclization of **28** with NBS gave **29b** with 4% *ee*. This limitation can be avoided by the stereospecific transhalogenation of 3-iodoterpenoid **24a** into the bromine derivative **28b** by lithiation (*t*-BuLi, 3.0 equiv) followed by bromination ($BrCF_2CF_2Br$, 3 equiv). The chlorine derivative **28c** (X = Cl) was also obtained using $ClCF_2CF_2Cl$ instead of $BrCF_2CF_2Br$. The enantioselective introduction of functional groups to the three-position of polycyclic terpenoids is useful for not only the synthesis of halogenated bioactive natural products but also derivation to a variety of chiral building blocks.

It is very interesting to compare the latter synthetic methodology with biosynthesis. The molecular weights of FeHeme and Vanadium haloperoxidases, which have been




**SCHEME 9.37** Intermolecular acetal-initiated polyene cyclization promoted by $SnCl_4$.

discovered in many marine organisms and which catalyze similar halocyclizations, are larger than 10,000 Da. In contrast, the chiral phosphoramidite **30** has a molecular weight of 951, which is just less than 1 wt% of its natural haloperoxidase. In sharp contrast, to the natural enzyme, this synthetic counterpart requires the use of stoichiometric amount to provide comparable yields of cyclized products.

### 9.3.5 "Chiral Carbocation"-Induced Polyene Cyclizations

Intramolecular acetal-initiated cationic polyene cyclization was first reported by W. S. Johnson's group [12]. High diastereoselectivity has been achieved using a chiral acetal at the terminal position. While intramolecular acetal-initiated polyene cyclization had been studied over the years, an intermolecular version had not been developed. However, in early 2007, Loh's group reported the first *intermolecular* version of the chiral acetal-initiated polyene cyclization (Scheme 9.37) [50]. The reaction of homogeranylbenzene derivatives with benzaldehyde cyclic acetals was promoted by $SnCl_4$ to give the desired cyclization products in 65–89% yield with 81–86% *ds*. The use of benzaldehyde cyclic acetals effectively provided the desired dicyclization products, and the monocyclization products were not detected. The benzyl ether moieties of the cyclization product can be easily functionalized to give several optically active tricyclic compounds. Importantly, this intermolecular process does not require the incorporation of the acetal group into the substrate, and this enables the acyclic precursors to have a variety of structures.

### 9.3.6 Stereoselective Cyclizations of Homo(polyprenyl)arene Analogs

In 2006, Yamamoto–Ishihara's group reported highly diastereoselective polycyclization of homo(polyprenyl)arene analogs bearing terminal siloxyvinyl groups catalyzed by tin(IV) chloride (10 mol%) (Scheme 9.38) [51]. The cyclizations of *tert*-butyldiphenylsilyl and triisopropylsilyl polyenol ethers gave 4α(equatorial)- and 4β(axial)-siloxypolycycles as major isomers, respectively. The strong nucleophilicity of *pro*-C(9), a (6*E*)-geometry, and bulky silyl group effectively favored the 4α-preference via transition state TS-**33**, whereas the weak nucleophilicity of pro-C(9), a (6*Z*)-geometry, and less steric hindrance of a silyl group favored the 4β-preference via transition state TS-**34**.

In 2010, Loh's group reported a highly efficient catalytic enantioselective polyene cyclization [52]. An α-ketoester was demonstrated to initiate enantioselective cationic polyene cyclization catalyzed by a $Sc(OTf)_3$–Pybox Lewis acid catalyst (Scheme 9.39).

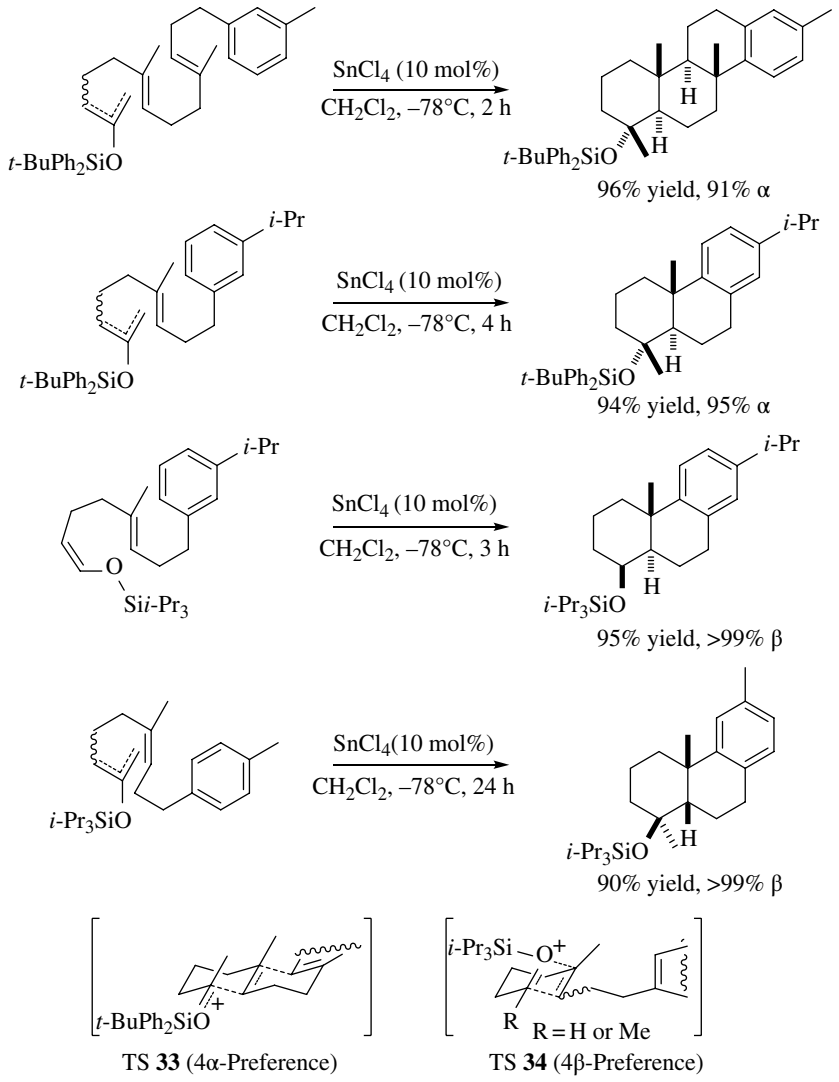
MacMillan's group reported the first catalytic enantioselective cyclization strategy for accessing steroidal and terpenoidal frameworks using organocatalysis [53]. This strategy represents an ambient temperature protocol, which is unprecedented in SOMO activation catalysis with respect to carbon─carbon bond formation (Scheme 9.40).

Furthermore, Jacobsen's group reported the development of a new thiourea catalyst for the enantioselective bicyclization of hydroxylactams [54]. The enantioselective cationic polycyclization reactions catalyzed by bifunctional thiourea derivatives appear to engage stabilizing π–cation interactions as a principal element of enantioselectivity (Scheme 9.41).

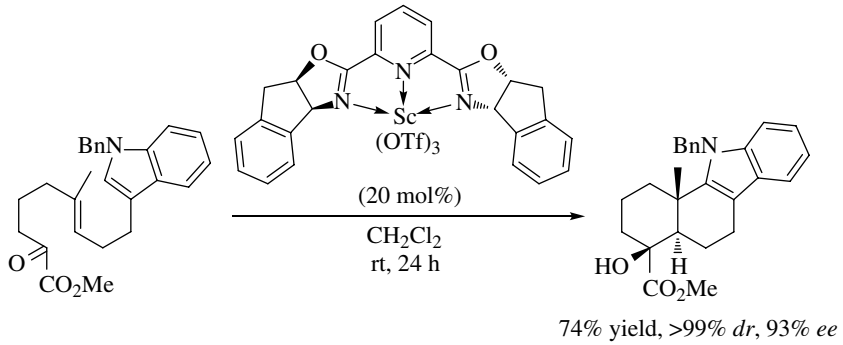
These catalytic enantioselective polyene cyclizations have been accomplished through the use of substrates with the appropriate functional groups on the reactive sites, such as aldehydes and hydroxylactams. Therefore, these methods cannot be applied to the enantioselective cyclization of simple isoprenoids with a terminal isoprenyl group.

## 9.4 BIOMIMETIC TOTAL SYNTHESIS OF TERPENES AND STEROIDS THROUGH POLYENE CYCLIZATION

All-*E* oligoprenols, from *E*-geraniol (*E*-diprenol) to *E*-solanesol (all-*E* nonaprenol), are important naturally occurring compounds not only in their own right but also biosynthetic precursors of many thousands of complex isoprenoids as well as prenylated proteins and carbohydrates. In addition, it has been postulated that oligoprenol phosphates

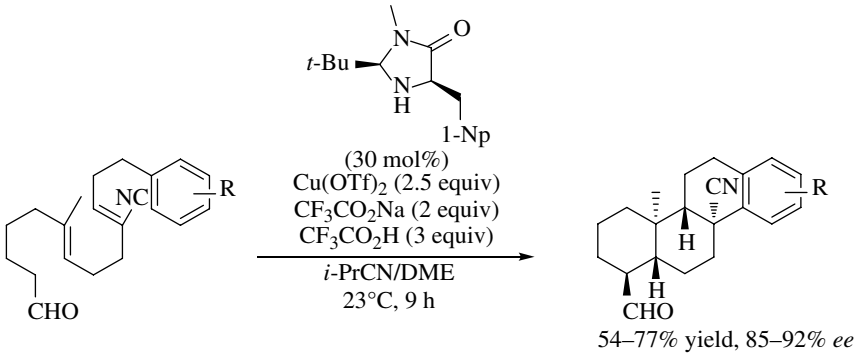



**SCHEME 9.38** Diastereoselective polycyclization of homo(polyprenyl)arene analogs bearing terminal siloxyvinyl groups.

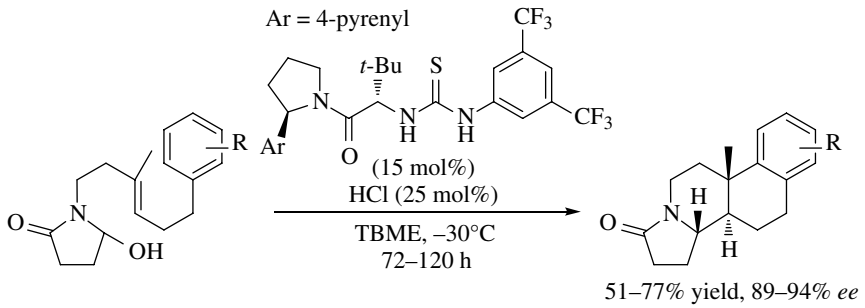



**SCHEME 9.39** Enantioselective polyene cyclization catalyzed by chiral Lewis acid.

may have been important membrane and cell components in the early development of life. The biosynthesis of oligoprenols occurs by a 5-carbon homologation process (prenylation) in which a prenyl (or oligoprenyl) pyrophosphate-derived cation attaches to the terminal olefinic carbon of the 5-carbon species 4-methyl-3-butenyl pyrophosphate. Corey's group has developed an efficient, convergent, and general route for the synthesis of all-*E* oligoprenols that parallels the




**SCHEME 9.40** Enantioselective polyene cyclization via organo-SOMO catalysis.




**SCHEME 9.41** Enantioselective thiourea-catalyzed cationic polycyclization.

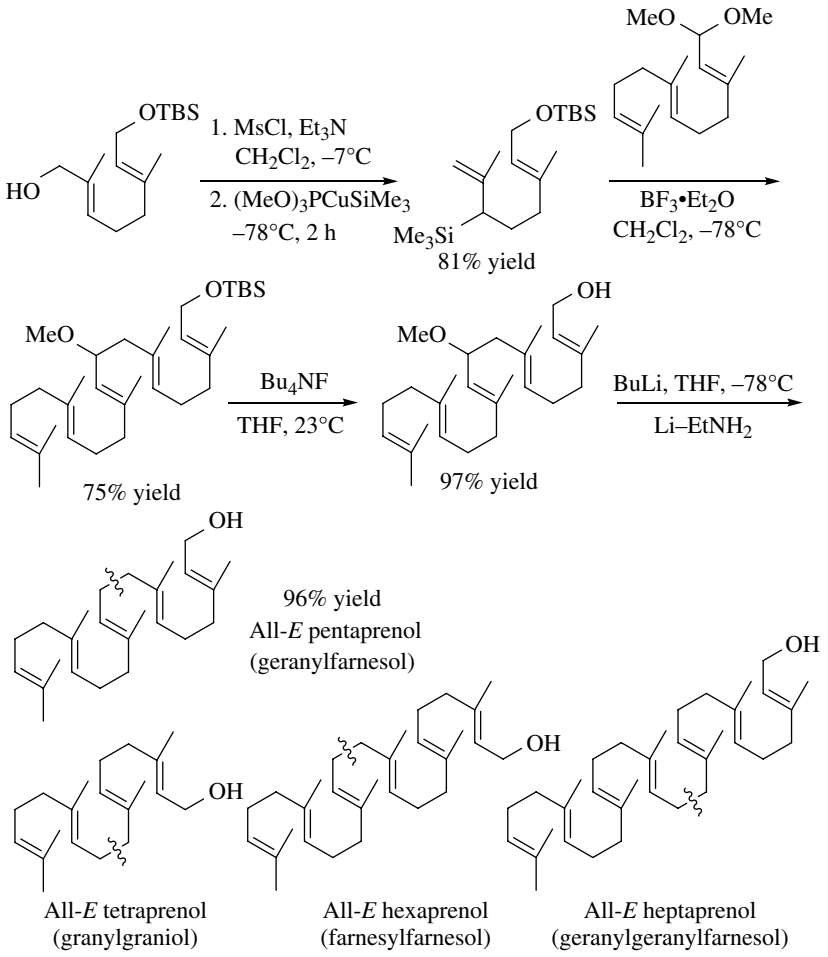
biosynthetic process because it is both cationic and highly *E*-stereoselective [55]. The synthesis is strategically powerful since it allows the coupling of two fragments each of which can have multiple prenyl units. Its generality has been demonstrated by the syntheses of all-*E* geranylgeraniol, geranylfarnesol, farnesylfarnesol, and heptaprenol. As a specific illustration, the synthesis of all-*E* pentaprenol by the described pathway is highlighted in Scheme 9.42.

The site-selective epoxidation of polyunsaturated substrates is a key process in the biosynthesis of several families of natural products, including steroids and triterpenoids (from 2,3-(*S*)-oxidosqualene), insect juvenile hormones (farnesoate or homofarnesoate terminal epoxides), and eicosanoids (e.g., leukotriene-$A_4$ or (11*R*,12*S*)-oxidoarachidonic acid). Corey's group has developed an effective strategy for the efficient site-selective epoxidation of polyolefinic isoprenoid alcohols based on the use of an internal control element for intramolecular reaction (Scheme 9.43) [56]. This approach is illustrated by its application to a series of polyisoprenoid alcohols (polyprenoids) at substrate concentration of 0.5 mM. Polyprenol substrates, which are having a phenol functionality at one terminus, can direct selective internal epoxidation at a double bond, which is positioned either four or five prenyl units away from the hydroxyphenyl terminal.

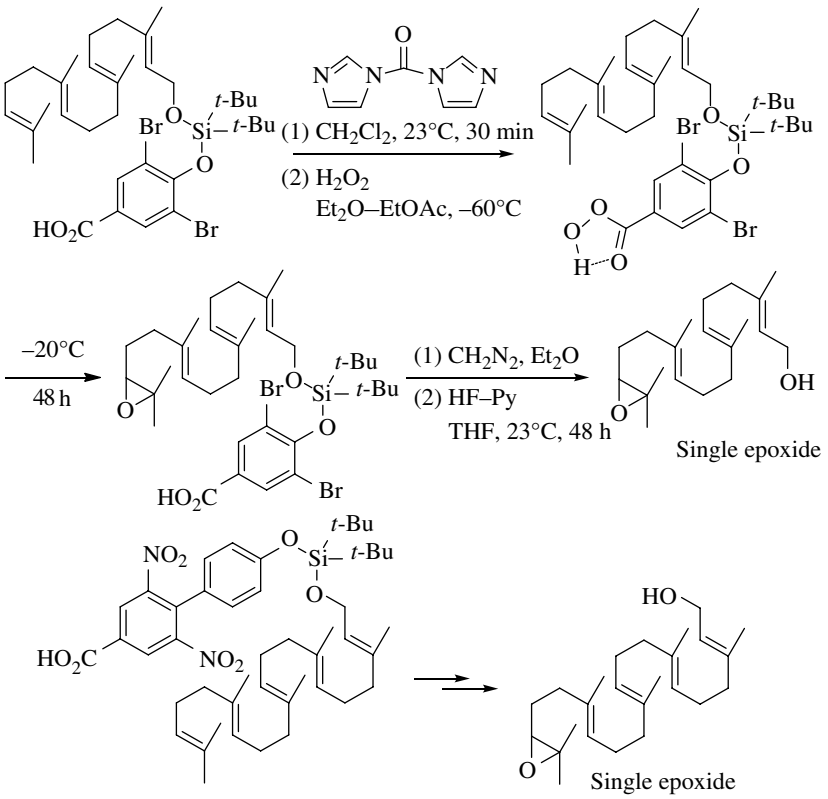
Corey's group has also demonstrated the power of epoxide-initiated, stereoselective cationic cyclizations, which are the nonenzymatic mimics of biosynthetic processes [17].

Serratenediol, a pentacyclic triterpenoid containing a unique seven-membered central ring has been concisely synthesized using double epoxide-initiated stereoselective cationic polycyclizations mediated by $MeAlCl_2$ as key steps (Scheme 9.44) [17h]. (+)-α-Onocerin has been also synthesized in four steps via double epoxide-initiated stereoselective polycyclizations (Scheme 9.44) [17i].

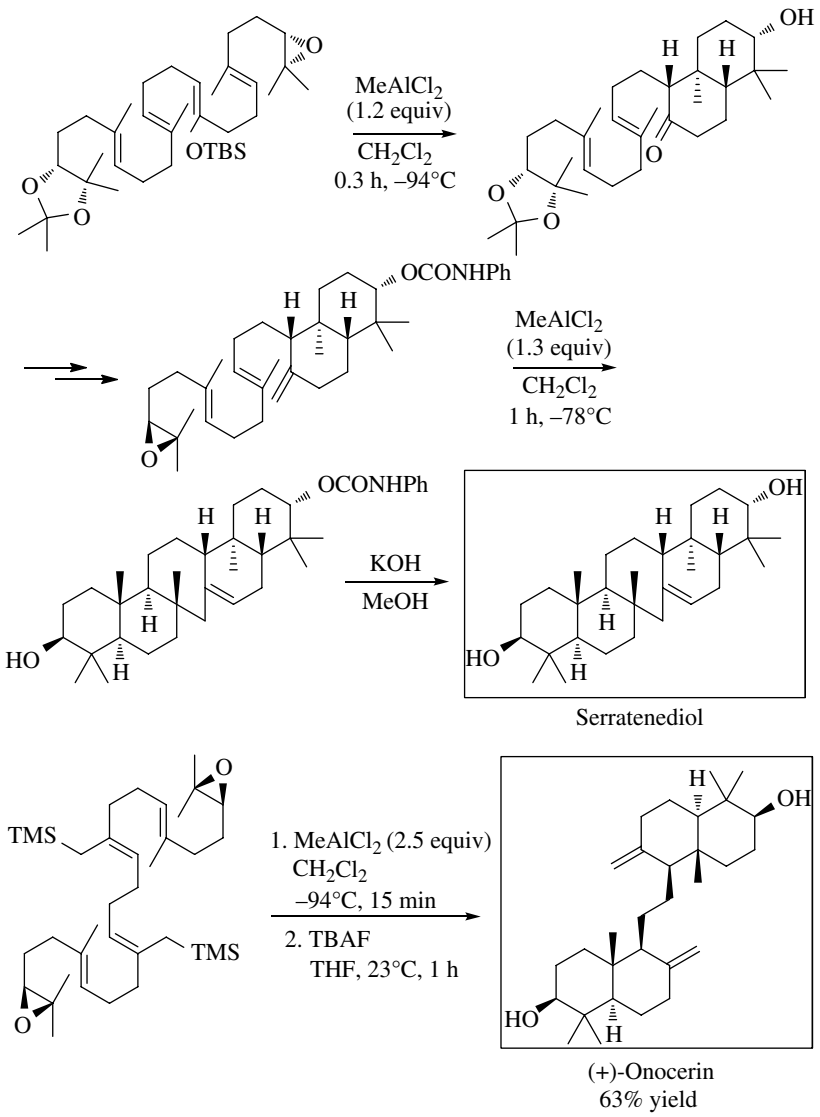
Since the determination of the structure of the citrus bitter principle limonin in 1960, the number of structurally defined members of this class of natural products (now called limonoids) has grown to several hundred. Corey's group reported the first enantioselective synthesis of a limonoid, the protolimonoid, by a route which is both short and stereocontrolled (Scheme 9.45) [17j]. Brief exposure of chiral epoxide **35** to 1.2 equiv of $MeAlCl_2$ at −78°C provided two diastereomeric tricyclic ketones in a 1.5 : 1.0 ratio with ketone **36** as the minor component. The predominating diastereomer in the mixture, in which the appendage α to the carbonyl is axially oriented, could be isomerized to **36** by treatment of the crude mixture with sodium ethoxide in ethanol. Overall, the cationic cyclization and epimerization permit the rapid stereoselective establishment of three rings and five stereocenters in 43% yield. Slow addition of a solution of AIBN and $Bu_3SnH$ to a heated solution of xanthate




**SCHEME 9.42** A general stereocontrolled, convergent synthesis of all-*E* oligoprenols.




**SCHEME 9.43** Site-selective epoxidation of polyprenoids.




**SCHEME 9.44** Total syntheses of serratenediol and (+)-onocerin.

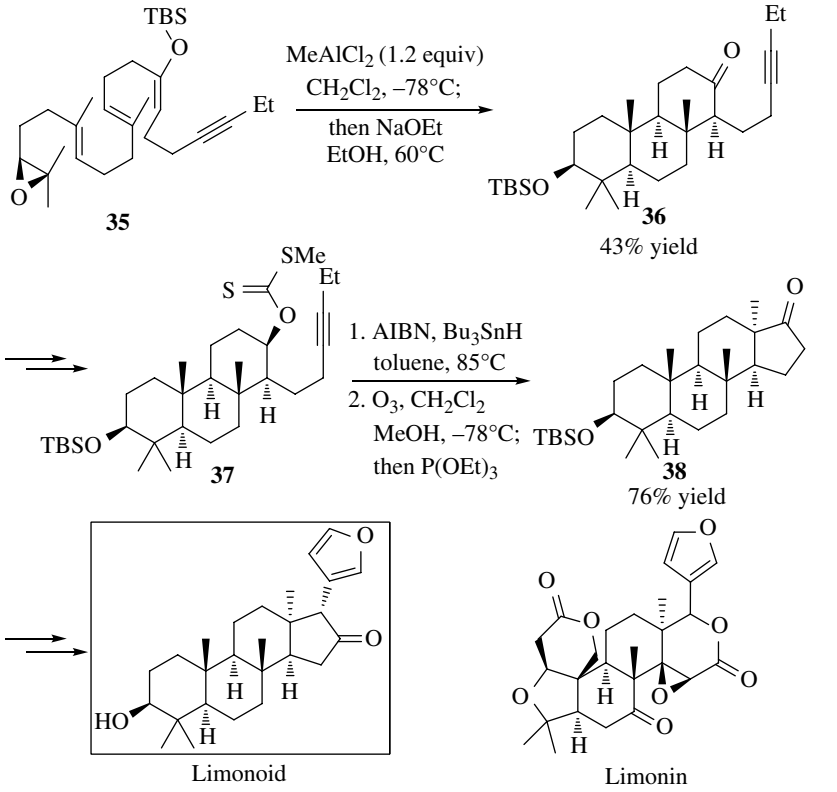
**37** resulted in smooth radical-mediated 5-*exo-dig* cyclization to form the tetracyclic ketone (2 : 1 ratio of *E*/*Z* isomers). The subsequent ozonolysis gave a single ketone, **38** (*cis* C/D ring junction), which was transformed to limonoid after several steps.

Two exceedingly short synthetic routes to the key intermediate **39** for the synthesis of the pentacyclic triterpene germanicol have been developed (Scheme 9.46) [17k]. In the first, (*S*)-epoxide **37** is transformed in just one step to tetracyclic intermediate **38**, which is converted to chiral **39** by treatment with polyphosphoric acid. The second synthetic route to **39** involves the two-stage acid-catalyzed cyclization of (*S*)-epoxide **40** via **41**.

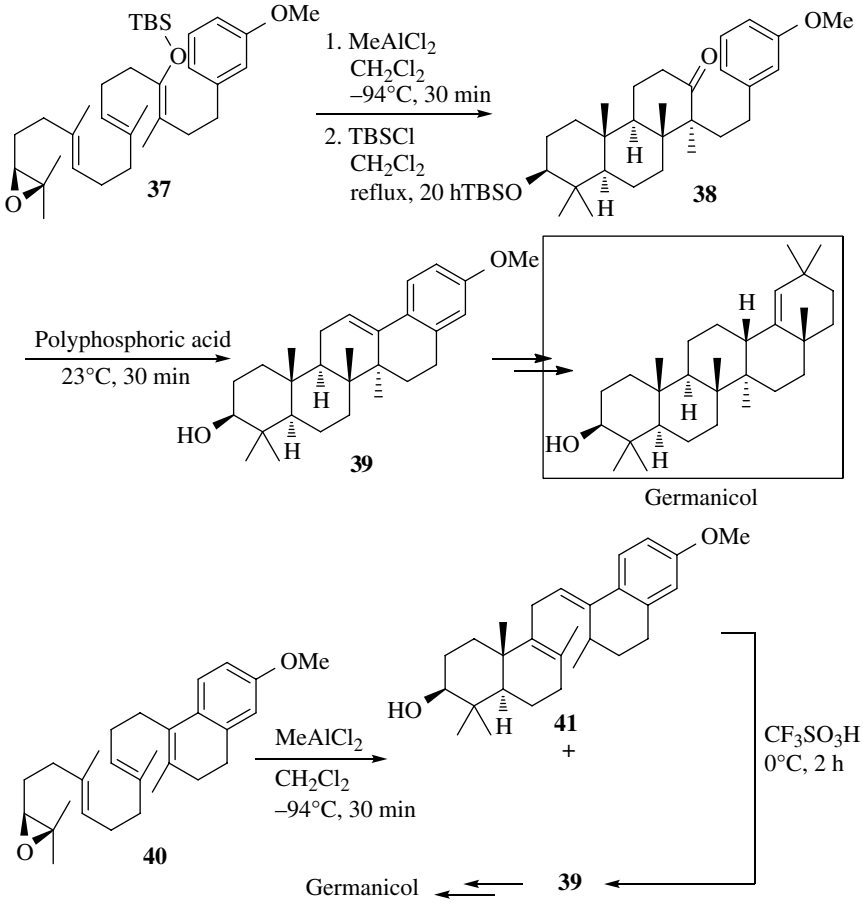
The direct, one-step pentacyclization of (*S*)-2,3-oxidosqualene to the pentacyclic triterpene lupeol is a remarkable example of biosynthetic efficiency. Lupeol has been synthesized through the diastereoselective tricyclization of the chiral epoxide and the subsequent monocyclization by Corey's group (Scheme 9.47) [17l]. One-step conversion of lupeol to the naturally occurring pentacyclic triterpenes germanicol, δ-amyrin, 18-*epi*-β-amyrin, α-amyrin, taraxasterol, and ψ-taraxasterol via cationic intermediates highlights the potency of the described synthetic plan.

The total synthesis of hongoquercin B has been completed in nine steps from farnesyl acetate using a double biomimetic strategy, a Pd(0)-catalyzed regioselective decarboxylative farnesyl migration, cycloaromatization to produce the resorcylate, and a cationic epoxydiene cyclization (Scheme 9.48). The single epoxyfarnesyl stereocenter was used to control all the remaining four stereocenters of the tetracyclic core [57].

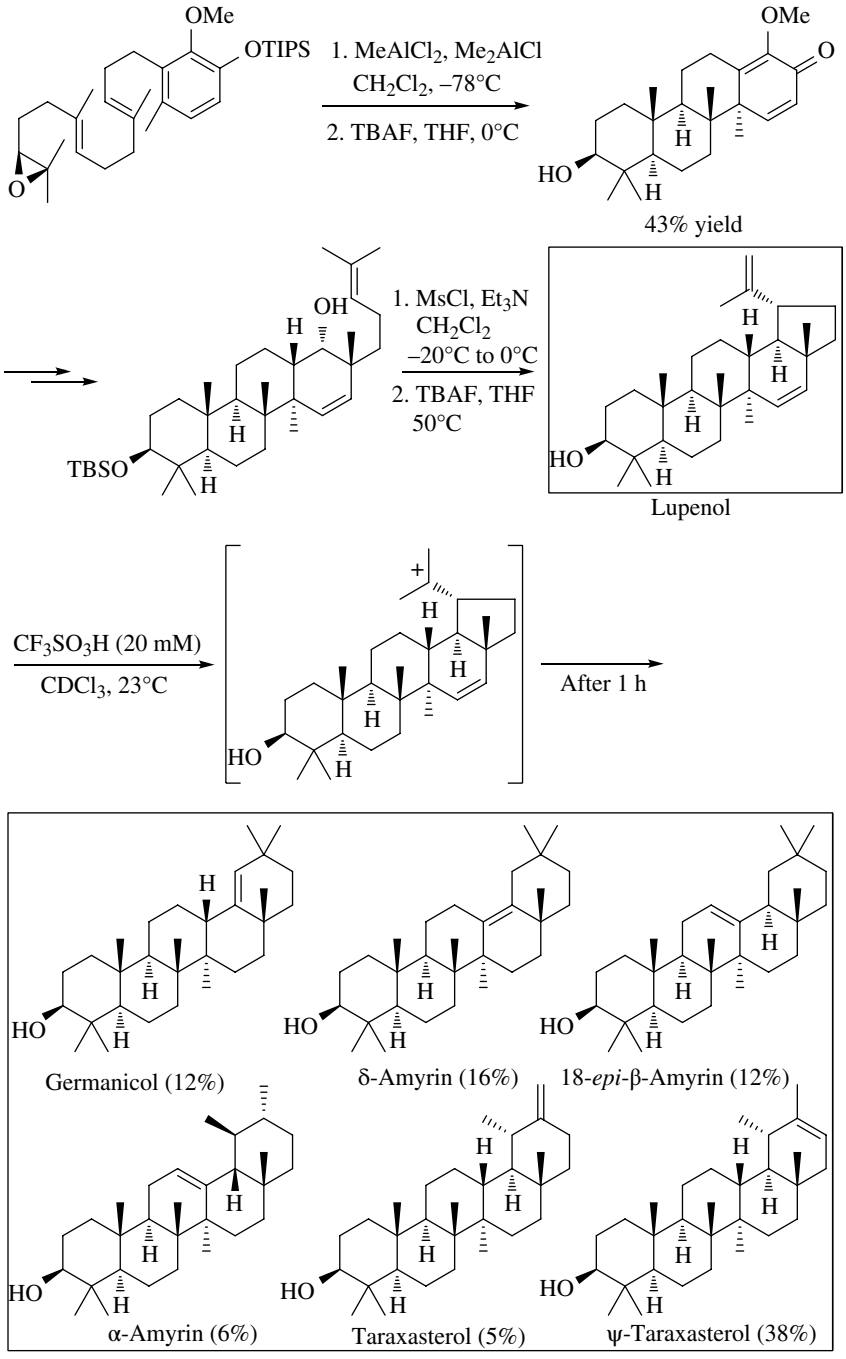
Yamamoto–Ishihara's group has demonstrated that chiral LBA **7**·$SnCl_4$ is an artificial cyclase that is useful for




**SCHEME 9.45** Total syntheses of limonoid.

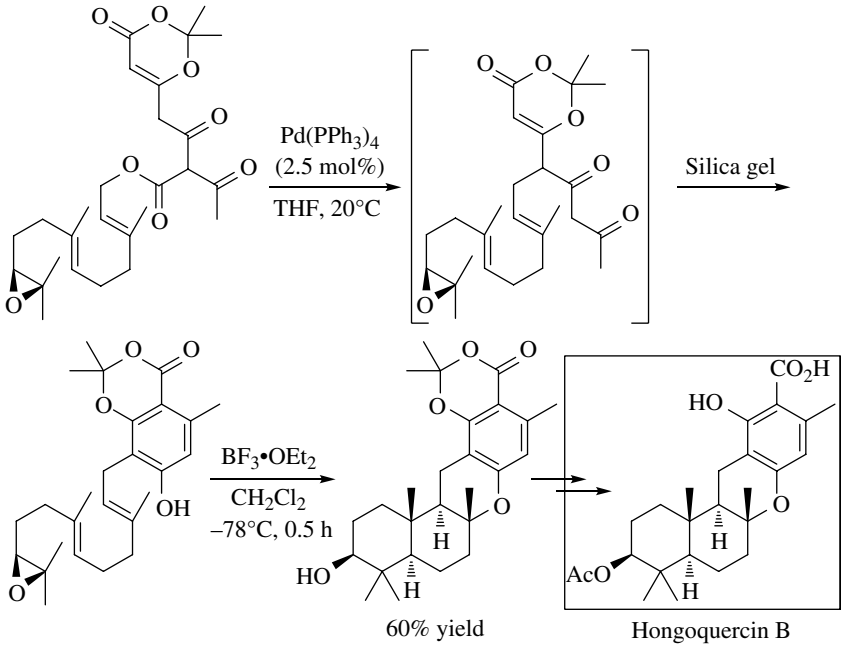



**SCHEME 9.46** Two routes for total syntheses of germanicol.

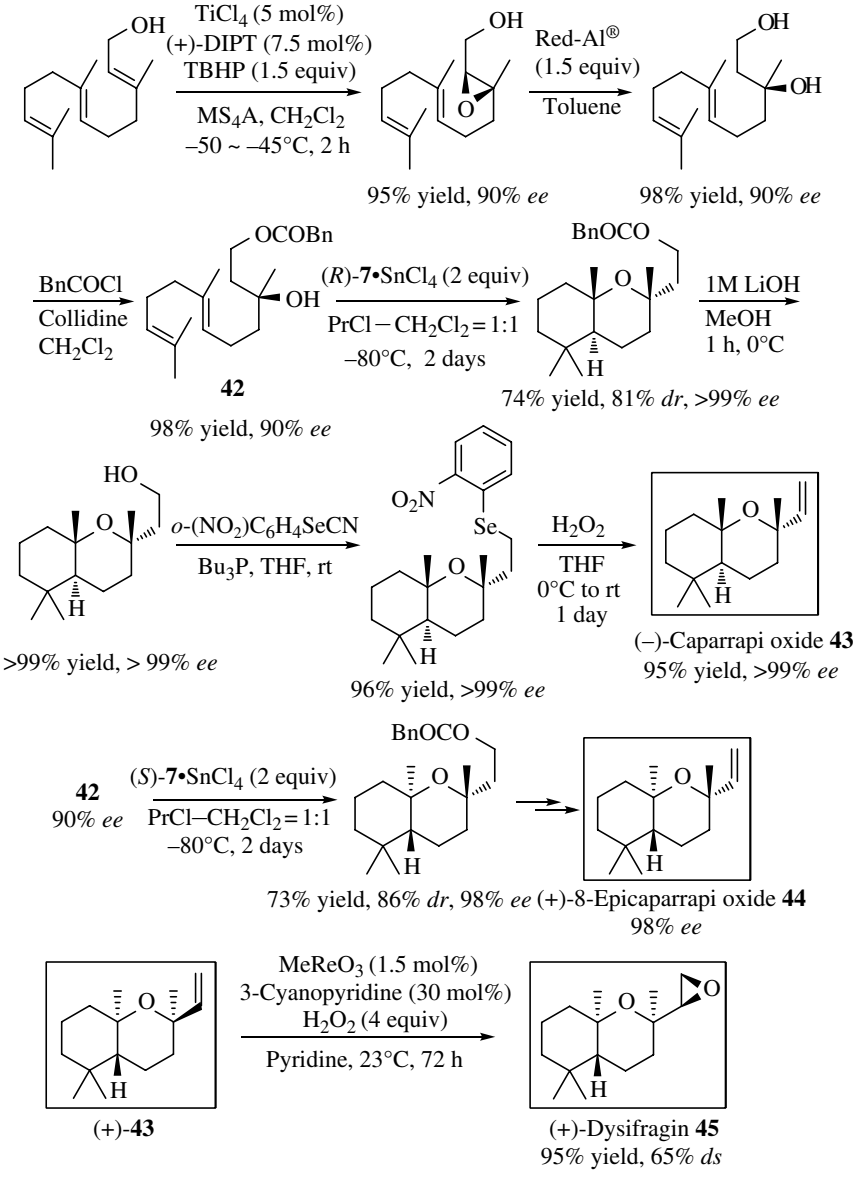



**SCHEME 9.47** Total synthesis of lupeol.

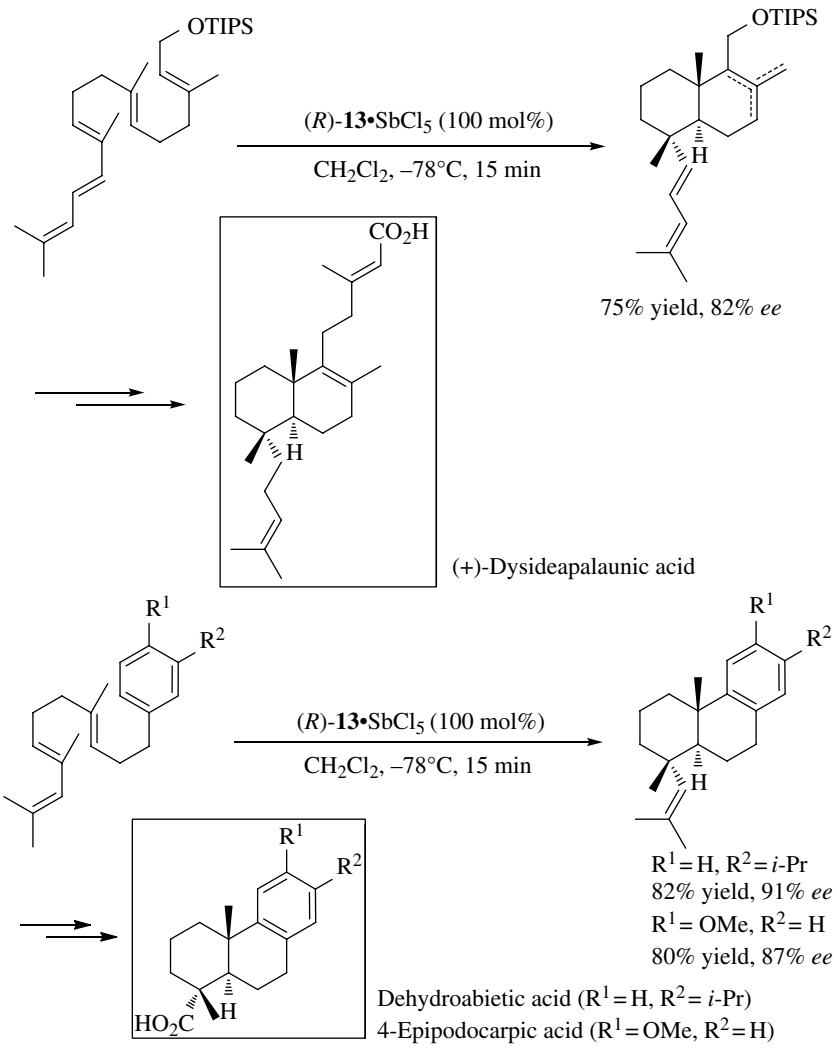
both optically active and racemic substrates (Scheme 9.49) [15h, i]. (−)-Caparrapi oxide **43** and (+)-8-epicaparrapi oxide **44** could be diastereoselectively synthesized from (*S*)-**42** in high yields by the reagent control of (*R*)-**7**·$SnCl_4$ and (*S*)-**7**·$SnCl_4$, respectively, regardless of the chirality of (*S*)-**42**. (*S*)-**42** was obtained from farnesol using Sharpless–Katsuki epoxidation as a key step (Scheme 9.49). Furthermore, in the direct cyclization of (±)-nerolidol induced by (*R*)-**7**·$SnCl_4$, (−)-**43** was obtained from (*S*)-nerolidol with 88% *ds* by reagent control, which overcome the substrate control, while (−)-**44** was obtained form (*R*)-nerolidol with greater than 99% *ds* by the double-asymmetric induction of substrate control and reagent control. However, the direct cyclization of (±)-nerolidol gave these bicyclic products in low yield due to acid sensitivity of substrates and products. (+)-Dysifragin **45** was obtained from (+)-**43** by the diastereoselective epoxidation catalyzed by $MeReO_3$ [15i].




**SCHEME 9.48** Total synthesis of hongoquercin B.




**SCHEME 9.49** Total syntheses of (–)-caparrapi oxide **43**, (+)-caparrapi oxide **43**, (+)-8-epicapparapi oxide **44**, and (+)-dysifragin **45**.



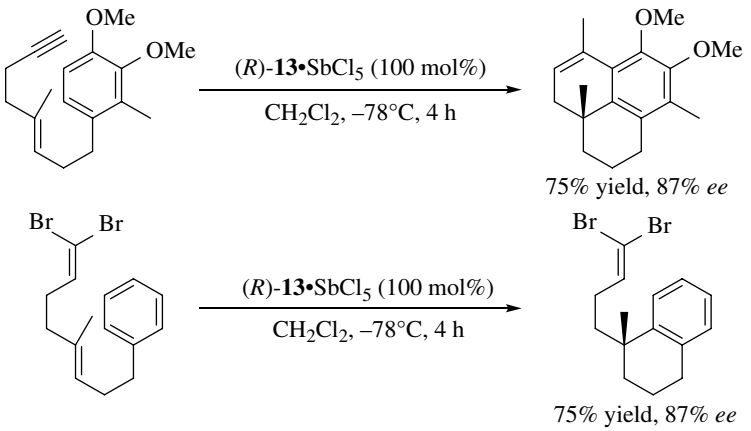

**SCHEME 9.50** Total syntheses of (+)-dysideapalaunic acid, dehydroabietic acid, and 4-epipodocarpic acid.

In 2014, Corey's group demonstrated the synthetic application of LBA (*R*)-**13**·$SbCl_5$ in catalyzed enantioselective polyene cyclization [21b] by three different ways in which the LBA could be used to initiate enantioselective, cationic polycyclizations at a nonterminal π-bond.

The first way involves activation of an internal double bond by an electron-supplying π-attachment [21b]. This type of process is quite useful, as is demonstrated by the especially simple, enantioselective syntheses of three well-known natural products. Thus, (+)-dysideapalaunic acid, dehydroabietic acid, and 4-epipodocarpic acid were synthesized through very short pathways including an enantioselective polyene cyclization under the influence of the LBA at −78°C for 15 min (Scheme 9.50).

The second way for achieving enantioselective cationic cyclization originating in an internal π-bond as illustrated in Scheme 9.51, which shows the cyclization by the LBA in a single step to the tricyclic product in 75% yield with 87% *ee* [21b]. This process is clearly initiated by protonation of the internal olefinic π-bond to form a bicyclic acetylene, which then undergoes a second (and slower) cyclization to generate the close core analog of pseudopterosin tricycle. The successful employment of this scenario is based on the lower proton affinity of C≡C triple bond relative to C═C double bond.

The third way of utilizing the LBA for the initiation of cationic cyclization at an internal π-bond is demonstrated by the process depicted in Scheme 9.51 [21b]. In this approach, bromine substituents at the terminal double bond are employed to enforce selective proton transfer from the LBA to the internal double bond, as takes place in the enantioselective conversion of the dibromodiene to the bicyclic product.




**SCHEME 9.51** Enantioselective cyclization reactions catalyzed by the LBA.

## 9.5 CONCLUSION

Enantio- and diastereoselective polyene cyclization reactions promoted by small-molecule artificial enzymes have been developed as key steps for the practical synthesis of polycyclic terpenoids based on biosynthetic pathways. Several examples as highlighted previously exist in the literature mimicking the all chair transition state of the nonsterol folding. In sharp contrast, there have been no successful examples of the polyene cyclization via a chair–boat transition state like sterol folding. In near future, more efficient and more effective catalytic biomimetic polyene cyclization reactions are expected to be developed.

## REFERENCES

1. (a) P. M. Dewick, *Medicinal Natural Products: A Biosynthetic Approach*, 2nd ed. John Wiley & Sons, Ltd, Chichester (2002) pp 167–289; (b) R. B. Woodward, K. Bloch, *J. Am. Chem. Soc.* 1953, 75, 2023; (c) G. Stork, A. W. Burgstahler, *J. Am. Chem. Soc.* 1955, 77, 5068; (d) A. Eshenmoser, L. Ruzicka, O. Jeger, D. Arigoni, *Helv. Chim. Acta* 1955, 38, 1890; (e) E. E. van Tamelen, *Pure Appl. Chem.* 1981, 53, 1259; (f) W. S. Johnson, *Tetrahedron* 1991, 47, xi; (g) K. U. Wendt, G. E. Schulz, E. J. Corey, D. R. Liu, *Angew. Chem. Int. Ed.* 2000, 39, 2812; (h) R. A. Yoder, J. N. Johnston, *Chem. Rev.* 2005, 105, 4730.
2. C. D. Poulter (ed.), *Comprehensive Natural Products Chemistry*, Vol. 5. Editors in chief D. Barton, K. Nakanishi, O. Meth-Cohn, Pergamon Press, Oxford (1999).
3. (a) G. Ohloff, The Fragrance of Ambergris in *Fragrance Chemistry*, ed. by E. T. Theimer, Academic Press, New York (1982), pp 535–573; (b) R. Decorzant, C. Vial, F. Naf, G. M. Whitesides, *Tetrahedron* 1987, 43, 1871; (c) I. C. Coste-Maniere, J. P. Zahra, B. Waegell, *Tetrahedron Lett.* 1988, 29, 1017; (d) A. A. Verstegen-Haaksma, H. J. Swarts, B. J. M. Jansen, A. Groot, *Tetrahedron* 1994, 50, 10095; (e) A. F. Barrero, J. Altarejos, E. J. Alvarez-Manzaneda, J. M. Ramos, S. Salido, *J. Org. Chem.* 1996, 61, 2215; (f)M. G. Bolster, B. M. F. Lagnel, B. J. M. Jansen, *Tetrahedron* 2001, 57, 8369.
4. (a) W. Fenical, O. McConnel, *Experientia* 1975, 31, 1004; (b) G. Cimino, S. DeStefeano, L. Minale, *Experientia* 1975, 31, 1117; (c) P. Djura, D. B. Stiele, B. Sullivan, J. Faulkner, E. Arnold, J. Clardy, *J. Org. Chem.* 1980, 45, 1435; (d) J. Rodriguez, E. Quinoa, R. Riguera, B. M. Peters, L. M. Abrell, P. Crewa, *Tetrahedron* 1992, 48, 6667.
5. A. F. Barrero, E. J. Alvarez-Manzaneda, R. Chahboun, M. Cortes, V. Armstrong, *Tetrahedron* 1999, 55, 15181.
6. (a) J. Rodriguez, E. Quinoa, R. Riguera, B. M. Peters, L. M. Abrell, P. Crewa, *Tetrahedron* 1992, 48, 6667; (b) M. T. Hamann, P. J. Scheuer, M. J. Kelly-Borges, *J. Org. Chem.* 1993, 58, 6565; (c) B. N. Navi, H. P. Perzanowski, R. A. Ross, T. R. Erdman, P. J. Scheuer, J. Finer, J. Clardy, *Pure Appl. Chem.* 1979, 51, 1893; (d) S. S. Nasu, B. K. S. Yeung, M. T. Hamann, P. J. Scheuer, M. J. Kelly-Borges, K. Goins, *J. Org. Chem.* 1995, 60, 7290.
7. For a review, see: B.-G. Wang, J. B. Gloer, N.-Y. Ji, J.-C. Zhao, *Chem. Rev.* 2013, 113, 3632.
8. (a) J. W. Blunt, B. R. Copp, M. H. G. Munro, P. T. Northcote, M. R. Prinsep, *Nat. Prod. Rep.* 2006, 23, 26; (b) J. W. Blunt, B. R. Copp, W.-P. Hu, M. H. G. Munro, P. T. Northcote, M. R. Prinsep, *Nat. Prod. Rep.* 2009, 26, 170; (c) J. W. Blunt, B. R. Copp, R. A. Keyzers, M. H. G. Munro, M. R. Prinsep, *Nat. Prod. Rep.* 2012, 29, 144.
9. For a review, see: A. Butler, M. Sandy, *Nature*, 2009, 460, 848.
10. (a) S. Yamamura, Y. Terada, *Tetrahedron Lett.* 1977, 18, 2171; (b) A. Bulter, J. N. Cartr-Franklin, *Nat. Prod. Rep.* 2004, 21, 180; (c) A. Yarnell, *Chem. Eng. News* 2006, 84, 12.
11. (a) E. E. van Tamelen, *Acc. Chem. Res.* 1968, 1, 111; (b) E. E. van Tamelen, *Acc. Chem. Res.* 1975, 8, 152.
12. (a) W. S. Johnson, *Acc. Chem. Res.* 1968, 1, 1; (b) W. S. Johnson, *Angew. Chem. Int. Ed.* 1976, 15, 9; (c) W. S. Johnson, *Bioorg. Chem.* 1976, 5, 51.
13. (a) L. E. Wolinsky, D. J. Faulkner, *J. Org. Chem.* 1976, 41, 597; (b) A. G. González, J. D. Martín, C. Pérez, M. A. Ramírez, *Tetrahedron Lett.* 1976, 17, 137; (c) Y. Yamaguchi, T. Uyehara,

T. Kato, *Tetrahedron Lett.* 1985, 26, 343;(d)J. N. Carter-Franklin, J. D. Parrish, R. A. Tschirret-Guth, R. D. Little, A. Butler, *J. Am. Chem. Soc.* 2003, 125, 3688.

14. (a) M. Nishizawa, H. Takenaka, Y. Hayashi, *J. Am. Chem. Soc.* 1984, 106, 4290; (b) M. Nishizawa, H. Takenaka, Y. Hayashi, *J. Org. Chem.* 1986, 51, 806.
15. (a) K. Ishihara, S. Nakamura, H. Yamamoto, *J. Am. Chem. Soc.* 1999, 121, 4906; (b) S. Nakamura, K. Ishihara, H. Yamamoto, *J. Am. Chem. Soc.* 2000, 122, 8131; (c) K. Ishihara, H. Ishibashi, H. Yamamoto, *J. Am. Chem. Soc.* 2001, 123, 1505; (d) K. Ishihara, H. Ishibashi, H. Yamamoto, *J. Am. Chem. Soc.* 2002, 124, 3647; (e) K. Ishihara, D. Nakashima, Y. Hiraiwa, H. Yamamoto, *J. Am. Chem. Soc.* 2003, 125, 25; (f) K. Kumazawa, K. Ishihara, H. Yamamoto, *Org. Lett.* 2004, 6, 2551; (g) H. Ishibashi, K. Ishihara, H. Yamamoto, *J. Am. Chem. Soc.* 2004, 126, 11122; (h) M. Uyanik, H. Ishibashi, K. Ishihara, H. Yamamoto, *Org. Lett.* 2005, 7, 1601; (i) M. Uyanik, H. Ishibashi, K. Ishihara, H. Yamamoto, *Bioorg. Med. Chem.* 2005, 13, 5055.
16. For a review, see: R. A. Yoder, J. N. Johnston, *Chem. Rev.* 2005, 105, 4730.
17. (a) E. J. Corey, M. A. Tius, J. Das, *J. Am. Chem. Soc.* 1980, 102, 1742; (b) E. J. Corey, J. G. Reid, A. G. Myers, R. W. Hahl, *J. Am. Chem. Soc.* 1987, 109, 918; (c) E. J. Corey, J. Lee, *J. Am. Chem. Soc.* 1993, 115, 8873; (d) E. J. Corey, H. B. Wood, *J. Am. Chem. Soc.* 1996, 118, 11982; (e) E. J. Corey, D. S. Staas, *J. Am. Chem. Soc.* 1997, 119, 9929; (f) E. J. Corey, D. D. Staas, *J. Am. Chem. Soc.* 1998, 120, 3526; (g) A. X. Huang, Z. Xiong, E. J. Corey, *J. Am. Chem. Soc.* 1999, 121, 9999; (h) J. Zhang, E. J. Corey, *Org. Lett.* 2001, 3, 3215; (i) Y. Mi, J. V. Schreiber, E. J. Corey, *J. Am. Chem. Soc.* 2002, 124, 11290; (j) D. C. Behenna, E. J. Corey, *J. Am. Chem. Soc.* 2008, 130, 6720; (k) K. Surendra, E. J. Corey, *J. Am. Chem. Soc.* 2008, 130, 8865; (l) K. Surendra, E. J. Corey, *J. Am. Chem. Soc.* 2009, 131, 13928; (m) R. A. Shenvi, E. J. Corey, *Org. Lett.* 2010, 12, 3548.
18. D. C. Braddock, J. S. Marklew, K. M. Foote, A. J. P. White, *Chirality* 2013, 25, 692.
19. F. E. King, T. J. King, J. G. Topliss, *J. Chem. Soc.* 1957, 573.
20. B. K. Banik, A. K. Chakraborti, U. R. Ghatak, *J. Chem. Res. (S)* 1986, 406.
21. (a) K. Surendra, E. J. Corey, *J. Am. Chem. Soc.* 2012, 134, 11992; (b) K. Surendra, G. Rajendar, E. J. Corey, *J. Am. Chem. Soc.* 2014, 136, 642.
22. (a) For the use of triphenylphosphonium triflate as a Brønsted acid catalyst, see: H. Iwahashi, T. Oka, A. Abiko, *Chem. Lett.* 2008, 37, 708; (b) A. Sakakura, K. Ishihara, *Chem. Rec.* 2015, 15, 728–742.
23. (a) A. Sakakura, M. Sakuma, K. Ishihara, *Org. Lett.* 2011, 13, 3130; (b) M. Sakuma, A. Sakakura, K. Ishihara, *Org. Lett.* 2013, 15, 2838.
24. For selected recent examples, see: (a) S. A. Snyder, D. S. Treitler, A. P. Brucks, *J. Am. Chem. Soc.* 2010, 132, 14303; (b) K. Surendra, E. J. Corey, *J. Am. Chem. Soc.* 2009, 131, 13928.
25. C.-C. Chen, Y.-L. Huang, P.-Y. Yeh, J.-C. Ou, *Planta Med.* 2003, 69, 964.
26. (a) Y. Ohfune, N. Kurokawa, *Tetrahedron Lett.* 1985, 26, 5307; (b) R. C. Larnck, T. R. Hightower, *J. Org. Chem.* 1993, 58, 5298; (c) S. H. Kang, J. H. Lee, S. B. Lee, *Tetrahedron Lett.* 1998, 39, 59; (d) C. Jonasson, A. Horvath, J. E. Baeckvall, *J. Am. Chem. Soc.* 2000, 122, 9600; (e) S. P. Chavan, A. K. Shamia, *Tetrahedron Lett.* 2001, 42, 4923; (f) M. Tiecco, L. Testaferri, A. Temperini, L. Bagnoli, F. Marini, C. Santi, *Synlett* 2001, 1767; (g) M. GruUadauria, C. Aprile, R. Noto, *Tetrahedron Lett.* 2002, 43, 1669; (h) M. Curini, F. Epifano, M. C. MarcoiuUio, F. Montanari, *Synlett* 2004, 2, 368.
27. (a) M. F. Anscll, M. H. Palmer, *Q. Rev. (Lond.)* 1964, 18, 211; (b) M. Tiecco, L. Testaferri, M. Tingoli, *Tetrahedron* 1993, 49, 5351; (c) R. S. Mali, K. N. Babu, *Helv. Chim. Acta* 2002, 85, 3525; (d) K. Miura, J. Hayashida, T. Takahashi, H. Nishikori, A. Hosomi, *J. Organomet. Chem.* 2003, 686, 242; (e) Y. Zhou, L. K. Woo, R. J. Angelici, *Appl. Catal. A: Gen.* 2007, 333, 238.
28. L. Coulombel, E. Duñach, *Synth. Commun.* 2005, 35, 153.
29. K. B. Upar, S. J. Mishra, S. P. Nalawade, S. A. Singh, R. P. Khandare, S. V. Bhat, *Tetrahedron Asymmetry* 2009, 20, 1637.
30. For selected examples, see: (a) H. B. Kagan, J. C. Fiaud, in *Topics in Stereochemistry*, Vol. 18, ed. by E. L. Eliel, S. H. Wilen, John Wiley & Sons, Inc., New York (1988), pp 249–330; (b) J. M. Keith, J. F. Larrow, E. N. Jacobsen, *Adv. Synth. Catal.* 2001, 343, 5; (c) V. P. Krasnov, D. A. Gruzdev, G. L. Levit, *Eur. J. Org. Chem.* 2012, 1471; (d) C. E. Müller, P. R. Schreiner, *Angew. Chem. Int. Ed.* 2011, 50, 6012; (e) J. E. Taylor, S. D. Bull, J. M. J. Williams, *Chem. Soc. Rev.* 2012, 41, 2109; (f) E. Vedejs, M. Jure, *Angew. Chem. Int. Ed.* 2005, 44, 3974.
31. For recent advances, see: (a) A. Peschiulli, B. Procuranti, C. J. O'Connor, S. J. Connon, *Nat. Chem.* 2010, 2, 380; (b) V. D. Bumbu, V. B. Birman, *J. Am. Chem. Soc.* 2011, 133, 13902; (c) I. Čorić, B. List, *Nature* 2012, 483, 315; (d) Y. Wang, K. Zheng, R. Hong, *J. Am. Chem. Soc.* 2012, 134, 4096.
32. (a) J. H. Koh, M. G. Gagné, *Angew. Chem. Int. Ed.* 2004, 43, 3459; (b) J. H. Koh, C. Mascarenhas, M. R. Gagné, *Tetrahedron* 2004, 60, 7405; (c) For a review, see A. R. Chianese, S. J. Lee, M. R. Gagné, *Angew. Chem. Int. Ed.* 2007, 46, 4042; (d) L. Nelson, M. R. Gagné, *Organometallics* 2009, 28, 950; (e) J. G. Sokol, C. S. Korapala, P. S. White, J. J. Becker, M. R. Gagné, *Angew. Chem. Int. Ed.* 2011, 50, 5658; (f) W. D. Kerber, J. H. Koh, M. R. Gagné, *Org. Lett.* 2004, 6, 3013; (g) W. D. Kerber, M. R. Gagné, *Org. Lett.* 2005, 7, 3379; (h) J. A. Feducia, A. N. Campbell, M. Q. Doherty, M. R. Gagné, *J. Am. Chem. Soc.* 2006, 128, 13290; (i) C. A. Mullen, M. R. Gagné, *J. Am. Chem. Soc.* 2007, 129, 11880; (j) C. A. Mullen, A. N. Campbell, M. R. Gagné, *Angew. Chem. Int. Ed.* 2008, 47, 6011; (k) J. G. Sokol, N. A. Cochrane, J. J. Becker, M. R. Gagné, *Chem. Commun.* 2013, 49, 5046; (l) S.-B. Zhao, J. J. Becker, M. R. Gagné, *Organometallics* 2011, 30, 3926; (m) N. A. Cochrane, H. Nguyen, M. R. Gagné, *J. Am. Chem. Soc.* 2013, 135, 628; (n) H. Nguyen, M. R. Gagné, *ACS Catal.* 2014, 4, 855; (o) M. J. Geier, M. R. Gagné, *J. Am. Chem. Soc.* 2014, 136, 3032.
33. S. A. Snyder, D. S. Treitler, A. Schall, *Tetrahedron* 2010, 66, 4796.
34. S. G. Sethofer, T. Mayer, F. D. Toste, *J. Am. Chem. Soc.* 2010, 132, 8276.

35. (a) K. Surendra, W. Qiu, E. J. Corey, *J. Am. Chem. Soc.* 2011, 133, 9724; (b) W.-W. Qiu, K. Surendra, L. Yin, E. J. Corey, *Org. Lett.* 2011, 13, 5893.
36. J. W. Blunt, B. R. Copp, W.-P. Hu, M. H. G. Munro, P. T. Northcote, M. R. Prinsep, *Nat. Prod. Rep.* 2007, 24, 31.
37. (a) A. Sakakura, A. Ukai, K. Ishihara, *Nature* 2007, 445, 900; (b) A. Sakakura, K. Ishihara, *Chim. Oggi Chem. Today* 2007, 25, 9; (c) A. Sakakura, G. Shomi, A. Ukia, K. Ishihara, *Heterocycles* 2011, 82, 249. (d) A. Sakakura, K. Ishihara, Chem. Rec. 2015, 15, 728.
38. (a) S. H. Kang, S. B. Lee, C. M. Park, *J. Am. Chem. Soc.* 2003, 125, 15748; (b) S. H. Kang, C. M. Park, S. B. Lee, M. Kim, *Synlett* 2004, 1279; (c) S. H. Kang, S. Y. Kang, C. M. Park, H. Y. Kwon, M. Kim, *Pure Appl. Chem.* 2005, 77, 1269.
39. (a) G. Bellucci, C. Chiappe, R. Bianchini, D. Lenoir, R. Herges, *J. Am. Chem. Soc.* 1995, 117, 12001; (b) D. Lenoir, C. Chiappe, *Chem. Eur. J.* 2003, 9, 1036.
40. (a) R. S. Brown, R. W. Nagorski, A. J. Bennet, R. E. D. McClung, G. H. M. Aarts, M. Klobukowski, R. McDonald, B. D. Santarsiero, *J. Am. Chem. Soc.* 1994, 116, 2448; (b) A. A. Neverov, R. S. Brown, *J. Org. Chem.* 1996, 61, 962; (c) R. S. Brown, *Acc. Chem. Res.* 1997, 30, 131.
41. S. E. Denmark, M. T. Burk, A. J. Hoover, *J. Am. Chem. Soc.* 2010, 132, 1232.
42. S. A. Snyder, D. S. Treitler, A. P. Brucks, *Aldrichim. Acta* 2011, 44, 27.
43. E. E. van Tamelen, E. J. Hessler, *Chem. Commun.* 1966, 411.
44. (a) T. Kato, I. Ichinose, S. Kumazawa, Y. Kitahara, *Bioorg. Chem.* 1975, 4, 188; (b) T. Kato, I. Ichinose, A. Kamoshida, Y. Kitahara, *J. Chem. Soc. Chem. Commun.* 1976, 518; (c) T. Kato, K. Ishii, I. Ichinose, Y. Nakai, T. Kumagai, *J. Chem. Soc. Chem. Commun.* 1980, 1106; (d) T. Kato, M. Mochizuki, T. Hirono, S. Fujiwara, T. Uyehara, *J. Chem. Soc. Chem. Commun.* 1984, 1077; (e) Y. Yamaguchi, T. Uyehara, T. Kato, *Tetrahedron Lett.* 1985, 26, 343; (f) S. Fujiwara, K. Takeda, T. Uyehara, T. Kato, *Chem. Lett.* 1986, 1763; (g) T. Hirukawa, M. Oguchi, N. Yhoshikawa, T. Kato, *Chem. Lett.* 1992, 2343.
45. (a) S. A. Snyder, D. S. Treitler, *Angew. Chem. Int. Ed.* 2009, 48, 7899; (b) S. A. Snyder, D. S. Treitler, A. P. Brucks, *J. Am. Chem. Soc.* 2010, 132, 14303.
46. (a) Y. Sawamura, H. Nakatsuji, A. Sakakura, K. Ishihara, *Chem. Sci.* 2013, 4, 4181; (b) Y. Sawamura, H. Nakatsuji, M. Akakura, A. Sakakura, K. Ishihara, *Chirality* 2014, 26, 356; (c) H. Nakatsuji, Y. Sawamura, A. Sakakura, K. Ishihara, *Angew. Chem. Int. Ed.* 2014, 53, 6974.
47. (a) D. Leguern, G. Morel, A. Foucaud, *Tetrahedron Lett.* 1974, 15, 955; (b) M.-F. Chasle, E. Marchand, A. Foucaud, *Tetrahedron Lett.* 1971, 12, 963; (c) E. V. Jennings, K. Nikitin, Y. Ortin, D. G. Gilheany, *J. Am. Chem. Soc.* 2014, 136, 16217.
48. C. Recsei, B. Chan, C. S. P. McErlean, *J. Org. Chem.* 2014, 79, 880.
49. (a) R. B. Grossman, R. J. Trupp, *Can. J. Chem.* 1998, 76, 1233; (b) X.-L. Cui, R. S. Brown, *J. Org. Chem.* 2000, 65, 5653; (c) J. Haas, S. Piguel, T. Wirth, *Org. Lett.* 2002, 4, 297; (d) T. Fukuzumi, N. Shibata, M. Sugiura, S. Nakamura, T. Toru, *J. Fluor. Chem.* 2006, 127, 548.
50. Y.-J. Zhao, S.-S. Chng, T.-P. Loh, *J. Am. Chem. Soc.* 2007, 129, 492.
51. M. Uyanik, K. Ishihara, H. Yamamoto, *Org. Lett.* 2006, 8, 5649.
52. Y.-J. Zhao, B. Li, L.-J. S. Tan, Z.-L. Shen, T.-P. Loh, *J. Am. Chem. Soc.* 2010, 132, 10242.
53. S. Rendler, D. W. C. MacMillan, *J. Am. Chem. Soc.* 2010, 132, 5027.
54. R. R. Knowles, S. Lin, E. N. Jacobsen, *J. Am. Chem. Soc.* 2010, 132, 5030.
55. B. Radetich, E. J. Corey, *J. Am. Chem. Soc.* 2002, 124, 2430.
56. V. Gnanadesikan, E. J. Corey, *J. Am. Chem. Soc.* 2008, 130, 8089.
57. T. N. Barrett, A. G. M. Barrett, *J. Am. Chem. Soc.* 2014, 136, 17013.

# SECTION III

# SHIKIMIC ACID BIOSYNTHETIC PATHWAY

# 10

# LIGNANS, LIGNINS, AND RESVERATROLS

YU PENG
*State Key Laboratory of Applied Organic Chemistry, Lanzhou University, Lanzhou, China*

## 10.1 BIOSYNTHESIS

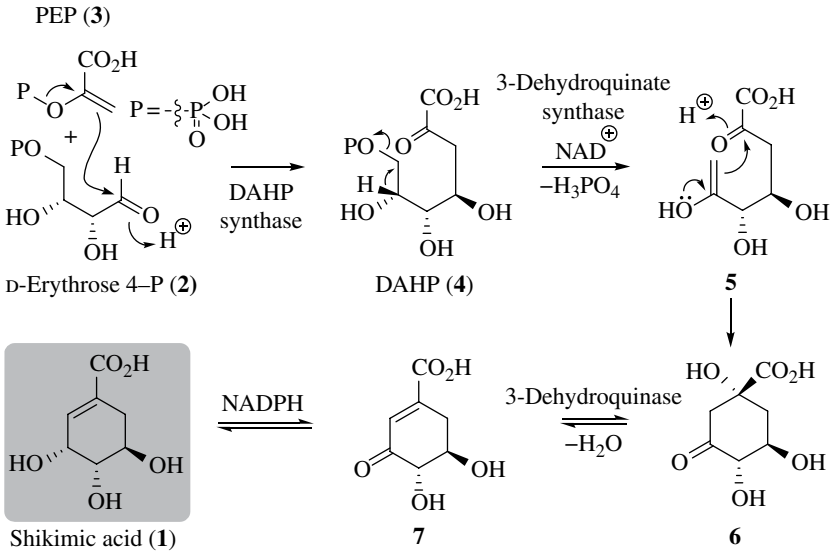
### 10.1.1 Primary Metabolism of Shikimic Acid and Aromatic Amino Acids

Shikimic acid (**1**) [1] was first isolated from the fruit of *Illicium religiosum* Sieb. et Zucc. in 1885 by Eykman [2]. Its relative and absolute configuration was not determined until in the 1930s by Karrer [3a], Fischer [3b–g], and Freudenberg [3h]. Its major role in the metabolism of several natural substances, known as the shikimic acid pathway, has been revealed [4] based on the pioneering work of Davis [5a], Sprinson [5b], and Gibson [5c]. This biosynthetic pathway starts from an intermolecular aldol-type condensation between D-erythrose 4-phosphate (**2**) and phosphoenolpyruvate (PEP, **3**) to give 3-deoxy-D-arabino-heptulosonic acid 7-phosphate (DAHP, **4**). This reaction is controlled by the enzyme DAHP synthase (Scheme 10.1) and establishes a new chiral center by *re*-face attack of PEP to **2**. The elimination of phosphoric acid from DAHP (**4**) followed by an intramolecular aldol reaction affords 3-dehydroquinic acid (**6**). This step constructs the carbon skeleton of shikimic acid (**1**) and actually involves an $NAD^+$/NADH-dependent redox reaction of **5** under the control of the enzyme 3-dehydroquinate synthase. Then, the dehydration catalyzed by the enzyme 3-dehydroquinase occurs to give 3-dehydroshikimic acid (**7**), which can be further converted to shikimic acid (**1**) by NADPH reduction.

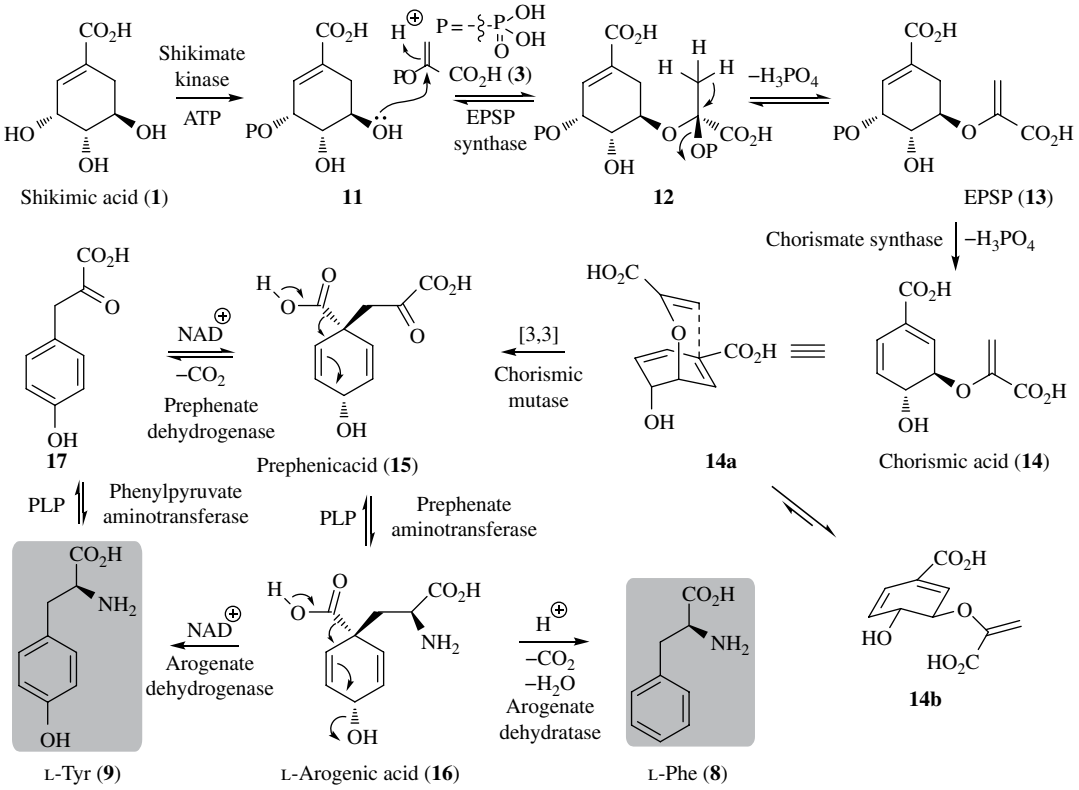
Aromatic compounds, especially the aromatic amino acids [6] L-phenylalanine (**8**), L-tyrosine (**9**), and L-tryptophan (**10**), could be synthesized through the shikimate pathway in microorganisms and plants. As shown in Scheme 10.2, an ATP-dependent phosphorylation of **1** provides shikimic acid 3-phosphate (**11**), which is further combined with PEP (**3**), catalyzed by the enzyme EPSP synthase under acidic conditions to give 3-enolpyruvylshikimic acid 3-phosphate (EPSP, **13**), via an addition–elimination reaction. The next step involves chorismate synthase-controlled 1,4-elimination of phosphoric acid on **13**, affording chorismic acid (**14**), a very important branchpoint compound in the shikimate pathway. A Claisen rearrangement of **14** delivers prephenic acid (**15**) that has already possessed the whole carbon backbone of the targeted phenylalanine and tyrosine. This reaction is facilitated and controlled by chorismate mutase via its binding with the pseudoaxial conformer **14a** of chorismic acid, which could develop to more stable transition state **14b**. Pyridoxal phosphate (PLP)-dependent transamination of **15** generates L-arogenic acid (**16**) [7], which can be further transformed into L-phenylalanine (**8**) and L-tyrosine (**9**) depending on the presence of dehydratase or dehydrogenase. The order of these reactions can vary. For example, the $NAD^+$-dependent decarboxylative aromatization prior to transamination of **15** could also occur, and the resulting 4-hydroxyphenyl pyruvic acid (**17**) is then converted to L-tyrosine (**9**) by phenyl pyruvate aminotransferase-controlled transamination.

Biosynthetic pathway of L-tryptophan (**10**) is shown in Scheme 10.3. The aforementioned chorismic acid (**14**) would participate in an $S_N2'$-type reaction, in which ammonia generated from glutamine acts as a nucleophile. The resultant 2-amino-2-deoxy-isochorismic acid (**18**) could be transformed

*From Biosynthesis to Total Synthesis: Strategies and Tactics for Natural Products*, First Edition. Edited by Alexandros L. Zografos.
© 2016 John Wiley & Sons, Inc. Published 2016 by John Wiley & Sons, Inc.

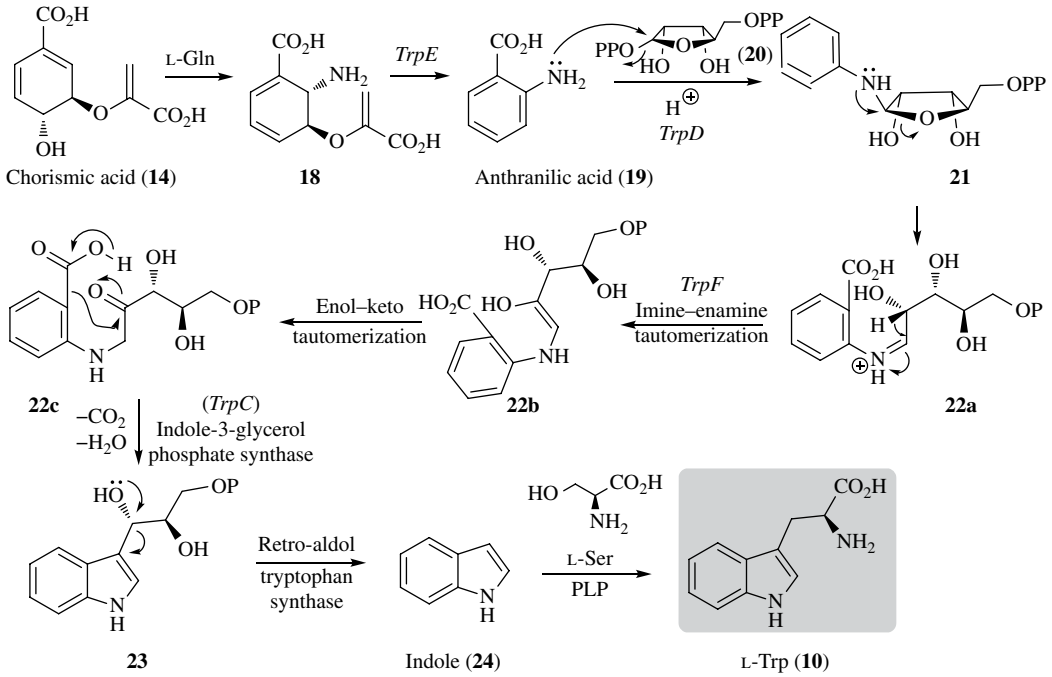



**SCHEME 10.1** Biosynthesis of shikimic acid (**1**).




**SCHEME 10.2** Biosynthetic pathway from shikimic acid (**1**) to L-phenylalanine (**8**) and L-tyrosine (**9**).

into anthranilic acid (**19**) through the elimination of pyruvic acid by 2-amino-2-deoxy isochorismate lyase (TrpE). Then anthranilic acid (**19**) would initiate a complex reaction sequence to form the desired L-tryptophan (**10**). The first step involves an $S_N2$-type reaction with phosphoribosyl diphosphate (**20**) catalyzed by anthranilate phosphoribosyl transferase (TrpD), and the furan ring of the generated **21** would open to produce iminium **22a** under the acidic conditions. The subsequent imine–enamine and enol–keto tautomerization under the control of phosphoribosyl anthranilate isomerase (TrpF) gives the ketone **22c**, which in turn could be converted to indole-3-glycerol phosphate (**23**) via a




**SCHEME 10.3** Biosynthetic pathway from shikimic acid (**1**) to L-tryptophan (**10**) via chorismic acid (**14**).

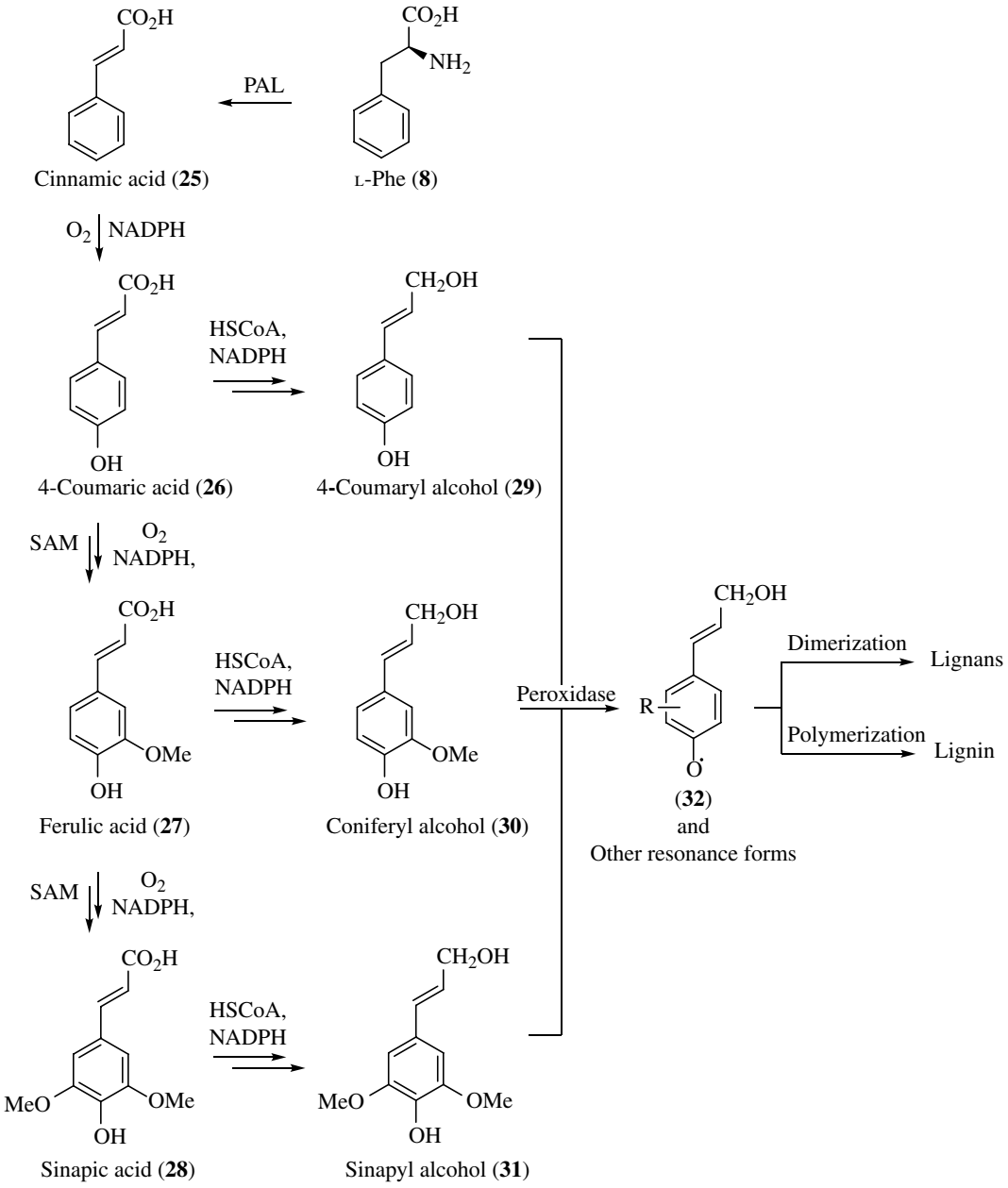
decarboxylative Friedel–Crafts-type cyclization catalyzed by TrpC. The L-tryptophan (**10**) is obtained eventually through the removal of side-chain ribosyl carbons via a retro–aldol reaction and the replacement of indole (**24**) by L-serine.

### 10.1.2 Lignans and Lignin

The downstream metabolites in the shikimic acid pathway mainly include lignans and lignin, and their biosynthesis [8] is shown in Scheme 10.4. Deamination of L-phenylalanine (**8**) catalyzed by the enzyme phenylalanine ammonia lyase (PAL) [9] generates cinnamic acid (**25**), which is further oxidized to 4-coumaric acid (**26**) through the NADPH-dependent hydroxylation. The similar hydroxylation and methylation on **26** by *S*-adenosyl methionine (SAM) give ferulic acid (**27**) and sinapic acid (**28**) sequentially. All of these three unsaturated acids transform into the corresponding 4-coumaryl alcohol (**29**), coniferyl alcohol (**30**), and sinapyl alcohol (**31**) through the NADPH-dependent reduction via coenzyme A esters. The peroxidase then achieves single-electron oxidation of the phenol group in these three allylic alcohols, and the generated radical species (**32**) along with other resonance forms dimerize or polymerize in stereocontrolled fashion, thus affording a variety of lignans or lignin.

Biosynthesis of some antimalarial lignans such as 8′-*epi*-aristoligone (**33**) from the roots of *Holostylis reniformis* [10a] had been investigated through detailed administration experiments with the radiolabeled precursors by Lopes and coworkers [10b]. Similar to the well-known biosynthetic pathway of lignans with oxygenation at C9 and C9′, [9-$^3H_1$] isoeugenol (**34**) resulting from the reduction of coniferyl alcohol [11] would generate O-centered radical **34A** and its resonance forms like **34B** and **34C** by enzymatic oxidation (Scheme 10.5). Regio- and stereospecific radical coupling then proceeded *in vivo* and provided the dimer **35** with the construction of C8—C8′ bond. The attack of water to one of quinone methides followed by the intramolecular Friedel–Crafts alkylation of the resultant phenol **36** to the remaining quinone methide afforded aryltetralol **37** in a highly diastereoselective fashion. After the establishment of the key C2—C7′ bond, the access to the optically active 8′-*epi*-aristoligone (**33**) only needed two steps of functional group transformations: oxidation and methylation of ketone **38**. The other lignans isolated from this genus of plant could be derived from this aryltetralone as well.

(−)-Podophyllotoxin (**39**) is a very important antitumor and antiviral agent that was isolated from *Podophyllum* species. As shown in Scheme 10.6, its biosynthesis begins with an analogous phenolic oxidative coupling of coniferyl alcohol (**40**). This C8—C8′ dimerization of radical species **40A** is controlled by dirigent protein [12] and thus stereospecific, affording bis-quinonemethide (**41**) that would further convert to neolignan (+)-pinoresinol (**42**). The stepwise reductive opening of tetrahydrofuran rings in **42** via the action of an NADPH-dependent bifunctional pinoresinol/lariciresinol reductase produces (−)-secoisolariciresinol (**44**), which is oxidized by $NAD^+$-dependent secoisolariciresinol dehydrogenase to give (−)-matairesinol (**45**). Notably, this biosynthetic route from **40** to **45** had been investigated in

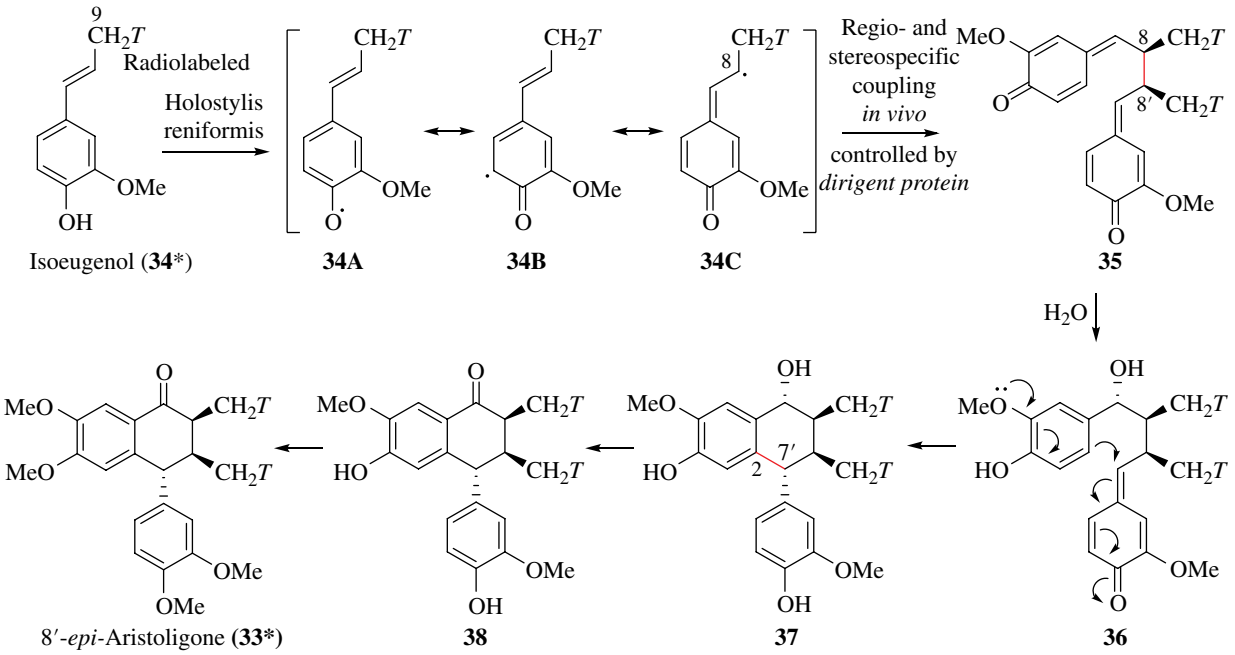



**SCHEME 10.4** Biosynthetic pathway from L-Phe to lignans and lignin.

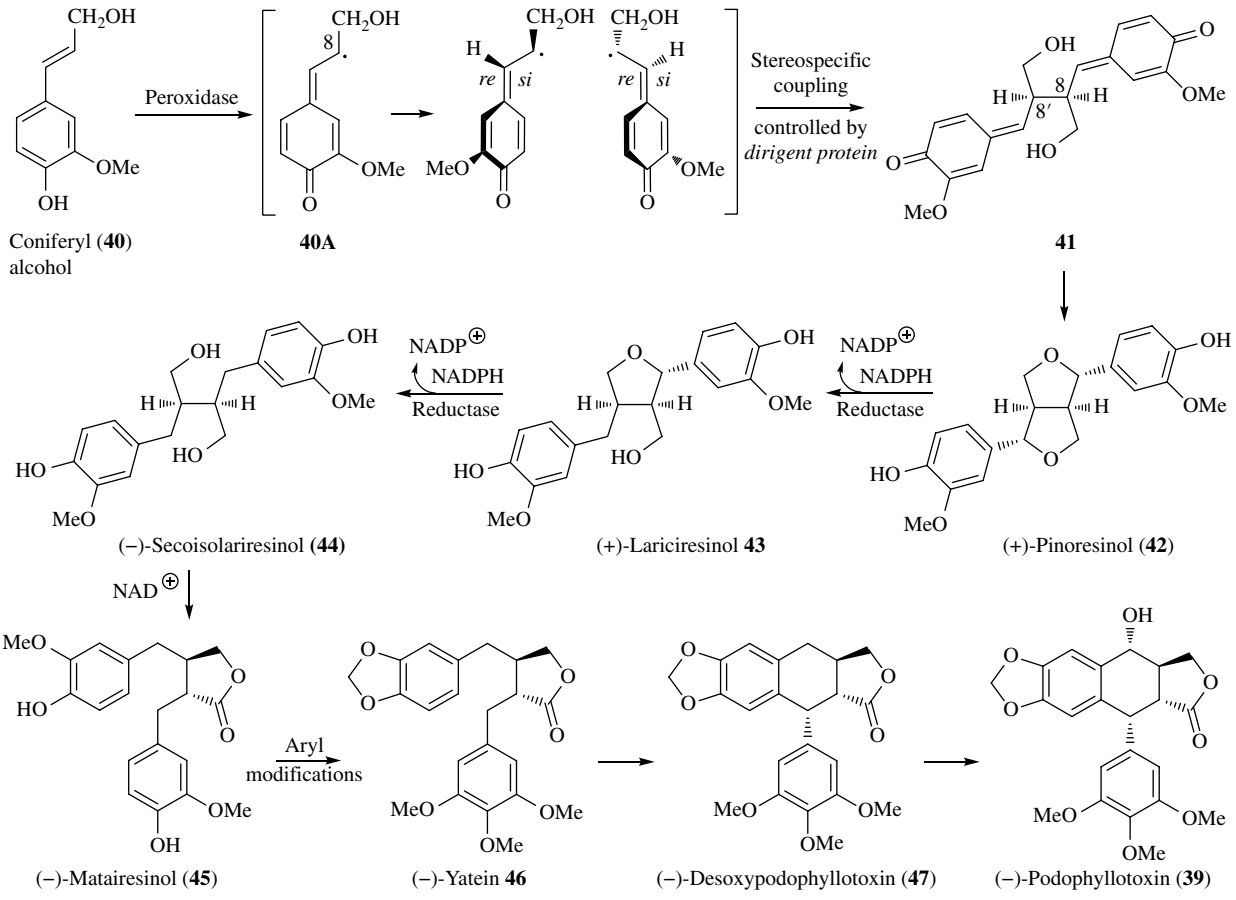
*Podophyllum peltatum*/*Linum flavum* by Lewis and coworkers [13a] using radiolabeled substrates, whereas (−)-matairesinol (**45**) that serves as a biosynthetic precursor for (−)-podophyllotoxin (**39**) had been also determined earlier by Dewick and coworkers [13b]. These late-stage transformations include modifications of two aryl rings and subsequent Friedel–Crafts alkylation of the resultant yatein (**46**) just like that described from **36** to **37** (Scheme 10.5). Finally, the regio- and stereoselective hydroxylation of (−)-deoxypodophyllotoxin (**47**) completes the biosynthesis of (−)-podophyllotoxin (**39**).

## 10.2 AUXILIARY-ASSISTED C($sp^3$)–H ARYLATION REACTIONS IN ORGANIC SYNTHESIS

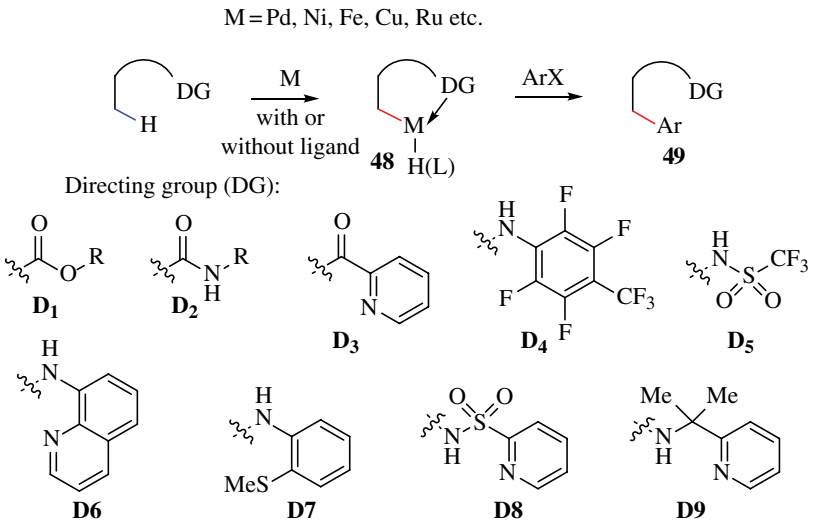
C—H bonds are ubiquitous in organic molecules, and therefore direct functionalization of substrates by activation of C—H bonds and subsequent transformation would eliminate the multiple steps and limitations associated with the preparation of functionalized starting materials. Over the past two decades, transition metal-catalyzed activation reactions of C—H bonds have opened a new dimension in synthetic




**SCHEME 10.5** Biosynthetic pathway to 7′-aryltetralol and aryltetralone lignans in *Holostylis reniformis*.




**SCHEME 10.6** Biosynthetic pathway from coniferyl alcohol (**40**) to (−)-podophyllotoxin (**39**) via (−)-matairesinol (**45**).

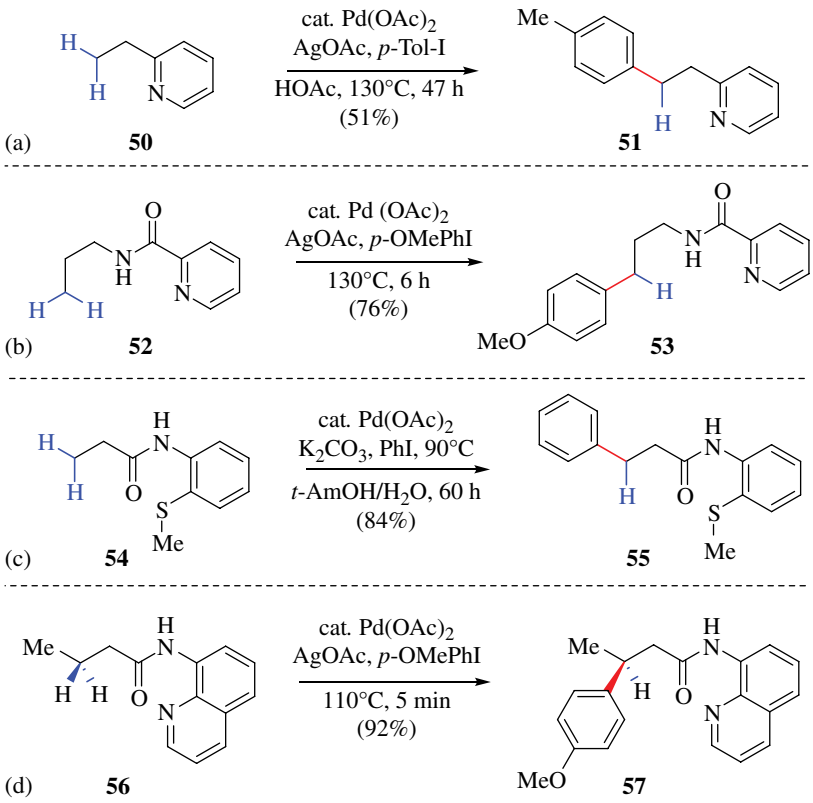



**SCHEME 10.7** Chelation-assisted C($sp^3$)─H arylation catalyzed by a transition metal.

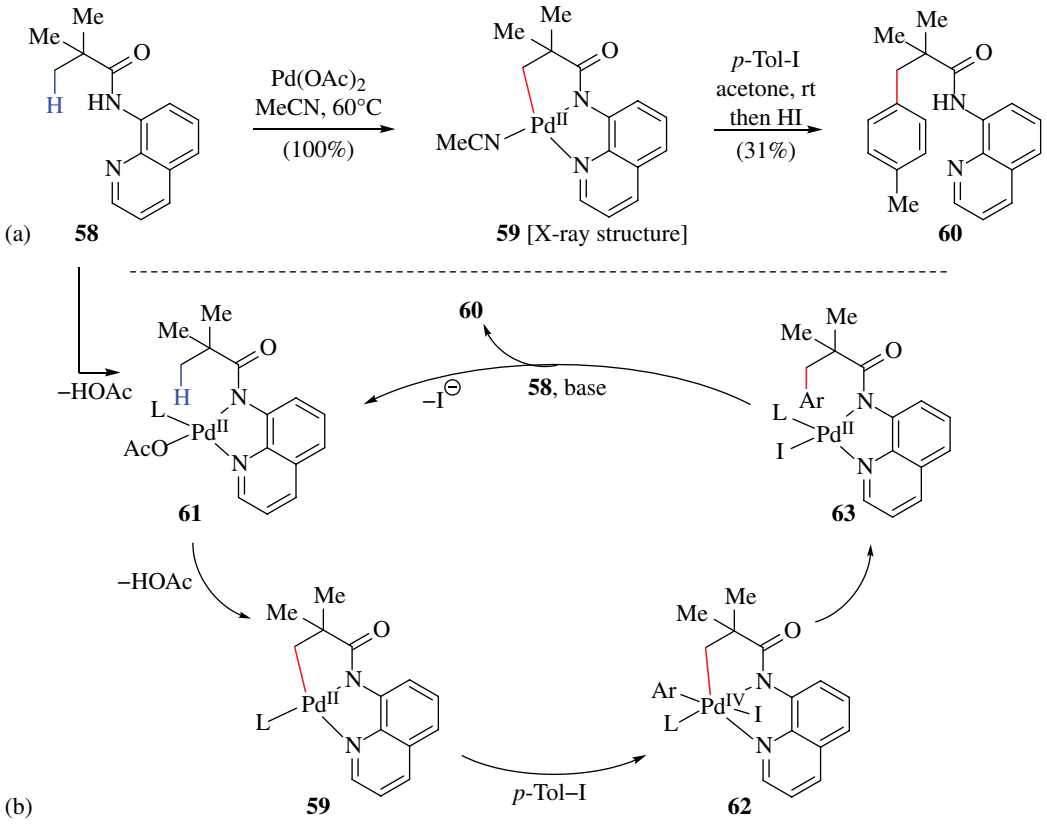
organic chemistry and provided novel perspectives in retrosynthesis [14]. In particular, direct functionalization of unactivated C($sp^3$)─H bonds remains underdeveloped and continues to be highly challenging due to the absence of stabilizing orbital interactions with the metal center, as is the case with C($sp^2$)─H bonds. Another issue is the control of regioselectivity because of the large number and diversity of C─H bonds in an organic compound. The use of a directing group with at least one heteroatom can overcome this problem by allowing the catalyst to come into proximity with the targeted C($sp^3$)─H bonds, via the formation of a thermodynamically stable 5- or 6-membered metallacyclic intermediate **48** (Scheme 10.7). The electrophilic reagents such as aryl halide (ArX) then react with this metal complex, affording eventually the arylation [15] product **49**. Some efficient monodentate directing groups include –ester, –amide (**$D_1$**~**$D_5$**), etc., and sometimes these weak coordinating groups [16] need an external ligand to lower the transition state energy in the C–H bond cleavage. Recently, bidentate directing groups [17] (e.g., **$D_6$**~**$D_9$**) have emerged as promising tools for C($sp^3$)─H arylation, and the assistance of the external ligand is not necessary owing to their innate strong capacity.

In 2005, Daugulis and Shabashov [18a] reported that the primary β-C($sp^3$)─H bond of 2-ethylpyridine (**50**) underwent a $Pd(OAc)_2$-catalyzed arylation, affording **51** in 51% yield (Scheme 10.8a). However, the scope of this unprecedented transformation was limited, especially as the auxiliary pyridine moiety cannot be easily removed. The similar but more efficient γ-C─H arylation of the amide **52** derived from the detachable picolinic acid was later demonstrated (Scheme 10.8b) [18b], offering an interesting method for the functionalization of aliphatic amines upon the hydrolysis of the resulting amides like **53**. Two important directing groups, that is, 8-aminoquinoline (AQ) and 2-methylthioaniline, were subsequently investigated in detail [18b, c]. As shown in Scheme 10.8c, primary β-C─H bond of 2-methylthioaniline-derived amide **54** was monoarylated with *p*-iodoanisole under the indicated conditions, giving **55** in 84% yield. While substantial β-methyl diarylation of AQ-derived amide always occurred, the corresponding secondary β-C─H monoarylation proceeded in a very fast reaction rate and high yield (Scheme 10.8d). Considering the relative difficulty of activating a methylene C($sp^3$)─H bond compared with methyl analogs, this type of transformation represented by **56** is remarkable. Both 2-methylthioaniline and AQ moieties can be removed under simple basic or acidic hydrolysis condition, therefore providing convenient approach for the synthesis of β-arylated carboxylic acids.

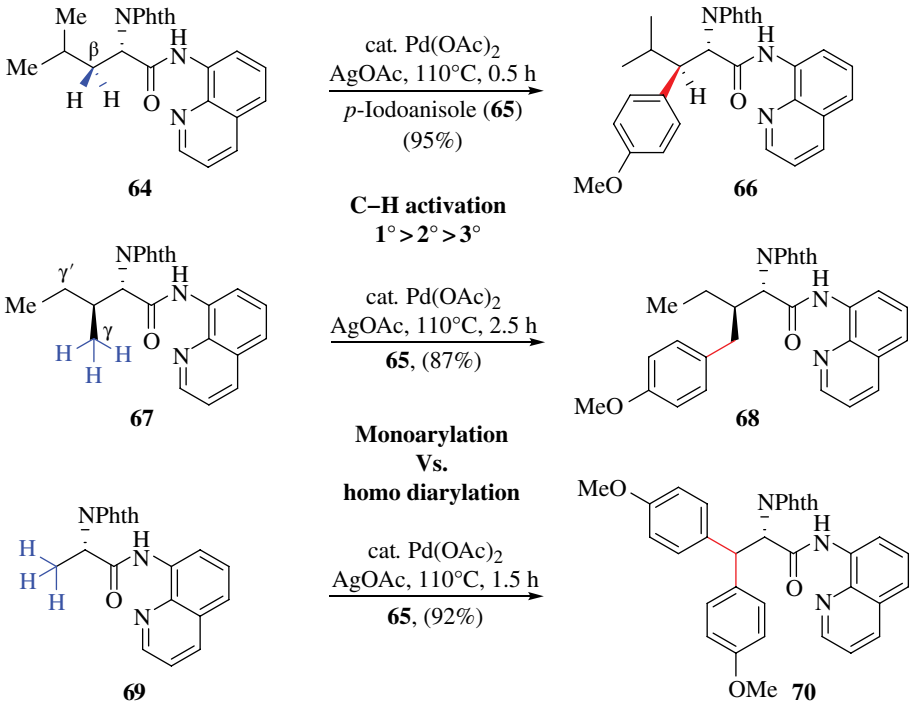
In order to get an insight into the mechanism of the aforementioned C($sp^3$)─H arylation, some intermediates were intercepted and characterized [18c]. For example, the reaction of 8-AQ pivalamide **58** with stoichiometric amount of $Pd(OAc)_2$ in MeCN produced the cyclopalladium complex **59** in quantitative yield (Scheme 10.9a). The structure of this Pd(II) complex was verified by single-crystal X-ray diffraction analysis, from which the formation of C($sp^3$)─Pd bond assisted by the bidentate AQ auxiliary could be observed clearly. This activated C─H bond in **59** was then reacted with *p*-tolyl iodide to generate β-arylated pivalamide **60**, thereby implying that complex **59** may be the reactive intermediate. The Pd-catalytic cycle is demonstrated in Scheme 10.9b: the initial reaction of $Pd(OAc)_2$ with **58** affords palladium amide **61**. The next step involves a rapid cyclopalladation of the *tert*-butyl group that would generate palladacycle **59** with the simultaneous release of HOAc. Oxidative addition of *p*-tolyl iodide to **59** affords Pd(IV) complex **62**, and its reductive elimination followed by ligand exchange of **63** with **58** produces the desired β-arylated pivalamide **60** accompanied with the regeneration of palladium amide **61**.




**SCHEME 10.8** Daugulis's pioneering arylation of C($sp^3$)—H bonds by directed Pd catalysis.




**SCHEME 10.9** The proposed Pd(II)/Pd(IV) catalytic cycle.

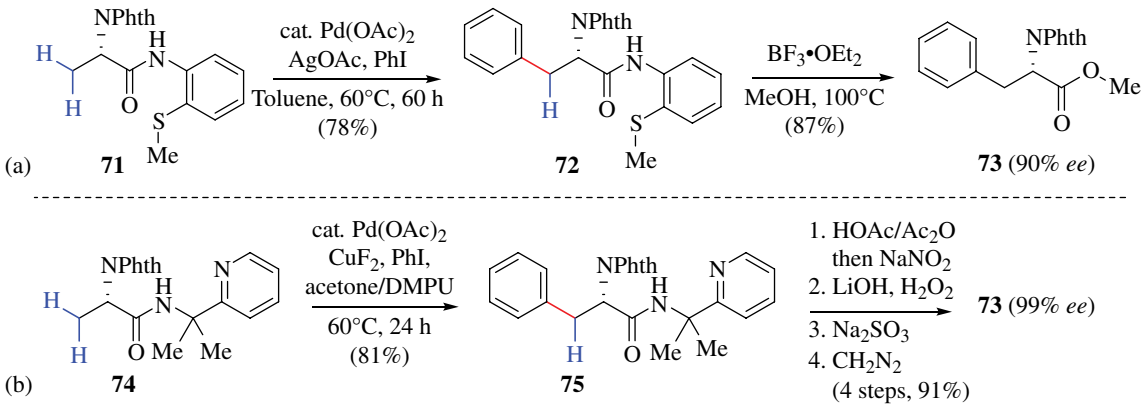



**SCHEME 10.10** Corey's pioneering synthesis of nonnatural α-amino acids by C($sp^3$)—H arylation.

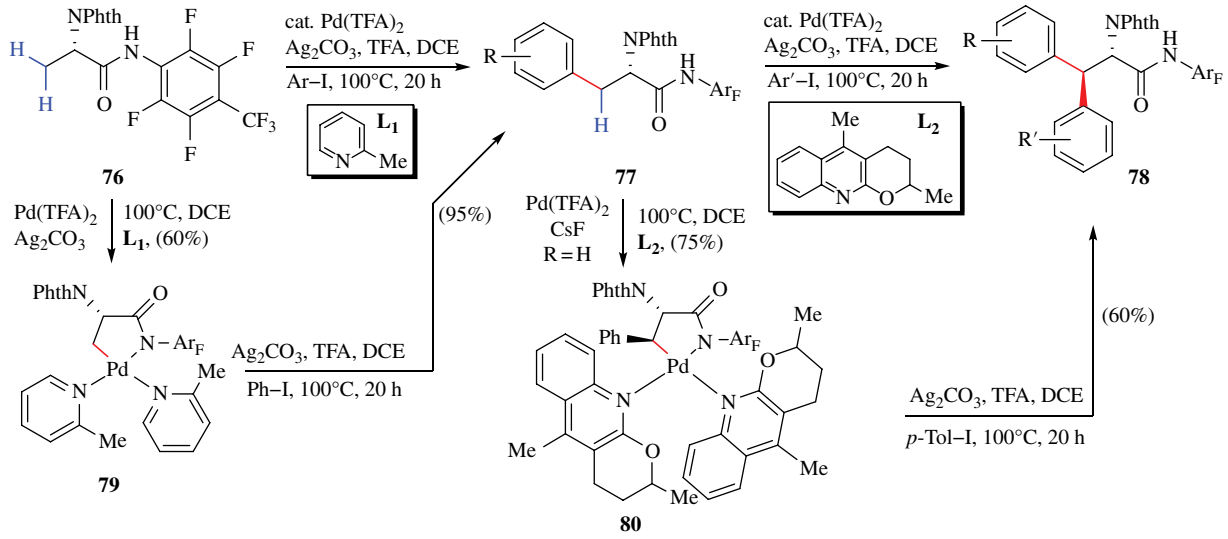
The seminal report by Daugulis and coworkers was rapidly adapted to the efficient and novel synthesis of various nonnatural α-amino acid derivatives. As shown in Scheme 10.10, Corey and coworkers [19] pioneeringly reported the Pd-catalyzed β-arylation of *N*-phthaloylated leucine amide **64** and demonstrated excellent regio- and diastereoselectivity during the access to **66** in 95% yield. This 8-AQ-guided C—C coupling method is also suitable for the C($sp^3$)—H arylation at the γ position as in the case of isoleucine amide **67**. The observed monoarylation selectivity (**68**) is attributed to steric hindrance of tertiary β-C—H bond and predominant insertion of palladium into methyl over γ-methylene group. When the alanine 8-AQ amide **69** was treated with catalytic amount of $Pd(OAc)_2$ and 1.5 equivalent of AgOAc in excess of *p*-iodoanisole (**65**), a *gem*-diarylation occurred, providing β-*p*-anisylated tyrosine derivative **70** in 92% yield.

Subsequently, other auxiliaries were investigated for primary β-C($sp^3$)—H monoarylation of α-amino acids. As shown in Scheme 10.11a, Daugulis and coworkers [20] reported that the use of 2-thiomethylaniline as a directing group allowed for a selective monophenylation of the methyl group in **71** under the Pd-catalyzed conditions, affording **72** in 78% yield. Unfortunately, the erosion of the optical purity was observed in the resulting phenylalanine methyl ester **73** upon the removal of this directing group by $BF_3{\cdot}OEt_2$. Thus, an alternative bidentate directing group derived from 2-(pyridin-2-yl-) isopropylamine (PIP) was developed by Shi and coworkers (Scheme 10.11b) [21]. This new pyridine-containing directing group indeed demonstrated superior selectivity for mono- versus diarylation of **74**, and the use of $CuF_2$ as a scavenger of the generated iodide further improved the yield of **75**. Importantly, the same phenylalanine methyl ester **73** could be obtained without any observable epimerization after a mild N-nitrosylation/hydrolysis sequence.

As mentioned earlier, these methods are powerful but have some limitations such as the uncontrolled β,β-homodiarylation of alanine derivative **70**. Moreover, the hypothetical stepwise route for β-Ar-β-Ar′-α-amino acids cannot be actually realized since the use of two different directing groups led to superfluous steps for the respective removal and installation, and especially the basic conditions utilized in the first arylation step have partially racemized the amino acid to 90% enantiomeric excess (e.g., **73**). Yu and coworkers [22] thus provided an ideal solution for this challenging problem by ligand-enabled tuning of the reactivity and selectivity in the C($sp^3$)—H bond arylation. As shown in Scheme 10.12, they chose auxiliary 2,3,5,6-tetrafluoro-4(trifluoromethyl)aniline as a sole directing group and 2-picoline ($\mathbf{L_1}$) as a monodentate and weak-coordinated ligand. The desired monoselective arylation of alanine-derived amide **76** occurred exclusively with high yield and complete reservation of optical purity. Diverse phenylalanine derivatives **77** with electron-rich or electron-poor groups in the *ortho*, *meta*, or *para* positions can be synthesized by this protocol. A tricyclic quinoline ($\mathbf{L_2}$) was identified as the second ligand for the subsequent arylation of the secondary



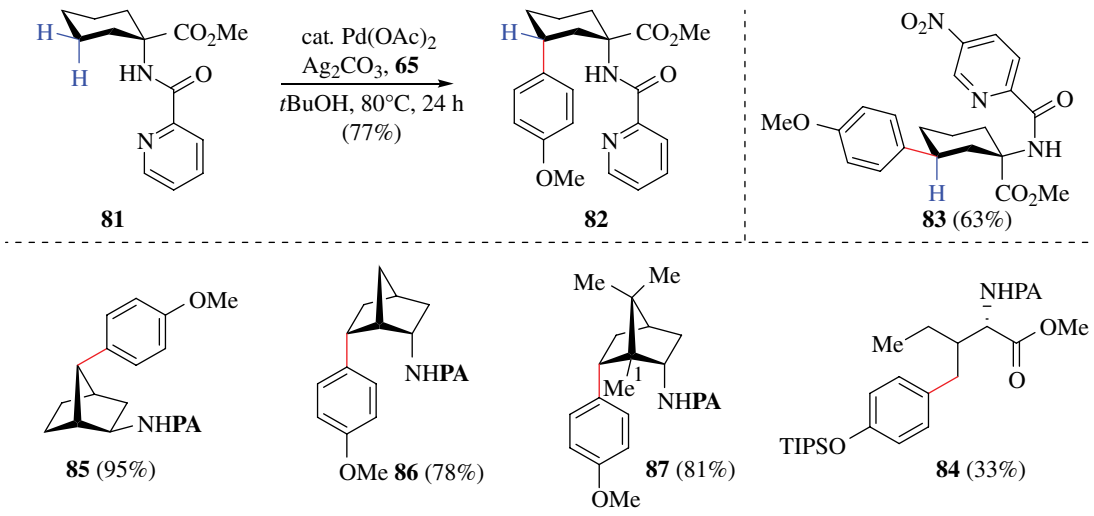

**SCHEME 10.11** Synthesis of phenylalanine derivatives through β-methyl monoarylation (a) with 2-thiomethylaniline and (b) with PIP.



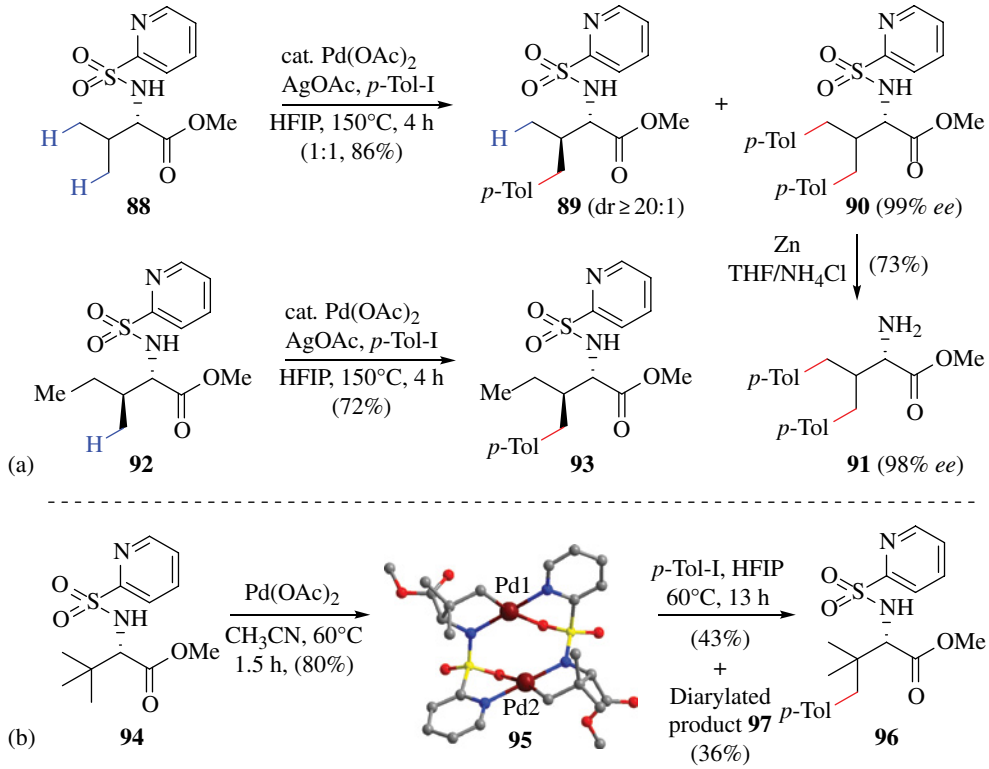

**SCHEME 10.12** Yu's diverse synthesis of β-Ar-β-Ar′-α-amino acids enabled by a ligand-controlled sequential C(sp³)—H diarylation.

β-C(sp³)—H in the resulting **77**. Thus, a series of β-Ar-β-Ar′-alanine-derived amides **78** could be generated in high yield and excellent diastereoselectivity. High performance of this unique ligand is attributed to further increase of the electron-donating ability of its alkoxy group because the conformation of the lone pairs on the oxygen atom in $\mathbf{L_2}$ is rigidified to favor π-conjugation with the quinoline ring. Interestingly, this sequential hetero-diarylation of a methyl group in an alanine derivative could proceed in one pot with the aid of these two ligands, and both configurations of the newly formed β-chiral center can be also accessed by choosing the order in which two distinct aryl groups are introduced. More importantly, two key C(sp³)—H insertion intermediates **79** and **80** had been characterized, and their formation is consistent with the general Pd(II)/Pd(IV) catalytic cycle (Scheme 10.9) where Pd(II) cleaves the C—H bond first. These two Pd complexes can serve as the precatalysts and undergo subsequent oxidative addition with an aryl iodide, eventually realizing the primary and secondary β-C(sp³)—H arylations, respectively.

The discovery of a picolinamide (PA)-directed C(sp³)—H functionalization by Daugulis [18b] was further adapted to γ-methylene arylation of α-amino acid derivatives by Chen and coworkers [23]. As shown in Scheme 10.13, monoarylation of cyclohexylamino acid **81** with 4-iodoanisole (**65**) under milder conditions than the original one gave **82** stereoselectively in 77% yield. The electron-withdrawing substituent on the pyridine ring of the PA led to a decrease in the arylation yield, as represented by product **83** with *p*-$NO_2$-PA. Compared to AQ-directed monoarylation of isoleucine amide **67** (Scheme 10.10), the present method gave an inferior result as demonstrated in the case of **84**. However, this C(sp³)—H arylation system can be extended to a wide range of aliphatic amines especially with some bridged scaffolds. For example, *p*-anisylation of the *exo*-2-aminonorbornane occurred exclusively at the proximal γ-C—H position,



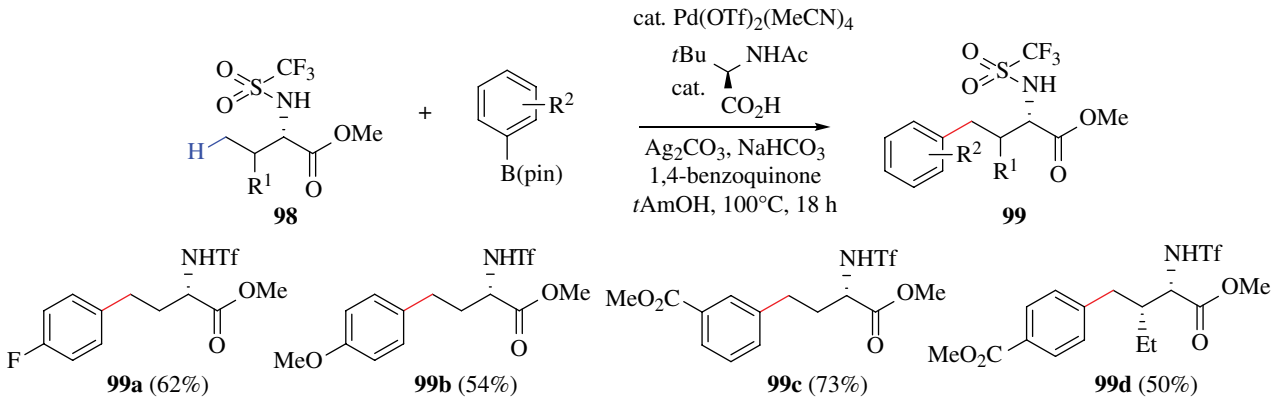

**SCHEME 10.13** Stereoselective synthesis of aliphatic amines through γ-methylene arylation.



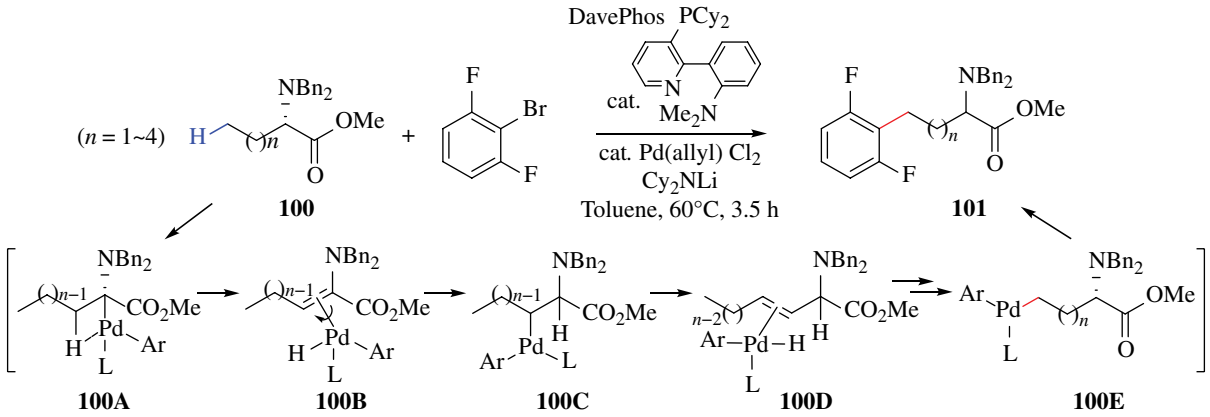

**SCHEME 10.14** Pd-catalyzed *N*-(2-pyridyl)sulfonyl-directed γ-C($sp^3$)—H arylation of α-amino acid esters.

affording **85** in 95% yield, whereas the *endo*-analog gave the product **86** of arylation exclusively at the axial γ-C—H position. The *endo*-bornylamine was also selectively arylated at the axial γ-C—H position to give **87** instead of seemingly preferential 1-methyl group.

Carretero and coworkers [24] developed an easily installed and removable *N*-(2-pyridyl) sulfonyl directing group and thereafter demonstrated its successful application in the γ-arylation of native amino acid esters. As shown in Scheme 10.14a, the reaction of *N*-(2-pyridyl)sulfonamide of L-valine methyl ester (**88**) with *p*-iodotoluene resulted in a 1:1 mixture of the γ-monoarylated product **89** and the γ-bisarylated product **90**, whose ratio can be further adjusted by the amount of the iodide. It is noteworthy that γ-monoarylation occurred exclusively at the pro-S methyl group, thus providing **89** with excellent diastereoselectivity. The chiral




**SCHEME 10.15** Ligand-enabled cross coupling of γ-C(sp³)─H bonds in triflyl-protected amino acid esters with arylboron reagents.

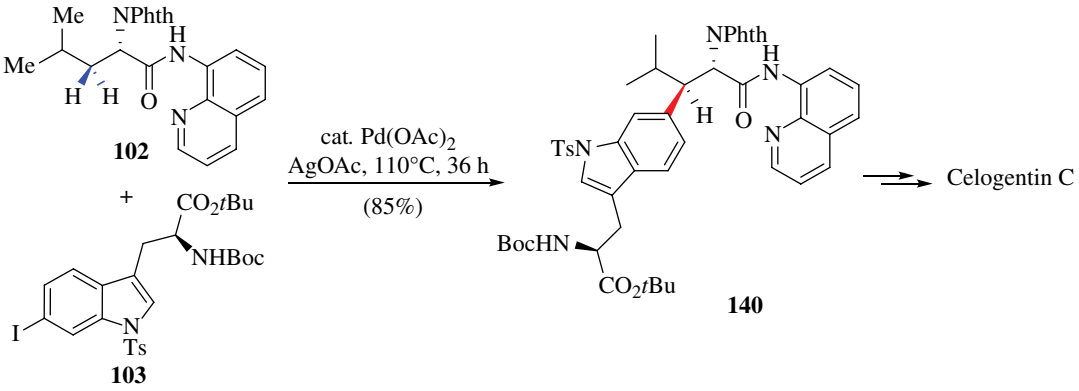



**SCHEME 10.16** Long-range arylation of primary C(sp³)─H bonds through Pd migration.

integrity of natural amino acid was preserved during this Pd-catalyzed process since very high enantiopurity of **90** was determined by HPLC. Importantly, only less than 2% of racemization in the free **91**, resulting from one-step reductive elimination of 2-pyridylsulfonyl moiety, could be observed. In analogy to AQ-directed γ-monoarylation of isoleucine amide **92**, this directing group also preferred to activate methyl group and generated **93** in 72% yield. In order to gain some mechanistic insights into this C(sp³)─H arylation, stoichiometric reaction of *N*-(2-pyridyl)sulfonyl *tert*-leucine methyl ester **94** with $Pd(OAc)_2$ was carried out (Scheme 10.14b). A novel bimetallic five-membered ring palladacycle complex **95** was isolated and determined by X-ray diffraction analysis. Its crystal structure clearly indicated that one C─H bond of *tert*-butyl group is activated due to the formation of C─Pd bond assisted by the bidentate 2-pyridylsulfonyl moiety. This palladacycle complex **95** was indeed able to react with *p*-iodotoluene, leading to an almost equimolar mixture of the monoarylated and bisarylated product **96** and **97** in 79% overall yield.

Unlike the typical C(sp³)─H activation reaction promoted by strong coordinating directing groups mentioned earlier, Pd-catalyzed arylation of C(sp³)─H bonds in triflyl-protected amines cannot take place because of the lack of strong σ-chelation. Yu and coworkers [25] found that incorporation of a mono-*N*-protected amino acid (MPAA) ligand enabled the successful realization of the desired transformation (Scheme 10.15). This dramatic acceleration of C(sp³)─H activation step could be attributed to the cooperation of the weak coordinating triflimide-derived imidate with the MPAA ligand on the Pd(II) center, thus lowering the transition state energy. The Ac-D-*t*Leu-OH was found to be better and more economical ligand for the efficient cross coupling of L-amino ester **98** with a wide variety of arylboronic acid pinacol esters, as exemplified in the cases of **99a–d**. This unique reaction was believed to proceed via a Pd(II)/Pd(0) catalytic cycle assisted by the oxidant 1,4-benzoquinone.

As shown in Scheme 10.16, Baudoin and coworkers [26] reported a general Pd-catalyzed longer-range (γ to ζ) arylation of α-amino acid esters with aryl bromides, which predominantly occurs at the terminal position of a linear alkyl chain to afford higher homologs of arylalanines after debenzylation. For example, 1-bromo-2,6-difluorobenzene can react with the readily available dibenzyl-protected homo-alanine methyl




**SCHEME 10.17** Biomimetic synthesis of celogentin C through a Pd-catalyzed 6-indolylation of β-C($sp^3$)-H bond of leucine amide.

ester **100** under the catalysis of $[Pd(\eta^3\text{-allyl})Cl]_2$ and DavePhos as the ligand, giving homoarylalanine methyl ester **101** in synthetically useful yield. The mechanism of this method is different from that of directing group-guided C($sp^3$)─H arylation, and a plausible process is demonstrated in Scheme 10.16 (bottom). The transmetallation of lithium enolate generated under the condition of $Cy_2NLi$ forms palladium enolate **100A**, which in turn converts to π-complex **100B** through β-hydride elimination. The subsequent rotation insertion of the Pd hydride species into the olefin provided Pd homoenolate **100C**, thus completing Pd migration from α to β position. This interesting Pd walk [27] along the alkyl chain proceeds and not ends until the terminal Pd─C bond is formed. The eventual reductive elimination of the intermediate **100E** furnishes the synthesis of homoarylalanine methyl ester **101**. Some issues exist in this remote C($sp^3$)─H arylation reaction: all products obtained are racemic due to the formation of intermediacy olefin; the aryl bromides bearing an *ortho*-electronegative group must be utilized since the formation of a strong Ar─Pd bond would disfavor the immediate reductive elimination to generate α-aryl aminoester, thus allowing the desired Pd migration to occur smoothly by the indicated cascade.

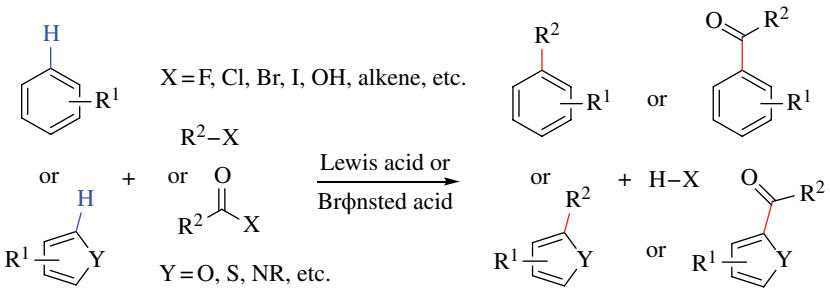
The development of C─H functionalization has innovated the disconnection fashion toward the synthesis of complex molecules, especially natural products [28]. As shown in Scheme 10.17, Chen and Feng [29] demonstrated the first application of a Pd-catalyzed β-C($sp^3$)─H arylation of 8-AQ amide to achieve the total synthesis of celogentin C, a bicyclic nonribosomal peptide possessing inhibitory activity ($IC_{50}$ = 0.8 μM) against tubulin polymerization. The 8-AQ-directed coupling of *N*-phthaloylleucine amide **102** and 6-iodotryptophan derivative **103** gave rise to **104** in 85% yield and a gram scale application. The observed *erythro* stereochemistry in the arylated products **104** is due to exclusive formation of the *trans*-palladacycle intermediate. Notably, this key assembly of Leu–Trp linkage is inspired by the proposed natural enzymatic pathway, and therefore this C($sp^3$)─H arylation strategy is envisaged as a biomimetic route.

More interesting examples focusing on the total synthesis of lignans will be found in Section 10.4.

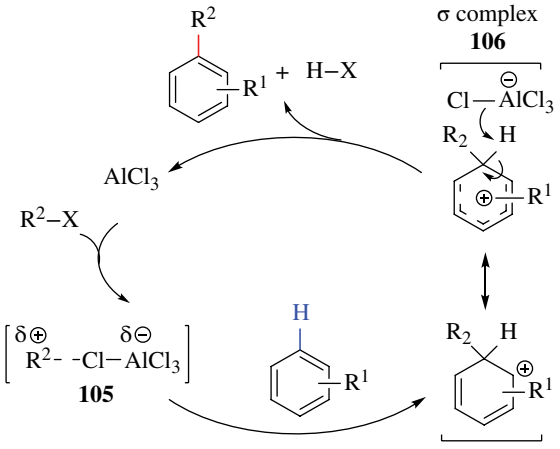
## 10.3 FRIEDEL–CRAFTS REACTIONS IN ORGANIC SYNTHESIS

In 1877, Charles Friedel and James Mason Crafts [30a, b] corporately discovered that treatment of amyl chloride with aluminum strips in benzene led to the formation of amylbenzene. This type of transformation was found to be general for alkyl halides and aromatics under the catalysis of Lewis acid. Along with the discovery of the closely related acylation [30c, d], these two men are best remembered by Friedel–Crafts reaction that bears their names. With various modern modifications that appeared in the literature, including enantioselective variants [31], Friedel–Crafts alkylation and acylation have already become one of the most powerful C─C bond forming reactions in organic chemistry [32]. These methods are recognized to date as of fundamental importance not only in academia but also in industry [33]. As shown in Scheme 10.18, some heteroaromatics, instead of the aryl component or alcohol, and alkenes instead of halides can be used as suitable substrates. Also, other common Lewis acids like $BF_3$, $TiCl_4$, $SnCl_4$, $Sc(OTf)_3$, etc., and Brønsted acids such as HF, $H_2SO_4$, and superacids (e.g., $HF{\cdot}SbF_5$, $HSO_3{\cdot}SbF_5$) can also be used as catalysts.

Friedel–Crafts reaction is essentially electrophilic aromatic substitution (EAS), and the generally accepted mechanism [34] is explained based on its alkylation variant as an example in Scheme 10.19. The whole catalytic cycle begins with the coordination of $AlCl_3$ to the alkylating agent $R^2X$ to generate a polar addition complex **105**, whose polarization extent depends on the type of the alkyl group. The subsequent electrophilic addition of this initial complex with the aromatic ring will result in the formation of Wheland or σ-complex **106**. This rate-determining step disrupts the aromaticity, and therefore the fast loss of a proton will occur to afford the




**SCHEME 10.18** Friedel–Crafts alkylation and acylation.




**SCHEME 10.19** The mechanism of Friedel–Crafts alkylation.

alkylative product with the rearomatization and the regeneration of the catalyst $AlCl_3$. Friedel–Crafts acylation proceeds according to a similar mechanism. Notably, this EAS mechanism involving the carbocationic intermediate salt [35] had been supported strongly by the classic work of Olah [36], where the stable boron trifluoride–ethylfluoride and trifluoride–formylfluoride complexes of the mesitylene were isolated.

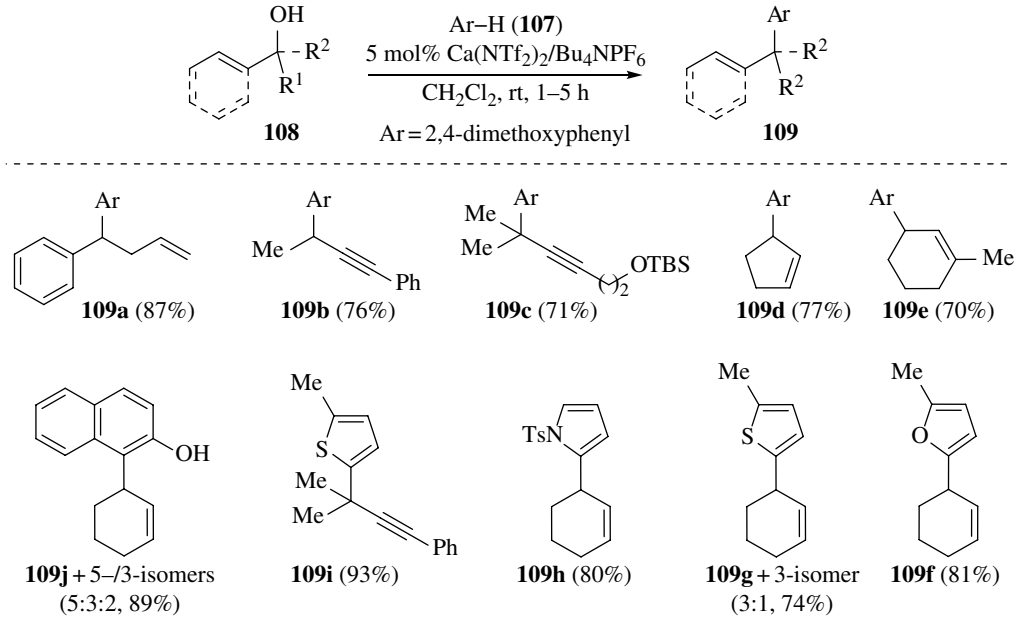
Now, significant advances of Friedel–Crafts reaction have appeared, including the developments of new catalysis and methods for the efficient intermolecular and intramolecular reactions. Some recent examples will be accounted for in the following section, with an emphasis on the control of diastereoselectivity and enantioselectivity.

There are some significant drawbacks in the original Friedel–Crafts reaction: the use of toxic alkyl halides combined with superstoichiometric amount of the acid provides excess of waste that is very harmful to the environment. Moreover, the general harsh reaction conditions result in low functional group tolerance. The use of alcohols as electrophiles could bring ecologically beneficial arylations since water is the only by-product after the transformation. On the other hand, considering the ready availability and low cost, calcium among the alkaline earth metals appears particularly promising for sustainable catalysis.

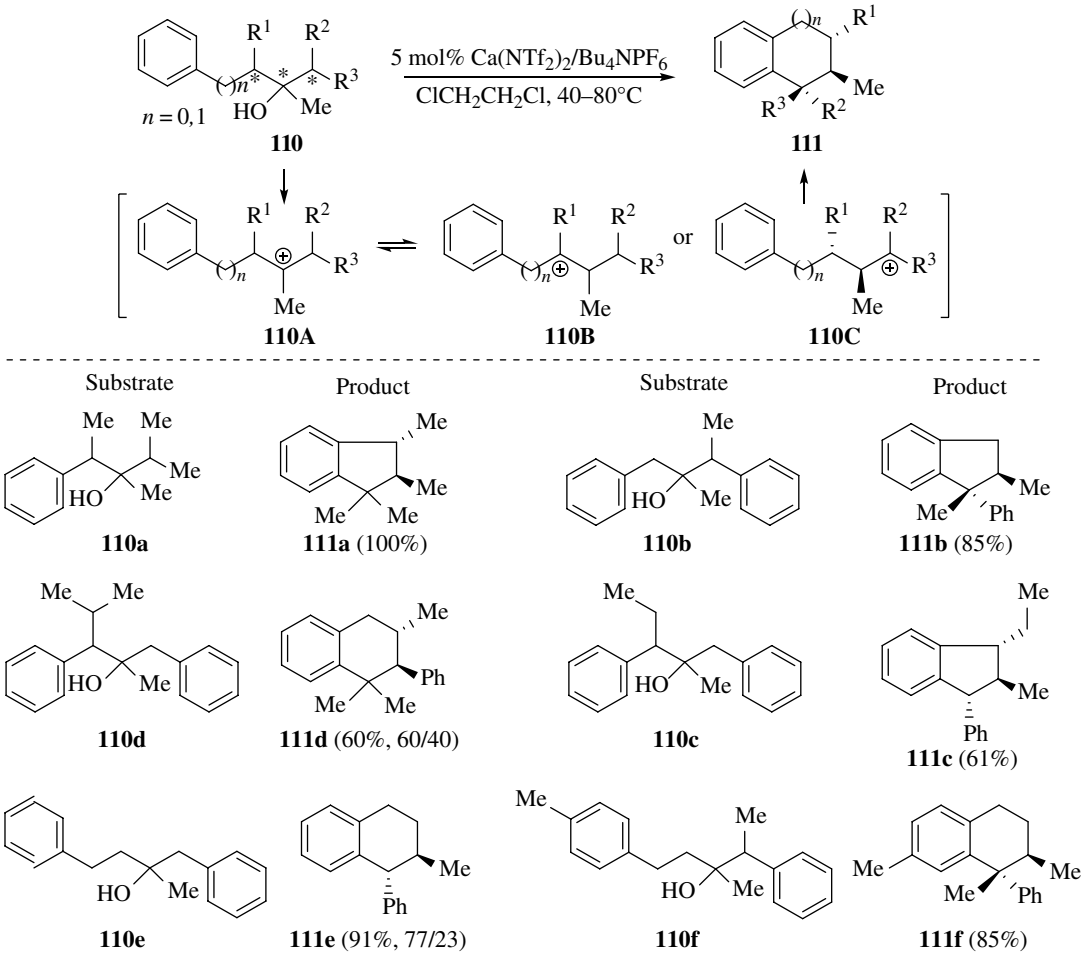
Accordingly, Niggemann and coworkers [37a] identified a Ca-based catalytic system, which allows the facile alkylation of electron-rich arenes with secondary and tertiary benzylic, allylic, and propargylic alcohols at room temperature (Scheme 10.20). The superior performance of this new catalyst is attributed to the weakly coordinating triflimidate counterion [38], whose highly delocalized nature and steric hindrance lead to high positive charge density on the Ca(II) center, thus enhancing its Lewis acid character. The unique capacity of calcium [37b] was further proved by the control experiments, which demonstrated that other related $M(NTf_2)_n$ Lewis acids ($n$ = 2, M = Mg, Ba; $n$ = 1, M = Li) and $HNTf_2$ displayed none or a little catalytic activity. The additive $Bu_4NPF_6$ is also necessary for the potential generation of more soluble and reactive $Ca(NTf_2)_2{\cdot}PF_6$ species.

With this air- and moisture-tolerant protocol in hand, resorcinol dimethyl ether (**107**) was treated with a series of activated alcohols (**108**). While the arylations of the secondary benzylic and propargylic alcohols were completed within one hour to give **109a** and **109b** in good yields exclusively at *o*,*p*-positional regioselectivity, the successful formation of an all-carbon quaternary center tethered to OTBS ether was surprising since this acid labile moiety in **109c** often collapses under the common Friedel–Crafts alkylation conditions. The arylations of cyclic alcohols also proceeded smoothly although the conversion of tertiary allylic alcohol would always give the rearrangement product like **109e** via the allylic transposition. 2-Cyclohexen-1-ol also served as an efficient alkylating reagent for the typical 5-membered heteroarenes (**109f–h**), and moderate regioselectivity was observed on the alkylation of 5-methylthiophene. Interestingly, complete regioselectivity could be restored in the case of tertiary propargylic alcohol, affording **109i** in excellent yield. Alkylation of β-naphthol can also be obtained albeit in poorer regioselectivity as demonstrated in the **109j**.

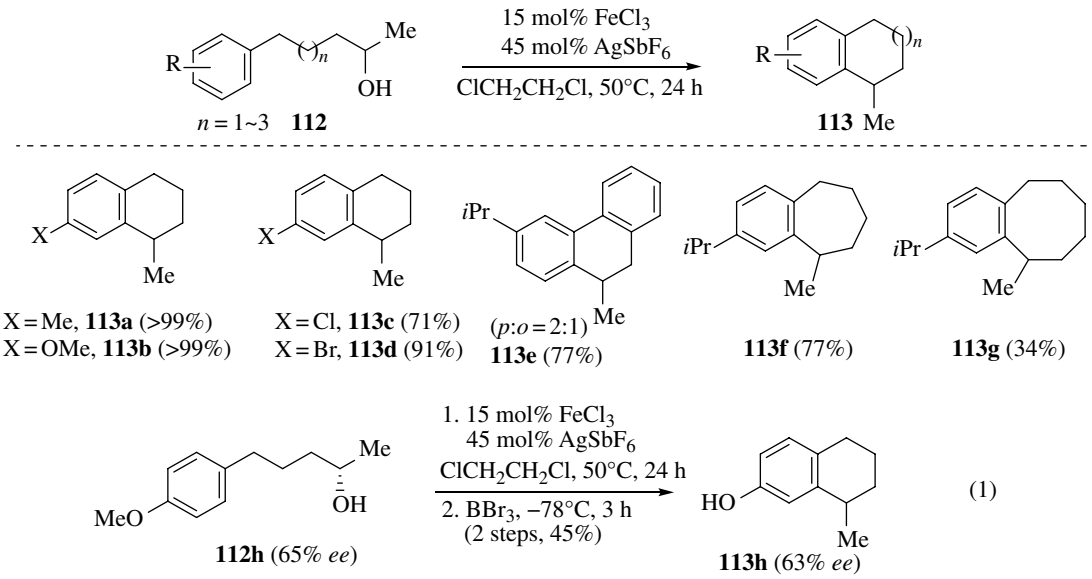
This mild Friedel–Crafts alkylation was expeditiously extended to highly regio- and diastereoselective intramolecular version at elevated temperature by the same research group [39], thus allowing an easy access to tetralin and indane skeletons in good yields (Scheme 10.21). This reaction starts




**SCHEME 10.20** Calcium-catalyzed intermolecular Friedel–Crafts alkylation with π-activated alcohols.




**SCHEME 10.21** Calcium-catalyzed intramolecular Friedel–Crafts alkylation with alcohols.

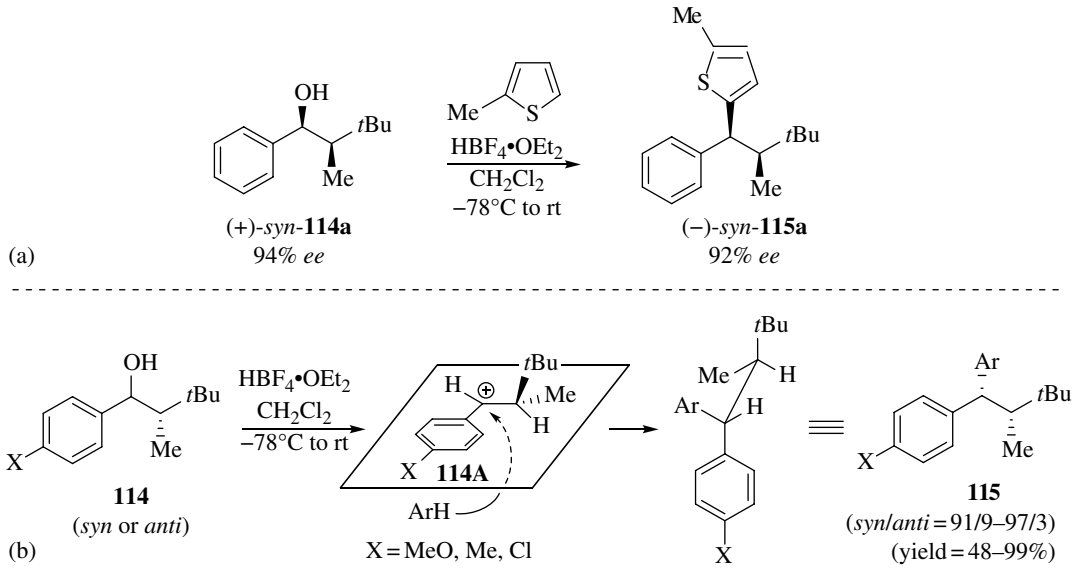



**SCHEME 10.22** Iron-catalyzed intramolecular Friedel–Crafts alkylation with unactivated alcohols.

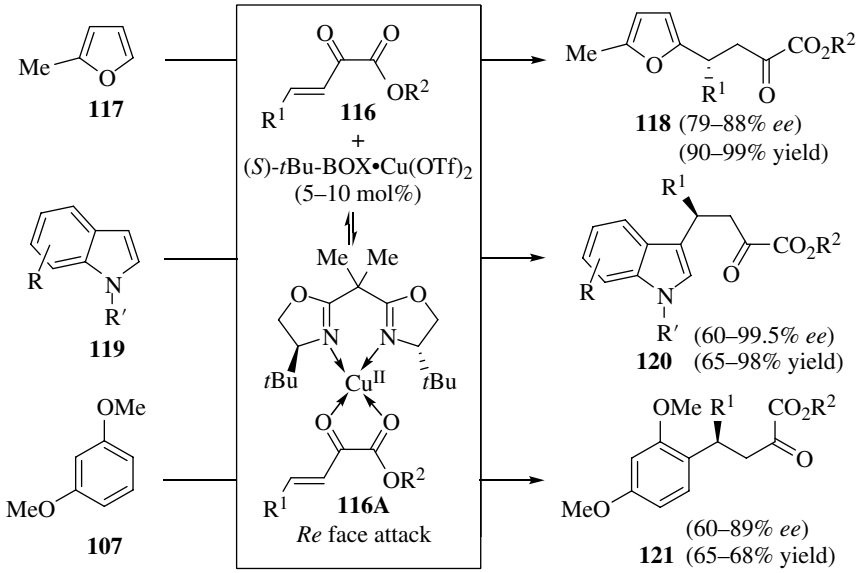
with a calcium-catalyzed efficient dehydroxylation of benzyl carbinols. The initially generated carbocation **110A** rearranges to the related carbocation **110B** or **110C** by either a hydride shift or an elimination–reprotonation sequence, rather than the usual direct cyclization with the tethered arene moiety. Regardless of stereochemistry in the starting material, this equilibrium leads to the thermodynamically most favorable **110C** with *trans*-configuration, which in turn eventually cyclizes to give the regio- and diastereoisomeric pure products **111**. The quantitative formation of indane **111a** with complete diastereoselectivity strongly supported the aforementioned hypothesis, whereas **111b** showed a preference for closure at the more stable tertiary benzylic carbocation. Interestingly, the all-*trans*-substituted indane **111c** with the opposite regioselectivity was instead produced when the methyl group was replaced by ethyl group in **110c**. More surprisingly, benzyl carbinol **110d** generated by the further attachment of a methyl group on **110c** afforded the tetralin **111d** albeit with the moderate yield and low diastereoselectivity under the identical calcium analysis. These results suggest that the regio- and diastereoselectivity of the present Friedel–Crafts-type cyclization is governed by subtle changes of the substitution pattern in the reactive carbocationic intermediates. Regioselective cyclization to the six-membered tetralins was generally preferred over indane formation, as demonstrated in the additional examples **111e** and **111f** in which moderate to good diastereoselectivities were still observed.

In 2014, Cook and coworkers [40] developed an iron-catalyzed direct cyclization with unactivated secondary alcohols (Scheme 10.22). This mild intramolecular Friedel–Crafts alkylation demonstrated high efficiency, as exemplified in the cases of **113a** and **113b** with almost quantitative yields. When the aromatic ring carries deactivating substituents like a halogen, good yields were still obtained (71% for **113c** and 91% for **113d**). The substrate scope was also expanded to the dihydrophenathrene **113e** but with modest regioselectivity. Interestingly, attempts to close a five-membered ring resulted in substantial elimination product (not shown), whereas the traditionally more difficult to close, seven-membered ring **113f** proceeded smoothly. Even larger, much more challenging closure of eight-membered ring **113g** can also be realized in fairly good yield. More importantly, the stereochemical information in enantioenriched **112h** was almost transferred to the optical active tetralin **113h** (Scheme 10.22) [40]. This conversion is in sharp contrast to the formation of racemic **113h** under the traditional conditions utilizing sulfuric acid as the catalyst.

Previously, Bach and coworkers [41] also reported retainment of stereochemical integrity during intermolecular Friedel–Crafts alkylation. As shown in Scheme 10.23a, when enantiomerically enriched benzylic alcohol (+)-**114a** was subjected to weak Brønsted acid $HBF_4{\cdot}OEt_2$ followed by the addition of 2-methylthiophene, the product (−)-**115h** with a slight erosion of enantiomeric excess was obtained in excellent yield. Other electron-rich arenes and heteroarenes (e.g., resorcinol dimethyl ether, *N*-tosylpyrrole, benzofuran) are suitable for this kinetically controlled condition and could also convert to the respective *syn*-1,1-diarylalkanes **115** in moderate to excellent yields regardless of the employment of *syn*- or *anti*-oriented alcohols **114** (Scheme 10.23b). The observed stereoconvergent reaction and its extremely high diastereoselectivity were attributed to the formation of α-branched benzylic carbocation **114A**, where the attack from a nucleophile ArH at the prostereogenic center occurs preferably from the bottom face of the




**SCHEME 10.23** Diastereoselective intermolecular Friedel–Crafts alkylation via chiral α-branched benzylic carbocations.

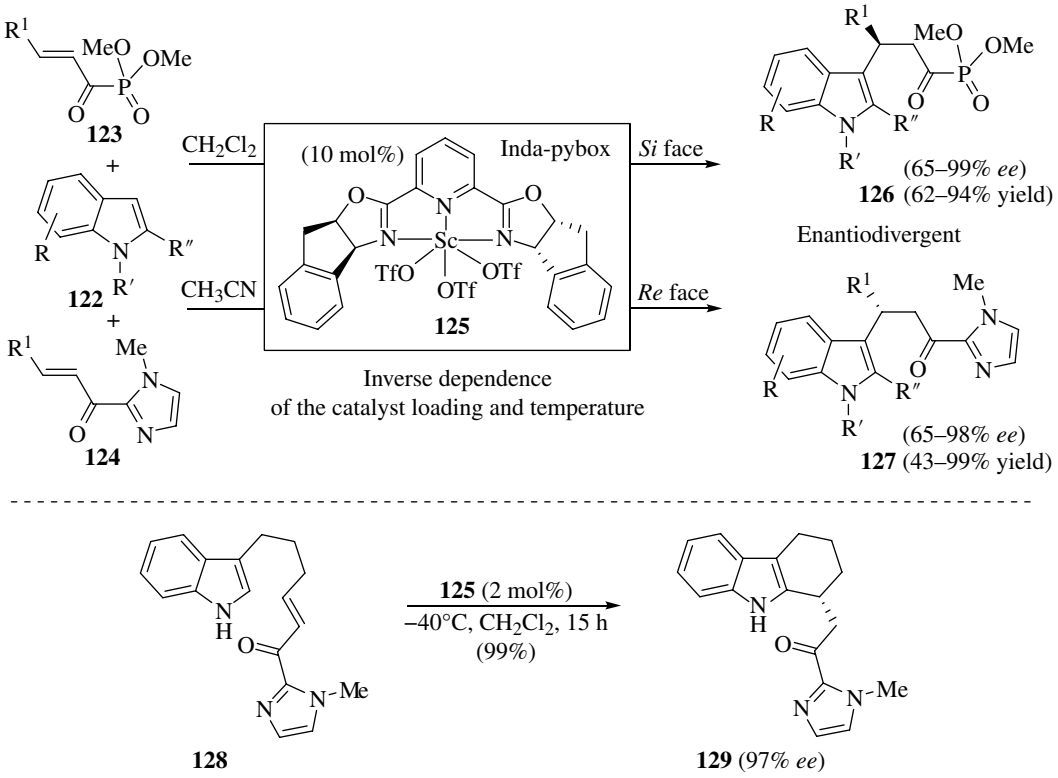



**SCHEME 10.24** Enantioselective Friedel–Crafts alkylation catalyzed by a chiral copper complex.

depicted plane. Notably, the conformation adopted by this type of carbocations had been elucidated by NMR studies on the long-lived intermediates in superacidic medium.

Besides performing diastereoselective reactions using chiral staring materials, optically active catalyst-controlled enantioselective Friedel–Crafts alkylation [31] can also be served as an alternative to provide chiral products. Great advances have been demonstrated in this hot field within the last decade. Generally, three strategies have been successfully utilized to achieve catalytic asymmetric Friedel–Crafts alkylation. The first one involves the use of chiral Lewis acids, where a chiral ligand is coordinated to the Lewis acid, and the second one uses Brønsted acids with a chiral counterion. Both catalyses are based on the enantioselective noncovalent interaction of the acidic site with O or N lone-pair electrons in the alkylating reagents. A third type of activation belongs to organocatalysis based on covalent interaction, in which a chiral primary or secondary amine catalyst would react with α,β-unsaturated carbonyl compound to form an iminium species that is ready for nucleophilic attack by the arenes.

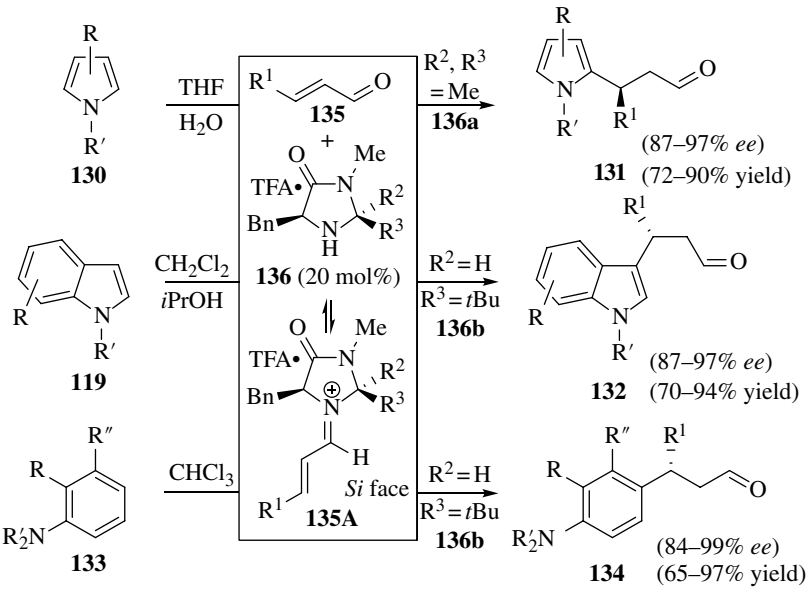
As shown in Scheme 10.24, Jørgensen and coworkers [42] used the (*S*)-*t*Bu-BOX·Cu(OTf)$_2$ complex [43] as a chiral Lewis acid to develop the first catalytic asymmetric




**SCHEME 10.25** Enantiodivergent Friedel–Crafts alkylation catalyzed by a chiral scandium complex.

Friedel–Crafts alkylation. The origin of enantioselectivity is postulated to derive from coordination of β,γ-unsaturated-α-ketone (**116**) to the copper catalyst in a bidentate fashion, leading to a square-planar intermediate **116A**, where the *re*-face of the C═C double bond is primarily available for the nucleophilic attack by the arenes since a severe shielding effect on the *Si*-face by the bulky *tert*-butyl group occurs. The support of this mechanistic assumption first came from asymmetric Friedel–Crafts alkylations of 2-methylfuran **117** in high yields and good enantioselectivities. Indole framework **119** as a "privileged" structure or pharmacophore gave generally excellent enantioselectivities, and up to 99.5% *ee* of the optically active indole derivatives **120** were obtained. Besides heteroaromatic compounds, other electron-rich benzenes such as resorcinol dimethyl ether (**107**) can take part in this asymmetric Friedel–Crafts alkylations of activated alkenes, albeit with slightly lower yields and enantioselectivities.

Evans and coworkers [44] expanded the scope of enantioselective Friedel–Crafts alkylation of indoles **122** through the utilization of a series of β-substituted α,β-unsaturated phosphonates **123** and α,β-unsaturated 2-acyl imidazoles **124** (Scheme 10.25). The active catalyst was proposed to be the respective complex of these enones in a bidentate fashion with bis(oxazolinyl)pyridine–scandium(III) triflate **125**. Generally, this asymmetric addition reaction was found to be more versatile with α,β-unsaturated 2-acyl imidazoles **124**, and the resulting optical active acyl imidazoles **127** could be easily converted to indole derivatives bearing more diverse functionalities such as ester, amide, carboxylic acid, ketone, and aldehyde. More interestingly, unsaturated 2-acyl imidazoles **124** produced the opposite enantiomer of the newly formed stereocenter as was seen in the corresponding reaction with acyl phosphonates **123** catalyzed by the same **125**. This enantiodivergent outcome could be attributed to the difference of binding modes: 2-acyl imidazoles **124** were able to adopt the seven-coordinate pentagonal bipyramidal coordination geometry, whereas the more bulky acyl phosphonates **123** involved octahedral coordination with the catalyst **125** [44]. In addition, more loading of the catalyst on acyl imidazoles **124** led to the decrease of enantioselectivity (20 mol%, 78% *ee*, 50 mol%, 11% *ee*) even turnover in asymmetric induction (100 mol%, −31% *ee*), rather than the usually flat catalyst profile with **123**. The inverse relationship between reaction temperature and enantioselectivity of these two activated alkenes was observed as well. The intramolecular alkylation of 2-acyl imidazole-tethered indole **128** proceeded smoothly with as little as only 2 mol% of **125**, affording the tetrahydrocarbazole **129** in excellent yield and enantioselectivity. Attempts to extend this remarkable transformation to the synthesis of five- or seven-membered ring were unsuccessful.

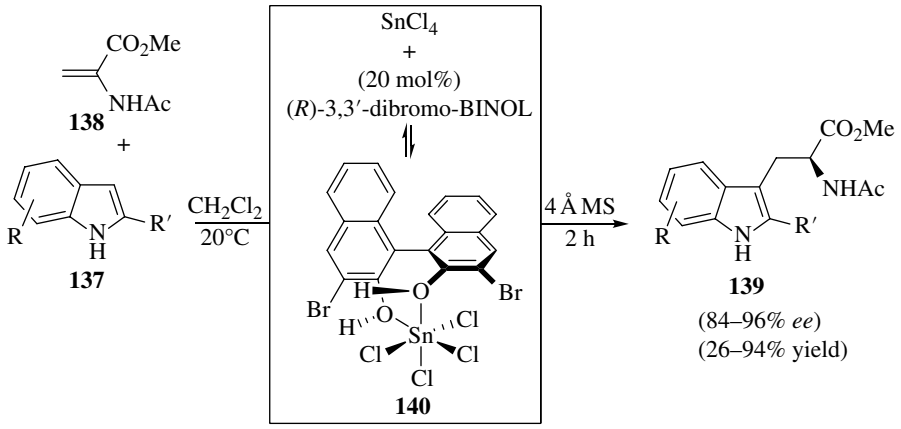



**SCHEME 10.26** Enantioselective Friedel–Crafts alkylation catalyzed by chiral imidazolidinone·TFA salts.

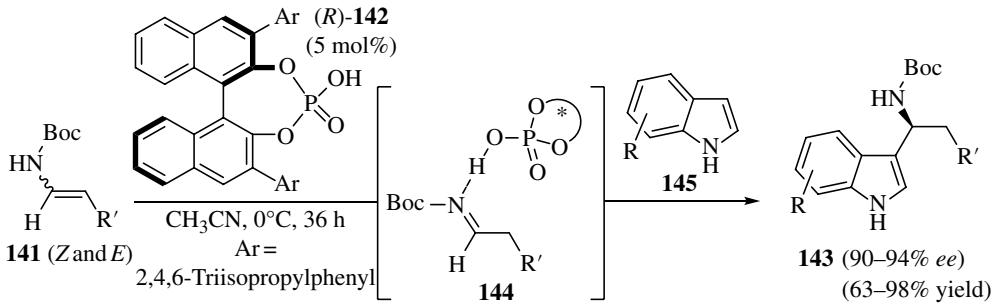
As shown in Scheme 10.26, MacMillan and coworkers [45] first developed organocatalytic asymmetric Friedel–Crafts alkylation of pyrroles **130**, indoles **119**, and electron-rich benzenes **133** with α,β-unsaturated aldehydes **135** in high yields and enantioselectivities approaching in general the 90% *ee*. Conjugate pyrrole addition occurs through the LUMO-lowering activation of α,β-unsaturated aldehydes via the reversible formation of iminium ion **135A** with the chiral benzyl imidazolidinone·TFA salt **136a**. No products arising from 1,2-addition were observed since steric constraints were imposed by this catalyst framework, which further enforced high enantiocontrol levels of *Si*-face in the 1,4-addition instead. This novel iminium catalysis featuring an aerobic atmosphere, the use of wet solvents, and inexpensive bench-stable material was extended to indole nucleophiles **119**. However, poor reaction rate and enantioselectivity were observed after the addition of *N*-methylindole to (*E*)-crotonaldehyde catalyzed by **136a**. This result was expected since the indole nucleophile is significantly less activated toward electrophilic substitution than the pyrrole. The insightful analysis of computational iminium ion mode [45b] led to the invention of the powerful (2*S*,5*S*)-5-benzyl-2-*tert*-butyl-imidazolidinone **136b**, which enabled the Friedel–Crafts alkylation of various aldehydes and indoles **119** including those bearing electron-withdrawing substituents. In most of examined cases, products **132** demonstrated good to excellent enantioselectivities and efficiency, even on a large reaction scale. Moreover, this iminium activation strategy by **136b** was also advanced to the enantioselective conjugate addition of anilines **133** to **135** at subambient temperature, leading to products **134** with bis-benzylic stereogenicity, a structural motif broadly found in the natural products and drug candidates.

All of the aforementioned methods can only establish a new stereogenic center at the β-position of the conjugate acceptor, albeit asymmetric construction of the corresponding α center is highly demanded. In 2011, Reisman and coworkers [46] applied the *in situ* generated (*R*)-BINOL·$SnCl_4$ complex as a chiral Lewis acid-assisted Brønsted acid (LBA) [47], to develop the first tandem Friedel–Crafts conjugate addition/asymmetric protonation reaction between 2-substituted indoles **137** and methyl 2-acetamidoacrylate **138** (Scheme 10.27). Through the optimized conditions (20 mol% of (*R*)-3,3-dibromo-BINOL, one equivalent of $SnCl_4$, and room temperature), a range of indoles **137** including electron-deficient ones delivered a series of tryptophans **139** in high enantioselectivity. Along with the orthogonal hydrolysis of the acetamide and methyl ester groups in **139**, these synthetic unnatural tryptophan derivatives can serve as important building blocks for the total synthesis of the related natural products. Mechanistically, this convergent transformation commenced with Friedel–Crafts conjugate alkylation/rearomatization, and the resulting intermediacy Sn enolate would be protonated enantioselectively by catalytically generated (*R*)-BINOL·$SnCl_4$ **140** to give the desired products **139**.

Despite their scarcity, asymmetric additions to electron-rich alkenes have also appeared in the literature. For example, Terada and coworkers [48a] reported the first enantioselective Friedel–Crafts reaction of enecarbamates **141** catalyzed by (*R*)-BINOL-derived monophosphoric acid **142** [49] (Scheme 10.28). This method provided an efficient access to highly enantioenriched 1-indolyl-1-alkylamine derivatives that have pharmaceutical and biological importance. Notably, the geometric isomers **141**(*Z*) and **141**(*E*) afforded the optical active amine **143** with the almost same



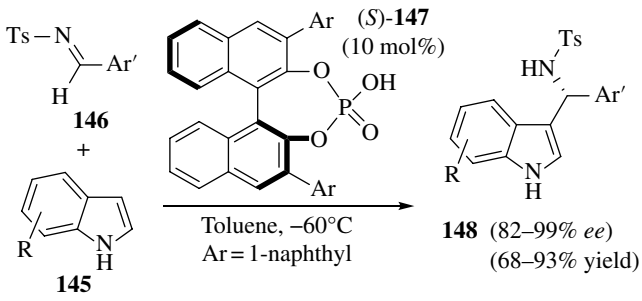

**SCHEME 10.27** Enantioselective tandem Friedel–Crafts conjugate addition/asymmetric protonation catalyzed by (*R*)-3,3-dibromo-BINOL·$SnCl_4$ complex.




**SCHEME 10.28** Enantioselective Friedel–Crafts reaction of indoles with enecarbamates catalyzed by a chiral monophosphoric acid.

enantiocontrol level, implying that their reactions proceeded through the common intermediate **144**. This intermediate is composed of chiral phosphoric acid (*R*)-**142** and an imine that would be generated by the protonation of enecarbamates **141**. This protonation via ionic transition states is expected to be the rate-determining step. Isomer **141**(*Z*) allows higher reactivity demonstrated from the faster reaction rate and the better yield of **143** after the enantio-discriminable attack of indoles **145** to **144**. This mechanistic assumption had been supported by the solvent effect, in which the highly polar and protophobic $CH_3CN$ provide the best result. Identification of the imine as the actual reactant led to the discovery of its direct use in the enantioselective Friedel–Crafts, as exemplified in the earlier work by Terada [48b], in which catalytic asymmetric additions of 2-methoxyfuran to aromatic *N*-Boc aldimines were demonstrated.

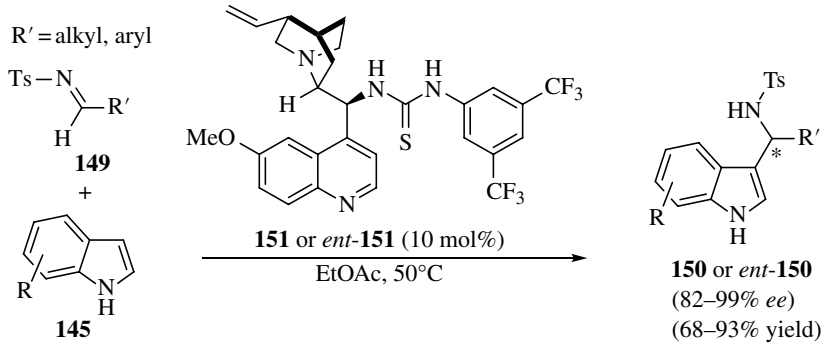
As shown in Scheme 10.29, You and coworkers [50] disclosed the enantioselective aza-Friedel–Crafts reaction of indoles **145** with *N*-sulfonyl aldimines **146** by a (*S*)-BINOL-derived phosphoric acid **147**. Their reactions in toluene completed within several hours for most of the substrates, providing a series of 3-indolyl methanamine derivatives **148** with up to >99% *ee* and the opposite absolute configuration from the previously described method. Unfortunately, when



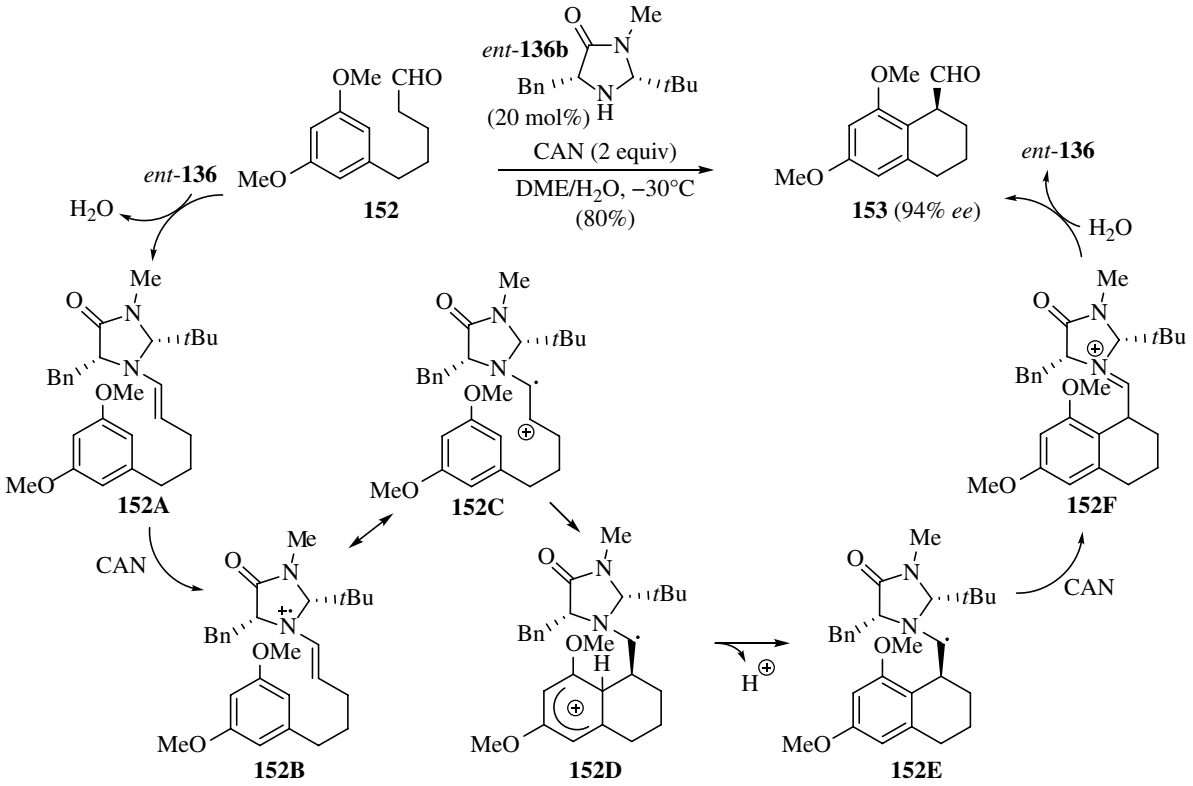

**SCHEME 10.29** Enantioselective aza-Friedel–Crafts reaction of indoles with imines catalyzed by a chiral monophosphoric acid.

the aliphatic *N*-Ts aldimine was evaluated, only moderate yield and enantioselectivity were observed. The plausible reasons are its weakly electrophilic nature and easy tautomerization to the corresponding enamine.

This challenging problem was addressed by Deng and coworkers [51] by the use of 9-thiourea cinchona alkaloids as acid–base bifunctional catalysts. As shown in Scheme 10.30, the enantioselective aza-Friedel–Crafts reaction proceeded through a network of hydrogen bonding interactions between indoles **145** and *N*-Ts aldimines **149**




**SCHEME 10.30** Enantiodivergent aza-Friedel–Crafts reaction of indoles with imines catalyzed by bifunctional 9-thiourea cinchona alkaloids.




**SCHEME 10.31** Enantioselective intramolecular Friedel–Crafts α-arylation of aldehydes.

assisted by the catalyst, and either an enantiomer of the desired 3-indolyl methanamines **150** could be obtained by the choice of quinine-derived **151** or quinidine-derived *ent*-**151**. With wide scope for both indole and imines and by utilizing an easily available organocatalyst, this method represents a practically useful enantioselective approach for the access to optical active amines **150**.

In 2009, Nicolaou and coworkers [52] applied chiral 5-benzyl-2-*tert*-butyl-imidazolidinones (MacMillan's catalysts) [45] to develop asymmetric Friedel–Crafts-type α-arylation of aldehydes via the enamine intermediate formed under the condition of cerium ammonium nitrate (CAN) as an oxidant. As shown in Scheme 10.31, 5-(3,5-dimethoxyphenyl)pentanal **152** was treated with *ent*-**136b** and CAN in wet DME, and the chiral bicyclic aldehyde **153** was obtained in 94% *ee* and 80% yield. A plausible mechanism for this transformation has been proposed: The aldehyde **152** is activated by secondary amine *ent*-**136b**, and the resulting enamine **152A** converts to radical cation **152B** through single-electron transfer (SET) oxidation by CAN. This highly reactive species would establish an equilibrium with its resonance form **152C**, which rapidly collapses to

σ-complex **152D** via a Friedel–Crafts-type cyclization. This intramolecular attack from the aromatic nucleus occurs from the *Si*-face of enamine intermediate **152B**, thus establishing the absolute configuration of the newly formed stereogenic center. Rearomatization by the loss of a proton generates the radical **152E**, which undergoes a second SET oxidation with CAN to afford iminium species **152F**. The final hydrolysis affords the chiral aldehyde **153** with the regeneration of *ent*-**136b** that enters into the next round of the catalytic cycle.

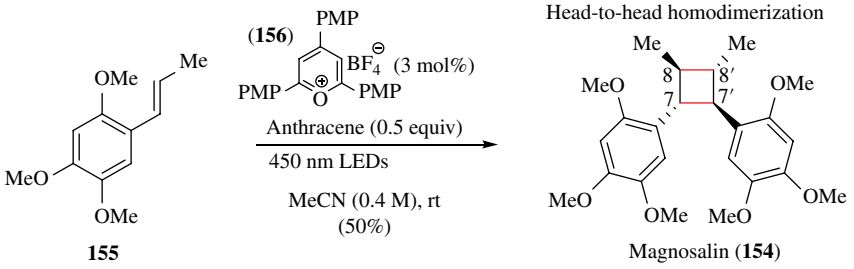
## 10.4 TOTAL SYNTHESIS OF LIGNANS BY C(sp³)─H ARYLATION REACTIONS

The magnosalin (**154**) [53], a typical all-*trans*-cyclobutane lignan, was isolated from *Piper clusii* and has notable inhibitory activity toward nitric oxide synthase (NOS) enzymes ($IC_{50}$ = 5.9 μM) [54]. The biosynthesis of this kind of $C_2$-symmetric natural products has been proposed to occur via the regioselective homodimerization of the requisite styrene [55]. Nicewicz and coworkers developed an organic single-electron oxidant–electron relay (ER) system to control the desired head-to-head dimerization under visible light [56]. As shown in Scheme 10.32, by using 2,4,6-tris(4-methoxyphenyl) pyrylium tetrafluoroborate (**156**) as a photooxidant and anthracene as an aromatic ER, *E*-asarone (**155**) was smoothly converted to magnosalin (**154**) with the irradiation of 450 nm LEDs, thus completing its biomimetic synthesis in one step [57].

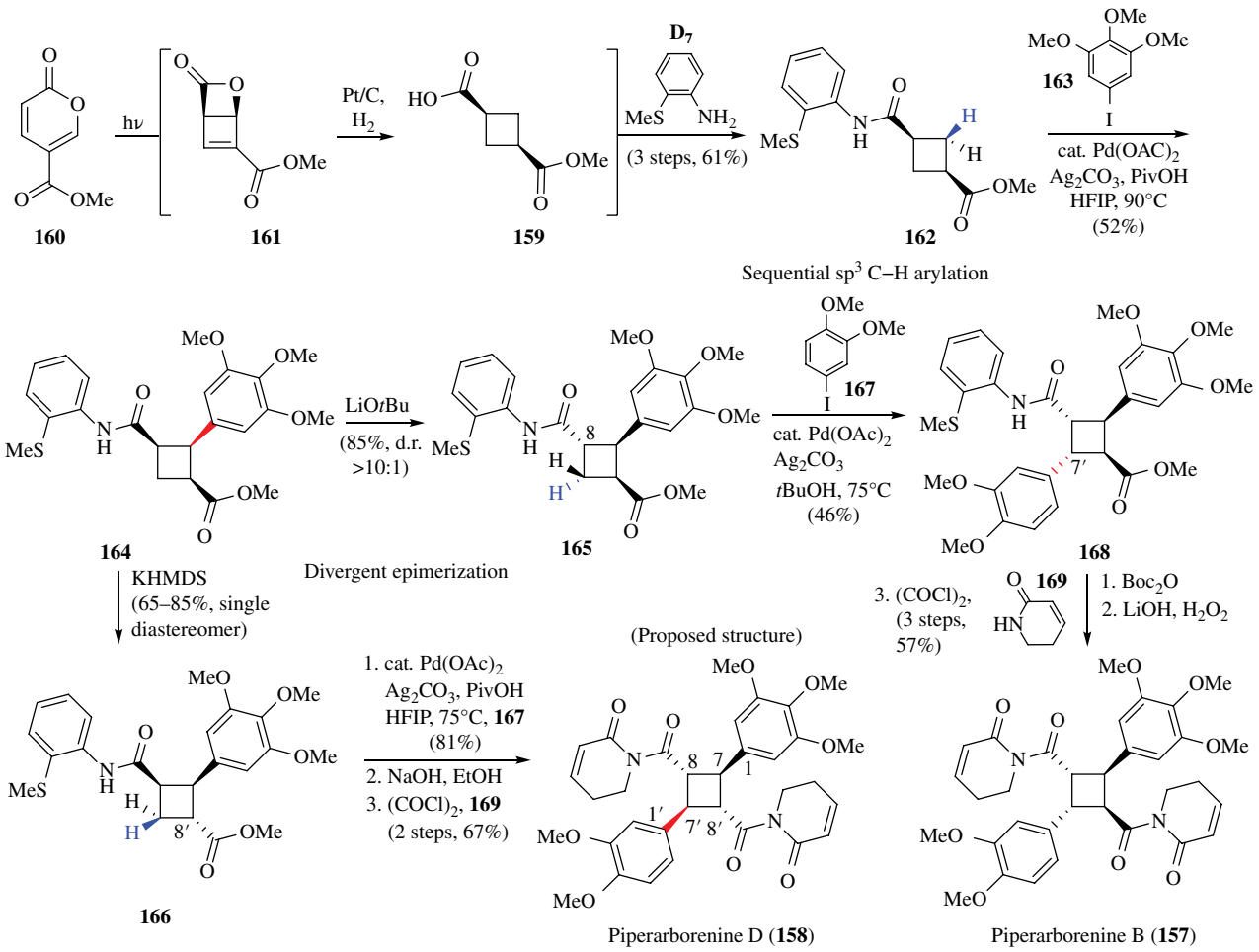
The aforementioned method, though elegant, cannot be adapted to the synthesis of head-to-tail homodimerization- or heterodimerization-derived cyclobutane lignans, such as piperarborenine B (**157**) [58a] and D (**158**) [58b], both of which were isolated from the stems of the creeping shrub *Piper arborescens* and exhibit *in vitro* cytotoxicity against P-388, HT-29, and A-549 cancer cell lines ($IC_{50}$ < 4 μg/ml) [58b]. They are assumed to arise from the head-to-tail heterodimerization of piplartine-type monomers, with *cis–trans–cis* and *trans–trans–trans* stereochemistry, respectively. However, a biomimetic [2+2] photocycloaddition fashion is certainly problematic since homodimerization and head-to-head dimerization and *E*/*Z* isomerization would lead to a variety of structures and stereoisomers. Inspired by the pioneering studies about cross coupling of sp³ C─H bonds with aryl iodides by Daugulis [18c], Baran and coworkers devised the first cyclobutane C─H arylation to solve the preparation of this kind of pseudosymmetrical lignans [59].

As shown in Scheme 10.33, this novel synthesis commenced with the efficient preparation of 1,3-*cis*-substituted cyclobutane dicarboxylate **159**, which required an 8-step and nonstereocontrolled route in the previous literature. Alternatively, the photochemical 4π-electrocyclization of methyl coumalate (**160**) gave photopyrone **161** [60], which was converted to the desired **159** as a single diastereomer via hydrogenation with Pt/C. The subsequent coupling of this carboxylic acid with 2-aminothioanisole as a directing group (DG) afforded the amide **162** in 61% overall yield and thus set the stage for the challenging arylation of cyclobutane C─H bond. After the initial plague and therefore significant optimization, the addition of hexafluoroisopropanol (HFIP) and pivalic acid was found to be critical to this Pd-catalyzed 3,4,5-trimethoxyphenylation of sp³ C─H bond. Notably, the first arylation could be executed on gram scale, and the all-*cis* cyclobutane **164** was isolated in 52% yield with only trace of overarylated by-product formed, which could be attributed to steric effect endowed with methyl ester and DG.

With the common intermediate **164** secured, attention was then turned to its divergent epimerization. Its treatment with LiO*t*Bu in nonpolar toluene resulted in the inversion of C8 stereocenter with high diastereoselectivity, whereas the exposure of **164** to excess of potassium hexamethyldisilazane (KHMDS) led to C8′ epimerization exclusively. The easy access to either epimer (**165** or **166**) guaranteed the second arylation events. To this end, C─H coupling of **165** with 3,4-dimethoxyiodobenzene (**167**) provided tetrasubstituted cyclobutane **168** in 46% yield under the similar catalytic conditions except the employment of *t*BuOH at high concentration and exclusion of HFIP and pivalic acid. It is noteworthy that excellent regioselectivity guided by the DG was observed for this arylation at the methylene C7′─H bond over the tertiary benzylic C7─H bond. In order to remain intact, the hydrolysis of the generated stereotetrad **168** for the installation of two dihydropyridone rings needs



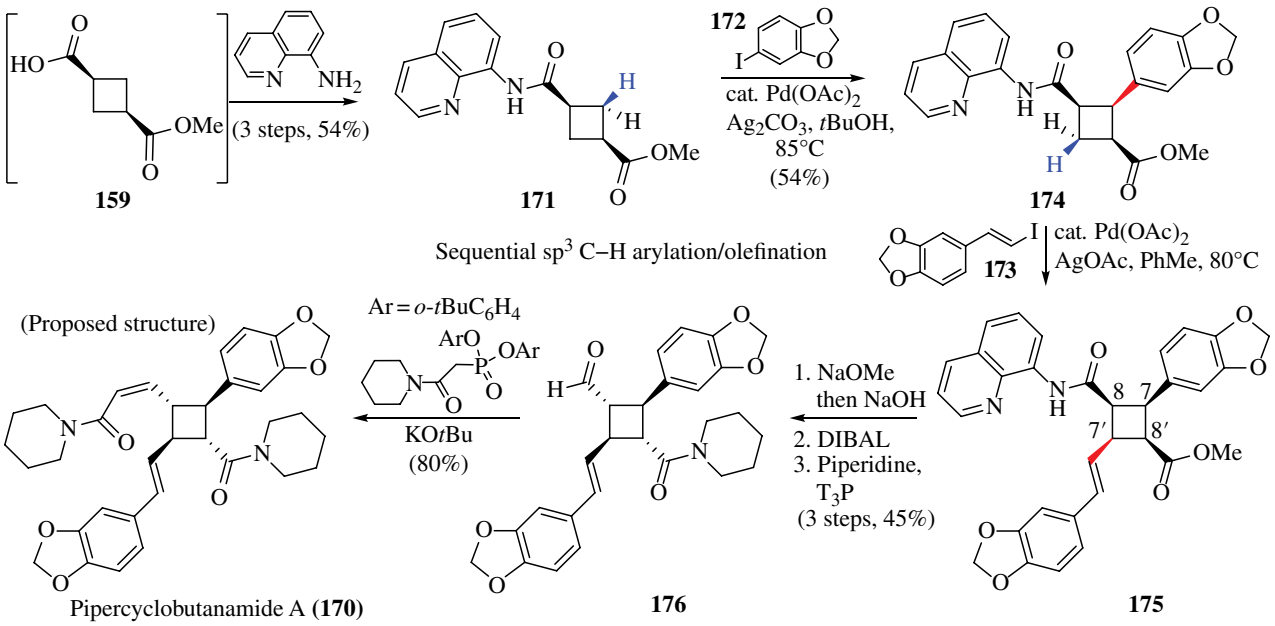

**SCHEME 10.32** Biomimetic synthesis of magnosalin via photoinduced electron transfer.




**SCHEME 10.33** Total synthesis of piperarborenines B and D enabled by double cyclobutane C–H arylations.

to be performed under mild conditions. Thus, the DG within **168** was first carbamoylated with $Boc_2O$ according to the protocol developed by Evans [61] and cleaved with *in situ* generated $Li_2O_2$. The methyl ester hydrolyzed as well under the aforementioned conditions, and the resultant biscarboxylic acid was then converted to the corresponding acid chloride followed by the heating with dihydropyridone (**169**), eventually affording piperarborenines B (**157**) in 57% overall yield. The next pursuit to the stereoisomeric piperarborenines D (**158**) was conducted from the second round of C–H arylation of epimer **166** with **167**. The desired cross coupling proceeded under the conditions analogous to that of **162** but with more facility, presumably due to *trans* orientation of the ester group and the DG. The harsh condition with NaOH in hot ethanol caused complete inversion of C8 stereocenter and full hydrolysis of this diarylation product, affording the biscarboxylic acid with all-*trans* cyclobutane skeleton in 86% yield. The final conversion to bis-acid chloride and coupling with **169** resulted in the proposed structure of piperarborenines D (**158**) in 78% yield. Unfortunately, NMR spectra of synthetic sample did not match the original data given for **158** in the isolation report [58b]. Its real structure was reassigned as a head-to-head dimer through the independent synthesis featuring intramolecular [2+2] photocycloaddition by Baran and coworkers [59].

As an extension of cyclobutane C–H functionalization strategy (Scheme 10.34), Baran et al. [62] also completed the synthesis of pipercyclobutanamide A (**170**), which was first isolated from the fruits of the black pepper, *Piper nigrum*, by Fujiwara and coworkers [63a]. In 2006, Tezuka [63b] reisolated **170** and demonstrated a selective inhibition of cytochrome P450 2D6 (CYP2D6). This molecule contains a styrene motif on the cyclobutane ring and thereby was envisioned as an opportunity to develop C–H olefination chemistry by Baran and coworkers. Based on the previous facile access of 1,3-*cis*-substituted cyclobutane dicarboxylate **159**, the desired C–H olefination precursor **171** was obtained in a single operation and 54% overall yield. In this case, 8-AQ was chosen as a directing group since it demonstrated higher reactivity compared to 2-aminothioanisole in a model study. However, bis(olefination) of **171** proceeded favorably due to smaller vinyl iodide **173**

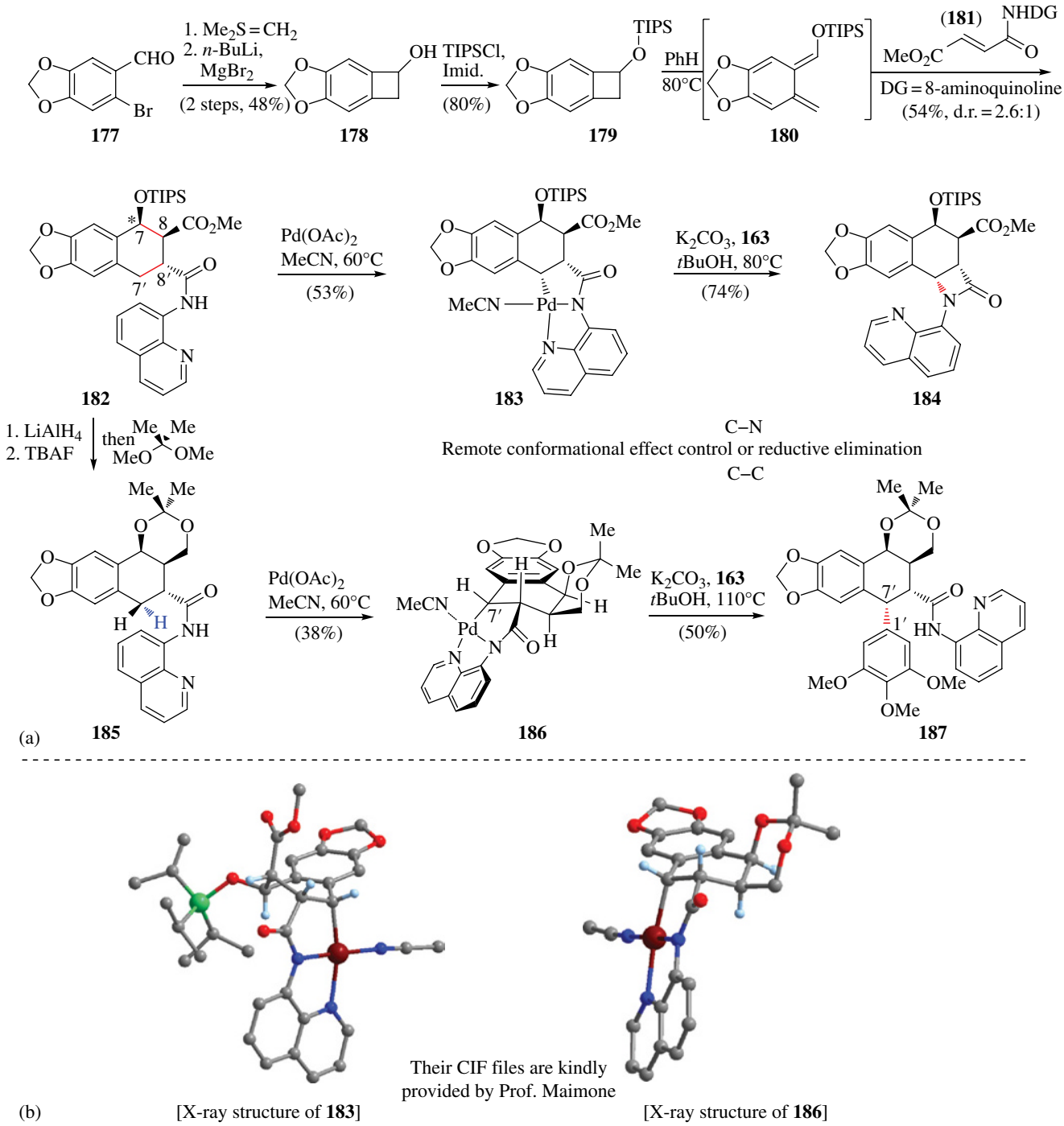



**SCHEME 10.34** Total synthesis of pipercyclobutanamide A enabled by sequential sp³ C─H arylation and olefination.

relative to 1-iodo-3,4-methylenedioxybenzene (**172**), and therefore the sequence of cyclobutane C─H functionalization had to be altered. Indeed, monoarylation with **172** followed by the olefination at C7′ afforded all-*cis* cyclobutane **175** through judicious choice of the silver salts as the base and solvents. The next double epimerization of quite strained **175** at C8 and C8′ let to thermodynamically stable all-*trans* cyclobutane by the use of two equivalents of NaOMe. The further hydrolysis of ester group gave the corresponding carboxylic acid, which could convert to its anion form by DIBAL and therefore actually act as an innate protecting group for the subsequent selective reduction of 8-AQ motif. Notably, this direct reduction of secondary amide to aldehyde group is probably resulted from the chelation of 8-AQ and represents a new method for the cleavage of this DG developed by Daugulis [18b, c]. With distinct aldehyde and carboxylic acid functional groups in hand, the elaboration of two side chains within the cyclobutane could be implemented severally. Thus, the condensation with piperidine promoted by propylphosphonic anhydride ($T_3P$) provided amide **176** in 45% overall yield. Finally, the installation of the unusual *cis*-unsaturated amide motif in pipercyclobutanamide A (**170**) was accomplished through the Horner–Wadsworth–Emmons (HWE) olefination of the remained aldehyde group in **176** with Ando's phosphonate [64] in 80% yield. Unfortunately again, NMR data of synthetic pipercyclobutanamide A (**170**) did not match the original spectra reported for this natural product [63a]. Its real structure was actually assigned as constitutionally isomeric cyclohexene-containing natural product chabamide from the same plant, according to careful comparison of NMR data of synthetic sample with that of natural **170** by Tang and coworkers [65].

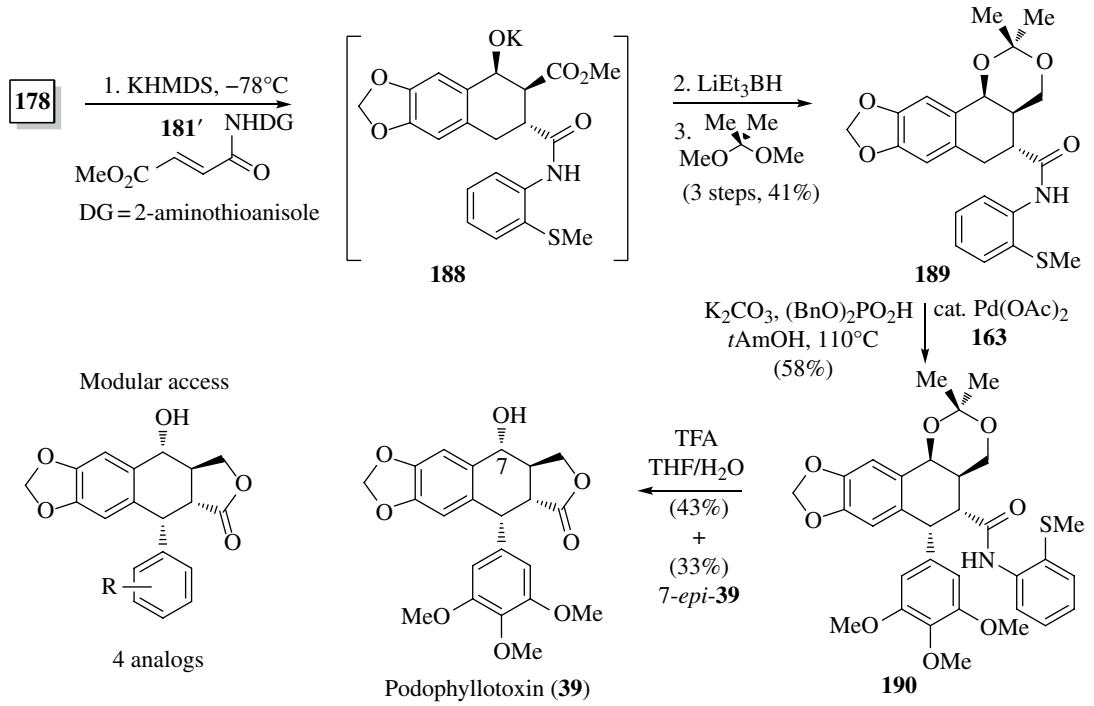
Very recently, Maimone and coworkers also reported a C─H arylation approach to the aryltetralin lignans [66] and completed a short total synthesis of racemic podophyllotoxin (**39**) as a prototypical member. This plant-derived compound can serve as a starting material for the widely used type II topoisomerase-targeting drugs etoposide (VP-16) and teniposide, which have been used for the treatment of lung and testicular cancer, lymphoma, leukemia, and Kaposi's sarcomas [67]. The efficient supply of **39** and especially the preparation of diverse analog are still in high demand although there has been significant progress about their synthesis in the past several decades [68]. Maimone's inspiration also came from the pioneering methodology in the field of amide-directed, Pd-catalyzed C(sp³)─H arylation, as discussed in Section 10.2.

As shown in Scheme 10.35a, this distinct synthesis began with the scalable preparation of benzocyclobutenol silyl ether **178** from 6-bromopiperonal (**177**) through epoxidation, cyclization, and silylation procedure [69]. The subsequent thermal cycloaddition of **179**, via an *o*-quinodimethane intermediate **180**, with fumarate-derived amide **181** afforded C─H functionalization precursor **182** albeit in moderate yield and diastereoselectivity. As expected, when this amide is subjected to stoichiometric $Pd(OAc)_2$ in hot $CH_3CN$, the $Pd^{II}$ complex **183** was formed in 53% yield. However, upon the exposure of this intermediate with C7′─H activation to excess of 3,4,5-trimethoxyiodobenzene (**163**) under the usual arylation condition, β-lactam **184** was obtained exclusively in 75% yield, instead of the expected




**SCHEME 10.35** (a) Initially attempted synthesis of podophyllotoxin enabled by a C($sp^3$)─H arylation and (b) crystal structures of the corresponding palladium complexes.

C─C coupling product. After the careful inspection of the crystal structure (**183**, Scheme 10.35b), the unusual conformation of the cyclohexene-type ring within this Pd complex was identified. In order to accommodate the palladacycle and put the bulky OTIPS group in an equatorial position, the twist-boat conformation must be adopted, therefore leading to the highly crowed environment surrounding the underside of this ring. The $Pd^{IV}$ species from oxidative addition of aryl iodide is difficult to generate, and even if generated, the following C─C reductive elimination would cause significant strain. Regardless, competing C─N coupling predominated on this precursor. Maimone and coworkers realized that an




**SCHEME 10.36** Short total synthesis of podophyllotoxin enabled by a Pd-catalyzed C($sp^3$)─H arylation.

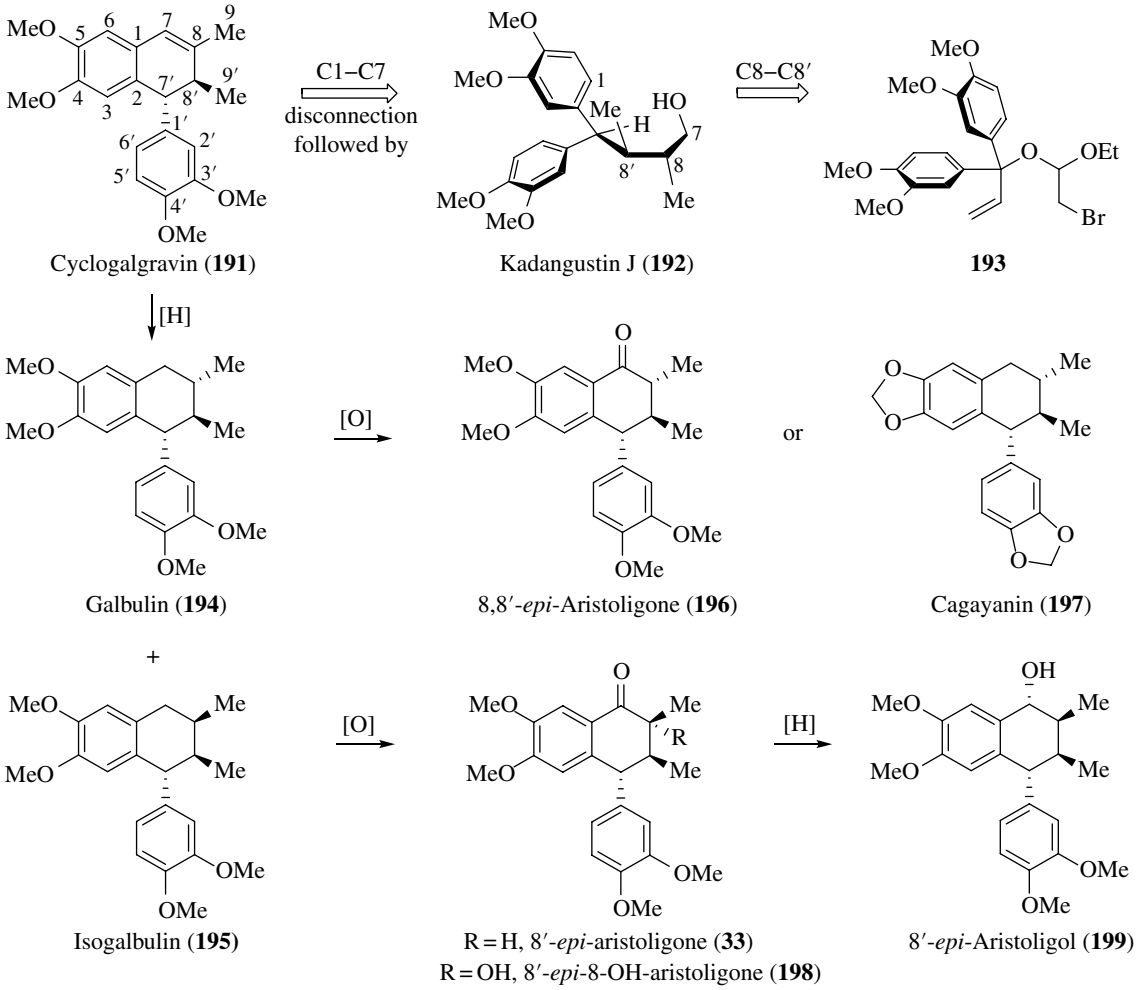
adjustment of conformation must be undertaken and then moved forward to the synthesis of precursor **185** by an ester reduction/desilylation/ketalization sequence. Analogous C─H palladation afforded square-planar $Pd^{II}$ complex **186**, whose X-ray crystal structure revealed that the rigid acetonide locks the cyclohexene-type ring into a half-chair-like conformation. The facile establishment of axial C7′─$C_{aryl}$ bond within **187** is thus expected since this palladacycle is forced away from the underside of the six-membered ring. Indeed, treatment of **186** with excess of **163** under the similar conditions gave the desired arylated product **187** in 53% yield.

Before moving to catalytic C─H arylation reaction, the previous route to **185** was modified for the efficient synthesis of the final target (Scheme 10.36). Deprotonation of free cyclobutanol **178** with KHMDS triggered a low-temperature *o*-quinodimethane generation [70], and a subsequent highly diastereoselective cycloaddition with 2-methylthioaniline-containing amide **181′**. The generated ester **188** was directly reduced by superhydride, and the following ketalization of the resultant diol with dimethoxypropane afforded C─H arylation precursor **189** in 41% overall yield. Incorporation of dibenzyl phosphate [71] as an additive and the replacement of *t*BuOH by *t*AmOH led to the successful C─H arylation of **189** in a catalytic fashion and 58% yield. The remaining task for the synthesis of podophyllotoxin (**39**) is removal of the DG, deprotection of acetonide, and the formation of *trans*-lactone moiety, which can be done in one-pot by simply stirring **190** in TFA/THF aqueous solution, thus affording **39** in 43% yield along with 33% of 7-*epi*-**39**. Equally important, this late-stage C─H arylation strategy allowed for the fast access to some arene-modified podophyllotoxins, which are not easily semisynthesized from the natural product itself.

## 10.5 TOTAL SYNTHESIS OF LIGNANS AND POLYMERIC RESVERATROL BY FRIEDEL–CRAFTS REACTIONS

Inspired by the biosynthetic pathways mentioned in Section 10.1.2, Peng and coworkers [72a] disclosed a collective synthesis [73] of several 2,7′-cyclolignans featuring a novel C1─C7 disconnection (Scheme 10.37) for cyclogalgravin [74a, i] (**191**) since the correlation of this aryltetralene with kadangustin J (**192**) could be envisioned despite its different source of isolation (*Kadsura angustifolia*) (Lem.) A. C. Smith [74b]. Construction of C8─C8′ bond within **192** could be realized through a Ueno–Stork radical cyclization reaction [75] of **193**, since this strategy had been adopted in the total synthesis of related sacidumlignans A and D by the same group previously [72b].

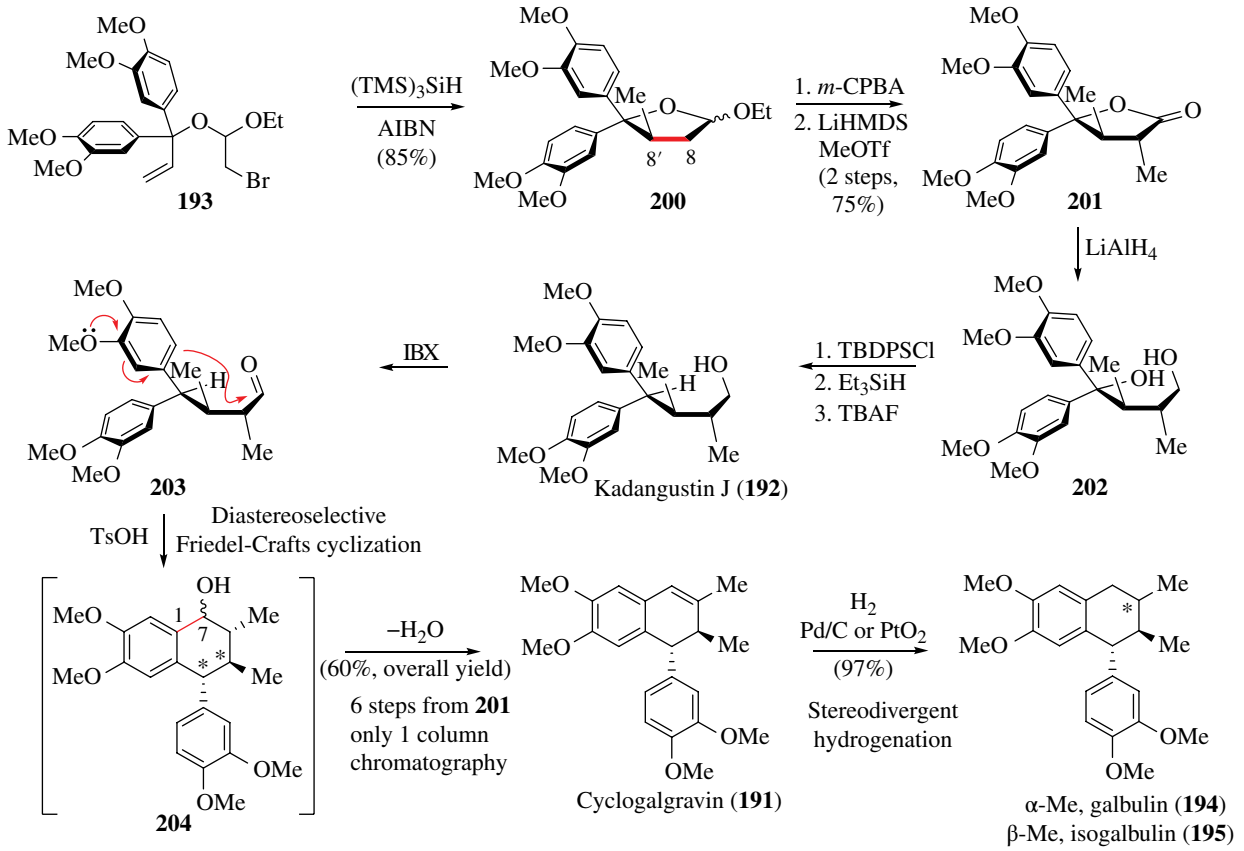
Cyclogalgravin (**191**) then can be served as a common intermediate for collective synthesis of stereodivergent aryltetralins and aryltetralones [(**33**, **194–199**)] with *anti–anti* or *(anti–)syn–anti* arrangement of substituents in tetrahydronaphthalene (THN) skeleton through a series of redox reactions. In particular, the first racemic syntheses of




**SCHEME 10.37** Synthetic tactic of 2,7′-cyclolignan class and their correlation.

8,8′-*epi*-aristoligone (**196**) [10a], 8′-*epi*-aristoligone (**33**) [10a], 8′-*epi*-8-OH-aristoligone (**198**) [74i], and 8′-*epi*-aristoligol (**199**) [74i] with three and four consecutive all-carbon stereocenters have been achieved during this endeavor, and their structures and relative configurations are confirmed accordingly.

As shown in Scheme 10.38, the desired Ueno–Stork radical cyclization of β-bromo acetal **193** for the construction of C8–C8′ bond proceeded smoothly under $(TMS)_3SiH$/AIBN condition, affording cyclic acetal **200** as a mixture of inconsequential diastereomers in 85% yield. Oxidation of **200** mediated by *m*-CPBA and $BF_3{\bullet}Et_2O$ [76] followed by highly diastereoselective methylation of the resulting γ-lactone under shown conditions, provided **201** in 75% isolated yield. The complete reduction of lactone **201** by $LiAlH_4$ afforded diol **202**, which has a superfluous hydroxyl group compared to the structure of kadangustin J (**192**). Thus, diol **202** was first selectively protected as its monosilyl ether in which the untouched tertiary alcohol group was then removed by $Et_3SiH$ followed by deprotection of the resulting TBDPS ether, to give kadangustin J (**192**) in 92% yield over four steps (from **201**). Oxidation of **192** by IBX provided aldehyde **203**, which set the stage for the intramolecular Friedel–Crafts-type, dehydrative cyclization reaction [77]. Pleasingly, this key cascade triggered by substoichiometric amount of TsOH demonstrated excellent diastereotopic differentiation of veratryl group (*anti*-relationship with Me around dihydronaphthalene backbone) with concomitant construction of C1—C7 bond, and eventually cyclogalgravin (**191**) was obtained in 66% yield over two steps. More importantly, each step in the whole sequence (from **201** to **191**) was run in gram scale, and more than 2 g of cyclogalgravin (**191**) as a linchpin was prepared. Diastereodivergent hydrogenation of the unfunctionalized trisubstituted olefin within **191** was then investigated. The heterogeneous conditions mediated by 5% Pd/C can almost quantitatively lead to galbulin (**194**) [74c, d], whereas hydrogenation under Adams catalyst ($PtO_2$) can give the 1.7:1 mixture of **194** and isogalbulin (**195**) [74e, f], from which the desired **195** bearing *syn–anti* substituents in THN framework could be separated by

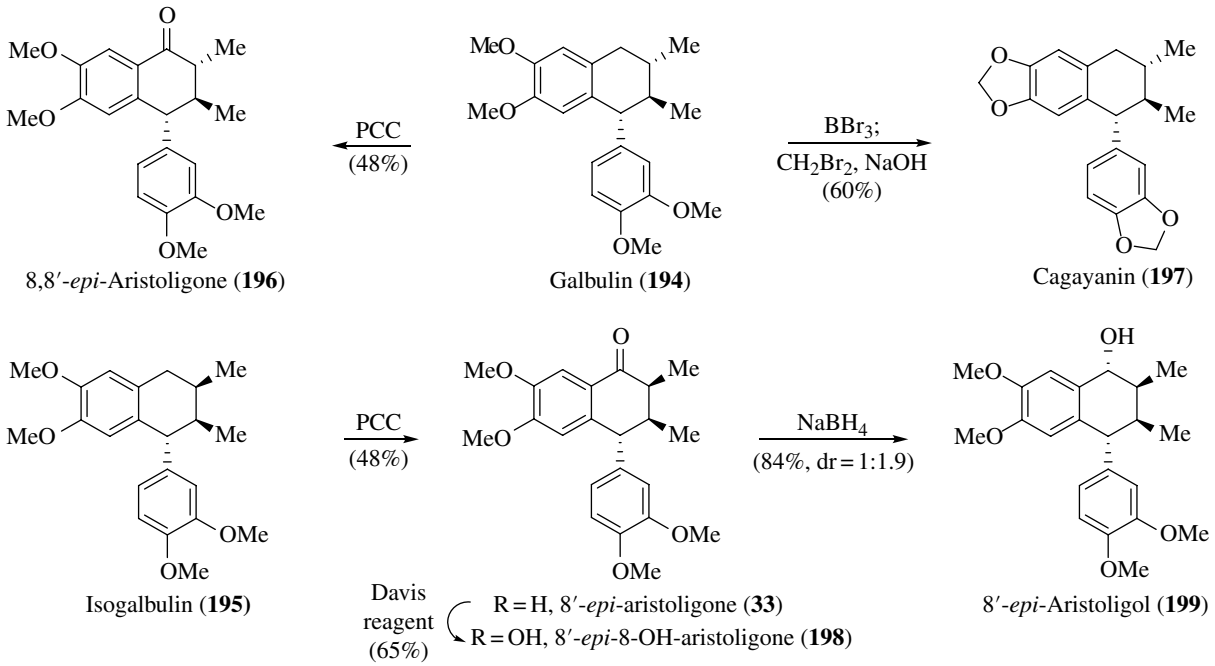



**SCHEME 10.38** Total synthesis of galbulin and isogalbulin via cyclogalgravin and kadangustin J.

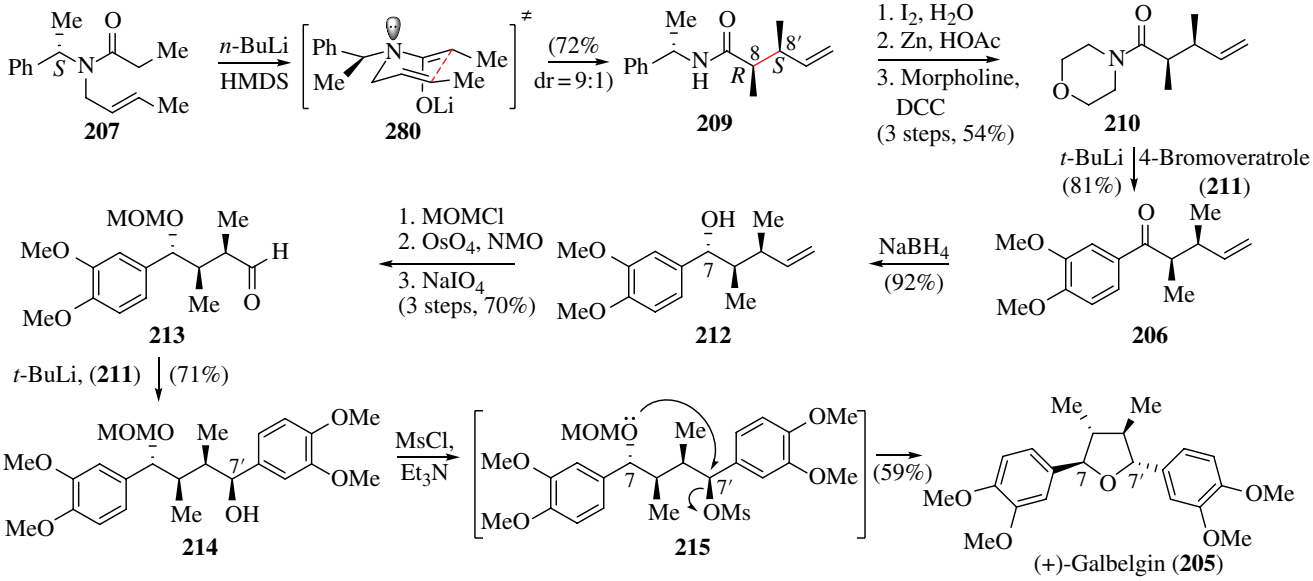
fractional recrystallization. With these two aryltetralins in hand, subsequent collective synthesis of stereodivergent 2,7′-cyclolignans (**33**, **196–199**) could be guaranteed.

As shown in Scheme 10.39, the first synthesis of 8,8′-*epi*-aristoligone (**196**) via benzylic C─H oxidation at C7 in galbulin (**194**) was achieved in 48% isolated yield under the condition of PCC and Celite [78]. The access to cagayanin (**197**) [74g, h] with common *anti–anti* substituents appended to THN framework was realized by the global cleavage of methoxy groups in **194** with $BBr_3$ and subsequent double methylenation of the resulting bis-catechol with $CH_2Br_2$ under basic condition. It is noteworthy that this route features in step-economic, late-stage functional group conversion instead of previous parallel synthesis [79] starting from the corresponding precursor with methylenedioxy group. Similar C─H oxidation of isogalbulin (**195**) gave rise to the first synthetic sample of 8′-*epi*-aristoligone (**33**), which paved the way for the unified synthesis of 8′-*epi*-8-OH-aristoligone (**198**) and 8′-*epi*-aristoligol (**199**) bearing two *syn*-methyls. Highly diastereoselective (dr = 20:1) hydroxylation of ketone **33** enabled by the combination of KHMDS and (+)-(2*R*,8*aS*)-camphorsulfonyl oxaziridine [80] led to 8′-*epi*-8-OH-aristoligone (**198**) in 65% yield. Its structure assignment of the first synthetic sample was verified by its single-crystal structure analysis. Finally, the first synthesis of 8′-*epi*-aristoligol (**199**) with four continuous stereocenters was also achieved in 29% yield from **33** by $NaBH_4$ reduction, accompanied with the formation of its 7-epimer in 55% yield.

Barker and coworkers [81a] constructed C8─C8′ bond employing aza-Claisen rearrangement [82], and asymmetric synthesis of three structurally distinct lignans, namely, (−)-cyclogalgravin (**191**), (−)-kadangustin J (**192**), and (+)-galbelgin (**205**) [83], was achieved by using the resultant common chiral precursor **206** (Schemes 10.40, 10.41, and 10.42). The formation of these divergent lignans is dependent on the substitution pattern in the aryl rings, and careful choice of protecting group on the key benzylic hydroxyl group at C7 is essential. Based on their previous racemic synthesis of tetrahydrofuran lignans [81b], the amide **207** that was generated from (*S*)-α-methylbenzylamine, propionyl chloride, and (*E*)-crotyl bromide was subjected into LiHMDS in toluene at 140°C. The aza-Claisen rearrangement of **207** proceeded smoothly, presumably through chair transition state **208** shown in Scheme 10.40, affording *syn*-dimethylamide **209** in 65% yield. Notably, this key transformation for the construction of C8─C8′ bond is highly *syn*-selective since none of the *anti*-diastereoisomers were

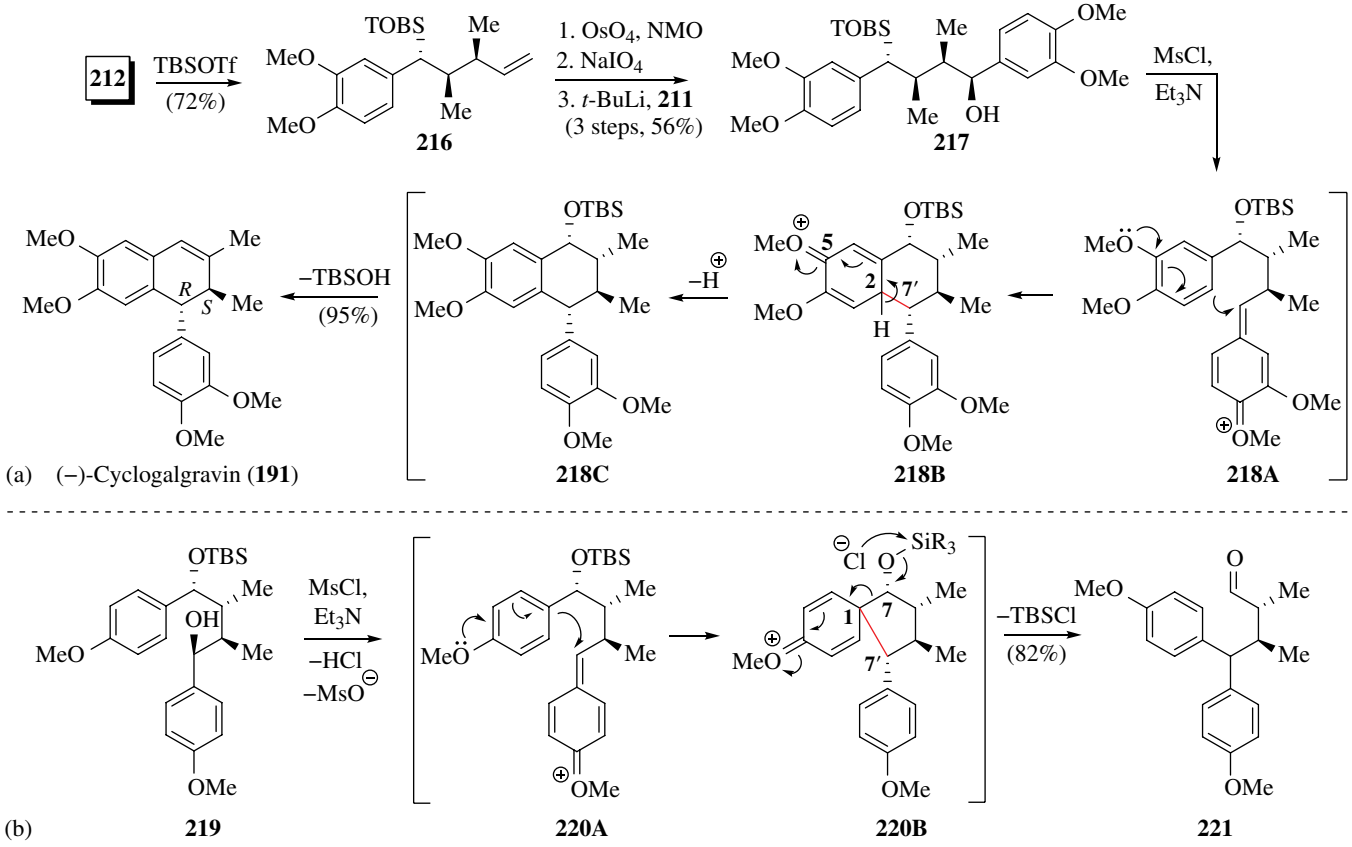



**SCHEME 10.39** Collective synthesis of 7′-aryltetralol and aryltetralone lignans.




**SCHEME 10.40** Total synthesis of the tetrahydrofuran lignan (+)-galbelgin.

observed under the aforementioned conditions. The removal of chiral auxiliary group followed by the condensation of the resulting acid with morpholine gave amide **210** in 54% overall yield. The introduction of the veratrole group was realized through the addition of morpholine amide **210** by the corresponding lithium reagent. The generated ketone **206** was further reduced with $NaBH_4$ to afford alcohol **212** as a single diastereoisomer in 92% yield. This alcohol was then protected as the MOM ether which was converted to aldehyde **213** in 70% overall yield via dihydroxylation of the terminal alkene and the subsequent oxidative cleavage. The incorporation of another veratrole group still relied on the addition of aldehyde **213** by lithiated 4-bromoveratrole (**211**), producing alcohol **214** also as a single diastereoisomer at C7 stereocenter in 71% yield. With all the necessary carbons installed, the ring closure of **214** was then investigated. Upon simple exposure of **214** to MsCl and $Et_3N$, intramolecular nucleophilic attack of the resultant free hydroxyl



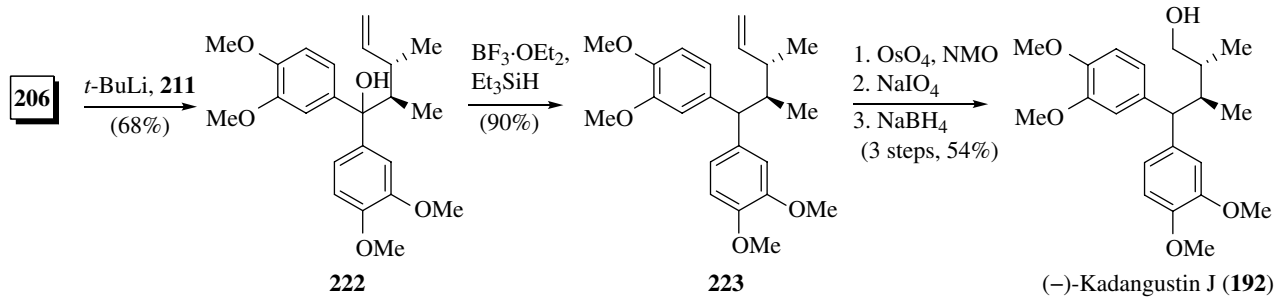

**SCHEME 10.41** Divergent cyclizations based on the variation of substitution pattern in the aryl rings.

group on the mesylate within **215** furnished (+)-galbelgin (**205**) in 59% yield.

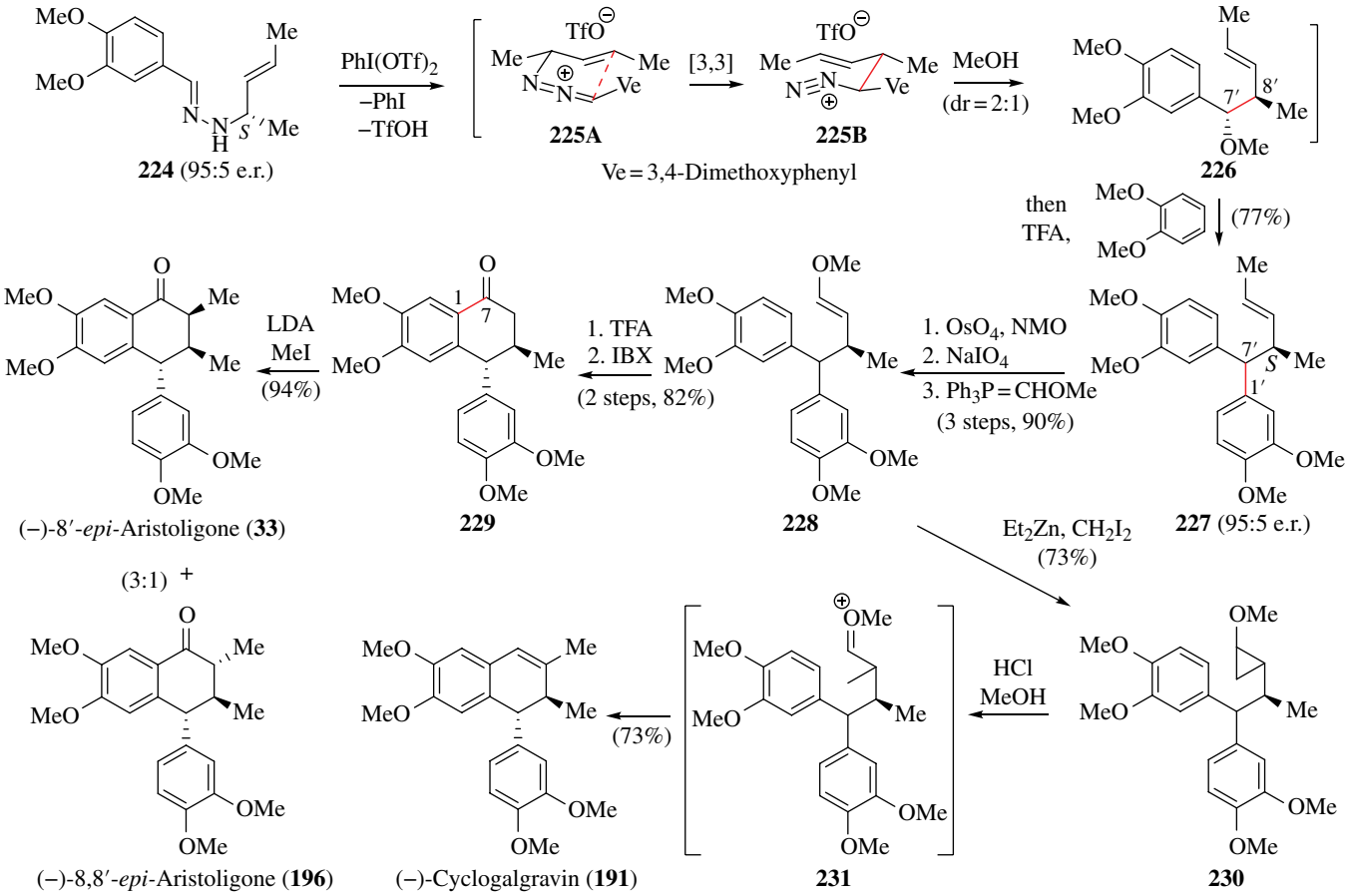
As shown in Scheme 10.41a, the same intermediate **212** can be protected as the TBS ether **216** and converted to the cyclization precursor **217** in 54% overall yield, via a similar protocol as the one described for **214**. Surprisingly, (−)-cyclogalgravin (**191**) was instead obtained in almost quantitative yield upon the exposure of **217** to MsCl and $Et_3N$. The plausible mechanism is demonstrated for the cascade reaction from **217** to **191**. In this case, the diastereoselective attack of quinone methide in **218A** by C2 that is *para* to the C5 methoxy group occurs favorably before the generated HCl from the mesylate formation cleaves O─Si bond, thus constituting the biomimetic construction of C2─C7′ bond according to previous biogenesis studies [10b] (see Scheme 10.5). The resultant **218B** rearomatizes to give THN **218C**, which then undergoes elimination of *tert*-butyldimethylsilanol to form (−)-cyclogalgravin (**191**) [74a] eventually. Optical rotation of the natural substance cyclogalgravin *ent*-**191** [84] was found to be the opposite to the synthetic one; thus its absolute configuration was determined to be (7′*S*,8′*R*). Interestingly, replacement of the veratrole group by *para*-methoxy phenyl group causes a distinct cyclization of the resultant alcohol **219** (Scheme 10.41b). The *ipso*-attack of quinone methide in **220A** by C1 occurs instead, and generated spirocycle **220B** then rearomatizes through the cleavages of O─Si bond and C1─C7 bond, to afford 4,4′-diaryl butanal **221**, which is resembling the structure of kadangustin J (**192**).

Although highly efficient, this transformation could not be further elaborated to the natural kadangustin (**192**) and a different approach was developed. Thus, the tertiary alcohol **222** was first prepared by the addition of lithiate **211** to the common precursor **206** (Scheme 10.42), and the subsequent reductive deoxygenation and the redox manipulation to the terminal double bond completed the total synthesis of enantiomer of the natural (+)-kadangustin J (**192**) [74b].

In 2013, Thomson and coworkers [85a] completed the asymmetric synthesis of (−)-8′-*epi*-aristoligone (**33**) and (−)-cyclogalgravin (**191**) by their one-pot oxidative [3,3] sigmatropic rearrangement/Friedel–Crafts arylation [85b]. As shown in Scheme 10.43, treatment of optically enriched *N*-allylhydrazone (**224**, 95:5 e.r.) with $PhI(OTf)_2$ in the presence of MeOH gave methyl ether **226** with the construction of C7′─C8′ bond, presumably through a chair-like transition state **225A** and diazonium **225B**. This diastereoselectivity for **226** is moderate but inconsequential since subsequent addition of 1,2-dimethoxybenzene and




**SCHEME 10.42** Total synthesis of the neolignan (–)-kadangustin J (**192**).




**SCHEME 10.43** Thomson's stereocontrolled synthesis of tetralone- and dihydronaphthlene-type lignans by an oxidative [3,3] rearrangement/Friedel–Crafts arylation cascade.

trifluoroacetic acid led to benzhydryl derivative **227** in 77% overall yield. More importantly, the complete transfer of chirality in **224** (95:5 e.r.) was observed during this hypervalent iodide-initiated cascade for **227**. After the establishment of C1′—C7′ bond, the remaining C1—C7 bond needed to forge via the methyl enol ether **228**, which was prepared over three steps involving oxidative alkene cleavage and Wittig olefination. Upon the exposure of **228** to the aqueous TFA, highly diastereoselective Friedel–Crafts cyclization analogous to Peng's route [72b] (see Scheme 10.38) occurred, and the resulting benzylic alcohol was further oxidized to the tetralone **229** in 82% overall yield. Methylation of **229** under kinetically controlled condition delivered (–)-8′-*epi*-aristoligone (**33**) and its C8 epimer, (–)-8,8′-*epi*-aristoligone (**196**), in a 3:1 ratio and 94% overall yield. The common intermediate **228** was also intercepted through its cyclopropanation under conditions developed by Shi et al. [86], and the generated oxycyclopropane **230** [87] was smoothly

converted to (−)-cyclogalgravin (**191**) [74a] by simple heating in a mixture of HCl and methanol, presumably via an intermediate aldehyde **231** that undergoes facile cyclization and elimination of methanol.

Resveratrol (**232**), the simplest polyphenol natural product [88], was originally isolated from the roots of white hellebore [89] and later from more than 72 different plants including grapevines. Several biological activities of resveratrol (**232**) have been demonstrated, including cardiovascular protective, antiaging, anti-inflammatory, and tumor suppressant [90]. Hundreds of resveratrol-based dimers and oligomers have also been found in nature [91], and some of them exhibited additional properties such as HIV inhibition [92]. However, the further investigation of these promising effects was hampered by the inability of their isolation in sufficient quantity. Laboratory synthesis could thus be a solution to this problem [88, 93], and early progress was mainly focused on the biomimetic synthesis [94] based on the biogenesis of this oligostilbene family. Their biosynthesis hypothesis *in vivo* is attributed to oxidative coupling between resveratrol-derived mesomers such as $M_5$, $M_8$, and $M_{10}$ under enzymatic catalysis (Scheme 10.44a). The diversity in which the described radical coupling modes can occur describes the existing carbogenic complexity within resveratrol oligomers and explains the difficulty to achieve their stereocontrol biomimetic synthesis *in vitro*. For example, δ-viniferin (**233**) could be generated in various yields upon the exposure of resveratrol itself to either peroxidase [95a] or inorganic oxidants [95b] (Scheme 10.44b), whereas highly toxic $Tl(NO_3)_3$ provided ε-viniferin (**234**) in 60% yield [95c].

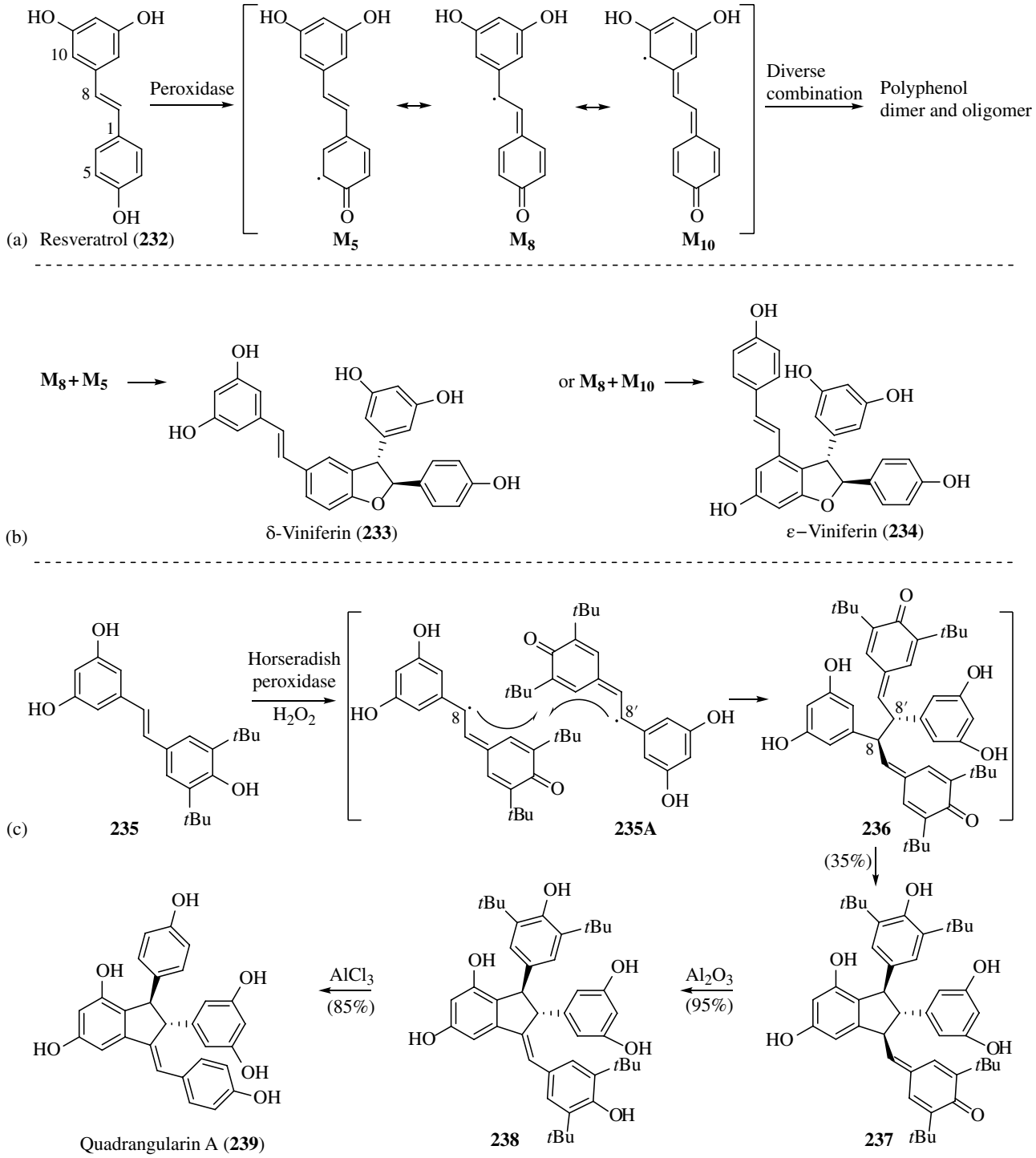
In 2006, Hou and coworkers reported a landmark work in this field (Scheme 10.44c) [96a]. Inspired by the research from Wallis et al. [96b], they placed the bulky *t*-butyl group on the C3 and C5 positions of resveratrol and therefore achieved horseradish peroxidase-catalyzed regioselective homodimerization of **235** via radical species **235A**. The generated *meso*-intermediate **236** underwent stereoselective 5-*exo*-*trig* cyclization through stereoselective Friedel–Crafts alkylation of the *p*-quinone methide moiety, affording *trans*,*trans*-trisubstituted indane **237** in 35% yield along with two minor trimers. The subsequent tautomerization gave **238** as a single *E* isomer in 95% yield, and final removal of all the *t*-butyl groups within **238** provided the racemic quadrangularin A (**239**) in 85% yield.

The aforementioned biosynthetic and biomimetic explorations suffered from some significant limitations: unregiocontrolled oxidative coupling always leads to a complex mixture from which the desired product is only available in low yield and nonnatural analogs predominate; those methods generally can produce single dimeric member but do not possess the strategic power to deliver a family-level solution for all frameworks especially including higher-order structures. In 2007, Snyder, Zografos, and coworkers [97] filled this gap and established an elegant approach for the collective synthesis [73] of several resveratrol dimers and oligomers (Scheme 10.45).

Snyder's inspiration came from his careful inspection to every structure within this class of natural products, seeking for some clues that might identify an alternate synthetic approach. His team found that one key feature appeared to reside in a few natural products such as pauciflorol F (**241**) [98a], diptoindonesin D (**242**) [98b], and cassigarol B (**243**) [98c], all of which possess an odd number of aromatic rings. This fact suggested that the building block **240** with three aryl rings arrayed in the same core structure could enable access to these sesquimers by reagent control and in turn to dimeric ampelopsin D (**244**) [98d], ampelopsin F (**245**) [98e], quadrangularin A (**239**) [98f], pallidol (**246**) [98g, h], and tetrameric ampelopsin H (**247**) [98d]. To this end, utilizing such a unique starting point, diverse carbogenic complexity represented by central 5-, 6-, and 7-membered rings and [3.3.0]-, [3.2.1]-, and [3.2.2]-bicycles would be established through orchestrated cascades based on Friedel–Crafts reaction. This daring hypothesis has been proved to be true by Snyder et al., and the following sections will detail their wonderful campaign.

One of these privileged precursors **240** is biaryl alcohol **240a**, which can be prepared from 3,5-dimethoxybenzaldehyde (**248**) through simple functional group manipulations (to **249**) in combination with HWE olefination (to **250**) and nucleophilic addition as shown in Scheme 10.46. Notably, the whole sequence proceeded smoothly even when conducted on scales up to 50 g, and no chromatographic separations were required for any of those steps. Upon the exposure of this key intermediate to a stoichiometric amount of TFA, a cascade featuring cation generation (**251A**), regio- and stereoselective cyclization, and stereoselective capture of the newly formed cation (**251B**) afforded *trans*,*trans*-trisubstituted indane **251C** that can be converted to alcohol **252** under basic work-up conditions in 75% overall yield. Oxidation of **252** by Dess–Martin periodinane and then $BBr_3$-mediated global demethylation delivered the typical sesquimer pauciflorol F (**241**) in 83% two-step yield.

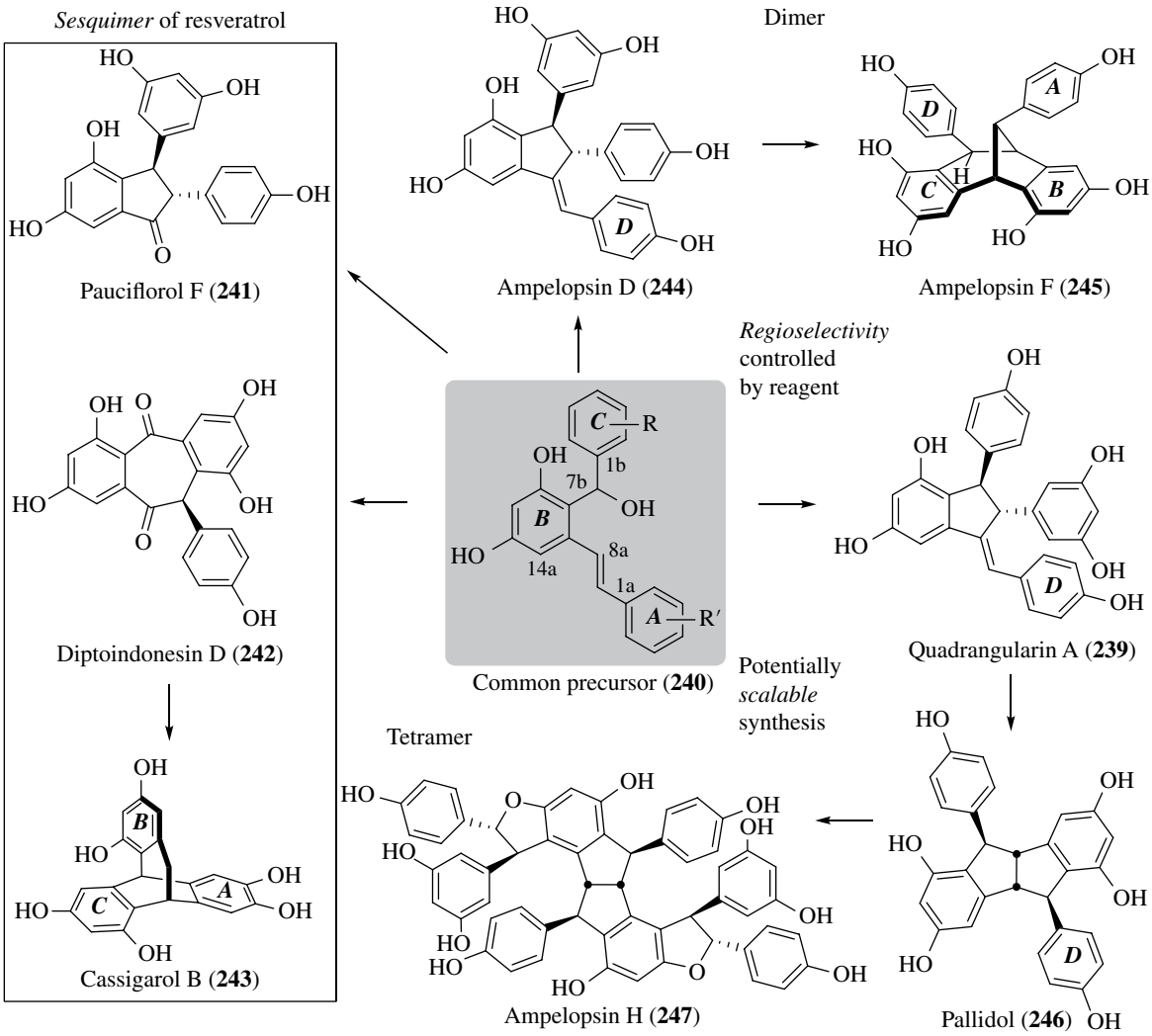
Next, another sesquimer diptoindonesin D (**242**) bearing a seven-membered carbocycle was also attempted to access from the oxidized form of the privileged precursor **240a**. As shown in Scheme 10.47, when the diaryl ketone **253** was subjected to $Br_2$, the bromocycloheptanone (not shown) was produced following an electrophilic activation of the double bond/7-*exo*-*trig* cyclization sequence. Further exposure of this labile intermediate to AgOAc in acetic acid generated benzyl cation **254A** that was intramolecularly trapped by the adjacent phenyl group to produce **254B** instead of reacting intermolecularly with acetate. The following regioselective cyclopropane opening induced by *ortho*- and *para*-disposed methoxy groups within **254B** and a terminating attack of acetate to the resulting *p*-quinone methide afforded the product **255** with the transposition of the phenyl group. The




**SCHEME 10.44** Biosynthesis of resveratrol-derived natural products and biomimetic dimerization strategy. (a) Biosynthetic pathway. (b) Direct but uncontrolled dimerization under peroxidase, laccase, or inorganic oxidants, and (c) Biomimetic radical dimerization *in vitro* based on the structurally modified resveratrol $[\mathbf{M_8}+\mathbf{M_{8'}}]$.

cleavage of the acetate in **255** and oxidation of the resultant alcohol led to diptoindonesin D analog (**256**) in 77% yield.

Although this serendipitous discovery featuring thermodynamically favored phenonium shift is unique and interesting, the pursuing for natural product itself forced Snyder et al. to look for other electrophile-initiated cascade in order to access the correct architecture connectivity. Indeed, when the epoxide functionality was installed onto

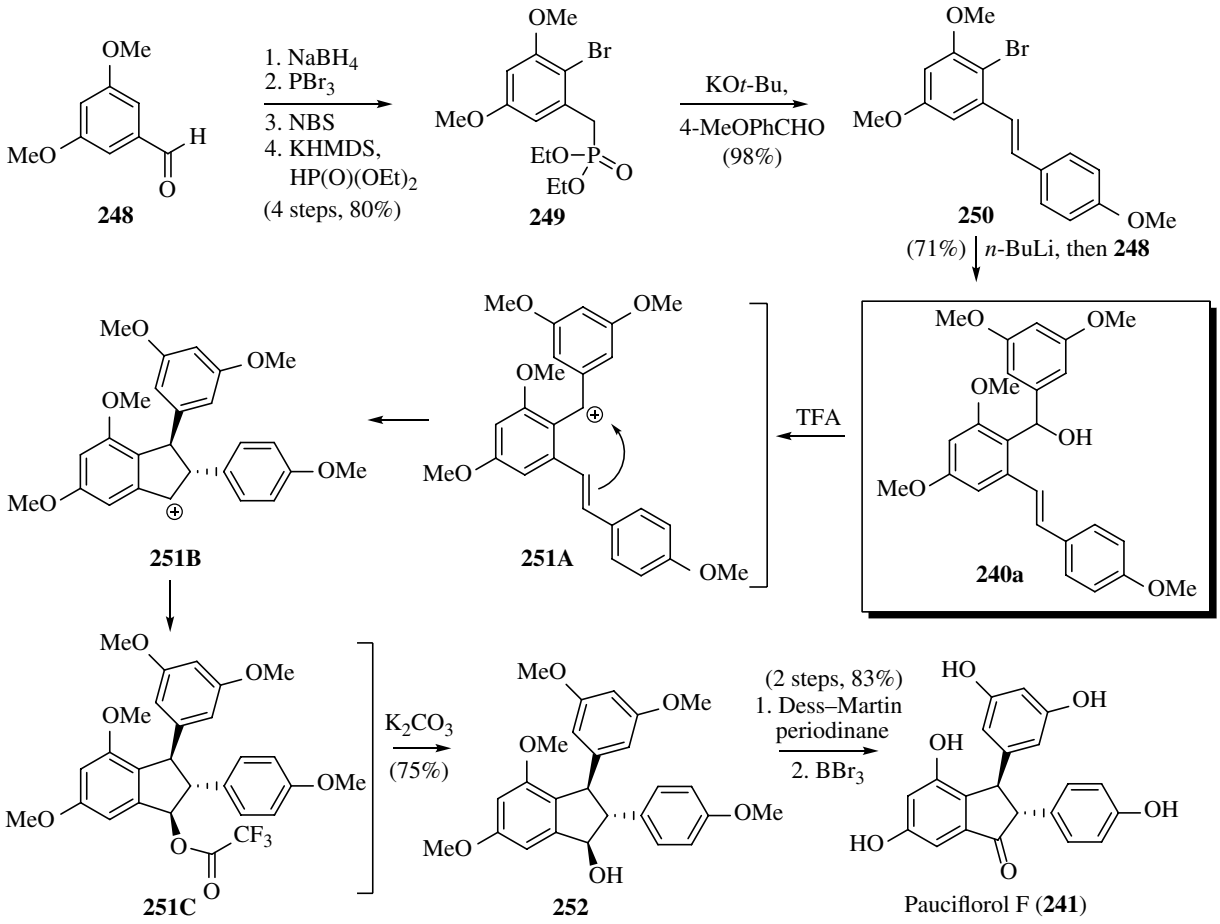



**SCHEME 10.45** Snyder's collective synthesis strategy for resveratrol oligomers from the alternate precursors (**240**).

the double bond by 1,1,1-trifluorodimethyldioxirane, the spontaneous 7-*endo-tet* cyclization of **257A** occurred, directly providing protected hemsleyanol E (**258**) albeit in 34% yield. The subsequent oxidation completed the synthesis of permethylated diptoindonesin D (**259**) in almost quantitative yield. Disappointedly, all the attempts to obtain natural product hemsleyanol E [98i] and diptoindonesin D were unsuccessful.

The third sesquimer cassigarol B (**243**) with a [3.2.2]-bicyclic skeleton was also synthesized from the analogous precursor **240b** (Scheme 10.48a). Although cassigarol B possesses ring systems reminiscent of resveratrol-based structures, such a connection was not suggested by those isolation chemists [98c]. Snyder thought that the desired bicyclic skeleton could be accessed by the forge of C2a─C7b bond in a dibenzocycloheptane intermediate, which is easily available from **240b** according to the previous synthesis for diptoindonesin D. The adjustment of reaction conditions combined with the innate reactivity imparted by the 3,4-dimethoxy group indeed realized this hypothesis. Upon the exposure of **240b** in a mixture of 33% HBr in AcOH at room temperature, the benzylic alcohol was initially exchanged to either a bromide or acetate (**260A**) followed by a proton-initiated Friedel–Crafts cyclization. The generated **260B** proceeded through a second Friedel–Crafts cyclization of the *p*-quinone methide moiety derived from B ring, affording permethylated cassigarol B (**261**) in one-pot 74% yield. It is noteworthy that two strategic bonds (C2b─C7a and then C2a─C7b) were sequentially established in this cascade promoted by the simple reagent. Finally, $BBr_3$-induced global demethylation delivered the unique sesquimer cassigarol B (**243**) in 87% yield. Two cassigarol B analogs (**262** and **263**, Scheme 10.48b) were also synthesized successfully starting from methyl ether of **240b**.

This campaign next moved to resveratrol dimer series. Niwa and coworkers [99] had already found that the

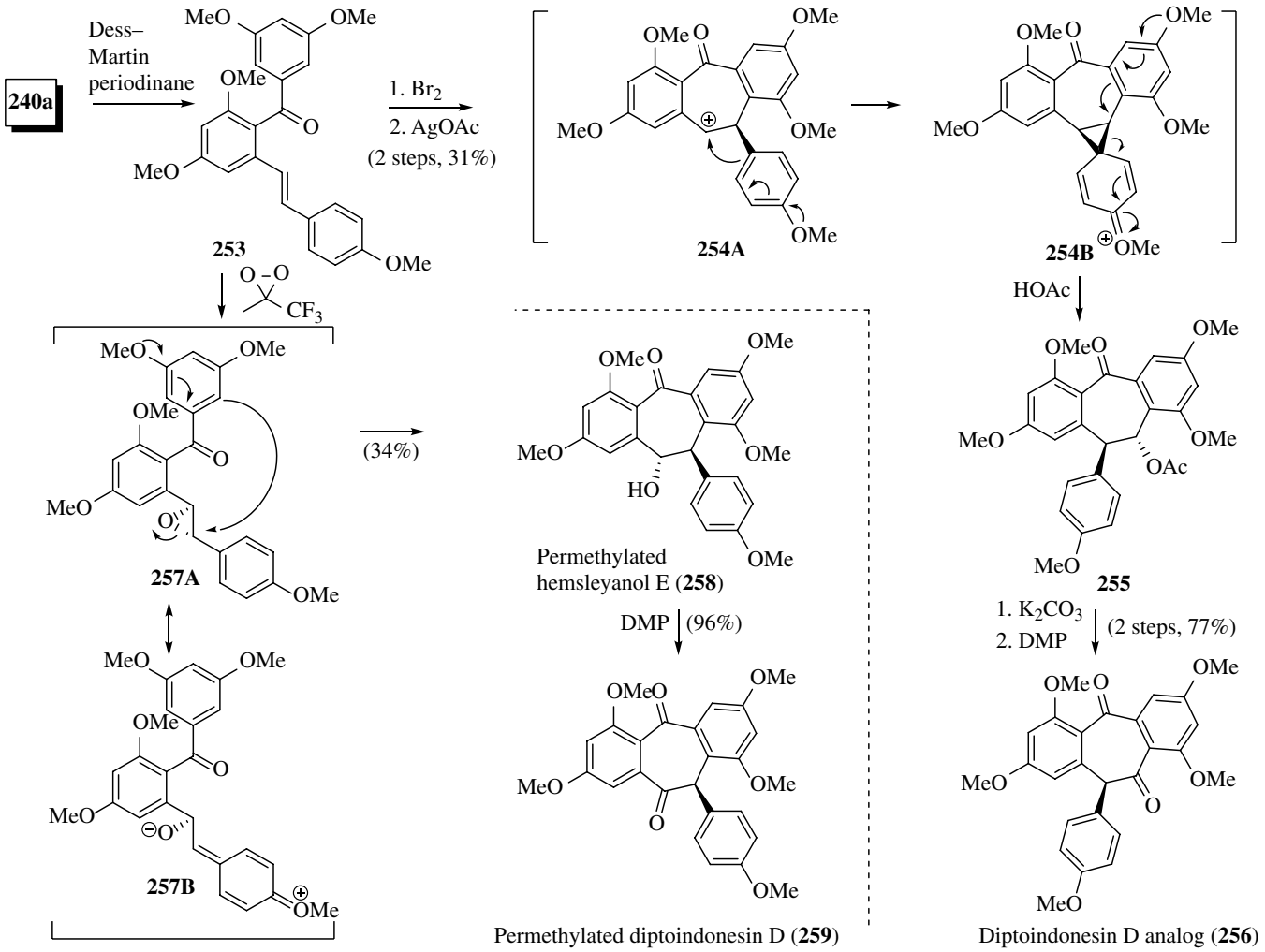



**SCHEME 10.46** Acid-promoted cyclization of triaryl precursor **240a** for the total synthesis of pauciflorol F.

treatment of ε-viniferin (**234**) by acid can produce the important intermediate **264**, from which two pathways could proceed (Scheme 10.49). The simple elimination of benzyl proton generated ampelopsin D (**244**) in 14% yield (path a), whereas the transannular attack of quinone methide moiety within **264** by *cis*-disposed aryl group gave ampelopsin F (**245**) in higher yield (path b).

This uncontrolled therefore low-yield approach encouraged Snyder et al. to improve its efficiency through other electrophile-initiated cascades. As shown in Scheme 10.50, the previously generated cation **251B** during the synthesis for pauciflorol F (**241**) could be intercepted with *p*-methoxy-α-toluenethiol, thus affording tetraaryl intermediate **265** in 57% yield. This thioether was oxidized to the sulfone and then converted to the permethylated ampelopsin D (**266**) in 41% yield through Ramberg–Bäcklund reaction [100a] under Meyer's modified conditions [100b]. $BBr_3$-mediated global demethylation furnished the ampelopsin D (**244**) in 86% yield. Pleasingly, upon the exposure of **266** to NBS, the tribromide (**268**) bearing the desired [3.2.1]-bicycle was obtained in 89% yield via the intermediacy **267** resembling **264** in Scheme 10.49. The same deprotection using $BBr_3$ accomplished the synthesis ampelopsin F (**245**) with high efficiency.

The structure of quadrangularin A (**239**) is different from that of ampelopsin F (**245**) only in the array of pendant phenol rings on the indane core, and thus it could be access from the corresponding precursor **240c** in the same manner. Indeed as shown in Scheme 10.51, the permethylated quadrangularin A (**269**) was produced in 25% overall yield following a similar route for **266**. The final deprotection using $BBr_3$ completed the total synthesis of quadrangularin A (**239**) in 75% yield. The regio- and stereoselective bromination of **269** delivered quinone methide **270**, which was attacked by the vicinal 3,5-dimethoxy-benzene ring to afford the tribromide **271** with a [3.3.0]-bicycle framework in 80% yield. The eventual hydrogenolysis and cleavage of all six methyl ethers completed the synthesis of pallidol (**246**) in 63% yield. Notably, although the incorporation of those Br atoms in the aforementioned cascade violated the viewpoint of atom economy for an ideal synthesis, they (two aryl bromine atoms at least) played a critical role in ensuring that attachment of the benzyl Br atom and the following ring closure leading to either **268** or **271** were stereoselective.

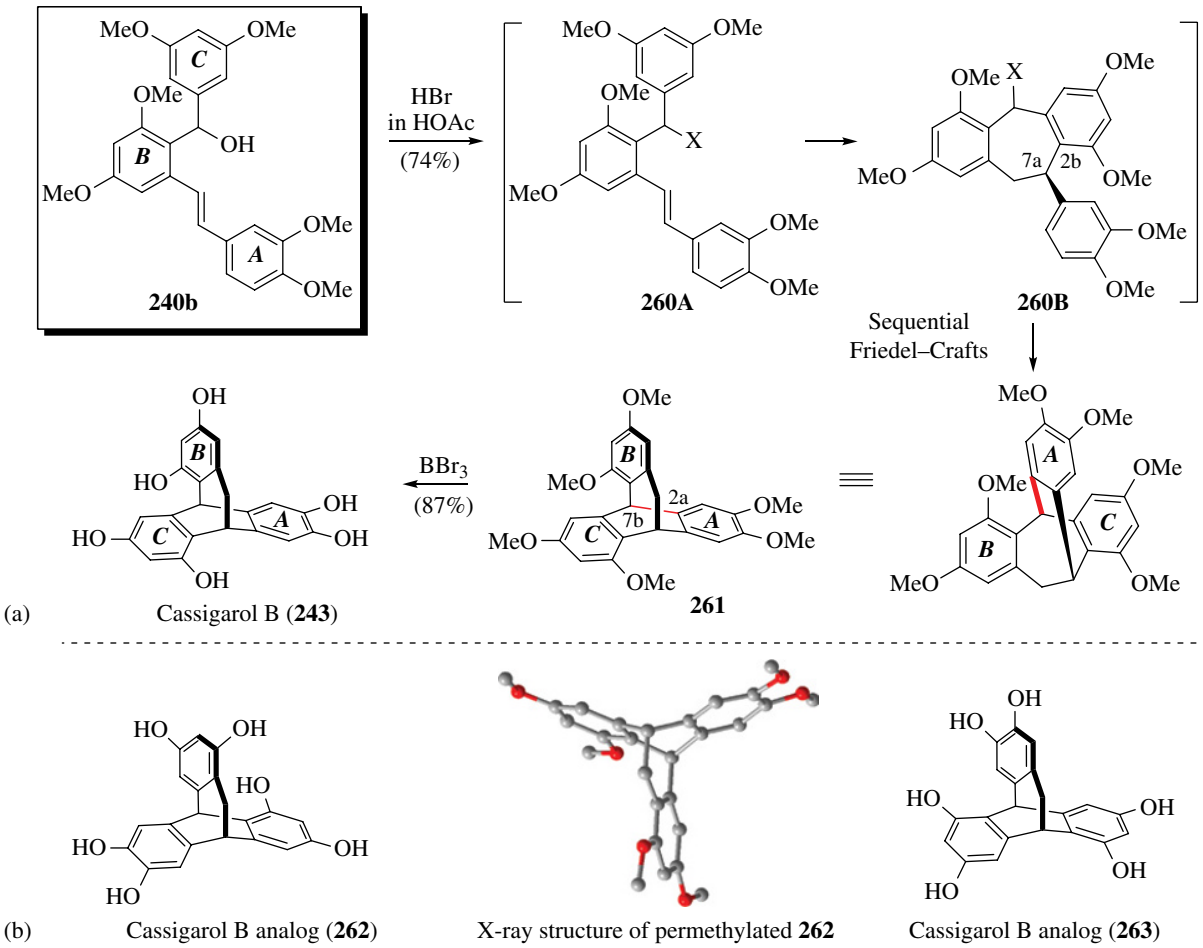



**SCHEME 10.47** Total syntheses of protected hemsleyanol E, diptoindonesin D, and analog via bromonium or epoxide-initiated cascade sequence from the precursor **240a**.

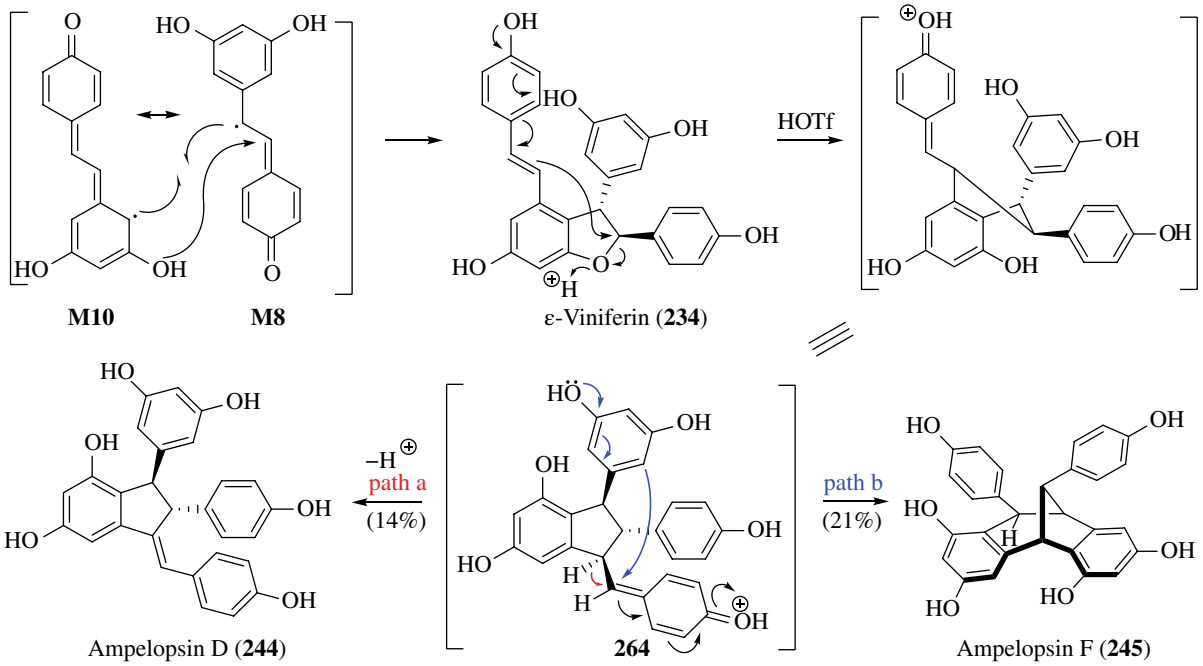
Equally important, the aryl bromides within **268** and **271** also served as a versatile handle for the construction of dihydrofuran rings that generally exist in the higher-order resveratrol oligomers such as ampelopsin H (**247**).

To this end, the tertiary bromine atom within **271** was efficiently and selectively removed under catalytic photoredox conditions (Scheme 10.52). The subsequent double lithiation of the resultant $C_2$-symmetric dibromide **272** followed by the addition of 3,5-dimethoxybenzaldehyde gave the dibenzyl alcohol that was subjected to oxidation by Dess–Martin periodinane and protecting group exchange to afford diketone **273** with high efficiency (4 steps, 70% overall yield). One-carbon homologation employing Corey–Chaykovsky epoxidation [101] and $ZnI_2$-mediated rearrangement [102] provided bisaldehyde **274** and its diastereoisomer in 77% combined yield. The major isomer **274** could be enriched (up to 21:1 ratio) through the epimerization of the mixture under KHMDS. The nucleophilic addition of bisaldehyde **274** by *p*-benzyloxy-phenylmagnesium provided all the necessary carbons for the target molecule. Hydrogenation over catalytic Pd/C then excised the benzyl ethers, and stereoselective formation of *trans*-disposed dihydrofuran rings within the resulting polyphenol gave this sophisticated resveratrol tetramer, ampelopsin H (**247**).

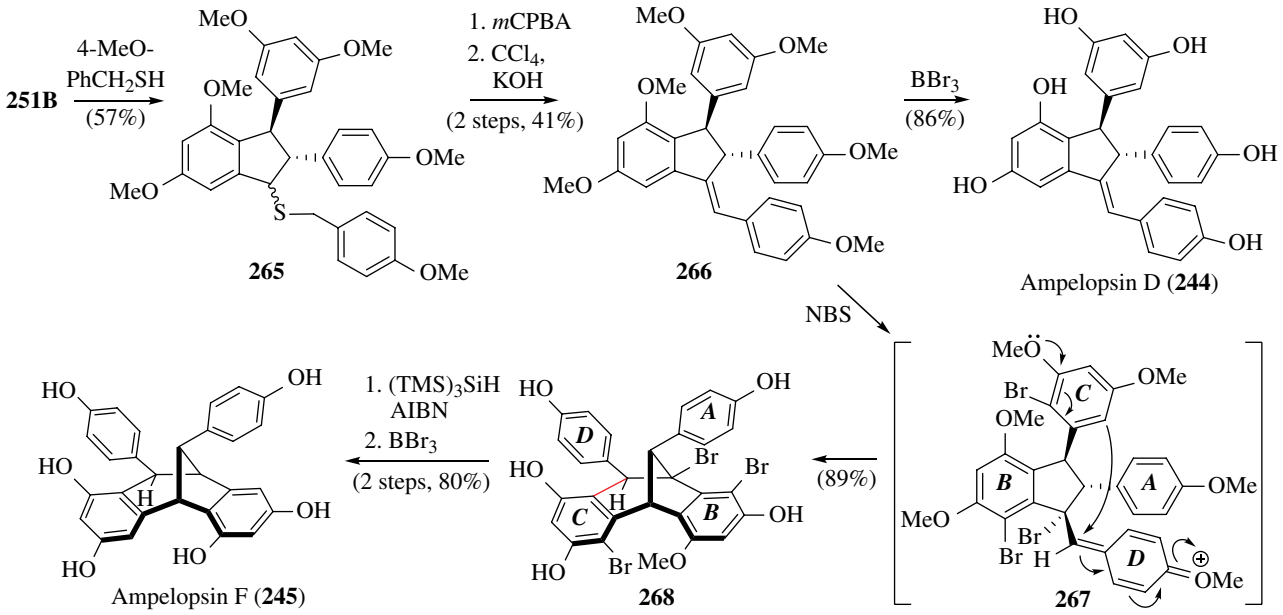
There are some noteworthy features in this campaign for the resveratrol oligomers: (i) a common sesquimer **240** instead of resveratrol itself was identified as the privileged precursor, which can realize the efficient synthesis of the diverse members, potentially the entire class; (ii) this synthesis is programmable and modular, therefore allowing the convenient access to unnatural analogs for broader biochemical screening; (iii) the invention of reagent-controlled orchestrated cascade sequences with the excellent chemo- and regioselectivity; (iv) it is a hybrid of retrosynthetic analysis [103] and diversity-oriented synthesis (DOS)



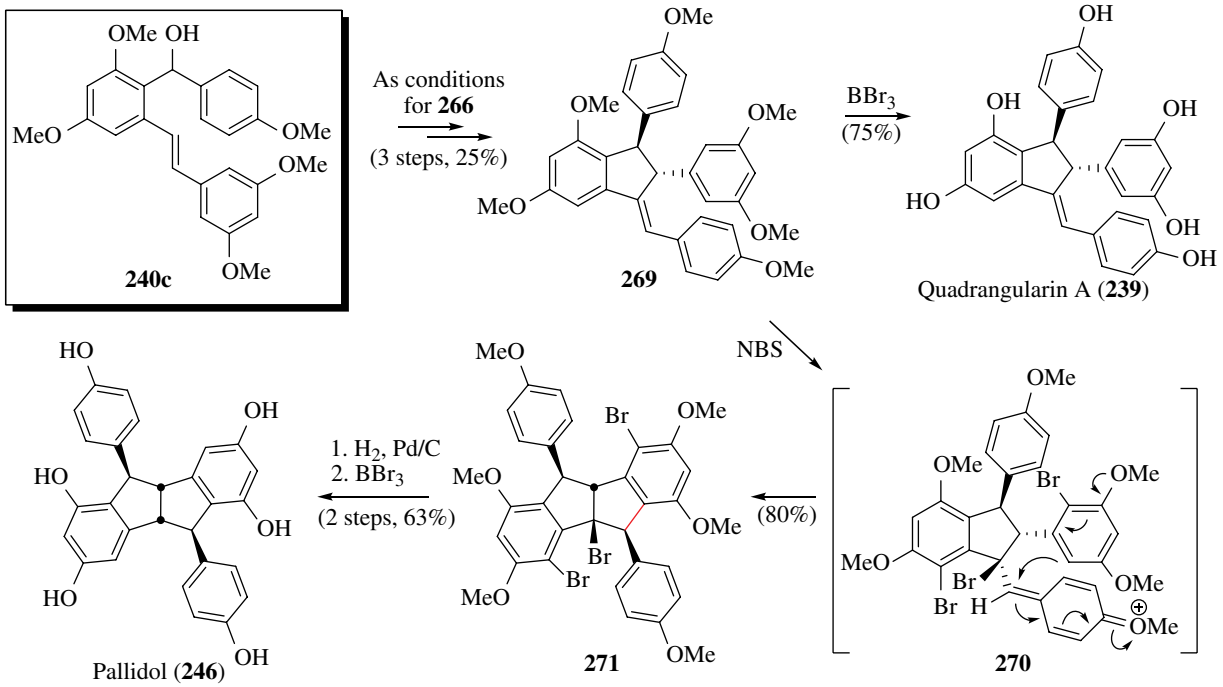

**SCHEME 10.48** Diverse synthesis of (a) cassigarol B and (b) analogs via proton-initiated cascade from the precursor **240b**.




**SCHEME 10.49** The plausible biogenesis relationship between ε-viniferin, ampelopsin D, and ampelopsin F via acid-promoted rearrangement.




**SCHEME 10.50** Unified synthesis of ampelopsin D and ampelopsin F via the intermediacy **266**.

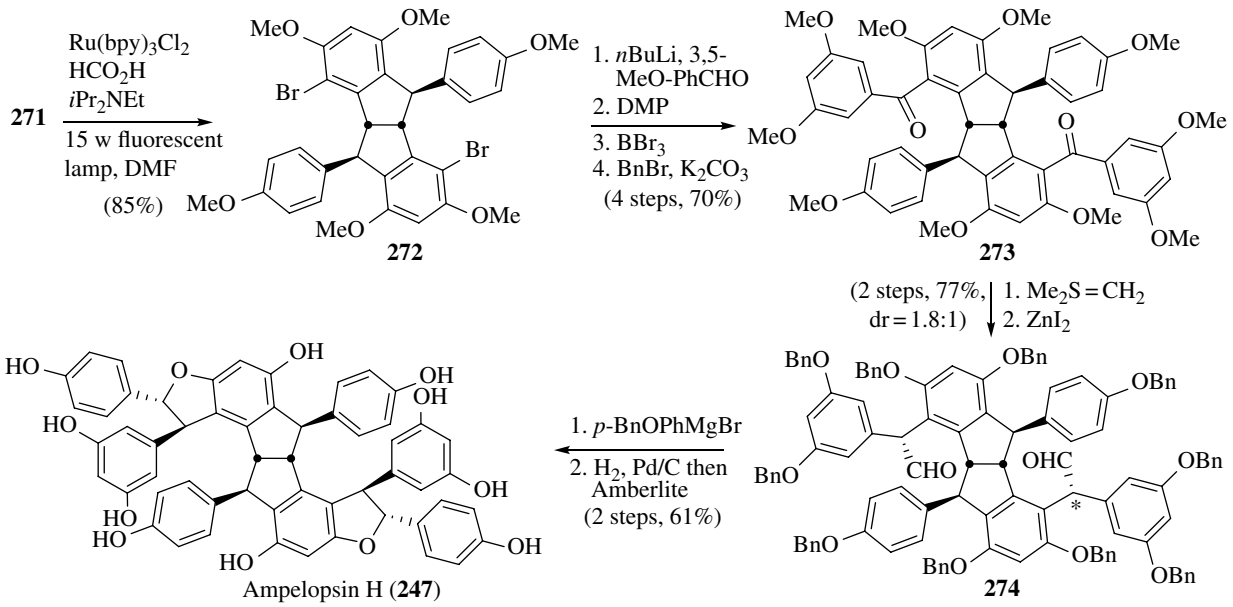



**SCHEME 10.51** Unified synthesis of quadrangularin A and pallidol via bromonium-initiated cascade starting from the precursor **240c**.

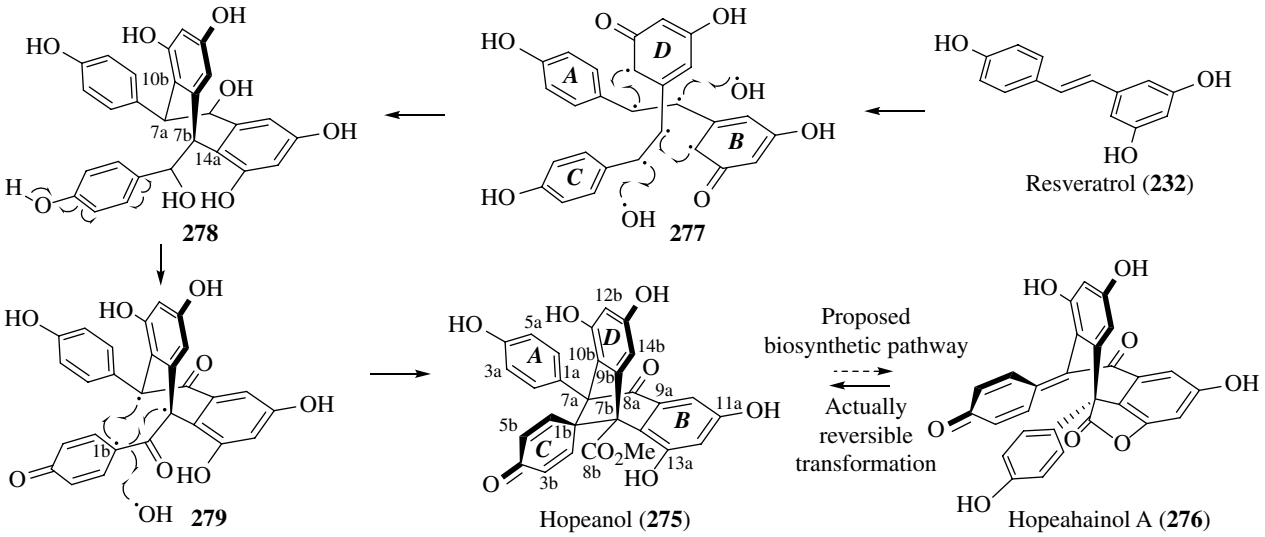
[104]; and (v) the overall strategy could be extended to the synthesis of other oligomer natural product families.

The following content will be focused on the discussion about the total synthesis of several resveratrol dimers with unique skeletons.

Hopeanol (**275**, Scheme 10.53) and hopeahainol A (**276**), which belong to rearranged resveratrol dimers with the novel carbon skeleton, were isolated from the stem bark of *Hopea exalata* Lin, Yang, and Hsue in 2006 and subsequently from *Hopea hainanensis* in 2008 by Tan and coworkers [105]. Hopeanol (**275**) with a constrained and partially dearomatized bicyclic core is proved to be a potent cytotoxic agent against a series of human cancer cell lines (KB, AGS, Hela, BEL-7402, SW1116, and BGC-803, $IC_{50} = 0.52–19.36\,\mu M$),

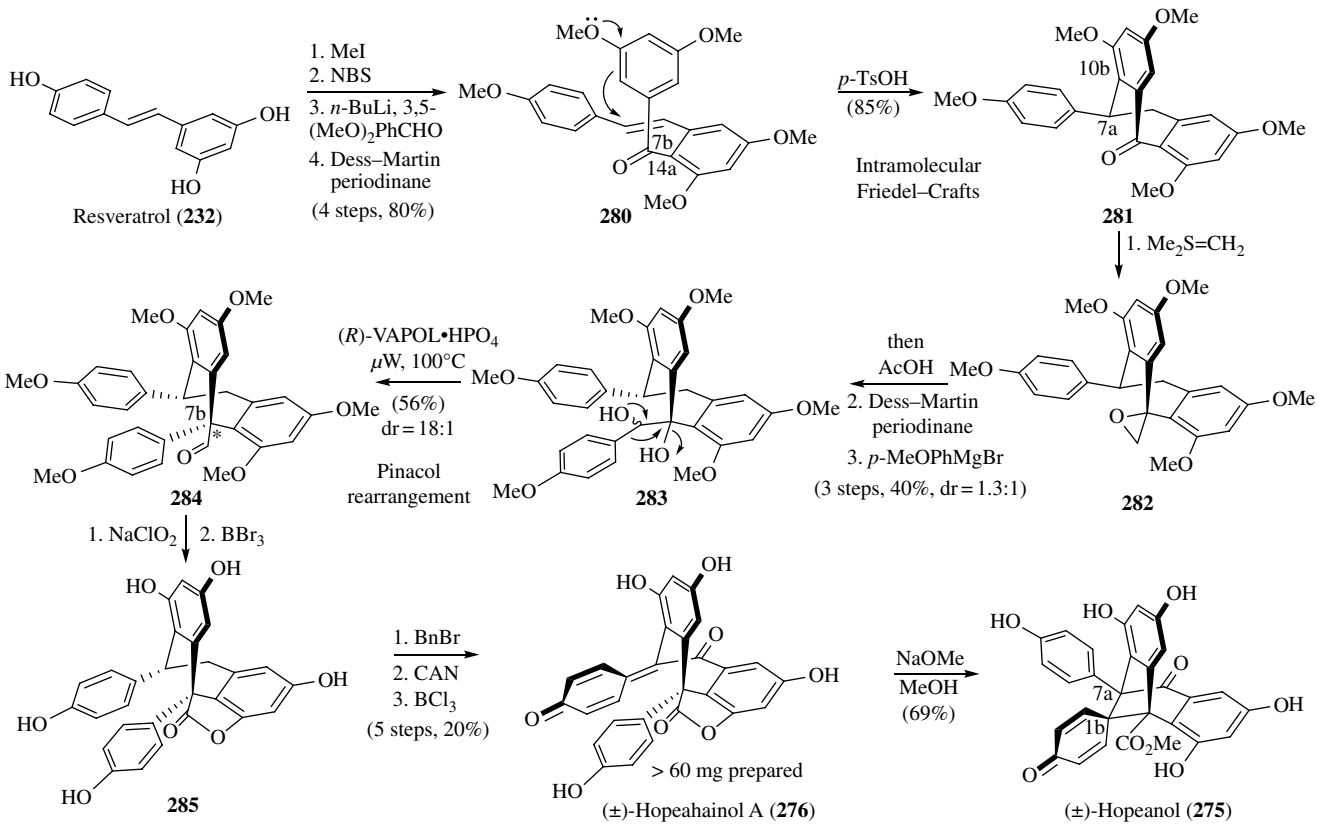



**SCHEME 10.52** Programmable synthesis of ampelopsin H based on brominated pallidol (**271**).




**SCHEME 10.53** Structures of hopeanol and hopeahainol A and their biosynthesis hypothesis.

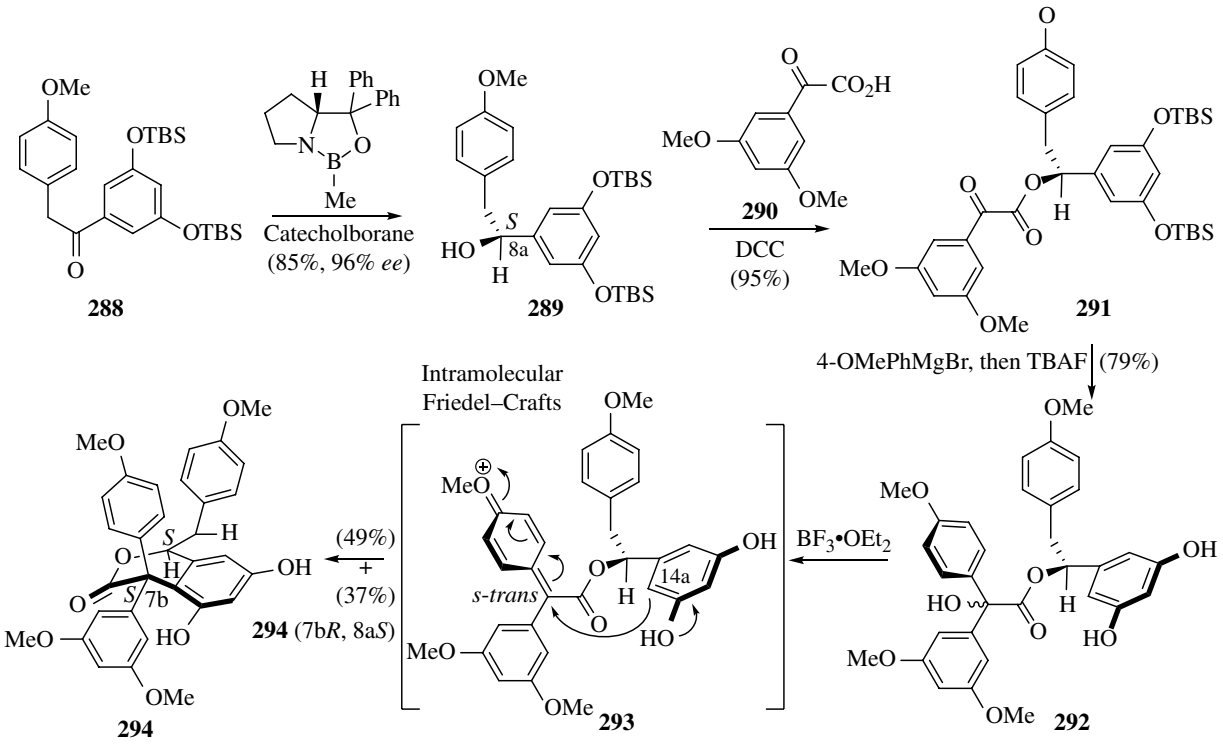
whereas hopeahainol A (**276**) exhibited inhibitory activity against acetylcholinesterase (AChE), which can degrade acetylcholine to its inactive metabolite choline and therefore has emerged as a promising target for the management of Alzheimer's disease (AD). In addition, hopeahainol A (**276**) demonstrated the $IC_{50}$ value of 4.33 μM that is comparable to that of huperzine A, a presently exploited drug for the treatment of AD. Their molecular structures and relative configurations were elucidated through extensive analysis of the spectroscopic data and single-crystal X-ray spectroscopy of permethylated derivative of **276**, and the absolute configuration of C7b in **276** had been assigned as *S* by computational methods [105b]. Their plausible biogenetic pathway was supposed to start from oxidative coupling of two resveratrol monomers through radical intermediate **277**, and both C7a—C10b and C14a—C7b bonds within the architecture **278** could be forged. The subsequent oxidation of the two benzyl hydroxyl groups would generate radical species **279**, where radical can recombine and the migration of ring C would next occur with the formation of C7a—C1b and C7b—C1b bonds, eventually leading to hopeanol (**275**) upon further oxidation of C8b and methyl esterification of the resulting carboxylic acid. Inspired by this migration event for the efficient formation of C7b quaternary carbon center, Snyder and coworkers [106] devised an elegant Pinacol rearrangement as a key step for their biomimetic synthesis of




**SCHEME 10.54** Snyder's biomimetic synthesis of racemic hopeahainol A and hopeanol.

racemic hopeahainol A (**276**). However, original proposed biosynthetic transformation from hopeanol (**275**) to hopeahainol A (**276**) did not work in the lab, and instead the reversed conversion from **276** to **275** proceeded smoothly upon the treatment with a base, as demonstrated in the first syntheses of hopeanol to hopeahainol A in their racemic forms by Nicolaou and Chen in 2009 [107a].

Snyder's biomimetic synthesis toward hopeahainol A (**276**) began with commercially available resveratrol, and diaryl ketone **280** could be obtained in 80% overall yield with the construction of C7b─C14a bond (Scheme 10.54) [106]. The secondary strategic bond (C7a─C10b) was established by TsOH-induced intramolecular Friedel–Crafts alkylation, affording to dibenzocycloheptanone **281** in 85% yield. After some unsuccessful attempts on functionalization of the ketone carbonyl group, they found that the reaction sequence from **281** to **283** via intermediacy epoxide **282** was rewarded. This was accomplished, through a stereoselective Corey–Chaykovsky epoxidation, followed by an AcOH-mediated ring opening of the resulting labile epoxide and oxidation by Dess–Martin periodinate. The generated α-hydroxyaldehyde was attacked by *para*-methoxyphenylmagnesium bromide, leading to the key diols **283** as a mixture of two separable diastereomers (dr = 1.3:1) in 40% overall yield. With the precursors **283** in hand, the critical Pinacol rearrangement was investigated. Pleasingly, many Brønsted and Lewis acids can promote the expected migration of *para*-methoxyphenyl group, but the yield and diastereoselectivity of this cascade were moderate. The chiral phosphoric acid was proved to a solution to this issue, even for slow-reacting minor diol diastereomer. Specifically, when the mixture **283** was stirred with one equivalent of (*R*) or (*S*)-Vapol·$HPO_4$ in chloroform at 100°C under microwave irradiation for 1 h, the neopentyl aldehyde **284** was indeed produced in 56% yield and 18:1 diastereocontrol in favor of the desired stereochemistry of quaternary C7b center. The final stages of this route were focused on the formation of γ-lactone and the pendant regioselective oxidation of the *para*-substituted aromatic ring. Thus, this sterically hindered aldehyde was converted into a carboxylic acid followed by the treatment of $BBr_3$, delivering **285**. The remaining ketone located at C8a was able to be introduced only with excess of ceric ammonium nitrate (CAN) on its pentabenzylated derivative. The resulting tetrabenzylated hopeahainol A was deprotected with $BCl_3$ to afford hopeahainol A (**276**) eventually in 20% overall yield. The hopeanol (**275**) was next obtained in 69% yield upon exposure of **276** to one equivalent NaOMe in MeOH at room temperature. This facile transformation could be attributed to the subtle conformation change after rupture of γ-lactone ring within **276**, that is, the



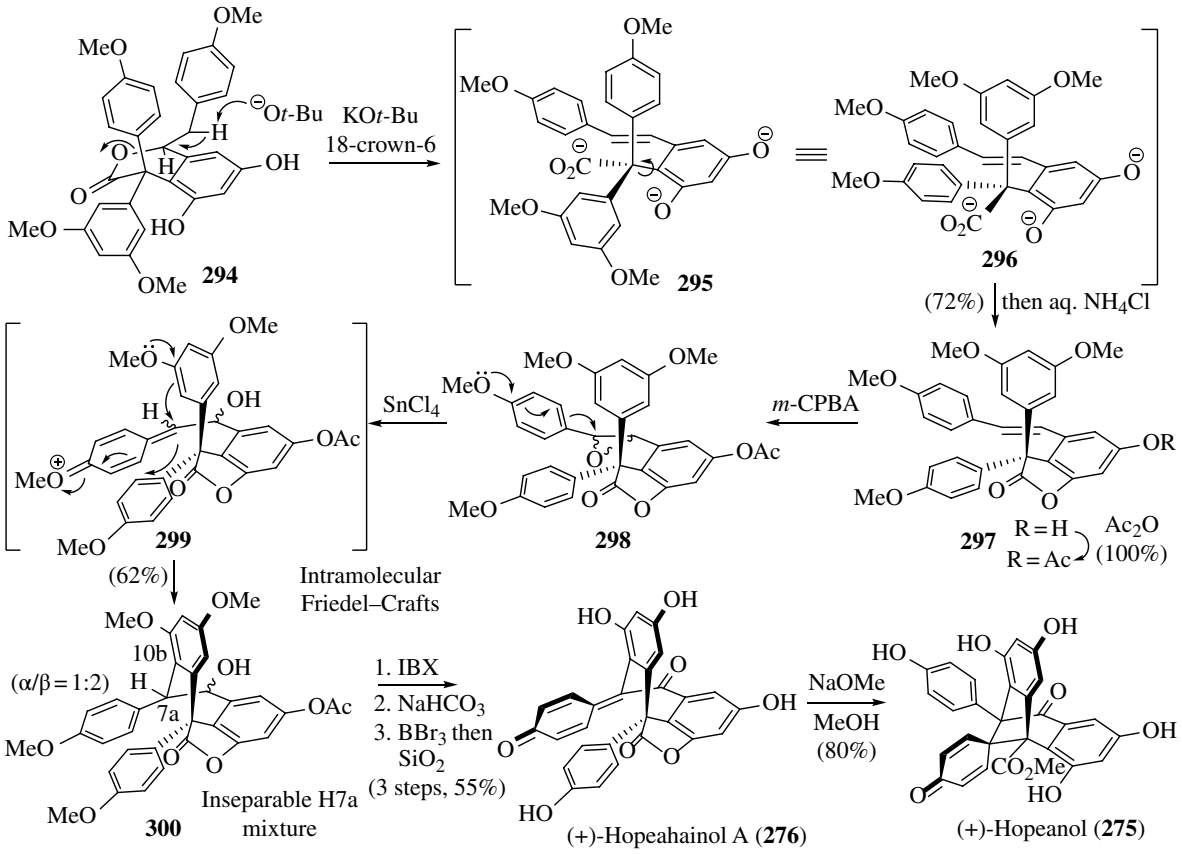

**SCHEME 10.55** Synthesis of δ-lactone **294** bearing C7b(*S*) stereocenter.

resulting flexible conformation makes C7a and C1b proximal to allow the establishment of the last strategic bond.

Snyder's total synthesis had some appealing elements: (i) it is redox economic; (ii) the route to hopeahainol A (**276**) is nine steps long from easily available **281** with the 4% overall yield; (iii) it has potential for scalable synthesis [108] since they had prepared over 60 mg of **276** along with 180 mg of its benzyl-protected precursor so far; (iv) it has a substrate- and site-specific oxidation chemistry; and (v) it is a biomimetic synthesis given the constructions of C7b—C14a, C7a—C10b, and C1b—C7a(b) bonds and meanwhile possesses biogenetic relevance with other resveratrol-derived dimers such as heimiol A (**286**) and hopeahainol D (**287**), which will be discussed in Schemes 10.57 and 10.58.

Nicolaou and coworkers completed the enantioselective synthesis of these two natural products molecules through a short and equally efficient route (12 steps from commercially available material with the 4% overall yield) involving a series of cascade reactions and novel skeletal rearrangements [107b]. This unique route commenced with a CBS asymmetric reduction of ketone **288** that is easily generated from the resveratrol monomer (Scheme 10.55). The chiral benzylic alcohol **289** was obtained in 85% yield and 95% *ee* in the presence of one equivalent of catecholborane and catalytic amount of (*R*)-(+)-2-methyl-CBS-oxazaborolidine. This newly formed C8a center would be served as a chiral source by which other stereocenters within the architecture of **275** could be generated successively through its induction. The esterification of the aforementioned optical secondary alcohol **289** with α-ketoacid **290** mediated by DCC gave α-ketoester **291** in almost quantitative yield. The addition of 4-methoxyphenylmagnesium bromide to **291** afforded diphenolic hydroxyester **292** as an inconsequential mixture in 79% yield after desilylation of the resulting bis-OTBS intermediate. Notably, the assembly of the resveratrol dimeric derivative **292** already bears all the necessary carbons for the advancement to the final targets; thus the stage was set for the establishment of the strategic C7b—C14a bond. The subjection of **292** into $BF_3{\cdot}Et_2O$ in $CH_2Cl_2$ at room temperature furnished six-membered ring lactone **294** in 49% yield, presumably through *s-trans* transition state **293**. This intramolecular Friedel–Crafts alkylation also gave another diastereomeric product **294** (7b*R*, 8a*S*) in 37% yield, which resulted from the attack of phenol on the *p*-quinone methide via energetically somewhat high *s-cis* transition state. Notably, X-ray crystallographic analysis of *ent*-**294** that was analogously prepared by using the antipodal CBS catalyst through the route outlined in the Scheme 10.55 confirmed its structure.

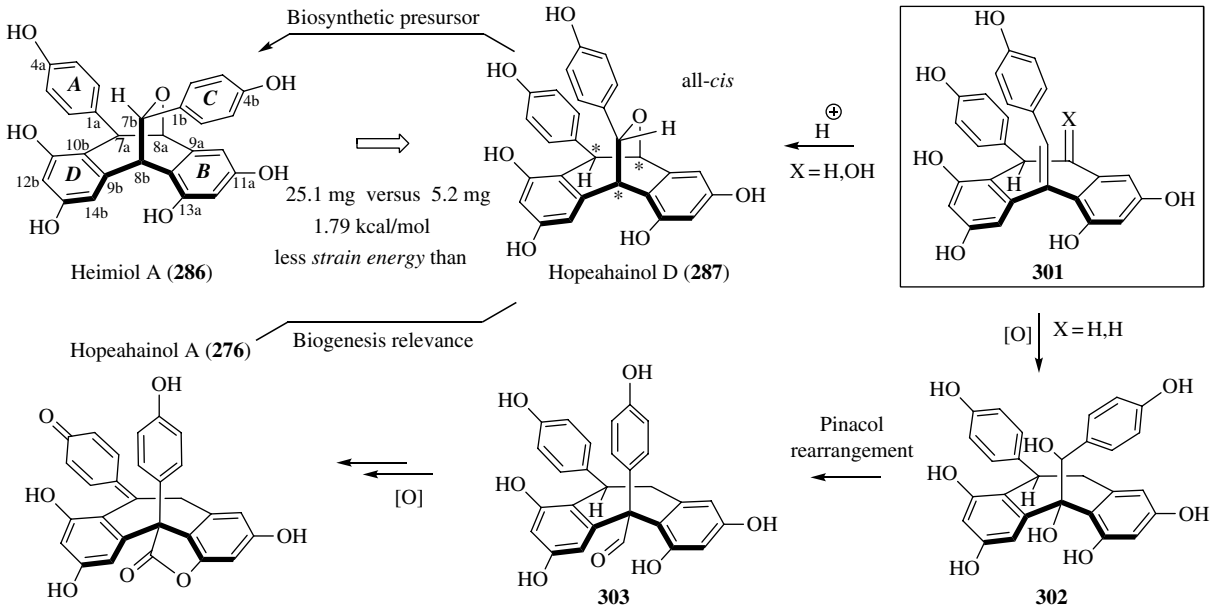
With chiral intermediate **294** structurally secured, its advancement to the hopeahainol A (**276**) and hopeanol (**275**) was undertaken, as shown in Scheme 10.56. Exposure of δ-lactone **294** to excess of KO*t*Bu and 18-crown-6 in THF led, upon quenching with aqueous $NH_4Cl$ solution, to




**SCHEME 10.56** Nicolaou and Chen's total synthesis of (+)-hopeahainol A and (+)-hopeanol.

olefinic γ-lactone **297** bearing the sole quaternary stereocenter C7b in 72% yield. This cascade was thought to proceed through anion formation, β-elimination, and ring closure of trianion **296** generated from the rotation of the C7b─C14a bond within conformer **295**. The remaining phenolic group in stilbene γ-lactone **297** was then protected as its acetate in quantitative yield, and this resulting olefinic product was subjected to epoxidation with *m*-CPBA to afford **298** as a mixture of diastereomers (ca. 1:1). The construction of the key the strategic C7a─C10b bond was realized through another cascade, which is made of epoxide ring opening promoted by $SnCl_4$ and intramolecular attack of the generated *p*-quinone methide **299** by 3,5-dimethoxyphenyl group, affording **300** in 62% yield. The major diastereoisomer of **300** was successfully elaborated into (+)-hopeahainol A (**39**) according to carefully chosen oxidation and deprotection conditions. In contrast to the proposed biosynthetic relationship between **275** and **276** by isolation chemists [105b], only conversion of (+)-hopeahainol A (**276**) to (+)-hopeanol (**275**) could be realized under alkaline methanolysis condition. It is noteworthy that the aforementioned sequence from **294** also served to synthesize the unnatural antipodes of these two natural products from **294** (7b*R*, 8a*S*) or *ent*-**294**, therefore constituting an enantiodivergent synthesis enabled by some reagent-controlled cascades during the Nicolaou and Chen's campaign.

Heimiol A (**286**), which is a resveratrol dimer with a unique [3.2.2] oxabicycle skeleton that is bearing four continuous chiral centers and possessing some antioxidant activity, was isolated from the heartwood of *Neobalanocarpus heimii* in 2001 by Weber and coworkers [109a]. Eight years later, Tan's team reisolated 25.1 mg of the same compound but from the stem wood of *Hopea hainanensis* [109b] along with 5.2 mg of hopeahainol D (**287**) that structurally differs from **296** only in the orientation of ring C at C7b (Scheme 10.57). Given the relative amount of **286** and **287** obtained by the isolation team and the indicated strain difference according to subsequent calculations with B3LYP functional in conjunction with the 6-31G(d) basis set by Snyder coworkers [110], hopeahainol D (**287**) was proposed as a biosynthetic precursor to heimiol A (**286**). Furthermore, Snyder anticipated that hopeahainol D (**287**) could be generated from **301** by a proton cyclization event, and this type of intermediates with a seven-membered ring could be served as a common precursor en route (via **302** and **303**) to the hopeahainol A (**276**) following the synthetic steps as demonstrated in Scheme 10.54.

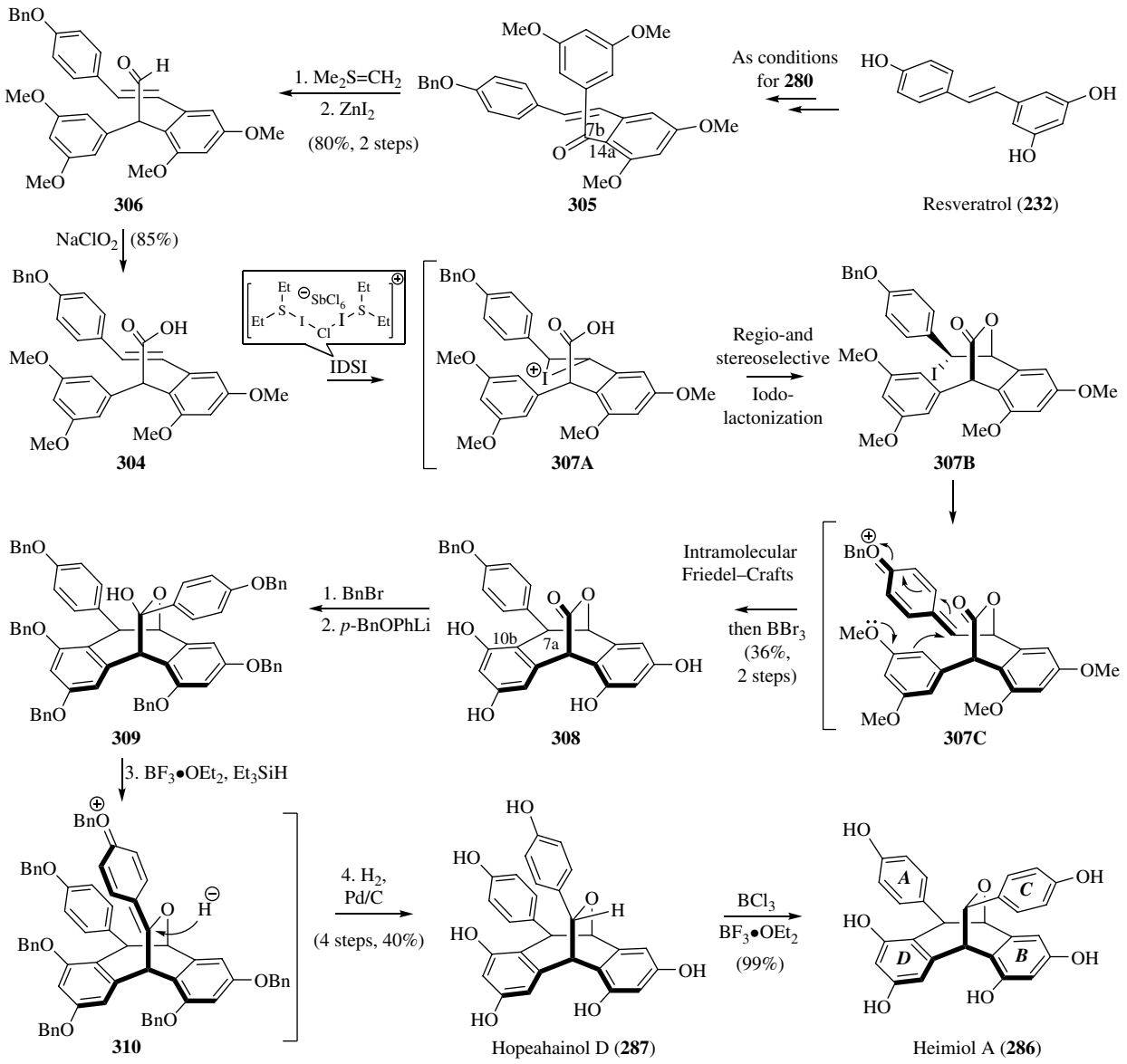



**SCHEME 10.57** Structures of heimiol A and hopeahainol D and their biosynthesis hypothesis.

Though very appealing, however, the aforementioned idea was not easily implemented in the lab. The synthetic challenge of these two molecules comes from arraying two aromatic rings (A and C) and a bridging oxygen atom on the same side of a compact and constrained seven-membered carbocyclic core. The lessons learned from the facile construction of major resveratrol oligomers with a *trans* disposition of groups cannot guide the access of more unique *cis*-disposed frameworks of hopeahainol D (**287**) and heimiol A (**286**). Eventually, Snyder invented an iodolactonization/Friedel–Crafts cascade to establish the whole [3.2.2] oxabicycle with the requisite all-*cis* stereochemistry from an acyclic precursor **304**.

As shown in Scheme 10.58, the diaryl ketone **305** with a privileged scaffold that has demonstrated its value during the synthetic efforts for the related family members of resveratrol oligomers was chosen as the starting material following the standard procedure developed by Snyder's laboratory. One-carbon homologation employing Corey–Chaykovsky epoxidation [101] and $ZnI_2$-mediated rearrangement [102] provided aldehyde **306** in 80% yield. With the carboxylic acid **304** generated by Pinnick oxidation in hand, the designed cascade (**304**→methyl ether of **308**) was then investigated. Initial results were disappointed since over- and/or nonselective halogenations predominated under some routine conditions such as $I_2$, NIS, etc. After extensive optimization, they found that $(Et_2SI)_2Cl{\cdot}SbCl_6$ (IDSI), a unique iodonium source developed by themselves [111], can suppress the normal electrophilic aromatic substitution reactions with the electron-rich systems. In this way, the desired bicyclic lactone with all *cis*-stereochemistry could be produced in one-pot reaction, and notably the whole cascade (**307A**→**307B**→**307C**) was smoothly completed at 25°C in only 2 min with the sequential formation of both C8a─O and C7a─C10b bonds. Upon this critical step accomplished, the methyl ethers were then removed by exposure to $BBr_3$, giving tetraphenol **308** in 36% overall yield. Reprotection of **308** with benzyl bromide under basic condition followed by the nucleophilic addition of the resulting pentabenzyl lactone with *para*-benzoxyphenyl lithium afforded the tertiary alcohol **309** as a single stereoisomer. The excellent diastereoselectivity during the incorporation of C ring could be attributed to superior diastereotopic discrimination of the bridged lactone carbonyl group to the bulk nucleophile. The same trend was also observed in the subsequent reductive deoxygenation reaction to **310**, even with the smallest hydride, and the hydrogenation of the resulting perbenzylated hopeahainol D under catalytic Pd/C furnished racemic hopeahainol D (**287**) in 40% overall yield. Finally, epimerization of C7b stereocenter within **287** through a retro-Friedel–Crafts/Friedel–Crafts reaction proceeded under the combination condition of $BF_3{\cdot}Et_2O$ and $BCl_3$, and the thermodynamic stable heimiol A (**286**) was indeed obtained in almost quantitative yield, supporting their biogenetic synthesis hypothesis at the outset.

There are some noteworthy highlights in the conquest of hopeahainol D (**287**) and heimiol A (**286**) by Snyder and coworkers: (i) it is fully stereocontrolled and concise with only 9 and 10 operations from conveniently available **305**; (ii) a potential biogenetic relationship between **287** and **286** is established first and therefore constitutes a rare example using thermodynamic strain energy to dictate synthetic plan; (iii) a reagent-controlled cascade for the construction of the entire [3.2.2] oxabicycle with a unique all-*cis* stereochemistry of substituents from an acyclic precursor is developed;




**SCHEME 10.58** Snyder's total synthesis of hopeahainol D and heimiol A.

and (iv) it is also a DOS [104] since the strategy for **287** and **286** has already been assessed to other relevant dimeric resveratrol analogs even with a highly strained [3.2.1] bicycle core.

## 10.6 CONCLUSION

Despite significant achievements in method development, the application of C($sp^3$)─H functionalization logic to the synthesis of structurally complex natural products is still in its infancy compared to that of the more "classic" Friedel–Crafts reactions [C($sp^2$)─H alkylation and acylation]. The innate C($sp^3$)─H functionalizations instead of usual strategy utilizing a removable/modifiable or traceless directing group would be a promising direction in the pursuit of "ideal synthesis." Highly enantioselective C($sp^3$)─H functionalization either on the intermolecular or intramolecular occasion remains a formidable challenge in the near future.

## REFERENCES

1. (a) S. Jiang, G. Singh, *Tetrahedron* 1998, **54**, 4697; (b) M. M. Campbell, M. Sainsbury, P. A. Searle, *Synthesis* 1993, 179; (c) B. A. Bohm, *Chem. Rev.* 1965, **65**, 435.
2. J. F. Eykman, *Recl. Tray. Chim. Pays-Bas* 1885, **4**, 32.
3. (a) P. Karrer, K. P. Link, *Helv. Chim. Acta* 1927, **10**, 794; (b) H. O. L. Fischer, G. Dangschat, *Ber. Deutsch. Chem. Ges.* 1932, **65**, 1009; (c) H. O. L. Fischer, G. Dangschat, *Helv. Chim. Acta* 1934, **17**, 1196; (d) H. O. L. Fischer, G. Dangschat, *Helv.*

*Chim. Acta* 1934, **17**, 1200; (e) H. O. L. Fischer, G. Dangschat, *Helv. Chim. Acta* 1935, **18**, 1204; (f) H. O. L. Fischer, G. Dangschat, *Helv. Chim. Acta* 1935, **18**, 1206; (g) H. O. L. Fischer, G. Dangschat, *Helv. Chim. Acta* 1937, **20**, 705; (h) K. Freudenberg, H. Meisenheimer, J. T. Lane, E. Plankenhorn, *Liebigs Ann. Chem.* 1940, **543**, 162.

4. (a) H. G. Floss, *Nat. Prod. Rep.* 1997, **14**, 433; (b) P. M. Dewick, *Nat. Prod. Rep.* 1998, **15**, 17; (c) A. R. Knaggs, *Nat. Prod. Rep.* 1999, **16**, 525; (d) A. R. Knaggs, *Nat. Prod. Rep.* 2000, **17**, 269; (e) P. M. Dewick, *Medicinal Natural Products: A Biosynthetic Approach*, John Wiley & Sons Ltd, West Sussex (2002), p. 121.
5. (a) B. D. Davis, *Adv. Enzymol.* 1955, **16**, 287; (b) D. B. Sprinson, *Adv. Carbohydr. Chem.* 1961, **15**, 235; (c) F. Gibson, J. Pittard, *Bact. Rev.* 1968, **32**, 468.
6. G. A. Sprenger, in *Amino Acids Biosynthesis—Pathways, Regulations and Metabolic Engineering* (Ed.: V. F. Wendisch), Springer-Verlag, Berlin/Heidelberg (2006), p. 93.
7. H. Maeda, H. Yoo, N. Dudareva, *Nat. Chem. Biol.* 2011, **7**, 19.
8. (a) L. B. Davin, N. G. Lewis, *Phytochem. Rev.* 2003, **2**, 257; (b) T. Umezawa, *Phytochem. Rev.* 2003, **2**, 371; (c) L. B. Davin, N. G. Lewis, *Curr. Opin. Biotechnol.* 2005, **16**, 398.
9. L. Poppe, J. Rétey, *Angew. Chem.* 2005, **117**, 3734; *Angew. Chem. Int. Ed.* 2005, **44**, 3668.
10. (a) T. da Silva, L. M. X. Lopes, *Phytochemistry* 2004, **65**, 751; (b) G. B. Messiano, T. da Silva, I. R. Nascimento, L. M. X. Lopes, *Phytochemistry* 2009, **70**, 590.
11. For its biosynthesis, see: T. Koeduka, E. Fridman, D. R. Gang, D. G. Vassao, B. L. Jackson, C. M. Kish, I. Orlova, S. M. Spassova, N. G. Lewis, J. P. Noel, T. J. Baiga, N. Dudareva, E. Pichersky, *Proc. Natl. Acad. Sci. U.S.A.* 2006, **103**, 10128.
12. L. B. Davin, H.-B. Wang, A. L. Crowell, D. L. Bedgar, D. M. Martin, S. Sarkanen, N. G. Lewis, *Science* 1997, **275**, 362.
13. (a) Z.-Q. Xia, M. A. Costa, J. Proctor, L. B. Davin, N. G. Lewis, *Phytochemistry* 2000, **55**, 537; (b) A. J. Broomhead, M. M. A. Rahman, P. M. Dewick, D. E. Jackson, J. A. Lucas, *Phytochemistry* 1991, **30**, 1489.
14. For some leading reviews, see: (a) *Review of C–H Activation. Topics in Current Chemistry*, **292**. (Ed.: J.-Q. Yu, Z. Shi), Springer-Verlag, Berlin/Heidelberg (2010); (b) C. Jia, T. Kitamura, Y. Fujiwara, *Acc. Chem. Res.* 2001, **34**, 633; (c) X. Chen, K. M. Engle, D.-H. Wang, J.-Q. Yu, *Angew. Chem.* 2009, **121**, 5196; *Angew. Chem. Int. Ed.* 2009, **48**, 5094; (d) R. Giri, B.-F. Shi, K. M. Engle, N. Maugel, J.-Q. Yu, *Chem. Soc. Rev.* 2009, **38**, 3242; (e) T. W. Lyons, M. S. Sanford, *Chem. Rev.* 2010, **100**, 1147; (f) T. Brueckl, R. D. Baxter, Y. Ishihara, P. S. Baran, *Acc. Chem. Res.* 2012, **45**, 826.
15. O. Daugulis, H. Q. Do, D. Shabashov, *Acc. Chem. Res.* 2009, **42**, 1074.
16. K. M. Engle, T.-S. Mei, M. Wasa, J.-Q. Yu, *Acc. Chem. Res.* 2012, **45**, 788.
17. G. Rouquet, N. Chatani, *Angew. Chem.* 2013, **125**, 11942; *Angew. Chem. Int. Ed.* 2013, **52**, 11726.
18. (a) D. Shabashov, O. Daugulis, *Org. Lett.* 2005, **7**, 3657; (b) V. G. Zaitsev, D. Shabashov, O. Daugulis, *J. Am. Chem. Soc.* 2005, **127**, 13154; (c) D. Shabashov, O. Daugulis, *J. Am. Chem. Soc.* 2010, **132**, 3965.
19. B. V. S. Reddy, L. R. Reddy, E. J. Corey, *Org. Lett.* 2006, **8**, 3391.
20. L. D. Tran, O. Daugulis, *Angew. Chem.* 2012, **124**, 5278; *Angew. Chem. Int. Ed.* 2012, **51**, 5188.
21. Q. Zhang, K. Chen, W. Rao, Y. Zhang, F.-J. Chen, B.-F. Shi, *Angew. Chem.* 2013, **125**, 13833; *Angew. Chem. Int. Ed.* 2013, **52**, 13588.
22. J. He, S. Li, Y. Deng, H. Fu, B. N. Laforteza, J. E. Spangler, A. Homs, J.-Q. Yu, *Science* 2014, **343**, 1216.
23. G. He, G. Chen, *Angew. Chem.* 2011, **123**, 5298; *Angew. Chem. Int. Ed.* 2011, **50**, 5192.
24. N. Rodríguez, J. A. Romero-Revilla, M. Á. Fernández-Ibáñez, J. C. Carretero, *Chem. Sci.* 2013, **4**, 175.
25. K. S. L. Chan, M. Wasa, L. Chu, B. N. Laforteza, M. Miura, J.-Q. Yu, *Nat. Chem.* 2014, **6**, 146.
26. S. Aspin, A.-S. Goutierre, P. Larini, R. Jazzar, O. Baudoin, *Angew. Chem.* 2012, **124**, 10966; *Angew. Chem. Int. Ed.* 2012, **51**, 10808.
27. (a) J. E. Ney, J. P. Wolfe, *J. Am. Chem. Soc.* 2005, **127**, 8644; (b) B. J. Stokes, S. M. Opra, M. S. Sigman, *J. Am. Chem. Soc.* 2012, **134**, 11408.
28. For some leading reviews, see: (a) K. Godula, D. Sames, *Science* 2006, **312**, 67; (b) H. M. L. Davies, J. R. Manning, *Nature* 2008, **451**, 417; (c) L. McMurray, F. O'Hara, M. J. Gaunt, *Chem. Soc. Rev.* 2011, **40**, 1885; (d) W. R. Gutekunst, P. S. Baran, *Chem. Soc. Rev.* 2011, **40**, 1976; (e) J. Yamaguchi, A. D. Yamaguchi, K. Itami, *Angew. Chem.* 2012, **124**, 9092; *Angew. Chem. Int. Ed.* 2012, **51**, 8960; (f) D. Y. K. Chen, S. W. Youn, *Chem. Eur. J.* 2012, **18**, 9452; (g) J. Wencel-Delod, F. Glorius, *Nat. Chem.* 2013, **5**, 369.
29. Y. Feng, G. Chen, *Angew. Chem.* 2010, **122**, 970; *Angew. Chem. Int. Ed.* 2010, **49**, 958.
30. (a) C. Friedel, J. M. Crafts, *J. Chem. Soc*. 1877, **32**, 725; (b) C. Friedel, J. M. Crafts, *Bull. Soc. Chim. Fr.* 1877, **27**, 530; (c) J. M. Crafts, E. Ador, *Ber.* 1877, **10**, 2173; (d) J. M. Crafts, E. Ador, *Bull. Soc. Chim. Fr.* 1880, **10**, 531.
31. (a) T. B. Poulsen, K. A. Jørgensen, *Chem. Rev.* 2008, **108**, 2903; (b) S.-L. You, Q. Cai, M. Zeng, *Chem. Soc. Rev.* 2009, **38**, 2190; (c) M. Bandini, A. Umani-Ronchi, *Catalytic Asymmetric Friedel–Crafts Alkylation*, Wiley-VCH, Weinheim, (2009).
32. (a) N. O. Calloway, *Chem. Rev.* 1935, **17**, 327; (b) C. C. Price, *Org. React.* 1946, 1; (c) E. Berliner, *Org. React.* 1949, 229; (d) P. H. Calloway, *Chem. Rev.* 1955, **55**, 229; (e) G. A. Olah, *Friedel–Crafts Chemistry*, John Wiley & Sons, New York (1973); (f) R. A. Roberts, A. A. Khalaf, *Friedel–Crafts Alkylation Chemistry: A Century of Discovery*, Wiley-Interscience, New York (1984); (g) G. Sartori, R. Maggi, *Chem. Rev.* 2006, **106**, 1077; (h) G. Sartori, R. Maggi, *Chem. Rev.* 2011, **111**, PR181.
33. (a) H.-G. Franck, *Industrial Aromatic Chemistry*, Springer-Verlag, Berlin (1988); (b) M. Rueping, B. J. Nachtsheim, *Beil. J. Org. Chem.* 2010, **6**, doi:10.3762/bjoc.6.6.
34. (a) H. C. Brown, M. Grayson, *J. Am. Chem. Soc.* 1953, **75**, 6285; (b) H. C. Brown, H. Jungk, *J. Am. Chem. Soc.* 1955, **77**, 5584.

35. (a) G. A. Olah, *J. Am. Chem. Soc.* 1972, **94**, 808; (b) G. A. Olah, K. K. Laali, Q. Wang, G. K. S. Prakash, *Onium Ions*, Wiley: Hoboken/New York, (1998); (c) R. R. Naredla, D. A. Klumpp, *Chem. Rev.* 2013, **113**, 6905.
36. (a) G. A. Olah, S. Kuhn, A. Pavláth, *Nature* 1956, **178**, 693; (b) G. A. Olah, S. Kuhn, *Nature* 1956, **178**, 1344.
37. (a) M. Niggemann, M. J. Meel, *Angew. Chem.* 2010, **122**, 3761; *Angew. Chem. Int. Ed.* 2010, **49**, 3684; (b) J.-M. Begouin, M. Niggemann, *Chem.-Eur. J.* 2013, **19**, 8030.
38. S. Antoniotti, V. Dalla, E. Duñach, *Angew. Chem.* 2010, **122**, 8032; *Angew. Chem. Int. Ed.* 2010, **49**, 7860.
39. J.-M. Begouin, F. Capitta, X. Wu, M. Niggemann, *Org. Lett.* 2013, **15**, 1370.
40. L. R. Jefferies, S. P. Cook, *Org. Lett.* 2014, **16**, 2026.
41. (a) F. Mühlthau, O. Schuster, T. Bach, *J. Am. Chem. Soc.* 2005, **127**, 9348; (b) F. Mühlthau, D. Stadler, A. Goeppert, G. A. Olah, G. K. S. Prakash, T. Bach, *J. Am. Chem. Soc.* 2006, **128**, 9668.
42. K. B. Jensen, J. Thorhauge, R. G. Hazell, K. A. Jørgensen, *Angew. Chem.* 2001, **113**, 164; *Angew. Chem. Int. Ed.* 2001, **40**, 160.
43. For leading reviews, see:(a) J. S. Johnson, D. A. Evans, *Acc. Chem. Res.* 2000, **33**, 325; (b) D. A. Evans, T. Rovis, J. S. Johnson, *Pure Appl. Chem.* 1999, **71**, 1407.
44. D. A. Evans, K. R. Fandrick, H.-J. Song, K. A. Scheidt, R. Xu, *J. Am. Chem. Soc.* 2007, **129**, 10029.
45. (a) N. A. Paras, D. W. C. MacMillan, *J. Am. Chem. Soc.* 2001, **123**, 4370; (b) J. F. Autin, D. W. C. MacMillan, *J. Am. Chem. Soc.* 2002, **124**, 1172; (c) N. A. Paras, D. W. C. MacMillan, *J. Am. Chem. Soc.* 2002, **124**, 7894.
46. (a) M. E. Kieffer, L. M. Repka, S. E. Reisman, *J. Am. Chem. Soc.* 2012, **134**, 5131; for a similar report, see: (b) N. Fu, L. Zhang, J. Li, S. Luo, J.-P. Chen, *Angew. Chem.* 2011, **123**, 11653; *Angew. Chem. Int. Ed.* 2011, **50**, 11451.
47. For a review of combined acid catalysis, see: H. Yamamoto, K. Futatsugi, *Angew. Chem.* 2005, **117**, 1958; *Angew. Chem. Int. Ed.* 2005, **44**, 1924.
48. (a) M. Terada, K. Sorimachi, *J. Am. Chem. Soc.* 2007, **129**, 292; (b) D. Uraguchi, K. Sorimachi, M. Terada, *J. Am. Chem. Soc.* 2004, **126**, 11804.
49. (a) S. J. Connon, *Angew. Chem.* 2006, **118**, 4013; *Angew. Chem. Int. Ed.* 2006, **45**, 3909; (b) T. Akiyama, *Chem. Rev.* 2007, **107**, 5744.
50. Q. Kang, Z.-A. Zhao, S.-L. You, *J. Am. Chem. Soc.* 2007, **129**, 1484.
51. Y.-Q. Wang, J. Song, R. Hong, H. Li, L. Deng, *J. Am. Chem. Soc.* 2006, **128**, 8156.
52. (a) K. C. Nicolaou, R. Reingruber, D. Sarlah, S. Bräse, *J. Am. Chem. Soc.* 2009, **131**, 2086; for the correction, see: (b) *J. Am. Chem. Soc.* 2009, **131**, 6640; for another independent studies, see: (c) J. C. Conrad, J. Kong, B. N. Laforteza, D. W. C. MacMillan, *J. Am. Chem. Soc.* 2009, **131**, 11640; for computational studies, see: (d) J. M. Um, O. Gutierrez, F. Schoenebeck, K. N. Houk, D. W. C. MacMillan, *J. Am. Chem. Soc.* 2010, **132**, 6001.
53. (a) S. Malhotra, S. Koul, S. Taheja, P. Pushpangadan, K. Dhar, *Phytochemistry* 1990, **29**, 2733; (b) R. N. Mahindru, S. C. Taneja, K. L. Dhar, R. T. Brown, *Phytochemistry* 1993, **32**, 1073.
54. J. Rhu, H. Son, S. Lee, D. Sohn, *Bioorg. Med. Chem. Lett.* 2002, **12**, 649.
55. Q. Wang, C. Terreaux, A. Marston, R. Tan, K. Hostettmann, *Phytochemistry* 2000, **54**, 909.
56. M. Riener, D. A. Nicewicz, *Chem. Sci.* 2013, **4**, 2625.
57. For the previous synthesis using ultraviolet light in 15% yield, see: S. Yamamura, M. Niwa, M. Nonoyama, Y. Terada, *Tetrahedron Lett.* 1978, **19**, 4891.
58. (a) F.-P. Lee, Y.-C. Chen, J.-J. Chen, I.-L. Tsai, I.-S. Chen, *Helv. Chim. Acta* 2004, **87**, 463; (b) I.-L. Tsai, F.-P. Lee, C.-C. Wu, C.-Y. Duh, T. Ishikawa, J.-J. Chen, Y.-C. Chen, H. Seki, I.-S. Chen, *Planta Med.* 2005, **71**, 535.
59. W. R. Gutekunst, P. S. Baran, *J. Am. Chem. Soc.* 2011, **133**, 19076.
60. H. Javaheripour, D. C. Neckers, *J. Am. Chem. Soc.* 1977, **42**, 1844.
61. D. A. Evans, P. H. Carter, C. J. Dinsmore, J. C. Barrow, J. L. Katz, D. W. Kung, *Tetrahedron Lett.* 1997, **38**, 4535.
62. (a) W. R. Gutekunst, R. Gianatassio, P. S. Baran, *Angew. Chem.* 2012, **124**, 7625; *Angew. Chem. Int. Ed.* 2012, **51**, 7507; (b) W. R. Gutekunst, P. S. Baran, *J. Org. Chem.* 2014, **79**, 2430.
63. (a) Y. Fujiwara, K. Naithou, T. Miyazaki, K. Hashimoto, K. Mori, Y. Yamamoto, *Tetrahedron Lett.* 2001, **42**, 2497; (b) S. Tsukamoto, K. Tomise, K. Miyakawa, B. C. Cha, T. Abe, T. Hamada, H. Hirota, T. Ohta, *Bioorg. Med. Chem.* 2002, **10**, 2981.
64. K. Ando, S. Nagaya, Y. Tarumi, *Tetrahedron Lett.* 2009, **50**, 5689.
65. R. Liu, M. Zhang, T. P. Wyche, G. N. Winston-McPherson, T. S. Bugni, W. Tang, *Angew. Chem.* 2012, **124**, 7621; *Angew. Chem. Int. Ed.* 2012, **51**, 7503.
66. C. P. Ting, T. J. Maimone, *Angew. Chem.* 2014, **126**, 3179; *Angew. Chem. Int. Ed.* 2014, **53**, 3115.
67. H. F. Stähelin, A. von Wartburg, *Cancer Res.* 1991, **51**, 5.
68. For a review, see: J. D. Sellars, P. G. Steel, *Eur. J. Org. Chem.* 2007, 3815.
69. E. Akgün, E. M. B. Glinski, K. L. Dhawan, T. Durst, *J. Org. Chem.* 1981, **46**, 2730.
70. W. Choy, H. Yang, *J. Org. Chem.* 1988, **53**, 5796.
71. (a) S.-Y. Zhang, G. He, W. A. Nack, Y. Zhao, Q. Li, G. Chen, *J. Am. Chem. Soc.* 2013, **135**, 2124; (b) K. Chen, F. Hu, S.-Q. Zhang, B.-F. Shi, *Chem. Sci.* 2013, **4**, 3906.
72. (a) J.-J. Zhang, C.-S. Yan, Y. Peng, Z.-B. Luo, X.-B. Xu, Y. W. Wang, *Org. Biomol. Chem.* 2013, **11**, 2498; (b) Y. Peng, Z.-B. Luo, J.-J. Zhang, L. Luo, Y. W. Wang, *Org. Biomol. Chem.* 2013, **11**, 7574.
73. E. E. Anagnostaki, A. L. Zografos, *Chem. Soc. Rev.* 2012, **41**, 5613.
74. For corresponding natural products, see: [cyclogalgravin (**191**)] (a) S. F. Fonseca, L. T. Nielsen, E. A. Ruveda, *Phytochemistry* 1979, **18**, 1703; [kadangustin J (**192**)] (b) X.-M. Gao, J.-X. Pu, S.-X. Huang, L.-M. Yang, H. Huang, W.-L. Xiao, Y.-T. Zheng, H.-D. Sun, *J. Nat. Prod.* 2008, **71**, 558; [galbulin (**194**)] (c) C. K. Hughes, E. Ritchie, *Aust.*

*J. Chem.* 1954, **7**, 104; (d) E. K. Nemethy, R. Lago, D. Hawkins, M. Calvin, *Phytochemistry* 1986, **25**, 959; [isogalbulin (**195**)] (e) A. W. Schrecker, J. L. Hartwell, *J. Am. Chem. Soc.* 1955, **77**, 432; (f) J.-S. Liu, M.-F. Huang, Y.-L. Gao, J. A. Findlay, *Can. J. Chem.* 1981, **59**, 1680; [cagayanin (**197**)] (g) Y.-H. Kuo, R.-E. Wu, *J. Chin. Chem. Soc. (Taipei)* 1985, **32**, 177; (h) Y.-H. Kuo, S.-T. Lin and R.-E. Wu, *Chem. Pharm. Bull.* 1989, **37**, 2310; [8′-*epi*-8-OH-aristoligone (**198**) and 8′-*epi*-aristoligol (**199**)] (i) T. da Silva, L. M. X. Lopes, *Phytochemistry* 2006, **67**, 929.

75. (a) Y. Ueno, K. Chino, M. Watanabe, O. Moriya, M. Okawara, *J. Am. Chem. Soc*. 1982, **104**, 5564; (b) G. Stork, Mook, R., Jr.; S. A. Biller, S. D. Rychnovsky, *J. Am. Chem. Soc.* 1983, **105**, 3741; for reviews, see: (c) G. Stork, *Bull. Chem. Soc. Jpn.* 1988, **61**, 149; (d) G. Stork, *Bull. Soc. Chim. Fr.* 1990, **127**, 675; (e) X. J. Salom-Roig, F. Dénès, P. Renaud, *Synthesis* 2004, 1903.
76. P. A. Grieco, T. Oguri, Y. Yokoyama, *Tetrahedron Lett.* 1978, **19**, 419.
77. (a) D. F. Taber, W. Tian, *J. Org. Chem.* 2008, **73**, 7560; (b) J. R. Butler, C. Wang, J. Bian, J. M. Ready, *J. Am. Chem. Soc.* 2011, **133**, 9956.
78. H. W. Thompson, D. J. Long, *J. Org. Chem.* 1988, **53**, 4201.
79. P. K. Datta, C. Yau, T. S. Hooper, B. L. Yvon, J. L. Charlton, *J. Org. Chem.* 2001, **66**, 8606.
80. (a) F. A. Davis, A. C. Sheppard, B.-C. Chen, M. S. Haque, *J. Am. Chem. Soc.* 1990, **112**, 6679; (b) F. A. Davis, M. C. Weismiller, *J. Org. Chem.* 1990, **55**, 3715.
81. (a) C. E. Rye, D. Barker, *J. Org. Chem.* 2011, **76**, 6636; (b) C. E. Rye, D. Barker, *Synlett* 2009, 3315.
82. (a) T. Tsunoda, O. Sasaki, S. Itô, *Tetrahedron Lett.* 1990, **31**, 727; (b) T. Tsunoda, M. Sakai, O. Sasaki, Y. Sako, Y. Hondo, S. Itô, *Tetrahedron Lett.* 1992, **33**, 1651.
83. N. P. Lopes, M. J. Kato, M. Yoshida, *Phytochemistry* 1999, **51**, 29.
84. M. Miyazawa, H. Kasahara, H. Kameoka, *Nat. Prod. Lett.* 1996, **8**, 25.
85. (a) J. C. T. Reddel, K. E. Lutz, A. B. Diagne, R. J. Thomson, *Angew. Chem.* 2014, **126**, 1419; *Angew. Chem. Int. Ed.* 2014, **53**, 1395; (b) K. E. Lutz, R. J. Thomson, *Angew. Chem.* 2011, **123**, 4529; *Angew. Chem. Int. Ed.* 2011, **50**, 4437.
86. Z. Q. Yang, J. C. Lorenz, Y. Shi, *Tetrahedron Lett.* 1998, **39**, 8621.
87. E. Wenkert, *Acc. Chem. Res.* 1980, **13**, 27.
88. (a) S. Quideau, D. Deffieux, C. Douat-Casassus, L. Pouységu, *Angew. Chem.* 2011, **123**, 610; *Angew. Chem. Int. Ed.* 2011, **50**, 586; (b) S. A. Snyder, in *Biomimetic Organic Synthesis* (Ed.: E. Poupon, B. Nay), Wiley-VCH, Weinheim (2011), p. 695; (c) K. C. Nicolaou, J. C. Chen, *Classics in Total Synthesis III-Further Targets, Strategies, Methods*, Wiley-VCH, Weinheim (2011), p. 566.
89. M. Takaoka, *Proc. Imp. Acad. Tokyo* 1940, **16**, 405.
90. (a) M. Jang, L. Cai, G. O. Udeani, K. V. Slowing, C. F. Thomas, C. W. W. Beecher, H. H. S. Fong, N. R. Farnsworth, A. D. Kinghorn, R. G. Mehta, R. C. Moon, J. M. Pezzuto, *Science* 1997, **275**, 218; (b) J. G. Wood, B. Rogina, S. Lavu, K. Howitz, S. L. Helfand, M. Tatar, D. Sinclair, *Nature* 2004, **430**, 686; for a review, see: (c) F. Orallo, *Curr. Med. Chem.* 2008, **15**, 1887.
91. (a) S. Sotheeswaran, V. Pasupathy, *Phytochemistry* 1993, **32**, 1083; (b) S. Quideau, D. Deffieux, C. Douat-Casassus, L. Pouységu, *Angew. Chem.* 2011, **123**, 610; *Angew. Chem. Int. Ed.* 2011, **50**, 586; (c) C. Rivière, A. D. Pawlus, J.-M. Mérillon, *Nat. Prod. Rep.* 2012, **29**, 1317.
92. J.-R. Dai, Y. F. Hallock, J. H. Cardellina, M. R. Boyd, *J. Nat. Prod.* 1998, **61**, 351.
93. S. A. Snyder, A. M. ElSohly, F. Kontes, *Nat. Prod. Rep.* 2011, **28**, 897.
94. S. S. Velu, I. Buniyamin, L. K. Ching, F. Feroz, I. Noorbatcha, L. C. Gee, K. Awang, I. A. Wahab, J.-F. F. Weber, *Chem. Eur. J.* 2008, **14**, 11376.
95. (a) P. Langcake, R. J. Pryce, *J. Chem. Soc. Chem. Commun.* 1977, 208; (b) M. Sako, H. Hosokawa, T. Ito, M. Iinuma, *J. Org. Chem.* 2004, **69**, 2598; (c) Y. Takaya, K. Terashima, J. Ito, Y.-H. He, M. Tateoka, N. Yamaguchi, M. Niwa, *Tetrahedron* 2005, **61**,10285.
96. (a) W. Li, H. Li, Y. Li, Z. Hou, *Angew. Chem.* 2006, **118**, 7771; *Angew. Chem. Int. Ed.* 2006, **45**, 7609; (b) K. V. Sarkanen, A. F. A. Wallis, *J. Chem. Soc. Perkin Trans.* **1** 1973, 1878.
97. (a) S. A. Snyder, A. L. Zografos, Y. Lin, *Angew. Chem.* 2007, **119**, 8334; *Angew. Chem. Int. Ed.* 2007, **46**, 8186; (b) S. A. Snyder, S. P. Breazzano, A. G. Ross, Y. Lin, A. L. Zografos, *J. Am. Chem. Soc*. 2009, **131**, 1753. (c) S. A. Snyder, A. Gollner, M. Chiriac, *Nature* 2011, **474**, 461.
98. For the isolation and characterization of these natural products, see: [paucifloral F (**241**)] (a) J. Ito, T. Tanaka, M. Iinuma, K. Nakaya, Y. Takahashi, R. Sawa, J. Murata, D. Darnaedi, *J. Nat. Prod.* 2004, **67**, 932; [diptoindonesin D (**242**)] (b) Sahadin, E. H. Hakim, L. D. Juliawaty, Y. M. Syah, L. bin Din, E. L. Ghisalberti, J. Latip, I. M. Said, S. A. Achmad, *Z. Naturforsch., C: Biosci.* 2005, **60**, 723; [cassigarol B (**243**)] (c) K. Baba, K. Maeda, Y. Tabata, M. Doi, M. Kozawa, *Chem. Pharm. Bull.* 1988, **36**, 2977; [ampelopsin D (**244**) and ampelopsin H (**247**)] (d) Y. Oshima, Y. Ueno, *Phytochemistry* 1993, **33**, 179; [ampelopsin F (**245**)] (e) H.-F. Luo, L.-P. Zhang, C.-Q. Hu, *Tetrahedron* 2001, **57**, 4849; [quadrangularin A (**239**)] (f) S. A. Adesanya, R. Nia, T. M. Martin, N. Boukamcha, A. Montagnac, M. Pais, *J. Nat. Prod.* 1999, **62**,1694; [pallidol (**246**)] (g) M. A. Khan, S. G. Nabi, S. Prakash, A. Zaman, *Phytochemistry* 1986, **25**, 1945; (h) B. Supudompol, K. Likhitwitayawuid, P. J. Houghton, *Phytochemistry* 2004, **65**, 2589; [hemsleyanol E] (i) T. Tanaka, T. Ito, K. Nakaya, M. Iinuma, Y. Takahashi, H. Naganawa, S. Riswan, *Heterocycles* 2001, **55**, 729.
99. Y. Takaya, K.-X. Yan, K. Terashima, J. Ito, M. Niwa, *Tetrahedron* 2002, **58**, 7259.
100. (a) R. J. K. Taylor, *Chem. Commun.* 1999, 217; (b) C. Y. Meyers, A. M. Malte, W. S. Matthews, *J. Am. Chem. Soc.* 1969, **91**, 7510.
101. E. J. Corey, M. Chaykovsky, *J. Am. Chem. Soc.* 1965, **87**, 1353.
102. N. J. Bach, E. C. Kornfeld, N. D. Jones, M. O. Chaney, D. E. Dorman, J. W. Paschal, J. A. Clemens, E. B. Smalstig, *J. Med. Chem.* 1980, **23**, 481.

103. E. J. Corey, X.-M. Cheng, *The Logic of Chemical Synthesis*, John Wiley & Sons: New York, (1989).

104. (a) S. L. Schreiber, *Science* 2000, **287**, 964; (b) M. D. Burke, S. L. Schreiber, *Angew. Chem.* 2004, **116**, 48; *Angew. Chem. Int. Ed.* 2004, **43**, 46.

105. (a) H. M. Ge, C. Xu, X. T. Wang, B. Huang, R. X. Tan, *Eur. J. Org. Chem.* 2006, 5551; (b) H. M. Ge, C. H. Zhu, D. H. Shi, L. D. Zhang, D. Q. Xie, J. Yang, S. W. Ng, R. X. Tan, *Chem. Eur. J.* 2008, **14**, 376.

106. S. A. Snyder, S. B. Thomas, A. C. Mayer, S. P. Breazzano, *Angew. Chem.* 2012, **124**, 4156; *Angew. Chem. Int. Ed.* 2012, **51**, 4080.

107. (a) K. C. Nicolaou, R. T. Wu, Q. Kang, D. Y.-K. Chen, *Angew. Chem.* 2009, **121**, 3492; *Angew. Chem. Int. Ed.* 2009, **48**, 3440; (b) K. C. Nicolaou, Q. Kang, R. T. Wu, C. S. Lim, D. Y.-K. Chen, *J. Am. Chem. Soc.* 2010, **132**, 7540.

108. C. A. Kuttruff, M. D. Eastgate, P. S. Baran, *Nat. Prod. Rep.* 2014, **31**, 419.

109. (a) J.-F. F. Weber, I. A. Wahab, A. Marzuki, N. A. Thomas, A. A. Kadir, A. H. A. Hadi, K. Awang, A. A. Latiff, P. Richomme, J. Delaunay, *Tetrahedron Lett.* 2001, **42**, 4895; (b) H. M. Ge, W.-H. Yang, J. Zhang, R. X. Tan, *J. Agric. Food Chem.* 2009, **57**, 5756.

110. S. A. Snyder, N. E. Wright, J. J. Pflueger, S. P. Breazzano, *Angew. Chem.* 2011, **123**, 8788; *Angew. Chem. Int. Ed.* 2011, **50**, 8629.

111. S. A. Snyder, D. S. Treitler, A. P. Brucks, *J. Am. Chem. Soc.* 2010, **132**, 14303.

# SECTION IV

# MIXED BIOSYNTHETIC PATHWAYS–THE STORY OF ALKALOIDS

# 11

# ORNITHINE AND LYSINE ALKALOIDS

SEBASTIAN BRAUCH, WOUTER S. VELDMATE, AND FLORIS P. J. T. RUTJES
*Institute for Molecules and Materials, Radboud University Nijmegen, Nijmegen, The Netherlands*

## 11.1 BIOSYNTHESIS OF L-ORNITHINE AND L-LYSINE ALKALOIDS

Alkaloids, low-molecular-weight, heterocyclic organic compounds containing nitrogen in a negative oxidation state, represent a highly diverse class of secondary metabolites that occur in a variety of organisms, such as fungi, bacteria, and animals but predominately in higher plants (e.g., *Apocynaceae*, *Asteraceae*, *Solanaceae*, etc.). It is estimated that approximately up to 20% of all plant species contain alkaloids. Most of these compounds exhibit a pronounced biological activity, which makes them highly attractive for the application as pharmaceuticals (e.g., galanthamine, quinine, berberine, vincristine), stimulants (e.g., caffeine, nicotine), narcotics (e.g., cocaine, morphine), and poisons (e.g., coniine, strychnine) [1–3].

In general, most alkaloids are condensation products of decarboxylated amino acids with nonnitrogenous structural moieties derived from the acetate, shikimate, or deoxyxylulose phosphate pathway. Besides the proteinogenic amino acids L-phenylalanine (L-Phe), L-tyrosine (L-Thy), L-tryptophan (L-Trp), L-histidine (L-His), and L-lysine (L-Lys), the nonproteinogenic amino acid L-ornithine (L-Orn) serves as the main precursor in alkaloid biosynthesis leading to different classes of alkaloids with a common carbon skeleton depending on the amino acid precursor [4]. However, in contrast to most secondary metabolites, the different classes of alkaloids originate from unique biosynthetic pathways [5]. In recent years, extensive efforts using either genomic approaches (e.g., expressed sequence tag databases, DNA microarrays, proteome analysis) or feeding experiments with isotopically labeled precursors shed light on these highly complex intracellular processes. The results of these studies leading to a profound knowledge of the different alkaloid biosynthetic pathways will be the focal point of the first part of the forthcoming chapter highlighting the biosynthesis of L-Orn- and L-Lys-derived alkaloids.

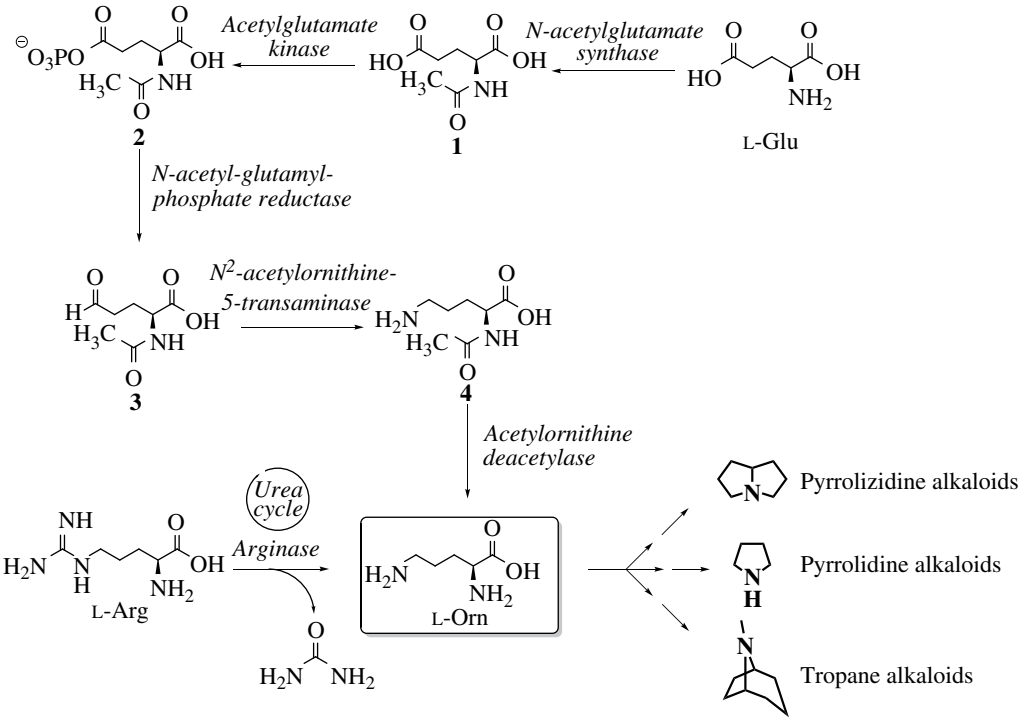
### 11.1.1 Biosynthetic Formation of Alkaloids Derived from L-Ornithine

Although not coded for by DNA, L-Orn is present in both plants and animals. In animals, it originates from the urea cycle, where it is the product of the enzymatic conversion of L-arginine (L-Arg) by the enzyme arginase (EC 3.5.3.1) (Scheme 11.1). In plants, L-Orn is predominately formed from L-glutamic acid (L-Glu), which is converted first into *N*-acetyl-L-Glu (**1**) by *N*-acetylglutamate synthase (EC 2.3.1.1) [6–8]. The next steps involve the formation of *N*-acetyl-L-glutamyl-5-phosphate (**2**) catalyzed by acetylglutamate kinase (EC 2.7.2.8) and reduction by *N*-acetyl-γ-glutamyl-phosphate reductase (EC 1.2.1.38) leading to *N*-acetyl-L-glutamyl-5-semialdehyde (**3**) followed by the $N^2$-acetylornithine 5-transaminase (EC 2.6.1.11)-catalyzed transamination reaction between semialdehyde **3** and L-Glu affording $N^2$-acetylornithine (**4**). Finally, cleavage of the acetyl group by acetylornithine deacetylase (EC 3.5.1.16) yields L-Orn, which acts as the amino acid precursor for various structurally related alkaloids with a common five-membered pyrrolidine ring, namely, pyrrolidine, pyrrolizidine, and tropane alkaloids [9].

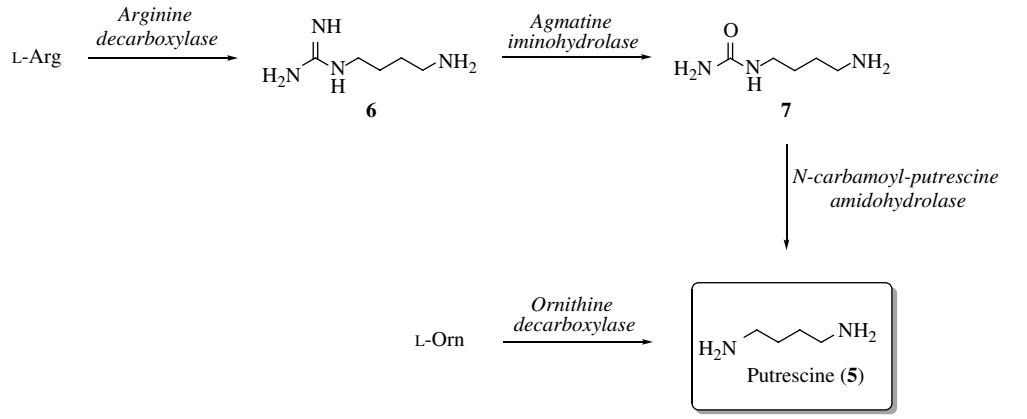
*From Biosynthesis to Total Synthesis: Strategies and Tactics for Natural Products*, First Edition. Edited by Alexandros L. Zografos.
© 2016 John Wiley & Sons, Inc. Published 2016 by John Wiley & Sons, Inc.

The first step in the biosynthesis of these types of alkaloids involves the formation of putrescine (**5**, IUPAC: butane-1,4-diamine), a foul-smelling compound owing its name to its occurrence in putrefying animal flesh. Two major pathways for the production of putrescine are known (Scheme 11.2): either via direct decarboxylation of L-Orn by ornithine decarboxylase (EC 4.1.1.17) with the cofactor pyridoxal phosphate (PLP) or indirectly from L-Arg, which bypasses L-Orn [10–12]. The later route relies on the decarboxylation of L-Arg by PLP-dependent arginine decarboxylase (EC 4.1.1.19). Next, the resulting agmatine (**6**) is hydrolyzed by agmatine iminohydrolase (EC 3.5.3.12). The resulting *N*-carbamoyl-putrescine (**7**) is then converted into putrescine by hydrolysis of the urea moiety via *N*-carbamoyl-putrescine amidohydrolase (EC 3.5.1.53). In animals and some human and phytopathogenic fungi, putrescine is produced solely from L-Orn, whereas in bacteria, other fungi, and higher plants, both pathways are involved.

Putrescine is an important link between primary and secondary metabolisms. It acts as a branch point for various biosynthetic pathways leading to a structurally diverse set of metabolites. Besides being an important intermediate in pyrrolidine, pyrrolizidine, and tropane alkaloid biosynthesis, putrescine can be converted into spermidine (**8**) and spermine




**SCHEME 11.1** Biosynthesis of L-ornithine.




**SCHEME 11.2** The biosynthesis of putrescine, the gateway to ornithine alkaloids.

(**9**) by the action of spermidine synthase (EC 2.5.1.16) and spermine synthase (EC 2.5.1.22), respectively (Scheme 11.3) [13]. These polyamines owe their name to their original isolation source, human semen, and they play a vital role in cellular metabolism. Both conversions require the presence of decarboxylated *S*-adenosyl methionine (dcSAM), which donates the aminopropyl group. Another polyamine derived from putrescine is homospermidine (**13**), which is formed either from two putrescine molecules or from one molecule each of putrescine and spermidine (Scheme 11.3) [14]. Both reactions are catalyzed by the $NAD^+$-dependent enzyme homospermidine synthase (EC 2.5.1.44) and involve the $NAD^+$-dependent dehydrogenation of putrescine (or spermidine), transfer of the 4-aminobutylidene group from dehydroputrescine **10** (or dehydrospermidine **11**) to a second molecule of putrescine, and reduction of the intermediate imine **12** to form the symmetric triamine homospermidine, which is the first pathway-specific intermediate in pyrrolizidine alkaloid biosynthesis. However, the genes and enzymes involved in the formation of the bicyclic skeleton present in these pyrrolizidine alkaloids, which constitute a class of secondary metabolites predominately occurring in plants and being thought of as acting in plant defense against herbivores, have not been characterized so far [14]. Most likely the biosynthesis involves the participation of a diamino oxidase catalyzing the oxidative deamination of homospermidine leading to a five-membered cyclic iminium ion (**14**) after immediate intramolecular Schiff-base formation (Scheme 11.3) [9, 14–16]. After a subsequent second oxidative deamination step of the remaining terminal amine, the enolate anion of the resulting aldehyde **15** may attack the postulated iminium ion to furnish the characteristic bicyclic structure of pyrrolizidine alkaloids in an intramolecular Mannich reaction. This bicyclic intermediate (**16**) is the precursor for about 400 different, structurally related pyrrolizidine alkaloids that have been identified in the meantime. For example, the corresponding pyrrolizidine alcohols (so-called necine base), such as lindelofidine (**17**) or retronecine (**19**), can be further esterified with various mono- or dicarboxylic acids (so-called necic acids, which are derived biosynthetically predominately from L-leucine, L-isoleucine, or L-valine) to yield, for example, cyanaustraline (**18**) from **17** and (–)-trachelanthic acid (derived from L-valine [17]) or senecionine from **20** and senecic acid (derived from L-isoleucine [18]).

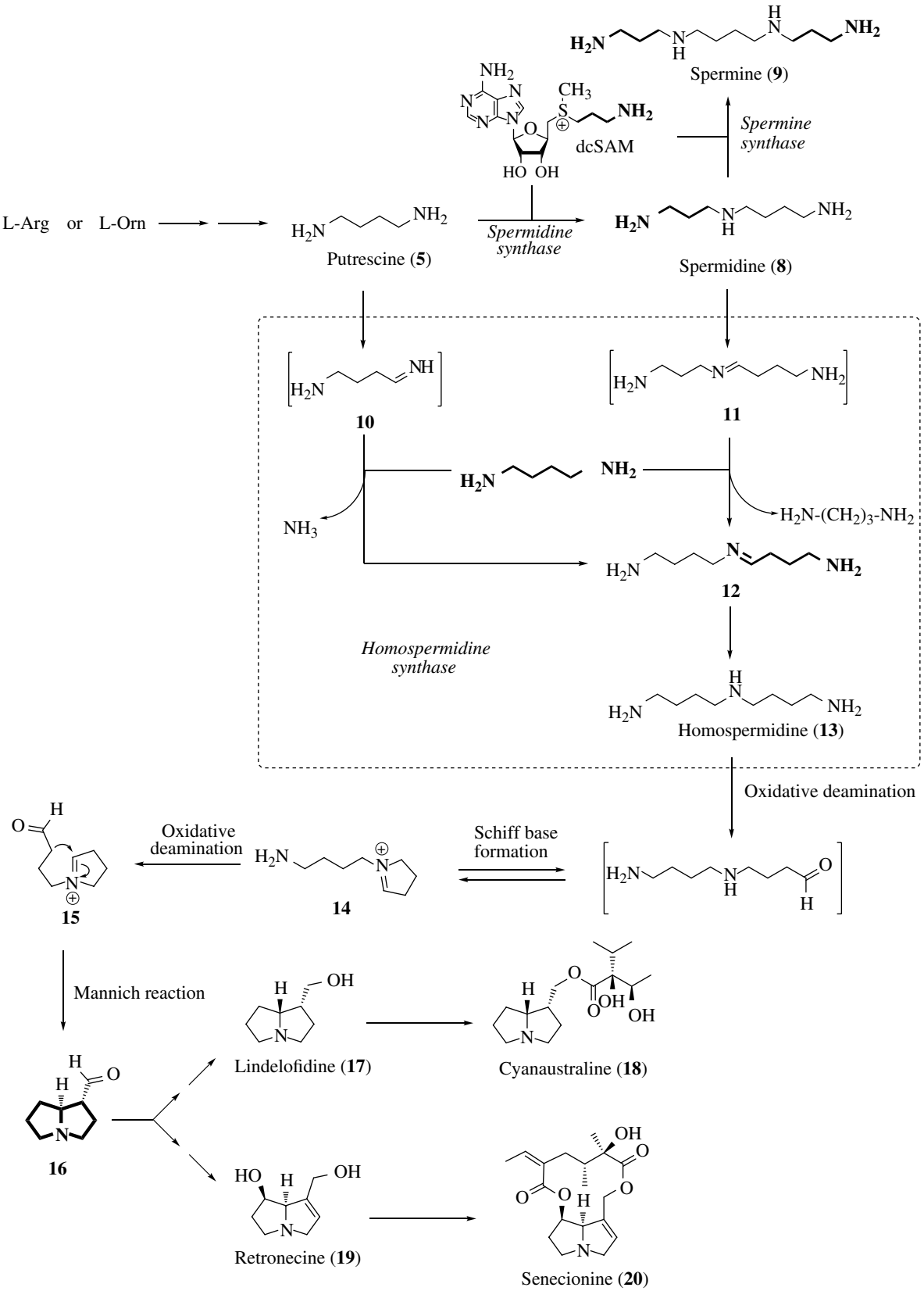
The first committed biosynthetic step toward pyrrolidine and tropane alkaloids involves N-methylation of putrescine to furnish *N*-methylputrescine (**21**) by SAM-dependent putrescine *N*-methyltransferase (EC 2.1.1.53) (Scheme 11.4) [9, 19, 20]. Oxidative deamination by *N*-methylputrescine oxidase (EC 1.4.3.21) affords 4-methylaminobutanal (**22**), which spontaneously cyclizes to furnish the corresponding *N*-methyl-$\Delta^1$-pyrrolinium cation (**23**) via intramolecular Schiff-base formation. Although no enzymes have been identified catalyzing the subsequent biosynthetic steps, from feeding experiments, it was suggested that the previously formed iminium ion, which is highly susceptible to nucleophilic attack, might react with the enolate anion of acetyl coenzyme A (acetyl-CoA) in a Mannich reaction to afford 1-methylpyrrolidine-2-acetyl-CoA (**24a/b**).

After subsequent Claisen condensation with a second equivalent acetyl-CoA, 4-(1-methyl-pyrrolidin-2-yl)-3-oxobutanoyl-CoA **25a/b** is formed, the link between pyrrolidine and tropane alkaloid biosynthesis. From this intermediate, characteristic pyrrolidine alkaloids, such as hygrine (**26**) and cuscohygrine (**27**), two alkaloids commonly found in coca leaves [9], are formed either directly by hydrolysis and subsequent decarboxylation (for **26**) or via an additional Mannich reaction with the aforementioned *N*-methyl-$\Delta^1$-pyrrolinium cation (**23**) followed by hydrolysis and decarboxylation (**27**).

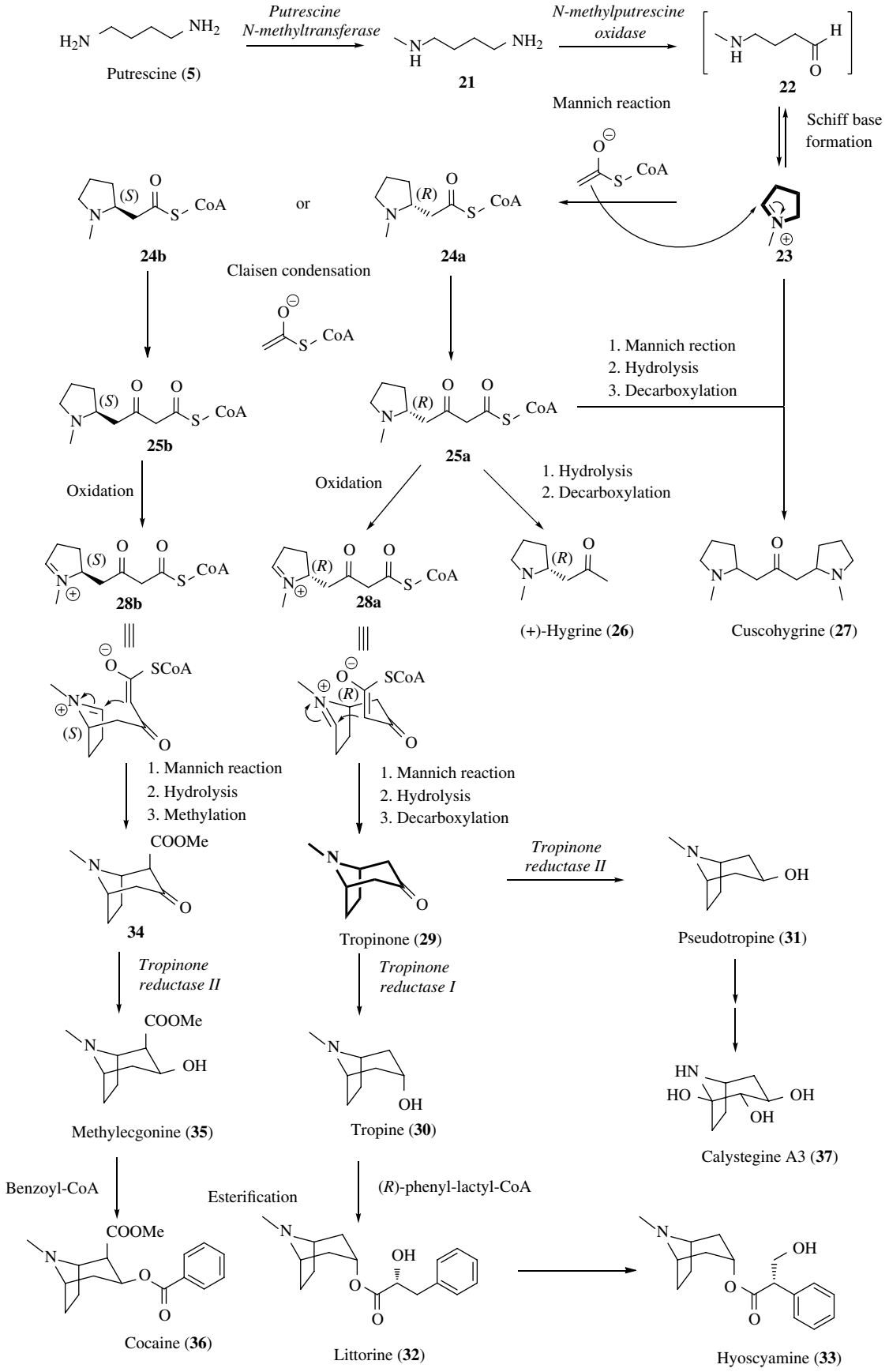
From the intermediate 4-(1-methylpyrrolidin-2-yl)-3-oxobutanoyl-CoA (**25a/b**), the biosynthetic pathway toward the bicyclic tropane alkaloids is supposed to proceed via a subsequent oxidation step generating the pyrrolinium cation **28a/b** [9, 19, 20]. Next, the common tropane alkaloid skeleton is formed in an intramolecular Mannich reaction between the formed imine moiety and the enolate anion of the 3-oxobutanoyl-CoA side chain. Subsequent hydrolysis and decarboxylation afford the bicyclic tropinone **29**, which is reduced either by the NADPH-dependent enzyme tropinone reductase I (EC 1.1.1.206) to tropine **30** (axial hydroxyl group) or by tropinone reductase II (EC 1.1.1.236) to pseudotropine **31** (equatorial hydroxyl group). Subsequent modification of the hydroxyl group affords a variety of structurally related tropane alkaloids. For example, esterification of tropine (**30**) with L-Phe-derived (*R*)-phenyl-lactyl-CoA affords littorine (**32**), a tropane alkaloid that can be isolated from *Atropa belladonna* (commonly known as deadly nightshade) [21], a plant being well known for its high toxicity. Especially the foliage and berries of *A. belladonna* contain high levels of tropane alkaloids, for example, L-hyoscyamine (**33**), which contributes to the observed severe toxicity. Biosynthetically this toxin is derived from littorine, which first undergoes radical rearrangement after one-electron oxidation (presumably catalyzed by a cytochrome P450 enzyme) to yield after subsequent reduction the tropate ester L-hyoscyamine (**33**) [9, 20].

Alternatively, other tropane alkaloids (here cocaine) are obtained if no decarboxylation occurs after the intramolecular Mannich reaction of **28b**. Subsequent hydrolysis and methylation afford the methyl ester **34**, which is reduced stereospecifically to methylecgonine (**35**). Esterification with benzoyl-CoA (derived from L-Phe [22]) yields cocaine (**36**), the well-known central nervous system stimulant present in leaves of the coca plant [9].

Other important secondary metabolites, which can be considered as tropane alkaloids, are the recently discovered




**SCHEME 11.3** The biosynthetic route toward the pyrrolizidine skeleton found in ornithine alkaloids.




**SCHEME 11.4** The biosynthetic route toward the pyrrolidine and tropane skeleton found in ornithine alkaloids.

calystegines, selective glycosidase inhibitors that are currently under investigation in respect to their applicability as drugs against the AIDS virus HIV [23, 24]. For example, calystegine A3 (**37**), one of the first calystegines isolated from *Calystegia sepium* and *A. belladonna* in 1990, is equipped with three hydroxyl groups at various positions of the nortropane skeleton (tropane without N-methyl group), whereas the hydroxyl group on C-3 was found to be equatorial. Consequently, it was postulated that calystegines originate biosynthetically from pseudotropine (**31**) [25, 26].

### 11.1.2 Biosynthetic Formation of Alkaloids Derived from L-Lysine

As a consequence of one additional methylene group present in the side chain of the homolog amino acid L-Lys in comparison with L-Orn, the corresponding piperidine, quinolizidine, indolizidine, and lycopodium alkaloids contain a six-membered piperidine ring instead of a five-membered pyrrolidine ring. Moreover, the fact that both L-Lys and L-Orn exhibit a quiet similar chemical reactivity enables L-Lys to undergo similar metabolic conversions as outlined in the previous chapter for the biosynthesis of alkaloids derived from L-Orn.

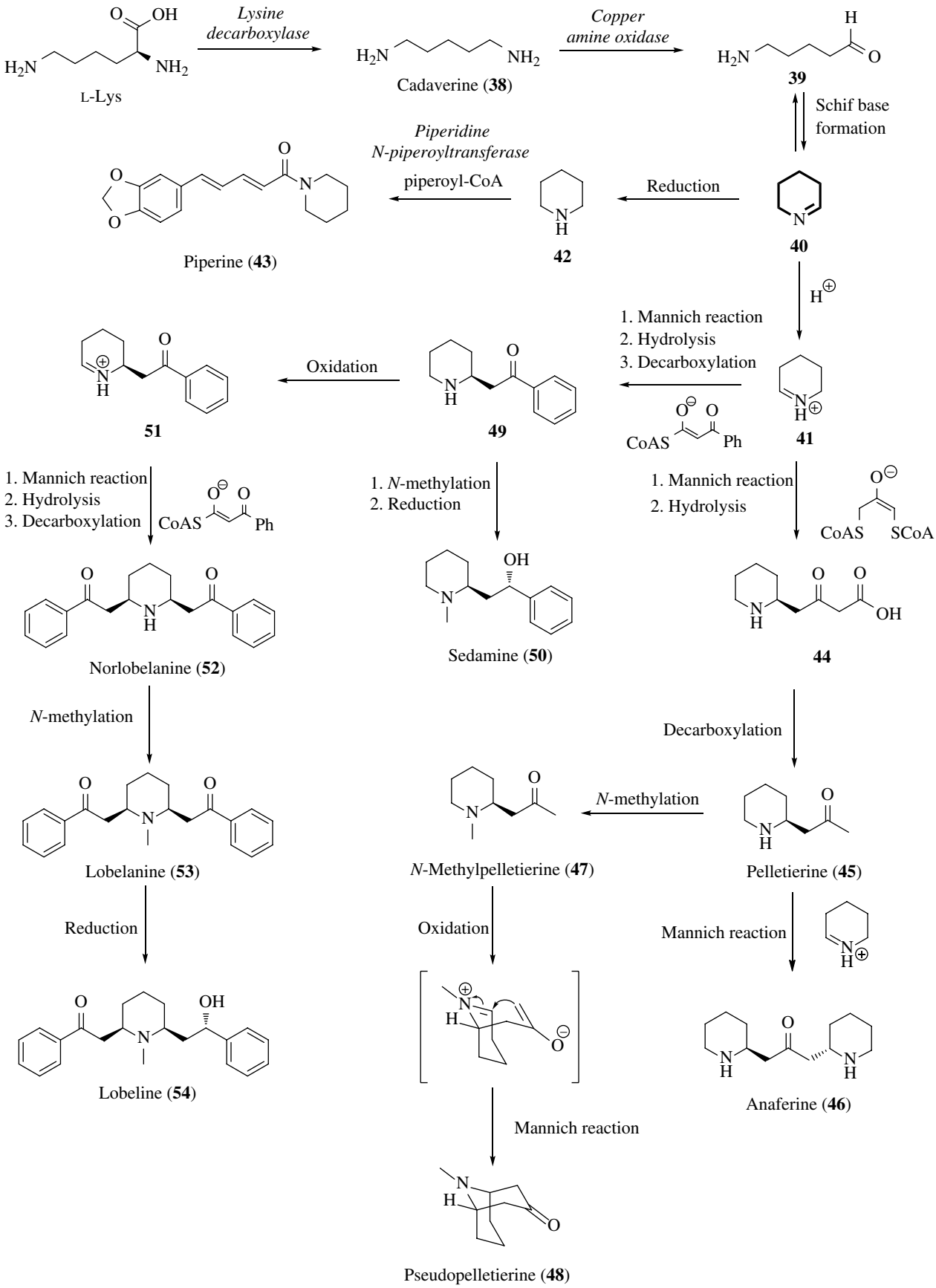
The first step in the biosynthesis of piperidine, quinolizidine, and lycopodium alkaloids is the PLP-assisted decarboxylation of L-Lys to the diamine cadaverine (**38**) by lysine decarboxylase (EC 4.1.1.18) (Scheme 11.5) [9, 27]. Similar to putrescine, this foul-smelling compound is associated with putrefying animal tissue as one might expect by hearing its name. Next, oxidative deamination of cadaverine by copper amine oxidase (EC 1.4.1.22) yields 5-aminopentanal (**39**), which spontaneously cyclizes to furnish $\Delta^1$-piperideine (**40**). The corresponding $\Delta^1$-piperideinium cation (**41**), probably the universal intermediate in piperidine, quinolizidine, and lycopodium alkaloid biosynthesis, is susceptible to nucleophilic attack much like its *N*-methyl-$\Delta^1$-pyrrolinium cation counterpart in pyrrolidine and tropane alkaloid biosynthesis. Moreover, $\Delta^1$-piperideine (**40**) might be reduced to piperidine (**42**), which now in turn might serve as nucleophilic species. For example, condensation of piperidine (**42**) with piperoyl-CoA catalyzed by piperidine *N*-piperoyltransferase (EC 2.3.1.145) yields piperine (**43**), the main alkaloid found in black pepper where it is responsible for the characteristic pungent taste.

If not reduced to piperidine, the $\Delta^1$-piperideinium cation (**41**) can serve as substrate in an intermolecular Mannich reaction with the enolate anion, for example, of acetonedicarboxylic acid bisCoA ester or benzoylacetyl-CoA serving as the nucleophile. Although no enzyme activities associated with these steps have been characterized so far, the biosynthetic route toward the alkaloid pelletierine (**45**) from imine **41** is supposed to involve a Mannich reaction with acetonedicarboxylic acid bisCoA ester followed by hydrolysis and decarboxylation [28]. Similar to the aforementioned formation of cuscohygrine (**27**), a second Mannich reaction between imine **41** and pelletierine **45** leads to the dimeric alkaloid anaferine (**46**). Moreover, pelletierine (**45**) can be methylated to *N*-methyl-pelletierine (**47**). Subsequent oxidation may induce an intramolecular Mannich reaction leading to the bicyclic pseudopelletierine (**48**), the homolog of tropinone [29].

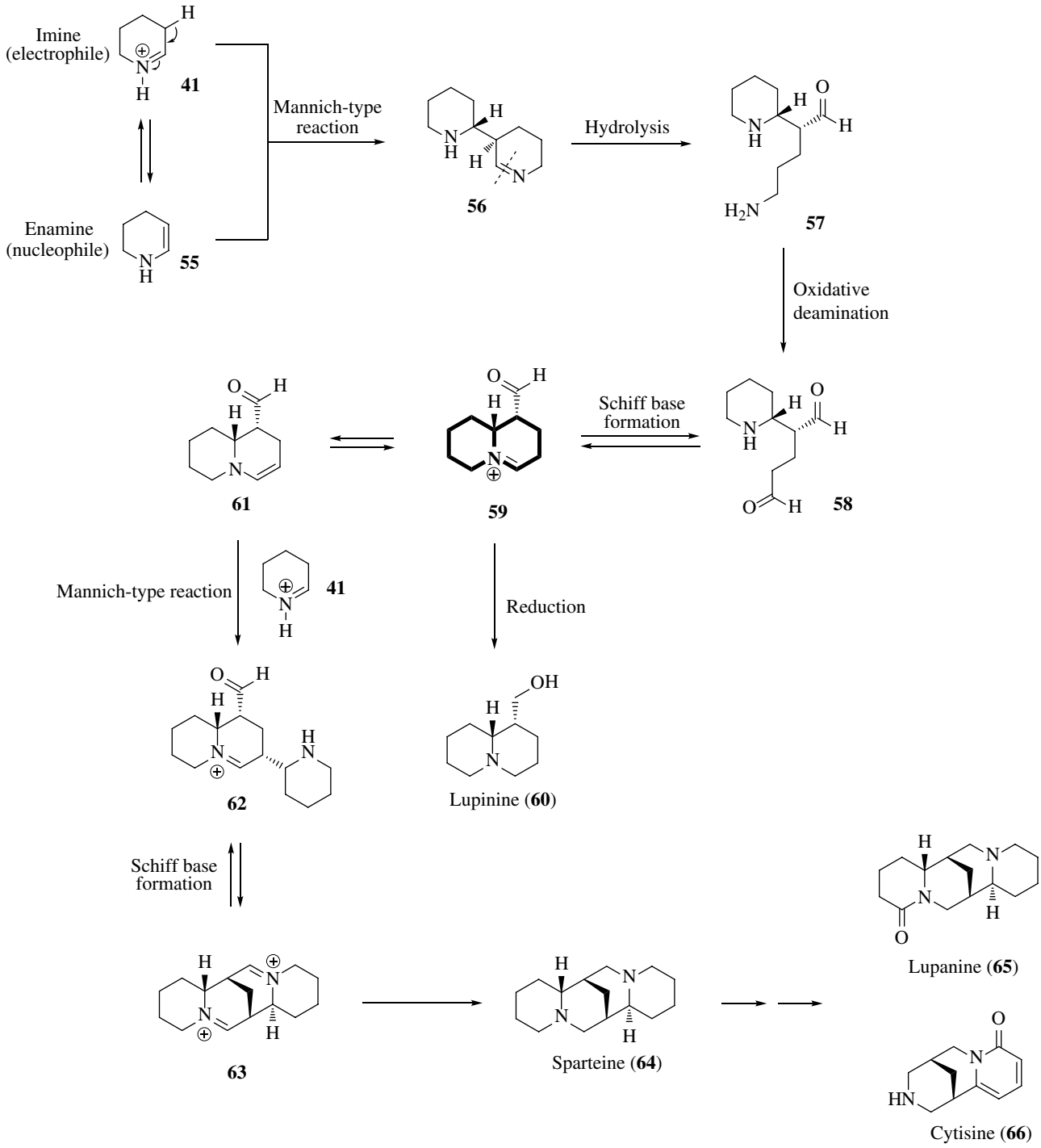
If benzoylacetyl-CoA, an intermediate in the β-oxidation of cinnamic acid [30], instead of acetonedicarboxylic acid bisCoA ester participates in the Mannich reaction with imine **41**, (*S*)-1-phenyl-2-(piperidin-2-yl)ethanone **49** is formed after subsequent hydrolysis and decarboxylation. Then, intermediate **49** either is reduced selectively to sedamine (**50**) after methylation of the secondary amine or is oxidized to the corresponding imine **51**, which yields *cis*-norlobelanine (**52**) upon reaction with a second equivalent benzoylacetyl-CoA.

Methylation of the secondary amine of *cis*-norlobelanine (**52**) affords lobelanine (**53**), a precursor of the alkaloid lobeline (**54**), which is obtained upon selective reduction of a single carbonyl group and is commonly applied as a smoking cessation aid [9].

Another nucleophile able to react with the $\Delta^1$-piperideinium cation (**41**) in a Mannich-type reaction is the tautomeric enamine $\Delta^2$-piperideine **55** to yield tetrahydroanabasine **56** (Scheme 11.6). After hydrolysis of the imine moiety and subsequent oxidative deamination of the primary amine, the fused bicyclic quinolizidine skeleton (**59**) is formed via Schiff-base formation. However, in contrast to the biosynthesis of other alkaloids, such as tropane or pyrrolidine alkaloids, the mechanisms of quinolizidine alkaloid biosynthesis are only marginally explored yet [9, 16, 27, 31, 32]. For example, stereoselective reduction of the remaining carbonyl group probably leads to the formation of the quinolizidine alkaloid lupinine (**60**), a bitter-tasting alkaloid present in *Lupinus*. Alternatively, the bicyclic intermediate **59** might tautomerize into its corresponding enamine **61**. Then, this highly nucleophilic enamine is able to stereoselectively add to the $\Delta^1$-piperideinium cation (**41**), again in a Mannich-type reaction, to furnish upon subsequent intramolecular formation of a Schiff base between the secondary amine and the remaining carbonyl group the intermediate didehydrosparteinium cation (**63**). Subsequent reduction leads to sparteine (**64**), one of the major alkaloids isolated from Scotch broom (*Cytisus scoparius*), which acts as an antiarrhythmic agent [33]. However, it is not approved for human use by the FDA due to its severe toxicity. Moreover, the intermediate didehydrosparteinium cation (**63**) is supposed to be part of the biosynthesis of other polycyclic lupine alkaloids, such as lupanine (**65**) and cytosine (**66**). Although no enzyme activities catalyzing these steps have been discovered, labeling studies supported this biosynthetic hypothesis. Intermediates following cadaverine have not been isolated, though. It has been suggested



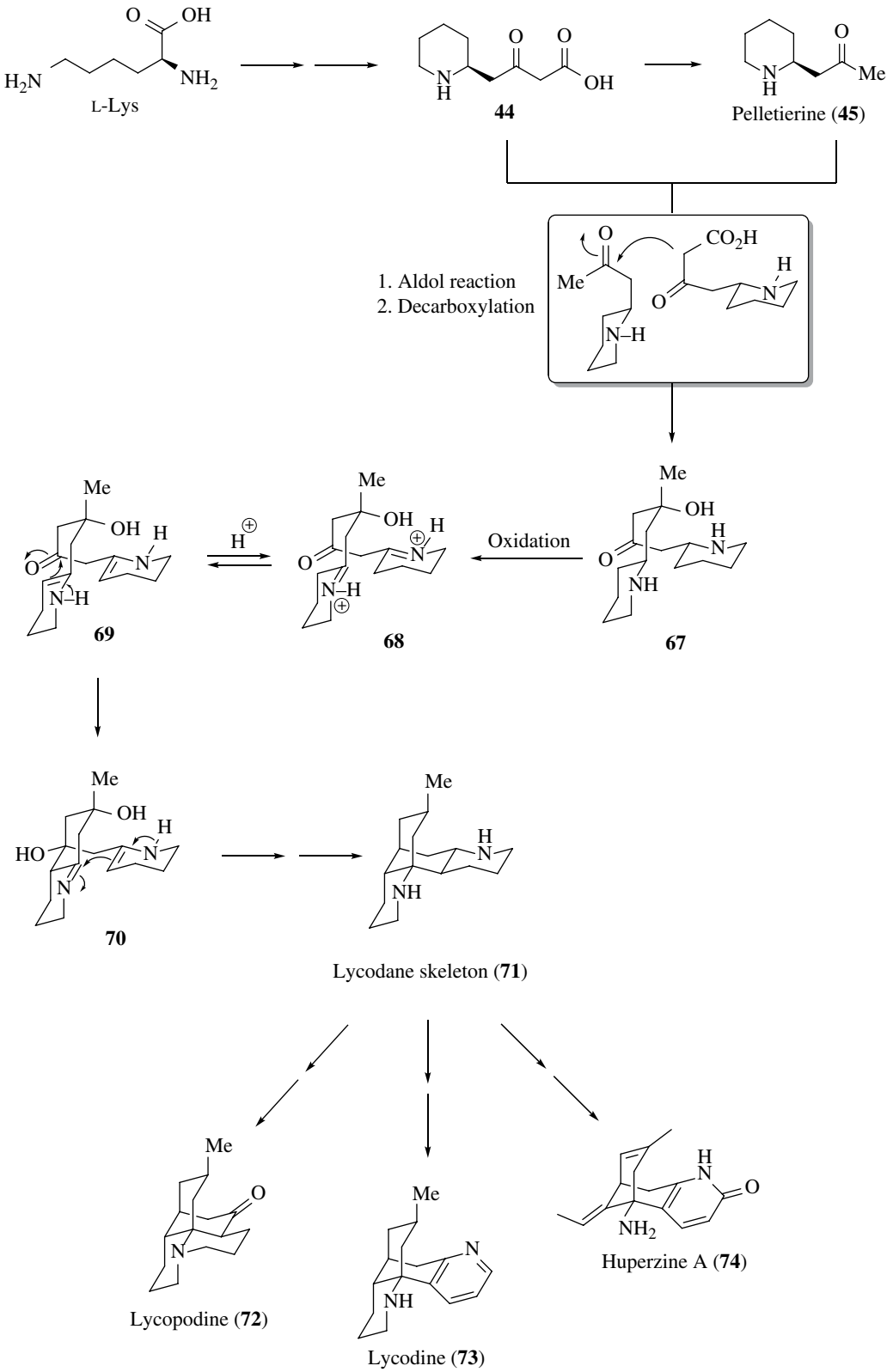

**SCHEME 11.5** The biosynthetic route toward the piperidine skeleton found in lysine alkaloids.




**SCHEME 11.6** The biosynthetic route toward quinolizidine alkaloids derived from the amino acid lysine.

that the subsequent steps occur in a channeled fashion, with the intermediates remaining enzyme-bound [34].

The biosynthesis of lycopodium, quinolizine, pyridine, or α-pyridone-type alkaloids isolated from *Lycopodium* species, shares some common steps with the biosynthesis of the previously mentioned piperidine alkaloids [28, 35, 36]. The first general intermediate for all lycopodium alkaloids is the piperidine alkaloid pelletierine (**45**). Again, besides the enzymes being involved in the synthesis of 5-aminopentanal (**39**), which cyclizes to $\Delta^1$-piperideine **40**, no pathway-specific enzymes have been identified until now. However, feeding studies with isotopically labeled L-Lys and isolation of some intermediates from plant material suggest that pelletierine **45** is first condensed with the intermediary formed β-ketoester (**44**) in an aldol-type reaction followed by decarboxylation (**67**) (Scheme 11.7).




**SCHEME 11.7** The biosynthetic route toward lycopodium alkaloids derived from the amino acid lysine.

Subsequent oxidation might lead to the formation of the bisimine **68**, which tautomerizes to its corresponding enamine **69**. Next, intramolecular tandem cyclization may lead to the formation of the tetracyclic lycodane skeleton (**71**), which is supposed to act as the central intermediate in the biosynthetic pathway from which different classes of lycopodium alkaloids are accessible. For example, a variety of oxidative modifications catalyzed presumably by cytochrome P450 enzymes or 2-oxoglutarate-dependent dioxygenases may lead to the formation of lycopodine (**72**), lycodine (**73**), or huperzine A (**74**). The latter being a reversible binding acetylcholinesterase inhibitor that has been studied in the treatment of Alzheimer's disease, however, up to now, no clear evidence supports its routine therapeutic use [37, 38].

Instead of cadaverine, the first committed biosynthetic step toward indolizidine alkaloids involves oxidative deamination of the ε-amino group of L-Lys by L-Lys 6-dehydrogenase (EC 1.4.1.18) to yield L-2-aminoadipate-6-semialdehyde (**75**), which spontaneously cyclizes to furnish $\Delta^1$-piperideine-6-L-carboxylate (**76**) (Scheme 11.8) [9, 39]. Subsequent reduction of the imine affords L-pipecolic acid (**77**). Alternatively, in some organisms, L-pipecolic acid might be produced via oxidative deamination of the α-amino group of L-Lys by L-Lys oxidase (EC 1.4.3.14), leading to 6-amino-2-oxohexanoate (**78**), which immediately cyclizes to yield $\Delta^1$-piperideine-2-carboxylate (**79**), and stereoselective reduction by $\Delta^1$-piperideine-2-carboxylate reductase (EC 1.5.1.21) [40–43]. After subsequent formation of pipecolyl-CoA (**80**), Claisen condensation with acetyl-CoA affords 4-(piperidin-2-yl)-3-oxobutanoyl-CoA (**81**). Although no details are known concerning the mechanism of the ring closure, the characteristic bicyclic skeleton (fused five- and six-membered ring) of indolizidine alkaloids is most likely formed via an intermediate amide (**82**) or imine (**83**). The resulting 1-indolizidinone (**84**), a central intermediate in the biosynthesis of various indolizidine alkaloids, can be converted in a series of consecutive hydroxylation, reduction, and oxidation steps into swainsonine (**85**) or castanospermine (**86**). Both polyhydroxylated indolizidines, which were originally isolated from *Swainsona* and *Castanospermum*, exhibit a pronounced activity against the HIV due to their ability to inhibit glycosidases involved in glycoprotein biosynthesis [44, 45]. Other alkaloids like slaframine (**87**), a mycotoxin first isolated from the plant pathogen *Rhizoctonia leguminicola*, might require additional transamination and acylation steps.

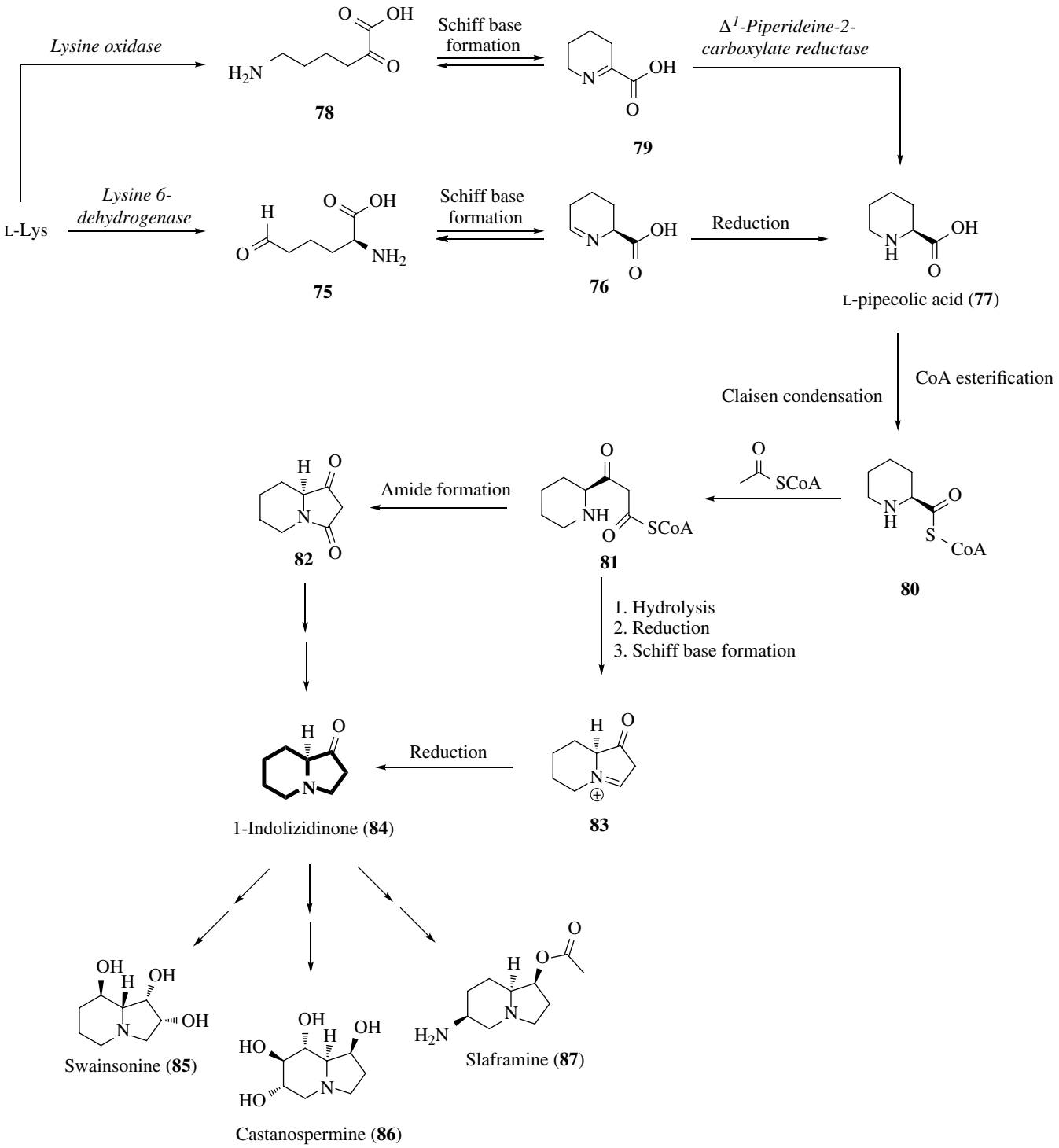
As it gets obvious from the previous paragraphs, the formation of the unique carbon skeleton present in lysine and ornithine alkaloids is based on only a limited amount of chemical transformations. In general, the condensation reaction between an amine and an aldehyde or ketone forming a Schiff base (imine) is one of the key steps toward the formation of these heterocyclic structures. Another important reaction, which plays a vital role throughout alkaloid biosynthesis, is the Mannich reaction. Here, the highly electrophilic iminium ion formed upon condensation of an amine and a carbonyl group is able to react with a variety of suitable nucleophiles, which is reflected by the unique and diverse carbon skeletons present in these alkaloids.

Nowadays, the mechanisms underlying the Mannich reaction are well understood, and conditions have been developed that enable to run these reactions with high yields under very mild conditions with ultimate regio- and stereoselectivity. This might be the reason why biomimetic strategies utilizing the Mannich reaction in the total synthesis of this class of secondary metabolites have been of particular success. For example, the tropinone synthesis by Robinson and Schöpf is probably the first total synthesis of a natural product that mimics essential elements of its biosynthesis (see Section 11.3). Other more recent examples that involve the Mannich reaction as key step in the total synthesis of L-Lys- and L-Orn-derived alkaloids include a variety of piperidine (e.g., dihydropinidine, anabasine), indolizidine (e.g., gephyrotoxin 167B, pumiliotoxin 251D), quinolizidine (e.g., lasubine II, epimyrtine), and lycopodium alkaloids (e.g., lycopodine, lycoflexine) (Figure 11.1). Before a more detailed description of the total syntheses of some of these secondary metabolites is given highlighting the impact of the Mannich reaction in creating the characteristic heterocyclic alkaloid skeleton, in the forthcoming chapter, we wish to introduce the basic concepts of the (asymmetric) Mannich reaction.

## 11.2 THE ASYMMETRIC MANNICH REACTION IN ORGANIC SYNTHESIS

The α-aminoalkylation of CH-acidic compounds, commonly known as Mannich reaction, was first described by Carl Mannich in 1912 [46]. In principle, the Mannich reaction can be considered as an Aldol-type reaction, whereas one of the carbonyl compounds is interchanged for an intermediary formed imine, which is generated upon condensation of a nonenolizable aldehyde with a primary or secondary amine. The corresponding iminium intermediate is highly susceptible to nucleophilic attack by a variety of different nucleophiles, such as enolized ketones, leading to β-aminoketones (Scheme 11.9). These so-called Mannich bases are highly versatile intermediates in organic synthesis, for example, Michael acceptors, β-amino alcohols, or functionalized carbonyl compounds are easily accessible (Scheme 11.10). Moreover, some of these Mannich bases and derivatives thereof exhibit a pronounced pharmacological activity and are used routinely in medicine (Figure 11.2) [47].

In contrast to the classic intramolecular Mannich reaction, which is well established, for example, in the synthesis of natural products [48], the insufficient stereocontrol and the formation of undesired by-products due to the harsh




**SCHEME 11.8** The biosynthetic route toward indolizidine alkaloids derived from the amino acid lysine.

reaction conditions and prolonged reaction times required, from a modern viewpoint, limit the applicability of the classic intermolecular Mannich reaction despite its great potential to create new C–C bonds. To overcome these limitations, modern versions of the intermolecular Mannich reaction were consequently developed, which employ preformed imines and enolates (indirect Mannich reaction) [47]. The increased concentration of the reactive intermediates present in the reaction mixture reduces the required reaction time and temperature, hence minimizing the extent of occurring side reactions. But probably the most impressive impact on the Mannich reaction has the addition of a chiral catalyst,

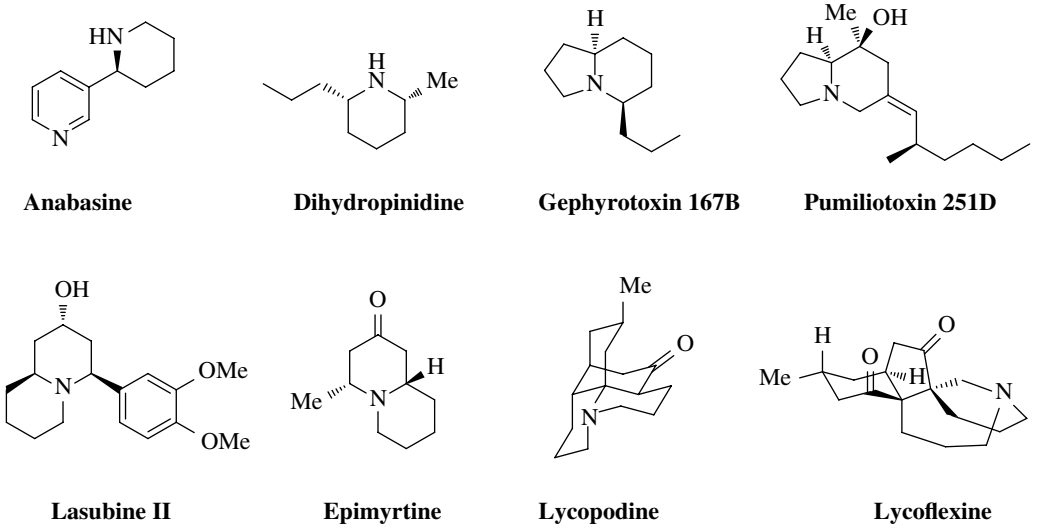
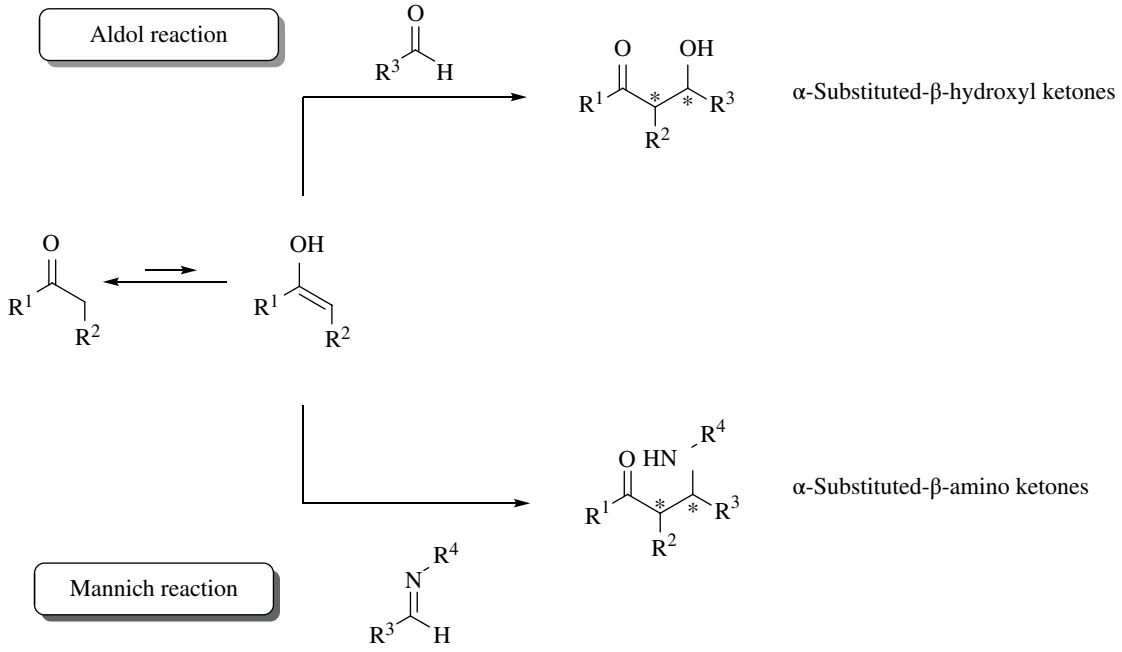



**FIGURE 11.1** Recent examples of L-ornithine- and L-lysine-derived alkaloids, which involve the Mannich reaction as key step in the total synthesis toward these alkaloids.

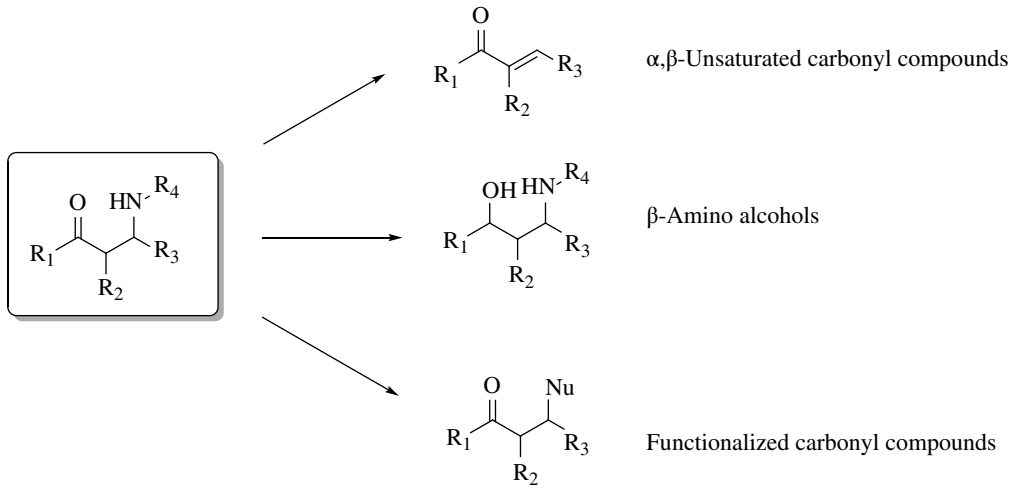



**SCHEME 11.9** The formation of new C–C bonds–aldol vs. Mannich reactions.

which additionally allows to control the stereochemical outcome of the reaction. Almost 90 years had passed since the discovery of Carl Mannich, when Shibasaki and colleagues disclosed the first catalytic asymmetric Mannich reaction combining paraformaldehyde, pyrrolidine, and propiophenone in the presence of the heterobimetallic catalyst **88** (Scheme 11.11) [49]. Despite the very low yields and modest enantioselectivity, this example prompted further developments in that field. Since that seminal publication, many different types of catalysts have been reported that promote the Mannich reaction in a highly enantio- and diastereoselective manner including chiral amines, Brønsted bases, Brønsted acids, transition metals, and biocatalysts [50–56].

### 11.2.1 Chiral Amines as Catalysts in Asymmetric Mannich Reactions

Based on the mechanistic hypotheses that the nucleophilic addition of chiral enamines, formed from ketones and chiral amines, onto imines is sufficiently faster compared with the




**SCHEME 11.10** Mannich bases—important synthetic intermediates.

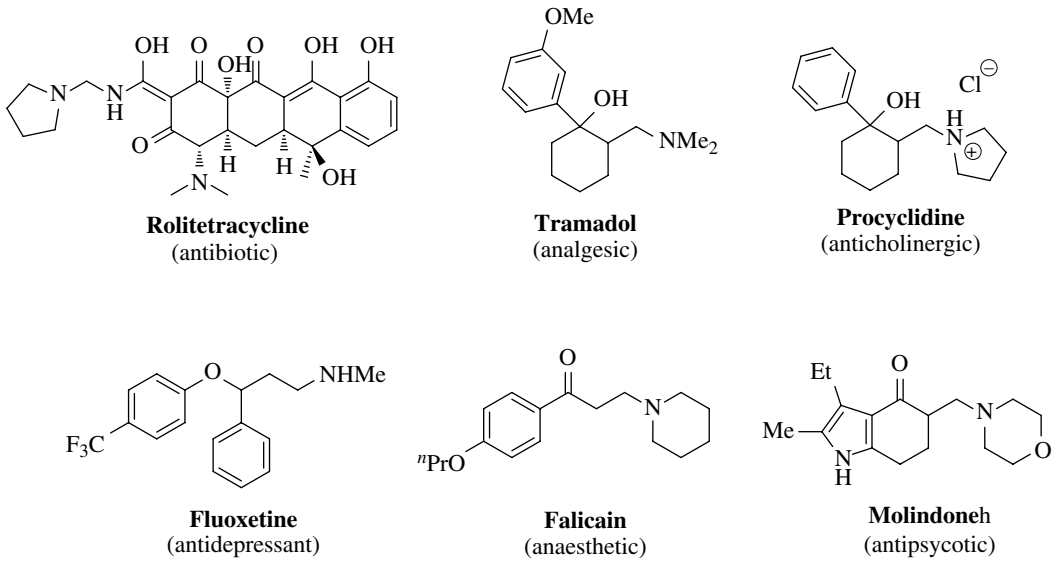
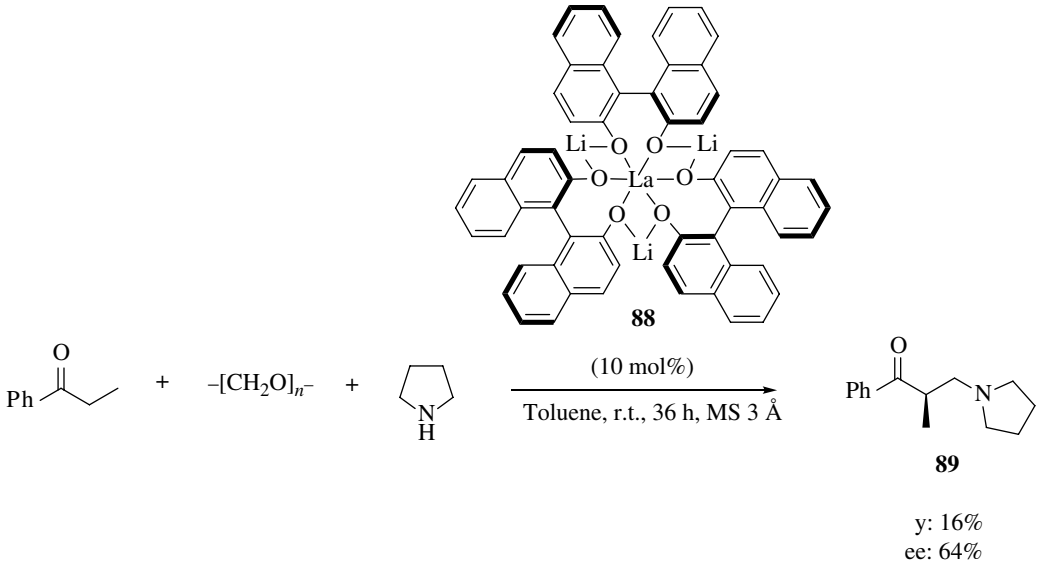


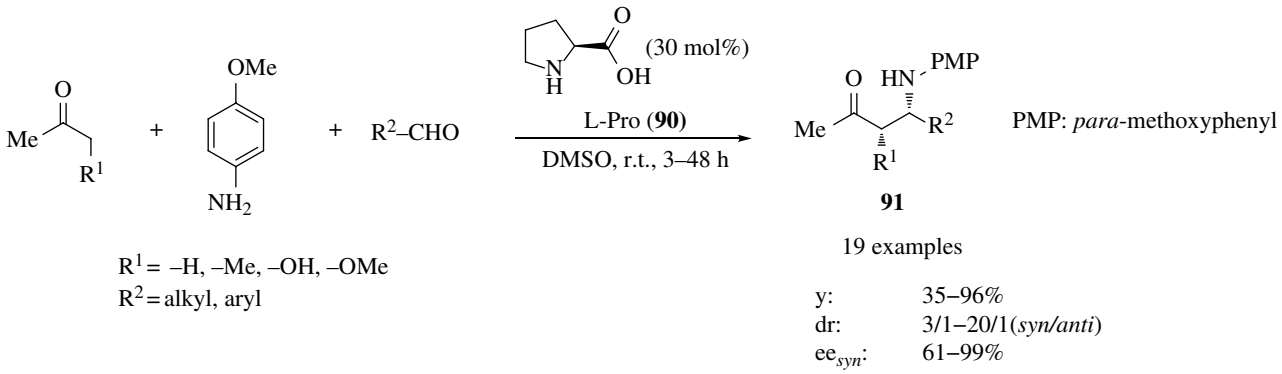

**FIGURE 11.2** Application of Mannich bases and derivatives thereof in medicine.

addition onto aldehydes and that the formation of electrophilic imines is substantially faster than the concurrent aldolization, List and coworkers investigated whether the catalytic three-component Mannich reaction between an aldehyde, a primary amine, and a ketone can be performed in an asymmetric fashion utilizing chiral amine catalysts. They found that L-proline (**90**) effectively catalyzed the Mannich reaction between *p*-nitrobenzaldehyde, *p*-anisidine, and acetone to afford the corresponding Mannich base **91** in 50% yield and 94% ee (Scheme 11.12) [57]. Subsequent scope and limitation studies of the L-proline catalyzed direct Mannich reaction utilizing a variety of different ketones, aldehydes, and *p*-anisidine confirmed the general applicability of this approach affording the corresponding Mannich bases in 35–96% yield with excellent enantio- and diastereoselectivity [58].

Although, simple acyclic amino acids, such as L-serine, L-alanine, L-valine, etc., proved to be similarly effective in promoting the asymmetric Mannich reaction [59], since the pioneering work by List and collaborators, L-proline has been the catalyst of choice probably due the fact that it has performed well in a multitude of cases besides its availability and low costs [60–62]. However, the application of L-proline is not without its flaws. As with other organocatalysts, typically high catalyst loadings of up to 30 mol% are required. Additionally, reactions have to be executed in very polar solvents, such as DMSO, DMF, MeOH, or $H_2O$, due to its poor solubility. To overcome some of these limitations, novel



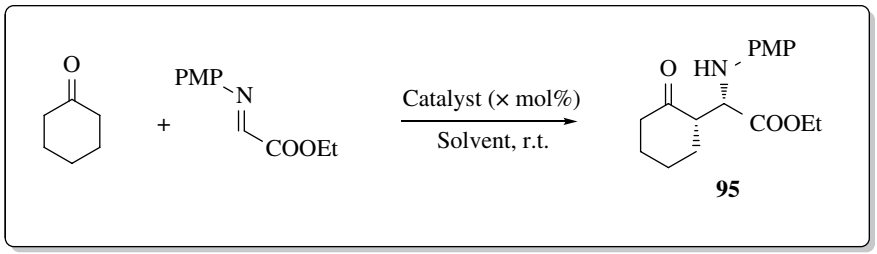

**SCHEME 11.11** The first catalytic asymmetric Mannich reaction.



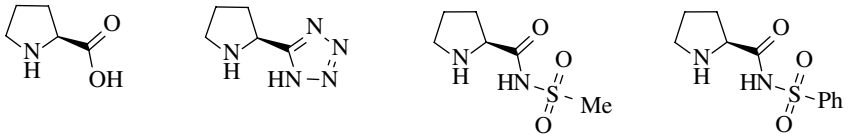

**SCHEME 11.12** Proline-catalyzed asymmetric Mannich reaction.

L-proline-based catalysts were consequently developed. For example, the incorporation of a tetrazole moiety, which is widely applied in medicinal chemistry as a carboxylic acid bioisostere, increased the solubility of the proline tetrazole catalyst **92** in more lipophilic solvents (e.g., $CH_2Cl_2$) [63]. Furthermore, besides catalyst loading (only 1 mol% is required), the reaction time could be reduced tremendously when compared to the classical L-proline-catalyzed version without affecting the enantioselectivity of the reaction. Other carboxylic acid surrogates, which also have been incorporated into L-proline, are acylsulfonamides (Scheme 11.13, **93** and **94**). However, despite an increased solubility in lipophilic solvents, this type of proline analogs requires an equally high catalyst loading (around 20 mol%) to obtain high enantioselectivities [63].

Except for increasing the solubility and the catalytic efficiency of L-proline, modifications on the pyrrolidine ring may additionally change the stereochemical outcome of the asymmetric Mannich reaction from *syn*-selective to *anti*-selective by fixing the enamine transition state in a different conformation. For example, Barbas and coworkers found that (3*R*,5*R*)-5-methyl-3-pyrrolidinecarboxylic acid (**96**) catalyzes the Mannich reaction between various aldehydes and *N-para*-methoxyphenyl (PMP)-protected iminoglyoxylates affording the corresponding *anti*-β-amino aldehydes in high stereoselectivities (Scheme 11.14) [64]. This completely inverted stereochemical outcome presumably is based on the preferred s-*cis* conformation of the (*E*)-enamine transition state as a result of steric interactions between a substituent in 5-position of the pyrrolidine ring (here methyl), which is unable to initiate proton transfer to the imine, and the allyl moiety. Attack of the enamine occurs from the *re*-face (*re* if substituent R is of highest priority) onto the *si*-face of the (*E*)-imine resulting in the formation of the corresponding *anti*-diastereomers. In this particular case, attack on the *si*-face of the imine is controlled by proton transfer from the carboxylic acid to the nitrogen of the imine, which increases the electrophilicity of the imine.




**95**




| | **90** | **92** | **93** | **94** |
|---|---|---|---|---|
| Catalyst loading (mol%) | 20 | 1 | 20 | 20 |
| Solvent | DMSO | $CH_2Cl_2$ | $CH_2Cl_2$ | THF |
| Reaction time (h) | 24 | 16 | 24 | 24 |
| Yield (%) | 81 | 70 | 82 | 87 |
| dr (*syn*/*anti*) | >19/1 | >19/1 | >19/1 | >19/1 |
| $ee_{syn}$ (%) | >99 | >99 | 96 | >99 |

**SCHEME 11.13** Application of more lipophilic L-proline derivatives in the asymmetric Mannich reaction.

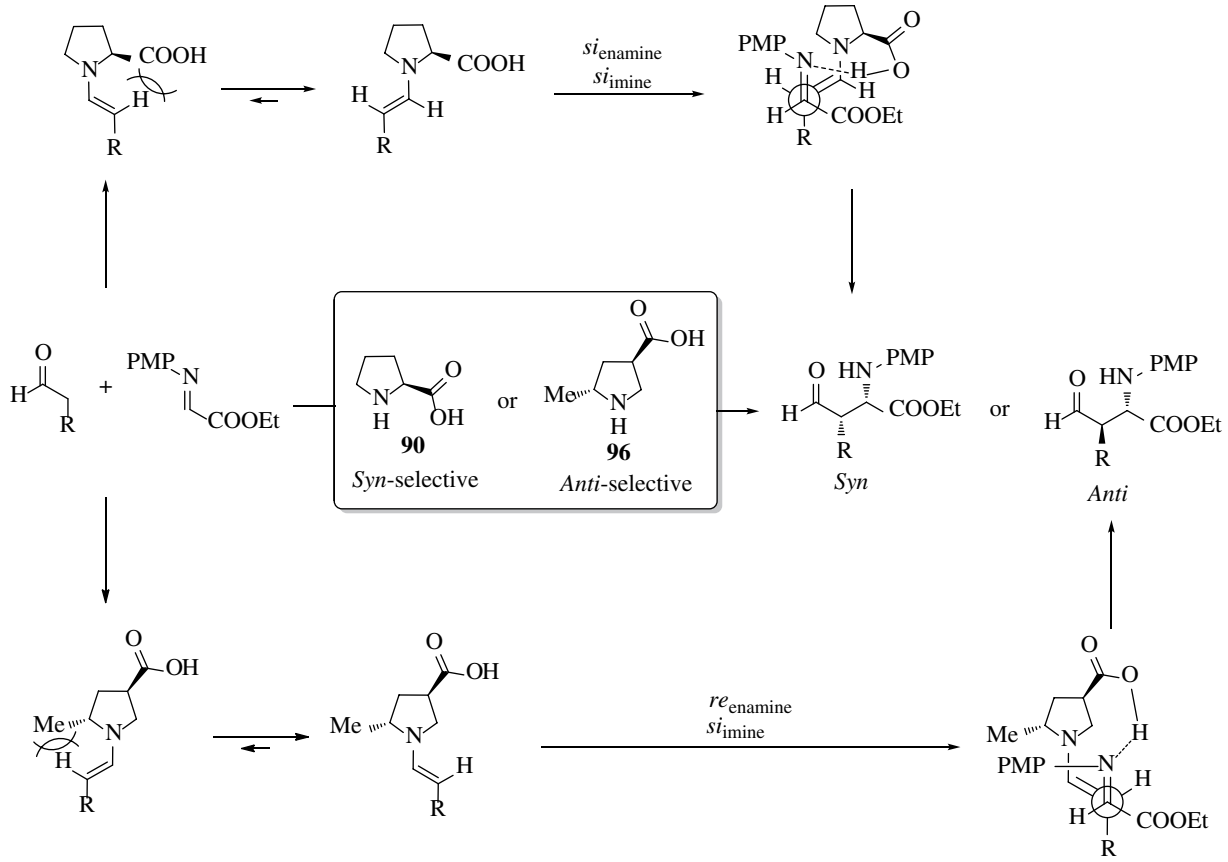
If C–C bond formation occurs at the *si*-face of the enamine (in the case of L-proline as catalyst), the corresponding *syn* diastereomers are formed.

However, this type of catalyst was unable to effectively catalyze the Mannich reaction between ketones and *N*-PMP-protected α-imino esters. This observation might originate from the very slow formation of the enamine due to steric interactions between the ketone and the methyl group of **96**. If the methyl group is omitted though, the corresponding (*R*)-3-pyrrolidinecarboxylic acid (**97**) was found to effectively catalyze the Mannich reaction affording the *anti*-diastereomer with high stereoselectivities (Scheme 11.15) [65]. Although the s-*cis* conformation and the s-*trans* conformation of the (*E*)-enamine have similar free energies, C–C bond formation should proceed from the s-*cis* conformer due to the spatial proximity of the nucleophilic carbon of the enamine and the electrophilic imine.

Other proline-derived catalysts promoting the selective formation of the *anti*-diastereomer have been developed, for example, by the groups of Maruoka (axially chiral amino sulfonamides **98**, $C_2$ symmetric chiral pyrrolidine-based amino sulfonamides **99**) [66, 67] and Córdova (diarylprolinols **100**) [68], among others, involving Coulombic or steric interactions (or both) as well to lock the transition state in the conformation required for stereoselective catalysis (Figure 11.3).

Although very good chemical yields and stereoselectivities can be accomplished, these catalytic processes still require rather high catalyst loadings. Moreover, after the reaction, both catalyst and product need to be separated from the reaction mixture by time-, waste- and cost-intensive techniques. Immobilization of the catalyst, which facilitates separation from the reaction mixture and recycling of the catalyst, consequently may lead to more ecological sustainable processes [69]. For example, the Mannich reaction between acetone and *N*-PMP-imine afforded the corresponding β-aminoketone **102** in 81% yield and 96% ee when utilizing a PEG-bound proline catalyst (**101**), which was prepared from (2*S*, 4*R*)-4-hydroxyproline (Scheme 11.16) [70]. However, the reaction requires a high catalyst loading (30%) and prolonged reaction times (72 h). Recycling of the catalyst by filtration and subsequent reuse did not affect the enantioselectivity of the reaction, although a decreased yield for each cycle was detected.

Thinking one step further, the incorporation of an immobilized proline catalyst into a continuous flow reactor might improve the performance of the asymmetric Mannich reaction because some Mannich products are rather labile and often suffer from degradation or epimerization upon purification [71]. Besides an increased process efficiency, for example, by reducing the amount of solvents needed, by-products formed and hence purification steps required, the application of flow chemical processes, in general, exhibits a variety of unique advantages over classical batch processes: (i) increased reaction rates, selectivity, and yields, due to rapid mixing and optimized thermal management; (ii) accessibility of exothermic and runaway reactions, as a consequence of the unparalleled heat transfer properties; and (iii) increased safety, as flow reactors provide a safe, self-contained environment to carry out reactions, which might be hazardous in batch because of



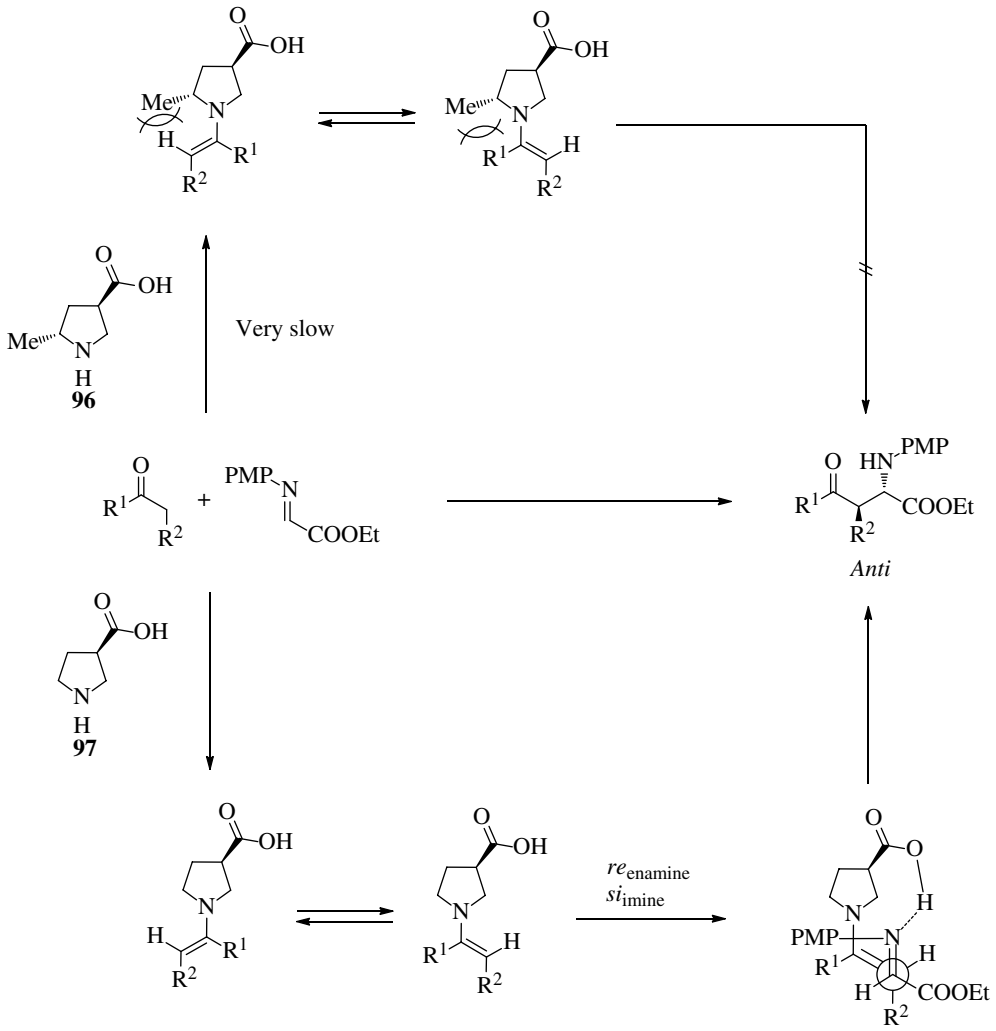

**SCHEME 11.14** Postulated transition states leading to the formation of either the *syn*- or *anti*-diastereomer.

the necessity of large amounts of toxic or explosive reagents [72]. The first asymmetric Mannich reaction that was performed under continuous flow utilizing an immobilized proline catalyst was reported by the lab of Pericàs. Here, the polymeric matrix was functionalized with (2*S*, 4*R*)-4-hydroxyproline using the well-established copper-catalyzed azide alkyne cycloaddition reaction (CuAAC) combining readily available azido-modified polystyrene and *O*-propargyl hydroxyproline [73]. Based on this approach, the authors were able to produce up to 7.8 mmol of the desired Mannich product using 0.46 mmol catalytic resin (5.9%) without the need of an additional purification step (except for evaporation of the solvent and starting aldehyde) (Scheme 11.17).

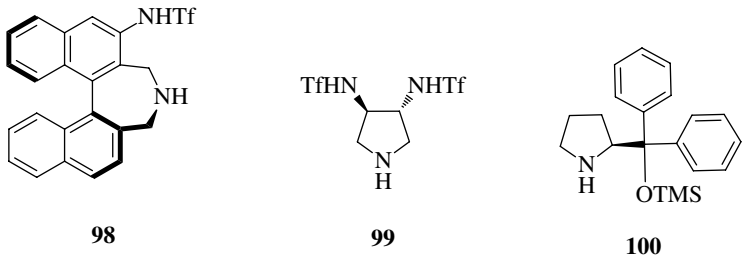
The same group was also able to establish a continuous flow process leading to the formation of the *anti*-Mannich product with high diastereo- and enantioselectivities. Here, instead of immobilized (2*S*, 4*R*)-4-hydroxyproline **103**, polystyrene-supported (3*S*, 4*S*)-3-amino-4-hydroxypyrrolidine **106** was used as catalyst (Scheme 11.18) [74].

### 11.2.2 Chiral Brønsted Bases as Catalysts in Asymmetric Mannich Reactions

As outlined previously, the reaction between an enantiomerically pure enamine and an imine induces the stereoselective formation of a new C–C bond during the course of the asymmetric Mannich reaction. In this case, protonation of the imine seems essential to enhance its electrophilicity and to facilitate the nucleophilic attack on the resulting iminium ion. On the other hand, it is also possible to react a neutral imine with a carbon nucleophile in a Mannich reaction. However, this approach is often limited to imines that are equipped with an electron-withdrawing substituent on the imine nitrogen to increase the electrophilicity of the imine. The nucleophile, most often an active methylene compound, forms upon deprotonation with a chiral tertiary amine a chiral ion pair that attacks the electrophilic Mannich acceptor in an highly enantioselective fashion. Only a few examples rely solely on Brønsted base interactions for asymmetric catalysis, though [75, 76]. For example, Jørgensen and coworkers described the highly diastereo- and enantioselective Mannich reaction combining α-aryl-substituted cyanoacetates and *N*-Boc-protected iminoglyoxylates in the presence of the chiral tertiary amine catalyst **108**, which is derived from naturally occurring optical pure quinidine (Scheme 11.19). Besides a variety of α-aryl-substituted cyanoacetates, cyclic β-ketoesters were tolerated as well as substrates in the catalytic process leading to the corresponding Mannich products in excellent yields and stereoselectivities [77].



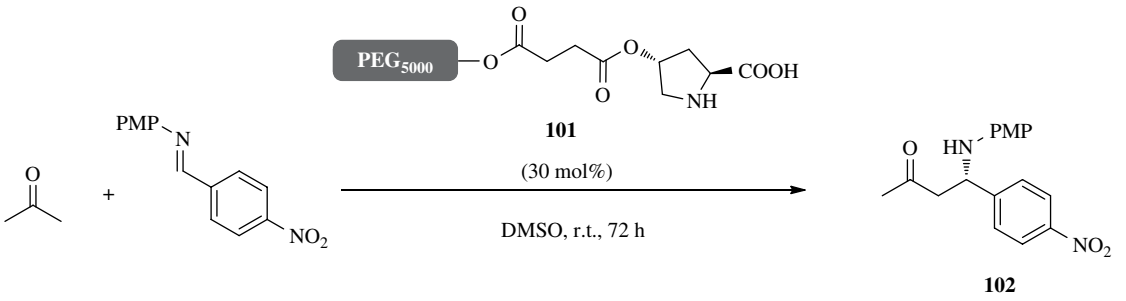

**SCHEME 11.15** *Anti*-selective Mannich reaction between ketones and N-PMP-protected α-imino esters.




**98** **99** **100**

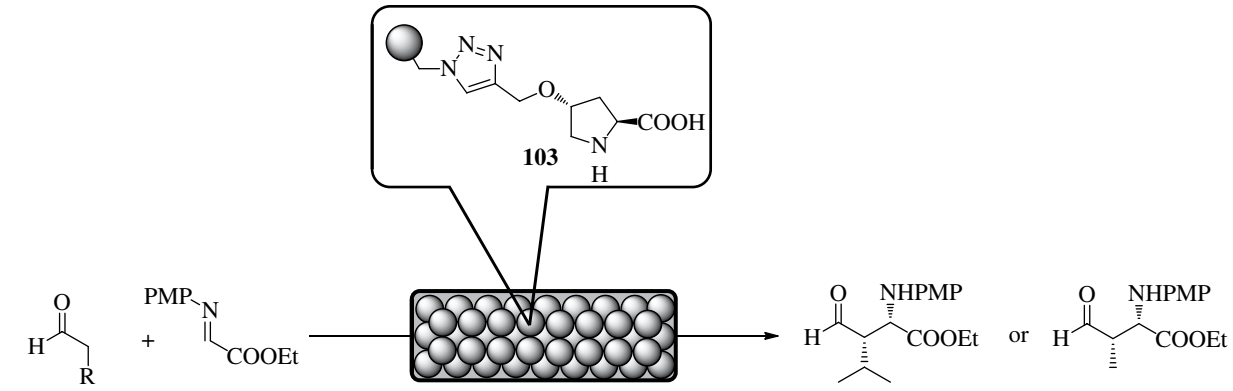
**FIGURE 11.3** Examples of highly *anti*-selective catalysts for the asymmetric Mannich reaction.

In general, most chiral Brønsted base catalysts are equipped with an additional hydrogen bond donor (Brønsted acid), which activates the electrophile. Moreover, coordination of both the nucleophile and electrophile to the rigid chiral backbone of the bifunctional catalyst via hydrogen bonding and a basic tertiary amine anchors the electrophile and nucleophile in an optimal transition state, which seems essential for the highly stereoselective and predictable formation of a new C–C bond. In this respect, alkaloids from *Cinchona* and derivatives thereof have been studied in various enantioselective transformations. These types of alkaloids contain a quinuclidine ring and a hydroxyl group attached to a chiral carbon, which contribute to their bifunctional catalytic property. For example, cinchonine (**110**) has been successfully employed in the asymmetric Mannich reaction between β-ketoesters and acyl aryl imines (Scheme 11.20) [78].




1st cycle: 81% yield, 96% ee
2nd cycle: 71% yield, 96% ee
3rd cycle: 64% yiedl, 97% ee

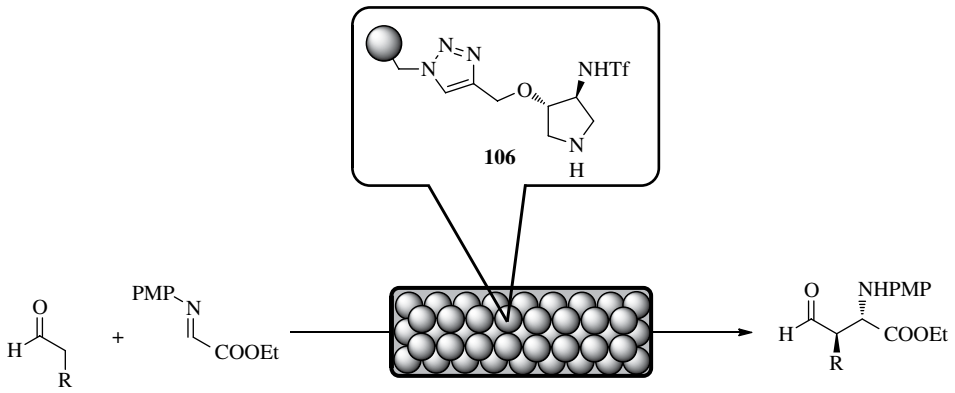
**SCHEME 11.16** Asymmetric Mannich reaction catalyzed by a polymer-supported proline catalyst.




7.8 mmol
dr > 97/3
> 99% ee

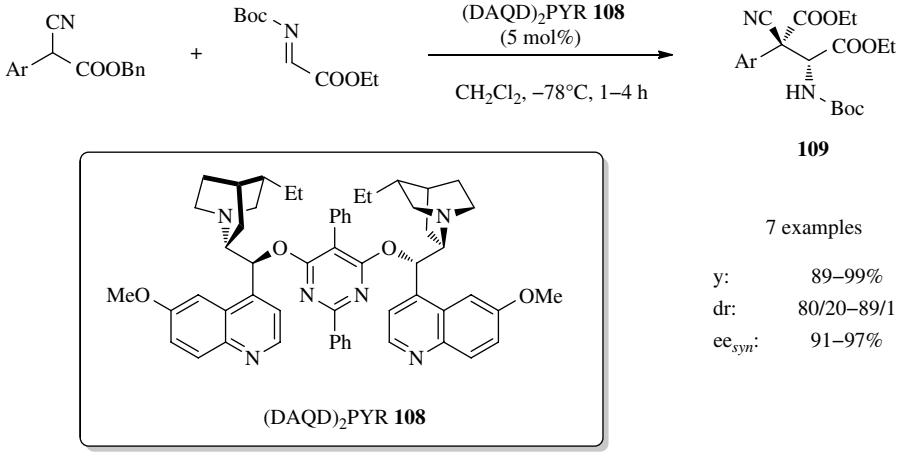
6.6 mmol
dr > 97/3
> 99% ee

**SCHEME 11.17** Production of *syn*-Mannich products from aldehydes in continuous flow.

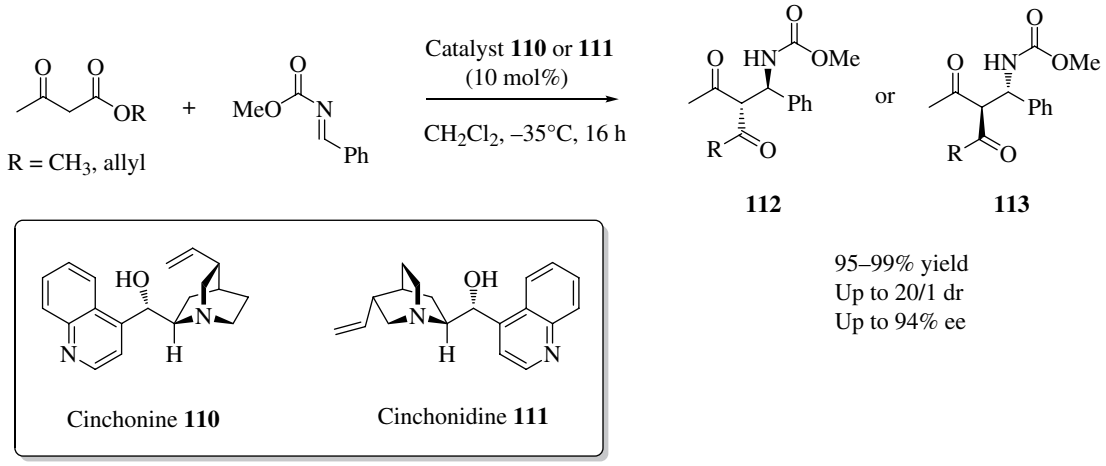



Up to 16.7 mmol
" dr = 93/7
" 97% ee

**SCHEME 11.18** Production of *anti*-Mannich products from aldehydes in continuous flow.




**SCHEME 11.19** Brønsted base-catalyzed asymmetric Mannich reaction.



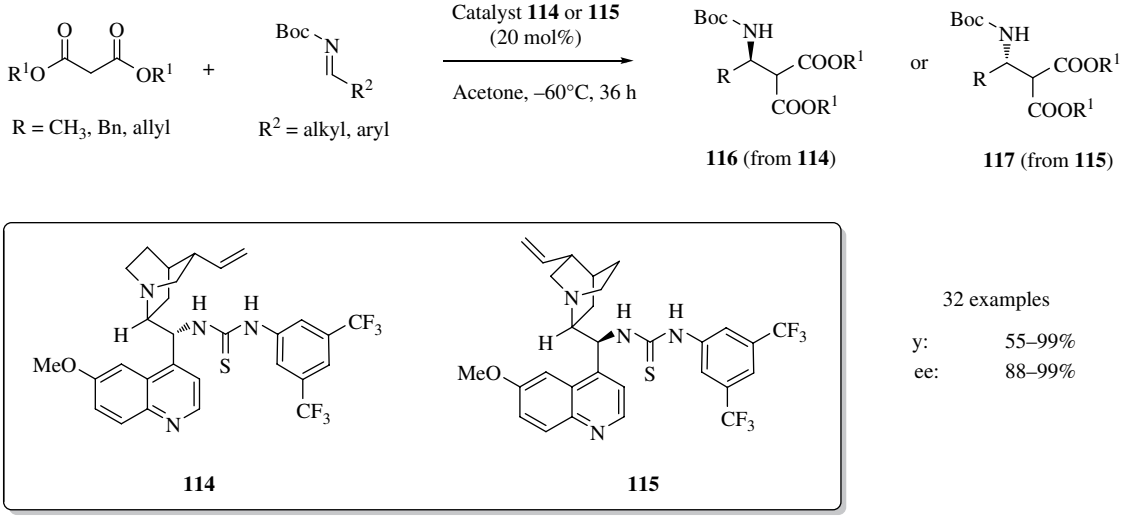

**SCHEME 11.20** Cinchona alkaloids as catalysts in the asymmetric Mannich reaction.

In addition, the opposite enantiomer of the Mannich product (**113**) was easily accessible using the pseudoenantiomer cinchonidine (**111**) instead as catalyst [78].

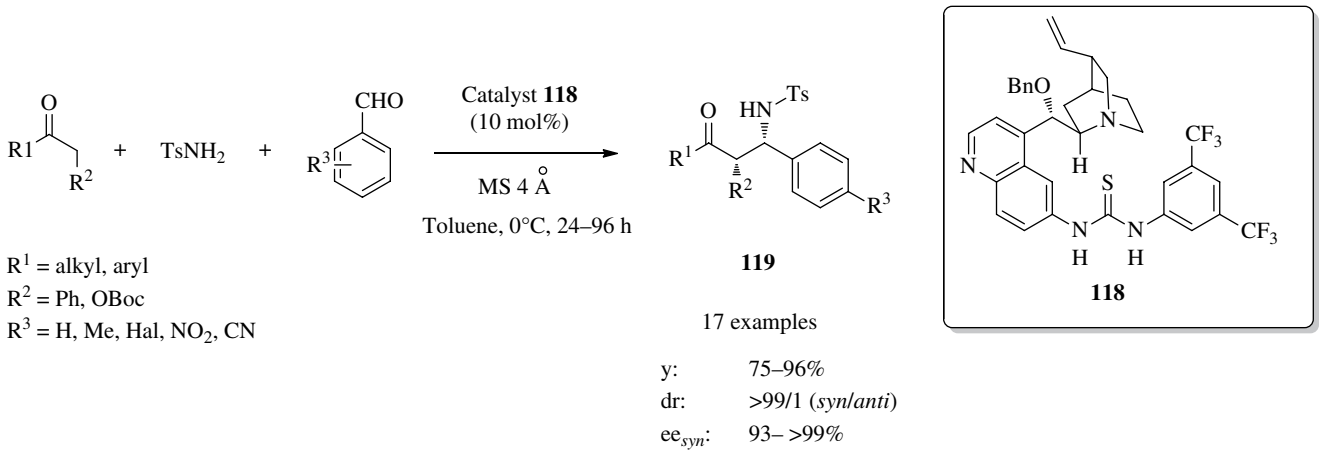
The catalytic performance of these cinchona alkaloids could be improved significantly by incorporating a urea or thiourea moiety, which are well known for their superior hydrogen-bonding activity, and an electron-withdrawing group adjunct to the (thio)urea moiety. For example, Deng and coworkers investigated the Mannich reaction between various *N*-Boc-protected imines and malonate diesters. After optimization of the reaction conditions, the desired products were obtained in excellent yields and enantioselectivities utilizing the quinidine-derived thiourea catalysts **114** and the quinine-derived thiourea catalysts **115**, which affords the opposite enantiomer (Scheme 11.21) [79].

However, the tolerated substrate scope of this methodology is rather low being limited to only substituted 1,3-dicarbonyl compounds. This limited applicability was improved recently by the lab of Zhao, which developed a bifunctional quinidine thiourea catalyst (**118**) able to promote the highly diastereo- and enantioselective Mannich reaction between aromatic aldehydes, *para*-toluenesulfonamide, and unfunctionalized ketones (Scheme 11.22) [80].

The dual activation mode of the aforementioned cinchona alkaloid-derived thiourea catalysts proved to be highly effective in catalyzing the asymmetric Mannich reaction, among other transformations. These findings prompted the development of new, more simple bifunctional chiral catalysts that are predominately based on *trans*-1,2-diaminocyclohexane. For example, the application of the thiourea catalyst **120**, which was developed by Takemoto and coworkers, afforded upon the reaction of *N*-Boc-protected imines with diethyl malonate the desired chiral amines in good chemical yields (up to 91%) and enantioselectivities (98% ee) (Scheme 11.23) [81]. The catalytic mechanism presumably involves deprotonation and coordination of the active carbonyl compound by the chiral tertiary amine moiety. The formed enolate then attacks the *si*-face of the




**SCHEME 11.21** Bifunctional cinchona alkaloid/thiourea-catalyzed asymmetric Mannich reaction.

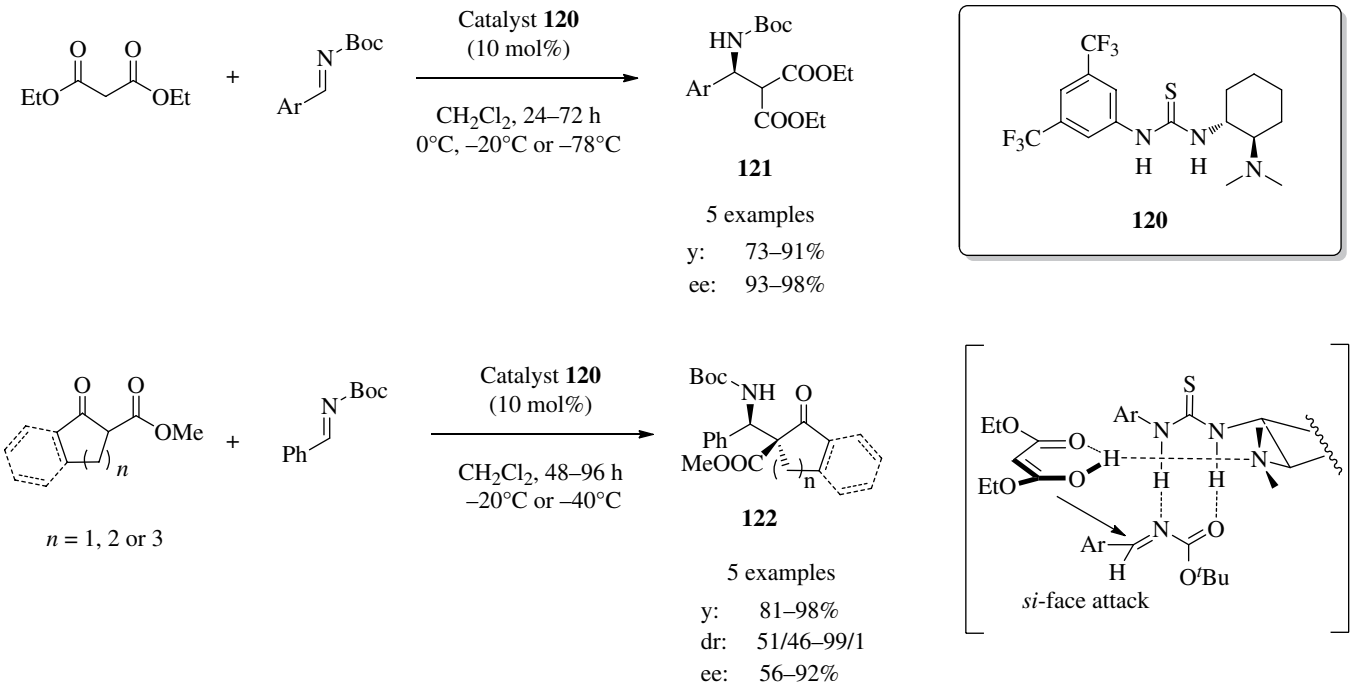



**SCHEME 11.22** Three-component direct asymmetric Mannich reaction catalyzed by a bifunctional quinidine thiourea catalyst.

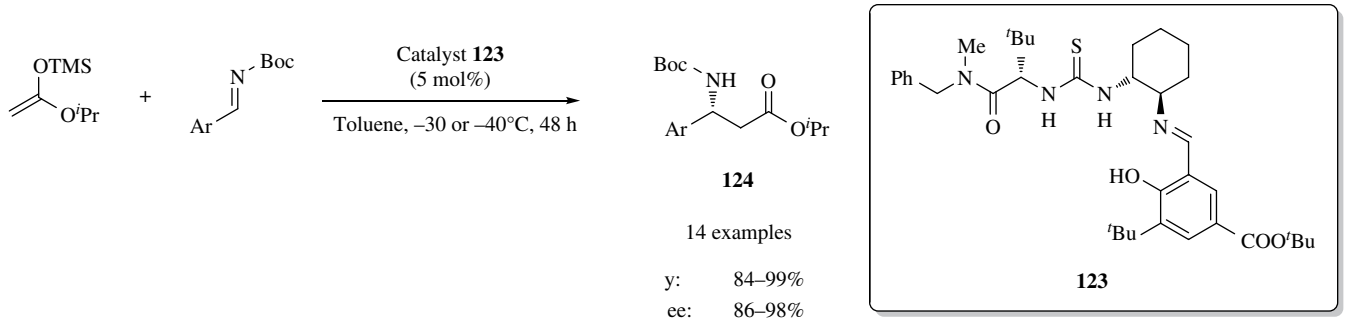
imine, which is coordinated and activated by the thiourea functionality via hydrogen bonding. However, upon the reaction of *N*-Boc-protected imines with prochiral nucleophiles, no diastereoselectivity was observed, which might be a result of epimerization during the reaction. To prevent epimerization, cyclic 1,3-dicarbonyl compounds having a substituent at the C-2 position were employed as substrates. A series of cyclic substrates were tested in the Mannich reaction with thiourea catalyst **120**, but the observed selectivities varied much [81].

It must be noted that chiral thiourea catalysts have been used earlier to catalyze the asymmetric Mannich reaction. Jacobsen and Wenzel reported the enantioselective synthesis of *N*-Boc-protected β-amino acids from silyl ketene acetals and *N*-Boc-protected imines using the thiourea catalyst **123** (Scheme 11.24). Here, the chiral thiourea-derived Brønsted acid catalyst (the application of chiral Brønsted acids in the asymmetric Mannich reaction will be discussed in more detail in the forthcoming chapter) coordinates the imine via hydrogen bonding and helps to distinguish between the enantiotopic faces of the imine. The reaction performed extremely well at low temperatures (−40 to −30°C), which suppressed the noncatalytic (racemic) pathway leading to the desired Mannich products [82].

More recently, guanidines have emerged as versatile catalysts in various organic transformations. Besides their strong Brønsted basicity, guanidines additionally can function as hydrogen bond donors as well. These features prompted the development of chiral guanidines, which can be used as catalyst in asymmetric reactions [83–85]. However, the application of guanidine-derived catalysts has only been marginally explored yet in the Mannich reaction. For example, the bicyclic guanidine catalyst **125**, which was developed by the lab of Tan, catalyzed the stereoselective



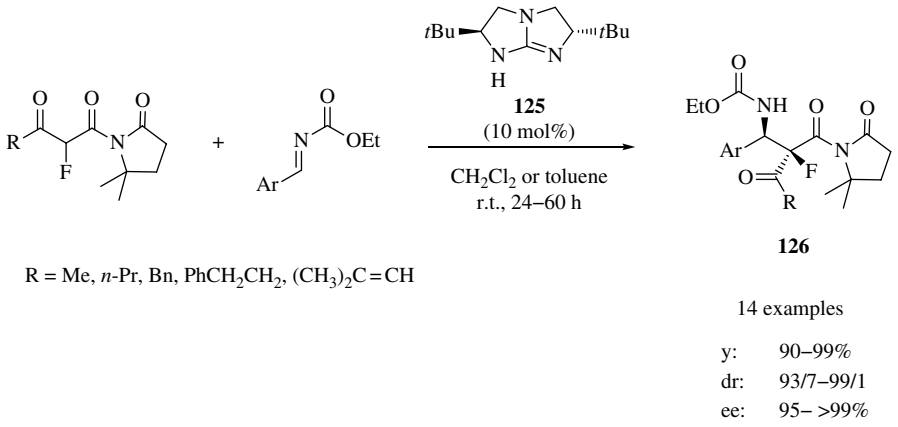

**SCHEME 11.23** Chiral thiourea-catalyzed asymmetric Mannich reaction.



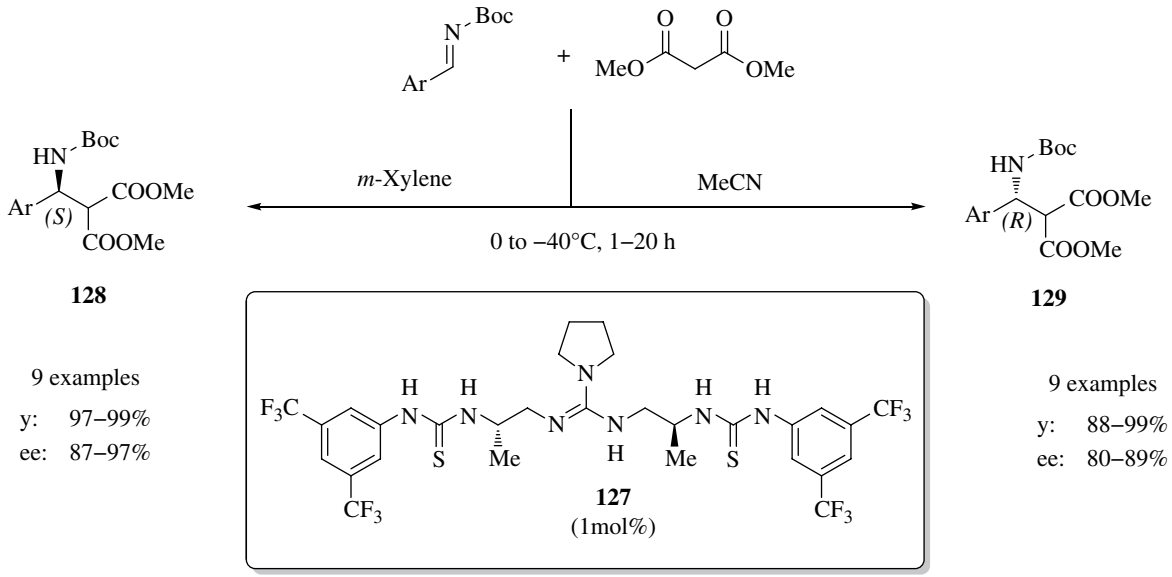

**SCHEME 11.24** Chiral thiourea-catalyzed asymmetric Mannich reaction between silyl ketene acetals and imines.

C–C bond formation between *N*-Eoc-protected imines and β-keto acetyloxazolidinone [86]. Excellent results were obtained with imines bearing either an electron-withdrawing or an electron-donating aryl group. Furthermore, the outlined protocol tolerated β-keto acetyloxazolidinone with different aliphatic substituents. Although longer reaction times were required, no adverse effect on neither the diastereo- nor enantioselectivity could be detected (Scheme 11.25).

Connecting a thiourea moiety to a guanidinium base can improve catalysis further. Nagasawa and coworkers described the application of such an open-chain guanidine/bisthiourea organocatalyst **127** in the asymmetric Mannich reaction between *N*-Boc-protected imines and dimethyl malonate [87]. The stereochemical outcome of the reaction was strongly influenced by the reaction medium. In nonpolar solvents, such as *m*-xylene, predominately the *S*-enantiomers were formed, whereas in polar solvents like acetonitrile, almost exclusively the *R*-enantiomers were obtained. Both isomers were generally obtained in enantioselectivities exceeding 80% ee (Scheme 11.26). Based on kinetic analyses, the authors speculated that the solvent-dependent stereodiscrimination is controlled by an enthalpy–entropy compensation. Moreover, control experiments with derivatives of **127** lacking either the thiourea or the Brønsted basic guanidine moiety proved that the bifunctional character is essential for catalysis. If the basic guanidine moiety is omitted, no products could be isolated, whereas the absence of the thiourea moiety affords the product in excellent chemical yield, however, as a racemic mixture [87].




**SCHEME 11.25** Chiral guanidine-catalyzed asymmetric Mannich reaction.

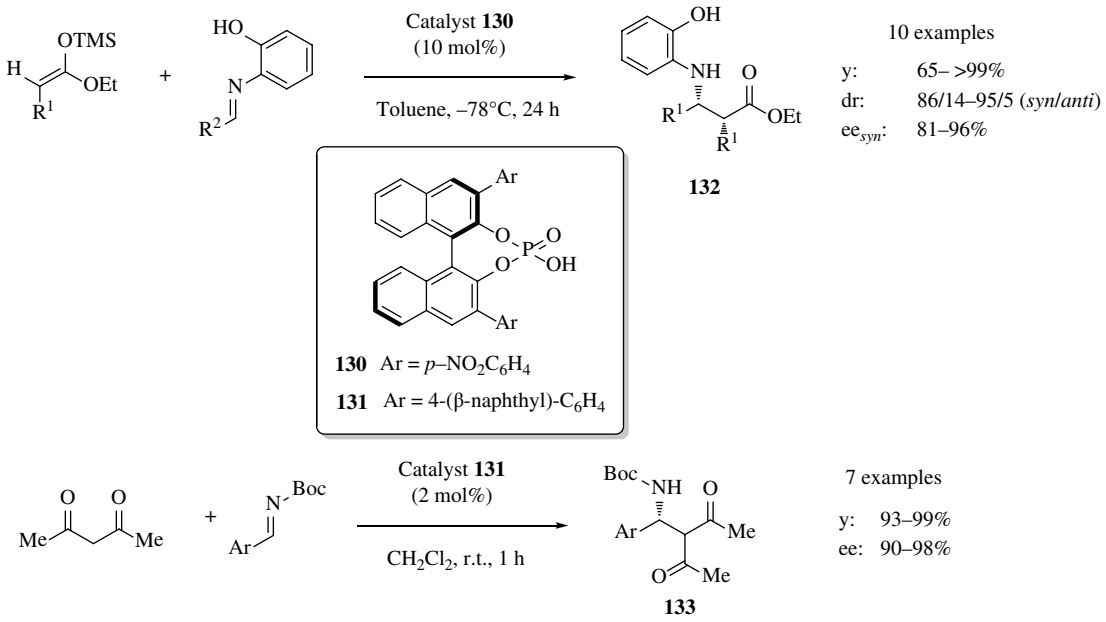



**SCHEME 11.26** Bifunctional chiral guanidine/bisthiourea-catalyzed asymmetric Mannich reaction.

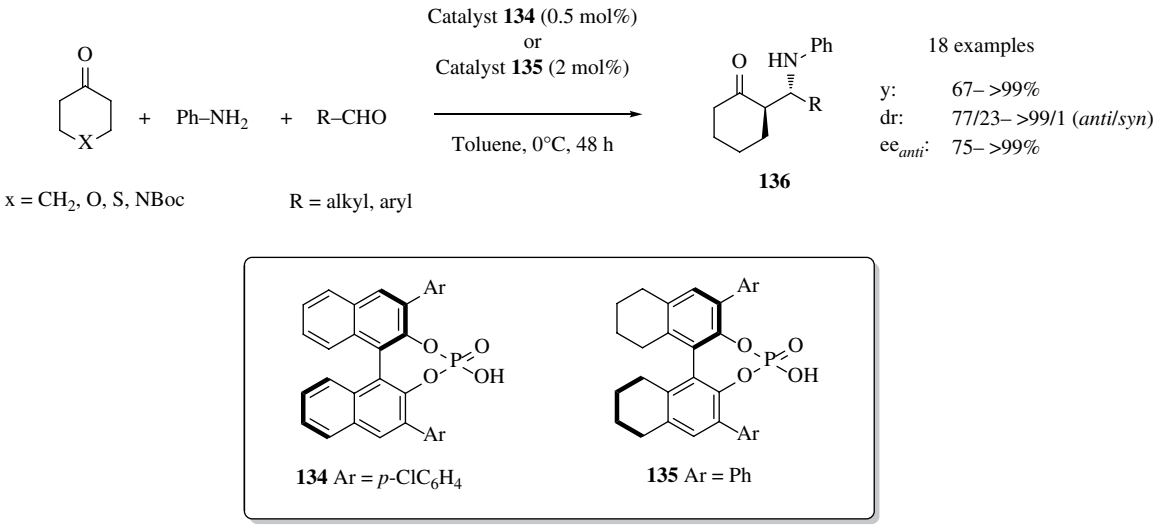
### 11.2.3 Chiral Brønsted Acids as Catalysts in Asymmetric Mannich Reactions

As outlined in the previous paragraph, chiral Brønsted base organocatalysts appear to be most effective when equipped with an additional Brønsted acidic moiety, for example, hydrogen bond donors like (thio)urea. Apparently, both functionalities catalyze the asymmetric Mannich reaction in a cooperative fashion, that is, simultaneous activation of both the nucleophile and the electrophile. However, activation of the electrophile can also be accomplished with a single, enantiomerically pure Brønsted acid. In this respect, readily available chiral phosphoric acids are most commonly applied [88–90]. In 2004, the groups of Akiyama and Terada independently from each other reported the first asymmetric Mannich reaction of silyl ketene acetals or acetyl acetone with imines utilizing chiral phosphoric acid catalysts, which are derived from 1,1′-bi-2-naphthol (BINOL) (Scheme 11.27) [91–93]. Besides activation of the imine via hydrogen bonding, the phosphoryl oxygen creates a Brønsted basic site, which is additionally involved in substrate binding. Moreover, fine-tuning of the substituent pattern at the 3,3′-position of the BINOL backbone, which creates a chiral substrate recognition site, is essential for obtaining high diastereo- and enantioselectivities [94].

The scope of the Brønsted acid-catalyzed asymmetric Mannich reaction was later extended by Gong and colleagues, which used instead of silyl ketene acetals or acetyl acetone simple ketones as nucleophiles [95]. The combination of various cycloketones, phenylamines, and aldehydes in the presence of the chiral phosphoric acid catalyst **134** or **135**, respectively, afforded the corresponding *anti*-Mannich products in high yields with good enantioselectivities (75–98% ee)



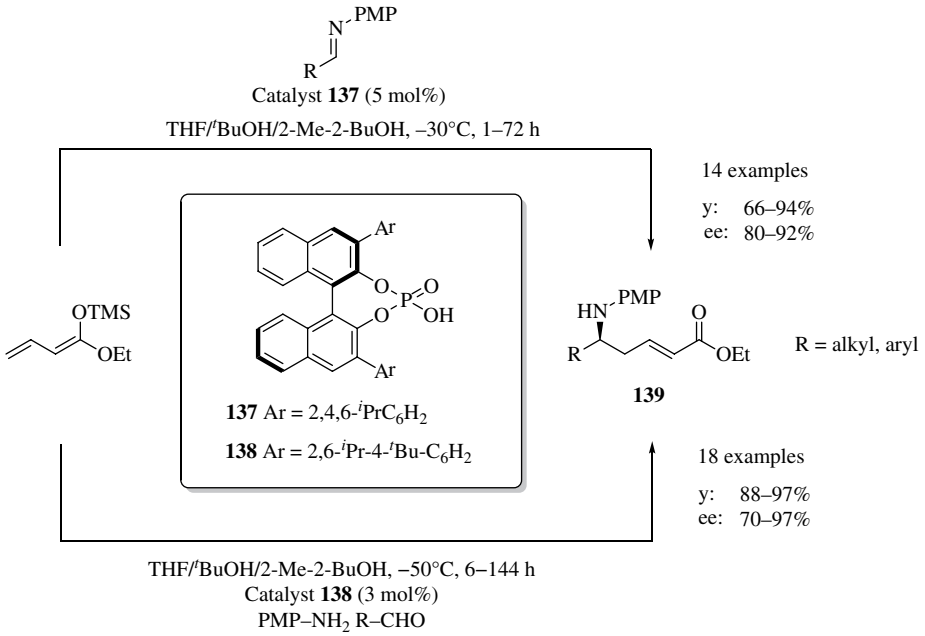

**SCHEME 11.27** Asymmetric Mannich reaction catalyzed by chiral phosphoric acids.



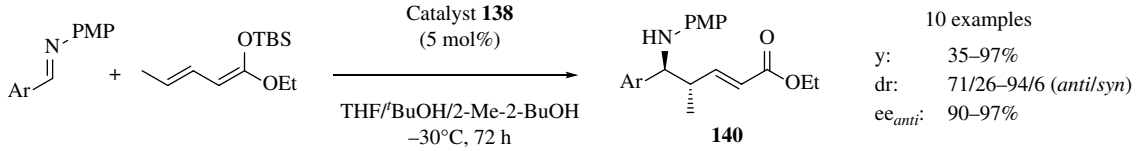

**SCHEME 11.28** Three-component asymmetric Mannich reaction catalyzed by chiral phosphoric acids.

and diastereoselectivities (4/1 to 49/1) depending strongly on the nature of the substituent on benzaldehyde (Scheme 11.28).

Similar BINOL-derived phosphoric acids were also found to effectively catalyze the asymmetric vinylogous Mannich reaction. Sickert and Schneider reported that various *N*-PMP-protected imines react with acyclic silyl dienolates in the presence of the Brønsted acid catalyst **137** to afford the desired δ-amino α,β-unsaturated carboxylic esters (**139**) in good yields (83–94%) with complete regioselectivity and high enantioselectivities (80–92% ee) (Scheme 11.29) [96]. Remarkably, the one-pot three-component process (i.e., imine is formed *in situ*) is comparable to the two-component process with preformed imines. Later on, the same group described a superior second-generation catalyst (**138**) for the three-component asymmetric vinylogous Mannich reaction, which afforded the desired δ-amino α,β-unsaturated carboxylic esters in high yields (up to 97%) and enantioselectivities (in general >90% ee) over a wide range of substrates (Scheme 11.29) [97]. Moreover, γ-substituted silyl dienolates proved to be suitable nucleophiles in the vinylogous Mannich reaction, leading to the formation of γ-substituted δ-amino α,β-unsaturated carboxylic esters (**140**) with two stereocenters in modest yields (35–97%) though but good *anti*-diastereoselectivities (up to 94/6) and




**SCHEME 11.29** Vinylogous asymmetric Mannich reaction catalyzed by chiral phosphoric acids.

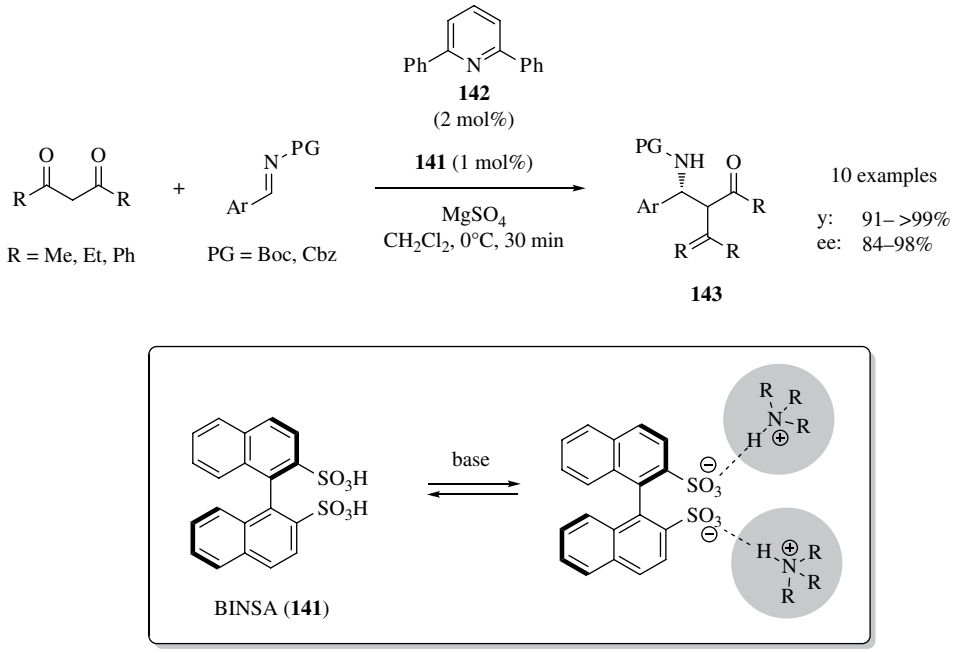



**SCHEME 11.30** Vinylogous asymmetric Mannich reaction between γ-substituted silyl dienolates and imines.

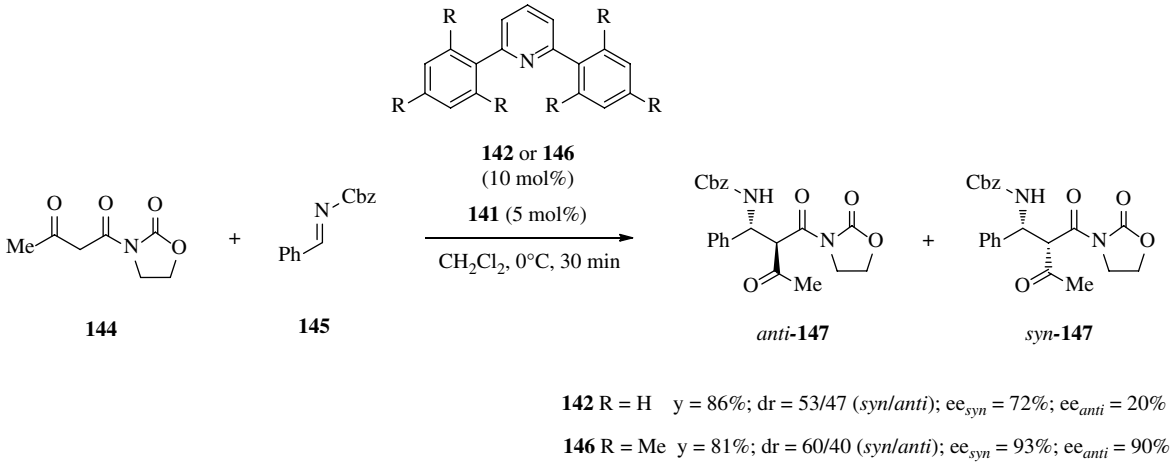
enantioselectivities (>90% ee) (Scheme 11.30) [97]. Additionally, besides cocrystallization of phosphoric acid **138** and *N*-benzylidene-4-methoxyaniline, NMR spectroscopic and mass spectrometric investigations were conducted to reveal the mechanism of the vinylogous Mannich reaction and the origin of the observed stereoinduction. The proposed catalytic cycle involves the formation of an iminium ion BINOL phosphate complex. Here, one of the 3-aryl groups shields the *re*-face of the iminium ion, hence directing the nucleophilic attack onto the opposite *si*-face [97].

In general, bulky substituents at the 3,3′-position of the BINOL backbone are required to achieve good selectivities in asymmetric catalysis. This laborious catalyst fine-tuning can be simplified when chiral 1,1′-binaphthyl-2,2′-disulfonic acid (BINSA, **141**) is used instead of the aforementioned BINOL-derived chiral phosphoric acids. Complexation with a suitable achiral amine enables to tune the bulkiness and Brønsted acidity *in situ* [98]. Based on this approach, Ishihara and coworkers combined various *N*-Boc- or *N*-Cbz-protected imines and acetyl acetone in the presence of BINSA (1 mol%) and 2,6-diphenylpyridine (**142**, 2 mol%) to afford the corresponding Mannich products in excellent yields and enantioselectivities (Scheme 11.31) [98]. However, the catalyst proved ineffective in promoting the stereoselective reaction between *N*-Cbz-protected imine **145** and 3-acetoacetyl-2-oxazolidinone (**144**). The reaction was quickly optimized by changing the achiral amine. If 2,6-dimesitylpyridine (**146**) instead of 2,6-diphenylpyridine (**142**) was used, the desired Mannich product could be isolated in 81% yield and 93% ee (Scheme 11.32) [98].

The best stereocontrol achieved in a Mannich reaction utilizing a chiral Brønsted acid catalyst so far was reported by Zhang and coworkers [99]. A small library of double axially chiral bisphosphorylimides was synthesized, whereas (*R*,*R*)-3,3′-bis(1-naphthyl)-BINOL bisphosphorylimide **148** proved to be most efficient catalyzing the asymmetric Mannich reaction between cyclohexanone, aniline, and *para*-nitrobenzaldehyde. The desired *syn*-β-amino ketone could be isolated in excellent yield (99%) exclusively as the *syn*-diastereomer (dr > 99/1) with excellent enantioselectivity (99% ee). Then, the scope of the catalyst was further explored by changing the aldehyde component. Benzaldehyde derivatives with both electron-withdrawing and electron-donating substituents afforded exclusively the *syn*-Mannich products in high yields and excellent enantioselectivities (Scheme 11.33). Moreover, the reaction was also shown to




**SCHEME 11.31** Brønsted acid–base combined salt catalyst for the asymmetric Mannich reaction.

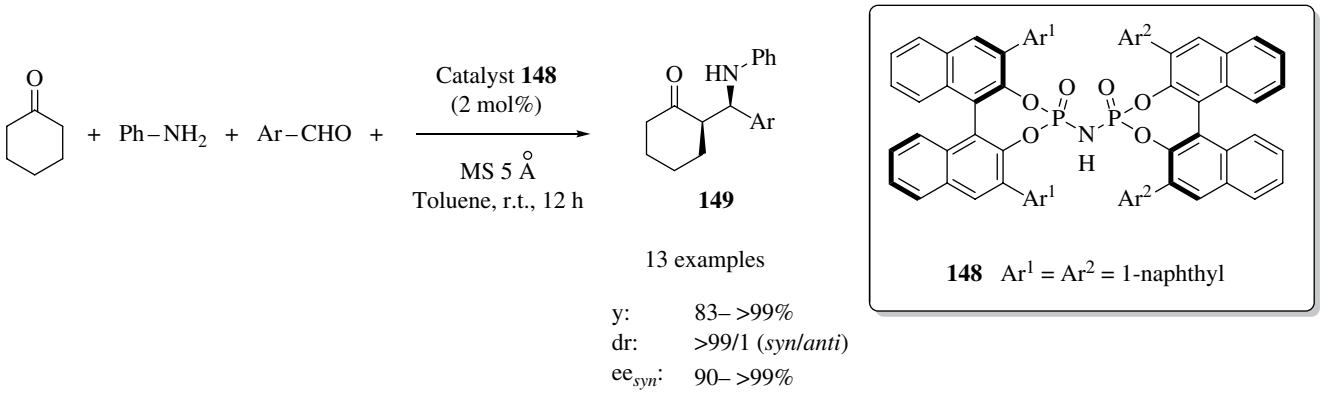



**SCHEME 11.32** Effect of the achiral amine counterpart in the Brønsted acid–base combined salt-catalyzed asymmetric Mannich reaction.

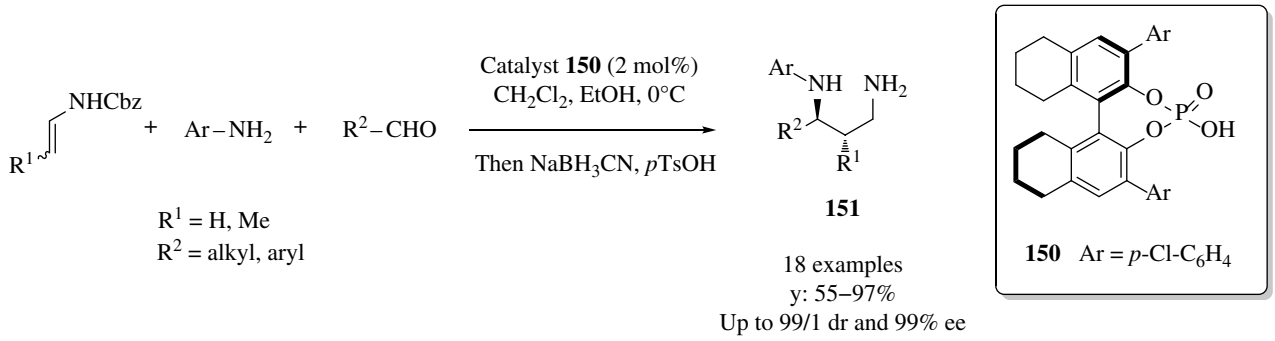
work on a gram scale without any loss of selectivity, which might open up the application of this methodology for the large-scale production of important synthetic intermediates.

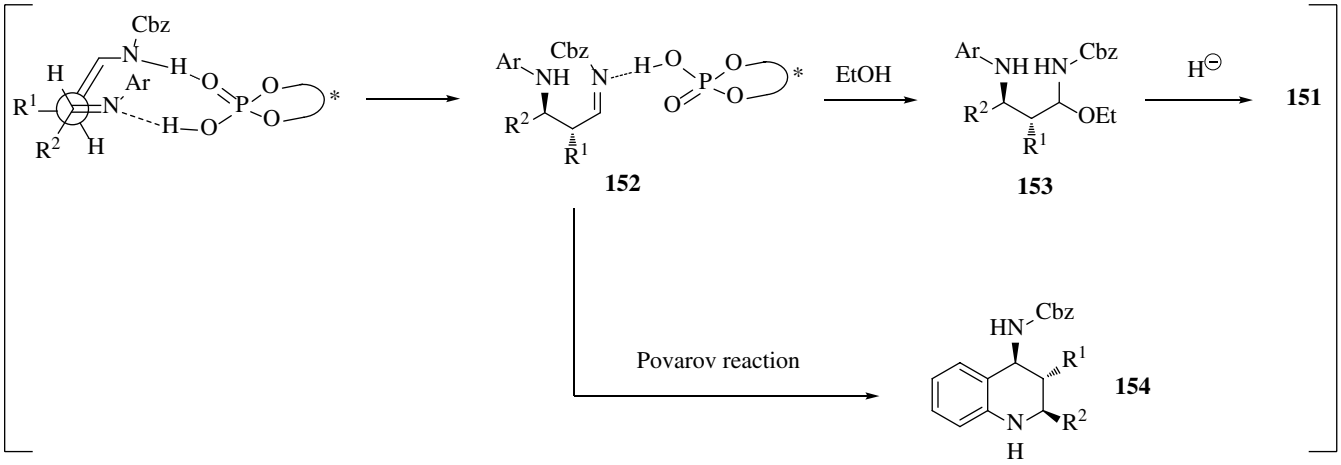
Chiral Brønsted acids have also been shown to effectively catalyze the Mannich reaction between aldehydes, anilines, and enecarbamates [100]. Here, the application of enecarbamates as nucleophilic species instead of ketones gives access to enantioenriched 1,3-diamines after subsequent reduction *in situ* with sodium cyanoborohydride. The potential of this approach was demonstrated by reacting various aromatic or aliphatic aldehydes and substituted enecarbamates with *para*-nitroaniline in the presence of the chiral phosphoric acid catalyst **150** (Scheme 11.34).

In general, good chemical yields (74–97%) and enantioselectivities (76–90% ee) were obtained. The application of substituted enecarbamates afforded the desired Mannich products in good yields with high *anti*-diastereoselectivities (dr > 95/5) and enantioselectivities (83–99% ee) regardless of the configuration of the enecarbamate. Probably *E*/*Z* isomerization is sufficiently faster than addition to the imine. Presumably, the chiral phosphoric acid catalyst **150** activates both imine and enecarbamate. Then, nucleophilic attack on the *si*-face of the *in situ* formed imine results in the formation of a new C–C bond and two stereocenters. Afterward, the *N*-acyl iminium intermediate **152** is trapped by ethanol resulting in the formation of aminoether **153**,




**SCHEME 11.33** Chiral bisphosphorylimides as catalyst in the asymmetric Mannich reaction.



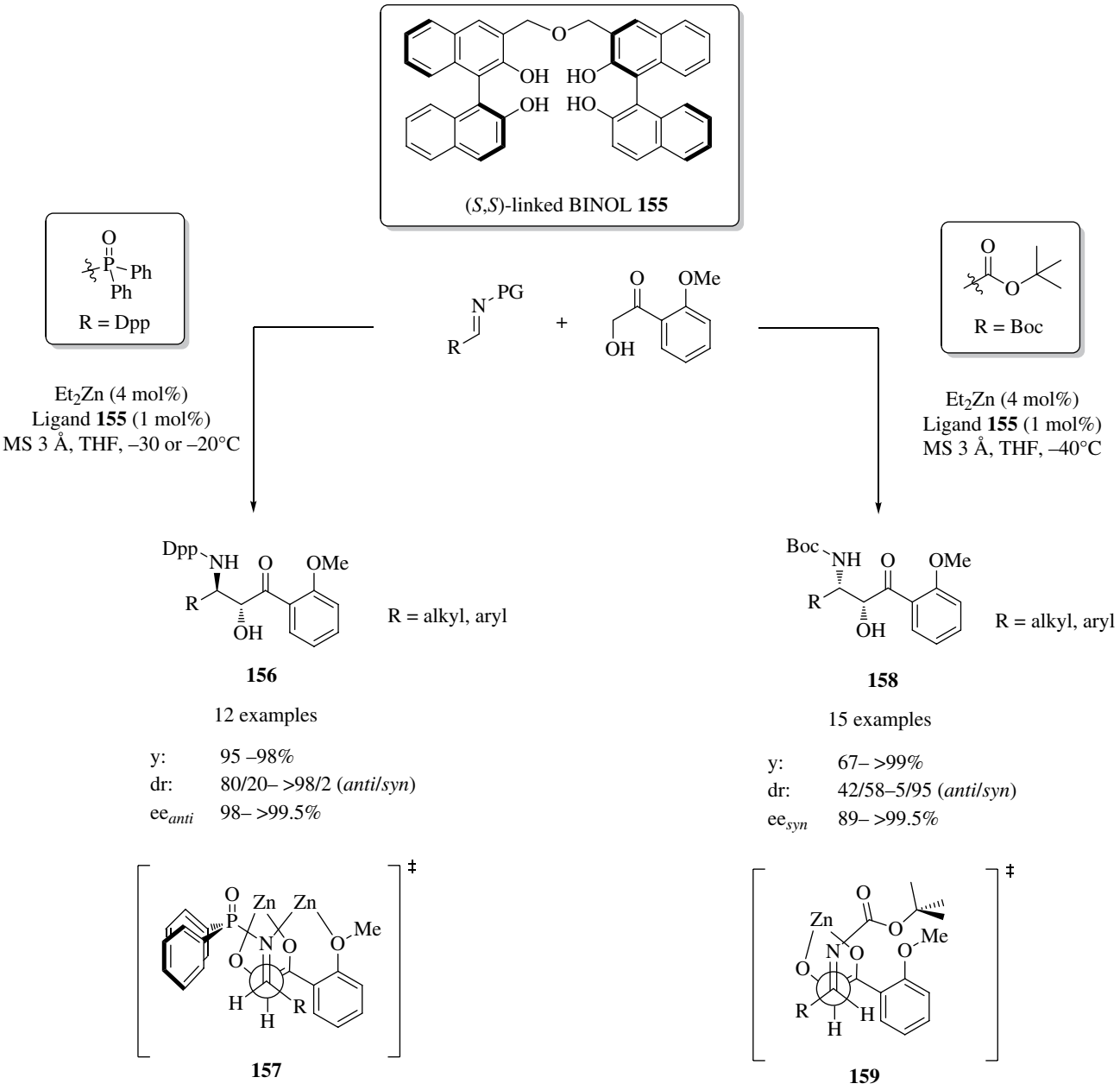




**SCHEME 11.34** Synthesis of *anti*-1,3-diamines in an asymmetric Mannich-type reaction.

which is reduced *in situ* to give the corresponding 1,3-diamine. Interestingly, if no ethanol is present in the reaction mixture, the *N*-acyl iminium intermediate **152** is intramolecularly trapped in an aza-Friedel–Crafts reaction to yield tetrahydroquinoline **154** (Povarov reaction [101]), which suggests that nucleophilic attack of ethanol onto the *N*-acyl iminium intermediate **152** interrupts the classical Povarov pathway.

### 11.2.4 Organometallic Catalysts in Asymmetric Mannich Reactions

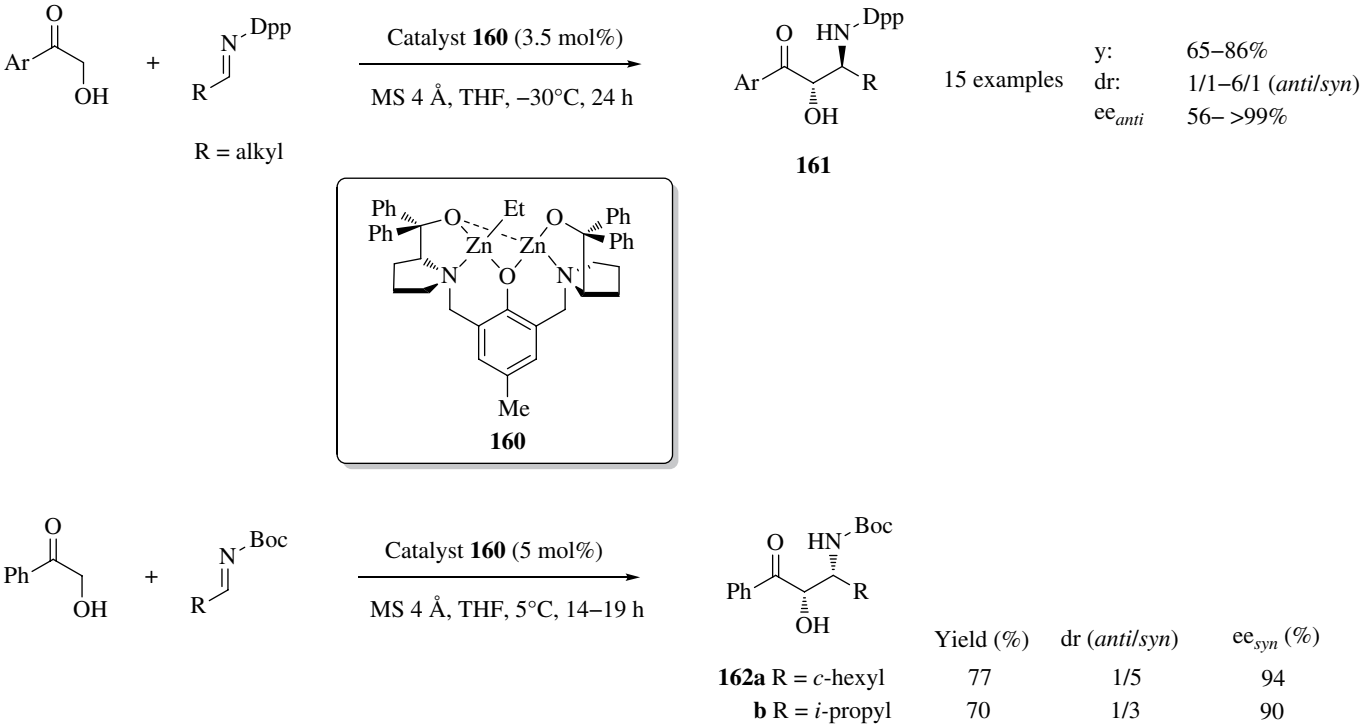
The application of chiral metal complexes in asymmetric catalysis has a long-standing tradition in creating novel C–C bonds in a highly stereoselective fashion due to the facile tunability of the catalyst [102–104]. In general, the metal center functions as Lewis acid that, in case of the Mannich reaction,




**SCHEME 11.35** N-Protective group-dependent highly *anti*- and *syn*-selective Mannich reaction.

predominately activates either the electrophilic imine, the nucleophilic carbonyl compound, or both simultaneously. Moreover, the metal center is most often coordinated by a Brønsted basic ligand, which deprotonates the metal-complexed carbonyl component. Due to steric interactions with the chiral ligands, nucleophilic attack of the enolate onto the imine is solely favored on either the *re*- or *si*-site, which explains the observed stereochemical outcome of the reaction. Consequently, the fine-tuning of the electronic and steric properties of the catalyst is essential to obtain good selectivities [105].

The first example of an asymmetric Mannich reaction, which is based on the application of a chiral organometallic catalyst, was reported by Shibasaki and colleagues using the heterobimetallic catalyst **88** affording the desired Mannich product in a rather modest enantioselectivity though, as stated previously (Scheme 11.11) [49]. A few years later, the same group disclosed a catalyst system formed from linked BINOLs (e.g., **155**) and diethyl zinc, which catalyzed the Mannich reaction between α-hydroxyketones and *N*-diphenylphosphinoyl (Dpp) imines affording almost exclusively the corresponding *anti*-*N*-protected-α-hydroxyl-β-amino ketones (**156**) in excellent yields and enantioselectivities (Scheme 11.35) [106]. Although a variety of *N*-Dpp-protected imines were tolerated as substrates in the Mannich reaction, the




| | Yield (%) | dr (*anti*/*syn*) | $ee_{syn}$ (%) |
|---|---|---|---|
| **162a** R = *c*-hexyl | 77 | 1/5 | 94 |
| **b** R = *i*-propyl | 70 | 1/3 | 90 |

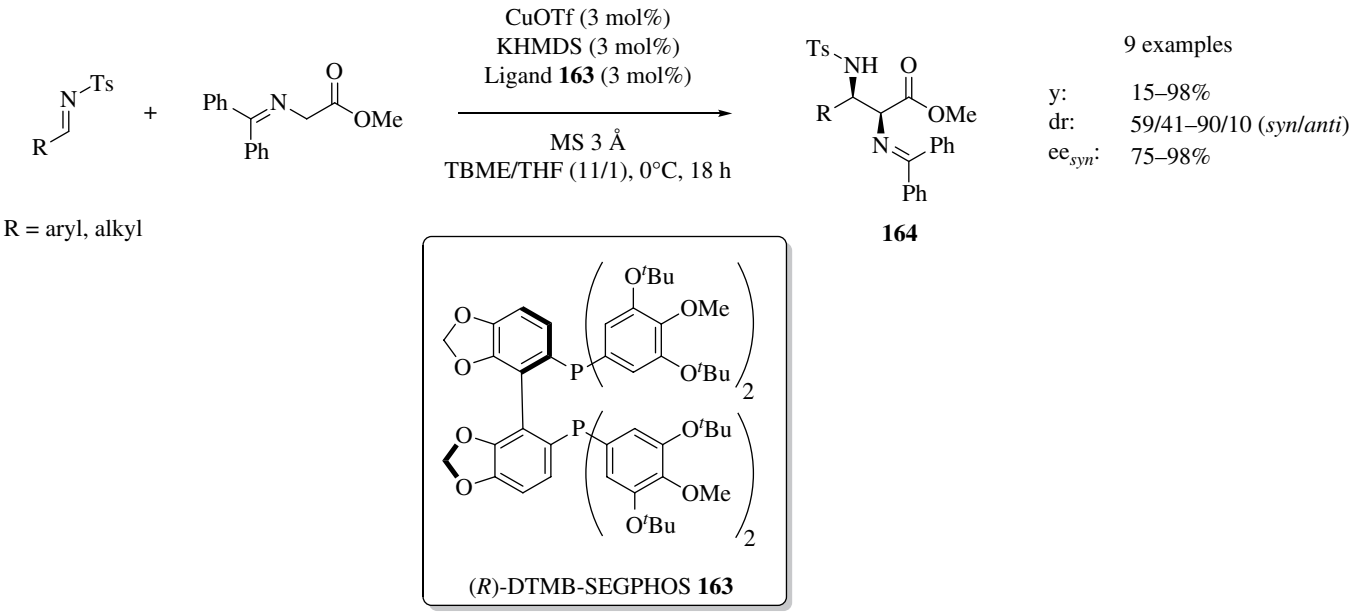
**SCHEME 11.36** Highly *anti*- and *syn*-selective Mannich reaction catalyzed by a dinuclear zinc complex.

*ortho*-methoxy group was found to be essential to achieve high enantioselectivities. This suggests that the methoxy substituent coordinates to the metal center, which additionally fixes the transition state in a conformation favoring attack onto the *re*-face of the intermediate Zn-enolate (**157**, Scheme 11.35). Remarkably, if *N*-Boc-protected imines instead of *N*-Dpp-protected imines were treated under similar reaction conditions with α-hydroxyketones, diethyl zinc, and BINOL ligand **155**, the selectivity of the Mannich reaction was completely opposed affording predominately the *syn*-diastereomer (**158**) in high yields and excellent enantioselectivities (Scheme 11.35) [107].

This drastic change in the stereochemical outcome of the reaction might be linked to changes in the spatial orientation of the imine in the transition state, which is dependent on the stereochemical properties of the N-protective group. Based on CSI-MS analysis of the Zn/BINOL complex in the presence of hydroxyketone, the authors suggested that a heptanuclear Zn/BINOL/ketone oligomer serves as the catalytic active species. The zinc phenoxide deprotonates the ketone to furnish the nucleophilic enolate. At the same time, zinc acts as Lewis acid to simultaneously activate the imine. To minimize steric repulsions between the enolate and the Dpp-protective group, attack of the imine occurs from the *si*-face to the *re*-face of the enolate *via* transition state **157**. When using the less bulky *N*-Boc-protective group, the facial selectivity of the imine is determined by the steric interaction between the substituent of the imine and the enolate now favoring attack from the *re*-face of the imine to the *re*-face of the enolate *via* transition state **159**.

Later, the substrate scope of a complementary Mannich reaction was extended by Trost and colleagues utilizing the (*S*,*S*)-dinuclear zinc complex **160**. They successfully demonstrated that, under similar reaction conditions as reported by Shibasaki, various *N*-Dpp-protected imines derived from enolizable ketones furnish upon the reaction with various α-hydroxyketones in the presence of catalyst **160** the corresponding *anti*-*N*-protected-α-hydroxyl-β-amino ketones (**161**) in good yields with good diastereoselectivities and good to excellent enantioselectivities (Scheme 11.36) [108]. Application of the (*R*,*R*)-dinuclear zinc complex consequently afforded the enantiomeric product in comparable yield and diastereoselectivity. The authors hypothesized that the same mechanism that was suggested by the group of Shibasaki accounts for the observed *anti*-stereoselectivity. Not surprisingly, if aliphatic *N*-Boc-protected imines were used instead, the corresponding *syn*-*N*-protected-α-hydroxyl-β-amino ketones (**162**) were isolated in good yields with good diastereoselectivities and excellent enantioselectivities (Scheme 11.36).

Recently, the synthesis of enantioenriched 1,2-diamino acid derivatives [109, 110] was reported by Kobayashi and colleagues combining a glycine Schiff base and an imine in an asymmetric Mannich-type reaction [111]. To achieve simultaneous activation and deprotonation of the glycine Schiff base, which was hypothesized to be a crucial feature

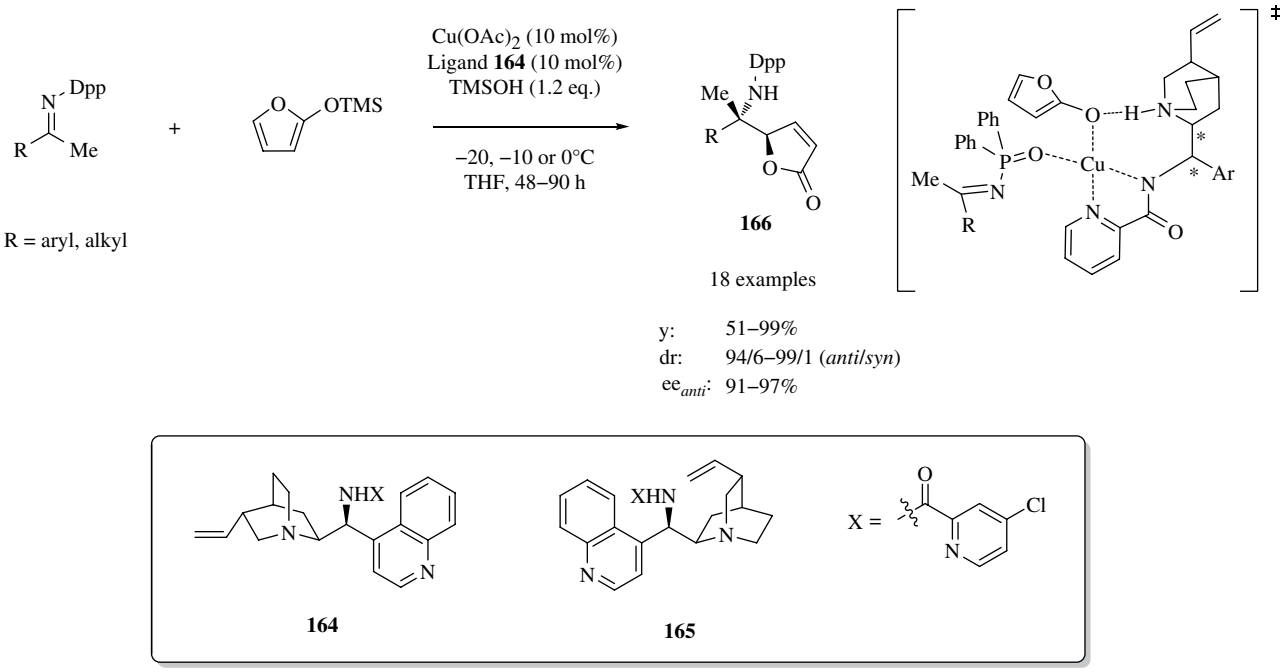



**SCHEME 11.37** Chiral CuHMDS-catalyzed asymmetric Mannich reaction affording *syn*-1,2-diamino acid.

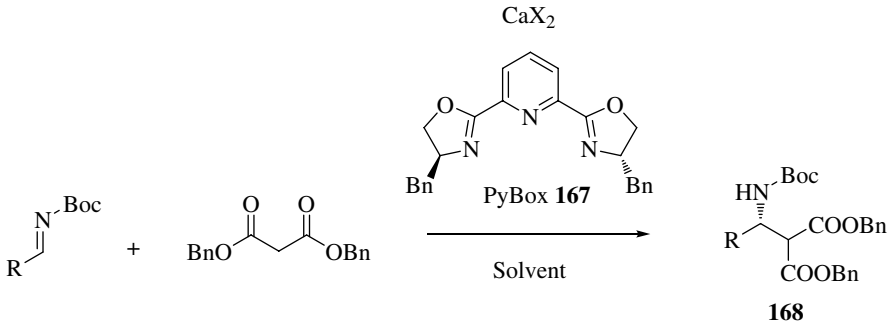
to obtain good selectivities in the Mannich reaction, a chiral copper(I) hexamethyldisilazide (CuHMDS) was prepared *in situ* from copper(I) triflate and KHMDS in the presence of the chiral phosphine ligand (*R*)-DTBM-BIPHEP (**163**). Such chiral metal amides should be well suited for catalyzing the asymmetric Mannich reaction because they have both a Lewis acidic (metal center) and a Brønsted basic moiety (amide). The reaction proceeded well with various aromatic imines affording the desired Mannich adducts in modest to excellent yields and stereoselectivities (Scheme 11.37). An aliphatic imine was also tested. Although the yield was rather modest, the reaction proceeded with good stereoselectivity. Noteworthy, if isolated CuHMDS was used as the copper source instead of being formed *in situ*, the Mannich reaction proceeded smoothly; however, almost no stereoinduction was observed. The authors suggest that CuHMDS forms upon isolation of stable aggregates, which might prevent the formation of an active chiral CuHMDS complex.

The application of less reactive ketimines (imines derived from ketones) as substrates in the asymmetric (vinylogous) Mannich reaction is only marginally explored yet in comparison with the application of imines that are derived from simple aldehydes. Most recently, the group of Nakamura disclosed a highly diastereo- and enantioselective vinylogous Mannich reaction combining siloxyfurans and various *N*-Dpp-protected ketimines utilizing a chiral copper complex [112]. In the presence of 10 mol% $Cu(OAc)_2$, 10 mol% of a chiral ligand (**164**), which is derived from the cinchona alkaloid 9-amino-9-deoxy-*epi*-cinchonidine, and trimethylsilyl alcohol (TMSOH), the corresponding δ-amino-δ,δ-disubstituted-α,β-unsaturated carbonyl compounds (**166**) were obtained in good to excellent yields exclusively as the *anti*-diastereomer with excellent enantioselectivities (Scheme 11.38). Moreover, the opposite enantiomer was easily accessible in good yields and excellent selectivities when changing the cinchona alkaloid-derived ligand from **164** to **165**, which is derived from 9-amino-9-deoxy-*epi*-cinchonine. Based on a mechanistic proposal and the stereochemical outcome of the reaction, the authors suggested a transition state in which copper is coordinated by two nitrogen atoms (from the cinchona ligand) and two oxygen atoms (one each from the Dpp-protective group and dienolate) in a square planar manner. From this mechanistic drawing, the dienolate can only approach the *re*-face of the ketamine.

The application of chiral group 2 alkaline earth metals (Ca, Sr, Ba) as catalysts in various chemical processes is an emerging field in asymmetric catalysis due to their natural abundance, specific electronic properties (strong Brønsted basicity and mild Lewis acidity), and environmental sustainability in comparison with transition metal catalysts [113–115]. For example, Kobayashi and coworkers disclosed a Ca–pyridinebisoxazoline (PyBox) complex, prepared *in situ* by heating $Ca(O^iPr)_2$ and ligand **167** in dry xylene, which catalyzed the asymmetric Mannich reaction between *N*-Boc-protected imines and dibenzyl malonates (Scheme 11.39) [116]. Although the reaction was completed within 2 h affording the desired Mannich products in good to very good yields, the observed moderate enantioselectivities and substrate scope limit the further applicability of this approach. The moderate stereocontrol of the described catalyst system might be explained by partial decomplexation of the Ca–PyBox complex. Hence, free calcium alkoxide could catalyze the racemic addition of malonates to *N*-Boc-protected




**SCHEME 11.38** Chiral cinchona alkaloid amide/copper(II)-catalyzed asymmetric Mannich reaction.



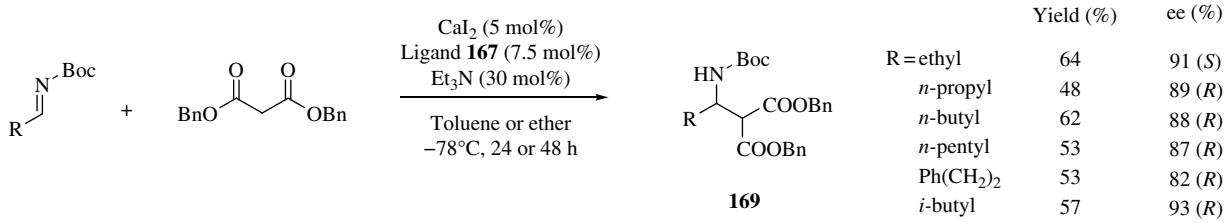

**Method A**
$Ca(O^iPr)_2$ (10 mol%)
Ligand **167** (15 mol%)
Xylene, –20°C, 2 h

**Method B**
$CaI_2$ (5 mol%)
Ligand **167** (7.5 mol%)
$Et_3N$ (30 mol%)
Toluene, –78°C, 2 h

| | Yield (%) Method A/B | ee (%) Method A/B |
|---|---|---|
| R = Ph | 90/89 | 73/92 |
| *o*-$MeC_6H_4$ | 90/86 | 77/84 |
| *m*-$MeC_6H_4$ | 93/91 | 71/88 |
| *p*-$MeOC_6H_4$ | 75/71 | 75/81 |
| *p*-$ClC_6H_4$ | 82/87 | 61/90 |
| *p*-$FC_6H_4$ | 91/88 | 72/91 |
| 3,4-$(OCH_2O)C_6H_3$ | 92/66 | 67/84 |
| 2-furyl | 95/99 | 76/92 |
| 2-thienyl | 89/76 | 54/96 |

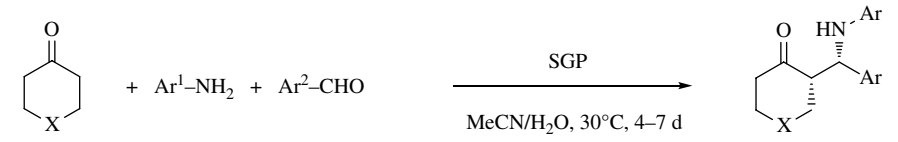
**SCHEME 11.39** Chiral Ca–PyBox-catalyzed asymmetric Mannich reaction: Substrate scope of aromatic imines.

imines. The scope of this methodology could be improved by changing the calcium salt. After screening several calcium salts and reaction conditions, the lab of Kobayashi identified a chiral calcium iodide catalyst, which is derived from calcium iodide and PyBox ligand 1**67**, which afforded the desired Mannich products from *N*-Boc-protected imines and dibenzyl malonates in good to excellent yields with very good enantioselectivities (Scheme 11.39) [117]. Moreover,




| | Yield (%) | ee (%) |
|---|---|---|
| R = ethyl | 64 | 91 (*S*) |
| *n*-propyl | 48 | 89 (*R*) |
| *n*-butyl | 62 | 88 (*R*) |
| *n*-pentyl | 53 | 87 (*R*) |
| $Ph(CH_2)_2$ | 53 | 82 (*R*) |
| *i*-butyl | 57 | 93 (*R*) |

**SCHEME 11.40** Chiral Ca–PyBox-catalyzed asymmetric Mannich reaction: Substrate scope of aliphatic imines.




**SCHEME 11.41** First biocatalytic asymmetric Mannich reaction.

aliphatic imines were tolerated as substrates after further optimization of the reaction conditions. The desired Mannich products were obtained in very good enantioselectivities but modest yields, though. Interestingly, except for the propionaldehyde-derived imine, enantioselective formation of the opposite enantiomers was observed (Scheme 11.40).

### 11.2.5 Biocatalytic Asymmetric Mannich Reactions

In general, the application of enzymes as biocatalyst in chemical transformation has several advantages over classical organo- or metal-catalyzed processes, such as (i) mild reaction conditions (ambient temperature and pressure); (ii) environmentally compatible and biodegradable catalysts; (iii) accessibility of the catalysts from renewable raw materials; (iv) high chemo-, regio-, and stereoselectivities; (v) no need for functional group activation or protection; and (vi) no contamination with traces of metals. Therefore, the implementation of biocatalysis in industrial chemical processes may lead to more environmentally benign and profitable processes involving fewer steps and consequently less waste production [118–121]. Despite these advantages over the aforementioned organo- or metal-catalyzed processes, recent efforts identifying a suitable biocatalyst promoting the asymmetric Mannich reaction showed only limited success. Li et al. screened a variety of different lipases toward their ability to effectively catalyze the direct Mannich reaction between acetone, aniline, and *p*-nitrobenzaldehyde. In this respect, utilizing lipase from *Mucor miehei* (MML) afforded the desired Mannich product in 72% yield, whereas only 8% of the product was isolated when denatured enzyme was used as negative control, which proved the promotive effect of the enzyme [122]. Moreover, the substrate scope and the recyclability of the biocatalyst were investigated. A variety of different aromatic aldehydes were found to be tolerated in the lipase-catalyzed direct Mannich reaction, and the catalyst could be recovered and reused at least six times without a significant loss of activity. The major drawback of this approach, however, relies on the complete inability to induce any significant enantioselectivity [122].

Later on, the same group was able to identify a lipase from *Candida rugosa*, which was able to promote the direct Mannich reaction between aniline, *p*-nitrobenzaldehyde, and various ketones, such as cyclohexanone, 2-butanone, and 1-hydroxy-2-propanone. Although most of the products could be isolated in moderate to very good chemical yields, the obtained diastereoselectivities are generally low (dr ≤ 3/1) [123]. Similar results on the enzyme-catalyzed Mannich reaction were reported by other groups using trypsin [124] or alcalase [125], respectively.

The first biocatalytic asymmetric Mannich reaction was reported recently by Guan and colleagues. They found that protease type XIV from *Streptomyces griseus* was able to catalyze the Mannich reaction between cyclohexanone, *p*-nitrobenzaldehyde, and aniline in moderate yields though but in good diastereo- and enantioselectivities (dr = 85/15 *syn*/*anti*; 82% ee) (Scheme 11.41) [126]. Remarkably, control experiments with metal ion or urea-denatured enzyme still afforded the Mannich product in high yields (≥51% yield) compared to the blank reaction without enzyme (28% yield), but almost all stereoselectivity was lost. These

findings indicate that the amino acids of the protein were still able to catalyze the Mannich reaction; however, the natural fold is responsible for the stereoselectivity of the reaction. To test the scope of the reaction, various aromatic aldehydes with electron-donating or electron-withdrawing substituents and different anilines were evaluated in the enzyme-catalyzed asymmetric Mannich reaction. In general, the best chemical yields and stereoselectivities were obtained with compounds containing an electron-withdrawing substituent [126].

Although the observed selectivities varied much, investigations toward a highly selective asymmetric Mannich reaction, which is promoted by a biocatalyst, most certainly will be intensified due to the versatile application possibilities of the Mannich products, leading to environmentally more benign products. This, however, is extremely challenging due to the myriad of potential biocatalysts available. An alternative approach to screening enzyme libraries for a certain activity would be to identify an enzyme with a promising activity and to optimize its performance via site-directed mutagenesis. Instead of using isolated single enzymes, a crude extract of an organism can also serve as a highly versatile biocatalyst for various transformations. For example, most recently, Guan et al. found that a crude extract of the earthworm species *Eisenia foetida*, commonly known as red worm, is able to promote various organic transformations, such as the Henry, Biginelli, aza-Diels–Alder, asymmetric Aldol, and asymmetric Mannich reaction [127].

During the past 15 years, developments in the field of asymmetric Mannich reactions were not only restricted to catalyst design or reaction optimization, as outlined comprehensively in the previous chapter, but also on applying the established methodologies to natural product total synthesis. Here, especially the synthesis of N-heterocyclic compounds, such as alkaloids, benefited substantially from this progress in performing Mannich reactions in a highly stereocontrolled fashion. In the forthcoming chapter, we wish to highlight recent developments in the total synthesis of L-Lys- and L-Orn-derived alkaloids, but not without giving first credit to the pioneers in this field, namely, Sir Robert Robinson and Clemens Schöpf.

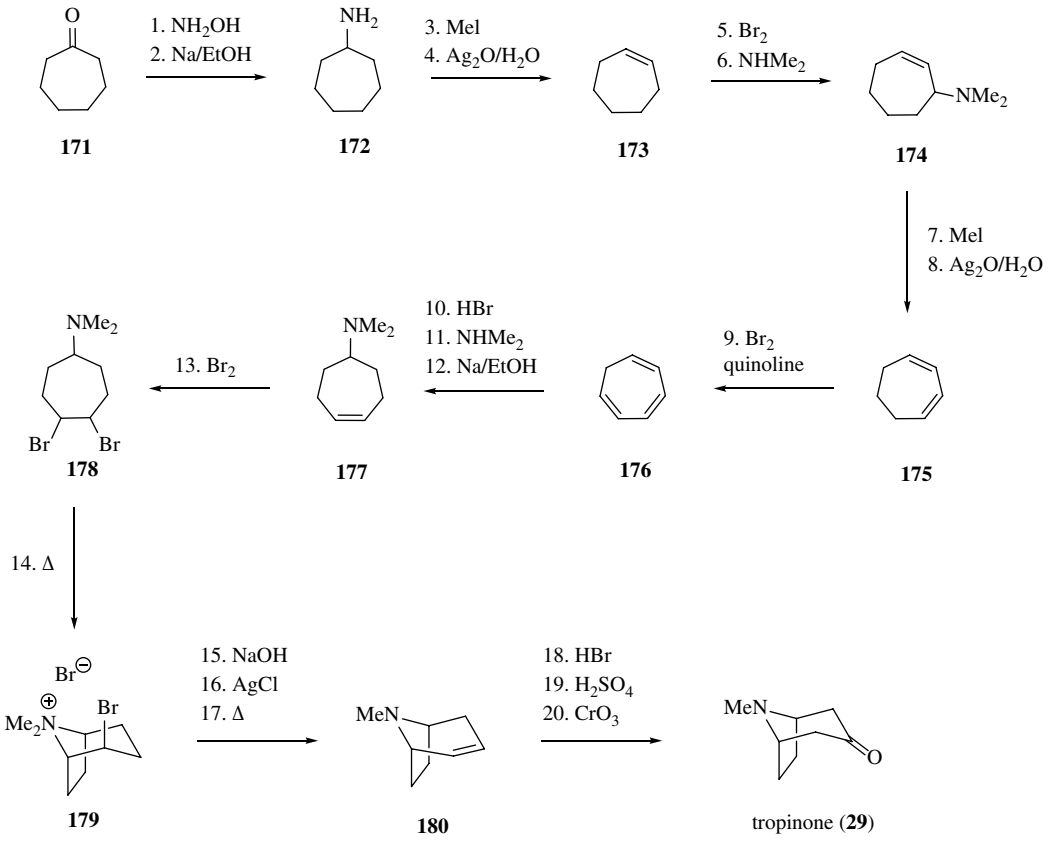
## 11.3 MANNICH AND RELATED REACTIONS IN THE TOTAL SYNTHESIS OF L-LYSINE- AND L-ORNITHINE-DERIVED ALKALOIDS

Although *Solanaceae* plant extracts (e.g.. mandrake, henbane, belladonna, etc.), among others, which contain high amounts of tropane alkaloids, have been used since centuries in medicine, the isolation and identification of the principle components contributing to the observed pharmacological activities lasted until the mid-nineteenth century. At that time, the structural elucidation of these alkaloids proved to be rather challenging, though. The extensive work done by Willstätter at the beginning of the twentieth century on the total synthesis of tropinone and related tropane alkaloids, in the end, verified the chemical structure of some of these alkaloids. Starting from cycloheptanone (**171**), tropinone could be synthesized in a very elegant, straightforward reaction sequence in 0.75% overall yield in 20 steps (Scheme 11.42) [128–130].

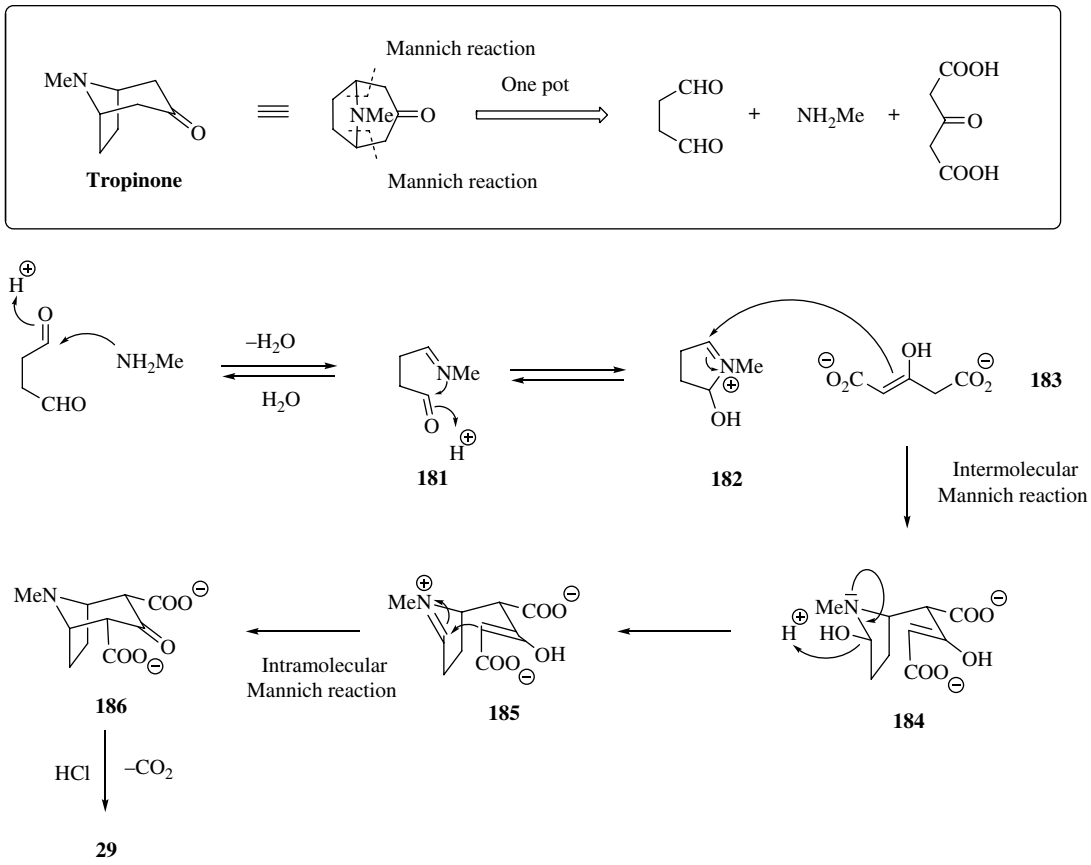
However, this remarkable achievement, considering the chemical capabilities at the turn of the nineteenth century, has been strongly outshone by Robinson's one-pot, biomimetic total synthesis of tropinone (**29**), which mimics the conditions and mechanistic principles of its putative biosynthesis (i.e., ambient reaction temperature, physiological pH, water as solvent, probable or known biological metabolites as substrates). Based on the symmetry and architecture of tropinone, Robinson hypothesized that tropinone might originate from succindialdehyde, *N*-methylamine, and a reactive acetone equivalent. Indeed, under physiological pH using calcium acetonedicarboxylate (**183**) as reactive acetone equivalent, tropinone could be isolated in 42% yield (Scheme 11.43) [131]. The reaction can be considered as a double Mannich condensation, whereas the enol tautomer of calcium acetonedicarboxylate nucleophilically attacks the intermediary dihydropyrrolium **182**, formed upon condensation of succindialdehyde and *N*-methylamine, in an intermolecular Mannich reaction. Subsequent loss of water generates an iminium ion (**185**), which is highly susceptible to nucleophilic attack by the enolate to furnish in an intramolecular Mannich reaction tropinone dicarboxylate (**186**). Upon acidification, carbon dioxide is released to afford tropinone (**29**). Due to its simplicity, Robinson proposed that this process is also employed in the plant involving an amino acid precursor (L-Orn) affording the pyrrolidine ring moiety and a reactive acetone equivalent, which furnishes C-2, C-3, and C-4 of the tropane skeleton, a hypothesis that is still held to be true [132].

Later, Robinson's approach was improved substantially by Schöpf in the early 1930s when he realized that only slight changes of the pH affect the yield of the reaction. After in-depth studies concerning the optimal reaction conditions, buffered conditions using a citrate buffer (pH = 5) where found to double the initial yield of the reaction [133]. Therefore, the synthesis of tropinone from succindialdehyde, *N*-methylamine, and acetonedicarboxylate is nowadays commonly referred to as Robinson–Schöpf condensation.

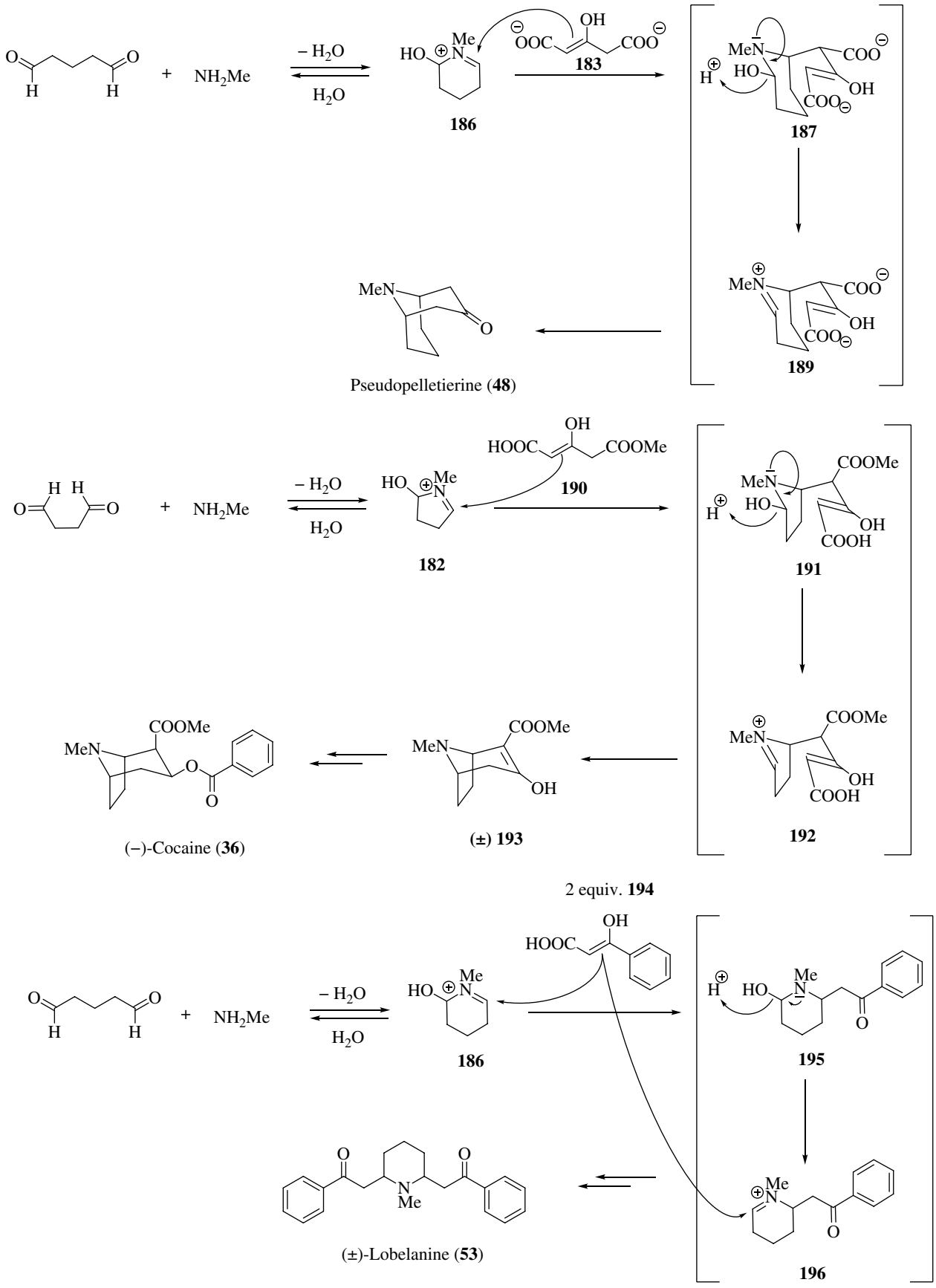
Based on this simple one-step route to tropinone developed by Robinson, other alkaloids with a common piperidine or pyrrolidine ring moiety became easily accessible. For example, only a few years after the initial discovery of the tropinone synthesis, Robinson developed an analogous one-step synthesis of pseudopelletierine (**48**), a ring homolog of tropinone, involving a consecutive inter- and



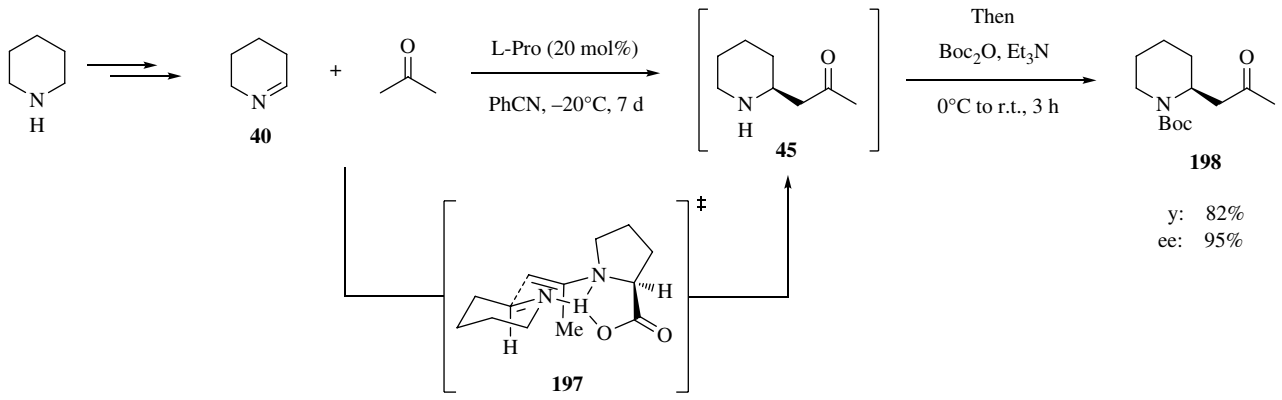

**SCHEME 11.42** First tropinone total synthesis by Willstätter [128, 129].




**SCHEME 11.43** Revised tropinone synthesis by Robinson [131, 132] and Schöpf [133].




**SCHEME 11.44** Adopting Robinson's principle: Synthesis of pseudopelletierine, (±)-lobelanine, and (–)-cocaine.




**SCHEME 11.45** One-step total synthesis of (+)-pelletierine employing an asymmetric Mannich reaction.

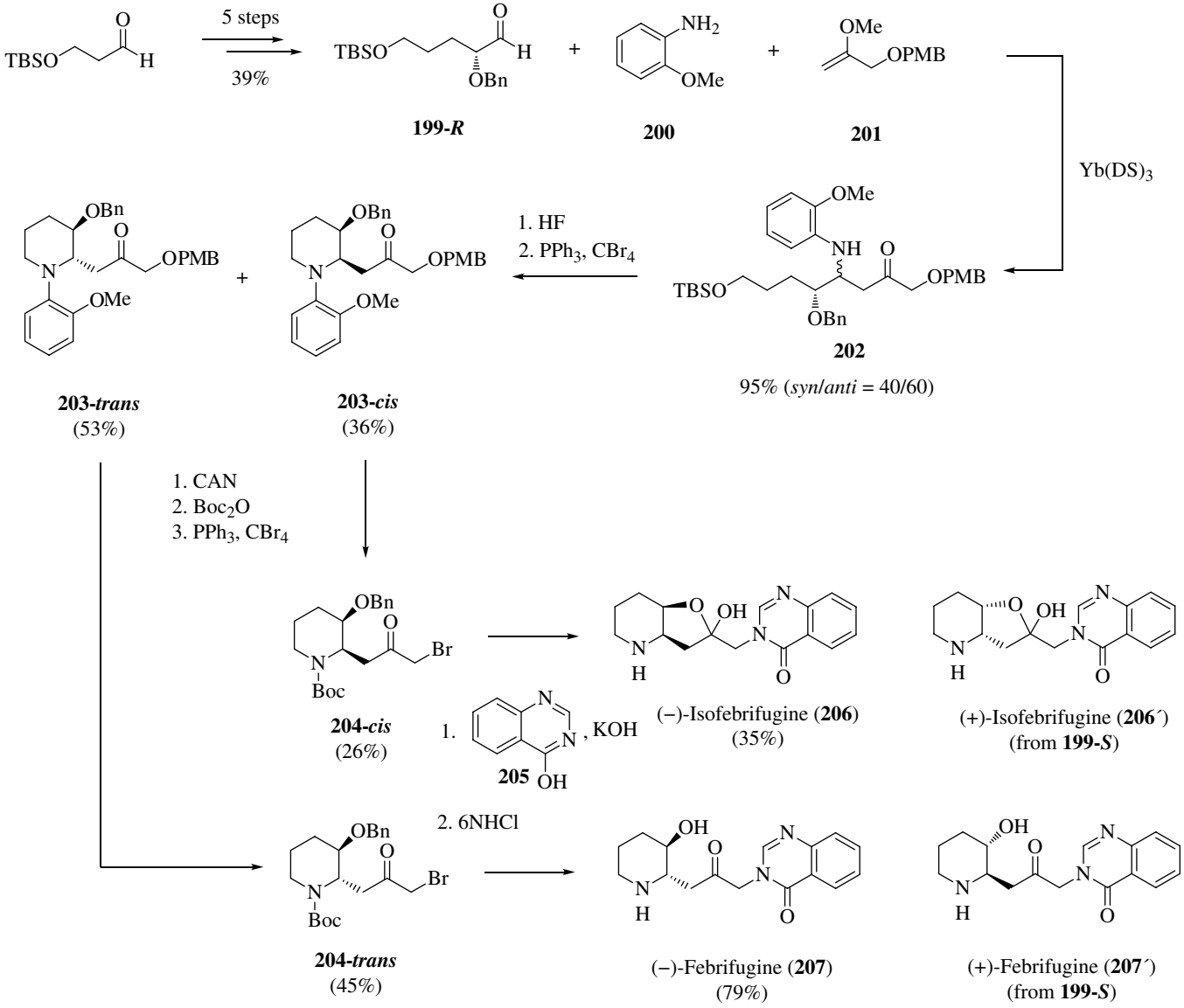
intramolecular Mannich reaction, by simply exchanging succindialdehyde for glutaraldehyde (Scheme 11.44) [134]. Again, Schöpf and colleagues were able to significantly improve this process by performing the reaction under buffered conditions (phosphate buffer, pH = 7) using excess acetonedicarboxylic acid, which afforded pseudopelletierine in 95% yield [135]. However, reinvestigations of the formation of pseudopelletierine by Cope showed some discrepancies between their results and the data reported by Schöpf. Using similar conditions as reported previously by Schöpf, Cope isolated only traces of pseudopelletierine. After optimization of the conditions, the maximum yield was found to be 45–57% under slightly acidic conditions (pH = 2–4.5) after 4 h reaction time [136].

Moreover, if acetonedicarboxylic acid monomethyl ester (**190**) is used as reactive acetone equivalent instead of acetonedicarboxylic acid (**183**) in the Robinson–Schöpf condensation, (±)-2-carbomethoxytropinone (**193**) can be obtained, which can be converted either into (−)-cocaine or (+)-cocaine (**36**) in three subsequent steps (separation of both epimers of **193** via crystallization with either (+)-tartaric acid or (–)-tartaric acid, reduction of the carbonyl group, and benzylation) (Scheme 11.44) [137].

Monocyclic piperidine or pyrrolidine alkaloids are also accessible in a Robinson–Schöpf-type condensation if substituted acetone monocarboxylic acids are used as reactive acetone equivalent. For example, the reaction of glutardialdehyde, methylamine, and two equivalents 3-keto-3-phenylpropionic acid (**194**) under slightly acidic conditions (pH = 4) afforded (±)-lobelanine (**53**) in 90% yield (Scheme 11.44). Here, the reaction presumably proceeds via intermediate **195**, which is formed in an initial intermolecular Mannich reaction between glutardialdehyde, methylamine, and one equivalent **194**. Under the applied reaction conditions, water is eliminated. The formed iminium ion **196** is prone to nucleophilic attack by a second equivalent **194** to furnish the piperidine alkaloid (±)-lobelanine [132, 134].

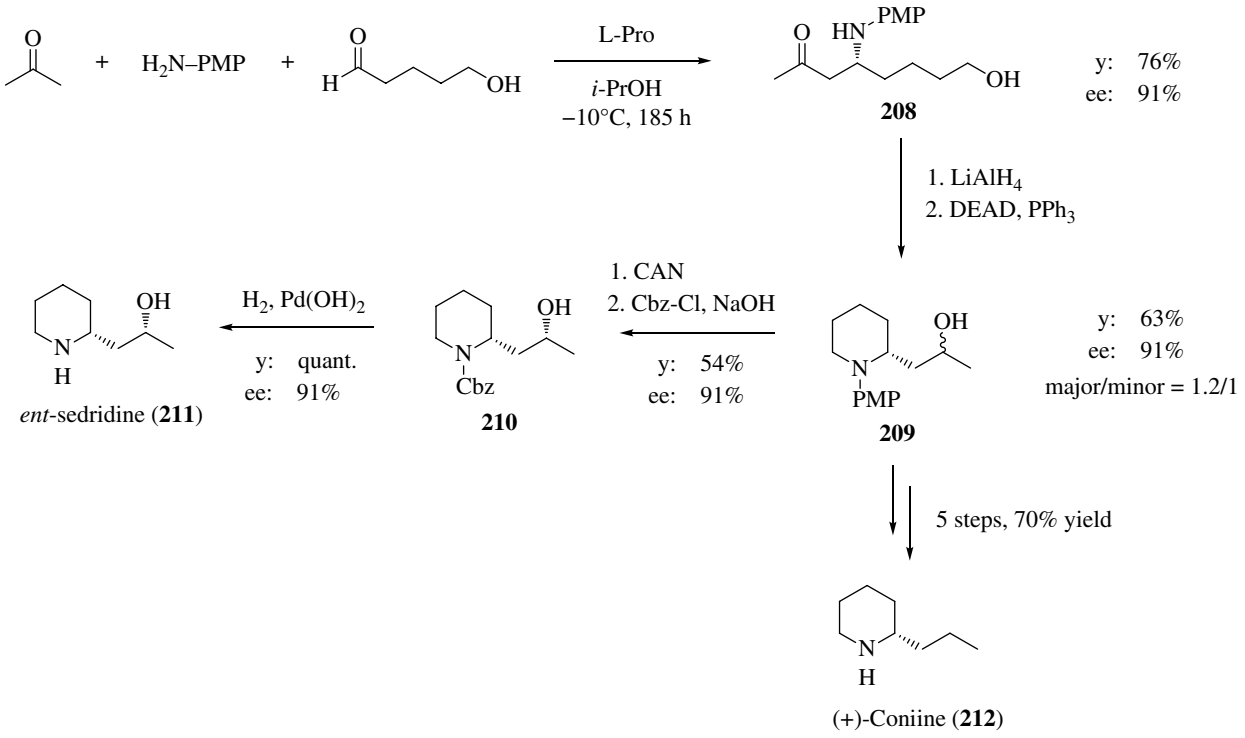
Similar to the synthesis of lobelanine, other piperidine and pyrrolidine alkaloids have been prepared in a one-pot process, such as hygrine [138, 139], pelletierine [140–143], nicotine [144, 145], and anabasine [146], among others. Despite the simplicity of the outlined methodology, which is based on the Mannich reaction, these alkaloids could be isolated only as racemic mixtures, though. The enantioselective syntheses of these natural products, which have been accomplished in the meantime, however, require multiple synthetic and purification steps. Hence, the synthesis of members of this structurally highly diverse class of natural products would most certainly benefit greatly from the combination of the principles developed by Robinson and Schöpf and organocatalysis to promote the asymmetric Mannich reaction. In this respect, the synthetic effort might be reduced tremendously, and both enantiomers might become easily accessible by simply changing the catalyst. Moreover, the high convergence of the Mannich reaction might facilitate the synthesis of alkaloid derivatives by varying the starting materials of the reaction. For example, Bella and coworkers reported the first asymmetric total synthesis of (+)-pelletierine (**45**) and derivatives thereof, which utilizes an asymmetric Mannich reaction as key step. The combination of acetone and $\Delta^1$-piperideine (**40**), which can be obtained via piperidine-*N*-chlorination and subsequent base-mediated elimination of HCl, in the presence of 20 mol% L-proline as catalyst afforded (+)-pelletierine (**45**) in a single step in good yield (82%) and excellent enantioselectivity (95% ee) (Scheme 11.45) [147]. To facilitate purification and HPLC analysis, the secondary amine was protected *in situ* with $Boc_2O$. This biomimetic approach is superior to other asymmetric syntheses published in recent years, which require at least three to five synthetic steps [148, 149].

The method of Bella is a supreme example of how the organocatalytic asymmetric Mannich reaction can facilitate the synthesis of simple pyrrolidine or piperidine alkaloids starting from achiral starting materials. Therefore, in the subsequent paragraphs, we wish to review recent efforts made by various research groups to implement an organocatalytic asymmetric Mannich reaction as key step in the total synthesis of alkaloids, predominately derived from L-Orn and L-Lys.




**SCHEME 11.46** Asymmetric total synthesis of febrifugine and isofebrifugine.

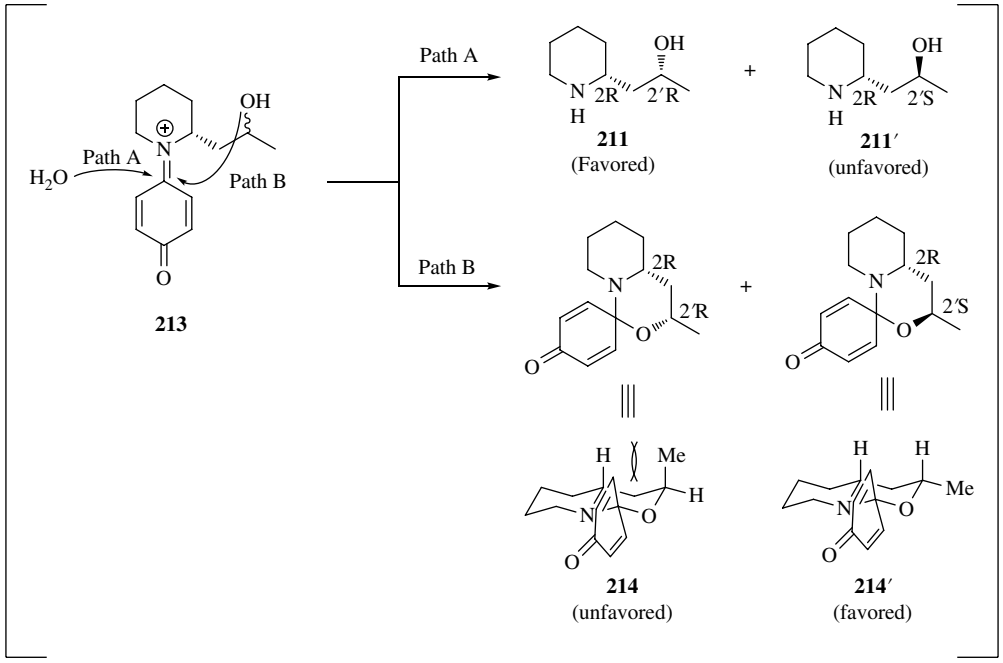
The total synthesis of the antimalarial alkaloids febrifugine (**207**) and isofebrifugine (**206**) by Kobayashi is probably the first example of the implementation of a catalytic Mannich-type reaction in the synthetic planning (Scheme 11.46) [150]. Febrifugine was disconnected into 4-hydroxyquinazoline (**205**) and bromoacetone **204**. The latter one was accessible from 2-methoxyaniline (**200**), chiral aldehyde **199,** and vinyl ether **201** in a Mannich-type reaction, which proceeded smoothly in the presence of 10 mol% of the achiral catalyst ytterbium(III) dodecyl sulfate ($Yb(DS)_3$) in water, to afford the corresponding β-amino ketone **202** in 95% yield. After cleavage of the TBS-protective group and subsequent bromination (Appel reaction), piperidine **203** could be isolated in overall 89% yield. Then, both diastereomers were separated and treated individually with ceric ammonium nitrate (CAN), $Boc_2O$, and $PPh_3/CBr_4$ to furnish either bromoacetone **204**-*cis* or **204**-*trans*. Finally, coupling of bromoacetone **204** with 4-hydroxyquinazoline (**205**) followed by the removal of the protective groups afforded febrifugine **207** (from **204**-*trans*) and isofebrifugine **206** (from **204**-*cis*) in 7 and 1% overall yield, respectively, over 13 steps. However, comparison of the optical rotation of (2′*S*,3′*R*)-febrifugine **207** and (2′*R*,3′*R*)-isofebrifugine **206** with values reported in the literature indicated that the originally proposed configuration was wrong. Therefore, the synthesis was repeated with aldehyde **199**-*S*, and the physical data of the corresponding (2′*R*,3′*S*)-febrifugine **207**′ and (2′*S*,3′*S*)-isofebrifugine **206**′ matched those reported in the literature.



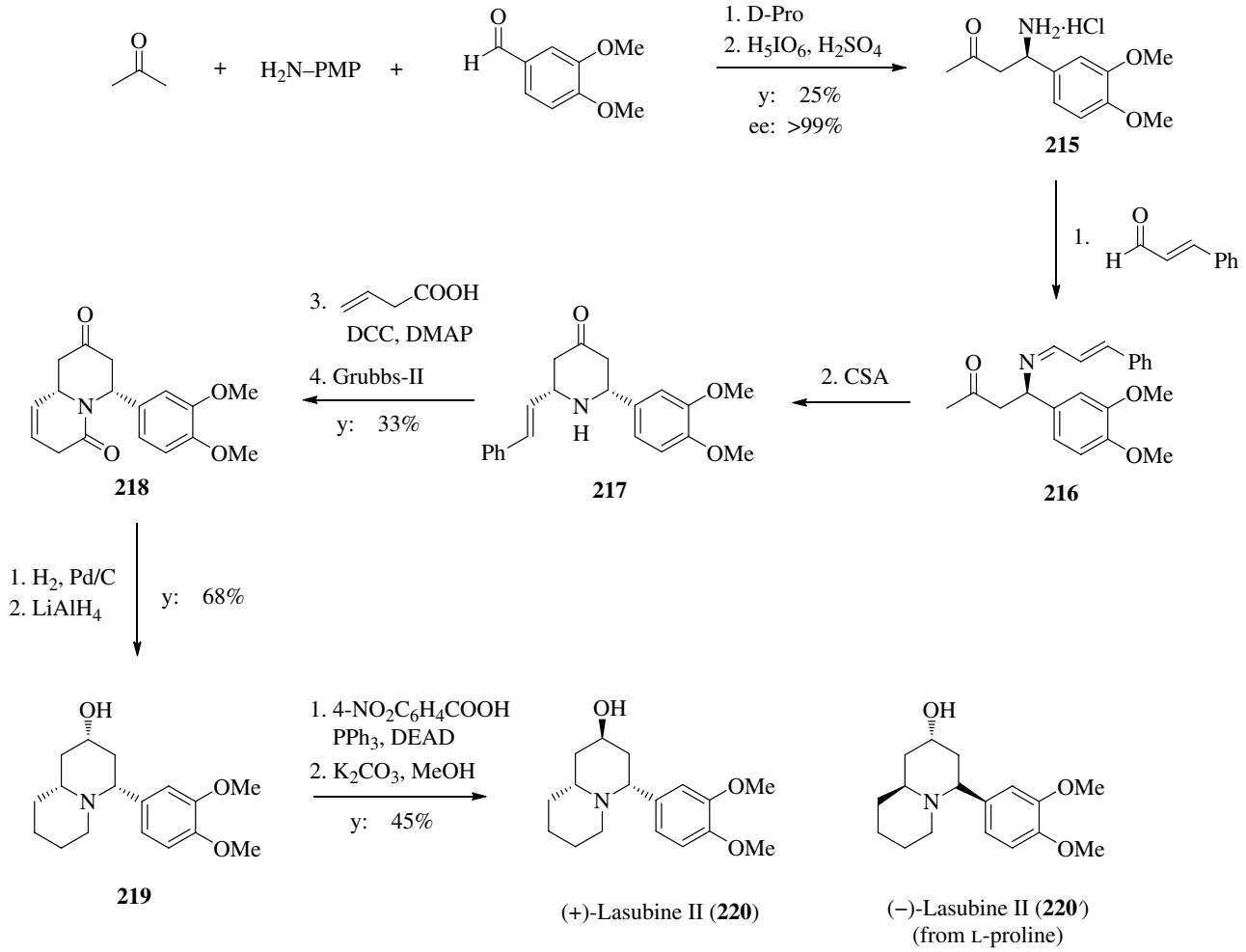

**SCHEME 11.47** Asymmetric total synthesis of *ent*-sedridine and (+)-coniine.

Instead of an achiral catalyst to promote the Mannich or Mannich-type reaction, chiral catalysts have been used as well to facilitate the stereoselective formation of a new C–C bond. For example, an enantiomer of the piperidine alkaloid sedridine, *ent*-sedridine (**211**), was synthesized by the lab of Itoh in six steps and 34% overall yield (Scheme 11.47) [151]. First, it was envisioned to combine acetone, 4-hydroxybutanal, and *p*-anisidine in an asymmetric Mannich reaction to afford β-amino ketone **208**. For this purpose, various reaction conditions were initially screened, and the reaction was found to proceed extremely well at −10°C in *i*-propanol in the presence of 30 mol% L-proline (76% yield, 91% ee). Afterward the β-amino ketone **208** was reduced, and the epimeric mixture was subsequently treated with DEAD and $PPh_3$ to yield piperidine **209**. After removal of the PMP-protective group, subsequent protection of the secondary amine with CbzCl afforded surprisingly compound **210** as a single diastereomer. Initially, deprotection and subsequent protection of the secondary amine were aimed at to facilitate the identification of the stereochemistry of compound **210**. However, upon oxidation with CAN, quinonoid intermediate **213** is formed, which is supposed to undergo either hydrolysis affording compound **211** and its epimer **211′** or intramolecular attack of the hydroxyl group to give the cyclized products **214** or its epimer **214′**. Due to unfavorable steric interactions, the authors stated that the (2*R*,2′*R*)-epimer of **213** is transformed directly into **211**, whereas the (2*R*,2′*S*)-epimer of **213** may cyclize to yield **214′** without the formation of **211′** upon hydrolysis (Scheme 11.48) [151]. Subsequent removal of the cyclic by-product enables the isolation of pure **210** as a single diastereomer. Finally, compound **210** was converted into *ent*-sedridine (**211**) by reductive cleavage of the Cbz group. Alternatively, intermediate **209** can be converted into (+)-coniine (**212**) in 35% overall yield over eight steps (from *p*-anisidine) [152].

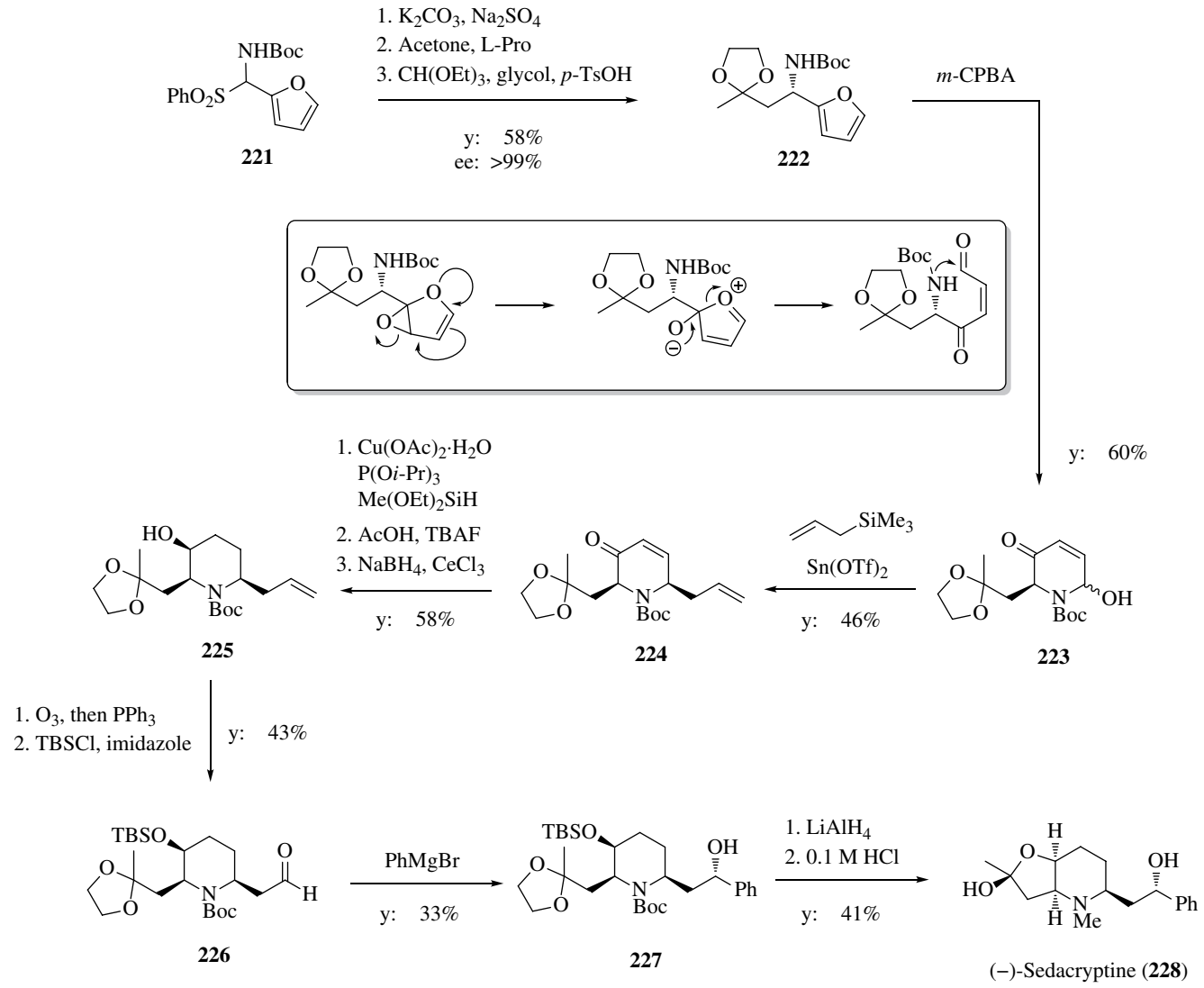
The proline-catalyzed Mannich reaction has also been employed in the synthesis of both enantiomers of lasubine II. Starting from commercially available starting materials, (+)-lasubine II (**220**) was obtained in 2.5% overall yield over 10 steps using D-proline in the initial asymmetric Mannich reaction (Scheme 11.49) [153]. First, acetone, *p*-anisidine, and veratryl aldehyde were condensed in a Mannich reaction followed by removal of the PMP-protective group to afford β-amino ketone **215** as a single enantiomer. Condensation of amine **215** with cinnamaldehyde afforded imine **216**, which can undergo intramolecular Mannich cyclization to afford diastereoselectively piperidinone **217**. Then, acylation of the secondary amine with vinylacetic acid and subsequent ring-closing metathesis furnished the quinolizidine backbone (**218**) of lasubine II. Hydrogenation of the double bond followed by the reduction of both carbonyl groups afforded (+)-2-*epi*-lasubine II (**219**), which was finally converted into (+)-lasubine II (**220**) under Mitsunobu conditions and subsequent ester hydrolysis. If L-proline was used instead, the natural (−)-lasubine II (**220′**) was obtained in an identical pathway [153].




**SCHEME 11.48** Plausible mechanism for the formation of compound **210** as a single diastereomer.




**SCHEME 11.49** Asymmetric total synthesis of (+)- and (−)-lasubine II.



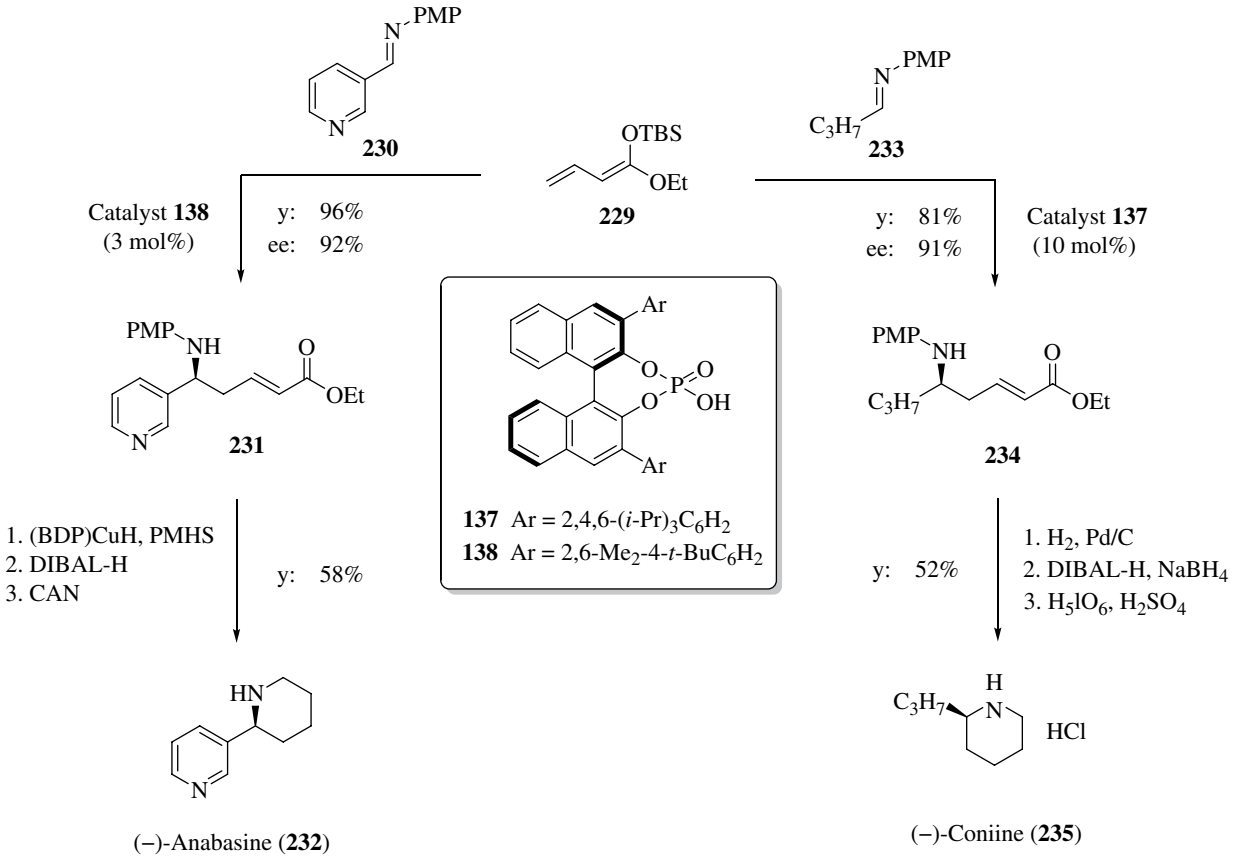

**SCHEME 11.50** Asymmetric total synthesis of (−)-sedacryptine.

Alternatively, natural (−)-lasubine II (**220′**) was also accessible in 1.3% overall yield over 15 steps employing an L-proline-catalyzed Mannich reaction, Maruoka allylation, and aza-Michael addition as the key steps [154].

Recently the total synthesis of natural (−)-sedacryptine (**228**) was accomplished in an organocatalyzed Mannich/aza-Achmatowicz/*N*-acyliminium ion reaction sequence in 0.6% overall yield over 14 steps (Scheme 11.50) [155].

Retrosynthetic analysis revealed piperidinone **223**, which was accessible from sulfone **221** via asymmetric Mannich reaction, protection of the carbonyl group, and aza-Achmatowicz reaction, to be a promising intermediate toward (−)-sedacryptine (**228**). Then, addition of allyltrimethylsilane to the *in situ* formed *N*-acyliminium ion afforded the *cis*-substituted piperidinone **224** as single diastereomer. Compound **225**, which was subjected to ozonolysis, was obtained upon conjugate reduction of the double bond followed by reduction of the remaining carbonyl group. After subsequent silylation with TBSCl, the aldehyde **226** could be isolated in pure form. The 2-hydroxy-2-phenylethyl substituent of (−)-sedacryptine was introduced via Grignard reaction and the resulting diastereomers were separated. Subsequently, the (2*S*,3*S*,6*S*)-diastereomer **227** was treated with $LiAlH_4$, which simultaneously removed the TBS group and reduced the carbamate. Finally, cleavage of the acetal protective group and isomerization of the resulting hemiacetal furnished (−)-sedacryptine (**228**).

An asymmetric version of the vinylogous Mannich reaction has also been implemented in the total synthesis of various alkaloids. For example, Schneider and coworkers combined *N*-*p*-methoxyphenylnicotinimine **230** and the acyclic silyl dienolate **229** in the presence of 3 mol% of a chiral



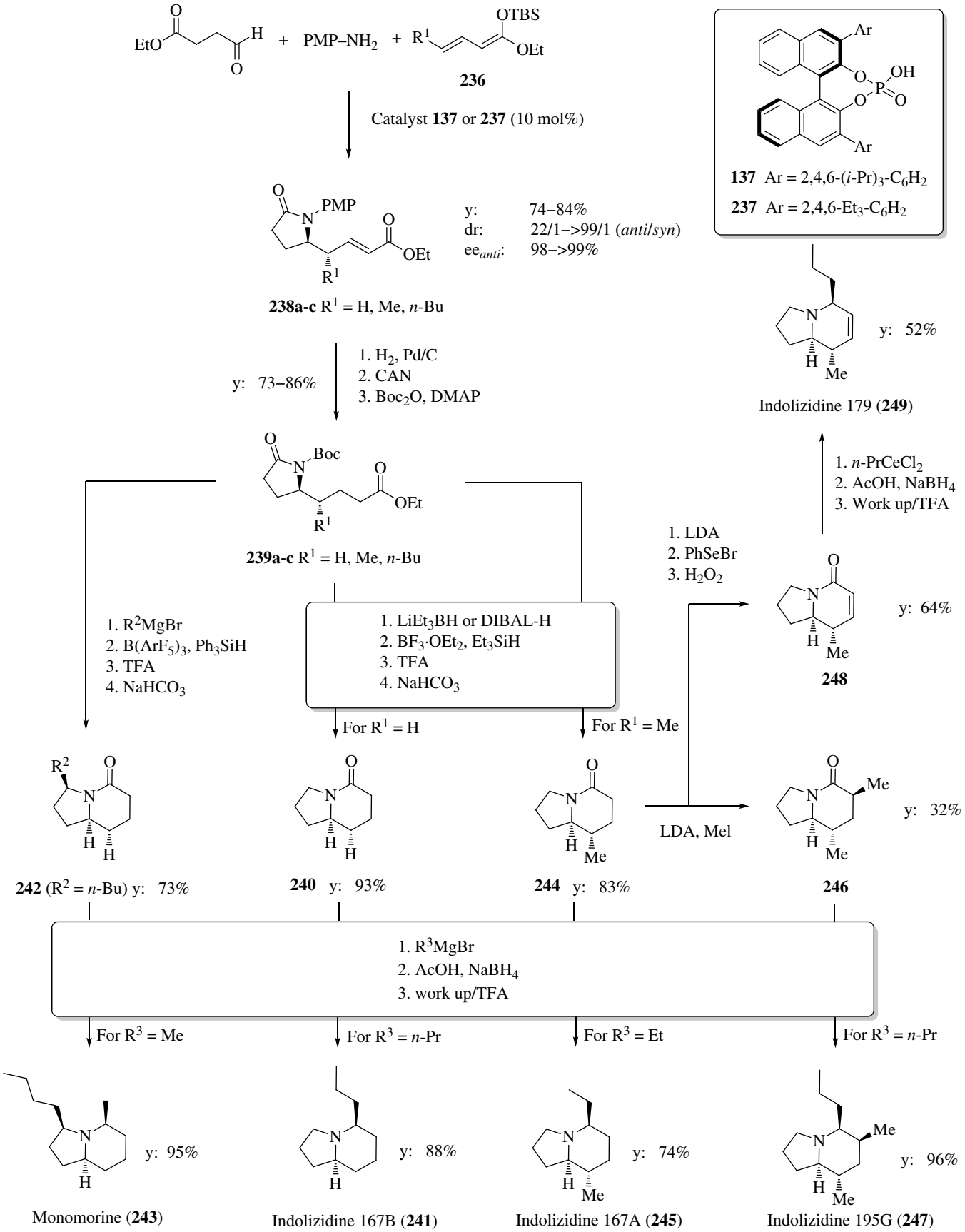

**SCHEME 11.51** Asymmetric total synthesis of (–)-anabasine and (–)-coniine employing an asymmetric vinylogous Mannich reaction as key step.

BINOL-derived phosphoric acid catalyst affording the β-amino ketone (**231**) in 96% yield and 92% ee (Scheme 11.51) [156]. The total synthesis of (–)-anabasine (**232**) was completed in three more steps in 55% overall yield: (i) reduction of the conjugated double bond, (ii) reduction of the ester moiety with an excess DIBAL-H resulting in the formation of the piperidine ring, and (iii) removal of the PMP-protective group.

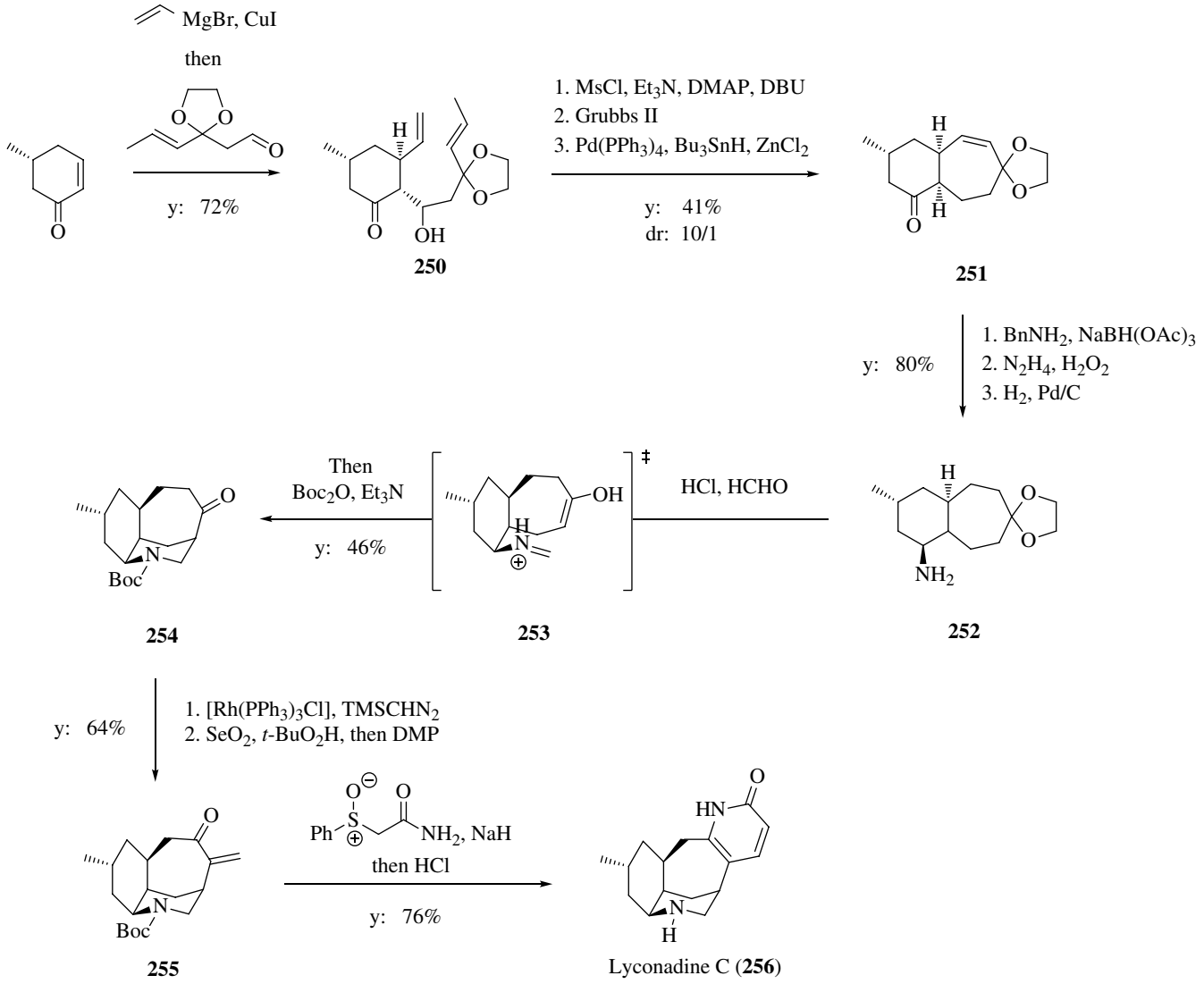
The same approach can be used to effectively synthesize (–)-coniine (**235**) in four steps in 42% overall yield on a multigram scale in less than 3 h (Scheme 11.51) [157]. For this purpose, instead of imine **230**, the *N*-PMP-protected imine **233** derived from butyric aldehyde was used in the initial vinylogous Mannich reaction (Scheme 11.51). Similar to the previously outlined protocol leading to (–)-anabasine (**232**), the resulting β-amino ketone (**234**) can be transferred into (–)-coniine (**235**).

Based on the Brønsted acid-catalyzed asymmetric vinylogous Mannich reaction, the lab of Schneider developed a highly flexible approach to access a variety of naturally and nonnaturally occurring indolizidine alkaloids, in general, in 11 steps in overall yields exceeding 36% (Scheme 11.52) [158, 159]. To set up the first two stereocenters of the indolizidine core, an ester-functionalized imine was chosen to react with the acyclic silyl dienolate **236** in the vinylogous Mannich reaction, which would readily cyclize to furnish the intermediate γ-lactam (**238**) in good yields and excellent enantioselectivities on a multigram scale (Scheme 11.52). Subsequent reduction of the double bond, removal of the PMP-protective group, and protection of the secondary amine with $Boc_2O$ afforded the general intermediate **239**, which can be converted either into 5-monosubstituted (e.g., (+)-indolizidine 167B **241**), 3,5-disubstituted (e.g., (+)-monomorine **243**), 5,8-disubstituted (e.g., (+)-indolizidine 167A **245**), 5,6,8-trisubstituted (e.g., indolizidine 195G **247**), or 6,7-dihydro-indolizidines (e.g., indolizidine 179 **249**).

The aforementioned synthetic examples clearly show that the incorporation of a catalytic asymmetric Mannich or Mannich-type reaction facilitates the synthesis of these types of natural products in terms of reducing the number of synthetic steps required and improving the overall yields. However, this approach has been only marginally explored yet and so far is rather limited to mono- or bicyclic alkaloids,




**SCHEME 11.52** A flexible approach toward the total synthesis of various indolizidine alkaloids based on the asymmetric vinylogous Mannich reaction as key step.



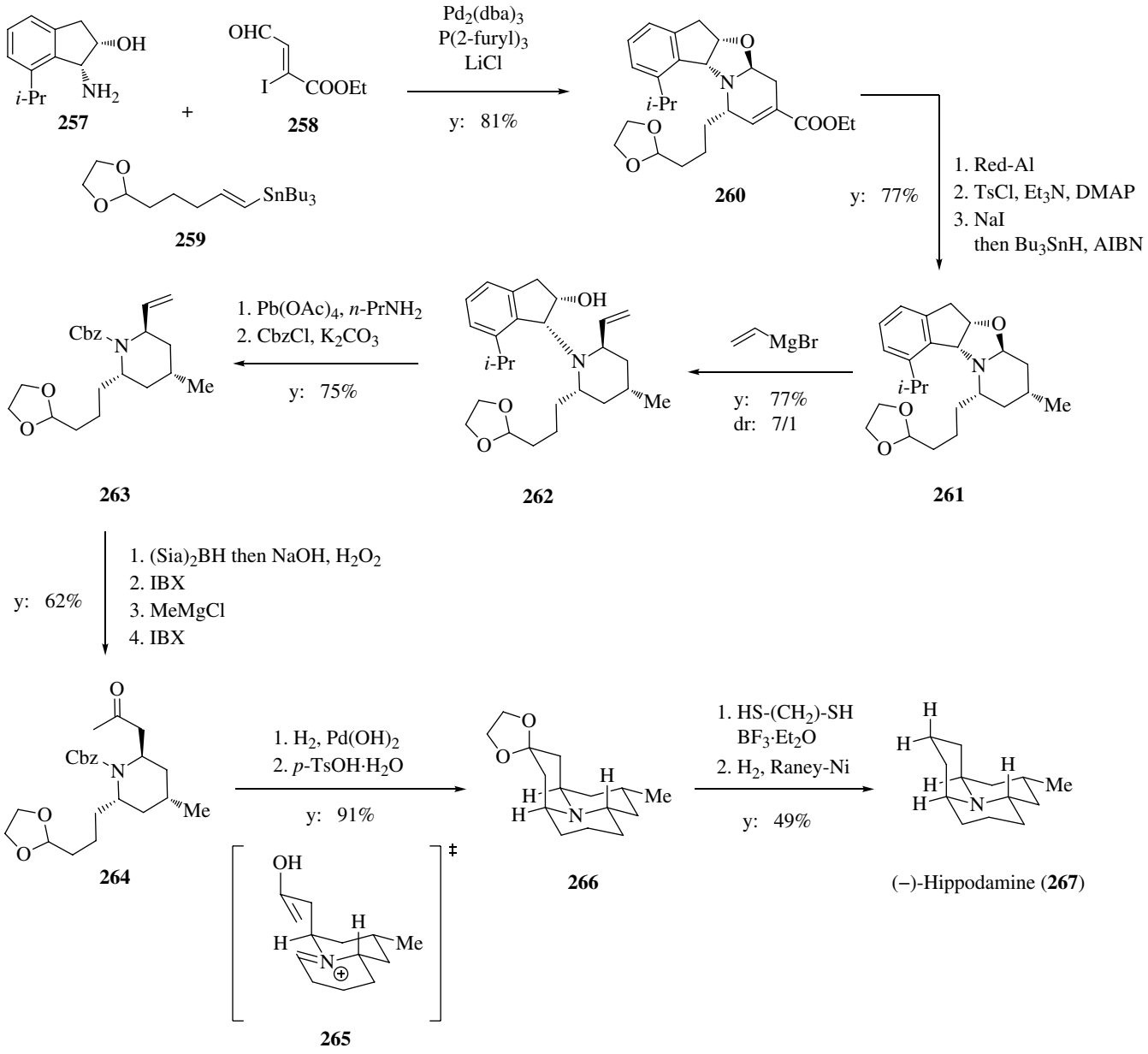

**SCHEME 11.53** Asymmetric total synthesis of lyconadine C.

such as piperidine and indolizidine alkaloids. An intramolecular version of the Mannich reaction, on the other hand, has been utilized quiet routinely in the total synthesis of more complex alkaloids derived from L-Orn and L-Lys, predominately lycopodium alkaloids, though.

In this respect, the imine electrophile and the nucleophile are fixed in a spatial orientation, which is necessary for the stereoselective C–C bond formation, making the addition of a chiral catalyst unnecessary. As an example, here we wish to highlight only the most recent examples of the incorporation of an intramolecular Mannich reaction in the enantioselective total synthesis of L-Lys-derived alkaloids, namely, (−)-hippodamine (**267**) and (−)-lyconadine C (**256**). The latter was accessible from the bicyclic intermediate **252** in a tandem ketal removal/Mannich reaction to furnish the tricyclic core structure **254** (Scheme 11.53) [160]. Subsequent methylenation, allylic oxidation, and introduction of the pyridone moiety according to a procedure by Fukuyama and Yokoshima afforded natural (−)-lyconadine C (**256**) in 5% overall yield over 11 steps.

The azaphenalene core of (−)-hippodamine (**267**), a defense alkaloid secreted by the ladybird beetle, can be constructed via an asymmetric azaelectrocyclization and subsequent Mannich cyclization (Scheme 11.54) as key steps [161].

First, the combination of 6,6-ethylenedioxy-1-hexenylstannane (**259**), (−)-7-isopropyl-*cis*-1-amino-2-indanol (**257**), and ethyl (*Z*)-2-iodo-4-oxobutenoate (**258**) in a three-component 6π-azaelectrocyclization reaction furnished the chiral piperidine **260** as a single stereoisomer. Then, reduction of the conjugated double bond followed by chemoselective reduction of the ester and subsequent

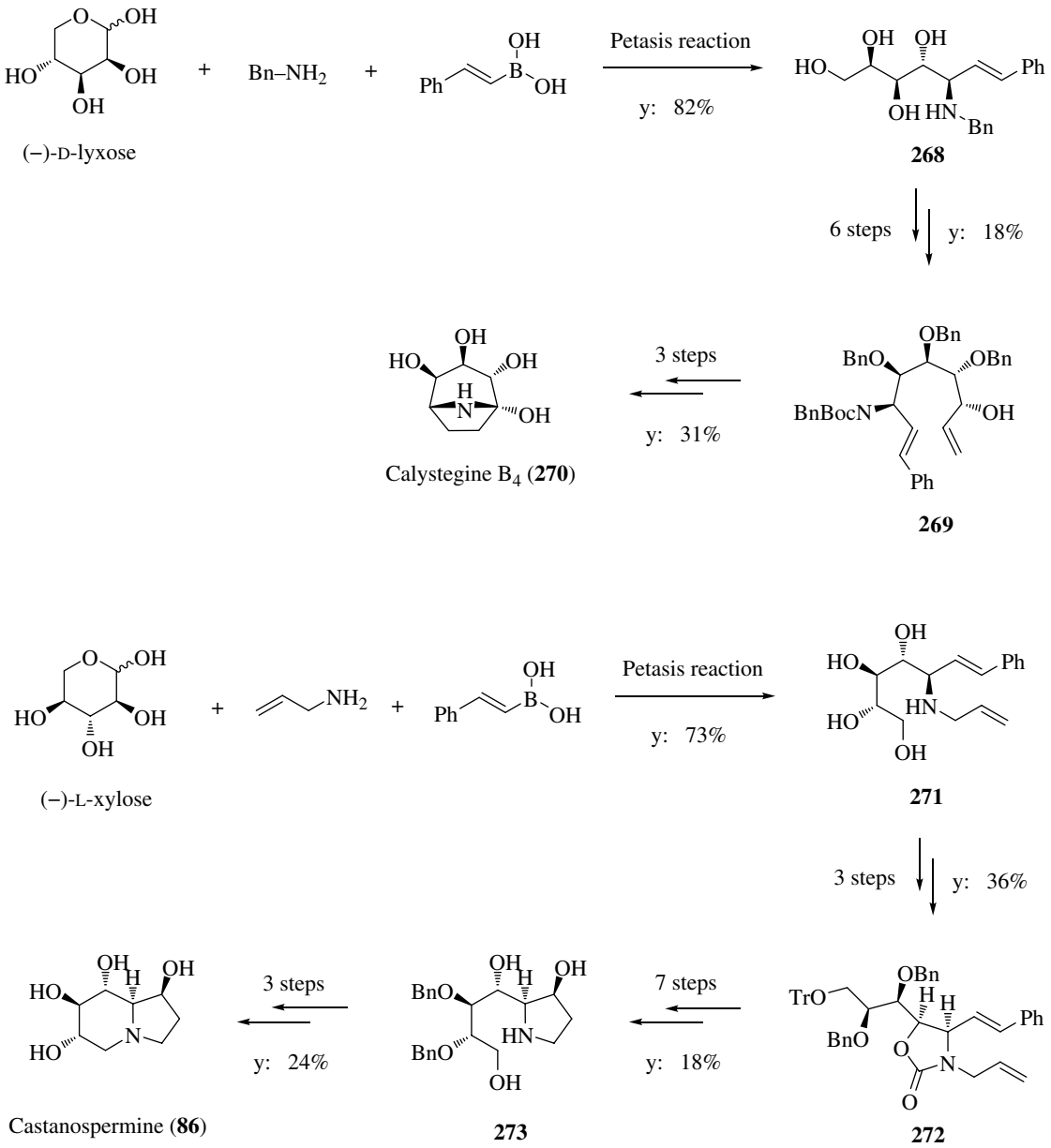



**SCHEME 11.54** Asymmetric total synthesis of (−)-hippodamine.

deoxygenation afforded intermediate **261**. Treatment of aminal **261** with vinylmagnesium bromide gave the vinylated piperidine **262** in good selectivity. After removal of the indanol moiety, the secondary amine was protected with CbzCl, and the methyl ketone was introduced in a four-step sequence. After reductive cleavage of the Cbz-protective group, the resulting piperidine underwent smoothly Mannich cyclization under acidic conditions to furnish the natural (−)-hippodamine (**267**) after subsequent deoxygenation via dithioketalization–desulfurization in 10% overall yield over 16 steps.

For a more comprehensive overview on recent applications of the Mannich cyclization in alkaloid total synthesis, the interested reader should refer to excellent reviews by Rinner [36] and Poupon [162].

Moreover, recently the boronic acid Mannich reaction, mostly referred to as Petasis reaction [163, 164], has evolved as a powerful entry to polyhydroxylated pyrrolizidine, indolizidine, and tropane alkaloids, among others [165, 166]. For example, Pyne and coworkers disclosed a short total synthesis of calystegine $B_4$ (**270**) starting from (−)-D-lyxose in 4.7% overall yield (Scheme 11.55), which involved, besides a ring-closing metathesis, the Petasis reaction as key step [167]. In a similar fashion, castanospermine (**86**) was prepared in 14 steps from (−)-L-xylose in 1.5% overall yield (Scheme 11.55) [168].




**SCHEME 11.55** Asymmetric total synthesis of polyhydroxylated alkaloids employing the Petasis–Mannich reaction as key step.

## 11.4 CONCLUSION

There is no doubt that the field of natural product synthesis benefited tremendously from the versatility and robustness of the Mannich reaction in constructing N-heterocyclic compounds. Since the pioneering work by Robinson and Schöpf almost a century ago, the concept of employing the Mannich or a Mannich-type reaction as key synthetic step has not only been limited to the total synthesis of L-Orn- or L-Lys-derived alkaloids, as outlined comprehensively in the previous chapter, but also alkaloids derived from other amino acid or non-amino acid precursors have been synthesized in a similar fashion [169, 170]. As developments continue, especially in the field of intermolecular asymmetric Mannich reactions, the toolbox of suitable catalysts and reactions is constantly extended, which enables to access novel frameworks found in alkaloids in an highly stereoselective fashion. Moreover, due to convergence and the atom efficiency of the Mannich reaction, an advanced adoption of this methodology in natural product synthesis will most certainly reduce the amount of synthetic steps required and might facilitate the synthesis of natural product analogs for lead optimization purposes in drug discovery programs.

## REFERENCES


1. G. A. Cordell, M. L. Quinn-Beattie, N. R. Farnsworth, *Phytother. Res.* 2001, **15**, 183–205.
2. M. Hesse, *Alkaloids: Nature's Curse or Blessing*. 1st Edition, John Wiley & Sons, Ltd, Weinheim (2002).
3. M. Wink, Ecological roles of alkaloids, in *Modern Alkaloids: Structure, Isolation, Synthesis and Biology*, 1st Edition (Eds. E. Fattorusso and O. Taglialatela-Scafati), John Wiley & Sons, Ltd, Weinheim (2008), pp. 3–24.
4. M. F. Roberts, D. Strack, M. Wink, *Annual Plant Reviews* 2010, **40**, 20–91.
5. J. Ziegler, P. J. Facchini, *Annu. Rev. Plant Biol.* 2008, **59**, 735–769.
6. G. McKay, P. D. Shargool, *Plant Sci. Lett.* 1977, **9**, 189–193.
7. M. E. Jones, *J. Nutr.* 1985, **115**, 509–515.
8. G. Wu, F. W. Bazer, T. A. Davis, S. W. Kim, P. Li, J. M. Rhoads, M. C. Satterfield, S. B. Smith, T. E. Spencer, Y. Yin, *Amino Acids*, 2009, **37**, 153–168.
9. P. W. Dewick, *Medicinal Natural Products. A Biosynthetic Approach*. 2nd Edition, John Wiley & Sons, Ltd, Chichester (2002).
10. T. A. Smith, *Ann. NY Acad. Sci.* 1970, **171**, 988–1001.
11. C. White Tabor, H. Tabor, *Annu. Rev. Biochem.* 1976, **45**, 285–306.
12. N. Bagni, A. Tassoni, *Amino Acids* 2001, **20**, 301–317.
13. C. White Tabor, H. Tabor, *Annu. Rev. Biochem.* 1984, **53**, 749–790.
14. T. Hartmann, D. Ober, *Top. Curr. Chem.* 2000, **209**, 207–243.
15. D. J. Robins, *Chem. Soc. Rev.* 1989, **18**, 375–408.
16. D. S. Seigler, (1998) Pyrrolizidine, quinolizidine, and indolizidine alkaloids, in *Plant Secondary Metabolism*, 1st edition (Ed. D. S. Seigler), Springer Science and Business Media, New York (1998), pp. 546–567.
17. S. Weber, W. Eisenreich, A. Bacher, T. Hartmann, *Phytochemistry* 1999, **50**, 1005–1014.
18. D. H. G. Crout, N. M. Davies, E. H. Smith, D. Whitehouse, *J. Chem. Soc. Perkin 1* 1972, **5**, 671–680.
19. T. Hemscheidt, *Top. Curr. Chem.* 2009, **209**, 175–206.
20. A. J. Humphrey, D. O'Hagan, *Nat. Prod. Rep.* 2001, **18**, 494–502.
21. F. Nakanishi, K. Sasaki, K. Shimomura, *Plant Cell Rep.* 1998, **18**, 249–251.
22. C. Hertweck, B. S. Moore, *Tetrahedron* 2000, **56**, 9115–9120.
23. B. Dräger, *Nat. Prod. Rep.* 2004, **21**, 211–223.
24. S. Biastoff, B. Dräger, Calystegines, in *The Alkaloids. Chemistry and Biology*, Vol. **64** (Ed. G. A. Cordell), Academic Press, Oxford (2007), pp. 49–102.
25. A. Goldmann, M. L. Milat, P. H. Ducrot, J. Y. Lallemand, M. Maille, A. Lepingle, I. Charpin, D. Tepfer, *Phytochemistry*, 1990, **29**, 2125–2127.
26. R. J. Molyneux, R. J. Nash, N. Asano, The chemistry and biological activity of calystegines and related nortropane alkaloids, in *Alkaloids: Chemical and Biological Perspectives*, Vol. **11** (Ed. S. W. Pelletier), Pergamon, Oxford (1996), pp. 303–343.
27. S. Bunsupa, M. Yamazaki, K. Saito, *Front. Plant Sci.* 2012, **3**:239, doi:10.3389/fpls.2012.00239.
28. X. Ma, D. R. Gang, *Nat. Prod. Rep.* 2004, **21**, 752–772.
29. J.-C. Braekman, R. N, Gupta, D. B. MacLean, I. D. Spenser, *Can. J. Chem.* 1972, **50**, 2591–2602.
30. L. F. Mao, C. Chu, H. Schulz, *Biochemistry* 1994, **33**, 3320–3326.
31. W. M. Golebiewski, I. Spenser, *Can. J. Chem.* 1988, **66**, 1734–1748.
32. S. Ohmiya, K. Saito, I. Murakoshi, Lupine alkaloids, in *The Alkaloids. Chemistry and Pharmacology*, Vol. **47** (Ed. G. A. Cordell), Academic Press, Oxford (1995), pp. 1–114.
33. T. Schmeller, M. Wink, Utilization of alkaloids in modern medicine, in *Alkaloids: Biochemistry. Ecology and Medicinal Applications* (Eds. M. F. Roberts and M. Wink), Plenum Press, New York (1998), pp. 435–459.
34. M. Wink, *Planta Medica*, 1987, **53**, 509–514.
35. M. Kitajima, H. Takayama, *Top. Curr. Chem.* 2012, **309**, 1–32.
36. P. Siengalewicz, J. Mulzer, U. Rinner, *Lycopodium* alkaloids—synthetic highlights and recent developments, in *The Alkaloids: Chemistry and Biology*, Vol. **72** (Ed. H.-J. Knölker), Academic Press, Oxford (2013), pp. 1–151.
37. D.-Y. Zhu, C.-H. Tan, Y.-M. Li, The overview of studies on huperzine A: a natural drug for the treatment of Alzheimer's disease, in *Medicinal Chemistry of Bioactive Natural Products*, 1st edition (Eds. X.-T. Liang and W.-S. Fang), John Wiley & Sons, Inc, Hoboken (2006), pp. 143–182.
38. B.-S. Wang, H. Wang, Z.-H. Wie, Y.-Y. Song, L. Zhang, H.-Z. Chen, *J. Neural. Transm.* 2009, **116**, 457–465.
39. C. M. Harris, M. J. Schneider, F. S. Ungemach, J. E. Hill, T. M. Harris, *J. Am. Chem. Soc.* 1988, **110**, 940–949.
40. H. P. Broquist, *Annu. Rev. Nutr.* 1991, **11**, 435–448.
41. R. N. Gupta, I. D. Spenser *J. Biol. Chem.* 1969, **244**, 88–94.
42. T. M. Zabriskie, M. D. Jackson, *Nat. Prod. Rep.* 2000, **17**, 85–97.
43. M. He, *J. Ind. Microbiol. Biotechnol.* 2006, **33**, 401–407.
44. D. C. Montefiori, W. E. Robinson Jr., W. M. Mitchell, *Proc. Natl. Acad. Sci. U.S.A*, 1988, **85**, 9248–9252.
45. A. A. Watson, G. W. J. Fleet, N. Asano, R. J. Molyneux, R. J. Nash, *Phytochemistry* 2001, **56**, 265–295.
46. C. Mannich, W. Krösche, *Arch. Pharm.* 1912, **250**, 647–667.
47. M. Arend, B. Westermann, N. Risch, *Angew. Chem. Int. Ed.* 1998, **37**, 1044–1070.
48. L. E. Overman, D. J. Ricca, The intramolecular Mannich and related reactions, in *Comprehensive Organic Synthesis*, Vol. **2** (Eds. B. M. Trost, I. Fleming and C. H. Heathcock), Pergamon, Oxford (1991), pp. 1007–1046.
49. S. Yamasaki, T. Iida, M. Shibasaki, *Tetrahedron Lett.* 1999, **40**, 307–310.
50. A. Córdova, Examples of metal-free direct catalytic asymmetric Mannich-type reactions using aminocatalysis, in *Stereoselective*

*Organocatalysis: Bond Formation Methodologies and Activation Modes*, 1st edition (Ed. R. R. Torres), John Wiley & Sons, Inc, Hoboken (2013), pp. 129–146.

51. C. de Graaff, E. Ruijter, R. V. A. Orru, *Chem. Soc. Rev.* 2012, **41**, 3969–4009.
52. S. Kobayashi, Y. Mori, J. S. Fossey, M. M. Salter, *Chem. Rev.* 2011, **111**, 2626–2704.
53. J. M. M. Verkade, L. J. C. van Hemert, P. J. L. M. Quaedflieg, F. P. J. T. Rutjes, *Chem. Soc. Rev.* 2008, **37**, 29–41.
54. S. Mukherjee, J. W. Yang, S. Hoffmann, B. List, *Chem. Rev.* 2007, **107**, 5471–5569.
55. A. Ting, S. E. Schaus, *Eur. J. Org. Chem.* 2007, 5797–5815.
56. A. Córdova, *Acc. Chem. Res.* 2004, **37**, 102–112.
57. B. List, *J. Am. Chem. Soc.* 2000, **122**, 9336–9337.
58. B. List, P. Pojarliev, W. T. Biller, H. J. Martin, *J. Am. Chem. Soc.* 2002, **124**, 827–833.
59. I. Ibrahem, W. Zou, M. Engqvist, Y. Xu, A. Córdova, *Chem. Eur. J.* 2005, **11**, 7024–7029.
60. H. Kotsuki, H. Ikishima, A. Okuyama, *Heterocycles* 2008, **75**, 493–529.
61. H. Kotsuki, H. Ikishima, A. Okuyama, *Heterocycles* 2008, **75**, 757–797.
62. B. List, *Tetrahedron* 2002, **58**, 5573–5590.
63. A. J. A. Cobb, D. M. Shaw, D. A. Longbottom, J. B. Gold, S. V. Ley, *Org. Biomol. Chem.* 2005, **3**, 84–96.
64. S. Mitsumori, H. Zhang, P. H. -Y. Cheong, K. N. Houk, F. Tanaka, C. F. Barbas III, *J. Am. Chem. Soc.* 2006, **128**, 1040–1041.
65. H. Zhang, M. Mifsud, F. Tanaka, C. F. Barbas III, *J. Am. Chem. Soc.* 2006, **128**, 9630–9631.
66. T. Kano, Y. Yamaguchi, O. Tokuda, K. Maruoka, *J. Am. Chem. Soc.* 2005, **127**, 16408–16409.
67. T. Kano, Y. Hato, K. Maruoka, *Tetrahedron Lett.* 2006, **47**, 8467–8469.
68. I. Ibrahem, A. Córdova, *Chem. Commun.* 2006, 1760–1762.
69. For a general overview concerning solid-supported proline organocatalysts and their applications see: M. Gruttadauria, F. Giacalone, R. Noto, *Chem. Soc. Rev.* 2008, **37**, 1666–1688.
70. M. Benaglia, M. Cinquini, F. Cozzi, A. Puglisi, G. Celentano, *Adv. Synth. Catal.* 2002, **344**, 533–542.
71. For a general overview concerning stereoselective reactions in flow refer to: A. Puglisi, M. Benaglia, V. Chiroli, *Green Chem.* 2013, **15**, 1790–1813.
72. B. P. Mason, K. E. Price, J. L. Steinbacher, A. R. Bogdan, D. T. McQuade, *Chem. Rev.* 2007, **107**, 2300–2318.
73. E. Alza, C. Rodríguez-Escrich, S. Sayalero, A. Bastero, M. A. Pericàs, *Chem. Eur. J.* 2009, **15**, 10167–10172.
74. R. Martín-Rapún, S. Sayalero, M. A. Pericàs, *Green Chem.* 2013, **15**, 3295–3301.
75. A. Ting, J. M. Goss, N. T. McDougal, S. E. Schaus, *Top. Curr. Chem.* 2010, **291**, 145–200.
76. C. Palomo, M. Oiarbide, R. Rosa López, *Chem. Soc. Rev.* 2009, **38**, 632–653.
77. T. B. Poulsen, C. Alemparte, S. Saaby, M. Bella, K. A. Jørgensen, *Angew. Chem. Int. Ed.* 2005, **44**, 2896–2899.
78. S. Lou, B. M. Taoka, A. Ting, S. E. Schaus, *J. Am. Chem. Soc.* 2005, **127**, 11257–11257.
79. J. Song, Y. Wang, L. Deng, *J. Am. Chem. Soc.* 2006, **128**, 6048–6049.
80. Q. Guo, J. C. -G. Zhao, *Org. Lett.* 2013, **15**, 508–511.
81. Y. Yamaoka, H. Miyabe, Y. Yasui, Y. Takemoto, *Synthesis*, 2007, **16**, 2571–2575.
82. A. G. Wenzel, E. N. Jacobsen, *J. Am. Chem. Soc.* 2002, **124**, 12964–12965.
83. M. P. Coles, *Chem. Commun.* 2009, 3659–3676.
84. D. Leow, C.-H. Tan, *Synlett*, 2010, **11**, 1589–1605.
85. P. Selig, *Synthesis* 2013, **45**, 703–718.
86. Y. Pan, Y. Zhao, T. Ma, Y. Yang, H. Liu, Z. Jiang, C.-H. Tan, *Chem. Eur. J.* 2010, **16**, 779–782.
87. Y. Sohtome, S. Tanaka, K. Takada, T. Yamaguchi, K. Nagasawa, *Angew. Chem. Int. Ed.* 2010, **49**, 9254–9257.
88. M. Terada, *Synthesis*, 2010, **12**, 1929–1982.
89. A. Zamfir, S. Schenker, M. Freund, S. B. Tsogoeva, *Org. Biomol. Chem.* 2010, **8**, 5262–5276.
90. D. Kampen, C. M. Reisinger, B. List, *Top. Curr. Chem.* 2010, **291**, 395–456.
91. T. Akiyama, J. Itoh, K. Yokota, K. Fuchibe, *Angew. Chem. Int. Ed.* 2004, **43**, 1566–1568
92. M. Yamanaka, J. Itoh, K. Fuchibe, T. Akiyama, *J. Am. Chem. Soc.* 2007, **129**, 6756–6764.
93. D. Uraguchi, M. Terada, *J. Am. Chem. Soc.*, 2004, **126**, 5356–5357.
94. For comprehensive mechanistic investigations regarding imine reactions catalysed by chiral BINOL-phosphoric acids see: L. Simón, J. M. Goodman, *J. Org. Chem.* 2011, **76**, 1775–1788.
95. Q.-X. Guo, H. Liu, C. Guo, S.-W. Luo, Y. Gu, L.-Z. Gong, *J. Am. Chem. Soc.* 2007, **129**, 3790–3791.
96. M. Sickert, C. Schneider, *Angew. Chem. Int. Ed.* 2008, **47**, 3631–3634.
97. M. Sickert, F. Abels, M. Lang, J. Sieler, C. Birkemeyer, C. Schneider, *Chem. Eur. J.* 2010, **16**, 2806–2818.
98. M. Hatano, T. Maki, K. Moriyama, M. Arinobe, K. Ishihara, *J. Am. Chem. Soc.* 2008, **130**, 16858–16860.
99. Y.-Y. Chen, Y.-J. Jiang, Y.-S. Fan, D. Sha, Q. Wang, G. Zhang, L. Zheng, S. Zhang, *Tetrahedron: Asymmetry*, 2012, **23**, 904–909.
100. G. Dagousset, F. Drouet, G. Masson, J. Zhu, *Org. Lett.* 2009, **11**, 5546–5549.
101. For a comprehensive overview on the chemistry of the Povarov reaction see: V. V. Kouznetsov, *Tetrahedron* 2009, **65**, 2721–2750.
102. B. M. Trost, *Angew. Chem. Int. Ed.* 1995, **34**, 259–281.
103. E. N. Jacobsen, A. Pfaltz, H. Yamamoto (Eds.) *Comprehensive Asymmetric Catalysis*, Springer, Berlin (1999).
104. J. Christoffers, G. Koripelly, A. Rosiak, M. Rössle, *Synthesis* 2007, **9**, 1279–1300.
105. For a comprehensive overview on metal-catalyzed asymmetric Mannich reactions see: B. Karimi, D. Enders, E. Jafari, *Synthesis* 2013, **45**, 2769–2812.

106. S. Matsunaga, N. Kumagai, S. Harada, M. Shibasaki, *J. Am. Chem. Soc.* 2003, **125**, 4712–4713.
107. S. Matsunaga, T. Yoshida, H. Morimoto, N. Kumagai, M. Shibasaki, *J. Am. Chem. Soc.* 2004, **126**, 8777–8785.
108. B. M. Trost, J. Jaratjaroonphong, V. Reutrakul, *J. Am. Chem. Soc.* 2006, **128**, 2778–2779.
109. A. Viso, R. Fernández de la Pradilla, A. García, A. Flores, *Chem. Rev.* 2005, **105**, 3167–3196.
110. R. Gómez Arrayás, J. C. Carretero, *Chem. Soc. Rev.* 2009, **38**, 1940–1948.
111. Y. Yamashita, S. Yoshimoto, K. Masuda, S. Kobayashi, *Asian J. Org. Chem.* 2012, **1**, 327–330.
112. M. Hayashi, M. Sano, Y. Funahashi, S. Nakamura, *Angew. Chem. Int. Ed.* 2013, **52**, 5557–5560.
113. S. Kobayashi, Y. Yamashita, *Acc. Chem. Res.* 2011, **44**, 58–71.
114. Y. Yamashita, T. Tsubogo, S. Kobayashi, *Chem. Sci.* 2012, **3**, 967–975.
115. T. Tsubogo, Y. Yamashita, S. Kobayashi, *Top. Organomet. Chem.* 2013, **45**, 243–270.
116. T. Poisson, T. Tsubogo, Y. Yamashita, S. Kobayashi, *J. Org. Chem.* 2010, **75**, 963–965.
117. T. Tsubogo, S. Shimizu, S. Kobayashi, *Chem. Asian J.* 2013, **8**, 872–876.
118. R. A. Sheldon, *Chem. Commun.* 2008, 3352–3365.
119. R. Wohlgemuth, *Curr. Opin. Biotechnol.* 2010, **21**, 713–724.
120. P. J. Dunn, *Chem. Soc. Rev.* 2012, **41**, 1452–1461.
121. R. A. Sheldon, *Chem. Soc. Rev.* 2012, **41**, 1437–1451.
122. K. Li, T. He, C. Li, X.-W. Feng, N. Wang, X.-Q. Yu, *Green Chem.* 2009, **11**, 777–779.
123. T. He, K. Li, M.-Y. Wu, X.-W. Feng, N. Wang, H.-Y. Wang, C. Li, X.-Q. Yu, *J. Mol. Catal. B: Enzym.* 2010, **67**, 189–194.
124. S.-J. Chai, Y.-F. Lai, H. Zheng, P.-F. Zhang, *Helv. Chim. Acta*, 2010, **93**, 2231–2236.
125. M. López-Iglesias, E. Busto, V. Gotor, V. Gotor-Fernández, *Adv. Synth. Catal.* 2011, **353**, 2345–2353.
126. Y. Xue, L.-P. Li, Y.-H. He, Z. Guan, *Sci. Rep.* 2012, **2**, doi:10.1038/srep00761.
127. Z. Guan, Y.-L. Chen, Y. Yuan, J. Song, D.-C. Yang, Y. Xue, Y.-H. He, *PLoS One* 2014, **9**(8), e105284.
128. R. Willstätter, *Liebigs Ann. Chem.* 1901, **317**, 204–265.
129. R. Willstätter, *Liebigs Ann. Chem.* 1901, **317**, 307–374.
130. R. Willstätter, *Liebigs Ann. Chem.* 1903, **326**, 1–22.
131. R. Robinson, *J. Chem. Soc., Trans.* 1917, **111**, 762–768.
132. R. Robinson, *J. Chem. Soc., Trans.* 1917, **111**, 876–899.
133. C. Schöpf, G. Lehmann, *Liebigs Ann. Chem.* 1935, **518**, 1–37.
134. R. C. Menzies, R. Robinson, *J. Chem. Soc., Trans.* 1924, **125**, 2163–2168.
135. C. Schöpf, *Angew. Chem.* 1937, **50**, 779–790.
136. A. C. Cope, H. L. Dryden Jr., C. G. Overberger, A. A. D'Addieco, *J. Am. Chem. Soc.* 1951, **73**, 3416–3418.
137. J. F. Casale, *Forensic Sci. Int.* 1987, **33**, 275–298.
138. E. F. L. J. Anet, G. K. Hughes, E. Ritchie, *Nature* 1949, **163**, 289.
139. E. F. L. J. Anet, G. K. Hughes, E. Ritchie, *Aust. J. Sci. Res. A* 1949, **2**, 616–621.
140. E. Anet, G. K. Hughes, E. Ritchie, *Nature*, 1949, **164**, 501.
141. E. F. L. J. Anet, G. K. Hughes, E. Ritchie, *Aust. J. Sci. Res. A* 1950, **3**, 616–621.
142. C. Schöpf, *Angew. Chem.* 1949, **61**, 31–32.
143. C. Schöpf, F. Braun, K. Burkhardt, G. Dummer, H. Müller, *Liebigs Ann. Chem.* 1959, **626**, 123–133.
144. E. Leete, *J. Chem. Soc., Chem. Commun.* 1972, 1091.
145. E. Leete, S. A. S. Leete, *J. Org. Chem.* 1978, **43**, 2122–2125.
146. C. Schöpf, *Angew. Chem.* 1947, **59**, 29–30.
147. M. R. Monaco, P. Renzi, D. M. S. Schietroma, M. Bella, *Org. Lett.* 2011, **13**, 4546–4549.
148. T. K. Beng, R. E. Gawley, *J. Am. Chem. Soc.* 2010, **132**, 12216–12217.
149. G. Cheng, X. Wang, D. Su, H. Liu, F. Liu, Y. Hu, *J. Org. Chem.* 2010, **75**, 1911–1916.
150. S. Kobayashi, M. Ueno, R. Suzuki, H. Ishitani, H.-S. Kim, Y. Wataya, *J. Org. Chem.* 1999, **64**, 6833–6841.
151. T. Itoh, K. Nishimura, K. Nagata, Yokoya, M. *Synlett* 2006, 2207–2210.
152. K. Nagata, K. Nishimura, M. Yokoya, T. Itoh, *Heterocycles*, 2006, **70**, 335–344.
153. J. M. M. Verkade, F. van der Pijl, M. M. J. H. P. Willems, P. J. L. M. Quaedflieg, F. L. van Delft, F. P. J. T. Rutjes, *J. Org. Chem.* 2009, **74**, 3207–3210.
154. S. Chandrasekhar, R. V. N. S. Murali, C. Raji Reddy, *Tetrahedron Lett.* 2009, **50**, 5686–5688.
155. F. van der Pijl, R. K. Harmel, G. J. G. Richelle, P. Janssen, F. L. van Delft, F. P. J. T. Rutjes, *Org. Lett.* 2014, **16**, 2038–2041.
156. D. S. Giera, M. Sickert, C. Schneider, *Synthesis* 2009, 3797–3802.
157. F. Abels, C. Schneider, *Synthesis* 2011, 4050–4058.
158. F. Abels, C. Lindemann, E. Koch, C. Schneider, *Org. Lett.* 2012, **14**, 5972–5975.
159. F. Abels, C. Lindemann, C. Schneider, *Chem. Eur. J.* 2014, **20**, 1964–1979.
160. Y. Yang, C. W. Haskins, W. Zhang, P. Leng Low, M. Dai, *Angew. Chem. Int. Ed.* 2014, **53**, 3922–3925.
161. S. Fujita, T. Sakaguchi, T. Kobayashi, H. Tsuchikawa, S. Katsumura, *Org. Lett.* 2013, **15**, 2758–2761.
162. E. Poupon, R. Salame, L. -H. Yan, Biomimetic synthesis of ornithine/arginine and lysine-derived alkaloids: selected examples, in *Biomimetic Organic Synthesis*, 1st Edition (Eds. E. Poupon and B. Nay), John Wiley & Sons, Ltd, Weinheim (2011), pp. 3–60.
163. N. A. Petasis, Multicomponent reactions with organoboron compounds, in *Multicomponent Reactions*, 1st Edition (Eds. J. Zhu and H. Bienaymé), John Wiley & Sons, Ltd, Weinheim (2005), pp. 199–223.

164. N. R. Candeias, F. Montalbano, P. M. S. D. Cal, P. M. P. Gois, *Chem. Rev.* 2010, **110**, 6169–6193.

165. S. G. Pyne, C. W. G. Au, A. S. Davis, I. R. Morgan, T. Ritthiwigrom, A. Yazici, *Pure Appl. Chem.* 2008, **80**, 751–762.

166. S. G. Pyne, A. S. Davis, T. Ritthiwigrom, C. W. G. Au, K. Savaspun, M. Wotherspoon, *Pure Appl. Chem.* 2013, **85**, 1215–1225.

167. P. Moosophon, M. C. Baird, S. Kanokmedhakul, S. G. Pyne, *Eur. J. Org. Chem.* 2010, 3337–3344.

168. T. Machan, A. S. Davis, B. Liawruangrath, S. G. Pyne, *Tetrahedron* 2008, **64**, 2725–2732.

169. J. Hájíček, *Chem. Listy*, 2004, **98**, 1096–1111.

170. S. F. Martin, Strategies for the synthesis of alkaloids and novel nitrogen heterocycles, in *Advances in Heterocyclic Chemistry*, Vol. **110** (Ed. A. R. Katritzky), Academic Press, Oxford (2013), pp. 73–117.

# 12

# TYROSINE ALKALOIDS

Uwe Rinner[1,2] and Mario Waser[1]

[1] *Institute of Organic Chemistry, Johannes Kepler University Linz, Linz, Austria*
[2] *Department of Chemistry, College of Science, Sultan Qaboos University, Muscat, Oman*
**This chapter is dedicated to Prof. Tomas Hudlicky, on the occasion of his 65th birthday in recognition of his synthetic contributions to tyrosine-derived alkaloids, and on a more personal note (U.R.), in appreciation for his friendship and support.*

## 12.1 INTRODUCTION

Tyrosine (**1**) serves as substrate for the biosynthesis of a variety of structurally diverse natural products, and some of these secondary metabolites are of great pharmacologic, historic, and economic importance. To name a few, dopamine and adrenaline are well-known second messengers. Mescaline is a naturally occurring psychedelic alkaloid that has been used by some Native American tribes for several thousands of years in religious ceremonies. Morphine and structurally related opiates are important analgesics and invaluable in palliative care. Colchicine is used as effective medication against gout, while several Amaryllidaceae alkaloids are in clinical trial studies against various types of cancer.

This chapter provides an overview of the most important biosynthetic pathways leading to tyrosine alkaloids. Furthermore, synthetic approaches toward members of this class of secondary metabolites, mainly tetrahydroisoquinoline alkaloids and opiates, are outlined in the third section of this chapter. Very often, the structural diversity of tyrosine-derived secondary metabolites arises from different oxidative aryl–aryl coupling reactions. Thus, special emphasis is devoted to this highly important reaction throughout this section. Furthermore, the second section discusses various methods that have been elaborated to allow the formation of aryl–aryl bonds. Additionally, the chemical syntheses described within the third section have also been chosen in such a way as to present and discuss interesting strategies for the crucial aryl–aryl coupling reaction.

The main focus of this chapter rests on the discussion of biosynthetic routes and biomimetic synthesis. Detailed information on the enzymatic mechanisms is omitted. Also, the huge amount of research results and scientific contributions available on tyrosine-derived alkaloids does not allow an in-depth coverage of the field. References to book chapters, review articles, and research papers are included for further literature study.

## 12.2 BIOSYNTHESIS OF TYROSINE-DERIVED ALKALOIDS

The following section provides an overview of the most important biosynthetic routes leading to prominent tyrosine-derived alkaloids. Throughout the chapter, alkaloids are categorized as outlined in Figure 12.1. A schematic overview of the biosynthetic routes described herein concludes this section. Names of enzymes that have been identified to catalyze specific reactions are included in the reaction schemes.

### 12.2.1 Phenylethylamines

The most simple tyrosine-derived secondary metabolites are phenylethylamines with adrenaline and mescaline as prominent members. The biosynthetic route leading to these biologically important secondary metabolites and neurotransmitters is outlined in Scheme 12.1.

*From Biosynthesis to Total Synthesis: Strategies and Tactics for Natural Products*, First Edition. Edited by Alexandros L. Zografos.
© 2016 John Wiley & Sons, Inc. Published 2016 by John Wiley & Sons, Inc.

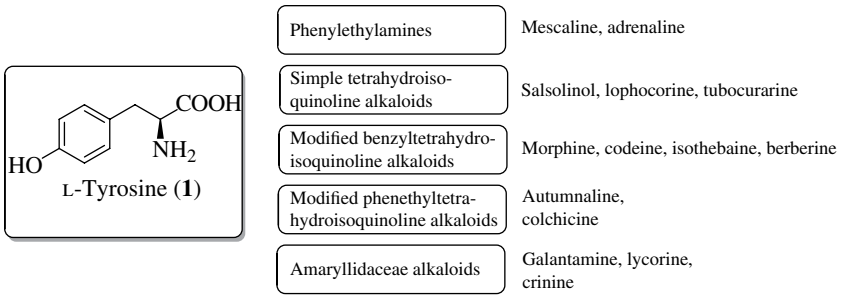
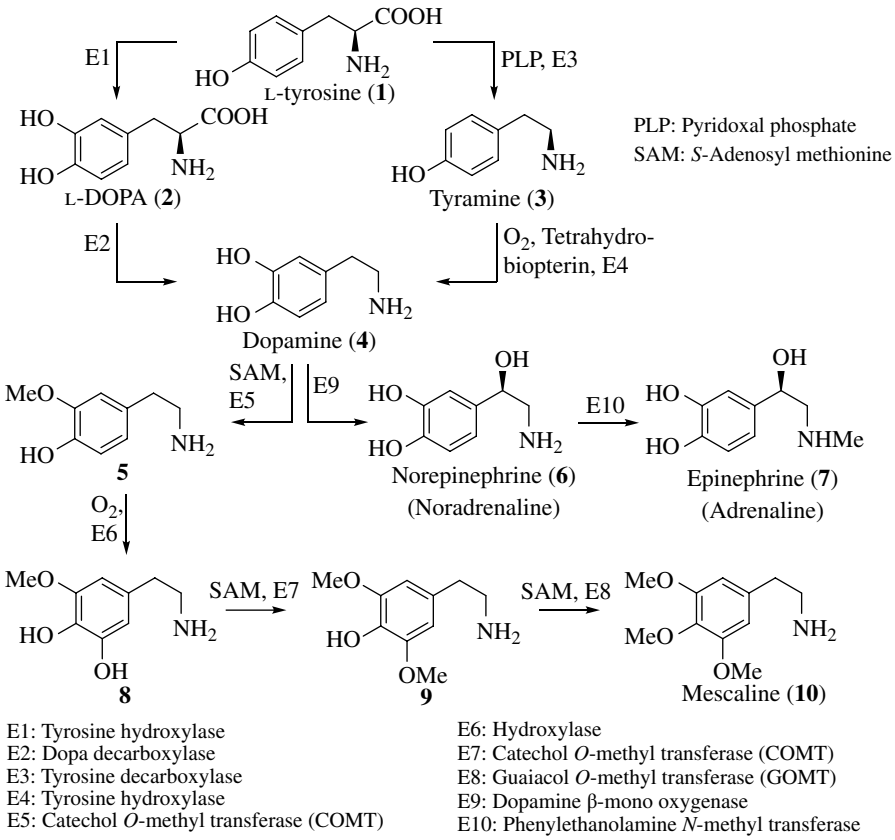



**FIGURE 12.1** Classification of tyrosine-derived secondary metabolites.




**SCHEME 12.1** Biosynthesis of adrenaline (**7**) and mescaline (**10**).

Dopamine (**4**) serves as key intermediate in the biosynthesis of the stress hormone adrenaline (**7**). Two different routes are available for the biosynthesis of **4** from tyrosine (**1**). Hydroxylation of the aromatic ring, catalyzed by tyrosine hydroxylase, affords L-DOPA (**2**), which is converted to dopamine (**4**) via a decarboxylation step. Alternatively, tyrosine decarboxylase-mediated decarboxylation of tyrosine delivers tyramine that can be hydroxylated to afford the important bioactive intermediate **4**. Hydroxylation of the benzylic position in **4** then leads to the formation of norepinephrine, also known as noradrenaline (**6**), which upon methylation of the amine is converted to epinephrine (adrenaline, **7**) [1].

Phenylethylamines and catecholamines are of crucial importance for many physiological processes [2]. L-DOPA (**2**) serves as precursor for dopamine, which acts as neurotransmitter in the human brain. Dopamine is associated with reward-motivated behavior and cognitive alertness, and the compound is linked to controlling the release of other important hormones. In contrast to dopamine (**4**), L-DOPA is able to cross the blood–brain barrier, and it is used to increase the concentration of dopamine in the brain in patients suffering from Parkinson's disease [3].

Norepinephrine (noradrenalin, **6**) acts as powerful peripheral vasoconstrictor, and similarly to its methylated congener epinephrine (adrenalin, **7**), the neurotransmitter

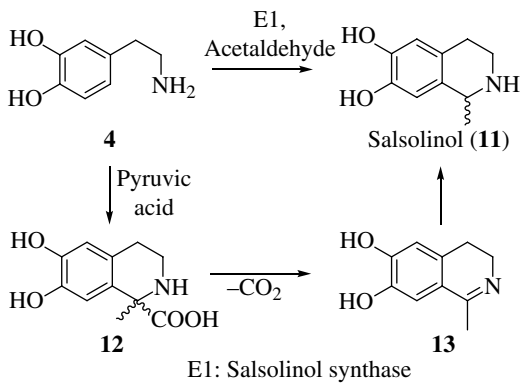
is able to restore blood pressure in case of acute hypotension [4]. Epinephrine furthermore affects glycogen breakdown and increases metabolic processes, which produce energy in emergency situations.

Because of the pronounced biological activity of phenylethylamines and catecholamines, structurally related derivatives of these important neurotransmitters also trigger distinct physiological responses. Mescaline (**10**), isolated from the peyote cactus (*Lophophora williamsii*), is one of the best-known hallucinogenic alkaloids. Peyote has been used by Native American tribes in religious ceremonies to establish contact with spirits and gods for thousands of years [5, 6]. Mescaline (**10**) is biosynthetically derived from dopamine (**4**) as also outlined in Scheme 12.1 [7]. Methylation of one phenolic hydroxyl group (**5**) is followed by hydroxylation of the aromatic ring (**8**) before two subsequent methylation steps afford the hallucinogenic natural product (**10**).

### 12.2.2 Simple Tetrahydroisoquinoline Alkaloids

Simple tetrahydroisoquinoline alkaloids are obtained upon condensation of phenylethylamines and catecholamines with carbonyl compounds. In a subsequent Mannich-like reaction, the biosynthetic equivalent to a Pictet–Spengler reaction, the heterocyclic ring system is established. Numerous examples of simple tetrahydroisoquinoline alkaloids have been isolated from different plant sources. Several of these tyrosine-derived secondary metabolites exhibit intriguing biological and physiological properties, due to their structural relationship to catecholamines and phenylethylamines.

Exemplarily, the biosynthesis of salsolinol (**11**) is outlined in Scheme 12.2. Salsolinol has been isolated from various plant sources, such as the cacao plant [8], banana fruits [9], marine sponges [10], and several *Corydalis* species (Papaveraceae) [11]. Generally, tetrahydroisoquinoline alkaloids can be obtained via condensation of the corresponding phenylethylamine with an aldehyde (top line, Scheme 12.2) and subsequent Pictet–Spengler reaction, or alternatively via condensation of the requisite ketoacid, followed by cyclization and loss of carbon dioxide (bottom line, Scheme 12.2). A remarkable reaction sequence is used to remove the carboxyl moiety. Instead of employing a simple decarboxylation step, an oxidative protocol, consisting of the initial formation of an imine as intermediate, is used. Reduction of the imine then releases the tetrahydroisoquinoline alkaloid. Interestingly, both pathways are used in living systems to produce this class of tyrosine-derived alkaloids [12]. Enzymes involved in the reaction sequence have not been identified so far.




**SCHEME 12.2** Biosynthesis of salsolinol (**11**).

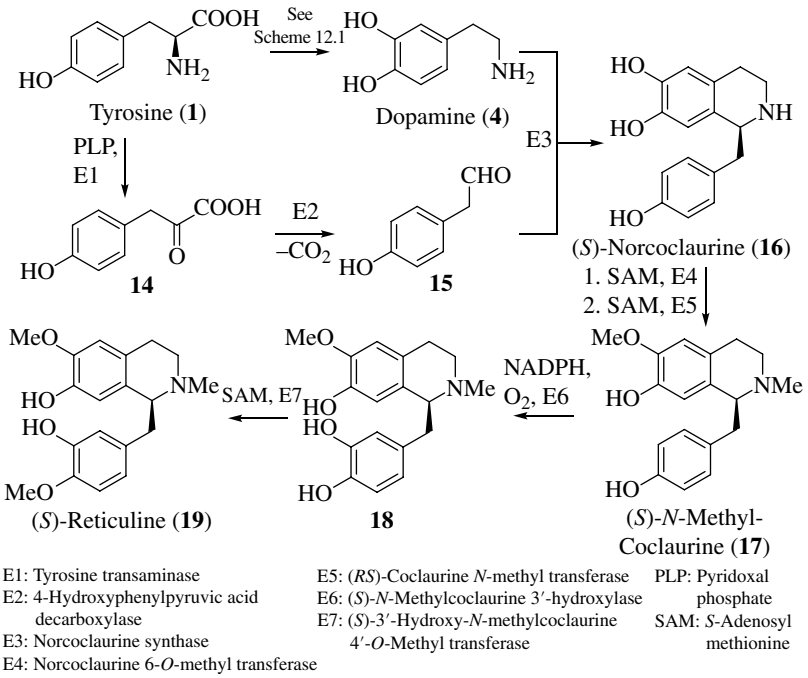
Salsolinol has also been isolated from human urine and blood, especially after consumption of alcoholic beverages [13]. There, the alkaloid is formed via condensation of dopamine and ethanol-derived acetaldehyde.

### 12.2.3 Modified Benzyltetrahydroisoquinoline Alkaloids

The condensation of dopamine (**4**) with phenylethyl units and subsequent cyclization result in the formation of benzyltetrahydroisoquinoline alkaloids. These initial reaction steps are identical to those discussed for the formation of simple tetrahydroisoquinoline alkaloids. However, the additional aromatic ring allows further modification, and a variety of structurally diverse classes of alkaloids are obtained via different aryl–aryl coupling reactions. Among others, protoberberine alkaloids, porphine alkaloids, and the most important class of opium alkaloids can be summarized as modified benzyltetrahydroisoquinoline alkaloids.

The manifold possibilities for the elaboration of structurally intriguing natural products via the aforementioned oxidative aryl–aryl coupling reactions emphasize the importance of phenolic coupling reactions in the biosynthesis of tyrosine-derived alkaloids. This important reaction not only plays a significant role in the biosynthesis of benzyltetrahydroisoquinoline alkaloids but also for the construction of phenethylisoquinoline alkaloids and Amaryllidaceae constituents, discussed in the following sections.

The biosynthesis of benzyltetrahydroisoquinoline alkaloids has been thoroughly studied—mainly because of the medicinal and commercial importance of opium alkaloids—and commences with the preparation of (*S*)-reticuline (**19**). Reticuline then presents a point of divergence and as starting point for the biosynthesis of the previously named tyrosine-derived alkaloids with different skeletal structures [14–16]. The route to (*S*)-reticuline is outlined in Scheme 12.3. Both reaction partners for the condensation reaction and formation of (*S*)-norcoclaurine (**16**) are derived from tyrosine. The aromatic portions in (*S*)-reticuline (**19**) possess an *ortho*-dihydroxylation pattern as present in dopamine (**4**). However, only the northern portion in **19** is derived from dopamine, and the second hydroxyl functionality in the southern part is introduced after the formation of the tetrahydroisoquinoline ring system. The synthesis of the southern portion in




**SCHEME 12.3** Biosynthesis of (*S*)-reticuline (**19**).

reticuline begins with transamination of tyrosine, followed by decarboxylation of the resulting 4-hydroxyphenylpyruvic acid [17]. Next, condensation with dopamine and subsequent cyclization result in the stereoselective formation of (*S*)-norcoclaurine (**16**). Methylation of one of the phenolic hydroxyl moieties and the basic heterocyclic nitrogen produces (*S*)-*N*-methyl-coclaurine (**17**), which is hydroxylated (**18**) and methylated to deliver (*S*)-reticuline (**19**), the key intermediate in the biosynthesis of benzyltetrahydroisoquinoline alkaloids.

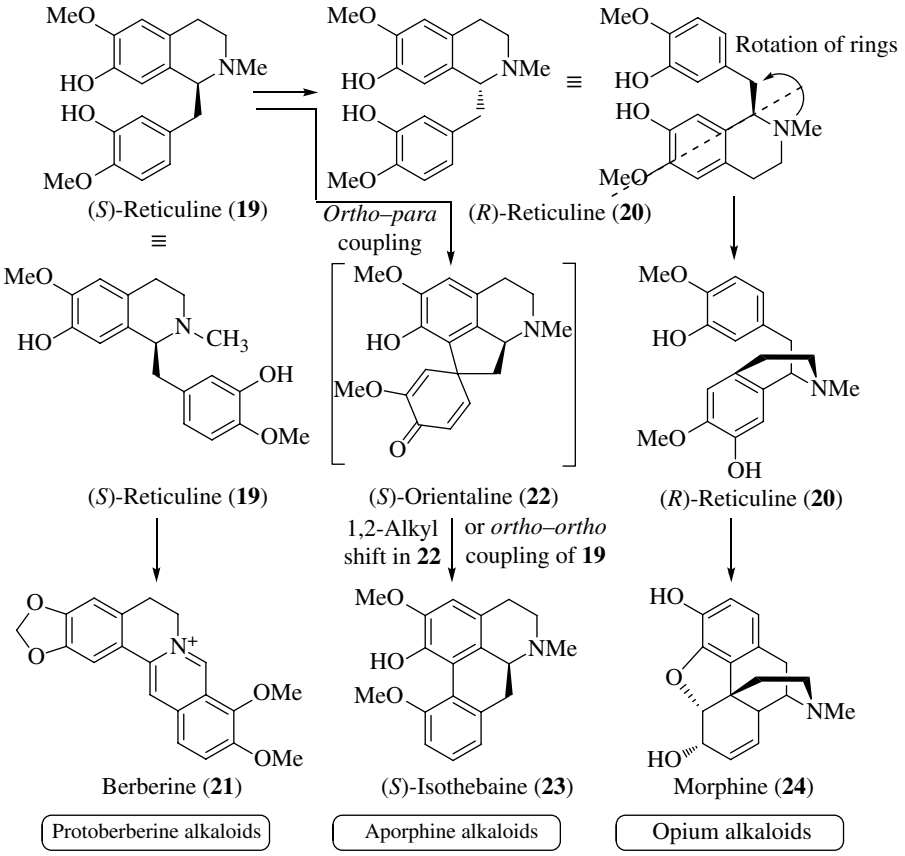
As pointed out earlier, the structural diversity of this class of tyrosine-derived secondary metabolites arises from different aryl coupling reactions. The biosynthetic pathway to alkaloids of the protoberberine skeleton, as well as the aporphine and morphine skeleton, is outlined in Scheme 12.4 [14]. While protoberberine [18] and aporphine alkaloids [19–21] are obtained from (*S*)-reticuline (**19**), opium alkaloids are biosynthesized from the enantiomeric (*R*)-configured natural product (**20**).

Oxidation of the *N*-methyl group in (*S*)-reticuline (**19**) to the corresponding iminium ion and subsequent Mannich-like cyclization afford the protoberberine skeleton. This oxidative process requires molecular oxygen and releases hydrogen peroxide. In order to obtain berberine (**21**), another oxidation step is required, which again releases hydrogen peroxide into the medium. Various structurally modified classes of alkaloids are derived from the protoberberine skeleton. A detailed discussion of these fascinating natural products exceeds the scope of this chapter; however, a short summary of possible structures is provided in Scheme 12.5. Alkaloids of the protoberberine skeleton as well as follow-up products have been isolated from various species of the Berberidaceae and the Ranunculaceae plant families [18].

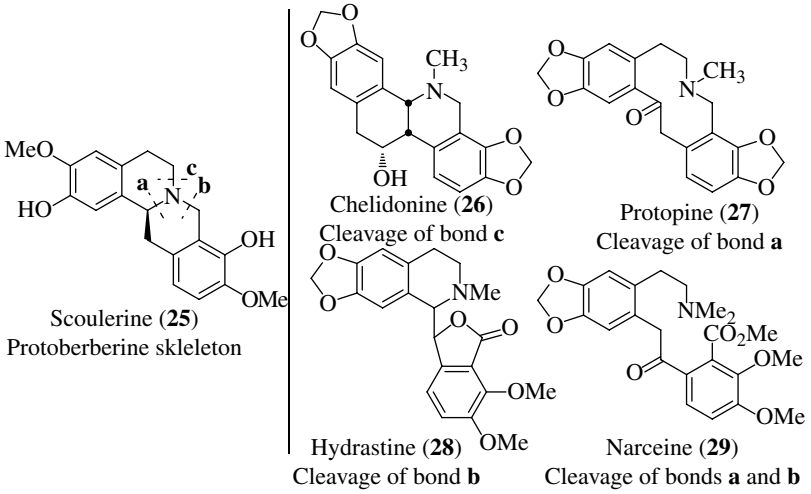
Oxidative coupling between the positions *ortho* and *para* to the phenol moieties in **19** leads to (*S*)-orientaline (**22**). A subsequent 1,2-alkyl shift then establishes the aporphine ring system (isothebaine, **23**) [22]. Alternatively, aporphine alkaloids can directly be obtained from (*S*)-reticuline (**19**) via an oxidative *ortho–ortho* coupling reaction. Alkaloids possessing the aporphine skeleton have been isolated from members of the Ranunculaceae plant family. Furthermore, some *Papaver* species are known to produce aporphine alkaloids in significant quantities [23, 24].

Morphinans present by far the most important class of reticuline-derived natural products. In contrast to alkaloids of the protoberberine and aporphine skeleton, opium alkaloids are biosynthesized from (*R*)-reticuline (**20**) via an *ortho–para* coupling reaction. For better comprehension, the structure of (*R*)-reticuline (**20**) has been redrawn to highlight the position of the oxidative coupling reaction and to clearly picture the emerging morphine skeleton (**24**). Because of the pronounced medicinal and economic importance, opium alkaloids are discussed in detail in the following.

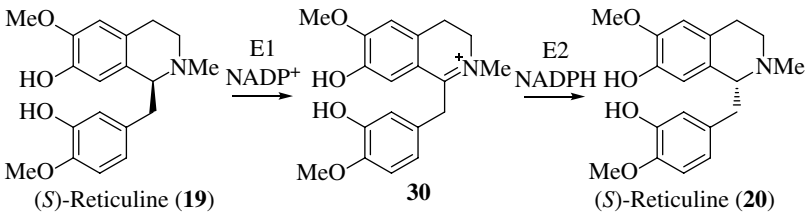
As pointed out earlier, opium alkaloids are derived from (*R*)-reticuline (**19**). As shown in Scheme 12.6, the stereocenter in (*S*)-reticuline is inverted via an oxidation/reduction sequence and intermediary formation of iminium ion **30** [25]. Next, both aromatic rings in (*R*)-reticuline (**20**) are oxidized to the corresponding diradical (Scheme 12.7), which readily undergoes the *ortho–para* coupling to afford the



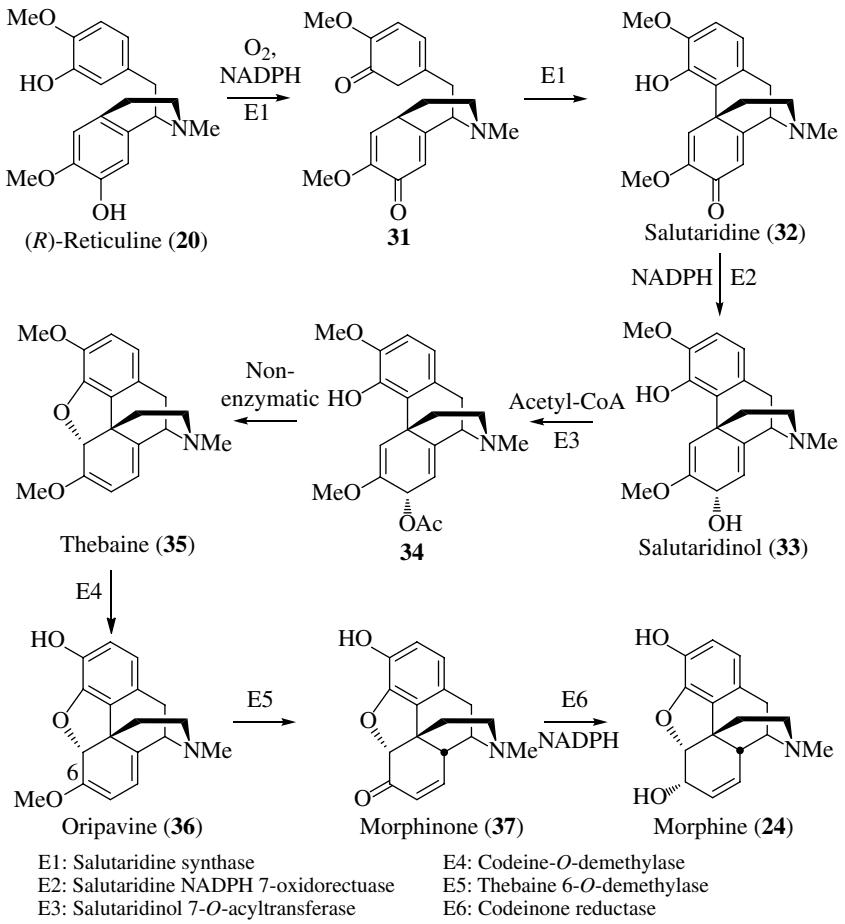

**SCHEME 12.4** Biosynthetic route to various alkaloids from (*S*)-reticuline (**19**) and (*R*)-reticuline (**20**).




**SCHEME 12.5** Protoberberine-derived alkaloids.




**SCHEME 12.6** Conversion of (*S*)-reticuline (**19**) in (*R*)-reticuline (**20**).




**SCHEME 12.7** Biosynthesis of morphine (**24**). NADPH, nicotinamide adenine dinucleotide phosphate.

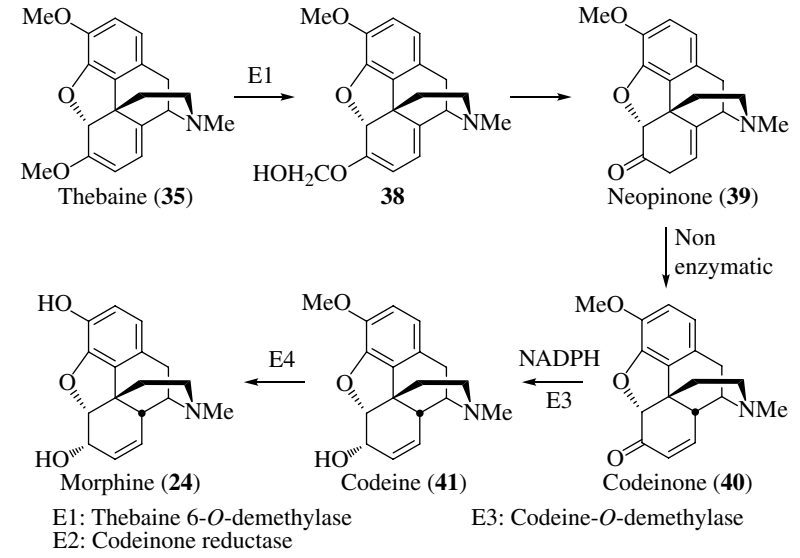
dienone salutaridine (**32**). Stereoselective reduction of the carbonyl functionality (**33**) is followed by an acetylation (**34**), which prepares the system for the subsequent nonenzymatic nucleophilic attack of the phenolic hydroxyl moiety and formation of the dihydrofuran ring (thebaine, **35**). Subsequent cleavage of the phenolic methyl ether (oripavine, **36**) and the C6 enol ether with concomitant formation of the α,β-unsaturated ketone provides morphinone (**37**), which delivers morphine (**24**) after reduction of the carbonyl moiety [26].

The route shown in Scheme 12.7 has been confirmed for some poppy plants [26]. However, a more common route from thebaine (**35**) toward morphine is outlined in Scheme 12.8 [27]. Cleavage of the enol ether, most probably via a hydroxylation step (**38**), affords neopinone (**39**). Migration of the double bond to the more stable conjugated position gives codeinone (**40**), which is converted to codeine (**41**) by means of an NADPH-dependent reduction. Morphine is obtained after cleavage of the phenolic methyl ether, probably via the same hydroxylation mechanism, which delivers neopinone (**39**) a few steps earlier.

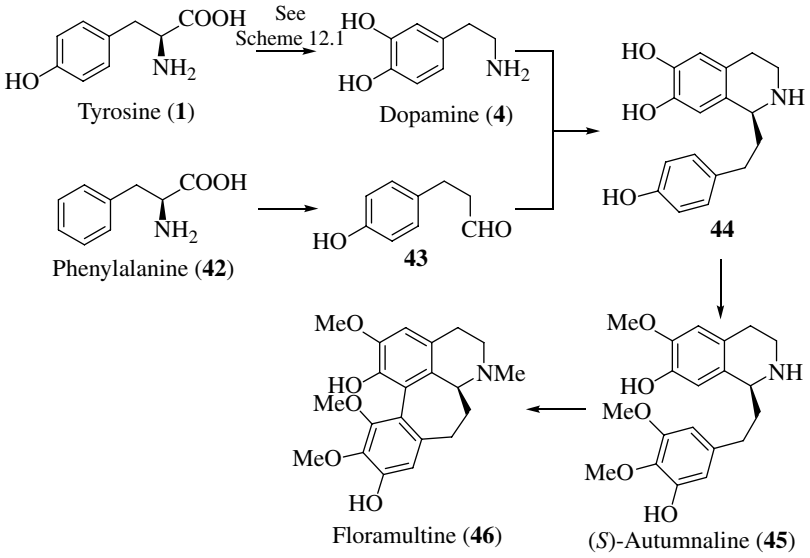
Noteworthy, a late-stage demethylation is quite uncommon. A possible explanation for this unusual biosynthetic peculiarity might be the protecting group nature of the methyl ether, which prevents other oxidative coupling reactions during the preparation of morphine.

### 12.2.4 Phenethylisoquinoline Alkaloids

Phenethylisoquinoline alkaloids constitute another important group of tyrosine-derived secondary metabolites. This class of natural products with colchicine (**54**) as most prominent member is obtained when aldehyde **43** is employed in a condensation reaction with dopamine, followed by a Pictet–Spengler cyclization reaction. The difference to benzyltetrahydroisoquinoline alkaloids is an additional carbon between the tetrahydroisoquinoline core and the aromatic ring. As outlined in Scheme 12.9, aldehyde **43** is derived from phenylalanine (**42**) via intermediary formation of 4-hydroxycinnamaldehyde. The formation of the tetrahydroisoquinoline system **44** from dopamine (**4**) and 4-hydroxydihydrocinnamaldehyde (**43**) is followed




**SCHEME 12.8** Main route to morphine (**24**) from thebaine (**35**).

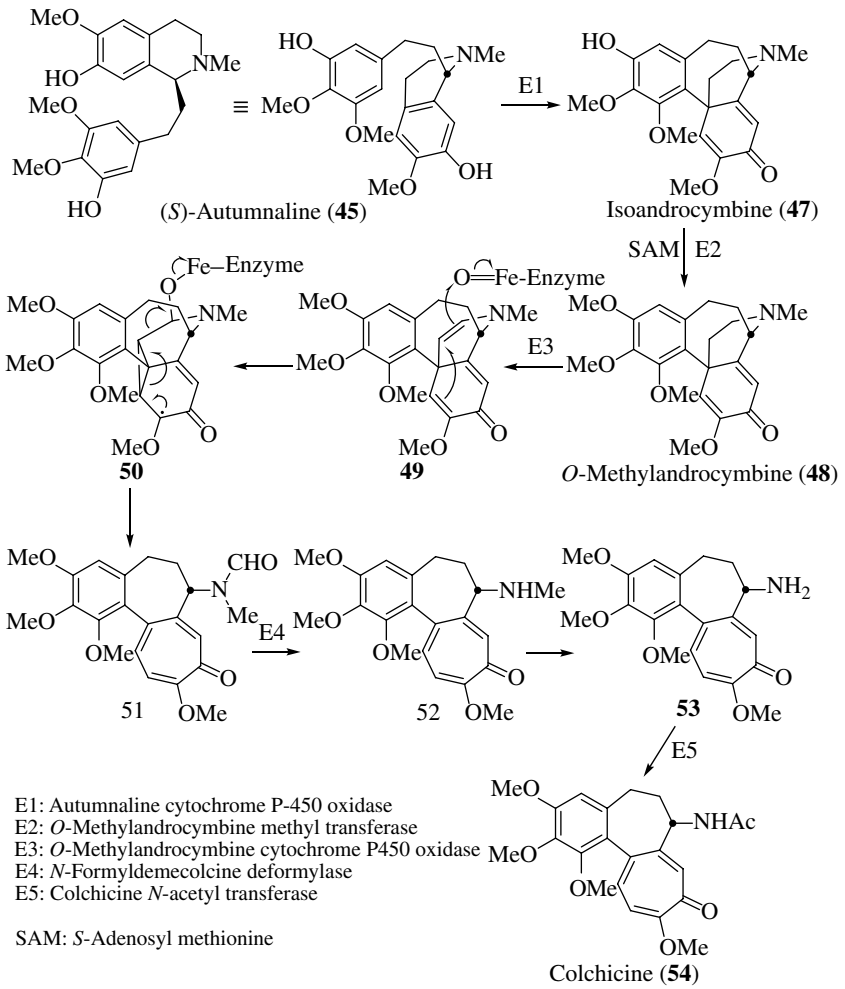



**SCHEME 12.9** Route toward autumnaline (**45**) and phenethylisoquinoline alkaloids.

by hydroxylation and methylation steps and delivers (*S*)-autumnaline (**45**) as key intermediate in the preparation of various phenethylisoquinoline alkaloids [28]. Enzymes responsible for the transformations have not been identified yet.

As demonstrated for the biosynthesis of benzyltetrahydroisoquinoline alkaloids in the previous section of this chapter, different aryl–aryl coupling reactions affect structurally diverse carbon skeletons for the resulting secondary metabolites. As shown in Scheme 12.9, oxidative phenolic *ortho–para* coupling of autumnaline results in the formation of floramultine (**46**), a prominent member of the homoaporphine family of alkaloids, which can be isolated from several families of higher plants [29].

The proposed biosynthetic route from (*S*)-autumnaline (**45**) to colchicine (**54**), the most prominent member of the phenethylisoquinoline alkaloids, is depicted in Scheme 12.10. Colchicine has been originally isolated from the poisonous plant *Colchicum autumnale* L., the autumn crocus or meadow saffron, by Pelletier and Caventou [30] as early as 1820, but the biologically interesting natural product is also found in other species of *Colchicum* [31, 32]. Colchicine (**54**) is characterized by an unusual tropolone ring, which is biosynthetically derived from an interesting rearrangement, discussed later in more detail. With the lack of a basic nitrogen and its unique tropolone system, colchicine holds a special place among tyrosine-derived alkaloids. Besides




**SCHEME 12.10** Biosynthesis of colchicine (**54**) from autumnaline (**45**).

its unique structural features, the natural product also stands out in respect to its biological properties. Formulations of meadow saffron have been used in the treatment of gout for more than 2000 years [33, 34].

Oxidative *para–para* coupling of autumnaline (**45**) delivers the dienone isoandrocymbine (**47**), which is *O*-methylated in the subsequent enzymatic step. This very same *para–para* coupling reaction has also been biosynthetically employed in the route to reticuline (**19**), key intermediate for the preparation of morphine and other important tyrosine-derived alkaloids (see Section 12.2.3). Next, the tropolone ring is established via the aforementioned skeletal rearrangement. Most likely, this process is achieved by a cytochrome P-450-mediated oxidation with subsequent formation of an intermediary cyclopropane ring (**50**). Opening of the three-membered ring with concomitant skeletal rearrangement affords the aromatic tropolone ring (**51**). This remarkable cascade reaction not only establishes the carbon framework of colchicine, but the rearrangement is also responsible for the removal of the nitrogen atom from the ring system and the formation of a purely carbocyclic skeleton. The final steps in the biosynthesis of colchicine are the refunctionalization of the nitrogen and involve a deformylation (**52**), an oxidative demethylation (**53**), and installation of the *N*-acetyl moiety (**54**) [35].

Because of the unprecedented tropolone ring, the structure elucidation of colchicine has been a highly challenging problem. In 1945, 125 years after its isolation, Dewar proposed the correct structure for this important alkaloid [36], which was confirmed by X-ray analysis a few years later [37]. The elucidation of the biosynthetic route proved to be equally troublesome. The currently accepted biosynthetic route has been deduced from extensive labeling experiments [38–43].

### 12.2.5 Amaryllidaceae Alkaloids

The final biosynthetic section of this chapter is devoted to the field of Amaryllidaceae alkaloids, which are common secondary metabolites in plants of the daffodil and narcissus

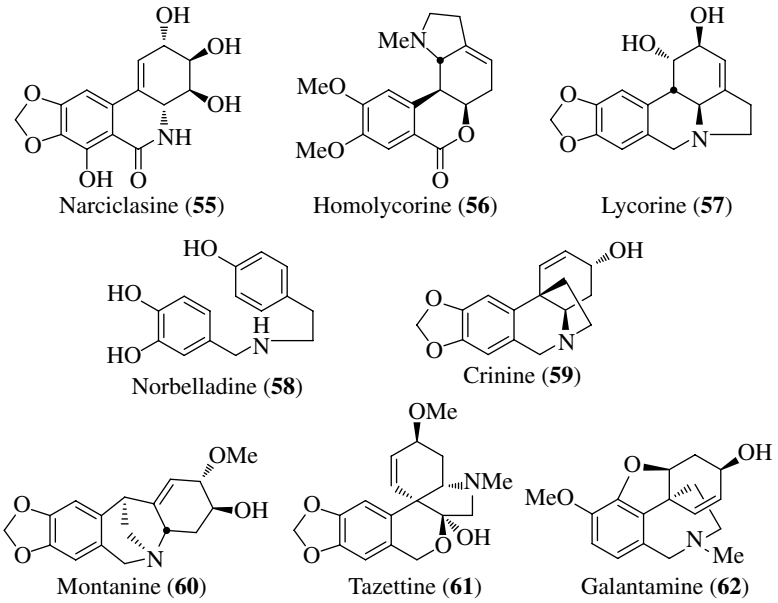
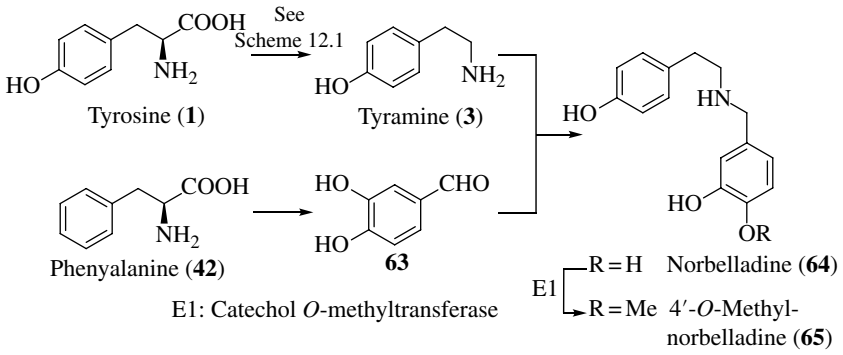



**FIGURE 12.2** Examples of Amaryllidaceae alkaloids.




**SCHEME 12.11** Biosynthesis of 4′-*O*-methylnorbelladine (**65**).

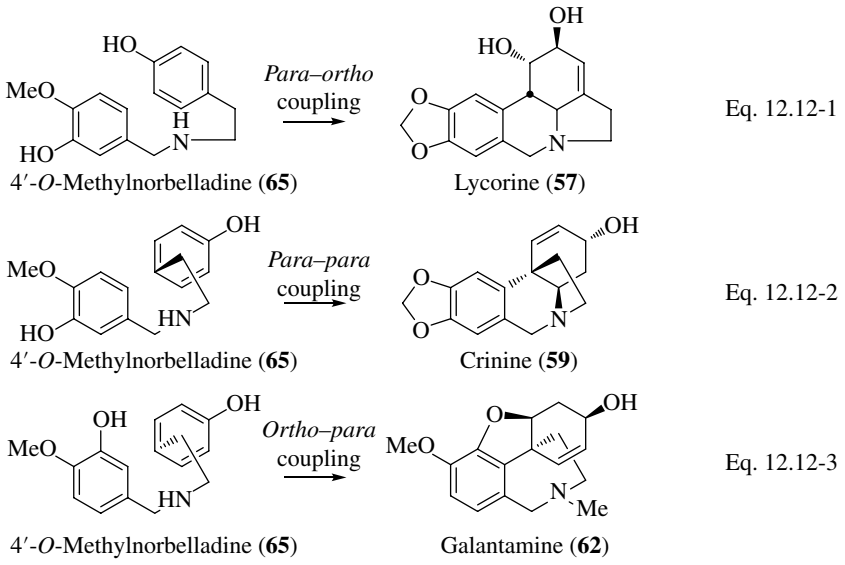
family. Amaryllidaceae alkaloids are structurally extremely diverse, and members of these families have been organized in several subfamilies [44]. The most important subtypes of Amaryllidaceae alkaloids are shown in Figure 12.2.

Despite their structural differences, all Amaryllidaceae alkaloids are biosynthetically derived from 4′-*O*-methylnorbelladine (**65**), and the variety arises from different oxidative coupling reactions of this key intermediate.

Several members of the Amaryllidaceae family of alkaloids display pronounced biological activities, and some Amaryllidaceae plants have played an important role in traditional herbal medicine for the treatment of various ailments. The most prominent examples of Amaryllidaceae alkaloids of biological relevance are narciclasine (**55**) and its congeners (pancratistatin and 7-deoxypancratistatin) and galantamine (**62**) (also commonly spelled galanthamine). These natural products also find application in modern medicine, and in this respect, pancratistatin is used in clinical trial against several human cancer lines [45–47], while galantamine plays an important role in the treatment of Alzheimer's disease [48, 49].

The biosynthesis of 4′-*O*-methylnorbelladine (**65**), the common biosynthetic intermediate for all Amaryllidaceae alkaloids, is straightforward, and the route is outlined in Scheme 12.11. Tyrosine is converted to tyramine (**3**) and the amine is then reacted with phenylalanine-derived dihydroxylated aldehyde **63**. The short biosynthetic sequence is then concluded after methylation of one of the phenolic hydroxyl moieties in **64**.

Despite the great importance of some members of the Amaryllidaceae family of alkaloids, only limited information on the subsequent steps of their biosynthesis is available to date. However, in analogy to other classes of secondary metabolites presented within this chapter, the diversity of 4′-*O*-methylnorbelladine (**65**)-derived natural products can easily be explained by means of different oxidative phenolic



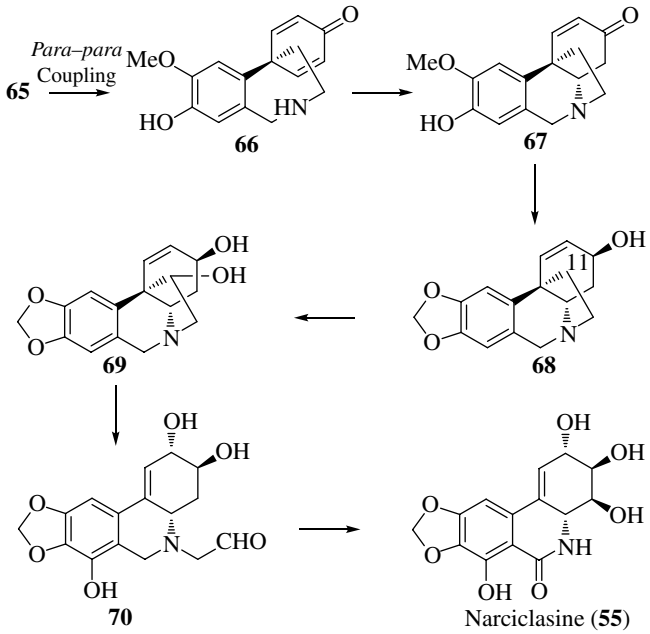

**SCHEME 12.12** Biosynthesis of Amaryllidaceae alkaloids via different aryl–aryl coupling reactions of 4′-*O*-methylnorbelladine (**65**).

coupling reactions as outlined in Scheme 12.12 on three classes of Amaryllidaceae alkaloids. While *para–ortho* coupling of **65** ultimately leads to lycorine (**57**) and structurally related Amaryllidaceae alkaloids (Eq. 12.12-1, Scheme 12.12), *para–para* coupling produces alkaloids of the crinine skeleton as shown in Equation 12.12-2, Scheme 12.12. Galantamine is biosynthetically accessible via *ortho–para* coupling of **65** as outlined in Equation 12.12.3, Scheme 12.12.

Chemical routes to narciclasine and 7-deoxypancratistatin (narciclasine type) as well as galantamine are described in the synthetic section of this chapter. The biosyntheses of these two types of Amaryllidaceae alkaloids are described in the following, while the discussion of other interesting classes of Amaryllidaceae constituents is omitted.

As pointed out earlier, only limited information is available regarding the biosynthesis of Amaryllidaceae alkaloids, and enzymes responsible for specific transformations have not been isolated or identified. The pathways outlined in the following are working models, which need further refinement or experimental proof.

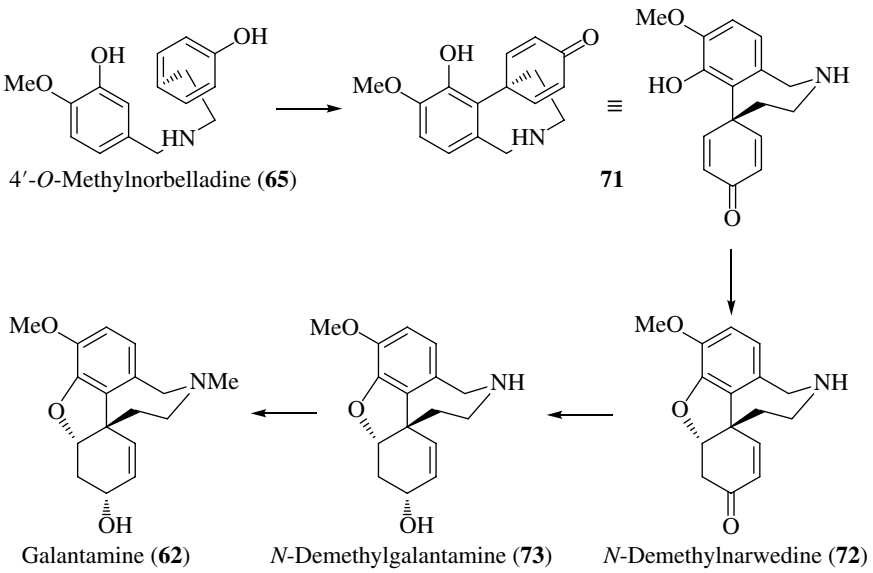
The proposed biosynthesis of narciclasine (**55**) is outlined in Scheme 12.13. The pathway is based on results obtained by Fuganti and coworkers who carried out radioactive labeling studies in the early 1970s [50–52], as well as by Pettit and coworkers who performed tissue culture studies on the Amaryllidaceae plant *Hymenocallis littoralis* [53]. Oxidative *para–para* coupling of 4′-*O*-methylnorbelladine (**65**) delivers dienone **66**, which serves as precursor for the nucleophilic attack of the basic nitrogen with concomitant elaboration of a six-membered ring (**67**). Next, reduction of the carbonyl moiety and elaboration of the methylenedioxy motif on the aromatic ring afford intermediate **68** possessing



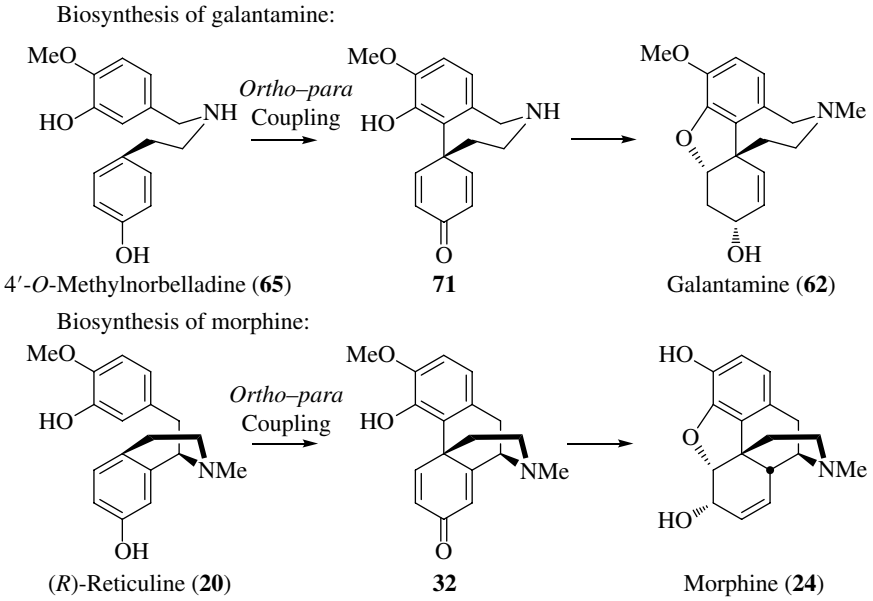

**SCHEME 12.13** Proposed biosynthesis of narciclasine (**55**).

the crinine ring system. The following steps are devoted to the late-stage removal of the C2 bridge present in the crinine skeleton, initiated by the oxidation of C11 in **68** (Amaryllidaceae numbering). Hydroxylation of the aromatic ring and the conduritol ring concludes the biosynthesis of this biologically potent Amaryllidaceae alkaloid.

A little more is known about the biosynthesis of galantamine (**62**). Early biosynthetic investigations date back as far as the late 1960s and early 1970s, when Fuganti observed the incorporation of 4′-*O*-methylnorbelladine (**65**) into galantamine [54] and Bhandarkar and Kirby reported the



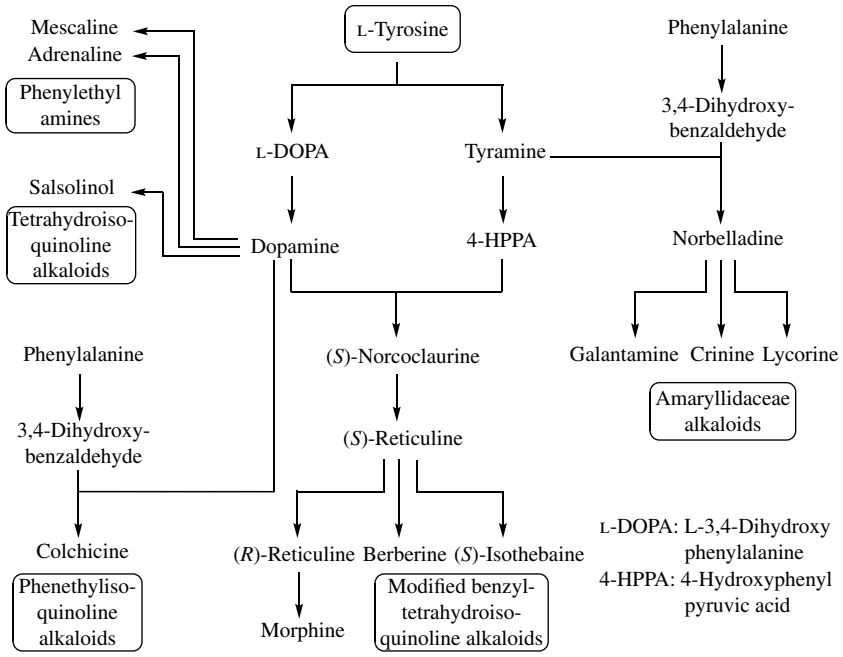

**SCHEME 12.14** Biosynthesis of galantamine (**62**).




**SCHEME 12.15** Comparison of the biosynthesis of galantamine (**62**) and morphine (**24**).

incorporation of [$^3$H]-narwedine into **65** [55]. In the late 1990s, Zenk and coworkers slightly modified the originally proposed pathway [56]. As shown in Scheme 12.14, *ortho–para* coupling of **65** affords dienone **71**, differing from **66** (Scheme 12.13) only in the position of the phenolic hydroxyl moiety. This reaction is possibly catalyzed by a cytochrome P-450-dependent oxidase, as such enzymes have been identified to catalyze oxidative phenolic coupling reactions, for example, in the biosynthesis of reticuline [57–59]. Next, spontaneous nucleophilic attack of the phenolic hydroxyl group onto the enone moiety results in the formation of *N*-demethylnarwedine (**72**), which is converted to galantamine (**62**) via reduction of the carbonyl group (**73**), and methylation of the nitrogen.

The biosynthesis of galantamine (**62**) is closely related to the biosynthesis of morphine (**24**) as illustrated in Scheme 12.15. Key steps in both routes are an *ortho–para* coupling of the requisite phenol, probably both catalyzed by cytochrome P-450-dependent enzymes, as well as a spontaneous nucleophilic attack of the phenolic hydroxyl moiety onto the highly reactive enone with concomitant formation of the dihydrofuran ring. The slightly more




**SCHEME 12.16** Simplified biosynthetic route to tyrosine-derived secondary metabolites.

complex structure of opioids results from the additional six-membered ring present in the substrate employed in the oxidative phenolic coupling reaction.

### 12.2.6 Biosynthetic Overview of Tyrosine-Derived Alkaloids

All major pathways toward tyrosine-derived secondary metabolites discussed within the biosynthetic section of this chapter are summarized in Scheme 12.16. The great structural diversity of this important class of natural products arises from a very limited set of chemical transformations. Except for the extremely simple catecholamines and phenylethylamines, tyrosine-derived alkaloids are generally formed via condensation of two aromatic substrates, facultatively followed by a Pictet–Spengler-type ring closing reaction. Next, the key oxidative phenolic coupling reaction then introduces structural complexity and serves as convenient tool for the elaboration of different alkaloid frameworks.

## 12.3 ARYL–ARYL COUPLING REACTIONS

Aryl–aryl coupling reactions play an utmost important role in the biosynthesis and the chemical synthesis of many tyrosine-derived alkaloids. Furthermore, the biaryl substructure is a common motif in natural products and unnatural derivatives of great scientific or industrial importance. Many compounds such as antibiotics, anticancer drugs, agrochemicals, or liquid crystals contain aryl–aryl bonds, and efficient protocols for the generation of these structural subunits are essential for the large-scale production of such compounds.

Because of the intrinsic importance of aryl–aryl coupling reactions, this field has received considerable attention from academic and industrial chemists for more than hundred years. Since the pioneering work of Pschorr, Ullmann, and others [60–62], procedures for the generation of biaryl systems have continuously evolved. Today, unsymmetrical biaryl systems with a variety of functional groups can be accessed, which would have been impossible to prepare only a few decades ago.

This section of the book chapter is devoted to a brief discussion of different methods and protocols that have been developed to grant access to biaryl systems. The classification of different types of coupling reactions is often difficult and not fully consistent for several reasons: In some cases the mechanistic pathway of the reaction has not been completely understood. In other cases, several metals are involved, which does not allow an unambiguous categorization. Additionally, very often similar results are obtained when different metals are employed in the requisite coupling reaction. Thus, specific reactions are not always limited to certain metals.

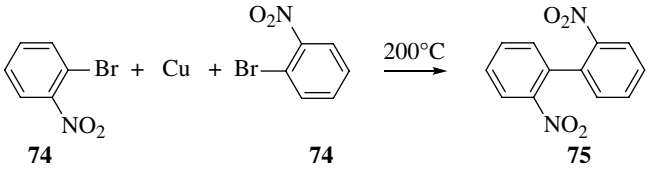
Clearly, this section is not intended to completely cover the huge field of aryl–aryl coupling methods but should provide a representative overview of different reactions. Additionally, oxidative protocols are discussed in the third section of this chapter dealing with the synthesis of tyrosine-derived alkaloids.

Mechanistic discussions have been omitted to a large extent. Over the last few years, excellent review articles have been published and the reader is invited to further investigate this interesting research field by consulting these articles [63–70].

### 12.3.1 Copper-Mediated Aryl–Aryl Bond Forming Reactions

In 1901, Ullmann reported a method for the aryl–aryl coupling of aromatic halides [62]. He observed that reaction of one or more nitro-groups, containing aromatic halides are converted to the corresponding biaryl derivatives as shown in Scheme 12.17. The exact mechanistic course of the Ullmann reaction has not yet been fully elucidated to date, and two possible pathways are currently considered, which deliver the biaryl species either via radical intermediates or via the formation of aryl copper species. As aryl copper species have been isolated before on several occasions, the second pathway seems more likely.

Originally, high temperatures, up to 200°C or more, were required in order to obtain substantial amounts of the desired adducts, which constituted a major disadvantage and limitation on the scope of the reaction. The use of activated copper or addition of copper salts [71] and the use of dimethylformamide as solvent allowed the reaction to proceed at synthetically practical temperatures (as low as 85°C). Additionally, activation with ultrasound is possible [72].



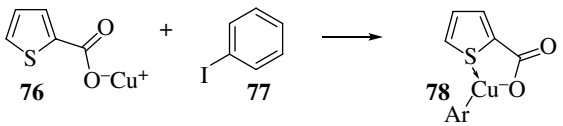

**SCHEME 12.17** Ullmann's copper-mediated formation of biaryls.

With the application of copper(I)-thiophene-2-carboxylate (CuTC; **76**), Liebeskind was able to access substituted biaryls and heterobiaryls at room temperature [73]. The thiophene derivative serves as ligating substituent (Eq. 12.18-1, Scheme 12.18) and mediates the formation of the required aryl copper species. An intramolecular example of such a CuTC-promoted Ullmann reaction in the preparation of tricycle **80** is outlined in Equation 12.18-2, Scheme 12.18.

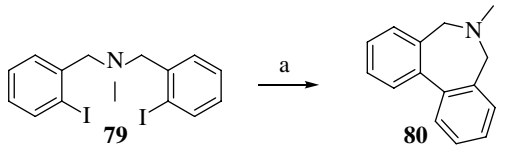
The Ullmann reaction has been employed in the syntheses of numerous symmetrical natural compounds and biaryl ligands. With Meyers' synthesis of mastigophorene A (not shown), a representative example is outlined in Equation 12.18-3, Scheme 12.18 [74].

The Ullmann reaction has also been successfully employed in the preparation of unsymmetrical biaryl compounds. However, the results are often not satisfying, and such reactions are only applicable to a limited type of substrates where both coupling partners clearly differ in reactivity (electron-rich vs. electron-poor aromatic substrates) and steric demands. Usually, the less reactive coupling partner also must be used in excess.

Ziegler reported a modification of the Ullmann protocol that takes advantage of the chelating properties of nitrogen- or sulfur-containing substituents. These chelating groups serve to stabilize preformed aryl copper species [75]. This modification involves the lithiation of aryl halides with

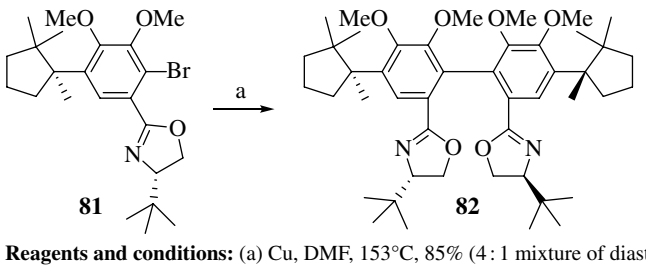



Eq. 12.18-1




Eq. 12.18-2

**Reagents and conditions:** (a) **78**, NMP. rt, 15 h, 88%




Eq. 12.18-3

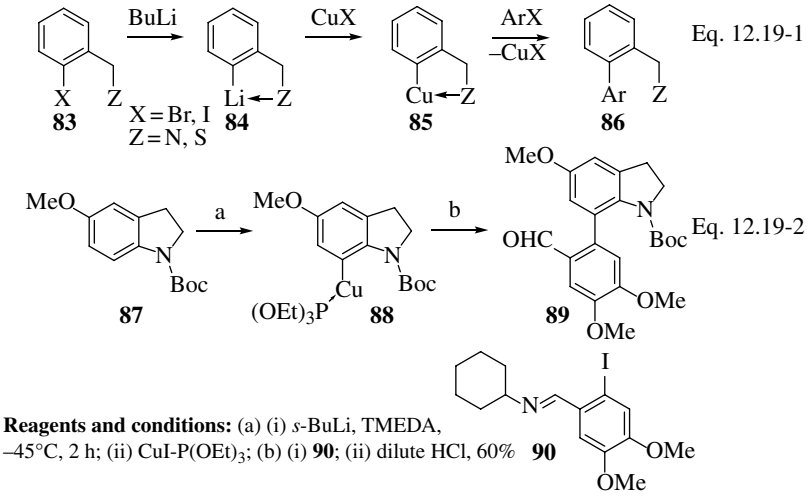
**Reagents and conditions:** (a) Cu, DMF, 153°C, 85% (4 : 1 mixture of diastereomers, favoring **82**)

**SCHEME 12.18** CuTC-mediated Ullmann-type reaction and application of the Ullmann reaction in the synthesis of natural products.

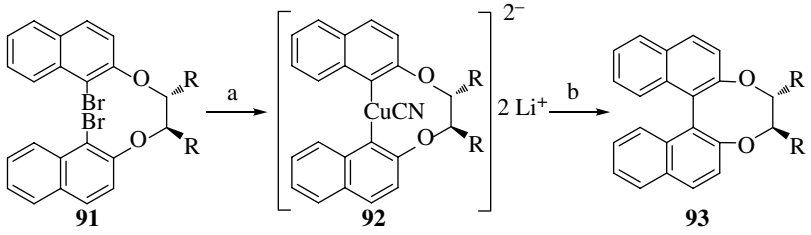
concomitant formation of the corresponding aryl anion prior to the addition of copper(I) salts. Thus, the reaction mechanistically slightly differs from the previously discussed coupling protocols. The Ziegler modification of the Ullmann reaction is outlined in Scheme 12.19 (Eq. 12.19-1), along with its application in Flippin's synthesis of tortuosine (not shown), an antitumor Amaryllidaceae pyrrolophenanthridinium alkaloid (Eq. 12.19-2) [76].

Lipshutz employed copper cyanide in the oxidative aryl coupling reaction and was able to prepare biaryl systems in good overall yield [77]. The method, involving a higher-order organocuprate intermediate, delivers the coupled adduct after exposure to oxygen (Scheme 12.20).

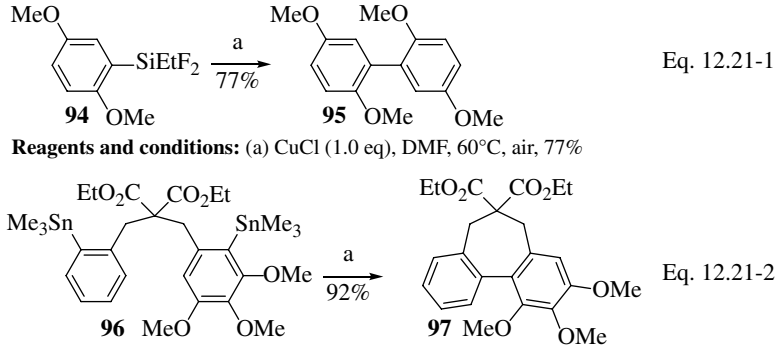
A variety of different protocols have been developed for the copper-promoted aryl–aryl coupling of silicon [78] and tin [79, 80] or boron derivatives instead of the corresponding aryl halides, exemplarily outlined in Scheme 12.21. A discussion of these protocols is omitted, and the reader is referred to the cited literature for more information.



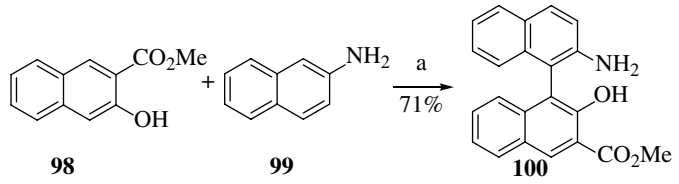

**SCHEME 12.19** Ziegler modification of the Ullmann reaction and its application in synthesis.




**SCHEME 12.20** Higher-order organocuprates in the formation of biaryl compounds.

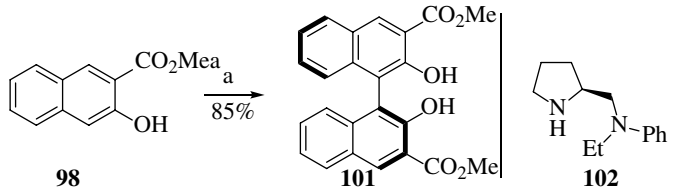



**SCHEME 12.21** Copper-mediated aryl–aryl coupling of organosilicon compounds and stannanes.



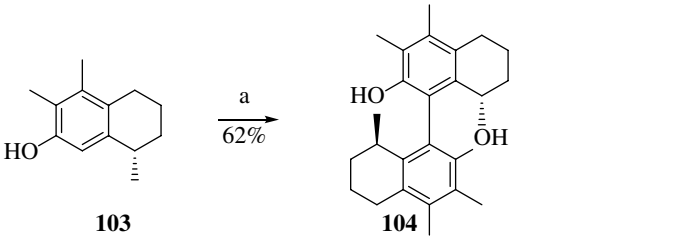

Eq. 12.22-1

**Reagents and conditions:** (a) $CuCl_2$•$PhCH(NH_2)CH_3$, 71%




Eq. 12.22-2

**Reagents and conditions:** (a) Cu(OH)Cl•**102** (10 mol%), $O_2$, $CH_2Cl_2$, rt, 24 h, 85%, 78% *ee*




Eq. 12.22-3

**Reagents and conditions:** (a) $K_3Fe(CN)_6$ (0.7 eq.), NaOH, $Et_2O$, $O_2$, 22°C, 2 h, 62%

**SCHEME 12.22** Copper(II) salt-mediated and copper(II) salt-catalyzed couplings of aromatic substrates.

Copper(II) salts and also Fe(III) salts have been successfully employed in the oxidative coupling of aromatic compounds, mainly for the formation of binaphthyl derivatives. These protocols utilize either stoichiometric or catalytic amounts of copper(II) and facilitate symmetrical as well as unsymmetrical coupling.

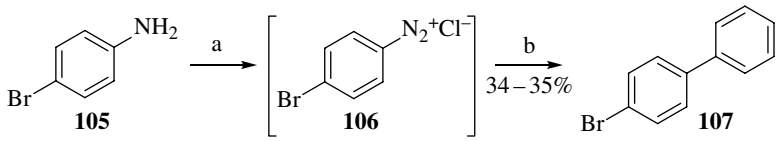
Two copper(II)-mediated coupling reactions and one Fe(III)-catalyzed reaction are outlined in Scheme 12.22. An example of the stoichiometric use of $CuCl_2$ in the oxidative coupling of phenol **98** and amine **99** is shown in Equation 12.22-1, Scheme 12.22 [81]. This reaction also demonstrates the potential of copper-mediated processes in the formation of unsymmetrical adducts (with the formation of only minor amounts of homodimers as side products). The authors supported their experimental findings with calculations of the frontier orbital interactions and showed that the HOMO and LUMO interaction with the SOMO of the initially formed radical is favored in differently substituted coupling partners. The success of the reaction also strongly depends on the additive and the yield dropped significantly when the reaction was carried out without the chelating primary amine.

Catalytic amounts of copper salts can be employed when co-oxidants are present in the reaction medium or when the reaction is carried out under an oxygen atmosphere (Eq. 12.22-2) [82]. Furthermore, the utilization of chiral bases allows the isolation of the desired adducts with significant levels of enantiomeric excess.

Fe(III) salts have also been used in oxidative aryl–aryl bond forming reactions and present an environmentally and biologically more satisfying approach [83]. In analogy to the copper-mediated reaction, Fe(III) salts can either be employed stoichiometrically or in catalytic amounts as shown in Equation 12.22-3, Scheme 12.22, with $K_3Fe(CN)_6$, when co-oxidants are present. In some cases, the use of (Fe) III salts resulted in the formation of problematic emulsions during aqueous work-up of the reaction mixture. It is possible to circumvent this problem by the utilization of solid-supported iron salts [84].

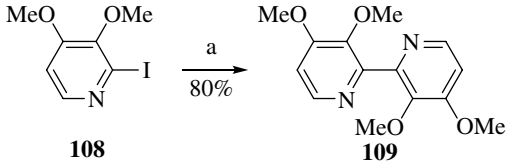
Another, especially historically important copper-mediated radical aryl–aryl bond forming reaction is the Pschorr reaction (Gomberg–Bachmann reaction), which has been first described in 1896 for the preparation of phenanthrene and its derivatives [85]. Later, in 1924, Gomberg and Bachmann described an intermolecular version of this reaction and prepared several biphenyl derivatives in moderate yield [86]. The reaction is initiated by formation of diazonium salts from aromatic amines, which release nitrogen upon reaction with copper salts. The intermediary formed aryl radial then undergoes the desired coupling reaction and allows the isolation of biaryl compounds. An example of such a reaction is outlined in Scheme 12.23 [87].

The Pschorr or Gomberg–Bachmann reaction is only rarely used. Reaction conditions are harsh, and it is often difficult to prepare the requisite amines as starting material.



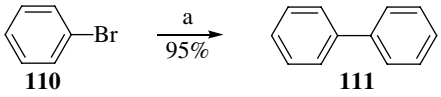

**Reagents and conditions:** (a) HCl, $NaNO_2$; (b) NaOH, $H_2O$, benzene, 0–5°C, 34–35%.

**SCHEME 12.23** Aryl–aryl coupling via diazonium salts.




Eq. 12.24-1

**Reagents and conditions:** (a) $NiCl_2$, $PPh_3$, Zn, DMF, 50°C, 1.5 h, 80%




Eq. 12.24-2

**Reagents and conditions:** (a) EtOH, $NiBr_2 \cdot 3H_2O$, 0.2 A, stainless steel electrode, rt, 95%

**SCHEME 12.24** Ni-catalyzed aryl–aryl coupling protocols.

More importantly, the intermediary formed diazonium salts are unstable and the reaction poses a hazard when carried out on large scale. Additionally, as evidenced by the example shown in Scheme 12.23, yields are generally low.

### 12.3.2 Nickel-Mediated Aryl–Aryl Bond Forming Reactions

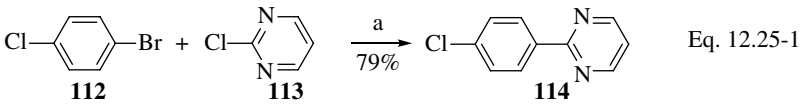
The utilization of nickel considerably increased the scope and the practicability of aryl–aryl bond forming reactions. During the course of the reaction, Ni(0) inserts in carbon–halogen bonds before the desired biaryl compound is released after the subsequent reaction of the activated species with the requisite coupling partner. Nickel-mediated coupling reactions have been carried out with stoichiometric amounts of Ni(0) or, more commonly, with catalytic amounts in the presence of reagents that are suited to efficiently recover the metal.

Typical aryl–aryl coupling reactions that utilize catalytic amounts of Ni(II) salts are outlined in Scheme 12.24. Zinc metal was used to reduce Ni(II) to the catalytically active Ni(0) species in the homocoupling of dimethoxypyridine **108** and the efficient synthesis of dimer **109** (Eq. 12.24-1) [88]. Alternatively, nickel salts can also efficiently be reduced by means of electrochemical methods. As shown in Equation 12.24-2, Troupel and coworkers were able to recover Ni(0) on a steel electrode and isolated the coupling products in excellent yield [89]. Comparable studies were carried out with slightly more complex substrates and confirmed that the coupling reaction can be carried out in the presence of esters, methoxy groups, and nitriles [90].

Nickel-promoted or nickel-catalyzed reactions are well suited for the preparation of unsymmetrical biaryls via cross coupling. A variety of different protocols have been developed, and a small selection of reactions is outlined in Scheme 12.25. The aryl coupling shown in Equation 12.25-1 is a nice example of an electrochemical protocol where the coupling chemoselectively takes place at the more active bromide while the chloride in halide **112** does not participate in the coupling reaction [90].

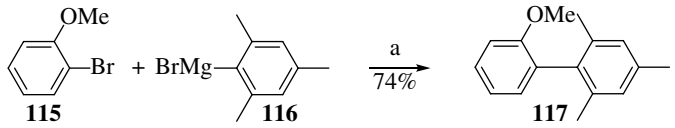
In 1972, Kumada [91] and Corriu [92] independently reported the selective nickel-catalyzed cross-coupling reaction of Grignard reagents and aryl (and vinyl) halides. Findings by these groups outlined the importance of the phosphine ligands and their spatial configuration on the outcome of the reaction. An example of this elegant and highly efficient protocol is shown in Equation 12.25-2 [91, 93]. Later, the scope of the Kumada cross-coupling reaction was extended by the utilization of palladium as discussed in the following section. The possibility to differentiate between bromides and chlorides further increased the versatility of this nickel-catalyzed process. Such an example is shown in Equation 12.25-3 [94].

Two examples for nickel-catalyzed cross-coupling reactions of triflates and mesylates with the requisite zinc and boron species are outlined in Scheme 12.26. In 1994, Snieckus reported the Ni(0)-catalyzed reaction of aryl zinc reagents with aryl triflates and obtained the desired biaryl compounds in



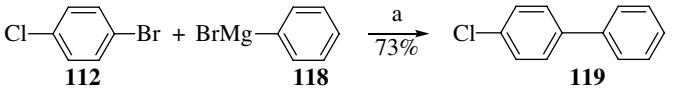

Eq. 12.25-1

**Reagent and conditions:** (a) $FeBr_2$ (0.3 eq.), $NiBr_2$•Bpy, DMF/py (4 : 1), $NBu_4BF_4$, Fe-anode, 79%




Eq. 12.25-2

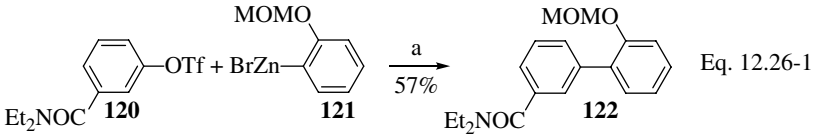
**Reagents and conditions:** (a) $NiCl_2$ (dppp) (1%), THF, 74%




Eq. 12.25-3

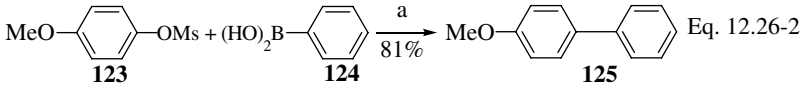
**Reagents and conditions:** (a) $NiCl_2$ (5%), 73%

**SCHEME 12.25** Nickel-catalyzed cross-coupling protocols.




Eq. 12.26-1

**Reagents and conditions:** (a) $Ni(acac)_2$ (10%), *i*PrMgCl, THF, rt, 57%




Eq. 12.26-2

**Reagents and conditions:** (a) $NiCl_2$ (dppf), Zn, $K_3PO_4$, dioxane, 81%

**SCHEME 12.26** Nickel-catalyzed cross-coupling protocols.

good yield (Eq. 12.26-1) [95]. This method furthermore showed tolerance for a variety of functional groups. Another example by Percec is shown in Equation 12.26-2 [96]. Exposure of mesylates to arylboronic acids in the presence of nickel catalysts, zinc as reducing agent, and potassium phosphate resulted in the isolation of various biaryls.

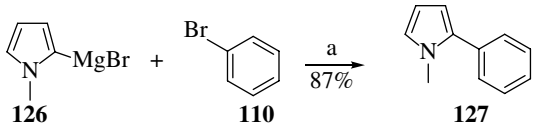
### 12.3.3 Palladium-Mediated Aryl–Aryl Bond Forming Reactions

Today, palladium-catalyzed reactions play a most important role in the formation of aryl–aryl bonds. The utilization of palladium (and other elements of the platinum group) enabled the development of mild and efficient protocols for the coupling of aromatic substrates with a diverse substitution pattern and different functional groups.

Since the potential of palladium in the aryl–aryl bond formation became obvious, numerous research groups became engaged in this field and helped with the elaboration of new protocols, which were designed to solve certain specific problems or to improve existing methods.

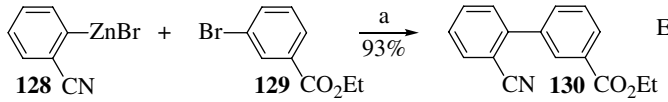
The success story of palladium catalysis initially began with the direct adaption of nickel-catalyzed processes. Palladium-catalyzed cross-coupling reactions of aromatic Grignard species were first reported in 1976 by Ishikawa [97]. A few years later, Kumada published the palladium-catalyzed cross coupling of pyrroles with aromatic Grignard species (Eq. 12.27-1, Scheme 12.27) and also of organozinc compounds [98]. The example shown in Equation 12.27-2, Scheme 12.27 was reported by Rieke and coworker [99]. Because of the lower reactivity of organozinc derivatives, higher selectivities are obtained than with the corresponding organomagnesium compounds while a variety of functional groups are tolerated.

A variety of different organometallic compounds have been evaluated as coupling partners in the palladium-catalyzed cross-coupling reaction, including mercury, germanium, lead, antimony, silicon, tin, and boron derivatives. Lack of reactivity or pronounced toxicity prevented the large-scale application or general use of some metals, and the discussion of these studies is omitted. Organosilicon derivatives have been studied to some extent, and an example of an aryl–aryl coupling reaction of aryl(fluoro)silane **131** and iodide **132** is outlined in Scheme 12.28 [100]. The reaction follows the general pathway of palladium-catalyzed aryl–aryl couplings. Potassium fluoride is required to




Eq. 12.27-1

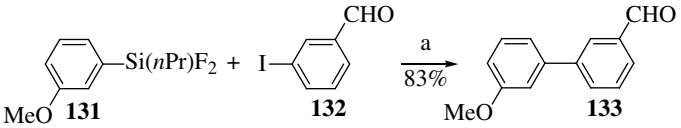
**Reagents and conditions:** (a) $PdCl_2(dppb)$ (1.1%), THF, reflux, 1 h, 87%




Eq. 12.27-2

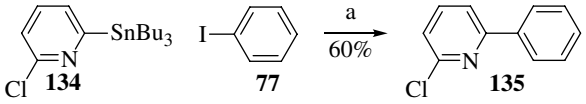
**Reagents and conditions:** (a) $Pd(PPh_3)_4$ (5%), THF, rt, 3 h, 93%

**SCHEME 12.27** Early examples of palladium cross-coupling reactions of organomagnesium and organozinc derivatives.




**Reagents and conditions:** (a) $(\eta^3\text{-}C_3H_5PdCl)_2$, KF (2 eq.), DMF, 100°C, 15 h, 83%

**SCHEME 12.28** Application of organosilicon derivatives in palladium-catalyzed aryl–aryl couplings.




**Reagents and conditions:** (a) $Pd(PPh_3)_4$ ( 5%), xylene, reflux, 12 h, 60%

**SCHEME 12.29** Stille cross-coupling reaction.

generate the corresponding anionic pentacoordinate aryl (fluoro)silicate, which then reacts by means of an oxidative addition with the requisite aryl palladium species. Next, reductive elimination releases the desired biaryl derivative.

While silyl ethers are commonly used as protecting groups for hydroxyl moieties, the formation of carbon–silicon bonds is often troublesome, which limits the scope of the coupling protocol discussed earlier.

Organotin derivatives are stable and relatively easy to prepare. In 1977, Kosugi and Migita reported the palladium-catalyzed allylation of aromatic halides with allyltributyltin [101]. One year later, Stille published a protocol for the preparation of ketones by means of a palladium-catalyzed reaction of acid chlorides and organotin compounds [102, 103]. Over the next few years, protocols for the palladium-catalyzed coupling reaction of organotin derivatives were improved and allowed the general preparation of unsymmetrical biaryl derivatives [104]. One example of the Stille coupling (alternatively also referred to as Migita–Kosugi–Stille coupling) is outlined in Scheme 12.29 [105].

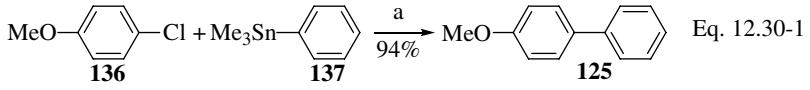
The mechanism of the Stille reaction follows the general route of palladium-catalyzed couplings and involves oxidative addition of the palladium(0) species into the aryl–halogen bond, followed by transmetallation and reductive elimination. A great advantage of the Stille reaction is that either Pd(0) or Pd(II) can be employed as catalyst. If Pd(II) is used, the transition metal is reduced to the catalytically active species by the organotin compound.

The outcome of the Stille coupling can be further improved by the addition of small amounts of CuI to the reaction mixture. The intermediary formed organocopper species is more reactive than the corresponding organostannane, resulting in an over hundredfold rate increase [106].

The Stille reaction has been evaluated with a variety of different leaving groups on the aromatic ring, which resulted in a great extension of the versatility of this palladium-catalyzed process. Generally, bromides and iodides are ideal leaving groups. Chlorides have also been successfully employed in coupling reactions, but rates and yield are often lower. An example of a high yielding coupling reaction of chloride **136** with aryl stannane **137** is shown in Equation 12.30-1, Scheme 12.30 [107]. Cesium fluoride was added for the activation of the fluorophilic tin. Triflates are good leaving groups and organotriflates have commonly been employed in Stille couplings (see Eq. 12.30-2, Scheme 12.30) [108]. A few coupling reactions have been reported, which utilize hypervalent iodine substituents (Eq. 12.30-3) [109] or phosphates as leaving groups (Eq. 12.30-4) [110].

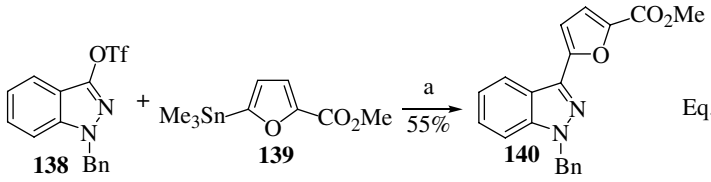
The versatility of the Stille coupling reaction has been further improved by the introduction of polymer-supported catalysts or substrates. A discussion of these protocols is omitted.

Despite all advantages pointed out earlier and the great improvement of unsymmetrical aryl–aryl coupling protocols, a major disadvantage of the Stille coupling remains the



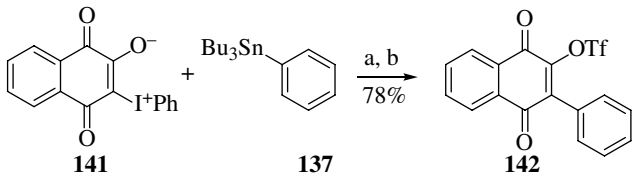

Eq. 12.30-1

**Reagents and conditions:** (a) $[Pd_2(dba)_3]$ (1.5%), P*t*$Bu_3$ (6%), CsF, dioxane, 100°C, 48 h, 94%



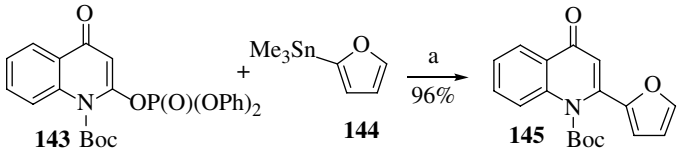

Eq. 12.30-2

**Reagents and conditions:** (a) $Pd(PPh_3)_4$, dioxane, reflux, 55%




Eq. 12.30-3

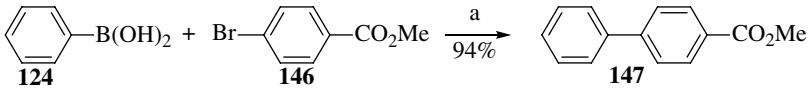
**Reagents and conditions:** (a) $Pd(PPh_3)_4$, CuI, DMF, rt; (b) $Tf_2O$, $NEt_3$, 78% (2 steps)




Eq. 12.30-4

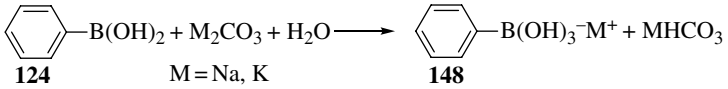
**Reagents and conditions:** (a) $Pd(PPh_3)_4$(0.05 eq.), LiCl (3 eq.), **144** (2 eq.), THF, reflux, 96%

**SCHEME 12.30** Different leaving groups in the Stille coupling reaction.




**Reagents and conditions:** (a) $Pd(PPh_3)_4$, $Na_2CO_3$, $C_6H_6$, reflux, 6 h, 94%

**SCHEME 12.31** First example of the Suzuki coupling reaction.




**SCHEME 12.32** Trihydroxyphenylboronate anion as catalytically active species in the Suzuki coupling.

high toxicity of organostannanes and their environmental hazard. Shortly after the initial reports by Stille on the palladium-catalyzed coupling reaction of stannanes, Suzuki published an example of a palladium-catalyzed coupling reaction with a boronic acid as nucleophilic partner [111–113]. This first example of a Suzuki coupling (often referred to as Suzuki–Miyaura cross-coupling reaction) is shown in Scheme 12.31. Together with the Stille coupling, the Suzuki coupling belongs to the most important palladium-catalyzed protocols for the elaboration of C—C bonds.

Similar to other palladium-catalyzed reactions, the Suzuki coupling commences with insertion of the catalytically active Pd(0) species and is followed by transmetallation and a final reductive elimination. The pH of the reaction medium is of crucial importance, and it is commonly believed (and supported by kinetic investigations) that the trihydroxyphenylboronate anion (see Scheme 12.32) is the catalytically active species.

The Suzuki coupling has been successfully employed in the homocoupling of aryl derivatives, and two examples are shown in Scheme 12.33. As outlined in Equation 12.33-1, the reaction has been applied to the preparation of binaphthyls [114]. Wong prepared thiophene derivatives via boroxine **153**. The phenanthrene derivative **155** serves as ligand for palladium and helped to regenerate the catalytically active Pd(0) species (Eq. 12.33-2) [115]. In both cases, the boronic ester is converted to the corresponding boronic acid under the basic reaction conditions. As the installation of the

boronic acid originally required harsh reaction conditions, such as exposure of the corresponding halide to butyl lithium, other methods might be better suited for the formation of homodimers.

More commonly, the Suzuki reaction is used for the preparation of unsymmetrical biaryls and other adducts. While the preparation of the boronic acid or ester often requires harsh conditions, the requisite coupling partner might easily be accessible and prepared under mild conditions, which allows the incorporation of various functional groups as evidenced by the examples shown in Scheme 12.33 with the cross coupling of thiophene derivatives (Eq. 12.33-2) and in Scheme 12.34. The preparation of an indole derivative bearing an ester moiety is outlined in Equation 12.34-1 [116]. Primary amines have also been employed in Suzuki cross-coupling reactions. However, in some cases, as shown in Equation 12.34-2, deamination occurs [117]. Ferrocene derivatives and aldehydes can be utilized in the Suzuki cross coupling. Imrie performed a study with a variety of different ferrocenes and was able to obtain the desired adducts in moderate to good yield. An example of a difficult substrate is shown in Equation 12.34-3 [118]. Aryl chromium complexes have also been used in Suzuki–Miyaura cross-coupling reactions, and they seem well-accepted substrates and suited for the preparation of biaryl compounds with axial chirality (Eq. 12.34-4) [119].

The scope of the Suzuki cross-coupling reaction has been further increased by the utilization of novel boron derivatives. The synthesis of these coupling precursors has also been simplified as they are accessible from aromatic halides by means of a palladium-catalyzed procedure, which is more tolerant to functional groups than the original lithiation protocol. Examples of aromatic boron species are shown in Figure 12.3. A detailed account on boron species employed in Suzuki couplings has recently been published [120].

Additionally, and similar to the previously discussed Stille reaction, various leaving groups have been employed in Suzuki cross-coupling reactions. The Suzuki reaction can be carried out with bromides, iodides, and, usually with slightly lower yield, chlorides. Triflates and related sulfonates are perfectly suited to act as leaving groups, and occasionally, the application of diazonium salts or phosphates has been reported [63].

The choice of ligands has a great influence on the outcome of Suzuki–Miyaura coupling reactions. While great results have been obtained with triphenylphosphine as ligand for palladium, electron-rich ligands are often better suited, especially in the reaction with substrates lacking reactivity. A variety of different ligands have been prepared, designed to increase the reactivity. These ligands work either by modifying the electronic properties of the palladium species or by increasing steric bulk around the catalyst, thus favoring the formation of coordinatively unsaturated complexes. Novel ligands include bis(diphenylphosphino)alkyl ligands such as 1,1′-bis(diphenylphosphinoferrocene (dppf; **182**), bis(diphenylphosphino)butane (dppb; **183**), or bis[1,2-bis(diphenylphosphino)ethane (DIPHOS; **185**). Additionally, trialkylphosphine (**180**), aryl-dialkylphosphine (**181**), *N*-heterocyclic carbene ligands (**186**), or palladacycles (**187**) have been employed in the Suzuki reaction. A small selection is outlined in Figure 12.3 [63].

New developments in the Suzuki cross-coupling reaction include the application of microwave, polymer-bound catalysts, nanoparticles, and ionic liquids as reaction medium. A discussion of these methods exceeds the scope of this chapter.

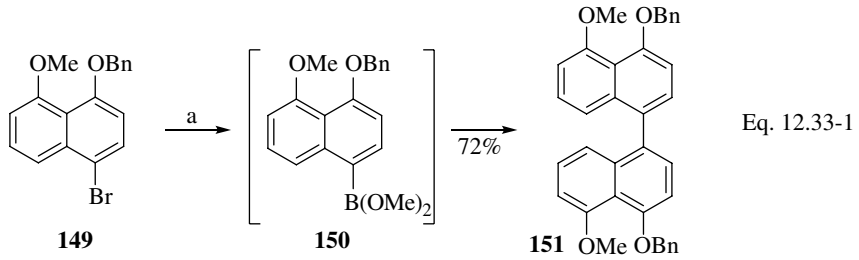
### 12.3.4 Transition Metal-Catalyzed Couplings of Nonactivated Aryl Compounds

Over the last few years, functionalization by means of C—H activation has gained considerable importance for several reasons, including atom economy, the drastic decrease of undesired by-products, and reduced costs for the preparation of substrates, which are often available in fewer steps. In this respect, recent efforts were devoted to the elaboration of efficient protocols for the direct transition metal-catalyzed aryl–aryl bond formation of nonactivated aromatic substrates [63, 68, 69].

The direct oxidative coupling of two nonactivated aryl systems is rarely used for the elaboration of biaryls and, in most cases, thermodynamically not favored because of the C—H bond strength in aromatic compounds. The preparation of biphenyl by means of a homocoupling of benzene with concomitant release of hydrogen is disfavored by 13.8 kJ/mol [121]. However, among others, Sasson reported the palladium-catalyzed formation of biphenyl from benzene, along with minor amounts of acetate **189** as by-product (Eq. 12.35-1). In this experiment, a complex mixture of different metals was employed, which should facilitate the rapid generation of the active Pd(II) species by increasing the $O_2$ concentration in the solution [122]. The successful formation of bipyridine derivative **191** is outlined in Equation 12.35-2 [123] (Scheme 12.35).

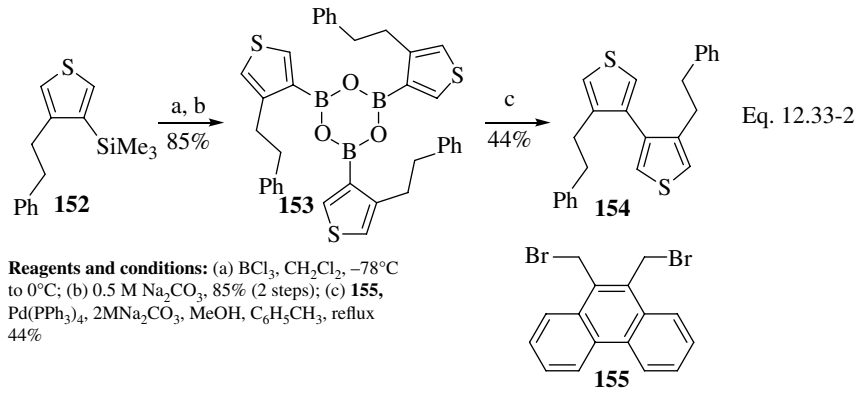
More commonly, the transition metal-catalyzed coupling of aryl halides with nonfunctionalized aromatic substrates has been used for the preparation of unsymmetrical biaryl systems. Different strategies have been developed over the last few years. One very elegant approach utilizes directing groups on aromatic substrates. The lone pair of the requisite heteroatom coordinates to the transition metal and promotes the arylation reaction via intermediary formation of a five- or six-membered metallacycle.

Two examples of such directing group-mediated arylation reactions are shown in Scheme 12.36. Palladium-catalyzed arylation of 2-phenylphenol affords adduct **194** in excellent yield (Eq. 12.36-1). If iodide **193** is used in excess




Eq. 12.33-1

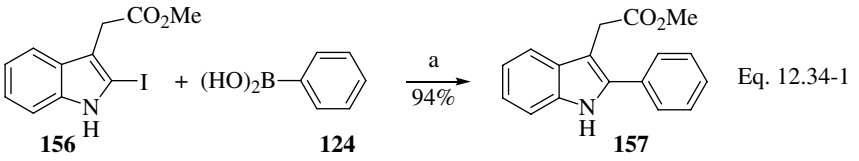
**Reagents and conditions:** (a) (i) *n*BuLi (0.5 eq.), THF, –78°C; $B(OMe)_3$, 12 h, –78°C to rt; (ii) $C_6H_5CH_3$, $Et_2O$, $H_2O$, $Na_2CO_3$, $Pd(PPh_3)_4$, reflux, 12 h, 72%




Eq. 12.33-2

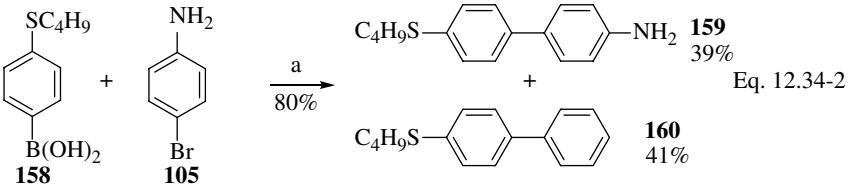
**Reagents and conditions:** (a) $BCl_3$, $CH_2Cl_2$, –78°C to 0°C; (b) 0.5 M $Na_2CO_3$, 85% (2 steps); (c) **155,** $Pd(PPh_3)_4$, $2MNa_2CO_3$, MeOH, $C_6H_5CH_3$, reflux 44%

**SCHEME 12.33** Formation of homodimers via the Suzuki reaction.



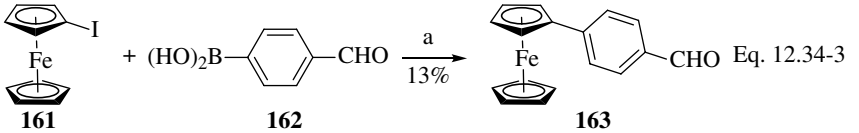

Eq. 12.34-1

**Reagents and conditions:** (a) $Pd(OAc)_2$ (5%), $K_2CO_3$ (2.5 eq.), aetone, $H_2O$, 65°C, 94%



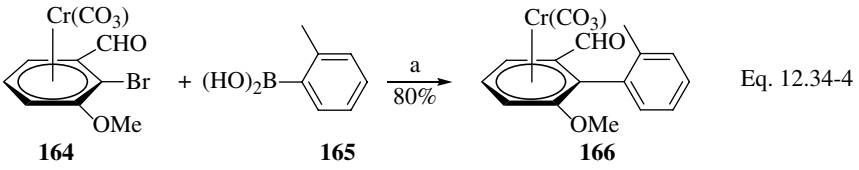

Eq. 12.34-2

**Reagents and conditions:** (a) $Pd(OAc)_2$, $Na_2CO_3$, DME, $H_2O$, 24 h, 13%, 80%




Eq. 12.34-3

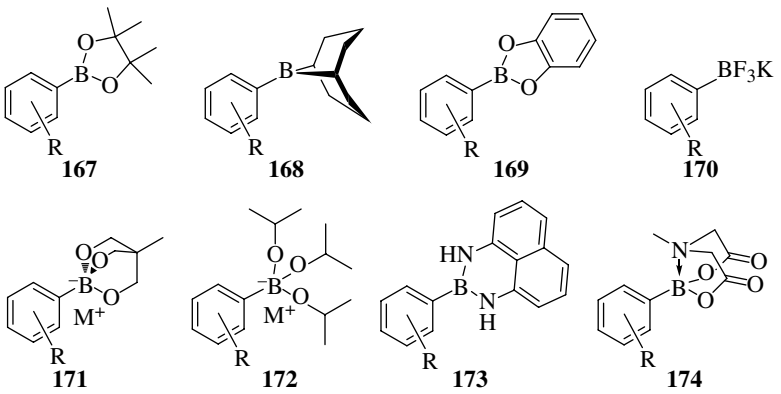
**Reagents and conditions:** (a) $Pd(OAc)_2$ (4%), $Na_2CO_3$, EtOH, $H_2O$, 24 h, 13%



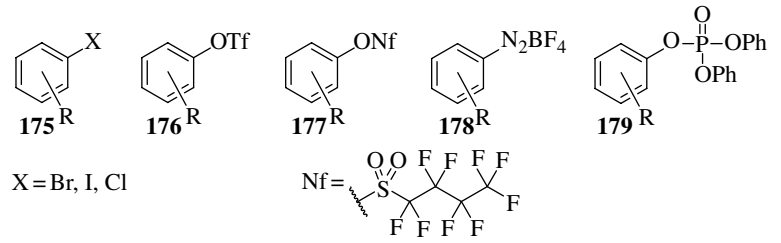

Eq. 12.34-4

**SCHEME 12.34** Functional group tolerance of the Suzuki reaction.

Boron species for the suzuki coupling:




Possible leaving groups:




Novel ligands for palladium:

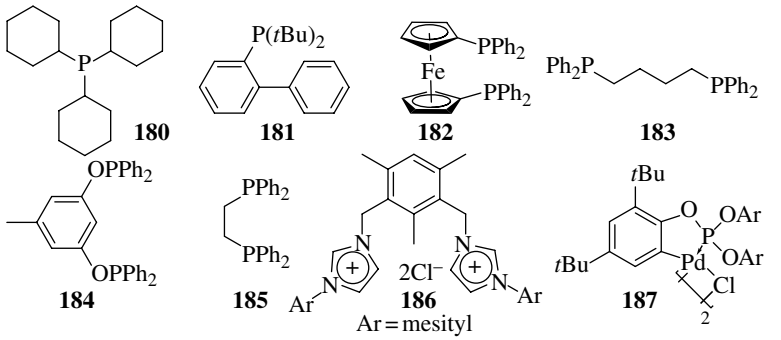
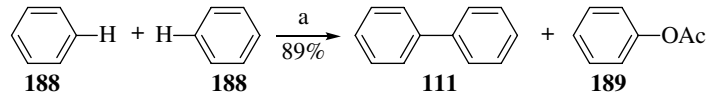
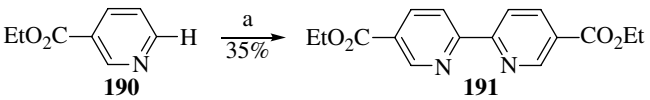



**FIGURE 12.3** Novel boron derivatives, leaving groups, and ligands for the Suzuki coupling.




Eq. 12.35-1

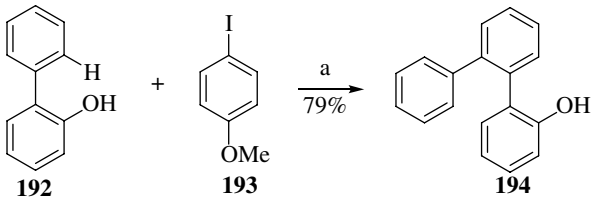
**Reagents and conditions:** (a) $PdCl_2$ (7%), $Zr(OAc)_4$ (2%), $Mn(OAc)_2$ (1.8%), $Co(OAc)_2$ (1.8%), acac (3.1%), HOAc, NaOAc, $O_2$ (10 atm), 105°C, 89%




Eq. 12.35-2

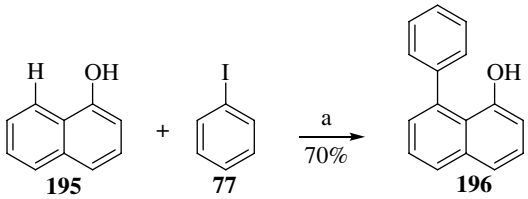
**Reagents and conditions:** (a) Pd/C (10%), reflux, 6 days, 35%

**SCHEME 12.35** Oxidative aryl–aryl formation of nonactivated aromatic substrates.




Eq. 12.36-1

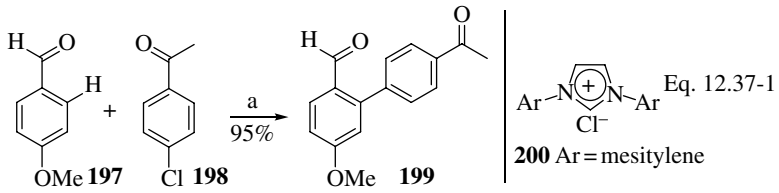
**Reagents and conditions:** (a) $Pd(OAc)_2$ (5%), **193** (1.2 eq.), $Cs_2CO_3$ (1.2 eq.), molecular sieves, DMF, 100°C, 79%




Eq. 12.36-2

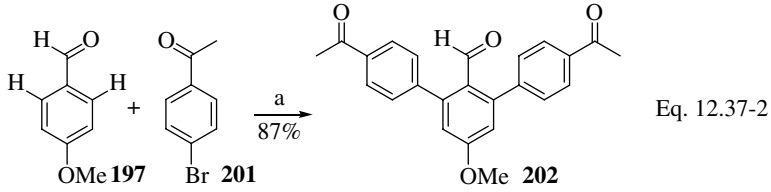
**Reagents and conditions:** (a) $Pd(OAc)_2$ (2.5 %), $Cs_2CO_3$, DMF, 110°C, 70%

**SCHEME 12.36** Directing group-assisted arylation of aromatic substrates.




Eq. 12.37-1

**Reagents and conditions:** (a) $Pd(OAc)_2$ (1%), **200**, $Cs_2CO_3$, dioxane, 80°C, 95%




Eq. 12.37-2

**Reagents and conditions:** (a) $Pd(OAc)_2$ (1%), **200**, $Cs_2CO_3$, dioxane, 80°C, 87%

**SCHEME 12.37** Aldehydes as directing group—arylation of benzaldehydes.

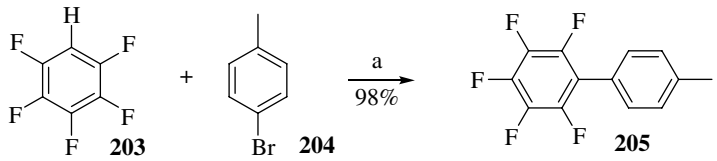
(4.0 eq.), the corresponding diarylated compound is formed as main product. In complete analogy, naphthol **196** was arylated with iodobenzene (**77**) and **196** was isolated in good yield (Eq. 12.36-2) [124].

Aldehydes also serve as suitable directing group, and the arylation of *p*-methoxybenzaldehyde is shown in Scheme 12.37. The coupling was carried out in the presence of palladium as catalyst and an electron-rich carbene ligand (**200**).

Thus, the authors were also able to successfully employ aryl halides in the palladium-catalyzed coupling reaction to form monoarylated product **199** (Eq. 12.37-1). When the more reactive bromide **201** was used, diarylation occurred and **202** was obtained as major product (Eq. 12.37-2) [125].

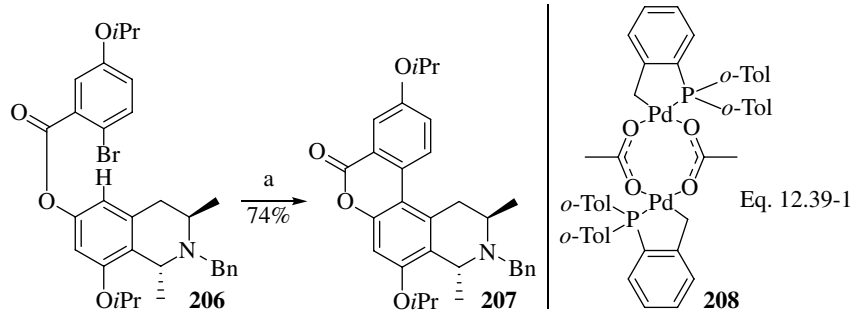
Numerous examples with ethers, amines, imines, oxazolines, and pyrazoles, just to name a few, have been reported and give evidence of the synthetic versatility of this method. The intermolecular arylation of nonactivated electron-deficient aromatic substrates is possible by means of a palladium-catalyzed protocol. Fagnou and coworkers reported the arylation of pentafluorobenzene in excellent yield as shown in Scheme 12.38 [126]. The authors employed different halides as coupling partner for the fluorinated species and were even able to convert chlorides into the corresponding adducts in good yield (57% isolated yield when *p*-methyl chlorobenzene was used). Additionally, different mono-, di-, and trifluorides were converted to biaryl products.

Very often, the intramolecular direct arylation delivers excellent results, and this methodology has been successfully employed in the preparation of natural products. The idea behind this protocol is simple and takes advantage of the close spatial arrangement of the intermediary formed palladium complex and the nonactivated aromatic moiety. Additionally, chelating groups facilitate the reaction.



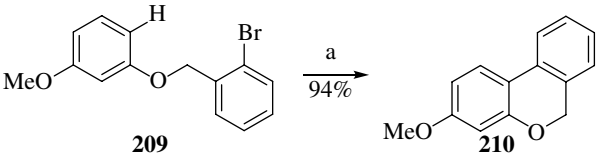

**Reagents and conditions:** (a) $Pd(OAc)_2$ (5%), $P(tBu)_2Me\text{-}HBF_4$, $K_2CO_3$, DMA, 120°C, 98%

**SCHEME 12.38** Intermolecular arylation of fluorinated substrates.



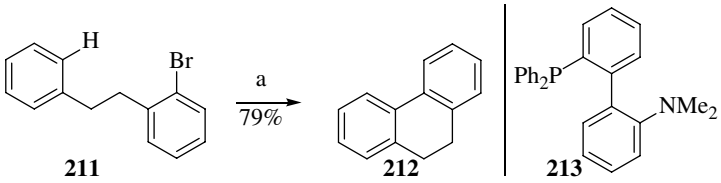

Eq. 12.39-1

**Reagents and conditions:** (a) **208** (10%), NaOAc, DMA, 140°C, 74%




Eq. 12.39-2

**Reagents and conditions:** (a) $Pd(OAc)_2$, **213**, $K_2CO_3$ (2 eq.), DMA, 145°C, 10 h, 94%




Eq. 12.39-3

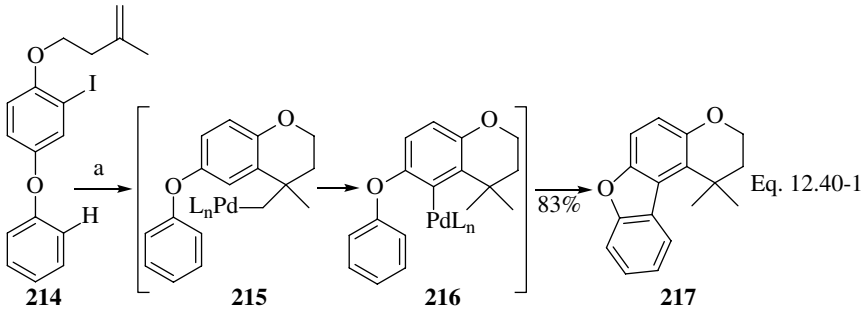
**Reagents and conditions:** (a) $Pd(OAc)_2$, **213**, $K_2CO_3$ (2 eq.), DMA, 135°C, 79%

**SCHEME 12.39** Intramolecular arylation using nonfunctionalized arenes.

As shown in Equation 12.39-1, Scheme 12.39, ester groups are perfectly suited as temporary linker for the intramolecular palladium-catalyzed aryl coupling reaction. After the successful aryl–aryl bond formation, cleavage of the ester releases the desired adduct as demonstrated by Bringmann in his preparation of the antimalarial naphthylisoquinoline alkaloid korupensamine B [127, 128]. Fagnou reported the synthesis of a variety of biaryl compounds [129, 130]. Two examples are shown in Scheme 12.39. While Equation 12.39-2 describes the application of a phenyl ether, which is capable of serving as ligand in the palladium complex, the intramolecular aryl–aryl bond formation in bromide **211** is an impressive example of the synthetic potential of this method, for substrates lacking heteroatoms with lone pairs (Eq. 12.39-3). The use of electron-rich carbene ligands furthermore allowed the transformation of aryl chlorides in excellent yield [130].

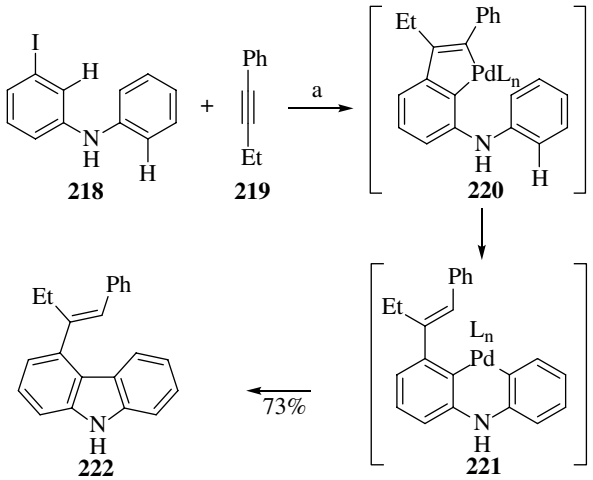
A different strategy and very elegant approach combines the palladium insertion into an aryl halide, subsequent Heck reaction, and an intramolecular arylation through C─H activation. In 2004, Larock published the synthesis of various polycycles by utilizing such a tandem protocol [131]. The sequence leading to tetracycle **217** is shown in Equation 12.40-1, Scheme 12.40. The sequential palladium-catalyzed reactions allow the efficient elaboration of complex polycyclic frameworks, which are commonly observed in natural products.

One year later, Larock reported the preparation of various carbazole derivatives by using the same conditions



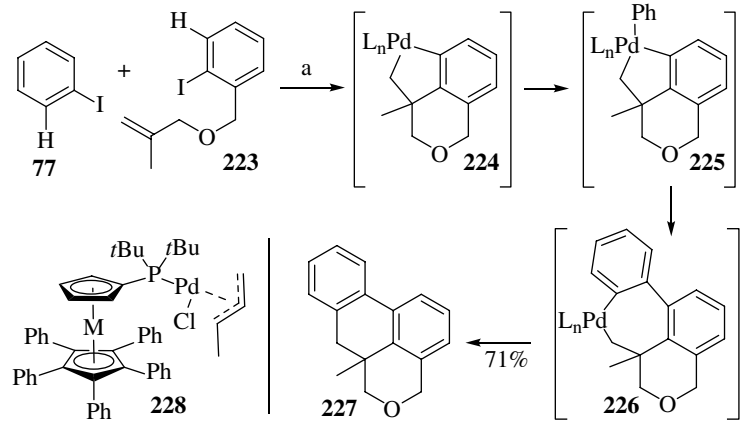

Eq. 12.40-1

**Reagents and conditions:** (a) $Pd(OAc)_2$ (5%), dppm, CsOPiv, DMF, 90°C, 83%




Eq. 12.40-2

**Reagents and conditions:** (a) $Pd(OAc)_2$ (5%), dppm, CsOPiv, DMF, 100°C, 73%




Eq. 12.40-3

**Reagents and conditions:** (a) **228**, KO*t*Bu, CsOPiv, $Cs_2CO_3$, DMF, 100°C, 18 h, 71%

**SCHEME 12.40** Palladium-catalyzed cascade reactions.

as outlined earlier [132]. As shown in Equation 12.40-2, palladium-catalyzed reaction of iodophenyl anilines and internal alkynes proceeded via the initial palladium insertion into the aryl halide bond, followed by Heck reaction and subsequent C─H activation with palladium migration from the vinylic position and formation of intermediate **220**. The desired carbazole is then formed by means of another C─H activation of the remaining aromatic moiety and a final reductive elimination step.

Recently, an impressive palladium-catalyzed cascade reaction was published by the Lautens group as shown in Equation 12.40-3, Scheme 12.40 [133]. Generally, the reaction cascade can either start with iodide **77** or **223**. The route shown in Equation 12.40-3 commences with the insertion of the palladium catalyst into the aryl–iodide bond of iodide **223**. The whole sequence includes oxidative insertion of the palladium species into the aryl–halogen bond, two C─H activation steps, and a final reductive elimination.

The preparation of tetracycle **227** from two simple building blocks in one transition metal-catalyzed cascade reaction clearly outlines the potential of this protocol in the elaboration of complex natural products.

## 12.4 SYNTHESIS OF TYROSINE-DERIVED ALKALOIDS

The following section is devoted to the discussion of selected chemical syntheses of tyrosine-derived alkaloids. The great variety of these biologically and structurally fascinating natural products complicates or even renders any attempt to comprehensively cover this field and to present a complete overview of synthetic achievements impossible. The section is organized in a similar fashion as the section on biosynthetic routes to tyrosine-derived secondary metabolites. Syntheses of the most prominent members of each class of alkaloids are described in detail.

During the discussion of the biosynthetic pathways toward tyrosine-derived metabolites, the importance of aryl–aryl couplings and oxidative phenolic coupling reactions becomes obvious, and the most important methods for the aryl–aryl bond formation are outlined in the previous section. Because of the predominant importance of coupling reactions in the biosynthesis and synthesis of tyrosine-derived metabolites, the subsequent section covers biomimetic synthetic achievements with interesting or unusual protocols for the coupling of the ring motifs.

### 12.4.1 Synthesis of Modified Benzyltetrahydroisoquinoline Alkaloids

Morphine and its congeners play a unique role in alkaloid history, and this fascinating natural product has attracted humans for at least 5000 years, as evidenced by excavations of the Sumerians that date back as far back as 3000 B.C. [134]. Because of its societal, historical, and medicinal importance, opium alkaloids have also gained considerable attention from the scientific community. Morphine has already been isolated in 1805 by Sertürner [135]—approximately 25 years before Wöhler's synthesis of urea, which marks the beginning of organic chemistry. The structure elucidation of morphine constitutes a masterpiece of logic deduction and reasoning, and the precise structural assignment was finally resolved in 1923 [11, 136, 137], 120 years after the isolation of the natural product [138].

Even more than 60 years after the first total synthesis of morphine by Gates [139, 140], the ongoing interest of synthetic chemists in the natural product is evidenced by the numerous approaches to the morphinan skeleton, as well as formal and total syntheses of the natural product. The progress in morphine synthesis has been reviewed on several occasions [141–143].

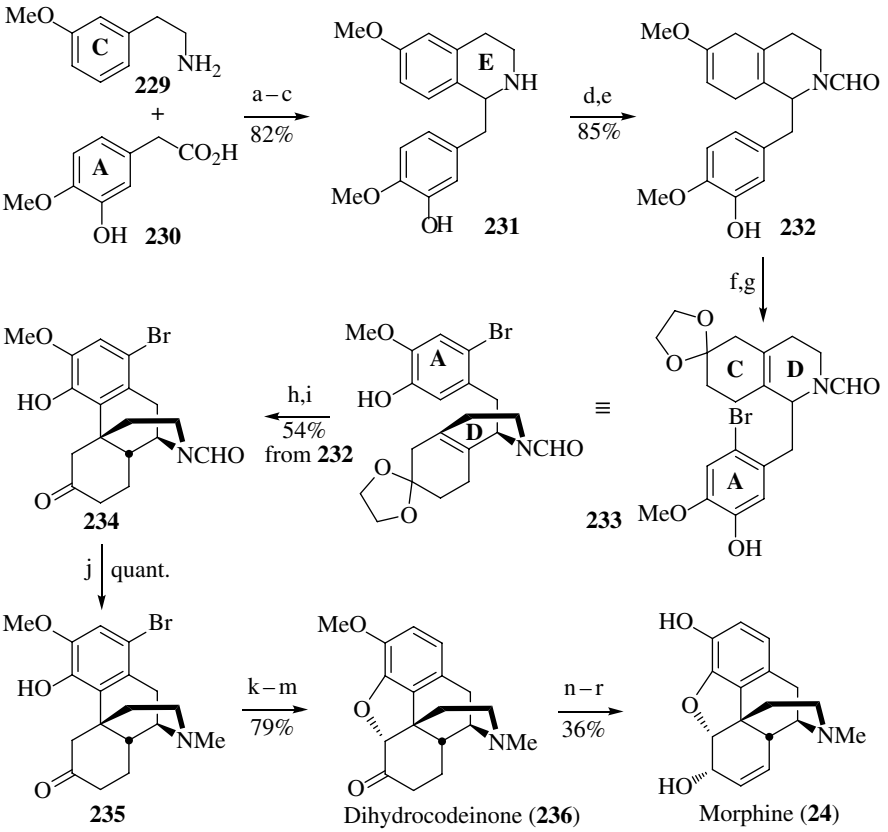
Herein, three syntheses of morphine or related alkaloids are discussed in detail, which utilize completely different protocols for the coupling of the ring motifs of the alkaloid. Rice published a biomimetic approach with an acid-mediated electrophilic cyclization strategy as key step [144]. Mulzer employed a Friedel–Crafts acylation and a Robinson annulation to construct the phenanthrenone ring system [145]. The D ring of the alkaloid was elaborated with a 1,4-cuprate addition as key step. In his most recent contribution to morphine research, Hudlicky employed a Diels–Alder cycloaddition reaction to construct the ABCE ring system of the natural product. The requisite diene was obtained after oxidative dearomatization of the A ring precursor [146].

(±)-*Morphine; Rice, 1980*: In 1980, Rice achieved a short and highly efficient synthesis of morphine [144, 147]. The route, outlined in Scheme 12.41, closely follows the biosynthetic pathway and features an electrophilic cyclization reaction as first described by Grewe (**233** to **234**) as key step for the closure of the B ring [148]. Although this route was published nearly 35 years ago, Rice's synthesis of morphine still stands out in respect to brevity and overall efficiency and is considered a milestone achievement in morphine research.

The route commenced with the condensation of amine **229** and carboxylic acid **230** at 200 °C. Subsequent Bischler–Napieralski reaction and sodium borohydride reduction established the C/D ring system of morphine and delivered tetrahydroisoquinoline **231** in good yield. Next, Birch reduction and *N*-formylation afforded enol ether **232**, which was converted into the corresponding ketal before reaction with bromine allowed the isolation of the cyclization precursor. The halide in **233** serves to protect the *para* position in the aromatic ring in the subsequent acid-mediated electrophilic cyclization reaction—a common strategy that has also been applied by other research groups in their endeavors toward morphine and related alkaloids.

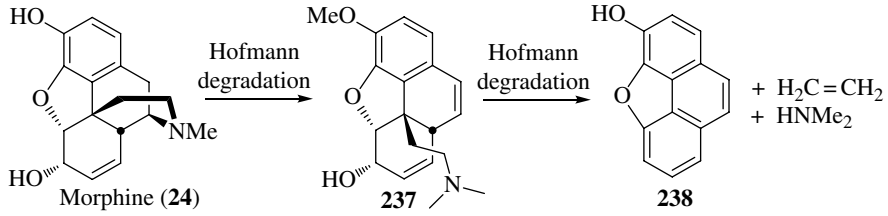
As mentioned earlier, the crucial formation of the B ring of morphine was accomplished by applying conditions previously reported by Grewe [148]. Exposure of **233** to formic acid released the β,γ-unsaturated ketone and subsequent reaction with $NH_4 \cdot HF$ facilitated the ring closure (**234**). Reductive amination allowed the isolation of phenol **235**, which was used to elaborate the dihydrofuran moiety via bromination of the α-position of the ketone (C5) and subsequent nucleophilic attack of the deprotonated phenol. This strategy was inspired by the pioneering work of Tschudi and Gates who presented the first total synthesis of morphine in 1952 [139, 140]. Next, hydrogenation of the aryl bromide in the presence of formaldehyde delivered dihydrocodeinone (**236**) in good overall yield.

As dihydrocodeinone has been converted to morphine before, this hydrogenation concludes the formal synthesis of this important alkaloid. The completion of the synthetic route included the conversion of the tertiary amine into the corresponding carbamate before the C7–C8 unsaturation




**Reagents and conditions:** (a) 200°C, 2 h; (b) $POCl_3$, MeCN; (c) $NaCNBH_3$, MeOH; (d) Li, $NH_3$, THF, *t*BuOH; (e) PhOCHO, EtOAc, Δ; (f) $(CH_2OH)_2$, THF, $MeSO_3H$; (g) $CH_3CONHBr$, 0°C; (h) $HCO_2H$, $H_2O$; (i) $NH_4F{\cdot}HF$, $CF_3SO_3H$; (j) (i) MeOH, HCl, reflux, (ii) $NH_3$, $H_2O$, *i*PrOH; (k) $Br_2$, HOAc; (l) NaOH, $CHCl_3$; (m) $H_2$, HOAc, HCHO; (n) EtOCOCl, $C_6H_6$, reflux; (o) PhSeCl, EtOAc, HCl; (p) $NaIO_4$, EtOAc, $H_2O$; (q) LAH, THF, reflux; (r) (i) $BBr_3$, $CHCl_3$, (ii) $NH_3$.

**SCHEME 12.41** Rice's biomimetic synthesis of morphine (**24**).

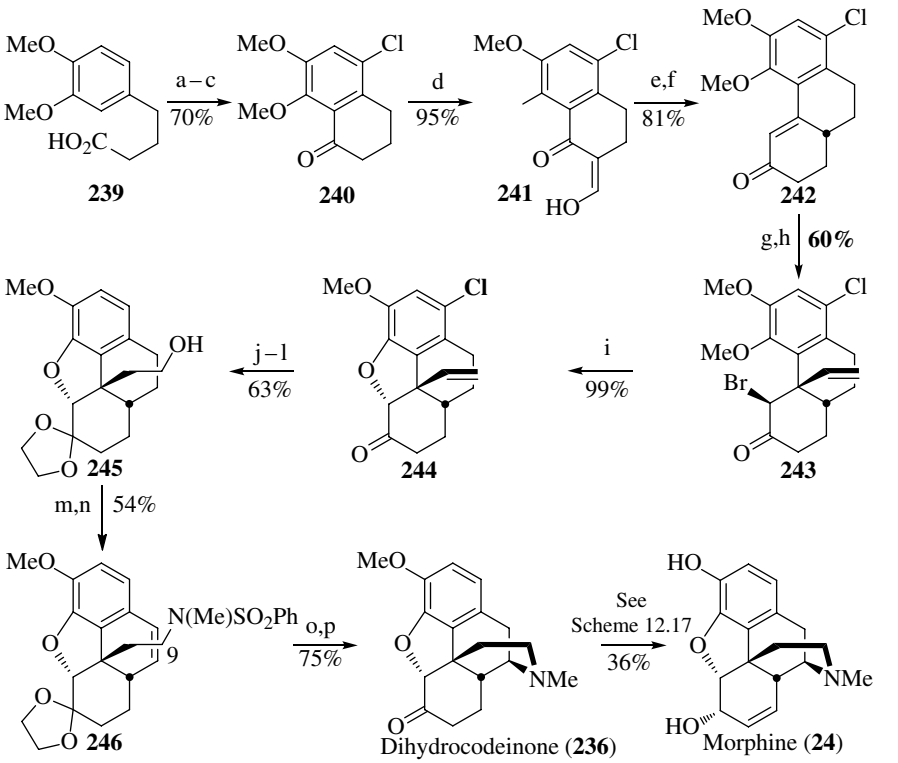



**SCHEME 12.42** Early degradation study of morphine (**24**).

was installed via preparation of the 7-phenylseleno derivative, followed by the well-established oxidation–elimination protocol. Reduction of the enone and the ethyl carbamate and treatment of the resulting codeine with boron tribromide then allowed the isolation of morphine (**24**) [149, 150].

(–)-*Morphine; Mulzer, 1996*: Mulzer and Trauner published a conceptually completely different synthesis of morphine [145, 151]. The route does not follow the biomimetic synthesis of the natural product but was inspired by early degradation studies, which ultimately helped to achieve the structure elucidation of morphine and related alkaloids. As outlined in Scheme 12.42, double Hofmann degradation of morphine afforded oxygenated phenanthrene **238** and ethene (a detailed account of the structure elucidation of morphine is provided in Ref. [138]). Mulzer's approach formally constitutes the reversal of the Hofmann degradation protocol.

Most other approaches toward the title alkaloid featured Heck reactions [152], Claisen rearrangements [153], or Diels–Alder reactions [139, 154]—Mulzer's route is the only one so far that utilized a 1,4-cuprate addition to install



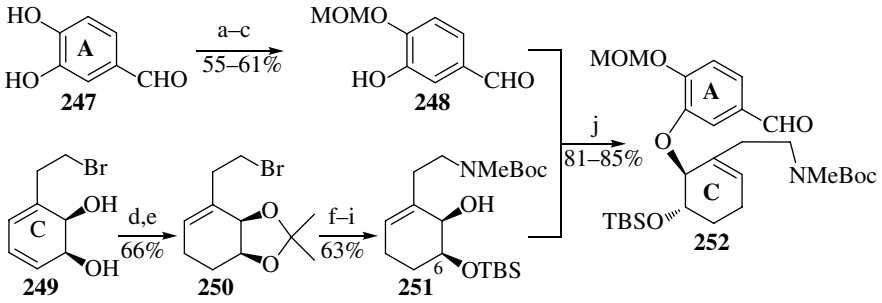

**Reagents and conditions:** (a) $Cl_2$, AcOH, 99%; (b) $(COCl)_2$, $C_6H_6$, reflux; (c) $SnCl_4$, $C_6H_6$, 0°C, 71% (2 steps); (d) $HCO_2Me$, NaOMe, $C_6H_6$, 95%; (e) methyl vinyl ketone, $NEt_3$, MeOH, (f) KOH, dioxane, $H_2O$, 81% (2 steps); (g) ($H_2C{=}CH_2$) CuMgCl, THF, –78°C to 0°C; TMSCl, $NEt_3$, 0°C to 25°C; (h) NBS, THF, 60% (2 steps) (i) DMF, 140°C, 99%; (j) TMSCl, $(CH_2OH)_2$, $CH_2Cl_2$, 92%; (k) $BH_3{\bullet}SMe_2$, THF; $H_2O_2$, NaOH, 70%; (l) Raney-Ni, MeOH, KOH, 98%; (m) $PhSO_2NHMe$, ADDP, $Bu_3P$, 81%; (n) NBS, $(PhCO_2)_2$, $CCl_4$, $NEt_3$, reflux, 67%; (o) Li, $NH_3$, THF, *t*-BuOH, –78°C, 79%; (p) HCl (3N), 90°C, 95%.

**SCHEME 12.43** Mulzer's synthesis of morphine (**24**).

the C13 quaternary center and to mimic the Hofmann degradation pathway.

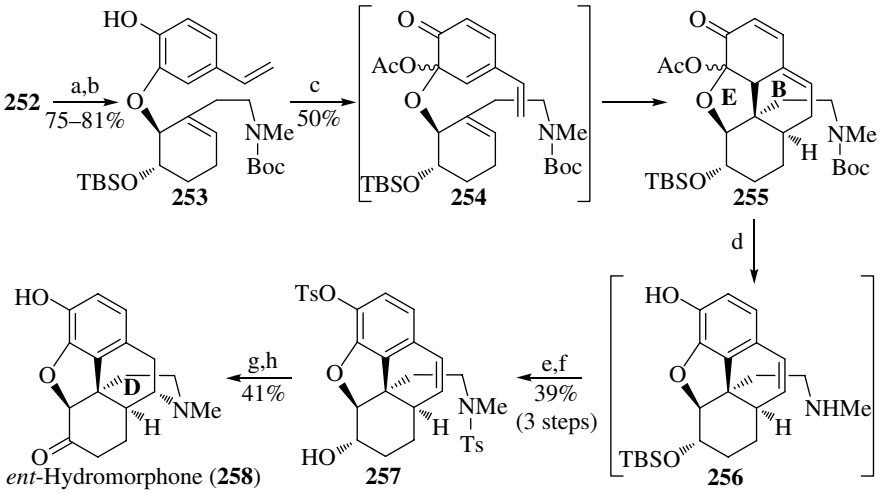
As outlined in Scheme 12.43, the initial steps of the synthesis were devoted to the elaboration of phenanthrenone **242**, which served as substrate for the intended key cuprate addition reaction. Subsequent cuprate addition should then establish the quaternary C13 center and install the handle to establish the D ring of the alkaloid.

The synthesis began with conversion of carboxylic acid **239** to tetralone **240** via chlorination of the aromatic ring, followed by Friedel–Crafts acylation. Next, activation of **240** as its formyl derivative (**241**), Robinson annulation, and a retro-Claisen reaction allowed the isolation of phenanthrenone **242** in excellent overall yield. The racemic mixture was resolved by chromatography on cellulose triacetate, and the optically pure material was employed in the key 1,4-cuprate addition. Reaction of enone **242** with $(CH_2{=}CH_2)_2CuMgCl$ and subsequent trapping of the intermediary enolate afforded α-bromoketone **243** in good yield as 3 : 1 mixture with its α-epimer, after treatment of the silyl enol ether with *N*-bromosuccinimide (NBS). When heated in DMF to 140 °C, **243** smoothly delivered dihydrobenzofuran **244**, while the undesired α-epimer did not undergo cyclization. With **244** in hand, the stage was set for the elaboration of the piperidine ring. Ketalization of the carbonyl moiety in **244** was followed by a hydroboration/oxidation sequence of the terminal alkene, resulting in the isolation of the corresponding primary alcohol. Raney nickel-mediated dechlorination of the aromatic A ring then afforded advanced intermediate **245**, which was converted to secomorphinan **246** via a variant of the Mitsunobu reaction, and subsequent reaction with NBS, which installed the benzylic double bond and paved the way for the final bond formation between the nitrogen and C9. This synthetic operation was carried out following a protocol published by Parker [155]. Reaction of **246** with lithium in liquid ammonia furnished the closure of the piperidine ring of morphine and concomitantly resulted in reductive desulfonation. Dihydrocodeinone (**236**) was obtained after deketalization under acidic conditions, and this final operation concluded the formal synthesis of



**Reagents and conditions:** (a) $Ac_2O$, NaOH, THF, 0°C, 82–85%; (b) MOMCl, $K_2CO_3$, DMF, 0°C to rt, 76–80%; (c) $K_2CO_3$, MeOH, 88–90%; (d) potassium azodicarboxylate, AcOH, MeOH, 0°C, 83%; (e) 2, 2-dimethoxypropane, acetone, *p*-TsOH, 80%; (f) $MeNH_2$, $K_2CO_3$, THF, sealed tube, 93%; (g) HCl (1.3M), EtOH; (h) $(Boc)_2O$, $NaHCO_3$, EtOH, 74% (2 steps); (i) TBSCl, imidazole, $CH_2Cl_2$, –78°C to rt, 92%; (j) TMAD, $PBu_3$, 81–85%.

**SCHEME 12.44** Hudlicky's synthesis of *ent*-hydromorphone (**258**)—part 1.



**Reagents and conditions:** (a) $CH_3PPh_3Br$, *n*-BuLi, THF, –78°C to rt, then reflux, 82–88%; (b) $ZnBr_2$, $CH_3(CH_2)_{10}CH_2SH$, $CH_2Cl_2$, 10 min, 92%; (c) $Pb(OAc)_4$, $ClCH_2CH_2Cl$, reflux, 50%; (d) TFA, $CH_2Cl_2$, 0°C; (e) TsCl, $Et_3N$, $CH_2Cl_2$, 0°C to rt, 45% (2 steps); (f) TBAF, THF, 86%; (g) Li, *t*-BuOH, $NH_3$ (liq), THF, –78°C, 10 min, 93%; (h) *t*-BuOK, PhCOPh, toluene, 85°C, 44%.

**SCHEME 12.45** Hudlicky's synthesis of *ent*-hydromorphone (**258**)—part 2.

morphine. The conversion of dihydrocodeinone (**236**) to morphine (**24**) has been reported by Rice and coworkers and is described in the previous section and outlined in Scheme 12.41 [149, 150].

Mulzer's elegant synthesis of morphine is characterized by a stepwise elaboration of the ring motives in the natural product. While the biosynthetic pathway comprises an oxidative phenolic coupling, Mulzer employed a highly efficient Friedel–Crafts acylation to establish the C12─C13 bond. Additionally, the implementation of observations from degradation studies represents an interesting alternative strategy to the exploitation of biomimetic pathways for natural product synthesis.

ent-*Hydromorphone; Hudlicky, 2014*: Very recently, Hudlicky presented a concise route to *ent*-hydromorphone (**258**), which takes advantage of a biocatalytically derived chiral synthon as starting material [146]. The route, outlined in Schemes 12.44 and 12.45, features an oxidative dearomatization with a subsequent intramolecular [4+2] cycloaddition as key step and represents a creative strategy for the elaboration of the morphinan skeleton. So far, only one other approach has been reported, which employed a Diels–Alder cycloaddition in the construction of the B ring of morphine [154]. The strategy reported by Hudlicky represents an interesting and valuable alternative to oxidative phenolic coupling reactions or palladium-catalyzed protocols.

The synthesis of the synthons for the A and C ring of the natural product and the preparation of the substrate for the crucial oxidative dearomatization/intramolecular [4+2] cycloaddition key step are shown in Scheme 12.44.

The synthesis of the aromatic A ring of morphine commenced from 3,4-dihydroxybenzaldehyde (**247**). Monoacetylation of **247** was followed by protection of the remaining phenolic hydroxyl moiety as its MOM ether. Hydrolysis of the acetate under mild conditions then allowed the isolation of arene **248** in good overall yield.

The preparation of the C ring of the alkaloid took advantage of whole-cell fermentation of arenes with recombinant *Escherichia coli* JM 109 (pDTG601A) [156], which delivers the corresponding cyclohexadiene diols from the corresponding inexpensive aromatic starting materials [157, 158]. Dihydroxylation of β-bromoethylbenzene delivered cyclohexadiene **249**, which was immediately employed in a selective reduction of the sterically less congested double bond with potassium azodicarboxylate, before protection of the diol moiety as its acetonide furnished bromide **250**. Nucleophilic displacement of the bromide with methylamine was followed by hydrolysis of the acetonide under acidic conditions and installation of a Boc-protecting group on the secondary amine. Silylation of the more accessible, distal hydroxyl functionality (C6, morphine numbering) concluded the synthesis of the C ring synthon of the natural product (**251**) and paved the way for the preparation of intermediate **252**. This material was obtained in good yield after coupling of alcohol **251** with phenol **248** by means of a Mitsunobu protocol.

With key intermediate **252** in hand, Hudlicky turned his attention to the crucial oxidative dearomatization/intramolecular [4+2] cycloaddition sequence (Scheme 12.45). Thus, the carbonyl moiety in **252** was converted to the requisite terminal alkene via reaction with methyltriphenylphosphonium bromide, before the MOM ether was cleaved under acidic conditions. Reaction of the free phenol in cyclization precursor **253** with lead tetraacetate resulted in the desired arene oxidation and isolation of cycloaddition product **255** in 50% yield, via intermediary formed dienone **254**. Interestingly, **255** was formed as sole cycloaddition product, and the product of the endocyclic cycloaddition reaction was only observed once in minor amounts, probably because of unfavorable steric interactions.

Next, exposure of **255** to trifluoroacetic acid resulted in rearomatization of the A ring of morphine and cleavage of the carbamate (**256**), which prepared the substrate for the intended hydroamination and elaboration of the D ring of the title compound. All attempts failed to achieve ring closure from **255**, either via aminomercuration or addition of lithium amide, and the material was converted to the corresponding tosyl amide before the ethylamino bridge was established. The cyclization was accomplished by addition of lithium to **257** and delivered the desired product in excellent yield. Oxidation of the secondary alcohol with benzophenone and *t*-BuOK allowed the isolation of *ent*-hydromorphone (**258**) in 12 steps from β-bromoethylbenzene.

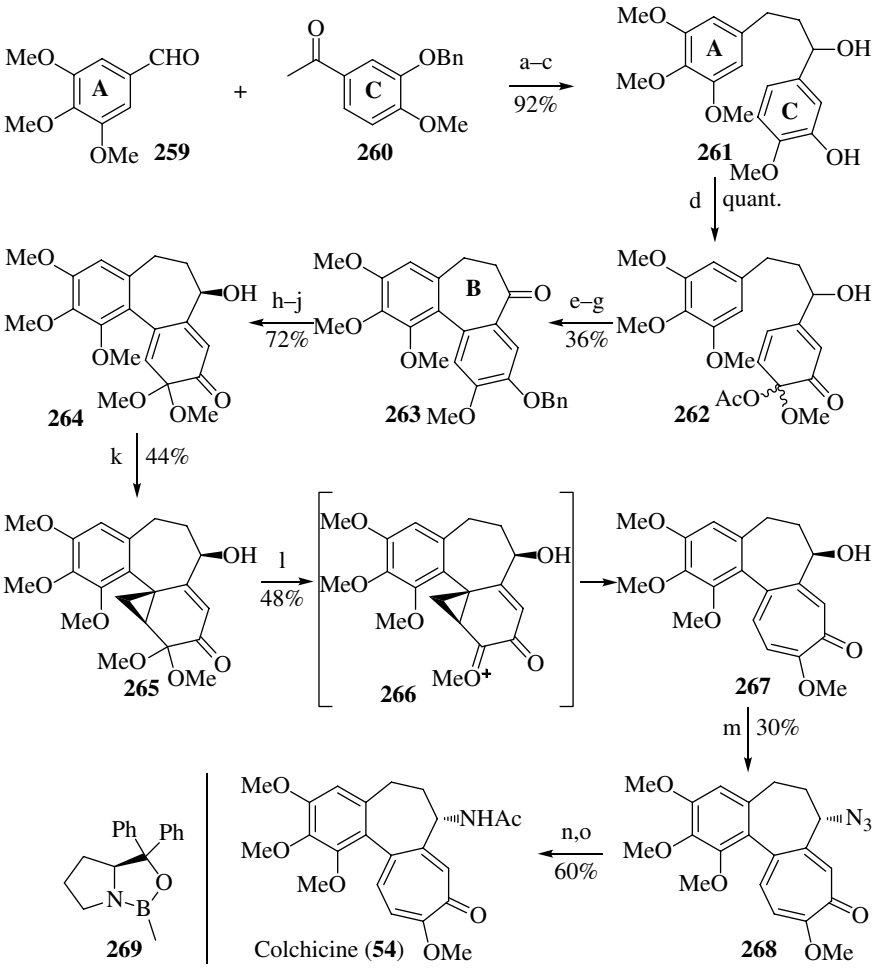
### 12.4.2 Synthesis of Phenethylisoquinoline Alkaloids

Several genera of the Liliaceae plant family have been identified to produce the secondary metabolite autumnaline (**45**), which also serves as key intermediate in the biosynthesis of a variety of phenethylisoquinoline alkaloids (see Schemes 12.9 and 12.10). Colchicine (**54**), derived from autumnaline (**45**) via a remarkable ring-expanding rearrangement, is the most prominent member of this class of tyrosine-derived alkaloids.

Colchicine (**54**) has first been isolated by Pelletier and Caventou as early as 1820, only a few years after the isolation of morphine by Sertürner [135]. Because of its highly promising cytotoxic and anti-inflammatory properties, colchicine is employed during acute attacks of gout. Furthermore, the compound is also used as anticancer agent. The natural product has received considerable attention from the synthetic community, and even today, the alkaloid represents a challenging target. The first total synthesis was published in 1959 by Eschenmoser [159], and since then, several highly interesting syntheses of this remarkable natural product [31] and other phenethylisoquinoline alkaloids [32] have been reported.

In the following section, Banwell's synthesis of colchicine is discussed in detail [160]. The route features a biomimetic ring enlargement as key step. The ring system is elaborated via an oxidative coupling approach. Key steps of other approaches that utilize oxidative coupling reactions for the elaboration of the colchicine ring system are briefly outlined.

(−)-*Colchicine; Banwell, 1996*: In 1996, Banwell reported a concise biomimetic synthesis of colchicine (**54**) [160]. The route, in analogy to Tobinaga's [161] and Evans' [162, 163] approaches, features a ring enlargement strategy for the elaboration of the seven-membered C ring of the natural product. The synthesis, outlined in Scheme 12.46, starts with condensation of trimethoxybenzaldehyde (**259**) and acetophenone **260**. Hydrogenation of the resulting enone and reduction of the carbonyl moiety delivered 1,3-diarylpropanol (**261**) in excellent yield. This material was converted to cyclohexadienone **262** with lead tetraacetate via a Wessely oxidation of the phenol [164], and this material successfully delivered tricyclic ketone **263** by means of a cationic cyclization and subsequent protection of the resulting phenol and Ley oxidation. The synthetic strategy envisaged installation of the acetamido side chain via a Mitsunobu reaction with azide as nucleophile at a later stage. The requisite stereoselective reduction of the carbonyl moiety to the (*R*)-configured alcohol was achieved with the chiral CBS reagent in stoichiometric quantities. Next, debenzylation allowed the isolation of the corresponding phenol, which served as substrate for the second phenol oxidation. Exposure of the free phenol to $Tl(NO_3)_3$ (Taylor–McKillop oxidation) [165] afforded the desired cyclohexadienone **264**, which was




**Reagents and conditions:** (a) NaOH, MeOH, 96%; (b) $H_2$, Pd/C, EtOAc, 15°C, 96%; (c) $NaBH_4$, THF, MeOH, 96%; (d) $Pb(OAc)_4$, 3Å molecular sieves, $CH_2Cl_2$, 15°C, 100%; (e) $CF_3CO_2H$, 3Å molecular sieves, THF, $C_6H_6$, 0°C, 42%; (f) BnBr, MeCN, 88%; (g) NMO, TPAP, 4Å molecular sieves, $CH_2Cl_2$, 15°C, 98%; (h) **269**, $BH_3$, THF, 15°C, 88%; (i) $H_2$, Pd, Pd/C, EtOAc, 15°C, 99%; (j) $Tl(NO_3)_3$, MeOH, –20°C, 83%; (k) $Me_3S(O)I$, NaH, DMSO, 54%; (l) $CF_3CO_2H$, $CH_2Cl_2$, 15°C, 48%; (m) DIAD, $PPh_3$, $Zn(N_3)_2$•2py, THF, 15°C, 30%; (n) $PPh_3$, $H_2O$, THF, 15°C; (o) $Ac_2O$, py, 60% (over 2 steps).

**SCHEME 12.46** Banwell's synthesis of (−)-colchicine (**54**).

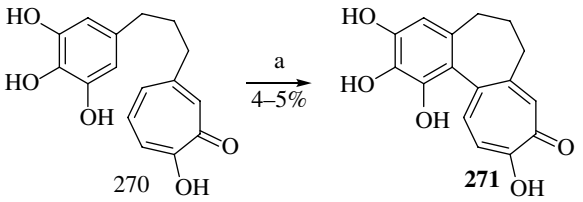
treated with dimethylsulfoxonium methylide to produce cyclopropane **265** in fair yield but excellent 98% *ee* after one crystallization.

With cyclopropane **265** in hand, the envisaged biomimetic ring enlargement could be attempted. When treated with trifluoroacetic acid, cyclopropane **265** underwent ring expansion and delivered the 6,7,7-ring system, probably via oxonium species **266**. This protocol elegantly afforded the tropolone system with the correct oxidation state and the correct regiochemical arrangement of the oxygen functionalities.

After the successful elaboration of the 6,7,7-ring system of colchicine, the only remaining synthetic operation was the installation of the acetamide moiety. Alcohol **267** was allowed to react with diisopropyl azodicarboxylate (DIAD), triphenylphosphine, and azide to afford the requisite amine with the correct stereochemical configuration after subsequent Staudinger reduction. Colchicine (**54**) was isolated after exposure of the amine to acetic anhydride in pyridine.

As pointed out earlier, of all approaches published so far, Banwell's route is the closest to the proposed biosynthetic pathway and also highlights the importance and relevance of oxidative coupling reactions in the preparation of tyrosine-derived alkaloids. Such oxidative coupling reactions have also been used in other approaches. Quite early, Scott [166] employed an oxidative coupling of **270** in his synthesis of desacetamidocolchiceine, Equation 12.47-1, Scheme 12.47 (colchiceine varies from colchicine in the methoxy substituent on the tropolone ring, colchiceine bears a hydroxyl

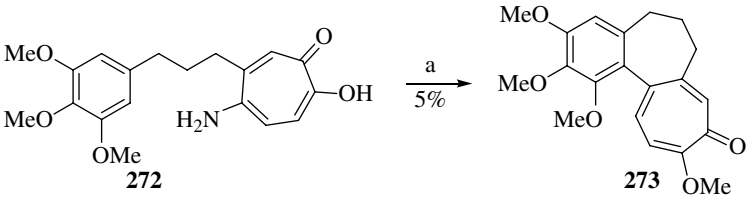
Desacetmidocolchiceine; Scott et al. [166]:




Eq. 12.47-1

**Reagents and conditions:** (a) $FeCl_3 \bullet 6H_2O$, $H_2SO_4$ (6 N), EtOH, $CHCl_3$ 4–5%.

Desacetmidocolchiceine; Kaneko and Matsui [167]:




Eq. 12.47-2

**Reagents and conditions:** (a) Isoamylnitrite, $H_2SO_4$ (conc), 7–10°C; then Cu, dioxane, rt, 24 h, 5%.

**SCHEME 12.47** Key steps in Scott's and Kaneko's syntheses of desacetamidocolchiceine.

group). Cyclization precursor **270** was allowed to react with $FeCl_3$ in aqueous sulfuric acid in a biphasic mixture with ethanol and chloroform, and the desired material was isolated in 4–5% yield. Various other conditions have been employed, including sodium iodate, lead dioxide, and potassium ferricyanide, but these conditions did not allow the isolation of **271** because of competing oxidative cleavage of the ring system.

A few years later, Kaneko reported a slightly modified approach toward desacetamidocolchiceine [167]. As shown in Equation 12.47-2, Scheme 12.47, the route featured the diazotation of amine **272**, followed by addition of copper powder to the reaction mixture. This protocol allowed the isolation of **273** in 5% yield.

The key step of Tobinaga's synthesis of desacetamidocolchicine [161] is outlined in Equation 12.48-1, Scheme 12.48. The synthetic strategy relied on the erroneous assumption of Anet and Robinson that the biosynthesis of colchicine proceeds via spirocyclic intermediates such as **275** [168]. This spirocyclic dienone was obtained in 80% yield from **274** via anodic oxidation in the presence of $HBF_4$. Reduction of the carbonyl moiety was followed by a Simmons–Smith cyclopropanation, which afforded the precursor for the key ring enlargement reaction after Jones oxidation of the secondary alcohol (**276**). Exposure of **276** to a mixture of acetic anhydride and sulfuric acid resulted in the opening of the cyclopropyl ring with concomitant formation of the tropolone system (**277**). This sequence is superior to the oxidative coupling protocol as described earlier and allows the isolation of substantial amounts of the desired target.

Evans devised a highly similar route (Eq. 12.48-2, Scheme 12.48) and achieved the synthesis of trimethylcolchicinic acid (not shown in the scheme—the compound possesses an amino functionality instead to the methyl ester in **281**) [162, 163]. The main difference to Tobinaga's route is the installation of the cyclopropyl ring prior to the elaboration of the fused ring system. The key cyclopropyl opening and ring enlargement could be carried out in a one- or two-step procedure, delivering the desired 6,7,7-fused ring system in excellent yield under mild reaction conditions. Noteworthy, besides **280**, Evans also obtained the double-bond isomer with the corresponding α,β-unsaturated ester. This material could be successfully equilibrated to the more stable desired tropolone system.

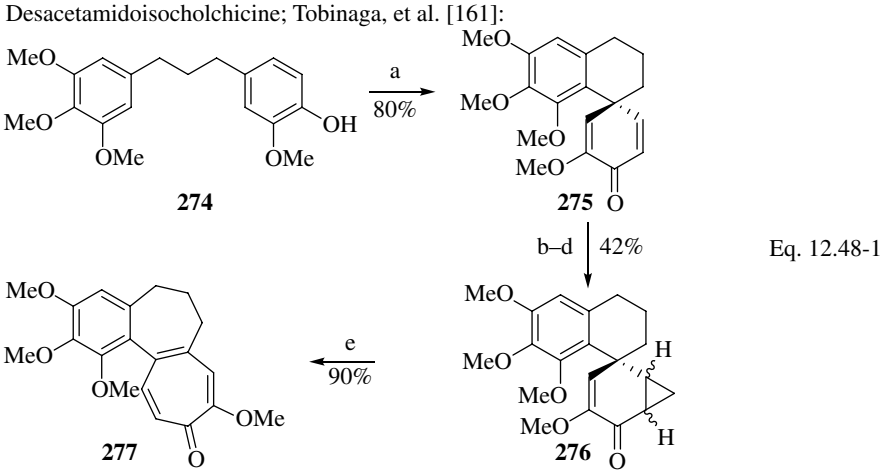
### 12.4.3 Synthesis of Amaryllidaceae Alkaloids

The Amaryllidaceae plant family comprises of approximately 75 genera, and so far more than 1100 species have been identified. Members of this highly diverse plant family are endemic in most tropic and temperate areas of the world, and several Amaryllidaceae species have been employed in traditional herbal folk medicine to cure serious health conditions and various diseases [169].

Amaryllidaceae species have been identified as rich source of structurally intriguing tyrosine-derived secondary metabolites. The great structural diversity of Amaryllidaceae alkaloids is rationalized by the different possibilities to connect the aromatic portions of 4′-*O*-methylnorbelladine as outlined in the biosynthetic section of this chapter.

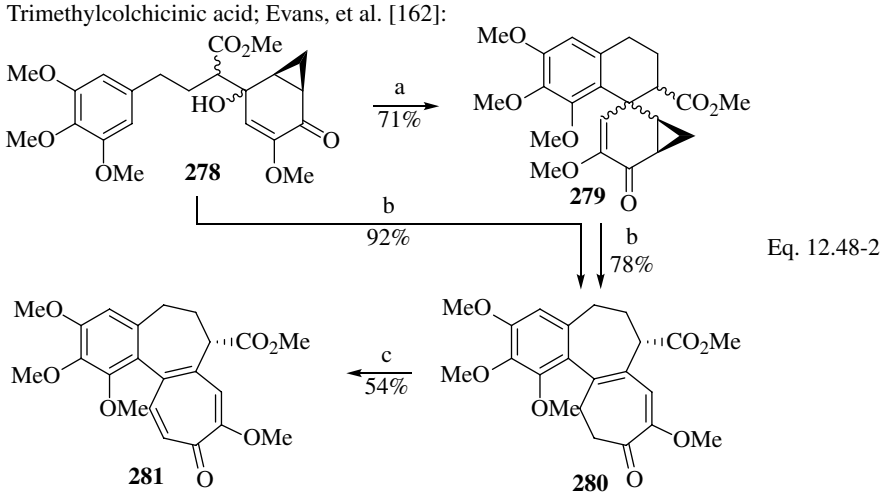
This section is devoted to the discussion of selected syntheses of biologically intriguing Amaryllidaceae constituents—a more comprehensive overview of Amaryllidaceae alkaloids can be obtained from recent review articles [44, 45, 48, 170]. Narciclasine (**55**) is one of the major secondary metabolites of various *Narcissus* species,

Desacetamidoisocholchicine; Tobinaga, et al. [161]:




**Reagents and conditions:** (a) anodic oxidation, $HBF_4$, MeCN, 0.92–1.00 V, 20 min, 80%; (b) $NaBH_4$; (c) $CH_2I_2$, Zn/Cu couple; (d) Jones oxidation, 42% (e) $Ac_2O$, $H_2SO_4$, 90%.

Trimethylcolchicinic acid; Evans, et al. [162]:



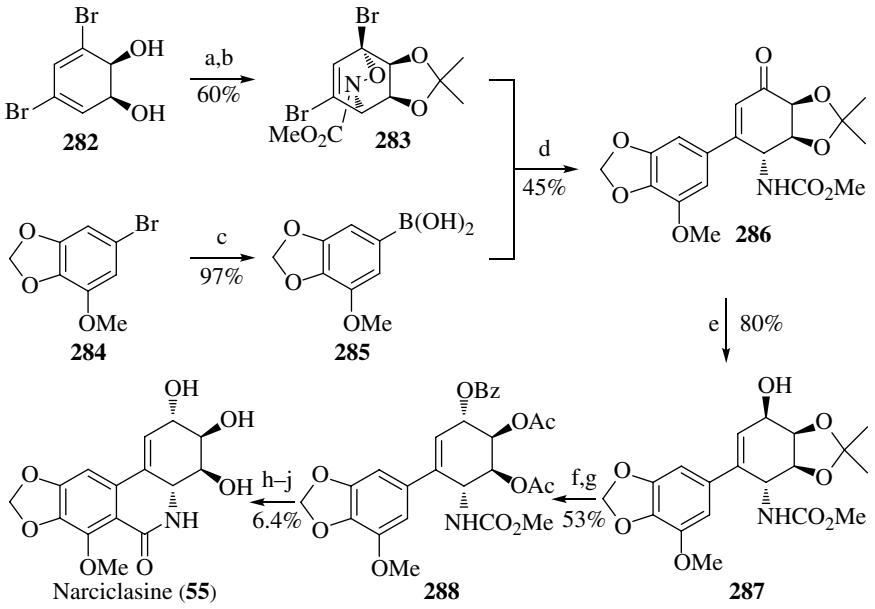

**Reagents and conditions:** (a) $CF_3CO_2H$, rt, 71%; (b) $CF_3CO_2H$, rf; (c) DDQ, $C_6H_6$, reflux, 54%.

**SCHEME 12.48** Key steps in Tobinaga's and Evans' synthesis of colchicine derivatives.

and the natural product and its congener 7-deoxypancratistatin (**298**) have been identified as highly potent cytotoxic metabolites with potential applications in cancer chemotherapy [45, 46]. Galantamine (**62**), isolated from the Caucasian snowdrop (*Galanthus woronowii*), exhibits selective, competitive, and reversible inhibition of acetylcholinesterase and serves as an allosteric modulator of the neuronal nicotinic receptor for acetylcholine. The compound is used in the treatment of Alzheimer's disease [48, 49].

A truly biomimetic route to alkaloids of the narciclasine type has not been published yet. Nevertheless, very interesting protocols for the coupling of the six-membered ring motifs have been employed in the preparation of these compounds. Transition metal-catalyzed coupling reactions play an important role in the preparation of Amaryllidaceae alkaloids, and Hudlicky's synthesis of narciclasine highlights this approach [171, 172]. Keck utilized radical reactions and his route to 7-deoxypancratistatin has been chosen to emphasize the importance of radical protocols [173, 174]. Galantamine is structurally perfectly suited for the application of oxidative coupling protocols. Barton and Kirby's route to the alkaloids is discussed in detail [175], followed by a short overview of key steps in the preparation of this important natural product by other research groups.

(+)-*Narciclasine; Hudlicky, 1999*: In his synthesis of narciclasine (**55**), Hudlicky employed biocatalytically derived cyclohexadiene diol **282** as starting material and synthon for the oxygenated conduramine ring of the Amaryllidaceae constituent (Scheme 12.49) [171, 172]. Their oxygenation pattern makes cyclohexadiene diols perfect starting materials for the preparation of Amaryllidaceae constituents and other highly oxygenated natural products. Diol **282**, obtained from whole-cell oxidation of *m*-dibromobenzene with recombinant *E. coli* JM 109 (pDTG601A), was converted to




**Reagents and conditions:** (a) DMP, acetone, *p*-TsOH(cat.); (b) $NaIO_4$, methyl carbamate, MeOH, 0°C to rt, 60% (2 steps); (c) *t*-BuLi, $B(OEt)_3$, THF, –78°C, 97%; (d) $Pd(PPh_3)_4$ (0.03%), $Na_2CO_3$, $C_6H_6$, EtOH, $H_2O$, reflux; $Mo(CO)_6$, reflux, 45%; (e) $CeCl_3$, $NaBH_4$, MeOH, 0°C, 80%; (f) DEAD, $Bu_3P$, BzOH, THF, 75%; (g) Dowex 50X8-100, MeOH; $Ac_2O$, py, DMAP, 70% (h) $Tf_2O$, DMAP, $CH_2Cl_2$, 0°C 41%; (i) Amberlyst A21, MeOH, 80%; (j) LiCl, DMF, 120°C, 20%.

**SCHEME 12.49** Hudlicky's synthesis of narciclasine (**55**).

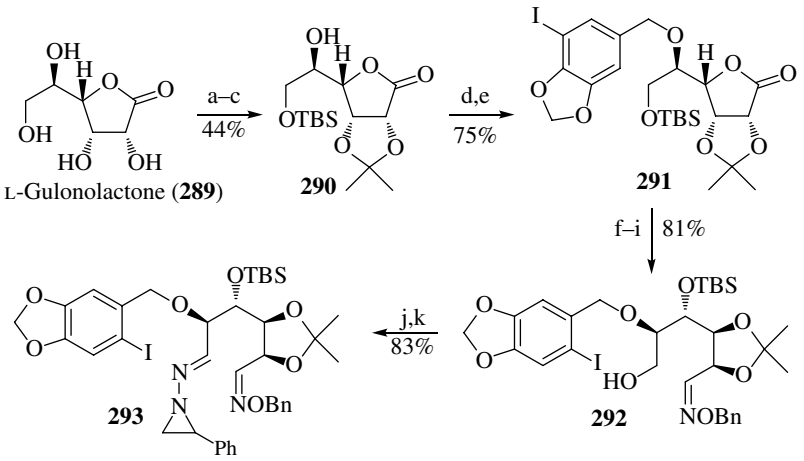
its acetonide before a nitroso-Diels–Alder reaction allowed the isolation of cycloadduct **283** in good overall yield. The initial strategy envisaged reduction of the N—O bond and subsequent Suzuki coupling with boronic acid **285**. However, as all attempts to reduce the N—O bond under Keck's [176] conditions resulted in the predominant formation of the fully dehalogenated material, the strategy was slightly altered and the Suzuki coupling was carried out prior to the cleavage of the labile N—O bond. This reaction could even be elegantly carried out in a one-pot procedure, and enone **286** was obtained in 45% yield when $Mo(CO)_6$ and acetonitrile were added to the reaction mixture after the Suzuki coupling was finished. Luche reduction of the enone delivered the alcohol **287** and the stereochemistry at C2 was corrected via a Mitsunobu inversion.

Next, as final synthetic operation, the phenanthridone skeleton had to be established. The carbamate moiety, introduced during the hetero-Diels–Alder cycloaddition reaction, was ideally suited for a modified Bischler–Napieralski reaction. This Bischler–Napieralski protocol has been developed by Banwell [177] a few years earlier and employed on structurally related Amaryllidaceae constituents. Before the reaction could be carried out, the acetonide moiety had to be cleaved and the hydroxyl functionalities were protected as acetates to prevent the formation of undesired side products. With this substrate in hand, Banwell's conditions afforded the phenanthridone skeleton in 60% yield. The ester groups were cleaved with Amberlyst resin in methanol, and the phenolic ether was removed with LiCl in DMF at elevated temperatures.

Several syntheses of Amaryllidaceae alkaloids with palladium-catalyzed coupling reactions have been reported in the literature. Hudlicky presented a highly efficient route to narciclasine and was able to demonstrate the great potential of transition metal-catalyzed reactions in the preparation of Amaryllidaceae alkaloids. Furthermore, he successfully demonstrated the advantage of combining enzymatic methods and traditional synthetic chemistry.

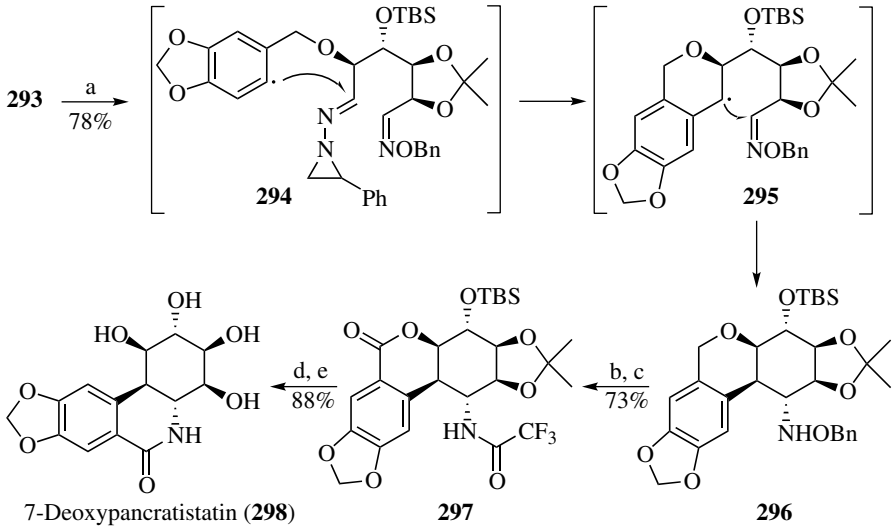
*7-Deoxypancratistatin; Keck, 1998*: In 1995, Keck reported his first synthesis of 7-deoxypancratistatin (**298**) with a radical cyclization as key step [178]. A few years later, a second-generation synthesis of this important Amaryllidaceae constituent was reported [173]. The route, outlined in Schemes 12.50 and 12.51, started from inexpensive and commercially available L-gulonolactone (**289**) and featured a highly efficient radical cyclization cascade, which established two ring systems of the natural product. This radical cyclization protocol is quite unique in the preparation of Amaryllidaceae alkaloids and constitutes an interesting alternative to commonly employed coupling protocols.

The preparation of key intermediate **293**, required for the radical cyclization cascade, is shown in Scheme 12.50. L-Gulonolactone (**289**) was converted to secondary alcohol **290** via a literature-known procedure, including protection




**Reagents and conditions:** (a) 2,2-dimethoxypropane, acetone, *p*-TSOH, 79%; (b) HOAc, $H_2O$, 79%; (c) TBSCl, imidazole, DMF, –40°C, 71%; (d) 6-iodopiperonol, NaH, $CCl_3CCN$, 0°C; (e) TfOH, THF, 0°C, 75% (over 2 steps); (f) L-selectride, $CH_2Cl_2$, –78°C; (g) HCl•$H_2NOBn$, py, 96% (over 2 steps); (h) TBSOTf, 2,6-lutidine, $CH_2Cl_2$, 0°C; (i) HF•py, THF, 84% (over 2 steps); (j) TPAP, NMO, 4Å molecular sieves; (k) 1-amino-2-phenylhydrazine, EtOH, 0°C, 83% (over 2 steps).

**SCHEME 12.50** Keck's synthesis of 7-deoxypancratistatin (**298**)—part 1.



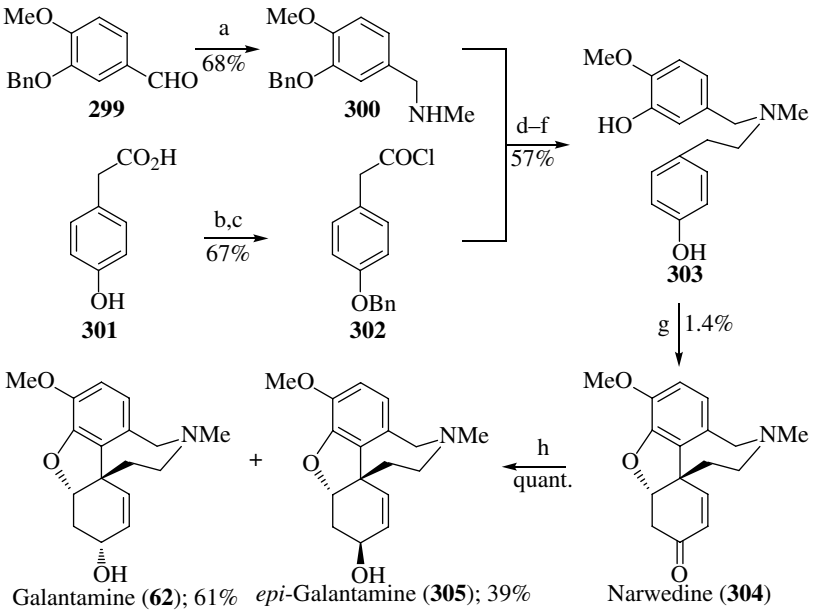

**Reagents and conditions:** (a) $Ph_3SnH$, AIBN, $C_6H_6$, reflux, 78%; (b) $SmI_2$; TFAA, THF, 60°C, 88%; (c) PCC, $CH_2Cl_2$, 83%; (d) $BF_3$•$Et_2O$; (e) $K_2CO_3$, MeOH, 88% (two steps).

**SCHEME 12.51** Keck's synthesis of 7-deoxypancratistatin (**298**)—part 2.

of the hydroxyl functionalities as bis-acetonide, followed by selective cleavage of the less stable acetal, and installation of a silyl ether on the primary alcohol. Next, the trichloroacetimidate of iodopiperonol was used to alkylate the secondary hydroxyl functionality in **290** and lactone **291** was isolated in good yield. Reduction of the lactone with L-selectride and subsequent formation of the corresponding *O*-benzyloxime were followed by silylation of the secondary alcohol and desilylation of the primary hydroxyl group (**292**). The preparation of the substrate for the radical cascade reaction was concluded after Ley oxidation of the primary alcohol and elaboration of the crucial aziridinylamine (**293**).

With key intermediate **293** in hand, the radical cascade reaction could be investigated (Scheme 12.51). When allowed to react with $Ph_3SnH$ and AIBN in refluxing benzene, the desired cyclization product was obtained in excellent 78% yield. This beautiful radical cyclization cascade is mechanistically outlined in Scheme 12.51.

Initial formation of the aryl radical is followed by attack of this reactive species onto the aziridinylamine in a 6-exo




**Reagents and conditions:** (a) $MeNH_2$, MeOH; $KBH_4$, 67%; (b) KOH, BnCl, EtOH, reflux, 67%; (c) $(COCl)_2$, $C_6H_6$, quant.; (d) **300** and **302**, $C_6H_6$, 85%; (e) LAH, $Et_2O$, reflux, 88%; (f) $H_2$, Pd/C, MeOH, $H_2O$, HCl; $NaHCO_3$, 76%; (g) $K_3Fe(CN)_6$, $H_2O$, $NaHCO_3$, 1.4%; (h) LAH, $Et_2O$ quant.

**SCHEME 12.52** Barton and Kirby's synthesis of galantamine (**62**).

cyclization. The formation of styrene and nitrogen serves as driving force for this elegant process, first developed by Kim and coworkers [179]. This first cyclization reaction generated radical species **295** as intermediate, which has been shown to readily undergo another 6-exo cyclization reaction in Keck's first-generation synthesis of the title compound [178]. The nitrogen of the benzyloxime moiety furthermore served as synthon for the elaboration of the lactam ring at a later stage of the synthesis. Noteworthy, **296** was obtained as single isolable isomer after this remarkable radical cyclization cascade, which presents a valuable alternative to other coupling protocols usually employed in the preparation of Amaryllidaceae alkaloids.

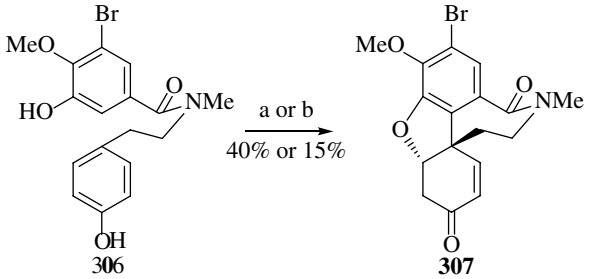
The completion of the synthesis required oxidation of the benzylic position and subsequent lactone–lactam rearrangement. This strategy has been commonly employed in the synthesis of Amaryllidaceae alkaloids and has been developed by Danishefsky in the first total synthesis of pancratistatin [180]. Reductive cleavage of the N─O bond in **296** with $SmI_2$ and installation of the trifluoroacetamide in a one-pot procedure were followed by PCC oxidation of the benzylic ether to afford lactone **297**. The acetonide moiety and the silyl ether were removed with $BF_3 \cdot Et_2O$ and the resulting triol was treated with $K_2CO_3$ in methanol, resulting in the aforementioned rearrangement of the lactone to the more stable lactam. 7-Deoxypancratistatin (**298**) was isolated in excellent overall yield and only 13 linear steps from iodopiperonol.

*Galantamine; Barton and Kirby, 1960*: As pointed out earlier, two main strategies have been employed in the preparation of galantamine (**62**), namely, the biomimetic approach utilizing an oxidative phenol coupling as key step and transition metal-catalyzed protocols, such as the Heck reaction [48]. Barton was the first to propose the biosynthetic route to galantamine and reported that all Amaryllidaceae alkaloids could be traced back to the same biosynthetic precursor, namely, 4′-*O*-methylnorbelladine (**65**) [181]. A few years later, in 1960, Barton and Kirby presented a biomimetic synthesis of **62** with an oxidative coupling as key step [175, 182].

The route is outlined in Scheme 12.52. Reductive amination of benzaldehyde **299** delivered secondary amine **300** as synthon for the A ring of the natural product. Next, **300** was acetylated with acid chloride **302**, readily available from commercially available *p*-hydroxyphenylacetic acid (**301**), to afford **303** as the precursor for the key oxidative coupling reaction.

The transformation of **303** into narwedine (**304**) proved troublesome. Various oxidizing reagents were evaluated but all attempts resulted in the polymerization of the starting material and only minute amounts of narwedine (**304**) could be detected in the reaction mixtures. Manganese dioxide, lead dioxide, and silver oxide did not allow the isolation of appreciable amounts of coupling product. When a solution of $K_3[Fe(CN)_6]$ was employed in the oxidative cyclization, 1.4% of narwedine was obtained.

Galantamine; Kametani et al. [183]; Vlahov et al. [187]:

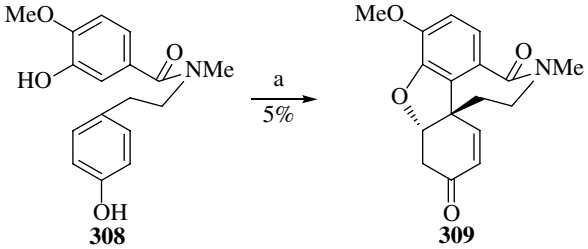



306 307

Eq. 12.53-1

**Reagents and conditions:** (a) $K_3Fe(CN)_6$, $H_2O$, $NaHCO_3$, 60°C, 1.5 h; 40%; (b) same as (a) 15%.

Galantamine; Kametani et al. [188]:




308 309

Eq. 12.53-2

**Reagents and conditions:** (a) $K_3Fe(CN)_6$, $H_2O$, $CHCl_3$, $NaHCO_3$, 60°C, 1.5 h; 5%;

**SCHEME 12.53** Oxidative coupling reactions in Kametani's and Vlahov's synthesis of galantamine (**62**).

Reduction of the carbonyl moiety in narwedine (**304**) with lithium aluminum hydride completed the synthesis of galantamine. The Amaryllidaceae alkaloid was obtained in quantitative yield as 6 : 4 mixture with its epimer.

Barton and Kirby's achievement paved the way for more intense investigations on oxidative phenol coupling protocols, and in the following, a series of papers were published dealing with this important reaction. Some of these examples are outlined in the following.

A few years after Barton and Kirby's synthesis of galantamine, Kametani published a route to the alkaloid, which also featured a $K_3[Fe(CN)_6]$-mediated oxidative coupling as key step (Eq. 12.53-1, Scheme 12.53) [183, 184]. Kametani employed bromide **306** as substrate for the coupling reaction in order to block the *para* position and to force the coupling reaction to proceed at the unblocked *ortho* position. Furthermore, instead of utilizing a substrate with a basic nitrogen, the corresponding amide was employed in the reaction, following findings by Franck [185] and Abramovitch [186] who reported that yields can be significantly improved when the basic nitrogens are protected.

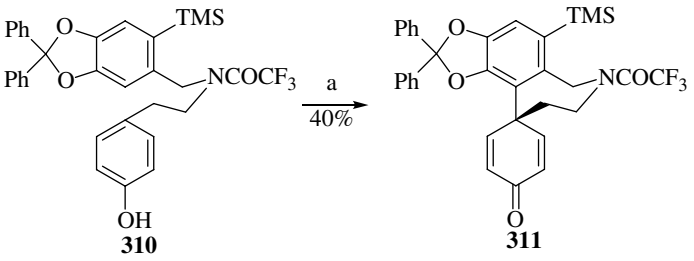
Kametani obtained 40% yield in the key oxidative coupling reaction. Later, Vlahov [187] repeated the key step but was unable to confirm previously reported results and only obtained moderate 15% of **307**, which still significantly exceeds the initial results obtained by Barton and Kirby. As shown in Equation 12.53-2, Scheme 12.53, when a slightly modified substrate lacking the halide on the aromatic portion (**308**) was used, the desired product was obtained in disappointing 5% yield [188, 189].

Kita employed a hypervalent iodine species for the oxidative cyclization of phenol **310** as shown in Equation 12.54-1, Scheme 12.54 [190]. When allowed to react with phenyliodine(III) bis(trifluoroacetate) (PIFA), **310** delivered the desired galantamine skeleton in 40% yield. The cyclization most likely proceeds via the initial reaction of the phenolic oxygen with the hypervalent iodine reagent and subsequent nucleophilic attack of the second electron-rich aromatic ring onto the intermediary formed cation radical intermediate. Kita and coworkers outlined the importance of the fluorinated solvent. When carried out in benzene or dichloromethane, the desired product was not formed. A similar oxidative coupling protocol has been successfully employed by the authors for other Amaryllidaceae alkaloids [191].

Another interesting example of an oxidative phenolic coupling reaction was reported by Koga and coworkers in 1977 (Eq. 12.54-2, Scheme 12.54) [192]. Exposure of chiral ester **312** to three equivalents of $Mn(acac)_3$ in acetonitrile allowed the isolation of adduct **313** in 49% isolated yield. Koga's efforts resulted in the first enantioselective total synthesis of the biologically highly interesting Amaryllidaceae alkaloid.

The synthetic potential of electrochemical oxidation protocols for the oxidative phenolic coupling has been discussed earlier for the preparation of colchicine (see Tobinaga's route, Eq. 12.48-1, Scheme 12.48). Vlahov was able to successfully employ an electrochemical protocol as key step in the preparation of galantamine [193]. Bromide **314** was utilized in the anodic oxidation. The halide served to block

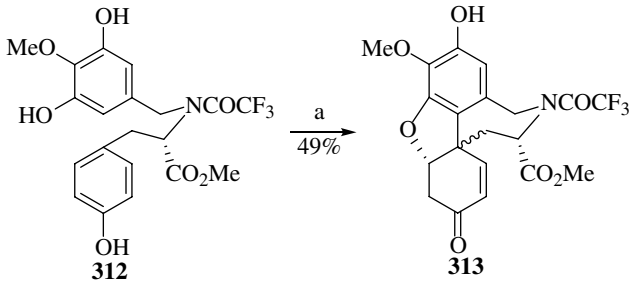
Galantamine; Kita et al. [191]:




Eq. 12.54-1

**Reagents and conditions:** (a) PIFA, $CF_3CH_2OH$, –40°C, 40%

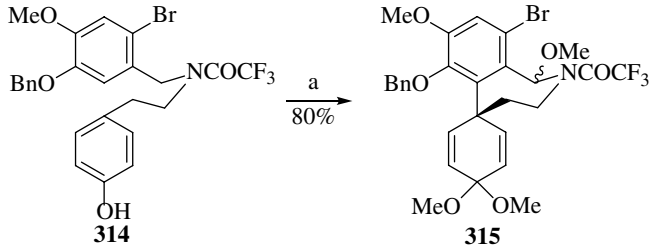
Galantamine; Koga et al. [192]:




Eq. 12.54-2

**Reagents and conditions:** (a) $Mn(acac)_3$, 49%.

Galantamine; Vlahov et al. [193]:




Eq. 12.54-3

**Reagents and conditions:** (a) anodic oxidation 1.15 V, Pt-electrode, MeOH, $CH_3CN$, $AgNO_3$, 80%.

**SCHEME 12.54** Oxidative coupling reactions in Kita's, Koga's, and Vlahov's synthesis of galantamine (**62**).

the *para* position and to trigger the coupling at the *ortho* position (Eq. 12.54-3, Scheme 12.54). The material was dissolved in acetonitrile, which contained minor amounts of methanol, and the substrate was electrolyzed in a three-compartment cell with platinum electrodes and dry lithium perchlorate as supporting electrode. The working potential was maintained at 1.15 V with reference to an Ag electrode, yielding in the isolation of adduct **315** in excellent 80% yield. Noteworthy, the process also resulted in the oxidation of the benzylic position at C10.

Several other protocols have been reported. For further information, review articles on Amaryllidaceae alkaloids and galantamine should be consulted [48].

## 12.5 CONCLUSION

Tyrosine serves as substrate for the biosynthesis of important natural products. Historically, morphine and mescaline have attracted considerable attention from ancient cultures, and these compounds have played a crucial role in human history. Morphine and structurally related opiates are important analgesics and invaluable in palliative care. Colchicine, galantamine, and Amaryllidaceae alkaloids are other examples of tyrosine-derived secondary metabolites of great medicinal importance.

Because of their pronounced biological activities, tyrosine-derived alkaloids also belong to the first natural products, which have been isolated from plant sources, and these early scientific achievements substantially helped to advance the newly emerging scientific disciplines. The ongoing interest in the isolation, biological evaluation, and synthesis of tyrosine-derived secondary metabolites is a clear indication for their great importance.

Certain alkaloids of this highly diverse class of natural products continue to be a testing ground for the development of novel synthetic methods. Throughout the chapter, the importance of aryl–aryl coupling reactions in the biosynthetic pathways and the chemical syntheses of tyrosine-derived metabolites has been communicated. These natural

products have played an important role in the development of oxidative coupling protocols as well as transition metal-catalyzed procedures. Furthermore, some tyrosine-derived secondary metabolites, most worthy morphine and its congeners, are an important testing ground for synthetic methodology in general. With the enormous activity in this field, we can look forward to some exciting developments and synthetic achievements in the near future.

## REFERENCES


1. M. Goodall, N. Kirshner, *J. Biol. Chem.* 1957, **226**, 213–221.
2. D. Goldstein, *Clin. Auton. Res.* 2010, **20**, 331–352.
3. M. R. Luquin, P. J. Garcia-Ruiz, M. J. Marti, A. Rojo, L. Vela, F. J. Grandas, M. Bravo-Utrera, J. A. Burguera, J. R. Chacon, V. M. Campos-Arillo, C. Duran-Herrera, J. M. Fernandez-Garcia, R. Garcia-Ramos, J. C. Gomez-Esteban, J. Gutierrez, J. Juni, M. Mata, J. C. Martinez-Castrillo, J. Olivares, R. Ribacoba-Montero, D. Santos-Garcia, M. Sierra, C. Valero-Merino, *Rev. Neurol.* 2012, **55**, 669–688.
4. D. L. Wong, T. C. Tai, D. C. Wong-Faull, R. Claycomb, E. G. Meloni, K. M. Myers, W. A. Carlezon, R. Kvetnansky, *Cel. Mol. Neurobiol.* 2012, **32**, 737–748.
5. J. G. Bruhn, P. A. G. M. De Smet, H. R. El-Seedi, O. Beck, *Lancet* 2002, **359**, 1866.
6. H. R. El-Seedi, P. A. G. M. De Smet, O. Beck, G. Possnert, J. G. Bruhn, *J. Ethnopharmacol.* 2005, **101**, 238–242.
7. S. Agurell, J. Lundström, F. Sandberg, *Tetrahedron Lett.* 1967, **8**, 2433–2435.
8. R. M. Riggin, P. T. Kissinger, *J. Agric. Food Chem.* 1976, **24**, 900.
9. R. M. Riggin, M. J. Mccarthy, P. T. Kissinger, *J. Agric. Food Chem.* 1976, **24**, 189–191.
10. Y. Nagasawa, R. Ueoka, R. Yamanokuchi, N. Horiuchi, T. Ikeda, H. Rotinsulu, R. E. P. Mangindaan, K. Ukai, H. Kobayashi, M. Namikoshi, H. Hirota, H. Yokosawa, S. Tsukamoto, *Chem. Pharm. Bull.* 2011, **59**, 287–290.
11. K. Iwasa, M. Kamigauchi, N. Takao, *Phytochemistry* 1991, **30**, 2973–2975.
12. B. Mravec, *Physiol. Res.* 2006, **55**, 353–364.
13. P. Dostert, M. Strolin Benedetti, V. Bellotti, C. Allievi, G. Dordain, *J. Neural Transm. Gen. Section JNT* 1990, **81**, 215–223.
14. J. Ziegler, P. J. Facchini, R. Geißler, J. Schmidt, C. Ammer, R. Kramell, S. Voigtländer, A. Gesell, S. Pienkny, W. Brandt, *Phytochemistry* 2009, **70**, 1696–1707.
15. J. M. Hagel, P. J. Facchini, *Plant Cell Physiol.* 2013, **54**, 647–672.
16. D. K. Liscombe, P. J. Facchini, *Curr. Opin. Biotechnol.* 2008, **19**, 173–180.
17. E. J. Lee, P. J. Facchini, *Plant Physiol.* 2011, **157**, 1067–1078.
18. E. V. Leitao Da-Cunha, I. M. Fechine, D. N. Guedes, J. M. Barbosa-Filho, M. Sobral Da Silva, Protoberberine Alkaloids, in *The Alkaloids: Chemistry and Biology*, G. A. Cordell, Editor. Academic Press: Amsterdam (2005), p. 1–75.
19. H. Guinaudeau, M. Leboeuf, A. Cave, *J. Nat. Prod.* 1975, **38**, 275–338.
20. H. Guinaudeau, M. Leboeuf, A. Cavé, *J. Nat. Prod.* 1979, **42**, 325–360.
21. C. Stevigny, C. Bailly, J. Quetin-Leclercq, *Curr. Med. Chem. AntiCancer Agents* 2005, **5**, 173–182.
22. A. R. Battersby, T. J. Brocksom, R. Ramage, *J. Chem. Soc. D* 1969, 464–465.
23. T. Serbetci, G. Sariyar, S. Michel, N. Ozhatay, F. Tillequin, *Biochem. Syst. Ecol.* 2009, **37**, 501–503.
24. A. Langlois, D. A. Mulholland, N. R. Crouch, O. M. Grace, *Biochem. Syst. Ecol.* 2004, **32**, 1087–1090.
25. K. Hirata, C. Poeaknapo, J. Schmidt, M. H. Zenk, *Phytochemistry* 2004, **65**, 1039–1046.
26. E. Brochmann-Hanssen, *Planta Med.* 1984, **50**, 343–345.
27. A. Onoyovwe, J. M. Hagel, X. Chen, M. F. Khan, D. C. Schriemer, P. J. Facchini, *Plant Cell* 2013, **25**, 4110–4122.
28. P. Paul, M. Halder, S. Jha, Alkaloids Derived from Tyrosine: Penethylisoquinoline (Autumnaline, Colchicine), in *Natural Products*, K. G. Ramawat and J.-M. Mérillon, Editors. Springer: Berlin/Heidelberg (2013), p. 461–478.
29. E. Tojo, *J. Nat. Prod.* 1989, **52**, 909–921.
30. P. J. Pelletier, J. B. Caventou, *Ann. Chim. Phys.* 1820, **14**, 69–81.
31. T. Graening, H. G. Schmalz, *Angew. Chem. Int. Ed.* 2004, **43**, 3230–3256.
32. N. S. Sitnikov, A. Y. Fedorov, *Russ. Chem. Rev.* 2013, **82**, 393–411.
33. C. P. Bryan, H. Joachim, *The Papyrus Ebers*, London: G. Bles (1930), p. 167.
34. P. Dioscorides, *De materia medica*. Altertumswissenschaftliche Texte und Studien, Hildesheim/New York: Olms-Weidmann. **38**, (2005), p. 540.
35. M. Rueffer, M. H. Zenk, *Febs Lett.* 1998, **438**, 111–113.
36. M. J. S. Dewar, *Nature*, 1945, **155**, 141–142.
37. M. V. King, J. L. Devries, R. Pepinsky, *Acta Crystallogr.* 1952, **5**, 437–440.
38. E. Leete, *Tetrahedron Lett*. 1965, 333–336.
39. E. Leete, P. E. Nemeth, *J. Am. Chem. Soc.* 1961, **83**, 2192–2194.
40. P. W. Sheldrake, K. E. Suckling, R. N. Woodhouse, A. J. Murtagh, R. B. Herbert, A. C. Barker, J. Staunton, A. R. Battersby, *J. Chem. Soc., Perkin Trans.* **1**, 1998, 3003–3009.
41. E. Mcdonald, R. Robert, R. N. Woodhouse, E. W. Underhill, L. R. Wetter, A. R. Battersby, *J. Chem. Soc., Perkin Trans. 1* 1998, 2979–2987.
42. R. N. Woodhouse, E. Mcdonald, R. Ramage, A. R. Battersby, *J. Chem. Soc., Perkin Trans.* **1** 1998, 2995–3001.
43. A. C. Barker, D. R. Julian, R. Ramage, R. N. Woodhouse, G. Hardy, E. Mcdonald, A. R. Battersby, *J. Chem. Soc., Perkin Trans.* **1** 1998, 2989–2994.

44. Z. Jin, X.-H. Xu, Amaryllidaceae Alkaloids, in *Natural Products*, K. G. Ramawat and J.-M. Mérillon, Editors. Springer: Berlin/Heidelberg (2013), p. 479–522.
45. A. Kornienko, A. Evidente, *Chem. Rev.* 2008, **108**, 1982–2014.
46. G. Van Goietsenoven, V. Mathieu, F. Lefranc, A. Kornienko, A. Evidente, R. Kiss, *Med. Res. Rev.* 2013, **33**, 439–455.
47. L. Ingrassia, F. Lefranc, V. Mathieu, F. Darro, R. Kiss, *Transl. Oncol.* 2008, **1**, 1–13.
48. J. Marco-Contelles, M. D. Carreiras, C. Rodriguez, M. Villarroya, A. G. Garcia, *Chem. Rev.* 2006, **106**, 116–133.
49. C. Loy, L. Schneider, *Cochrane Database Syst. Rev.* 2006, CD001747.
50. C. Fuganti, M. Mazza, *J. Chem. Soc. Chem. Commun.* 1972, **4**, 239.
51. C. Fuganti, M. Mazza, *J. Chem. Soc. D* 1971, 1388–1389.
52. C. Fuganti, J. Staunton, A. R. Battersby, *J. Chem. Soc. D* 1971, 1154–1155.
53. R. A. Backkaus, G. R. Pettit III, D. S. Huang, G. R. Pettit, G. Groszek, J. C. Odgers, J. Ho, A. Meerow, *Acta Horticult.* 1992, **306**, 364–366.
54. C. Fuganti, *Chim. Ind.* 1969, **51**, 1254–1255.
55. J. K. Bhandarkar, G. W. Kirby, *J. Chem. Soc. C*, 1970, 1224–1227.
56. J. Eichhorn, T. Takada, Y. Kita, M. H. Zenk, *Phytochemistry* 1998, **49**, 1037–1047.
57. M. H. Zenk, R. Gerardy, R. Stadler, *J. Chem. Soc. Chem. Commun.* 1989, **22**, 1725–1727.
58. P. F. X. Kraus, T. M. Kutchan, *Proc. Natl. Acad. Sci. U. S. A.* 1995, **92**, 2071–2075.
59. A. Nasreen, M. Rueffer, M. H. Zenk, *Tetrahedron Lett.* 1996, **37**, 8161–8164.
60. F. Ullmann, G. Meyer, O. Loewenthal, E. Gilli, *Justus Liebigs Ann. Chem.* 1904, **332**, 38–81.
61. F. Ullmann, W. R. Forgan, *Ber. Dtsch. Chem. Ges.* 1901, **34**, 3802–3805.
62. F. Ullmann, J. Bielecki, *Ber. Dtsch. Chem. Ges.* 1901, **34**, 2174–2185.
63. J. Hassan, M. Sévignon, C. Gozzi, E. Schulz, M. Lemaire, *Chem. Rev.* 2002, **102**, 1359–1470.
64. V. Ritleng, C. Sirlin, M. Pfeffer, *Chem. Rev.* 2002, **102**, 1731–1770.
65. G. Dyker, *Angew. Chem. Int. Ed.* 1999, **38**, 1698–1712.
66. A. M. Norberg, L. Sanchez, R. E. Maleczka, *Curr. Opin. Drug Discov. Devel.* 2008, **11**, 853–869.
67. J.-P. Corbet, G. Mignani, *Chem. Rev.* 2006, **106**, 2651–2710.
68. D. Alberico, M. E. Scott, M. Lautens, *Chem. Rev.* 2007, **107**, 174–238.
69. S. L. You, J. B. Xia, *Top. Curr. Chem.* 2010, **292**, 165–194.
70. L. Bai, J. X. Wang, *Curr. Org. Chem.* 2005, **9**, 535–553.
71. D. H. R. Barton, J.-P. Finet, J. Khamsi, *Tetrahedron Lett.* 1987, **28**, 887–890.
72. J. Lindley, T. J. Mason, J. P. Lorimer, *Ultrasonics* 1987, **25**, 45–48.
73. S. Zhang, D. Zhang, L. S. Liebeskind, *J. Org. Chem.* 1997, **62**, 2312–2313.
74. A. P. Degnan, A. I. Meyers, *J. Am. Chem. Soc.* 1999, **121**, 2762–2769.
75. F. E. Ziegler, I. Chliwner, K. W. Fowler, S. J. Kanfer, S. J. Kuo, N. D. Sinha, *J. Am. Chem. Soc.* 1980, **102**, 790–798.
76. L. M. Stark, X. F. Lin, L. A. Flippin, *J. Org. Chem.* 2000, **65**, 3227–3230.
77. B. H. Lipshutz, F. Kayser, Z.-P. Liu, *Angew. Chem. Int. Ed.* 1994, **33**, 1842–1844.
78. Y. Nishihara, K. Ikegashira, F. Toriyama, A. Mori, T. Hiyama, *Bull. Chem. Soc. Jpn.* 2000, **73**, 985–990.
79. E. Piers, J. G. K. Yee, P. L. Gladstone, *Org. Lett.* 2000, **2**, 481–484.
80. G. Harada, M. Yoshida, M. Iyoda, *Chem. Lett.* 2000, **29**, 160–161.
81. M. Smrcina, S. Vyskocil, B. Maca, M. Polasek, T. A. Claxton, A. P. Abbott, P. Kocovsky, *J. Org. Chem.* 1994, **59**, 2156–2163.
82. M. Nakajima, I. Miyoshi, K. Kanayama, S.-I. Hashimoto, M. Noji, K. Koga, *J. Org. Chem.* 1999, **64**, 2264–2271.
83. B. Feringa, H. Wynberg, *J. Org. Chem.* 1981, **46**, 2547–2557.
84. F. Toda, K. Tanaka, S. Iwata, *J. Org. Chem.* 1989, **54**, 3007–3009.
85. R. Pschorr, *Ber. Dtsch. Chem. Ges.* 1896, **29**, 496–501.
86. M. Gomberg, W. E. Bachmann, *J. Am. Chem. Soc.* 1924, **46**, 2339–2343.
87. M. Gomberg, W. E. Bachmann, *Org. Synth.* 1928, **8**, 42.
88. F. Trécourt, M. Mallet, O. Mongin, B. Gervais, G. Quéguiner, *Tetrahedron* 1993, **49**, 8373–8380.
89. V. Courtois, R. Barhdadi, S. Condon, M. Troupel, *Tetrahedron Lett.* 1999, **40**, 5993–5996.
90. C. Gosmini, J. Y. Nédélec, J. Périchon, *Tetrahedron Lett.* 2000, **41**, 201–203.
91. K. Tamao, K. Sumitani, M. Kumada, *J. Am. Chem. Soc.* 1972, **94**, 4374–4376.
92. J. P. Corriu, J. P. Masse, *J. Chem. Soc. Chem. Commun.* 1972, **3**, 144–148.
93. M. Kumada, *Pure Appl. Chem.* 1980, **52**, 669–679.
94. Y. Ikoma, K. Ando, Y. Naoi, T. Akiyama, A. Sugimori, *Synth. Commun.* 1991, **21**, 481–487.
95. C. A. Quesnelle, O. B. Familoni, V. Snieckus, *Synlett* 1994 349–350.
96. V. Percec, J.-Y. Bae, D. H. Hill, *J. Org. Chem.* 1995, **60**, 1060–1065.
97. A. Sekiya, N. Ishikawa, *J. Organomet. Chem.* 1976, **118**, 349–354.
98. A. Minato, K. Tamao, T. Hayashi, K. Suzuki, M. Kumada, *Tetrahedron Lett.* 1981, **22**, 5319–5322.
99. L. Zhu, R. M. Wehmeyer, R. D. Rieke, *J. Org. Chem.* 1991, **56**, 1445–1453.
100. Y. Hatanaka, K.-I. Goda, Y. Okahara, T. Hiyama, *Tetrahedron* 1994, **50**, 8301–8316.

101. M. Kosugi, K. Sasazawa, Y. Shimizu, T. Migita, *Chem. Lett.* 1977, **6**, 301–302.
102. D. Milstein, J. K. Stille, *J. Am. Chem. Soc.* 1978, **100**, 3636–3638.
103. M. M. Heravi, E. Hashemi, F. Azimian, *Tetrahedron* 2014, **70**, 7–21.
104. J. K. Stille, *Angew. Chem. Int. Ed.* 1986, **25**, 508–524.
105. S. Choppin, P. Gros, Y. Fort, *Org. Lett.* 2000, **2**, 803–805.
106. V. Farina, S. Kapadia, B. Krishnan, C. Wang, L. S. Liebeskind, *J. Org. Chem.* 1994, **59**, 5905–5911.
107. A. F. Littke, G. C. Fu, *Angew. Chem. Int. Ed.* 1999, **38**, 2411–2413.
108. D. W. Gordon, *Synlett*, 1998 1065–1066.
109. K. W. Stagliano, H. C. Malinakova, *Tetrahedron Lett.* 1997, **38**, 6617–6620.
110. C. Buon, P. Bouyssou, G. Coudert, *Tetrahedron Lett.* 1999, **40**, 701–702.
111. N. Miyaura, A. Suzuki, *J. Chem. Soc. Chem. Commun.* 1979, 866–867.
112. N. Miyaura, K. Yamada, A. Suzuki, *Tetrahedron Lett.* 1979, **20**, 3437–3440.
113. N. Miyaura, T. Yanagi, A. Suzuki, *Synth. Commun.* 1981, **11**, 513–519.
114. N. G. Andersen, S. P. Maddaford, B. A. Keay, *J. Org. Chem.* 1996, **61**, 9556–9559.
115. X.-S. Ye, H. N. C. Wong, *J. Org. Chem.* 1997, **62**, 1940–1954.
116. H. Tokuyama, Y. Kaburagi, X. Chen, T. Fukuyama, *Synthesis* 2000, 429–434.
117. M. Hird, A. J. Seed, K. J. Toyne, *Synlett*, 1999, 438–440.
118. C. Imrie, C. Loubser, P. W. Engelbrecht, C. Mccleland, *J. Chem. Soc., Perkin Trans.* **1** 1999, 2513–2523.
119. K. Kamikawa, T. Watanabe, M. Uemura, *Synlett*, 1995, 1040–1042.
120. A. J. J. Lennox, G. C. Lloyd-Jones, *Chem. Soc. Rev.* 2014, **43**, 412–443.
121. R. Dasgupta, B. R. Maiti, *Ind. Eng. Chem. Process. Des. Dev.* 1986, **25**, 381–386.
122. S. Mukhopadhyay, G. Rothenberg, G. Lando, K. Agbaria, M. Kazanci, Y. Sasson, *Adv. Synth. Catal.* 2001, **343**, 455–459.
123. G. R. Newkome, J. Gross, A. K. Patri, *J. Org. Chem.* 1997, **62**, 3013–3014.
124. T. Satoh, Y. Kawamura, M. Miura, M. Nomura, *Angew. Chem. Int. Ed.* 1997, **36**, 1740–1742.
125. N. Gürbüz, I. Özdemir, B. Çetinkaya, *Tetrahedron Lett.* 2005, **46**, 2273–2277.
126. M. Lafrance, C. N. Rowley, T. K. Woo, K. Fagnou, *J. Am. Chem. Soc.* 2006, **128**, 8754–8756.
127. G. Bringmann, M. Ochse, *Synlett* 1998, 1294–1296.
128. G. Bringmann, M. Ochse, R. Götz, *J. Org. Chem.* 2000, **65**, 2069–2077.
129. L.-C. Campeau, M. Parisien, M. Leblanc, K. Fagnou, *J. Am. Chem. Soc.* 2004, **126**, 9186–9187.
130. L.-C. Campeau, P. Thansandote, K. Fagnou, *Org. Lett.* 2005, **7**, 1857–1860.
131. Q. Huang, A. Fazio, G. Dai, M. A. Campo, R. C. Larock, *J. Am. Chem. Soc.* 2004, **126**, 7460–7461.
132. J. Zhao, R. C. Larock, *Org. Lett.* 2005, **7**, 701–704.
133. M. Sickert, H. Weinstabl, B. Peters, X. Hou, M. Lautens, *Angew. Chem. Int. Ed.* 2004, **53**, 5147–5151.
134. M. Booth, *Opium: A History*, 1st U.S. ed., New York: St. Martin's Press (1998), p. 381.
135. F. W. Sertürner, *J. Pharm. Aerzte Apoth. Chem.* 1805, **13**, 234.
136. J. M. Gulland, R. Robinson, *J. Chem. Soc.* 1923, **123**, 980–998.
137. J. M. Gulland, R. Robinson, *Mem. Proc. Manch. Lit. Philos. Soc.* 1925, **69**, 79.
138. G. Butora, T. Hudlicky, The Story of Morphine Structure Elucidation: One Hundred Years of Deductive Reasoning, in *Organic Synthesis: Theory and Applications*, T. Hudlicky, Editor. JAI Press: Greenwich, CT (1989), p. 1–51.
139. M. Gates, G. Tschudi, *J. Am. Chem. Soc.* 1952, **74**, 1109–1110.
140. M. Gates, G. Tschudi, *J. Am. Chem. Soc.* 1956, **78**, 1380–1393.
141. U. Rinner, T. Hudlicky, *Alkaloid Synth.* 2012, **309**, 33–66.
142. J. Zezula, T. Hudlicky, *Synlett* 2005, 388–405.
143. B. H. Novak, T. Hudlicky, J. W. Reed, J. Mulzer, D. Trauner, *Curr. Org. Chem.* 2000, **4**, 343–362.
144. K. C. Rice, *J. Org. Chem.* 1980, **45**, 3135–3137.
145. J. Mulzer, G. Durner, D. Trauner, *Angew. Chem. Int. Ed.* 1996, **35**, 2830–2832.
146. V. Varghese, T. Hudlicky, *Angew. Chem. Int. Ed.* 2014, **53**, 4355–4358.
147. J. D. White, G. Caravatti, T. B. Kline, E. Edstrom, K. C. Rice, A. Brossi, *Tetrahedron* 1983, **39**, 2393–2397.
148. R. Grewe, W. Friedrichsen, *Chem. Ber. Recl.* 1967, **100**, 1550–1558.
149. K. C. Rice, *J. Med. Chem.* 1977, **20**, 164–165.
150. I. Iijima, K. C. Rice, J. V. Silverton, *Heterocycles* 1977, **6**, 1157–1165.
151. J. Mulzer, D. Trauner, *Chirality* 1999, **11**, 475–482.
152. C. Y. Hong, N. Kado, L. E. Overman, *J. Am. Chem. Soc.* 1993, **115**, 11028–11029.
153. P. J. Parsons, C. S. Penkett, A. J. Shell, *Chem. Rev.* 1996, **96**, 195–206.
154. M. A. Tius, M. A. Kerr, *J. Am. Chem. Soc.* 1992, **114**, 5959–5966.
155. K. A. Parker, D. Fokas, *J. Am. Chem. Soc.* 1992, **114**, 9688–9689.
156. G. J. Zylstra, D. T. Gibson, *J. Biol. Chem.* 1989, **264**, 14940–14946.
157. T. Hudlicky, D. Gonzalez, D. T. Gibson, *Aldrichimica Acta* 1999, **32**, 35–62.
158. U. Rinner, Chiral Pool Synthesis: Chiral Pool Syntheses from cis-Cyclohexadiene Diols, in *Comprehensive Chirality*,

Editors-in-Chief: M. C. Erick and Y. Hisashi, Editors. Elsevier: Amsterdam (2012), p. 240–267.

159. J. Schreiber, W. Leimgruber, M. Pesaro, P. Schudel, A. Eschenmoser, *Angew. Chem. Int. Ed.* 1959, **71**, 637–640.
160. M. G. Banwell, *Pure Appl. Chem.* 1996, **68**, 539–542.
161. E. Kotani, F. Miyazaki, S. Tobinaga, *J. Chem. Soc. Chem. Commun.* 1974, 300–301.
162. D. A. Evans, D. J. Hart, P. M. Koelsch, *J. Am. Chem. Soc.* 1978, **100**, 4594–4595.
163. D. A. Evans, S. P. Tanis, D. J. Hart, *J. Am. Chem. Soc.* 1981, **103**, 5813–5821.
164. G. Billek, J. Swoboda, F. Wessely, *Tetrahedron* 1962, **18**, 909–915.
165. A. Mckillop, D. H. Perry, M. Edwards, S. Antus, L. Farkas, M. Nogradi, E. C. Taylor, *J. Org. Chem.* 1976, **41**, 282–287.
166. A. I. Scott, F. Mccapra, R. L. Buchanan, A. C. Day, D. W. Young, *Tetrahedron* 1965, **21**, 3605–3631.
167. S. I. Kaneko, M. Matsui, *Agric. Biol. Chem.* 1968, **32**, 995–1001.
168. R. Robinson, *The Structural Relations of Natural products*. Weizmann Memorial Lectures, Oxford: Clarendon Press (1955), p. 150.
169. J. L. Hartwell, *Lloydia* 1967, **30**, 379–436.
170. U. Rinner, T. Hudlicky, *Synlett* 2005, 365–387.
171. D. Gonzalez, T. Martinot, T. Hudlicky, *Tetrahedron Lett.* 1999, **40**, 3077–3080.
172. T. Hudlicky, U. Rinner, D. Gonzalez, H. Akgun, S. Schilling, P. Siengalewicz, T. A. Martinot, G. R. Pettit, *J. Org. Chem.* 2002, **67**, 8726–8743.
173. G. E. Keck, T. T. Wager, S. F. Mchardy, *J. Org. Chem.* 1998, **63**, 9164–9165.
174. G. E. Keck, T. T. Wager, J. F. D. Rodriquez, *J. Am. Chem. Soc.* 1999, **121**, 5176–5190.
175. D. H. R. Barton, G. W. Kirby, *Proc. Chem. Soc. Lond.* 1960, 392–393.
176. G. E. Keck, S. Fleming, D. Nickell, P. Weider, *Synth. Commun.* 1979, **9**, 281–286.
177. M. G. Banwell, B. D. Bissett, S. Busato, C. J. Cowden, D. C. R. Hockless, J. W. Holman, R. W. Read, A. W. Wu, *J. Chem. Soc. Chem. Commun.* 1995, 2551–2553.
178. G. E. Keck, S. F. Mchardy, J. A. Murry, *J. Am. Chem. Soc.* 1995, **117**, 7289–7290.
179. S. Kim, I. S. Kee, S. Lee, *J. Am. Chem. Soc.* 1991, **113**, 9882–9883.
180. S. Danishefsky, J. Y. Lee, *J. Am. Chem. Soc.* 1989, **111**, 4829–4837.
181. D. H. R. Barton, T. Cohen, *Festschrift Prof. Dr. Arthur Stoll zum siebzigsten Geburtstag 8. Januar 1957. Arbeiten aus dem Gebiet der Naturstoffchemie*, Basel: Birkhäuser (**1957**), p. 293.
182. D. H. R. Barton, G. W. Kirby, *J. Chem. Soc.* 1962, 806–817.
183. T. Kametani, K. Yamaki, H. Yagi, K. Fukumoto, *J. Chem. Soc. C* 1969, 2602–2605.
184. T. Kametani, K. Yamaki, H. Yagi, K. Fukomuto, *J. Chem. Soc. D* 1969, 425–426.
185. B. Franck, H. I. Lubs, G. Dunkelma, *Angew. Chem. Int. Ed.* 1967, **6**, 969–970.
186. R. A. Abramovitch, S. Takahashi, *Chem. Ind.* 1963, 1039–1040.
187. R. Vlahov, D. Krikorian, G. Spassov, M. Chinova, I. Vlahov, S. Parushev, G. Snatzke, L. Ernst, K. Kieslich, W.-R. Abraham, W. S. Sheldrick, *Tetrahedron* 1989, **45**, 3329–3345.
188. T. Kametani, K. Shishido, E. Hayashi, C. Seino, T. Kohno, S. Shibuya, K. Fukumoto, *J. Org. Chem.* 1971, **36**, 1295–1297.
189. T. Kametani, C. Seino, K. Yamaki, S. Shibuya, K. Fukumoto, K. Kigasawa, F. Satoh, M. Hiiragi, T. Hayasaka, *J. Chem. Soc. C* 1971, 1043–1047.
190. Y. Kita, M. Arisawa, M. Gyoten, M. Nakajima, R. Hamada, H. Tohma, T. Takada, *J. Org. Chem.* 1998, **63**, 6625–6633.
191. Y. Kita, T. Takada, M. Gyoten, H. Tohma, M. H. Zenk, J. Eichhorn, *J. Org. Chem.* 1996, **61**, 5857–5864.
192. K. Shimizu, K. Tomioka, S. I. Yamada, K. Koga, *Heterocycles* 1977, **8**, 277–282.
193. D. Krikorian, R. Vlahov, S. Parushev, M. Chinova, I. Vlahov, H.-J. Schäfer, H. Duddeck, G. Snatzke, *Tetrahedron Lett.* 1984, **25**, 2969–2972.

# 13

# HISTIDINE AND HISTIDINE-LIKE ALKALOIDS

IAN S. YOUNG
*Bristol-Myers Squibb Company, Chemical Development, New Brunswick, NJ, USA*

## 13.1 INTRODUCTION

The amino acid L-histidine (**1**) was first isolated by German biochemist Albrecht Kossel in 1896 [1] (Fig. 13.1). Kossel's work with proteins and nucleic acids contributed significantly to our knowledge of cellular chemistry, and for this he was awarded the 1910 Nobel Prize in Physiology and Medicine. The side chain of histidine makes this amino acid unique from a chemistry perspective, as the p$K_a$ of the imidazole (~6.0) allows it to act as both a proton donor and acceptor at physiological pH. As a result, the imidazole side chain of histidine assumes diverse roles in many biological processes. Some of the most important functions are involvement in the catalytic triad of hydrolase and transferase enzymes [2, 3], presence in enzyme metal binding sites (commonly with cysteine) [4], and assistance with iron coordination in hemoglobin [5].

Histidine is one of the 22 proteinogenic amino acids and there has been debate regarding whether or not it is essential for humans. A 1957 report by Rose based on nitrogen balance studies suggested that histidine was nonessential for humans [6] but this was later revised to suggest that histidine was only essential for children [7]. Additional studies led again to modification of histidine's classification, and it is now considered (with some controversy [8]) essential for adults as well [9, 10]. Humans obtain histidine through consumption of protein-rich foods that produce histidine biosynthetically or consume organisms that do.

## 13.2 BIOSYNTHESIS

The biosynthesis of histidine in organisms of lesser complexity (archaea, gram-positive bacteria, and lesser eukaryotes) has been extensively studied since the 1950s [11, 12], although efforts in plants did not really commence until the 1990s [13]. It has been determined for the most part that the process to produce histidine is conserved and proceeds through a 10-step linear route (Scheme 13.1). In this pathway, some enzymes may assume a bifunctional role.

The sequence begins with the condensation of ATP (**2**) and **3**, catalyzed by *N*′-5′-phosphoribosyl-ATP transferase. Then, a hydrolase enzyme converts the triphosphate to the monophosphate via the addition of water to yield **4**. The same hydrolase enzyme utilizes water to open the purine ring of **4** to produce imidazole-containing intermediate **5**. At first glance, it may be assumed that this is the imidazole that is present in histidine, but this is not the case. An enzyme-catalyzed Amadori reaction (internal redox) results in ketone **6**. The imidazole of histidine is then formed by the reaction of **6** with ammonia to yield **8**. Ammonia could be incorporated directly, or an ammonia equivalent could be supplied from glutamine. The expelled **7** is then recycled back into the purine biosynthetic pathway. Step 6 of the process involves enzyme-catalyzed dehydration to produce ketone **9**. An aminotransferase-catalyzed reductive amination uses glutamate (converted to α-ketoglutarate) as the ammonia source and installs the primary amine of **10**. The same enzyme that causes dehydration of **8** to **9** may

*From Biosynthesis to Total Synthesis: Strategies and Tactics for Natural Products*, First Edition. Edited by Alexandros L. Zografos.
© 2016 John Wiley & Sons, Inc. Published 2016 by John Wiley & Sons, Inc.

be responsible for hydrolysis of the phosphate to yield **10**. Histidinol **10** is then oxidized by a two-step process that proceeds through the unstable histidinal, with NAD+ used as a cofactor. The same enzyme is utilized for both oxidations, likely to prevent degradation of the unstable aldehyde intermediate. Overall, 10 steps are required to arrive at L-histidine **1** from progenitors **2** and **3**.

Imidazole natural products, especially those derived biosynthetically from histidine, make up a small portion of the alkaloids found in nature. The majority of these alkaloids are thought to be produced from two histidine metabolites: (1) histamine (**11**), which results from histidine decarboxylase-catalyzed decarboxylation [14], and (2) urocanic acid (**12**), generated from the histidine ammonia-lyase-catalyzed [15] elimination of ammonia (Fig. 13.2).

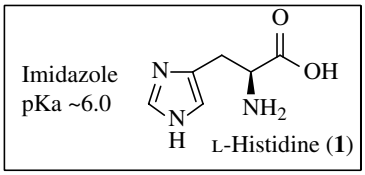
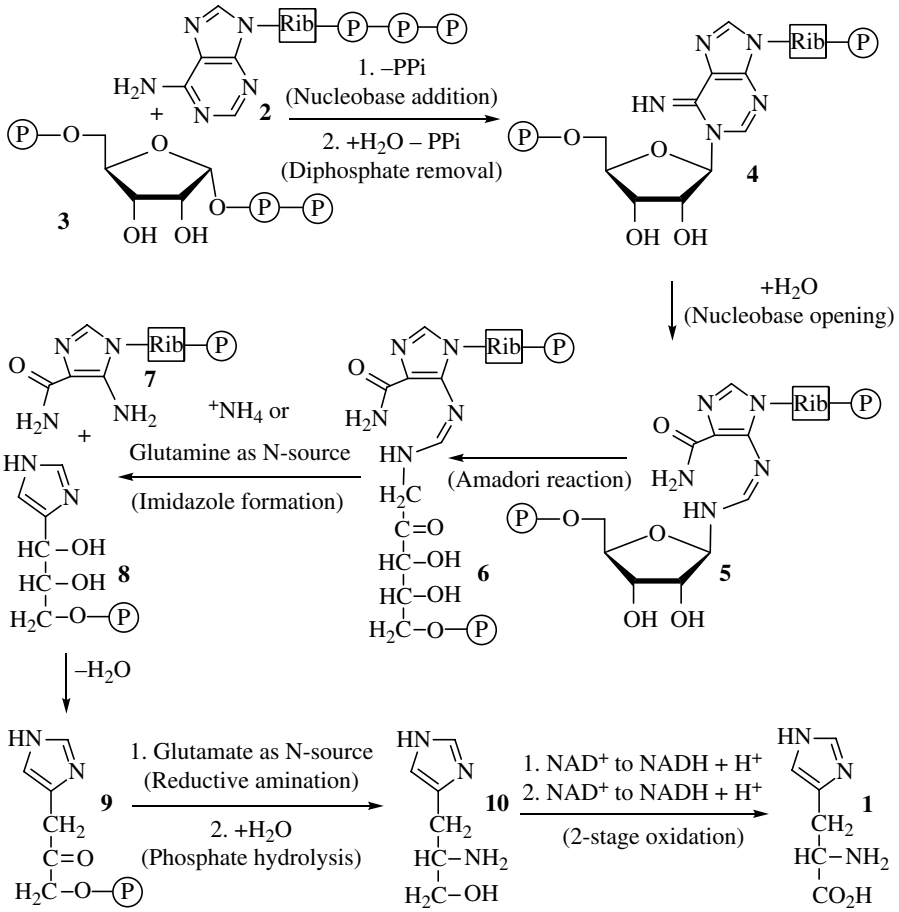



**FIGURE 13.1** The molecular structure of L-histidine amino acid.

A number of simple histamine-derived alkaloids exist in nature and are generally assumed to arise through acylation of the primary nitrogen. Figure 13.2 displays a selection (**13–15**) of these natural products. Very little has been done with respect to biosynthetic studies for these simple histamine amides. In 1971, O'Donovan performed the first tracer study to examine the biosynthesis of an imidazole alkaloid [16]. The origin of dolicotheline (**14**), assumed to be formed from histamine (**11**) and isovaleric acid, was studied by independently injecting (2-$^{14}$C)-histidine (**1**), (2-$^{14}$C)-leucine (**19**), and sodium (1-$^{14}$C)-isovalerate (**21**) into three different cacti (Scheme 13.2). After 3 weeks, dolicotheline was isolated via standard methods and then digested into isovaleric acid and histamine to determine the fragment responsible for the radioactivity. It was found that the dolicotheline isolated from each cactus had significant incorporation of the radiolabeled substrate (between 2 and 4%). These results suggest that histamine (derived from histidine) and isovaleric acid (known to be derived from leucine via **20**) are biosynthetic progenitors.




**SCHEME 13.1** Ten-step biosynthesis of L-histidine. Rib, ribose; P, phosphate.

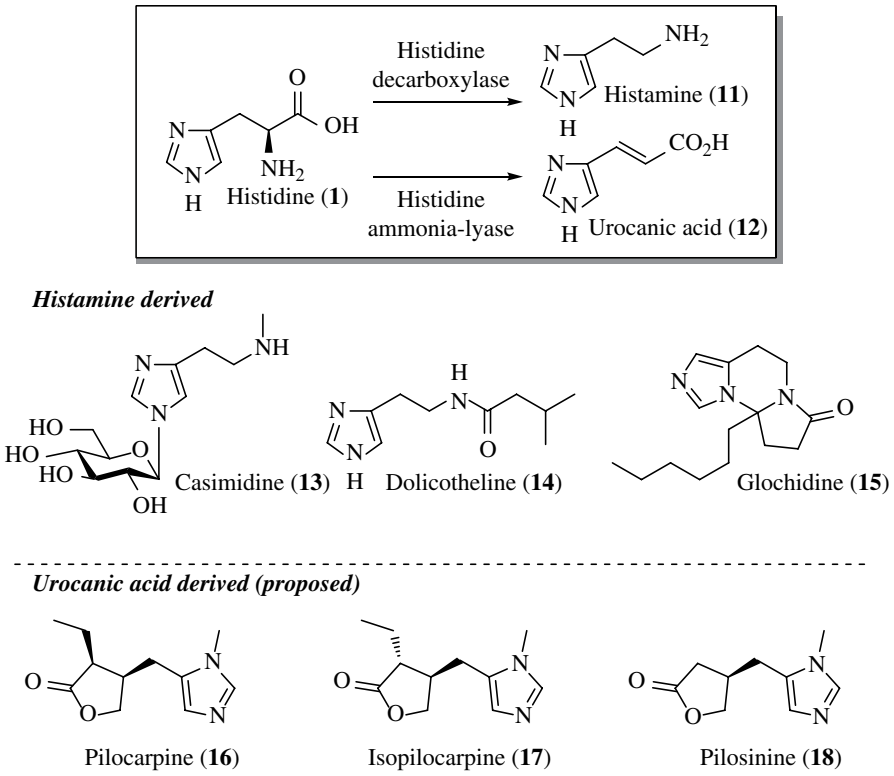
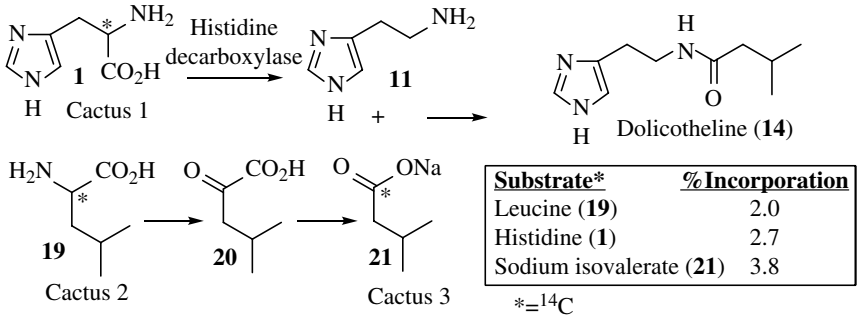



**FIGURE 13.2** Common enzyme-catalyzed transformations of histidine and compounds that may arise from histamine and urocanic acid.

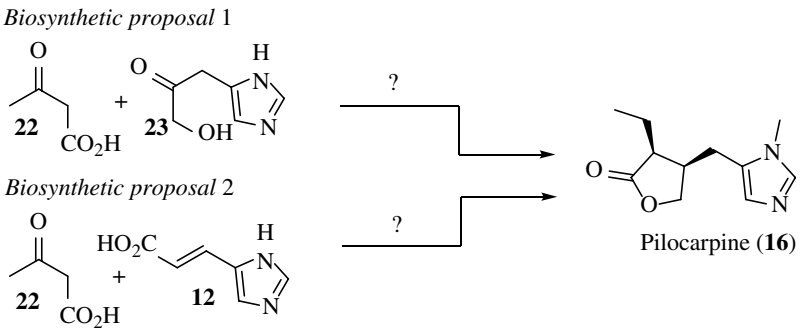



| Substrate* | %Incorporation |
|---|---|
| Leucine (**19**) | 2.0 |
| Histidine (**1**) | 2.7 |
| Sodium isovalerate (**21**) | 3.8 |

**SCHEME 13.2** Biosynthetic study of dolicotheline using radiolabeled amino acids.

Pilocarpine (**16**) [17] (Fig. 13.2), a highly studied imidazole-containing natural product, potentially could arise from the histidine metabolite urocanic acid (**12**). The intense interest in this alkaloid stems from its diverse range of medicinal properties. Pilocarpine has been investigated as a treatment for xerostomia (dry mouth) [18] and to stimulate sweat production [19]. Due to a lack of selectivity in the body though, it has been relegated mainly to the use as an antiglaucoma medicine [20]. As a result of these potential medicinal applications, there has been much synthetic effort toward this natural product [21]. The main synthetic challenge toward pilocarpine is designing a route that will minimize epimerization of the ethyl group to yield isopilocarpine (**17**).

The most abundant source of pilocarpine is the leaves of the jaborandi species of plant, native to north and northeast Brazil. Due to pilocarpine's interesting physiological effects, this plant has been extensively harvested and as a result is now listed as endangered [22]. Studies by Abreu have been directed toward producing pilocarpine using cell lines/suspensions on scales that would have the potential to satisfy the current need [23]. To date, very little is known about the biosynthetic pathway that produces pilocarpine. Proposal that utilizes **22** and **23** [24] and **22** and **12** [25] as key intermediates has been put forth (Scheme 13.3), but no conclusive evidence derived from using radiolabeled substrates has been reported.




**SCHEME 13.3** Potential starting materials in the biosynthesis of pilocarpine.

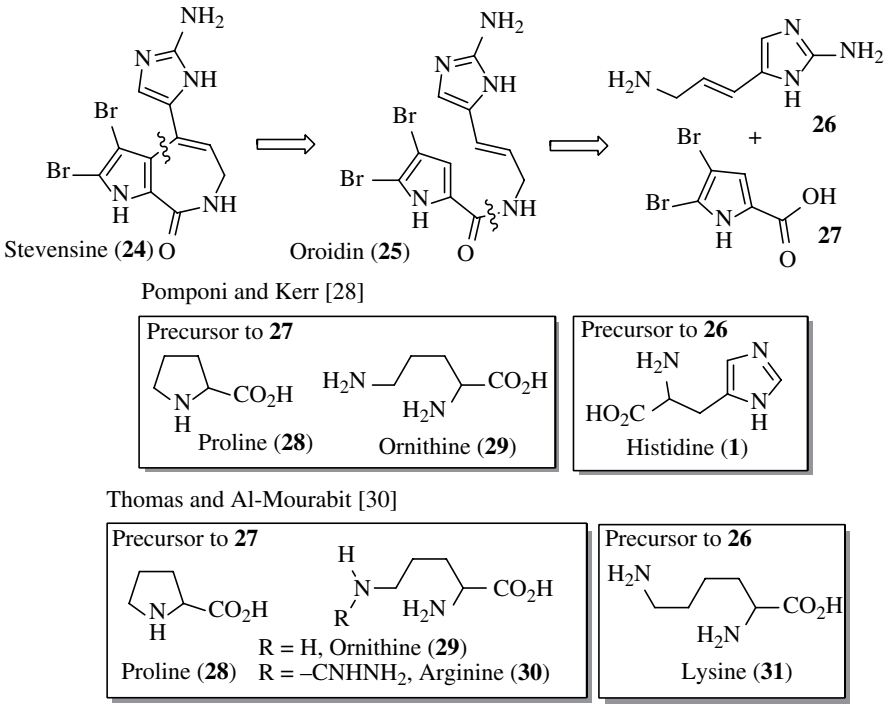



**FIGURE 13.3** Biosynthetic precursors to oroidin based on radiolabeled feeding studies.

Despite the intense effort directed at determining the biosynthetic origin of histidine in various organisms, minimal studies have been conducted with respect to the generation of natural products thought to be derived from this amino acid. The work outlined earlier represents the bulk of this research.

Another class of natural products that contain the imidazole nucleus, although in the 2-amino form, is the marine sponge-derived pyrrole–imidazole alkaloids (PIAs) [26]. Similar to the natural products discussed earlier, the biosynthesis of even the simplest members such as oroidin has not been extensively studied. This is in part due to the difficulty in designing the appropriate systems to mimic aquatic environments, in comparison to those needed to study biosynthesis of terrestrial alkaloids in plants [27]. In 1999, Kerr reported the first biosynthetic investigation toward a PIA in sponge-derived cell cultures (*T. morchella*) in which $^{14}$C-radiolabeled amino acids were used [28]. Stevensine (**24**), the compound of study, is assumed to be derived from cyclization of oroidin (**25**) [29], which after dissection of the peptide bond yields the precursors 4,5-dibromopyrrole-2-carboxylic acid (**27**) and 3-amino-1-(2-aminoimidazolyl)-prop-1-ene (**26**) (Fig. 13.3). Support for **26** and **27** being substrates in the biosynthesis of oroidin and thus stevensine comes from the fact that all of these compounds can be found to together in the sponge extract. Kerr proposed that the pyrrole-containing **27** is derived from either proline (**28**) or ornithine (**29**) and the aminoimidazole fragment results from either histidine (**1**) or arginine (**30**). Feeding experiments produced radioactive stevensine when labeled proline/ornithine (pyrrole precursors) or histidine (aminoimidazole precursor) was provided in the medium. Although the histidine result was rational based on the fact that both the amino acid and product **26** contain an imidazole, an extra

carbon must be incorporated into histidine to yield **26** and no biological pathways were known at the time that could effect this conversion.

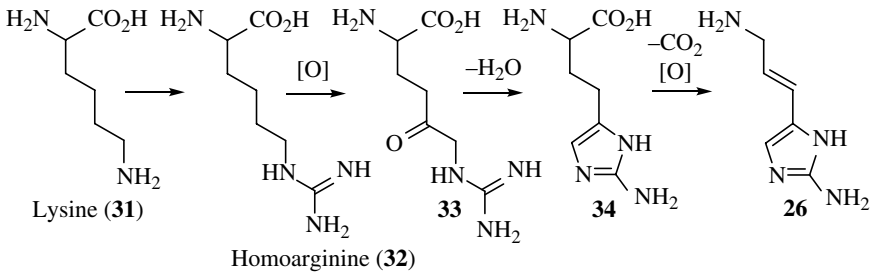
One year after the Kerr report, Lindel and Köck hypothesized that lysine (**31**) could actually be the biosynthetic precursor to imidazole-containing **26** [31]. It was not until 11 years later that this proposal was actually validated by the groups of Thomas and Al-Mourabit [30] (Fig. 13.3). In this instance, intact sponge in an environment that mimicked a natural habitat was employed to study the biosynthesis of oroidin, as opposed to the sponge cell cultures utilized by Kerr. Similar to Kerr, they found that the pyrrole portion **27** is derived from proline (**28**) and ornithine (**29**), as well as arginine (**30**), which is known to convert to ornithine in the urea cycle. In contrast though, they found that the aminoimidazole-containing **26** is derived from lysine (**31**), and no radioactivity was detected when labeled histidine was provided. Scheme 13.4 provides a possible pathway for the conversion of lysine to **26**, with the majority of these transformations being observed in other biological cycles [32]. Although the Thomas/Al-Mourabit results suggest that the PIAs are not histidine derived, we have decided to modify the chapter title to include "histidine-like" alkaloids as well.

Although both Kerr and Thomas/Al-Mourabit probed the biogenetic origin of oroidin, before 2012 there was only speculation (although logical) that oroidin was a precursor to the more complex dimeric PIAs in nature. Using cell-free enzyme preparations from the sponges *Agelas sceptrum* and *Stylissa caribica* and 7-$^{15}$N-oroidin (**25**), Molinski and Romo observed that after incubation for only 30 min, two major products were obtained: benzosceptrin C (**35**; Scheme 13.5) and nagelamide H (not depicted) [33]. Incorporation of the $^{15}$N-labeled oroidin into the natural products was confirmed by both HRMS and NMR. It is hypothesized that this coupling proceeds by a single-electron transfer process, catalyzed by a cytochrome P450 enzyme.

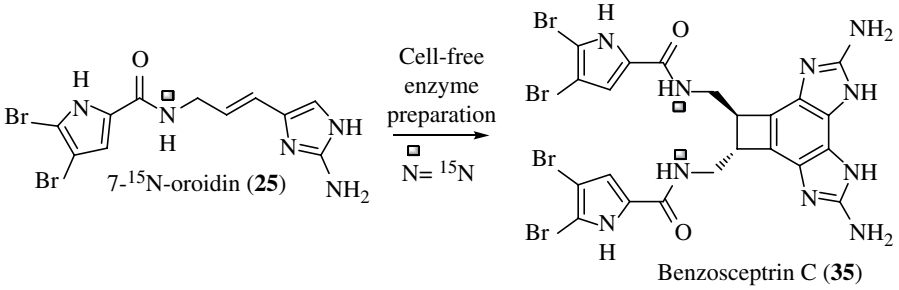
Although the number of studies using (radio) labeled substrates in an attempt to confirm the generation of these PIAs in nature is limited, numerous biosynthetic hypotheses occupy the chemical/synthetic literature [34, 35]. These proposals represent all levels of the complexity spectrum for this family, from simple cyclic compounds derived from an oroidin monomer to those that result from dimerization of oroidin and further cyclizations. To prevent this chapter from occupying the whole book, only two examples will be presented in this subsection to serve as a general overview.

The ability of the 2-aminoimidazole **36/37** to tautomerize allows it to incorporate both electrophilic and nucleophilic sites into the molecule simultaneously (Fig. 13.4). This concept is further emphasized when considering the vinylogous compound **38/39** (**26**), which is thought to make up the basic building block of the PIAs (oroidin). This ambiphilic reactivity allows for the vast number of speculative cyclization and dimerization pathways.

In 1977, Sharma proposed the following hypothesis for dibromophakellin (**44**) formation in nature [36] (Scheme 13.6). Starting from dihydrooroidin **40** (presumed to be derived from reduction of oroidin (**25**)), oxidation of the amide nitrogen would induce attack by the nucleophilic 2-aminoimidazole to form tricyclic intermediate **43**. The resulting iminium is then




**SCHEME 13.4** Proposed conversion of lysine to aminoimidazole-containing **26**.




**SCHEME 13.5** Study of benzosceptrin C biosynthesis using $^{15}$N-oroidin.

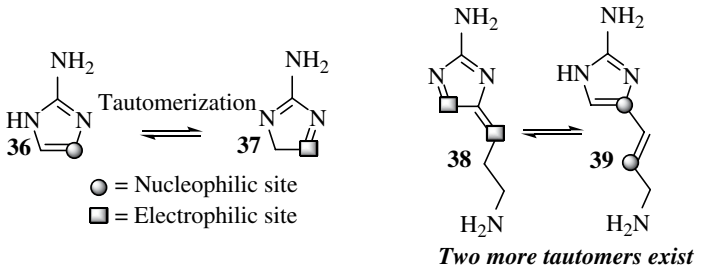
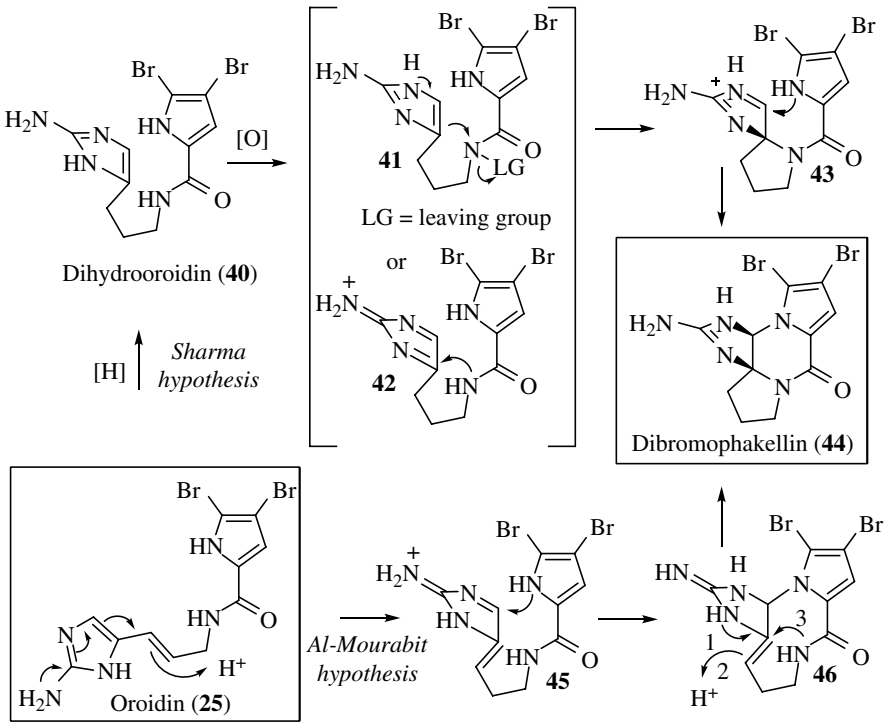



**FIGURE 13.4** Ambiphilic reactivity of (vinyl) 2-aminoimidazoles.

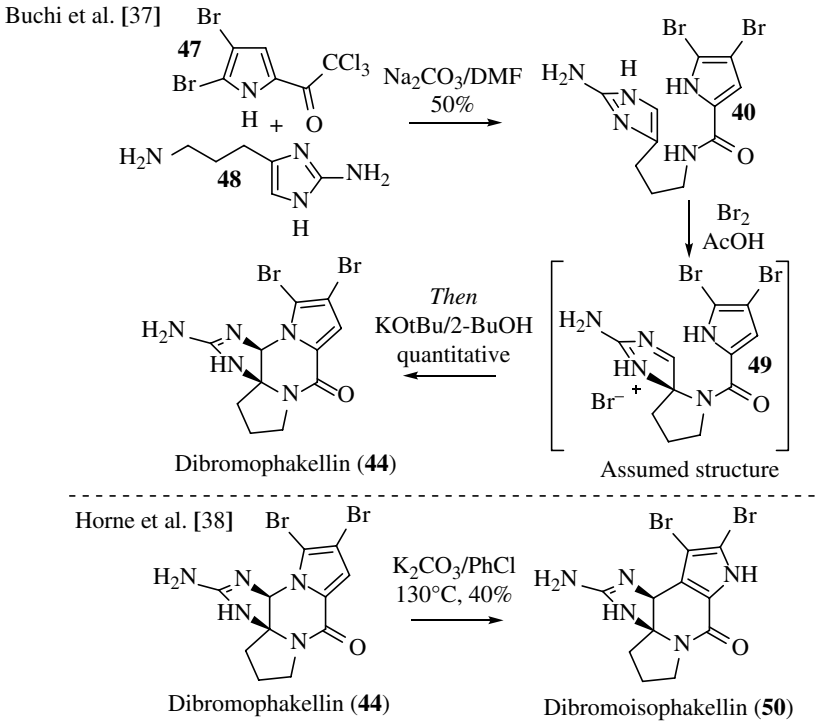



**SCHEME 13.6** Biosynthetic proposals to dibromophakellin from Sharma and Al-Mourabit.

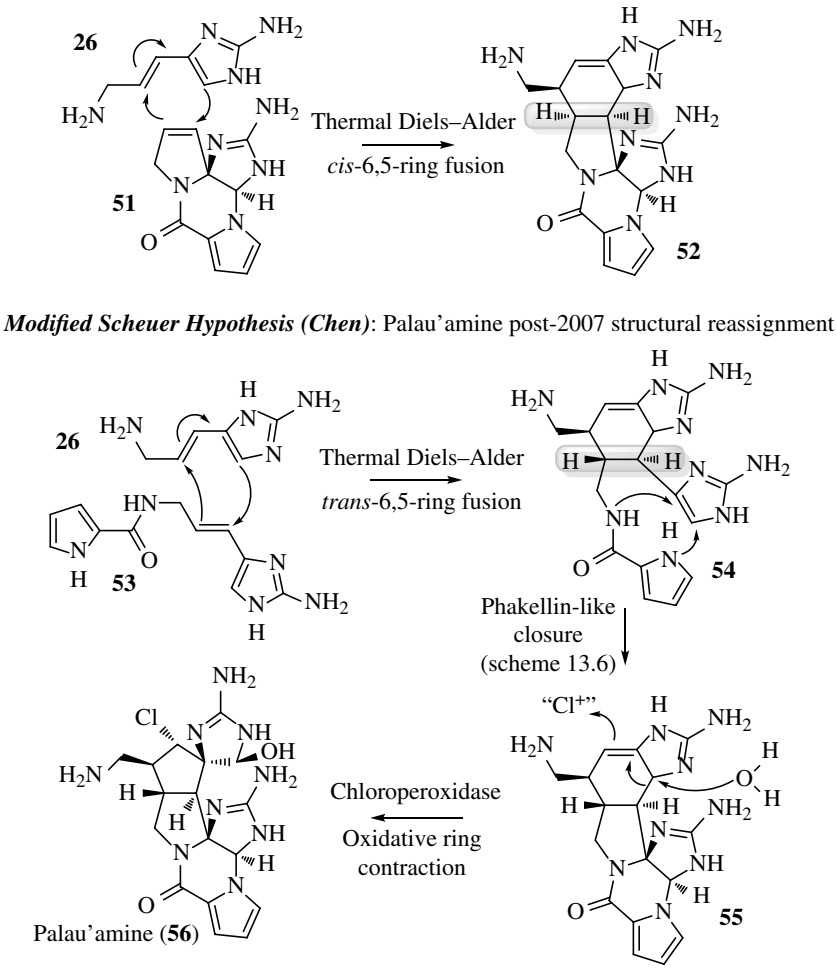
intercepted by the pyrrole nitrogen to form the natural product, although it is also possible that oxidation occurs at the aminoimidazole to form the electrophilic azafulvene-containing **42**, which then undergoes two subsequent nucleophilic additions to form the tetracyclic natural product. An alternative proposal for the formation of **44** directly from oroidin has been proposed by Potier and Al-Mourabit [34]. This hypothesis does not require prior reduction to dihydrooroidin and instead takes place by a series of tautomerizations.

This oxidation hypothesis was put to practice by Buchi in 1982 in an elegant synthesis of dibromophakellin [37] (Scheme 13.7). After coupling of pyrrole **47** and aminoimidazole **48** to yield dihydrooroidin (**40**), oxidation with bromine in acetic acid produced an insoluble material that was not fully characterized but was assumed to be compound **49**. Treatment of **49** with base then led to quantitative conversion to dibromophakellin. Horne later improved the process by utilizing NBS in TFA and directly treating the reaction mixture with triethylamine [38]. Horne also demonstrated that dibromophakellin could be converted to another natural product, dibromoisophakellin (**50**), by heating in the presence of base (Scheme 13.7).

This conversion of **44** to **50** was presented for a specific reason, as it highlights a unified premise for the PIAs: the assumed biogenetic relationship/conversion between members. Scheme 13.8 displays two biosynthetic proposals toward a more complex member of the PIAs, palau'amine (**56**). This scheme was offered to emphasize another reoccurring idea, the fact that the same simple building blocks are thought to be used to construct many of the PIAs in nature. The original proposal by Scheuer [39] for palau'amine utilized a cycloaddition between an oxidized form of phakellin (**51**) and vinyl imidazole-containing **26**, which is thought to be a building block of clathroidin (**53**) (Scheme 13.8).




**SCHEME 13.7** Buchi's biomimetic synthesis of dibromophakellin and conversion of **44** to dibromoisophakellin by Horne.




**SCHEME 13.8** Two examples of palau'amine biosynthetic proposals that differ due to the need to install either the *cis*-5,5 or *trans*-5,5 ring junction.

Intermediate **52** could then be converted to the *cis*-5,5 ring system of palau'amine by a chloro-peroxidase-mediated ring contraction (see proposal by Chen in the following). After the structure of palau'amine was reassigned to *trans*-5,5 in 2007 [40–42], Chen published an alternative proposal that would generate the *trans*-5,5 system within the natural product [43]. Now, Diels–Alder reaction between **26** and clathroidin occurs prior to cyclization of **53** to phakellin. These two themes (natural product interconversion and conserved building blocks) will be commonplace in the last section of this chapter, which will also highlight two key concepts in the realm of PIA synthesis: (1) atom economy and (2) protecting-group-free synthesis. An introduction to these concepts follows.

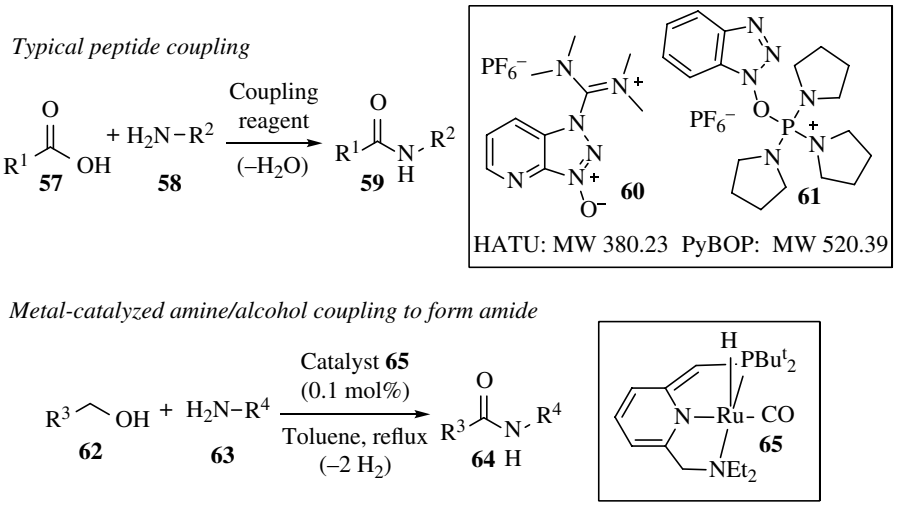
## 13.3 ATOM ECONOMY AND PROTECTING-GROUP-FREE CHEMISTRY

A regular discussion, especially among nonsynthetic chemists, is that we are now able to prepare any natural product if enough time, money, and manpower are invested. This "brute-force" approach, although not always elegant, can in many cases lead to inefficient syntheses [44]. As a practicing synthetic chemist reading this chapter you are aware that once a natural product is made for the first time, efforts toward that target do not cease. The challenges associated with total synthesis are almost endless, as in theory, the current preparation of a molecule can always be done better. Whether it is being from a yield, material throughput, step count, or cost perspective, chemists are always trying to outdo those who have come before them. In 1975, Hendrickson suggested that an ideal synthesis should (i) create a complex skeleton from simpler starting materials, (ii) link synthon molecules via construction reactions, (iii) start from available small molecules, (iv) involve no intermediary refunctionalizations, and (v) lead directly to the structure of the target, not only in skeleton but also in correctly placed functionality [45]. Twenty-one years later, Wender offered an even more daunting definition of an ideal synthesis in which "the target molecule is prepared from readily available, inexpensive starting materials in one simple, safe, environmentally acceptable and resource-effective operation that proceeds quickly and in quantitative yield" [46].

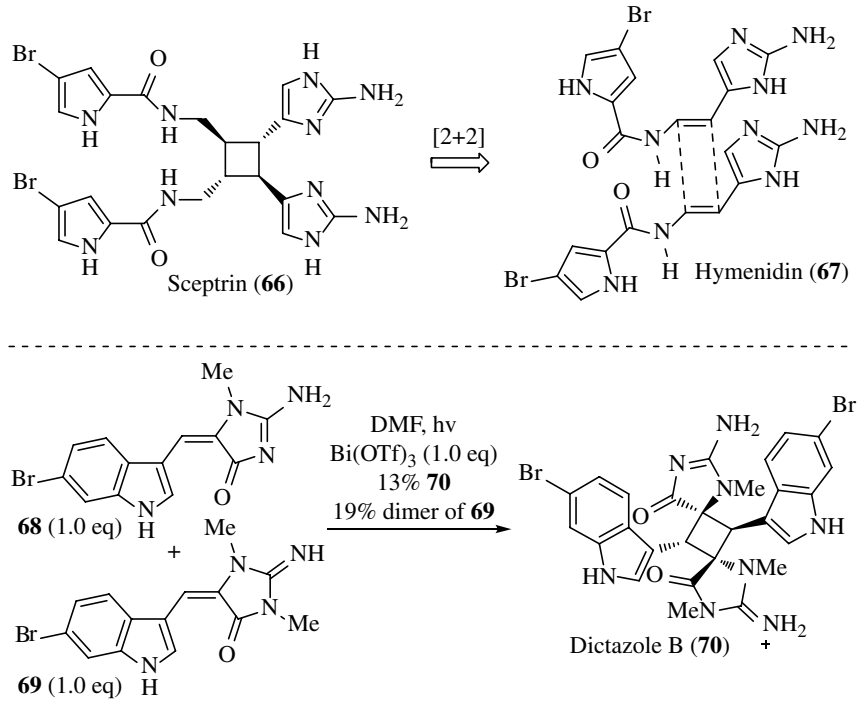
In an attempt to quantify the "ideality" of a synthetic route, the Baran lab created a formula that considers such factors as formation reactions (C─C and C─heteroatom bonds) and strategic redox steps as positive, and nonstrategic redox, functional group interconversions and protecting-group manipulations as unproductive [47]. Upon assessment of a number of syntheses from their own laboratory (high 83% ambiguine, and low 32%, palau'amine), it was found that, as expected, our field has significant room to be innovative and improve upon past results. Although we may never be able to obtain "ideality" at the levels suggested by Hendrickson and Wender, the motivation to try encourages the synthetic chemist to identify deficiencies in how we practice our craft and inspires us to further evolve our field.

The prevalence of certain terms in the chemical literature suggests that we have begun to identify areas that can offer improvement with respect to synthetic efficiency. Many of these themes such as "redox" [48], "step" [49], and "atom" [50] are followed by "economy" [51], which derives in part from the Greek word for "management." The ideals of "green chemistry" [52] and "protecting-group-free" synthesis [53, 54] are also receiving significant attention. Although all of these concepts have profound impact on the ideality of a synthesis, two topics (atom economy and protecting-group-free synthesis) will be discussed in more detail.

Atom economy (AE) can serve as an alternative to overall chemical yield or step count to assess the efficiency of a single transformation or synthetic route. The concept of AE in academic settings was not given full appreciation until Trost elevated the notion through a 1991 thought-provoking perspective [50]. Where the importance of AE has always been recognized is in the pharmaceutical or fine chemical industries, where the production of compounds may be on the scale of several metric tons [55]. The large amounts of waste that are generated during execution of a multistep process are costly to dispose of and can have environmental impact. Thus, syntheses evolve to minimize the amount of waste generated as the development stage of the project advances. The content of Trost's manuscript began to change the way that Academics think about chemical reactions (although step count and overall yield still tend to dominate in a total synthesis arena), and much work has been aimed at developing more atom-economical processes. Atom economy in a broad sense is a measure of what percentage of the atoms in the starting materials and reagents are present in the product. Solvents are typically excluded but are given more attention when considering the related topic of "green chemistry." A generic peptide coupling will be used to highlight this concept [56] (Scheme 13.9). The overall change with respect to reactants is the net loss of low molecular weight water, so at first glance it appears that this is a fairly atom-economical process. But one must consider all the reagents in the flask, and the shortcomings of traditional dehydrating agents such as *N*,*N*′-dicyclohexylcarbodiimide (DCC, MW = 206.18) have led to the development and use of more exotic (and massive) reagents (e.g., HATU (**60**) MW = 380.23 or PyBOP (**61**) MW = 520.39). These alternative reagents are commonly utilized due to their superior reaction profiles, whether from a yield, rate, racemization, or impurity minimization perspective. With these benefits comes a cost: the requirement for the use of a stoichiometric amount of a high molecular weight reagent, the atoms of which will not be incorporated into the product. These inefficiencies have been recognized and in 2007 Milstein reported that by utilizing




**SCHEME 13.9** Atom uneconomical peptide bond formation and alternative catalytic method.




**SCHEME 13.10** Proposed atom-economical dimerization of hymenidin to produce sceptrin and photochemical union of **68** and **69** to yield dictazole B.

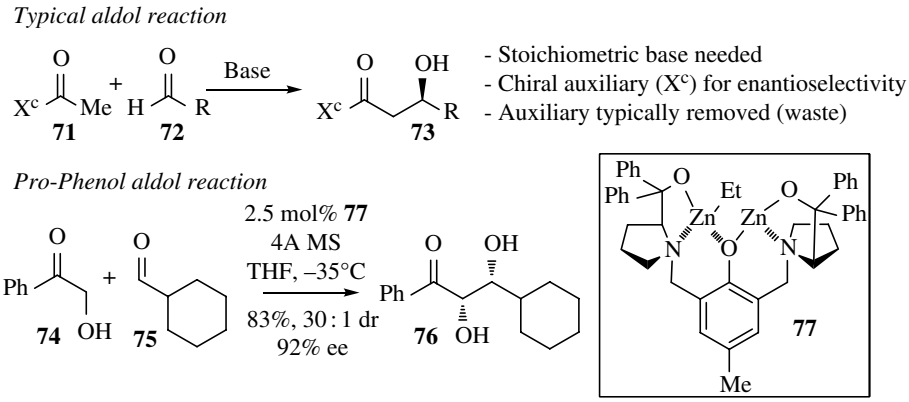
only 0.1 mol% of catalyst **65**, an amide bond could be generated directly from an amine (**63**) and alcohol (**62**) [57]. The stoichiometric by-product in this process is only two equivalents of hydrogen. Although this transformation was limited to primary amines (secondary led to ester formation), it served as inspiration for research into more atom-efficient peptide couplings. In 2013, Kang reported a metal-catalyzed peptide bond formation from nitriles and alcohols that proceeded with 100% AE [58].

The Diels–Alder reaction (and cycloadditions in general) [59] is commonly utilized to represent atom-economical processes. In many examples, heat or light drives these reactions and all atoms present in the flask end up in the product (solvent excluded). Biosynthetic hypotheses based on cycloadditions for the PIAs sceptrin (**66**) ([2+2]) [60] and ageliferin ([4+2], not depicted) [61] from hymenidin (**67**) highlight this point (Scheme 13.10). Some facts suggest that it is unlikely that sceptrin is formed by a light-catalyzed

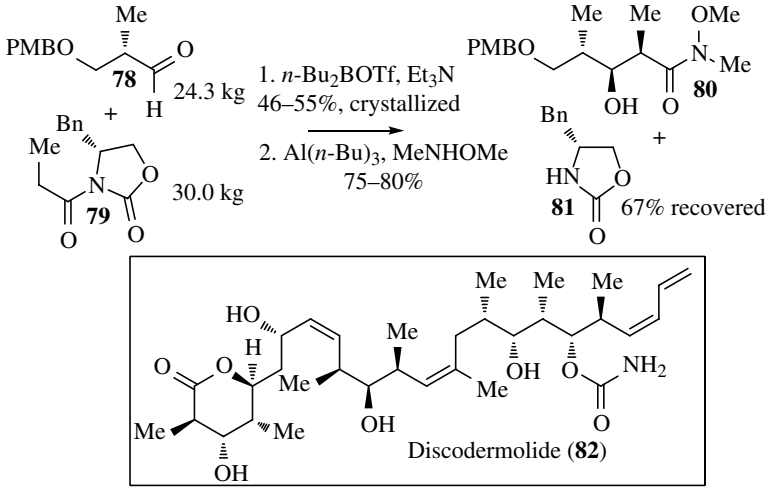
[2+2] cycloaddition: (i) the sponge that produces sceptrin is found at a depth where sunlight will have trouble penetrating and (ii) sceptrin exists in a nonracemic state (suggesting enzyme involvement). This knowledge has not dissuaded numerous groups from attempting to prepare sceptrin and ageliferin directly from hymenidin, but to date, none of these attempts have been successful, although the recent synthesis of dictazole B (**70**) [62] via a light-induced [2+2] dimerization of **68** and **69** should offer encouragement to further pursue these endeavors.

The aldol reaction is another class of reactions used to highlight AE, as all the atoms in the reactants end up in the product. One should note though that this transformation comes with a number of caveats. Typically, a stoichiometric base is required to form the reactive enolate, and for many asymmetric aldols, a chiral auxiliary is utilized. Although this auxiliary is present in the product after the reaction, it is usually cleaved in a subsequent step and discarded to waste. An example of innovation to address both of these issues is the asymmetric aldol reaction using a zinc–Pro-Phenol catalyst (**77**) developed by Trost [63]. Catalyst **77** (2.5%) serves both as base and chiral controller, and its use yielded **76** in high yield, *dr* and *ee* (Scheme 13.11). One minor shortcoming of the reaction from an AE perspective is that a slight excess of the nucleophilic partner is sometimes necessary. Trost exploited the use of this catalyst for the total synthesis of the complex macrolide laulimalide [64]. Please see review by Bartlett for other examples of how the use of transition metal catalysts has increased AE for a number of reaction classes [65].

Even with more atom-economical, catalytic, asymmetric aldol options available, the use of chiral auxiliaries on large scale should not always be avoided based on the perception of poor AE. The following example toward discodermolide (**82**) from Novartis Process Chemistry, where AE, process greenness, and waste minimization are of great concern, demonstrates that aldol transformations with auxiliaries are possible on multi-kg scale [66] (Scheme 13.12). After aldol reaction and cleavage of the chiral controller to produce **80**, they were able to recover **81** in 67% yield via crystallization.




**SCHEME 13.11** Shortcomings of a typical aldol reaction from an atom economy perspective and catalytic, asymmetric aldol reaction.




**SCHEME 13.12** Large-scale asymmetric aldol reaction with chiral auxiliary recovery.

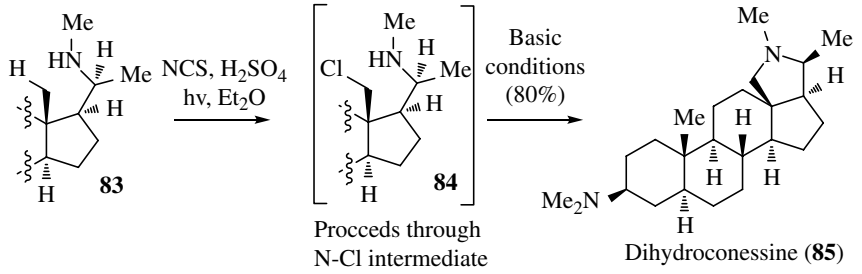
The ability to produce a natural product with the complexity of discodermolide on Process Chemistry scale demonstrates how our field has evolved from an efficiency standpoint and with a newfound aptitude to take on challenges [67] that would seem impossible in the not-so-distant past.

As is the case for the Zn–Pro-Phenol aldol reaction described earlier, the development of catalytic reactions that remove the need for stoichiometric reagents is of paramount importance with respect to AE. Trost has been a major contributor in this field, and an overview of some of his labs contributions should provide a reference for the impact of homogeneous catalysis on AE [68, 69]. Other modes of catalysis, such as organocatalysis, have also played an important role in the union of two substrates into product with high AE [70].

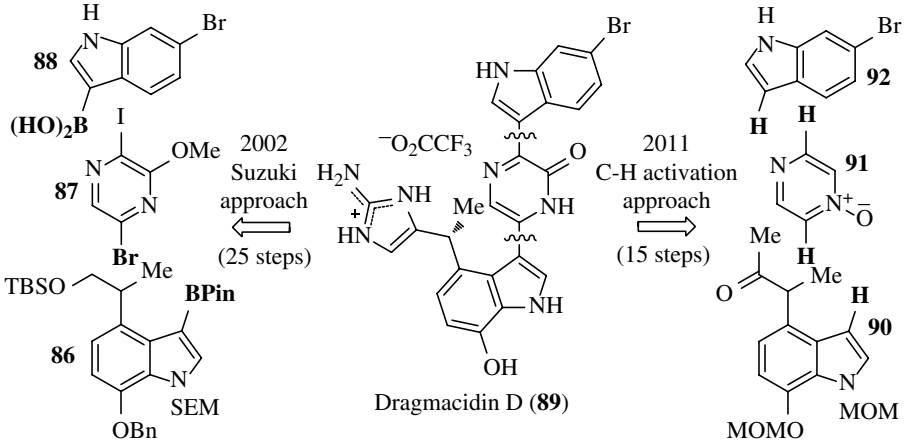
A general class of reactions that has the potential to greatly increase AE is C─H activation chemistry [71]. C─H activation is a broad term and generally refers to direct conversion of a C─H bond to a C─C or C─heteroatom bond. This is not a new concept with Corey's synthesis of dihydroconessine (**85**) in 1958 representing an early example [72] (Scheme 13.13). A Hofmann–Löffler–Freytag reaction was utilized to convert a C─H bond to a C─Cl bond, with the installed chloride being displaced by the proximal amine after exposure to base.

In the past 10 years, other classes of C─H activation, especially those based on cross-coupling methodologies, have been extensively developed and showcased in the field of natural product synthesis. To highlight how powerful C─H activation can be with respect to AE, the example of dragmacidin D will be used. Standard cross couplings in which both coupling partners are functionalized have changed the way we think about synthesis [73]. They offer new retrosynthetic disconnections [74] and for the most part proceed with predictable reactivity and in a reliable manner. One downside is that prefunctionalization of both coupling partners is often necessary, adding steps and diminishing AE as these reactivity handles are often not found in the coupled product. Stoltz's synthesis of dragmacidin D (**89**) in 2002 couples prefunctionalized substrates **86–88** via two subsequent Suzuki reactions to prepare the core of the natural product [75] (Scheme 13.14). Using this strategy, a total of 25 steps were required to complete the target.

In 2002, C─H functionalization in the realm of natural product synthesis had hardly been realized, and Stoltz's synthesis stands as a great achievement with respect to technology available at that time. Only 9 years later, the synthesis of dragmacidin D by Yamaguchi and Itami [76] demonstrates how the state of the art of organic chemistry has quickly evolved (Scheme 13.14). Through two C─H




**SCHEME 13.13** Early example of C–H activation by Corey.




**SCHEME 13.14** Comparison of dragmacidin D syntheses.

activation events, they were able to forge the same two key aryl–aryl bonds between substrates **90–92**. Although not the only reason, the absence of the need for prefunctionalization of the coupling partners was a key contributor to the Itami synthesis requiring 10 less steps.

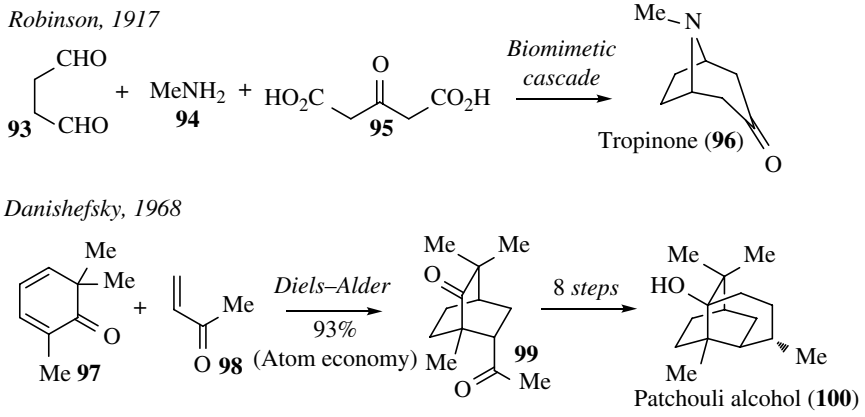
This section on C─H activation is in no way meant to be comprehensive and should serve only to highlight the potential power of this concept for increasing AE. For a thorough summary on the topic of C─H activation in natural product synthesis, please refer to these recent reviews [77, 78].

When the term "protecting-group-free" (PGF) synthesis is discussed in the context of this chapter, it encompasses more than just a synthesis that happens to proceed without protecting groups (PGs). Instead, it represents an alternative way to think about and plan the construction of molecules. In many cases for PGF synthesis to become reality, chemists must expand their toolbox through the invention of new chemistry/reactions. In other examples, the outcome is realized by using the innate "unmasked" reactivity of a functional group in a way not before imagined (or anticipated) [79]. This spirit of discovery, in combination with routes based on biosynthetic hypotheses, has greatly elevated the status and prevalence of PGF synthesis. Intense interest/effort into pushing the boundaries of PGF synthesis began around the mid-2000s.

One example of an early PGF synthesis is Robinson's 1917 landmark synthesis of tropinone **96** [80] (Scheme 13.15). By the combination of succinaldehyde **93**, methylamine **94**, and acetone dicarboxylic acid **95**, tropinone resulted from what can be assumed to be a biomimetic process [81]. Another classic PGF synthesis is Danishefsky's 1968 preparation of patchouli alcohol (**100**) [82]. The atom-economical first step of this sequence, the Diels–Alder reaction of diene **97** and methyl vinyl ketone (**98**), is one of but not the only reason this example was chosen. Not to take away from the beauty of Danishefsky's synthesis, functionality contained within patchouli alcohol is minimal and as a result limited PG usage would be expected. Also, during the decades of the two syntheses the use of PGs (and the number of varieties available) [83] was only a fraction of what is known today. To put things into perspective, the report of using a *tert*-butyldimethylsilyl (TBS) group for the protection of alcohols was not published until 1972 [84], 4 years after Danishefsky's synthesis of patchouli alcohol. For comparison, only 35 years later (2007), the fourth edition of Greene's *Protective Groups in Organic Synthesis* is now composed of over 1000 pages [85].

The strong promotion of PGF synthesis is not meant to condemn the use of PGs in the preparation of a target molecule. The invention of the numerous PGs currently available has allowed organic chemist to quickly advance our knowledge of chemical reactivity, by modulating functionality that might interfere with the intended study. Also PGs provide a layer of security that allows for synthetic problems to be overcome more rapidly. A perusal of the total synthesis literature should convince you that many of the greatest accomplishments in the past 50 years would not have been accomplished without the use of blocking groups [86], and as a result, their value for advancing our field cannot be quantified. But as the field matures further and we as a discipline continue to battle, the notion that "with enough money/resources we can make anything" (which may be true), we must continue to improve and advance the way we do synthesis. Making 1 mg of a natural product in an academic lab is a noble achievement and can represent the fruits of many years of hard labor. But again, someone will always ask, "what is the value of making 1 mg of compound **X**?" Increasing synthetic efficiency presents the opportunity to make significant quantities (*vide infra*) to allow for biological testing, if the molecule renders itself to such characteristics. More importantly, in all but the most straightforward syntheses, new chemistry/reactivity will be discovered, and these learnings are then added to our knowledge/strategy database.

Based on the concept of AE, the use of PGs is not favorable, as the atoms of the PG are ultimately discarded to waste. In certain cases, judicious selection of the PG negates

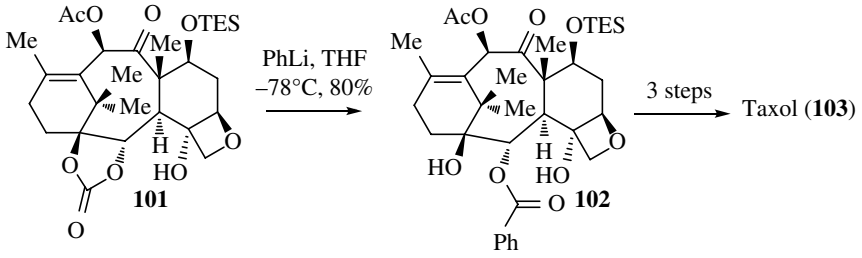



**SCHEME 13.15** Early examples of protecting-group-free synthesis.

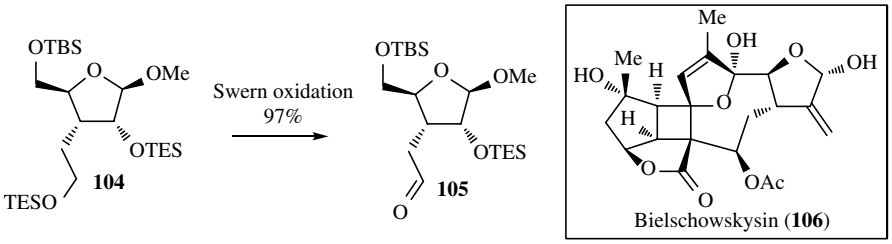
this inefficiency. Nicolaou's synthesis of Taxol® (**103**; see Scheme 13.20 for structure) incorporates the atoms of the PG into the molecule (in this case it is only a C═O) (Scheme 13.16) [87], and after thinking about this example further, one may wonder if this cyclic carbonate should be classified as a PG at all.

Another criticism that the employment of PGs faces is that their use increases step count, as both protection and deprotection steps are typically required. This impact can be minimized by the use of fairly labile PGs such as TMS, which can be removed with acidic work-ups, but this is not typical, and in general PGs require enhanced stability to survive a variety of synthetic transformations. Mulzer in his studies toward bielschowskysin (**106**) [88] took advantage of the fact that primary TES ethers are directly converted to aldehydes upon subjection to Swern conditions (Scheme 13.17). Besides the fact that this strategy does not invoke an additional step for TES removal (as the alcohol needed to be oxidized anyways), it also offers a chemoselective advantage, as only the primary TES group reacts under these conditions. This negates the challenges that are often encountered when trying to selectively install/remove a PG on comparable functional groups or in similar chemical environments. It might seem that these two examples are out of place in a section dedicated to PGF synthesis, but they are included to help emphasize the overall theme of this chapter. Even when using PGs, which have been given a negative connotation with respect to overall synthetic efficiency, there is the ability to be innovative and minimize impact on ideality.

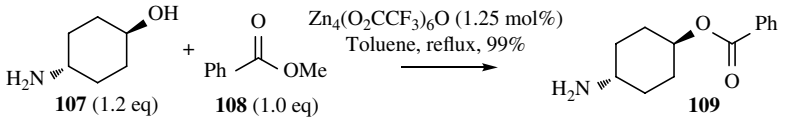
Crucial to the implementation of PGF synthesis is the concept of selectivity [89], specifically site and chemoselectivity. Chemoselectivity has been referred to as "the mother of invention" [90], and advancements in this concept have been strong drivers for the expansion of the field of PGF synthesis. We are typically taught throughout our organic chemistry education that amines are more nucleophilic than alcohols (barring steric or electronic factors that may exert heavy influence). As a result, if both functionalities are present in a molecule, for most reagents amine protection will be needed to selectively modify the alcohol. Intense efforts have been aimed at changing this reactivity preference, and one example is the report by Oshima and Mashima [91]. It was found that by using a Zn-complex catalyst, which is thought to increase the oxophilicity of the acylating reagent, they could induce a high yielding acylation of the hydroxyl group contained within **107** (Scheme 13.18), without resorting to protection of the primary amine.



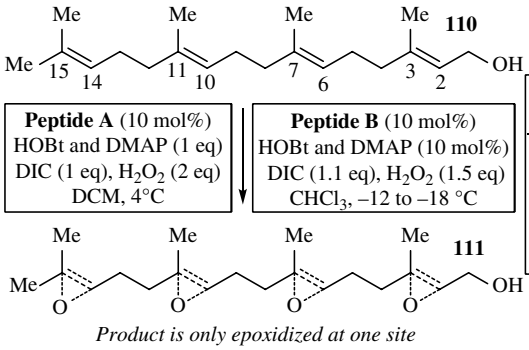

**SCHEME 13.16** Incorporation of atoms of protecting group into molecule.




**SCHEME 13.17** Strategic removal of protecting group without adding to step count.




**SCHEME 13.18** Reversal in selectivity induced by Zn catalyst to favor O-acylation.




| Peptide or oxidant | *Selectivity* 14,15- | 10,11- | 6,7- | 2,3- |
|---|---|---|---|---|
| ***m*-CPBA** | 3.1 | 3.1 | 2.5 | 1.0 |
| **A** | 1.0 | 1.0 | 1.0 | **>100** |
| **B** | 1.0 | 1.8 | **13.2** | 1.5 |

**SCHEME 13.19** Site-selective epoxidation of polyene substrate using small peptide catalysts.

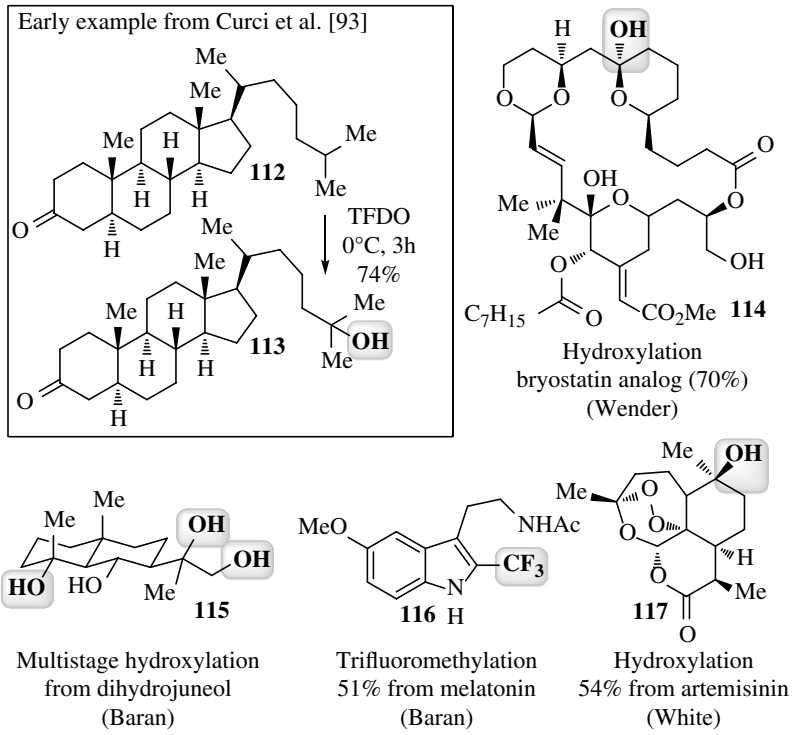
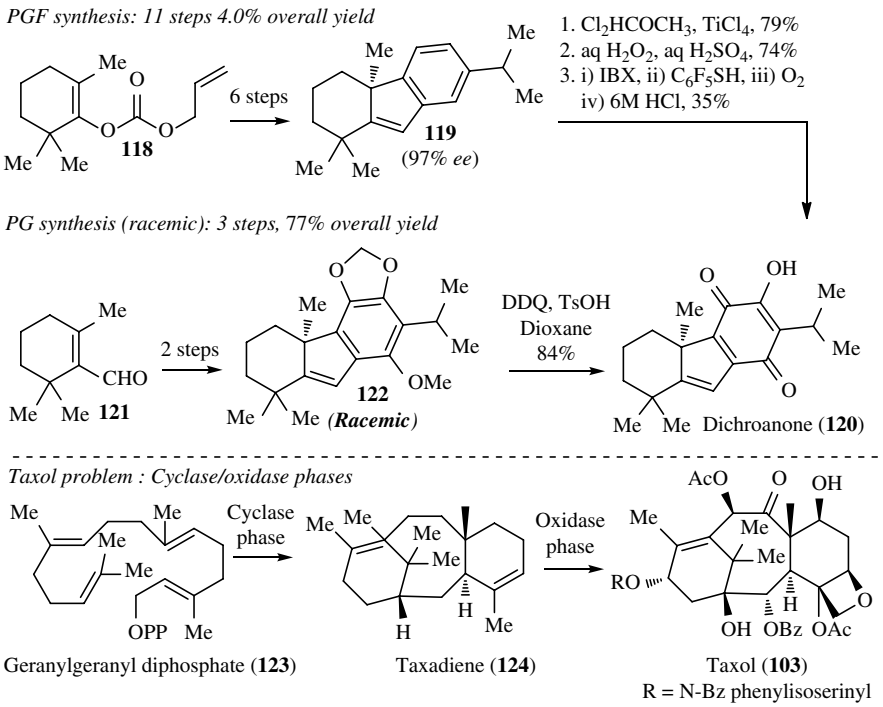



**FIGURE 13.5** Examples of site-specific, late-stage functionalizations.

The Miller group has done significant work in developing site-specific reactions in polyfunctionalized substrates. Key to their success is their exploitation of small peptide catalysts. The example in Scheme 13.19 demonstrates the use of an aspartate-containing pentapeptide (not depicted) for the site-selective epoxidation of geranylgeraniol (**110**) [92]. With *m*-CPBA as the oxidant, this epoxidation has poor site specificity, but by using one of two peptide catalysts, selectivity for the 2,3- or 6,7-double bond is realized.

The modification of complex natural products and advanced intermediates highlights the importance of both site- and chemoselective reactions. The benefits from a strategy standpoint are immense, with one advantage being that natural products can be selectively derivatized to prepare analogs for biological testing. Implementation of this concept will negate the necessity to develop an independent multistep synthesis to access these compounds. Also in the realm of natural product total synthesis, late-stage installation of a functional group will limit the need to carry this functionality through numerous steps in a "protected" state. For either of these strategies to be put to practice, selective reactions that proceed with a high degree of predictability must be developed. The synthetic community has made significant progress in the field, with early work in the area of site-selective C–H oxidation by Curci serving as inspiration (**112** to **113**; Fig. 13.5) [93].




**SCHEME 13.20** Comparison of PGF and PG syntheses of dichroanone and the Taxol® problem.

Alternative examples of selective, late-stage functionalizations are also included to demonstrate the generality of this concept [94–97]. Although the majority of these instances result in the installation of a hydroxyl group, recent work has focused on incorporating other functionalities [96]. For a comprehensive summary of late-stage natural product (and analog) functionalization, please refer to the review by Romo [98].

One point to clarify is that the absence of PGs from a synthesis does not always lead to the most efficient preparation of a molecule (from a step count and yield perspective). The comparison of two syntheses of the diterpenoid dichroanone (**120**) highlights this fact (Scheme 13.20), but what should be taken into account from this example is that value other than shorter syntheses may be realized when PGs are excluded. In 2006, Stoltz and McFadden reported a total synthesis of dichroanone [99] that showcased the group's asymmetric allylation methodology [100]. Their synthesis can be considered to mimic the two-stage cyclase/oxidase strategy that is under investigation in other terpene molecules such as Taxol (**103**) [101] and consists of constructing the unfunctionalized carbon backbone **124** and then selectively oxidizing the core to provide the desired natural product. Although the yield for Stoltz's three-stage oxidation sequence was only 20% (overall: 11 steps, 4% yield), it represented a new strategy to approach molecules of this family and provides the synthetic practitioner with additional disconnections when designing syntheses. For comparison, a 2009 *racemic* synthesis of dichroanone by Alvarez-Manzaneda that incorporated the oxygenation into the starting material in protected form required only three steps and proceeded in 77% overall yield [102]. This second example demonstrates the level of security and utility that PGs can provide. It must be emphasized that the purpose of the Stoltz synthesis was not to produce the world's supply of dichroanone but instead to demonstrate the synthetic utility of a methodology and to advance our field by developing new chemistry. PGF synthesis in this case required substantial optimization to afford late-stage functionalization, but the potential advantages conceived by such a strategy justify this endeavor. This point will be presented again when the total synthesis of the axinellamines is discussed.

Figure 13.6 shows some examples of natural products (**125–130**) that have been recently prepared without the need for PGs [103–108]. Many key examples prior to 2009 have been previously reviewed [53, 54]. As can be observed, these molecules do not share common structural features, highlighting the current generality of the state of PGF synthesis. Also under each structure is the exceptional yield and meager step count for the preparation of these targets. With the overall yield of multistep syntheses commonly being less than 1% (whether using PGs or not), these results demonstrate the vast progress the art of total synthesis has made in recent years toward increasing ideality/efficiency and silencing our critics.

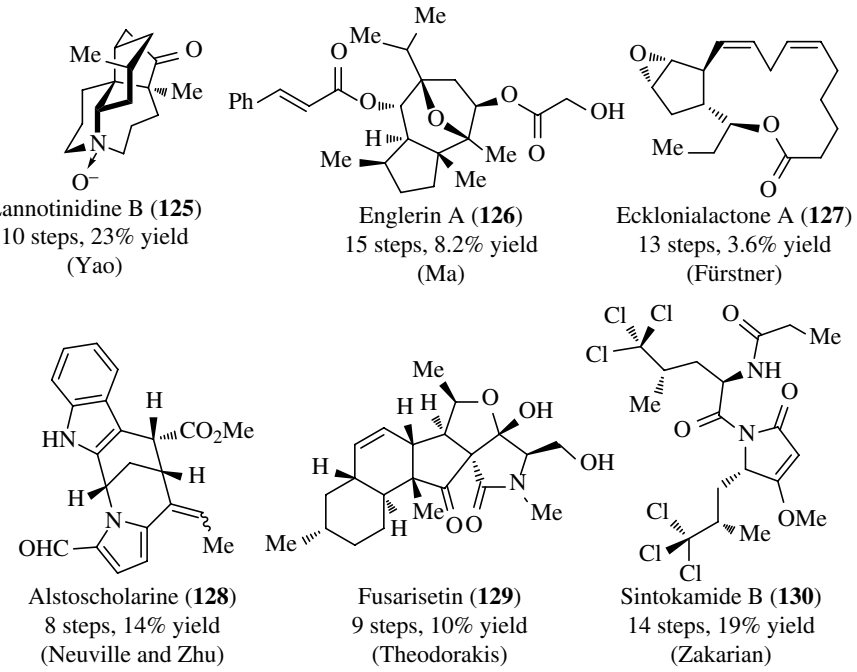



**FIGURE 13.6** A selection of natural products that have been prepared without protecting groups post-2009.

## 13.4 CHALLENGING THE BOUNDARIES OF SYNTHESIS: PIAs

The PIAs are a class of marine natural products whose members display vast structural diversity [26] (for examples, see Fig. 13.7). Oroidin (**25**), the presumed building block to the more complex compounds, and stylissadine A (**131**) represent both ends of the complexity spectrum. As expected, these molecules present significant synthetic challenges due to their highly nitrogenous structures (C : N is ~2 : 1 for many examples). These difficulties are further emphasized if one envisions attempting PGF manipulations. The most well-known molecule in the family is arguably palau'amine (**56**), due to initial reports of promising biological activity [109] and a structural reassignment in 2007 (14 years after isolation). Three groups independently suggested that the *cis*-[3,3,0] ring system should be revised to *trans*-[3,3,0] [40–42]. This fusion is not common in nature, and the reason for this becomes obvious upon building a plastic model of the molecule; the *trans*-5,5 ring system is so strained that it is prone to rupture. While this reassignment elevated the perceived complexity of palau'amine to an even greater level, it served to allow for simplification of the biogenetic relationship between the tetra- and hexacyclic PIAs. The originally proposed *cis*-stereochemistry of palau'amine's cyclopentane ring did not match the other tetracyclic family members, and as a result, the hexacyclic family members required distinct biosynthetic hypotheses [39]. In the following, examples will be presented that highlight the concepts of this chapter (biosynthesis, atom economy, and protecting-group-free synthesis) in the context of PIA synthesis.

After completing the PGF synthesis of sceptrin (**66**) in 2004 [110], Baran focused his attention on the next member on the PIA complexity spectrum, ageliferin (**132**) [111]. Upon examination of the isolation data, it was found that sceptrin and ageliferin were always found together in the sponge extract, with ageliferin being present to a lesser degree. Three distinct pathways for the rupture of the sceptrin cyclobutane to yield ageliferin were proposed [112]. Experimentally, it was found that heating sceptrin in water with microwave irradiation led to a PGF and AE conversion to ageliferin and epimeric nagelamide E (**133**) (Scheme 13.21). Computational examination of the mechanism suggests that this transformation proceeds through dication/diradical intermediate **134** [113].

Baran also postulated that these simpler dimeric PIAs could be precursors to the more advanced tetracyclic and hexacyclic family members. Key to this hypothesis was the common putative intermediate pre-axinellamine (**139**), which hypothetically could be produced from both the rearrangement of sceptrin (**66**) or ageliferin (**132**) (Scheme 13.22) [114]. Oxidative ring expansion (sceptrin) or contraction (ageliferin) induced by either electrophilic oxygen or chlorine, respectively, would lead to formation of the highly functionalized cyclopentane core (**137**) of this hypothetical compound. Further oxidation of the aminoimidazole would then yield pre-axinellamine (**139**).

Baran suggested that through differing hydration states, pre-axinellamine (**139**) could lead to multiple members of

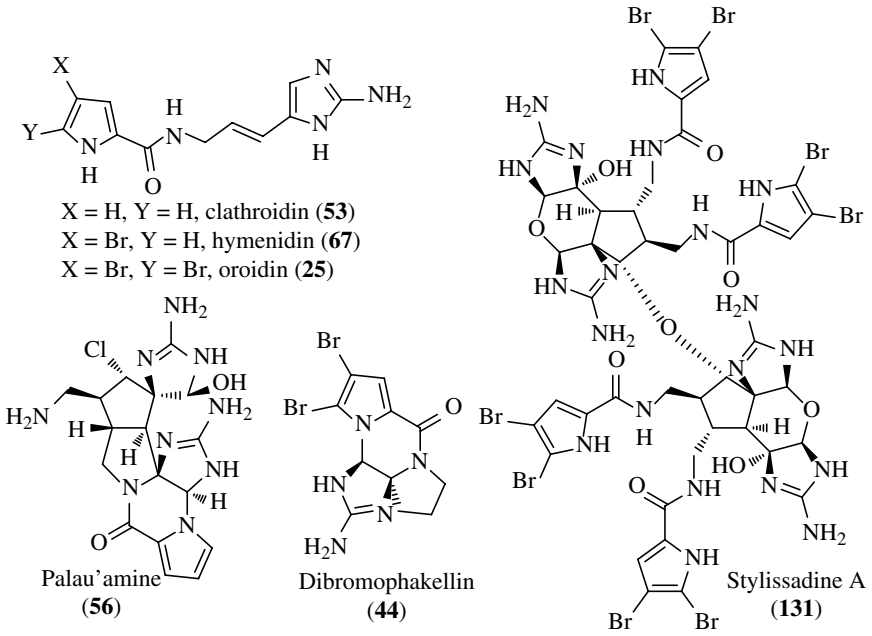
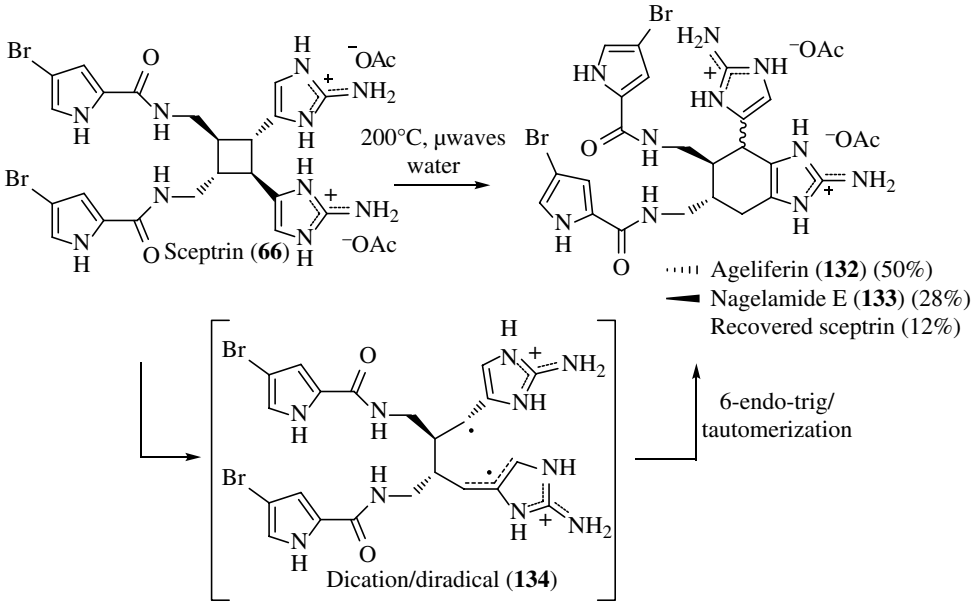


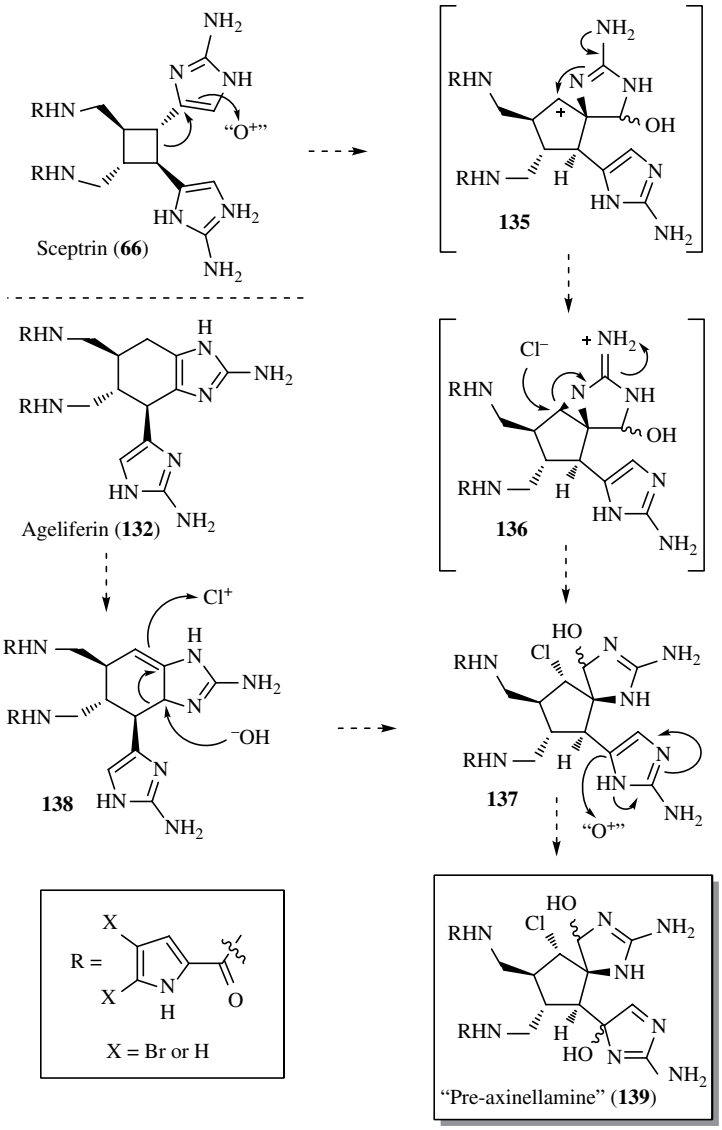

**FIGURE 13.7** A small selection of pyrrole–imidazole alkaloids to display family structural diversity.




**SCHEME 13.21** Conversion of sceptrin to ageliferin by rupture of the cyclobutane.

the tetra- and hexacyclic PIAs (Scheme 13.23) [114]. The cyclization modes that would produce three natural products, konbu'acidin (**140**), massadine chloride (**141**), and axinellamine A (**142**), are depicted. For this strategy to be tested, access to pre-axinellamine would be required. It was thought that pre-axinellamine would immediately cyclize and be unstable and nonisolable, so the unoxidized version, 1,9-dideoxy-pre-axinellamine (**143**), was nominated as the synthetic target to test this theory.

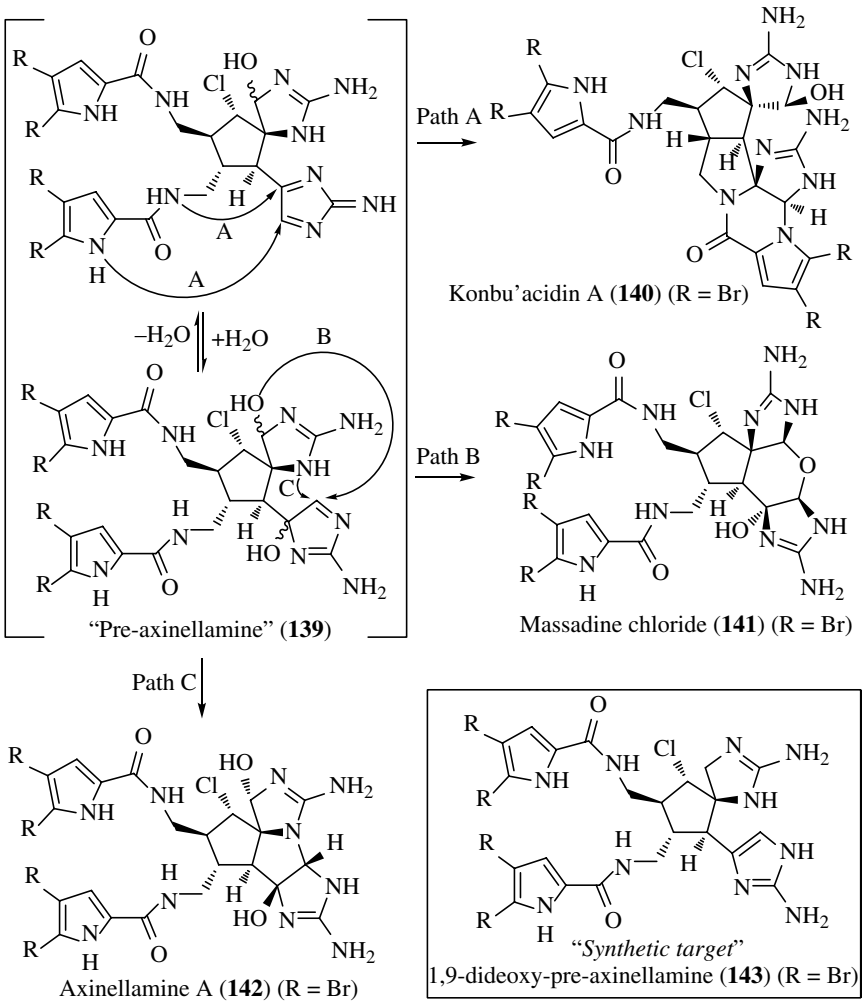
Baran's synthesis of 1,9-dideoxy-pre-axinellamine is outlined in Scheme 13.24 [115]. To form the densely functionalized cyclopentane ring of the natural product family, a cyclohexane to cyclopentane ring contraction strategy was utilized. Diels–Alder reaction of diene **144** and dimethyl fumarate (**145**) produced **146** and set the relative stereochemistry of three stereocenters. After conversions of the esters of **146** to azides, the TIPS was exchanged for a PMB group. This unproductive PG manipulation was necessary as the




**SCHEME 13.22** Baran's hypotheses for the generation of pre-axinellamine from both sceptrin and ageliferin.

steric bulk imparted by TIPS hindered subsequent reactions. Oxidative cleavage of the double bond utilizing ozone produced a linear intermediate, which was then subsequently α-brominated to yield **148**. These α-halogens were necessary to serve as synthetic handles for guanidine installation at a later stage. After intramolecular aldol reaction to form the highly functionalized cyclopentane **149**, selective Br/Cl exchange and PMB removal led to compound **150**. Treatment of this diol with sulfuryl chloride not only eliminated the tertiary alcohol to produce the requisite enone of **151**, but also led to chlorine installation by $S_N2$ displacement of the now secondary allylic alcohol (as the sulfate) by chloride. After ketone reduction, bis-Boc-guanidine was installed through displacement of the allylic bromide. Treatment of **152** with IBX reformed the enone system and induced aza-Michael addition to form the spirocenter found within the target molecule. The facial selectivity for the desired diastereomer in this transformation was poor and under most conditions the undesired diastereomer was exclusively formed. Running the reaction at elevated temperatures could afford a best-case scenario 1.3 : 1 dr with respect to the desired compound. At this point, all stereocenters of the cyclopentane ring had been correctly set, and the remaining α-chloroketone was utilized as a handle for installation of the aminoimidazole. Global Boc-protection was then utilized as a method to prepare a compound (**154**) that could be more readily purified. The product from one-pot azide reduction and subsequent acylation of the resulting amines with **155** was globally deprotected with TFA to yield the target compound, 1,9-dideoxy-pre-axinellamine (**143**).

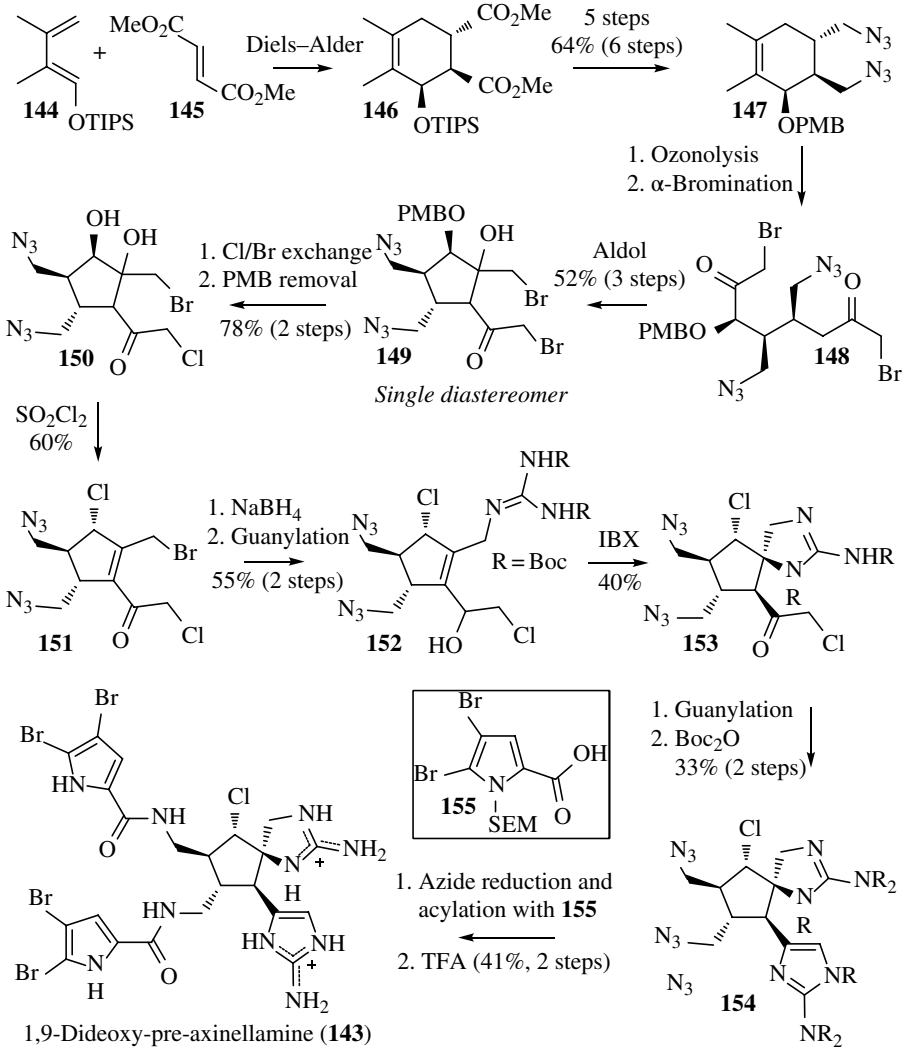
Significant effort was then directed at converting 1,9-dideoxy-pre-axinellamine to tetra-/hexacyclic cores of



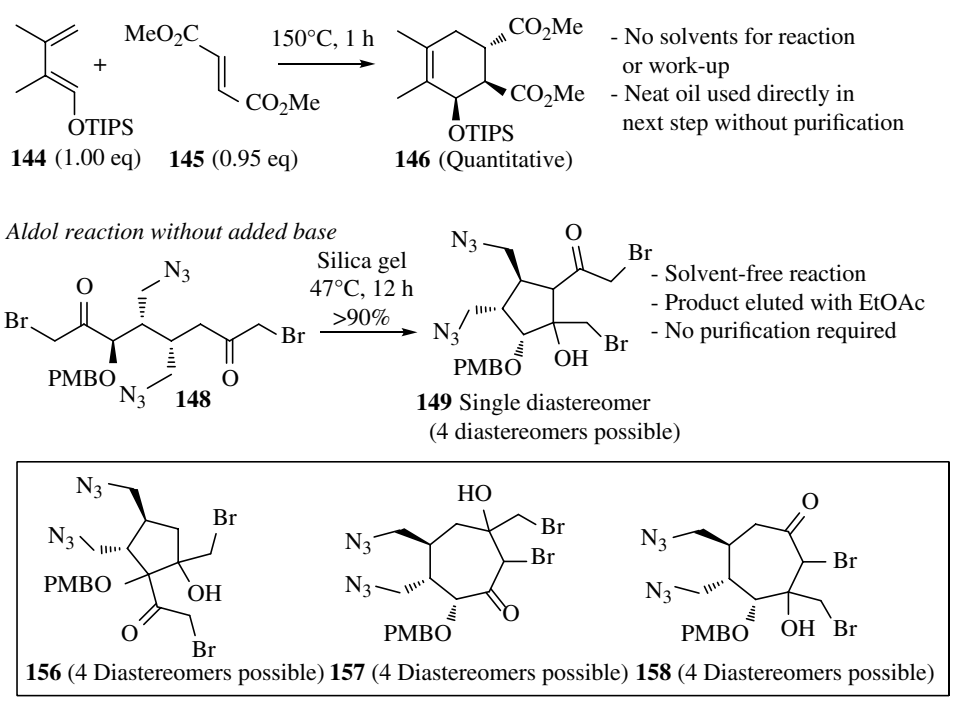

**SCHEME 13.23** Proposed conversion of "pre-axinellamine" to other pyrrole–imidazole alkaloids.

the PIAs through closure modes induced by oxidation of the double bond of the aminoimidazole (such as in Scheme 13.23). Unfortunately, no such conditions could be found that affected such transformations despite extensive screening. One may notice that many of the intermediates in Scheme 13.24 contain PGs and may wonder what this chemistry is doing in a chapter dedicated to PGF synthesis. The PGF portion of Baran's work toward the PIAs will be presented in detail when describing the target-directed syntheses of the natural products. In the following, two reactions from Scheme 13.24 will be highlighted to demonstrate the concept of atom economy in the realm of complex natural product synthesis.

To set the relative stereochemistry of the densely functionalized cyclopentane core found within the natural products, contraction of a cyclohexene ring was utilized. The cyclohexene was formed in quantitative yield via a Diels–Alder reaction of **144** and dimethyl fumarate (**145**), without the need for solvent or catalyst (Scheme 13.25). This conversion represents a truly atom-economical reaction, as the product could be directly used in the subsequent step without purification or work-up. Another example of an AE transformation involves conversion of linear product (**148**) (resulting from cyclohexene **146** after five steps) to the requisite cyclopenta(e)ne. This transformation was complicated by the fact that the molecule had four potential sites of enolization and due to the stereochemistry already present in the molecule, 16 products were possible (**149**, **156–158**). Enolizations induced by base exclusively produced a single but unidentified 7-membered ring diastereomer (**157**). It was noticed that column purification of linear precursor **148** surprisingly led to small amounts of the desired 5-membered **149** being present in isolated **148**. This inspired the development of a silica gel-catalyzed aldol reaction in which **148** was directly adsorbed onto silica gel, and the dry solid heated to 47°C (Scheme 13.25). Amazingly, compound **149** was isolated in >90% yield as a pure, single, unidentified diastereomer by simply washing the product off the silica gel with ethyl acetate. This aldol reaction is an example where stoichiometric base/catalyst was not necessary. The relative




**SCHEME 13.24** Synthesis of 1,9-dideoxy-pre-axinellamine (**143**). Trifluoroacetate counterions have been omitted for clarity.



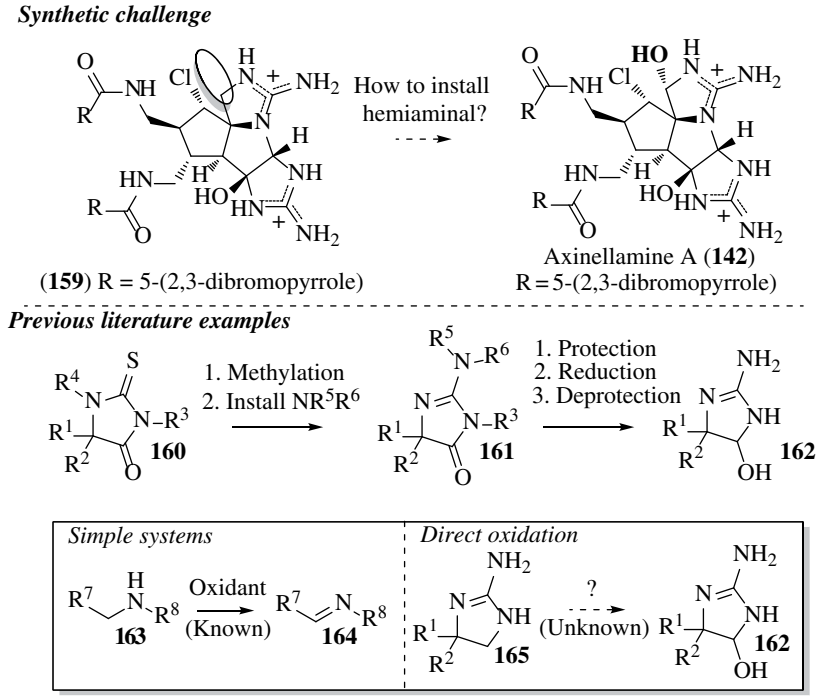

**SCHEME 13.25** Atom-economical reactions from the synthesis of 1,9-dideoxy-pre-axinellamine.

stereochemistry of the two newly formed stereocenters was inconsequential, as it would be subsequently lost via installation of a double bond.

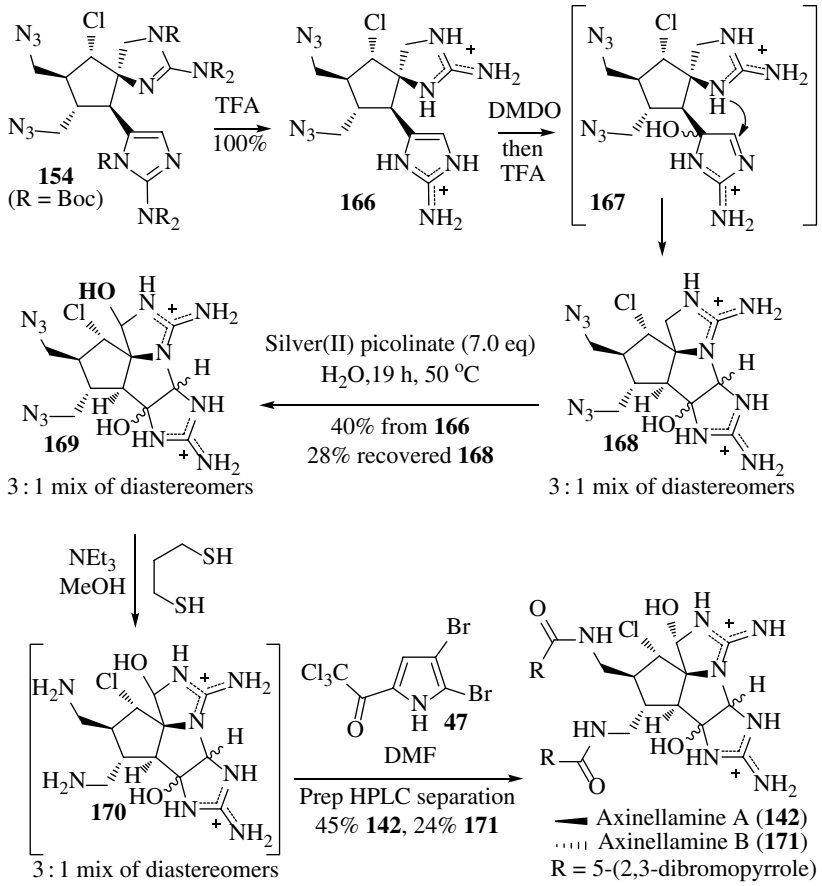
In contrast to what one may anticipate when formulating a synthesis of the PIAs, Baran actually performed his PGF portions of the synthesis when the basic nitrogens were installed. One example from the Baran's PIA work that pushes the boundary of both PGF synthesis and chemoselectivity is the late-stage installation of the cyclic guanidine hemiaminal (**159** to **142**) (Scheme 13.26) [116]. In a previous attempt toward the *cis*-structure of palau'amine, Overman installed this functionality via S-alkylation of a thiohydantoin (**160**), displacement of the thioether with an appropriately protected amine and then reduction of **161** to **162** [117] (Scheme 13.26). While effective, a number of steps were required to deal with the PGs necessary to implement this strategy. Baran hypothesized that late-stage installation of the hemiaminal would minimize the need to protect this highly labile functionality. Although examples of oxidation of simple secondary amines (**163**) to imines (**164**) were known [118], at the time the literature contained no such reports that utilized cyclic guanidines (**165**).

To prepare the substrate necessary to test this late-stage hemiaminal installation strategy in the context of the total synthesis of the axinellamines, Baran utilized an intermediate (**154**) from the 1,9-dideoxy-pre-axinellamine synthesis. Treatment of **154** with TFA led to the fully deprotected compound **166**, which when treated with DMDO led to oxidation of the aminoimidazole double bond to produce a diastereomeric mixture of diols. This material was not isolated but instead directly treated with TFA to induce closure (through the imine) to yield two tetracyclic cores corresponding to both axinellamines A and B (**168**). It was found through experimentation that hemiaminal installation was required at this stage, as performing it as the final step highlighted the instability of pyrroles to many oxidation conditions. After extensive screening, it was determined that silver(II) picolinate [119] could oxidize the methylene of the cyclic guanidine with a high degree of chemoselectivity on a substrate lacking PGs (**168** to **169**) (Scheme 13.27). Silver(II) picolinate led to minimal overoxidation to the imidazolidinone, even with extended reaction times and the use of excess oxidant. This overoxidation was the major issue that rendered other oxidants nonviable. It is interesting to note that the oxidation was not successful on a variety of protected versions of **168** and if a less risky PG strategy was utilized, this transformation may not have been discovered. Finally, reduction of the azides found within **169** with propanedithiol and acylation with the trichloroacetylpyrrole **47** led to the pair of natural product (**142/171**), which could then be separated by preparative HPLC chromatography. As noted earlier, the final four transformations, two of which are oxidations, were carried out on highly nitrogenous substrates without the need for protecting groups.

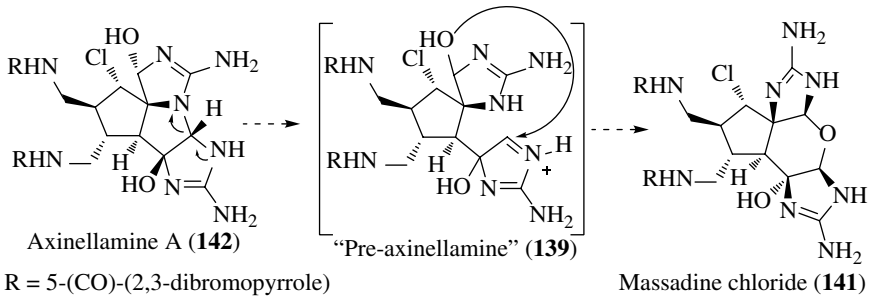
After completing the synthesis of the axinellamines, Baran attempted to convert members of the axinellamines directly to massadine chloride (**141**). It was hoped that fragmentation of the aminal present in the axinellamines would lead to




**SCHEME 13.26** Literature method for installing hemiaminal and direct oxidation proposal.




**SCHEME 13.27** Synthesis of the axinellamines featuring selective oxidation of cyclic guanidine methylene with silver(II) picolinate as a key step. Trifluoroacetate counterions have been omitted for clarity.

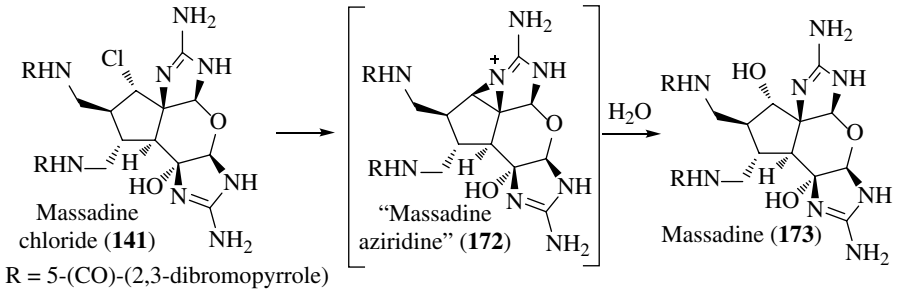



**SCHEME 13.28** Proposed conversion of axinellamine A to massadine chloride through pre-axinellamine.

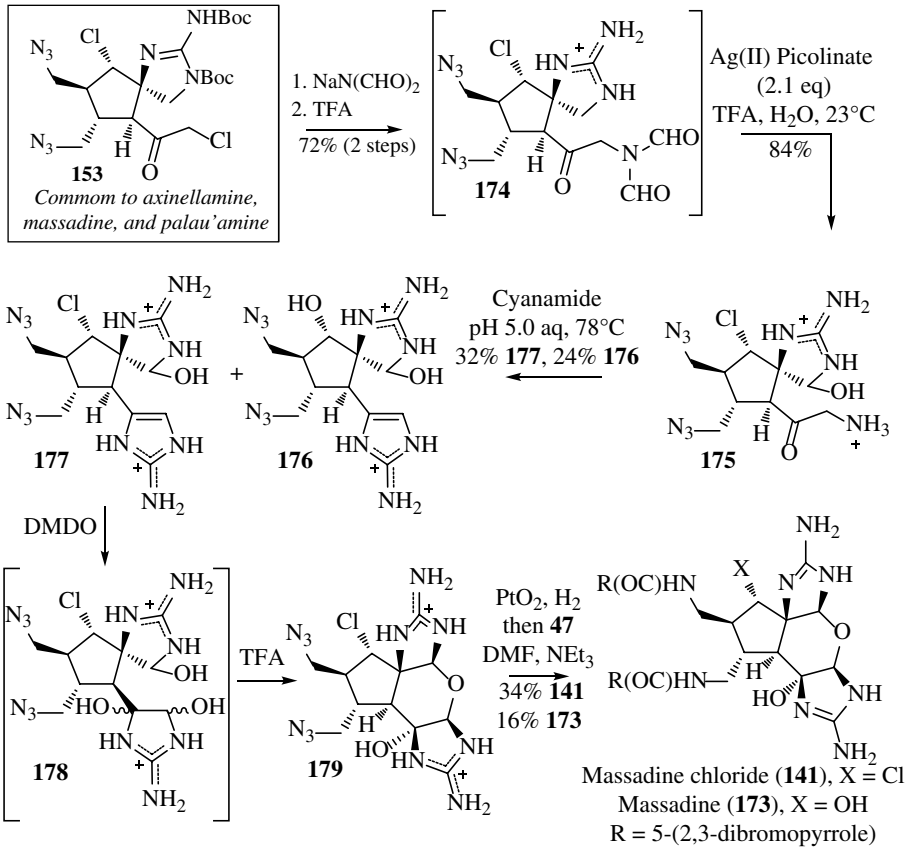
pre-axinellamine (**139**), the key component of the Baran lab's biosynthetic hypothesis (Scheme 13.23). Intermediate **139** would then have the opportunity to close via the hemiaminal oxygen to form massadine chloride (Scheme 13.28) or through involvement of the pyrrole to form one of the other hexacyclic family members. Although conditions could not be found to afford this transformation, if successful, it would represent a completely AE and PGF conversion to access the more advanced members of the PIAs.

As it has been observed with other members of the PIAs, there is a significant propensity of one natural product to convert to another. Massadine chloride (**141**) [120] was isolated 4 years after massadine (**173**) [121], as the –Cl to –OH conversion occurs readily in nature and during the isolation process. This conversion is assumed to go through the putative intermediate massadine aziridine (**172**) (Scheme 13.29) [122]. The reason this is observed for the massadine series and not other members of the PIA family is postulated to be due to the dihedral angle between the adjacent guanidine and chloro functionality in massadine tetracyclic core.

During the synthesis of the massadines [123], the hemiaminal was required to be installed prior to DMDO

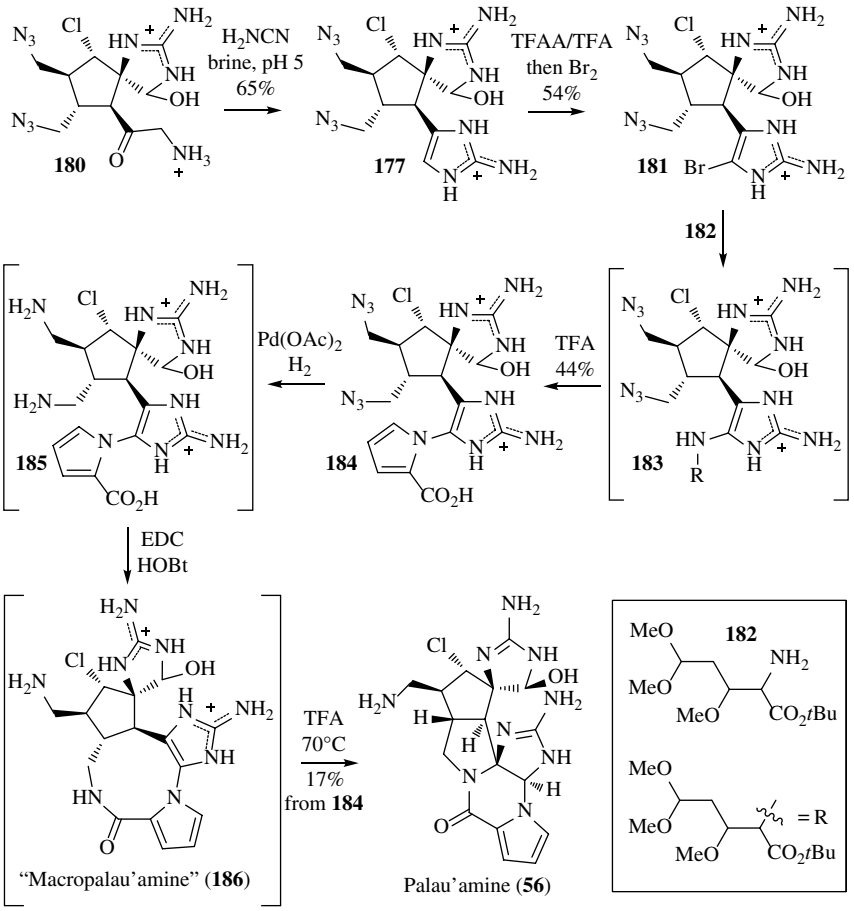



**SCHEME 13.29** Conversion of massadine chloride to massadine proceeding through intermediate massadine aziridine.




**SCHEME 13.30** Utilization of an axinellamine intermediate (**153**) for a divergent total synthesis of massadine (chloride). TFA counterions have been omitted for clarity.

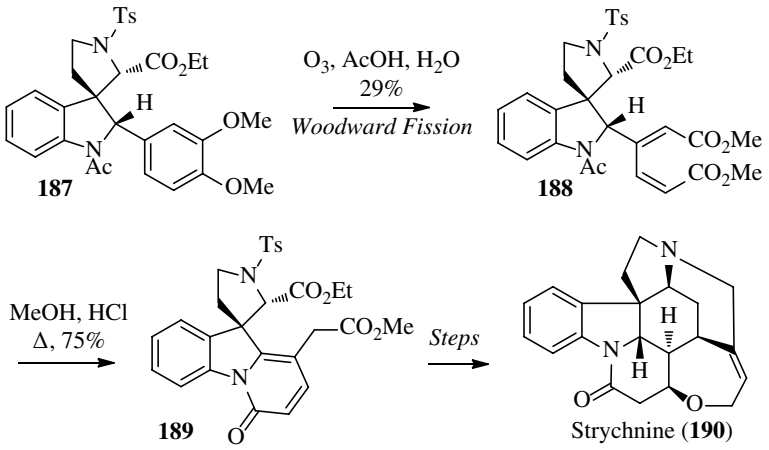
oxidation of the aminoimidazole double bond, as closure of the hemiaminal oxygen needed to occur with preference over the cyclic guanidine nitrogen. Experimentally, it was found that the hemiaminal needed to be introduced prior to forming the aminoimidazole, as the imidazole double bond was not compatible with the silver(II) picolinate. Since this key oxidation was occurring at a much earlier stage of the synthesis, it was desirable to increase the yield of this transformation to facilitate material throughput. It was found that inclusion of 10 vol% TFA in the aqueous silver(II) oxidation of **174** was beneficial. This addition led to higher yields, as evidenced by its full reactant conversion in less than 20 min, even when the reaction is performed at room temperature with only 2.1 eq of the oxidant (compare to conditions in scheme 13.27). Upon treatment of **175** with aqueous cyanamide, a ~1 : 1 mixture of the desired product **177** and the compound resulting from chloride to hydroxyl exchange (**176**) resulted (Scheme 13.30). Although both the –OH and –Cl could be advanced to natural products (massadine and massadine chloride, respectively), more control would be necessary when utilizing a similar strategy toward palau'amine (*vide infra*; Scheme 13.31), as only the –Cl-containing compounds are known in the hexacyclic family members. Oxidation of the imidazole double bond contained




**SCHEME 13.31** Final five steps in palau'amine synthesis proceed without the need for protecting groups. Trifluoroacetate counterions are omitted for clarity.

within **177** with DMDO and treatment with TFA now led to exclusive closure of the hemiaminal hydroxyl group (vs. cyclic guanidine nitrogen) to form the tetracyclic core of the massadines. This fortunate outcome alleviated the need to protect the cyclic guanidine to prevent the unwanted axinellamine closure. Azide reduction and acylation of the resulting primary amines then yielded a mixture of massadine and massadine chloride, which were separated by preparative HPLC.

With regard to PGF synthesis, the final sequence in Baran's synthesis of palau'amine is quite remarkable [124]. Palau'amine on paper has an elevated level of synthetic challenge for three reasons: (1) the *trans*-5,5 ring system is highly strained; (2) the pyrrole is embedded within the core and as a result must be installed at an earlier stage; and (3) the two primary amines resulting from azide reduction must be differentiated during the synthesis. Beginning with compound **180**, Baran installed the aminoimidazole with cyanamide, but in contrast to this process in the massadine synthesis, the reaction was run in saturated brine. The high concentration of the chloride anion prevented unwanted Cl/OH conversion (as observed in the massadine synthesis; Scheme 13.30) and allowed for the desired chloro-containing product to be isolated in 65% yield (Scheme 13.31). Treatment of **177** with bromine installed an electrophilic handle (iminoyl bromide) for installation of the pyrrole through a nucleophilic process. Due to the weak nucleophilicity of the pyrrole nitrogen, a surrogate **182** was utilized, which after treatment with acid formed compound **184**. After reduction of both azides, treatment with EDC fortunately led to amide formation with the desired amine to form the entropy-reducing cyclic intermediate termed "macropalau'amine (**186**)." Despite the immense strain of the ring system that would result from transannular closure, all that was required for conversion to the natural product was heating **186** in TFA. Although PGs were not required for the final five-step sequence, it should be mentioned that in almost all transformation TFA was present to prevent degradation of the unstable intermediates. It was noted during isolation that palau'amine was prone to rapid decomposition above pH 6.5 [109], so the conditions that could be employed in the end game were limited.




**SCHEME 13.32** "Woodward fission" that allowed for completion of strychnine total synthesis.

The majority of Baran's work toward the PIAs utilized "pre-axinellamine" as a foundation. While this presumed reactive species could not be generated directly, or as an intermediate via the conversion of one natural product to another (axinellamine A (**142**) to massadine chloride (**141**); Scheme 13.28), we cannot rule out Mother Nature using this strategy for the preparation of the more complex PIAs. Despite if "pre-axinellamine" exists or not, one must recognize the value of logically planned retrosyntheses guided by biosynthetic hypotheses. As Baran mentions [114], this outcome bears resemblance to Woodward's 1954 synthesis of strychnine (**190**) [125] (Scheme 13.32).

Woodward based his strategy on the premise that strychnine was generated biogenetically by oxidative fission of the electron-rich aromatic ring present in **187**. It has since been determined that strychnine is not produced in nature by this pathway [126]. Regardless, this "Woodward fission" idea allowed for what is regarded as one of the greatest accomplishments in total synthesis.

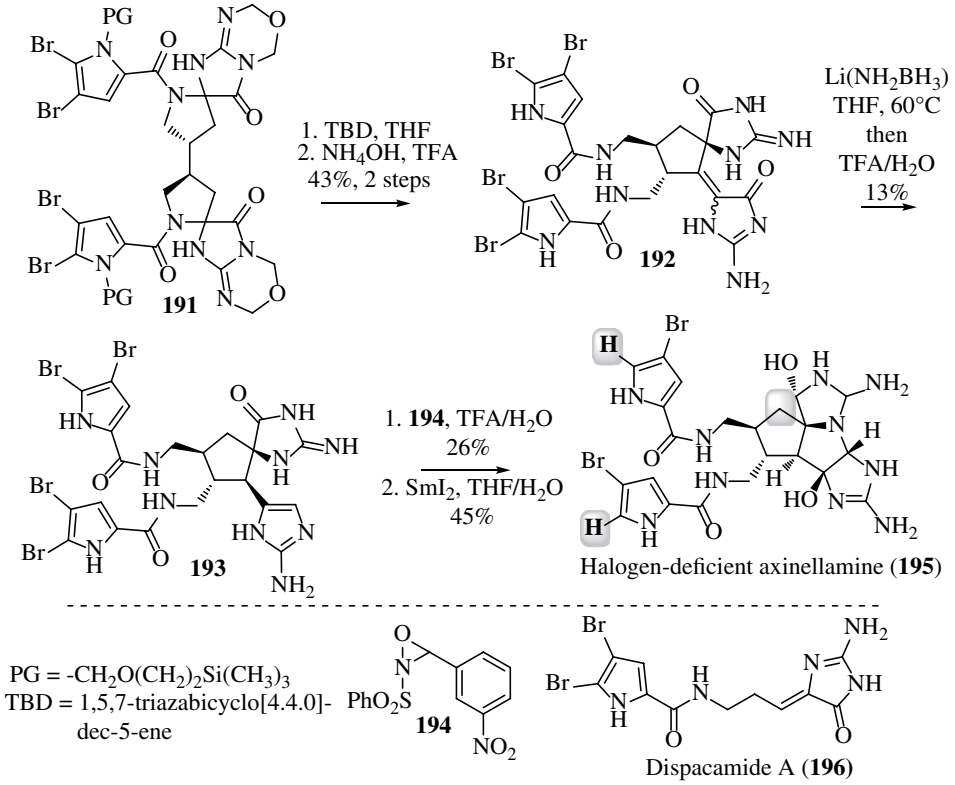
Groups other than Baran's have contributed significantly to the development of chemistry directed toward the total synthesis of the PIAs. Harran utilized a symmetry-based strategy to prepare "axinellamine deficient in halogens" (**195**) (Scheme 13.33), with the positions of the missing halogens highlighted [127]. Although compound **191** does contain PGs, the remarkable final three steps do not and so it was decided to include this example. Compound **191** represents a dimeric dispacamide (**196**) derivative, which upon treatment with the base TBD and subsequent PG removal yielded enamide **192**. The enamide carbonyl was then selectively deoxygenated and treated with TFA to induce double-bond migration to form the aminoimidazole **193**. The undesired diastereomer was the major product in this step and contributed to the modest yield. Imidazole oxidation with oxaziridine **194** led to closure to the tetracyclic core of the axinellamines. Finally, treatment with an excess of samarium iodide led to slow reduction of the C1 carbonyl, with accompanied undesired pyrrole-C2 debromination. Overall, only 13 steps were required to arrive at **195**, demonstrating the efficiency of this approach. Harran also utilized symmetry-based strategies for the synthesis of ageliferin [128] and in studies toward palau'amine [129].

Horne was able to provide support for the biosynthetic hypothesis that mauritiamine (**197**) results from dimerization of an oroidin-like species. Upon examination of the natural product structure, it appears to be the union of oroidin (**25**) and dispacamide (**196**) (Scheme 13.34). Horne was able to dimerize vinyl aminoimidazole **26** under oxidative conditions to provide the core of mauritiamine (**199**) [130]. After installation of the dibromopyrroles via acylation, the natural product was realized in six steps from ornithine methyl ester (**198**), without the need for PGs.

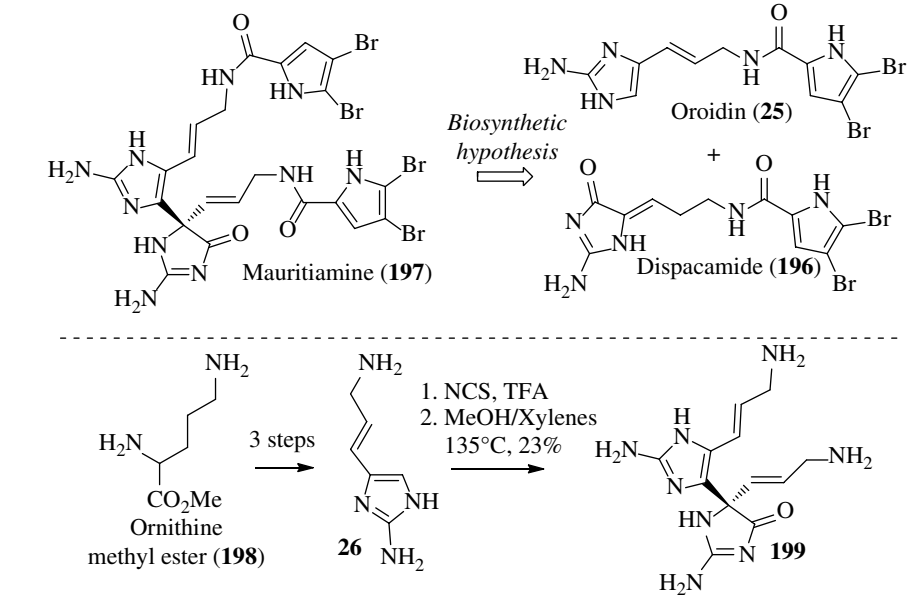
An alternative cyclization strategy toward dibromophakellin (**44**) was reported by Feldman [131]. Subjection of a thiolated dihydrooroidin derivative (**200**) to Pummerer conditions induced closure to tetracycle **201** (Scheme 13.35). Oxidation with ceric ammonium nitrate led to the cyclic urea-containing natural product dibromophakellistatin (**202**), which could be converted to dibromophakellin in two steps. This represents a complimentary PGF mode of closure to that developed by Buchi/Horne (Scheme 13.7). Feldman is currently attempting to apply this strategy to the synthesis of the more complex PIAs such as palau'amine (**56**) [132].

## 13.5 CONCLUSION

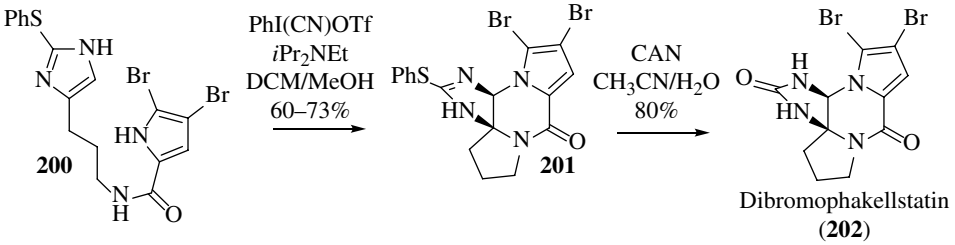
The PIA chemistry presented in this chapter represents only a minor portion of the extensive work directed at synthesizing these complex targets. To find examples that encompass either atom-economical processes or protecting-group-free transformations was a challenging task, due in part to the nitrogen-rich nature of these natural products. In all cases, the development of new strategies/chemistry was necessary, without which the




**SCHEME 13.33** Harran's synthesis of halogen-deficient axinellamine via symmetry-based strategy.




**SCHEME 13.34** Horne's protecting-group-free total synthesis of mauritiamine.




**SCHEME 13.35** Feldman's Pummerer route to dibromophakellstatin, which was advanced to dibromophakellin (**44**).

synthesis of these compounds may still not be realized. To put things in perspective, an analysis of Baran's ideality ranking of targets completed in his lab demonstrates that the four least "ideal" synthetic routes are toward PIAs [palau'amine (**56**, 32%), axinellamine A (**142**, 36%), massadine Cl (**141**, 36%), and sceptrin (**66**, 36%)] [47]. It should be noted that an improved synthesis of a derivative of key intermediate **174** used to prepare **56**, **141**, and **142** was reported in 2011 [133]. Through the use of this alternative route, the ideality of the synthesis of the axinellamines was greatly increased to 63%. This result suggests that there is still substantial room for improvement in the arena of PIA preparation, a challenge that the synthesis community has already eagerly accepted.

## REFERENCES


1. A. Kossel, *Zeit. Physiol. Chem.* 1896–1897, **22**, 176–187.
2. G. Dodson, A. Wlodawer, *Trends Biochem. Sci.* 1998, **23**, 347–352.
3. L. Polgár, *Cell. Mol. Life Sci.* 2005, **62**, 2161–2172.
4. A. Battistoni, F. Pacello, A. P. Mazzetti, C. Capo, J. S. Kroll, P. R. Langford, A. Sansone, G. Donnarumma, P. Valenti, G. Rotilio, *J. Biol. Chem.* 2001, **276**, 30315–30325.
5. L. T. Rozum, F. Taketa, *Marq. Med. Rev.* 1965, **31**, 33.
6. W. C. Rose, *Nutr. Abstr. Rev.* 1957, **27**, 631–647.
7. S. E. Snyderman, A. Boyer, E. Roitman, L. E. Holt, P. H. Prose, *Pediatrics* 1963, **31**, 786–801.
8. P. van Ruitenbeek, A. Sambeth, A. Vermeeren, S. N. Young, W. J. Reidel, *Brit. J. Pharmacol.* 2009, **157**, 91–103.
9. J. D. Kopple, M. E. Swendseid, *J. Clin. Investig.* 1975, **55**, 881–891.
10. V. R. Young, *J. Nutr.* 1994, **124**, 1517S–1523S.
11. P. Alifano, R. Fani, P. Liò, A. Lazcano, M. Bazzicalupo, M. S. Carlomagno, C. B. Bruni, *Microbiol. Rev.* 1996, **60**, 44–69.
12. R. K. Kulis-Horn, M. Persicke, J. Kalinowski, *Microb. Biotechnol.* 2013, **7**, 5–25.
13. A. Stepansky, T. Leustek, *Amino Acids*, 2006, **30**, 127–142.
14. H. M. R. Epps, *Biochem. J.* 1945, **39**, 42–46.
15. M. Suchi, H. Sano, H. Mizuno, Y. Wada, *Genomics* 1995, **29**, 98–104.
16. H. Horan, D. G. O'Donovan, *J. Chem. Soc. (C)* 1971, 2083–2085.
17. A. P. Santo, P. R. H. Moreno, *Natural Products*, Springer: New York (2013), pp. 861–882.
18. R. G. Hendrickson, A. P. Morocco, M. I. Greenberg, *J. Emerg. Med.* 2004, **26**, 429–432.
19. S. Basu, M. Mitra, A. Ghosh, *Clin. Biochem.* 2013, **28**, 433–435.
20. S. E. Norell, P.-A. Granström, *Brit. J. Ophthalmol.* 1980, **64**, 137–141.
21. S. G. Davies, P. M. Roberts, P. T. Stephenson, H. R. Storr, J. E. Thomson, *Tetrahedron* 2009, **65**, 8283–8296, and references within.
22. C. U. B. Pinheiro, *Econ. Bot.* 1997, **51**, 49–58.
23. I. N. Abreu, N. L. Andreazza, A. C. H. F. Sawaya, M. N. Eberlin, P. Mazzafera, *Plant Biol.* 2009, **9**, 793–799.
24. L. Maat, H. C. Beyerman, *The Alkaloids: Chemistry and Pharmacology*, vol **22**. Academic Press: New York (1984), pp. 281–333.
25. E. Brochmann-Hanssen, M. A. Nunes, C. K. Olah, *Planta Med.* 1975, **28**, 1–5.
26. B. Forte, B. Malgesini, C. Piutti, F. Quartieri, A. Scolaro, G. Paper, *Mar. Drugs*, 2009, **7**, 705–753.
27. T. L. Simmons, R. C. Coates, B. R. Clark, N. Engene, D. Gonzalez, E. Esquenazi, P. C. Dorrestein, W. H. Gerwick, *Proc. Natl. Acad. Sci. U.S.A.*, 2008, **105**, 4587–4594.
28. P. Andrade, R. Willoughby, S. A. Pomponi, R. G. Kerr, *Tetrahedron Lett.* 1999, **40**, 4775–4778.
29. K. F. Albizati, D. J. Faulkner, *J. Org. Chem.* 1985, **50**, 4163–4164.
30. G. Genta-Jouve, N. Cachet, S. Holderight, F. Oberhänsli, J.-L. Teyssié, R. Jeffree, A. Al Mourabit, O. P. Thomas, *ChemBioChem*, 2011, **12**, 2298–2301.
31. T. Lindel, M. Hochgürtel, M. Assmann, M. Köck, *J. Nat. Prod.* 2000, **63**, 1566–1569.
32. A. Gravel, E. Poupon, *Nat. Prod. Rep.* 2010, **27**, 32–56.
33. E. P. Stout, B. I. Morinaka, Y.-G. Wang, D. Romo, T. F. Molinksi, *J. Nat. Prod.* 2012, **75**, 527–530.
34. A. Al-Mourabit, P. Potier, *Eur. J. Org. Chem.* 2001, 237–243.
35. A. Al-Mourabit, M. A. Zancanella, S. Tilvi, D. Romo, *Nat. Prod. Rep.* 2011, **28**, 1229–1260.
36. G. Sharma, B. Magdoff-Fairchild, *J. Org. Chem.* 1977, **42**, 4118–4124.
37. L. H. Foley, G. Büchi, *J. Am. Chem. Soc.* 1982, **104**, 1776–1777.
38. K. J. Wiese, K. Yakushijin, D. A. Horne, *Tetrahedron Lett.* 2002, **43**, 5135–5136.
39. R. B. Kinnel, H.-P. Gehrken, R. Swali, G. Skoropowski, P. J. Scheuer, *J. Org. Chem.* 1998, **63**, 3281–3286.
40. M. Köck, A. Grube, *Angew. Chem. Int. Ed.* 2007, **46**, 2320–2324.
41. M. S. Buchanan, A. R. Carroll, R. J. Quinn, *Tetrahedron Lett.* 2007, **48**, 4573–4574.
42. H. Kobaysashi, K. Kitamura, K. Nagai, Y. Nakao, N. Fusetani, R. W. M. van Soest, S. Matsunaga, *Tetrahedron Lett.* 2007, **48**, 2127–2129.
43. Z. Ma, J. Lu, X. Wang, C. Chen, *Chem. Commun.* 2011, **47**, 427–429.
44. J. Mulzer, *Nat. Prod. Rep.* 2014, **31**, 595–603.
45. J. B. Hendrickson, *J. Am. Chem. Soc.* 1975, **97**, 5784–5800.
46. P. A. Wender, *Chem. Rev.* 1996, **96**, 1–2.
47. T. Gaich, P. S. Baran, *J. Org. Chem.* 2010, **75**, 4657–4673.
48. N. Z. Burns, P. S. Baran, R. W. Hoffmann, *Angew. Chem. Int. Ed.* 2009, **48**, 2854–2867.
49. P. A. Wender, V. A. Verma, T. J. Paxton, T. H. Pillow, *Acc. Chem. Res.* 2008, **41**, 40–49.
50. B. M. Trost, *Science*, 1991, **254**, 1471–1477.

51. T. Newhouse, P. S. Baran, R. W. Hoffmann, *Chem. Soc. Rev.* 2009, **38**, 3010–3021.
52. K. Sanderson, *Nature*, 2011, **469**, 18–20.
53. R. W. Hoffmann, *Synthesis*, 2006, 3531–3541.
54. I. S. Young, P. S. Baran, *Nat. Chem.* 2009, **1**, 193–205.
55. R. A. Sheldon, *Green Chem.* 2007, **9**, 1273–1283.
56. E. Valeur, M. Bradley, *Chem. Soc. Rev.* 2009, **38**, 606–631.
57. C. Gunanathan, Y. Ben-David, D. Milstein, *Science* 2007, **317**, 790–792.
58. B. Kang, Z. Fu, S. H. Hong, *J. Am. Chem. Soc.* 2013, **135**, 11704–11707.
59. N. Nishiwaki, *Methods and Applications of Cycloaddition Reactions in Organic Syntheses*. John Wiley & Sons, Inc: New York (2014), pp. 1–672.
60. R. P. Walker, D. J. Faulkner, D. Van Engen, J. Clardy, *J. Am. Chem. Soc.* 1981, **103**, 6773–6775.
61. P. A. Keifer, R. E. Schwartz, M. E. S. Koker, R. G. Hughes, D. Rittschof, K. L. Rinehart, *J. Org. Chem.* 1991, **56**, 2965–2975.
62. A. Skiredj, M. A. Beniddir, D. Joseph, K. Leblanc, G. Bernadat, L. Evanno, E. Poupon, *Angew. Chem. Int. Ed.* 2014, **53**, 6419–6424.
63. B. M. Trost, H. Ito, E. R. Silcoff, *J. Am. Chem. Soc.* 2001, **123**, 3367–3368.
64. B. M. Trost, D. Amans, W. M. Seganish, C. K. Chung, *J. Am. Chem. Soc.* 2009, **131**, 17087–17089.
65. M. Bartlett, *Chem. N. Z.*, 2012, 11–16.
66. S. J. Mickel, et al. *Org. Proc. Res. Develop.* 2004, **8**, 92–100.
67. C. A. Kuttruff, M. D. Eastgate, P. S. Baran, *Nat. Prod. Rep.* 2014, **31**, 419–432.
68. B. M. Trost, *Angew. Chem. Int. Ed.* 1995, **34**, 259–281.
69. B. M. Trost, *Acc. Chem. Res.* 2002, **35**, 695–705.
70. C. M. Marson, *Chem. Soc. Rev.* 2012, **41**, 7712–7722.
71. R. H. Crabtree, *J. Chem. Soc., Dalton Trans.* 2001, 2437–2450
72. E. J. Corey, W. R. Hertler, *J. Am. Chem. Soc.* 1958, **80**, 2903–2904.
73. C. C. C. Johansson Seechurn, M. O. Kitching, T. J. Colacot, V. Snieckus, *Angew. Chem. Int. Ed.* 2012, **51**, 5062–5085.
74. E. J. Corey, X.-M. Cheng, *The Logic of Chemical Synthesis*, John Wiley & Sons, Inc.: New York (1995).
75. N. K. Garg, R. Sarpong, B. M. Stoltz, *J. Am. Chem. Soc.* 2002, **124**, 13179–13184.
76. D. Mandal, A. D. Yamaguchi, J. Yamaguchi, K. Itami, *J. Am. Chem. Soc.* 2011, **133**, 19660–19663.
77. J. Yamaguchi, K. Itami, A. D. Yamaguchi, *Angew. Chem. Int. Ed.* 2012, **51**, 8960–9009.
78. D. Y.-K. Chen, S. Won Youn, *Chem. – Eur. J.* 2012, **18**, 9452–9474.
79. P. S. Baran, T. J. Maimone, J. M. Richter, *Nature* 2007, **446**, 404–408.
80. R. A. Robinson, *J. Chem. Soc., Trans.* 1917, **111**, 762–768.
81. M. Razzak, J. K. De Brabander, *Nat. Chem. Biol.* 2011, **7**, 865–875.
82. S. Danishefsky, D. Dumas, *Chem. Commun.* 1968, 1287–1288.
83. P. J. Kocienski, *Protecting Groups*, 3rd Edition, Thieme: New York (2006), pp. 1–679.
84. E. J. Corey, A. Venkateswarlu, *J. Am. Chem. Soc.* 1972, **94**, 6190–6191.
85. P. G. M. Wuts, T. W. Greene, *Greene's Protective Groups in Organic Synthesis*, 4th Edition, John Wiley & Sons Inc.: New York (2007), pp. 1–1082.
86. K. C. Nicolaou, D. Vourloumis, N. Winssinger, P. S. Baran, *Angew. Chem. Int. Ed.* 2000, **39**, 44–122.
87. K. C. Nicolaou, Z. Yang, J. J. Liu, H. Ueno, P. G. Nantermet, R. K. Guy, C. F. Clalborne, J. Renaud, E. A. Couladouros, K. Paulvannan, E. J. Sorensen, *Nature* 1994, **367**, 630–634.
88. M. Himmelbauer, J.-B. Farcet, J. Gagnepain, J. Mulzer, *Org. Lett.* 2013, **15**, 3098–3101.
89. B. M. Trost, *Science* 1983, **219**, 245–250.
90. R. A. Shenvi, D. P. O'Malley, P. S. Baran, *Acc. Chem. Res.* 2009, **42**, 530–541.
91. T. Ohshima, T. Iwasaki, Y. Maegawa, A. Yoshiyama, K. Mashima, *J. Am. Chem. Soc.* 2008, **130**, 2944–2945.
92. P. A. Lichtor, S. J. Miller, *Nat. Chem.* 2012, **4**, 990–995.
93. R. Mello, M. Fiorentino, C. Fusco, R. Curci, *J. Am. Chem. Soc.* 1989, **111**, 6749–6757.
94. P. A. Wender, M. K. Hilinski, A. V. W. Mayweg, *Org. Lett.* 2005, **7**, 79–82.
95. K. Chen, P. S. Baran, *Nature* 2009, **459**, 824–828.
96. Y. Ji, T. Brueckl, R. D. Baxter, Y. Fujiwara, I. S. Seiple, S. Su, D. G. Blackmond, P. S. Baran, *Proc. Natl. Acad. Sci. U.S.A.* 2011, **108**, 14411–14415.
97. M. S. Chen, M. C. White, *Science* 2007, **318**, 783–787.
98. O. Robles, D. Romo, *Nat. Prod. Rep.* 2014, **31**, 318–334.
99. R. M. McFadden, B. M. Stoltz, *J. Am. Chem. Soc.* 2006, **128**, 7738–7739.
100. J. T. Mohr, D. C. Behenna, A. M. Harned, B. M. Stoltz, *Angew. Chem. Int. Ed.* 2005, **44**, 6924–6927.
101. Y. Ishihara, P. S. Baran, *Synlett* 2010, **12**, 1733–1745.
102. E. Alvarez-Manzaneda, R. Chahboun, E. Cabrera, E. Alvarez, R. Alvarez-Manzaneda, R. Meneses, H. Es-Samti, A. Fernández, *J. Org. Chem.* 2009, **74**, 3384–3388.
103. H. M. Ge, L.-D. Zhang, R. X. Tan, Z.-J. Yao, *J. Am. Chem. Soc.* 2012, **134**, 12323–12325.
104. Q. Zhou, X. Chen, D. Ma, *Angew. Chem. Int. Ed.* 2010, **49**, 3513–3516.
105. V. Hickmann, M. Alcarazo, A. Fürstner, *J. Am. Chem. Soc.* 2010, **132**, 11042–11044.
106. T. Gerfaud, C. Xie, L. Neuville, J. Zhu, *Angew. Chem. Int. Ed.* 2011, **50**, 3954–3957.
107. J. Xu, E. J. E. Caro-Diaz, L. Trzoss, E. A. Theodorakis, *J. Am. Chem. Soc.* 2012, **134**, 5072–5075.
108. Z. Gu, A. Zakarian, *Angew. Chem. Int. Ed.* 2010, **49**, 9702–9705.
109. R. B. Kinnel, H.-P. Gehrken, P. J. Scheuer, *J. Am. Chem. Soc.* 1993, **115**, 3376–3377.

110. P. S. Baran, A. L. Zografos, D. P. O'Malley, *J. Am. Chem. Soc.* 2004, **126**, 3726–3727.
111. J. Kobayashi, M. Tsuda, *Tetrahedron* 1990, **46**, 5579–5586.
112. P. S. Baran, D. P. O'Malley, A. L. Zografos, *Angew. Chem. Int. Ed.* 2004, **43**, 2674–2677.
113. B. H. Northrop, D. P. O'Malley, A. L. Zografos, P. S. Baran, K. N. Houk, *Angew. Chem. Int. Ed.* 2006, **45**, 4126–4130.
114. M. Köck, A. Grube, I. B. Seiple, P. S. Baran, *Angew. Chem. Int. Ed.* 2007, **46**, 6586–6594.
115. J. Yamaguchi, I. B. Seiple, I. S. Young, D. P. O'Malley, M. Maue, P. S. Baran, *Angew. Chem. Int. Ed.* 2008, **47**, 3578–3580.
116. D. P. O'Malley, J. Yamaguchi, I. S. Young, I. B. Seiple, P. S. Baran, *Angew. Chem. Int. Ed.* 2008, **47**, 3581–3583.
117. B. A. Lanman, L. E. Overman, R. Paulini, N. S. White, *J. Am. Chem. Soc.* 2007, **129**, 12896–12900.
118. H. Choi, M. P. Doyle, *Chem. Commun.* 2007, 745–747, and references within.
119. G. W. A. Fowles, R. W. Matthews, R. A. Walton, *J. Chem. Soc. (A)* 1968, 1108–1113.
120. A. Grube, S. Immel, P. S. Baran, M. Köck, *Angew. Chem. Int. Ed.* 2007, **46**, 6721–6724.
121. S. Nishimura, S. Matsunaga, M. Shibazaki, K. Suzuki, K. Furihata, R. W. M. van Soest, N. Fusetani, *Org. Lett.* 2003, **5**, 2255–2257.
122. S. Wang. A. S. Dilley, K. G. Poullennec, D. Romo, *Tetrahedron* 2006, **62**, 7155–7161.
123. S. Su, I. B. Seiple, I. S. Young, P. S. Baran, *J. Am. Chem. Soc.* 2008, **130**, 16490–16491.
124. I. B. Seiple, S. Su, I. S. Young, C. A. Lewis, J. Yamaguchi, P. S. Baran, *Angew. Chem. Int. Ed.* 2010, **49**, 1095–1098.
125. R. B. Woodward, M. P. Cava, W. D. Ollis, A. Hunger, H. U. Daeniker, K. Schenker, *J. Am. Chem. Soc.* 1954, **76**, 4749–4751.
126. S. I. Heimberger, A. I. Scott, *J. Chem. Soc., Chem. Commun.* 1973, 217–218.
127. H. Ding, A. G. Roberts, P. G. Harran, *Angew. Chem. Int. Ed.* 2012, **51**, 4340–4343.
128. H. Ding, A. G. Roberts, P. G. Harran, *Chem. Sci.* 2013, **4**, 303–306.
129. Q. Li, P. Hurley, H. Ding, A. G. Roberts, R. Akella, P. G. Harran, *J. Org. Chem.* 2009, **74**, 5909–5919.
130. A. Olofson, K. Yakushijin, D. A. Horne, *J. Org. Chem.* 1997, **62**, 7918–7919.
131. K. S. Feldman, A. P. Skoumbourdis, M. D. Fodor, *J. Org. Chem.* 2007, **72**, 8076–8086.
132. K. S. Feldman, A. Yimam Nuriye, J. Li, *J. Org. Chem.* 2011, **76**, 5042–5060.
133. S. Su, R. A. Rodriguez, P. S. Baran, *J. Am. Chem. Soc.* 2011, **133**, 13922–13925.

# 14

# ANTHRANILIC ACID–TRYPTOPHAN ALKALOIDS

ZHEN-YU TANG

*Department of Pharmaceutical Engineering, College of Chemistry and Chemical Engineering, Central South University, Changsha, China*

## 14.1 BIOSYNTHESIS

Anthranilic acid (or *o*-amino-benzoic acid) is an aromatic acid with the formula $C_7H_7NO_2$, which consists of a substituted benzene ring with two adjacent, or "*ortho*-" functional groups, a carboxylic acid, and an amine (Fig. 14.1). Anthranilic acid is biosynthesized from shikimic acid (for shikimic acid biosynthesis, see Chapter 10) following the chorismic acid-mediated pathway [1]. Based on its biosynthetic mechanism, shikimate is transformed to shikimate 3-phosphate with the consumption of one molecule of ATP, catalyzed by shikimate kinase. 5-Enolpyruvylshikimate-3-phosphate (EPSP) synthase is then catalyze the addition of phosphoenolpyruvate to 3-phospho-shikimate followed by the elimination of phosphate, which leads to EPSP. EPSP is further transformed into chorismate by chorismate synthase. Chorismate reacts with glutamine to afford the final product anthranilate and glutamate pyruvate catalyzed by anthranilate synthase (Fig. 14.1).

Phosphorylation of 3-hydroxyl group of shikimate by shikimate kinase (EC 2.7.1.71) with ATP as a cosubstrate initiates the biosynthesis pathway of anthranilic acid [2]. This step also presents the first step of the shikimate pathway, which is a metabolic route used by bacteria, fungi, and plants for the biosynthesis of many aromatic products such as lignins, alkaloids, flavonoids, benzoic acid, and plant hormones, in addition to the aromatic amino acids (phenylalanine, tyrosine, and tryptophan). The sequential EPSP synthesis is catalyzed by EPSP synthase (EC 2.5.1.19) through the addition of phosphoenolpyruvate to 3-phospho-shikimate followed elimination of phosphate. EPSP synthase belongs to the family of transferases, specifically to those transferring aryl or alkyl groups other than methyl groups. The gene encoding for EPSP synthase is found in the nucleus, but the location of the enzyme is in the chloroplast. The peptide sequence of EPSP synthase is 444 amino acids long, with an additional 72 amino acid transit peptide (for a total of 516 amino acids) [3]. The transit peptide sequence ensures the enzyme will be transported to the chloroplast. EPSP synthase is a monomeric enzyme (Fig. 14.2). It is composed of two domains, which are joined by protein strands. This strand acts as a hinge and can bring the two domains closer together. The enzyme first binds a molecule of shikimate-3-phosphate. Next a molecule of phosphoenolpyruvate binds to the enzyme's active site. After that, ligand bonding causes the two part of the enzyme to clamp down around the substrate in the active site and catalyzes the condensation reaction to produce EPSP. Herbicide, such as glyphosate, targets EPSP synthase by inhibiting the shikimate pathway [4].

Chorismate synthase (EC 4.4.3.5) catalyzes the 1,4-*trans* elimination of the phosphate group from EPSP to form chorismate. It requires the presence of a reduced flavin mononucleotide (FMNH2 or FADH2) for its activity. Chorismate synthase from various sources shows a high degree of sequence conservation of about 360–400 amino acid residues [5]. By now, nine structures have been solved for this class of enzymes. The X-ray crystal structure of chorismate synthase from *Mycobacterium tuberculosis* is a homotetramer with one FMN molecule noncovalently bound to each of the four monomers (Fig. 14.3). Each monomer is made up of 9 alpha helices and 18 beta strands, and the core is assembled in a unique beta–alpha–beta sandwich fold. The active sites for FMN binding are made up of clusters

*From Biosynthesis to Total Synthesis: Strategies and Tactics for Natural Products*, First Edition. Edited by Alexandros L. Zografos.
© 2016 John Wiley & Sons, Inc. Published 2016 by John Wiley & Sons, Inc.

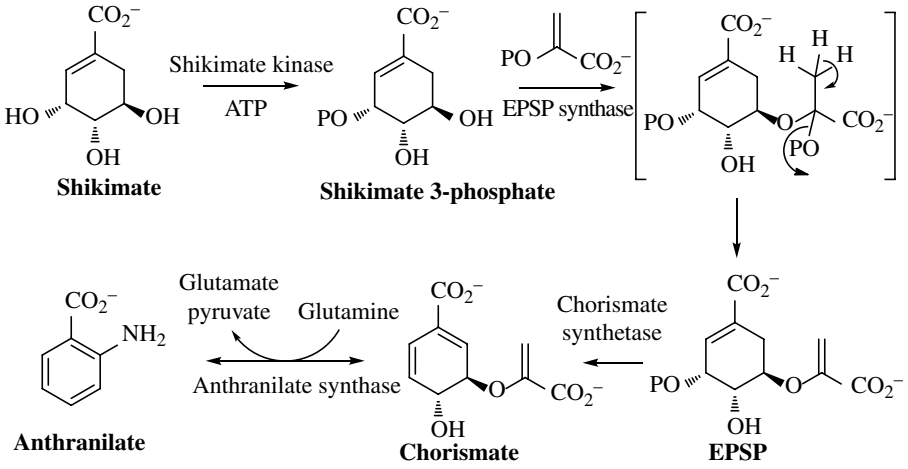



**FIGURE 14.1** Biosynthesis of anthranilate from shikimate.



**FIGURE 14.2** Ribbon diagram of EPSP synthase (EC 2.5.1.19). (*See insert for color representation of the figure.*)

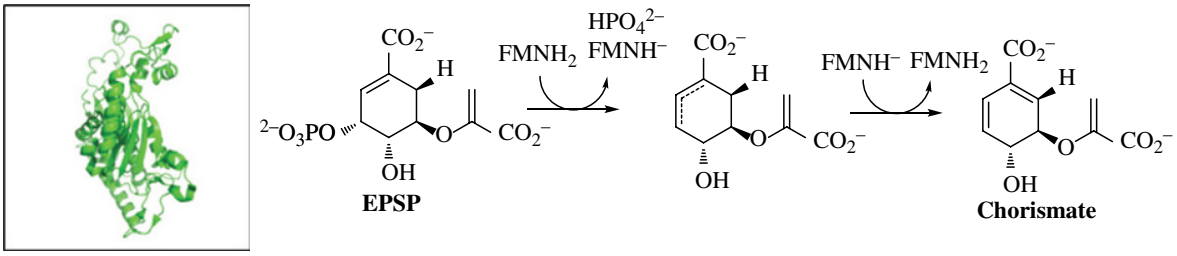



**FIGURE 14.3** Ribbon diagram of chorismate synthase and its mechanism.

of flexible loops, and the areas around those regions have highly positive electromagnetic potential. There are two histidine residues located at the active site, which are thought to protonate the reduced flavin molecule and the leaving phosphate group of the substrate. The mechanism of the 1,4-elimination of phosphate from EPSP is proceeded through the reduced flavin (FMN), which transfers an electron to the substrate resulting in cleavage of the C–O bond. How this flavin is obtained differs from one organism to another, and the process is not completely understood [6]. Following the binding of EPSP, the flavin reaction intermediate is formed, but this process is complete prior to EPSP consumption.

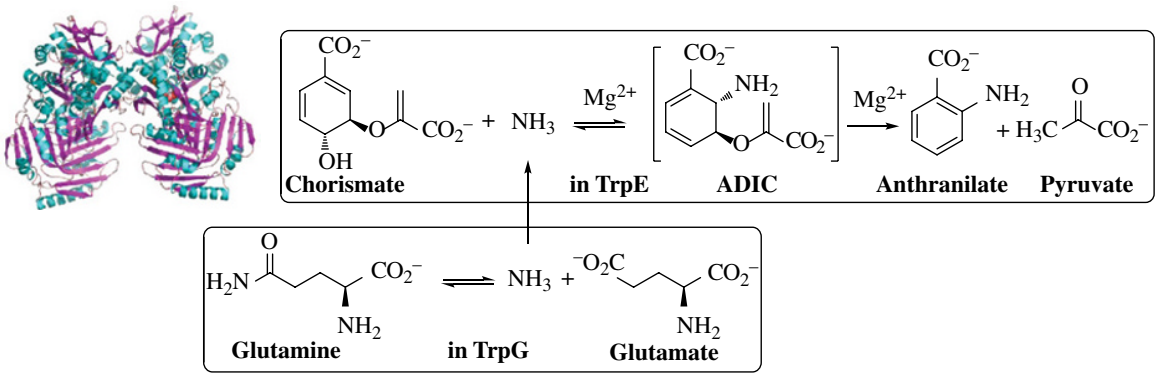



**FIGURE 14.4** Ribbon diagram of anthranilate synthase and its mechanism.

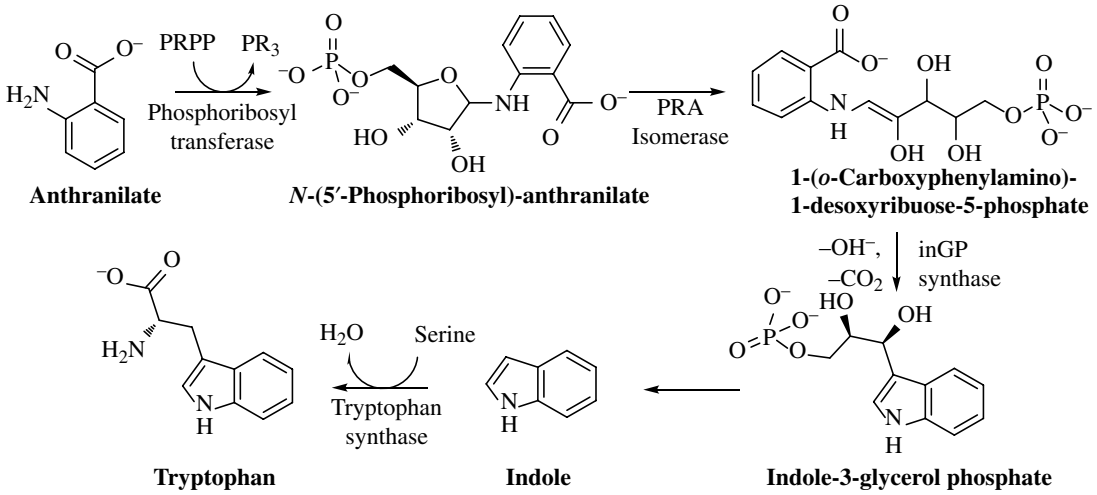



**FIGURE 14.5** Biosynthesis of tryptophan from anthranilate.

After EPSP is converted to chorismate, and after the phosphate has been released from the enzyme, the flavin immediate will decay [7]. The chorismate synthase enzyme can be divided into two categories based on how reduced FMN is obtained. Bifunctional chorismate synthase is present in fungi and requires a "second enzymatic activity, an NAD(P)H-dependent flavin reductase" [8]. Monofunctional chorismate synthase is found in plants and *Escherichia coli* and is only active in an anaerobic environment with "chemically or enzymatically reduced flavin." There is no net redox change in the reaction. The flavin molecule is not consumed during the reaction and merely acts as a catalyst.

Anthranilate synthase (EC 4.1.3.27) catalyzes the formation of anthranilate from chorismate and glutamine with pyruvate and glutamate being the other two products (Fig. 14.4). In the aromatization process of chorismate, a hydroxyl group and an enolpyruvyl group are eliminated by protonation. Deuterium experiments with $D_2O$ demonstrate that in the formation of the pyruvate, the third hydrogen of the methyl group arises from water and not by intramolecular shift of a hydrogen atom from the ring of chorismate [9]. The X-ray structure of the cooperative anthranilate synthase from *Salmonella typhimurium* is heterotetramer with the allosteric inhibitor tryptophan bound to a regulatory site in TrpE subunit. From the schematic model of anthranilate synthase (Fig. 14.4), ammonia produced by the glutaminase reaction of TrpG is presumed to pass through a tunnel to the active site of TrpE, where an aminodeoxyisochorismate (ADIC) synthase half-reaction leads to the formation of the enzyme-bound intermediate ADIC [10]. The enolpyruvyl group of ADIC is then eliminated as pyruvate from ADIC in the ADIC lyase half-reaction. Both half-reaction are $Mg^{2+}$ dependent and respond to allosteric inhibition by tryptophan.

Anthranilic acid is the precursor to the amino acid tryptophan via the attachment of phosphoribosyl pyrophosphate to the amine group to form *N*-(5′-phosphoribosyl)-anthranilate (PRA) (Fig. 14.5) [11]. The second step of the tryptophan biosynthesis is the PRA isomerization to 1-(*o*-carboxyphenylamino)-1-desoxyribuoso-5-phosphate (CdRP) by PRA isomerase. Further elimination of hydroxyl group and decarboxylation forms indole-3-glycerol phosphate (InGP) by InGP synthase. Tryptophan synthase catalyzes the final two




**FIGURE 14.6** Ribbon diagram of anthranilate transferase and PRA isomerase.

steps, the reversible formation of indole and glyceraldehyde 3-phosphate (G3P) from InGP and the irreversible condensation of indole and serine, to form tryptophan in a pyridoxal phosphate (PLP)-dependent reaction [12].

Anthranilate phosphoribosyl transferase (EC 2.4.2.18) (AnPRT) belongs to the class of transferase enzyme, which enacts the transfer of specific functional group (e.g., methyl or glycosyl group) from one molecule (called the donor) to another (called the acceptor). It transfer a ribose group between the basic functional group of anthranilate and 5-phospho-alpha-D-ribose 1-diphosphate (PRPP). AnPRT has four domains and its quaternary structure consists of two identical protein structures [13]. Each domain of AnPRT contains a magnesium ion and a pyrophosphate molecule as the active site. The secondary structure of AnPRT consists mainly of alpha helices with a beta sheet within each domain (Fig. 14.6).

PRA isomerase (EC 5.3.1.24) belongs to the family of isomerases, specifically those intramolecular oxidoreductases interconverting aldoses and ketoses. It catalyzes the reaction of converting *N*-(5-phospho-beta-D-ribosyl) anthranilate to 1-(2-carboxyphenylamino)-1-deoxy-D-ribulose-5-phosphate. PRA isomerase is monomeric and labile in most mesophilic microorganisms but dimeric and stable in the hyperthermophile *Thermotoga maritima* (tPRAI) [14]. tPRAI has a TIM barrel fold, whereas helix alpha5 in ePRAI is replaced by a loop. The subunits of tPRAI associate via the N-terminal faces of their central beta barrels. Two long, symmetry-related loops that protrude reciprocally into cavities of the other subunit provide for multiple hydrophobic interactions. Moreover, the side chains of the N-terminal methionines and the C-terminal leucines of both subunits are immobilized in a hydrophobic cluster, and the number of salt bridges is increased in tPRAI. These features appear to be mainly responsible for the high thermostability of tPRAI [15].

InGP synthase (EC 4.1.1.48) catalyzes the ring closure of an N-alkylated anthranilate to a 3-alkyl indole derivative releasing carbon dioxide and water. In some bacteria, InGP synthase is a single-chain enzyme. In others, such as *E. coli.*, it is the N-terminal domain of a bifunctional enzyme that also catalyzes PRA isomerase activity, the third step of tryptophan biosynthesis [16]. In fungi, InGP synthase is the central domain of a trifunctional enzyme that contains a PRA isomerase C-terminal domain and a glutamine amidotransferase (GATase) N-terminal domain. A structure of the InGP synthase domain of the bifunctional enzyme from the mesophilic bacterium *E. coli* (eIGPS) has been compared with the monomeric InGP synthase from the hyperthermophilic archaeon *Sulfolobus solfataricus* (sIGPS). Both are single-domain (beta/alpha) eight-barrel proteins, with one (eIGPS) or two (sIGPS) additional helices inserted before the first beta strand [17].

Tryptophan synthase catalyzes the last two steps of the biosynthesis of tryptophan. It is typically found as a $\alpha_2\beta_2$ tetramer. The α subunits catalyze the reversible formation of indole and G3P from InGP. The β subunits catalyze the irreversible condensation of indole and serine to form tryptophan in a PLP-dependent reaction. Each α active site is connected to a β active site in a process known as substrate channeling [18]. Figure 14.7 represents the stereo view of one αβ heterodimer of tryptophan [19]. The α subunit contains bound indole-3-propanol phosphate and β subunit contains L-serine, which forms aldimine with the coenzyme PLP. The orange sphere represents the course of tunnel running from the α to the β subunits. This tunnel is a 25 Å long hydrophobic channel contained within the enzyme allowing for the diffusion of indole. If the channel did not exist, the indole formed at α active site would quickly diffuse always and be lost to the cell as it is hydrophobic and can easily cross membranes.

Mechanism of tryptophan synthase is depicted in Figure 14.8. During the indole formation from the G3P elimination from InGP, the active sites of α subunit are the amino acid residues of Asp-60 and Glu-49. The formed indole is rapidly transferred to the active site of β subunit to react with serine to synthesize the tryptophan [20]. In the absence of L-serine, the coenzyme PLP is covalently bound to the amino group of Lys-87 of β subunit. Transmission between L-serine and PLP results in the formation of an external aldimine intermediate, and then deprotonation leads to a quinoid intermediate. This step is followed by the elimination of a water molecule to form an aminoacrylate intermediate. Condensation of the aminoacrylate intermediate with internal indole generates a second quinonoid intermediate that is protonated to produce a second external aldimine intermediate. Subsequently release of product, L-tryptophan, completes the catalytic cycle. The kinetic studies also reveal that the reaction of indole with serine at β subunit modulates the α reaction such that the formation of the aminoacrylate leads to a change in protein conformation that is transmitted to the α site to enhance the rate of InGP cleavage 150-fold [21].

For many organism (including humans), tryptophan is an essential amino acid. This means that although it is essential for human life, it cannot be synthesized by the organism and has to be delivered exogenously. Tryptophan acts as building blocks in protein biosynthesis [22]. In addition, as a primary

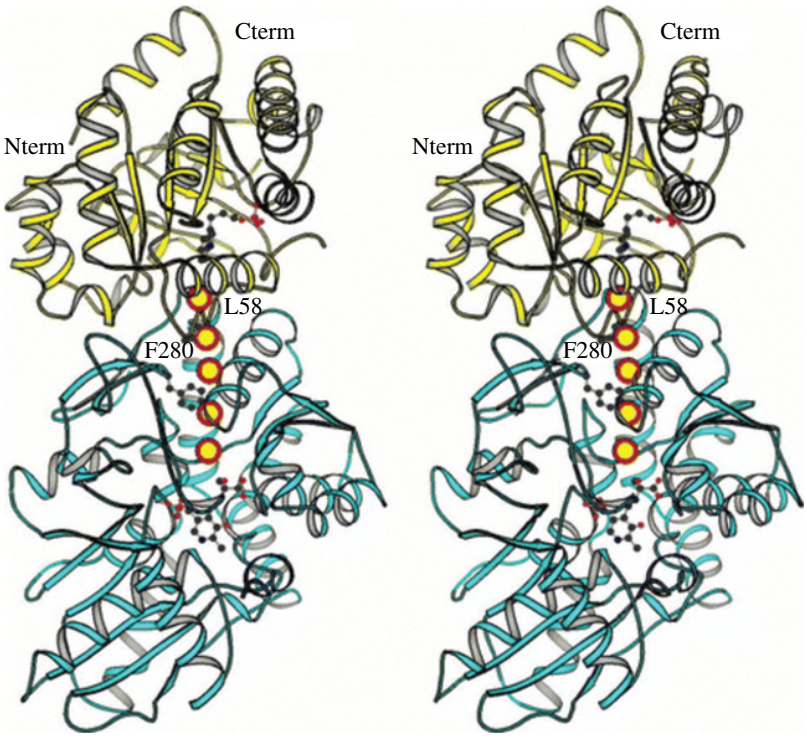



**FIGURE 14.7** Ribbon structure of tryptophan synthase.

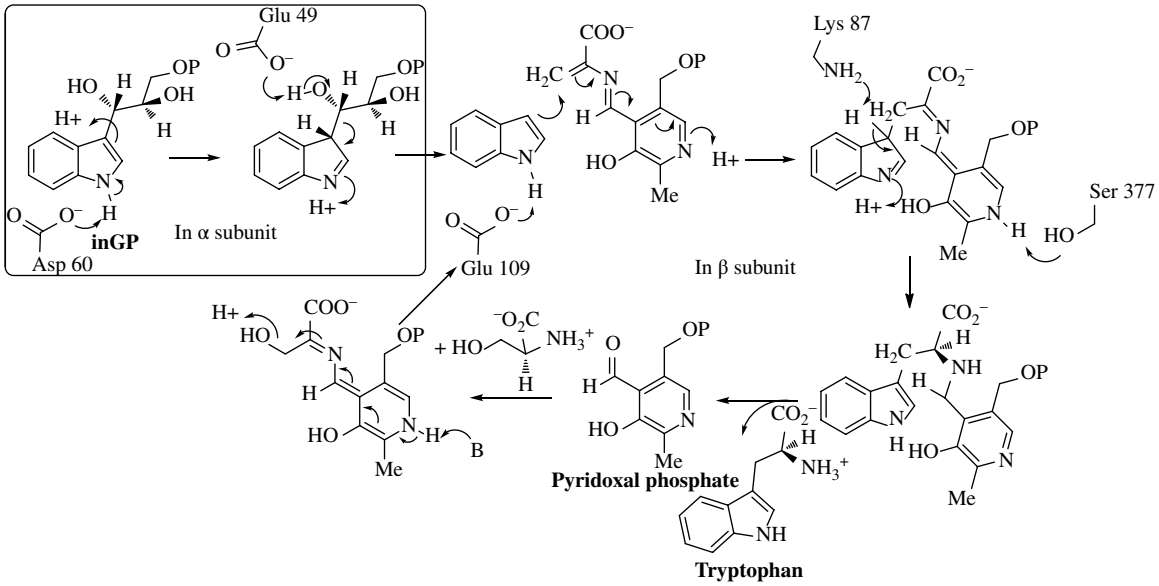



**FIGURE 14.8** Tryptophan synthase reaction mechanism.

metabolite, tryptophan functions as a biochemical precursor for the indole alkaloids [23]. Containing more than 4100 known different compounds, indole alkaloids are one of the largest classes of alkaloids [24]. Among them, some of the simplest and yet widespread indole derivatives are the biogenic amines tryptamine and 5-hydroxytryptamine (serotonin). Figure 14.9 lists selected examples of some simple indole alkaloids, which are biosynthesized from tryptophan. Following one of them, tryptophan is converted to serotonin via enzyme-aided sequential 5-position hydroxylation and amino acid decarboxylation [25]. Most of these small molecules have good biological activities. For example,

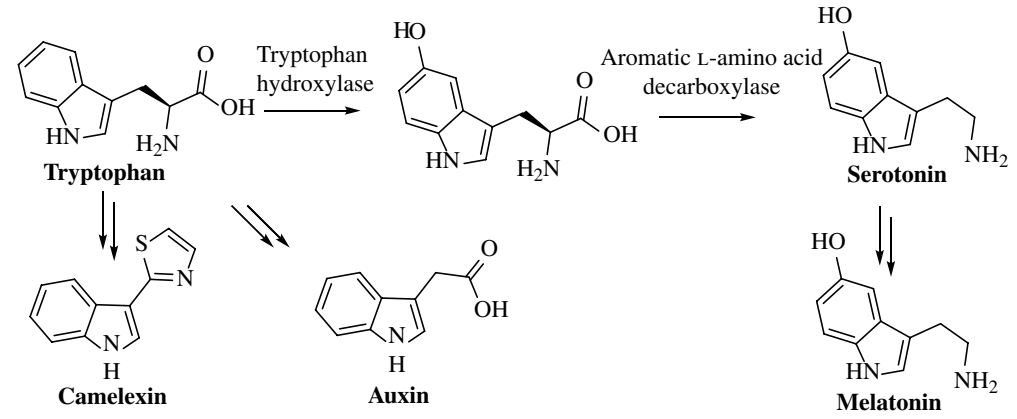



**FIGURE 14.9** Examples of simple indole alkaloids with tryptophan as bioprecursor.

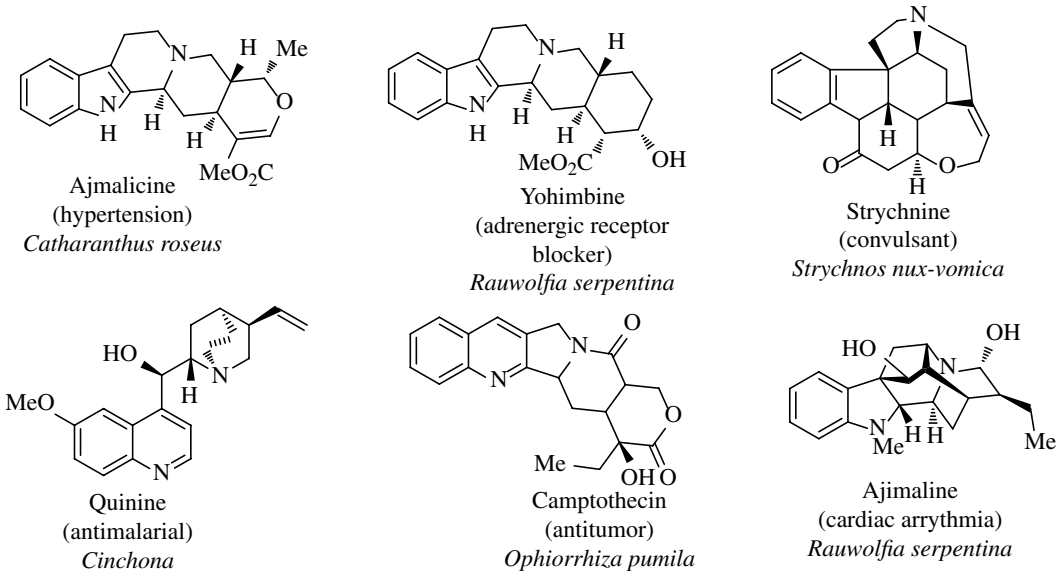



**FIGURE 14.10** Selected example of monoterpene indole alkaloids.

native auxin is found as plant growth hormone and serotonin is popularly regarded as a contributor of well-being and happiness [26].

Unlike its primary metabolite precursor, monoterpene indole alkaloids, which include isoprene groups, possess a range of highly diversified chemical structures and a wealth of biological activities [27]. Most monoterpene indole alkaloids include a C9 and C10 fragment originating from the secologanin. Depending on the structure of this fragment, these alkaloids belong to *Corynanthe*, *Iboga*, and *Aspidosperma* classes named by a typical genus or species of plant that contain such alkaloids. Monoterpene indole alkaloids are widely used as anticancer, antimalarial, and antiarrhythmic agents (Fig. 14.10) [28]. Due to their intrinsic biologic activities and potential as drug candidates, they have become important synthetic targets in last decades.

Biosynthesis of some classes of terpene indole alkaloids is well understood. In certain cases, many of the enzymes that are responsible for biosynthesis have been cloned and mechanistically studied. In other cases, biosynthesis pathway is only proposed based on the results of feeding studies with isotopically labeled substrates and from the structures of isolated biosynthetic intermediates. All terpene indole alkaloids are derived from tryptophan and the iridoid terpene secologanin (Fig. 14.11). Tryptophan decarboxylase, a pyridoxal-dependent enzyme [29], converts tryptophan to tryptamine [30]. The following strictosidine synthase-catalyzed Mannich reaction connects tryptamine and secologanin to yield strictosidine [31]. The *Apocynaceae*, *Loganiaceae*, *Rubiaceae*, and *Nyssaceae* families of plants each produce terpene indole alkaloids with dramatically diverse structures [32–34]. The mechanisms and control of

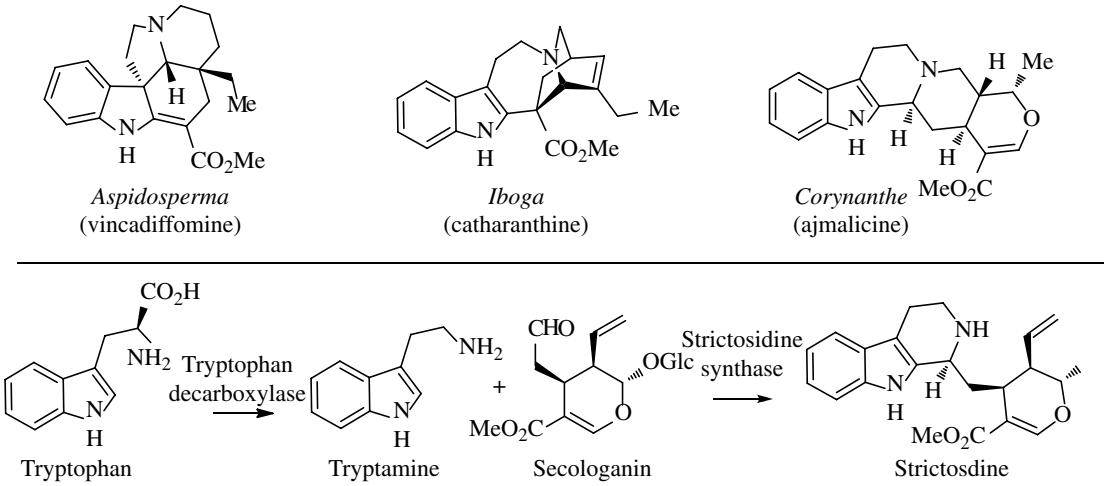



**FIGURE 14.11** Classes of terpene indole alkaloid derived from strictosidine.

the processes by which strictosidine rearranges into these diverse families of product remain one of the most fascinating problems in secondary metabolism. Even through the enzymes that catalyze those biotransformations remain unidentified, one can still propose biosynthetic pathway toward strychnine by isolation of intermediates from *Strychnos nux vomica* [35].

## 14.2 DIVERGENT SYNTHESIS–COLLECTIVE TOTAL SYNTHESIS

Today, organic chemists are able to synthesize almost any known natural product, given enough time, resources, and effort, via a strategy which is often called *target-oriented synthesis* [36]. In nature, biosynthesis normally starts from a limited library of simple precursors derived from primary metabolism to produce secondary metabolites with diversity and complexity based on specific enzymes. Over the last few decades, synthetic chemists are approaching novel synthetic targets in two different ways [37]. On one hand, they are trying to imitate existing proposed biosynthetic pathways through *biomimetic* target-oriented synthesis, and on the other, they are attempting to develop natural product-like compound libraries. For the latter endeavor, the term *diversity-oriented synthesis* was introduced [38]. Random production of structural complex and diverse small molecules through diversity-oriented synthesis is driving recent efforts to dissect biological pathways by imitating those used in genetics, where at first random mutations take place and then are screened in search of a particular cellular or organismic phenotype. Although this concept greatly enriched our synthetic libraries with "privileged molecular structures," it did not produce the anticipated results concerning their biological fingerprints, proving to be inadequate [39].

As a result, synthetic approaches have recently turned to the introduction of a novel term, called *collective total synthesis* [40]. Consider initially the fact that natural products are occupying biologically relevant chemical space by binding both their biosynthetic enzymes and their target macromolecules. Natural product families, as a result, can be envisioned as prevalidated libraries of functionally diverse structures. In these libraries, single compounds selectively modulate unrelated macromolecular targets [41]. The emergence of preparing diverse natural product scaffolds is firmly associated with the need of our society for more potent and selective biomodulators. In response, the synthetic approach of using just one synthetic or biosynthetic intermediate (common synthetic scaffold) that can be readily transformed to an array of diverse natural compounds is progressively gaining ground and is what was introduced above as *collective total synthesis* (Fig. 14.12).

Improvement of the understanding of complex biosynthetic pathways during the last two decades provided the opportunity for scientists to recognize additional common biosynthetic intermediates, which nature uses to access seemingly unrelated natural compounds. Striving to imitate this biosynthetic logic, organic chemists are called to connect natural product of the same or different families with common synthetic roots. These roots can either be a biosynthetically existing or a synthetically produced common scaffold.

Wishing to provide a deeper understanding of the synthetic tactics, which are used on the examples that will follow, some general guidelines on the design of a common synthetic scaffold are provided. These guidelines follow David W.C. MacMillan's tryptophan-derived monoterpene indole alkaloids syntheses as an example [39]:

a. *Selecting Targets*: The selection of novel targets consists one of the most crucial parts of a successful project. This challenging task presents in three ways for organic chemists: firstly the biological significance

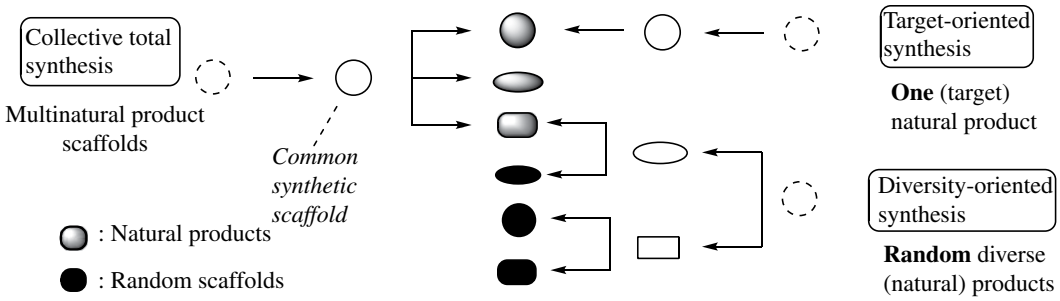



**FIGURE 14.12** Evolution in total synthesis from target to diversity-oriented synthesis and collective total synthesis.

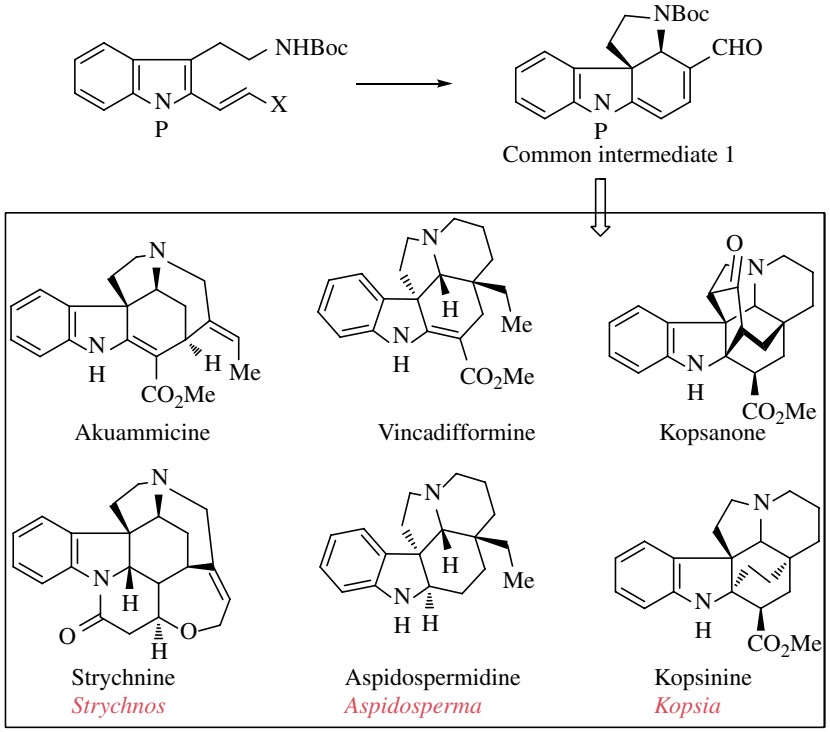



**FIGURE 14.13** Selected targets on David M. C. MacMillan's collective synthesis of terpene indole alkaloids.

of the targets must be considered, then the intriguing molecular complexity of the target molecule, and finally, the unanswered chemical problems that its structure might possess. In a *collective total synthesis* approach, an additional factor must be taken into account: the recognition of other targets/natural products fulfilling the above statements that still bear common structural characteristics. In MacMillan's synthesis, six structurally complex members of the *Strychnos*, *Aspidosperma*, and *Kopsia* families of alkaloids have been selected (Fig. 14.13) [42]. Each of them presents unique potent antibiotic properties and complex molecular architecture.

b. *Designing a common scaffold*: After selecting the appropriate group of targets, the identification of a common synthetic scaffold commences on the basis of common characteristics or general patterns. Such patterns must be presented in a specific class of compounds, for example, all compounds in Figure 14.13 are tryptophan-derived alkaloids with monoterpene indole core. Carefully examination of all isolated components within the same or other natural product families is essential for recognition of concrete oxidative states and different modes of diversification. Note that all cyclized compounds in Figure 14.13 contain one or more ring than the proposed common scaffold (**1**). Finally, the selection of the common scaffold should be delineated by the minimum number of necessary steps needed to build a common molecular skeleton. To realize this design, a highly efficient and enantioselective organocascade reaction was utilized to construct the common synthetic intermediate **1**.

c. *Adjusting the unified synthetic plan*: It is important that an economical approach (atom and step economy—Chapter 13 for more details on the topic) should be addressed by the whole synthetic plan. When a common scaffold is designed, different cyclization strategies to reach specific synthetic target are desirable. The attached protected amine and the aldehyde moiety of the common intermediate **1** served as points of diversification to access the whole variety of the described natural compounds. For example, the Wittig reaction on the aldehyde moiety of the benzyl protected **1**, reduction of the existing enamine and introduction of the appropriate side chain in the pyrrolidine moiety provided **4**. Heck reaction followed by deprotection completed the total synthesis of aspidospermine and its oxidized counterpart vincadifformine. More details about the different synthetic strategies to access these six different monoterpene indole alkaloids are included in the following section.

Syntheses targeting an advanced core structure for the construction of closely related natural products are frequently reported. The discovery of common scaffolds, however, and its application in the synthesis of structurally diverse natural products in the so-called "collective total synthesis" is much less present in the literature. In the following section some of the most elegant collective syntheses of indole and bisindole natural products are presented.

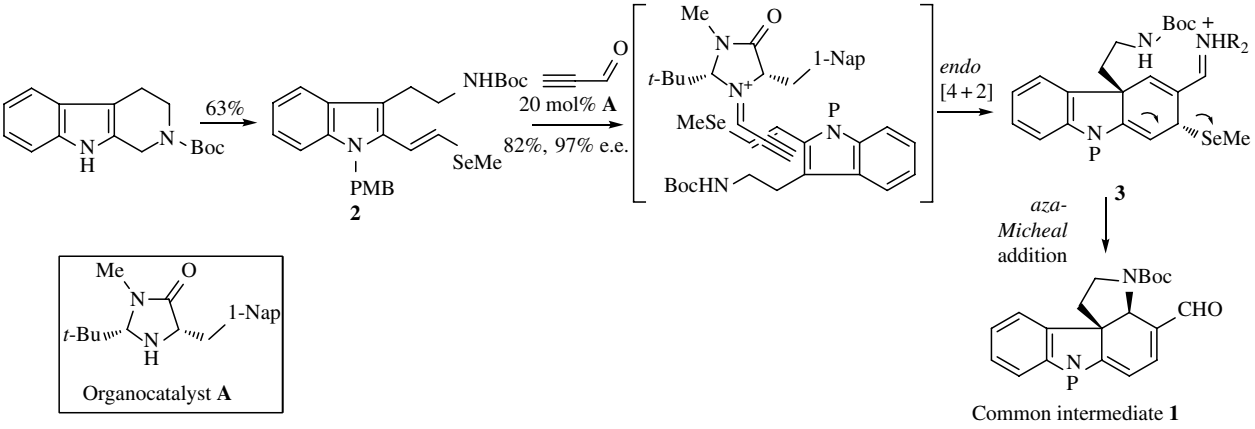
Until recently, organic chemists focused on the synthesis of one single molecular target, ignoring the numerous synthetic hurdles involved in this approach. Given the infinity of molecular complexity illustrated by nature, diversity-oriented synthesis brought into light the ability to access randomly diverse synthetic scaffolds. This was achieved by taking advantage of the usually numerous high yielding reactions that build upon existing functionalization. Not surprisingly, the evolution of the described methods that contributed to the discovery of collective total synthesis of natural products introduced a new era in providing natural product libraries by the utilization of common synthetic intermediates. Following this concept, the scientific community has witnessed tremendous advances on completing highly complex natural targets, contributing, for example, in expanding the drug leads arsenal, by minimizing the number of synthetic steps and increasing the product yields.

## 14.3 COLLECTIVE TOTAL SYNTHESIS OF TRYPTOPHAN-DERIVED ALKALOIDS

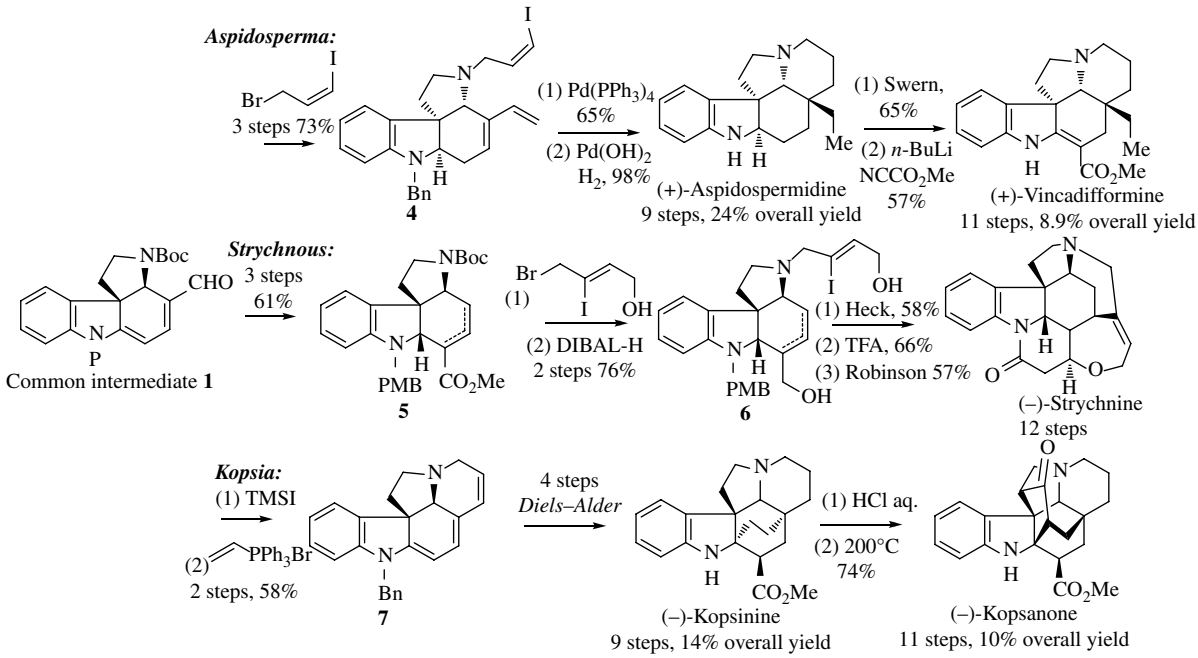
### 14.3.1 Monoterpene Indole Alkaloids

MacMillan's synthesis of monoterpene indole alkaloids as it was mentioned previously was based on the synthesis of common synthetic scaffold **1** [40]. The synthesis started from a highly efficient and enantioselective organocascade reaction to construct a common synthetic intermediate. In the presence of an imidazolidinone catalyst (A) [43], the key tetracyclic precursor **1** was accessed by exposure of the 2-(vinyl-1-selenomethyl) tryptamine system **2** to propynal (Scheme 14.1) [44]. As a key element of enantiocontrol, the acetylenic functionality of the catalyst-bound propynal was expected to partition away from the bulky *tert*-butyl group, leaving the naphthyl group effectively to shield the bottom face of the reacting alkyne. The activated dienophile then underwent *endo*-selective Diels–Alder cycloaddition with the substituted 2-vinyl indole **3**. By contrast with their previous studies, incorporation of organoselenide substitution instead of the methyl-sulfide analog permits a facile β-elimination and aza-Michael addition to deliver the highly enantioenriched spiroindoline core (**1**) (yield: 82%, ee: 97%) [45].

MacMillan's synthesis toward *Aspidosperma* alkaloids started from the allylation of the secondary amine of the spiroindoline core (**1**) and continued with a Wittig reaction to form intermediate **4** (Scheme 14.2). Then, intramolecular Heck reaction followed by hydrogenation of the double bond




**SCHEME 14.1** Synthesis of common intermediate **1**.




**SCHEME 14.2** MacMillan's synthesis of five members of natural indole alkaloids.

furnished (+)-aspidospermidine in nine steps and 24% overall yield. Swern oxidation of aspidospermidine and further treatment with *n*-butyllithium followed by methyl cyanoformate provided (+)-vincadifformine in 8.9% overall yield. Route to the *Strychnos* alkaloid was forged by decarbonylation by Wilkinson's catalyst, treatment with phosgene and methanol to introduce a carbomethoxy group, and DIBAL-H reduction to provide the unsaturated ester **5** in 61% yield (Scheme 14.2) [46]. Similarly, the allylation of **5** and Heck cyclization from the substrate **6** afforded the (−)-strychnine with a very short route [47]. Kopsia alkaloids differs in the bicycle[2,2,2]octane structure to the above compound. The diene-containing six-membered ring intermediate **7** was constructed by Wittig reaction. Further Diels–Alder reaction and reduction of double bond finished (−)-kopsinine synthesis in 14% overall yield [48]. Simple hydrolysis with aqueous hydrochloric acid and further heating without solvent finished (−)-kopsanone in only 11 chemical steps (Scheme 14.2). Even though the highly efficient (−)-akuammicine synthesis is not introduced here, MacMillan's synthesis toward six monoterpene indole alkaloids family member from the common intermediate (**1**) represents one of the most elegant collective synthesis examples and thus defines the term.

Collective total synthesis has been gathering more and more attention recently, Prof. Jieping Zhu's divergent synthesis toward five members of *Aspidosperma* alkaloids represent one of the most recent advancement (Fig. 14.14) [49]. The advantages in Prof. Zhu's synthesis plan include (i) to construct the indole unit at a late stage of the synthesis instead of using tryptamine or other indole-containing compounds as starting materials and (ii) to construct the polycyclic ring system by a one-pot domino cyclization process. They designed a functionalized cyclopentene derivative **8** as a common intermediate to reach topologically different structure by varying the nature of the substituents and their connectivity. This common intermediate **8** could be easily accessed by the direct decarboxylative coupling of the substituted potassium *o*-nitrophenylacetate **9** and vinyl triflate **10**.

Indeed the common intermediate **8** was accessible by the $[Pd(allyl)Cl]_2$/X-phos-catalyzed decarboxylative coupling reaction and in situ O-desilylation (TBAF) with 70% yield [50]. Goniomitine synthesis started from the Mitsunobu reaction to afford azido compound **11** (Scheme 14.3). The one-pot integrated *o*xidation/*r*eduction/*c*yclization (*i*ORC) sequential reaction was carried out to form the core structure of the final natural product. Ozonolysis of **11** in methanol at −78°C in the presence of $NaHCO_3$ followed by addition of $Me_2S$ and then activated zinc and $CaCl_2$ and heating finished the benzyl group protected goniomitine in 80% yield [51]. The intermediate **12** was isolated and fully characterized after the sole ozonolysis [52]. The presence of $CaCl_2$ was crucial for the reduction of the nitro and azido groups to provide diamino dicarbonyl intermediate **13**, which cyclized spontaneously to afford the intermediate **15** via the indole intermediate **14** [53]. Intramolecular attack of the indolyl nitrogen on the iminium from the face opposite to the ethyl substituent would diastereoselectively produce the *cis*-fused C/D ring system, thus completing the construction of benzyl group protect goniomitine. Further

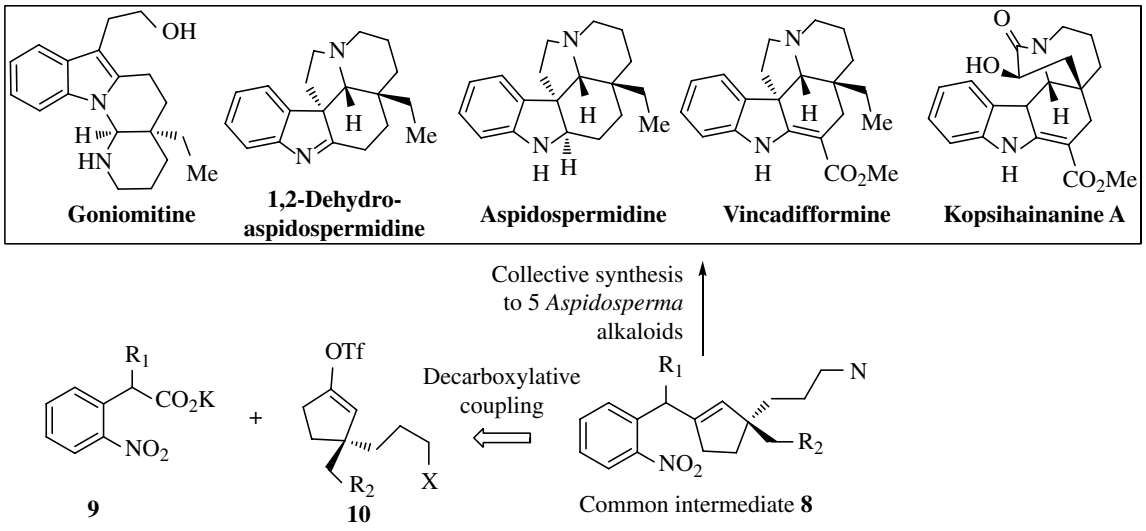
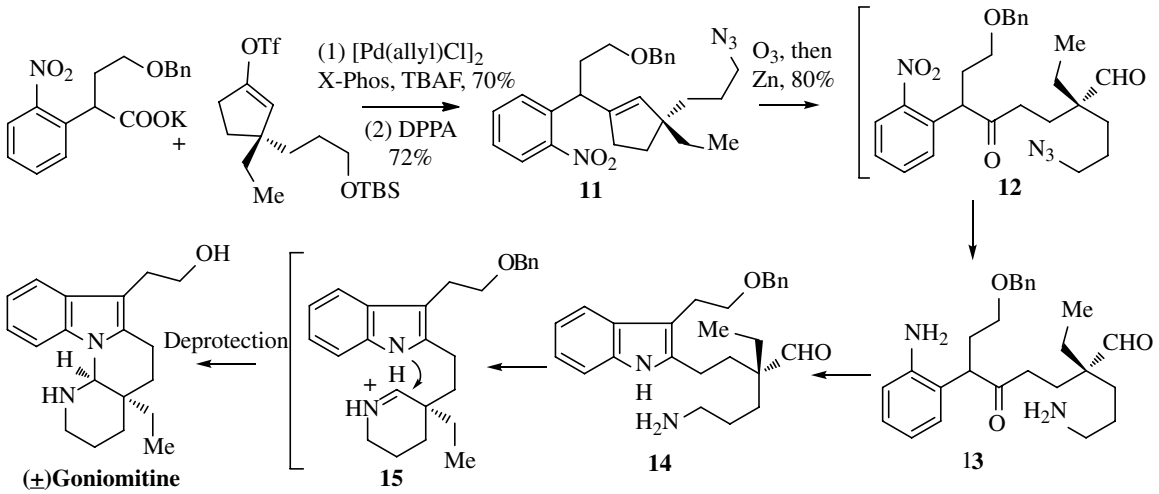



**FIGURE 14.14** Prof. Jieping Zhu's synthetic plan toward monoterpene indole alkaloids.



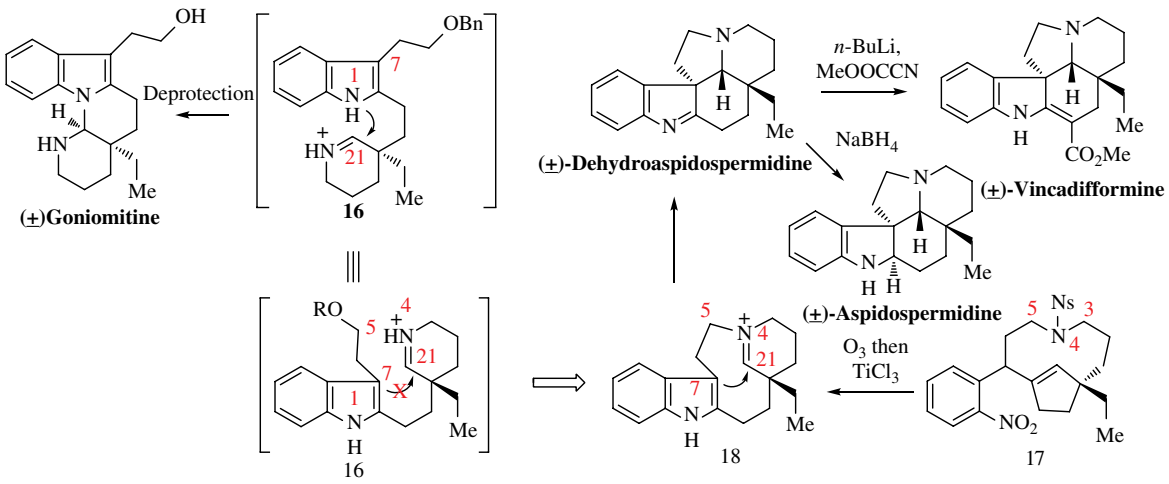

**SCHEME 14.3** Total synthesis of (±)-goniomitine.

sodium naphthalenide deprotection [54] of benzyl ether finished the natural product synthesis.

In the synthesis of goniomitine, an intramolecular nucleophilic addition of the indolyl nitrogen N1 to C21 of the putative iminium intermediate **15** was assumed to be the last step of *i*ORC sequence [55]. However, authors noticed that an alternative cyclization via nucleophilic addition of C7 (supposed to be more nucleophilic than N1) to C21 was not observed, most probably for steric reasons (Scheme 14.4). To channel the cyclization via the formation of the C7–C21 bond, authors planned to impose a geometric constraint by introducing a C5–N4 bond into the *i*ROC substrate. As expected, with the C5–N4 connected intermediate **17** in hand, authors successfully used the *i*ROC reaction to finish the synthesis of (±)-dehydroaspermidine in a beautiful step. Reduction of the nitro group with $TiCl_3$ in an ammonium acetate buffer rather than Zinc powder/$CaCl_2$ proved to be crucial for this cyclization to happen [55]. Further sodium borohydride reduction of (±)-dehydroaspermidine afforded (±)-aspidospermidine. Another treatment with *n*-butyl lithium and methyl cyanoformate provided (±)-vincadifformine in highly efficient way [40].

### 14.3.2 Bisindole Alkaloids

More than 200 bisindole alkaloids are known today. They are produced in living organism through dimerization of monomeric indole by the following reactions: Mannich reaction, Michael reaction, condensation of aldehydes with amines, oxidative coupling of tryptamines, and splitting of the functional group of one of the monomers. Bisindole alkaloids containing 2,2′-connectivity constitute a large




**SCHEME 14.4** New *i*ROC sequence and syntheses of 1,2-dehydroaspidospermidine, aspidospermidine, and vincadifformine.

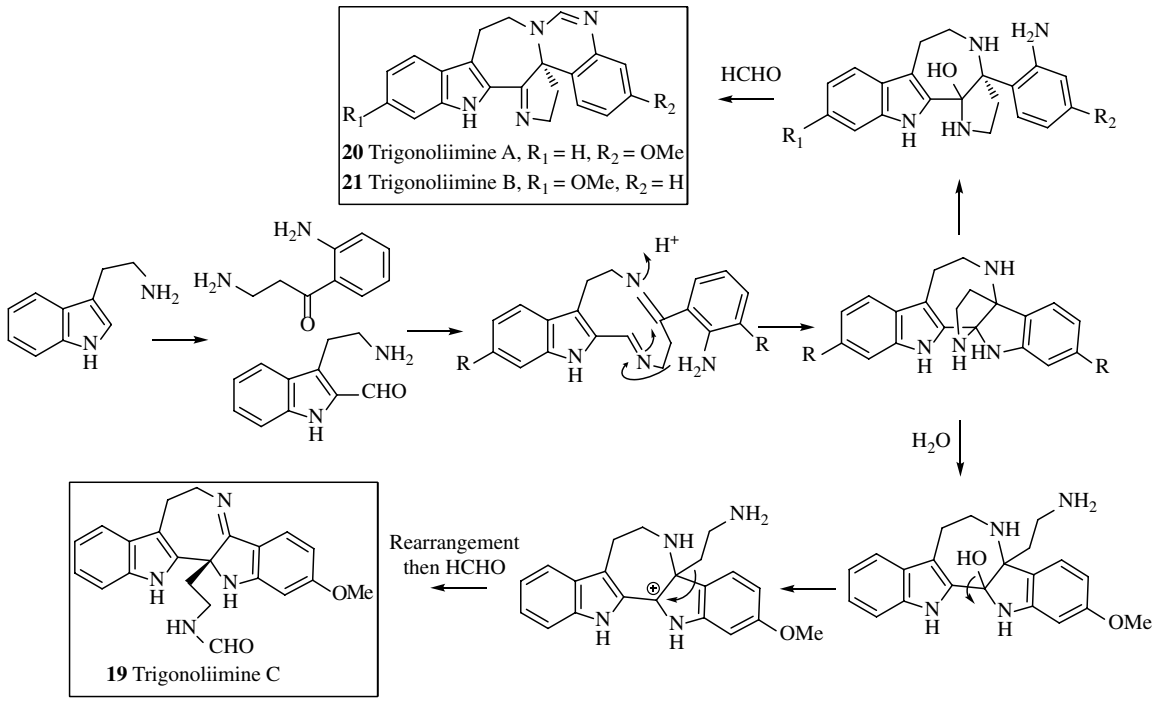
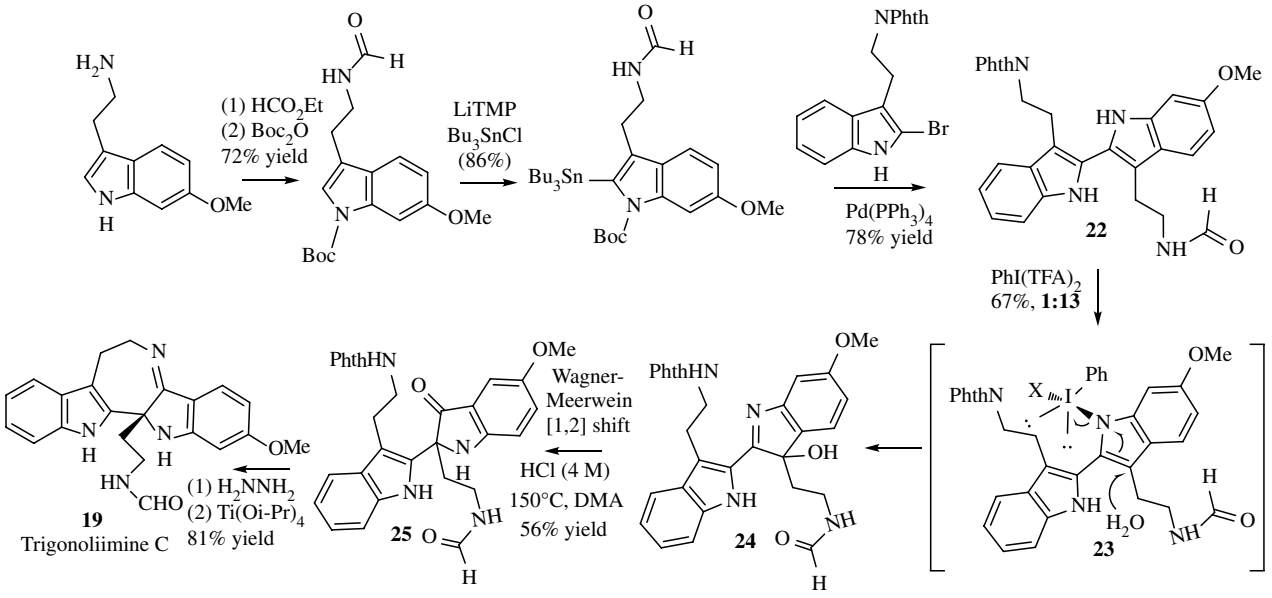



**FIGURE 14.15** Trigonoliimine A, B, and C and biosynthesis proposed by Hao.

number of natural products, which includes tryptamine-derived natural products. In 2010, Hao and coworker reported the isolation of 2,2′-linked bistryptamine alkaloids (+)-trigonoliimine A and B along with (−)-trigonoliimine C from the leaves of *Trigonostemon lii* Y.T. Chang collected in the Yunnan province of China (Fig. 14.15) [56]. From their biological studies of these alkaloids, trigonoliimine A showed modest activity in an anti-HIV assay ($EC_{50}$ = 0.95 μg/ml, TI = 7.9). Fascinated by their unique molecular structure, many research groups initiated synthetic programs aimed at their total syntheses. Among them, Prof. Uttam K. Tambar's group [57] and Prof. Mohammad Movassaghi's group [58] reported the first total syntheses almost at the same time. After that, Prof. Jieping Zhu [59] and Prof. Xiao-Jiang Hao [60] finished their syntheses based on different synthetic strategies.

In their isolation paper, Hao and coworkers proposed a biosynthesis that commenced with the coupling of tryptamine and kynuramine (Fig. 14.15). On the other hand, Prof. Uttam K. Tambar, coworker Xiangbing Qi, and Hongli Bao proposed an alternative biogenetic pathway, which involves an oxidative aryl–aryl coupling of two tryptamine derivatives to



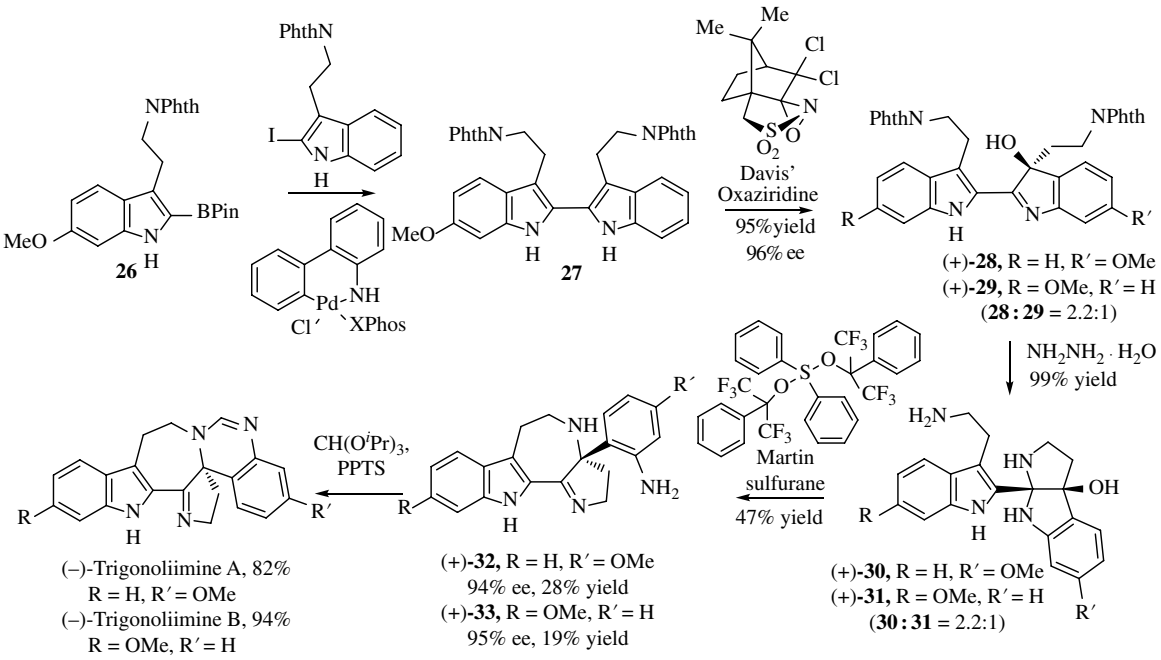

**SCHEME 14.5** Tambar's total synthesis toward (±)-trigonoliimine C.

generate 2,2′-binary tryptamine **22**. This intermediate is proposed to be converted to trigonoliimine scaffolds through a series of selective oxidative rearrangement shown in Scheme 14.5 [61]. Having as a basis this biosynthetic hypothesis, their total synthesis of (±)-trigonoliimine C started with a Stille cross-coupling between stannylindole and bromoindole, which was assembled from tryptamine in a two-step sequence. The following selective mono-oxidation on the electron-rich 6-methoxyindole system represented the first hurdle on their pathway.

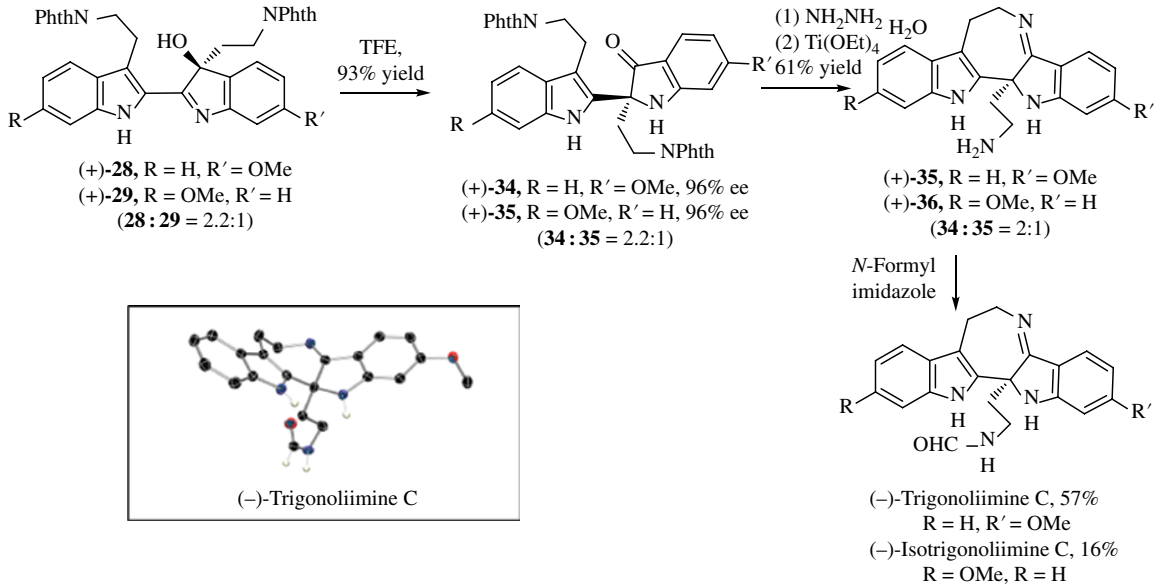
To their surprise, exposure of unsymmetrical bisindole **22** to a diverse set of oxidant led to the formation of the undesired mono-oxidation product, which installed a hydroxyl group on the nonsubstituted indole. For example, in presence of oxone, the undesired oxidation product was generated in a ratio of 6:1. After considerable experimentation, they discovered that iodine(III) reagents such as $PhI(OAc)_2$ and $PhI(TFA)_2$ preferentially produced the desired hydroxyindolenine **24** in a ratio up to 13:1. The favorable oxidation of methoxy-substituted indole system was attributed to the formation of covalent adduct **23**, which would be susceptible to intermolecular nucleophilic attack by a molecule of water. Several attempts were made to realize the enantioselective mono-oxidation of unsymmetrical bistryptamine **22** with chiral iodine(III) reagent unfortunately were failed [62]. The desired Wagner–Meerwein [1, 2] shift of alkyl group of intermediate **24** was firstly tested with Lewis acids such as $Sc(OTf)_3$ to give the opposite isomer to **23** regioselectively. Shift to the Bronsted acid, formic acid, gave considerable amount of the dehydroxylation product, bisindole **22**. Finally, HCl (4 M in dioxane) in wet dimethylacetamide at 150°C succeeded the transformation producing **25** as the only isomer in 56% yield. Further deprotection of phthalimide group with hydrazine and subsequent $Ti(Oi\text{-}Pr)_4$ mediated cyclization efficiently converted intermediate **25** into (±)-trigonoliimine C.

Almost at the same time, Prof. Mohammad Movassaghi and his coworker finished the first stereoselective synthesis of all members of (−)-trigonoliimine family and revised their absolute stereochemistry [58]. Movassaghi's synthesis started from the assembly of the bistryptamine heterodimer **27** via a Suzuki–Miyaura cross-coupling of the 6-methoxytryptamine borate derivative **26**, which was prepared by an iridium-catalyzed C2-borylation (Scheme 14.6) [63]. Suzuki–Miyaura cross-coupling of the unprotected tryptamine was unprecedented. Authors successfully synthesized the bistryptamine **27** by utilizing Buchwald's aminobiphenyl precatalyst [64] with silver phosphate salt as key parameters to afford the desired product in 63% yield. Following their plan enantioselective oxidation of 2,2′-bistryptamine derivative **27** was expected to install the first absolute stereocenter and serve as the key common scaffold to the stereoselective syntheses of all trigonoliimine families. By thorough experimentation, authors found that modification of bistrytamine electron density by N1-protection with various electron-withdrawing groups greatly altered its chemical property toward the desired region-selective oxidation. Finally, they discovered that (+)-((8,8-dichlorocamphoryl)-sulfonyl) oxaziridine (Davis' oxaziridine) [65] afforded hydroxyindolenines (+)-**28** and (+)-**29** (**28**:**29** = 2.2:1) in 95% yield and with an outstanding level of enantioselection for both isomers (96% ee).

Deprotection of the two amino groups of hydroxyindolenines spontaneously provided *cis*-fused aminals (+)-**30** and




**SCHEME 14.6** Movassaghi's enantioselective synthesis toward (–)-trigonoliimine A and B.




**SCHEME 14.7** Movassaghi's enantioselective synthesis toward (–)-trigonoliimine C.

(+)-**31**, the proposed precursors for trigonoliimine A and B, in 99% yield. Heating a solution of aminal (+)-**30** in trifluoroethanol (TFE) at 105°C provided the desired azepane (–)-**32** in 34% yield with significant drop in enantiomeric excess (15% ee). On the other hand, aminal (+)-**31** led to almost complete decomposition under the same condition. After careful studies, the authors found that treatment of a solution of aminals (+)-**30** and (+)-**31** in dichloromethane with the Martin sulfurane reagent [66] at −78°C provided the desired azepanes (–)-**32** and (–)-**33** in 47% combined yield (8 and 19% yield) with minimal erosion of enantiomeric excess (94% ee and 95% ee, respectively). Using optimal conditions, sequential treatment of pentacycle (–)-**32** with pyridinium *p*-toluenesulfonate (PPTS) and triisopropyl orthoformate in dichloromethane afforded (–)-trigonoliimine A in 82% yield. Under identical conditions, the pentacycle (–)-**33** was converted to (–)-trigonoliimine B in 94% yield.

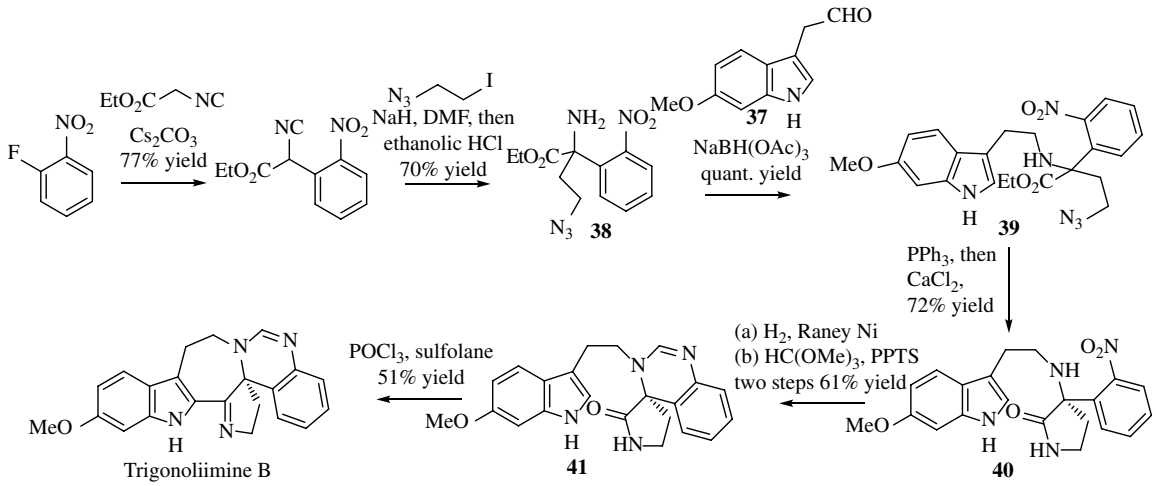
Wagner–Meerwein type 1,2-alkyl rearrangement was employed to access (–)-trigonoliimine C from the same hydroxyindolenines intermediate (Scheme 14.7) [67]. Heating

of hydroxyindolenines (+)-**28** and (+)-**29** in TFE at 102°C resulted in selective formation of the corresponding indoxyl (−)-**34** and (−)-**35** in 93% combined yield. The protection of the two amino groups in form of phthalimides during this rearrangement was critical in the overall efficiency and selectivity. Unveiling the two amino groups of indoxyls (−)-**34** and (−)-**35**, followed by condensative cyclization promoted by titanium ethoxide [68], provided the cyclic imine (−)-**36** and (−)-**37**. Treatment of these pentacyclic imines with *N*-formyl imidazole provided (−)-trigonoliimine C and (−)-isotrigonoliimine in 57 and 16% yield. All $^{1}H$ and $^{13}C$ NMR data for the synthetic trigonoliimines matched those provided in isolation report. The specific rotation and X-ray crystal structures of the synthetic trigonoliimines contradicted the results from isolation paper, especially in reversed optical rotation. Thus the stereochemistry of the natural products was revised.

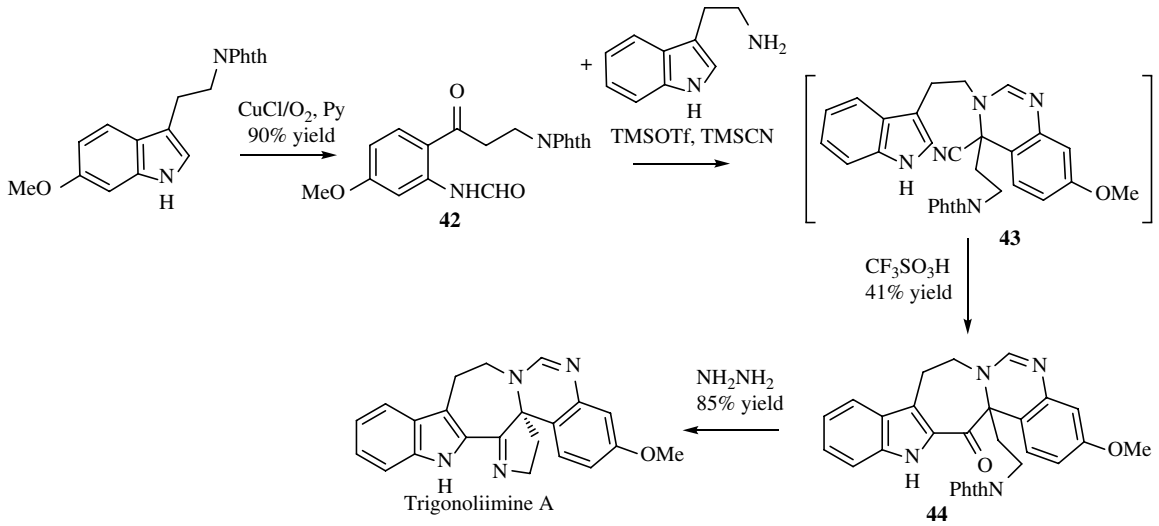
In a summary, both Tambar and Movassaghi's synthesis is based on the same biogenetic hypothesis through the selective oxidation and 1,2-alkyl migration strategy. Based on the same enantioselective oxidized common intermediate (+)-**28/29**, Movassaghi efficiently finished syntheses of all (−)-trigonoliimines in a diversified fashion. However, the regioselectivity in the oxidation of dissymmetric bistryptamine remained an issue. An alternative, nonbiomimetic and more target-oriented synthesis of trigonoliimine A was presented by Prof. Jieping Zhu and his coworkers that hinged on the sequential construction of the tricyclic ring system from simple α,α-disubstituted α-amino ester **38** (Scheme 14.8) [59]. Intermediate **38** was synthesized by sequential $S_NAr$ reaction between α-isocyanoacetate [69] and 2-fluoronitrobenzene, alkylation with 2-azidoiodoethane, and hydrolysis of isocyanide group in 54% yield (two steps combined) [70]. The aldehyde intermediate **37** was prepared by palladium-catalyzed heteroannulation between 2-iodo-5-methoxy aniline and 4-acetoxy butanal [71]. Reductive amination of aldehyde **37** with amine **38** under standard condition of $NaBH(OAc)_3$ to afford secondary amine **39** in quantitative yield. Staudinger reduction of **39** ($PPh_3$, $THF/H_2O$) and sequential treatment with $CaCl_2$ [72] were carried out to finish the first ring closure to afford γ-lactam intermediate **40**. Reduction of the nitro group by hydrogenation in Raney Nickel catalyst and following treatment with trimethyl orthoformate and PPTS yielded spirocycle **41** [58]. The final seven-member ring closure was envisioned to make use of the Bischler–Napieralski (BN) reaction [73]. Although the classic conditions including $POCl_3$/toluene/reflux did not afford the desired product, changing to a more polar solvent, as sulfolane took place smoothly to provide natural product of Trigonoliimine B in 51% yield.

A hypothesis of natural product biosynthesis can often provide an elegant access to their synthesis as illustrated by Movassaghi and Tambar's synthesis of trigonoliimine A–C. However, careful analysis of target structure can sometimes suggest an alternative laboratory synthesis that could be competitive to the biomimetic ones. Prof. Zhu's group accomplished an efficient nonbiomimetic-inspired total synthesis in seven steps from commercially available starting materials with an overall yield of 12%. In 2014, Prof. Xiao-Jiang Hao and coworkers finish the synthesis of (+)-trigonoliimine A in four steps via a Strecker/Houben–Hoesch sequence (Scheme 14.9) [60].

Prof. Hao's synthesis commenced with the copper(I) chloride-catalyzed oxidation of the tryptamine derivative to afford ketone **42** [74]. A three-component Strecker-type reaction was designed to react the ketone **42** with tryptamine and TMSCN to finish the first ring closure. After examining a series of both Lewis acid and Bronsted acids, the authors found a catalytic amount of TMSOTf promoted the transformation and afforded nitrile intermediate **43**, which is ready for the Houben–Hoesch-type cyclization [75]. Treatment by TfOH (trifluoromethanesulfonic acid) [76] in DCM and the




**SCHEME 14.8** Zhu's total synthesis toward trigonoliimine B.




**SCHEME 14.9** Prof. Hao's total synthesis toward trigonoliimine A.

hydrolysis of the resulting imine by saturated aqueous $NaHCO_3$ solution provided the ketone intermediate **44**. Since intermediate **43** is sensitive to basic or neutral environment and difficult to isolate, a modified one-pot procedure was applied to **42** to combine the Strecker-type reactions and Houben–Hoesch-type cyclization to afford **44** directly in 41% yield. The final deprotection of the phthalimide protecting group with hydrazine afforded trigonoliimine A in four steps with extreme atom economy.

From a synthetic chemist's view, total syntheses of trigonoliimine family alkaloid are not forbidden. In a very short time, the elegant syntheses toward the tryptamine-derived bisindole alkaloid trigonoliimine A–C were accomplished by different groups. According to their synthetic strategies, these syntheses could be categorized into two types: biomimetic and nonbiomimetic ones. Both Tambar and Movassaghi's synthesis plan came from biogenetic origins and finished in almost identical way. Selective oxidation and Wagner–Meerwein [1,2]-shift were applied to these syntheses. Among them, Movassaghi succeeded the first enantioselective synthesis of all the structural diversity within trigonoliimine families based on the common synthetic scaffolds concept described previously and revised their stereochemistry. Although both Zhu and Hao's syntheses are nonbiomimetic, their target-oriented synthesis proved to be highly efficient and short. With the presentation of these four elegant examples, we wish to demonstrate that well-designed different strategies can indeed provide solutions to complex chemical problems.

## REFERENCES


1. K. M. Hermann, L. M. Weaver, *Annu. Rev. Plant Physiol. Plant Mol. Biol.* 1999, **50**, 473–503.
2. H. Morell, D. B. Sprinson, *J. Biol. Chem.* 1968, **243**, 676–677.
3. C. S. Gasser, J. A. Winter, C. M. Hironaka, D. M. Shah, *J. Biol. Chem.* 1988, **263**, 4280–4287.
4. E. Schonbrun, S. Eschenburg, W. A. Shuttleworth, J. V. Schloss, J. N. Evans, W. Kabsch, *Proc. Natl. Acad. Sci. U.S.A.* 2001, **98**, 1376–1380.
5. A. Schaller, J. Schmid, U. Leiginger, N. Amrhein, *J. Biol. Chem.* 1991, **266**, 21434–21438.
6. P. Macheroux, J. R. Schmid, N. Amrhein, A. Schaller, *Planta* 1999, **207**, 325–334.
7. S. Bornemann, D. J. Lowe, R. N. Thorneley, *Biochemistry* 1996, **35**, 9907–9916.
8. F. Ely, J. E. Nunes, E. K. Schroder, J. Frazzon, M. S. Palma, D. S. Santos, L. A. Basso *BMC Biochem.* 2008, **9**, 13–29.
9. H. Tamir, P. R. Srinivasan, *Proc. Natl. Acad. Sci. U.S.A.* 1970, **66**, 547–551.
10. A. A. Morollo, M. J. Eck, *Nat. Struct. Biol.* 2001, **8**, 243–247.
11. T. E. Creighton, C. Yanofsky, *Methods Enzymol.* 1970, **17A**, 365–380.
12. E. R. Radwanski, R. L. Last, *Plant Cell* 1995, **7**, 921–934.
13. O. Mayans, A. Ivens, L. J. Nissen, K. Kirschner, M. Wilmanns, *EMBO J.* 2002, **21,** 3245–3254.
14. R. Thoma, M. Hennig, R. Sterner, K. Kirschner, *Structure* 2000, **8**, 265–276.
15. M. Hennig, R. Sterner, K. Kirschner, J. N. Jansonius, *Biochemistry* 1997, **36**, 6009–6016.
16. J. P. Priestle, M. G. Grutter, J. L. White, M. G. Vincent, M. Kania, E. Wilson, T. S. Jardetzky, K. Kirschner, J. N. Jansonius, *Proc. Natl. Acad. Sci. U.S.A.* 1987, **84**, 5690–5694.
17. M. Hennig, B. Darimont, R. Sterner, K. Kirschner, J. N. Jansonius, *Structure* 1995, **3**, 1295–1306.
18. X. Huang, H. M. Holden, F. M. Raushel, *Annu. Rev. Biochem.* 2001, **70**, 149–150.
19. T. T. Schneider, E. Gerhardt, M. Lee. P.-H. Liang, K. S. Anderson, I. Schlichting, *Biochemistry* 1998, **37**, 5394–5406.

20. A. N. Lane, K. Kirschner, *Biochemistry* 1991, **30**, 479–484.
21. K. S. Anderson, E. W. Miles, K. A. Johnson, *J. Biol. Chem.* 1991, **266**, 8020–8033.
22. S.E. O'Connor, J. J. Maresh, *Nat. Prod. Rep.* 2006, **23**, 532–547.
23. I. L. Knynyants, *Chemical Encyclopedia, Soviet Encyclopedia* p. 623 (1998).
24. D. S. Seigler, *Plant Secondary Metabolite*, Springer, Dordrecht, p **628**, (1998).
25. F. Cote, E. Thavenot, C. Fligny, *Proc. Natl. Acad. Sci. U.S.A.*, 2003, **100**, 13525–13530.
26. K. Palme, F. Nagy, *Cell* 2008, **133**, 31–32.
27. J. Leonard, *Nat. Prod. Rep.* 1999, **16**, 319–338.
28. G. A. Cordell, *The Alkaloids: Chemistry and Biology*, Academic Press, San Diego, Vol. **50**, p 260 (1998).
29. V. De Luca, C. Marineau, N. Brisson, *Proc. Natl. Acad. Sci. U.S.A.*, 1989, **86**, 2582–2586.
30. E. Leete, *Tetrahedron* 1961, **14**, 35–41.
31. T. P. Begley, *Encyclopedia of Chemical Biology*, John Wiley & Sons, Inc., Hoboken, p 5–7, (2009).
32. W. G. Kurz, K. B. Chatson, F. Constabel *Planta Med.* 1981, **42**, 22–31.
33. A. A. Qureshi, A. I. Scott, *Chem. Commun.* 1968, 948–950.
34. J. E. Saxton, *Nat. Prod. Rep.* 1984, **1**, 21–51.
35. S. I. Heimberger. I. Stanley, I. A. Scott, *J. Chem. Soc. Chem. Commun.* 1973, 217–218.
36. E. J. Corey, X.-M. Cheng, *The Logic of Chemical Synthesis*, Wiley, New York, (1989).
37. E. E. Anagnostaki, A. L. Zografos. *Chem. Soc. Rev.* 2012, **41**, 5613–5625.
38. S. L. Schreiber, *Science* 2000, **287**, 1964–1969.
39. T. Beghyn, R. Deprez-Poulain, N. Willand, B. Folleas, B. Deprez, *Chem. Biol. Drug Des.* 2008, **72**, 3–15.
40. S. B. Jones, B. Simmons, A. Mastracchio, D. W. C. MacMillan, *Nature* 2011, **475**, 183–188.
41. B. R. Stockwell, *Nature* 2004, **432**, 846–854.
42. J. Bonjoch, D. Sole, *Chem. Rev.* 2000, **100**, 3455–3482.
43. S. B. Jones, B. Simmons, D. W. C. MacMillan, *J. Am. Chem. Soc.* 2009, **131**, 13606–13607.
44. F. Gatta, D. Misiti, *J. Heterocycl. Chem.* 1987, **24**, 1183–1187.
45. P. J. Thomas, C. J. M. Stirling, *J. Chem. Soc. Perkin Trans. II* 1978, **11**, 1130–1134.
46. M. Prashad, L. Lavecchia, K. Prasad, O. Repic, *Synth. Commun.* 1995, **25**, 95–100.
47. F. A. L. Anet, R. Robinson, *Chem. Ind.* 1953, 245.
48. M. E. Kuehne, P. J. Seaton, *J. Org. Chem.* 1985, **50**, 4790–4796.
49. O. Wagnieres, Z. Xu, Q. Wang, J. Zhu, *J. Am. Chem. Soc.* 2014, **136**, 15102–15108.
50. Z. Xu, Q. Wang, J. Zhu, *Angew. Chem. Int. Ed.* 2013, **53**, 3272–3276.
51. S. L. Schreiber, R. E. Claus, J. Reagan. *Tetrahedron Lett.* 1982, **23**, 3867–3870.
52. G. C. Hirst, T. O. Johnson Jr., L. E. Overman, *J. Am. Chem. Soc.* 1993, **115**, 2992–2993.
53. R. J. Sundberg, W. J. Pitts, *J. Org. Chem.* 1991, **56**, 3048–3054.
54. M. T. Crimmina, M. Shamszad, A. E. Mattson, *Org. Lett.* 2010, **12**, 2614–2617.
55. S. A. Kozmin, T. Iwama, Y. Huang, V. H. Rawal, *J. Am. Chem. Soc.* 2002, **124**, 4628–4641.
56. C.-J. Tan, Y.-T. Di, Y.-H. Wang, Y. Zhang, Y.-K. Si, Q. Zhang, S. Gao, X.-J. Hu, X. Fang, S.-F. Li, S.-F. Li, X.-J. Hao. *Org. Lett.* 2010, **12**, 2370–2373.
57. X. Qi, H. Bao, U. K. Tambar, *J. Am. Chem. Soc.*, 2011, **133**, 10050–10053.
58. S. Han, M. Movassaghi, *J. Am. Chem. Soc.* 2011, **133**, 10768–10771.
59. T. Buyck, Q. Wang, J. Zhu, *Org. Lett.*, 2012, **14**, 1338–1341.
60. B. Zhao, X.-Y. Hao, J.-X. Zhang, S. Liu, X.-J. Hao. *Org. Lett.* 2013, **15**, 528–530.
61. A. R. Howard-Jones, C. T. Wash, *J. Am. Chem. Soc.* 2007, **129**, 11016–11017.
62. S. Quideau, G. Lyvinec, M. Marguerit, K. Bathany, A. Ozanne-Beaudenon, T. Buffeteau, D. Cavagnat, A. Chenede *Angew. Chem. Int. Ed.* 2009, **48**, 4605–4609.
63. T. Ishiyama, J. Takagi, K. Ishida, N. Miyaura, N. R. Anastasi, J. F. Hartwig. *J. Am. Chem. Soc.* 2002, **124**, 390–391.
64. T. Kinzel, Y. Zhang, S. L. Buchwald, *J. Am. Chem. Soc.* 2010, **132**, 14073–14075.
65. F. A. Davis, M. C. Weismiller, *J. Org. Chem.* 1990, **55**, 3715–3717.
66. J. C. Martin, R. J. Arhart, *J. Am. Chem. Soc.* 1971, **93**, 4327–4329.
67. G. Wagner, *Ber.* 1899, **32**, 2302.
68. G. Liu, D. A. Cogan, T. D. Owens, T. P. Tang, J. A. Ellman, *J. Org. Chem.* 1999, **64**, 1278–1281.
69. J. Zhu, *Eur. J. Org. Chem.* 2003, 1133–1144.
70. C. Lalli, M. J. Bouma, D. Bonne, G. Masson, J. Zhu, *Chem.-Eur. J.* 2011, **17**, 880–889.
71. C.-Y. Chen, D. R. Lieberman, R. D. Larsen, T. R. Verhoeven, P. J. Reider, *J. Org. Chem.* 1997, **62**, 2676–2677.
72. M. W. Bundesmann, S. B. Coffey, S. W. Wright, *Tetrahedron Lett.* 2010, **51**, 3879–3882.
73. W. M. Whaley, T. R. Govindachari, *Org. React.* 1951, **6**, 74–150.
74. J. Tsuji, H. Kezuka, H. Takayanagi, K. Yamamoto, *Bull. Chem. Soc. Jpn.* 1981, **54**, 2369.
75. Y. Sato, M. Yato, T. Ohwada, S. Saito, K. Shudo, *J. Am. Chem. Soc.* 1995, **117**, 3037–3043.
76. H. M. Colquhoun, D. F. Lewis, D. J. Williams, *Org. Lett.* 2001, **3**, 2337–2340.

# 15

# FUTURE DIRECTIONS OF MODERN ORGANIC SYNTHESIS

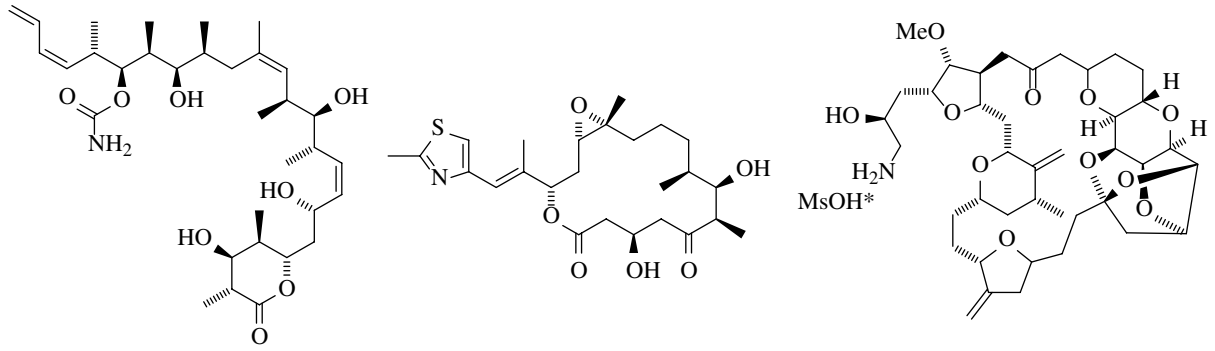
Jakob Pletz and Rolf Breinbauer
*Institute of Organic Chemistry, Technische Universität Graz, Graz, Austria*

## 15.1 INTRODUCTION

Total synthesis of natural products has seen several paradigm shifts over the last century [1]. Until the 1950s its main purpose was to provide the ultimate proof of the proposed structure of a complex natural product. Eschenmoser has pointed out that in this endeavor total synthesis was for a long time intellectually restrained to synthetic routes, which aimed at intermediates, which have been achieved in degradation studies of the natural products before [2]. With the advent of spectroscopic techniques such as UV, IR, NMR, and X-ray, which enabled the confirmation of the structural identity of synthesized and natural product, this aspect became obsolete, and synthetic chemists were free to pursue any creative way accessing the desired target compound. A new period started in which organic synthesis demonstrated that it could access the most challenging natural products. The total syntheses of vitamin B12 [3], palytoxin [4], brevetoxin [5], tetrodotoxin [6], or palau'amine [7] showed that organic chemistry has matured to a state in which any synthetic molecule can be successfully synthesized. These achievements not only gave a boost in confidence to the synthetic community but also set a crisis to the field of natural product synthesis, as it needed a new justification, why it remains important (and why it should be funded). First of all, total synthesis continues to be the inspiration and the best testing ground for new synthetic methods. Since the 1970s the groups of Evans [8], Masamune [9], and others have refined the synthetic methodology in stereoselective aldol chemistry to such a level that the synthesis of polyketide natural products has become a well tractable problem thanks to a richly filled tool box of reliable and predictable organic reactions. The trust the synthetic community has in Pd-catalyzed cross-coupling reactions has strongly been built on the numerous applications of these transformations in later stages of syntheses of complex natural products, demonstrating the excellent functional group tolerance of these reactions [10]. Since 2000, natural product synthesis has seen a new paradigm, in which the scalable access to natural products has emerged as an important goal [11]. Until then natural products as pharmaceuticals have either been isolated directly from natural sources (or fermentation broths) or have semisynthetically been produced by modification of natural products. In contrast, the Novartis synthesis of discodermolide (**1**) (60 g) [12], the Bayer–Schering synthesis of sagopilone (**2**) (8 kg) [13], and—probably most impressive—the total synthesis of the marketed drug Halaven® (**3**, eribulin mesylate) by Esai [14] have shown that natural products are now accessible on production scale by total synthesis (Fig. 15.1).

Along this endeavor synthetic organic chemists have also become more pragmatic in their choice of methods. While photochemistry, electrochemistry, or biocatalysis has been studied and practiced by specialized labs, who had the necessary equipment and expertise, it seems that these techniques are now increasingly adapted by synthetic groups and integrated in total syntheses, since the scope and limitations of these transformations have been better defined and low-cost experimental setups have been designed. Increasingly, synthetic routes are becoming richer in the used synthetic methodology and remind of the Reichstein vitamin C synthesis from 1934, in which after a heterogeneous hydrogenation

*From Biosynthesis to Total Synthesis: Strategies and Tactics for Natural Products*, First Edition. Edited by Alexandros L. Zografos.
© 2016 John Wiley & Sons, Inc. Published 2016 by John Wiley & Sons, Inc.



**(+)-Discodermolide** **Sagopilone** **Eribulin mesylate**

**1** **2** **3**

**FIGURE 15.1** Examples of natural product drug candidates produced via total synthesis on large scale.

using Ni a microbial oxidation with *Acetobacter oxidans* is followed by chemical oxidation with $KMnO_4$ [15].

For the field of the synthesis of natural products, we see the following new trends:

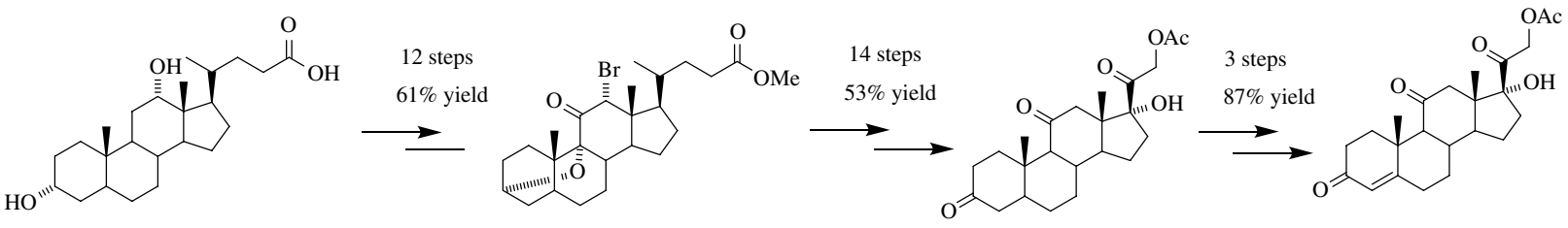
- New methodologies in the synthesis of total synthesis (photochemistry, electrochemistry, biocatalysis, etc.)
- Late-stage functionalization of core structures using highly selective chemical or biochemical methods
- Scalable synthesis of natural products (overcoming supply problems)
- Bioengineering for the production of natural products (and derivatives)
- Natural products as structural inspiration for new synthetic targets

## 15.2 ENZYMES IN ORGANIC SYNTHESIS: MERGING TOTAL SYNTHESIS WITH BIOSYNTHESIS

Mother Nature is undoubtedly regarded as the best synthetic chemist. Complex natural products are produced from simple starting materials available in form of sugars, fatty acids, or amino acids as carbon sources and converted to complex structures using multistep synthesis using a series of enzymes, which sometimes enable amazing transformations even in the context of highly functionalized substrates. It would be attractive if one could integrate such enzymes in organic synthesis and combine the advantages of chemical and biosynthetic methods. An instructive example how disruptive such an enzymatic transformation can be is the story of cortisone, which was identified as a wonder drug but which could only be isolated in minute amounts from natural sources. The Merck process group developed in 1953 the first industrial synthesis of cortisone, which starts from deoxycholic acid (**4**) as a starting material. In a series of transformations, the C=O moiety at C-12 is transposed to C-11 furnishing **5**, which was converted to intermediate **6**, from which a dehydrogenation sequence led to cortisone acetate (**7**). The overall synthetic sequence comprises 29 steps in an impressive overall yield of 28% [16]. This process was abandoned when Upjohn devised an alternative strategy in which starting from less expensive stigmasterol (**8**) as a starting material first progesterone (**9**) was produced in four steps. The critical installment of the 11-OH group in fantastic 90% yield was accomplished by microbial oxidation using *Rhizopus nigricans* microorganism, which is today performed on a multiton scale. With **10** in hand, the transformation to **7** is straightforward [17]. This process illustrates how the integration of enzymes into organic synthesis sequences allows for late-stage functionalization through unsurpassed chemoselectivity (Scheme 15.1).

Despite this early commercial success, it has taken considerable time that enzymes have become valuable tools for organic synthesis in the 1980s. Since then several enzyme classes such as hydrolases (especially lipases and esterases), hydroxynitrilases, ketoreductases, enoate reductases, aldolases, transaminases, nitrilases, Baeyer–Villiger monooxygenases, etc. have found widespread application in organic synthesis and even industrial application in the fine chemical industry [18–21]. Directed evolution has emerged as an efficient strategy to overcome common limitations of wild-type enzymes such as limited non-native substrate scope, limited stereoselectivity for non-native substrates, undesired absolute configuration, or stability problems regarding heat and organic solvents [22]. In the context of the total synthesis of natural products and complex target molecules, biocatalysis typically is used in the early stage of a synthetic sequence and most often for the synthesis of chiral building blocks [23]. Turner has recently proposed that the field of biocatalysis has to develop a catalog of reliable and predictive transformations, which will be integrated into the retrosynthetic considerations

Merck-process:



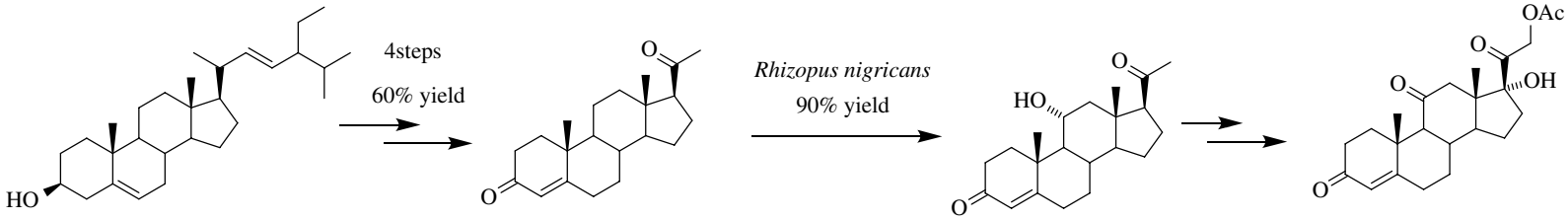

Deoxycholic acid
**4**

**5**

**6**

Cortisone acetate
**7**

Upjohn-process:




Stigmasterol
**8**

Progesteron
**9**

**10**

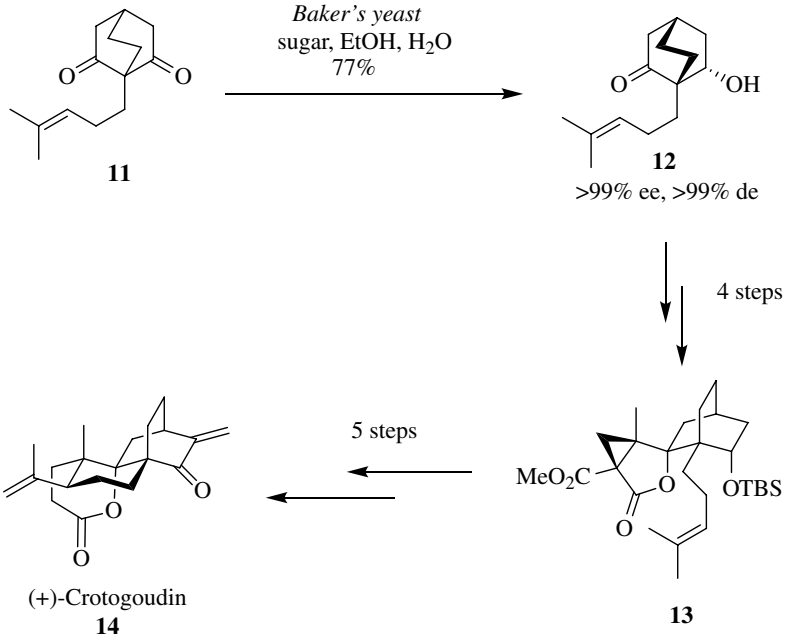
Cortisone acetate
**7**

**SCHEME 15.1** Commercial routes toward cortisone acetate (**7**).

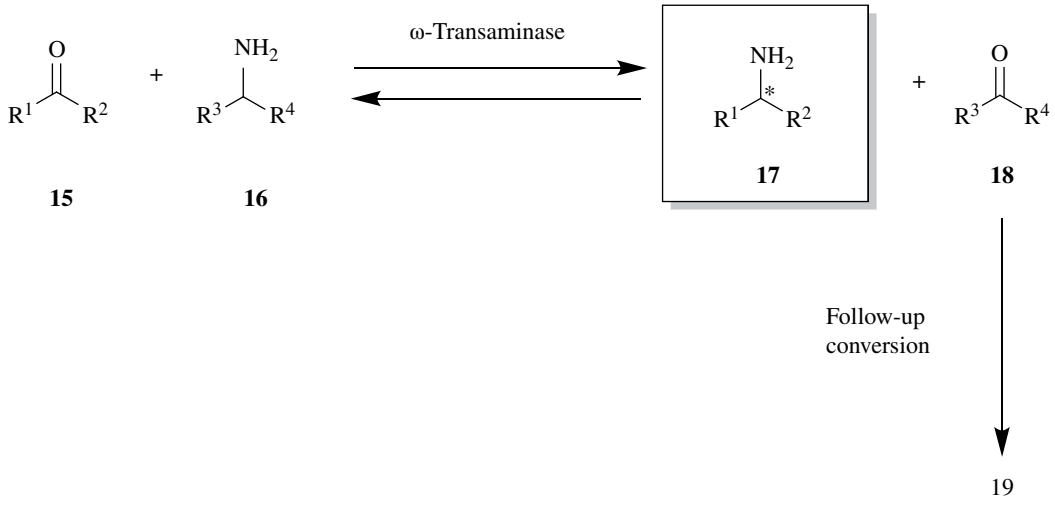
of synthetic chemists [24]. In this chapter, we want to highlight some recent applications, which demonstrate that the integration of biocatalytic steps can improve the elegance and synthetic efficiency dramatically.

The reduction of 1,3-diketones to β-hydroxyketones catalyzed by baker's yeast is one of the oldest biocatalytic transformations applied in organic synthesis. It is very simple to perform using inexpensive reagents, which can be purchased in any supermarket. Carreira showed an application of this transformation in their recent synthesis of the cytotoxic diterpene (+)-crotogoudin (**14**) (Scheme 15.2) [25]. Bicyclo[2.2.2] octa-2,6-dione **11** was treated with baker's yeast and sugar in water, furnishing *endo*-alcohol (−)-**12** in 77 % yield as a single enantio- and diastereomer. Further elaboration led to intermediate **13**, which in a $SmI_2$-mediated radical cyclopropane-opening/annulation/elimination cascade reaction delivered the tetracyclic carbon skeleton, which was further elaborated to target compound **14**.

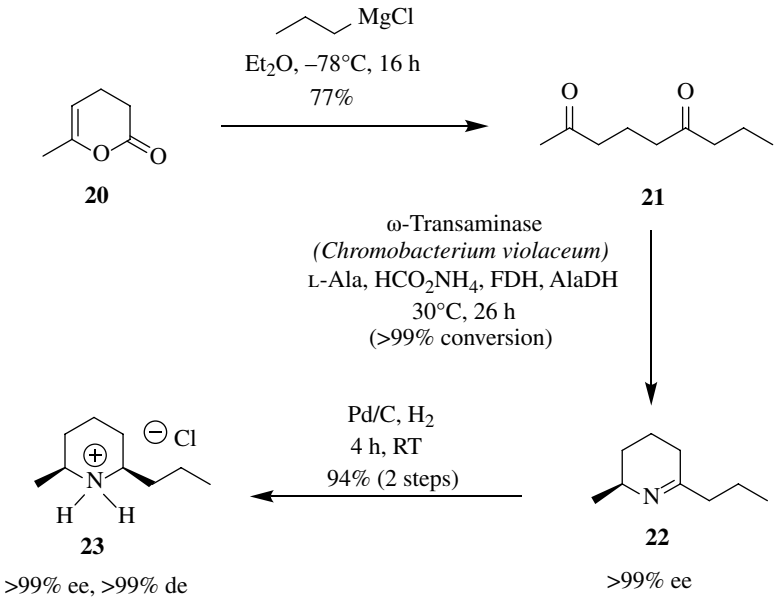
The enzyme class which has received the most increase in attention in industrial and synthetic applications since 2000 is ω-transaminases, in which a suitable inexpensive amino-donor **16** is used to convert a C=O group of a prochiral substrate **15** into chiral amine **17**. In order to shift the equilibrium to the desired amine product, the keto by-product **18** is usually converted in a second irreversible enzymatic step into an innocent side product **19** (Scheme 15.3).




**SCHEME 15.2** Synthesis of (+)-crotogoudin.




**SCHEME 15.3** ω-Transaminases for the synthesis of chiral amines.



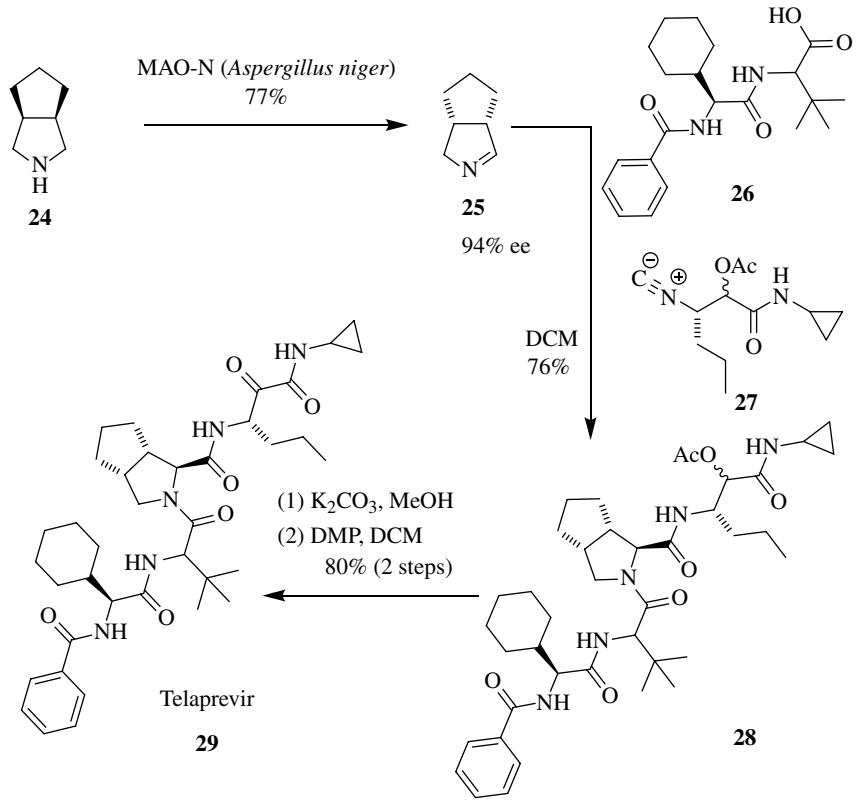

**SCHEME 15.4** Chemoenzymatic synthesis of (+)-dihydropinidine (**23**).

Kroutil presented a very nice application of an ω-transaminase in the synthesis of the natural alkaloid (+)-dihydropinidine **23** in a 3-step synthesis with 72% overall yield (Scheme 15.4) [26]. Commercially available pyranone **20** was converted into diketone **21**. Taking advantage of the superb regio- and enantioselectivity of the ω-transaminase from *Chromobacterium violaceum*, the less substituted ketone was converted into the (*S*)-amine, which spontaneously cyclized to imine **22**. As an amino donor L-alanine was used and the equilibrium shifted to full conversion by converting the resulting pyruvate side product with alanine dehydrogenase (AlaDH) to L-alanine, therefore recycling the amino donor and having ammonium formate as the ultimate nitrogen source. The subsequent catalytic hydrogenation of imine **22** with Pd/C occurred under complete diastereoselectivity producing the desired product **23**. The synthetic route is distinguished by its conciseness and its high atomic efficiency and optimal stereoselectivity.

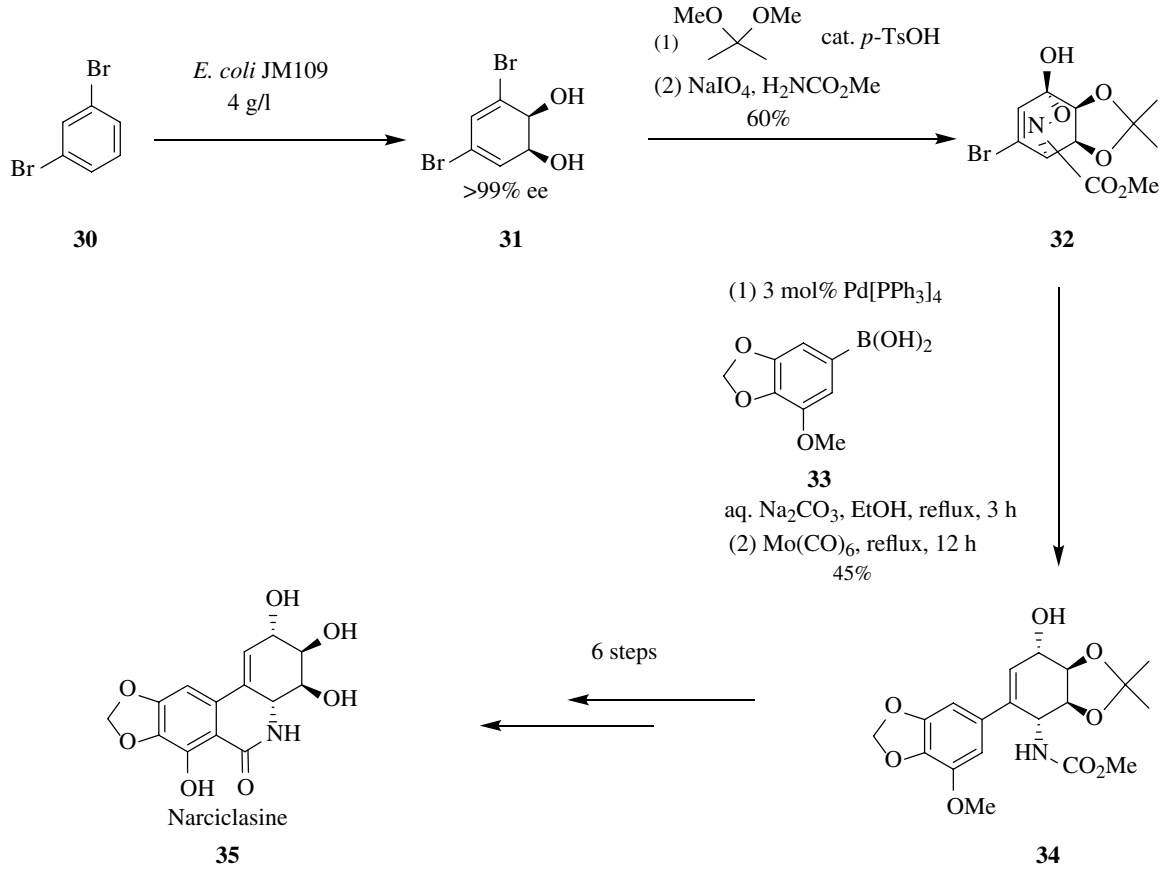
An impressive example demonstrating that an enzymatic step in combination with a multicomponent reaction allows the stereoselective assembly of complicated structures has been reported by Orru and Ruijter in the synthesis of the antihepatitis C virus (HCV) drug telaprevir (**29**) (Scheme 15.5) [27]. **29** is an inhibitor of HCV NS3 protease. The key transformation is an enzymatic desymmetrization of *meso*-pyrrolidine **24** by means of the monoamine oxidase N (MAO-N) from *Aspergillus niger* optimized by directed evolution in 94% ee and 77% yield. Chiral imine **25** is combined with carboxylic acid **26** and isonitrile **27** to undergo a Ugi-type 3-component reaction establishing **28** with the complete framework of the drug molecule in 76% yield. Cleavage of the acetate and oxidation of the resulting alcohol with Dess–Martin periodinane (DMP) produced telaprevir (**29**) in 80% over the last two steps. The total yield is 45% over the longest linear sequence starting from L-cyclohexylglycine methyl ester.

The enantioselective oxidation of a C–H bond is a very attractive strategic bond-formation strategy in organic synthesis for which we have unfortunately only few and rather limited chemical methods. In contrast microbial oxidation provides for certain structures an almost perfect solution, as has been demonstrated by the Upjohn cortisone process (see Scheme 15.1). Hudlicky and others have developed a very universal toolbox of microorganisms, which enable the scalable and highly enantioselective 1,2-dihydroxylation of substituted benzenes. The elegance of this method, which upon dearomatization not only generates two stereogenic centers but also several functional groups, which can be exploited for further derivatization, should first be illustrated in Hudlicky's synthesis of the *Amaryllidaceae* alkaloid narciclasine (**35**) (Scheme 15.6) [28]. Through whole-cell fermentation of 1,3-dibromobenzene (**30**) with toluene dioxygenase overexpressing organism *E. coli* JM109, the chiral diol **31** was produced in a fermentation yield of 4 g/L. As diol **31** is a rather unstable compound, it was immediately transformed into a ketal, which underwent a nitroso Diels–Alder reaction furnishing bicycle **32**, which could be transformed into narciclasine (**35**) in eight steps.

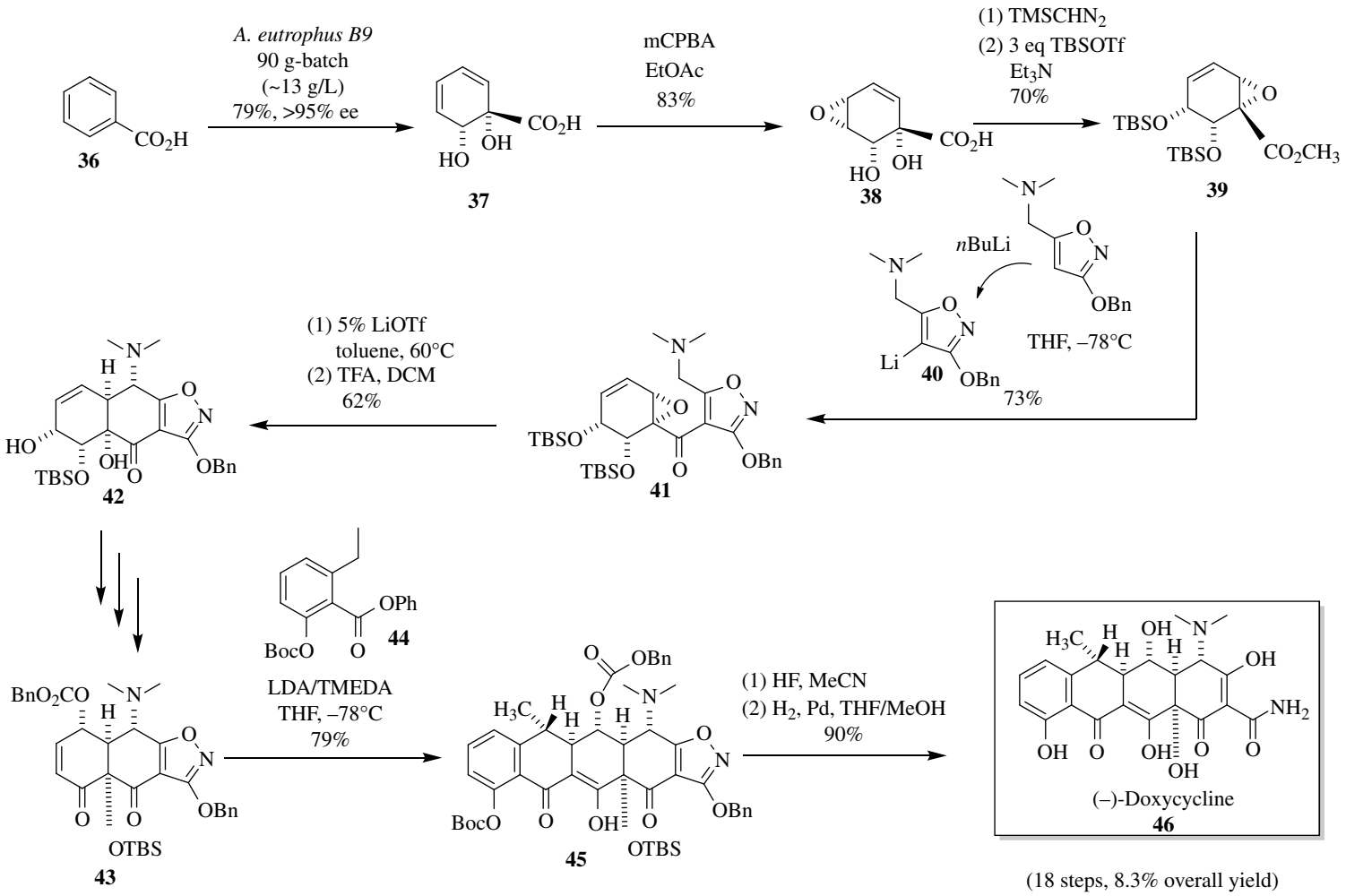
A different variant of this enzyme led to the dioxygenation of benzoic acid (**36**) to 1,2-diol 37, which served as the chiral starting material for Myers' synthesis of the antibiotic (+)-doxycycline (**46**) (Scheme 15.7) [29]. Functional group manipulation of **37** led to epoxide **39**, which was ligated with **40** to ketone **41**. In a Sommelet–Hauser-type rearrangement



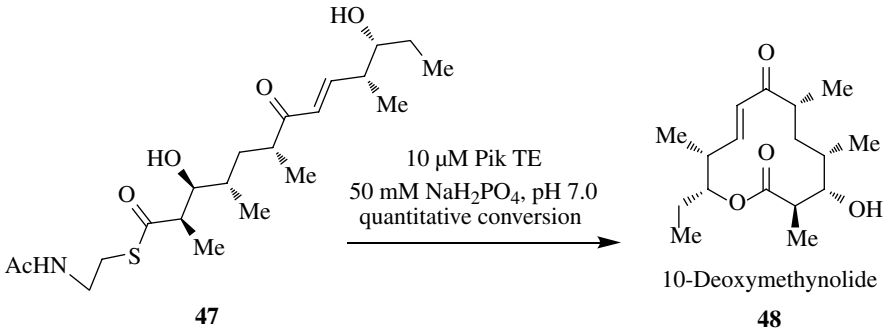

**SCHEME 15.5** Chemoenzymatic synthesis of telaprevir.




**SCHEME 15.6** Synthesis of narciclasine (**35**) using a fermentative 1,2-dioxygenation.




**SCHEME 15.7** Myers synthesis of (−)-doxycycline (**46**) using an enzymatic dihydroxylation.




47 48

**SCHEME 15.8** Thioesterase-catalyzed macrolactonization leading to 10-deoxymethynolide (**48**).

tricycle **42** was generated, which was elaborated to central building block **43**. The subsequent Michael addition followed by intramolecular enolate acylation proved effective for reagent **44** leading to (−)-doxycycline (**46**) and was quite universal for similar nucleophiles leading to differently substituted products. The unique tactics and practical elegance of their synthetic route allowed the Myers group to prepare hundreds of analogs, from which a clinical candidate was identified, which is now in Phase II clinical trials [30–32].

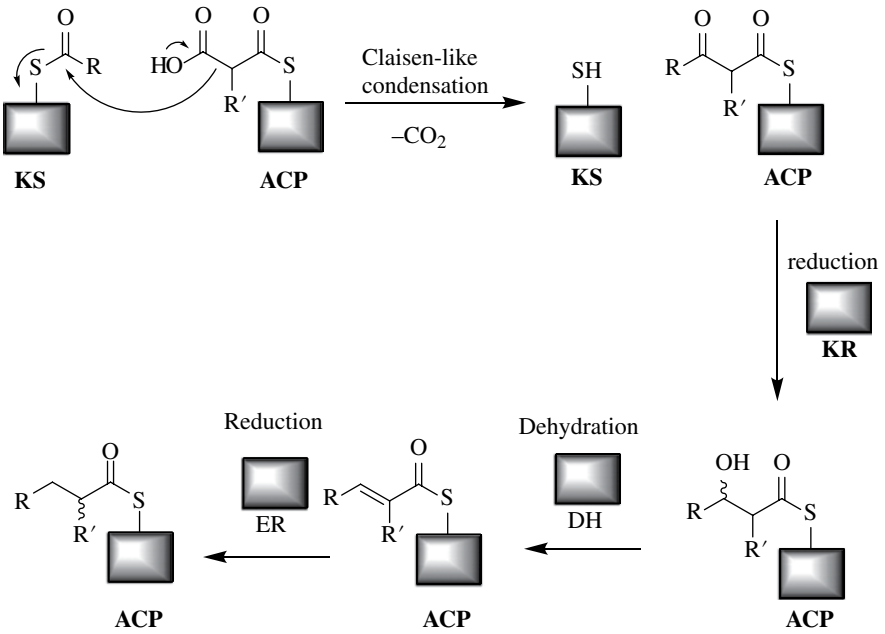
The examples described above highlight the impact of biocatalysis in the contribution of chiral building blocks or in stereoselective transformations in the early stages of a multistep synthesis, where the value of biocatalysis has been well documented. Ideally one would be able to use enzymes also in later stages of a multistep organic synthesis or for late-stage functionalization as it is characteristic for cellular biosynthesis processes using multienzyme complexes. However, this has so far been elusive to established biocatalysts for several reasons: natural enzymes with broader substrate scope typically prefer small substrates. If they are able to handle larger substrates then they typically have very narrow scope limited to the natural substrate. In addition, for larger substrates often an operational problem arises that they are often poorly soluble in the aqueous solvents, which are necessary for using enzymes. More recently, several groups have begun to isolate domains for the biosynthetic machinery of polyketide synthases (PKSs) and make them as reagents available [33]. One especially attractive candidate enzyme is thioesterase (TE), which as being part of PKS multienzyme complexes transforms acyclic precursors into macrolactones in polyketide biosynthesis. Aldrich et al. have used the TE of the Pikromycin (Pik) PKS system of *Streptomyces venezuelae* for the macrocyclization of the *N*-acetylcysteamine (SNAC) thioester of seco-10-deoxymethynolide **47** into 10-deoxymethynolide (**48**) as the exclusive product (Scheme 15.8) [34]. However, when they used non-native substrates such as the epimeric alcohols at C-7, no cyclization product was observed indicating that Pik TE is highly specific for its native substrate. Eguchi et al. could show that other TEs can be more tolerant in their substrate scope and have described that the vicenistatin (Vin) TE domain is able to catalyze the macrocyclization of ω-hydroxy fatty acid ethyl esters to afford 17- to 28-membered lactones [35]. One would hope that in the future a rather general TE domain will be identified or optimized via directed evolution, which could compete with the chemical Yamaguchi macrolactonization.

## 15.3 ENGINEERED BIOSYNTHESIS

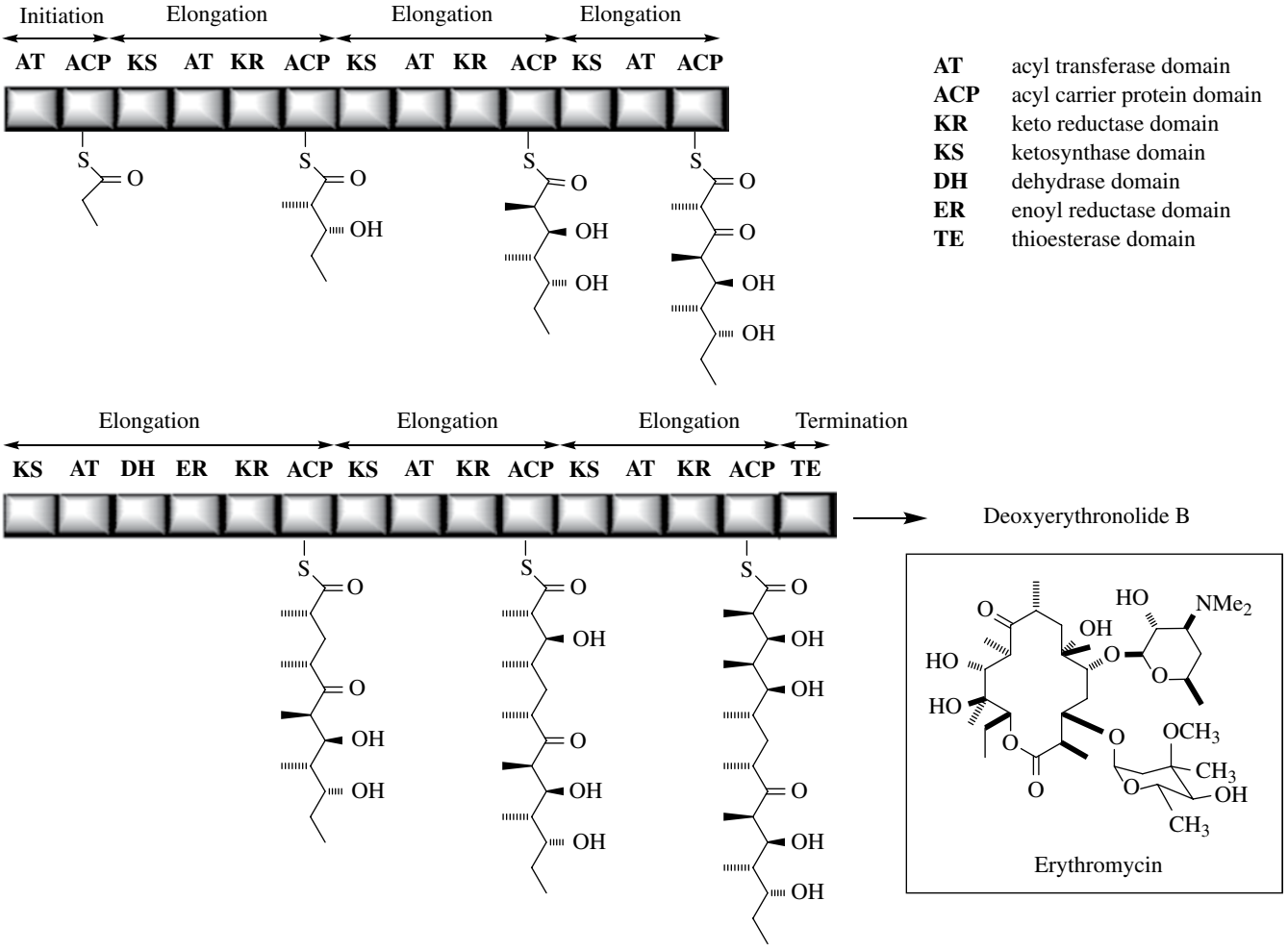
While the previous chapter has shown that single enzymatic steps can be of tremendous value for organic synthesis, it might be prudent to exploit the unsurpassed synthetic skills of Mother Nature by borrowing not only one enzyme but the complete biosynthetic machinery encoded in the genes of secondary metabolite producing microorganisms [36]. The synthesis of the antimalarial drug precursor artemisinic acid in engineered yeast by Keasling is an impressive example for this strategy [37]. Despite this also industrially relevant success, in practice the strategy of synthetic biology faces several challenges, such as identifying suitable production hosts for the manipulated gene clusters and strategies toward improving the production yields of structural variants of the wild-type natural products. In this chapter, we will highlight the current status of the field [38].

Polyketides constitute a large and diverse class of natural products with high structural complexity and various bioactivities. They present significant challenges for synthesis, and various synthetic and biosynthetic techniques have been used for their preparation and derivatization [39–41]. In their biosynthesis, polyketides are assembled by PKSs via a cascade of decarboxylative Claisen condensations of malonyl extender units and carboxylic acid thioesters [42]. After each extension cycle, the resulting β-keto thioester can be processed further by means of various enzymatic reactions to furnish a large variety of structures (Scheme 15.9). In this process, the growing polyketide chain is passed from one catalytic enzyme domain to the next eventually furnishing the final polyketide (Scheme 15.10).

The modular nature of this PKS has inspired biochemists to manipulate this biosynthetic machinery by exchanging PKS




**SCHEME 15.9** Key steps in the biosynthesis of polyketides.




**AT** acyl transferase domain
**ACP** acyl carrier protein domain
**KR** keto reductase domain
**KS** ketosynthase domain
**DH** dehydrase domain
**ER** enoyl reductase domain
**TE** thioesterase domain

**SCHEME 15.10** Synthesis of the aglycon deoxyerythronolide B in the biosynthesis of erythromycin.

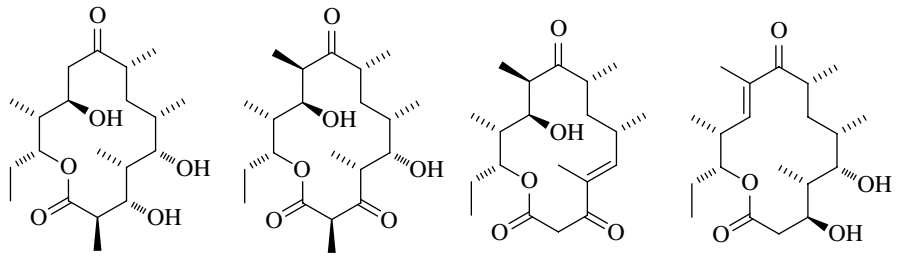


**FIGURE 15.2** Representative compounds synthesized by biosynthetic engineering of DEBS.

fragments, hence transplanting catalytic domains between different PKSs, making new derivatives and structural analogs accessible [43, 44]. There are four degrees of freedom in polyketide biosynthesis that can be independently manipulated by genetic engineering, taking advantage of the natural modularity of polyketide biosynthesis:

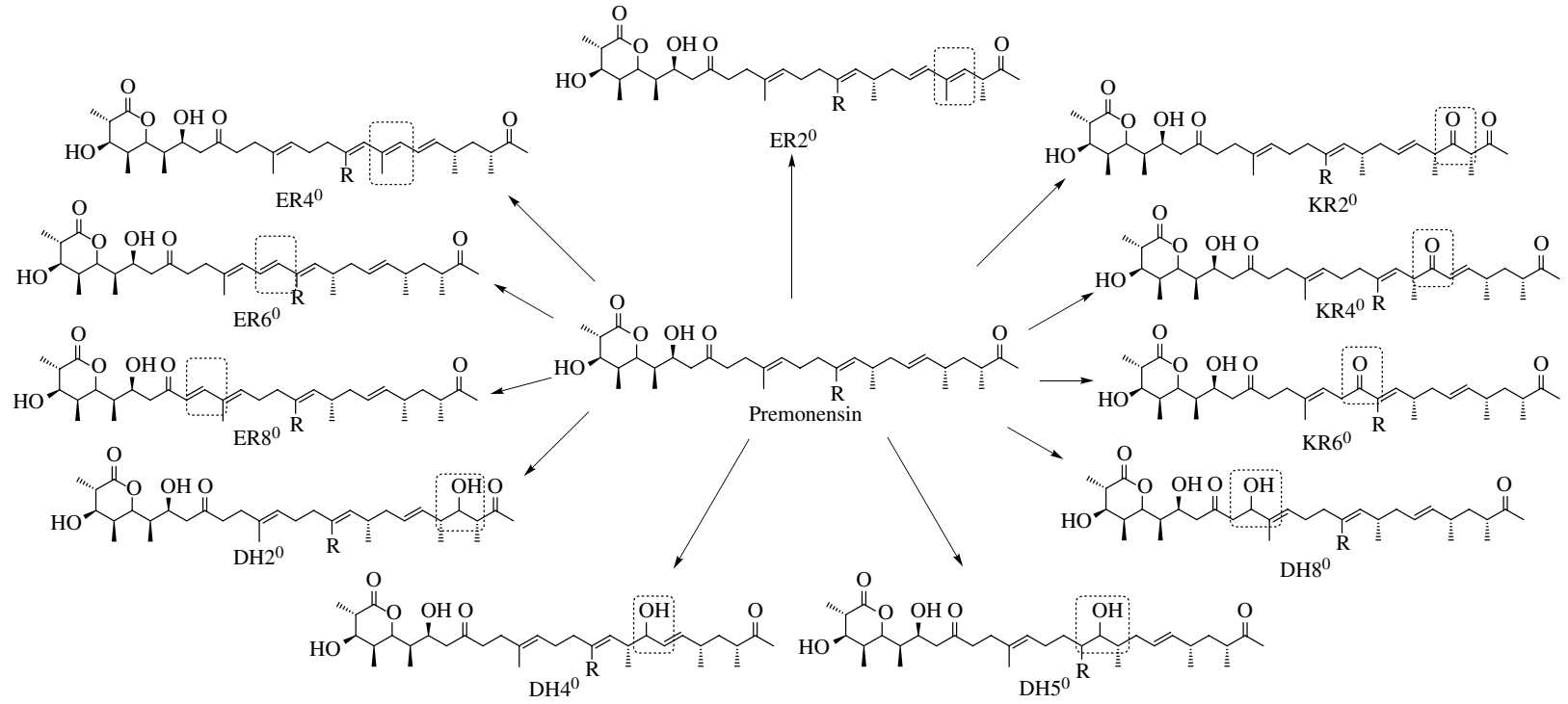
1. Length of the polyketide chain (determined by the number of modules that comprise the PKS)
2. Choice of primer and extender units (determined by the set of enzyme domains present in each module)
3. Degree of reduction of the polyketide backbone (determined by the set of enzyme domains present in each module)
4. Stereochemistry of centers carrying alkyl and hydroxyl substituents (locally controlled by enzyme domains that are responsible for generating the stereocenters in question)

For the success of this approach, it is essential that the manipulation of the modularity of the biosynthetic apparatus does not cause severe problems such that downstream modules in a PKS may not accept or process efficiently the anomalous product of an engineered upstream module.

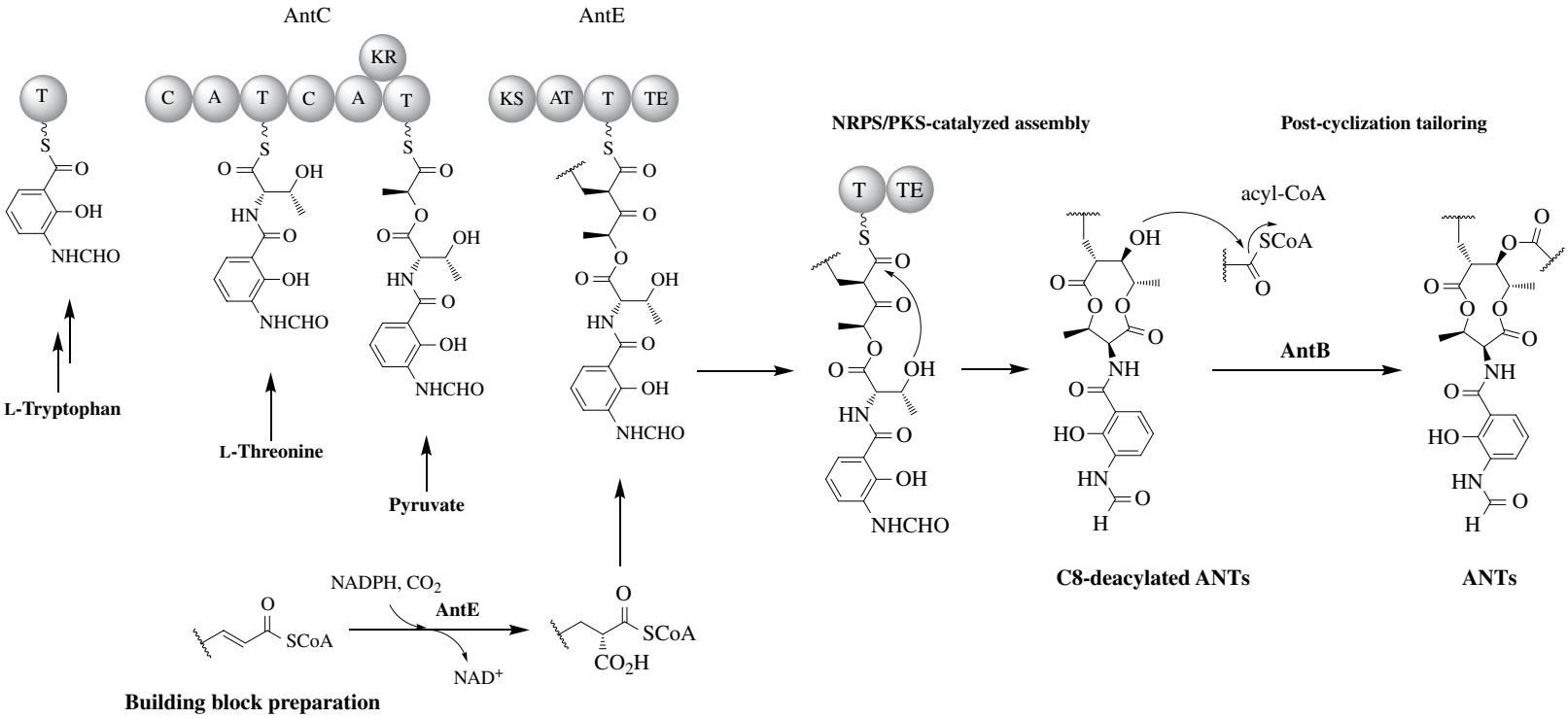
An early example in which such a bioengineering approach has been successfully attempted is the bioengineering of the 6-deoxyerythronolide B synthase (DEBS) [45]. The DEBS multienzyme complex consists of 3 large subunits (>300 kDa), each containing two modules (in total 28 catalytic domains). DNA manipulations were performed in *Escherichia coli* XL1 and *Streptomyces coelicolor* or *lividans* were used as the host for the production of polyketides. 50 compounds were produced in yields of 0.005–0.7% (relative to 6dEB under the same conditions) (Fig. 15.2). This was an impressive example for the potential power of this strategy, but it fades when one considers that theoretically the DEBS gene cluster could be permutated with the result of $10^7$ different compounds.

However, one disadvantage of this domain shuffling method is that many resulting hybrid PKSs are unproductive. An unresolved problem in this field is the limited insight into the structure and mode of action of the PKS. Schulz et al. presented the first example of using site-directed mutagenesis alone to systematically generate a library of polyketide structures [41]. The principle of the mutagenesis employed in their study was a deactivation of a targeted reductive domain. This minimally invasive strategy avoids the swapping of domains or modules of a PKS and thereby minimizes the deleterious side effects of the manipulation. By site-directed mutagenesis of monensin PKS they could generate 22 of the 32 theoretically predicted premonensin redox derivatives (Scheme 15.11).

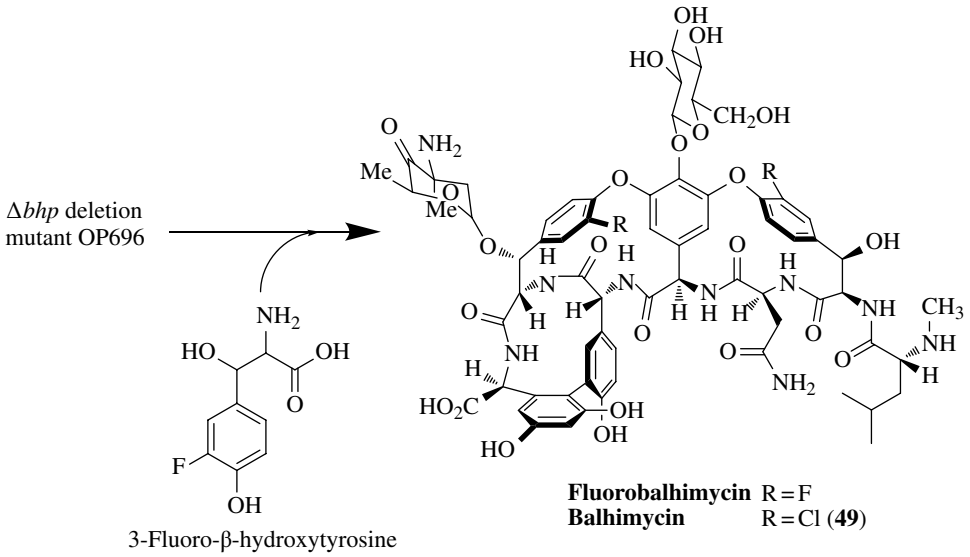
Natural product biosynthesis of polyketides, nonribosomal peptides, and their hybrids often follows a similar biosynthetic logic, involving the preparation of building blocks, backbone skeleton assembly catalyzed by PKS and/or nonribosomal peptide synthetase (NRPS), and post-tailoring for compound maturation. Liu et al. utilized this knowledge about the linear fashion of product assembly to apply combinatorial variation at different biosynthetic stages in antimycin (ANT) biosynthesis [46]. ANTs display a variety of biological activities and feature a nine-membered polyketide–peptide hybrid dilactone, which was proven to be a privileged structure by interacting with multiple protein targets. They engineered a strain of *Streptomyces sp.* NRRL 2288 so that it failed to produce mature ANTs but accumulated C-8 deacetylated ANTs (Scheme 15.12). Exploring the substrate compatibility of the hybrid NRPS/PKS system *in vivo*, they found it was amenable to variations both in the starter and extender units, allowing the so-called "mutasynthesis" introducing artificial building blocks accessed via chemical synthesis. AntD was found to be the most compatible PKS to date and was used to incorporate extender units, which could be linear, branching, cyclic, halogenated, and alkyne containing. They furthermore took advantage of the promiscuity of the acyltransferase AntB in order to attach acyl groups to C-8 for the diversity-oriented maturation of ANTs *in vitro*. Permutation of the C-8 deacetylated ANTs with the acyl donors from the CoA derivative library (25 members) produced 285 mature ANT variants (Scheme 15.12, 87.7% of the theoretical number). The acyl transfer generally proved highly effective, but the linear acyl transfer was found to be limited by length (with a range from two to ten carbon atoms). They selected 45 ANT derivatives for *in vitro* assays of cytotoxic activity against the mouse leukemia P388 cell line and antifungal activity against *Candida albicans*. All of the mature ANTs were biologically



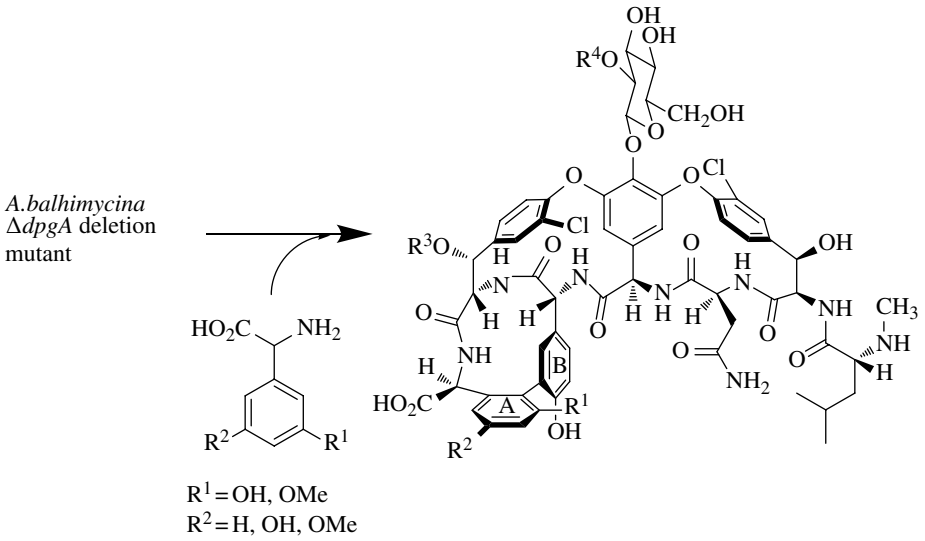

**SCHEME 15.11** Predicted structures of the premonensin redox derivatives obtained in this study. R=$CH_3$ (premonensin B).




**SCHEME 15.12** Biosynthetic pathway toward antimycins (ANTs), showing modular skeleton assembly, post-tailoring, and preparation of building blocks. KS=ketosynthase, TE=thioesterase, C=condensation, A=adenylation, T=thiolation domain, KR=ketoreductase.




**SCHEME 15.13** Pathway to fluorinated balhimycins by supplementation of mutant OP696.

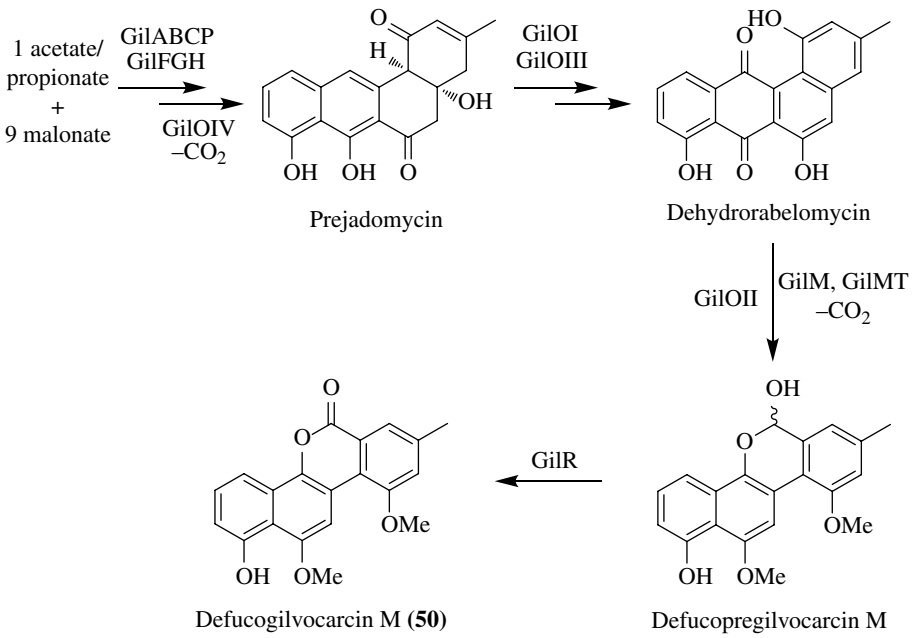



**SCHEME 15.14** Mutasynthetically generated balhimycins from supplementation of Δ*dpgA* mutant with substituted phenylglycines.

active and showed a wide range of cytotoxicity and antifungal activity. In total they generated 380 ANT-like products, of which 356 are new and introduced various functional groups. This multiplex combinatorial biosynthesis approach for the diversity-oriented biosynthesis of ANT-like compounds is a remarkable example for the generation of a library, which would synthetically have been effortful to come by.

Vancomycin is an antibiotic of last resort for life-threatening enterococcal and staphylococcal infections, such as methicillin-resistant *Staphylococcus aureus* (MRSA). Numerous natural and semisynthetic glycopeptide analogs have since been synthesized [47]. However, the main emphasis was placed on the modification of the peripheral features of vancomycin, but the characteristic tricyclic aglycon structure has remained mainly unchanged due to the demanding synthetic accessibility of the aglycon.

Suessmuth et al. have focused on the generation of molecular diversity in the vancomycin-type glycopeptide balhimycin (**49**, Scheme 15.13) [48]. They generated a Δ*bhp* deletion mutant (OP696) of *Amycolatopsis mediterranei*, which is deficient in β-hydroxytyrosine biosynthesis, the structural precursor of the two diastereomeric 3-chloro-β-hydroxytyrosine moieties. In mutasynthesis experiments, they supplemented OP969 with fluorinated analogs of β-hydroxytyrosine (Scheme 15.14) and obtained the respective fluorinated balhimycin derivatives, which were the first reported in vivo modified glycopeptides bearing nonnatural fluorine substituents.



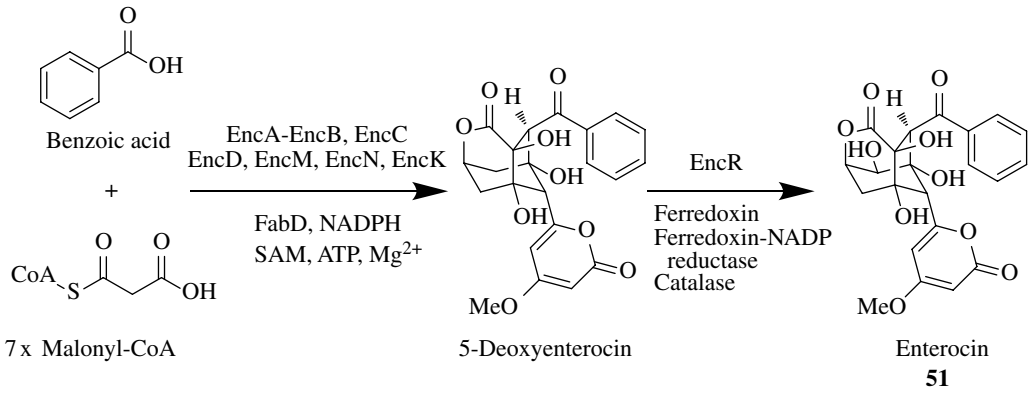

**SCHEME 15.15** Proposed biosynthetic pathway to defucogilvocarcin M (**50**).

Furthermore, Suessmuth et al. were able to generate diversity in the atropisomeric AB macrocycle of balhimycin (**49**), which is of crucial importance for the antibiotic activity [49]. In mutasynthesis experiments, they generated a series of vancomycin-type derivatives selectively modified at the C-terminal amino acid (*S*)-3,5-dihydroxyphenylglycine (DPg) by supplementation with various phenylglycines or their respective mandelic and phenylacetic acid analogs (Scheme 15.14). This example points out the strength of mutasynthesis in natural product-like library synthesis, since access to such compounds by synthetic routes would be extremely laborious. Similar mutasynthetic approaches were applied for the modification of the immunosuppressive agents rapamycin [50] and FK506 (tacrolimus) [51].

The members of the gilvocarcin group of natural products are renowned for their antitumor activities, a unique mode of action, and their low toxicities. The development as therapeutics is hampered by their intrinsic low solubility and furthermore by the reported chemical syntheses, which are unsuitable for the generation of a library of analogs. However, the combinatorial biosynthetic efforts to date have shown more promise. The continued advancement of such combinatorial biosynthetic approaches requires an in-depth knowledge of the underlying biosynthetic pathway. Rohr et al. investigated the exact sequence of biosynthetic events in gilvocarcin biosynthesis and reported a complete, one-pot, enzymatic total synthesis of defucogilvocarcin M (**50**, Scheme 15.15) [52]. They cloned the entire gilvocarcin V (GV) biosynthetic gene cluster and heterologously expressed it in *S. lividans* TK24. In order to gain a better understanding of the role of the gene products of GV biosynthesis and to elucidate the actual biosynthetic sequence of events, they focused on *in vitro* studies with selected pathway enzymes. By sequential interrogation of the pathway, enzymes with the respective intermediates as substrates, they were able identify the sequence of GV biosynthesis. They found that 15 enzymes are necessary to biosynthesize defucogilvocarcin M (Scheme 15.15) and used them subsequently in an one-pot enzymatic total synthesis of **50** starting from the natural substrates acetyl-CoA and malonyl-CoA.

Moore et al. reported the first *in vitro* assembly of a complete type II PKS enzymatic pathway and demonstrated the multienzyme total synthesis of the bacteriostatic agent enterocin [53]. They employed nine recombinant and three commercial proteins in a single reaction vessel along with the necessary cofactors (*S*-adenosyl-L-methionine (SAM), ATP, $Mg^{2+}$, and NADPH) to produce enterocin (**51**) from its primary metabolite precursors (benzoic acid and malonyl-CoA) (Scheme 15.16). This remarkable enzyme cascade generates 10 C–C bonds, 5 C–O bonds, and 7 chiral centers in impressive 25% yield.

Proteasome inhibitors receive widespread attention as promising treatment options in cancer chemotherapy. One of the most promising drug candidates of this class is salinosporamide A (**53**), isolated from the marine bacterium *Salinispora tropica* (Fig. 15.3) [54]. The densely functionalized γ-lactam-β-lactone pharmacophore is responsible for its irreversible binding to the β subunit of the 20S proteasome [55]. Moore et al. reported a biosynthetic synthesis of antiprotealide (**52**) and were furthermore able to generate other non-natural salinosporamide derivatives **54** with C-5 modifications




**SCHEME 15.16** The *in vitro* total biosynthesis of enterocin (**51**).

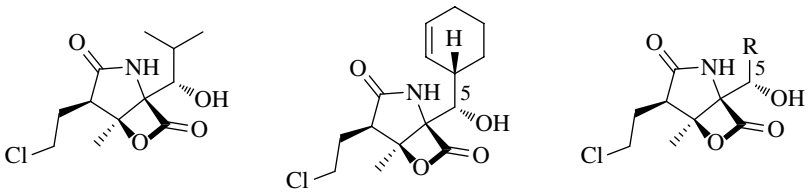



**FIGURE 15.3** Antiprotealide, salinosporamide A, and synthesized analogs.

by supplementation of a *S. tropica* salX$^-$ disruption mutant with nonproteinogenic cycloalkyl amino acids [56].

Organofluorines play an important role in medicinal chemistry, and estimates indicate that 20–30% of the pharmaceutical products on the market contain at least one fluorine atom [57, 58]. However, natural organofluorine compounds are exceedingly rare, and the pharmaceutical industry has not yet benefited from a microbial source of such compounds. The soil bacterium *Streptomyces cattleya* was found to produce fluoroacetate and 4-fluorothreonine, but the biological scope is limited to a single biological pathway that produces fluoroacetate [58, 59]. Identification of the fluorination enzyme FIA, responsible for C–F bond formation in *S. cattleya*, enabled the directed manipulation of biosynthetic pathways for the formation of fluorinated natural products.

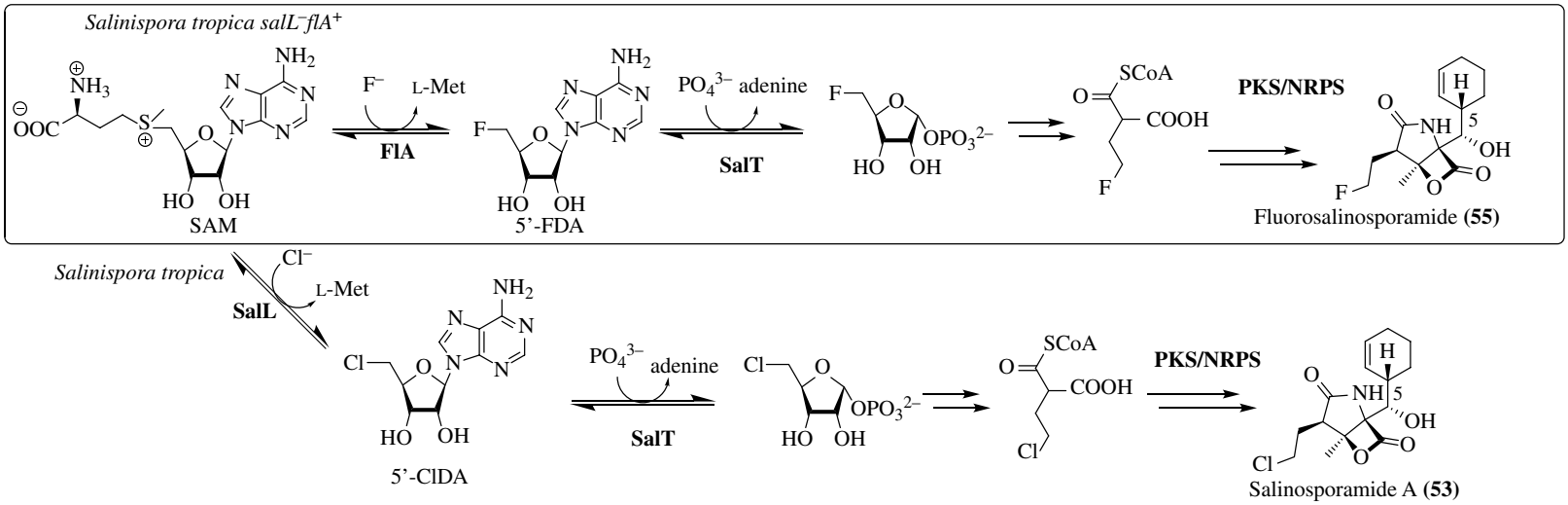
Moore et al. reported the first example whereby the fluorinase gene has been incorporated into a host organism by genetic engineering so that the heterologous host had the new capacity of producing a fluorinated natural product when grown in a culture containing inorganic fluoride [57]. They previously reported a standard mutasynthesis approach in which the chlorinase gene *salL* was inactivated and the resulting mutant converted the chemically complemented synthetic 5′-fluorodeoxyadenosine (5′-FDA), 5-fluororibose [60], and 4-fluorocrotonic acid [61] into fluorosalinosporamide (**55**). In the new approach they generated a *S. tropica* mutant in which the *salL* chlorinase gene was chromosomally replaced with the *S. cattleya flA* fluorinase gene. Cultivation of the salL$^-$flA$^+$ mutant in seawater-based medium supplemented with 2 mM potassium fluoride led to fluorosalinosporamide (**55**) production (Scheme 15.17). In order to minimize the toxic effect of the fluoride, potassium fluoride was added only when the culture reached an early to midexponential phase.

Recently Chang et al. showed that fluoroacetate can be used to incorporate fluorine into the polyketide backbone *in vitro* [58, 59].

Taken together the examples shown in this chapter indicate the potential of bioengineering for the synthesis of natural products and its analogs. While currently only a few specialized labs worldwide have the complete set of competencies at their disposal to perform this kind of research, it is realistic to believe that with continuous progress in genetic engineering and production hosts this technology will in the future become a tremendously useful addition to the toolbox of organic synthesis.

## 15.4 DIVERSITY-ORIENTED SYNTHESIS, BIOLOGY-ORIENTED SYNTHESIS, AND DIVERTED TOTAL SYNTHESIS

One major application of organic synthesis is the synthesis and development of small molecules, which are biologically active and control cellular events. These “molecular probes” have tremendous importance in biological research, since




**SCHEME 15.17** Fluorosalinosporamide engineering approach (top) and biosynthesis of salinosporamide A by *Salinispora tropica* (bottom)

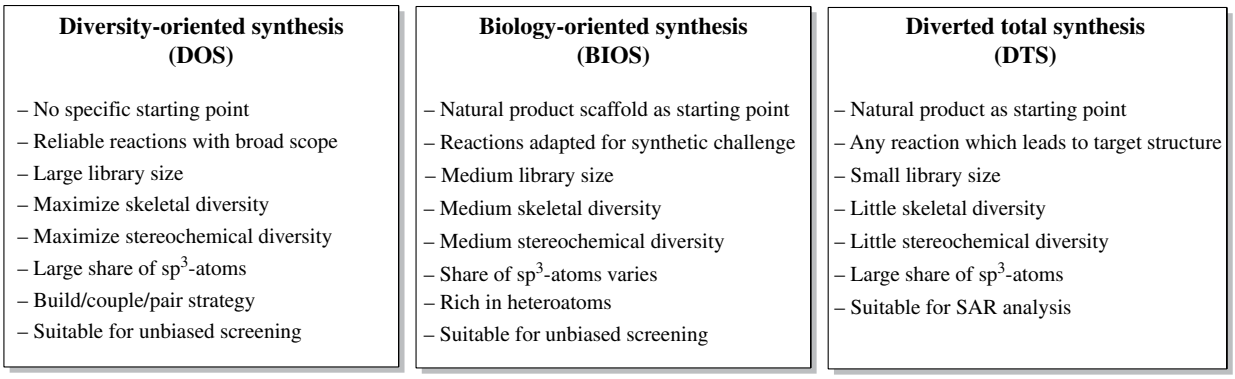


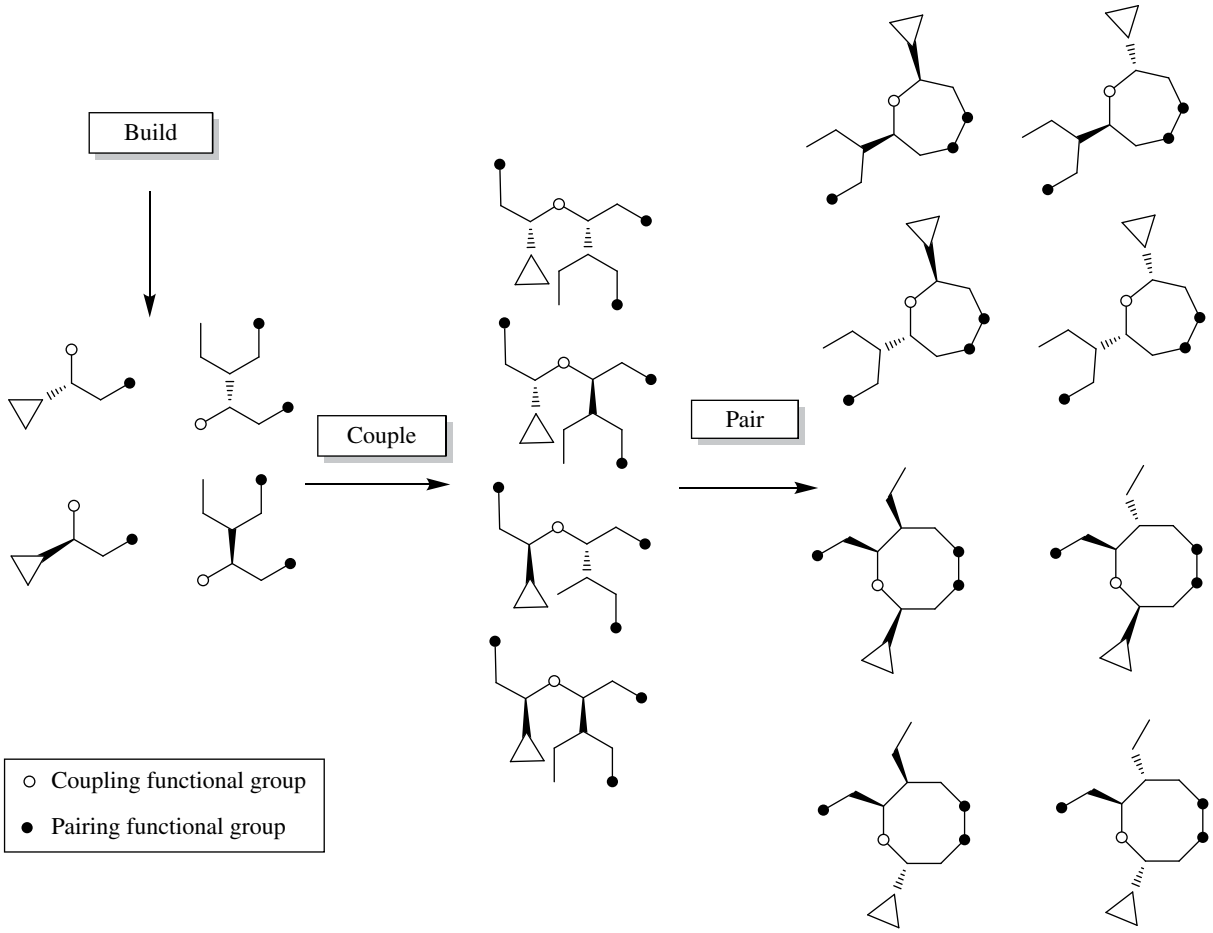

**FIGURE 15.4** Characteristic features of the strategies used for library design of biologically active compounds.

they allow the reversible, dose-dependent, time-controlled modulation of the action of a particular protein (or DNA) target, which is not possible with established genetic techniques. With these molecular probes, it is possible to characterize cellular pathways and validate proteins as drug targets. If such a protein emerges as a relevant target to treat a specific disease, the corresponding molecular probe can be developed into a drug, which benefits mankind. Along these efforts people have defined the goal that for each of the tens of thousands different proteins in a human cell, one specific small molecule probe should be identified. It is not clear if this goal will ever be reachable, but one could be optimistic when considering that the chemical universe of small molecules (compounds with MW <500, containing just the elements C, H, N, O, P, S, F, Cl, Br) is estimated to involve $10^{62}$ different molecules [62]. Considering that the high-throughput screening collection of a big pharma company contains just $10^6$ different compounds, people in the 1990s were excited about the concept of combinatorial chemistry, which produced compound libraries of similar size. When subjected to biological testing, these early combinatorial chemistry libraries proved to deliver disappointing results [63]. It was recognized that not the number of compounds is the success factor in library generation, but the creation of compounds, which belong to the biologically relevant region of the chemical universe, is important. In the last 15 years, three major concepts have emerged as valuable in addressing these issues and have produced exciting results in biological tests (Fig. 15.4).

### 15.4.1 Diversity-oriented Synthesis

Diversity-oriented synthesis (DOS) has been defined by Schreiber as the opposite to target-oriented synthesis (TOS) [64]. TOS is distinguished by aiming at the synthesis of a single defined product (most often a natural product). The synthetic route is developed using the concept of retrosynthetic analysis. In the forward direction any type of reaction, even if it is very specialized and has only limited scope, will be used as long as it leads to the target compound. In contrast, DOS aims at the synthesis of many molecules with ideally maximum structural, skeletal, functional, and stereochemical diversity. Preferably, the molecules contain many $sp^3$-atoms, which give the molecules a 3D shape overcoming the common "flatland" character of typical heteroarene compounds, which are overrepresented in established screening libraries. In the development of the synthetic strategy for DOS libraries, forward synthetic thinking is important and powerful synthetic transformations with large substrate scope, high functional group tolerance, and synthetic robustness (e.g., Pd-catalyzed cross-coupling, Diels–Alder reaction, amide formation, etc.) are preferred [65]. In its most recent formulation, DOS has seen the integration of a strategy called "Build/Couple/Pair" introduced by Schreiber [66]. In the first stage ("Build"), suitable building blocks are synthesized featuring both functional groups for coupling with other building blocks as well as pairing functional groups, which can be used in subsequent transformations. Ideally, these building blocks are provided as a full matrix of stereoisomers. In the second stage ("Couple"), the building blocks are coupled, providing all diastereomers. In the final stage ("Pair"), two or more functional groups (polar/polar, polar/nonpolar, nonpolar/nonpolar, etc.) are reacted with each other to result into skeletally and functional diverse products (Scheme 15.18) [66].

An important advantage of this strategy is that from its intrinsic design a full set of stereoisomers of each product is aimed for, which will give invaluable information about the structure–activity relationship in the biological testing phase as has been reported by Schreiber for [10.4.0]bicyclic products [67] and 3,4,5,6-tetrahydro-2*H*-benzo[*b*][1,5]oxazocines [68]. An example of this Build/Couple/Pair strategy of the Schreiber lab is highlighted in Scheme 15.19. A Petasis 3-component reaction between lactol **56**, amino acid ester **57**, and boronic acid **58** leads after alkylation with propargylic bromide (**59**) to the coupling product **60**, from which a series of "pairing" reactions generate skeletally diverse scaffolds **61–63**. The level of diversity and complexity can be even




**SCHEME 15.18** The concept of "Build/Couple/Pair" strategy in DOS.

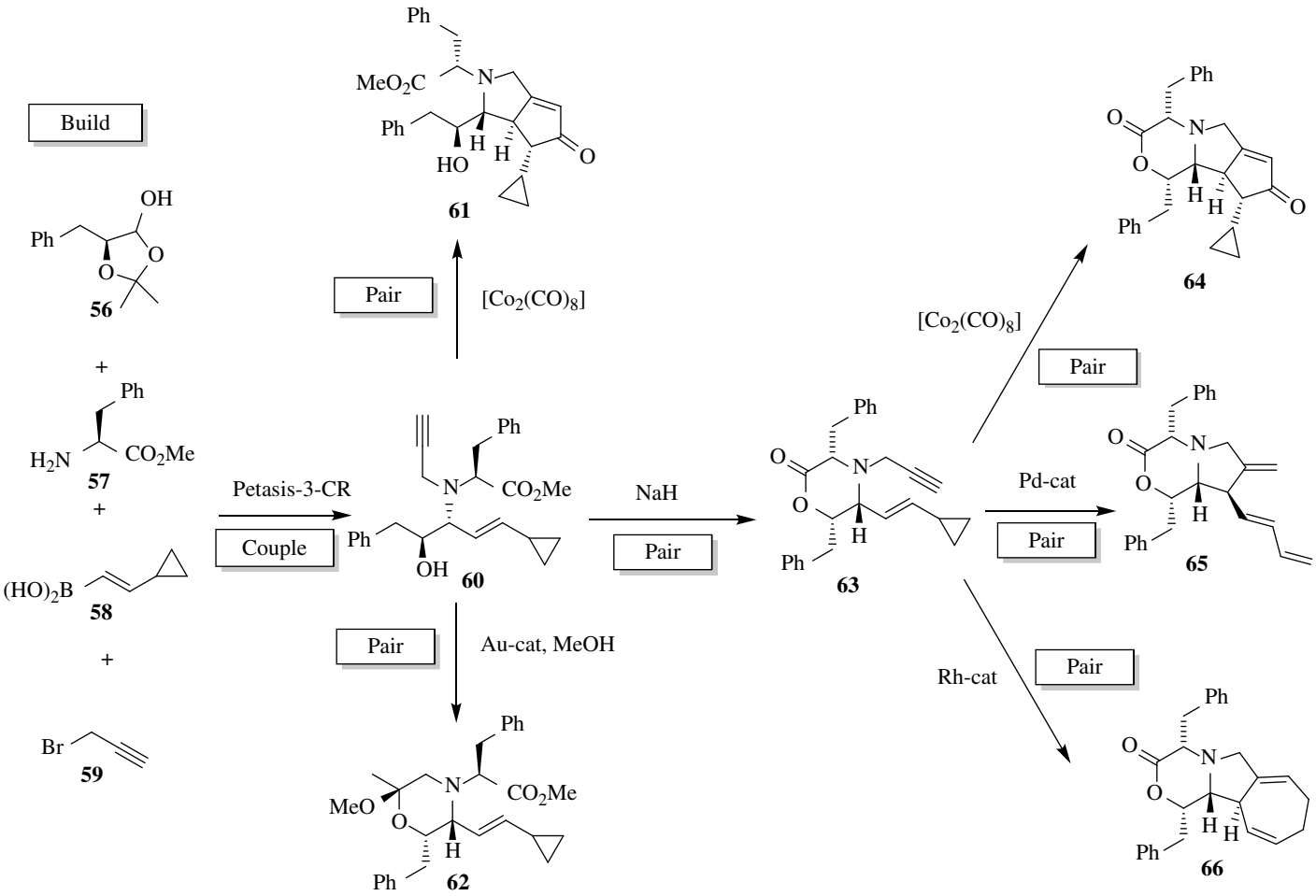
further increased by repeating the process of "pairing" reactions. For example, morpholine pairing product **63** can itself undergo subsequent "pairing" reactions, such as a Pauson–Khand reaction leading to **64**, a Pd-catalyzed isomerization to **65**, or a Rh(I)-catalyzed cycloaddition to bicyclo[5.3.0] product **66** [69, 70].

Importantly, there are now already several exciting hits coming out from the screening of these DOS libraries [71, 72]. For example, the modulator of the Sonic Hedgehog (shh) Pathway **67** [68] and the drug lead **68** [73] against Chagas disease caused by the parasite *Trypanosoma cruzi* have been developed by screening DOS-based libraries (Fig. 15.5).

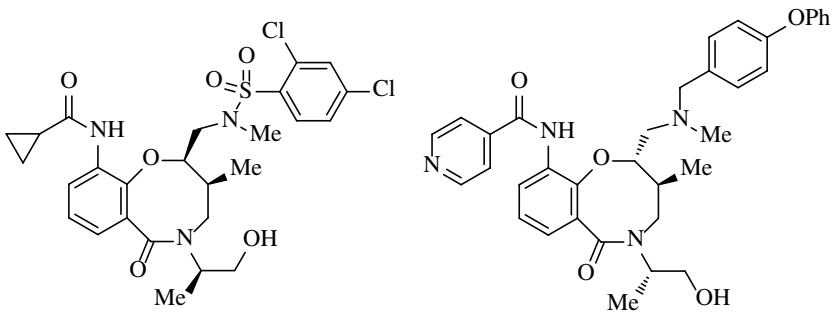
An impressive and simple solution to the generation of scaffold diversity, which conceptually is related to the "Build/Couple/Pair" strategy [74], has been given by Nelson [75]. In contrast to the example described in Scheme 15.19, where various pairing reactions with different catalysts and reagents were necessary to guarantee huge scaffold diversity, Nelson relied solely on olefin metathesis cascade reactions, which through clever design of the substrates led to an amazing scaffold diversity. Difunctional "propagating building blocks" are substituted with a fluorous-tagged linker, which will allow removal of excess of reagents at each stage by fluorous solid-phase extraction alone. The resulting intermediates such as **69–70** are appended with a "capping building block" producing substrates such as **71–76**, which are then subjected to metathesis cascade reaction, which leads to a highly diverse ensemble of different scaffolds, like **77–82** (Scheme 15.20). With a very small number of reactions greater than 80 scaffolds could be prepared, which represent a unique record in optimizing scaffold diversity.

### 15.4.2 Biology-oriented Synthesis

The second major concept, biology-oriented synthesis (BIOS), has its origin in the empirical observation that a very high portion of marketed drugs are either natural products, modified natural products, or inspired by natural products [76]. Waldmann and others have rationalized the success of natural products that natural products are by its very origin and purpose privileged compounds [77], which belong to the biologically relevant space of the chemical




**SCHEME 15.19** Build/Couple/Pair DOS synthesis using a Petasis 3-CR.



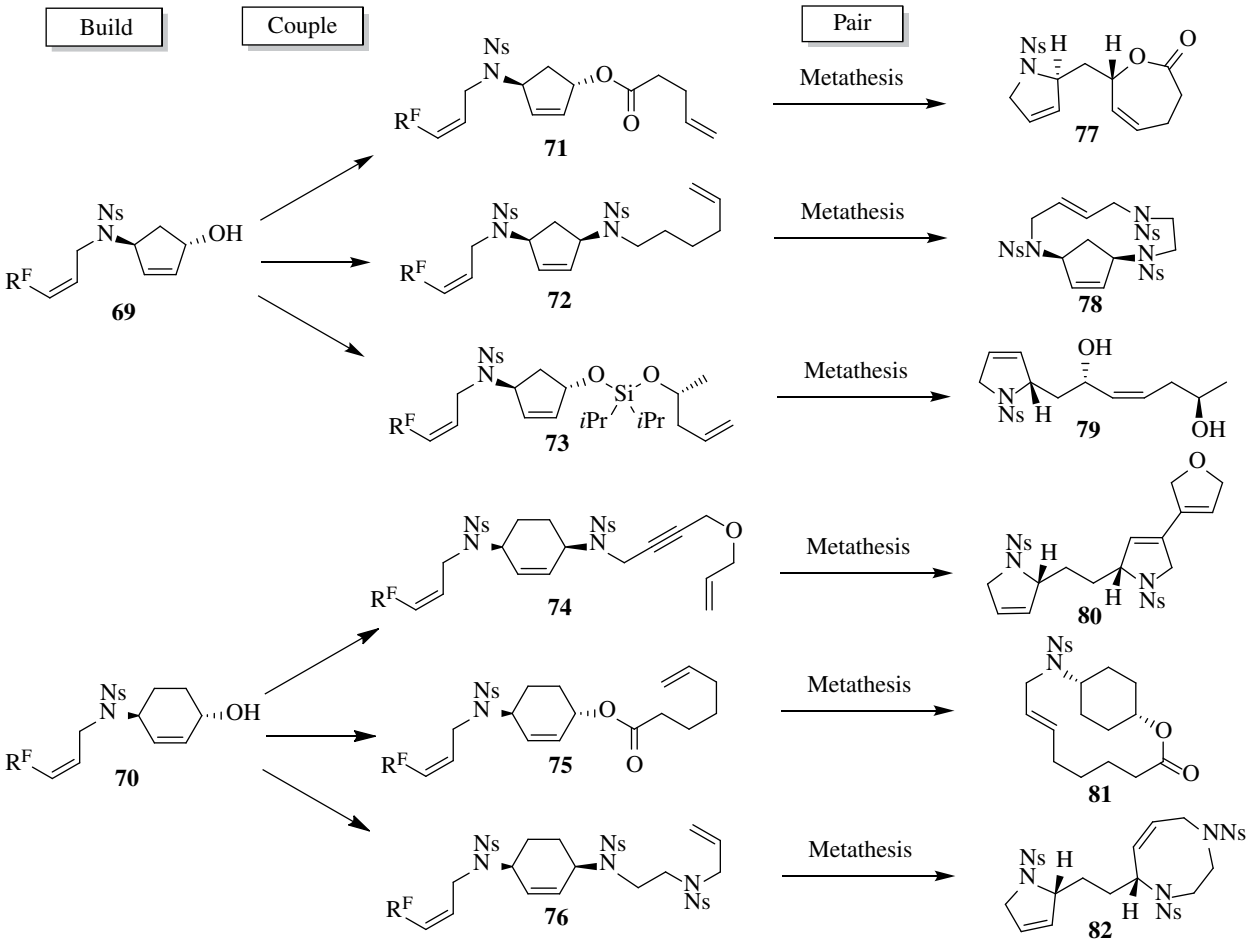
**67**

Secondary differentiation assays C3H10T1/2 cells $EC_{50}$ = 0.06 μM

**68**

*Trypanosoma cruzi* growth inhibition $IC_{50}$ = 16 nM

**FIGURE 15.5** Biologically active molecules identified by screening of DOS libraries.




**SCHEME 15.20** Representative examples of Nelson's highly scaffold-divergent synthesis.

universe [63, 78]. Natural products are produced biosynthetically by proteins of the host organism (plant, bacteria, etc.) to serve a biological function (e.g., defense against invading microbes, predators, or grazing animals) by binding to another protein receptor. Typically, this binding to the protein target has been optimized in an evolutionary process explaining the degree of sophistication of the structural and functional complexity of some natural products. Considering that there is a huge evolutionary, structural, and functional relationship between proteins of different species, functions, and purposes, Waldmann et al. have recognized that natural products are ideal starting points for the design of compound libraries for biological testing [63]. In a systematic chemoinformatics approach, they have defined a periodic table of natural product structures (scaffold of natural products, SCONP) [79, 80], which provides a frequency score of ring structures identified in natural product databases. These ring structures have served as starting points for library synthesis projects [81–83].

A very impressive achievement is the synthesis of a 2527-membered library by Shair et al. based on the alkaloid natural product galanthamine using an elegant biomimetic oxidative cyclization reaction, which has been made accessible on a solid-phase format (Scheme 15.21) [84]. Starting from a tyrosine derivative **83**, attached onto a solid support via an acid labile silyl ether linkage, adduct **85** was synthesized after coupling of building block **84** via reductive amination. In the following key step, a $PhI(OAc)_2$-mediated oxidative cyclization produced the spiroazepine ring. The newly generated dienone **86** was further elaborated via two Michael additions involving an internal phenolate and external S-nucleophile. Further O- and N-alkylation and imine formation of the keto group enabled the introduction of four different diversity elements. After cleavage from the solid support and biological screening of library **89** using a phenotypic assay, a library member was identified that perturbs the secretory pathway in mammalian cells—a process unrelated to the acetylcholine esterase inhibitory activity of the lead structure galanthamine. This compound, named secramine, was shown to inhibit the activation of the Rho GTPase Cdc42 [85]. Using a similar oxidative addition strategy, the Shair group has also prepared a 10,000-member large library of carpanones, which they also screened for phenotypic changes in vesicular trafficking [86]. By its clever combination of scaffold building and subsequent modification, in which each synthetic step contributes to the overall diversity of the library, the galanthamine and carpanone libraries by the Shair group have set a benchmark for library design in natural product-inspired libraries.

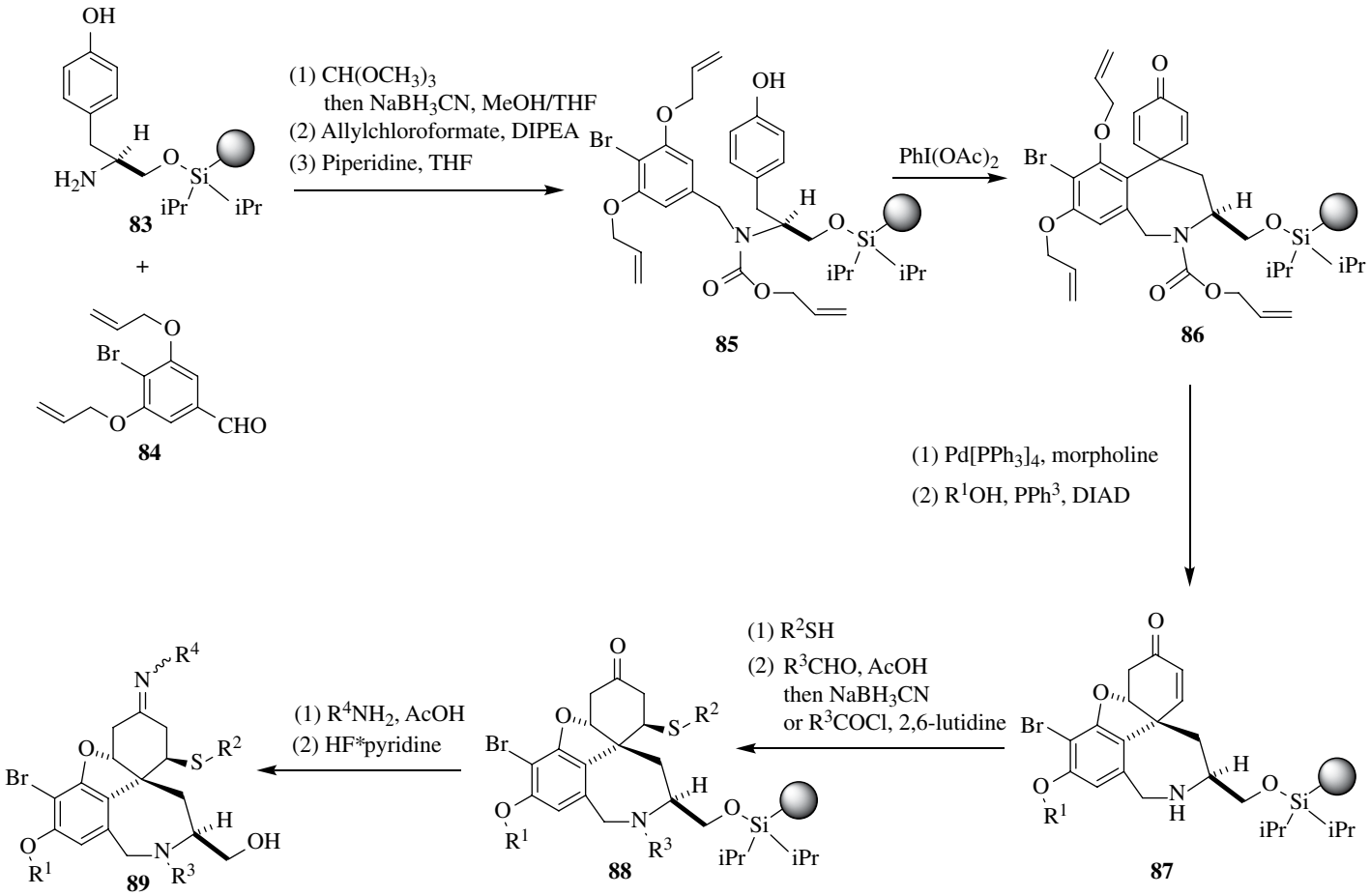
Waldmann and Kumar reported about an enantioselective [3+2]-cycloaddition of zwitterions generated from allene **91** and chiral phosphine catalyst **92** with cyclopentenones **90** to produce pentalenones **93**. Regioselective Baeyer–Villiger oxidation with bis(monoperoxyphthalate) hexahydrate (MMPP) produced a focused library of lactone **94** inspired by the natural product class of iridoids (Scheme 15.22). Among this limited set of 40 compounds, several biological hits were identified, which induced neuronal outgrowth and differentiation of neurons [87].

An impressive example for the power of cascade reactions has recently been reported by Waldmann and Kumar in a synthesis of a library of tetrahydroindolo[2,3-*a*]quinolizines **105** using 12 consecutive transformations in one pot [88]. The reaction starts with the formation of zwitterion **95**, which reacts with 3-formyl chromone **96** to pyran **97**. Michael addition of tryptamines **98** to **97** forms **99**. In a series of intramolecular reactions and rearrangements azadiene **102** forms, which reacts in a Pictet–Spengler cyclization to **103**, from which the centrocountins **105** result in impressive 20–88% overall yield (Scheme 15.23). By using a chiral Bronsted acid, the enantioselective synthesis is possible [89]. Centrocountin 1 (R = Me, $R^1$–$R^6$ = H) was characterized as a compound that modulates centrosome integrity showing the phenotype of multipolar mitotic spindles and multipolar cell division by targeting the centrosome-associated proteins nucleophosmin and Crm1 [88].

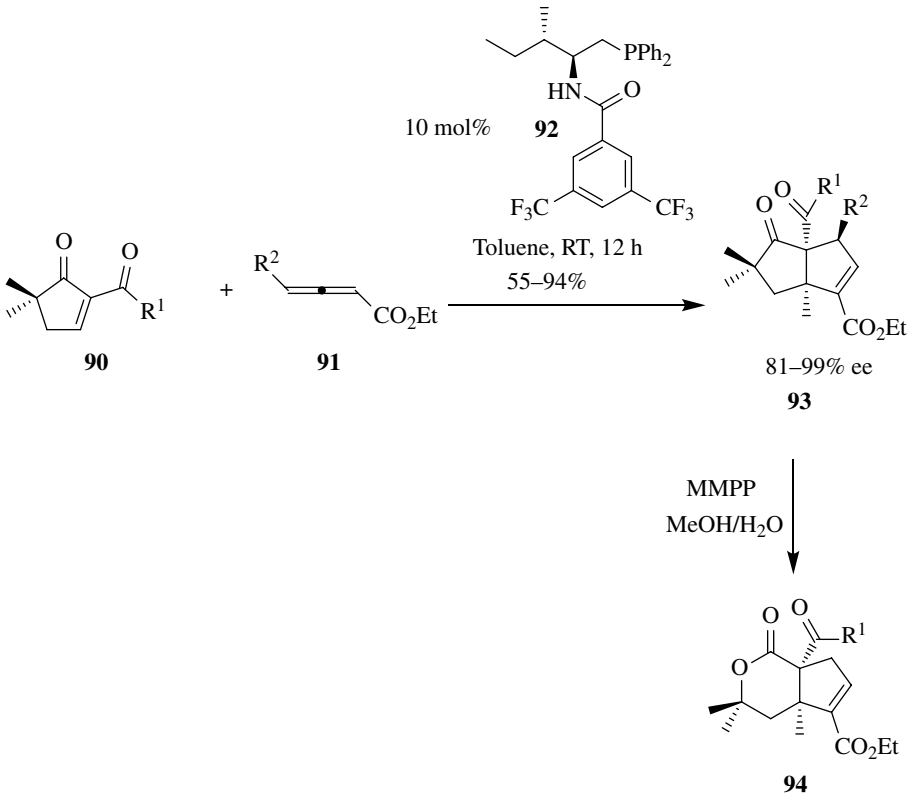
### 15.4.3 Diverted Total Synthesis

A concept even closer to TOS is diverted total synthesis (DTS) introduced by Danishefsky [90, 91]. DTS means that in the course of a natural product synthesis not only the target itself but—taking advantage of advanced intermediates—also analogs of the target compound with reduced or even higher complexity are synthesized. For example, the Wender group noticed in the context of their total synthesis of bryostatin 1 (**106**) that simplified analogs but still featuring the relevant pharmacophore, called "Bryologues" (**107**), showed even stronger cytotoxic behavior by binding to protein kinase C (PKC) (Fig. 15.6) [92].

Such analogs are highly welcome, as they give not only insight into the SAR of the original natural product but also are attractive lead structures for drug development, since they are better accessible and have often improved bioavailability. Another illustrative example is the DTS of the antimetastatic natural product migrastatin (**115**). In the course of their total synthesis and biological characterization of synthetic intermediates, Danishefsky recognized that the deletion of the glutarimide side chain as well as the α,β-unsaturated lactone moieties did not abrogate cell migration [93]. On the basis of this analysis, they selected candidate structures of much more simplified analogs of **115**. Among these cyclic ether **114** ("migrastatin ether") showed the most exciting biological data, being even more potent than the parent natural product **115** and increasing survival of breast cancer cell-treated mice. The synthesis starts with a Lewis acid-catalyzed cyclocondensation between aldehyde **108** and diene **109** furnishing pyranone **110** as a single diastereomer. Reduction and Ferrier




**SCHEME 15.21** Shair synthesis of a library of galanthamine analogs on solid phase.




**SCHEME 15.22** Synthesis of a library inspired by the natural product class iridoids.

rearrangement produced **111**, which was converted in an Appel reaction into allyl bromide **112**. Williamson ether synthesis with 6-hepten-1-ol delivered ether **113**, which underwent ring closing metathesis with Grubbs II catalyst forming a 14-membered cyclic ether, which after silyl deprotection produced migrastatin ether **114** (Scheme 15.24).

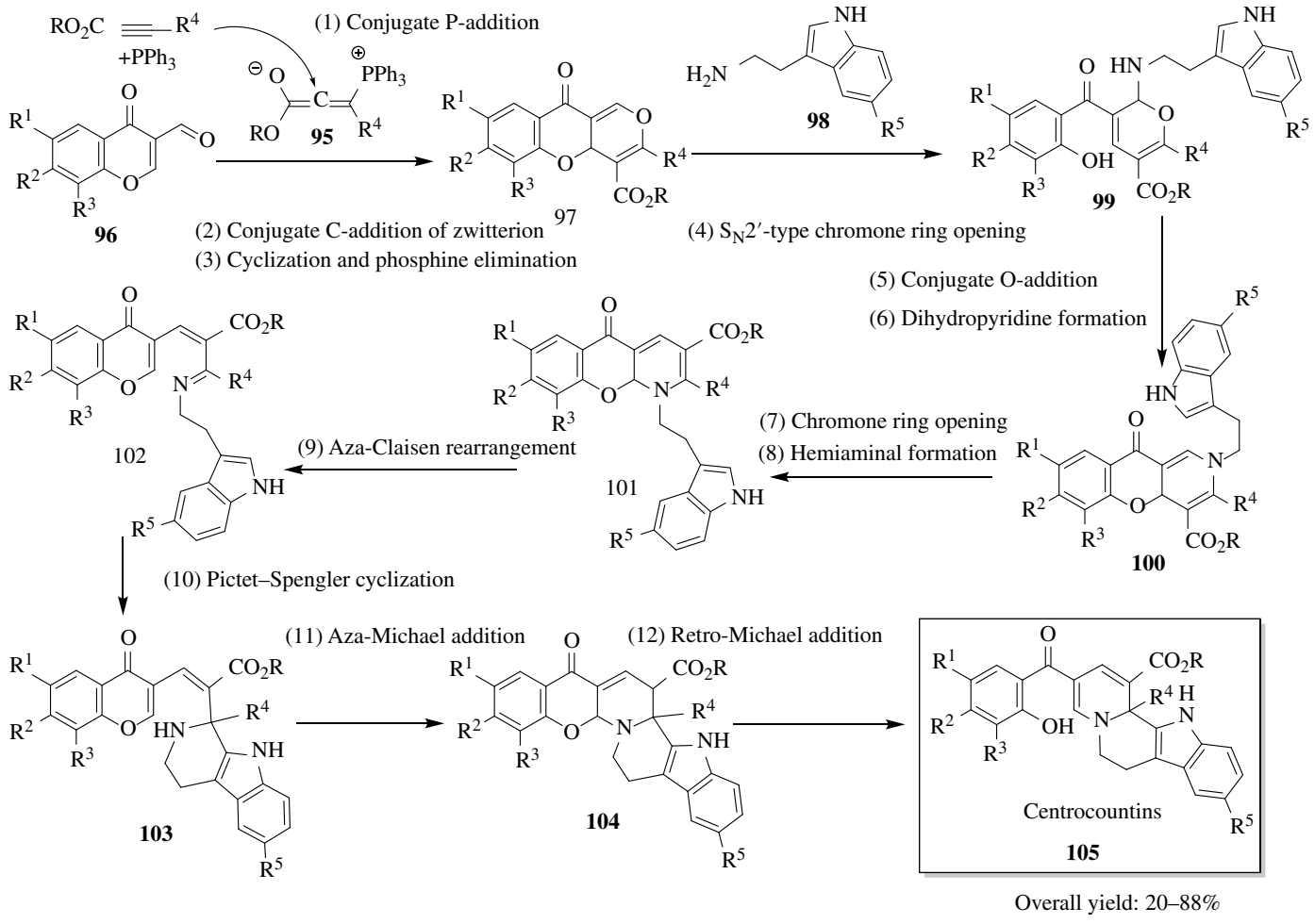
A recent extension of the DTS is the concept of "collective total synthesis," which has been introduced by MacMillan in 2011 [94]. Collective total synthesis aims for the generation of structurally diverse natural products by transformation of a common synthetic scaffold through biomimetic-like pathways [95]. MacMillan et al. employed the common tetracyclic scaffold **120** for the complex total synthesis of six different opium alkaloids of considerable structural complexity (Scheme 15.25) [94].

Snyder and Zografos have made remarkable use of a common synthetic scaffold during their efforts for the syntheses of oligomeric resveratrol natural compounds. They invented the scaffold **121**, which is distinct from the postulated biosynthetic precursor, and transformed it in reagent-controlled reaction cascades to 25 oligomeric natural products and analogs (Scheme 15.26) [96].

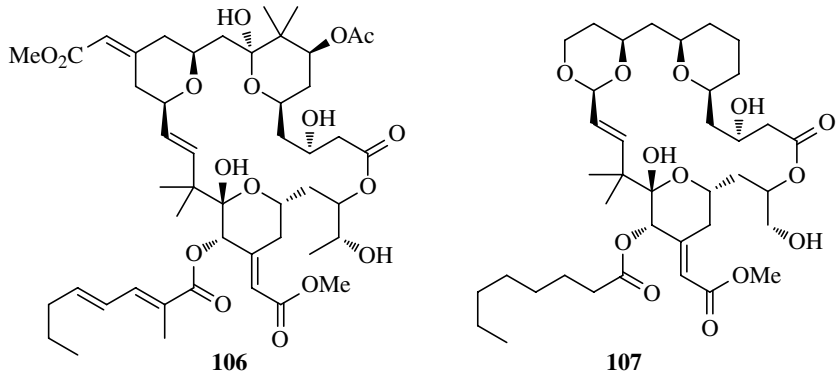
These two examples highlight the current state of the art of organic synthesis, in which it has finally become possible to merge the aims of total synthesis with the goals of diversified library synthesis, which only a decade ago have thought to be irreconcilable as they represented opposite extremes of the organic synthesis spectrum.

## 15.5 CONCLUSION

Even in the new millennium, total synthesis of natural products will remain a very important field in organic synthesis but will be different in its character than in the twentieth century. The priorities in this field will shift from being the first of synthesizing a new synthetic target of maximum difficulty and complexity to provide efficient and scalable routes to biologically relevant natural products. Biocatalysis and—in the future—bioengineering will become efficient tools, which will be integrated into synthetic sequences like other techniques such as photochemistry, electrochemistry, or transition metal catalysis. Besides the efforts to provide an efficient access to a single-target molecule, the emerging paradigm of synthesizing compound libraries following the DOS, BIOS, and DTS strategy will become even more popular, as it has proven to be such a rich source of biologically relevant molecules. All these efforts will profit from the continuous progress in the development of new synthetic methodology.




**SCHEME 15.23** Cascade synthesis of centrocountins (**105**).



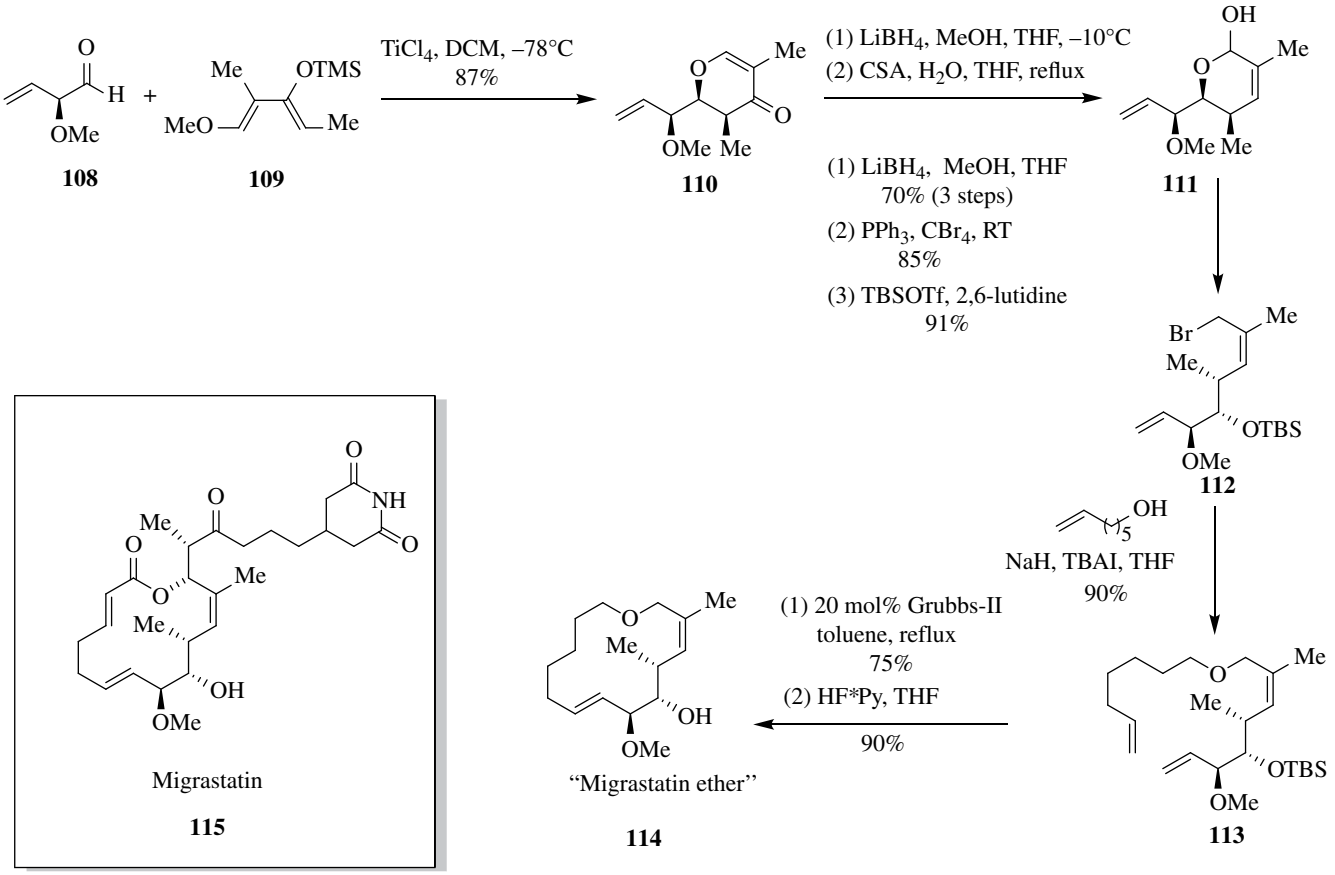
**106**

Bryostatin 1
PKC $K_i$ = 1.35 nM

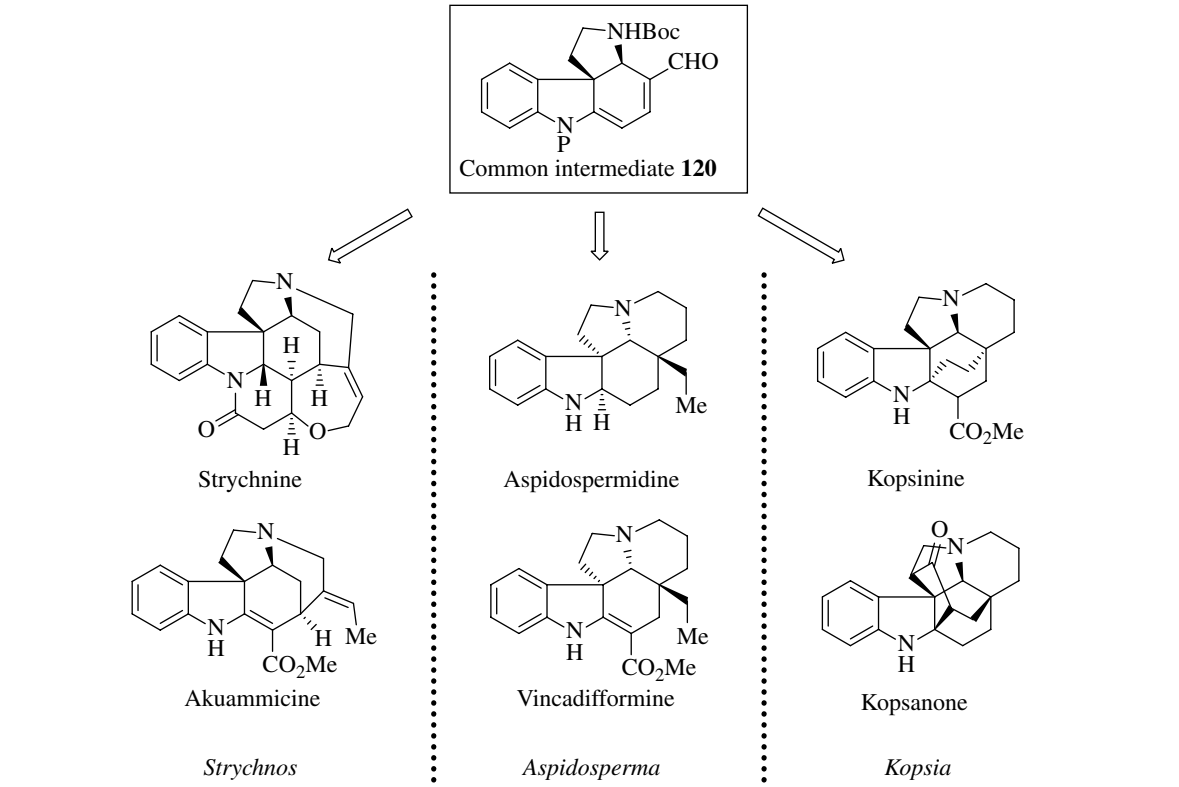
**107**

Bryologue
PKC $K_i$ = 0.25 nM

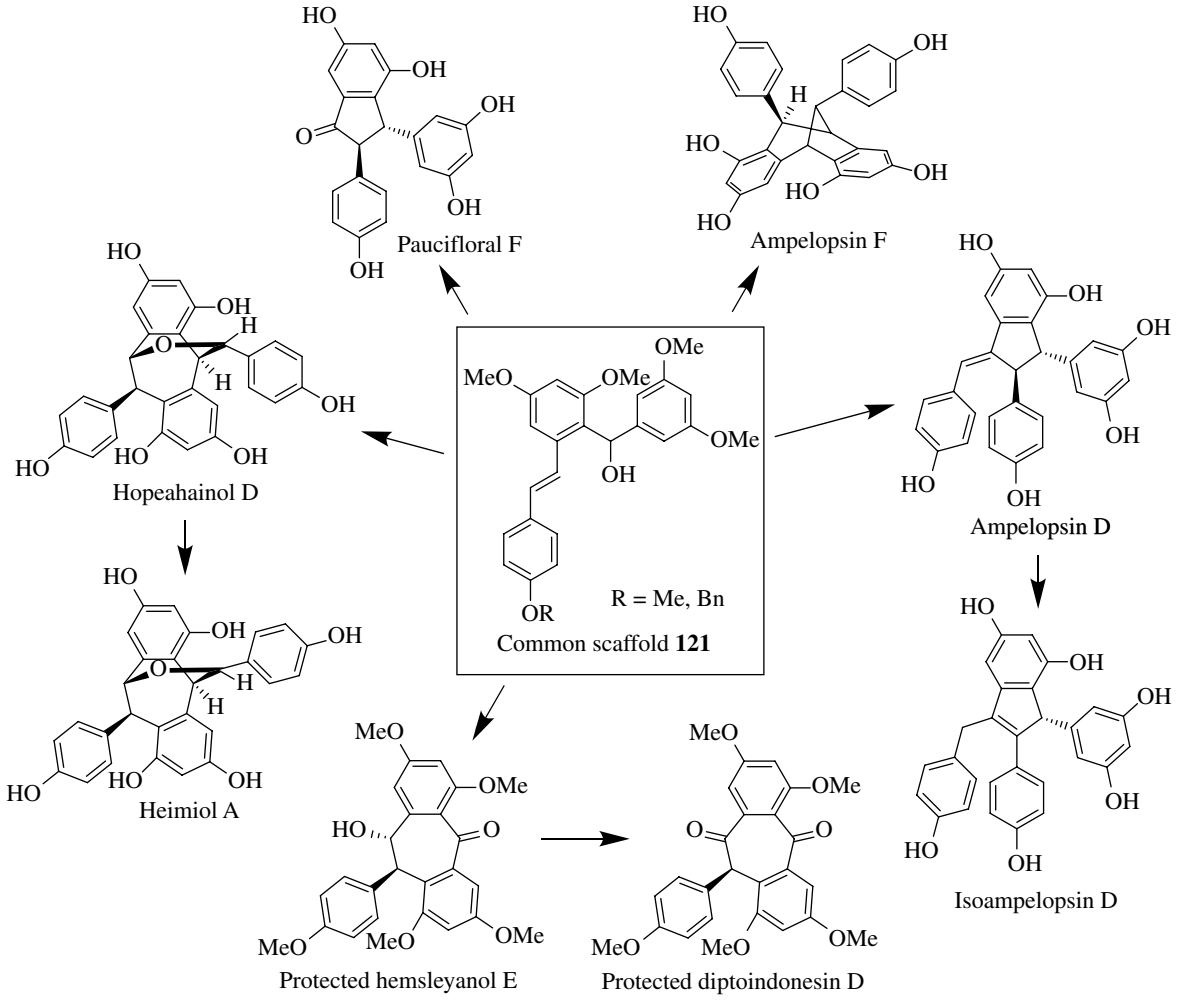
**FIGURE 15.6** Bryostatin (**106**) and bryologue (**107**).




**SCHEME 15.24** Synthesis of migrastatin analogs.




**SCHEME 15.25** Collective natural product synthesis of six structurally diverse *Strychnos*, *Aspidosperma*, and *Kopsia* alkaloids.




**SCHEME 15.26** Total syntheses of polymeric resveratrol natural products from common scaffold **121**.

## REFERENCES


1. R. W. Hoffmann, *Angew. Chem. Int. Ed.* 2013, **52**, 123–130.
2. A. Eschenmoser, *Naturwissenschaften* 1974, **61**, 513–525.
3. (a) R. B. Woodward, *Pure Appl. Chem.* 1973, **33**, 145–177; (b) A. Eschenmoser, C. E. Wintner, *Science* 1977, **196**, 1410–1420.
4. R. W. Armstrong, J.-M. Beau, S. H. Cheon, W. J. Christ, H. Fujioka, W.-H. Ham, L. D. Hawkinds, H. Jin, S. H. Kang, Y. Kishi, M. J. Martinelli, W. W. McWorther, Jr., M. Mizuno, M. Nakata, A. E. Stütz, F. X. Talamas, M. Taniguchi, J. A. Tinio, K. Ueda, J. Uenishi, J. B. White, M. Yonaga, *J. Am. Chem. Soc.* 1989, **111**, 7530–7533.
5. K. C. Nicolaou, Z. Yang, G.-Q. Shi, J. L. Gunzner, K. A. Agrios, P. Gärtner, *Nature* 1998, **392**, 264–269.
6. Y. Kishi, T. Fukuyama, M. Aratani, F. Nakatsubo, T. Goto, S. Inoue, H. Tanino, S. Sugiura, H. Kakoi, *J. Am. Chem. Soc.* 1972, **94**, 9219–9221.
7. I. B. Seiple, S. Su, I. S. Young, C. A. Lewis, J. Yamaguchi, P. S. Baran, *Angew. Chem. Int. Ed.* 2010, **49**, 1095–1098.
8. D. A. Evans, J. Batroli, T. L. Shi, *J. Am. Chem. Soc.* 1981, **103**, 2127–2129.
9. S. Masamune, S. Ali, D. L. Snitman, D. S. Garvey, *Angew. Chem. Int. Ed.* 1980, **19**, 557–558.
10. K. C. Nicolaou, P. G. Bulger, D. Sarlah, *Angew. Chem. Int. Ed.* 2005, **44**, 4442–4489.
11. C. A. Kutruff, M. D. Eastgate, P. S. Baran, *Nat. Prod. Rep.* 2014, **31**, 419–432.
12. S. J. Mickel, D. Niederer, R. Daeffler, A. Osmani, E. Kuesters, E. Schmid, K. Schaer, R. Gamboni, W. Chen, E. Loeser, F. R. Kinder Jr., K. Konigsberger, K. Prasad, T. M. Ramsey, O. Repic, R.-M. Wang, G. Florence, I. Lyothier, I. Paterson, *Org. Proc. Res. Dev.* 2004, **8**, 122–130.
13. U. Klar, J. Platzeck, *Synlett* 2012, **23**, 1291–1299.
14. (a) M. J. Yu, W. Zheng, B. M. Seletsky, *Nat. Prod. Rep.* 2013, **30**, 1158–1164; (b) K. L. Jackson, J. A. Henderson, A. J. Phillips, *Chem. Rev.* 2009, **109**, 3044–3079.
15. T. Reichstein, A. Grüssner, *Helv. Chim. Acta* 1934, **17**, 311–328.
16. S. H. Pines, *Org. Proc. Res. Dev.* 2004, **8**, 708–724.
17. J. A. Hogg, *Steroids* 1992, **57**, 593–615.
18. K. Faber, *Biotransformations in Organic Chemistry*, 6th ed., Springer, Heidelberg (2011).
19. K. Drauz, H. Gröger, O. May, *Enzyme Catalysis in Organic Synthesis*, 3rd ed., Wiley-VCH, Weinheim (2012).
20. B. M. Nestl, S. C. Hammer, B. A. Nebel, B. Hauer, *Angew. Chem. Int. Ed.* 2014, **53**, 3070–3095.
21. C. M. Clouthier, J. N. Pelletier, *Chem. Soc. Rev.* 2012, **41**, 1585–1605.
22. M. T. Reetz, *J. Am. Chem. Soc.* 2013, **135**, 12480–12496.
23. T. Fischer, J. Pietruszka, *Top. Curr. Chem.* 2010, **297**, 1–43.
24. N. J. Turner, E. O'Reilly, *Nat. Chem. Biol.* 2013, **9**, 285–288.
25. S. Breitler, E. M. Carreira, *Angew. Chem. Int. Ed.* 2013, **52**, 11168–11171.
26. R. C. Simon, B. Grischek, F. Zepeck, A. Steinreiber, F. Belaj, W. Kroutil, *Angew. Chem. Int. Ed.* 2012, **51**, 6713–6716.
27. A. Znabet, J. Zonneveld, E. Janssen, F. J. J. De Kanter, M. Helliwell, N. J. Turner, E. Ruijter, R. V. A. Orru, *Chem. Commun.* 2010, **46**, 7706–7708.
28. T. Hudlicky, U. Rinner, D. Gonzalez, H. Akgun, S. Schilling, P. Siengalewicz, T. A. Martinot, G. R. Pettit, *J. Org. Chem.* 2002, **67**, 8726–8743.
29. M. G. Charest, C. D. Lerner, J. D. Brubaker, D. R. Siegel, A. G. Myers, *Science* 2005, **308**, 395–398.
30. M. G. Charest, D. R. Siegel, A. G. Myers, *J. Am. Chem. Soc.* 2005, **127**, 8292–8293.
31. C. Sun, Q. Wang, J. D. Brubaker, P. M. Wright, C. D. Lerner, K. Noson, M. G. Charest, D. R. Siegel, Y.-M. Wang, A. G. Myers, *J. Am. Chem. Soc.* 2008, **130**, 17913–17927.
32. D. A. Kummer, D. Li, A. Dion, A. G. Myers, *Chem. Sci.* 2011, **2**, 1710–1718.
33. J. D. Mortison, D. H. Sherman, *J. Org. Chem.* 2010, **75**, 7041–7051.
34. C. C. Aldrich, L. Venkatraman, D. H. Sherman, R. A. Fecik, *J. Am. Chem. Soc.* 2005, **127**, 8910–8911.
35. F. Kudo, Y. Asou, M. Watanabe, T. Kitayama, T. Eguchi, *Synlett* 2012, **23**, 1843–1846.
36. J. D. Keasling, *Nature* 2012, **492**, 188–188.
37. D.-K. Ro, E. M. Paradise, M. Ouellet, K. J. Fisher, K. L. Newman, J. M. Ndungu, K. A. Ho, R. A. Eachus, T. S. Ham, J. Kirby, M. C. Y. Chang, T. Withers, Y. Shiba, R. Sarpong, J. D. Keasling, *Nature* 2006, **440**, 940–943.
38. J. M. Winter, Y. Tang, *Curr. Opin. Biotechnol.* 2012, **23**, 736–743.
39. A. Kirschning, F. Hahn, *Angew. Chem. Int. Ed.* 2012, **51**, 4012–4022.
40. M. Cummings, R. Breitling, E. Takano, *FEMS Microbiol. Lett.* 2014, **351**, 116–125.
41. S. Kushnir, U. Sundermann, S. Yahiaoui, A. Brockmeyer, P. Janning, F. Schulz, *Angew. Chem. Int. Ed.* 2012, **51**, 10664–10669.
42. B. Shen, R. Hutchinson, *Science* 1993, **262**, 1535–1540.
43. D. E. Cane, C. T. Walsh, C. Khosla, *Science* 1998, **282**, 63–68.
44. K. J. Weissman, P. F. Leadlay, *Nat. Rev. Microbiol.* 2005, **3**, 925–936.
45. R. McDaniel, A. Thamchaipenet, C. Gustafsson, H. Fu, M. Betlach, G. Ashley, *Proc. Natl. Acad. Sci. U.S.A.* 1999, **96**, 1846–1851.
46. Y. Yan, L. Zhang, Q. Zheng, Y. Han, H. Zhang, D. Zhang, T. Awakawa, I. Abe, W. Liu, *Angew. Chem. Int. Ed.* 2013, **52**, 12308–12312.
47. S. Blanchard, J. S. Thorson, *Curr. Opin. Chem. Biol.* 2006, **10**, 263–271.
48. S. Weist, B. Bister, O. Puk, D. Bischoff, S. Pelzer, G. J. Nicholson, W. Wohlleben, G. Jung, R. D. Suessmuth, *Angew. Chem. Int. Ed.* 2002, **41**, 3383–3385.
49. S. Weist, C. Kittel, D. Bischoff, B. Bister, V. Pfeiffer, G. J. Nicholson, W. Wohlleben, R. D. Suessmuth, *J. Am. Chem. Soc.* 2004, **126**, 5942–5943.

50. M. A. Gregory, H. Petkovic, R. E. Lill, S. J. Moss, B. Wilkinson, S. Gaisser, P. F. Leadlay, R. M. Sheridan, *Angew. Chem. Int. Ed.* 2005, **44**, 4757–4760.
51. S. Mo, D. H. Kim, J. H. Lee, J. W. Park, D. B. Basnet, Y. H. Ban, Y. J. Yoo, S.-W. Chen, S. R. Park, E. A. Choi, E. Kim, Y.-Y. Jin, S.-K. Lee, J. Y. Park, Y. Liu, M. O. Lee, K. S. Lee, S. J. Kim, D. Kim, B. C. Park, S.-G. Lee, H. J. Kwon, J.-W. Suh, B. S. Moore, S.-K. Lim, Y. J. Yoon, *J. Am. Chem. Soc.* 2011, **133**, 976–985.
52. P. Pahari, M. K. Kharel, M. D. Shepherd, S. G. van Lanen, J. Rohr, *Angew. Chem. Int. Ed.* 2012, **51**, 1216–1220.
53. Q. Cheng, L. Xiang, M. Izumikawa, D. Meluzzi, B. S. Moore, *Nat. Chem. Biol.* 2007, **3**, 557–558.
54. R. H. Feling, G. O. Buchanan, T. T. Mincer, C. A. Kauffman, P. R. Jensen, W. Fenical, *Angew. Chem. Int. Ed.* 2003, **42**, 355–357.
55. T. A. M. Gulder, B. S. Moore, *Angew. Chem. Int. Ed.* 2010, **49**, 9346–9367.
56. R. P. McGlinchey, M. Nett, A. S. Eustáquio, R. N. Asolkar, W. Fenical, B. S. Moore, *J. Am. Chem. Soc.* 2008, **130**, 7822–7823.
57. A. S. Eustáquio, D. O'Hagan, B. S. Moore, *J. Nat. Prod.* 2010, **73**, 378–382.
58. M. C. Walker, B. W. Thuronyi, L. K. Charkoudian, B. Lowry, C. Khosla, M. C. Y. Chang, *Science* 2013, **341**, 1089–1094.
59. M. C. Walker, M. C. Y. Chang, *Chem. Soc. Rev.* 2014, **43**, 6527–6536.
60. A. S. Eustáquio, B. S. Moore, *Angew. Chem. Int. Ed.* 2008, **47**, 3936–3938.
61. Y. Liu, C. Hazzard, A. S. Eustáquio, K. A. Reynolds, B. S. Moore, *J. Am. Chem. Soc.* 2009, **131**, 10376–10377.
62. R. S. Bohacek, C. McMartin, W. C. Guida, *Med. Res. Rev.* 1996, **16**, 3–50.
63. R. Breinbauer, I. R. Vetter, H. Waldmann, *Angew. Chem. Int. Ed.* 2002, **41**, 2878–2890.
64. S. L. Schreiber, *Science* 2000, **287**, 1964–1969.
65. M. D. Burke, S. L. Schreiber, *Angew. Chem. Int. Ed.* 2004, **43**, 46–58.
66. T. E. Nielsen, S. L. Schreiber, *Angew. Chem. Int. Ed.* 2008, **47**, 48–56.
67. Y. -k. Kim, M. A. Arai, T. Arai, J. O. Lamenzo, E. F. Dean III, N. Patterson, P. A. Clemons, S. L. Schreiber, *J. Am. Chem. Soc.* 2004, **126**, 14740–14745.
68. G. I. Schaefer, J. R. Perez, J. R. Duvall, B. Z. Stanton, A. F. Shamji, S. L. Schreiber, *J. Am. Chem. Soc.* 2013, **135**, 9675–9680.
69. N. Kumagai, G. Muncipinto, S. L. Schreiber, *Angew. Chem. Int. Ed.* 2006, **45**, 3635–3638.
70. G. Muncipinto, T. Kaya, J. A. Wilson, N. Kumagai, P. A. Clemons, S. L. Schreiber, *Org. Lett.* 2010, **12**, 5230–5233.
71. M. J. Wawer, K. Li, S. M. Gustafsdottir, V. Ljosa, N. E. Bodycombe, M. A. Marton, K. L. Sokolnicki, M.-A. Bray, M. M. Kemp, E. Winchester, B. Taylor, G. B. Grant, C. S.-Y. Hon, J. R. Duvall, J. A. Wilson, J. A. Bittker, V. Dancik, R. Narayan, A. Subramanian, W. Winckler, T. R. Golub, A. E. Carpenter, A. F. Shamji, S. L. Schreiber, P. A. Clemons, *Proc. Natl. Acad. Sci. U.S.A.* 2014, **111**, 10911–10916.
72. P. A. Clemons, J. A. Wilson, V. Dancik, S. Muller, H. A. Carrinski, B. K. Wagner, A. N. Koehler, S. L. Schreiber, *Proc. Natl. Acad. Sci. U.S.A.* 2011, **108**, 6817–6822.
73. S. Dandapani, A. R. Germain, I. Jewett, S. Le Quement, J.-C. Marie, G. Muncipinto, J. R. Duvall, L. C. Carmody, J. R. Perez, J. C. Engel, J. Gut, D. Kellar, J. L. Siqueira-Neto, J. H. McKerrow, M. Kaiser, A. Rodriguez, M. A. Plamer, M. Foley, S. L. Schreiber, B. Munoz, *ACS Med. Chem. Lett.* 2014, **5**, 149–153.
74. S. L. Schreiber, *Nature* 2009, **457**, 153–154.
75. D. Morton, S. Leach, C. Cordier, S. Warriner, A. Nelson, *Angew. Chem. Int. Ed.* 2009, **48**, 104–109.
76. D. J. Newman, G. M. Cragg, *J. Nat. Prod.* 2012, **75**, 311–335.
77. B. E. Evans, K. E. Rittle, M. G. Bock, R. M. DiPrado, R. M. Freidinger, W. L. Whitter, G. F. Lundell, D. F. Veber, P. S. Anderson, R. S. L. Chang, V. J. Lotti, D. J. Cerino, T. B. Chen, P. J. Kling, K. A. Kunkel, J. P. Springer, J. Hirshfield, *J. Med. Chem.* 1988, **31**, 2235–2246.
78. H. van Hattum, H. Waldmann, *J. Am. Chem. Soc.* 2014, **136**, 11853–11859.
79. M. A. Koch, A. Schuffenhauer, M. Scheck, S. Wetzel, M. Casaulta, A. Odermatt, P. Ertl, H. Waldmann, *Proc. Natl. Acad. Sci. U.S.A.* 2005, **102**, 17272–17277.
80. S. Wetzel, K. Klein, S. Renner, D. Rauh, T. I. Oprea, P. Mutzel, H. Waldmann, *Nat. Chem. Biol.* 2009, **5**, 581–583.
81. S. Wetzel, R. S. Bon, K. Kumar, H. Waldmann, *Angew. Chem. Int. Ed.* 2011, **50**, 10800–10826.
82. S. Rizzi, H. Waldmann, *Chem. Rev.* 2014, **114**, 4621–4639.
83. M. Mentel, R. Breinbauer, *Top. Curr. Chem.* 2007, **278**, 209–241.
84. H. E. Pelish, N. J. Westwood, Y. Feng, T. Kirchhausen, M. D. Shair, *J. Am. Chem. Soc.* 2001, **123**, 6740–6741.
85. H. E. Pelish, J. R. Peterson, S. B. Salvarezaa, E. Rodriguez-Boulan, J. L. Chen, M. Stamnes, E. Macia, Y. Feng, M. D. Shair, T. Kirchhausen, *Nat. Chem. Biol.* 2006, **2**, 39–46.
86. B. C. Goess, R. N. Hannoush, L. K. Chan, T. Kirchhausen, M. D. Shair, *J. Am. Chem. Soc.* 2006, **128**, 5391–5403.
87. P.-Y. Dakas, J. A. Parga, S. Höing, H. R. Schoeler, J. Sterneckert, K. Kumar, H. Waldmann, *Angew. Chem. Int. Ed.* 2013, **52**, 9576–9581.
88. H. Dueckert, V. Pries, V. Khedkar, S. Menninger, H. Bruss, A. W. Bird, Z. Maliga, A. Brockmeyer, P. Janning, A. Hyman, S. Grimme, M. Schürmann, H. Preut, K. Hübel, S. Ziegler, K. Kumar, H. Waldmann, *Nat. Chem. Biol.* 2012, **8**, 179–184.
89. V. Eschenbrenner-Lux, H. Dueckert, V. Khedkar, H. Bruss, H. Waldmann, K. Kumar, *Chem. Eur. J.* 2013, **19**, 2294–2304.
90. R. M. Wilson, S. J. Danishefsky, *J. Org. Chem.* 2006, **71**, 8329–8351.
91. A. M. Szpilman, E. M. Carreira, *Angew. Chem. Int. Ed.* 2010, **49**, 9592–9628.

92. P. A. Wender, J. L. Aryza, C. E. Bennett, F. C. Bi, S. E. Brenner, M. O. Clarke, J. C. Horan, C. Kann, E. Lacote, B. Lippa, P. G. Nell, T. M. Turner, *J. Am. Chem. Soc.* 2002, **124**, 13648–13649.

93. T. Oskarsson, P. Nagorny, I. J. Krauss, L. Perez, M. Mandal, G. Yang, O. Ouerfelli, D. Xiao, M. A. S. Moore, J. Massague, S. J. Danishefsky, *J. Am. Chem. Soc.* 2010, **132**, 3224–3228.

94. S. B. Jones, B. Simmons, A. Mastracchio, D. W. C. MacMillan, *Nature* 2011, **475**, 183–188.

95. E. E. Anagnostaki, A. L. Zografos, *Chem. Soc. Rev.* 2012, **41**, 5613–5625.

96. S. A. Snyder, S. P. Breazzano, A. G. Ross, Y. Lin, A. L. Zografos, *J. Am. Chem. Soc.* 2009, **131**, 1753–1765.

# INDEX

Note: Page numbers in *italic* and **bold** denotes figures and tables.


abudinol B, McDonald's second-generation synthesis, of, 179, *180*
*Acetobacter oxidans*, 520
acetyl-CoA carboxylase, 130
acetylenic esters, cycloisomerization reaction of, 270
*N*-acetyl oxazolidinones, 98
*O*-acetylquinine, 204, *205*
actinorhodin, 30, *30*
activated isoprene units, 196
acyclic monoterpenes, 197, *198*
acyl carrier protein (ACP), 23, 191
acyl-Pictet-Spengler reaction, 230, *231*
adenosine triphosphate (ATP), 1, *2*
adrenaline, 431, *432*
Alder-ene reaction, *246*
aldol reaction
  asymmetric aldehydes, 89–90
  chiral auxiliaries, 93–98
  chiral enolates, 90–93
  direct, 98–100
  mukaiyama, 100–106
  predict stereoselection, 88–89
  using chiral enolates, *97*
aldol–reduction reactions, *124*
alkaloids; *see also specific types*
  amaryllidaceae, 438, 439
    aryl radical, 465, 466
    carbamate moiety, 464
    7-deoxypancratistatin, 464, *465*
    galantamine, 440, *441,* 466–468, *467, 468*
    narciclasine, 440, 462, 463, *463*
    plant family, 462
  benzyltetrahydroisoquinoline
    biosynthesis, 433, *434*
    dihydrocodeinone, 456, 457
    ent-hydromorphone, 459–460
    morphinans, 434
    morphine, 456–458, *457–458*
    oxidation, 434
    possible structures, 434, *435*
    stereoselective reduction, 436, *436*
    thebaine, 436, *437*
  derived from Krebs cycle, 6–8, *7*
  lysine-derived alkaloids, 8
  nicotinic acid, 10
  NRPS metabolites and peptides, 10, *10*
  ornithine-derived alkaloids, 6–8
  tryptophan-derived alkaloid biosynthetic pathways, *9,* 9–10
  tyrosine-and phenylalanine-derived alkaloids, 8–10, *8–10*
alkene endocyclic bonds, metathesis reaction, *252*
all-*cis*-3,6,9,12, 15-octadecapentaenoic acid, 152
allene, 227, *227*
allenoate activations, 219
Alpine-Borane®, 110–111
amaryllidaceae alkaloids, 438, 439
  aryl radical, 465, 466
  carbamate moiety, 464
  7-deoxypancratistatin, 464, *465*
  galantamine, 440, *441,* 466–468, *467, 468*
  narciclasine, 440, 462, 463, *463*
  plant family, 462
amine-catalyzed cyclopropane activation, 213
*N*-amino cyclic carbamates (ACC), 49, *49*
aminodeoxyisochorismate (ADIC), 504
(*R*)-1-amino-2-methoxymethylpyrrolidine (RAMP), 45, *46*



*From Biosynthesis to Total Synthesis: Strategies and Tactics for Natural Products*, First Edition. Edited by Alexandros L. Zografos.


© 2016 John Wiley & Sons, Inc. Published 2016 by John Wiley & Sons, Inc.

(*S*)-1-amino-2-methoxymethylpyrrolidine (SAMP), 45, *46, 47*
8-aminoquinoline (AQ), 338, 340
amphotericin B, 21, *22*
anthranilic acid
  biosynthesis
    ADIC, 504
    chorismate synthase, 502, *503*
    ESPS, 502
    InGP synthase, 505
    monoterpene indole alkaloids, 507, *507*
    PRA isomerase, 505
    ribbon diagram, 504, *504*
    schematic model, 504, *504*
    shikimate pathway, 502, *503*
    simple indole alkaloids, 506, *507*
    terpene indole alkaloids, 507, *508*
    tryptophan, 504–505, *505*
  divergent synthesis–collective total synthesis
    adjusting unified synthetic plan, 510
    collective total synthesis, 508, *509*
    designing a common scaffold, 509
    selecting targets, *508,* 508–509
    target-oriented synthesis, 508
  tryptophan–derived alkaloids
    bisindole, 512–517, *513–517*
    monoterpene indole, 510–512, *511–513*
antimycin (ANT), 528, *530*
*anti*-selective Masamune–Abiko aldol reaction, *96*
2,3-*anti*-substituents with chelation control, *91*
2,3-*anti*-substitution (Felkin reinforcing), *91*
arachidonic acid, 135, *136, 142*
aristolochene synthase, crystal structure of, *240*
armatol A, Jamison's synthesis of, 179, *179*
aromadendrane sesquiterpenes, 267
aromatases (ARO), 30
aromatic amino acids
  Claisen rearrangement, 333
  pyridoxal phosphate, 333
  shikimate pathway, 333, *334*
*Artemisia annua*, 243
*Artemisia maritima*, 241
artemisinic acid, 244
artemisinin
  from *Artemisia annua*, 243–244
  biosynthesis of, *243*
aryl-aryl coupling reactions
  classification of different types, 442
  copper-mediated aryl-aryl bond forming reactions, 443–446
  intrinsic importance, 442
  nickel-mediated aryl-aryl bond forming reactions, 446–447
  palladium-mediated aryl-aryl bond forming reactions, 447–450
  transition metal-catalyzed coupling, 450, *452–455,* 453–456
α-santonin, 241
asperfuranone, 35, *36*
(+)-aspidospermidine, 230, *230*
asymmetric aldol reactions
  asymmetric aldehydes, 89–98
  basic models, 88–89
  direct aldol reactions, 98–100
  macrolides, total synthesis of
    asymmetric reduction, 117–120
    oxymercuration approach, 120–124
  Mukaiyama aldol reactions, 100–106
  stereoselective synthesis
    chemical reductions, 108–117
    enzymatic reduction, 107–108
    lewis base activation, *107*
asymmetric alkylation reactions, 44–49
asymmetric cycloisomerization
  diene, 259, 260
  of 1,6-enynes, 256
  with external nucleophiles, 256
  indicative cascades, *257*
  medium-size cyclopropane derivatives, *257*
asymmetric dihydroxylation (ADH), 176
asymmetric Mannich reaction, 392, *393–395,* 394
  biocatalytic, 413–414
  chiral amines as catalysts, 394–398, *395–400*
  chiral brønsted acids as catalysts, 404–408, *405–408*
  chiral brønsted bases as catalysts, 398, 399, 401–403, *401–404*
  organometallic catalysts, 408–413, *409–413*
asymmetric organocatalysis, 204–207
asymmetric phase-transfer catalysis, 220–225
atom economy, histidine
  aldol reaction, 482, *482*
  brute-force approach, 480
  C–H activation, *483,* 483–484
  chemoselectivity, 485
  C–H functionalization, 483
  concept, 480
  Diels–Alder reaction, 481
  generic peptide coupling, 480, *481*
  ideal synthesis, 480
  importance, 480
  incorporation, 485, *485*
  natural products, 487, *488*
  PGF *vs.* PG, 487, *487*
  protecting-group-free synthesis, 484, *484*
  site-selective epoxidation, 486, *486*
  stoichiometric base, 482, *482*
  strategic removal of protecting group, 485, *485*
  synthetic community, 486, *486*
  Zn-complex catalyst, 485, *485*
avian *trans*-FPPS, 236, *237*
axinellamines
  deficient in halogens, 497
  feature synthesis, 493, *494*
  utilization, 494, *494*
aziridination reactions, 220

Baylis-Hillman-type reactions, 219
benzaldehyde, 204, *205*
benzosceptrin C, 477, *478*
benzyltetrahydroisoquinoline alkaloids
  biosynthesis, 433, *434*
  dihydrocodeinone, 456, 457

benzyltetrahydroisoquinoline alkaloids (*cont'd*)
ent-hydromorphone, 459–460
morphinans, 434
morphine, 456–458, *457–458*
oxidation, 434
possible structures, 434, *435*
stereoselective reduction, 436, *436*
thebaine, 436, *437*
β-elimination pathway, 246
C–$H_a$ bond energy, 247
inducing asymmetry in, 248–250
palladium cycloisomerization chemistry, 248
palladium(II) salts, 247, *248*
BINAL-H, 108–109
biocatalytic asymmetric Mannich reactions, 413–414
biology-oriented synthesis (BIOS), 536
biomimetic total synthesis
achieving enantioselective cationic cyclization, 327, *328*
caparrapi oxide, 325, *326*
Corey's group, 321
double bond activation, 327
dysideapalaunic acid, 327, *327*
8-epicaparrapi oxide, 325, *326*
germanicol, 323, *324*
hongoquercin B, 323, *326*
limonoids, 321, *324*
lupeol, 323, *325*
oligoprenol phosphates, 319, 320
serratenediol, 321, *323*
site-selective epoxidation, 321, *322*
utilizing LBA, 327
biosynthesis
anthranilic acid
ADIC, 504
chorismate synthase, 502, *503*
ESPS, 502
InGP synthase, 505
monoterpene indole alkaloids, 507, *507*
PRA isomerase, 505
ribbon diagram, 504, *504*
schematic model, 504, *504*
shikimate pathway, 502, *503*
simple indole alkaloids, 506, *507*
terpene indole alkaloids, 507, *508*
tryptophan, 504–505, *505*
biomimetic strategy, and total synthesis, 12–13, *13*
carbohydrates, 1, *3*
chrysophanol, 34, *34*
diterpenes
abietanes, 279, *281*
biomimetic cyclization, 279, *282*
casbene, 279, *280*
cembrane, 279, *280*
clerodane, 283, *283*
labdane, 283, *283*
taxadienes, 279, *281*
transannular processes, 279
enterocin, 32, *32,* 33
epothilones, 37, *38*
formation of alkaloids
lysine, 388, *389–390,* 390, *391,* 392
ornithine, 383–385, *386–387,* 388
hirsutellones, 12, *13*
histidine
ambiphilic reactivity, 477, *478*
benzosceptrin C, 477, *478*
dibromophakellin, 477, *478*
dolicotheline, 474, *475*
enzyme-catalyzed transformations, 474, *475*
imidazole of, 473–474
lysine, 477
metabolites, 474
molecular structure, 473
ornithine, 477
oxidation hypothesis, 478, *479*
palau'amine biosynthetic proposals, 478, *479*
PIA, 476, 477
pilocarpine, 475, *476*
10-step linear route, 473, *474*
modern organic synthesis
biocatalytic transformations, 522
commercial routes toward cortisone acetate, 520, *521*
complex natural products, 520
crotogoudin, 522, *522*
dihydropinidine, chemoenzymatic synthesis, 523, *523*
doxycycline, 523, *525*
enantioselective oxidation, 523
enzyme classes, 520
irreversible enzymatic step, 522, *522*
Merck process group, 520
narciclasine, 523, *524*
telaprevir, chemoenzymatic synthesis, 523, *524*
thioesterase-catalyzed macrolactonization, 526, *526*
monoterpenes, 196–200, *197, 198*
norsolorinic acid, 33, *33*
polyketides, 21–23, *23*
soraphen, 87, *87*
terpenes, 3
terpenoids
active polycyclic compounds, 301, *301*
animals and higher plants, 296
bacterial membranes, 296–297
carbocycle, 298, *299*
C-4 methyl groups loss, 299, *300*
cyclizations, 297
cyclopropane moiety, 301
double bond modifications, 299, *300*
IPP, 296, *297*
lanosterol, 298, 299
Lys side chain, 302–303
phytosterols, 301, *301*
polycyclic, 296, *298, 299*
polycyclic natural compounds, 301, *302*
stereochemistry, 298

vanadium haloperoxidases, 302, *302*
Wagner–Meerwein ring, 297, *298*
to total synthesis
natural products, chemical space of, 10–11
pathways, 11–13
science of, 14–16
tyrosine
amaryllidaceae alkaloids, 438–442, *439–442*
classification, 431, *432*
modified benzyltetrahydroisoquinoline alkaloids, 433–436, *434–436*
phenethylisoquinoline alkaloids, 436–438, *437*, *438*
simple tetrahydroisoquinoline alkaloids, 433, *433*
bisabolene synthase, crystal structure of, *240*
bisabolyl cation, 244
bisindole alkaloids
biosynthesis, 513, *513*
Hao's total synthesis, 516, *517*
Movassaghi's synthesis, 514, *515,* 516
Strecker-type reaction, 516
synthetic chemist's view, 517
Tambar's total synthesis, 514, *514,* 516
trigonoliimine A, 512–513, *513*
Wagner–Meerwein type, *515,* 515–516
(−)-brasoside, 227–229, *228*
brevetoxin, 162, *163*
Brown's chlorodiisopinocampheylborane, 111
bryologues, 539
bryostatins, 38, *40*
Build/Couple/Pair, 535–536, *536, 537*

cadaverine, 392
Calvin cycle, 1, *2*
camphorsulfonic acid (CSA), 167
Cane-Celmer-Westley hypothesis, 162, 163
carbon–heteroatom bonds, *49*
catecholamines, 432
cationic gold(I)-catalyzed cycloisomerizations, 253
CBS (Corey, Bakshi, and Shibata) catalyst, 111–112
cerium ammonium nitrate (CAN), 352
chartreusin, 31, *32*
C($SP^3$)–H arylation reactions
8-aminoquinoline, 338
bidentate directing group, 338, 340
biomimetic synthesis of celogentin C, 344, *344*
chelation-assisted, 338, *338*
Daugulis's pioneering arylation, 338, *339*
direct functionalization, 336, 338
directing groups, 338, *339*
electrophilic reagents, 338
ligand-enabled cross coupling, 343, *343*
2-methylthioaniline, 338
MPAA, 343
nonnatural α-amino acid derivatives, 340, *340*
Pd-catalytic cycle, 338, *339*
Pd-catalyzed longer-range, 343, *343*
Pd-catalyzed *N*-(2-pyridyl)sulfonyl-directed, 342, *342*
Pd complexes, 341
Pd(II) complex structure, 338, *339*
picolinamide, 341
stereoselective synthesis of aliphatic amines, 341, *342*
synthesis of phenylalanine derivatives, 340, *341*
tricyclic quinoline, 340, 341
Yu's diverse synthesis, 340, *341*
C($SP^3$)–H coupling reactions
aryltetralin, 355
benzocyclobutenol silyl ether, 355, *356*
crystal structure, 356, *356*
head-to-head dimerization, 353
head-to-tail homodimerization, 353
magnosalin, 353, *353*
piperarborenines B and D, 353, *354*
pipercyclobutanamide A, 354, 355, *355*
pseudosymmetrical, 353
synthesis of podophyllotoxin, 357, *357*
chemoenzymatic synthesis
dihydropinidine, 523, *523*
telaprevir, 523, *524*
chemoselectivity, 485
chiral (bronsted) acids and H-bonding donors, 213–218
chiral amine-catalyzed Rauhut-Currier-type cyclization, 229, *229*
chiral Brønsted acids, 214
chiral Brønsted base-assisted Brønsted acids (chiral BBAs), 306, *306*
chiral bronsted/Lewis bases and nucleophilic catalysis, 218–220
chiral enol ester, 227, *227*
chiral enone, 227, *227*
chiral Lewis base catalysts, *223*
chiral tertiary amine-based nucleophilic catalysts, *221*
chiral (thio)urea organocatalysts, 216, *217*
chorismate synthase, 502, *503*
chrysanthemic acid, 202, *204*
chrysophanol, biosynthesis of, 34, *34*
*cis*-prenyltransferases, 236–237
Claisen-like condensation/reduction sequence, *115*
colchicine, 431
collective total synthesis, 508, *509*
copper-mediated aryl-aryl bond forming reactions, 443–446, *443–446*
Corey-Chaykovsky-type epoxidation, 220
Corey's total synthesis, of glabrescol, 176, *177*
costunolide, 241
cross coupling reactions, 143–145
cubebol-cubebenes sesquiterpenes, 267–270
cubebol natural products, cycloisomerization reaction for, 269
cyclases (CYC), 30
cyclic monoterpenes, 197–200, *198–200*
cyclobutenone, 69, *69*
cyclogalgravin, 357, 358, 359
cycloisomerization reaction
of acetylenic esters, 270
allylic substitution, *249*
asymmetric cycloisomerization, 256
biosynthetic correlation with sesquiterpene synthases, *245*
for cubebol natural products, 269

cycloisomerization reaction (*cont'd*)
definition, 244–245
enantioselective, *250*
enyne cycloisomerization
β-elimination pathway, *247,* 247–250
platinum and gold in metathesis, 252–257
proposed mechanisms, 245–247, 254
reductive elimination pathway, 250–252
labeling experiments for, 252
metal-catalyzed cycloisomerizations, 245, *246*
1,6-or 1,7-enynes, 249
remote alkene and, *249*
tether in, *248*
cyclooxygenases (COXs), 136
cyperolone, 273–275

10-deacetylbaccatin III, *4*
dehydroartemisinic acid, 244
3-deoxy-D-arabino-heptulosonic acid 7-phosphate (DAHP) synthase, 333, *334*
1-deoxy-D-xylulose-5-phosphate (DXP), 192
6-deoxyerythronolide B, 36, *36*
6-deoxyerythronolide B synthase (DEBS), 528
7-deoxyloganin, 226–227, *228*
deoxynivalenol, 244
biosynthesis of, *244*
D-erythrose 4-phosphate, 333
$\Delta^9$-desaturase system, 134
dibromophakellin
biosynthetic proposals, 477, *478*
Buchi's biomimetic synthesis, 478, *479*
dichroanone, 487, *487*
Diels–Alder reaction, 34
atom economy, histidine, 481
diterpenes
aglycones, 286, *286*
alcohol, 286, *286*
colombiasin A, 285, *286*
cycloadduct, 286, *286*
diene, 284, *285*
dienophile, 284, *285*
divinylallene, 286, *286*
ester, 286, *286*
pseudopterosin natural motifs, 286, *286*
symmetry-allowed process, 285
vinigrol, 286, *286*
PIAs, 491, *492*
diene cycloisomerization
asymmetric cycloisomerization, 259, 260
basic concept of, *258*
cationic platinum pincer complexes, 264
drawbacks, 257
enantioselectivities, *263*
hydrometalation, *258,* 259
hydrosilane additives, *262*
iron-catalyzed, *264*
nickel-catalyzed, *259*
palladium-catalyzed, *261,* 261–262
platinum pincer complexes, 264
precatalysts for, 262
rhodium-catalyzed, *260*
(*cis,cis*)-1,4-diene system, *141*
(5*S*,15*S*)-dihydroxy-6,13-*trans*-8,11-*cis*-eicosatetraenoic acid, 148, *148*
dimethylallyl diphosphate (DMAPP), 189, *190*
2,2-dimethyl-1,3-dioxan-5-one hydrazone, *48*
1,3-diols, asymmetric aldol reactions
asymmetric aldehydes, 89–98
basic models, 88–89
direct aldol reactions, 98–100
macrolides, total synthesis of
asymmetric reduction, 117–120
oxymercuration approach, 120–124
Mukaiyama aldol reactions, 100–106
stereoselective synthesis
chemical reductions, 108–117
enzymatic reductions, 107–108
lewis base activation, *107*
diterpenes, 189, *190*
biosynthesis
abietanes, 279, *281*
biomimetic cyclization, 279, *282*
casbene, 279, *280*
cembrane, 279, *280*
clerodane, 283, *283*
labdane, 283, *283*
taxadienes, 279, *281*
transannular processes, 279
Diels–Alder reaction and applications
aglycones, 286, *286*
alcohol, 286, *286*
colombiasin A, 285, *286*
cycloadduct, 286, *286*
diene, 284, *285*
dienophile, 284, *285*
divinylallene, 286, *286*
ester, 286, *286*
pseudopterosin natural motifs, 286, *286*
symmetry-allowed process, 285
vinigrol, 286, *286*
pericyclic reactions and applications, 291–293
diversity-oriented synthesis (DOS), 15–16, 533
biologically active molecules identified, 536, *538*
Build/Couple/Pair, 535–536, *536, 537*
characteristic features, 535, *535*
definition, 535
Nelson's highly scaffold-divergent synthesis, 536, *538*
synthetic strategy, 535
TOS, 535
diverted total synthesis (DTS), 539, 541, *542–544*
docosahexaenoic acid (DHA), 134, *134, 136*
dolicotheline, 474
DOS, *see* diversity-oriented synthesis (DOS)
doxycycline, Myers synthesis, 523, *525*
dragmacidin D, 483

echinopines, 271–273
eicosapentaenoic acid (EPA), 134, *134, 136, 143*
electrophilic cleavage, 247
electrophilic reagents, 307
enamine, 207–213, *212*
Enders alkylation
  applications of, 60–69
  attenols A and B, 66–68, *68*
  epothilones A and B, 65–66, *66*
  hydrazones, cleavage of, 46–47
  (+)-pectinatone, 60–62, *61*
  polyacetates, 47–49, *74–49*
  RAMP and SAMP Hydrazones, 45–46, *46*
  stigmatellin A, *62,* 62–63
  swinholide A, *63,* 63–64
energy supply, 1, *2*
engineered biosynthesis
  aglycon deoxyerythronolide B, 526, *527*
  ANTs, 528, *530*
  biosynthetic pathway, 532, *532*
  DEBS, 528
  disadvantage, 528
  fluorinase gene, 533
  fluorinated balhimycins pathway, 531, *531*
  fluorosalinosporamide engineering approach, 533, *534*
  gilvocarcin group, 532
  mutasynthesis, 528
  organofluorines, 533
  polyketides, 526, *527*
  premonensin redox derivatives, predicted structures, 528, *529*
  proteasome inhibitors, 532, 533
englerins, 271
enolate formation, *88*
5-Enolpyruvylshikimate-3-phosphate (EPSP) synthase
  gene encoding, 502
  ribbon diagram, 502, *503*
enshuol, Morimoto's total synthesis of, *178*
enterocin, biosynthesis of, 32, *32,* 33
enyne cycloisomerization
  β-elimination pathway, *247,* 247–250
  metallocyclopentene pathway, 245–246
  platinum and gold in metathesis, 252–257
  proposed mechanisms, 245–247, 254
  reductive elimination pathway, 250–252
enzyme commission (EC) number, 3
epothilones, biosynthesis of, 37, *38*
epoxide-opening reactions, 163
epoxy ester, 152
erythromycin A, 21, *22*
erythromycin, biosynthesis of, 36
eudesmyl cation, 241
Evans' alkylation
  amphidinolide G, 78–80, *78–80*
  amphidinolide H, 78–80, *78–80*
  amphidinolide $T_1$, 77–78, *77–78*
  diastereoselective alkylation, chiral auxiliaries for, 58–59, *58–59*
  isolaulimalide, 81–83
  neolaulimalide, 81–83
  preparation of, 57–58, *57–58*
Evans–Cornforth and Roush transition state, 88
Evans–Metternich aldol reaction, *97*
Evans–Metternich variation, 95
Evans–Tishchenko reduction, *116*

farnesyl diphosphate (FDP)
  crystallographic analysis, 239
  crystal structures, *238*
  diphosphate unit of, 239
  diverse sesquiterpene motifs, *237*
  formation, *237*
  ionization, 238
  isomerization, *239*
  sesquiterpene precursor, 236
  in sesquiterpenes, 238
fatty acids and lipids
  biosynthesis, 130
  condensation reactions, 131–133
  fatty acid synthase enzyme systems, 130–131, *131*, *132*
  fatty acyl synthases, structure models of, 133–134
  polyunsaturated fatty acids (PUFAs), *134*, 134–135, *135*
  Ω-3 and Ω-6 all-*Z* polyunsaturated fatty acids
    cross coupling reactions, 143–145
    polyyne semihydrogenation, 140–143, *141*, *142*, *143*
  ω-3 and ω-6 polyunsaturated fatty acids
    biosynthesis of, *134,* 134–135, *135*
    mediated oxidations of, 135–140, *138–141*
fatty acid synthase (FAS) enzyme systems, 130–131, *131*, *132*
FDP, *see* Farnesyl diphosphate (FDP)
Felkin model, 88, *90*
flavonoids, 6
Forsyth approach, 71, *71*
Friedel–Crafts reactions
  indoles, 210
  lignans
    acid-promoted cyclization, 363, *366*
    ampelopsin D unified synthesis, 366, *369*
    ampelopsin F unified synthesis, 366, *369*
    ampelopsin H programmable synthesis, 367, *370*
    7′-aryltetralol and aryltetralone, 359, *360*
    asymmetric synthesis, 359, *360*
    biomimetic dimerization strategy, 363, *364*
    cassigarol B diverse synthesis, 365, *368*
    cyclogalgravin, 357, 358
    2,7′-cyclolignans feature, 357, *358*
    diastereodivergent hydrogenation, 358
    diptoindonesin D total syntheses, 363, *367*
    divergent cyclizations, 361, *361*
    8′-*epi*-aristoligol, 359
    heimiol A structures, 372, *374*
    hopeahainol A structures, 369, *370*
    hopeahainol D structures, 372, *374*
    hopeanol structures, 369, *370*
    Nicolaou and Chen's total synthesis, 372, *373*
    oxidation of isogalbulin, 359
    pallidol unified synthesis, 366, *369*

Friedel–Crafts reactions (*cont'd*)
plausible biogenesis relationship, 366, *368*
plausible mechanism, 361
polyphenol natural product, 363
protected hemsleyanol E total syntheses, 363, *367*
quadrangularin A unified synthesis, 366, *369*
resveratrol-derived natural products, 363, *364*
Snyder's biomimetic synthesis, *371,* 373
Snyder's collective synthesis strategy, 363, *365*
Snyder's total synthesis, 374, *375*
synthesis of δ-lactone, 372, *372*
tertiary alcohol, 361
Thomson's stereocontrolled synthesis, 361, *362*
Ueno-Stork radical cyclization, 358, *359*
veratrole group, 360
organic synthesis
active catalyst, 349, *349*
advances, 345
alkylation and acylation, 344, *345*
arylations, 345
by (*R*)-BINOL-derived monophosphoric acid, 350, *351*
calcium-catalyzed intramolecular, 345, *346*
catalytic asymmetric, *348,* 348–349
cerium ammonium nitrate, 352, *352*
conjugate addition/asymmetric protonation catalyze, 350, *351*
cyclization, 347
diastereoselective intermolecular, 347, *348*
drawbacks, 345
formation of amylbenzene, 344
indoles with enecarbamates catalyze, 350, *351*
indoles with *N*-sulfonyl aldimines, 351, *351*
intramolecular attack, 353
iron-catalyzed intramolecular, 347, *347*
mechanism of alkylation, 344, *345*
network of hydrogen bonding interactions, 351–352, *352*
organocatalytic asymmetric, 350, *350*
function-oriented synthesis (FOS), *15,* 15–16

galbelgin, 359
galbonolide B, 36, *36*
gallic acids, 6
(+)-geniposide, 225–227, 227, *227*
geranyl diphosphate (GDP)
crystal structures, *238*
ionization, 236
in monoterpenes, 238
*trans*-prenyltransferases, 236
germacrane A hydroxylase, 240
germanicol, 323, *324*
gilvocarcins, 31, *32*
glabrescol, 176, *177,* 183
Corey's total synthesis of, 176, *177*
Hoye's synthesis of, 176, *177*
glucose, phosphorylation of, 1
glycolysis, 1–3, *3*
gold cycloisomerization
of 1,5-enynes, *254*
1,6-enynes-Prins cascade, 255
in metathesis reaction, 252–257
griseorhodin A, 31, *32*
gymnocin tetrahydropyran core, 183

Hajos–Parrish–Eder–Sauer–Wiechert reaction, *99*
Hayashi–Jorgensen catalysts, 208, 211
hemibrevetoxin B, Holton's synthesis of, 179, *180*
hemiterpenes, 189, *190*
herboxidiene, 70
15-HETE, 138, 150, *150*
heteroatom, 4
histidine
atom economy
aldol reaction, 482, *482*
brute-force approach, 480
C–H activation, *483,* 483–484
chemoselectivity, 485
C–H functionalization, 483
concept, 480
Diels–Alder reaction, 481
generic peptide coupling, 480, *481*
ideal synthesis, 480
importance, 480
incorporation, 485, *485*
natural products, 487, *488*
PGF *vs.* PG, 487, *487*
protecting-group-free synthesis, 484, *484*
site-selective epoxidation, 486, *486*
stoichiometric base, 482, *482*
strategic removal of protecting group, 485, *485*
synthetic community, 486, *486*
Zn-complex catalyst, 485, *485*
biosynthesis
ambiphilic reactivity, 477, *478*
benzosceptrin C, 477, *478*
dibromophakellin, 477, *478*
dolicotheline, 474, *475*
enzyme-catalyzed transformations, 474, *475*
imidazole of, 473–474
lysine, 477
metabolites, 474
molecular structure, 473
ornithine, 477
oxidation hypothesis, 478, *479*
palau'amine biosynthetic proposals, 478, *479*
PIA, 476, 477
pilocarpine, 475, *476*
10-step linear route, 473, *474*
functions, 473
PIAs
axinellamine deficient in halogens, 497, *498*
axinellamines feature synthesis, 493, *494*
Baran's hypotheses, 488, *490*
conversion of sceptrin, 488, *489*
1,9-dideoxy-pre-axinellamine synthesis, 491, *492*
Diels–Alder reaction, 491, *492*
literature method, 493, *493*

massadines, 494, *495*
oxidative ring expansion, 488
palau'amine synthesis, 496, *496*
pre-axinellamine conversion, 491, *491*
proposed conversion of axinellamine A, 494, *494*
structural diversity, 488, *489*
synthetic challenges, 488
Woodward fission, 497, *497*
side chain, 473
*Holostylis reniformis,* 335, *337*
Holton's synthesis, of hemibrevetoxin B, 179, *180*
Horner–Wadsworth–Emmons reaction, 153
Hoye's synthesis, of glabrescol, 176, *177*
hydrazine, 45, *46*
hydrazonesm, cleavage of, 46–47
hydroacylation cycloisomerization, of tetraenes, 268
hydrometalation, of dienes, *258*

IDP, *see* isopentenyl diphosphate (IDP)
ikarugamycin, 36, *36*
imidazole, 474
iminium, 207–213, *211*, *212*
indole-3-glycerol phosphate (InGP), 505
indoles, 210; *see also* Friedel–Crafts reactions
intramolecular Diels–Alder (IMDA) reaction, 12
iodolactone, 152
iridoids, 200–202, *200–202*
iron-catalyzed cycloisomerization, of trienes, *264*
isopentenyl diphosphate (IDP)
crystal structures, *238*
double bond, 236
spatial orientation, 236
isopentenyl diphosphate (IPP), 189, *190*

Jamison's dioxepanethyrsiferol synthesis, 180, *181*
Jamison's synthesis, of armatol A, 179, *179*

kadangustin J, 359
Kobayashi aldol reaction, *109*
Krebs cycle, 1–3, *3*

lactodehydrothyrsiferol, oxidative synthesis of, 181, *181*
lactone, 227, *227*
lanosterol, 298, 299
role of, 301
Leighton oxymercuration, *123*
leukotriene $B_4$, 146, *146*
leukotriene $B_5$, *158–159*, 158–160
Lewis acid-assisted chiral Brønsted acid (chiral LBA), 304, *304*, 306
Lewis acid-mediated epoxide cascade reaction, 179
Lewis acids, 99, *223*, 225
Lewis base activation, 104, *107*
lignans and lignins
biosynthesis, 335
pathway, 335, *336*
C($SP^3$)–H coupling reactions
aryltetralin, 355
benzocyclobutenol silyl ether, 355, *356*
crystal structure, 356, *356*
head-to-head dimerization, 353
head-to-tail homodimerization, 353
magnosalin, 353, *353*
piperarborenines B and D, 353, *354*
pipercyclobutanamide A, 354, 355, *355*
pseudosymmetrical, 353
synthesis of podophyllotoxin, 357, *357*
Friedel–Crafts reactions
acid-promoted cyclization, 363, *366*
ampelopsin D unified synthesis, 366, *369*
ampelopsin F unified synthesis, 366, *369*
ampelopsin H programmable synthesis, 367, *370*
7′-aryltetralol and aryltetralone, 359, *360*
asymmetric synthesis, 359, *360*
biomimetic dimerization strategy, 363, *364*
cassigarol B diverse synthesis, 365, *368*
cyclogalgravin, 357, 358
2,7′-cyclolignans feature, 357, *358*
diastereodivergent hydrogenation, 358
diptoindonesin D total syntheses, 363, *367*
divergent cyclizations, 361, *361*
8′-*epi*-aristoligol, 359
heimiol A structures, 372, *374*
hopeahainol A structures, 369, *370*
hopeahainol D structures, 372, *374*
hopeanol structures, 369, *370*
Nicolaou and Chen's total synthesis, 372, *373*
oxidation of isogalbulin, 359
pallidol unified synthesis, 366, *369*
plausible biogenesis relationship, 366, *368*
plausible mechanism, 361
polyphenol natural product, 363
protected hemsleyanol E total syntheses, 363, *367*
quadrangularin A unified synthesis, 366, *369*
resveratrol-derived natural products, 363, *364*
Snyder's biomimetic synthesis, *371*, 373
Snyder's collective synthesis strategy, 363, *365*
Snyder's total synthesis, 374, *375*
synthesis of δ-lactone, 372, *372*
tertiary alcohol, 361
Thomson's stereocontrolled synthesis, 361, *362*
Ueno-Stork radical cyclization, 358, *359*
veratrole group, 360
limonene, 197, 199, *200*, *201*
limonoids, 321, *324*
linoleic acid, 134, *134*
α-linolenic acid, 134, *134*, 135
linum flavum, 336
lipids, 130; *see also* fatty acids; polyunsaturated fatty acids (PUFAs)
lipoxin $A_4$, 148, *148*
lipoxygenases (LOXs), 136
littoralisone, 227, *227*
(−)-littoralisone, 227–229, *228*
L-lysine, *see* lysine
longilene peroxide, Morimoto's total synthesis of, 176, *178*

L-ornithine, *see* ornithine
lovastatin, 21, *22*
low-density lipoprotein (LDL), 192
L-phenylalanine
  biosynthetic pathway, 333, *334*
  deamination of, 335
L-tryptophan, *see* tryptophan
L-tyrosine, *see* tyrosine
lupeol, 323, *325*
lysine, 477
  asymmetric Mannich reaction, 392, *393–395*, 394
    biocatalytic, 413–414
    chiral amines as catalysts, 394–398, *395–400*
    chiral brønsted acids as catalysts, 404–408, *405–408*
    chiral brønsted bases as catalysts, 398, 399, 401–403, *401–404*
    organometallic catalysts, 408–413, *409–413*
  biosynthesis
    formation of alkaloids, 388, *389–390,* 390, *391,* 392
  Mannich and related reactions, 414, 417–419, *417–426,* 421–422, 424, 425
Lys side chain, 302–303

macrolactins, 38, *40*
macrolides, 87
magnesium monoperoxyphthalate hexahydrate (MMPP), 46
malonamate, 30
maresin 1, 146, *146*, 149, *149*
Marshall's reductive approach, 181, *182*
Martín's synthesis, of teurilene, 181, *182*
Maruoka-type ammonium salt catalysts, 224
Masamune's chiral 2,5-dimethylborolanes, 111–112
Masamune's (*R*)-mandelic acid-based auxiliary, *96*
McDonald's second-generation synthesis, of abudinol B, 179, *180*
mescaline, 431, *432*
metabolisms
  primary, 1, *2*
  secondary, 1–3, *2*
metal-catalyzed cycloisomerizations, 245, 246
metal-catalyzed enyne reactions, *246*
metallacyclopentenes, formation of, 246
metallocyclopentenes
  cleavage rearrangement products, *253*
  pathway, 245–246
$n^2$-metal pathway, 246
metathesis reaction
  from alkene endocyclic bonds, 252
  platinum and gold in, 252–257
methyl (5*Z*,8*Z*,10*E*,12*E*,14*Z*)-eicosapentanoate, 147, *147*
2-C-methyl-erythritol-4-phosphate (MEP), 192, *193*
methylglutaryl-CoA, 191
methylmalonate, 36
methyl phenyl ketene, 204, *205*
mevalonate-independent pathway, 192–193, *192–193*
mevalonic acid pathway, *191,* 191–192
(+)-mitsugashiwalactone, 229
modern organic synthesis
  BIOS, 536, 539, *540*
  DOS, 533
    biologically active molecules identified, 536, *538*
    Build/Couple/Pair, 535–536, *536*, *537*
    characteristic features, 535, *535*
    definition, 535
    Nelson's highly scaffold©divergent synthesis, 536, *538*
    synthetic strategy, 535
    TOS, 535
  DTS, 539, 541, *542–544*
  endeavor synthetic organic chemists, 519
  engineered biosynthesis
    aglycon deoxyerythronolide B, 526, *527*
    ANTs, 528, *530*
    DEBS, 528
    disadvantage, 528
    fluorinase gene, 533
    fluorinated balhimycins pathway, 531, *531*
    fluorosalinosporamide engineering approach, 533, *534*
    gilvocarcin group, 532
    mutasynthesis, 528
    organofluorines, 533
    polyketides, 526, *527*
    premonensin redox derivatives, predicted structures, 528, *529*
    proposed biosynthetic pathway, 532, *532*
    proteasome inhibitors, 532, 533
  natural product drug candidates, 519, *520*
  spectroscopic techniques, 519
  synthesis of natural products, 520
  total synthesis with biosynthesis
    biocatalytic transformations, 522
    commercial routes toward cortisone acetate, 520, *521*
    complex natural products, 520
    crotogoudin, 522, *522*
    dihydropinidine, chemoenzymatic synthesis, 523, *523*
    doxycycline, 523, *525*
    enantioselective oxidation, 523
    enzyme classes, 520
    irreversible enzymatic step, 522, *522*
    Merck process group, 520
    narciclasine, 523, *524*
    telaprevir, chemoenzymatic synthesis, 523, *524*
    thioesterase-catalyzed macrolactonization, 526, *526*
monensin, 162, *163*
mono-*N*-protected amino acid (MPAA), 343
monorhizopodin, Nicolaou synthesis of, *122*
monoterpene indole alkaloids, 507, *507*
  collective total synthesis, 511, *512*
  goniomitine total synthesis, 511–512, *512*
  Jieping Zhu's synthetic plan, 511, *512*
  MacMillan's synthesis, 510, *511*
monoterpenes, 189, *190*, 239
  acyclic monoterpenes, 197, *198*
  asymmetric organocatalysis, 204–207
  asymmetric phase-transfer catalysis, 220–225
  biosynthesis, 196–200, *197*, *198*
  chiral (brønsted) acids and H-bonding donors, 213–218
  chiral brønsted/Lewis bases and nucleophilic catalysis, 218–220
  cyclic monoterpenes, 197–200, *198–200*
  enamine, 207–213, *212*

iminium, 207–213, *211, 212*
iridoids, 200–202, *200–202*
irregular monoterpenes, 202–203, *204*
singly occupied molecular orbital activation, 207–213, *208*
morimoto's total synthesis
of enshuol, *178*
of longilene peroxide, 176, *178*
Moyori asymmetric transfer hydrogenation, 112–117
MPAA, *see* mono-*N*-protected amino acid (MPAA)
Mukaiyama aldol reaction, *90, 100,* 100–106, *102–106*
mupirocin, 38, *40*
murisolin, 162, *163*
mutational biosynthesis (MBS), 11
*Mycobacterium tuberculosis,* 238
mycoticin, 120–123, *123*
Myers' alkylation
carboxamides, 54–56
cylindrocyclophane A, 69, *70*
dictyostatin, 69–71, *70*
ephedrine carboxamides, **50**
herboxidiene/GEX 1A, 71–72, *72*
mandelalide A, 71–74, *72–73*
myxovirescin $A_1$, 74–75, *75*
(+)-pironetin, 75, *75*
pseudoephedrine auxiliary
β-branched primary alkyl iodides, **52**
carboxylic acids, 51, **53**
organolithium species, 51–53
pseudoephedrine carboxamides, **53**
reduction to corresponding alcohol, 51
pseudoephedrine carboxamides, **50,** 50–51, *51*
(+)-vittatalactone, 75–77, *76*
myxovirescin $A_1$, 74–75, *75*

Narasaka–Prasad reduction, *115*
narciclasine synthesis, 523, *524*
natural products, 10–11
NDP, *see* nerolidyl diphosphate (NDP)
nerolidyl diphosphate (NDP), 238–239, *239*
nickel-mediated aryl-aryl bond forming reactions, 446–447, *447*
nicotinamide adenine dinucleotide phosphate hydride (NADPH), 1, *2*
*N*-nitrosamine, 45, *46*
norepinephrine, 432–433
norsolorinic acid, biosynthesis of, 33, *33*
Noyori asymmetric transfer hydrogenation, *113*
*N*-(5-phosphoribosyl)-anthranilate (PRA), 505
π-nucleophiles, 179, *180*

oleic acid, 134, *134*
omaezakianol, Xiong's synthesis of, 178, *178*
oppolzer sultam-directed asymmetric synthesis, *syn*-aldol products, *96*
organic synthesis
$C(SP^3)$–H arylation reactions
8-aminoquinoline, 338
bidentate directing groups, 338, 340
biomimetic synthesis of celogentin C, 344, *344*
chelation-assisted, 338, *338*
Daugulis's pioneering arylation, 338, *339*
direct functionalization, 336, 338
directing groups, 338, *339*
electrophilic reagents, 338
ligand-enabled cross coupling, 343, *343*
2-methylthioaniline, 338
MPAA, 343
nonnatural α-amino acid derivatives, 340, *340*
Pd-catalytic cycle, 338, *339*
Pd-catalyzed longer-range, 343, *343*
Pd-catalyzed *N*-(2-pyridyl)sulfonyl-directed, 342, *342*
Pd complexes, 341
Pd(II) complex structure, 338, *339*
picolinamide, 341
stereoselective synthesis of aliphatic amines, 341, *342*
synthesis of phenylalanine derivatives, 340, *341*
tricyclic quinoline, 340, 341
Yu's diverse synthesis, 340, *341*
Friedel–Crafts reactions
active catalyst, 349, *349*
advances, 345
alkylation and acylation, 344, *345*
arylations, 345
by (*R*)-BINOL-derived monophosphoric acid, 350, *351*
calcium-catalyzed intramolecular, 345, *346*
catalytic asymmetric, *348,* 348–349
cerium ammonium nitrate, 352, *352*
conjugate addition/asymmetric protonation catalyze, 350, *351*
cyclization, 347
diastereoselective intermolecular, 347, *348*
drawbacks, 345
formation of amylbenzene, 344
indoles with enecarbamates catalyze, 350, *351*
indoles with *N*-sulfonyl aldimines, 351, *351*
intramolecular attack, 353
iron-catalyzed intramolecular, 347, *347*
mechanism of alkylation, 344, *345*
network of hydrogen bonding interactions, 351–352, *352*
organocatalytic asymmetric, 350, *350*
organocatalysis
alstoscholarine, 229
(+)-aspidospermidine, 230, *230*
(−)-brasoside and (−)-littoralisone, 227–229, *228*
classification of
acid-base properties, 204, *207*
activation modes, 204, *207*
(+)-geniposide and 7-deoxyloganin, 225–227, *227*
(+)-mitsugashiwalactone, 229
(+)-vincadifformine, 230, *230*
(+)-yohimbine, 230–231, *231*
ornithine
asymmetric Mannich reaction, 392, *393–395,* 394
biocatalytic, 413–414
chiral amines as catalysts, 394–398, *395–400*
chiral brønsted acids as catalysts, 404–408, *405–408*
chiral brønsted bases as catalysts, 398, 399, 401–403, *401–404*
organometallic catalysts, 408–413, *409–413*

ornithine (*cont'd*)
biosynthesis formation of alkaloids, 383–385, *386–387,* 388
Mannich and related reactions, 414, 417–419, *417–426,* 421–422, 424, 425
oxazolidinethione, *98*
oxepane, 168, 169
5-oxo-ETE, 153, *153*
oxytetracycline, 30

P450 acetyltransferase, 242
palladium-catalyzed cross coupling reactions, 146–149, *146–149*
palladium-catalyzed cycloisomerization, 247, *248,* 251, *261,* 261–262
palladium-mediated aryl-aryl bond forming reactions, 447–450, *448–450*
palmitic acid, 130
palmitoleic acid, 134, *134*
Panek's approach, 71, *71*
β-parinaric acid, 147, *147*
parthenolide, 240–241
parviflorin, *176,* 177
Paterson's Ipc strategy, chiral ketones, *95*
pathway of deoxyxylulose phosphate (DXP pathway), 189, *190*; *see also* mevalonate-independent pathway
Pauson-Khand reaction, 247
Payne rearrangement approach, 181, *182*
(+)-pectinatone, 60–62, *61*
pederin, 38, *40*
penicillin G, 10, *10*
pericyclic reactions and applications, 291–293
Petasis reaction, 425
phase-transfer catalysis (PTCs), 220–225
phase-transfer catalyst, 216
phenethylisoquinoline, 436–438, *437, 438*
autumnaline, 437, *437*
biosynthesis, 437, *437*
colchicine, 436, 437, *438*
dienone isoandrocymbine, 438
4′-*O*-methylnorbelladine, 438, *439*
phenethylisoquinoline alkaloids
alcohol, 461
colchicine, 460
desacetamidocolchicine, 462
phenylalanine ammonia lyase (PAL), 335
3-phosphoglyceraldehyde (3-PGAL), 1
3-phosphoglycerate (3-PGA), 1
photosynthetic machinery, 1, *2*
PIAs, *see* pyrrole-imidazole alkaloids (PIAs)
picolinamide (PA), 341
picrotoxane sesquiterpenes, 266–267
Pictet–Spengler reactions, 8
pikromycin (Pik), 526
pilocarpine, 475, *476*
pinacol, 255, *256*
piperarborenines B and D, 353, *354*
pipercyclobutanamide A, 354, *355*
(+)-pironetin, 75, *75*
*Plasmodium falciparum,* 243
platinum
in metathesis reaction, 252–257
propensity of, 253
platinum chloride, enyne metathesis catalyzed by, 253
platinum cycloisomerization, *254*
podophyllotoxin, 335
podophyllum peltatum, 336
polyacetates
iterative strategy for synthesis of, 47–48, *48*
secondary metabolisms, 4
polycyclic terpenoids, 296, *298, 299*
polyene cyclizations
chiral carbocation, 319
chiral halonium ion ($X^+$), 313–319, **314,** *314–319*
chiral metal ion, 308–313, *309–313*
chiral proton ($H^+$), 304–308, *304–308*
homo(polyprenyl)arene analogs, 319, *320, 321*
polyene propargylic alcohols, 268
polyethers
acid-mediated transformations, 176–179, *177–179*
biosynthesis
annonaceous acetogenins and terpene polyethers, 165–166, *166*
ionophore antibiotics, 162–165, *164*
marine ladder toxins, 165, *165*
cyclizations
under basic conditions, 181–182, *182–183*
in water, 182–183, *183*
epoxide reactivity and stereoselective synthesis
epoxide-opening reactions, 166–172
stereoselective epoxide synthesis, 172–174, *172–175*
epoxonium ion formation, 179–181, *180–181*
polyketides, 4, *5*
aflatoxins, 21, *22*
avermectin, 21, *22*
biosynthesis, 21–23, *23,* 526, *527*
*vs.* chemical synthesis, 87, *87*
daunorubicin, 21, *22*
erythromycin A, 21, *22*
lovastatin, 21, *22*
maitotoxin, 21, *22*
natural modularity, 528
natural product biosynthesis, 528
polyene amphotericin B, 21, *22*
synthesis of
asymmetric alkylation reactions, 44–49
Evans' alkylation, 56–60
Myers' alkylation, 49–56
tetracyclines, 21, *22*
polyketide synthases (PKSs), 23, 130, 526
classification, 23–25, 24
highly reducing, 25
nonreducing, 25
partially reducing (PR), 25
type I, 23, *24,* 33–39, *33–39*
type II, 23, *24, 28–32,* 28–33
type III, *24,* 25–28, *25–28*
polyunsaturated fatty acids (PUFAs), *134,* 134–135, *135*
biomimetic transformations, 149–153, *150–153*

palladium-catalyzed cross coupling reactions, 146–149, *146–149*
Ω-3 and Ω-6 all-*Z* polyunsaturated fatty acids
cross coupling reactions, 143–145
polyyne semihydrogenation, 140–143, *141, 142, 143*
ω-3 and ω-6 polyunsaturated fatty acids
biosynthesis of, *134,* 134–135, *135*
mediated oxidations of, 135–140, *138–141*
synthesis of
leukotriene B5, *158–159,* 158–160
prostaglandins, 153–158, *154–157*
polyyne semihydrogenation, 140–143, *141, 142, 143*
prenyltransferases, 236
primary metabolism
aromatic amino acids, 333–335, *334, 335*
shikimic acid, 333, *334*
primary metabolites, 1
prins-type reaction, 255
product template (PT) domain, 33
(*S*)-proline, 45, *46*
proline–catalyzed Mannich reaction, 419
prolinol, 45, *46*
prostaglandin, 153–158, *154–157*
prostaglandin $E_1$, 146, *146*
protectin D1, 149, *149*
protecting-group-free (PGF) synthesis, 484, *484*
pseudoephedrine carboxamides
hydrolysis of, **53**
into ketones, **54**
reduction of, **53**
pseudophenamine amides, **55**
(1*S,*2*S*)-and (1*R,*2*R*)-pseudophenamines, 54, 55
pyrethric acid, 202, *204*
pyrrole-imidazole alkaloids (PIAs)
axinellamine deficient in halogens, 497, *498*
axinellamines feature synthesis, 493, *494*
Baran's hypotheses, 488, *490*
conversion of sceptrin, 488, *489*
1,9-dideoxy-pre-axinellamine synthesis, 491, *492*
Diels–Alder reaction, 491, *492*
literature method, 493, *493*
massadines, 494, *495*
oxidative ring expansion, 488
palau'amine synthesis, 496, *496*
pre-axinellamine conversion, 491, *491*
proposed conversion of axinellamine A, 494, *494*
structural diversity, 488, *489*
synthetic challenges, 488
Woodward fission, 497, *497*
pyrrole–imidazole alkaloids (PIAs), 476, 477
pyruvic acid (PA), 1, *3*

quinidine, 204, *205*
quinine, 204, *205*

radicicol, 35, *36*
RAMP and SAMP hydrazones, 45–49
reductive elimination pathway, 246–247, 250–252
resorcylic acid lactones (RALs), 35, *36*
resveratrols, 6
rhizopodin, 118–119, *119–120*
Menche synthesis of, *120*
Paterson synthesis of, *120*
rhodium-catalyzed cycloisomerization, of dienes, *260*
rhodium-catalyzed enantioselective cycloisomerizations, *251*
ribulose-1,5-bisphosphate (RuBP), 1, *2*
Robinson's approach, 414
roxaticin A, 123–126
Rychnovsky's acetonide strategy, *124, 125*

*S*-adenosyl methionine (SAM), 335
Saksena–Evans reduction, *116*
secondary metabolisms, 1–3
alkaloids, 6–10
flavonoids, 6
gallic acids, 6
polyketides, 4, *5*
resveratrols, 6
terpenes, 4–6, *5, 6*
secondary metabolites, 1, 3–4
serratenediol, 321, *323*
sesquiterpenes, 189, *190*
aromadendrane sesquiterpenes, 267
biosynthesis, 236–244
α,β-unsaturated lactone functionality, 240
cubebol-cubebenes sesquiterpenes, 267–270, *269*
cycloisomerization reaction (*see* cycloisomerization reaction)
cyperolone, 273–275
diene cycloisomerization, 257–266
diverse production of, 239
diverse structures of, 276
echinopines, 271–273
englerins, 271
formation of, 239
picrotoxane sesquiterpenes, 266–267
synthases, 238
ventricos-7(13)-ene, 270–271
sesquiterpenoids, 240
sesterterpenes, 189, *190*
Shi asymmetric epoxidation, *174*
shikimic acid
biosynthesis, 333, *334*
biosynthetic
pathway, 333, *334*
isolation, 333
simple indole alkaloids, 506, *507*
simple tetrahydroisoquinoline alkaloids, 433, *433*
singlet oxygenene, 244
singly occupied molecular orbital (SOMO) activation, 207–213, *208*
$S_N2$-type reaction, 334, *335*
Sonogashira cross coupling reaction, *144,* 145
soraphen
of biosynthesis, 87, *87*
spirangien A, 117–118, *117–119*

starter unit transacylase (SAT), 33
steroids
  biomimetic total synthesis
    achieving enantioselective cationic cyclization, 327, *328*
    caparrapi oxide, 325, *326*
    Corey's group, 321
    double bond activation, 327
    dysideapalaunic acid, 327, *327*
    8-epicaparrapi oxide, 325, *326*
    germanicol, 323, *324*
    hongoquercin B, 323, *326*
    limonoids, 321, *324*
    lupeol, 323, *325*
    oligoprenol phosphates, 319, 320
    serratenediol, 321, *323*
    site-selective epoxidation, 321, *322*
    utilizing LBA, 327
α-and β-substituents, chelation control, *91*
Suzuki cross coupling reaction, *144,* 144–145
2,3-*syn*-substituents (Felkin opposing), *91*

*Tanacetum parthenium,* 240
target-oriented synthesis, 508
target-oriented synthesis (TOS), 15, 535
telomestatin, 10, *10*
terminal TE–Claisen cyclase (TE/CLC) domain, 33
terpenes, 4–6, *5, 6,* 189, *190*
terpenoids
  biomimetic total synthesis
    achieving enantioselective cationic cyclization, 327, *328*
    caparrapi oxide, 325, *326*
    Corey's group, 321
    double bond activation, 327
    dysideapalaunic acid, 327, *327*
    8-epicaparrapi oxide, 325, *326*
    germanicol, 323, *324*
    hongoquercin B, 323, *326*
    limonoids, 321, *324*
    lupeol, 323, *325*
    oligoprenol phosphates, 319, 320
    serratenediol, 321, *323*
    site-selective epoxidation, 321, *322*
    utilizing LBA, 327
  biosynthesis
    active polycyclic compounds, 301, *301*
    animals and higher plants, 296
    bacterial membranes, 296–297
    carbocycle, 298, *299*
    C-4 methyl groups loss, 299, *300*
    cyclizations, 297
    cyclopropane moiety, 301
    double bond modifications, 299, *300*
    IPP, 296, *297*
    lanosterol, 298, 299
    Lys side chain, 302–303
    phytosterols, 301, *301*
    polycyclic, 296, *298, 299*
    polycyclic natural compounds, 301, *302*
    stereochemistry, 298
    vanadium haloperoxidases, 302, *302*
    Wagner–Meerwein ring, 297, *298*
  bromine-containing polycyclic, 308
  diastereoselective polyene cyclizations, *303,* 303–304
  polyene cyclizations
    chiral carbocation, 319
    chiral halonium ion ($X^+$), 313–319, **314,** *314–319*
    chiral metal ion, 308–313, *309–313*
    chiral proton ($H^+$), 304–308, *304–308*
    homo(polyprenyl)arene analogs, 319, *320, 321*
terpenoid synthase fold, 239
tetracyclines, 21, *22*
tetraenes, hydroacylation cycloisomerization of, 268
tetrahydropyran, 168, 169
tetraterpenes, 189, *190*
thapsigargin, 242
  biosynthesis of, *243*
thiamine pyrophosphate (TPP), 192
thiazolidinethione, *98*
thioesterase (TE), 526
2-thiomethylaniline, 338, 340
thyrsiferol, 162, *163*
total synthesis
  diversity-oriented synthesis, 15–16
  evolution of, 14
  function-oriented synthesis, *15,* 15–16
  of spirangien A, 117–118, *117–119*
  strychnine, 14–15, *15*
transannular Diels-Alder (TADA) reaction, 289
*trans*-farnesyl diphosphate synthase
  crystal structures, *238*
*trans*-farnesyl pyrophosphate synthase
  prenyltransferase, 236
transition metal-catalyzed couplings, 450, *452–455,* 453–456
*trans*-prenyltransferases, 236
trichothecenes, 244
triene cycloisomerizations
  application, *265*
  iron-catalyzed cycloisomerization, *264*
  1,3,8,10-tetraenes, 265
triterpenes, 189, *190*
tryptophan
  biosynthetic pathway, 333, *335*
  bisindole
    biosynthesis, 513, *513*
    Hao's total synthesis, 516, *517*
    Movassaghi's synthesis, 514, *515,* 516
    Strecker-type reaction, 516
    synthetic chemist's view, 517
    Tambar's total synthesis, 514, *514,* 516
    trigonoliimine A, 512–513, *513*
    Wagner–Meerwein type, *515,* 515–516
  monoterpene indole
    collective total synthesis, 511, *512*

goniomitine total synthesis, 511–512, *512*
Jieping Zhu's synthetic plan, 511, *512*
MacMillan's synthesis, 510, *511*
synthasis
decarboxylase, 507
mechanism, 505, *506*
ribbon structure, 505, *506*
tyrosine
aryl-aryl coupling reactions
classification of different types, 442
copper-mediated aryl-aryl bond forming reactions, 443–446, *443–446*
intrinsic importance, 442
nickel-mediated aryl-aryl bond forming reactions, 446–447, *447*
palladium-mediated aryl-aryl bond forming reactions, 447–450, *448–450*
transition metal-catalyzed coupling, 450, *452–455,* 453–456
biosynthesis
amaryllidaceae alkaloids, 438–442, *439–442*
classification, 431, *432*
modified benzyltetrahydroisoquinoline alkaloids, 433–436, *434–436*
phenethylisoquinoline, 436–438, *437, 438*
phenylethylamines, 431–433
simple tetrahydroisoquinoline alkaloids, 433, *433*
biosynthetic pathway, 333, *334*
synthesis
amaryllidaceae alkaloids, 462–468, *463–468*
modified benzyltetrahydroisoquinoline alkaloids, 456–460, *457–459*
phenethylisoquinoline alkaloids, 460–462, *461–462*

Udwary–Merski algorithm (UMA), 33
Ueno-Stork radical cyclization, 358, *359*
unsaturated carboxylic acids, cyclization, 307, *307*

vade mecum, 1
vanadium haloperoxidases (V-HPO), 302, *302*
vancomycin, 531
vancomycin aglycone, 10, *10*
ventricos-7(13)-ene sesquiterpene, 270–271
V-HPO, *see* Vanadium haloperoxidases (V-HPO)
(+)-vincadifformine, 230, *230*
vinylmetal pathway, 246, 247
(+)-vittatalactone, 75–77, *76*
vomitoxin, 244

Wagner-Meerwein rearrangements, 197, 239
Westley's hypothesis, polyether biosynthesis, 162
wild-type metabolites, biosynthetic pathway of, 11, *12*

Xiong's synthesis, of omaezakianol, 178, *178*

(+)-yohimbine, 230–231, *231*

zearalenone, 35, *36*
Zimmerman–Traxler transition state, 88, 89, *89*
zwitterions, *254*

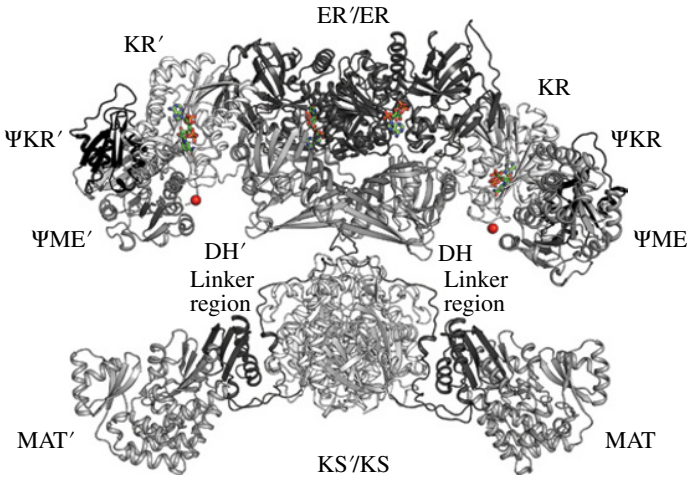



**FIGURE 3.1** An overview of the crystal structure of the multidomain porcine fatty acid synthase (FAS) dimer with domain names, $NADP^+$ (green/orange) and ACP/TE (red spheres) anchoring points (PDB: 2VZ9). Adapted from Maier et al. [10].

*From Biosynthesis to Total Synthesis: Strategies and Tactics for Natural Products*, First Edition. Edited by Alexandros L. Zografos.
© 2016 John Wiley & Sons, Inc. Published 2016 by John Wiley & Sons, Inc.

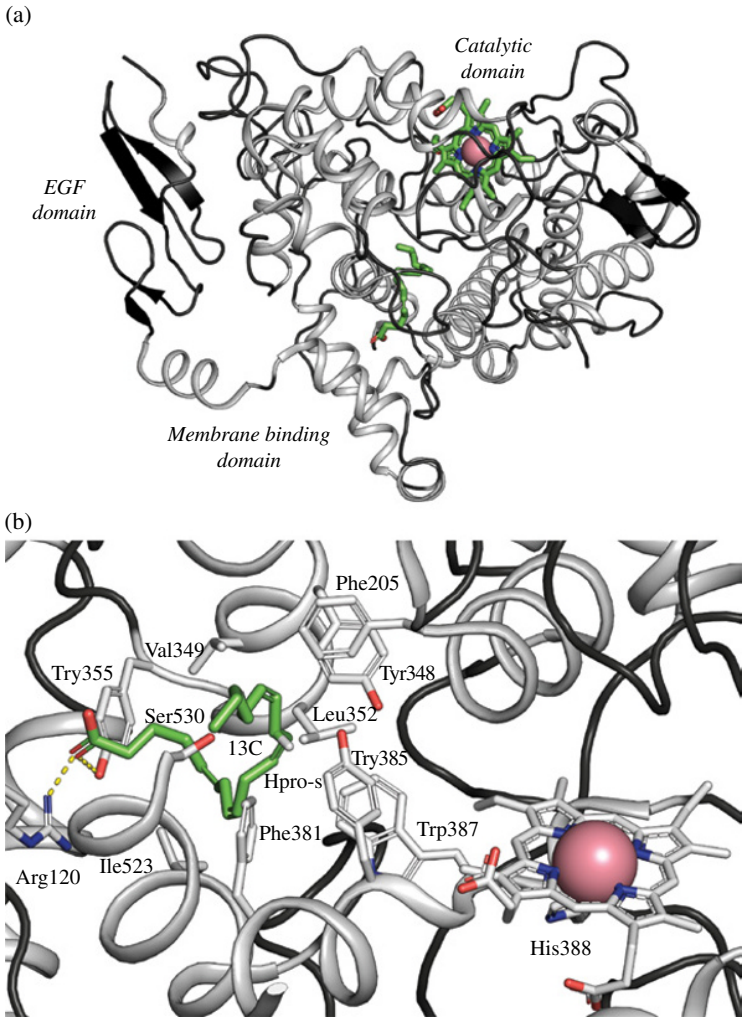



**FIGURE 3.4** The ovine $Co^{3+}$-COX-1 (PGHS-1) enzyme, with arachidonic acid (**8**) in the COX channel (PDB: 1DIY). (a) Structural overview showing the domains of monomeric COX-1. Arachidonic acid (**8**) and the $Co^{3+}$-protoporphyrin IX are shown in green. (b) The peroxidase active site of COX-1 with arachidonic acid (**8**) (green), important nearby residues, and the $Co^{3+}$-protoporphyrin IX. Phe209 has been omitted for clarity. Adapted from Malkowski et al. [25].

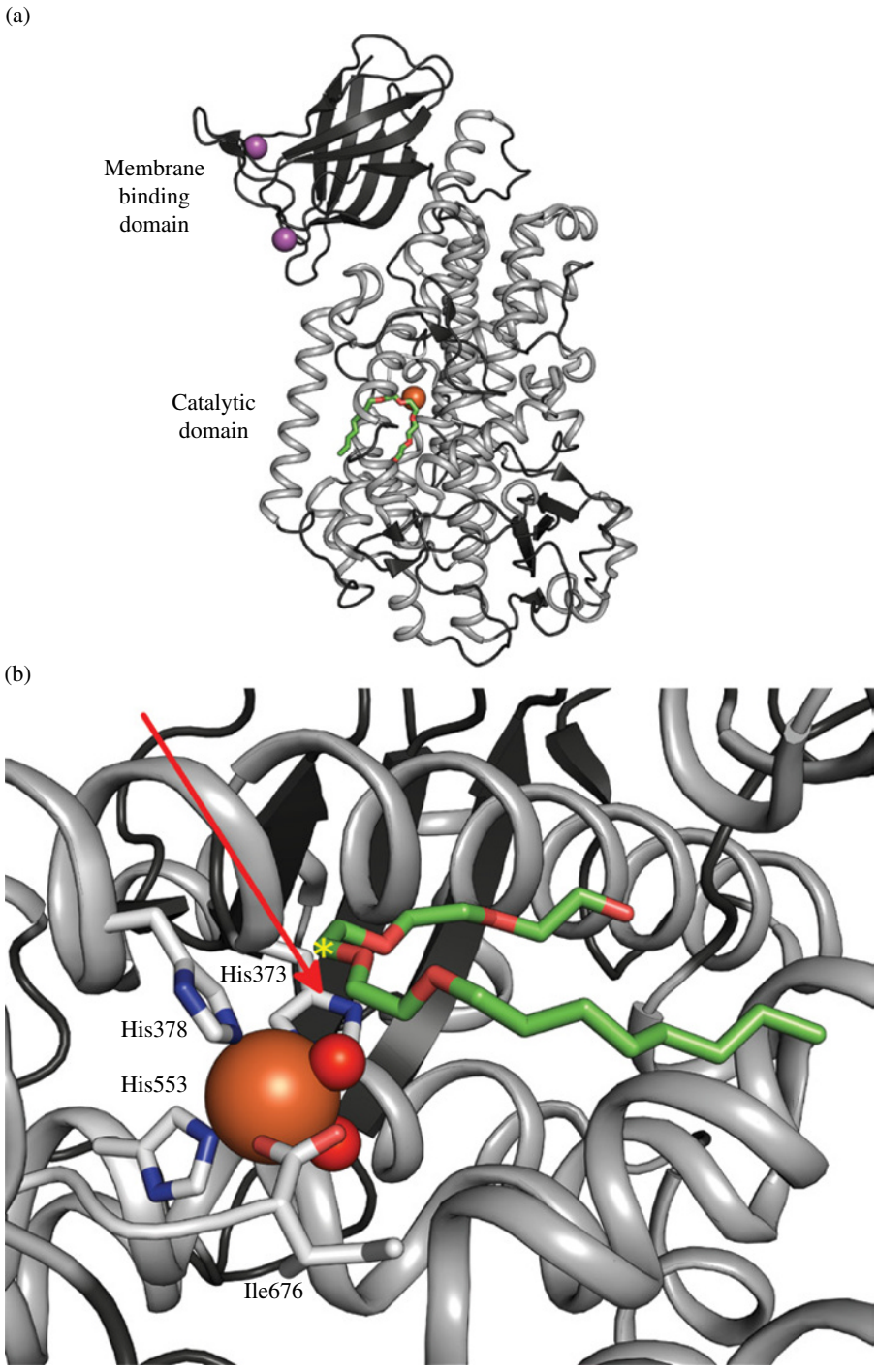



**FIGURE 3.5** The human LOX-15 enzyme bound to the substrate mimic octyl tetraethylene glycol ether (C8E4) (PDB: 4NRE). (a) Overview of the LOX-15 structure with domain names. $Ca^{2+}$ atoms are shown in purple, $Fe^{2+}$ atom in orange, and C8E4 in green. (b) Structure of the LOX-15 active site showing the nonheme $Fe^{2+}$ (orange) coordinated by three histidines, the C-terminal carboxylate and two water molecules. C8E4 is shown with green carbons. The yellow asterisk indicates the approximate position of the C13-carbon of arachidonic acid (**8**) when modeled into the C8E4 electron density. The red arrow denotes the direction and opening of the $O_2$ channel toward the active site. Adapted from Kobe et al. [28].

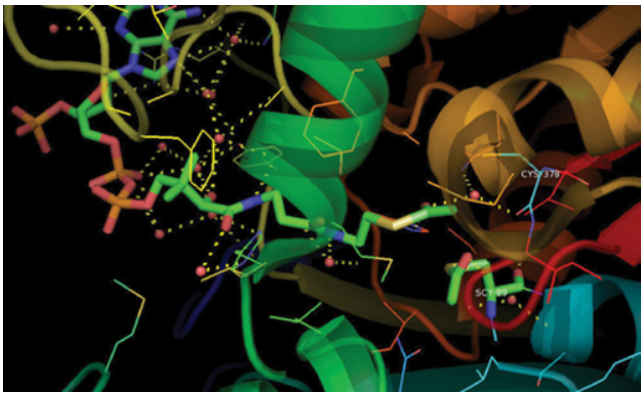


**FIGURE 5.4** Acetylated crystal structure of acetoacetyl-CoA transferase from *Zoogloea ramigera* cocrystallized with acetyl-CoA based on structural coordinates PDB: 1DM3 [10].

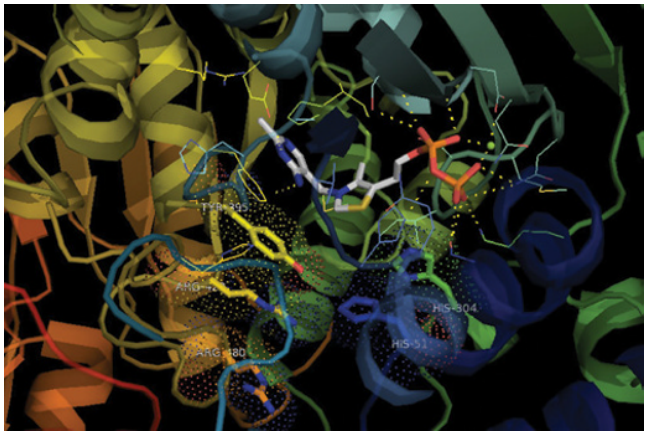


**FIGURE 5.5** Active site of DXP synthase from *D. radiodurans* based on structural coordinates PDB: 2O1X. TPP-cofactor is shown in stick colored by element, magnesium atom is shown as a green dot, active binding site of glyceraldehyde-3-phosphate is highlighted by dots [10a].

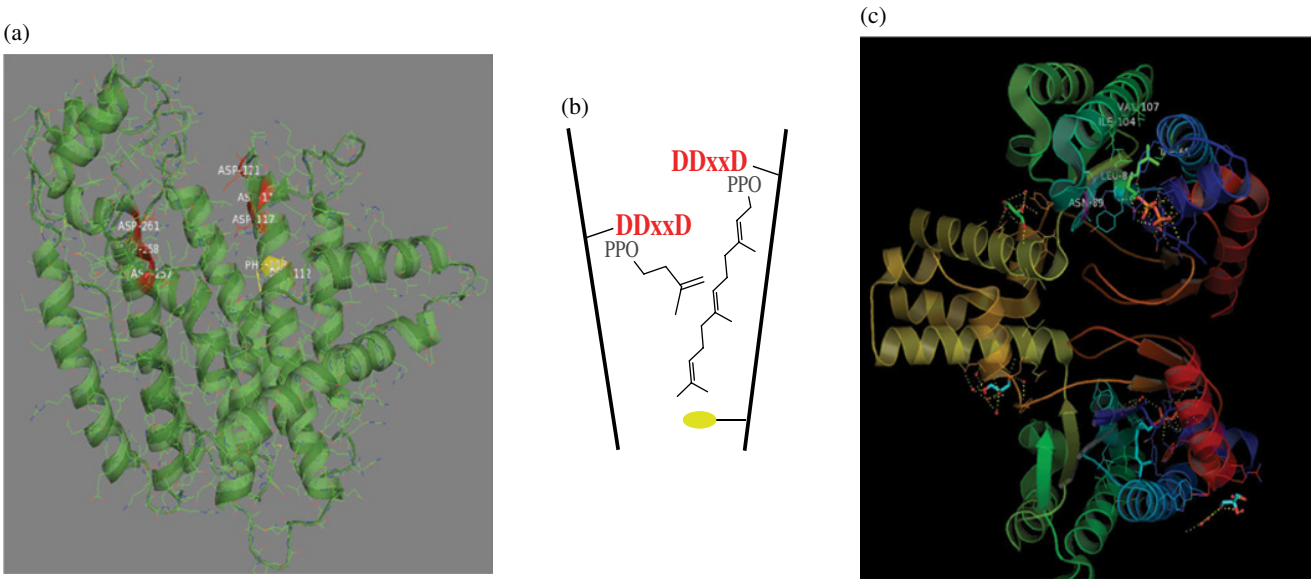



**FIGURE 7.2** (a) Crystal structure of avian *trans*-FPPS (in red conserved DDxxD areas; in yellow terminating FF residues) and (b) graphic animation of the active center of synthase enzymes; (c) crystal structure of *cis*-prenyltransferase Rv1086 producing *Z*,*E*-farnesyl diphosphate. Images created with PyMOL.

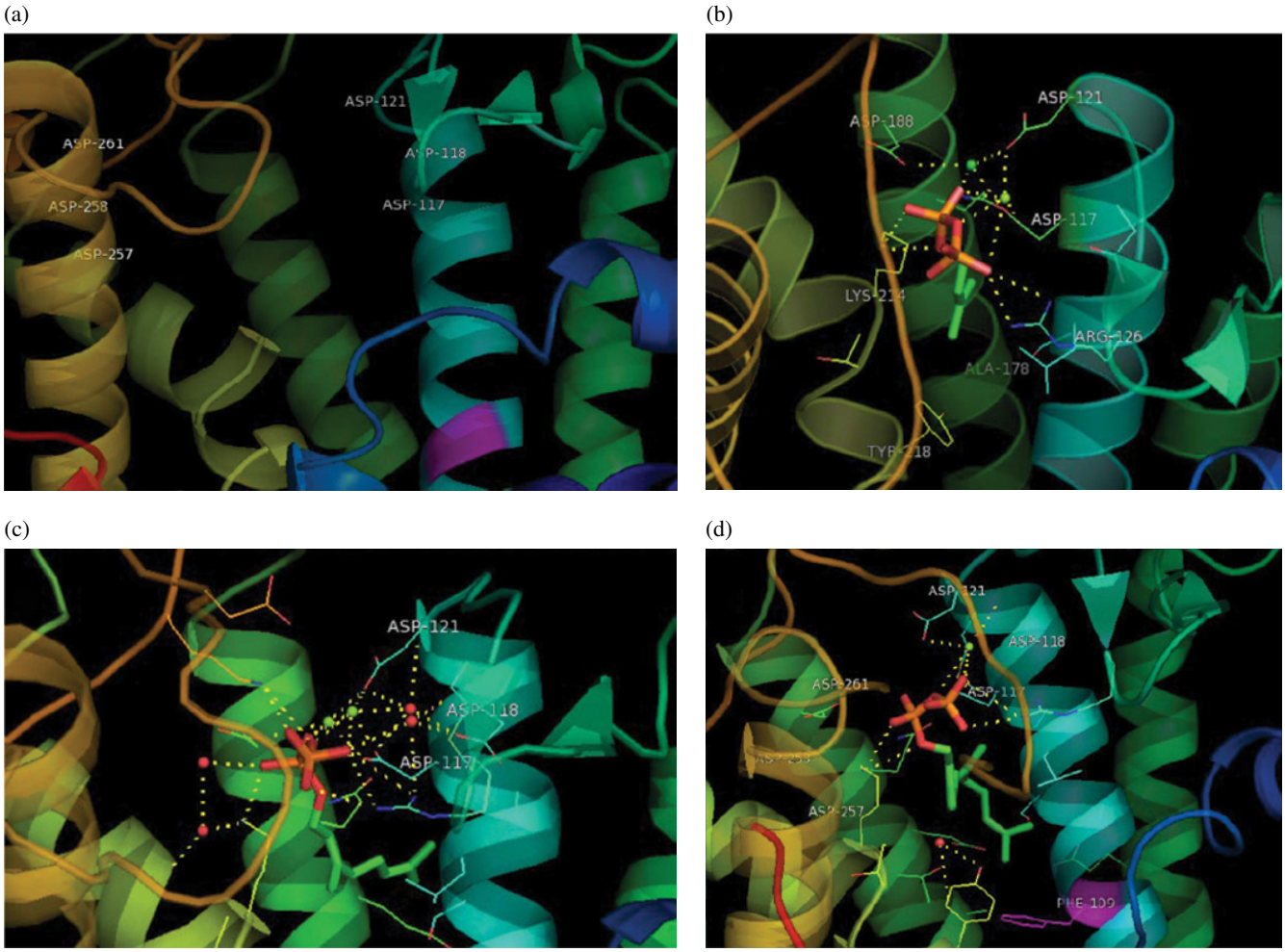



**FIGURE 7.3** Crystal structures of (a) *trans*-farnesyl diphosphate synthase; cocrystallized with (b) IDP, (c) GDP, (d) FDP (metal coordination and hydrogen bonds are shown as yellow dashed lines; magnesium anions are shown as green spheres, whereas red spheres are representing water molecules; terminating residue Phe109 is shown in magenta); Images created with PyMOL.

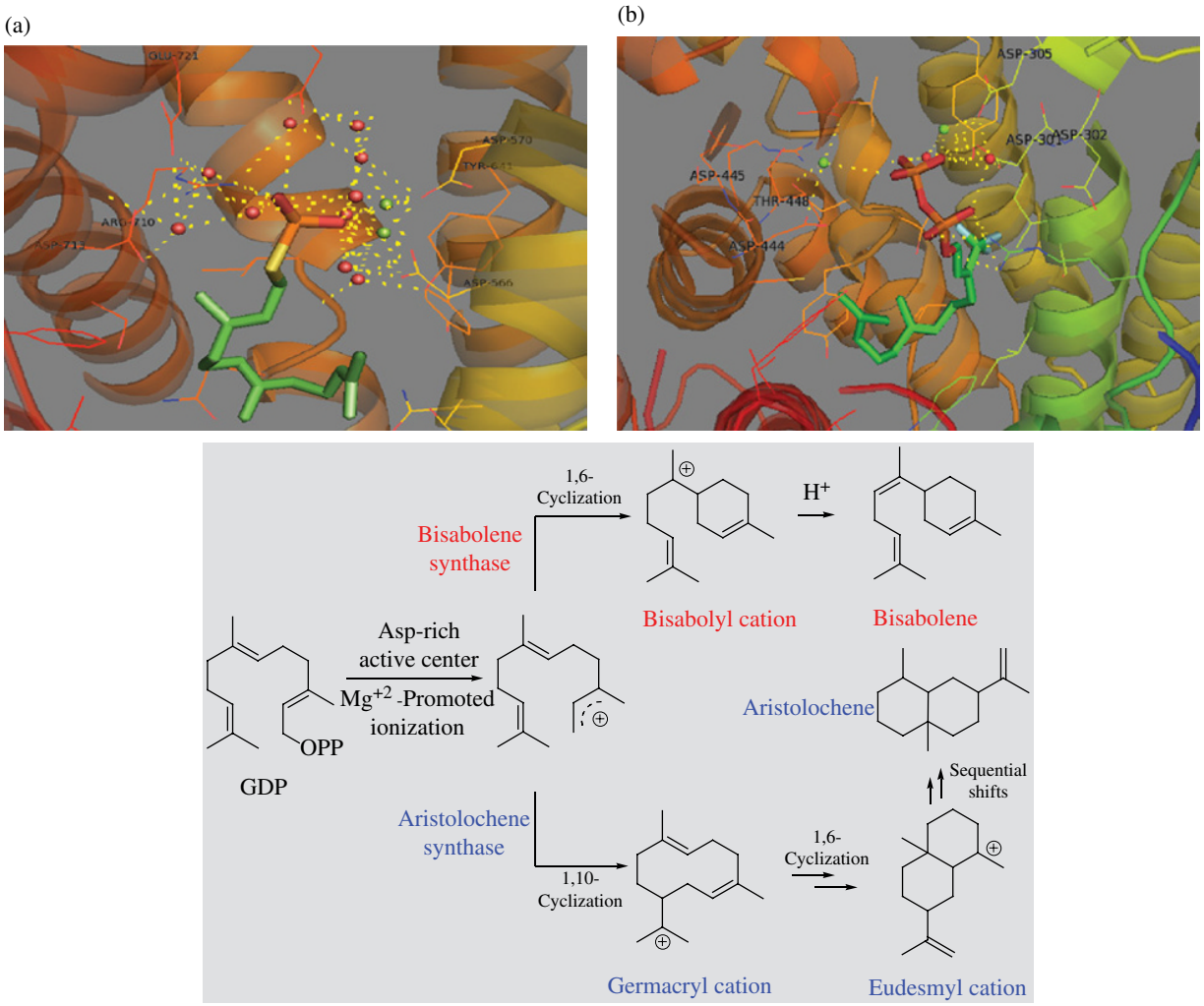
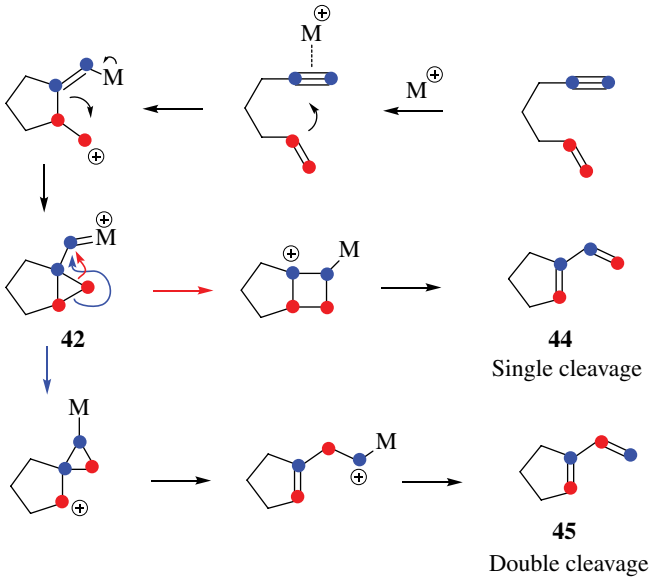



**FIGURE 7.4** Crystal structure of (a) bisabolene synthase active center bound to farnesyl diphosphate inhibitor; (b) aristolochene synthase cocrystallized with FDP (metal coordination and hydrogen bonds are shown as yellow dashed lines; magnesium anions are shown as green spheres, whereas red spheres are representing water molecules) and the proposed catalytic mechanisms for each cyclization; Images created with PyMOL.




**SCHEME 7.23** Single and double cleavage rearrangement products and a more detailed description of double cleavage product highlighted by the collapse of a metallocyclopentene.

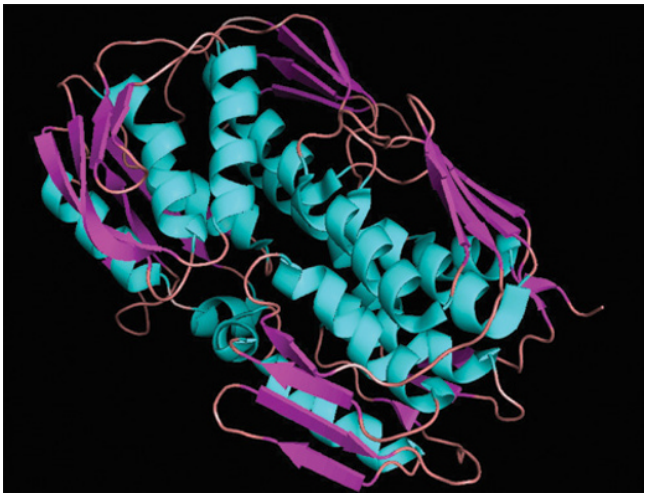


**FIGURE 14.2** Ribbon diagram of EPSP synthase (EC 2.5.1.19).

# WILEY END USER LICENSE AGREEMENT

Go to www.wiley.com/go/eula to access Wiley's ebook EULA.